DIGITAL COMMONS
@ UNIVERSITY OF SOUTH FLORIDA

University of South Florida
Digital Commons @ University of South Florida

KIP Talks and Conferences

Karst Information Portal

January 1997

Proceedings of the 12th International Congress of Speleology. Volume 1: Symposium 7, Physical Speleology & Symposium 8, Karst Geomorphology 12th International Congress of Speleology. Volume 1 Symposium 7, Physical Speleology & Symposium 8, Karst Geomorphology

Pierre-Yves Jeannin

Follow this and additional works at: https://digitalcommons.usf.edu/kip_talks

Recommended Citation
Jeannin, Pierre-Yves, "Proceedings of the 12th International Congress of Speleology. Volume 1: Symposium 7, Physical Speleology & Symposium 8, Karst Geomorphology 12th International Congress of Speleology. Volume 1 Symposium 7, Physical Speleology & Symposium 8, Karst Geomorphology" (1997). *KIP Talks and Conferences*. 121.
https://digitalcommons.usf.edu/kip_talks/121

This Conference Proceeding is brought to you for free and open access by the Karst Information Portal at Digital Commons @ University of South Florida. It has been accepted for inclusion in KIP Talks and Conferences by an authorized administrator of Digital Commons @ University of South Florida. For more information, please contact digitalcommons@usf.edu.

La Chaux-de-Fonds
Switzerland
10th – 17th August 1997

Proceedings of the 12th International Congress of Speleology

Volume 1

Symposium 7: Physical Speleology

Symposium 8: Karst Geomorphology

International Union of Speleology / Swiss Speleological Society

Swiss Speleological Society (SSS/SGH)

Proceedings of the 12th International Congress of Speleology

Volume 1

Symposium 7

Physical Speleology

&

Symposium 8

Karst Geomorphology

La Chaux-de-Fonds, Switzerland, 10-17.08.1997

Editor: Pierre-Yves Jeannin

Symposium 7: Physical Speleology

Symposium 8: Karst Geomorphology

Scientific coordinators: Thomas Bitterli
Wanda Stryjenska

Editorial board: Jörg Bäuchle
Volker Bäuchle
Chris Keller
Kurt Keller
Joëlle Salamin

Scientific committee:

Thomas Arbenz
Philippe Audra
Ian Chandler
Jean-Paul Graf
Stéphane Gogniat
Thomas Gubler
Thilo Herold
Beat Höchli
Nicole Höchli
George Huppert
Prisca Mariotta
Karlin Meyers
Michel Monbaron
Daniel Müller
Luc Perritaz
Sybille Rex
Dagmar Risen
Nicole Ruder
Daniela Spring
Hans Stünzi
George Veni
Sophie Verheyden
Michaela Wessicken
Andres Wildberger
William B. White

International Union of Speleology
Union Internationale de Spéléologie
Internationale Union für Speläologie

Swiss Speleological Society (SSS)
Société Suisse de Spéléologie (SSS)
Schweizerische Gesellschaft für Höhlenforschung (SGH)

United Nations Educational, Scientific and Cultural Organisation
Organisation des Nations Unies pour l'éducation, la science et la culture
United Nations Educational, Scientific and Cultural Organisation

International Association of Hydrogeologists (IAH)
Association Internationale des Hydrogéologues (AIH)

International Association of Hydrological Sciences (IAHS)
Association Internationale des Sciences Hydrologiques (AISH)

Swiss Academy of Sciences (SAS)
Académie Suisse des Sciences Naturelles (ASSN)
Schweizerische Akademie für Naturwissenschaften (SANW)

International Geographic Union
Union Géographique Internationale

International Association of Geomorphologists (I.A.G.)
Association Internationale des Géomorphologues (A.I.G.)

ISBN 2-88374-006-2 (Vol. 1)
ISBN 2-88374-012-7 (Vol. 1-6)

Publisher: Speleo Projects, Therwilerstr. 43, CH-4054 BASEL, Switzerland

Cover: Titanengang, Hölloch, Switzerland (Photo Ballmann/Widmer)

Sales: Bibliothèque de la Société Suisse de Spéléologie, c/o Bibliothèque de la Ville, Rue du Progrès 33, CH-2300 La Chaux-de-Fonds, Fax: 021 947 53 78, email: ssslib@vtx.ch

Printed in Switzerland

Papers published from the camera ready copies, prepared by the authors after reviewing by the members of the scientific committee. Despite this, the scientific board wishes to make clear that it shall take no responsability for any mistakes and omissions, or for the opinions stated by the authors.

Table of Contents

Symposium 7: Physical speleology

Session 1a: Karstic sediments and paleoclimate, *sedimentology*

Choppy Jacques & Dubois P. — Etude scientifique de la grotte de Clamouse (Hérault, France) ... 3

Pavuza Rudolf — Höhlensedimentologie in Österreich ... 7

Forgeot Olivier — Les méga-remplissages détritiques de la Cueva Fresca ... 9

Kadlec Jaroslav — Shape of fluvial pebbles in surface and subsurface streams from Moravian karst, Czech Republic ... 13

Allison Cara & Smart P. L. — The value of quarry records and monitoring excavation progress in the interpretation of sediment-filled caves in Eldon Hill Quarry, Derbyshire, England ... 16

Felisiak Ireneusz — Age and distribution of some karstic sediments from the Polish Jura and their implications for the age of the relief ... 17

Krekeler Mark P. S. *et al.* — Sedimentology, clay mineralogy, and geochemistry of cave sediment from Hard Baker Cave, Rockcastle County, Kentucky, USA ... 21

Summers Engel Annette *et al.* — A study of cave sediment from Movile Cave, Southern Dobrogea, Romania ... 25

Maltsev Vladimir A. *et al.* — Cave chemolithotrophic soils ... 29

Zupan Hajna Nadja — Mineral composition of clastic material in fault zones and open fissures in karst rocks, examples from SW Slovenia ... 33

Session 1b: Karstic sediments and paleoclimate, *dating, isotopes, paleomagnetism*

Tuccimei Paola *et al.* — Th/U dating of sea level controlled phreatic speleothems from caostal caves in Mallorca (Western Mediterranean) ... 37

Labau V. *et al.* — Speleothems dating using the thermoluminescence method ... 41

Ford Derek & Zambo L. — U series dating of phases of speleothem deposition and erosion in Baradla Cave, Aggtelek National Park, Hungary ... 44

Hercman Helena, *et al.* — Uranium-series dating of speleothems from Amaterska and Holstejnska caves, Moravian karst, Czech Republic ... 45

Linge Henriette & Lauritzen S.-E. — Potential use of uranium series dating of calcareous algae as a tool for dating paleo-watertables in maritime karst settings ... 49

Berstad Ida Malene *et al.* — U-series dating and stable isotope analysis of some last interglacial speleothems from north Norway ... 53

Holmgren K. *et al.* — Speleochronology, stable isotopes and laminae analysis of stalagmites from southern Africa ... 55

Mihevc Andrej & Lauritzen S.-E. — Absolute datations of speleothems and its speleomorphological significance from Divaska jama and Jazbina caves; Kras plateau, Slovenia ... 57

MacDonald William D. & Yonge C. J. — The isotope systematics of perennial cave ice in Northwestern Canada ... 60

Perrette Yves *et al.* — Enregistrement de l'activité charbonnière dans les spéléothèmes de Choranche (Vercors, France) ... 61

Shopov Yavor Y. *et al.* — Influence of the bedrock CO_2 on stable isotope records in cave calcites ... 65

Barredo Silvia P. *et al.* — Paleomagetic study in the Cuchillo Cura System, Neuquen Province, Argentina ... 69

Scherrer Nadim C. *et al.* — The palaeomagnetism of speleothems of Middle Quaternary age from northern Australia ... 73

Session 1c: Karstic sediments and paleoclimate, *paleoclimate*

Frisia Silvia *et al.*	Holocene paleoclimatic fluctuations recordedby stalagmite: Grotta di Ernesto (N Italy)	77
Gradzinski Michal, *et al.*	Environmental controls of origin of the annually varved calcite speleothems	81
Hercman Helena *et al.*	The antiquity of the famous Demianowska caves (Slovakia)	85
Hercman Helena & Walanus A.	Speleothem growth frequencies (PDF) as a climate record: problem of significance	87
Ford Derek C. *et al.*	A long interglacial and interstadial record in the North American mid-continent from vadose and phreatic speleothems, Jewel Cave and Wind Cave, South Dakota, U.S.A.	88
White William B.	Precise measurement of luminescence banding profiles in speleothems for paleoclimatic interpretation	89
Williams Paul W.	Evidence of glacial advances from New Zealand cave deposits	92
Verheyden Sophie *et al.*	L'oxygène et le carbone dans les concrétions nous informent-ils sur les climats passés ?	93
Pajón Morejon Jesús M.	Paleoclimate of the quaternary processes in the Western karst of Cuba: a quantitative characterization	97
Kempe Stephan & Hartmann J.	Excentriques capillaries: do they carry paleoclimatic information?	100
Lundberg Joyce	Paleoclimatic reconstruction and timing of sea level rise at the end of the Penultimate Glaciation, from detailed stable isotope study and TIMS dating of submerged Bahamian speleothem	101
Shopov Yavor Y.	Speleothem records of environmental changes in the past - Potential in comparison with the other paleoenvironmental archives and related UIS international programs 103	
Shopov Yavor Y. *et al.*	Speleothems as natural climatic stations with annual to daily resolution	105
Shopov Yavor Y. *et al.*	Speleothem luminescence proxy records of annual rainfall in the past. Evidences for "the Deluge" in speleothems	107
Shopov Yavor Y. *et al.*	Speleothem luminescence proxy records of geomagnetic field intensity	110
Shopov Yavor Y. *et al.*	Speleothem records of processes beyond the Solar System (supernova eruptions)	111

Session 2a: Cave morphology and genesis, *geological factors*

Sebela Stanka	Development of cave passages according to geological structure; example from Jama pod Pecno rebrijo, Slovenia	113
Leel-Ossy Szabolcs	Genesis of Jozsefhegy hydrothermal cave, Budapest	116
Sustersic France	Cave patterns North of the Planinsko polje (Slovenia)	117
Turchinov Igor	Lithological control of speleogenesis in the Pre-Carpathian region	121
Ruggieri Rosario	The Karst in the area of Matumbi Hills (Kilwa district, Tanzania). Hydrogeological characteristics and relationships between morphostructures and tectonic phases	125
Martin Philippe	Structures hiérarchiques dans le karst de la St Baume (Bouches du Rhône, Var, France)	129
Terlau Craig A. & Day M. J.	A comparison of the orientation of cave passages and surface tributary valleys in the karst of Southwestern Wisconsin, U.S.A.	133
Hof Alex	Labyrinthes et Sieben Hengste	137
Frumkin Amos	Classification and some morphometric features of salt caves	139
Farina Daniele & Gallerini G.	A karstic system in a semiallochtonous gypsum unit : the Legnanone caves (Marecchia valley, Italy): preliminary geological and hydrogeological features	143

Tarhule-Lips Rozemarijn F. A. & Ford D. C.	Morphologic studies of Bell hole development on Cayman Brac	146
Garasic Mladen	Some types of speleogenesis and speleohydrogeology in Dinaric karst area (Croatia, Europe)	147
Niggemann Stefan	Origin and development of caves in the Devonian massive limestone of the Rheinisches Schiefergebirge (Germany)	151
White Elizabeth L. & White W. B.	Mechanics of cave breakdown: relative importance of shear strength and fracture toughness	155
Knez Martin	Phreatic Channels in Velika dolina Collapse Doline (Skocjanske jame Caves, Slovenia)	156

Session 2b: Cave morphology and genesis, *hydrogeological factors*

Klimchouk Alexander	Artesian speleogenetic setting	157
Klimchouk Alexander	Speleogenetic effects of water density differences	161
Audra Philippe	Le rôle de la zone épinoyée dans la spéléogénèse	165
Kicinska Ditta	Reconstruction of paleoccurents in caves of the Bystra Valley (Tatra Mountains, Poland), on the basis of scallops and deposits analyses	168
Foltete Jacques	Hypothèse sur la genèse d'un siphon	169
Jaillet Stéphane	Hydrologie du système karstique du Rupt du Puits (Lorraine/Champagne, France) : fonctionnement du siphon aval	171
Vasileva Danica	The role of groundwater in the genesis of Resava cave	175
Lauritzen Stein-Erik *et al.*	Bell hole morphometry of a flank margin cave and possible genetic models: Lighthouse Cave, San Salvador, The Bahamas	178
Rossi Carlos *et al.*	Cave development along the water table in Corbe System (Sierra de Peñalabra, Cantabrian Mountains, Northern Spain)	179
Rossi Carlos *et al.*	Multiple paleo-water tables in Agujas Cave System (Sierra de Peñalabra, Cantabrian Mountains, Northern Spain): Criteria for recognition and model for vertical evolution	183
Galdenzi Sandro *et al.*	La corrosione di placchette calcaree ad opera di acque sulfuree: dati sperimentali in ambiente ipogeo	187

Session 3: Cave climatology

Mavlyudov Bulat R.	Caves climatic system	191
Jeannin Pierre-Yves *et al.*	Some concepts about heat transfer in karstic systems	195
Halliday William R.	Hyperthermic caves of the United States	199
De Paola Marco *et al.*	Misure di temperatura in due cavità carsiche nella formazione Gessoso-Solfifera dell'alto Crotonese (Italia meridionale)	202
Cigna Arrigo A.	Monitoring results in "Grotta Grande del Vento" (Frasassi, Ancona, Italy) and its visitors' capacity	203
Stoev Alexey *et al.*	Temperature anomalies formation and secular instability research of ice of atmospheric origin in the karst caves of North Albanian Alps	207
Pechhold Eberhard	CO_2 - Gehalte von Luft und Wasser im vadosen Karst und in der Bodenauflage	211
Mueller Robert J. & Day M. J.	Daily atmospheric variation within caves in southwestern Wisconsin, U.S.A.	215

Session 4a: Cave mineralogy, *minerals*

Maltsev Vladimir A. — Overview of cave minerals onthogeny ... 219

Martini Jacques E.J. — Pyrocoproite (Mg $(K,Na)_2P_2O_7$, monoclinic), a new mineral from Arnhem Cave (Namibia) derived from bat guano combustion ... 223

Hill Carol A. & Forti P. — The classification of cave minerals and speleothems ... 226

Viehmann Iosif *et al.* — Crystallographical observations on calcite rafts from three Romanian caves ... 227

Ghergari Lucretia *et al.* — Mineralogy of crusts and efflorescences from Humpleu cave system ... 231

Onac Bogdan Petroniu *et al.* — Deposition of black manganese and iron-rich sediments in Vântului Cave (Romania) ... 235

Turchinov Igor — Cave minerals of the Western Ukraine ... 239

Urbani Franco — Venezuelan cave minerals: a short overview ... 243

Session 4b: Cave mineralogy, *speleothems*

Frisia Silvia *et al.* — Aragonite precipitation at Grotte de Clamouse (Hérault, France): role of magnesium and driprate ... 247

Niggemann Stefan *et al.* — Aragonitic/calcitic coralloids in carbonate caves: evidence for solutions of different Mg influence ... 251

Perrette Yves *et al.* — Characterisation of speleothem crystalline fabrics by spectroscopic and digital image processing methods (Choranche, Vercors, France) ... 257

Tarhule-Lips Rozemarijn F. A. & Ford D. C. — Studies of speleothem dissolution on Cayman Brac and Isla de Mona ... 261

Van Beynen P. E. *et al.* — Chemical differences between light and dark coloured speleothem ... 262

Rowling Jill — Ribbon Helictites from Jenolan Caves, NSW Australia ... 263

Maltsev Vladimir A. — Stalactites, crystlactites, corlactites, tuflactites - 4 types of "stalactite-like" formations generated from cristallisation environments with different physical properties ... 267

Dublyansky Yuri V. & Pashenko S. E. — Cave Popcorn - An Aerosol speleothem ? ... 271

Gradzinski Michal *et al.* — Microbial agents of moonmilk calcification ... 275

Song Linhua — Classification of shields in Shihua Cave, Beijing ... 279

Symposium 8: Karst geomorphology

Session 1: Epikarstic zone: morphology, hydraulic behaviour and genesis

Goldie Helen S. Cox N. J. — Geomorphology of limestone pavements of some British, Irish and Swiss sites ... 285

Tyc Andrzej — Epikarstic features in zones affected by periglacial processes - example of the Silesian-Cracow Upland (Poland) ... 289

Puech Vincent & Jeannin P.-Y. — Contribution à la compréhension du fonctionnement hydraulique de l'épikarst : expériences d'arrosage sur le site de Bure (Jura, Suisse) ... 293

Sbai Abdelkader *et al.* — Intensité de la corrosion dans les sols du Jura méridional (France) - Note préliminaire ... 297

Liu Zaihua *et al.* — Carbon dioxide in soil and its drive to karst processes: A case study in transitional zone between North and South China ... 300

Clemens Torsten *et al.* — The influence of the Pco_2 on the chemical composition of karst spring water (Swabian Alb, SW Germany) 301

White William B. & White E. L. — A theoretical model for the distribution and transport of carbon dioxide in the epikarst 305

Klimchouk Alexander — The nature and principal characteristics of epikarst 306

Harlacher Christof *et al.* — Changes in chemical composition and physical parameters of water in an alpine karst system (Totes Gebirge, Steiermark, Austria) 307

Huntoon Peter W. — Definition and characteristics of stone forest epikarst aquifers in South China 311

Martini Sergio — Il ruolo dello strato limite turbolento nella morphogenesi dei rillenkarren 315

Sauter Martin — Determination of the hydraulic characteristics of the epikarst – Local and regional approaches 318

Song Linhua — Epikarst aquifer in Fengcong regions, South China 319

Session 2: Geotopes and human impact on karst

Ek Camille & Closson D. — Le karst en tant que contrainte physique en aménagement du territoire. Exemple de la commune de Sprimont (Belgique) 322

Pulina Marian *et al.* — Human impact on karst environment of the Silesian-Cracow region in South Poland 323

Gillieson David — Environmental change and human impact on the arid karst of the Nullarbor Plain, Australia 327

Grandgirard Vincent & Spicher M. — Les géotopes karstiques du canton de Fribourg (Suisse) 331

Session 3: Karst history of alpine caves

Audra Philippe — Réflexion sur les facteurs contrôlant la karstification dans l'Arc alpin 337

Denneborg Michael — Aufbau und Speleogenese eines hochalpinen Karstsystems (Kolkbläser-Monsterhöhle-System, Steinernes Meer, Österreich; L=43.4 km, HD= - 711 m) 341

Bini Alfredo *et al.* — Karst and glaciations in the Southern pre-alpine valleys 345

Bitterli Thomas & Jeannin P.-Y. — Entwicklungsgeschichte der Höhlen im Gebiet Hohgant - Sieben Hengste - Thunersee (Berner Oberland, Schweiz) 349

Loiseleur Bernard — Le synclinal oriental de Chartreuse (France) - Facteurs influant sur la genèse des grands réseaux 355

Vanara Nathalie & Maire R. — Neotectonique et spéléogenèse : application au massif pyrénéen des Arbailles (France) 359

Session 4a: Karst geomorphology, *karst & environment*

Furquim Scaleante Oscarlina A. — Geography and speleology 363

Pulina Marian & Glowacki P. — Reaction of the karst environment for acid rains (example: the massif of Snieznik - the Sudety Mountains, Polish and Czech sides) 366

Choppy Jacques — La tectonique et le karst 367

Singh Ramesh B. — Monitoring tropical geosystem, underground topography and potential water resources for sustainable development using geoinformatics - Indian case study 369

Veni George — The effects of aridity and topography on limestone cave development 373

Slabe Tadej — Cave rocky relief and its speleogenetical significance 377

Goggin Keith E. & Medville D. M. — Solutionally enlarged glacial striae on Ordovician dolomites in Western Wyoming, USA ... 381

Zhu Xuewen — Simultaneous systematic evolution of fenglin karst landforms ... 385

Kadlec Jaroslav — Reconstruction of the development of semiblind ponor valleys in Moravian karst based on geophysical surveying, Czech Republic ... 387

Hill Carol A. — Sulfuric acid karst: what is it good for? ... 390

Trofimova Elena — Karst denudation in Irkutsk Region ... 391

Lin Junshu *et al.* — Karst geomorphological process responses to climate ... 395

Session 4b: Karst geomorpholgy, regional studies

Perna Giuliano — Deep Messinian karst in Mediterranean area ... 397

Dimuccio Luca Antonio — Studio morphoevolutivo del fenomeno carsico dell'altopiano carbonatico di Cantanhede (a NW di Coimbra - Portogallo) ... 400

Choppy Jacques — Quelques observations sur les lapiaz de Majorque ... 401

Glazek Jerzy — Karst of the Tatra Mountains ... 405

Kostov Konstantin — Karst morphology in Bazovski part of Vratsa mountain (Stara Planina, NW Bulgaria) ... 409

Tamas Tudor & Vremir M. — Karstological investigations in the Middle Basin of Iada Valley (Padurea Craiului Mountains, Romania) ... 413

Otonicar Bojan — Macroscopic Upper Cretaceous paleokarstic features from SW Slovenia ... 417

Djurovic Predrag & Ljubojevic V. — Caves and karst areas in Serbia ... 421

Crochet Jean-Yves *et al.* — Le paléokarst polyphasé du Quercy (sud de la France) ... 424

Benischke Ralf, *et al.* — Speleological investigations in Saudi Arabia ... 425

Hobléa Fabien & Audra P. — Etude spéléo-karstologique du système Muruk-Bérénice (Monts Nakanaï; Papouasie-Nouvelle Guinée) : résultats de l'expédition de 1995 et perspectives pour 1998 ... 429

Song Linhua & Wang F. — Lunan Shilin landscape in China ... 433

Yonge Charles J. *et al.* — Speleogenesis of the coastal dune karst of SW Australia ... 436

Session 5: Vulcanospeleology and pseudokarst

Middleton Gregory & Halliday W. R. — Caves of the Republic of Mauritius, Indian Ocean ... 437

Loiseleur Bernard — Genèse de la dépression des Soulages (Causse de Sauveterre) : une explication nouvelle ... 441

Kempe Stephan — Lava falls: a major factor for the enlargements of lava tubes of the Kilauea and Hualalai, Hawaii ... 445

Kempe Stephan & Oberwinder M. — The upper Huehue flow (1801 eruption, Hualalai, Hawaii): an example of interacting lava flows yielding complex lava tube morphologies ... 449

Kempe Stephan *et al.* — Mapping lava flows by following their tubes: the Keauhou Trail / Ainahou Ranch Flow Field, Kilauea, Hawaii ... 453

Medville Douglas M. & Medville H. E. — Recent exploration of lava tube systems in Kona and on Mauna Loa, Hawaii ... 457

Halliday William R. — Unusual volcanic caves of Hawaï Island, Hawaïi ... 461

Gaál Lúdovít — The model of development of basalt caves by slope movements ... 464

Filippov Andrey G. — Gravity caves of Siberian platform ... 465

Eszterhás István — Konsequenzhöhlen in vulkanischen Gesteinen ... 469

Striebel Thomas & Schäferjohann V. — Karstification of sandstone in Central Europe: attempts to validate chemical solution by analyses of water and precipitates ... 473

Willems Luc — Karsts siliceux au Niger occidental ... 477

Havlicek David & Tasler R. — Pseudokarst process and speleothems in Bohemia Caves ... 481

Session 6: Glacial speleology

Badino Giovanni *et al.* — Present Status of Speleological Researches into the Patagonian Glaciers ... 483

Eraso Adolfo Romero *et al.* — Investigations on the endorreic drainage of the south east part of Vatnajökull glacier ... 485

Leszkiewicz Jan & Pulina M. — Hydrologic systems in carbonate karst and in subpolar glaciers. Similarities and differences ... 489

Krawczyk Wieslawa Ewa *et al.* — Similarity between karst hydrologic system of the Werenskiold Glacier (SW Spitsbergen) and a karst ... 493

Tremblay Marc & Gietl D. — Inlandsis 1994: glacial speleology into the Greenland icesheet ... 497

Swiss Speleological Society (SSS/SGH)

Proceedings of the 12th International Congress of Speleology

Volume 1

Symposium 7

Physical Speleology

La Chaux-de-Fonds, Switzerland, 10-17.08.1997

Swiss Speleological Society (SSS/SSH)

Proceedings of the 12th International Congress of Speleology

Volume 1

Symposium 7

Physical Speleology

La Chaux-de-Fonds, Switzerland, 10-17.08.1997

Étude scientifique de la grotte de Clamouse (Hérault, France)

par **Jacques Choppy** et **Paul Dubois**
182 rue de Vaugirard, F-75015 Paris - 1 rue des Grèzes, Impasse des Merlets, F-34070 Montpellier

Abstract: Scientific study of the grotte de Clamouse (Hérault, France)

Since the discovery of the Grotte de Clamouse in 1945, various observations had been made. In 1986 scientific research began to be organized. And in 1991 a pluridisciplinary study, mostly sedimentological, was started, and various complementary measures on air and water were made in the cave.

Simultaneously, observations in various fields came from the numerous cavers visiting the cave.

The Grotte de Clamouse is now a place where a large range of data permits a synthetic visions. And it is now the cave that has been most studied in France as far as physical speleology is concerned.

Résumé

Dès la découverte de la grotte de Clamouse, en 1945, furent faites diverses observation. En 1986, les recherches commencent d'être organisées. Et en 1991 débute une étude pluridisciplinaire essentiellement sédimentologique; mais en complément diverses mesures concernent l'eau et l'air dans la grotte.

Simultanément, la fréquentation active de la grotte a provoqué des observations dans des domaines très divers.

La grotte de Clamouse est maintenant le lieu d'un éventail de connaissances, permettant des visions synthétiques. Et c'est actuellement la grotte la plus étudiée de France en ce qui concerne la spéléologie physique.

La grotte de Clamouse (Hérault, France) est l'une des quelques grottes européennes dans lesquelles des études scientifiques de haut niveau sont en cours. La publication prévue (au moment où nous rédigeons cette note) des actes du Colloque tenu à Clamouse à l'occasion du cinquantenaire de la découverte spéléologique en fournira la bibliographie, qui aurait doublé le volume de cette note.

L'époque des observations

La découverte de la grotte de Clamouse en 1945 a vivement frappé les esprits : C'était en Europe à peu près la première cavité présentant une telle richesse de concrétionnement. Les traçages ont prouvé une liaison de plus de 14 kilomètres (distance considérable pour l'époque), l'eau franchissant l'importante faille du Larzac pour parvenir à l'émergence de Clamouse. Et une analyse du mondmilch de la grotte a montré qu'il était essentiellement composé de huntite, carbonate double de calcium et de magnésium, minéral récemment découvert.

Après l'aménagement touristique, et notamment à partir de 1968, se font des observations nouvelles :

-L'émergence est située aussi bas que possible, à la sortie des gorges de l'Hérault dans la plaine littorale, et la grotte suit la limite de cette plaine; elle apparaît donc comme un drain latéral du massif.

-L'examen des cristallisations de Clamouse a été déterminant pour découvrir leur étagement en altitude; celui-ci, confirmé dans d'autres grottes, est apparemment en relation avec un étagement microclimatique, qui défie encore nos moyens de mesure; ceci dans des conditions de confinement relativement poussées. Toutefois des mouvements d'air interviennent dans la localisation et l'orientation des cristaux «d'aragonite».

En 1986, la Société qui gère la grotte de Clamouse commence à promouvoir des recherches : mesures de CO_2, de températures. Dans la Cave de Vitalis (Hérault), qui se trouve dans l'amont du réseau fut observée pour la première fois cette nouvelle forme de concrétion que sont les baguettes de gours. Celles de la grotte de Clamouse, qui sont en aragonite, ont pour âme un filament organique probablement issu de la décomposition du guano de chauve-souris.

En 1990 débutent des datations uranium/thorium de concrétions, qui sont désormais au nombre de plusieurs dizaines; elles sont particulièrement nombreuses dans la zone d'entrée (partie aval de la grotte), où quatre niveaux de conduits de moins en moins élevés, perpendiculaires à la direction de l'Hérault, s'étagent en direction aval de ce fleuve. Ces datations montrent que les concrétions sont moins anciennes à mesure que l'on descend en altitude : Au niveau supérieur, leur âge dépasse souvent 350.000 ans, ce qui est la limite de la méthode uranium/thorium; par contre, dans les parties inondables lors des crues, le concrétionnement semble avoir débuté il y a 30 à 40.000 ans.

Une recherche multidisciplinaire

En 1991, la Société prend la décision de mener une recherche pluridisciplinaire sur la grotte, à laquelle plusieurs des meilleurs spécialistes européens adhèrent spontanément : belges, italiens, anglais, irlandais et français. Une matérialisation des stations topographiques est réalisée, qui permet désormais de localiser avec précision observations et points de mesure.

Cette recherche concerne surtout l'étude des remplissages, toujours grâce à des datations absolues, mais en mettant en oeuvre d'autres techniques :

- Cartographie des divers types de concrétionnements.

- Par photographie de mondmilchs au microscope électronique à balayage (M.E.B.) on a pu distinguer l'hydromagnésite, dont les cristaux ont la forme de plaques approximativement carrées (figure 1), tandis que la huntite est en plaques plus irrégulières. D'autres photographies au M.E.B. ont révélé l'existence de cristaux courbes de calcite (figure 2). Ces photographies montrent encore la présence de bactéries enkystées dans les concrétions, ce qui est désormais classique; mais aussi celle de filaments, qui sont vraisemblablement de nature biologique.

- Malgré leur aspect apparemment caractéristique, l'analyse au rayons X d'aiguilles « d'aragonite » a montré qu'elles sont souvent en calcite : Tout d'abord, grâce à des circonstances climatiques favorables, l'eau aurait mis en solution assez de dolomite pour que la cristallisation puisse se faire en aragonite.

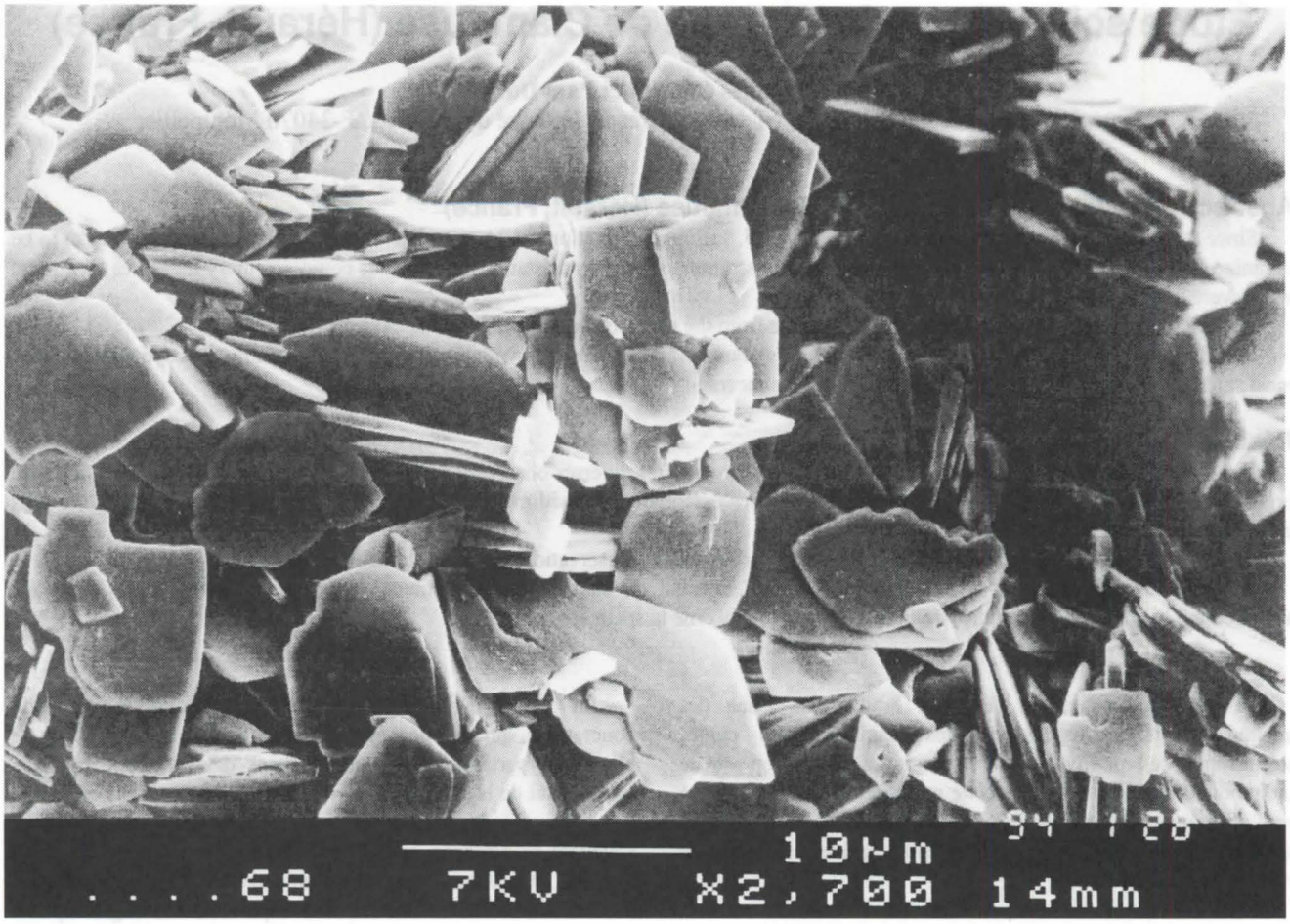

Figure 1 (photo Yves BODEUR au M.E.B.) : cristaux d'hydromagnésite, grossissement 5000

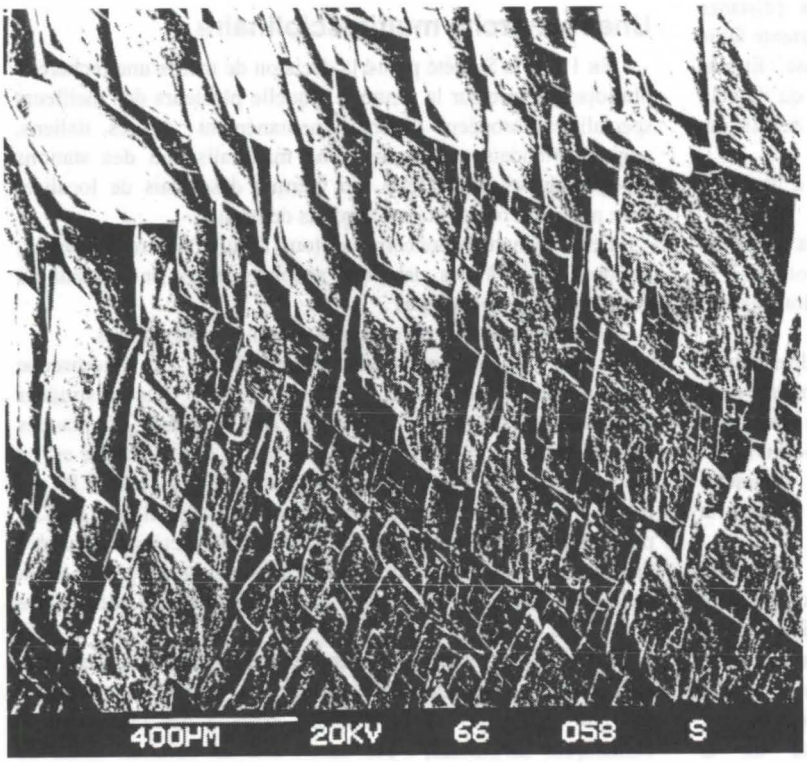

Figure 2 (photo Silvia FRISIA au M.E.B.) : cristaux courbes de calcite

Depuis plusieurs centaines d'années, ces conditions ne seraient plus remplies à Clamouse; et l'aragonite, instable, se serait transformée en calcite, au moins dans certains cas.

- Mesures de paléomagnétisme.

Par ailleurs, au moins quatre types de remplissages argileux étagés (figure 3) furent observés :

- Des placages d''halloysite (argile blanche d'origine volcanique) étagés sur 30 mètres d'altitude, qui recouvrent une argile rouge en un point.

-Une argile brune à l'éboulis terminal.

- Le dépôt d'argile grise des Terrasses est en forte pente vers le fond de la cavité; il semble donc indépendant du précédent.

- Enfin une argile assez rouge culmine à une altitude inférieure à celle des dépôts précédents.

Des mesures en cours visent à établir la chronologie relative de ces dépôts. Mais c'est surtout la première application d'une démarche nouvelle et riche de promesses : Une argile déposée par décantation a une extension plus générale que les autres sédiments de la grotte, et sa «signature» résulte nécessairement de la nature des sédiments extérieurs qui furent sa principale origine.

Des mesures du climat souterrain continuent d'être réalisées. Les températures de l'air de la grotte sont remarquablement homogènes, proches de 14,6 °C, sauf dans les zones particulièrement hautes (> 15 °C) ou basses (< 14 °C); ces températures sont vraisemblablement un peu supérieures à la « température du lieu ». Les températures des eaux stagnantes sont pratiquement égales à celles de l'air; ce qui montre un exceptionnel équilibrage thermique dans la grotte. Les pressions partielles de CO_2 sont décroissantes depuis le fond (0,53 % à l'éboulis terminal, 0,32 % en direction de l'entrée naturelle), avec un logique gradient décroissant en fonction de l'altitude dans une section de galerie. Le taux de radon est faible dans la grotte, n'atteignant en un point que 800 Bq/m^3.

Une station de mesure en continu, consacrée à l'eau de percolation (vitesse de transit, composition, etc.), est installée dans la grotte.

La source du Drac est, à l'amont de Clamouse, une émergence ascendante naturelle; lors des pompages de cette source, le rabattement est linéaire, ce qui prouve qu'une nappe captive contribue à son alimentation; cela est confirmé par l'observation de marées terrestres dans cet aquifère. La transmission du signal entre le Drac et Clamouse est 25 fois moins rapide lors d'un traçage que d'un pompage; ce rapport relativement faible entre transit de flux et transfert de pression montre que la circulation n'était pas entièrement en régime noyé lors du traçage.

De nouvelles observations

La fréquentation active de la grotte provoque de nouvelles observations :

- De nombreux indices prouvent qu'une importante colonie de chauve-souris d'au moins deux espèces occupait la grotte, mais qui a complètement disparu longtemps avant la découverte de celle-ci.

- Sortant d'un trou dans une paroi, une venue d'eau sous pression faisait un jet de 40 centimètres environ; puis, durant une période venait un jet d'eau et d'air, et enfin d'air seul avec sifflement; le jet d'eau reprenait au bout de 10 minutes environ.

- Une fracture courbe est visible près de l'éboulis terminal.

- Découverte de nouveaux sites d'aragonite coralloïde et d'une stalagmite d'aragonite; observation de fistuleuses et d'excentriques d'aragonite, tout ceci si l'on peut se fier à l'aspect macroscopique. Découverte de coupelles et de stalagmites à section triangulaire, nécessitant des conditions de confinement relativement sévères, et qui sont donc postérieures à l'établissement de celles-ci.

- Dans une zone relativement proche de la paroi extérieure, plusieurs stalactites proches ont été cassées à peu près au même

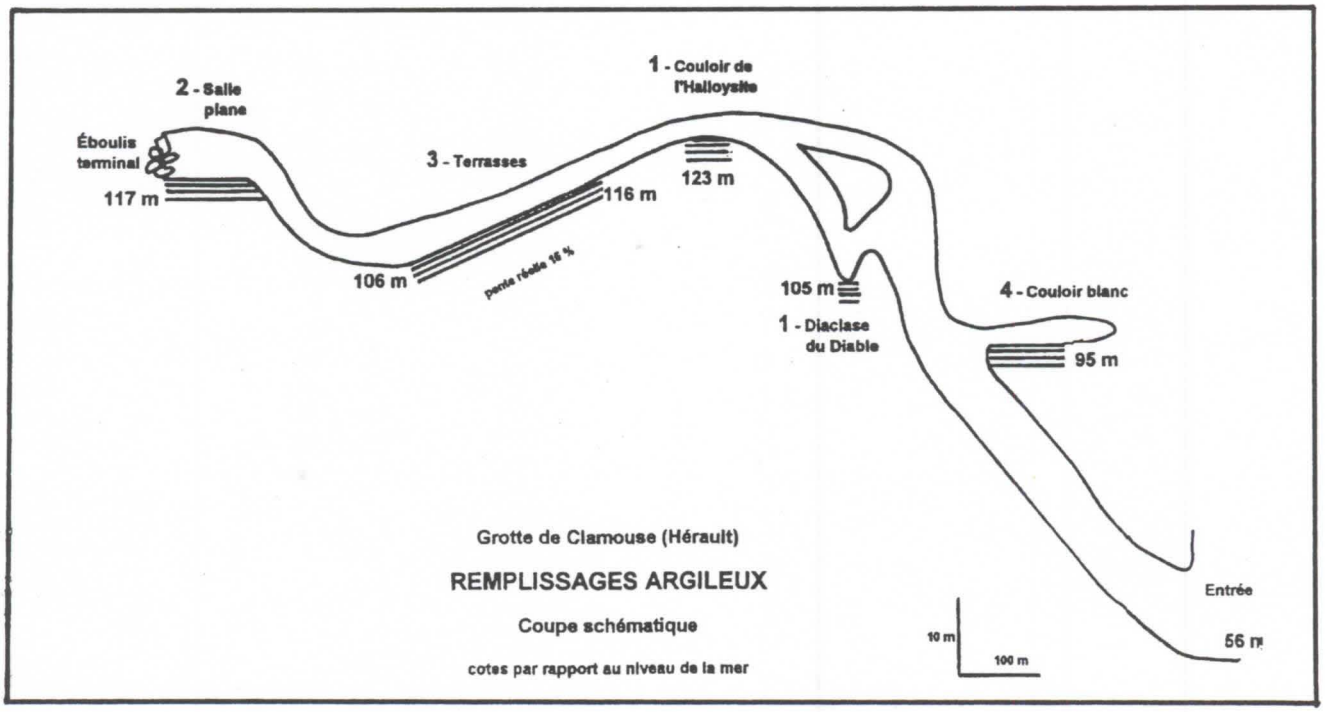

Figure 3 : grotte de Clamouse (Hérault), coupe longitudinale ultra-schématioque représentant les niveaux de remplissages argileux

niveau, et ont repoussé; leur fracture ne peut guère se comprendre que par l'ébranlement d'un tremblement de terre.

- Enfin, la grotte de Clamouse est le prototype d'une cavité *a priori* paradoxale : son plan est pour l'essentiel rectiligne, sans qu'à cette échelle une contrainte tectonique puisse être invoquée, alors que presque toutes les formes de creusement sont «phréatiques». Il faut considérer cette grotte comme typique d'un fonctionnement en régime noyé durant les crues, avec une érosion assez active pour imposer le plan général de la grotte, la vitesse demeurant toutefois suffisamment modérée pour que la roche encaissante, dolomitique, présente des formes de dissolution différentielle. À proximité de l'éboulis terminal, la section de conduit est celle d'un tube, résultat d'une action comparable dans une roche non dolomitique. En maigre, il est probable que le creusement était trop modéré pour que la morphologie en ait conservé les indices.

Conclusion

Les recherches dans la grotte de Clamouse ont été commandées par des observations plus ou moins ponctuelles ou les préoccupations des chercheurs qui ont participé.

Par le volume de ces recherches, Clamouse est maintenant le lieu d'un éventail de connaissances, qui en fait la grotte la plus étudiée de France en ce qui concerne la spéléologie physique. L'ensemble des résultats obtenus donne une vision tout à fait nouvelle de la grotte, liée pour une part à la transformation profonde des conceptions spéléologiques depuis 25 ans.

Les synthèses se font très progressivement mais il nous semble qu'un protocole pré-établi, probablement arbitraire, n'aurait pas permis d'avancer aussi vite dans la connaissance de la grotte.

Höhlensedimentologie in Österreich

von Rudolf Pavuza
Karst- und höhlenkundliche Abteilung, Naturhistorisches Museum Wien
Museumsplatz 1/10, A-1070 Wien, Österreich

Abstract

In the Austrian Eastern Alps extensive sedimentological investigations are conducted mainly in the course of a few paleontological and archeological excavations currently. Therefore the chance to encounter sediments of an age older than the late Pleistocene is comparatively small thus giving an insight only to the very last phases of cave development. Two examples from bear caves in the Austrian Alps will document this timespan where in one case some indications on very much older sediments could be observed. More vertical sedimentological information would help to clear up the chronology of the cave development remarkably thus demanding for more "pure" sedimentological excavations in the Alps.

Zusammenfassung

Umfangreichere höhlensedimentologische Untersuchungen werden in Österreich fast immer nur im Zusammenhang mit paläontologischen oder urgeschichtlichen Grabungen gemacht. Dadurch ist auch die Wahrscheinlichkeit, Höhlensedimente zu finden, die vor dem Jungpleistozän sedimentiert wurden, eher gering. An zwei Beispielen aus den Nördlichen Kalkalpen wird die sedimentologische Entwicklung von Bärenhöhlen kurz dokumentiert, wobei wenigstens in einem Fall ein Hinweis auf bedeutend ältere Sedimentanteile vorliegt. Bei einer größeren Zahl vertikaler Sedimentprofile - durch rein sedimentologische Grabungen - erschiene die aus speläochronologischer Sicht unverzichtbare Nachsuche nach älteren, früh- bis vorpleistozänen Sedimenten auch in den Alpen aussichtsreich.

1. Allgemeines

Das Hauptinteresse bei Höhlengrabungen in den Alpen ist zumeist ein paläontologisches oder urgeschichtliches. So interessiert etwa die Evolution des Höhlenbären, die spätpleistozän - holozäne Entwicklung der Höhlen, rekonstruiert anhand von Gastropodenfaunen oder auch die Frage der Nutzung der Höhlen durch den vorzeitlichen Menschen. Sedimentgeologische Arbeiten spielen dabei oft nur eine randliche Rolle. Dies hat, neben einem gewissen Mangel an interessierten Sedimentologen, auch seine Ursache in der Komplexität des Ablagerungsraumes „Höhle", der eine subtile Bearbeitung und Interpretation verlangt und oftmals nur mehrdeutige und damit wenig befriedigende Ergebnisse liefert.

2. Zielvorstellungen

Fraglos eine Hauptfragestellung der Speläologie ist diejenige nach dem Alter der Höhle. Daß Höhlensedimente, die ja in einen bereits lange vorher entstandenen Höhlenraum sedimentiert wurden, nur „Mindestalter" ergeben können (sofern eine Altersangabe überhaupt möglich ist), liegt auf der Hand. Trotzdem bieten sie oft den einzigen zeitlichen Anhaltspunkt, da auf dem Gebiet der gängigen und auch bewährten radiometrischen Alters-bestimmungsmethoden gerade im speläologisch relevanten Bereich noch eine breite Lücke klafft.

Paläontologische Nachweise präpleistozäner Besiedelungen von Höhlen sind in den österreichischen Alpen bislang praktisch ausgeblieben. So scheinen die Höhlensedimente bzw. Spuren älterer Sedimente im heutigen, im Pleistozän zumeist stark überarbeiteten Höhleninhalt das gegenwärtig einzige Bindeglied zu den initialen Phasen der Speläogenese darzustellen. Dabei ist neben einer möglichst großen Zahl von Aufschlüssen auch die Erarbeitung neuer Methoden gefragt, die dem sehr speziellen Ablagerungsraum „Höhle" Rechnung tragen.

3. Methodik

Neben den Standardmethoden der Korngrößenanalyse, der geologisch-petrographisch-paläontologischen Ansprache der Sediment-anteile und der Schwermineralanalyse gelangten bei den nachfolgenden Beispielen gelegentlich Isotopenmethoden zur Anwendung. Paläomagnetische Untersuchungen sind erst in Vorbereitung. Geoelektrische Prospektionen, die jedoch Erfahrung mit der Methode voraussetzen, bewährten sich in etlichen Fällen als wertvolle Hin-weise auf die bei der Grabung zu erwartenden Schichtmächtigkeiten. Bohrungen mit Handbohrgeräten waren bislang nur in einem einzigen, sehr speziellen Fall einer meterdicken geröllfreien Sedimentfüllung erfolgreich.

4. Beispiele aus den Alpen

Das Nixloch bei Losenstein

Diese voralpine Höhle (Österreichisches Höhlenverzeichnis: 1665/1) liegt im Ennstal unweit des Kalkalpennordrandes in Oberösterreich in einer Seehöhe von 780 m. Im Rahmen einer höhlenpaläontologisch - urgeschichtlichen Grabung der Universität Wien wurden durch den Verfasser (PAVUZA, 1992) sedimentologische Untersuchungen durchgeführt. Als wesentlichstes Ergebnis aus Sicht der Sedimentologie erscheint der Hinweis auf einen deutlichen Hiatus in tieferen Abschnitten des Profiles, wo in den basisnahen, völlig fossilfreien Lehmlagen stark erhöhte Anteile an allochthonem Material mit Chromspinell (der im Ostalpenraum in postkretazischen Sedi-menten nicht mehr aufscheint) in der Schwermineralfraktion (Abb. 1) nachgewiesen werden konnten. Geologisch erscheint es möglich, daß hier Reste eines alten, präpleistozänen Sedimentes vorliegen, über denen, deutlich abgesetzt, die pleistozänen Höhlenlehme mit ihrem Fossilinhalt (u.a. Höhlenbär) und in den oberen Lagen auch Steinwerkzeuge zur Ablagerung gelangten.

Leider wurde bei dieser paläontologischen Grabung weder die tiefste Lehmlage beprobt, noch wurden Proben für die hier aussichtsreich erscheinende paläomagnetische Untersuchung entnommen.

Aus diesen Daten ist wohl nicht der Schluß auf ein kreidezeitliches Alter der Höhle zulässig, wohl aber jener auf ein weit höheres als mittel- bis spätpleistozänes mit signifikant unterschiedlichen paläo-geographischen Gegebenheiten.

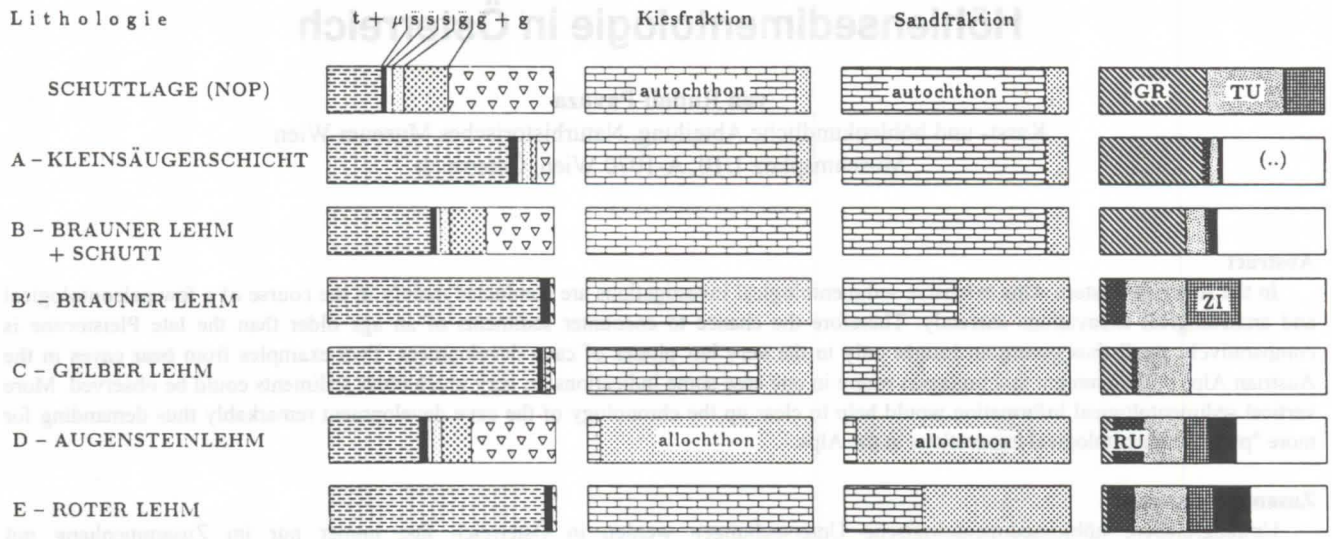

Abbildung 1: Sedimentgeologisches Profil aus dem Nixloch (Oberösterreich, Kat.Nr. 1665/1), Abkürzungen bei den Schwermineralen: GR=Granat, TU=Turmalin, ZI=Zirkon, RU=Rutil,Cr=Chromspinell (..)=übrige Minerale

Die Gamssulzenhöhle im Toten Gebirge

Im Gegensatz zum vorgenannten Beispiel befindet sich diese Höhle (Österreichisches Höhlenverzeichnis Nr.: 1637/3) in den Kalkhochalpen im Warscheneck in Oberösterreich in einer Seehöhe von 1300 m. Auch in diesem Fall begleiteten höhlensedimentologische Untersuchungen (PAVUZA, 1995) die Grabung. Im Unterschied zum Nixloch erfuhr das Höhlensediment der Gams-sulzenhöhle eine nahezu gänzliche Umlagerung im Jungpleistozän, sodaß präpleistzozäne Reste im Sediment allenfalls in geringen Spuren zu finden sind. Clusteranalysen mit granulometrischen und Schwermineraldaten ergaben überkreuzende Zusammenhänge zwischen den einzelnen Profilen und belegen so deren massive Durchmischung.

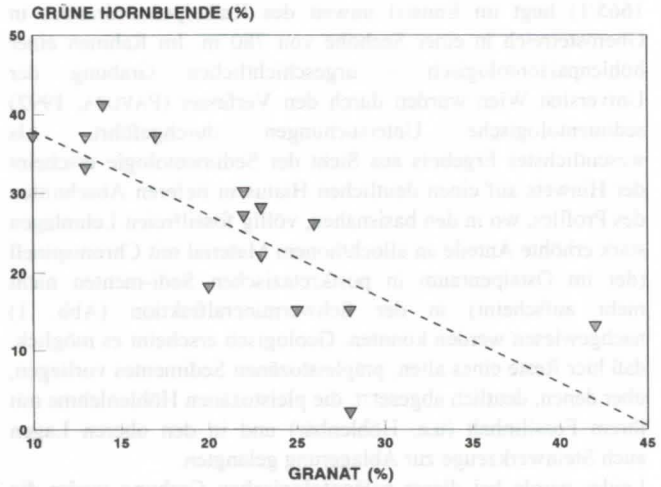

Abbildung 2: Zusammenhang von Granat- und Hornblendegehalt in den Quadranten D8/9, FG 8/9, D6/7 und F 6/7 der Gamssulzenhöhle (Oberösterreich, Kat.Nr. 1637/3)

Immerhin sind daraus aber wenigstens 2 differenzierte kristalline Liefergebiete abzuleiten, wie sich aus dem Dia-gramm „Granat-Hornblende" (Abb.2) ergibt. Die Punktverteilung im Diagramm illustriert die erwähnte Durchmischung nachhaltig.

5. Ausblick

Aus sedimentologischer Sicht erschiene es sinnvoll, in Zukunft im alpinen Karst auch rein sedimentologische Grabungen zu organisieren, also auch in Höhlen zu prospektieren, wo keine Hinweise auf paläontologisches oder urgeschichtliches Fundgut vorliegen. Entsprechend der naheliegenden Zielrichtung, möglichst alte Sedimente zu erfassen, um so einen Anknüpfungspunkt an die frühen Phasen der Höhlengenese zu erhalten, sollte ein Schwerpunkt dabei bei den bisher vernachlässigten basalen Sedimentabschnitten liegen. Auch paläomagnetische Methoden werden dabei aufgrund der zu erwartenden Zeitabschnitte (>700 000 a) zur Anwendung kommen. Für dieses Ziel wird aber fraglos eine ungleich größere Zahl an Vertikalprofilen erforderlich sein, als dies bei den paläontologischen Untersuchungen der Fall ist, da hier ja a priori keinerlei Hinweise auf die Erfolgsaussichten vorliegen. Freilich muß im Falle paläontologischer oder urgeschichtlicher Funde die Grabungsstrategie und -technik diesem Umstand Rechnung tragen und der Bergung dieses Fundgutes Vorrang einräumen.

6. Literatur

PAVUZA, R. 1992: Die Sedimentologie des Nixloches bei Losenstein-Ternberg (O.Ö.). *Mitt.Komm.Quartärforsch. Wien,8:17-19.*

PAVUZA R.1995:Die Sedimente der Gamssulzenhöhle (War-scheneck, Oberösterreich). *Mitt. Komm. Quartärforsch. Wien, 8:23-26.*

Les méga-remplissages détritiques de la Cueva Fresca

par Olivier Forgeot
4 résidence Géricault, 78150 Le Chesnay, France

Abstract
The Cueva Fresca (Cantabria - Spain) is a cave with many big galeries in canyon shape. The size of its canyons put this cave among the first ones in the world. The present text will talk about huge amounts of sand we can see all along these canyons, and which have probably filled all the cave in the past. The chaotic floor reveals us the location of these fillings and undermining phenomenas.

Résumé
La Cueva Fresca fait partie des grottes qui possèdent les plus grandes galeries en forme de canyon au monde. Cet exposé présente les gigantesques remplissages de sable qui ont probablement colmatés la cavité dans des temps très anciens. Le profil accidenté du sol actuel nous renseigne sur la position de ces remplissages souvent situés sous des éboulis ou entrecoupés par d'énormes soutirages.

Présentation géographique

La Cueva Fresca se développe dans le massif de Monte Llusias qui se trouve à l'Est de la cordillère cantabrique, elle-même située au Nord de la péninsule ibérique. Le sommet le plus proche de cette grotte est celui de Colina qui culmine à 1458 mètres d'altitude. L'entrée de la Cueva Fresca s'ouvre à 440 mètres d'altitude, en rive gauche et à une centaine de mètres au dessus du rio Asòn. L'entrée est au même niveau que la voûte des grandes galeries fossiles. Les eaux de la Cueva Fresca qui s'écoulent à l'étage inférieur, rejoignent directement le lit du rio Asòn au travers des éboulis de la vallée et finissent à une trentaine de kilomètres au Nord dans l'océan Atlantique. Le sud du massif de Monte Llusias sert de ligne de partage des eaux. Les pluies qui tombent au sud de cette ligne sont drainées par l'Ebre et évacuées vers la mer Méditerranée située à plus de quatre cents kilomètres au Sud-Est.

Présentation géologique

Un anticlinal dont l'axe est orienté du nord-est au sud-ouest fait apparaître, près d'Arredondo, le haut d'une épaisse série argilo-gréseuse wealdienne datée du Crétacé inférieur qui réalise un substratum imperméable. Au dessus de cette couche imperméable, nous trouvons les calcaires très purs à faciès urgonien du massif de Pena Lavalle, puis l'épaisse couche des grès d'Asòn dans lequel s'ouvre le profond ravin de Rolacia. Au sud du ravin, le massif de Colina est composé d'une alternance de séries gréseuses et de calcaires à rudistes et polypiers. Cette alternance forme ce que l'on appelle de complexe calcairo-gréseux d'Asòn daté de l'Aptien supérieur. Ce complexe repose sur le socle des grès d'Asòn qui constitue un écran imperméable entre les deux massifs. Le Val d'Asòn a été taillé à contre-pendage des massifs de Pena Lavalle et de Colina qui ont un pendage commun en pente douce vers le sud-est.

La Cueva Fresca a pour particularité de s'ouvrir exactement à l'intersection de la vallée et du plan de contact entre le complexe calcairo-gréseux supérieur et l'épais socle imperméable des grès d'Asòn. On remarquera qu'avec l'enfoncement du niveau hydrologique de base sous la contrainte du pendage du socle imperméable, l'entrée fossile de la Cueva Fresca est plus au nord que la résurgence de l'actif au niveau de la source du Manantial del Huerto del Rey.

Présentation historique

Les premières reconnaissances spéléologiques françaises dans cette région ont été effectuées dès 1958 par le spéléo-club de Dijon et dirigées par B. DE LORIOL. Les expéditions étaient placées sous l'autorité du Muséum National d'Histoire Naturel de Paris et du Laboratoire de géologie de la Faculté des sciences de Dijon. En 1964, le laminoir qui fait suite à la salle d'entrée fut désobstrué par l'équipe du Dr CASTIN, et le Canyon d'Exploration reconnu jusqu'au fossé du Bloc 64. L'immense réseau fossile fut exploré par le S.C.D. les années suivantes pour aboutir à la publication en 1975 d'une topographie globale. En 1968, C. MUGNIER soutint à l'université de Dijon une thèse sur le karst de la région d'Asòn qui deviendra la référence des travaux ultérieurs.

L'exploration reprit un deuxième souffle lors des années quatrevingts par l'arrivée de plusieurs groupes spéléos sur le terrain tel que le Spéléo-club de Chablis, les Spéléos Grenoblois du Club Alpin Français et le Spéléo-club de Paris du CAF Ile de France. La jonction entre la Sima Tibia (860m d'altitude) et la Cueva Fresca fut ainsi réalisée en 1990 par l'équipe de B. LISMONDE du S.G.CAF.

A coté de l'aspect sportif, le Spéléo-club de Paris démarre, dès 1988 sous l'impulsion de Ph. MORVERAND, le programme FRESCA d'étude scientifique sur ce réseau. Le développement fit un bond et dépassa les vingt cinq kilomètres en mai 1994. Depuis, des observations morphologiques sont régulièrement rapportées, des datations U/Th sont faites, et la compréhension de la spéléogénèse progresse.

Introduction

C'est une vue globale mais non exhaustive des remplissages de la Cueva Fresca qui amène à présenter, dans cet article, l'hypothèse du comblement total de ses canyons dans le passé. Ceci est observable aujourd'hui par la présence de méga-remplissages détritiques.

La première partie de cet exposé consistera à décrire les remplissages que l'on rencontre ou suppose lors d'une promenade d'environ deux kilomètres dans les grandes galeries entre l'entrée de la Cueva Fresca et le terminus du Canyon Rouge.

La deuxième partie discutera des remplissages observés, et des soutirages qui les séparent, face à l'hypothèse du colmatage de la Cueva Fresca dans des temps très anciens.

Observations de terrain

Après avoir franchi les deux laminoirs d'entrée de la Cueva Fresca, il faut escalader le muret d'un massif stalagmitique imposant et généré par les écoulements au travers des fractures de détente du massif calcaire à proximité de la vallée. En marchant plus profondément sous une large voûte rougeâtre et basse, nous débouchons sous le plafond et dans l'axe du Canyon d'Exploration. Une descente d'environ quarante mètres d'altitude sur une pente très glissante, puis le passage d'une première vire au dessus d'un profond fossé, nous permettent d'atteindre le fond horizontal du canyon d'exploration. Sur les parois du canyon, on remarquera de larges banquettes subconcaves et métriques.

Pour cette partie du Canyon d'Exploration, le soutirage aurait été effectué par le Réseau des Griffes qui s'ouvre en contrebas de la descente et sous la première vire. Les écoulements ont encroûté la pente d'une épaisse gangue de plusieurs couches de calcite comme l'a révélé le sondage effectué à la pioche. La calcification est supérieure aux cinquante centimètres creusés.

On notera toutes les montées et descentes qui s'observent le long des canyons. En poursuivant vers le fond, après être descendu au niveau bas du Bivouac, il faut à nouveau gravir une coulée calcitique sur environ trente mètres de dénivelé pour se retrouver près du plafond du Canyon d'Exploration. Après un court passage horizontal sous la voûte, il nous faut redescendre de plusieurs mètres parmi un chaos de blocs pour atteindre la vire du bloc 64. Cette vire nous fait passer au dessus d'un profond fossé. La progression continue par une galerie boueuse de quelques mètres de large qui permet de contourner le colmatage du Canyon d'Exploration et d'arriver au pied du Réseau du Caviar. La galerie principale du Réseau du Caviar contient un énorme remplissage de sable fin qui est soutiré à quelques endroits. Un léger dépot de galets s'observe dessus. Le sommet de ce remplissage est remarquablement horizontal sous une voûte présentant des formes de corrosion en chenal.

En amont du Réseau du Caviar se trouve le Canyon de l'Eboulis, où le Puits de l'Araignée a produit un soutirage.

Après avoir franchi la Vire de l'Araignée au dessus du confluent du Canyon de l'Eboulis et la galerie du Tracastin, il faut monter sur un chaos de blocs, où s'ouvre un peu plus loin le Puits du Sablier. Ce puits est une démonstration de la puissance des soutirages le long des canyons. En effet, ce gigantesque entonnoir, toujours actif par un écoulement qui perce le plafond, offre une coupe naturelle du remplissage et de la base rocheuse du canyon.

Nous arrivons maintenant dans la Cinquième Avenue. La morphologie de cette large galerie à voûte elliptique et la continuité topographique nous indiquent que nous sommes dans la suite du canyon qui est presque rempli jusqu'au plafond. Toutefois, l'analyse du remplissage est empêchée par un tapis de blocs d'effondrement. On remarquera les énormes lames de décollement le long des parois de la galerie qui trouvent probablement leur origine dans des phénomènes de détente lors de l'assèchement du réseau.

La Cinquième Avenue débouche à mi-hauteur dans l'immense salle Rabelais qui mesure de 80 à 120 mètres de diamètre et 108 mètres de haut. (MARQUET, 1995)
Le chaos de blocs sur lequel nous nous trouvons se poursuit tout autour de la salle. A la place d'un classique cône d'effondrement, on observe un énorme vide central qui suggère qu'un soutirage a eu lieu au centre de la salle.

De la salle Rabelais, partent le Canyon Nord et le Canyon Rouge. Nous nous dirigeons vers ce dernier et remarquons que la voûte de celui-ci est sensiblement à la même cote que celle de la Cinquième Avenue.

En descendant l'éboulis de la salle Rabelais vers le Canyon Rouge, à proximité du Passage du Shunt, nous pouvons observer les traces pariétales d'une corrosion sous remplissage avec de larges cannelures verticales.

Un peu plus loin dans le bas du Canyon Rouge, le passage peut se faire dans un surcreusement du canyon, et sous un plancher stalagmitique reposant sur une épaisseur d'environ deux mètres de sable siliceux blanc très fin. Toutefois, ce remplissage parait relativement jeune et fait probablement parti du dernier cycle remplissage-surcreusement du Canyon Rouge car il est lui-même contenu dans un surcreusement plus vaste. Dans le même secteur, on trouve environ trente mètres plus haut, un plancher stalagmitique daté d'environ 330 000 ans. (DELANNOY et MORVERAND, 1989)

Après avoir franchi le chaos de bloc au bas duquel se trouve le Canyon des Cupules qui mène vers le Grand Racourci et que nous laissons à notre gauche sous une strate inclinée, il nous faut gravir un deuxième chaos qui nous permet de prendre pied sur un remplisssage incliné et dont la forte pente verse dans le soutirage qui se développe tout du long de la paroi de gauche.

Toujours en nous dirigeant vers le sud, à mi-longueur du Canyon Rouge, le ressaut du Trou Blanc nous oblige à descendre un puits de dix mètres environ dans un remplissage de brèches gréseuses. Il nous faut alors passer sous le remplissage dans une galerie boueuse qui mène vers la suite du canyon. Peu après, l'escalade d'un talus d'une dizaine de mètres nous permet de remonter sur le remplissage. Nous progressons rapidement sur le sol plat quoique parsemé de blocs. Nous atteignons ensuite un chaos d'énormes blocs, où la trace nous indique le passage entre la parois de gauche et l'énorme monolithe.

En avançant plus en avant dans le Canyon Rouge, nous traversons l'immense et longiforme Salle du Monolithe (150 m x 50 m x 50m environ) qui doit probablement son existence à un phénomène d'effondrement de la voûte et des parois du canyon. On remarquera toutefois que ce chaos forme deux gigantesques banquettes d'une vingtaine de mètres de large de part et d'autre d'un surcreusement axial décamètrique. A l'autre extrémité, on retrouve un conduit qui ressemble bien au sommet d'un canyon remplis jusqu'à une dizaine de mètres de son plafond. Sur le sol, de grands gours fossiles sont remplis d'un sable qui ne réagit pas à l'acide. La voûte bien plus basse que celle de la Salle du Monolithe présente des coupoles métriques. Au bout de cette galerie, la suite s'effectue par un laminoir sous un épais plancher stalagmitique, le passage du Mille-Feuille. Ce plancher matérialise probablement un léger écoulement d'eau sur le colmatage d'un ancien siphon.

On ressort de ce laminoir dans un lac fossile où l'eau est remplacée par le brillant d'une dalle de calcite noire parfaitement horizontale et d'une dizaine de centimètres d'épaisseur. La galerie reprend la forme d'un canyon qui se poursuit jusqu'à la dernière salle dans laquelle descend sur la gauche un énorme éboulis d'une cinquantaine de mètres de haut et alimenté par une trémie suspendue dans le plafond. Revenons au bas de l'éboulis, nous retrouvons la suite du canyon dans l'axe du précédant. La promenade s'arrête malheureusement au bout d'une vingtaine de mètres sous un pittoresque plancher stalagmitique suspendu à plus de trois mètres de haut et soudé au milieu des parois du canyon qui sont écartées à cet endroit d'environ six mètres. Le remplissage qui servi d'échafaudage au plancher, a été partiellement déblayé.

On trouve de petits galets prismatiques scellés sous le concrétionnement. Le terminus actuel du Canyon Rouge se situe au niveau de ce second paléo-siphon derrière lequel la suite, indiquée par la présence d'un courant d'air, est interdite par une trémie.

Préambule

Un remplissage peut s'observer de plusieurs manières. On peut le remarquer par la présence d'une forme (talus, banquette, sol plat) ou par son absence (soutirage, plancher stalagmitique suspendu, trace pariétale de corrosion sous remplissage). Il peut être visible (coupe naturelle, sédiments) ou supposé (altimétrie anormalement haute avec couverture de blocs ou de calcite). On peut aussi le mettre en évidence, par exemple, en réalisant un sondage profond sous un encroûtement calcitique.

Discussion

La coupe schématique présentée sur la figure 1 présente un profil estimé des remplissages le long de l'axe qui va de l'entrée de la Cueva Fresca jusqu'au terminus du Canyon Rouge. A priori, en attendant les résultats des mesures fines d'altimétrie que le SCP à mis en chantier, on peut penser que les voûtes des canyons le long de cet axe sont quasiment à la même altitude, à une pente d'écoulement près.

Nous pouvons dresser la liste des talus en allant de l'entrée vers le fond. Nous rencontrons successivement le talus d'entrée, le talus entre le Lac et le bloc 64, le Réseau du Caviar, le talus entre le Canyon de l'Eboulis et l'arrivée du Grand Racourci, La Cinquième Avenue et son altimétrie haute, le pourtour de la Salle Rabelais formant un talus entre son centre et le début du Canyon Rouge, le remplissage peu après le chaos de départ du Grand Racourci et qui va jusqu'au Trou Blanc, la suite du remplissage après le Trou Blanc, les méga-banquettes de la salle du Monolithe, le remplissage de la galerie des Gours jusqu'à l'autre coté du laminoir du Mille-Feuille et le remplissage du tronçon de canyon terminal.

La caractéristique majeure de tous ces talus est qu'ils culminent à peu près tous à la même altitude et ce sur près de deux mille mètres de développement. Ceci incite donc à penser que ces talus sont le témoignage d'un même remplissage entrecoupé de creux provoqués par des soutirages postérieurs à la mise en place de ce méga-remplissage.

Pour que des creux puissent être considérés comme résultat d'un soutirage, il nous faut y remarquer l'action d'une galerie ou d'un réseau inférieur.

Ainsi, le premier creux évoqué, celui entre la descente d'entrée et la remontée après le Bivouac peut s'expliquer par l'action du réseau des Griffes qui communique en plusieurs endroit avec le Canyon d'Exploration et avec l'actif situé une cinquantaine de mètres plus bas. Le deuxième creux décrit correspond au fossé du Bloc 64 qui lui aussi communique avec l'actif. Le niveau bas du Canyon de l'Eboulis est probablement dû à l'action du Puits de l'Araignée qui s'écoule aussi vers l'actif. Le cône du Puits du Sablier, créé par la chute d'eau qui perce le plafond, mène aussi à l'actif. L'énorme creux de la Salle Rabelais reste encore une énigme, quoique un court tronçon de galerie partant de la base de la salle vers le Nord-Est soit suspecté d'avoir un rôle dans un phénomène de soutirage. Il ne faut pas oublier d'autre part l'action de galeries inférieures qui s'arrêtent sur les chaos périphériques de la Salle Rabelais. Ainsi, on remarquera que la trémie amont du méandre du Grand Bourbier n'est autre que le bord enfoui de la Salle Rabelais, et que la galerie de la rivière Tibia change de direction lorsqu'elle bute sur le bord de la salle Rabelais. On peut alors formuler l'hypothèse que la rivière Tibia lorsqu'elle était à moindre profondeur traversait la Salle Rabelais pour rejoindre le méandre du Grand Bourbier et aurait participé au déblaiement central de la salle. Puis son cours changea de direction pour emprunter le cheminement actuel plus au sud sous l'action conjointe de l'enfouissement, du pendage, de la fracturation et d'un éventuel effondrement dans la Salle Rabelais.

Le niveau bas de début du Canyon Rouge s'expliquerait par l'action du Canyon des Cupules, capturé sous une strate au pied du Canyon Rouge, et qui mène au bas du Canyon du Grand Racourci. Ce passage aurait pu drainer les eaux venant de l'ancienne rivière Tibia en les faisant remonter sur une centaine de mètres de la salle Rabelais vers le Canyon Rouge. L'évacuation aurait pu se faire par le Grand Racourci jusqu'au Canyon de l'Eboulis, contournant ainsi le remplissage de la Cinquième Avenue, en formant le Carrefour de l'Araignée (BIGOT, 1994).

Plus en amont dans le Canyon Rouge, nous avons le Trou Blanc qui présente avec son passage sous le sédiment un drain inférieur évident qui se dirige également vers le Grand Raccouci. Notons que l'actif actuel passe à cinquante mètres sous ce secteur...

La tranchée axiale de la salle du Monolithe fait penser à l'action d'un écoulement, mais cette zone est mal étudiée du fait de la difficulté à se déplacer dans ce gigantesque chaos.

Enfin dans la zone terminale, le niveau du remplissage est matérialisé par les planchers stalagmitiques fossiles suspendus. En dessous, le soutirage a été déblayé sur plusieurs mètres de haut sans qu'il y ait d'explication apparente. Nous pouvons seulement remarquer que cette zone du canyon se trouve à l'intersection d'une fracture qui lui est perpendiculaire et qui a généré la salle de la grande trémie. On peut donc supposer que la karstification s'est également produite dans un étage inférieur et soutire le remplissage de cette zone.

Les autres remplissages de la Cueva Fresca

On rencontre d'autres remplissages dans la Cueva Fresca, mais de nature bien différente de celle des remplissages sableux des grands canyons. Un premier type s'observe dans les étages supérieurs. Par exemple, à la cote +70m environ, le méandre au Plancher Percé comporte un remplissage de brèches bien nivelé. La Galerie du Marchand de Sable, suspendue à plus de quarante mètres au dessus du plafond des canyons, contient un remplissage alternant sables et brèches dont la coupe naturelle s'observe sur plus de dix mètres de hauteur (BIGOT,1992).

Un deuxième type de remplissage concerne les galets ovoïdes probalement d'origine fluviatile que l'on rencontre en grande quantité dans certains endroits de la Cueva Fresca (MORVERAND, 1992). Un épais remplissage de galets existe dans le Réseau des Galets situé dans le plafond du Canyon d'Exploration (GISSELBRECHT, 1991). Cette galerie relativement proche de la vallée et à une altitude voisine de l'entrée de la Cueva Fresca, permet d'étayer l'hypothèse d'une injection à partir du Val d'Asòn lorsque le Canyon d'Exploration était rempli presque jusqu'au plafond. Les caractéristiques des dépôts de galets en fonction de la distance de pénétration dans la grotte demandent à être étudiées. En effet, nous pensons avoir remarqué une décroissance des dépôts en allant vers le fond, pour terminer par une épaisseur de quelques galets polis au dessus de la masse sableuse et homogène du Réseau de Caviar à plus de cinq cents mètres de l'entrée. Les dépôts de galets mélangés à une matrice sableuse que l'on observe dans le Réseau des Griffes au pied du Canyon d'Exploration résulteraient par contre du soutirage effectué par ce réseau sur le paléoremplissage sableux recouvert de galets du Canyon d'Exploration aujourd'hui disparu.

Le Réseau des Galets suspendu presque à la verticale du Réseau des Griffes aurait ainsi conservé une partie du dépôt originel de galets.

Conclusion

La Cueva Fresca est une cavité complexe, chargée d'une longue histoire, et qui est très intéressante à étudier. D'une part pour la compréhension de la cavité elle-même, et d'autre part pour la compréhension de l'évolution du massif entier et de son interaction avec le Val d'Asòn.

Cet article a présenté le profil accidenté du sol le long d'un axe majeur de la Cueva Fresca. L'observation des creux et des bosses qui se succèdent permet de jeter un nouveau regard sur les gigantesques remplissages que l'on observe et d'en subodorer d'autres cachés par l'usure du temps, blocs tombés, calcification et soutirages par exemple. Cette démarche globale conforte l'hypothèse d'un quasi colmatage en des temps très anciens (> 330 000 ans) d'un beau canyon souterrain (20m x 50m x 2000m) sur toute sa longueur par un sable siliceux fin et homogène.

Références

Articles parus dans les différents numéros de la revue *'Sous le Plancher'* du Spéléo-club de Dijon, en autres tome 3 fasc. 4, tome 5 fasc. 1, tome 8 fasc. 2, et n°1987-2.

Articles parus dans les différents numéros de la revue *'Grottes & Gouffres'* du Spéléo-club de Paris, en autres n°111, 115, 116, 117, 119, 120, 122, 123, 124, 126, 130, et 134.

BIGOT, J.Y. 1992. Les remplissages des galerie bleue, lucarne, cinqième avenue de la Cueva Fresca. *Grottes & Gouffres* 126, 31-44.

BIGOT, J.Y. 1994. Les canyons de la Cueva Fresca en passant par le Grand Raccourci. *Grottes & Gouffres* 134, 15-28.

BIGOT, J.Y. & MORVERAND, Ph. 1994. A propos des canyons de la Cueva Fresca en particulier et ceux de la Cantabrie en général. Actes de la quatrième Rencontre d'Octobre, Pau 1994, *Publication du SCP*, 28-37.

CASTIN, P. & KIEFFER, J.P. 1975. Travaux dans le Val d'Asòn, *Spelunca*, 3 (1975) p 3.

DELANNOY, J.J. & MORVERAND, Ph. 1989. Contribution à la connaissance de la karstogénèse du massif de Pena Lavalle. *Grottes & Gouffres* 111, 9-21.

FORGEOT, O. 1996. Méga-remplissages détritiques dans la Cueva Fresca, Actes de la sixième Rencontre d' Octobre, Osselle 1996. *Publication du SCP*, 49-55.

GISSELBRECHT, O. 1991. Le réseau des Galets. *Grottes et Gouffres*, 120, 23-25.

MARQUET, P. 1995. Altimètrie à la Cueva Fresca. Rapport inédit.

MORVERAND, Ph. 1992. A propos de certains galets de la Cueva Fresca, Actes des Journées Pierre Chevalier. *Mémoires du Spéléo-club de Paris* 16, 217-222.

MUGNIER, C. 1969. Le karst de la région d'Asòn et son évolution morphologique. Thèse de troisième cycle de la Faculté de Dijon.

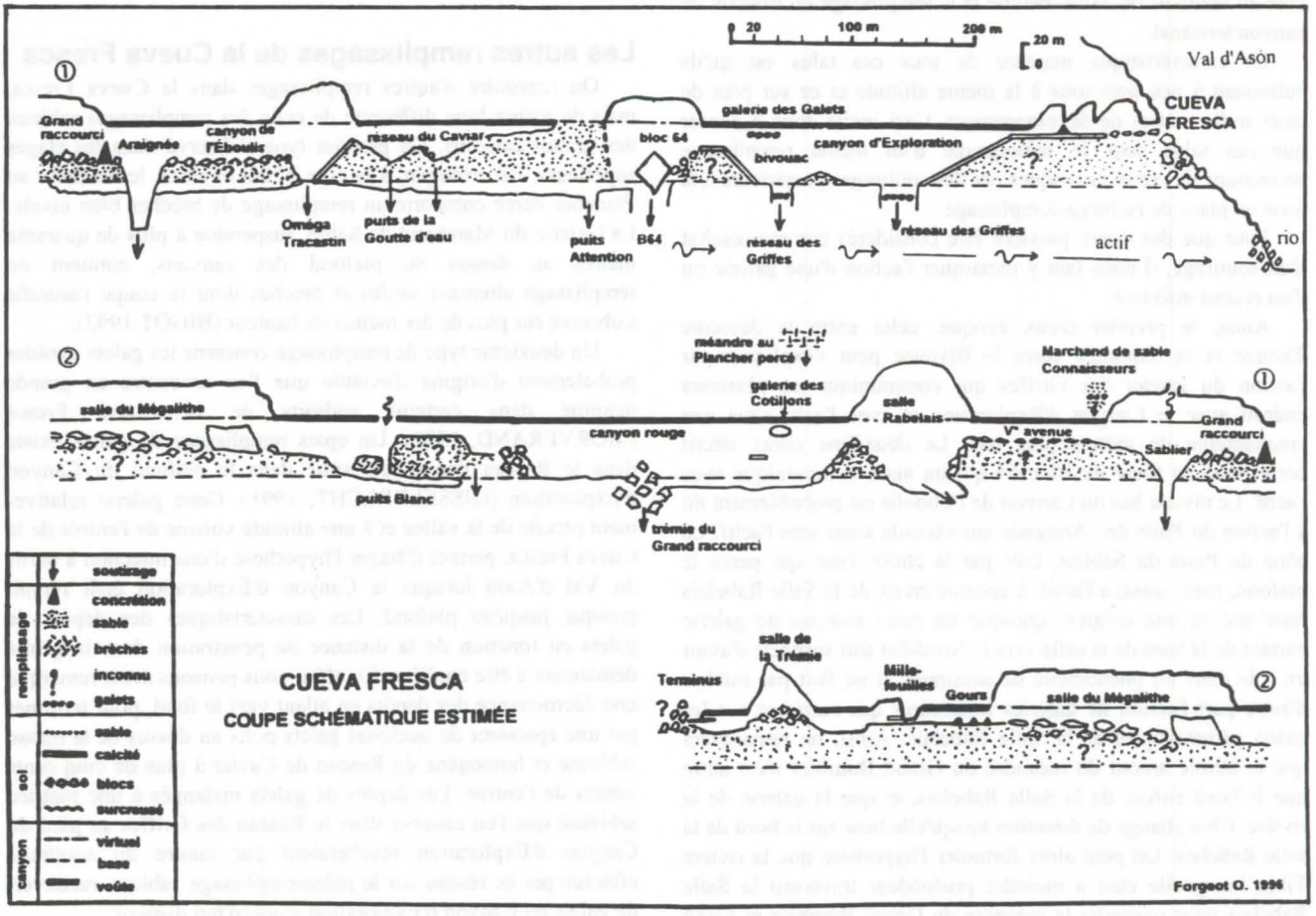

Figure 1 : Coupe schématique de la Cueva Fresca de l'entrée au terminus du Canyon Rouge

Shape of Fluvial Pebbles in Surface and Subsurface Streams from Moravian Karst, Czech Republic

Kadlec Jaroslav

Czech Geological Survey, 118 21 Prague, Czech Republic

Abstract

Streams draining karst areas often flow through caves which have significantly different hydraulic parameters than surface channels. Moravian Karst, Czech Republic, yields a good possibility to compare different degrees of reworking of pebbles transported by streams in surface and subsurface environments. For the study of the reworking of fluvially deposited pebbles, modern sediments of two streams flowing through the Moravian Karst cave systems were chosen. Almost 1700 greywacke pebbles (size interval 16-31.5 mm) were measured in total. The changes in shape and roundness of pebbles in the modern stream channel persuasively document the dependence of reworking of clasts of fluvial sediments on the hydraulic conditions.

1. Introduction

Karst environment is typical for its unique hydrologic conditions which have dominant influence on the means of transport and reworking of pebbles of fluvial sediments. Several authors studied the shape of pebbles in surface streams and the level of their reworking (see e.g. MILLS, 1979). Pebbles deposited by subsurface karstic streams were also investigated (e.g. BULL, 1978; KRANJC, 1981). KRANJC(1989, pp. 51-54) published a data set characterizing reworking of pebbles in a subsurface river flowing through the Škocjanske jame and Kaèna jama Caves in the Dinaric Karst. The set is complemented by three samples of a psephite collected from a surface stream at different distances in front of the cave. However, significant differences between reworking of pebbles in the surface and subsurface part of the stream are not apparent.

2. Geographical and geological setting of the Moravian Karst

The Moravian Karst is situated 200 km SE of Prague, the capital of the Czech Republic, and 20 km from the city of Brno (Fig. 1). The karst area formed by Devonian limestones has the shape of a belt 3 - 5 km wide and some 20 km long. The limestones are bounded by faults against non-karstic, Lower Carboniferous sediments in the north and in the east, and against Proterozoic granodiorites in the west. Streams flow across the Devonian limestones west, draining the area into the Svitava River (Fig. 2). The common feature of rivers flowing through the caves of Moravian Karst is the fact that a larger part of their catchment area is formed by non-karstic rocks of Lower Carboniferous age. On the boundary with the Devonian limestones the flows sink under the surface and continue through cave systems.

Figure 1 : Location of the Moravian Karst

The Moravian Karst yields an excellent possibility to compare different degrees of reworking of pebbles transported by streams in surface and subsurface environments. Reworking of fluvially deposited pebbles was first studied in modern sediments of the Bílá voda Stream, which flows through cave systems in the northern part of the Moravian Karst (Fig. 2). The catchment area of this stream is located to the NE of the karst area. The stream flows through the Lower Carboniferous greywackes, siltstones and shales. The length of its surface stream to the northern margin of the Moravian Karst is 18.5 km. Most of the pebbles transported by the Bílá voda Stream consist of fine- to medium-grained greywackes (83-98%), siltstones and shales are present in a much smaller scale (9-17%) and quartz can be found exceptionally in the psephitic fraction. On the northern rim of the limestone area the stream vertically sinks by 30 m into the Rasovna Cave. The underground river then continues through the cave systems (Fig. 2) with its gradient being 1.2%. .In the Amatérská Cave, the Bílá voda merges with a stream which vertically sinks in the Sloupsko-Šošùvské Caves - the Luha Stream and its tributaries. Waters of these two streams continue as the Punkva River through the Amatérská Cave towards the Macocha Chasm and Punkevní Caves. The sub

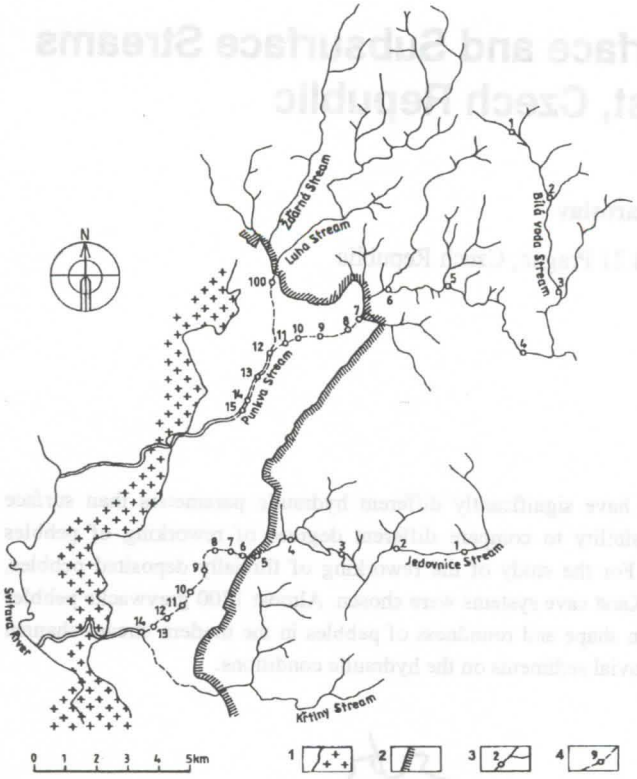

Figure 2 : The northern and central parts of the Moravian Karst; 1 - boundary between Devonian limestones and Proterozoic Brno massif, 2 - boundary between Devonian limestones and Lower Carboniferous non-karstic sediments, 3 - surface stream with a sampling point, 4 - subsurface stream with a sampling point

terranean river resurges on the bottom of the Pustý •leb Valley. The Punkva River then continues on the surface and meets the Svitava River.

The knowledge of greywacke pebble roundness gained by the study of the Bílá voda Stream sediments was tested on pebbles of modern sediments of the Jedovnice Stream. This stream flows through cave systems in the central part of the Moravian Karst (see Fig. 2). Its catchment area is located east of the karst area, being formed by greywackes, siltstones and shales. The catchment area is about a half of that of the Bílá voda Stream. The length of the surface reach of the stream is 11.5 km. Close to the boundary between limestones and non-karstic rocks, the stream vertically sinks by 90 m under the surface into the Rudické Propadání Cave. From this cave, the Jedovnice Stream proceeds to the Býèí skála Cave and resurges to the surface close to its mouth. The underground reach of the stream is 18.5 km long and has a gradient of 1.2 %. From the resurgence downstream, the Jedovnice Stream flows in a surface channel and finally meets the Svitava River after 4 km.

3. Roundness and shape determination of greywacke pebbles

The Bílá voda and Punkva streams

Reworking of the clasts during transportation both in the surface and underground channels of the Bílá voda and Punkva streams is expressed by the roundness and shape of the pebbles. Each sample consisted of 60 pebbles of greywacke from the size interval 16-31.5 mm. Roundness is determined by the ratio of the diameters of the largest and smallest circle drawn into the plane of the largest projection of a pebble (DOBKINS & FOLK, 1970). The resultant roundness value of the suite of 60 pebbles is expressed by the median of the set Figure 3-B shows that roundness in the surface flow gently rises downstream (samples 1-7). In places where short tributaries carrying less reworked pebbles enter the Bílá voda Stream, the roundness drops (samples 2, 4, 7). The profile of the flow rapidly changes in its character at the ponor of the Bílá voda Stream (fig.3-A), where the stream sinks vertically 30 m into Rasovna Cave. The hydrodynamic potential of the river increases and so does the rate of reworking of the pebbles. In the initial tract of the cave system, the stream flows through narrow places with long siphons often without open air surface at an increased velocity. The roundness of pebbles rapidly increases as a result of collisions with walls of narrow cave corridors. Also the more frequent collisions of pebbles with each other contribute to the rapidly increasing clast roundness. Another increase in the pebble roundness occurs after the confluence with the Luha Stream which transports more reworked clasts. The pebbles collected in a surface channel closely upstream of the ponor at the village of Sloup (sample 100) show a better roundness than those found closely upstream of the ponor of the Bílá voda Stream near the village of Holštejn (Fig.3-B). The steeper profile of the Luha Stream increases the hydrodynamic potential of the flow causing higher roundness of clasts.

It is not possible to reliably determine the roundness of pebbles in the surface flow of the Punkva Stream from its resurgence in the Pustý •leb Valley to its confluence with the Svitava River. Limestone and granitoid clasts dominate in the channel. One can assume that the roundness of pebbles in the surface flow of the Punkva Stream will not further increase, or, will increase only very slightly (see KRUMBEIN, 1941).

The shape of pebbles is determined by the ratio of all the three axes and calculated by a formula used by (DOBKINS & FOLK, 1970). The resultant value from each sampling point is expressed once again as a median of a set of 60 pebbles of the fraction 16-31.5 mm. Positive values represent a rodlike pebble shape, negative values an oblate shape. An obvious trend in flattening of pebbles can be seen from the source of the Bílá voda downstream (Fig. 3-C, samples 1-7). In places where short tributaries bring less reworked clasts, rodlike pebbles are more abundant (samples 2, 4). Continuous flattening downstream results from shortening of the shortest axes. This is caused by sliding of pebbles along the bottom of the channel. The flux pushes the clasts to the bottom by a

force opposite to hydraulic lift (BLATT *et al.*, 1972, p. 108). The same force causes imbrication of pebbles.

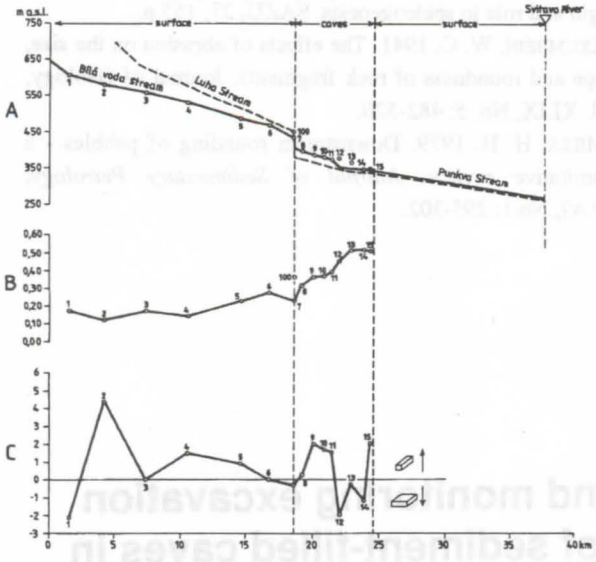

Figure 3 : A - gradient curves of the Luha, Bílá voda and Punkva streams with sampling points, B - roundness of the pebbles, C - shape of the pebbles

On the rim of the Moravian Karst where the Bílá voda Stream sinks into the karstic caverns, the hydraulic conditions change. The fluvial greywacke pebbles from the initial part of subsurface stream have significantly rodlike shapes (samples 9, 10,11). The increased velocity in the narrow underground channels and siphons lowers the pressure (DREYBRODT, 1988; KRANJC, 1989). Unlike the clasts in the surface channel these clasts are not being forced to the bottom of the channel. Pebbles in these parts of underground channels rotate around their long axes and obtain rodlike shapes. The next reach of the active stream channel is mostly unknown as it is situated 10-20 m below the Amatérská Cave. The Flood Corridor of the Amatérská Cave consists of vast passages active in the Holocene. In some of the extremely spacious passages, the hydraulic conditions were similar to those of a surface channel. In such reaches of the underground stream, the pebbles of greywackes were rapidly flattened due to the decrease in water velocity and increase in pressure (samples 12, 13 and 14). The last part of the underground flow of the Punkva River is formed by narrow channels and a 400 m long siphon between the Amatérská and Punkevní caves. The pebbles become rodlike again due to the previously described mechanism (sample 15).

The Jedovnice Stream

The roundness of greywacke pebles in the surface part of the Jedovnice stream increases in the downstream direction (Fig. 4-B). The same diagram shows that the roundness of pebbles increases in the cave system.

The shape of greywacke pebbles in the surface stream is clearly rodlike. Thinly bedded greywackes intersected by numerous joints are exposed in outcrops along the stream channel. Rodlike clasts get to the channel from the outcrops and no significant reworking occurs among them during the short transport. The first reach of the subsurface stream is formed by high, meandering corridors. The stream flows here with an open space above even during flood events. A gradual flattening of pebbles occurs in the sediments (Fig. 4 - C, samples 5,6,7,8,9). Narrow corridors and siphons several hundred metres long form the central part of the cave system. A different mode of pebble movement on stream bed occurs due to

the above described changed hydraulic conditions of flowing water. As a result, the pebbles acquire a distinctly rodlike character (samples 10,11). Downstream of the siphons, the underground flow runs through a large corridor, in which - similarly as in the large corridor of the Amatérská Cave - the greywacke pebbles become flat in shape (samples 12,13,14).

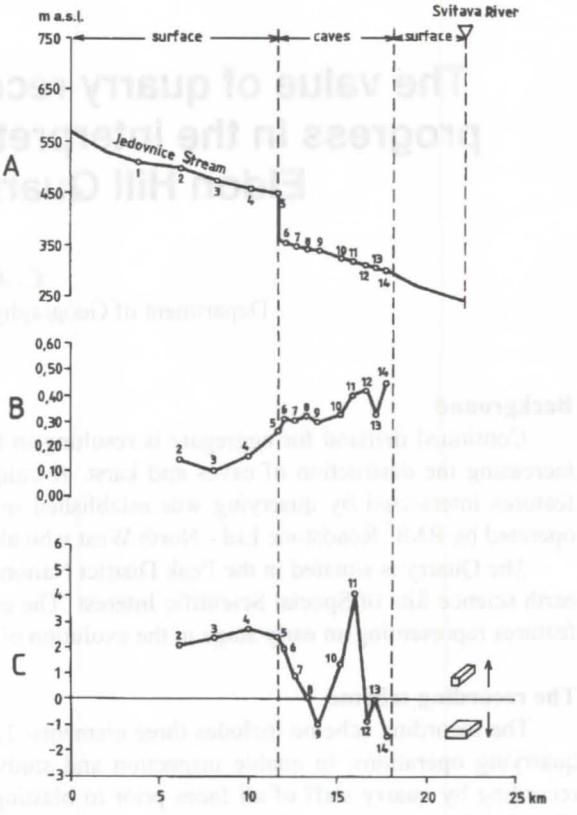

Figure 4: A - gradient curves of the Jedovnice Stream with sampling points, B - roundness of the pebbles, C - shape of the pebbles

4. Conclucion

The changes in shape and roundness of modern pebbles in the two streams flowing through the cave system of the Moravian Karst persuasively document the dependence of reworking of clasts of fluvial sediments on hydraulic conditions of the environment. These conditions control water flow in the surface and underground channels, which, in turn, determines the mode of fluvial pebble movement on channel bottom as well as the reworking of the pebbles.

Acknowledgments

The study of sediments of the Moravian Karst is supported by the Grant Agency of the Czech Republic (grant No. 205/93/0726) and U.S.-Czech Science and Technology Program (grant No. 95 051).

References

BULL, P. A. 1978. A study of stream gravels from a cave: Agen Allwedd, South Wales. *Zeitschrift für Geomorfologie*, 22, Heft 3: 275-296.

BLATT, H.; MIDDLETON, G. & R. MURRAY. 1972. Origin of sedimentary rocks. Prentice-Hall, 634 p.

DOBKINS, J. E. & R.L. FOLK. 1970. Shape development on Tahiti-Nui. *Journal of Sedimentary Petrology*, Vol.40, No.4: 1167-1203.

DREYBRODT, W. 1988 : Processes in karst systems. Physics, chemistry and geology: Springer-Verlag, 288 p.

KRANJC, A. A. 1981. Pebble investigation in Slovene caves (Yugoslavia). *Proc. 8th Int. Congress of Speleology*: 18-20.

KRANJC, A. A. 1989 : Recent fluvial cave sediments, their origin and role in speleogenesis. SAZU, 27, 155 p.

KRUMBEIN, W. C. 1941. The effects of abrasion on the size, shape and roundness of rock fragments. Journal of Geology, Vol. XLIX, No. 5: 482-520.

MILLS, H. H. 1979. Downstream rounding of pebbles - a quantitative review. *Journal of Sedimentary Petrology*, Vol.49, No.1: 295-302.

The value of quarry records and monitoring excavation progress in the interpretation of sediment-filled caves in Eldon Hill Quarry, Derbyshire, England

C. Allison, P.L. Smart

Department of Geography, University of Bristol, Bristol BS8 1SS

Background

Continued demand for aggregate is resulting in further expansion of limestone quarries in the U.K. thus potentially increasing the destruction of caves and karst. A unique scheme for the recording and documentation of cave and karst features intersected by quarrying was established in 1993 at Eldon Hill Quarry and continues to date. The Quarry is operated by RMC Roadstone Ltd - North West who also provide the sponsorship for the scheme.

The Quarry is situated in the Peak District National Park, Northern England and is included within the Castleton karst earth science Site of Special Scientific Interest. The quarry has intersected a large number of sediment-filled caves, fossil features representing an early stage in the evolution of the Castleton karst.

The recording scheme

The recording scheme includes three elements: 1) a procedure to alert scientists and cavers to features intersected by quarrying operations, to enable inspection and study before their subsequent destruction; 2) the routine photographic recording by quarry staff of all faces prior to blasting; 3) the archiving of rock quality logs obtained routinely from all blast drill-holes, together with the location and elevation of each drill-hole.

Results

The alert procedure has only operated once in a four year period (when an open void was intersected which enabled cavers to enter a 150m long cave system, Alsop's cave), but it has provided a framework allowing free access to sites of potential interest to both cavers and scientists, together with some financial and logistic support. It has also increased awareness of the significance of the cave sites among the quarry workforce.

A near complete photographic record of the progressively retreating quarry faces (usually at 10m intervals) has been obtained, although there are some problems with face identification and faces were not photographed prior to buffer blasting. The quality of this record is in some cases inadequate for detailed interpretation, often due to poor weather and light conditions, or inclusion of too wide a field of view. The use of marked drill holes for scale also proved inadequate. The photographic record enabled the gross morphology and distribution of intersected caves to be determined, but it did not enable interpretation of the stratigraphy and nature of the sediment infill, even where faces were especially cleaned.

Data for more than 2000 drill holes at 4.5m centres were obtained, offering the potential for very high resolution of distribution and extent of caves by use of a 3D visualisation package. However, many holes were deliberately deviated from the locations of known sediment filled caves or major joints to reduce drilling and blasting problems. There was also a problem in the unambiguous conversion of rock quality terms such as "rough drilling" and "clay and rock" into karstically meaningful categories, subcutaneous zone and gravel or boulder-filled cavity in these two cases.

Age and Distribution of some Karstic Sediments from the Polish Jura and their Implications for the Age of the Relief

Ireneusz Felisiak
University of Mining and Metallurgy, Faculty of Geology, Geophysics and Environmental Sciences
al. Mickiewicza 30, 30-059 Kraków, Poland

Abstract

Due to the lack of fossils, both the clay and heavy mineral assemblages were applied to the dating of both the Tertiary and Early Quaternary karst sediments in the Kraków Upland. Mineralogical criteria appeared to be the usefull age determination method. Preliminary results compared with the available palaeontological datings allow to revise the age of drainage system in the studied area which appears to be younger than previously proposed. The Late Pliocene-Early Eopleistocene was presumably the period of tectonic stabilization and planation whereas during Late Eopleistocene-Mesopleistocene quick uplift took place. This event is connected with rejuvenation of faults and with the general uplift of the area north from the Krzeszowice Graben.

Introduction

Relics of fossils in Tertiary and Early Quaternary karst sediments are relatively rare. Therefore, attempts are made to base their stratigraphy upon mineralogical criteria, particularly upon the composition of heavy and clay mineral assemblages. Preliminary results obtained for the Polish Jura are encouraging. The Polish Jura (PJ) is a NW-SE-trending belt of outcrops over which Oxfordian and Lower Kimmeridgian limestones are exposed.

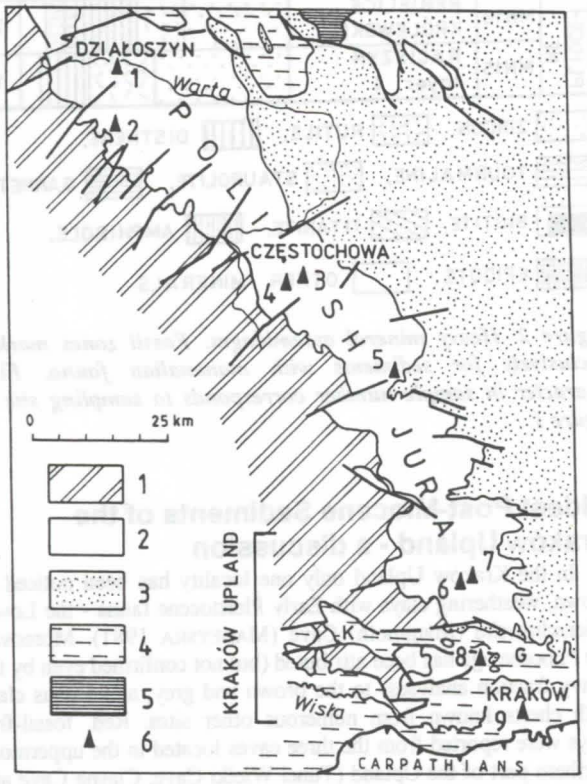

Figure 1. Simplified map of studied area: 1-9 sampling sites for heavy minerals analyses. Lithostratigraphy:1 - pre-Upper Jurassic, 2 - Upper Jurassic, 3 - Cretaceous, 4 - Miocene of the Carpathian Foredeep, 5 - continental Neogene, 6 - sampling sites. K G - Krzeszowice Graben.

The belt extends from Kraków through Częstochowa to Działoszyn (figure 1) and is the largest karst area in Poland. Its southern part is called "The Kraków Upland". It is cut by the latitudinal Krzeszowice Graben which marks the northern edge of the Carpathian Foredeep. In the area of Foredeep the karstified Oxfordian limestones are partly covered by marine Miocene clays.

The karst sediments in the studied area can be divided into the four age groups: 1. Eocene, 2. Oligocene and early Miocene, 3. Pliocene and Early Quaternary (Eopleistocene), 4. Meso- and, particularly, Neopleistocene. The absence of Middle and Late Miocene deposits is caused by marine transgression. In both the first and the second group sediments do not contain fossils and are locally covered by Middle Miocene strata (marine in SE and continental in NW parts of the studied area). The third group is palaeontologically dated but only in the NW part of the area. Finally, the fourth group has full palaeontological dating.

Denudation of Miocene clays cover as well as the initiation of recent river system took place in the Pliocene and Eopleistocene. Details of this process were studied in the SE part of the studied area (i.e. in the Kraków Upland) by DŻUŁYŃSKI *et al.*,(1966). The age limits proposed in their paper are rather hypothetical due to the absence of Pliocene and Early Quaternary fossils and had to be partly corrected (*cf.* MADEYSKA, 1977). Hence, applying the mineralogical criteria, the present author aims to ascertain which sediments in the vicinity of Kraków belong, in fact, to Pliocene and Eopleistocene. Although the study is based upon observations made in the NW part of the PJ, the uniform geological structure of pre-Tertiary basement allows to extend the conclusions to the SW part of the investigated area.

Summary of dated sediments

Eocene

The oldest sediments in the studied area are so called "moulding sands", i.e. red, clayey sands which crop out in the central part of the PJ. In the vicinity of Częstochowa these deposits fill numerous karstic depressions of diameters up to 1 km and depth over 45 m. In some places the sands are covered with continental Miocene strata. As the prevailing clay mineral of the moulding sands is kaolinite the sediments are regarded as products of warm and humid climat (GRADZIŃSKI, 1977). The heavy fraction is dominated by most resistive minerals: zircon, tourmaline and disthene, accompanied by rutile and staurolite. Garnet and epidote are rare or absent. The heavy mineral assemblage originates from the Cretaceous source rocks (KRYSOWSKA-IWASZKIEWICZ, 1974).

Oligocene - early Miocene

The second group of sediments includes green clays, rarely red and green clays with white sands and Oxfordian cherts (so called "Rudawa Beds") occurring only in the southern part of the studied area (Kraków Upland). The heavy mineral assemblage is identical with that of the first group but smectitic character of clay fraction implies more arid and somewhat cooler Oligocene climat (GRADZIŃSKI, 1962). Data from drill cores point out that deposition or, at least, redeposition of these clays proceeded up to Middle Miocene transgression (FELISIAK, 1992).

Pliocene and Eopleistocene

Sediments of the third group are red and brown clays and residual clays with mammalian fauna which represents MN15 - Q2 time span (Upper Ruscinian-Upper Biharian) (NADACHOWSKI *et al.*, 1991; GŁAZEK *et al.*, 1994). In the oldest strata (MN15 - Raciszyn-2, Layer No. 4; MN16 - Rębielice Królewskie-1) the heavy fraction is dominated by most resistive minerals: zircon, rutile and disthene accompanied by tourmaline and staurolite (figure 2; samples 1,2). Garnet contents do not exceed 0.3% but increases in younger strata, classified as MN17 (from 5% in Przymiłowice-3, Layer No. 4 up to 36% in Kielniki-3B) (figure 2; samples 3/1, 3/2, 4,1). In the Biharian (Q1+Q2) sediments perecentage of garnets varies from 25 to 45% (Kielniki-1 and -3A, Przymiłowice-2, Layer No. 5) whereas disthene, staurolite and zircon are accompanying minerals (figure 2; samples 3/3, 4/2,4/3). Unique component of these sediments is biotite found in clays from the Layer No. 3, Przymiłowice-2, beneath the silty clays of the Layer No. 4 with the MN17 zone fossils). Probably this mineral originates from redeposition of Miocene marine clays which contain both garnets and biotite.

The distinct increase of garnets content in continental sediments from the break of Pliocene and Pleistocene was observed also in the succession which fills the neighbouring Kleszczów Graben. Strata dated as Reuverian C (corresponding to the MN15) reveal 0-12% of garnets whereas in the overlying Łękińsko Formation their contents vary from 18 to 25% (KRZYSZKOWSKI & SZUCHNIK 1995).

Red colours of sediments dated as Pliocene and Pleistocene always have a brownish tint distinctly darker than the red colour of the "moulding sands". Independently on colour, the clay fraction is dominated by smectites accompanied by kaolinite. Illite and mixed-layer kaolinite/smectite are present in trace amounts. In the palaeontologically dated strata kaolinite predominates only in the Rębielice Królewskie-1 site and the fossil assemblage from this site, only, points out to the more warmer and more humid climat in comparison with the recent conditions (NADACHOWSKI, *unpub. report*, 1995).

Kaolinite also dominates in the brownish-red, fossil-free deposits from Dzibice which Pliocene age is inferred by position in stratigraphic sequence (BEDNAREK & LISZKOWSKI 1982) and confirmed by exceptionally low garnet concentration (below 0.6%, Dzibice-3 and -6; figure 2, samples 5/1,5/2). It seems that red, kaolinitic clays from the discussed group were derived mostly from the washing out of Eocene moulding sands-type sediments because available data usually indicate warm but not very humid, mediterranean-type palaeo-climate (GŁAZEK & SZYNKIEWICZ 1987; GŁAZEK *et al.* 1994).

Meso- and Neopleistocene

Sediments of this group show largest extent in the studied area. Lithologies include yellow and brown, clayey sands with common Oxfordian cherts, brown clays and residual (weathering) clays determined as *terra fusca* (BEDNAREK & LISZKOWSKI 1982) and redeposited loesses with limestone debris. Numerous cave sites are well-dated palaeontologically in the whole PJ area (*e.g.* MADEYSKA, 1981). Lithologically equivalent deposits cover the limestone outcrops and older karst sediments. The sands originated from the erosion of fluvioglacial sediments which were the source of large volumes of garnets and non-resistive minerals - amphiboles, pyroxenes, epidote, andalusite, silimanite) (KRYSOWSKA-IWASZKIEWICZ 1974). In the clay minerals assemblage smectites prevail over kaolinite whereas illite and mixed-layer smectite/kaolinite are trace components. Chlorites which indicate the contribution from moraine deposits (*op. cit.*) were found in X-ray patterns of clayey sands filling the sink-hole in Miocene gypsums in Kraków (Wola Duchacka, 58; figure 2, sample 9). Trace amounts of micas and feldspars were also found in this sample and in weathering clays from the Grzybowska Valley (figure 2, sample 8). Although chlorite is absent in the latter site, such mineralogical composition can also be regarded as indicative of contribution from moraine clays which were observed upslope, over the studied outcrop.

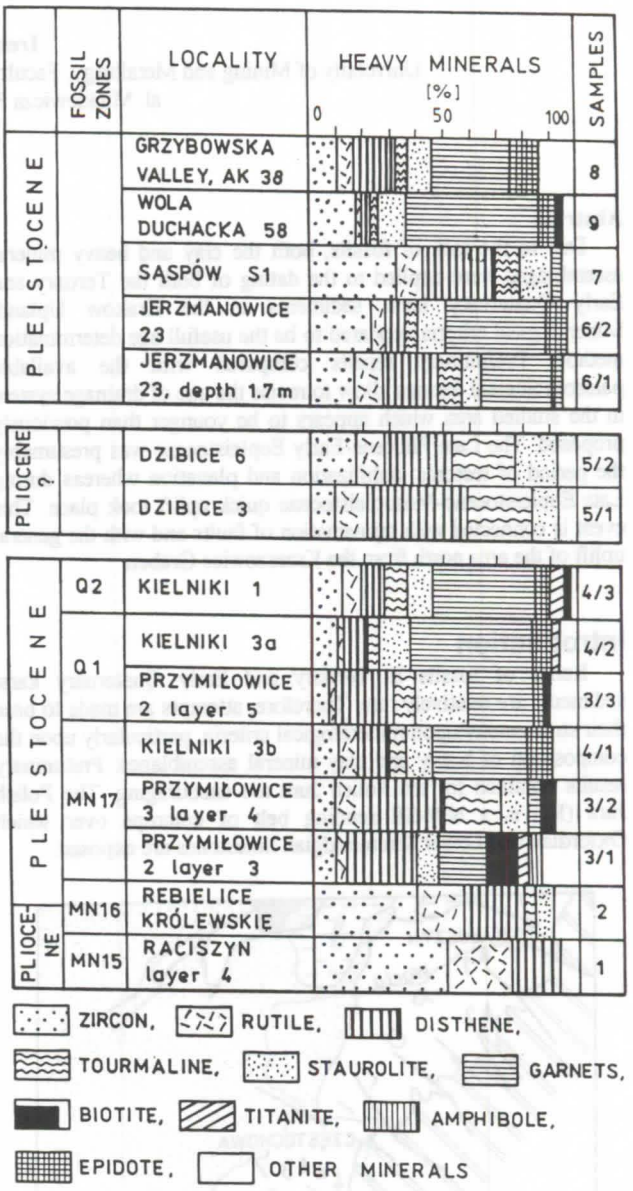

Figure 2. Heavy mineral assemblages. Fossil zones marked exclusively for sediments with mammalian fauna. First character in sample number corresponds to sampling site in figure 1.

Oldest Post-Miocene Sediments of the Kraków Upland - a discussion

In the Kraków Upland only one locality has been noticed of brown, weathering clays with Early Pleistocene fauna - the Lower Wierzchowska (Mammoth) Cave (MADEYSKA 1981). Moreover, the Pliocene age has been attributed (but not confirmed even by the heavy fraction analyses) to the brown and grey, arenaceous clays with cherts known from numerous other sites. Red, fossil-free clays were reported from the three caves located in the uppermost, northern part of the Upland (Tunel Wielki Cave, Ciasna Cave and Nad Jaskinią Niedostępną Shelter, MADEYSKA 1977).

The fourth site of red clays (and second with Eopleistocene fauna) was found close to the three mentioned above, in the Wierzchowska Górna Cave. Apart from light-red silts the younger, brown clay gritstone was encountered with clasts of dark-red clays. According to (NADACHOWSKI, *unpub. report*, 1985) the fossil *Glis*

sackdilligensis (Heller 1930) point to the Biharian. Red silts and clays can be older, even Pliocene. Analysis of heavy minerals is expected to provide solution. The clays contain kaolinite and mixed-layer kaolinite/smectite in equal proportions whereas in sample from the Ciasna Cave smectite dominates over kaolinite.

Relatively old (Eopleistocene?) can also be the clays over 11 m thick which fill the dellen of the Szklarka Valley in Jerzmanowice-23. The clays are brown and contain softened fragments of red clays. In mineralogical composition smectites prevail over kaolinite, similarly to the overlying brown, clayey sands with abundant Jurassic cherts. The latter deposits undoubtly belong to Meso- or Neopleistocene and contain much more garnets and epidotes (34.5 and 7.5%, respectively versus 27 and 4%, respectively in the clays; figure 2, samples 6/1,6/2).

Unexpected results were obtained for the clays from the adjacent Sąspów, from the dellen of the Sąspówka Valley which hosts the Ciasna and Tunel Wielki caves. Brown, arenaceous clays with abundant Oxfordian cherts consist of smectite with minor kaolinite and traces of feldspars and mixed-layer smectite/kaolinite. Heavy mineral assemblage contains very low amounts of garnets (3.3%) and is dominated by zircon, disthene and staurolite. Such composition corresponds to that of the oldest Pliocene sediments from the NW part of the PJ but also to that of the Rudawa Beds (*vidè* KRYSOWSKA-IWASZKIEWICZ, 1974; FELISIAK, 1992). Hence, it is more probable that sediments from Sąspów are residual products of weathering of the Jurassic limestones during Oligocene-early Miocene. Their original green or red-green colours changed to brown due to oxidation during Pleistocene. Such process can be observed in the Kryspinów quarry where green clays and weathering clays change colour to brown in the topmost part of the sequence and commonly grade into brown, clayey sands with cherts, typical of the Pleistocene (presumably Mesopleistocene). Traces of feldspars in sediments from Sąspów are easy to explain as same admixture was found in stratotype area of the Rudawa Beds.

The Pliocene age is also attributed traditionally to arenaceous clays with Jurassic cherts which were deposited upon the planated Miocene clays in the Krzeszowice Graben, in Pasternik (*vide* RUTKOWSKI 1996). The clays are grey and greyish-green with dark-red and violet spots and nests. Composition of clay assemblage is the same as that of the Rudawa Beds, i.e. mainly smectites accompanied by kaolinite and traces of illite. Almost identical sediments (more greenish and lacking the violet spots) underlie the Miocene clays in Pasternik, filling sub-Miocene karst paleovalley (FELISIAK, 1993). It seems that the arenaceous clays represent residuum left after weathering Oligocene-early Miocene of mainly Jurassic rocks and then transported to the south during post-Miocene deepening of river valleys in the northern part of the Kraków Upland. Currently run analyses of heavy fraction are expected to precise the period of redeposition: either the old concept on their Pliocene age will be confirmed (if garnets are absent) or redeposition period will have to be shifted to the Pleistocene (if garnets are abundant).

Conclusions on Dating of Fossil-Free Sediments

The results obtained prove the necessity of detailed mineralogical analysis of sediments and complex but thorough evaluation of the data because:

- dark-brown residual clays (so called *terra fusca*) may originate from Pliocene (MN15) but also from Mesopleistocene,
- dark-red colours are typical of sediments dated palaeontologically as MN16, MN17 and Q1 zones but pre-Miocene (including Eocene) residual deposits were multiply reworked and redeposited during Pliocene and Quaternary. Hence, carefull interpretation is recommended, particularly of the age of sediments low in garnets,
- high content of garnets in the karst deposits from the PJ is typical of the Quaternary but, theoretically, garnets, chlorites and micas may also be derived from the marine Miocene rocks (KRYSOWSKA-IWASZKIEWICZ, 1966) which shifts the potential age of the strata as far as to the Pliocene (inclusively),
- the presence of chlorites, micas and feldspars in clay fraction apart from garnets points to the Late Pleistocene age of the sediments (i.e. Elster$_2$ Glaciation in the studied area). Usually, these minerals are present in the finest fractions and, hence, can be identified only under the microscope or with the X-ray powder patterns.
- admixture of feldspars without garnets and micas may be misinterpreted as a result of glacial contribution and, hence, young age of sediment can be erroneously concluded.

The Age of Karst Sediments and the Age of Relief

According to DŻUŁYŃSKI *et al.* (1966), five levels of planation and rock terraces can be distinguished in the area of Kraków Upland (figure 3). The a-level is marked by rocky hills - monadnocs composed of Oxfordian massive limestones. The b-level is a Palaeogene (precisely Eocene) peneplain. The remaining c-, d- and e-levels are rock terraces of attributed Pliocene age with the c-level regarded as Middle Pliocene or older.

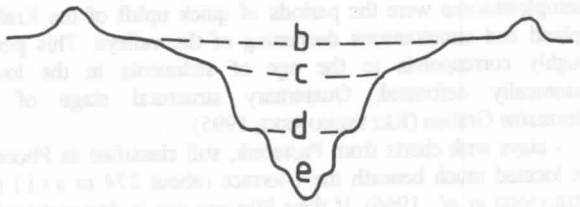

Figure 3. Scheme of the positions of peneplain and terraces (based on data after DŻUŁYŃSKI et al., 1966)

The proposed ages of the terraces were questioned for the first time basing on the analysis of age and distribution of karst sediments in caves of the Sąspów Valley (MADEYSKA, 1977). Red, fossil-free clays (Pliocene?) occur only in the caves of highest elevation (Ciasna, Tunel Wielki, Nad Jaskinia Niedostepna Shelter), related to the c-level (figure 4). In the adjacent Kluczwoda Valley the Wierzchowska Górna Cave with Biharian fauna can be attributed to the same c-level (elevation 390m a.s.l.). The Mammoth Cave with Early Pleistocene fauna (MADEYSKA, 1981) is located only 10 meters beneath. Thus, the concept on Late Pliocene or Early Quaternary age of the caves related to the c-level (MADEYSKA, 1977) is confirmed for this valley, as well.

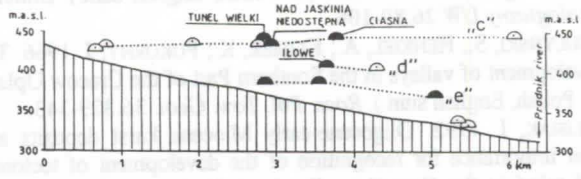

Figure 4. Vertical arrangement of caves and rock shelters in the Sąspówka Valley related to the recent Sąspówka River bed: c, d, e - terrace levels (after MADEYSKA 1977, simplified)

In the caves developed in both the d- and e-levels only Meso- and Neopleistocene sediments were encountered, with the latter dominating. These sediments were deposited in Pleistocene and the e-level was presumablyformed during the Holsteinian Glaciation. In one of the caves (Iłowa, d-level; figure 4) Oligocene-early Miocene green, smectitic clays were observed (FELISIAK, 1992). Their presence inferres the initiation of both valleys prior to the

Miocene transgression. It can also explain the probable initial age of discussed above clays from Sąspów which fill the dellen of the Sąspówka Valley.

Summary

The drainage system of the Kraków Upland was initiated in Oligocene-early Miocene, whereas river valleys north from the Krzeszowice Graben have been significantly deepened after the Miocene (Felisiak, 1992,1993). Preliminary results of the studies of oldest post-Miocene sediments in the Kraków Upland do not support the presence of brown residual clays which would correspond to sediments from Raciszyn dated as MN15 zone. According to MADEYSKA (1977), the age of removal of Miocene clays covering the valleys and deepening of the valleys is generally younger than that inferred by DŻUŁYŃSKI *et al.* (1966). Precisely:

- the c-terrace was formed presumably in the former Late Pliocene (MN16 and MN17 zones, Early Eopleistocene according to the recent stratigraphy). Its broad, trough-like shape suggests the tectonic stabilization and planation of the relief,
- both the d- and e-levels which are narrow ledges on the steep slopes of river valleys were developed in Pleistocene and the formation of e-level took place in the Eemian (MADEYSKA, 1977). Hence, it can be concluded that Late Eopleistocene and Mesopleistocene were the periods of quick uplift of the Krakow Upland and simultaneous deepening of the valleys. This period roughly corresponds to the age of sediments in the lower, tectonically deformed, Quaternary structural stage of the Kleszczów Graben (KRZYSZKOWSKI, 1995).
- clays with cherts from Pasternik, still classified as Pliocene, are located much beneath the c-terrace (about 274 m a.s.l.) (*c.f.* DŻUŁYŃSKI *et al.*, 1966). If their Pliocene age is demonstrated, it would prove that the mentioned above uplift of the Kraków Upland was connected with the rejuvenation of faults and with the uplift of the area north from the Krzeszowice Graben.

Acknowledgements

Sincere thanks are due to Prof. Adam Nadachowski (Polish Academy of Sciences, Kraków) for kind assistance during field work and for identification of fossils, and to Prof. Teresa Madeyska (Polish Academy of Sciences, Warsaw) for providing samples. Help is appreciated also from Mr. Adam Gaweł and Dr. Jerzy Czerny (University of Mining and Metallurgy, Kraków) for identification of clays and heavy minerals. Financial support of the research was provided by the University of Mining and Metallurgy Grants No. 10.140.338 and 10.140.543.

References

BEDNAREK, J. & LISZKOWSKI, J. 1982. The section of fossil weathering covers at Dzibice (In Polish, English sum.). *Biuletyn Geologiczny UW* 26:89-106.

DŻUŁYŃSKI, S.; HENKIEL, A.; KLIMEK, K.; POKORNY, J. 1966. The development of valleys in the Southern Part of the Cracow Upland (In Polish, English sum.). *Rocz. Pol. Tow. Geol.* 36:329-343.

FELISIAK, I. 1992. Oligocene-early Miocene karst deposits and their importance for recognition of the development of tectonics and relief in the Carpathian Foreland, Kraków region, Southern Poland (In Polish, English sum.). *Ann. Soc. Geol. Polon.* 62:173-207.

FELISIAK, I. 1993. Application of paleokarst studies in dating of tectonic events and morphology formation in an intensively faulted area (an example from the Carpathian Foredeep, Southern Poland). *Bull. de la Soc. geog. de Liege*, 29:129-133.

GŁAZEK, J. & SZYNKIEWICZ, A. 1987. Stratigraphy of the Late Tertiary and Early Quaternary Karst Deposits in Poland and their paleogeographic implications (In Polish, English sum.). In: *Problemy młodszego neogenu i eoplejstocenu w Polsce* p.113-130. Ossolineum, Wrocław.

GŁAZEK, J.; NADACHOWSKI, A.; SZYNKIEWICZ, A. 1994. Karst localities with Neogene and Quaternary Mammals on the Cracow - Częstochowa Upland. *Neogene and Quaternary Mammals of the Palaearctic Post-Conference Excursion Guide-Book, 22 May 1994.* Kraków

GRADZIŃSKI, R. 1962. Origin and development of subterranean Karst in the Southern Part of the Cracow Upland (In Polish, English sum.). *Rocz. Pol. Tow. Geol.* 32:429-492.

GRADZIŃSKI, R.1977. Sedimentation of "Moulding Sands" on karstified limestones in the middle part of Kraków-Wieluń Upland (In Polish, English sum.). *Zesz. Nauk. UŚ. 183. Kras i speleologia* 1(X):59-70. Katowice.

KRYSOWSKA-IWASZKIEWICZ, M.1966. Mineralogical and petrographical study of Cenozoic continental deposits of the Cracowian Upland. *Prace Mineral. PAN* 35, 69pp.

KRYSOWSKA-IWASZKIEWICZ, M. 1974. Heavy mineral assemblages in Miocene formation of the Silesian and Cracowian Regions. *Prace Geol. PAN* 36, 71pp.

KRZYSZKOWSKI, D. 1995. An outline of the Pleistocene stratigraphy of the Kleszczów Graben, Bełchatów Outcrop, Central Poland. *Quat. Sc. Rev.* 14:61-83.

KRZYSZKOWSKI & SZUCHNIK 1995. Pliocene-Pleistocene boundary in the Kleszczów Graben at Bełchatów, central Poland. *Jour. of Quat. Sc.* 10:45-58

MADEYSKA, T. 1977. The age differentiation of caves and their sediments of the Sąspowska Valley (In Polish, English sum.). *Zesz. Nauk. UŚ. 183. Kras i speleologia* 1(X):71-80. Katowice.

MADEYSKA, T. 1981. Le milieu naturel de l'homme du Paleolithique Moyen et Superieur en Pologne a la lumiere des recherches geologiques (In Polish, French resume). *Studia Geol. Pol.* 69, 125pp.

NADACHOWSKI, A. 1985. [Palaeontological opinion on bone relics sampled in the Wierzchowska Górna Cave]. *Unpub. report*, Archiv. Univ. Min. Metall., Kraków, (in Polish).

NADACHOWSKI, A. 1995. [Conclusions on palaeoclimate and palaeoenvironment of the selected Pliocene and Pleistocene sites in the Kraków-Częstochowa Jura based on gastropods and vertebrates faunas]. *Unpub. report*, Archiv. Univ. Min. Metall., Kraków, (in Polish)..

NADACHOWSKI, A.; WOLSAN, M.; GODAWA, J. 1991. New localities of Late Cenozoic faunas from Przymiłowice in the Craco-Wieluń Upland, Poland. *Acta zool. cracov.* 34:425-435.

RUTKOWSKI, J. 1996. On the polygenic character of the geomorphology of Cracow Region (S Poland). *Acta Geogr. Lodziensia*, 71:207-217.

Sedimentology, clay mineralogy, and geochemistry of cave sediment from Hard Baker Cave, Rockcastle County, Kentucky, USA

Mark P. S. Krekeler[1], Annette Summers Engel[1], Scott Engel[2], David Mixon[1], and Michael Ragsdale[1]
[1]University of Cincinnati, Department of Geology, Cincinnati, Ohio 45221-0013 USA
[2]Dames & Moore, Inc., 644 Linn Street, Cincinnati, Ohio 45203 USA

Abstract

An estimated 10 - 12 m of clastic cave sediment is preserved in Hard Baker Cave, Rockcastle County, Kentucky. The uppermost portion of the sediment is comprised of a thick, finely-laminated deposit, ranging from 30 cm to2+ m. A section of this deposit was studied to determine if there were any changes in texture, mineralogy, and chemistry of the unit, as well as to interpret what the controls of these variables were. Whole rock chemistry, as determined by X-ray fluorescence, shows no systematic enrichment or depletion of mobile elements. Chemical analyses of these sediments give a minimum chemical alteration index of 86-87, indicating that the sediment is highly evolved and has been through extensive chemical weathering prior to deposition in Hard Baker Cave. Therefore, the sediment in this cave can be used to investigate past weathering and soil development of the paleosurface before it was washed into the cave system.

Introduction

Cave sediment has been studied extensively from cave systems throughout the world. Basic reasoning behind sediment studies have been to determine 1) how the sediment accumulated in the cave, 2) from where the material came, and 3) what the sediment may reveal about the past. The present paper is concerned with these three points, addressing them using sediment stratigraphy, clay mineralogy, and sediment geochemisty. These data will test for past weathering conditions and indications of landscape evolution as they may have influenced the deposition of large quantities of sediment in this karst area.

Hard Baker Cave (figure 1; total length survey: 442.5 m) occurs in the Crooked Creek Drainage Basin, which occupies about 8% of Rockcastle County (O'DELL, 1992). This area lies near the edge of the Cumberland Plateau, where ridges (up to 150 m) are separated by narrow valleys. Streams dissect through Lower to Middle Pennsylvanian sandstone and shales and soluble Middle to Upper Mississippian limestones of the Newman Formation.

Most of Hard Baker Cave is characterized by large trunk passages, ranging from 1.5 - 2.0 m in height and width from 2 - 10 m in width. The cave is mainly developed in the Ste. Genevieve Limestone Member of the Newman Formation. The entrance pit (at 305 m above sea level) is approximately 3 m deep; at the bottom of this slope is the deepest point in the cave (at 291 m above sea level - refer to figure 1).

Sediment accumulations in the main trunk of Hard Baker cave are believed to be as much as 10 m in thickness. Investigations in Great Saltpetre Cave, which is located across the Crooked Creek valley at approximately the same elevation, suggest that sediment was deposited under similar flow regimes and that the materials in Great Saltpetre could correlate to those found in Hard Baker cave (KREKELER *et al.*, in press).

Materials and Methods

A well-exposed section of the upper-most deposit in Hard Baker Cave was described and sampled (figure 2). Samples of cave sediment were collected, whereby approximately 100g of sediment was placed in 800 mL beakers and suspended in distilled water. The <2.0 μm fraction from these beakers was collected and mounted on petrographic slides using the smear method of GIBBS (1968). Samples were X-rayed using a Siemens D-500 Diffractometer with Cu Kα radiation (XRD), with air-dried, ethylene glycol saturation, and heating at 375°C and 550°C treatments. Expandable clay minerals were modeled using the computer program NEWMOD® (REYNOLDS, 1985). Whole rock chemistry was analyzed using a Rigaku Wavelength Dispersive X-ray Fluorescence Spectrometer (XRF) for major elements.

Sediment Characteristics

Sedimentology

Overall, the clastic sediment in Hard Baker cave can be grouped into two categories: material deposited during high flow regimes and sediments deposited under low flow regimes. Materials capping the top of the sequence throughout the cave are typically silts and clays, whereas sediments at depth are characteristically coarser, containing sand and abundant gravel. Generally, cross-bedding in these deposits indicates paleoflow directions from north to south.

The top sediment (0-160 cm) of the deposit is characterized by finely-laminated silts and clays (figure 2). Sediment consists of approximately 85% to 95% clay and 5% to 15% silt. Silt grains are subangular to rounded. Measurements of light and dark banding couplets indicate that the bands are thicker towards the bottom. Dark bands contain more organic material than the lighter bands. No post-depositional burrowing or mechanical reworking are observed. Mudcracks are developed in only the top 10 - 15 cm of the sequence, ranging from 8-38 cm in width. Unidentified bones were found near the base of the sequence (M. PORTER, pers. comm.).

A gradational contact separates the laminated material from the lower unit. The sediment base is characterized by grains and pebbles of varying lithology (mostly quartz sand and quartzite pebble).

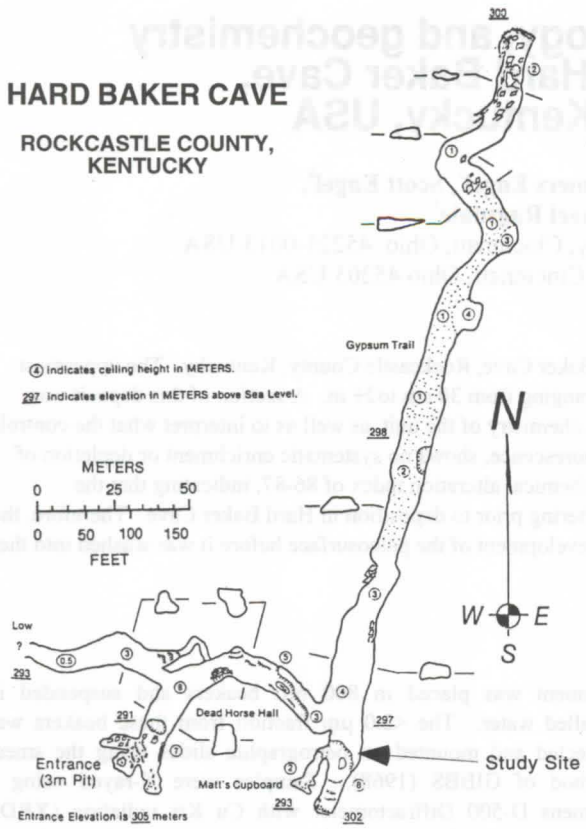

Figure 1. Map of Hard Baker Cave, Rockcastle County, Kentucky. Map courtesy of the Greater Cincinnati Grotto, Cincinnati, Ohio.

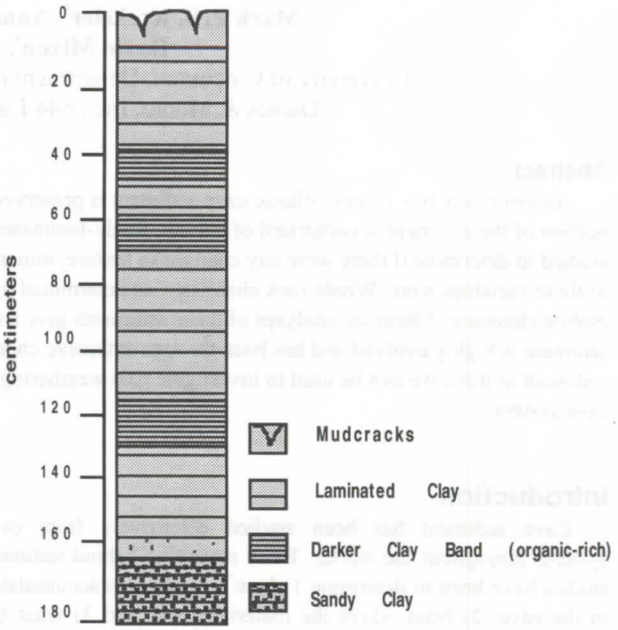

Figure 2. Stratigraphic column of cave sediment investigated for this paper. Total thickness is 180 cm.

The mineralogy of the silt fraction is composed dominantly of quartz and K-feldspar, with trace amounts of plagioclase, pyroxene, amphibole, altered biotite, and zircon. Quartz:feldspar ratios range from 1.5 to 3.3 and K-feldspar:plagioclase ratios are on the order of 30:1. Lithic fragments were observed occasionally and were identified as sandstone or chert.

Clay Mineralogy

Clay minerals in the sediment include kaolinite, illite (with minor interstratified smectite), vermiculite, lepidocrocite, goethite, R0 illite/smectite (I/S), and berthierine. Kaolinite is identified on the basis of a 7.14 Å (001) peak and a 3.56 Å (002) peak in air-dried sample. These peaks collapse upon heating at 550°C, confirming this mineral as kaolinite. Illite is identified on the basis of the ~10 Å peak which persisted through heating. Ethylene glycol treatment indicates that there is some smectite in the illite mineral structure. Using NEWMOD® (REYNOLDS, 1985), the mineral is modeled as an R3 structure with 93% illite layers and 7% smectite. Vermiculite is identified based on the presence of a ~14Å peak which expands to ~14.5 Å upon ethylene glycol treatment. After heating to 375°C, the 14 Å peak collapses to a ~12 to ~10 Å peak, verifying that the mineral as vermiculite. Lepidocrocite and goethite are identified by the presence of 6.22 Å and 4.17 Å peaks, respectively. The peaks of these minerals collapse upon heating to 375°C. R0 I/S is identified on the basis of a broad, poorly-defined peak at 16.83 Å. Traces of berthierine are identified by a ~7 Å peak which does not collapse upon heating to 550°C.

Clay mineralogy exhibits some variation with depth (figure 3). Throughout the section, as the amount of. Kaolinite is the

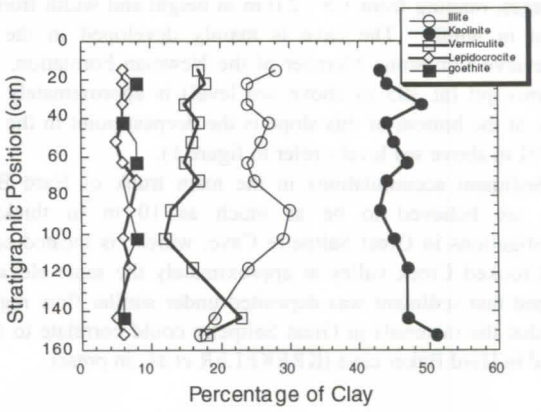

Figure 3. Variation of clay mineral percentages through laminated clay unit.

most abundant clay in the sequence, varying from 44-51%. Goethite and lepidocrocite show no systematic variation. Traces of berthierine and R0 I/S are detected in some samples throughout the section.

Geochemistry of Sediment

There is very little chemical variation within the sediment samples (table 1). No systematic increase or decrease of elemental abundance occurs. Of the elements analyzed, with the exception of SiO_2, none vary more than two per cent.

Values for CaO, Na_2O, K_2O, with respect to the Al_2O_3/TiO_2 ratio are constant. Additionally, the nearly constant Al_2O_3/TiO_2 ratio values between 18 and 20 are indicative of a single source region for the sediment.

We use the Chemical Index of Alteration (CIA) (NESBITT & YOUNG, 1982; McLENNAN, 1993) as an estimate of chemical weathering intensity. Typically, CIA values of world-wide surficial sediments range from essentially unweathered values on the order of 45 - 55 to completely weathered values near 100 (McLENNAN, 1993). The CIA is defined in molecular proportions as:

$$CIA = [Al_2O_3/(Al_2O_3 + CaO^* + Na_2O + K_2O)] \times 100$$

CaO^* is non-carbonate. Sediments from Hard Baker Cave are carbonate free and permit the application of this equation directly to our chemical data. Remobilization of elements in the spelean environment has been demonstrated to be negligible in sediments for this area (KREKELER *et al.*, in press). Therefore, using the molecular proportions from each sample, we obtained CIA values of 86-87 which indicate extensive weathering.

Interpretation of Sediment

Paleo-conditions to create sediment chemistry

The deposit we studied is sedimentologically, mineralogically, and chemically uniform. Specifically the ~2 m thick laminated clay sequence shows no significant changes in deposition, with the exception of the upper 10-15 cm where dessication is evident.

The uniformity of the Al_2O_3 / TiO_2 ratios indicates that there was a single sediment source for the laminated deposit in Hard Baker Cave. This ratio implies that any changes in mobile elements within the cave sediment would be indicative of changes in weathering intensity and climate on the surface. However, because no such changes are observed in the cave deposit, weathering conditions on the surface must have been relatively stable during the depositional sequence.

Speleogenic influences on sediment deposition

There are no apparent indications that the sediment was brought into the cave by any mechanism other than fluviokarstic drainage. Occasional cut-and-fill features in Hard Baker cave sediment suggest that some of the material was deposited and reworked in open channels. Additionally, cross-bedding in stratigraphically lower (and older) sands and gravels indicates that paleoflow was from the north to the south. The sediment sequence investigated for this study is located at a passage junction, where water and sediment would have been diverted westward, as delineated by elevations of modern passages. The nature of the laminated clay sequence supports that flow regimes were much decreased (to the point of ponding) during deposition at this locatity, and perhaps upstream and downstream, as well.

The lack of lithic carbonate material in the sediment can be explained in two ways (KREKELER *et al.*, in press). First, the carbonate clasts could have been deposited and dissolved post-depositionally. However, there are no indications that carbonate material has been leached from the sediment sequence. Second, it is possible that the drainage basin had not down-cut into the carbonate strata at the time of sediment transport and deposition in the cave system. The proposed scenario suggests that drainage at the time was not actively eroding carbonate material and thereby not contributing to the entrained sediment load of the streams (ENGEL & ENGEL, unpublished data). The present surface drainage, downcutting through the thick carbonate rock units, has developed base- level caves that having completely different passage morphology than Hard Baker Cave and similar caves at higher valley elevations (O'DELL, 1992; ENGEL, unpublished data).

An extensive survey of the cave levels in the Mammoth Cave region, Kentucky, was conducted by PALMER (1987). All major passages above 180 m in the Mammoth cave area have thick sequences of clastic cave sediment. These sediment packages often fill the passages to the ceilings and may be as thick as 25 m. These sequences are sands and gravels which are capped by silts and clays. However, the entrance of Hard Baker Cave occurs at 310 m above sea level, while most of the passages range between 300 and 291 m. PALMER (1987) states that the high cave levels of Mammoth show various stages of passage development and sediment filling, sometimes indicating slow fluvial entrenchment alternating with aggradation. Nevertheless, it is difficult to draw correlations between the two cave systems at present due to limited data and differences in local controls (i.e., stratigraphy, structure, etc.).

Presently, the timing of sediment deposition is not well established for Hard Baker Cave. Although paleomagnetism data have been collected, results are not yet interpreted (ENGEL, unpublished data). Furthermore, large and frequent speleothems are being investigated for age-dates. However, the sediment in Hard Baker Cave could be relatively old, predating continental glaciation for this region of the United States, as suggested by PALMER (1987), SASOWSKY & WHITE (1992), and SASOWSKY *et al.* (1995).

Significance of clay mineralogy for paleoclimatic inferences

The sediment in Hard Baker cave suggests that there was extensive chemical weathering occurring on the surface prior to transport and deposition in the cave, as supported by CIA values of 86-87 and clay mineralogy. The extremely evolved nature of the sediment chemistry and clay mineralogy implies that the area presently occupied by the Crooked Creek drainage basin was in a humid, temperate climate and a topographically well-drained region. The suite of clays are derived from pedogenic activty on sedimentary rocks, such as sandstone and shales, and are not the residue of carbonate dissolution.

Goethite and lepidocrocite are indicative of reductomorphic soils in temperate to tropical zones (DIXON & WEED, 1989). However, the meaning of the lepidocrocite and goethite ratio is not well understood. Hematite is also a common Fe-oxide in soils; however, the absence of hematite in the cave sediment suggests that goethite is favored pedogenically due to low temperatures, high water activity, and high organic matter content (SCHWERTMANN, 1971).

The presence of kaolinte implies that the landscape was older and mature, where the clay is inherited from primary Pennsylvanian-age shales (DIXON & WEED, 1989; KREKELER *et al.*, in press). GLENN (1960) suggests that kaolinte may be found in young glacially-derived soils where

loess is the widespread surface deposit. However, in this area of Kentucky, there are no significant loess deposits on the surface and only traces of glacial material in post-glacial drainages. This raises significant implications as to the timing of surface weathering and sediment flux into the cave system.

Acknowledgments

We thank Bill Simpson, Bill Carr, and John Wisher of the Great Saltpetre Committee (Greater Cincinnati Grotto) for field support and access to the cave. Thanks also go to members and the executive committee of the Greater Cincinnati Grotto, of the National Speleological Society for financial and field support. Special thanks go to the Wittenberg University Speleological Society for the use of caving equipment. We especially thank P. Mickler, R. Payn and M. Porter for long hours of help in the cave, as well as D. Helfin for extensive time in the lab.

References

DIXON,J.B. & S.B. WEED, eds. 1989: Minerals in Soil Environments. S.S.A. Book Series: 1. Soil Sci. Soc. Amer., Madison,1244p.

GIBBS, R.J. 1968. Clay mineral mounting techniques for X-ray diffraction analysis. *J. of Sed. Petrology*. 38: 242-244.

GLENN, R.C. 1960. Chemical weathering of layer silicate minerals in loess-derived Loring silt loam of Mississippi. Trans. Int. Cong. Soil Sci., 7th, 1960 (Madison, WI). IV: 523-531.

KREKELER, M. P. S.; SUMMERS ENGEL, A., ENGEL, S. MIXON, D. & M. RAGSDALE (in press) Mineralogy of cave sediment from Great Saltpetre Cave, Rockcastle County, Kentucky: detrital and authigenic minerals. *Clays and Clay Minerals*.

McLENNAN, S. M. 1993. Weathering and Global Denudation. *J. of Geology* . 101: 295-303.

NESBITT, H.W. & G.M. YOUNG. 1982. Early Proterozoic climates and plate motions inferred from major element chemistry of lutites. *Nature*. 299: 715-717.

O'DELL, G. A. 1992. Field Trip: Hydrology of the Crooked Creek region. *Karst-O-Rama Guidebook*. Greater Cincinnati Grotto, Cincinnati: 12-17.

PALMER, A.N. 1987. Cave levels and their interpretation. *NSS Bull*. 49: 50-66.

REYNOLDS, R.C. (Jr.). 1985. NEWMOD: a computer program for the calculation of one-dimensional diffraction patterns of mixed layered clays.

SASOWSKY, I. & W.WHITE. 1992. The role of stress release fractures in the development of cavernous porosity in carbonate aquifers. *Water Res. Res*. 30: 3523-3530.

SASOWSKY, I.; WHITE, W. & V. SCHMIDT. 1995. Determination of stream incision rate in the Appalachian Plateaus using cave-sediment magnetostratigraphy. *Geology*. 23 (5):415-418.

SCHWERTMANN, U. 1971. Transformation of hematite to goethite in soils. *Nature* (London). 232: 624-625.

Table 1. Chemical analyses as determined by XRF. Samples are delineated by depth in centimeters from the top of the described section. Chemical Index of Alteration (CIA) values are given below each sample respectively.

	15	22.5	33	42.5	52.5	63	72.5	87.5	102.5	117.5	143.5	152.5
SiO_2	59.54	59.68	61.15	59.56	61.57	59.20	58.85	57.68	62.64	59.26	63.23	65.74
TiO_2	0.96	0.98	0.97	0.95	0.96	0.95	0.95	0.96	0.94	0.97	0.95	0.93
Al_2O_3	19.13	19.04	18.61	19.07	18.50	19.20	19.29	19.50	18.28	19.29	18.17	17.49
FeO(t)	5.15	4.87	4.75	4.97	4.83	5.04	5.09	5.08	4.85	5.12	4.74	4.59
MnO	0.09	0.08	0.08	0.05	0.01	0.14	0.07	0.11	0.08	0.06	0.09	0.09
MgO	4.90	4.92	4.88	4.94	4.89	4.95	4.92	4.94	4.87	4.93	4.85	4.81
CaO	0.30	0.29	0.25	0.35	0.27	0.31	0.28	0.46	0.27	0.32	0.22	0.21
Na_2O	0.13	0.14	0.13	0.14	0.14	0.13	0.12	0.15	0.14	0.14	0.13	0.13
K_2O	2.43	2.44	2.40	2.41	2.39	2.46	2.40	2.46	2.36	2.45	2.27	2.23
P_2O_5	0.12	0.10	0.10	0.13	0.10	0.11	0.11	0.19	0.10	0.11	0.11	0.10
LOI	6.285	6.814	6.519	6.698	6.481	6.676	6.927	7.048	6.336	6.513	6.162	5.807
Total	99.035	99.354	99.839	99.268	100.24	99.166	99.007	98.578	100.87	99.163	100.92	102.13
CIA	**87**	**86**	**87**	**86**	**86**	**86**	**87**	**86**	**86**	**86**	**87**	**87**

A study of cave sediment from Movile Cave, Southern Dobrogea, Romania

Annette Summers Engel[1], Cristian Lascu[2], Adrian Badescu[1], Serban Sarbu[2], Ira Sasowsky[3], and Warren Huff[1]

[1]University of Cincinnati, Department of Geology, Cincinnati, Ohio 45221-0013 USA

[2]"Emil Racovita" Speleological Institute (G.E.S.S.), Str. Frumoasa 11, Bucharest 12, Romania

[3]University of Akron, Geology Department, Akron Ohio 44325-4101 USA

Abstract

The study of karst systems has benefited recently by cave sediment investigations, allowing new avenues for studies in speleogenesis, landform evolution, and paleoclimate. While the Movile Cave, located in Southern Dobrogea, Romania, has been the center of attention for the biospeological community with the discovery of the unique chemoautotropically-based ecosystem, Movile Cave has a complex geological evolution, as evidenced through cave sediment studies. This paper presents the cave sediment stratigraphy, mineralogy, and ages in order to determine the history of the cave system. Sediment of Movile Cave suggests fluviokarstic deposition, during the Brunhes Normal Polarity Chron (younger than 770 kya).

Introduction

Movile Cave, located several kilometers from the Black Sea coast in Southern Dobrogea, Romania, was discovered by accident in 1986 when an artificial shaft intercepted a cave passage at 18m below the surface (LASCU, 1989; figure 1). Much of the research done in the Movile has been to characterize the complex biotic system - the first cave ecosystem that does not derive its energy from photosynthesis (SARBU *et al.*, 1996). Instead, energy is derived from sulfide (H_2S)-laden waters and sulfur-oxidizing chemolithoautotrophic bacteria. Troglomorphic terrestrial and aquatic organisms, thirty-two of forty-seven being previously undescribed, have also been found in the Movile. It has been hypothesized that the cave has had no surface openings or surficial water contact since at least the end of the Late Miocene (5.2 - 5.5 mya) (LASCU, 1989; SARBU & POPA, 1992, SARBU & KANE, 1995).

However, sediment studies and other geologic investigations suggest that the cave has not been isolated since the Late Miocene but has had more recent sediment input (ENGEL, 1996; ENGEL & LASCU, 1996; ENGEL *et al.*,1996; ENGEL, unpublished). Sediment studies in caves throughout the world have revealed a number of depositional environments that, with spatial and temporal correlation, can lead to reliable interpretations of geomorphic evolution of karst terrains and the reconstruction of climatic history (MILSKE et al. 1983; OSBORNE, 1984). Therefore, the present paper is concerned with defining the speleogenesis of the Movile by using sediment within the cave. All evidence for this study is derived from cave sediment stratigraphy, clay mineralogy, paleontology, and paleomagnetism studies.

Geologic Setting

Movile Cave occupies a small portion of the eastern flank of the "Obanul de la Movile" (Movile Sinkhole), containing approximately 200 m of explored, dry upper level passages and 40 m of submerged airbells and passages in the lower level (figure 2). Both levels' passage morphologies show that the cave has had an initial phreatic origin (CONSTANTINESCU, 1989). The cave is developed in Sarmatian-age (~12.5 mya) oolitic and fossiliferous limestones deposited on the Moesian Platform. In the Mangalia area, there are numerous sinkholes and karstified carbonate outcrops, indicating a severe karstification event in the past, particularly during the Messinian Crisis (5.5- 5.2 mya) and possibly the Würmian glacial regression (LASCU, 1989; LASCU *et al.*, 1994). During the Quaternary, thick loess accumulations blanketed the region, thereby burying the karst and infilling sinkholes.

The lower level of the cave is inundated by thermal (20.9°C) water flowing at 5 l/s (SARBU & KANE, 1995), containing an abundance of sulfide (0.3 mMol/l), ammonium, and methane (SARBU & LASCU, in press). Thermomineral sulfurous springs dot the landscape as the water emerges from Sarmatian limestones through fissures and faults into valleys and the Black Sea. Isotopic comparisons with this water and other aquifers throughout the Mangalia region indicate that the origin of the thermal water in the Movile is from a deep aquifer in Jurassic and Cretaceous units (SARBU & POPA, 1992).

Figure 1: General location map for Movile Cave; the cave is located near the town of Mangalia.

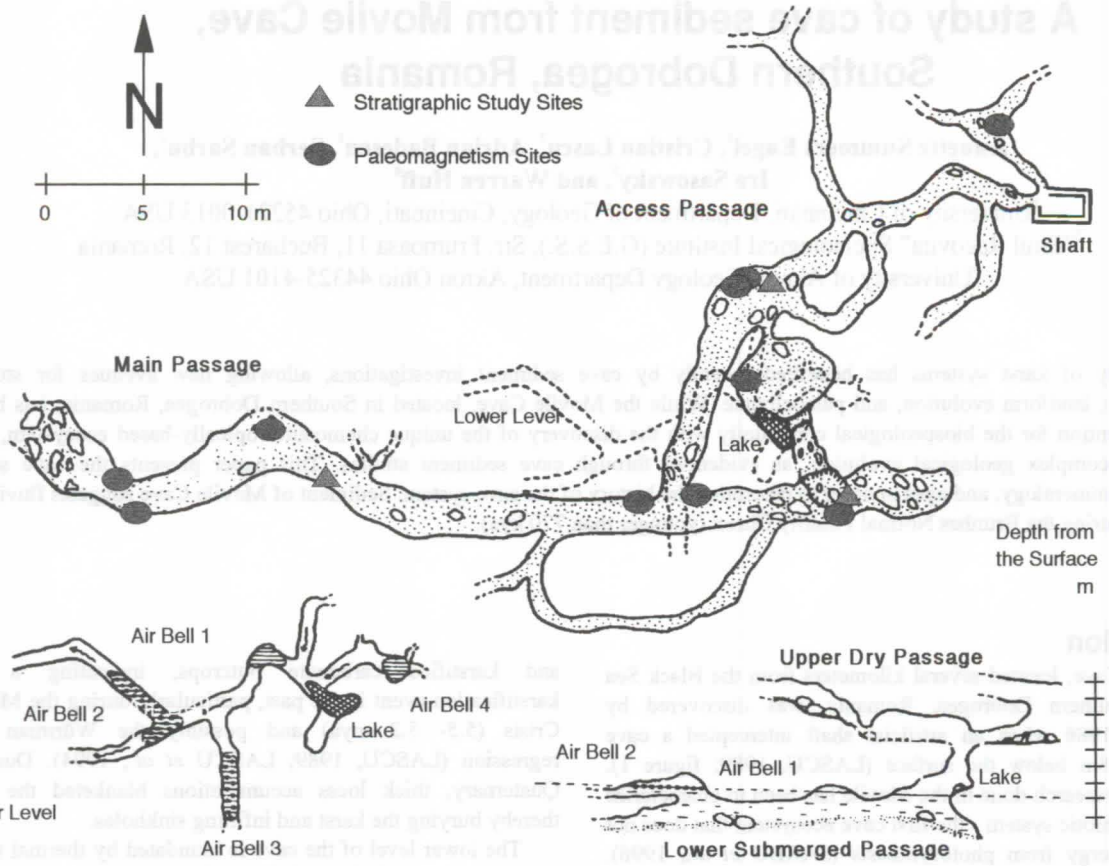

Figure 2: Map of Movile Cave, adapted from SARBU & POPA (1992). Stratigraphic and paleomagnetism sites are indicated.

Sediment and rock characteristics

Laboratory analysis of sediment and rock samples

Samples were collected from sites throughout the cave (floor and walls) where detailed stratigraphy and paleomagnetism were investigated (figure 2). Clay mineralogy was determined using X-ray diffraction techniques (XRD), starting with powder dispersions in 500 ml beakers. Solutions were centrifuged to obtain the <2mm fraction of materials. Smear mounts were made and analyzed using a Siemens D-500 X-ray Diffractometer with Cu Ka radiation. For each sample, XRD runs for air-dried, ethylene glycol treatment (to test for expandable clays), and heating to 375°C and 550°C (to determine kaolin group minerals and others that collapse with heat) were obtained.

Scanning electron microscopy (SEM) with an electron dispersive system (EDAX or EDS) work was done with numerous samples throughout the cave in order to distinguish depositional characteristics of the material and sediment microfabric. A JEOL JSM-T220 SEM with EDAX was used and samples had to be coated with a several angstrom thick layer of gold. An Hitachi S-246N SEM with EDS, infrared chamberscope, and Robinson detector was also used and samples did not need to be coated (operated in environmental mode).

Sediment mineralogy and fabric

Cave sediment can be described as *allochthonous,* having been derived from outside the cave system and then transported mechanically into it, or *autochthonous*, originating from within the cave by internal breakdown/corrosion processes. This study will differentiate the two sediment types.

Allochthonous clay-size sediment includes soil clay mineral assemblages similar to loess deposits: chlorite/vermiculite, (001) peak at ~14 Å (from XRD patterns); kaolinite/smectite, (001) peak at ~7 Å; R0 illite/smectite, (001) glycol treatment peak at 15.9-16.1 Å; R3 illite/smectite, (001) peak at 9.8-10.2 Å, and goethite, peak at 4.16 Å. These clay minerals do not result from carbonate dissolution. Sediment in larger size fractions (<2mm - 10cm) includes sub-rounded to angular carbonate clasts, clay clasts, sub-rounded to rounded quartz grains and pebbles, and fossil fragments. SEM photographs show that there is no compaction of clay flocks. The coarser sediment in the cave is distributed in gravel bed and bank deposits that mimic passage meandering. Slight clast imbrication and sediment sorting suggest water deposition; flow directions are generally from west to east in the upper level (refer to "Main Passage" on map).

Autochthonous sediment consists of very small portions of illite (peak at ~10.0 Å), kaolinite (peak at ~7 Å), and quartz, with great percentages of dolomite (peak at 2.89 Å). Most of the sediment >2mm are dolomitic ooids. SEM reveals zoned dolomite rhombs (5-20 mm in width) on the outer surfaces of the ooids, showing no signs of dissolution or instability. Some crystal faces have an abundance of adhering, spherical single and chained bacteria. The average diameter of the chained bacteria is 1 mm, with a connecting filament of approximately 1 mm. Bacteria chains, up to 20 mm long, rest in dents and depression on dolomite crystal faces.

Sediment collected from the bottom of the lower level consists predominately of the low-pH clay mineral alunite (distinctive peak at 3.01-2.99 Å). Aunite forms from the

alteration of pre-existing clay minerals (such as kaolinite and illite) in the presence of sulfuric acid (HILL, 1996).

Bedrock mineralogy and fabric

Rock samples were obtained from several localities inside the cave, as well as from surface outcrops in the surrounding region. The vast majority of the rocks from the surface consist of quartz, minor clays (<5% total volume), and calcite (peak at 3.04 Å). However, some rocks were composed of about 98% high magnesium calcite (peak at 3.02 Å). Rock samples collected from the cave shaft are composed of approximately 85% calcite and 10% dolomite (the remaining 5% being indistinguishable clays). Bedrock collected from inside the Movile, behind thick clay accumulations, is calcitic. However, bedrock sampled throughout the rest of the cave where there are no clay deposits reveal the main mineralogy to be dolomite.

Bedrock samples ~ 50 cm and 90 cm into the wall of the cave were analyzed by thin sections. Like HOROI (1994), the rock was found to be severely corroded. Where a considerable amount of porosity developed, dolomite filled the vugs. Whole ooids are shown also to be replaced by dolomite.

Age-dating Movile Cave sediment

Previous paleontological investigations

ENGEL & BADESCU (unpublished data), LASCU (pers. comm.), and STIUCA & ILINCA (1995) found vertebrate fauna containing micromammalian and aquatic taxa from sediment collected at various places throughout the cave. STIUCA & ILINCA (1995) identified the animals to include birch mice,. wood mice, steppe lemmings, bats, frogs, and fish. These animals are characteristic of a dry, open environment in association with species indicative of grassland and marsh. This fauna could not have been derived from in situ weathering of the Sarmatian-age carbonates, as terrestrial animals are not found in the units (GRIGORESCU *et al.*, 1986). Instead, the fossils were correlated to the late phase of the last glacial cycle (Würmian/Vistulian), which is approximately 24 to 12 kya., or Late Pleistocene.

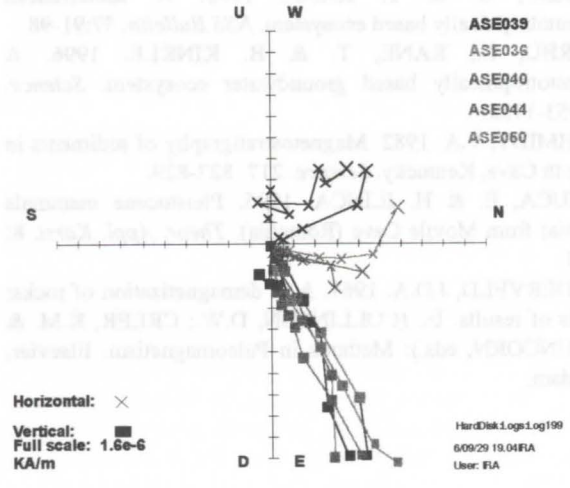

Figure 3 : Zijderveld plots for sediment from Movile Cave. These samples show a normal horizontal component and a positive (downward) inclination, indicating deposition during Brunhes Normal Polarity Chron (from 770 kya to present).

Paleomagnetism methodology and results

As described by SCHMIDT (1982), cave sediment can record paleomagnetic reversals in Earth's history. Oriented samples were collected at 10 sites (in the upper level of the cave at varying depths) using 2 cm plastic cubes. Two samples were taken from each locale. These samples were then subjected to a step-wise alternating-field (AF) demagnetization using a large-bore ScT cryogenic magnetometer interfaced with a computer to determine characteristic paleomagnetic directions.

Plots showing progressive removal of magnetic vectors, made after ZIJDERVELD (1967), reveal that most of the sediment showed very little post sampling viscous magnetization. Almost all of the samples display nearly straight-line intensity decay (demagnetization) towards the origin, indicating absence of a secondary component of magnetization. Higher coercivity steps indicate a normal horizontal component and a positive (downward) inclination (figure 3). Therefore, most of the sediment in Movile Cave has been deposited during the Brunhes Normal Polarity Chron prior 770 kya, being constrained by the Matuyama paleomagnetic reversal (IZZETT & OBRADOVICH, 1994). Based on the lack of deviations in demagnetization vectors, it is unlikely that the sediment was deposited during an older normal polarity event.

Interpretation of cave sediment

There are two main unconformities present in the Movile Cave, one being marked by the contact of the bedrock and sediment (as a primary unconformity) and the other being between allochthonous material and autochthonous sediment of modern processes. Specifically, the sediment/bedrock contact indicates that there is a large gap in time (roughly 12 million years). The sediment that has infilled the cave was deposited in a fluviokarstic drainage system. The clastic components of the sediment do not correlate to the cave host lithology, but instead resemble surface deposits, specifically aeolian sediment in fine size-fraction fabric and mineralogy and channel gravels with coarse foreign lithofragments. The proposal that a free-flowing stream, having originated from the surface, could have occupied the Movile upper level is supported by evidence of slightly imbricated clasts, sediment sorting and grading, and typical channel facies associations.

There is additional strong evidence that the Movile Cave (presently sealed) was in communication with the outside environment during certain times. Based on the paleomagnetic data, the cave was not receiving nor accumulating sediment prior to 770 kya, as constrained by the Matuyama-Brunhes geomagnetic boundary. If sediment was brought into the cave prior to this time, the material was either eroded or was not sampled. Furthermore, the vertebrate taxa found in the sediment indicate that there had to be a way for them to enter into the cave, probably by way of the associated sinkhole (STIUCA & ILINCA, 1995). These fossils have been constrained to 12 - 24 kya, and it is likely that the cave sediment is also from this time span.

The upper level of the Movile has been abandoned by free-flowing water and the lower level is presently occupied by sulfurous water. It is not known when sulfurous water inundated the lower level of the cave or how long the aquifer has existed. As indicated by the presence of alunite and isotopic

investigations done on the water and surrounding rock (SARBU, unpublished data), the process of sulfuric acid speleogenesis is actively enlarging the lower level of the cave. The process is accelerated by the high concentration of sulfide in the water and microbial oxidation of that sulfide to produce sulfuric acid. This speleogenetic mechanism has been associated with the formation of Carlsbad and Lechuguilla Caves in the southwestern United States (EGEMEIER, 1987; HILL, 1996). Alunite or other low - pH clays are absent in the upper level of the Movile, indicating that sulfurous water has not been in this portion of the cave.

Autochthonous dolomitic clay and associated residue from corroded wall rock in the upper level is attributed to condensation corrosion (ENGEL et al., 1996; ENGEL & LASCU, 1996; ENGEL, unpublished data; SARBU & LASCU, in review). This speleogenetic process is poorly understood, but the presence of corroded walls in the upper passages, the absence of water infiltration from the surface into the cave, temperature difference between the water in the lower level and the walls of the upper level, and the high CO_2 concentrations throughout the Movile all suggest that condensation corrosion is presently affecting the morphology of the upper level of the cave (SARBU & LASCU, in review). It is uncertain as to what is causing the precipitation of dolomite in place of the original calcitic host bedrock, although biogenic process may be influencing the mechanism. Also of importance is that the bedrock covered by thick clay accumulations is not dolomitized and shows no evidence of being corroded. This suggests that the clay was in place before severe corrosion of the bedrock began.

Acknowledgments

The authors of this paper would like to thank the members of G.E.S.S (Group for Underwater and Speleology Exploration), Bucharest, Romania, for field support and assistance. Appreciation is given to Dr. Ken Bladh (Wittenberg Univesity, Springfield, Ohio) and Dr. J. Lian (University of Cincinnati, Cincinnati, Ohio) for access to and help with scanning electron microscopes. Thanks are extended to S. Engel, M. Menard, R. Popa, M. Porter, and L. Trump for technical support. This research was funded by grants from the National Speleological Society, the Geological Society of America, and the University of Cincinnati.

References

CONSTANTINESCU, T. 1989. Considerations sur la zone karstique de "La Movile' (Mangalia, Dobrogea de Sud, Roumanie). *Misc. Speol. Rom.* 1:7-12.

EGEMEIER, S. 1987. A theory for the origin of Carlsbad Caverns. *NSS Bull.* 49: 73-76.

ENGEL, A.S. 1996. Scanning electron microscope images from fine-grained sediment in Movile Cave, Southern Dobrogea, Romania. *NSS Guidebook.* Salida, CO, 44.

ENGEL, A.S. & C. LASCU. 1996. Clays of Movile Cave, Southern Dobrogea, Romania: speleogenetic indicators of cavern formation. *Program and Abstracts of the 33rd Annual Meeting of the Clay Minerals Society* (Gatlinburg, TN), 53.

ENGEL, A.S.; HUFF, W., BADESCU, A., LASCU, C. & S. SARBU. 1996. Sediment studies from Movile Cave, South Dobrogea, Romania. *Geol. Soc. of America Abstracts with Programs. Annual Meeting* (Denver, CO), A-281.

GRIGORESCU, D.; CONSTANTINESCU, V. & L. DRAGOMIRESCU. 1986. A paleoecologic analysis of the Bassarabian (Middle Sarmatian) vertebrate association from Credinta and Ciobanita (Southern Dobrogea) based on the taphonomic characters processed through methods of numerical taxonomy. *Trav. Du Museum d' Hist. Naturella "Grigore Antipa"* 28: 275-283.

HILL, C. 1996: Geology of the Delaware Basin, Guadalupe, Apache, and Glass Mountains, West Texas and New Mexico. Midland: Permian Basin Section - SEPM, 478p.

HOROI, V. 1994. The corrosion process in "Pestera de la Movile" Cave (Southern Dobrugja - Romania). *Theor. Appl. Karstol.* 7: 187-191.

IZZETT, G.A. & J.D. OBRADOVICH. 1994. $^{40}Ar/^{39}Ar$ age constraints for the Jaramillo Normal Subchron and the Matuyama-Brunhes geomagnetic boundary. *J of Geophysical Res.* B99: 2925-2934.

LASCU, C. 1989. Paleogeographical and hydrogeological hypothesis regarding the origin of a peculiar cave fauna. *Misc. Speol. Rom.* 1:13-18.

LASCU, C.; POPA, R. & S. SARBU. 1994. Le karst de Movile (Dobrogea de Sud). *Rev. Roum. De Geographie.* 38: 85-94.

MILSKE, J.A.; ALEXANDER, E.C. (Jr.) & R. S. LIVELY. 1983. Clastic sediment in Mystery Cave, Southeastern Minnesota. *NSS Bull.* 45: 55-75.

OSBORNE, R.A.L. 1984. Lateral facies changes, unconformities and stratigraphic reversals: their significance for cave sediment stratigraphy. *Trans. British Cave Res. Assoc.* 11(3): 175-184.

SARBU, S. & C. LASCU. Condensation corrosion in Movile Cave, Romania. *NSS Bull.* (in review).

SARBU, S. & R. POPA. 1992. A unique chemoautotrophically based cave ecosystem. In: (CAMACHO, A., ed): The Natural History of Biospeology. Monografias Museo Nacional de Ciencias Naturales: Madrid, 637-666.

SARBU, S. & T. KANE. 1995. A subterranean chemoautotrophically based ecosystem. *NSS Bulletin.* 57:91-98.

SARBU, S.; KANE, T. & B. KINKLE. 1996. A chemoautotrophically based groundwater ecosystem. *Science.* 272: 1953-1955.

SCHMIDT, V.A. 1982. Magnetostratigraphy of sediments in Mammoth Cave, Kentucky. *Science.* 217: 827-829.

STIUCA, E. & H. ILINCA. 1995. Pleistocene mammals (Rodentia) from Movile Cave (Romania). *Theor. Appl. Karst.* 8: 157-161.

ZIJDERVELD, J.D.A. 1967. A.C. demagnetization of rocks: Analysis of results. In: (COLLINSON, D.W.; CREER, K.M. & S.K. RUNCORN, eds.): Methods in Paleomagnetism. Elsevier, Amsterdam.

Cave chemolithotrophic soils

Vladimir A. Maltsev[1], Viktor A. Korshunov[2], Andrei A. Semikolennykh[3],
[1]VNIIGEOSYSTEM institute. Moscow 121351, Yartsevskaya ul., 15-21, Russia
[2]Geology Department, Moscow State University Moscow, Tichvinsky pereulok, 9/12-4-86, Russia
[3] Soils Department, Moscow State University Moscow, Pervomaiskaya str., 94-133, Russia

Abstract

Geochemical and microbiological studies in the Cupp-Coutunn cave (Turkmenistan) show, that the fluffy red-colored coverings on the cave walls and roof, 1-20 cm thick, are not a kind of a residual sediment, but a complex organomineral media. This media, named "okher", has a very high biochemical activity. Okher appears to be a result of both strong corrosion and weathering of the rock, and a formation of secondary minerals. It also appears to be a basis of the feeding chain for higher organized flora and fauna.

Introduction

The biological redox processes are already proved to be a significant karstification factor, and the reason for some specific features of caves mineralogy. The so far studied cases mostly concern phreatic areas in caves where the sulfate reduction proceeds in deep phreas. Sometimes full bacterial sulfuric cycle was reported, with sulfatereduction in phreas, and sulfuroxidizing in dry areas [FORTI, 1988; BALL & JONES, 1990].

In spite of this, there are several caves known, that have no phreatic areas, but have active sulfuric processes in them. One of these caves is the Cupp-Coutunn cave in Turkmenistan, and it was selected as an object of the study.

Okher

The term "okher" came from the caver's jargon, as a name for red fluffy coverings on the floors and roofs of the cave, and is based on an untranslatable game of words. Up to 1993 it was taken as a residual of atmospheric corrosion [MALTSEV & SELF, 1992], but even the first studies shown, that it can't be so [SEMIKOLENNYKH & KORSHUNOV, 1994].

Okher vs. corrosion residues

If we compare okher to classic corrosion residues (for example, from Lechuguilla cave), we'll easily see two main differences:

a) In the corrosion residues we always see unaffected carcass of non-soluble minerals (especially alumosilicates), in which the original texture of the rock is saved recognizable. For the corrosion residues, known from Guadalopean caves, we can even see, that these residues are more likely simply weathered limestone - the texture has completely survived, so the volume of these "residues" is equal to the volume of the affected parent rock [CUNNINGHAM et.al., 1993; M.QUEEN, pers.comm.].

On the contrary, okher never keeps unaffected carcass of the limestone, because of much more acid conditions. All minerals, even silicates, completely re-crystallize, mostly forming new minerals, which were never found in the parent limestone. For example, fig. 1. shows rather large gibbsite crystals, generated in okher. The texture of the rock is lost completely, and the volume is changed greatly. For example, concentration of Fe_2O_3 in different layers of okher is 5.7%-28.3%, and in the parent limestone it never exceeds 0.5%. Even when converting volumes to weights (okher is fluffy, density of dried okher is about 0.2-0.6), the difference still remains great. The same is seen for silicates.

b) The corrosion residues are mineralogically passive. Okher, growing on pure carbonate substrate, is almost always covered by gypsum efflorescences, and even coatings. Disturbed okher noticeably smells of sulfuric gases, including H_2S. In spite of this, there are no visible mechanisms for transportation of sulfur to the okher location along the cave (no water flows, and no sulfuric gases in the air).

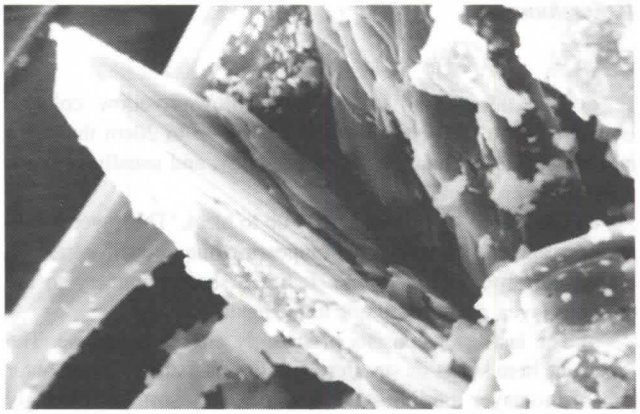

Figure 1. Gibbsite crystal in okher, 0.1 mm large, diagnosed via X-ray microzond. SEM photo by A.Semikolennykh.

These two features already allow to separate residues (passive product) form okher (active strata with complete re-working of everything).

Structure and morphology of okher

Okher is spread almost all over the cave, and its morphology and structure is variable, depending on the limestone composition, humidity, air circulation, etc.. But some generic features and typical structure exist.

Okher has no definite boundary with the limestone. Appearing as something fluffy and very porous on the surface, it becomes much more dense and sandy in the middle, then consequently transforms into altered limestone, and so on. The okher covering can be from a couple of millimeters thick up to 20cm and even more.

Okher is always well structured and has several layers. The main layers, listed below, have specific properties and can be found in almost any kind of okher (fig. 2).

a) The outer layer is thin (1-3mm.), and consists of gypsum sand, rarely forming a crust. This layer is usually present in thin okher (up to 2-3cm), and absent in thicker one. In the last case gypsum sand doesn't form a separate layer, but exist in next

layers. The boundary to the next layer is fuzzy. In places of strong seasonal humidity cycles, the gypsum may also be reworked into filamentary crystals [MALTSEV, 1996]

b) The second layer is red, extremely fluffy and porous, 1mm to 10cm thick. In thick okher this layer has a color trend - from browny inside to bright red outside. The boundary to the next layer is sharp. pH in this layer is in the range of 7-8.

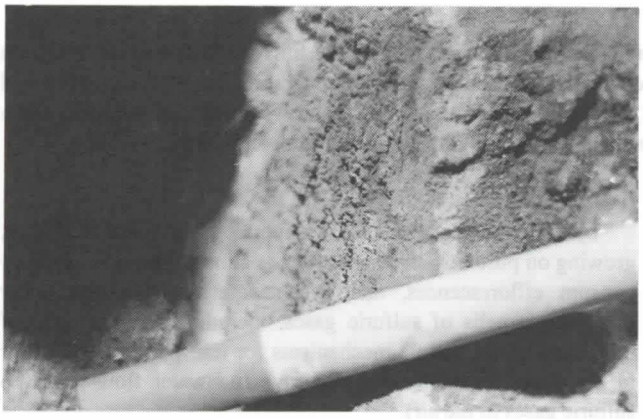

Figure 2. General view of the okher cross-section. Photo by V. Korshunov.

c) The third layer is yellow or browny-yellow colored. Usually it's the thickest layer, and can be up to 20cm thick. It's much more dense than the previous, sandy, and usually contains pieces of altered limestone.

d) The fourth layer is dark gray up to black. This layer is thin and unstable, possibly seasonal (appearing due to overmoistening during corresponding seasons). It has a sharp boundary to the previous layer, and a fuzzy one to the next.

e) The last layer consists of strongly altered limestone. The limestone here keeps its structure, but looses density. In the outer part of this layer the limestone becomes very soft, and strongly smells of sulfuric compounds when being broken. Deeper it consequently transits into normal limestone. pH on the contact of this layer with the previous is about 3.5-4, maybe even lower. The problem is, that the spatial distribution of pH is irregular, due to irregularity of bacterial communities, and all the measurements are to be made in situ - otherway the results are strongly distorted.

The pH data of the okher layers is to be compared to the pH data of the cave water. The meteoric water, coming along fractures, has pH about 6.5 in all the cases. The water in the pools has pH 7-7.5, the same as the water in the springs and in the artesian basin, both fed from the karst.

Okher covering is so delicate, that sometimes a thick red layer disconnects from the roof and falls, forming thick deposits. In these deposits only the top 10 cm look like the original okher, and in the deeper layers it changes into some dense, fat and plastic brown clay, and consequently - into also dense, fat and plastic blue clay.

Microbiology of okher

The key question - the source of the H_2S gas in the okher, in fact stays unresolved. There are many indirect evidences of SRB (sulfate reducing bacteria) activity in the deep layers of okher, but no direct ones. At the studied depth SRB (***Desulfotamaculum***) were found only in one sample. The source of the sulfur are bituminous inclusions in the limestone. Bacterial activity is the only known mechanism, due to which the sulfur is partly returned (see below). Therefore, SRB must be the main type of bacteria, utilizing the source sulfur. The question mostly is whether the SRB activity proceeds in limestone themselves, or only in the limestone near the cave. The first supposition has two

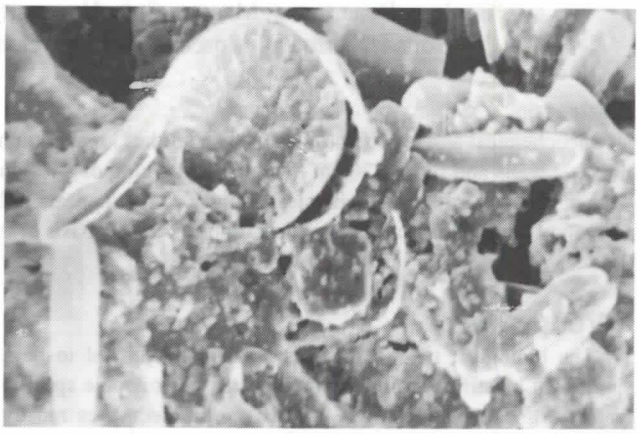

Figure 3. Diatomea in the outer layer of okher. Completely re-crystallized surrounding shows, that it's not residual. SEM photo by A.Semikolennykh.

pieces of evidences against it: No traces of the sulfur was found in springs, unloading from limestone; okher morphology too weakly correlates with fractures, which collect the H_2S gas, and this means, that it mostly appears near the cave, and is transported along the pores of the weathered limestone to deeper layers of the okher (porosity of the source limestone is extremely low). So, SRB must be mostly found in deeper layers, than it was sampled. Some evidences (mostly, studies of microflora, growing

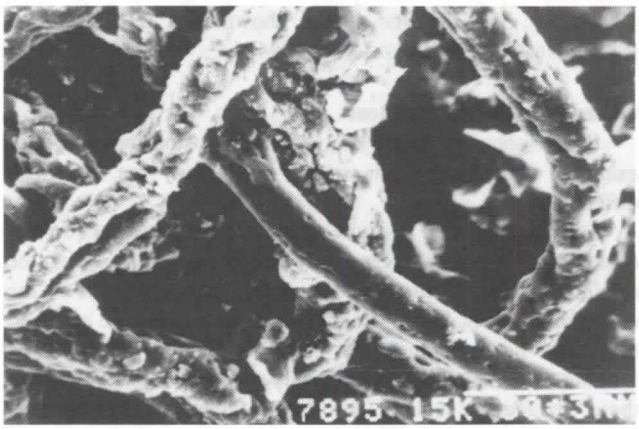

Figure 4. Simbios of mycoplasma and fungi (both undiagnosed) in the outer layer of okher. SEM photo by A.Semikolennykh.

on the candles left in caves), show, that utilizing of bituminous inclusions must be due not only to SRB, but also to ***Arthobacter, Rhodococcus, Mycobacterium***, found in all such samples.

On the contrary, another half of the sulfuric cycle is "opened", and proved. From the samples, taken from outer okher layers, using the Vacksman, Tausson and Birs media, there were exposed sulfuroxidating bacteria, particularly ***Thiobacillus ferrooxidans***, ***Th. thoioxidans***, and similar microorganisms. Their activity is enough for partial return of sulfur into the

corrosion cycle, and for enriching of the outer okher layers by Fe, providing the red coloring.

The sulfuroxidizing activity in the outer layer, returning the significant part of sulfur into the cyclic sulfuric corrosion of limestone, is an additional indirect evidence of SRB activity somewhere inside, because inside the okher pH falls to about 3, and free H_2SO4 exists, reacting with limestone, that consequently results in gypsum generation inside. Absence of this gypsum in middle layers of okher shows, that it must be destroyed by SRB.

The bacterial biomass from the okher is utilized by other organisms, giving a start to a long feeding chain. Immediately in okher several kinds of fungi (detected ***Penicillus sp., Aspergillus niger, Scopulariopsis sp***.), several protozoa, diatomea (fig.3, 4), etc. were found. In the massifs of fallen okher several kinds of mites and insects cab be found. It's possible also, that this chain

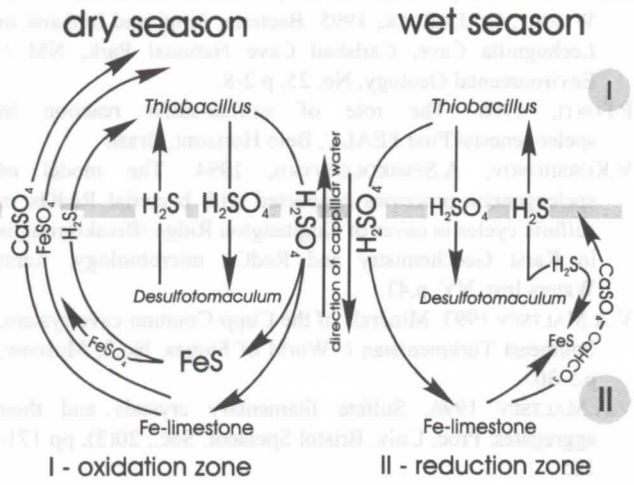

Figure 5. The seasonal iron and sulfur migration.

appears to be the chain, leading up to blind fishes, found in the under-plane drainage of the cave system (Kugitangtou blind loach), but some elements of this chain are still absent.

Looking at the details of the okher spatial distribution, we can find out, that there is some optimum between general high humidity of the cave area, and the oscillations of the humidity, caused by the seasonal cave wind inversions. Okher, developing within this optimum, is about one order more active, than the okher, developing in other areas of the cave. The diagram on fig. 5 illustrates the main relations between activities in the okher and the microclimatic conditions of the location.

Mineralogy of okher

Due to the fact that the okher layers have very different pH, and that the seasonal humidity cycle (and microbiology-driven cycles) result in cyclic migration of various ions through the pH barriers, all the matter is reworked. This reworking has several variants, but the general scheme is like the following.

Silicates, present in limestone mostly as quartz and micas, are transformed into kaolinite-like minerals in the middle layers of the okher, and further to gibbsite and illite in the outer layers. Gibbsite and illite co-existance may be explained with high-pH conditions, separating Si and Al. The same effect is known from the other parts of cave, where gibbsite and serpentine co-growth are known.

Iron is concentrated in the outer layer, mostly in the form of microcrystalline oxides - hematite, goetite, etc..

Gypsum (fig.6) is generated both in deep layers (metastabil), and outer layers (final). Calcite mostly disappears in the middle layers, and appears again in the outer layers, where it forms, together with gypsum, specific "sand". This sand, falling from

Figure 6. Okher corrosion. The white stripes are calcite veins, completely turned to gypsum in the outer layer of okher. The image height is about 40 cm. Photo by V.Maltsev.

the roofs, sometimes makes up sediments up to several metres thick, appearing as the product of the limestone corrosion by the okher.

High acidity in the deep okher layers causes some side effects when the cave intersects veins, or the cave wall is covered by products, which survived from the hydrothermal phase. Interactions between sulfuric acid, fluorite druses, silicate matter, and ore veins leads to generation of minerals, exotic for caves, like saukonite, fraipontite, serpentine, etc.

Okher as a kind of soil

So, okher is an active strata, providing the corrosion of limestone, gas and water exchange with atmosphere, alteration of the residual material, and biomass generation, that is used by other organisms. Due to this, okher certainly is to be classified not as a sediment, but as a special type of a soil, based on chemilititrophic bacteria.

Okher appears to be a significant corrosion factor. In some cave passages it provides up to 90% of the total corrosion. This can be estimated through the total quantity of the Fe and Si in the okher, compared to their contents in the parent limestone in the full volume of the passage. In such localities the okher corrosion forms specific morphologic types of the cave landscape - syr, red chinks, red tubes [SEMIKOLENNYKH et.al., 1996].

Okher exists not only in the Cupp-Coutunn cave. There are evidences of it's existance in Snezhshnaya deep cave in Caucasus, and also in some minor caves within ore mines, but this needs to be studied very carefully. In the Guadalopean caves the visual similarity appeared to be a visual convergence of very different phenomenas.

Related effects in the Cupp-Coutunn cave

The microbiological studies in the Cupp-Coutunn cave have not only shown the okher's microbiological origin. Some other corrosion and mineral generation factors definitely are also related to the activity of microorganisms. For example, it's the gypsum replacement by silicates in the Vodopadnyi chamber.

Figure 7. Gypsum replacement from inside by a foam-like silicate substance. Photo by V.Maltsev.

The gypsum gemmiforms (fig.7) are replaced from inside by some very porous foam-like silicate substance.

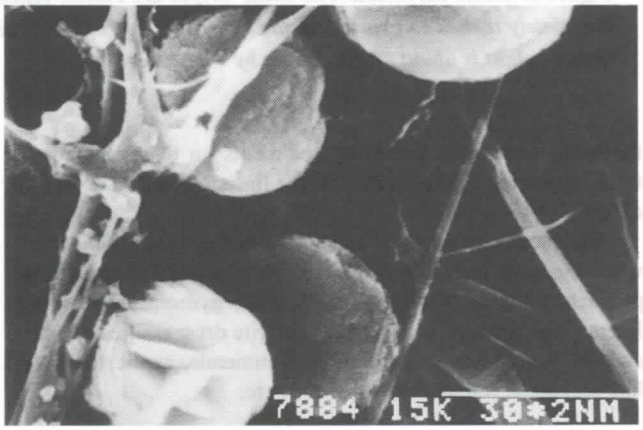

Figure 8. Celestite globules (those, where crystals are seen), silicate globules and threads from the foam, replacing gypsum gemmiforms from inside. SEM photo by A.Semikolennykh.

This substance, if studied closely, consists of celestite spherolites, amorphous silicate globules, amorphous silicate threads. The first of them may have any origin, but the last two - can only be biological. It can clearly be seen from the SEM photo on the fig. 8. There is no idea, what bacteria it could be. No growth in vitro was received, and no bacteria are known, leaving carcasses of Fe - Mg - silicate composition, very close to olivine.

There are several more similar phenomenas known, but all are completely unstudied. Certainly, microbiology must become one of the main trends in studying the cave systems like Cupp-Coutunn.

References

T.K.BALL & J.C.JONES, 1990. Speleogenesis in the Limestone Outcrup Worth of the South Wales Caalfield//Cave Science, 17(1), London

K.I.CUNNINGHAM., D.E.NORTHUP, A..M.POLLASTRO, W.J. WRIGHT, E.J.LAROCK, 1995. Bacteria, fungi and biokarst in Lechuguilla Cave, Carlsbad Cave National Park, NM // Environmental Geology, No. 25, p.2-8.

P.FORTI, 1988. The role of sulfide-sulfat reaction in speleogenesis//First FEALC, Belo Horizont, Brasil

V.KORSHUNOV, A.SEMIKOLENNYKH, 1994. The model of speleogenetic processes connected with bacterial RedOx in sulfuric cycles in caves of Kugitangtou Ridge//Breakthroughs in Karst Geochemistry and RedOx microbiology, Karst Waters Inst. NY, p.43.

V.A.MALTSEV 1993. Minerals of the Cupp-Coutunn cave system, Southeast Turkmenistan // World of Stones, No.2, Moscow, p.5-30.

V.A.MALTSEV 1996. Sulfate filamentary crystals and their aggregates: Proc. Univ. Bristol Spelaeol. Soc., 20(3), pp 171-185

V.A.MALTSEV & C.A.SELF, 1992. Cupp-Coutunn cave system, Turkmenia, Central Asia//Proc. Univ. Bristol Speleol.Soc., 19(2)-29

A.A.SEMIKOLENNYKH, V.A.MALTSEV, V.V.KORSHUNOV, 1996. The processes of biogenic sulfuric weathering in the caves of the Kugitangtou Ridge, Turkmenistan. In: Mineralogy and Life: Biomineral Interactions. Syktyvkar., p. 61.

Mineral composition of clastic material in fault zones and open fissures in karst rocks, examples from SW Slovenia

Nadja Zupan Hajna
Karst Research Institute ZRC SAZU, Titov trg 2, 6230 Postojna, Slovenia

Abstract

Three different types of clastic material may be distinguished based on its origin. The first type is infiltrated material into the open fissures from the surface. Mineral composition in that case depends on composition of rocks from were the weathering remains are originated. The second type is clastic material which is filled into opened fissures during floods of the caves, composition of it corresponds to the rocks composition of underground water flow watershed. Sediments could be enriched in calcite or dolomite clasts, these are actually small particles of limestone or dolomite from the walls of underground water passages. The third type of clastic material is significant for inner part of fault zones. This is clay size material, which was formed by tectonic compression of carbonate rocks. Tectonic clay consists almost entirely of calcite or dolomite and their admixture, depends on mineral composition of parent rocks.

Introduction

Fissures open within the fault zones due to tension and the fissured zones may be washed off or filled up by the deposits of various mechanical sediments, deriving either from the surface or by cave flood material. The fault zones are either opened or closed and their type controls whether there are infiltrated loams or tectonic clays. Tectonic clays are formed by compression of the carbonate rocks (PLACER, 1982). Tectonic clay has the same mineral composition as the rock comprising the fault zone, there could be only a bit more of minerals which are insoluble residues of the carbonate rocks. Mechanical sediments infiltrated into opened fissures may vary in respect to their mineral composition. They are the residues of different rocks weathering. Their mineral composition sometimes indicates their origin but usually it is very difficult because long lasting weathering disintegrates and shades a lot of primary minerals. Only the most resistant minerals to weathering remain such as quartz and heavy minerals. The less resistant minerals are replaced by secondary minerals like clay minerals and chlorites. Which are formed depends upon physical and chemical conditions in the environment. Sometimes within the same fissure minerals of different origin occur. Mixing appears when the water from the surface finds its way along the existing deposit and transports in a new mineral.

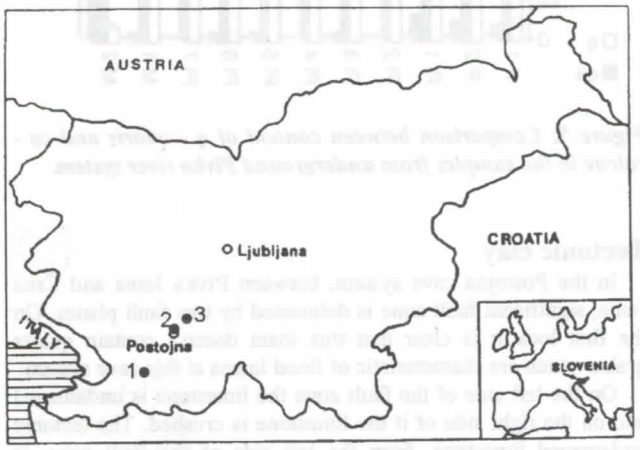

Figure 1: Position of 1 - Divača, 2 - Postojna cave system and 3 - Planina cave.

Infiltrated material is presented by the sample from the old cave near Divača, samples of flood loams, silt and clay size material, are from the same cave. From Postojna cave system and Planina cave flood material was also analysed as was tectonic clay from Postojna cave system (Figure 1).

All the samples were analysed by x - ray diffraction method and some of them in thin section. The quantity of the minerals is given in their respect to the height of the main peak of particular mineral and it is not absolute.

Infiltrated material

By denudation processes and percolating water a lot of different material could be infiltrated through the open fissures into the karst (KOGOVŠEK & ZUPAN, 1992). Mineral composition in that case depends on the composition of rocks from where the weathering remains originated. The mineral composition of red loam infiltrated into the cave below Divaški hrib, from the surface, is different from the mineral composition of flood loams in caves of the area (Figure 2).

Cave below Divaški hrib - red loam

During the construction of the motorway across the Karst the works uncovered an old cave, filled by two different types of clastic sediments (MIHEVC & ZUPAN HAJNA, 1996).

In the upper part of open profile in the cave red loam was seen. The sample consists of quartz 85 %, illite 5 %, gibbsite 4 %, kaolinite 2 %, hematite 2 %, chlorite 1 %, turmaline 1 % and traces of plagioclase. Due to mineral composition and position we know that this material is infiltrated into the cave from surface. The lower part of the profile was different in colour and mineral composition, it is typical mechanical cave sediment.

Legend for all figures

Samples: Postojna cave system: P 1 - Partizanski Rov, P 2 - Sp. Tartarus; Planina cave: Pl 1 - Rudolfov rov, Pl 2 - entrance, Pl 3 - Pivka channel, Pl 4 , Pl 5, Pl 6 - Slepič; Malni spring: M1 - upper, M 2 - lower. D 1, D 2 - cave below Divaški hrib.

Minerals: q - quartz, ca - calcite, il - illite, ka - kaolinite, kl - chlorite, mi - microclin, pl - plagioclase, g - goethite, h - hematite, d - dolomite, mu - muscovite.

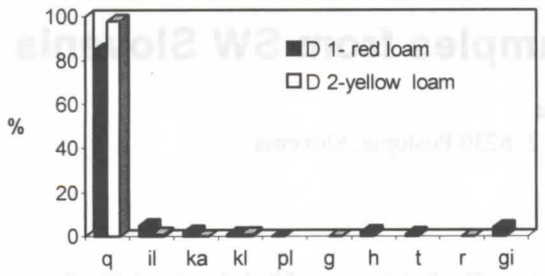

Figure 2: Comparison between mineral composition of infiltrated red loam and flood loam in the cave below Divaški hrib.

Flood loams

The mineral composition of flood loams in the caves depends in their origin. The first case is represented in the cave by allochthonous clastic sediments from the cave below Divaški hrib and in the second case are represented by flood loams and sands from Postojna cave system and Planina cave. In both cases the passages have developed in carbonate rocks but the waters flow from the non-karstic recharge area, where the rivers eroded Eocene flysch rocks and transported them into the caves (ZUPAN HAJNA, 1992).

Cave below Divaški hrib - yellow sand and loam

Cave filled with sediments was developed in Lower Paleocene limestone, according to the Basic geological map, sheet Gorica (BUSER, 1968).

Sample from the yellow part of the open profile consists from quartz 98 %, illite 1 %, chlorite 1 %; and traces of kaolinite, goethite, hornblende. This is the typical mineral composition of the cave sediment which has its origin in Eocene flysch rocks. The way of sediments sedimentation is also typical for the cave environment.

Postojna cave system and Planina cave

The entrance to Postojnska Jama is in the eastern border of Pivka basin; the bottom of the basin consists of Eocene flysch rocks; Postojnska Jama is developed in Upper Cretaceous carbonate rocks, according to the Basic geological map, sheet Postojna (BUSER, GRAD, PLENIČAR, 1967). The Pivka river transports into the cave sediments from the flysch recharge area. The river flows through lower levels of Postojna cave system and disappears in a siphon in Pivka Jama. From there its route is unknown up to Planinska Jama, a resurgence cave in the eastern part of Planinsko Polje, and to spring of Malni.

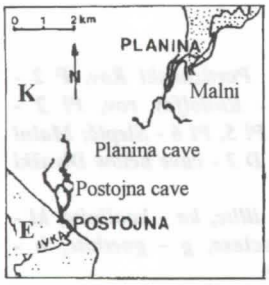

Figure 3:
Position of the Postojna cave system, Planina cave and Malni spring.

Legend
E - flysch
K - limestone, dolomite

The original rock of cave mechanical sediments is Eocene flysch; the Nanoščica river transports the detritus into the Pivka and further into Postojna cave system.

In the Postojna cave system and in Planina cave, Pivka and Rakov channel, the mineral associations are very similar, the quantity only varies a little. In some samples the quantity of carbonate minerals is unusually high, because it is known that the origin of the caves flood loams and sands is from non-carbonate rocks. Calcite can appear like cement but in analysed samples was presented in small grains, silt and clay size. These are small particles of limestone which were eroded from the cave walls.

%	q	ca	il	ka	kl	mi	pl	g	h	d	mu
P 1	86	5		1	1	1	1	1			4
P 2	73	7	3	2	3		3	7			3
Pl 1	40	10			4	12	10	10			14
Pl 2	81			1	4		2	6	1		5
Pl 3	81	2		1	2		9			4	1
Pl 4	81			1	3		9	4			2
Pl 5	78	2		1	2		8	4		3	2
Pl 6	78	2		1	1	4	3	2			9
Pl 7	79			2	3		13				2
M 1	85	2		3	3		3				4
M 2	7	84		1			1	1		4	1

Figure 4: Mineralogical compositions of flood loams and sands from Postojna cave system and Planina cave originated from Eocene flysch rocks, well expressed enrichment by calcite in same samples.

Enrichment on calcite is especially well expressed in cases where the water flows through narrow passages or in siphons where the water has mechanically eroded cave walls. In cases where water flows through big channels no enrichment of carbonate minerals is detected.

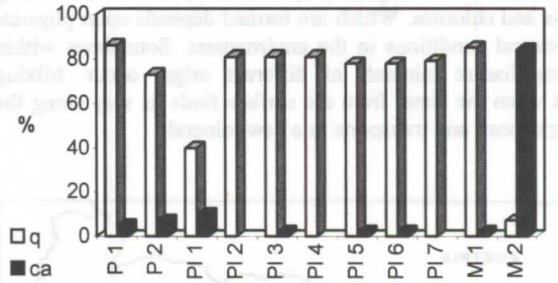

Figure 5: Comparison between content of q - quartz and ca - calcite in the samples from underground Pivka river system.

Tectonic clay

In the Postojna cave system, between Pivka Jama and Črna Jama, significant fault zone is delineated by two fault planes. On the first look it is clear that this loam doesn't contain quartz grains which are characteristic of flood loams at this cave system.

On the left side of the fault zone the limestone is undamaged and on the right side of it the limestone is crushed. The tectonic undamaged limestone, from the left side of the fault zone, is biomicritic with fragments of shells but on the contact of the fault plane a 1 cm thick red belt is presented. This red border is parallel to the main direction of fault plane and all the biomicritic limestone is recrystallized into sparite. The red colour is due to bigger concentration of less soluble iron and clay minerals which are concentrated on this recrystallized border.

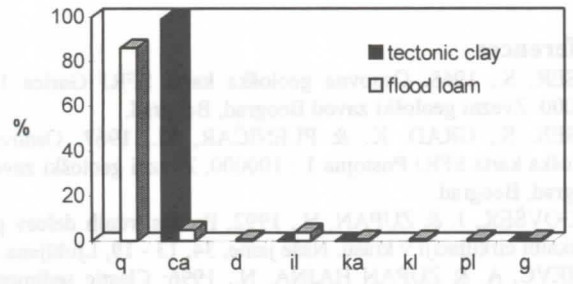

Figure 6: Comparison of the mineral composition of flood loam and tectonic clay from Postojna cave system.

Between both final fault planes is a 1 meter wide fissured zone which is consisted from several vertical laminas, about 1 cm wide. Between particular laminas yellow clay is situated (ZUPAN, 1989). Particular laminae consist of sparitic limestone. The yellow clay between them consists mostly of calcite. Goethite and kaolinite are presented only in traces (Figure 6).

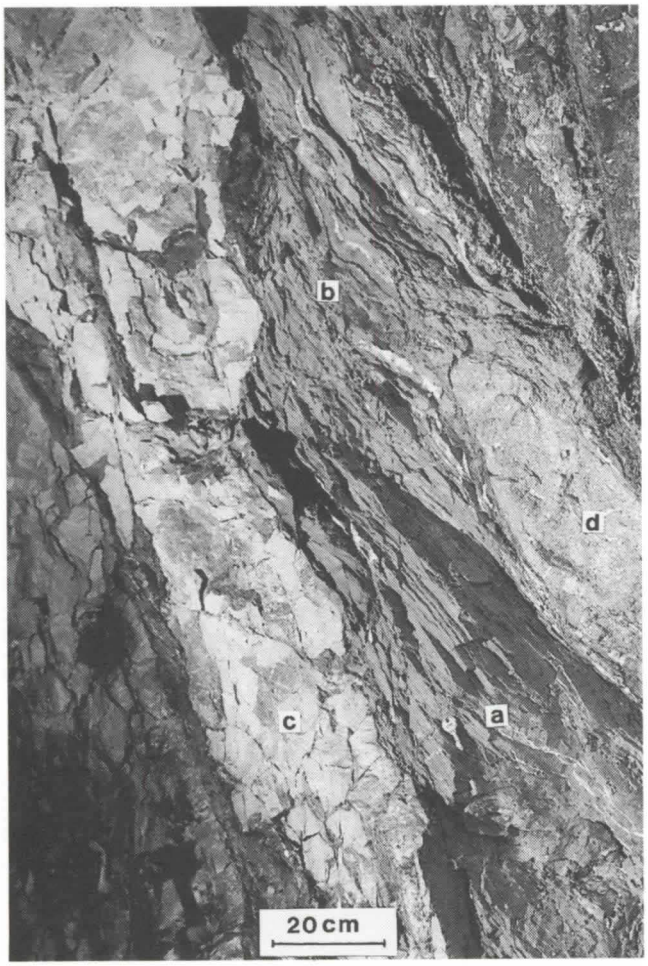

Figure 7: Fault zone from Postojna cave system a. tectonic laminated limestone, b. tectonic clay, c. undamaged limestone, d. tectonic breccia

Close to the fault plane the very porous structure disappears. Sparitic grains collapsed and clay is derived from the solid sparitic limestone, it has the same mineral composition as the limestone.

On the right side of fault zone, close to the main fault plane, where the tectonic sliding planes are seen, a red clay was analysed. By 90 % calcite prevails, there are some kaolinite and goethite, each 4 %, illite and hematite are represented in traces. In the red clay hematite is represented in traces and gives red colour to the clay.

The origin of the hematite is explained such that it is due to the tectonic pressure that squeezed the water out of the goethite and so hematite occurs.

The admixed minerals of the limestone, like illite, kaolinite and goethite, concentrate especially at the tectonic plane, where the carbonate solution is profoundly affected by the pressure.

Conclusion

Three different types of clastic material may be distinguished by their origin. In the caves opened by erosion processes or cut by dolines flood loam and sand originating from flysch sediments can be found. Yellow brown colour is typical of it, but sometimes when the flood sediments are near the surface the colour is changed to red. Due to diagenesis brown goethite is transformed to red hematite, but the association of minerals is different like in red soils from the surface. The mineral composition of red soils on karst can be totally different and depends on their origin. An opinion prevailed for a long time that in our karst in all the fissures and fault zones red loams are either "terra rossa", infiltrated from the surface, or yellow loams having their origin in flysch, transported by water flow. By microscope and x-ray analyses it was shown that this is not always the fact. Frequently within the fault zones tectonic clays are found, originating within the inner fault zone and having almost entirely carbonate structure.

The first type is infiltrated material into the open fissures by denudation processes and percolating water. Mineral composition in that case depends on composition of rocks from where the weathering remains are originated.

The second type is clastic material which was filled into opened fissures during floods, the composition of it corresponds to the rocks composition of underground water flow watershed. Quartz grains are characteristic of flood loams having the origin in non-carbonate rocks because of its properties. Sometimes some significant heavy minerals can be found. In that case the determination the origin is easier and better. But many mechanical sediments are composed of minerals which are the final product of weathering of different rocks but equal in respect to their mineral composition. In such cases their origin can not be determined.

Clastic sediments could be enriched on calcite or dolomite. These are actually small particles of limestone or dolomite from walls of the underground water passages. The content of carbonate minerals in allohtonous material has been presumed to be low but the x-ray analyses and analyses in thin sections have shown that carbonate contents in a lot of samples could increased to high values, from less then 5 % to more then 80 %.

Very high contents of carbonate minerals can be detected in tectonic clays. This third type of clastic material is significant for the inner part of fault zones in carbonate rocks. This is clay size material, formed by tectonic compression of carbonate rocks. Tectonic clay consists almost entirely of calcite or dolomite and their admixture, depends on mineral composition of the parent rocks.

Tectonic clay develops in limestone in such a way that under pressure the limestone recrystallizes. Where sparitic limestone occurs is more porous, especially at the active tectonic plane. Directly at the main tectonic plane a collapse of solid limestone structure appears. On the borders of the grains at first solution

occurs, later sparitic grains collapse and soft, unconsolidated clay occurs. Due to the origin, controlled by tectonic pressures, it is called tectonic clay. This term is not yet entirely clear, as in literature sometimes the expression milonite is used for technical crushed rock.

In tectonic clay not only calcite or dolomite are presented, depending in which carbonate rock the fault zone is developed, but also other minerals, which are admixture in them, may be found. Tectonic clays may be either yellow or red. Goethite gives the yellow colour, red colour is due to hematite in the places where the water had been squeezed out of goethite and it was transformed into hematite. This clay impedes the drainage within the fault zone this is why in such fault zones no karstification was recorded.

All of the described clastic sediments are characteristic for our karst, but their colour is not distinctive for their mineral composition and their origin. The colour of all three types depend on their mineral composition and on physical and chemical conditions in the environment. But the same colour is not necessary the same mineral composition and the knowledge of the mineral composition is not enough to declare the origin of the clastic sediments. Because at the end just the most resistant minerals and also the distinctive secondary minerals, for certain environments, are presented.

References

BUSER, S., 1968. Osnovna geološka karta SFRJ Gorica 1 : 100000. Zvezni geološki zavod Beograd, Beograd.

BUSER, S., GRAD, K. & PLENIČAR, M., 1967. Osnovna geološka karta SFRJ Postojna 1 : 100000. Zvezni geološki zavod Beograd, Beograd.

KOGOVŠEK, J. & ZUPAN, N., 1992. Prenos trdnih delcev pri vertikalni cirkulaciji v krasu. Naše jame, 34, 13 - 19, Ljubljana.

MIHEVC, A. & ZUPAN HAJNA, N., 1996: Clastic sediments from dolines and caves found during the construction of the motorway near Divača, on the classical Karst. Acta carsologica SAZU, 25, , Ljubljana.

PLACER, L.,1982. Tektonski razvoj idrijskega rudišča. Geologija 25/1, 7 - 94, Ljubljana.

ZUPAN, N., 1989. Mineralogija tektonske gline v Pivki jami. Acta carsologica SAZU, 18, 139 - 156, Ljubljana.

ZUPAN HAJNA, N., 1992. Mineralna sestava mehanskih sedimentov iz nekaterih delov slovenskega krasa. Acta carsologica SAZU, 21, 115 - 130, Ljubljana.

Th/U dating of sea level-controlled phreatic speleothems from coastal caves in Mallorca (Western Mediterranean)

by Paola Tuccimei[1], Joaquín Ginés[2], Angel Ginés[3] and Joan J. Fornós[2]

[1] Dip. Scienze Geologiche, Università "Roma Tre", Roma, Italy; [2] Dept. Ciències de la Terra, Univ. Illes Balears, Palma de Mallorca, Spain; [3] Museu Balear de Ciències Naturals, Sóller, Mallorca, Spain.

Abstract

Phreatic speleothems form today at the surface of the brackish pools existing inside littoral caves of Mallorca island (Western Mediterranean). Their occurrence directly identifies the height of the sea level at the time of carbonate deposition, because such pools are physically connected with sea waters. Therefore, ancient phreatic speleothems can be used to reconstruct the Mediterranean's fluctuations during the Pleistocene, since many alignments of these deposits are present in several caves of the studied area.

Some phreatic speleothems have been dated using the Th/U method in order to determine the position of the sea level during the Late Quaternary. Three high sea-stands have been recognized at different heights — between 1.4 and 2.5 meters above current sea level — in caves located in various sectors of the eastern coast of Mallorca. They date back to 83, 108 and 124 ka B.P. and can be related to several minor events within stage 5 of the marine oxygen isotope record.

Differences in height of about 1 meter can be observed in samples corresponding to the same sea paleolevel. Those which are particularly well-documented pertain to substage 5e, with higher elevations towards the northernmost localities. These altimetrical disturbances could be explained in terms of a tectonic tilt of the investigated area, and they can also be inferred from other stratigraphical and geological evidence.

Resumen

Es posible constatar la formación actual de espeleotemas freáticos en la superficie de los lagos salobres de numerosas cuevas costeras en la isla de Mallorca (Mediterráneo occidental). Su presencia registra la altura del nivel marino en el momento de la deposición de estos carbonatos freáticos, habida cuenta de que dichos lagos subterráneos están conectados físicamente con las aguas marinas. Por lo tanto, los depósitos antiguos de espeleotemas freáticos pueden ser utilizados para reconstruir las fluctuaciones del Mediterráneo durante el Pleistoceno, ya que abundantes alineaciones de estos espeleotemas existen en diversas cuevas del área en estudio.

Se han datado algunos espeleotemas freáticos, usando el método Th/U, con la intención de determinar la posición del nivel marino durante el Pleistoceno Superior. Tres estabilizaciones altas del Mediterráneo han sido reconocidas a diferentes alturas — entre 1,4 y 2,5 metros por encima del actual nivel marino — en cuevas localizadas en distintos sectores de la costa oriental de Mallorca. Dichas estabilizaciones se remontan a edades de 83, 108 y 124 ka B.P. pudiendo ser relacionadas con algunos eventos menores dentro del estadio 5 del registro marino de isótopos de oxígeno.

Diferencias de altitud de hasta 1 metro pueden observarse en muestras pertenecientes al mismo paleonivel marino, estando particularmente bien documentadas las correspondientes al subestadio isotópico 5e, el cual presenta altitudes mayores en las localidades más septentrionales. Estas anomalías altimétricas deben ser explicadas en base a un basculamiento tectónico del área investigada, tal como se desprende también a partir de otras evidencias estratigráficas y geológicas.

1. Introduction

Mallorca is a mostly carbonate island of the western Mediterranean basin that shows very interesting coastal karst features in its different natural regions. A lot of karstic littoral caves are developed all around, mainly along the eastern areas of the island. Such cavities have undergone a complex morphological evolution during Pleistocene times and contain deposits that include breccias with paleontological remains, and speleothems. This material is of great speleo-chronological and paleoclimatic interest (GINÉS & GINÉS, 1986; 1995) due to the fact that its deposition was frequently affected by Quaternary sea level oscillations.

This paper deals with a set of chronological information supplied by sea-controlled phreatic speleothems related to Pleistocene marine paleolevels. In this respect, a programme of isotopical studies of these speleothems has been developed over the last three years, including Th/U datings which are

2. Phreatic speleothems in Mallorcan caves

The littoral karstic areas of Mallorca present many caves partially drowned by brackish waters (GINÉS, 1995) as a consequence of post-glacial sea level rising. Partial drowning of such coastal caverns creates subterranean brackish pools that sometimes reach great dimensions. This happens to be a coastal phreatic environment controlled by the sea level, where periodical water oscillations take place adjusted to minor sea level changes like tides.

A great number of different kinds of phreatic speleothems are associated to this singular geochemical environment. Today, the formation of calcite rafts on the surface of these hypogean pools is often found, as well as conspicuous bulky overgrowths developed on the cave walls and also around those stalagmites or stalactites situated in the current fluctuation range of the water-table (POMAR *et al.*, 1979). Phreatic crystallizations of calcite and aragonite located a few meters over the level of present day brackish ponds are common too (GINÉS *et al.*, 1981b); through the bands of speleothems marked by them, former marine levels of stabilization corresponding to glacial-eustatic sea risings are recorded.

Most of the phreatic crystallizations, both the ancient and the

present day ones, overgrow over pre-existent common vadose speleothems and adopt bulky morphologies. Sometimes these carbonate coatings are belt-like forms developed around stalagmites and columns. In many cases, especially when the phreatic overgrowth affect the hanging tip of stalactites, the original speleothem morphology can be greatly modified. Occasionally, some floating calcite rafts are also trapped between the growth layers of these subhorizontal phreatic coatings.

Phreatic speleothems of Mallorcan caves offer a great morphological, textural and mineralogical variety, as was showed in several publications (GINÉS *et al.*, 1981b; POMAR *et al.*, 1976). These authors pointed out the paleoclimatic significance of their mineralogy by relating the presence of aragonite to warmer events which, in beach sediments, results in the appearance of malacological termophile fauna typical of the Eutyrrhenian (Riss - Würm interglacial).

The main interest in such processes of carbonate precipitation is that ancient positive fluctuations of the sea level, corresponding to interglacial periods, have been recorded inside numerous coastal caves by means of strictly horizontal alignments of phreatic speleothems. The formation of this kind of crystalline deposits is related to paleolevels attained by the groundwater table as a result of glacial-eustatic sea oscillations (GINÉS *et al.*, 1981a; POMAR *et al.*, 1987).

In the case of Mallorca, a great number of phreatic crystallization paleolevels have been observed between the current sea level and +40 meters above. In some papers (GINÉS & GINÉS, 1974), the feasibility of altimetrically correlating these deposits with ancient coastlines corresponding to the middle and upper Pleistocene has been considered. These coast-lines have been identified by means of the stratigraphic and paleontological study of the fossil Pleistocene beaches of the island, which are well-known due to the Quaternary research of BUTZER (1975) and CUERDA (1975).

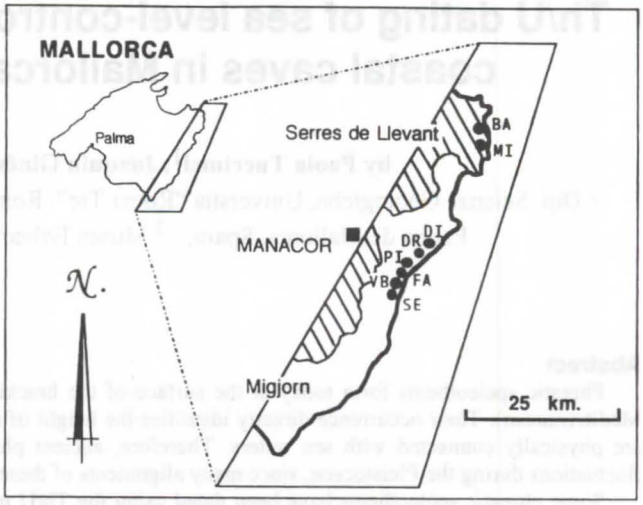

Figure 1: Location map of investigated caves. *BA: Cova de na Barxa; MI: Cova de na Mitjana; both in Capdepera municipality.*
DI: Cova del Dimoni; DR: Coves del Drac; PI: Coves del Pirata; FA: Cova de Cala Falcó; VB: Cova de Cala Varques B; SE: Cova des Serral; all of them in Manacor municipality.

On the basis of the above mentioned background, GINÉS & GINÉS (1974) formerly suggested that the phreatic crystallizations

locality	*sample*	*height a.s.l. (m)*	U (ppb)	$^{234}U/^{238}U$	$^{234}U/^{238}U_0$	$^{230}Th/^{232}Th$	$^{230}Th/^{234}U$	Age (ka)
Cv. C. Varques B	VB-D1 #	+1.4	228 ± 10	2.113 ± 0.099	2.41 ± 0.13	inf.	0.567 ± 0.025	83.4 ± 5.1
Cv. de Cala Falcó	FA-D2a #	+1.9	542 ± 5	1.378 ± 0.003	—	12.3 ± 0.2	—	—
	FA-D2b #	+1.9	651 ± 4	—	1.528 ± 0.037	—	0.554 ± 0.023	83.9 ± 5.0
Cova des Serral	SE-D2a #	+1.5	174 ± 1	1.466 ± 0.002	1.656 ± 0.011	137 ± 2	—	—
	SE-D2b *	+ 1.5	200 ± 4	1.453 ± 0.032	1.639 ± 0.046	240 ± 45	0.705 ± 0.019	121.3 ± 5.6
Coves del Pirata	PI-D1 *	+2.1	262 ± 9	1.663 ± 0.062	1.959 ± 0.092	inf.	0.745 ± 0.035	130.4 ± 14.0
Cova del Dimoni	DI-D1 *	+2.5	1273 ± 48	1.090 ± 0.018	1.126 ± 0.025	inf.	0.676 ± 0.032	119.7 ± 10.0
	DI-D2 *	+2.5	2640 ± 77	1.185 ± 0.013	1.255 ± 0.018	257.3 ± 25.4	0.660 ± 0.020	112.9 ± 5.8
	DI-D3 *	+2.5	1887 ± 45	1.108 ± 0.015	1.147 ± 0.020	inf.	0.638 ± 0.020	107.9 ± 5.7
Cova de na Barxa	BA-D3a *	+2.4	582 ± 22	1.095 ± 0.036	1.164 ± 0.063	16.9 ± 1.9	0.847 ± 0.045	<193.0 ± 33 §
	BA-D3b *	+2.4	423 ± 19	1.430 ± 0.070	1.612 ± 0.103	inf.	0.715 ± 0.045	124.7 ± 14.0
Cv. de na Mitjana	MI-D1a *	+3.9	128 ± 9	0.791 ± 0.067	—	inf.	1.340 ± 0.112	—
	MI-D1b *	+3.9	52 ± 6	2.091 ± 0.257	—	inf.	10.403 ± 1.098	—
	MI-D2 *	+4.9	146 ± 4	1.057 ± 0.019	1.110 ± 0.037	46.85 ± 5.29	0.894 ± 0.024	231.9 ± 28
	MI-D3 *	+5.8	169 ± 1	0.972 ± 0.028	0.937 ± 0.035	51	0.972 ± 0.035	> 300.7
Coves del Drac	DR-D4 *	+3.3	2888 ± 84	1.039 ± 0.016	—	inf.	1.038 ± 0.040	> 350

\# mass spectrometry * alpha counting
§ $^{230}Th/^{232}Th$ activity ratio is < 20, thus the true age is lower than the measured age (193 ka)

Table I: Data on localities and obtained samples, as well as analytical results of the dating programme.

situated 30 meters above the present sea level should go back at least to the Mindel - Riss interglacial. In 1981 a preliminary isotopical dating programme on Mallorcan phreatic speleothems was started. The analyses were carried out using the Uranium series method, and confirmed the previously stablished chronological model, with regard to altimetric correlations between phreatic speleothems and Pleistocene beach deposits. The results of this absolute dating programme yield ages that range from 3.9 ka (clearly post-glacial crystallizations) to above 350 ka, reaching the limits of this method (HENNIG *et al.*, 1981; GINÉS & GINÉS, 1989, 1993a, 1993b). The sampled phreatic crystallizations younger than 250 ka show good correlation with the climatic events that involve a sea level similar or higher than the present-day one (stages 1, 5 and 7, which correspond to warm pulsations); the samples that reveal ages above 300 ka (paleolevels higher than 30 meters a.s.l.) have to be assigned at least to the stages 9 or 11 of the marine oxygen isotope record established by SHACKELTON & OPDYKE (1973).

3. Sampled localities

Eight caves (Figure 1) were investigated in order to collect phreatic speleothems pertaining to several high sea-paleolevels. Most of these caves are developed on the post-orogenic upper Miocene calcarenites from the Migjorn platform area of Mallorca, whereas only two among the studied caves — Cova de na Barxa and Cova de na Mirjana — are located in folded Jurassic limestones that mainly integrate the Serres de Llevant mountain range.

Samples were obtained from phreatic speleothems that record several marine high-standings ranging from 1.4 to 5.8 meters above current sea level, with most situated between 1.4 and 2.5 meters a.s.l. Data about cave's names, samples obtained, and heights of paleo sea-levels represented in each locality are gathered in Table I.

In spite of the fact that detailed mineralogical and textural studies of the dated samples are still lacking, calcite seems the main constituent of these speleothems; however, some of them are aragonitic, like samples from Cova del Dimoni that are a spectacular phreatic coating of aragonite needles.

Altimetrical information on Pleistocenic beach deposits in Mallorca (BUTZER, 1975; CUERDA, 1975) suggest that marine paleolevels recorded by the analyzed speleothems must belong to upper and middle Pleistocene high-standings, fitting presumably in the range of applicability of Th/U dating method. In this context, the present dating programme of Mallorcan phreatic speleothems has been carried out in order to attain chronological information on the studied caves, as well as more precision on the late Pleistocenic sea level history of the Mediterranean.

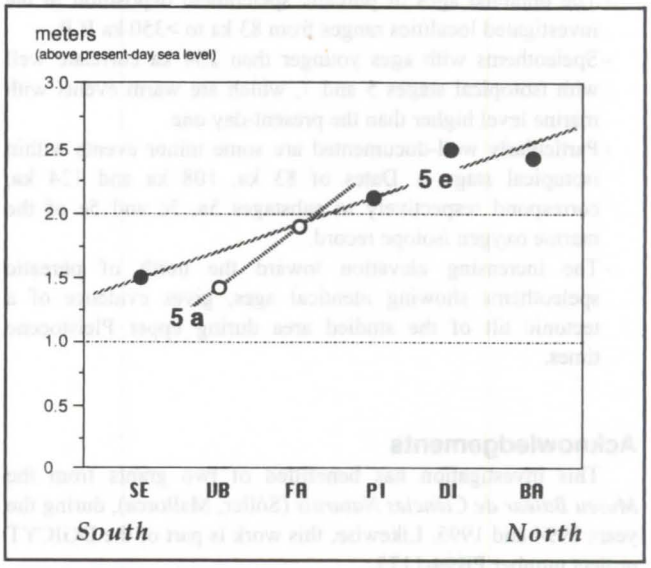

Figure 3: Increasing elevation toward the north of dated phreatic speleothems pertaining to several substages of the last interglacial event.

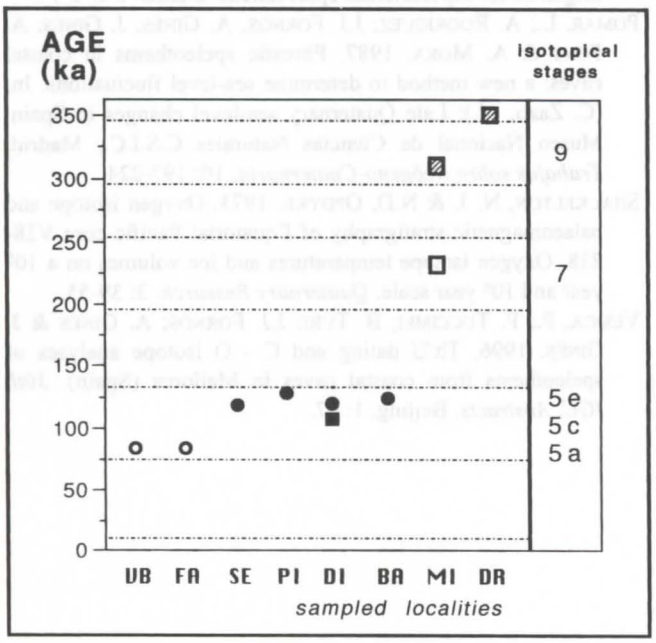

Figure 2: Th/U ages of phreatic speleothems studied in this dating programme. Caves are plotted in the same order as in Table I.

4. Dating results

Absolute dating of collected samples were performed by means of Uranium series methods (VESICA *et al.*, 1996); results are compiled in Table I. Calculated ages range from 83 ka to >350 ka, showing good agreement with stages 5 and 7 of the oxygen isotope record that correspond with events of high sea level (Figure 2). A sample from Coves del Drac, which age exceeds the dating limits of the method, must pertain at least to climatic stage 9.

Particularly well-represented are high-standings at ages of 83 ka, 108 ka and 124 ka B.P., dates that correlate quite well with the ages usually asigned to substages 5a, 5c and 5e of marine isotope record (SHACKELTON & OPDYKE, 1973). These data document three main Mediterranean sea level stabilizations at heights between 1.4 and 2.5 meters a.s.l. corresponding to the last interglacial event. Our data are also in agreement with the ages of the marine terraces from Campo de Tiro, in the Bay of Palma de Mallorca, recently dated by U-series methods (HILLAIRE-MARCEL *et al.*, 1996). These units yielded ages of 135 and 117 ka, and can be altimetrically correlated with our phreatic crystallizations paleolevels, since the oldest beach deposit culminates at +3 meters a.s.l.

The fact that the same paleolevel becomes recorded in diverse localities at different heights above current marine level, is evidence of a tectonic tilt of the investigated area. In this sense,

phreatic speleothem paleolevels belonging to stages 5a, 5c and 5e are recorded at higher elevations in northernmost localities (Figure 3).

Data brought forward by the present dating programme confirm a previously established geomorphological assumption that correlates phreatic speleothems of coastal Mallorcan caves with sea level high-standings related to interglacial events. Specially interesting are phreatic speleothems in order to contribute to the knowledge of Mediterranean sea level history during upper and middle Pleistocene times.

5. Conclusions

Results of these investigations on speleochronology of coastal caves in Mallorca island can be summarised as follows:

- The obtained ages of phreatic speleothem deposition in the investigated localities ranges from 83 ka to >350 ka B.P.
- Speleothems with ages younger than 250 ka correlate well with isotopical stages 5 and 7, which are warm events with marine level higher than the present-day one.
- Particularly well-documented are some minor events within isotopical stage 5. Dates of 83 ka, 108 ka and 124 ka, correspond respectively to substages 5a, 5c and 5e of the marine oxygen isotope record.
- The increasing elevation toward the north of phreatic speleothems showing identical ages, gives evidence of a tectonic tilt of the studied area during upper Pleistocene times.

Acknowledgements

This investigation has benefitted of two grants from the *Museu Balear de Ciències Naturals* (Sóller, Mallorca), during the years 1994 and 1995. Likewise, this work is part of the DGICYT project number PB94-1175.

References

BUTZER, K. W. 1975. Pleistocene littoral-sedimentary cycles of the Mediterranean basin: a Mallorquin view. In: (K.W. Butzer & G.L. Isaac, eds.): *After the Australopithecines: stratigraphy, ecology and culture change in the Middle Pleistocene*. Chicago: 25-71.

CUERDA, J. 1975. Los tiempos cuaternarios en Baleares. Instituto de Estudios Baleáricos, Palma de Mallorca, 304 p.

GINÉS, A. & J. GINÉS. 1974. Consideraciones sobre los mecanismos de fosilización de la Cova de sa Bassa Blanca y su paralelismo con formaciones marinas del Cuaternario. *Boll. Soc. Hist. Nat. Balears.* 19: 11-28.

GINÉS, A. & J. GINÉS. 1986. On the interest of speleochronological studies in karstified islands. The case of Mallorca (Spain). *Com. 9º Cong. Int. Espeleol.*, Barcelona, 1: 297-300.

GINÉS, A. & J. GINÉS. 1989. Absolute dating of phreatic speleothems from coastal caves of Mallorca (Spain). *Proc. 10th Int. Congress Speleol.*, Budapest, 1: 191-193.

GINÉS, A.; J. GINÉS & L. POMAR. 1981a. Phreatic speleothems in coastal caves of Majorca (Spain) as indicators of Mediterranean Pleistocene paleolevels. *Proc. 8th Int. Congress Speleol.*, Bowling Green, 2: 533-536.

GINÉS, J. 1995. L'endocarst de Mallorca: els mecanismes espeleogenètics / Mallorca's endokarst: the speleogenetic mechanisms. In: (A. Ginés & J. Ginés, eds.): El carst i les coves de Mallorca / Karst and caves in Mallorca. *Endins*. 20 / *Mon. Soc. Hist. Nat. Balears*. 3: 71-86.

GINÉS, J. & A. GINÉS. 1993a. Speleochronological approach to some coastal caves from "Cap Vermell" area in Mallorca island (Spain). *Proc. XI Int. Congress Speleol.*, Beijing, 56-59.

GINÉS, J. & A. GINÉS. 1993b. Dataciones isotópicas de espeleotemas freáticos recolectados en cuevas costeras de Mallorca (España). *Endins*. 19: 9-15.

GINÉS, J. & A. GINÉS. 1995. Aspectes espeleocronològics del carst de Mallorca / Speleochronological aspects of karst in Mallorca. In: (A. Ginés & J. Ginés, eds.): El carst i les coves de Mallorca / Karst and caves in Mallorca. *Endins*. 20 / *Mon. Soc. Hist. Nat. Balears*. 3: 99-112.

GINÉS, J.; GINÉS, A. & POMAR, L. 1981b. Morphological and mineralogical features of phreatic speleothems occurring in coastal caves of Majorca (Spain). *Proc. 8th Int. Congress Speleol.*, Bowling Green, 2: 529-532.

HENNIG, G. J.; A. GINÉS; J. GINÉS & L. POMAR. 1981. Avance de los resultados obtenidos mediante datación isotópica de algunos espeleotemas subacuáticos mallorquines. *Endins*. 8: 91-93.

HILLAIRE-MARCEL, C.; C. GARIÉPY; B. GHALEB; J.L. GOY; C. ZAZO & J. CUERDA. 1996. U-series measurements in Tyrrhenian deposits from Mallorca - Further evidence for two last-interglacial high sea levels in the Balearic islands. *Quaternary Science Reviews*, 15: 53-62.

POMAR, L.; A. GINÉS & R. FONTARNAU. 1976. Las cristalizaciones freáticas. *Endins*. 3: 3-25.

POMAR, L.; A. GINÉS & J. GINÉS. 1979. Morfología, estructura y origen de los espeleotemas epiacuáticos. *Endins*. 5-6: 3-17.

POMAR, L.; A. RODRÍGUEZ; J.J. FORNÓS; A. GINÉS; J. GINÉS; A. FONT & A. MORA. 1987. Phreatic speleothems in coastal caves: a new method to determine sea-level fluctuations. In: (C. Zazo, ed.): Late Quaternary sea-level changes in Spain. Museo Nacional de Ciencias Naturales C.S.I.C., Madrid, *Trabajos sobre Neógeno-Cuaternario*, 10: 197-224.

SHACKELTON, N. J. & N.D. OPDYKE. 1973. Oxygen isotope and palaeomagnetic stratigraphy of Equatorial Pacific core V28-238: Oxygen isotope temperatures and ice volumes on a 10^5 year and 10^6 year scale. *Quaternary Research*. 3: 39-55.

VESICA, P.; P. TUCCIMEI; B. TURI; J.J. FORNÓS; A. GINÉS & J. GINÉS. 1996. Th/U dating and C - O isotope analyses of speleothems from coastal caves in Mallorca (Spain). *30th IGC, Abstracts*, Beijing, 1: 87.

Speleothems dating using the thermoluminescence method

V. Labau, E. Gaspar, T. Paunica
Institute of Physics and Nuclear Engineering, Bucharest, Romania

Abstract

The thermoluminescence method was used to determine the age of a stalagmite from Wind Cave, Padurea Craiului Mountains. When certain crystallized inorganic substances are exposed to ionizing radiations and then warmed until a certain temperature characteristic of each material , they emit a luminous radiation. In order to establish the geological age, the natural thermoluminescence of the calcite and the natural dose accumulated during geological time were measured. It was necessary also to determine the yearly dose due to the radiation emitted by the natural radioactive elements (U, Th, K) present in very small quantities in speleothems. The accumulated natural dose was of 55 934 Gy. The samples was warmed at 450° C. For the artificial irradiation of the calcite samples, a beta radiation source from ^{90}Sr - ^{90}Y was used. The age of the stalagmite was 59,052 ± 9,600 years.

1. Introduction

The thermoluminescence (TL) method is based on the thermoluminescence phenomenon which consists in the fact that certain crystallized inorganic substances, when they are exposed to ionizing radiation and then warmed until a certain temperature characteristic of each material, they emit a luminous radiation.

The intensity of the emitted light is proportional to the radiation dose on which the substance has been exposed.

The establishing of the age in geology by the TL method is based on the fact that the geological materials contain certain minerals which have thermoluminescent properties and may be used as an integrator dosimeter. Such a mineral is also the calcite which is the main constituent of the stalactites and stalagmites.

The event which is dated by the TL method is the moment of the crystallization of calcium carbonate. From that moment the material is exposed to the radiation emitted by the natural radioactive elements (U, Th, K) which are found in the matrix. In the course of a year, because of the integrated character in the material is accumulated the dose (d) named the yearly dose. During the geological time, T, is accumulated the dose Dn = d × T which represents the accumulated natural dose.

From this relation of accumulation of the natural dose one can determine the geological age (T) as follows:

$$T = \frac{Dn}{d} \qquad (1)$$

The age of a stalagmite fragment collected from Wind Cave Romania, was determined using the TL method.

2. The calcite thermoluminescence

In order to establish the geological age, it is necessary to measure the natural thermoluminescence (NTL). For this determination, we have used a the thermoluminescence curve. The TL curve represents the temperature variations of the luminous flux emitted by the matrix progressively warmed from the environmental temperature until a maximum pre-established temperature (~ 450°C).

Figure 1 presents the natural thermoluminescence (NTL) and artificial thermoluminescence (ATL) curves obtained for the studied stalagmite. The NTL curve is due to the calcite irradiation by the natural elements (U, Th, K) contained in very small quantities in the stalagmite. The NTL curve presents a lonely peak situated at a temperature of about 320°C.

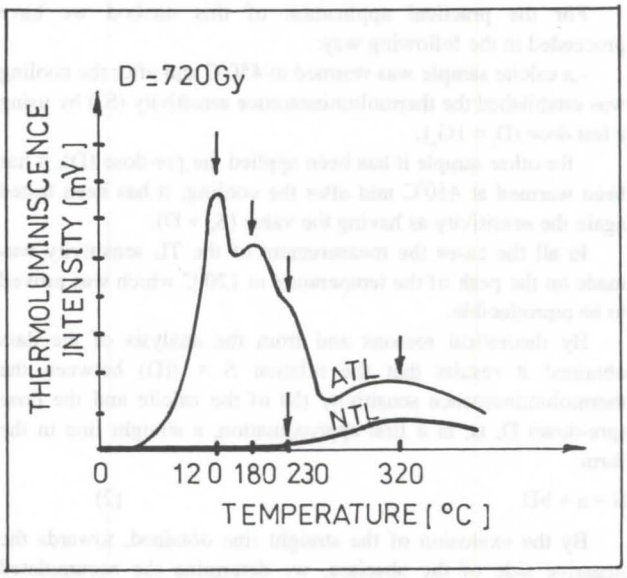

Figure 1: Natural and artificial termoluminescence curves for the studied stalagmite

The artificial thermoluminescence curve (ATL) may be obtained by artificial irradiation using a beta or gamma radiation source. The ATL curve presents peaks in evidence at the temperatures of 120° C , 180° C and 320° C . It also presents a peak at the temperature of 230° C but less in evidence. The peak from the temperature of 120°C is unstable and disappears comparatively soon, when the irradiated sample is stored a long time at the room temperature. During geological time, because of the thermic agitation, the peaks from the middle temperature (180°C and 230°C) present a decline (fading) which may lead to their disappearance.

For these reasons, the peaks from the low temperatures (120°C) and middle ones (180° and 230°C) don't appear in the natural thermoluminescence curve (NTL) . By irradiation with ionizing radiation , the thermoluminescence sensitivity of the peaks from the low and middle temperatures increases. This is due to the supplimentary flaws caused by the irradiation of the calcite (ZELLER, 1968).

3. The determination of the natural accumulated dose

In order to determine geological age it is necessary to establish the natural dose (Dn), accumulated during the geological time, T. The Dn dose is established by the measurement of the NTL and the dose conversion. For this purpose it would be normal to use the peak from the high temperature (320°C). But this maxima although being stable, cannot be used at the measurement of the thermoluminescence in dosimetric purposes because its intensity depends not only on the absorbed radiation dose but also on other uncontrollable factors.

In order to establish the Dn dose we used a method based on the combined action of the pre-irradiation (pre-dose) and warming (at 450°C) on the thermoluminescence at low and middle temperatures of the calcite.

For the stalagmite we have studied, the effect was an increasing of the thermoluminescence sensitivity at low and middle temperatures, proportional to the dose (pre-dose).

For the practical application of this method we have proceeded in the following way:

- a calcite sample was warmed at 450°C and after the cooling was established the thermoluminescence sensitivity (S_N) by using a test dose ($D_t = 1G_y$);
- for other sample it has been applied the pre-dose (D), it has been warmed at 450°C and after the cooling, it has been tested again the sensitivity as having the value ($S_N + D$).

In all the cases the measurement of the TL sensitivity was made on the peak of the temperature at 120°C which was proved to be reproducible.

By theoretical reasons and from the analysis of the data obtained it results that the relation S = f(D) between the thermoluminescence sensitivity (S) of the calcite and the dose (pre-dose) D, is, in a first approximation, a straight line in the form:

$$S = a + bD \qquad (2)$$

By the extension of the straight line obtained, towards the negative side of the abscissa, we determine the accumulated natural dose, Dn (fig. 2).

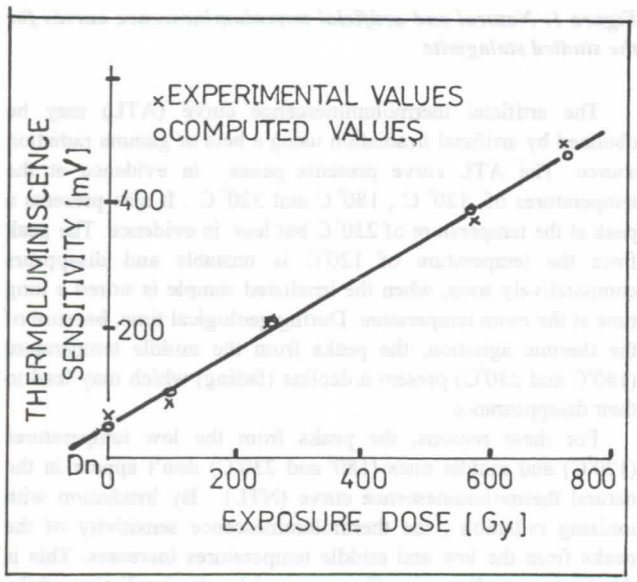

Figure 2: The thermoluminescence sensitivity versus the dose

4. The determination of the yearly dose

As it results from the relation (1) in order to establish the age it is also necessary to determine the yearly dose (d) due to the radiation emitted by natural radioactive elements (U, Th, K) present in very small quantities in speleothems.

The yearly dose of the stalagmite was determined indirectly from the natural radioactive elements content using a conversion table concentration - dose. (AITKEN & all, 1968)

The radioactive natural elements content was established using the neutron activation analysis method. Thus, the radioactive elements content was: U = 0.3 ppm; Th = 0.0 ppm and K = 0.01 %. From the conversion of this radioactive content, the yearly dose resulted:

$$d = 94.72 \times 10^{-5} \text{ Gy/y.} \qquad (3)$$

5. The experiment

For the thermoluminescence measurement the stalagmite fragment was transformed by crushing, grinding and sieving in a microcrystalline powder. The diameter of the microcrystals used in this experiment varried between 80 and 160 μm.

For natural (NTL) and artificial (ATL) thermoluminescence measurements, the same quantity of microcrystaline power was used. The dosimetrical information was put in evidence at the TL using a conventional apparatus for detector TL measurements, type Mark IV TLD Reader.

The thermoluminescence curve was determined by using a X-Y recorder. As a measure of the TL intensity one can take the peak height from 120°C temperature. For the artificial irradiation of the calcite samples, a beta radiation source from ^{90}Sr - ^{90}Y was used. TL curve was recorded after calcite samples irradiation, directly.

For the determination of the accumulated natural dose (Dn) we have used the "predose" method described above. As a measure of the TL sensitivity we used the heigth of the peak from 120°C obtained after calcite irradiation at a dose test of 1 Gy. The samples warming at 450°C was made with the same Mark IV apparatus. The samples warming was repeated 4 times in order to eliminate the residual TL influence on calcite sensitivity.

6. Experimental results

In order to establish the growth of the calcite TL sensitivity depending on the dose (predose), separately calcite samples were irradiated at growing doses. The irradiation doses used (D) and the TL sensitiviy resulting are presented in table no. 1. The irradiation dose (D) is expressed in Gy and the thermoluminescence sensitivity (S) in mV

D (Gy)	S (mV)
0	45
105	90
270	210
570	380
720	500

Table 1: Irradiation doses and thermoluminescence sensitivity

The thermoluminescence sensitivity versus the dose (predose) D is presented in fig.2.

From these data one can see that the relation S = f(D) between the calcite thermoluminescence sensitivity and the dose (predose) is a straight line.

The calculation of this straight line is given by the relation:

$$S = 35.233 + 0.6299\ D \qquad (4)$$

The accumulated natural dose is obtained extending the straight line until the X axis, where S = 0:

$$Dn = 55\ 934\ Gy \qquad (5)$$

The geological age of the studied speleotheme was determined using the natural accumulated dose established as above and the yearly dose. From these data it results the age of the stalagmite: 59,052 ± 9,600 years.

References

AITKEN, M. J., ZIMMERMAN, D. W. & FLEMING, S. J. 1968. Thermoluminescent dating of Ancient Pottery. *Nature.* 219: 442-445.

ZELLER, E. J. 1968. Geologic Age Determination by Thermoluminescence. In: (D. J. Mc Dougall): Thermoluminescence of Geological Materials. Academic Press, London & New York, 311 p.

U series dating of phases of speleothem deposition and erosion in Baradla Cave, Aggtelek National Park, Hungary

Derek Ford, Department of Geography
McMaster University, Hamilton, ON, Canada L8S 4K1
Laszlo Zambo, Department of Geography
Eotvos Lorand University, Budapest 1024, Hungary

The Domica-Baradla System

The cave system of Domica (in Slovakia) and Aggtelek-Baradla (in Hungary) is comprised principally of a large, low gradient, river passage. The rocks is densely fractured limestone and dolomitic limestones of Perno-Triassic age that became kartisfied hills in the late Cretaceous and early Tertiary and were then partially buried by clastic sediments. During exhumation a stable watertable was established in the karst; the river passage formed along it, fed by tributary streams collecting on surviving clastics to west. In its downstream section (Baradla Cave) the stream flow for most of the hydrologic year is now captured to younger passages at a lower elevation but there is still significant flooding occasion. The passage is well decorated with speleothem including (i) large columns and bosses actively growing in recesses sheltered from modern floods; (ii) large to very large columns that were toppled, broken and eroded by ancient floods in the bedrock channel; (iii) think flowstones and small stalagmites on bedrock and detrital terraces, and (iv) small stalagmites growing at the edges of the modern bedrock channel.

U series dating

Twelve small calcite samples were taken from points in toppled or broken speleothems between 0 and 3 m above the modern channel. They have been dated by the $^{230}Th/^{234}U$ method, using alpha spectrometry. The uranium content is very low (0.04-0.1 ppm). This is typical where the speleothem feedwaters are derived only from pure limestones (as at Baradla), rather than from limestones with shales or shaly interbeds; it makes accurate dating difficult. In addition, the speleothems contain much detrital thorium from the floodwaters, as indicated by $^{230}Th/^{232}Th$ ratios generally < 10; as a consequence it is not possible to determine precisely how much ^{230}Th has been created by decay of ^{234}U since deposition. Despite these difficulties twenty uncorrected $^{230}Th/^{234}U$ ages display a clear pattern of successive growth periods that correlates well with the published records of periodicity for a set of 500 dates from speleothems in NW Europe.

Conclusions

Our conclusions are (1) little or no speleothem in the Baradla river passage is older than the Last Interglacial (Isotope Stage 5, Riss-Würm); (2) most rapid and abundant growth occurred during the Last Interglacial and the Holocene. There were few floods during the Last Interglacial. This permitted large speleothems to grow in the channel. The Holocene deposits are comparatively small in volume except where they are overgrowths onto the Last Interglacial bosses and columns; (e) during the Lower Würm stadials and interstadials (isotope Stages 4 and 3) the passage was aggraded by river-laid pebbles, sands and clays, forming terraces. There was calciate deposition, at diminished rates, on the terraces and on columns and bosses standing in the channel. (4) There was little or no speleothem deposition during the main Würm cold stage (isotope stage 2). (4) The passage was swept by major floods that removed most clastic terrace deposits and toppled the large speleothem columns and bosses. This flood period probably correlates with the cold climate of the main Würm but could be a consequence of primary forest removal by early human settlers.

Uranium-Series Dating of Speleothems from Amaterska and Holstejnska Caves, Moravian Karst, Czech Republic

Helena Hercman[1], Stein-Erik Lauritzen[2], Jerzy Glazek[3], Jan Vit[4]
[1] Institute of Geological Sciences, Polish Academy of Sciences,
ul.Zwirki i Wigury 93, 02-089 Warszawa, Poland
[2] Department of Geology, Bergen University,
Allegaten 41, N-5007 Bergen, Norway
[3] Institute of Geology, Adam Mickiewicz University,
ul. Makow Polnych 16, Poznan, Poland
[4] Czech Geological Survey, Klárov 3, 118 21 Praha 1, Czech Republic

Abstract

Speleothems were sampled from Holstynska and Amaterska caves, The Moravian Karst, for Uranium-series dating and stratigraphic analysis. Dates spanning from present-day (i.e. actively growing speleothems) to beyond the limit of the method (350 ka, α-particle counting) have been identified. In all, 4 phases of clastic sedimentation, interrupted by massive speleothem deposition was found in the paleoponor cave, Holsteijnska cave.

1. Introduction

The Moravian Karst is located north of Brno, in the Czech Republic. Geologically, it belongs to the Bohemian Massif, geomorphologically to the Western part of Drohawska Upland. Well developed karst features are widespread in the Devonian limestones. The classical karst forms are concentrated within an area of about 100 km^2. The most abundant karst formations can be found in the northern part of the Moravian Karst between the karst canyons of Suchy and Pusty Zleb.

2. Holsteijnska Cave

This part of the Moravian Karst contains the Holstejnska paleoponor Cave, which was discovered in 1966. The cave was almost completly choked with sediments, and all the presently known galleries (600 m) have been excavated by members of the local caving society. The cave passage itself consists of a very wide trunk passage with an almost totally flat roof. Walls and ceiling are only sporadically exposed along the excavated galleries. The passage cross-section suggests that the profile is in part developed as a classical water-table cave passage, possibly by paragenesis. Stratigraphic sections of the infilling sediments are well exposed on the walls of the artificial galleries. We have identified 3 sequences of sediments (I, II and III). The oldest consists of strongly weathered gravels. This gravel deposit probably filled the passage completely, but was eroded at a later stage. The second sequence consists of red coloured silt and gravel. The youngest, uppermost deposit consists almost entirely of silt. The three sequences are separated by speleothem. These speleothem layers consists of broken flowstones blocks, sometimes overturned. Twenty-eight subsamples were collected from the galleries in Holstejnska Cave and were dated with the U-Series method (Fig. 2). Three periods of speleothem deposition may be recognized from the data (Table 1)

3. Amaterska Cave

Amaterska Cave is one of the most famous caves in Moravian Karst. It is a horizontal river cave, several kilometers long, and is a part of the underground course of the Punkva river. Eleven speleothem samples were dated with the U-Series method. We can distinguish 4 periods of speleothems deposition (Table 1). The results are compiled in Figure 1.

4. Discussion

Based on the dating results we may suggest a time scale for the development of the Holstejnska and Amaterska Caves (Fig. 2). The speleogenetic history of the Holstejnska Cave began more than 350 ka ago. After development of the main passage, there was a first episode of clastic sedimentation. The passage was most probably completely filled with fluvial gravels and sands. Later, these sediments were partially eroded. Into the empty space, before 350 ka ago, the first recognizable speleothem deposition began. Erosion episodes probably occurred in between speleothem deposition. After deposition of phase 2H (speleothems), the strongest erosional and depositional cycle occurred. Most of the sediments and speleothems which filled the cave passage were destroyed and redeposited. Then, the youngest speleothem deposition (lH) started. Quite recently, yet another depositional phase occurred, when a layer of gray silt covered

Table 1: Speleothem growth zones, based on U-series dating of flowstones and stalagmites in Holstejnska (H) and Amaterska (A) caves

Period	Time Range, ka	Comments	Marine Isotope Stage
1H	9-16		1 & 2
2H	100-145		2
3H	150-300	Possibly 2 phases of growth	7 and/or interstadials of 8
4H	> 350		9 or older
1A	0-10		1
2A	45-80		interstadials in 3 & 4, und 5a?
3A	90-140		5
4A	180-200		7

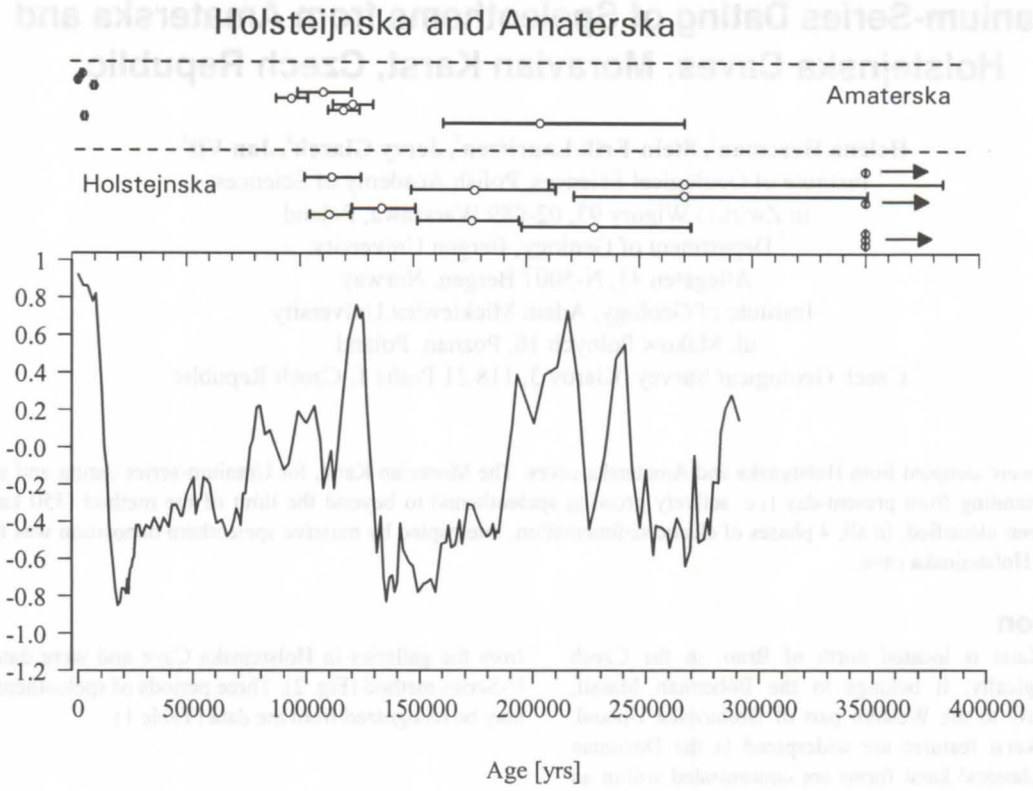

Fig. 1: Comparison between the U-series dating results from Amaterska and Holstejnska caves with the marine oxygen isotope stages. Arrows indicate infinite ages, with lower error limit (1 σ) shown. All error bars are 1 σ.

Holocene speleothems (Fig. 3).

The maximum age of speleothems so far found in Amaterska cave is 250-300 ka (Fig. 2). After a phase of large rockfalls, the first recognizable phase of speleothem deposition began (4A). These speleothems cement the breakdown blocks together. The next phase of speleothem deposition occured at 140-90 ka (3A) after a period of sand sedimentation. This was the main phase of speleothem deposition, and correspond to the last interglacial. The massive flowstones from this phase are 0.5-2 m thick. A period of erosion, followed by deposition of sands and gravels occured after this. The underground river (Punkva) reached its present level by cutting through about 4 m of older sediments. Then, the youngest speleothem deposition started (1A). At this time, speleothem deposition was rapid. Columnar stalagmites which are more than 3m tall have grown on top of the older sediments. Chronologically, they cover all of the Holocene. At the beginning the growth rate was ca. 240 mm/ka, but after about 5 ka it increased to 750 mm/ka.

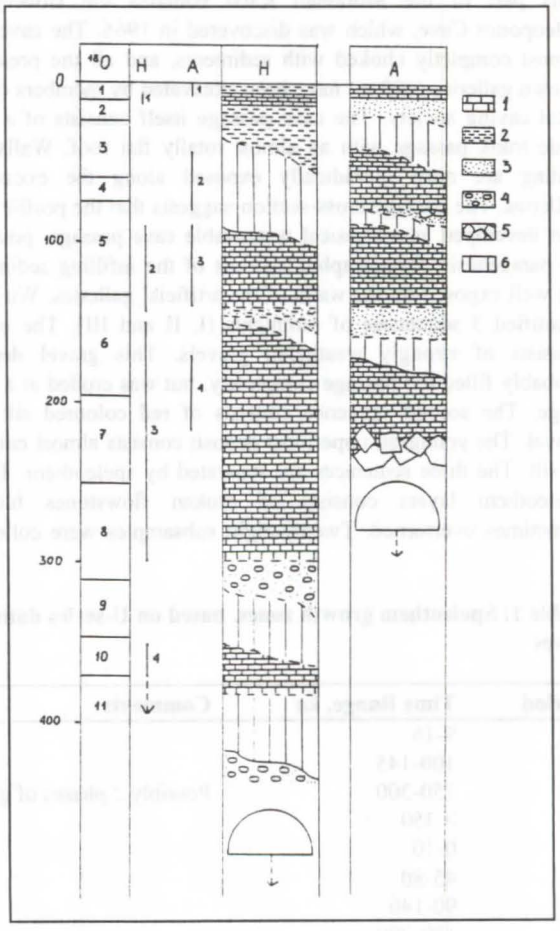

Fig. 2: Development of Holstejnska (H) and Amaterska (A) caves during the last ³350 ka. First column: Oxygen Isotope stages. Second Column: Growth range of speleothems. Legend: 1) Flowstone/stalagmite deposition, 2) Clay/silt, 3) Sand, 4) Gravel, 5) Breakdown, 6) Hiatus. Semicircle symbol: Placement of passage formation (speleogenesis sensu stricto).

Conclusions

The two caves of the Moravian karst that we have investigated, display proliferent speleothem deposits that are suitable for Uranium-series dating. The samples are also suitable for stable isotope work, as Holocene stalagmites may grow up to more than 3m in height, corresponding to an average growth rate of 0.3 mm/year. maximum speleothem ages go beyond the limit of the dating method (> 350 ka by a-particle counting). Further work will focus on attaining higher time-resolution (TIMS-dating), stable isotope stratigraphy and palaeomagnetic investigation of the older parts of the sequences.

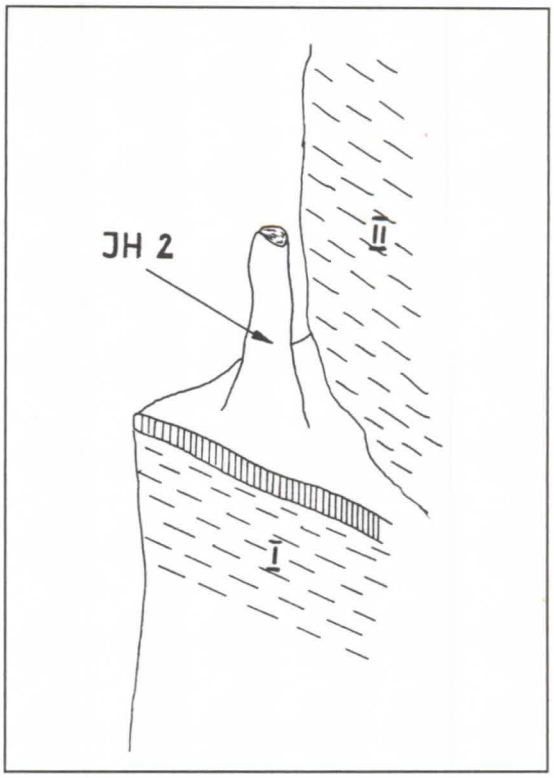

Fig. 3: Late-Glacial to holocene stalagmite column that was covered by later (Holocene) sediments. The sample was exposed during construction of the artificial gallery.

Potential use of uranium series dating of calcareous algae as a tool for dating paleo-watertables in maritime karst settings

Henriette Linge & Stein-Erik Lauritzen
Department of Geology, Bergen University
Allegt. 41, 5007 Bergen, Norway

Abstract
Calcareous algae which are sessile, marine organisms occur sometimes on cave walls in coastal karst and indicate minimum high sea stands. We investigate the possibility for applying uranium series dating to such deposits. Calcareous algae from Kapp Ekholm, Svalbard, has been evaluated for dating potential. The material display quite high uranium content which means that precise ages may be obtained from small samples, provided that they are unaffected by weathering processes. Because of difficulties in the accurate identification of the fossil algae only generic names (i.e. *Lithothamnium*) are used. This technique is also applied to algae situated in the twilight zone of a paleospring cave, north Norway.

Introduction

Numerous morphological indicators of paleo-watertables may be identified in karst caves (e.g. watertable corrosion notches, vadose-phreatic boundaries, and clastic sediment deposits and erosion levels in them). Dating of paleo-watertables in coastal karst can be used for construction of shoreline displacement diagrams, on the assumption that the cave system is situated below the upper marine limit in the area.

Such watertable markers may be dated providing that they are associated with datable deposits like speleothems, calcareous concretions, bone and shell fragments, or cap mud containing organic material. *In situ*, vadose speleothem deposits gives a maximum level of the paleo-watertable. Precipitation of calcareous concretions occurs in water-saturated sediments shortly after deposition of the sediments (HILLAIRE-MARCEL & CAUSSE, 1989) and gives a minimum level for paleo-watertables. If the precipitation occurs in the epiphreatic zone this might result in stratigraphically inverted ages under falling watertable conditions. Bone and shell fragments predate the last sedimentation cycle; the relation between the level of deposition and the watertable depends on the type of transport mechanism. Deposition of cap mud is related to stagnant phreatic/epiphreatic conditions (WORTHINGTON, 1991) and dating gives an age to a minimum level of the watertable.

We have investigated the possibility of using calcareous algae from cave walls as datable (minimum) watertable indicators. They have the advantage over other biogenic deposits in caves (i.e. bones and shells) that they are sessile organisms and often preserved *in situ*.

Calcareous algae (buildups) have been used as biological indicators of sea level fluctuations by several authors, e.g. LABOREL *et al.* (1994) ^{14}C dated of *Lithophyllum lichenoides*, and estimated sea level fluctuations during the last 4500 years in southwest France and Corsica, BOYD (1986) interpreted paleoenvironment from the occurrence of *Lithothamnium sp.* rhodoliths in late Quaternary raised coastal sediments, Irvine, Ayrshire, AKPAN and FARROW (1984) estimated depth of deposition and SARTORETTO *et al.* (1996) ^{14}C dated several calcareous algae species, which they correlate with bathymetric position.

Age estimates of high sea level stands can be compared with paleo-watertables in the adjacent cave system. This is a way of connecting paleo-watertables to sea level and also a test of what processes that governed changes in former watertables. Alternatives to high sea level stands are bedrock control, ice-contact damming and local sediment-choked passages/springs.

Uncertain factors associated with the use of calcareous algae in the estimation of sea level are at what depth the algae grew and whether dating is possible with known methods. The depth of growth depends on several factors, and the growth depth today in an area is not necessarily representative for former periods. Temperature and light are the main controls, determining depth and geographical distribution of calcareous algae (ADEY, 1970).

One example is the species *Lithothamnium glaciale* (Kjellman) that is found in northern Norway and in fjords in southern Norway (fig. 1). It is common in the sublittoral zone but is also found in the lower littoral zone in shady pools and runnels (RUENESS, 1977; IRVINE & CHAMBERLAIN, 1994).

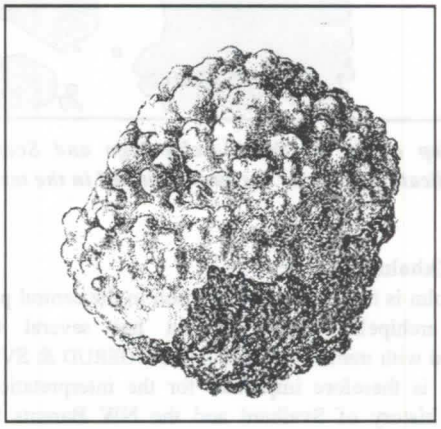

Fig. 1 Lithothamnium sp., after Oltmanns (1922).

The upper growth limit is controlled by sea level but also competition between different floral-species (light conditions), substrate and water quality. The lower growth limit is mainly determined by light intensity, in Norwegian waters algae growth is seldom present deeper than 40-50 m (RUENESS, 1977). In the case of twilight zone caves, encrusting calcareous algae may live near the low tide level due to the low light intensity.

Site and sample descriptions

a) Kjøpsvik caves

The caves of Kjøpsvik (fig. 2), northern Norway, have been studied intensively lately by LAURITSEN (in prep.), NESE

(1996), NESE & LAURITZEN (1996), LAURITSEN & LAURITZEN (1996) and LAURITZEN & LAURITSEN (1995).

Nygrotta (fig 3) is a sediment-choked paleospring situated 60 m a.s.l. and was until recently covered beneath a talus slope. The cave entrance is filled with bones and large amounts of mollusc shells. The bedrock walls around the entrance is covered with calcareous crusts consisting of white calcareous algae.

The main cave, Storsteinshola, which once drained to the paleospring, possesses several distinct paleo-watertables and also large paragenetic features developed up to a level corresponding to Nygrotta.

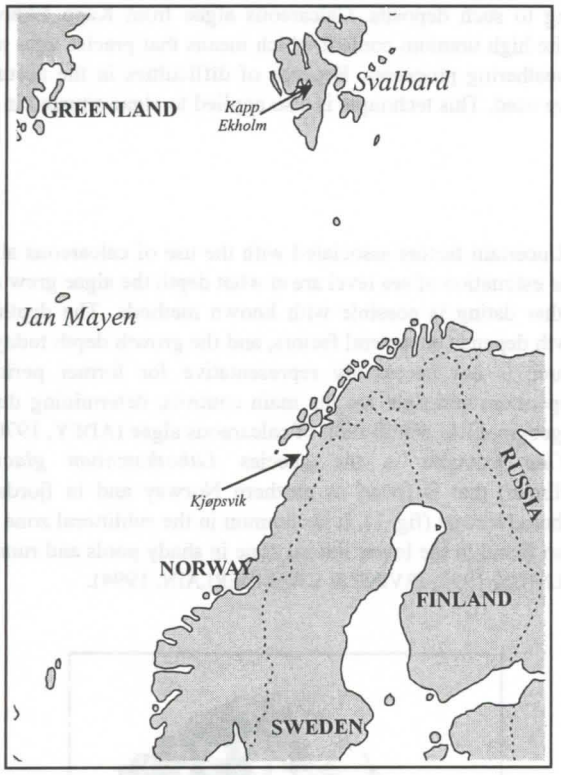

Fig. 2 Map of the Svalbard archipelago and Scandinavia, arrows indicate location of the sites discribed in the text.

b) Kapp Ekholm, Svalbard

Kapp Ekholm is the only known section in the central part of the Svalbard archipelago (fig. 2) that has several till beds interlayered with marine sediments (MANGERUD & SVENDSEN, 1992) and is therefore important for the interpretation of the glaciation history of Svalbard and the NW Barents Sea. The oldest marine unit is thought to be Eemian and the chronology is mainly based on luminescence and radiocarbon dating together with amino acid estimates and biostratigraphy.

The chronology from MANGERUD and SVENDSEN (1992) is used as reference when evaluating the obtained uranium series age estimates. Calcareous algae are found in the Eemian, Kapp Ekholm interstadial (ca 40-60 ka) and the Holocene sediments. Several types of calcareous algae (*Lithothamnium*) have been analysed from these three units, and we use their uranium series systematics as examples (LINGE, 1996).

c) General sample description

Living calcareous algae are pink, but fossil specimens are white or light red-brown. Both encrusting and free living (rhodoliths) species have been analysed. The crust of white fossil algae is normally less then 10 mm thick, and less than 3 mm for the red-brown type. Encrusting species may envelope stones, shells and other calcareous algae. Microstructures has been studied with SEM. XRD analysis show calcite with small amounts of aragonite.

Analytical results

Lithothamnium sp. precipitates calcite and small amounts of aragonite and usually have a high content of magnesium and iron. The reliability of dates obtained from calcareous algae is dependent of in what way uranium is incorporated in the calcareous crusts and which processes affect the material after burial/ subaerial exponation. It is therefore necessary to establish criteria for reliability and to test samples with known ages.

Analysis of recent calcareous algae (from Kragerø, south Norway) have a uranium content of 1.5 ppm and a $^{234}U/^{238}U$ activity ratio of 1.15 ±0.03, indicating that the organisms have a high *in vivo* U-content which is in isotopic equilibrium with seawater.

The study of Holocene, Weichselian and Eemian calcareous algae from Kapp Ekholm, Svalbard, shows a generally high uranium content and a large spread in $^{234}U/^{238}U$ activity ratio values. Nevertheless, there is no distinct trend in the $^{234}U/^{238}U$ values. Together with the observed deviation from the global marine $^{234}U/^{238}U$ activity ratio, this indicates that the algae represents open systems with *post mortem* uranium uptake from the pore water in the surrounding sediments. Table 1 shows the obtained results.

Investigation of the individual samples with SEM reveals traces of early biogenic cementation, but interpretation of the microstructures is difficult due to the lack of species control.

With the observed enrichment of uranium compared with recent calcareous algae, it is expected that the calculated U/Th ages would be younger than the "true" ages.

Discussion and preliminary conclusion

Calcareous algae from Kapp Ekholm yields overestimated ages compared with the chronology developed from MANGERUD and SVENDSEN (1992) (fig. 4). This can be explained with loss of uranium with time, but contradicts the observed enrichment relative to the modern algae. The uranium content differs strongly between samples and subsamples and it is therefore a need for evaluating the material. Full evaluation requires a larger set of data than present. *Post mortem* uranium uptake is evident from the $^{234}U/^{238}U$ activity ratio and is most probably associated with organic matrix in the calcite skeleton. Loss of uranium is due to normal weathering processes.

The material often displays early biogenic cementation (ALEXANDERSSON, 1974; MOBERLY, 1968, 1970, 1973) which allow testing of the degree of preservation. This biogenic cementation can be observed with SEM and is usually believed to be of short duration in normal calcite undersaturated marine environment. Here shoreline displacement and burial of the material comes convenient. The residence time the in marine environment may have been less than a few thousand years and hence the cementation is preserved.

If the material can be dated safely, age estimates of former high sea stands during deglaciation can be obtained. Twilight zone caves implies severe light conditions for growth of calcareous red algae, and growth might only have been possible close to the low tide level. The difference between high and low tide can be considered to be site specific and time independent. Linking of former sea level with paleo-watertables might therefore be both possible and useful, combining both speleogenesis and deglaciation history of an area.

Tab. 1 Uranium series results from calcareous algae from Kapp Ekholm, Svalbard. As shown in figure 4, the estimated ages are older than the assumed formation ages at the site. This discrepancy might be due to loss of uranium, but the general high uranium content together with the measured $^{234}U/^{238}U$ ratio indicates uranium uptake from a meteoric water source.*

age*	sample no.	lab. no.	U-content (ppm)	$^{234}U/^{238}U$	$^{230}Th/^{234}U$	$^{230}Th/^{232}Th$	calculated age (ka)
Holocene	1988-523	1067	2.17 ±0.04	1.19 ±0.02	0.125 ±0.008	21.0	14.39 ±0.97
	1988-318	1182	8.55 ±0.10	1.62 ±0.01	0.106 ±0.006	>1000	12.03 ±0.68
Kapp Ekholm interstadial (40-60 ka)	1988-714	1016	6.72 ±0.11	1.79 ±0.02	0.515 ±0.014	>1000	73.77 ±2.77
	1988-712	1169	10.4 ±0.1	1.50 ±0.01	0.561 ±0.009	>1000	84.42 ±2.02
	1988-713	1185	3.00 ±0.08	1.42 ±0.04	—	—	—
	1988-094	1324	8.12 ±0.11	1.88 ±0.02	0.239 ±0.011	>1000	28.98 ±1.54
	1988-713	1325	2.99 ±0.05	1.37 ±0.03	0.443 ±0.017	>1000	61.67 ±3.16
redeposited from Eeemian	1988-681	1015	26.7 ±1.2	1.17 ±0.02	0.784 ±0.063	450	155.95 ±30.50
	1988-681	1170	12.4 ±0.2	1.29 ±0.01	0.949 ±0.015	>1000	245.01 ±13.32
	1988-681	1183	31.8 ±0.4	1.22 ±0.01	0.817 ±0.007	>1000	168.31 ±17.25
Eemian	1988-679	1068	17.9 ±0.3	1.57 ±0.01	1.400 ±0.031	>1000	>350
	1988-108	1184	17.0 ±0.4	1.57 ±0.02	0.968 ±0.042	>1000	233.70 ±32.91
	1988-688	1186	2.57 ±0.05	1.55 ±0.03	—	—	—
	1988-524	1326	4.14 ±0.20	1.80 ±0.09	1.066 ±0.262	>1000	>350
	1988-108	1346	18.8 ±0.4	1.53 ±0.02	0.974 ±0.021	>1000	241.27 ±16.84

* after the chronology published by MANGERUD and SVENDSEN (1992)

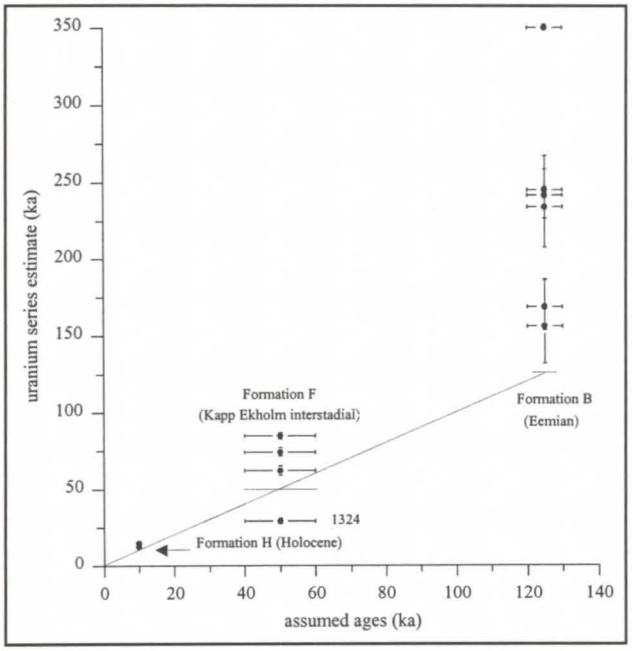

Fig. 4 Uranium series ages from calcareous algae from Kapp Ekholm plotted against formation ages from MANGERUD and SVENDSEN (1992). The solid line represents coherent ages.

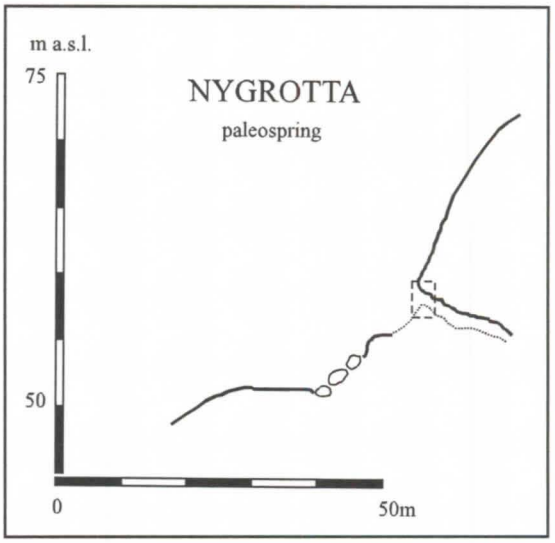

Fig. 5 Vertical cross section of Nygrotta. Box form indicates zone of algae growth. Modified from Nese (1996).

Algae crusts cover the walls and ceiling approximately one meter beyond the Nygrotta cave entrance and also large parts of the marble walls adjacent to the entrance. Dating of the calcareous algae from this site are in process and will be presented at the symposium.

Since the algae are relatively young (i.e. from the deglaciation period) and most probably well preserved due to the recently removed talus cover, precise uranium series ages might be obtained. The problem of possible overestimated ages calculated from Kapp Ekholm might also be absent. Hence, precise calendar ages of a former high sea stand at approximately 60 m a.s.l. will give the age of the corresponding paleo-watertable in the Storsteinshola cave system in Kjøpsvik.

References

AKPAN, E.B. & FARROW, G.E. 1984. Depth of deposition of early Holocene raised sediments at Irvine dedused from algal borings in mollusc shells. *Scott. J. Geol.* 20 (2): 237-247.

ALEXANDERSSON, T. 1974. Carbonate cementation in coralline algal nodules in the Skagerrak, North Sea: biochemical precipitation in undersaturated waters. *Journal of Sedimentary Petrology* 44 (1): 7-26.

BOYD, W.E. 1986. Fossil *Lithothamnium* (calcareous algae) rhodoliths from late Quaternary raised coastal sediments, Irvine, Ayrshire. *Scott. J. Geol.* 22 (2): 165-177.

HILLAIRE-MARCEL, C. & CAUSSE, C. 1989. Chronologie Th/U des concrétions calcaires des varves du lac glaciaire de Deschaillons (Wisconsinien inférieur). *Canadian Journal of Earth Science* 26: 1041-1052.

IRVINE, L.M. & CHAMBERLAIN, Y.M. 1994. Seaweeds of the British Isles, Vol.1 Rhodophyta, Part 2B Corallinales, Hildenbrandiales. The Natural History Museum, London. 276 p.

LABOREL, J., MORHANGE, C., LAFONT, R., LE CAMPION, J., LABOREL-DEGUEN, F. & SARTORETTO, S. 1994. Biological evidence of sea-level rise during the last 4500 years on the rocky coasts of continental southwestern France and Corsica. *Marine Geology* 120: 203-223.

LAURITSEN, Å. (in prep.). Geomorfologisk utvikling av grottesystemene i Kjøpsvik, Nordland. Cand.scient.-thesis. Department of Geology, Bergen University.

LAURITSEN, Å. & LAURITZEN, S.-E. 1996. Quaternary cave and landform development in the Tysfjord region, north Norway. *Karst Waters Institute Special Publication* 2: 73-77.

LAURITZEN, S.-E. & LAURITSEN, Å. 1995. Differential diagnosis of paragenetic and vadose canyons. *Cave and Karst Science* 21:, 55-59.

LINGE, H.C. 1996. Uranseriedatering av bivalver, kalkalger og torv fra noen arktiske lokaliteter. Cand.scient.-thesis, Department of Geology, Bergen University, 125 p.

MANGERUD, J. & SVENDSEN, J.I. 1992. The Last Interglacial-Glacial Period on Spitsbergen, Svalbard. *Quaternary Science Reviews* 11: 633-664.

MOBERLY, R.JR. 1968. Composition of magnesian calcites of algae and pelecypods by electron microprobe analysis. *Sedimentology* 11: 61-82.

MOBERLY, R.JR. 1970. Microprobe study of diagenesis in calcareous algae. *Sedimentology* 14: 113-123.

MOBERLY, R.JR. 1973. Rapid chamber-filling growth of marine aragonite and Mg-calcite. *Journal of Sedimentary Petrology* 43 (3): 634-635.

NESE, H. 1996. Sedimentologisk utvikling av grottesystemene i Kjøpsvik, Nordland. Cand.scient.-thesis. Department of Geology, Bergen University, 157 p.

NESE, H. & LAURITZEN, S.-E. 1996. Quaternary stratigraphy of the Storsteinshola cave system, Kjøpsvik, north Norway. *Karst Waters Institute Special Publication* 2: 116-120.

OLTMANNS, F. 1922. Morphologie und Biologie der Algen. Verlag von Gustav Fisher, Jena, 439 p.

RUENESS, J. 1977. Norsk algeflora. p. 1-23 and 54-63. Universitetsforlaget, Oslo.

SARTORETTO, S., VERLAQUE, M. & LABOREL, J. 1996. Age of settlement and accumulation rate of submarine "coralligène" (-10 to -60 m) of the northwestern Mediterranean Sea; relation to Holocene rise in sea level. *Marine Geology* 130: 317-331.

WORTHINGTON, S.R.H. 1991. Karst hydrology of the Candian Rocky Mountains. Ph.D.-thesis, McMaster University, 370 p.

U- series dating and stable isotope analysis of some last interglacial speleothems from north Norway

Ida Malene Berstad, Sølvi Einevoll and Stein Erik Lauritzen
Department of Geology, Bergen University
Allegt. 41, 5007 Bergen, Norway

Abstract

Stalagmites from a karst cave in north Norway were dated by the U-series technique and analysed for isotopic equilibrium. The purpose of the study is to use stable isotopes for paleoenviroment reconstruction for North Norway, emphasizing Last Interglacial material. This study is in progress, so only preliminary results are reported here.

Introduction

Provided that the speleothem grew in isotopic equilibrium with the feeding dripwater, the $\delta^{18}O$ signal along the growth axis is a paleoclimatic proxy. Combined with U-series dating, a time series of paleoprecipitation changes can be made (Schwarcz 1996). This study aims at the last interglacial time-window.

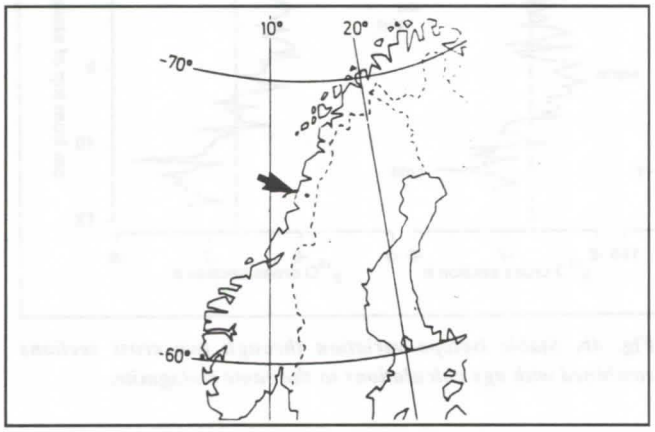

Fig.1.Key map to the investigated area.

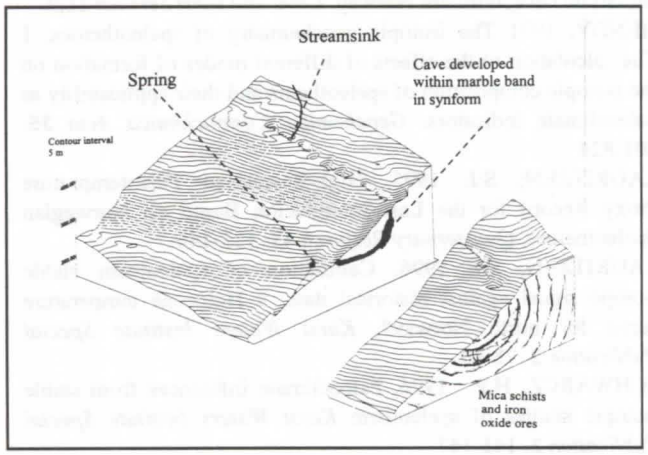

Fig. 2. Topographic and geologic setting of the investigated cave.

Background

The cave from which the speleothems were sampled, is located at Mo i Rana, at the Arctic Circle (66°20' N) (fig. 1) The thin band of steeply dipping marble was almost totally occupied by the 1,3 km long and 104m deep cave (fig. 2). A sinking stream runs through the marble band, but the percolation water which precipitate speleothems has to penetrate trough 100 m thick strata of mica schist and iron oxide ores on its way down to the marble band. The cave has previously been studied with respect to percolation water hydrology, cave microclimate, and stable isotopes (Einevoll & Lauritzen 1994). In addition, an almost complete time-series of Holocene $\delta^{18}O$ changes has been made. This $\delta^{18}O$ curve was calibrated against temperature changes during the last 250 years, and transformed into a temperature curve for the last 8500 years (Lauritzen 1996).

Material

Previous sampling by Einevoll & Gard provide material for screening with respect to U-series age and isotopic systematics. After preliminary screening, three specimens were selected, dated and tested in detail for isotopic equilibrium. According to the Hendy (1979) criteria, the isotopic composition within a single growth layer band must be practically invariant with respect to $\delta^{18}O$, and at the same time, $\delta^{18}O$ and $\delta^{13}C$ values within the same layer must be uncorrelated. Previously, speleothem dates up to beyond 350 ka (the limit of α- particle dating) have been found in the cave. The problem was to identify specimens that grew in isotopic equilibrium (i.e. Hendy, 1971), and at the same time covers the time window of the last interglacial.
One sample which were dated to be from the last interglacial, was tested for $\delta^{18}O$ variation trough a cross section.

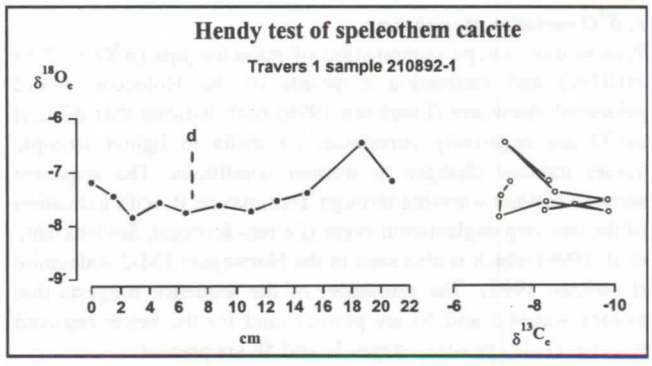

Fig. 3 Test of isotopic equilibrium.

Sample	ULB No	U-cons. ppm	$^{234}U/^{238}U$	$^{230}Th/^{234}U$	$^{230}Th/^{232}Th$	Age (ka)	+/-1 σ (ka)
210892-1 top	1507	0,86	1,30	0,671	370	113,8	+5,83 /-5,55
210892-1	1508	0.83	1.35	0.712	664	124.8	+8.24 /-7.72
210893-1	1673	1.01	1.32	0.743	457	135.5	+5.23 /-5.01
210892-1	1674	1.26	1.34	0.727	998	129.9	+4.97 /-4.74
210892.1	1675	1.31	1.33	0.710	399	124.8	+4.74 /-4.56
210892-1	1555	1.92	1.38	0.748	48	136.0	+10.91 /-10.01
210892-1 bottom	1556	2,91	1,45	0,774	358	143,6	+11,41 /-10,44

Table. 1. U- series age of sample 210892-1 in Stratigraphic order

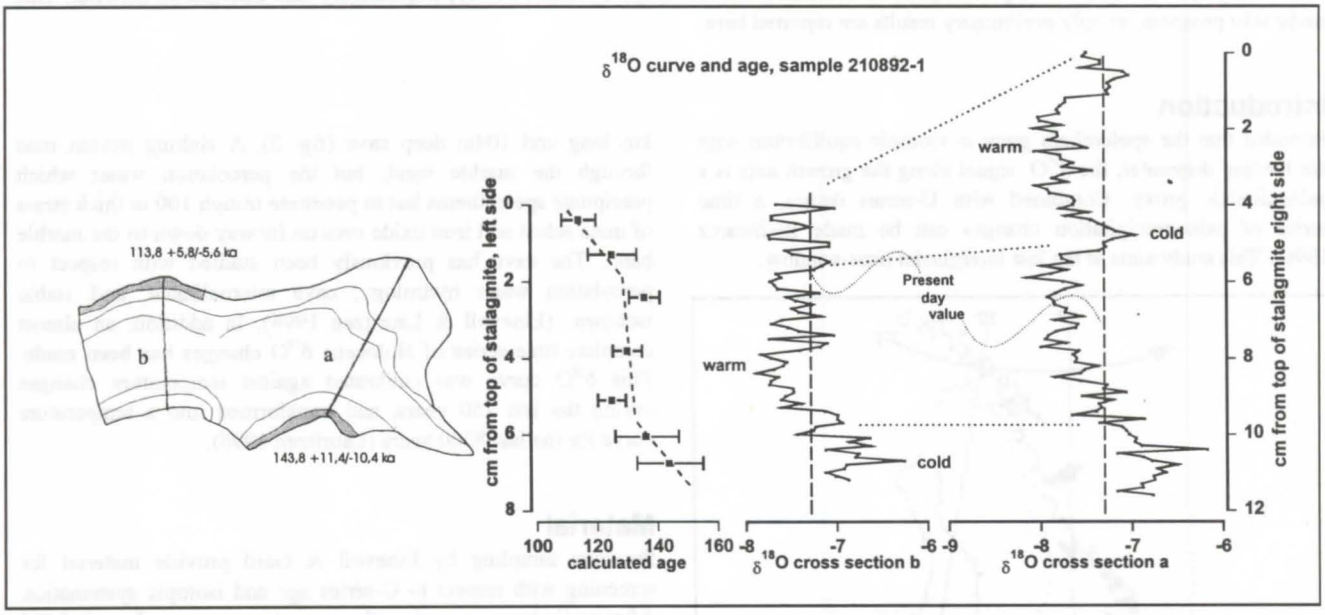

Fig. 4a. The investigated stalagmite

Fig. 4b. Stable isotope variation through two cross sections combined with age calculations in the same stalagmite.

Results and discussion

a. U- series dates

α- particle dating ($^{230}Th/^{234}U$) of sample 210892-1 yielded the growth-rate curve shown in Fig. 4b. The sample grew through Termination II through to at least isotope stage 5c

b. Stable isotopes- test of isotopic equilibrium.

The sample was tested for isotopic equilibrium according to the Hendy criteria, $\delta^{18}O$ along single growth bands varies by less than 0.5‰ in the vicinity of the drip-point. Also, the $\delta^{18}O$ vic. $\delta^{13}C$ varies unsystematically and lacks correlation (Fig. 3.). We therefore infer that stratigraphic sampling along the two traverses shown in Fig. 4a, will represent calcite growth in isotopic equilibrium with the dripwater.

c. $\delta^{18}O$ variation trough time

Present day isotope composition of stalactite tips ($\delta^{18}O$ = -7.33 ±0.07‰) and calibration constants of the Holocene record presented elsewhere (Lauritzen 1996) both indicate that ΔT and $\Delta\delta^{18}O$ are negatively correlated, i.e shifts to lighter isotopic values indicate changes to warmer conditions. The sequence shows a distinct warming through Termination II, with indication of the two step deglaciation event (Zeifen- Kattegat, Seidenkrantz et al. 1996) which is also seen in the Norwegian FM-2 stalagmite (Lauritzen 1995). The remainder of the sequence suggests that isotope stages 5 and 5d are present (and for the better resolved traverse a) also possibly stages 5c and 5b are present.

References

EINEVOLL, S. AND LAURITZEN, S.E 1994 Calibration of stable isotope and temperature signal in the percolation zone of a sub-arctic cave, northern Norway. *Cave and karst Science* **21**,9.

HENDY, 1971 The isotopic geochemistry of speleothemes. 1 The calculation of the effects of different modes of formation on the isotopic composition of speleothems and their applicability as paleoclimaic indicators. *Geochemica Cosmochimica Acta* **35**: 801-824

LAURITZEN; S:E 1995. High-Resolution Paleotemprature Proxy Record for the Last Interglacion Based on Norwegian Speleothemes. *Quarternary Resfarch* **43**: 133-146

LAURITZEN, S.E 1996. Calibration of speleothem stable isotope signal against historical data: a Holocene temperature curve for north Norway?, *Karst Waters Institute Special Publication* **2**: 78-80

SCHWARCZ, H.P. 1996, Paleoclimate inferences from stable isotopic studies of speleothem *Karst Waters Institute Special Publication* **2**: 145-147

SEIDENKRANZ, M.S. AND NINE OTHERS, 1996 Two-Step Deglaciation at the Oxygen Isotope Stage 6/5e Transition: the Zeifen-Kattegat Climate Oscillation. *Qarternary Science Reviews*, Vol.**15**, pp. 63-75

Speleochronology, stable isotopes and laminae analysis of stalagmites from southern Africa

by K. Holmgren[1], W. Karlén[2], S. E. Lauritzen[1], J. Lee-Thorp[3], T. C. Partridge[4], P. A. Shaw[5] and P. D. Tyson[4]

1) Department of Geology, University of Bergen, Allégt. 41, 5007 Bergen, Norway
2) Department of Physical Geography, Stockholm University, S-10691 Stockholm, Sweden
3) Department of Archaeology, University of Cape Town, Private Bag, Rondebosch, Cape 7700, South Africa
4) Climatology Research Group, University of the Witwatersrand, Wits 2050, Johannesburg, South Africa
5) Department of Environmental Science, University of Luton, Park Square, Luton LU1 3JU, UK

Abstract

Holocene and Pleistocene speleothems from South Africa, Botswana and Tanzania have been uranium-series dated and analysed on their stable isotopic content. Most of the stalagmites sampled are composed of finely laminated dense calcium carbonate. The structure and periodicity of the growth laminae are presently being analysed. New results from this study are presented and compared with data already available.

1. Introduction

Speleothems are often suitable climate archives and provide an option to obtain terrestrial high-resolution palaeoclimatic records from all over the world (SCHWARCZ, 1986). During the last twenty years several highly resolved palaeorecords from ice cores from Antarctica and Greenland have been presented and inferences have been drawn regarding global Late Quaternary climatic changes, global symmetry and driving forces (LOWELL *et al.*, 1995). There is an urgent need to obtain good quality terrestrial records of equally high resolution from low latitudes in order to test hypotheses about global climate changes and forcing factors. It is hoped that this recently initiated project will contribute such information through detailed analysis of speleothems from Tanzania, Botswana and South Africa.

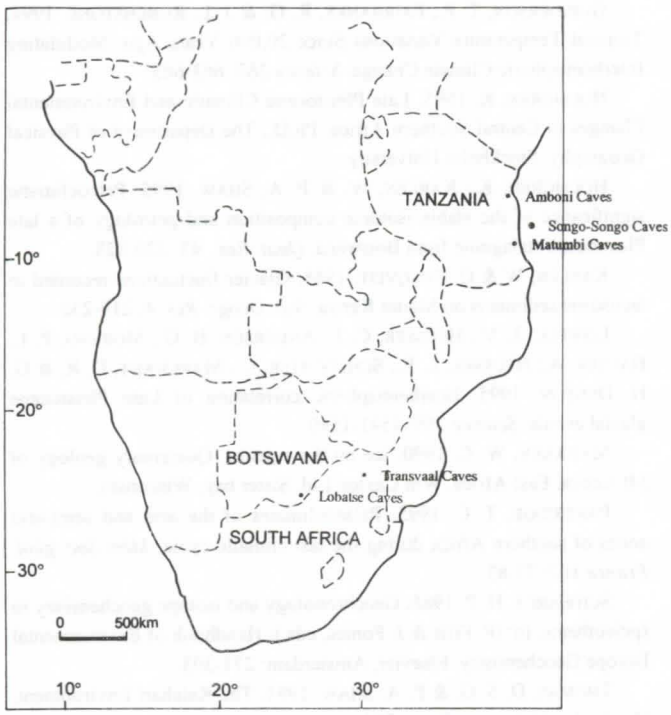

Figure 1: Map of southern Africa showing the locations of caves mentioned in the text.

2. Tanzania

Tanzania is situated just south of the equator and has a tropical climate influenced by the seasonal latitudinal movements of the Intertropical Convergence Zone and the monsoonal winds. Previous theories that climate in the tropics remained stable during the last ice ages have been proven incorrect (GUILDERSON *et al.*, 1994). Very few terrestrial high-resolution climate data have so far been presented from this region, but studies from caves from Somalia and Zaire (BROOK *et al.*, 1990), glacier studies from Mt Kenya (KARLÉN & ROSQVIST, 1988; MAHANEY, 1990), and lake studies from Kenya and Tanzania (BONNEFILLE *et al.*, 1995) generally suggest wetter conditions during the Eemian interglacial, aridity and cooler temperatures during the last deglaciation, wetter conditions at the Pleistocene-Holocene transition, a climate optimum in the early Holocene and since then a trend toward drier climates.

We have sampled stalagmites from cave systems along the Tanzanian coast; the Amboni Caves and the Matumbi Caves, and from caves on a small coral island outside the coast; the Songo-Songo Island (figure 1). Uranium-series dating so far has yielded ages from recent to the Last Glacial Maximum and from 38 to 34 ka (1000 years) (figure 2). The stalagmites are well laminated, with growth rates varying from 0.5 mm per 100 years for the Holocene samples, to 7 mm per 100 years for one that grew between 38 and 34 ka. Considering the high growth rate on the latter it is expected that a yearly resolution will be obtained from the laminae analysis and a 10 year resolution from the stable isotope analysis. This work is in progress.

3. Botswana and South Africa

The speleothems studied from Botswana and South Africa are from cave systems in semi-arid central southern Africa (figure 1). This region is of interest due to its transitional position between the summer rainfall zone to the north, the winter rainfall zone to the south, the semi-arid Kalahari Basin to the west and the more humid plateau to the east. Clearly, the climate and the borders of these zones have varied in response to past global climate changes. The limitations of most of the previous palaeoenvironmental data available are poor chronological control, low time resolution, and poor continuity (THOMAS & SHAW, 1991; PARTRIDGE, 1995).

Uranium-series dating, close-interval stable oxygen and carbon isotope measurements ($\delta^{18}O$, $\delta^{13}C$), and petrologic analyses carried out on one 33-cm-high stalagmite were reported

to provide a palaeoclimatic and palaeoecologic record for the period 50-20 ka (HOLMGREN, 1995; HOLMGREN *et al.*, 1995) (figure 2). The $\delta^{18}O$ record was interpreted as reflecting relative temperature variations, and comparing it with data from other palaeoenvironmental sites in central southern Africa, a regional decrease in temperatures from 50 ka, to a minimum during the Last Glacial Maximum, was confirmed. The $\delta^{13}C$ record in speleothems is governed by several factors, among which is the relative influence of C_3 and C_4 vegetation in the region (SCHWARCZ, 1986). This distribution is climatically controlled. As a working hypothesis we propose that the Lobatse $\delta^{13}C$ record reflects regional shifts in vegetation characteristics, supporting a model that involves an enhancement of the westerlies and an equatorward displacement of the subtropical convergence, which leads to increased influence of the winter rainfall belt in the Southern Kalahari, and to drier conditions in the Middle and Northern Kalahari (COCKROFT *et al.*, 1987). Subsequent dating and stable isotope analysis of cores from a 1.5-m-high stalagmite, LII2, confirm parts of previous interpretations and contradicts others, emphasizing the importance of cross-checking. Further work on material from Lobatse to test the validity of the data is in progress.

Speleothem samples have recently been collected from Ficus Cave and Cold Air Cave in Transvaal in South Africa. These caves lie in the same climate region and the same bedrock formation as Lobatse Caves. Hence, the results from studies of speleothems from these caves are expected to test the robustness and regional validity of the Lobatse data. The first uranium-series datings of the South African speleothems have yielded ages from Late Holocene to the present, from the end of the last glacial and from isotope stage 5a (figure 2). Thus, material is available both for comparison with the Lobatse record and for extending the record in time. The young Holocene-to-recent stalagmite has grown at a rate of 15 mm per 100 years and will be tested against the meteorological record.

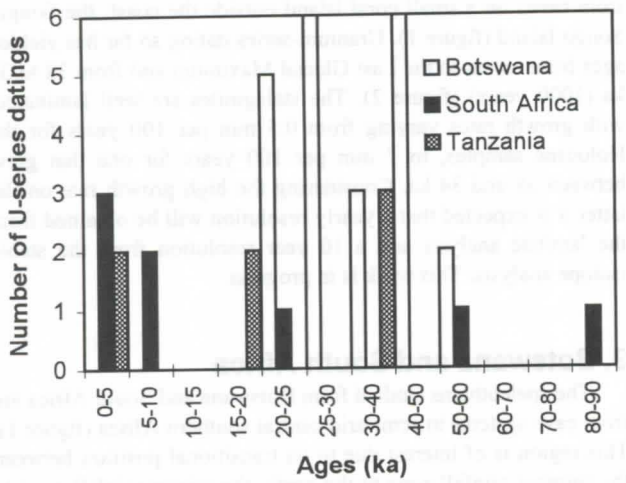

Figure 2: Age frequency distribution of speleothems from Botswana, South Africa and Tanzania.

4. Discussion

Speleothems are one of few potential archives for preserving palaeoenvironmental data in semi-arid regions, their validity is not yet fully explored. However, no archives are perfect and several problems are connected with semi-arid and tropical speleothems. They often possess parts that have suffered from re-solution, this can cause open system conditions and invalidate both the age dating and the stable isotope analyses. They can be composed of aragonite or calcite, or be a mixture of both. It is important to decide whether the structure, wheter calcite or aragonite, is of primary or secondary origin before any firm conclusions can be drawn regarding past environmental conditions.

These problems are best elucidated and overcome by appropriate selection of samples, by analysing several speleothems from the same locality and by performing a variety of analyses upon them. With this approach there may be a conflict between scientific interests and conservative interests. However, thanks to development of new techniques, smaller samples are needed.

5. Conclusions

Uranium-series dating of speleothems from Tanzania, Botswana and South Africa has yielded ages from 90 ka to the present. Most of the speleothems analysed are composed of compact, laminated, pure calcium carbonate. The prospect of obtaining high-resolution palaeoclimatic records from the on-going analyses is most encouraging.

References

BONNEFILLE, R.; RIOLLET, G.; BUCHET, G.; ICOLE, M.; LAFONT, R.; ARNOLD, M. & D. JOLLY. 1995. Glacial/Interglacial Record from Intertropical Africa, High-Resolution Pollen and Carbon Data at Rusaka, Burundi. *Quat. Sci. Rev.* 14: 917-936.

BROOK, G. A.; BURNEY, D. A. & J. B. COWART. 1990. Desert paleoenvironmental data from cave speleothems with examples from the Chihuahuan, Somali-Chalbi, and Kalahari deserts. *Palaeogeogr., Palaeoclim., Palaeoecol.* 76: 311-329.

COCKROFT, M. J.; WILKINSON, M. J. & P. D. TYSON. 1987. The application of a present-day climatic model to the late Quaternary in southern Africa. *Clim. Change* 10: 161-191.

GUILDERSON, T. P.; FAIRBANKS, R. G. & J. L. RUBENSTONE. 1994. Tropical Temperature Variations Since 20,000 Years Ago: Modulating Interhemispheric Climate Change. *Science* 263: 663-665.

HOLMGREN, K. 1995. Late Pleistocene Climatic and Environmental Changes in Central Southern Africa. Ph.D., The Department of Physical Geography, Stockholm University.

HOLMGREN, K.; KARLEN, W. & P. A. SHAW. 1995. Paleoclimatic significance of the stable isotopic composition and petrology of a late Pleistocene stalagmite from Botswana. *Quat. Res.* 43: 320-328.

KARLÉN, W & G. ROSQVIST. 1988. Glacier fluctuations recorded in lacustrine sediments on Mount Kenya. *Nat. Geogr. Res.* 4: 219-232.

LOWELL, T. V.; HEUSSER, C. J.; ANDERSEN, B. G.; MORENO, P. I.; HAUSER, A.; HEUSSER, L. E.; SCHLÜCHTER, C.; MARCHANT, D. R. & G. H. DENTON. 1995. Interhemispheric correlation of Late Pleistocene glacial events. *Science* 269: 1541-1549.

MAHANEY, W. C. 1990. Ice on the equator: Quaternary geology of Mt Kenya, East Africa. Wm Caxton Ltd. Sister bay, Wisconsin.

PARTRIDGE, T. C. 1995. Palaeoclimates of the arid and semi-arid zones of southern Africa during the last climatic cycle. *Mém Soc. géol. France* 167: 77-83.

SCHWARCZ, H. P. 1986. Geochronology and isotope geochemistry in speleothems. In: (P. Fritz & J. Fontes, eds.): Handbook of Environmental Isotope Geochemistry. Elsevier, Amsterdam: 271-303.

THOMAS, D. S. G. & P. A. SHAW. 1991. The Kalahari Environment. Cambridge University Press, 284 p.

Absolute datations of speleothems and its speleomorphological significance from Divaška jama and Jazbina caves; Kras plateau, Slovenia

Andrej Mihevc*, Stein-Erik Lauritzen**
*Inštitut za raziskovanje krasa ZRC SAZU, Titov trg 2, 66230 Postojna, Slovenia
**Institute of Geology, University of Bergen, Allegaten 41, N-5007 Bergen, Norway

Abstract

Various speleothems, including tall stalagmites and massive flowstone deposits from the Kras plateau, Western Slovenia have been sampled and dated with the $^{230}Th/^{234}U$ method by α-particle counting. Results of datations on speleothems in two caves, Divaška jama cave and Jazbina v Rovnah are presented. Sampling focused on the morphological evidence of the late Pleistocene and morphological impact of colder climate in caves.

In Divaška jama three periods of growth of flowstone were recorded. The oldest flowstone was deposited between two phases of sedimentation of flood loam, before 350 Ka, and are out of range of dating method. Intensive growth of thick large stalagmites is recordet at 240 -170 Ka. The newest deposition started on gravel after last glaciation, around 16 Ka B.P.

In Jazbina v Rovnah cave some flowstone crusts were deposited at about 240 Ka B.P. Flowstone was later fractured, scattered and arranged in a circle due to cryoturbation. On that stalagmite start to grow at 43 ±2 Ka. Growth was continuos till present, showing change of flowstone colour at 14,9 ±0,9 Ka. Another stalagmite analysed, started to grow at 16 ±0,6 Ka, having hiatuses in the bottom part, most distinct at 10,6 ±0,2 - 9,3 ±0,2 Ka, probably showing climatic changes of younger Dryas.

Dating allows us to connect some morphological evidence from caves with climatic changes of the late Pleistocene.

Introduction

Kras is about 50 km long and to 20 km wide karst surface, rising from elevations about 250 m on NW to elevations about 600 m in SE part.

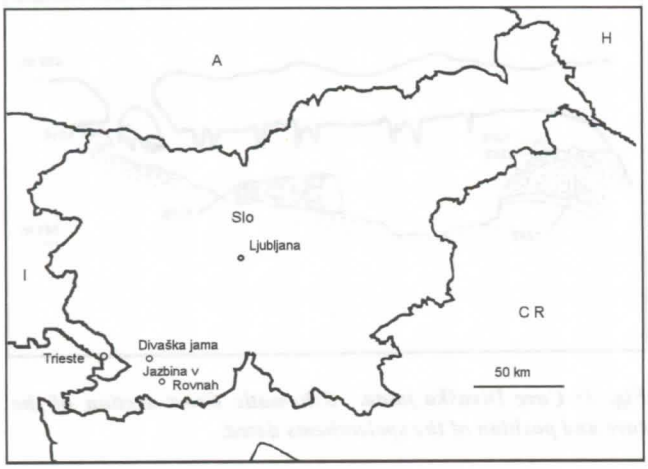

Figure1: Position of two caves in the W part of Slovenia.

The karstification of mostly Cretaceous limestone started after its uplift in the Oligocene. There is about 300 m of the vadoze zone accessible and there are caves formed in all elevations from the surface to the sea level and below. Some caves have been filled with allogenic sediments, originating from the impermeable surroundings which were later partly eroded. Different allochtonous sediment are showing different phases in the development of the karst but give no absolute datations of them.

There are few absolute dates of speleothems available for the Kras. First datations, with ^{14}C were done by Gospodarič (1980) in Škocjanske jame and Vilenica cave, these were followed with U series dating on a stalagmite from Grotta Gigante by Cucchi and Forti (1989), and by Zupan (1991), datations from Skocjanske jame, Lipiska jama cave, cave Vilenica and cave Mejame, but no more than 8 speleothems were dated by both methods.

Here we present some results of the speleothem U series dating from Jazbina cave and Divaška jama. Samples were dissolved in concentrated HNO_3. A $^{228}Th/^{232}U$ spike was added as an internal standard for control of the chemical yields. U and Th nuclides were separated by ion exchange chromatography in columns. After purification steps both fractions were electroplated on steel disks, and counted to measure alpha particle activity. Ages were calculated from isotope activity ratios using standard algorithms (Ivanovich & Harmon 1982, 1992; Lauritzen, 1991). The error is based on counting statistics. For the samples contaminated with detritic ^{230}Th correction was done on the equation suggested by Schwarcz (1980) with correction factor B_0= 1.5. Samples were prepared and dated in the U-series laboratory in Bergen. These results are preliminary, as there are not all the datations from larger area evaluated yet.

Work was conducted through collaboration between the Department of Geology, University of Bergen and the Institute of Karst Research from Postojna in a frame of PEP III, The Afro-European Transect (PANASH) and with financial support of University in Bergen and Slovene Ministry for Science and Technology.

Description of sampling points and samples

Jazbina v Rovnah is 2000 m long and 130 m deep cave with the entrance at an altitude of 483 m. The cave is reaching the lowest point in this part of the karst, 350 m respectively. Cave is a three dimensional maze of phreatic channels and there is little flood loam, characteristic of many other caves in vicinity.

Samples, already broken stalagmites from two parts of the cave were taken. A 238 cm long stalagmite C 228 grew in the depth of about 125 m, on the unstable debris. The parts of broken column were collected and the foot of column removed from the rock. The speleothem was split unhalves, showing, that it was composed of 224 cm tall stalagmite and a straw which joined the

stalagmite and after that started to grow thicker. Thickness of the stalagmite varied, from 7 cm at bottom to maximum 11 cm at 70 cm.

Several subsamples of white or transparent flowstone were cut of the stalagmite and dated, giving good results due to low ^{232}Th contamination and high uranium content. Stalagmite start to grow at 16 ±0,6 Ka (sample number 1396). Bottom parts show two distinctive hiatuses. The more important is the second, at 17 cm, where two subsamples were taken. As the samples weight more than 30 grams, their centres were 3 cm apart. Lower (1288), was dated to 10 ±0,2 Ka, the one above hiatus (1385) to 9 ±0,2 Ka. The hiatus is distinctive, marked with thin red layer, below it flowstone is compact and translucent, above it turns to white, more thicker lamina. Stalagmite became thicker too, which may be connected with increased water inflow. Growth was then disturbed several times, but only one hiatus at 151 cm is marked with thin layer of red soil A subsample was taken at 149 cm (1292), dated to 7,6 ±0.2 Ka. The subsample at 211 cm (1398), showed age of 5,5 ±0.2 Ka. All these data give the same growth rate of 0.03 mm/y.

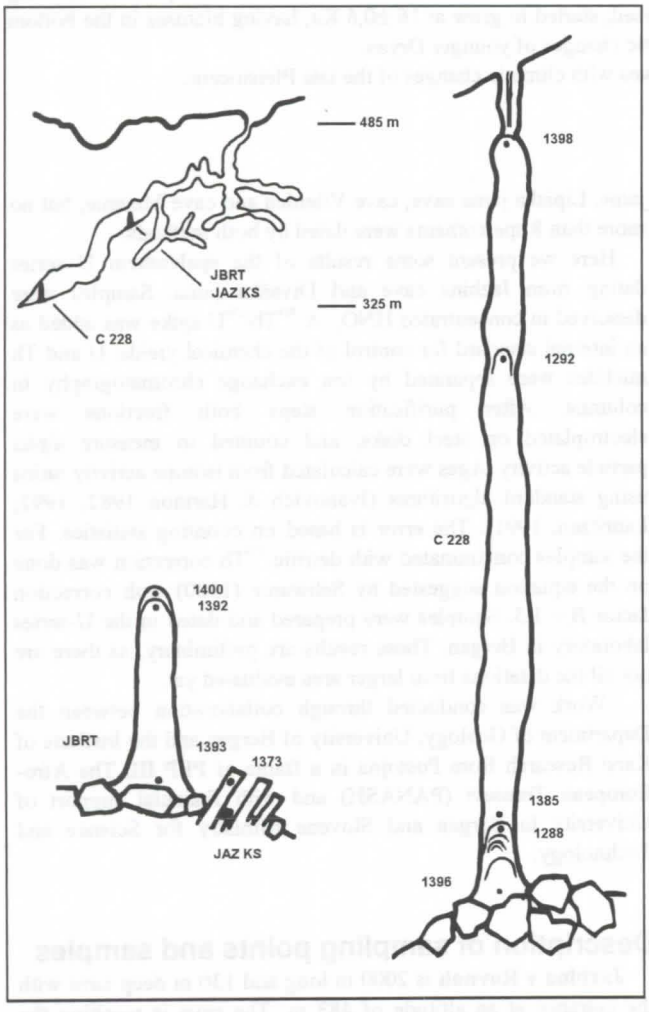

Figure 2: Cave Jazbina v Rovnah. Schematic cross section, position of the dated speleothems and subsample numbers on the speleothems.

The second stalactite was growing in the depth of about 75 m below the entrance. It grew on the loose rocks and broken flowstone crusts, which have been moved and arranged into polygon, with flakes of crusts been in near vertical position, obviously due to cryoturbation. Both broken parts of the stalagmite and ist base were sampled as well as the parts of the cryoturbated crusts.

A sample of the crust dated (1373) gave age of 240 +40 -30 Ka. The result is not very reliable as there is some contamination with detritic Th.

Stalactite has a dark brown crystalline laminated flowstone with a distinctive change to white flowstone 2 cm below the top. Three samples were analysed showing age (1393) at bottom 43 ±2 Ka and (1392), age 14,9 ±0,9 Ka at 48 cm, below the hiatus. Growth rate of that part of stalagmite was 0.016 mm/y. Above the hiatus the flowstone change to white and translucent. The top 1 cm thick layer of flowstone (1400)was dated to 4,9 ±0.5 Ka. The growth rate of this white flowstone is an order of magnitude lower, being only 0,0013 mm/y.

Divaška jama is 670 m long cave, accessible parts of galleries are to 20 m wide and high. The generations of fluvial sediments and flowstone in the cave were studied by Gospodarič (1984), but do absolute datations were made. Its galleries are at elevation from 350 - 410 m, while surface is at elevations of 450 m and the actual underground rivers flowing in the nearest cave at elevation of 156 m a.s.l. (Mihevc 1984).

Most extensive sediment in the cave is a more than 30 m thick laminated flood loam which filled up most of the cave. Loam was deposited at least in two phases, separated with a period of erosion and deposition of the flowstone. On the top of flood loam sequence in some places angular gravel was deposited.

Entrance to the cave is a collapse which split the cave gallery. From it to SW the gallery is open, towards NE gallery is filled, partly with rock blocks, partly with fluvial sediments, covering a massive flowstone too.

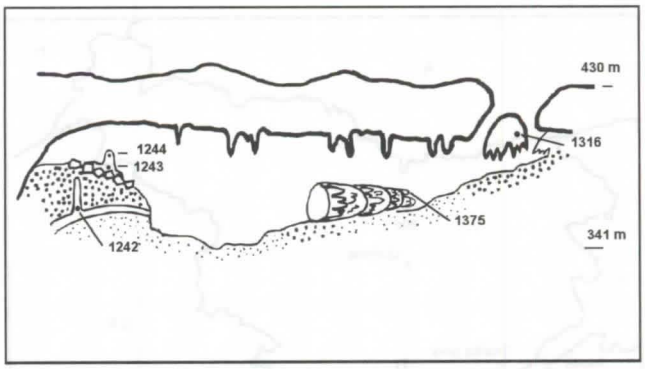

Fig. 3: Cave Divaška jama. Schematic Cross section of the cave and position of the speleothems dated.

A sample was taken from the massive flowstone at the collapse entrance of the cave. The age of the sample (1316) was 243 +81-47 Ka.

The flowstone from a top of small parasitic stalagmite growing on 12 m high, more than 3 m thick fallen stalagmite Harambaša was taken (1375). It showed the age of 176 +17 -15 Ka, which gives the time of its collapse.

In Žibernova dvorana 39 cm long stalagmite and flowstone crust grown between two phases of flood loam deposition. Subsample (1242) was taken from its base and dated to more than 350 Ka.

In Pretnerjeva dvorana a stalagmite grew on the angular pebbles and boulders, which partly cover the upper laminated loam. The surface of sediment is eroded making more than of 10 m relief. Base of the stalagmite (1243) gave age of 16 ±1 Ka. The top of the stalagmite (1244) was also dated, showing age of 7 ±0,8 Ka. The growth rate of the speleothem was low, 0,008

mm/y only. The reason for that is probably a high ceiling, which caused the splitting of the droplets and spraying them around a process which a thin crust of flowstone covering the gravel in vicinity.

Discussion

These speleothems and ages calculated from them are enough to give us some instructions for future work and to show some events in development of the caves studied.

Sampling concentrated on the tall stalagmites from caves, which were not influenced by sinking rivers floods or sedimentation during the end of Pleistocene. The speleothems growing on such a deposits are in most cases badly contaminated with detritic ^{232}Th, so datations are not very reliable.

The datations we conducted and presented in this paper show, that the growth of tall stalagmites after last glaciation start at about 16 Ka bp. This ages we found in Jazbina cave at stalagmite C228. At stalagmite JBRT from the same cave, the change in colour of speleothem and lower growth rate after 14.9 ±0,9Ka can also mark the same climatic change. At stalagmite C228 a evident hiatus in its lower part is possibly marking the Younger Dryas.

In Divaška jama same age, 16 ±1 Ka, is expressed in the sample 1243, taken from the base stalagmite which grew on angular pebbles and loam indicating a cold period of washing away the sediments.

Kras was not glaciated during the cold periods of Pleistocene. Most of it was above the tree line, and the snow line was at the elevation of about 1200 m, but small glaciers were only 20 km away. Low temperatures, poor vegetation and thin soil didn't create good conditions for flowstone deposition in the caves, so in cold periods washing of older sediments from caves prevailed, undermining the flowstone growing on them too. Through some entrances cold air could penetrate deep in the underground, shattering the older flowstone crusts or cause flaking of the cave walls or ceilings and causing frost movements.

In Jazbina, the JBRT stalagmite was growing on such a shattered crust arranged into frost polygon. As the crust was 250 Ka old it was deposited in M/R interglacial. After that, in Riss the crust was broken and cryoturbated. Reason for that could very low temperatures of that glaciation or a larger entrance to the cave. Later that entrance was closed, making possible the growth of the stalagmite JBRT during cold Würm climate.

Divaška jama has complex history. In the cave there are two sedimentation phases, but older than the reach of the dating method. In the cave sinter was deposed between the two sedimentation phases before 350 Ka, but the fastest it seems was the deposition in M/R interglacial. The flowstone at what is now entrance to the cave grew at that time. To the same warm period also belongs the large stalagmite which collapsed at 176 Ka, which can be connected with new, Riss cold period which stopped deposition of flowstone and started the washing of the sediments from the base of stalagmite. Collapse of the ceiling and opening of the entrance occurred much later, probably in the Holocene.

References

CUCCHI, F., P. FORTI, 1991: The first absolute datation of a speleothem from Trieste Karst. *Acta carsologica* 18, Ljubljana, 53-64.

GOSPODARIČ, R. 1985: O Speleogenezi Divaške jame in Trhlovce., *Acta carsologica* 13, Ljubljana, 5 - 32.

IVANOVICH, M. & HARMON, R. S., 1992: Uranium series Disequilibrium. Aplications to Earth, marine and Environmental sciences. Clarendon Press, Oxford, 1-910.

KRANJC, A.; J. KOGOVŠEK & S. ŠEBELA, (1992): les Concretionnements de la grotte de Skocjanske (Slovenie) et les changements climatiques. Karst et evolutions climatiques, Bordeaux 355-361,.

LAURITZEN, S. E. 1991: "Age4U2U" Program for Reading ADCAM energy $^{234}Uranium$ ages. Turbo Pascal Code, 5000 lines.

MIHEVC, A. 1984: Nova spoznanja o Kačni jami. *Naše jame* 26, Ljubljana,11-20.

MIHEVC, A. 1994: Contact karst of Brkini hills. *Acta carsologica* 23, (1994), pp. Ljubljana.100-109,

SCHWARCZ, H. P., 1980: Absolute age determination of archaeological sites by uranium dating of travertines. Archaeometry, 22, 3-4.

ZUPAN, N. 1991: Flowstone datations in Slovenia. *Acta carsologica* 20, Ljubljana, 187-204.

Sample.	Sample description	U ppm	$^{234}U/^{238}U$	$^{230}Th/^{234}U$	$^{230}Th/^{232}Th$	Age (Ka) ±1 σ
	Jazbina cave					
1396	C228, base of stalagmite	1.56	2.642	0.139	1084	16.1 ±0.6
1288	C228, below hiatus at 17 cm	1.54	2.597	0.094	660.2	10.6 ±0.2
1385	C228, abowe hiatus at 21 cm	1.6	2.48	0.083	10000	9.3 ±0.2
1292	C228, stalagmite at 149 cm	1.8	2.418	0.068	10000	7.6 ±0.2
1398	C228, stalagmite at 211 cm	1.6	2.432	0.050	10000	5.5 ±0.2
1373	JAZ KS, cryoturbated crust	0.364	1.43	0.931	14.08	240 +40 -30
1393	JBRT1, base of stalagmite	0.26	1.289	0.332	10000	43.1 ±2
1392	JBRT3, stalagmite at 48,5 cm	0.62	1.095	0.128	10000	14.9 ±0.9
1400	JBRT4, stalagmite at 49,8 cm	0.586	1.29	0.044	10000	4.9 ±0.5
	Divaška jama cave					
1242	stalagmite between loam	0.25	1026	1.019	10000	>350
1243	base of small stalagmite	0.24	0.976	0.140	258.0	16.42 ±1 -1
1244	top of small stalagmite	0.20	0.988	0.066	10000	7.48 ±0.8 -0.8
1375	top of collapsed stalagmite	0.24	1.087	0.827	23.966	176.34 +17 -15
1316	flowstone at the entrance	0.06	1.09	0.928	10.372	243.70 +81 -47

Table 1. Uranium series disequilibrium dates of speleothems from caves Jazbina and Divaška jama.

The Isotope Systematics of Perennial Cave Ice in Northwestern Canada

William D. MacDonald[2] and Charles J. Yonge[1,2]

[1]EIUDP, Universitas Sam Ratulangi , PO Box 1357, Manado 95013, Sulawesi Utara, Indonesia. E-mail Yonge@manado.wasantara.net.id. [2]Alberta Karst Institute, Box 8213, Canmore, Alberta, Canada.

Resume

Les glaces permanant de quatre grottes à l'intérieur et à l'est du territoire du "Canadian Great Divide" produisent un $\delta^{18}O$ et un δD plus positives en comparaison avec les précipitations annuelles significatives dans la région. De plus, dans un graphique $\delta^{18}O$ δD, ces données se situent en dessous et le long des lignes ayant une pente moins forte que la Ligne d'Eau Météorlogique Globale. Pour expliquer ces phénomenes observés, nous proposons le processus suivant: un fractionnement isotopique entre la vapeur et la glace, qui change le signal isotopique de la vapeur d'eau en saison chaude, quand se condense le givre à l'entrée des grottes. La chute du givre sur le sol de la grotte à travers une surcharge mécanique, à laquelle s'ajoute la glace qui provient du suintement de l'eau au sol (avec une composition isotopique annuelle significative), résulte en une formation massive de glace de composition multiple. Cette composition multiple est ce qui est observé dans les charactéristiques et les liaisons trouvées. De telles découvertes ont des implications pour l'interprétation climatique des grottes de glaces anciennes, et pourraient aussi contribuer à la compréhension des systèmes d'évaporation et de précipitation qui traversent les chaînes montagneuses.

Cave Ice Isotopic Composition Which Does Not Fall on the Global Meteoric Water Line

Stable isotope measurements, $\delta^{18}O$ and δD, were made on perennial ice from several ice caves in western North America. Three striking features of the data emerge, especially for cave sites west of the Great Divide: firstly, all $\delta^{18}O$ and δD points lie on or to the right of the Global Meteoric Water Line (GMWL), secondly, those points lie on positive slopes less than the GMWL, and thirdly, the ice is more enriched in the "heavy" isotopes than expected. Caves from east of the Great Divide are compared to those on the coastal, eastern side, the latter exhibiting trends more concordant with the GMWL. The cave ice trend away from the GMWL is in general made up of three components. The nearest (and most depleted in ^{18}O and D) points to the GMWL are from seepage or ground water, followed by those from massive floor ice. Finally, hoar ice formed on the walls and ceiling of the cave are most enriched in ^{18}O and D and lie the furthest off the GMWL. The western Caves exhibit isotope enrichments more than that expected for vapour-water-ice fractionation (an enrichment in the ice of around 3‰ in $\delta^{18}O$ and around 14‰ in δD over a water condensate), whereas our hoar frost samples enrichments of up to 8‰ in $\delta^{18}O$ and 60‰ in δD are observed. Therefore, while vapour-ice fractionation must occur, there needs to be an additional enriched moisture source. Water condensed from the cave atmosphere is generally a mean annual average of precipitation falling at the site, and is positively correlated with the site's mean annual temperature, and we might expect the cave ice to be derived from this source except that it is too depleted. Hoar ice therefore appears to be growing mostly from warm moist air entering the cave during the summer months. This warm air being enriched in ^{18}O and D over that of the mean annual average, and being able to carry more moisture than cooler air, supplies the additional moisture source required.

Ice Genesis in the Caves West of the Great Divide

Moist, warm air enriched in ^{18}O and D enters the cave subliming as hoar frost on the walls and ceiling. Over the warm part of the year the hoar builds up to such an extent that it becomes overloaded and falls to the floor. Along with seepage, melting and recrystallization, it reforms as massive floor ice. As a result, this massive ice has a mixed composition between mean annual seepage and warm-season derived hoar ice. For example we determine that 10°C vapour entering the cave and sublimating as hoar ice would yield a mixing line slope less than the GMWL (around 7.1), with enrichments of about 8‰ in $\delta^{18}O$ and 55‰ in δD, which fits our field data very well.

Perennial Cave Ice as Proxy Climate Indicators

How might these results be applied to paleoclimatology? Serendipity Cave in the Crows Nest Pass contains a 15-meter thick plug of massive ice, where guano trapped at a depth of 14.3 meters yields a carbon-14 date of 970 years BP. This site clearly offers the opportunity for an extremely detailed study of the last 1000 years or so, assuming that the isotopic composition of the ice can be interpreted climatologically. While the scenarios can be complex, we find that the caves encountering lower mean annual site temperatures contain massive ice that is more enriched in ^{18}O and D compared to caves sited in a higher temperature regime. It therefore seems to be the extent of hoar ice from warm-season air masses that dominates the changes observed in the composition of massive cave ice. Swings in isotope composition in cave ice sections, interpreted as warming/cooling trends, would then be in the opposite direction to conventional glacial or polar cap cores.

Analysis of ice from Caves west of the Great Divide yields a very different picture; data generally fall close to the GMWL and unusual isotopic enrichments are not observed, actually the reverse. Here, winter snow falling into the cave entrances is preserved in ponded cold air. Recrystallization enhanced by summer rain results in massive ice, but not a complete homogenization of the layers. This means that a muted record of precipitation is recorded and this offers some potential as a proxy paleoclimate indicator. We would interpret swings in isotopic composition in the same way as for polar and glacial ice cores, and thus opposite to records from the eastern divide caves. That is to say that isotope depletion would be associated with a lowering of temperature and vice versa (although we recognize further complexity when considering glacial/interglacial climate transitions). In essence though it appears that we studying two trends; ice derived directly from a vapour source (east divide regime) and ice derived from a water/ice source(west divide regime). Our investigation of perennial cave as proxy climate indicators continues.

Enregistrement de l'activité charbonnière dans les spéléothèmes de Choranche (Vercors, France)

par Yves Perrette, Jean-Jacques Delannoy, Dominique Genty, Jean-Luc Destombes et Yves Quinif
Université Joseph Fourier, Institut de Géographie Alpine, Grenoble (France)
U.R.A. 723 du C.N.R.S., Laboratoire d'hydrologie et de géochimie isotopique, Orsay (France)
U.R.A. 249 du C.N.R.S., Laboratoire de Spectrométrie Hertzienne, Lille (France)
Centre d'Etude et de Recherche Appliquée au Karst, Mons (Belgique).

Abstract

The study of the summital part of an active speleothem extracted from the Coufin-Chevaline cave (Choranche, Vercors, France) permits one to establish a link between the impact of human activities on the plateau des Coulmes karst and crystalline characteristics. The application of different methods (digital image processing, laser reflectance and laser induced luminescence) helps to describe crystalline inclusions (charcoals and clays) and crystalline fabrics. The yearly alternantions allows us to validate the quality of the speleothem recording. We show how the internal structure of speleothem keeps the mark of charcoal burning developement during the XIXth century. This study points out the possibilities offered by speleothems in the precise definition of environemental evolutions.

Résumé

L'étude de la partie sommitale d'une stalagmite active de Coufin-Chevaline (Choranche, Vercors, France) a permis d'établir une relation entre l'impact des occupations humaines sur le plateau karstique des Coulmes et diverses caractéristiques de la fabrique cristalline. L'application de différentes méthodes (traitement numérique d'image, mesure de la réflectance et de la luminescence laser) a aidé à la description fine des différentes fabriques cristallines et inclusions intercristallines (charbons de bois, argiles). Le comptage des alternances annuelles continues sur cette partie, a permis de valider la relation entre les modifications cristallines et les activités humaines, notamment le développement des charbonnières durant le XIXème siècle. Cette étude montre les possibilités qu'offrent les spéléothèmes dans la définition des conditions environnementales sur un pas de temps historique.

mots clés : spéléothèmes, lamines, impacts anthropiques, Vercors, France

Introduction

L'intérêt révélé par les concrétions endokarstiques – spéléothèmes – dans les études paléoenvironnementales est aujourd'hui reconnu. Au travers de leur présence/absence, comme au travers des datations isotopiques U/Th ou ^{14}C leur prise en compte est devenue habituelle. Depuis le début des années 1990, les informations contenues dans la structure interne des spéléothèmes sont de plus en plus étudiées (WHITE, W. et BRENAN, S., 1989 ; MAIRE, R., 1990 ; GENTY, D., 1992, 1994 ; ROUSSEAU, L., 1992 ; BAKER, A. et al., 1993 ; SHOPOV, Y.-Y. & al., 1990, 1991, 1994). La meilleure compréhension du transfert des informations environnementales dans cette structure interne permet aujourd'hui d'utiliser l'outil "spéléothème" en vue de la connaissance des évolutions environnementales passées.

L'objet de cet article est de présenter la démarche qui a permis de déceler l'empreinte laissée par les activités humaines développées sur le plateau des Coulmes (Vercors, France) depuis la période de la Renaissance (acception historique). Après avoir présenté brièvement les méthodes utilisées lors de cette étude, nous poserons les hypothèses qui ont sous-tendu ce travail. Enfin, par le biais de l'étude stratigraphique fine d'un échantillon stalagmitique prélevé dans la grotte de Coufin-Chevaline (Choranche, Vercors, France), nous verrons comment la calcite a enregistré l'évolution environnementale connue de ce massif.

1. Présentation du site et de la méthode

Les différents aspects méthodologiques de ce travail qui font l'objet d'une autre communication (PERRETTE, Y. & al., 1997) ne seront pas décrits précisément ici.

1.1. Site d'échantillonnage

Le carottage a été réalisé verticalement sur un édifice stalagmitique de type tam-tam de la salle de la Cathédrale du réseau de Coufin-Chevaline (Choranche, Vercors, France). Plusieurs raisons ont déterminées le choix de cette salle et de cet édifice. La raison nécessaire à cette étude est l'accueil et l'intérêt porté à nos travaux par Mr Mantovani et son équipe de guides. Cette salle est située dans la partie touristique du réseau spéléologique. L'édifice est donc à proximité de l'escarpement qui forme le cirque de Choranche (fig. 1). La décompression importante dans cette partie du massif doit, en ouvrant le réseau de fissuration, laisser circuler des particules diverses qui seront piégées dans le dépôt carbonaté. L'ancienneté de cette salle (DELANNOY, J.-J. & al., 1988), sa stabilité mécanique permettent de considérer le fonctionnement de l'édifice comme étant stable durant la période considérée. L'édifice carotté est actif ce qui permet un calage chronologique "par le haut". Pour clore cette liste non-exhaustive des raisons ayant guidé ce choix, on peut rappeler que le plateau des Coulmes est étudié depuis le début des années 1980 par des karstologues (DELANNOY, J.-J., 1981) mais aussi des palynologues (THIEBAULT, S.,1991), préhistoriens (BINTZ, P , 1980 in DELANNOY, J.-J. & al., 1988), etc.

L'étude relatée ici s'est donc attachée à la lecture des informations paléoenvironnementales contenues dans la partie sommitale de l'échantillon (fig. 1). Pour cela différents outils ont été utilisés en vue de la stratigraphie fine de l'échantillon.

1.2. Méthode

Après sciage , la section verticale a été polie en vue de l'analyse stratigraphique. Celle-ci s'est attachée à la description pétrographique de l'échantillon en observant tout particulièrement le type de fabrique cristalline, la coalescence intercristalline, la couleur et l'opacité de la calcite ainsi que les diverses inclusions piégées dans le réseau cristallin. Les observations ont été réalisées à la loupe binoculaire avec un grossissement de 4× à 40×. De nombreux comptages d'alternances ont été réalisés ce qui a permis d'évaluer l'âge approximatif des différentes informations. Ce comptage a été manuel dans un premier temps, puis assisté par ordinateur selon la méthode développée par GENTY, D. (1992).

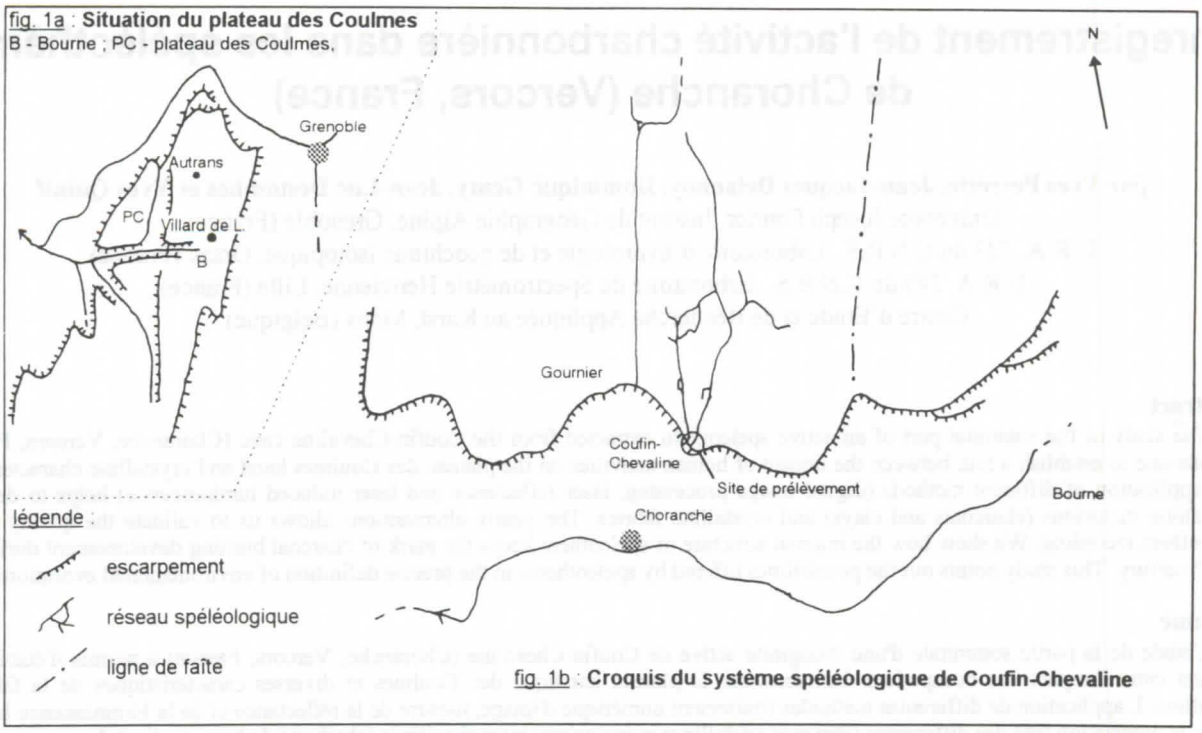

Figure 1 : Situation de Choranche et site de prélèvement.

Afin de diversifier les données collectées lors de la stratigraphie, différentes méthodes spectroscopiques ont été mises en oeuvre : mesure de la réflectance laser, de la luminescence laser (excitation à λ = 450 nm, mesure pour $\lambda > 550$ nm). Afin de valider certaines observations, des déterminations à la sonde Raman ont été réalisées. L'utilisation de ces outils variés en vue de la stratigraphie fine de l'échantillon a nécessité de clarifier les apports et limites de chacun d'eux dans ce type d'objectifs. La démarche ayant conduit à limiter leurs apports, à envisager leur articulation au sein de cette étude fait l'objet d'une communication dans ce même congrès.

2. Hypothèses et connaissances sous-tendant l'analyse stratigraphique

Un certain nombre de connaissances acquises depuis le début des années 90, d'hypothèses relatives au site étudié nous ont permis de lire les informations spéléothémiques. La première a déjà été énoncée; il s'agit de l'homogénéité du mode de fonctionnement de l'édifice durant la période considérée. Poser cette hypothèse permet de considérer que les évolutions révélées dans la croissance, dans les couleurs de la calcite sont "directement" imputables à des modifications environnementales.

La deuxième hypothèse est relative à la notion d'impluvium du spéléothème. On suppose que les informations collectées sont globales. Cette globalité est envisageable en raison du pendage généralement peu important des strates du massif.

La troisième hypothèse est relative à la mise en place des alternances et à l'incidence des acides humiques dans la croissance des spéléothèmes. En 1992, D. Genty montre au travers de l'étude d'une stalagmite actuelle du tunnel de Godarville (Belgique) que l'annualité des alternances – lamine sombre et compacte (D.C.L.) et lamine claire et poreuse (W.P.L.) - est due à la différenciation entre deux phases de croissance : l'une rapide (W.P.L.) et l'autre lente (D.C.L.). Ces deux phases sont corrélées, dans le cas du tunnel de Godarville, aux variations de l'excédent hydrique. Depuis, la variation de la luminescence dans l'ultra-violet des différentes lamines a été étudié (Baker, A. & al., 1993 ; White, W. et Brenan, E.-S., 1989 ; Shopov Y.-Y. & al., 1990, 1991, 1994). Cette luminescence est imputable à la présence d'acides humiques. Le rôle de ces macromolécules n'est pas encore bien cerné. Au cours de cette étude on considère que la mise en place des alternances est causée par le couple excédent hydrique/présence d'acides organiques. Cette hypothèse est essentielle dans la compréhension des évolutions de la couleur macroscopique ainsi que dans la domination de telle ou telle lamine dans l'alternance.

La quatrième des hypothèses majeures sous-tendant cette étude est liée à l'hypothèse précédente. On associe couleur macroscopique[1] et porosité cristalline, porosité cristalline et présence du couple acides humiques/excédent hydrique.

Ces différentes hypothèses ont permis de mettre en évidence diverses informations relatives aux évolutions environnementales du plateau des Coulmes depuis le XVème siècle jusqu'à aujourd'hui.

3 . Observations et interprétations

La figure 2 présente les principales observations collectées lors de l'analyse stratigraphique de la partie sommitale de l'échantillon stalagmitique prélevé dans la salle de la Cathédrale du réseau de Coufin-Chevaline. Avant de voir de quelle façon l'évolution historique environnementale du plateau des Coulmes a marqué la cristallisation du spéléothème étudié, on peut décrire quelques résultats important.

3.1. Résultats globaux

On peut dans un premier temps chercher à interpréter l'évolution globale de la couleur macroscopique de la calcite. De la zone (a4) vers le sommet on passe d'une calcite blanche laiteuse (dominante WPL) à une calcite pure transparente (dominante DCL). Le passage d'un faciès à l'autre semble se faire progressivement au sein de la zone (a2). Cette évolution progressive est révélée par la modification continue de

[1] On ne se réfère ici qu'aux spéléothèmes dont la coloration n'est pas imputable à la présence d'oxydes de fer de cuivre, etc.

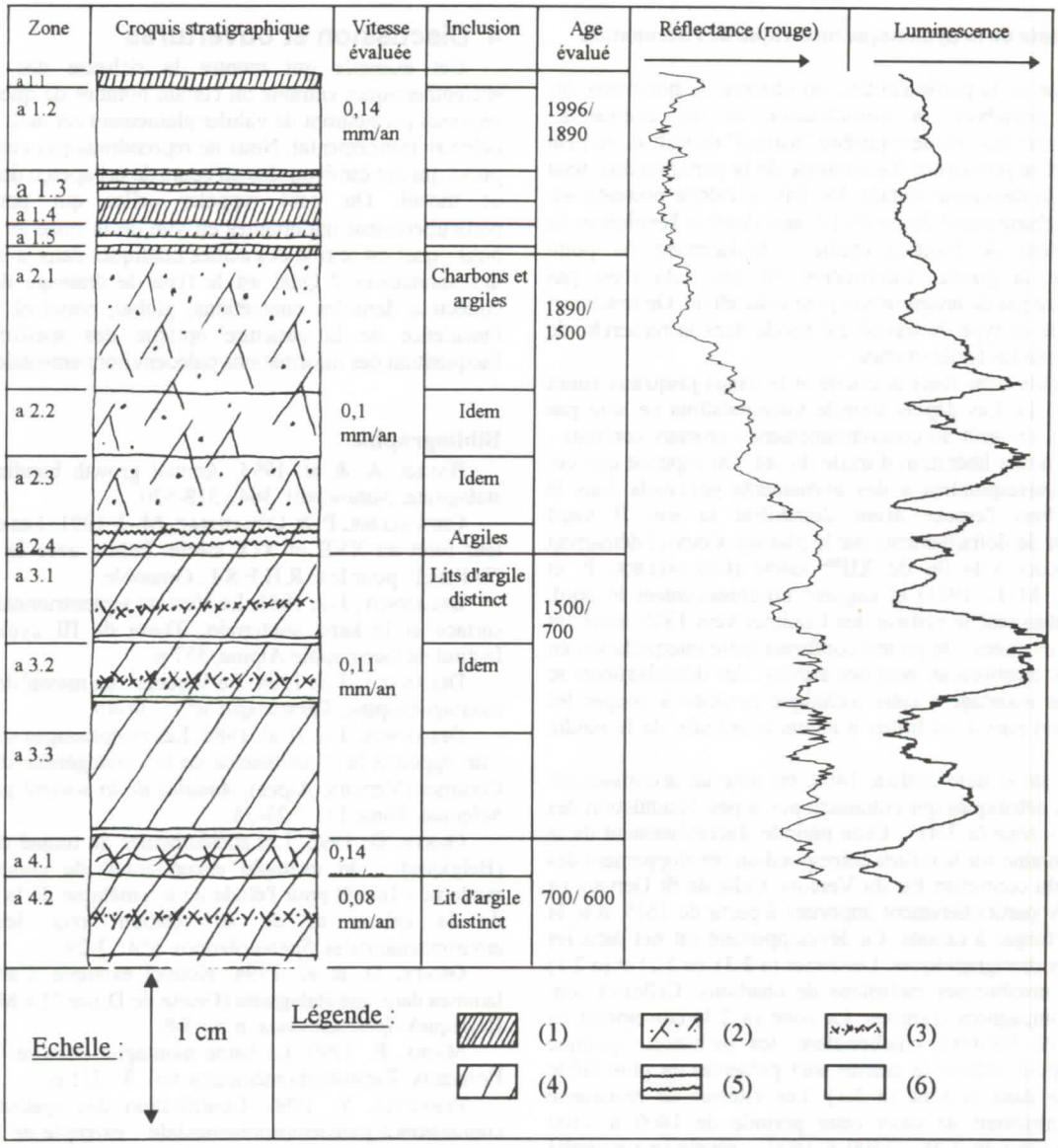

Figure 2 : Principaux résultats de l'analyse stratigraphique de la partie sommitale de l'échantillon étudié

Légende (1) Calcite blanche transparente à dominante WPL ; (2) Mauvaise coalescence cristalline avec grandes faces de cristaux et inclusions ; (3) Zone à mauvaise coalescence engendrée par un niveau d'argile ; (4) Calcite blanche laiteuse opaque, dominante WPL ; (5) Zone à alternances ondulées ; (6) Calcite pure et transparente, dominante DCL

l'enregistrement de la réflectance dans le rouge. Cette mesure donne des informations sur la couleur de la surface étudiée mais aussi sur sa structure optique. La zone (a2) dont la couleur grise provient des nombreuses inclusions de charbons (confirmé par analyse à la sonde Raman), masque cette transition.

La connaissance de l'évolution environnementale du plateau nous permet de valider les hypothèses posées lors de ce travail. On envisage donc cela comme une modification du couvert végétal et/ou comme une modification globale de la valeur des excédents hydriques. Il n'est sans doute pas nécessaire de trancher entre ces deux hypothèses qui semblent intimement liées. Quoiqu'il en soit, la connaissance historique de l'occupation du plateau des Coulmes permet d'opter pour l'évolution du couvert végétal. Durant le développement de l'activité des charbonnière, la forêt en place, majoritairement constituée d'essences résineuses a été peu à peu remplacée par du taillis - caducifolié - permettant un rendement suffisant quantitativement et qualitativement. Les études palynologiques confirment bien la dominance des espèces résineuses dans cette partie du Vercors à la fin de l'holocène (THIEBAULT, S. 1991). L'optimum climatique de 1300 ans révélé par les études historiques est lui aussi marqué dans la calcite : la translucidité de la zone (a3.1), révélé par l'observation des échantillons mais aussi par les mesures de réflectance et de luminescence est interprétable comme une modification de la structure optique de l'échantillon. De fait, la baisse de signal enregistré dans cette zone n'est pas imputable à la couleur macroscopique qui y est homogène La modification serait ici due à la baisse de l'excédent hydrique.

On le voit, la structure cristalline de la calcite comme le type d'alternance révèlent de nombreuses informations. L'étude des vitesses de croissance, très globale ne permet pas d'affiner ces interprétations. On peut simplement noter que les vitesses de croissances entre les zones (a1) et (a3) sont assez proches bien que l'une soit constituée d'alternances à dominante DCL et l'autre d'alternances à dominante WPL. De plus, l'étude fine des alternances de la zone (a1) a montré que les séquences constituées de dominantes DCL correspondaient aux vitesses de croissance les plus importantes (de 0,2 contre moins de 0,08 mm/an). L'exploitation de cette partie des informations spéléothémiques est en cours de réalisation. L'intérêt majeur de ce type d'étude ne se situe pas dans cette relecture des évolutions environnementales mais dans la lecture de leurs interactions avec l'occupation humaine du plateau des Coulmes.

3.2. Empreinte de la dynamique historique de l'occupation humaine

A la base de la partie étudiée, on observe de nombreux lits détritiques perturbant la cristallisation et les alternances. Occupation humaine ou déséquilibre "naturel" du milieu, on peut difficilement se prononcer. Le contexte de la partie étudiée tend plutôt vers la deuxième lecture. De fait, la calcite présente au-dessous un changement de faciès lié sans doute à l'évolution du fonctionnement de l'édifice étudié : déplacement du point d'impact de la goutte. Information en soi, cela n'est pas exploitable au pas de temps retenu pour cette étude. On touche ici une limite de ce type de travail qui réside dans la recherche de continuité dans les faciès étudiés.

On remonte donc dans la calcite et le temps jusqu'aux zones (a3.2) et (a3.1). Les dépôts d'argile intercristallins ne sont pas imputables à un arrêt du concrétionnement - cristaux continus - mais plutôt à une libération d'argile du sol. On suppose que ces libérations correspondent à des événements ponctuels dans le temps et dans l'espace ayant déstabilisé le sol. Il s'agit certainement de défrichements sur le plateau. Ceux-ci démarrent au sud-Vercors à la fin du XIIème siècle (CHEVALLIER, P. et COUAILHAC, M.-J., 1991) et gagnent progressivement le nord. Ainsi, ils atteignent le plateau des Coulmes vers 1300 selon les croissances évaluées. On pourra confirmer cette interprétation en décelant des charbons au sein des argiles : les défrichements se faisaient par essartage ; cette technique consiste à couper les arbres (taillis) puis à les brûler à même le sol afin de le rendre plus fertile.

A partir de la date évaluée 1400, on note un accroissement des niveaux détritiques qui entraînent peu à peu l'ondulation des alternances - zone (a 2.4) -. Cette période d'accroissement de la pression humaine sur le milieu correspond au développement des communes du contrefort Est du Vercors. Celle de St Gervais va jouer un rôle particulièrement important à partir de 1619 avec la création de forges à canons. Ce développement est net dans les observations stratigraphiques. Les zones (a 2.3), (a 2.2) et (a 2.1) recèlent de nombreuses inclusions de charbons. Celles-ci sont parfois accompagnées d'argiles. La zone (a 2.3) correspond au démarrage de l'activité charbonnière, les inclusions quoique suffisantes pour colorer la calcite sont présentes en plus faible quantité que dans la zone (a 2.1). Les vitesses de croissance évaluées permettent de caler cette période de 1400 à 1500 environ. La zone (a 2.2) – 1500 à 1600 – révèle une quantité assez faible de charbons, ralentissement ou déplacement de l'activité? La zone (a 2.1) correspond au maximum de l'activité qui cesse brutalement à la fin du XIXème siècle. Cette période correspond de même à la pente maximum de la réflectance et à la chute de la luminescence attribué à la modification du couvert végétal. Tout cela tend à montrer l'incidence du fonctionnement des forges et autres industries ayant contribué à écouler le charbon produit sur le plateau des Coulmes ; les forges de St Gervais cessent toute activité en 1869.

La zone (a 1) correspond à l'histoire de l'occupation humaine de ce siècle. La zone (a 1.6) correspond à la relaxation du système face au déséquilibre du à l'activité charbonnière ; celui-ci n'a pas été étudié en détail. Nous sommes néanmoins conscients de l'intérêt de cette information : cette relaxation est-elle propre au système karstique, à cet édifice, est-il possible de retrouver ce type d'indicateurs dans tous les édifices laminés ? En ce qui concerne la croissance globalement plus rapide, on peut la corréler à la fin du petit âge glaciaire. Les inclusions quasiment inexistantes révèlent l'histoire de la dépression de l'homme sur ce milieu. La pureté de la calcite n'est pas expliquée vraiment. Une hypothèse plausible tend à l'imputer à l'absence de sol et à la production très discontinue d'acides humiques. Cette hypothèse pose problème face à l'étendue de ce phénomène qui est relevé dans de nombreux autres massifs.

4. Discussion et ouvertures

Cet exemple qui montre la richesse des informations spéléothémiques entraîne un certain nombre de questions. Leurs réponses permettront de valider pleinement cet outil de recherche paléoenvironnemental. Nous ne reprendrons pas ces questions et pistes qui ont été évoquées au cours de cet aperçu des résultats de ce travail. On peut rappeler celles qui nous semblent particulièrement importantes en vue de la mise au point de cet outil : quel est le rôle des acides humiques dans la mise en place des alternances ? Quel est le type de drainage des particules collectées dans les concrétions, global, ponctuel ? Quelle est l'incidence de la structure optique des spéléothèmes dans l'acquisition des informations paléoenvironnementales ?

Bibliographie

BAKER, A. & al. 1993. Annual growth banding in a cave stalagmite. *Nature*. vol. 364 :.518-520.

CHEVALLIER, P. & COUAILHAC, M.-J. 1991. Les dauphinois et leur forêt au XVII et XIX siècle. Publié avec le concours de l'U.P.M.F. pour le C.R.H.E.S.I.. Grenoble.

DELANNOY, J.-J. 1981. Le Vercors septentrionnal : le karst de surface et le karst souterrain. Thèse de III cycle. Grenoble. Institut de Géographie Alpine, 537 p.

DELANNOY, J.-J. 1984. Le Vercors : un massif de la moyenne montagne alpine. *Karstologia*. n°3 :. 34-45.

DELANNOY, J.-J. & al. 1988. Les remplissages spéléologiques : un apport à la connaissance de la karstogénèse du massif des Coulmes (Vercors, Alpes). *Annales de la société géologique de belgique*. Tome 111 : .21-38.

GENTY, D. 1992. Les spéléothèmes du tunnel de Godarville (Belgique) - un exemple exceptionnel de concrétionnement moderne - Intérêt pour l'étude de la cinétique de la précipitation de la calcite et de sa relation avec les variations environnementales. *Spéléochronos*. n°4 :.3-29.

GENTY, D. & al. 1994. Nouvel exemple d'alternances de lamines dans une stalagmite (Grotte de Dinan "La Merveilleuse", Belgique). *Spéléochronos*. n°5 :.3-8.

MAIRE, R. 1990. La haute montagne calcaire. Thèse d'état, Bordeaux. Karstologia mémoires. vol..3 : 731 p.

PERRETTE, Y. 1996. Contribution des spéléothèmes à la connaissance paléoenvironnementale : exemple de l'étude de la structure interne d'une stalagmite du réseau de Coufin-Chevaline (Choranche, Vercors, France). Mémoire de maîtrise dirigé par Delannoy, J.-J.. Université Joseph Fourier. Grenoble I. Grenoble 188 p.

PERRETTE, Y. & al. 1997. Characterisation of speleothem crystalline fabrics by spectroscopic and digital image processing methods (Choranche, Vercors, France). *Proc. of the Internationnal Speleological Congres*, symposium 07.

ROUSSEAU, L. 1992. Etude physico-chimique et minéralogique des planchers stalagmitiques du pléistocène moyen. Doctorat du museum national d'histoire naturelle à l'institut de paléontologie humaine, Paris.

SHOPOV, Y.-Y. & al. 1990. Microzonality of luminescence of cave flowstones as a new indirect index of solar activity. *Comptes rendus de l'Académie bulgare des Sciences*, Tome 43-7 : 9-12.

SHOPOV Y.-Y. & al. 1991. One new indirect solar activity index. *Geomagnetism and Aeronomy*, vol.31, n°5,.739-740.

SHOPOV, Y.-Y. & al. 1994. Luminescent microbanding in speleothems : high-resolution chronology and paleoclimate. *Geology*. vol.22 :.404-410.

THIEBAULT, S. 1991. Approche de l'environnement végétal préhistorique pendant la fin du tardiglaciaire et l'Holocène entre Alpes et Jura par l'analyse anthracologique,. *Quaternaire*. vol. 2 : 49-58.

WHITE, W. & BRENNAN, E.-S. 1989. Luminescence of speleothems due to fulvic acid and other activators. *Proc. of the Internationnal Speleological Congress*, vol.10 : .212-214.

Influence of the Bedrock CO_2 on Stable Isotope Records in Cave Calcites

By Yavor Y. Shopov, Ludmil T. Tsankov
Section Speleology & Faculty of Physics, University of Sofia, James Baucher 5, Sofia 1164, Bulgaria, E-mail: YYShopov@Phys.Uni-Sofia.BG

Charles J. Yonge, H.P.Roy Krouse
Dept. of Physics & Astronomy, University of Calgary, Calgary,Alberta T2N 1N4, Canada

A.J. Timothy Jull
NSF- Arizona AMS Facility, Physics building 81, The University of Arizona, Tucson, Arizona 85721, USA

Abstract

This paper is a first study of the influence of variations of bedrock fraction in speleothem calcite on $\delta^{18}O$ and $\delta^{13}C$ records in speleothems. It is demonstrated that this influence can explain all $\delta^{13}C$ variations and can produce a substantial part of $\delta^{18}O$ variations in speleothems.

In both $\delta^{13}C$ and $\delta^{18}O$ records higher surface temperature produces higher values in the speleothem, because the bedrock itself has high positive values of both $\delta^{13}C$ and $\delta^{18}O$.

Introduction

Speleothems (stalactites, stalagmites, etc.) are secondary cave calcite aggregates growing continuously up to a million years. They incorporate in their structure number of impurities, elements and isotopes which held important paleoenvironmental information (SHOPOV ET AL., 1991, SHOPOV, 1996). Once formed, the speleothems preserve these records and they can be read out by different techniques. Speleothems are formed at almost constant temperature and humidity and remain unchanged with time. The speleothem records can be read with a remarkably high resolution (SHOPOV ET AL, 1994). So the speleothems appear to be one of the best paleoenvironmental archives known so far.

Paleoclimatic Records by Stable Isotopes

Records of stable isotopes δD, $\delta^{13}C$ and $\delta^{18}O$ in speleothems hold paleoclimatic information. δD and $\delta^{18}O$ values in precipitations are function of the air temperature (FAURE, 1987). δD from fluid inclusions in speleothems gives good records (YONGE ET AL., 1985) of the paleotemperature during speleothem growth, because there is no isotopic exchange with the bedrock. Far more complicated are the records of $\delta^{13}C$ and $\delta^{18}O$ in speleothems, because they can be supplied both from the surface and from the bedrock. The influence of the bedrock fraction (which varies from 6 to 85%) in these records usually is underestimated because it is considered to be constant with the time (SCHWARCZ, 1986, HARMON ET AL, 1978, TALMA ET AL., 1992). But JAKUCS (1977) demonstrated that the bedrock fraction in the karst waters varies several times with the climatic variations (during glacial-interglacial transitions), due to the variations of non-carbonate karst denudation produced by acids (mainly biogenic) and other inorganic minerals. Other factor producing variations of the bedrock fraction arises from the fact that the saturation degree of karst solutions (by bedrock calcite) depends exponentially on the temperature, because the dissolving rate has the same functional dependence.

Traditional explanation of $\delta^{13}C$ variations by C3-C4 type plants variations (TALMA, 1992) cannot explain the observed temperature dependence of $\delta^{13}C$ (SHOPOV ET AL., 1994, SHOPOV ET AL. in press) in the speleothems.

This paper is a first study of the influence of the variations of bedrock $\delta^{13}C$ and $\delta^{18}O$ fraction in speleothem calcite. Bedrock itself does not contain any ^{14}C because it is completely decayed due to the old age of bedrocks, so the bedrock fraction in speleothems is called "dead carbon".The ^{14}C concentration is good tracer of the bedrock carbon fraction in speleothems. It can be determined experimentally. ^{14}C and ^{13}C have similar isotopic behavior (fractionation) in the karst environment; so the dead carbon fraction of ^{14}C is identical to the bedrock fraction of ^{13}C in speleothems.

Determination of the fraction of modern and "dead" (bedrock) carbon in speleothem calcite can be achieved by two methods:

1. By ^{14}C and independent absolute dating:
Measured ^{14}C activity from a speleothem of age t_r is:

$$A_m = A_0 \exp(-\lambda t_m)$$

Real (specific) ^{14}C activity which should be obtained from calcite of the same age, but containing 100% modern carbon (at times of its precipitation) is:

$$A_r = A_0 \exp(-\lambda t_r),$$

where t_m is the measured ^{14}C age and t_r is the real age of the speleothem, determined by an independent absolute dating method, λ is the decay constant of ^{14}C and A_0 is the initial activity of the modern ^{14}C.

$$A_m = A_r . M , \qquad (0)$$

where M is fraction of modern carbon in the speleothem or seepage water. Therefore:

$$M = \exp [-\lambda(t_m - t_r)], \qquad (1)$$

and the fraction of "dead" carbon in the speleothem or seepage water is:

$$D = 1 - M, \qquad (2)$$

or

$$D = 1 - \exp[-\lambda(t_m - t_r)] \quad (3)$$

A precise determination of participation of modern and "dead" carbon in speleothem calcite can be done using eq.(1) and (3).

2. By measurements of $\delta^{13}C$ of the bedrock ($\delta^{13}C_r$), soil water ($\delta^{13}C_s$), cave seepage waters ($\delta^{13}C_{mw}$) or speleothem ($\delta^{13}C_m$):

$$\delta^{13}C_m = M \cdot \delta^{13}C_s + (1 - M) \cdot \delta^{13}C_r \quad (4)$$

and

$$M = (\delta^{13}C_m - \delta^{13}C_r) / (\delta^{13}C_s - \delta^{13}C_r) \quad (5)$$

Determination of participation of modern and bedrock carbon in speleothem calcite (presuming that $\delta^{13}C_s$ did not changed significantly from present day value) can be done using eqs. (5) and (2). Obtained data can be used to derive a precise estimate for the absolute age of the speleothem by eq.(0) from ^{14}C dating and a determination of M (by measuring $\delta^{13}C_s$, $\delta^{13}C_r$ and $\delta^{13}C_m$) of the same sample.

In the case when data on $\delta^{13}C_r$ are not available its average value for marine sediments of 0.6 ± 1.55 Per. mil. PDB can be used .

Equation (4) can be used to calculate $\delta^{13}C_s$ or $\delta^{13}C_r$ and system of these equations (for several samples from one cave) to calculate both.

For $\delta^{18}O$ equation (4) has the form:

$$\delta^{18}O_m = M \cdot \delta^{18}O_s + (1 - M) \cdot \delta^{18}O_r \quad (6)$$

Close to $\delta^{18}O_s$ is $\delta^{18}O_p$ for precipitation, which can be calculated from average annual surface temperature from the equation:

$$\delta^{18}O_p = s \cdot T - i, \quad (7)$$

where T is the air temperature [^{0}C], s- is the slope of the linear dependence and i- is its intercept. s- and i- must be determined experimentally for every region. For Calgary region (including Rats Nest and Castleguard caves) this equation have the form:

$$\delta^{18}O_p = 0.38 \cdot T - 19.5 \quad \text{(eq.(6) of YONGE ET AL (in press)).}$$

This equation is regional and using it here for calculation of Table 1 is just to illustrate the bedrock influence on speleothem $\delta^{18}O_m$.

Climate	Glacial	Periglacial	Temperate	Mediterr.	Tropical	Desert
Average Annual Air Temperature (^{0}C)						
	0	0	8	15	25	25
Participation of Bedrock Carbon in speleothems (calculated after JAKUCS 1977) dissolved by:						
Inorganic CO2	9	5	9	8	2.5	15
Acids	9	20	30	33	47	55
Total bedrock CO2	18	25	39	41	49.5	70
Active (modern) Carbon						
Surface CO2	82	75	61	59	50.5	30
Additional CO_2 in respect to bounded (%), for 300 mg/l $CaCO_3$						
	27	27	33.9	41.6	55.1	55.1
Calculated equilibrium participation in speleothem calcite (%)						
Dead C	48	52	57.6	56.6	58.5	73
Active C	52	48	42.4	43.4	41.5	27
Calculated equilibrium $\delta^{13}C$ (PDB) in speleothem calcite (for $\delta^{13}C$ = 0 Per. mil. PDB for bedrock and $\delta^{13}C$ =-10 for soil CO_2)[1]						
	-5.2	-4.8	-4.2	-4.4	-4.2	-2.7
(for $\delta^{13}C$ = 0 Per. mil. PDB for bedrock and $\delta^{13}C$ =-16.7 for soil CO_2)[2]						
	-8.6	-8	-7.1	-7.2	-6.9	-4.5
Calculated $\delta^{18}O$ (SMOW) in precipitation for given temperatures[3]						
	-19.5	-19.5	-16.5	-13.8	-10	-10
Calculated equilibrium $\delta^{18}O$ (SMOW) in speleothem calcite (for rock $\delta^{18}O$ = 28.6 Per mil. (SMOW))						
in (SMOW)	3.6	5.5	9.5	10.2	12.6	18.2
in (PDB)	-26.4	-24.6	-20.7	-20	-17.7	-12.3

Table 1. Origin of CO_2 in karst denudation and speleothem calcite and calculated values of $\delta^{13}C$ and $\delta^{18}O$ in speleothem calcite with given contend of bedrock and modern carbon:

[1]- this value of soil $\delta^{13}C$ is calculated from $\delta^{13}C$ of cave seepage waters and modern speleothems in Rats Nest cave (our data) and Castleguard cave, Alberta, Canada (after GASCOYNE & NELSON, 1983) with correction for "dead" carbon derived from ^{14}C and U/Th dates.

[2]- average value of soil $\delta^{13}C$ measured by TALMA & VOGEL, (1992) above Cango caves, South Africa.

[3]- calculated by equation (6) of YONGE ET AL., (in press).

These equations were used to calculate Tables 1 and 2. To estimate the bedrock carbon fraction (equilibrium participation) in Table 1 we took into account, that the amount of additional CO_2 necessary to dissolve one unit of bedrock $CaCO_3$ is temperature dependent (JAKUCS, 1977). All additional CO_2 is modern, while 50% of bonded CO_2 (in dissolved $CaCO_3$) is bedrock and 50% is modern carbon. Tables 1 and 2 suggest that variations of the fraction of the bedrock carbon in speleothems can explain all variations of $\delta^{13}C$, without involving any changes in C3 and C4 plant types. This influence can produce a substantial part of $\delta^{18}O$ variations in speleothems. $\delta^{18}O$ records probably are result of both variations of bedrock fraction in the speleothem and variations produced by temperature and rainfall variations.

In both $\delta^{13}C$ and $\delta^{18}O$ records higher surface temperature produces higher bedrock participation (due to higher non-carbonate denudation (JAKUCS, 1977) producing higher fraction of bedrock carbon) and higher values in the speleothem, because the bedrock has positive values of both $\delta^{13}C$ and $\delta^{18}O$. Higher temperatures also produce higher degree of saturation of percolating solutions by bedrock carbonate, because the saturation rate depends exponentially on the temperature.

In some semi-arid regions like Israel the observed negative correlation between paleotemperature and $\delta^{18}O_m$ is due to local air circulation peculiarities (FRUMKIN ET AL., 1996).

Some speleothems exhibit negative correlation between $\delta^{13}C_m$ and paleotemperature (SHOPOV ET AL, in press). It can be explained by the following way: Main part of CO_2 in karst waters come from soils (JAKUCS, 1977). In soils there are two sources of CO_2 (FAURE, 1987):

(1) respiratory, which is enriched by ^{13}C, and
(2) CO_2 formed by soil decomposition (which is depleted to ^{13}C).

The rate of soil decomposition (producing CO_2 of type (2)) is exponentially dependent on temperature thus producing anticorrelation between $\delta^{13}C_m$ and paleotemperature. In average the amount of CO_2 of types (1) and (2) in soils is equal (FAURE, 1987). But in some places type (2) can dominate if the region is covered only by grass and is heated directly by solar irradiation. Indeed the region with such negative correlation is covered by grass and soil temperature reach 55°C during summer times (SHOPOV ET AL., in press).

Evidently in such cases with negative correlation described dependencies prevail over bedrock fraction variations.

Sample	Modern C [%]	"Dead" C [%]	$\delta^{13}C_m$ [PDB]	$\delta^{13}C_s$ [PDB]	$\delta^{13}C_r$ [PDB]	$\delta^{18}O_{rc}$ [SMOW]	$\delta^{18}O_m$ [SMOW]	$\delta^{18}O_c$ [SMOW]
Temperate region- Rats Nest cave, Alberta, Canada (T_{av} = 2.8°C) (Precipitation $\delta^{18}O_p$ = -18.4 SMOW, bedrock $\delta^{13}C_r$ = 2.82 PDB)								
RNC-1w	93.2±0.5	6.8±0.5	-8.9	-9.8c	2.82m	28.7	-19.1	
RNC-2w	92±0.5	8.0±0.5	-8.9	-9.9c	2.82m	32.1	-19.5	
RNC-3w	85.7±0.5	14.3±0.5	-8.7	-10.6c	2.82m	26.0	-19.5	
RNC-F3	53.9	46.1	-3.66*	N.A.	2.82m	N.A.	14.51	
RNC-G2	52.1	47.9	-3.35*	-10.1	2.82m	N.A.	13.87	
Periglacial Region:-Castleguard cave, Alberta, Canada (T_{av} =-2.1°C) (Precipitation $\delta^{18}O_p$ = -20.3 SMOW, bedrock $\delta^{18}O_c$ = +28.6 SMOW presumed) (calculated after GASCOYNE & NELSON, 1983)								
GG1	36	64	0	-5.9c	3.3c	N.A.	14.5	11
GG2	29.5	70.5	-0.6	-10.0c	3.3c	N.A.	14.6	14.2
GG2Ew	60	40	-4.1	-9.0c	3.3c	N.A.	N.A.	-0.7
Semi-desert Region:-Cango caves, South Africa, (T_{av} = 17.5°C) (Precipitation $\delta^{18}O_p$ = -12.9 SMOW (calculated), presumed bedrock $\delta^{13}C_r$ = 0 PDB) (calculated after TALMA & VOGEL,1992)								
V3	38.3±4x	61.7±7x	-6.4	-16.7m ±2			25.4	
drip w							-5.2 -5.8	

Table 2. Sources of Carbon and Oxygen in speleothem calcite. Content of modern and "dead" carbon in seepage water and speleothems, calculated from precise ^{14}C and U/Th dating by eqs.(1) and (3) and

^{x}- from measured $\delta^{13}C_s$, $\delta^{13}C_r$ and $\delta^{13}C_m$ after eqs.(5) and (2). All isotope data are in Per. mil. Indices mean: m- measured, s- soil, r- bedrock, c- calculated from eq.(4) or (6), or systems of these equations, p- precipitation, rc- calculated bedrock content, w- water sample, av- average annual,

*- this value is obtained from a place near the ^{14}C sampling place, but not from the same material. $\delta^{18}O_p$ is calculated by equation (6) of YONGE ET. AL., (in press).

Conclusion

The influence of variations of the bedrock fraction in speleothem calcite on $\delta^{13}C$ and $\delta^{18}O$ records can explain all observable $\delta^{13}C$ variations and can produce a substantial part of $\delta^{18}O$ variations in speleothems.

Acknowledgements

A part of this research was supported by Research Grant 439 to Y. Shopov from Bulgarian Science Research foundation. We thank to Dr. D.C. Ford, Dr. H.P. Schwarcz and Dr. J. Bland for the support of this research.

References

FAURE G. 1987: Principles of isotope geology, (sec. edition), John Willey & Sons.

FRUMKIN A., FORD D.C., SCHWARCZ H.P. 1996: Paleoclimatic record from the Mediterranean desert border karst, Israel. In Lauritzen S.E. (Ed.): Climate Change. The Karst Record.: 35, KWI, Bergen.

GACKOYNE M., NELSON D.E. 1983: Growth mechanisms of recent speleothems from Castleguard cave, Columbus Icefields, Alberta, Canada, infered from a comparison of U-series and C-14 Age Data. Arctic and Alpine Research, 15, 4:537-542.

HARMON R.S., THOMPSON P., SCHWARCZ H., FORD D.C. 1978: Late Pleistocene Paleoclimates of North America as inferred from stable isotope studies of speleothems. Quaternary Research, 9, 54-70.

JAKUCS, L. 1977: Morphogenetics of Karst Regions, Akademie Kiado 323pp.

SCHWARCZ H.P. 1986: In: Handbook of Environmental Isotope Geochemistry, part B: 397-421. Elsevier, New York.

SHOPOV Y.Y., DERMENDJIEV V., BUYUKLIEV G., 1991: Astrophysical Effects and Solar- Terrestrial Relationships Recorded by the Convencional Indirect Indexes and the new LLMZA index of the Solar Activity in the Past in S. Radicella and K. Serafimov (Eds.): ICSU Round Table on Space and Solar influences on the Environment: 55-72.

SHOPOV Y.Y.,FORD D.C., SCHWARCZ H.P. 1994: Luminescent Microbanding in speleothems: High resolution chronology and paleoclimate.Geology, v.22: 407-410, May 1994.

SHOPOV Y.Y., 1996: Speleothem records of Environmental Changes in the Past- Potential in Comparison with the other Paleoenvironmental Archives and Related UIS International Programs.- in book "Climatic Change – the Karst Record", Ed. by S.E.Lauritzen. KWI, Bergen: 148-149

SHOPOV Y.Y., FORD D.C., YONGE C., MACDONALD W., GEORGIEV L., SANAMBRIA M., DERMENDJIEV V., BENDEREV A., BUYUKLIEV G., GEORGIEV S., DELCHEV M., SIRAKOVA M. (in press): High Resolution Records of Climatic Variations and Solar Forcing from the Luminescence of Speleothems from Duhlata cave, Bosnek, Bulgaria, Cold Water cave, Iowa,US and Rats Nest cave,Calgary, Canada. in Y.Daoxian (Ed.): Geology, Climate and Karst Formation – IGCP 299 final report.

TALMA A.S., VOGEL J.C. 1992: Late Quaternary paleotemperatures Derived from a Speleothem from Cango Caves, Cave Province, South Africa. Quaternary Research, 37: 203-213.

YONGE C.J., FORD D.C., GRAY J., SCHWARCS H.P. 1985: Stable isotope studies of cave seepage water. – Chemical Geology,58:97-105.

YONGE C.J., NORMAN A.L., KROUSE H.R. (in press): Isotopic composition of precipitation at Calgary, Alberta, Canada.

Paleomagnetic study in the Cuchillo Cura System Neuquen Province, Argentina

Barredo, S.P. [1] **, A. Balbi** [2] **y G. Ré** [3]

[1] CONICET. Universidad de Buenos Aires. Facultad de Ciencias Exactas y Naturales. Pabellón II. Grupo Espeleológico Argentino (**GEA**). E-mail: silvia@tango.gl.fcen.uba.ar

[2] Universidad de Buenos Aires. Facultad de Ciencias Exactas y Naturales. Pabellón II. Grupo Espeleológico Argentino (**GEA**)

[3] Laboratorio de Paleomagnetismo "Ing. Valencio". Universidad de Buenos Aires. Facultad de Ciencias Exactas y Naturales. Pabellón II. E-mail: indio@tango.gl.fcen.uba.ar

Abstract

This work was focused on the evaluation of the Paleomagnetic Method applied to the speleological analysis of the Cuchillo Cura System. This system is composed of a number of different caves partially disconnected and fully developed in the limestones of the Lower Oxfordian (La Manga Formation).

Although the isolated primary components are widely dispersed, the preliminary results suggest a normal polarity for those sites situated in the El Arenal Cave. It was also possible to establish the main responsible for this magnetization: Magnetite; and to determine that the remanent magnetization of cave sediments might include secondary components of a possibly viscous origin.

This method could be essential to understand the origin and the evolution of these caves but it can not be considered as the most appropriate for those partially evolved karsts. The devices used to pick the samples produce irreparable holes and the fact that the stalactites or stalagmites are removed makes this method one of the least advisable in terms of cave protection.

Resumen

El objetivo del trabajo es la evaluación del método Paleomagnético aplicado al análisis del sistema Cuchillo-Curá. Dicho sistema está compuesto por varias cuevas parcialmente desconectadas entre sí y totalmente desarrolladas en las calizas de la Formación La Manga, de edad oxfordiana inferior.

A pesar de la dispersión de las componentes primarias, los resultados preliminares indican polaridad normal para la cueva de El Arenal. También fue posible determinar el principal mineral responsable de esta magnetización: magnetita y la presencia de componentes viscosas como componentes secundarias.

Si bien este método podría ser esencial para entender el origen y evolución de estas cuevas, se estima que no es el más adecuado, si estas están parcialmente desarrolladas. Los dispositivos que se utilizan para extraer las muestras producen orificios irrecuperables y, la necesidad de extraer estalactitas y estalagmitas para completar las secuencias hacen de esta herramienta una de las menos recomendables si se trata además de preservar las cuevas con toda su belleza..

Introduction

The Cuchillo Cura System has one of the most important karst records of Argentina. In spite of this, the system is not large and comprises an area of approximately 2 km^2. Composed of four caves, the system has exquisite speleothems and important fauna which make of this karst a valuable mean of understanding the related processes.

The origin of the Cuchillo-Cura caves is likely to be due to solution processes that occurred during Pleistocene times under a favourable climate. This climate was drastically changed to arid conditions during the last phases of the Andean Orogeny resulting in the present day inactive karst system. Regarding rock deformation induced by the tertiary tectonism, the present upward growing corresponds to the collapse of blocks along the joints. Periodically these caves are flooded by waters from nearby lakes, but this had no influence in the karst evolution.

The paleomagnetic method has been widely applied in Southamerica for geological studies but rarely for speleological matters, specially in Argentina. Difficulties exist with samples extraction, which modifies essentially the natural features of the fragile environment in in such little caves.

A first study has been conducted in this country with the purpose of analysing the method efficiency for such rocks, the probability of an accurate dating. Furthermore, we wanted to know the needed sampling density and the resulting consequences for the caves.

The preliminary results are discussed in this paper.

Geologic setting

The cave system under study is located along the western side of the Neuquen basin in the Cuchillo Cura range, 10 km south from Las Lajas town in the Neuquen Province, Argentina (see Fig. 1). The geographical coordinates are: latitude 38° 37' 25" south, and longitude 70° 23' 03" west. Situated at 900 m above sea level, the climate is semiarid with a mean annual rainfall between 200 and 250 mm per year, and temperatures that vary from 20° to 6° Celsius for the warmest and coldest months respectively. The cave air temperature is below 10° C, the humidity nearly 100 % and slight wind currents have been detected for some of them.

The geology of this region has been described by GROEBER (1946) and many others. Mainly Jurassic and Cretaceous rocks form part of the sedimentary infill of the basin which covers almost the whole province.

Alternating marine and continental deposits characterise the depositional story of the basin, developed over a Paleozoic to Triassic heterogeneous basement; only during tertiary times there were volcanic and pyroclastic events of basaltic and andesitic nature.

Light-coloured limestones, sandstones and gypsum are Los Tábanos, Lotena, La Manga and Auquilco formations, which are surrounded by a basaltic plateau. These units comprise oolitic fossiliferous and medium grained limestones, greenish-grey fine grained sandstones with carbonate cement and important fossils, and finally an evaporite sequence (gypsum) interfingered by thin bedded stromatolitic limestones. All of them range in age from middle Callovian to Kimmeridgian. The structure consists of a huge east-northeast dipping anticline cut by northeast trending faults and a number of minor high angled joints with northeast – southwest and southeast – northwest strike.

The La Manga carbonatic facies (mainly packstones) is the primary cave-bearing unit which holds four caves known as El Gendarme, El Templo, El Arenal and Los Cabritos. They are situated in the northern flank of an anticline dipping 15°.

Fig. 1: Regional map of the Cuchillo Cura system.

Speleologic setting

The caves are Pleistocene in age as inferred by ELZEARD (1987). They were developed under the strong control of joints, as suggested by the strike of the main and lateral galleries which are disposed in a reticulate array. In spite of this, only two caves are physically connected: El Gendarme-El Templo.

The modern system is inactive due to the non favourable climate and bears no apparent relationship to the present topography or stream patterns. But in earlier times under a more humid and cold period, when La Manga was still undeformed, the caves were developed in the phreatic zone and water-table zone. The system evolved to its maturity building carbonate speleothems of a fine and wild beauty. They occur as calcium carbonate stalactites, stalagmites and columns, calcite cave pearls, calcium cascades lavish decorations as crust deposits coating the bedrock, carbonate floors composed of flowstones with swirls and ripples which appear to represent the growth at former pond surfaces, and fluvial

like travertine terraces. All these deposits suggest cyclicity in their evolution. Subsequently, the last phases of the Andean orogeny led to an episode of tectonism resulting in the uplifting and tilting of the formation, followed by a climatic change to current conditions. The cave system is developed vertically, favoured by the collapse of blocks along the joints but bounded by bedding planes (ELZEARD, 1987).

Methodology and resulting data

Speleothem deposits contain a weak but measurable magnetic remanence. As they are free from the depositional effects, which cause the shallowing of the inclinations, provide a valuable mean of studying a part of the karst history.

For this study, we used a complete stalactite of 40 cm long and a collection of only 6 samples picked in a sequential order which partially cover a whole determined sequence. They were used as a preliminary study focused mainly on the applicability of this tool and the direct consequences for the environment.

The speleothems were collected in El Arenal cave, where the existence of a profuse carbonate speleothem deposit gave the opportunity of a relatively easy sampling. Basically, this latter was held using a Brunton compass for the orientation and a pickaxe for the main extraction. The targets were always from hidden corners or the thickening backwards steps of the floor terraces to avoid the disgusting look of a sampled place.

The magnetic susceptibility (J0) for each of the present minerals and the natural remanent magnetism (NRM) were measured for the whole collection. Samples were then subjected to a stepwise demagnetization up to 700° (see adjoining table in fig. 2). Some of them were also subjected to stepwise alternating field demagnetization up to 80 mT (see fig. 2). The remanence was measured on a cryogenic magnetometer with the purpose of isolating the primary remanent magnetism which is the NRM - SRM (secondary remanent magnetism); this was later added during the geological history of the rock (VALENCIO, 1980; BARREDO, 1992). The collection showed a hard and stable remanence and a median destructive temperature of 575° C (see fig. 2) indicating magnetite as the main magnetic carrier of the remanence. In addition, hematite occurs as a secondary magnetic mineral. After removing the viscous components, it was possible to determine the polarity of these rocks – negative – which is normal for South Hemisphere. The paleopole could not be established due to the insufficient number of samples.

Discussion

As suggested above, it is possible to constrain the age of the cave using this method. But for the particular case of this study, the number of samples was not enough for a complete paleomagnetic study; therefore the paleopole could not be established. Despite this, the final data led us to arrive to a very important point. In caves of little development (2 km^2 for the whole system and only 383 m^2 for El Arenal Cave) a dense sampling oriented to a more statistically precise data implies a partial destruction of the little cavern and parallely the modification of the ecosystem. This latter is produced by gases emanated from the oil drill in a quite reduced space with no air circulation what implies certain risk for the local fauna. We could confirm it as some specimens died some days after the initial sampling work. On the other hand, if a pickaxe is used bigger holes are made to produce an oriented sample from where a cube can later be extracted. This is still more destructive for the natural beauty of such concretions considering that they are poor in number, little developed and quite separated one from each other.

Previous works like the one in Querey, south east of France (LEVEQUE & SEVKET, 1991), arrived to the same conclusions; in the Cuchillo Cura case, a complete study could imply the irrecoverable modification of the natural scene of one of the biggest systems of the country.

Conclusions

- The speleothems contain key information about the characteristics of the earth's magnetic field during their deposition.
- The main magnetic carrier is magnetite accompanied by hematite as a secondary mineral.
- The study shows normal polarity for the analysed sequence.
- It is possible to conclude that the age of the caves could be determined through this method if a more dense sampling is held.
- For the case of Cuchillo Cura or any other poorly developed cavern this tool is not advisable.
- Sampling should take into consideration the preservation of the natural beauty of the cave environment.

Sample	J0	NRM	CT° (≈ 575°)
EA1	2.10	15	0.5
EA2	1.65	15	25
EA3	2.35	25	10
EA4	1.80	40	20
M6	1.85	65	20
M5	2.00	5	10

References:
EAn= Stalactitic sample
Mn= Sequential sample
J0= Magnetic susceptibility (x 10^{-6} Gauss/Oe)
NRM=Natural Remanent Magnetism (Emu x $10^{-7}/cm^3$)
CT°= Curie temperature

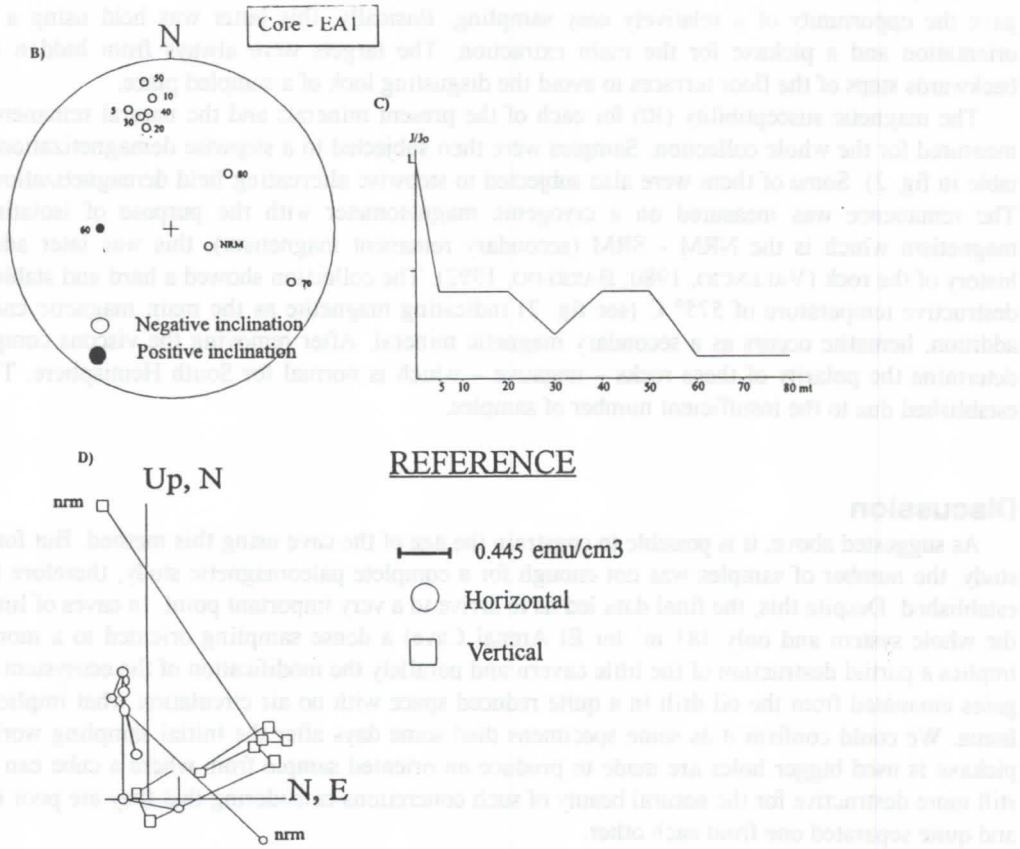

Fig. 2: ***A) Table of demagnetization; B) Stereographics projection; C) Normalized demagnetization curve; D) Zijderverg diagram.***

References

BARREDO, S. P. 1992. Estudio paleomagnético de las sedimentitas cretácicas de las Formaciones Castillo y Matasiete en la comarca del cañadón homónimo. Thesis of the University of Buenos Aires. Unpublished.

ELZEARD, L. 1987. Geología del sistema de cavernas del cordón Cuchillo - Curá. Salamanca Bulletin GEA, v. III: 3-11. Argentina.

GROEBER, P. 1946. Observaciones geológicas a lo largo del meridiano 70. Hoja Chos Malal. Rev. Soc. Geol. Arg., Buenos Aires, 1 (2): 177-208.

LEVEQUE, F.& S. SEVKET,. 1991. Polarité, magnétique de remplissages karstiques paléogènes du Querey (Sud-Ouest de la France). C.R. Acad. París, t.312, Série II: 1431-1438.

VALENCIO, D. 1980. El magnetismo de las rocas. Eudeba 351 p.

The palaeomagnetism of speleothems of Middle Quaternary age from northern Australia

N.C. Scherrer[1], M.J. Fischer[2], S.J. Gale[2], R.N. Drysdale[3] and H. Heijnis[4]

[1]Department of Geography and Planning, The University of New England, Armidale, New South Wales 2351, Australia; Current address: Mineralogisch-petrographisches Institut, Universität Bern, Baltzerstrasse 1, CH-3012 Bern, Switzerland

[2]Department of Geography, The University of Sydney, Sydney, New South Wales 2006, Australia

[3]Department of Geography, The University of Newcastle, Callaghan, New South Wales 2308, Australia

[4]Environmental Radiochemistry Laboratory, Australian Nuclear Science and Technology Organisation, Private Mail Bag 1, Menai, New South Wales 2234, Australia

Abstract

Palaeomagnetic analysis of a flowstone interbedded with fluvial deposits in Ten Truck Cave in the Barkly karst of northwest Queensland, Australia, has provided a record of secular variations in the direction of the Earth's magnetic field. Dating of the speleothem by uranium-series methods has proven difficult because of detrital contamination and the preferential leaching of isotopes from the deposit. However, it is cautiously considered that deposition took place at around 140 500 ± 55 500/40 500 before the present. This record represents the first evidence of palaeosecular variation for the Australian non-dipole field for any time prior to the Late Quaternary. The results demonstrate the considerable potential of speleothems as a source of datable and high resolution palaeomagnetic methods.

Introduction

The longest existing records of secular variations in palaeomagnetism from Australia extend back only ~16 200 years before present. One way of extending our knowledge of palaeosecular variation (PSV) beyond this is to exploit the potential of speleothems to preserve a reliable record of magnetic changes at a site. The ability to date speleothems using uranium-series methods allows such records to be placed in a reliable chronological framework.

Orientated samples of two conformable flowstone units, TTC1 (lower) and TTC2 (upper), were therefore obtained from an interbedded sequence of carbonate and clastic sediments located in Ten Truck Cave (18°43'S, 138°07'E) in the Barkly karst region of northwest Queensland.

Methods

Seventy-five orientated specimens were obtained from eight stratigraphic levels of TTC1 and a further 109 specimens were taken from seven stratigraphic levels of TTC2. The intensity and direction of the natural remanent magnetisation (NRM) of each specimen were measured using a spinner magnetometer. Eight pilot specimens from TTC1 and nine from TTC2 were demagnetised using a biaxial, tumbling, alternating field (AF) demagnetiser. All remaining specimens were demagnetised to the optimum level of demagnetisation, determined according to the behaviour of the pilot specimens, and then remeasured.

The age of the samples was assessed using the $^{230}Th/^{234}U$ disequilibrium method. Unfortunately, both TTC1 and TTC2 contained detritus. This may have introduced uranium and thorium into the carbonate of the speleothem, thus invalidating the assumption of a system which is closed with respect to ^{230}Th and ^{234}U and in which all the ^{230}Th in the deposit is the product of the decay of ^{234}U. In the case of TTC1, the detrital content was so high that the sample was considered unsuitable for analysis. Investigations were therefore restricted to nine specimens taken from the full depth of TTC2.

In order to minimise the amount of thorium derived from the non-calcareous fraction of the flowstone in the solutions made up for analysis, the specimens were prepared by dissolution in dilute nitric acid. The $^{230}Th/^{232}Th$ ratios of the digestions may be used to assess the extent of detrital contamination. Since thorium bonded onto detritus will contain isotopes which are not necessarily the product of radioactive decay, the presence of the long-lived parent isotope ^{232}Th in a speleothem provides clear evidence of detrital contamination. With one exception, the $^{230}Th/^{232}Th$ ratios in TTC2 all lie below 5, that is, in the highly contaminated category of FORD & WILLIAMS (1989, p. 360). The $^{234}U/^{232}Th$ ratios of the weak leaches are also less than 5. By comparison, other contaminated speleothems ($^{230}Th/^{232}Th < 20$) from the Barkly karst possess $^{234}U/^{232}Th$ ratios in excess of 600.

The upper two specimens from TTC2 displayed $^{230}Th/^{234}U$ ratios > 1. Since uranium is much more soluble in freshwater than thorium, this suggests that some ^{234}U has been removed by post-depositional leaching. These two specimens were therefore omitted from further analyses. The remaining specimens were assumed not to have been affected by leaching.

Plots of $^{238}U/^{232}Th$ vs $^{234}U/^{232}Th$ and $^{234}U/^{232}Th$ vs $^{230}Th/^{232}Th$ provide a means of representing patterns of mixing between authigenic calcite (with a high uranium content relative to ^{232}Th) and non-calcareous material (which generally has a low uranium content relative to ^{232}Th). Plotting the results of the analyses in this fashion reveals straight-line relationships with a $^{234}U/^{238}U$ ratio of 2.038±0.243 and a $^{230}Th/^{234}U$ ratio of 0.803±0.154. Both relationships are strongly indicative of a single source of uranium uptake which remained constant throughout the period of deposition of the speleothem.

Results

1. Uranium-series analysis: the corrected $^{234}U/^{238}U$ and $^{230}Th/^{234}U$ values yield an age of 144 500 ± 55 500/ 40 500 years.
2. Palaeomagnetic analysis: all except four of the specimens from TTC1 showed a normal polarity magnetisation, suggesting deposition during the present Brunhes normal polarity chron (<0.78 Ma). The demagnetisation process appears to have disrupted the magnetic signature of some specimens from TTC1. Clustering significantly worsened with demagnetisation and the AF-cleaned dataset exhibited excessively large α_{95} values. The magnetic signal of TTC1

cannot therefore be considered to be a reliable indicator of the PSV of the Earth's magnetic field. Despite this, the data have been plotted in sequence with those of TTC2 (Figure 1). Fisher mean directions and associated error bars have been plotted only where $K > 2$. Further interpretation of the data in terms of geomagnetic PSV has not been undertaken.

As with TTC1, all the specimens from TTC2 showed negative inclinations, suggesting deposition in the last 0.78 Ma. TTC2 possessed relatively high magnetic intensities, a minimum of 12 specimens per stratigraphic level, good clustering of magnetic directions at each level and independent age calibration based on uranium-series dating. It therefore exhibited considerable potential for the provision of a reliable record of PSV. The AF-cleaned declination and inclination data are plotted against depth in Figure 1.

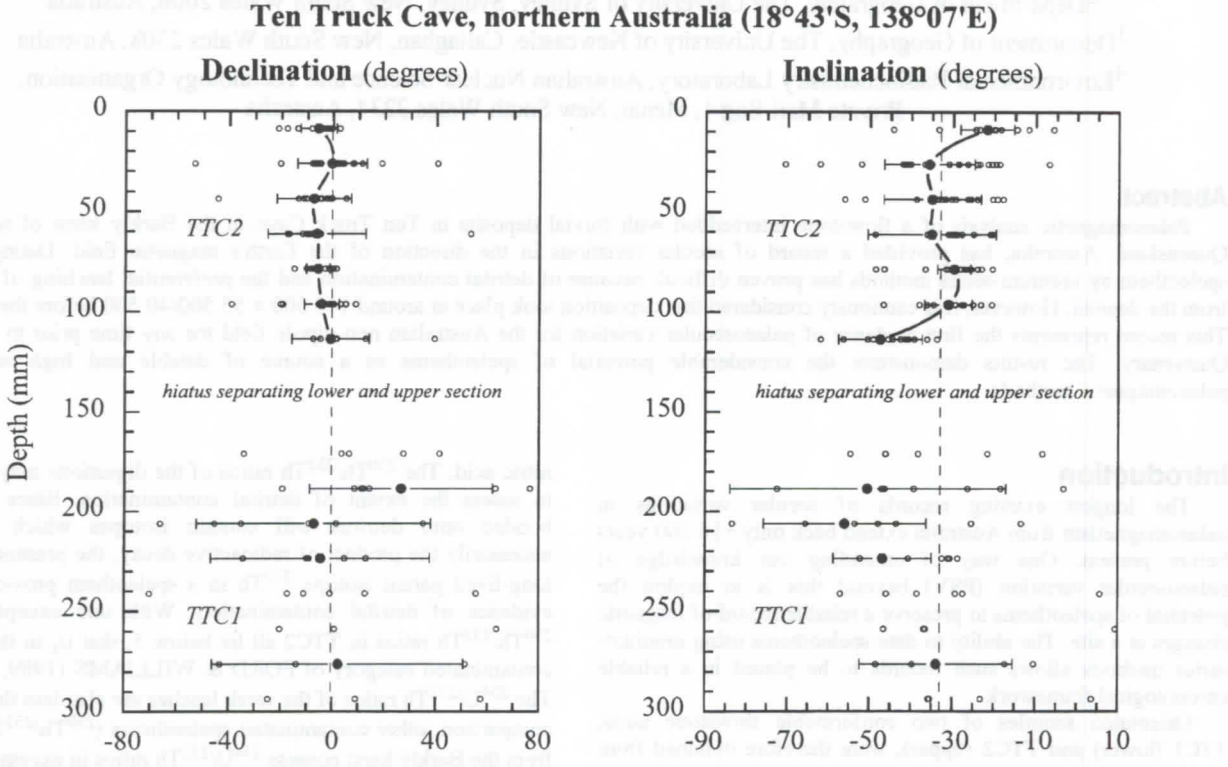

Figure 1. The magnetic declination and inclination of TTC1 and TTC2. The signal of each individual specimen has been plotted as a small open circle, whilst Fisher means for each level have been represented as solid circles connected by a smooth line. Circular standard deviations are shown as horizontal error bars ($s_{Inc} = a_{95}$; $s_{Dec} = a_{95}/\cos Inc$).

Discussion

Figure 1 represents the first record of PSV from prior to the Late Quaternary from anywhere in Australia. Records of similar age are available from New Zealand (TURNER & LYONS, 1986; PILLANS & WRIGHT, 1990), but these show no similarities with those from Ten Truck Cave, probably because the sites lie in separate regions of the non-dipole field.

The resultant curves of inclination and declination exhibit a relatively small amplitude. This may be interpreted in three possible ways:

1. The sample has grown very slowly and the specimen height of 17.5 mm is insufficient to resolve the PSV of the geomagnetic field. The signal is therefore an average approximating to the direction of an axially-geocentric dipole field.
2. The sample has grown very rapidly, as is possible in tropical climates, but the record is too short to depict significant fluctuations of the directional components of the geomagnetic field.
3. The sample recorded apparently stable geomagnetic field directions over a long time interval.

Whilst suggestion 1 could be tested by decreasing the specimen size and measuring sub-specimens on a more sensitive cryogenic magnetometer, PSV records from other parts of Australia covering the last ~16 ka show similarly low amplitudes of declination and inclination. If this is characteristic of the non-dipole field in the Australian region, possibility 3 cannot be ruled out. Option 2 seems unlikely since the finely-laminated stratigraphy of the flowstone suggests that the sample grew over a relatively long time period. Using the AF-cleaned dataset, a mean inclination of -33.7° has been calculated for the whole of TTC2. This is close to the -34.1° expected for an axially-geocentric dipole field at this latitude (18°43'S) and may indicate that the sample was deposited over a period of several thousand years, the time required to equalise secular variations in the Earth's magnetic field. A significantly steeper mean inclination of -42.4° for the NRM dataset is most probably the consequence of a viscous overprint acquired by grains of low coercivity through exposure to a changing ambient field. Support for this interpretation comes from the 1995 inclination at the site of -48.3° (computed using the international geomagnetic reference field). This appears to confirm that demagnetisation of all specimens in an applied field of 10 mT has effectively removed the viscous remanent magnetisation and isolated the primary magnetisation. Plotting the Fisher mean directions of each stratum as virtual geomagnetic poles (pole positions calculated on the assumption that the palaeomagnetic direction of each stratum is the product of a dipolar geomagnetic field) reveals little movement, with positions closely clustered around the

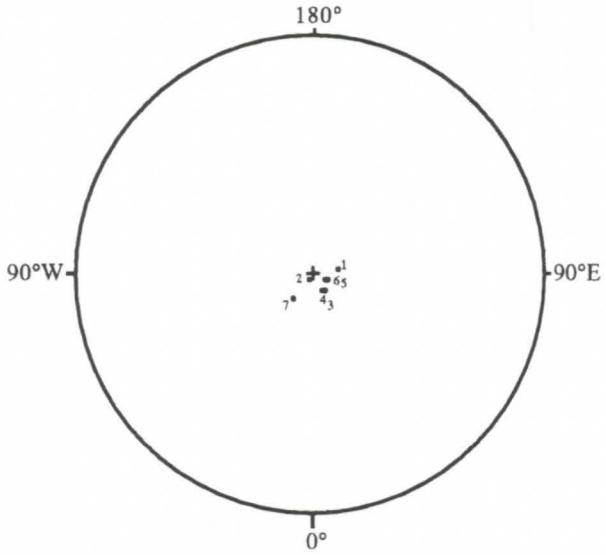

Figure 2. Virtual geomagnetic pole positions (1 is the most recent) based on the Fisher mean directions of each stratigraphic level for the AF-cleaned dataset of sample TTC2. The positions are plotted on a polar equal area projection.

Conclusions

This paper reports the first investigation in Australia of speleothems as sources of PSV information. The results reveal the considerable potential of the method as a means of obtaining datable and high resolution palaeomagnetic records. Figure 1 represents the first PSV curve which has been compiled for the Australian non-dipole field for any time prior to the Late Quaternary. Such information is of immense value both in terms of understanding geomagnetic field behaviour and in providing the foundations of a novel method of dating stably magnetised material.

Acknowledgements

We gratefully acknowledge logistical support for this work from the Musselbrook Reserve Scientific Study organised by the Royal Geographical Society of Queensland and, in particular, from Mr K.N. Teys. We should also like to thank the Australian Research Council and The University of New England for financial assistance. MJF acknowledges the support of an Australian Postgraduate Award and an Australian Institute of Nuclear Science and Engineering Postgraduate Research Supplement. This is contribution number 7 of the Barkly Karst Project.

References

FORD, D.C. & WILLIAMS, P.W. 1989. *Karst Geomorphology and Hydrology.* Unwin Hyman, London, 601 pp.

PILLANS, B. & WRIGHT, I. 1990. 500 000-year paleomagnetic record from New Zealand loess. *Quaternary Research* 33, 178-187.

TURNER, G.M. & LYONS, R.G. 1986. A palaeomagnetic secular variation record from *c.* 120 000 yr-old New Zealand cave sediments. *Geophysical Journal of the Royal Astronomical Society* 87, 1181-1192.

Holocene palaeoclimatic fluctuations recorded by stalagmites: Grotta di Ernesto (northeastern Italy)

Silvia Frisia[1], Andrea Borsato[1], Baruch Spiro[2], Tim Heaton[2], Yiming Huang[3], Frank McDermott[4] and Gianpaolo Dalmeri[1]

1. Museo Tridentino di Scienze Naturali, via Calepina 14, 38100 Trento, Italy. 2. NERC Isotope Geoscience Laboratory, Keyworth, Nottingham, NG12 5GG, UK. 3. Department of Earth Sciences, Open University, Milton Keynes MK7 6AA, UK. 4. University College Dublin, Belfield Dublin 4, Ireland

Abstract

Speleothems from Grotta di Ernesto, located in the now temperate and humid Pre-Alps of Trentino (northeastern Italy), preserve records of climatic changes that occurred in the last 11,000 years, and their effects on the cultural evolution of prehistoric man.

The TIMS (thermal ionisation mass spectrometry) U-series dating of speleothem calcite, continuous stable isotope profile, and calcite texture analyses on axial slabs of a stalagmite, inform on the nature of Holocene climatic changes for the last 8,500 years. The most marked climatic events recorded in the cave speleothem are the Holocene hypsithermal (7,650 to 5,300 years B.P.), the Medieval warming, and the Little Ice Age cooling.

Riassunto

Gli speleotemi della Grotta di Ernesto, situata nelle Pre Alpi del Trentino, hanno registrato il susseguirsi dei cambiamenti climatici avvenuti negli ultimi 11,000 anni. Questi hanno influito sull'evoluzione culturale dell'uomo preistorico, causando la frequentazione o l'abbandono dei siti di alta montagna.

Le datazioni col metodo U/Th, unite alle analisi degli isotopi stabili in serie continua lungo l'asse di una stalagmite e correlate con le analisi tessiturali hanno permesso di identificare la natura dei cambiamenti climatici Olocenici per gli ultimi 8,500 anni, separando periodi freddi e secchi da quelli caldi e umidi. Gli eventi più marcati riconosciuti sono l'*Optimum* climatico olocenico (7,650 a 5,300 anni B.P.), la fase calda Medioevale e il periodo freddo della Piccola Età Glaciale.

1. Introduction

Paleoclimatic reconstruction applied to archaeological sites inform on the environment and on the impact of climatic changes on human culture. One of the most common unknowns is the reason for the prehistoric abandonment of large areas, such as Mesa Verde in the North American Southwest, which needs highly refined and precise information about the past climate to be solved. The present study is one such refined reconstruction for the Holocene through the physico-chemical characteristic of a stalagmite from a prehistoric site, Grotta di Ernesto in northern Italy.

Speleothems are climate-sensitive deposits which record paleoclimatic changes with annual resolution on decadal to millennial scales (FORD & WILLIAMS, 1989; GASCOYNE, 1992), and can be precisely dated by U/Th thermal ionisation mass spectrometry (TIMS) (IVANOVICH & HARMON, 1993). With respect to other proxy data, speleothems have the advantage of carrying a continuous record through isotope composition ($\delta^{13}C$; $\delta^{18}O$) and textures (FRISIA & BORSATO, 1997) of sequential growth layers.

The $\delta^{18}O$ of speleothem calcite precipitated in stable isotopic equilibrium theoretically allows to calculate mean annual paleotemperatures by using the carbonate temperature equation of FRIEDMANN & O'NEILL (1977):

$$T(°C) = 16 - 4.14\,(\delta^{18}O_c - \delta^{18}O_w) + 0.13(\delta^{18}O_c - \delta^{18}O_w)^2 \quad (1)$$

where the subscripts c and w refer, respectively, to calcite and precipitating water. By substituting T°C with 6.5°C (i.e. the present temperature in Grotta di Ernesto) in equation (1), a difference of +1‰ in $\delta^{18}Oc$ should correspond to a change in past temperature of -4.06°C, provided that the $\delta^{18}Ow$ of the precipitating water remained the same. However, this is not the case. The $\delta^{18}O_w$ of rainwater is also temperature dependent and combines its effect on the calcite-water fractionation equation. Therefore, without knowing the original $\delta^{18}O_w$ it remains impossible to calculate the exact temperatures for the past through the sole $\delta^{18}O_c$.

The $\delta^{13}C$ values of speleothem carbonates provides a parallel record of climate-controlled changes. The carbon isotopic composition of seepage water is influenced by the uptake of soil-CO_2. For most of the Holocene, in temperate, preAlpine settings the vegetation likely consisted wholly of C_3 type plants. Seepage water which has uptaken soil-CO_2 derived from the decay of C_3 plant components commonly precipitates speleothem calcite with $\delta^{13}C$ values ranging between -13 to -11 ‰ (CERLING & HAY, 1986). However, within C_3 species, large variations in the isotopic signature are induced by fluctuations in water availability and temperature. Under drought conditions C_3 plants show enrichment in ^{13}C in comparison to non-limiting water availability (BRUGNOLI & LAUTERI, 1991), which corresponds to a shift towards more positive values of the $\delta^{13}C$ of seepage water and, consequently, of speleothem calcite.

Calcite textures are another proxy indicator of drip rate and degree of supersaturation of the seepage waters (GONZALEZ *et al.*, 1992, JONES & KAHLE, 1993; FRISIA & BORSATO, 1997), which, when correlated with isotope data, underpin the interpretation of climate changes in terms of water availability.

2. Cave description

Roadcut works in 1983 exposed the entrance to the Grotta di Ernesto at an elevation of 1167 m a.s.l. (Long. 11° 39' 28" Lat. 45° 58' 37") in Valsugana valley (Trentino, northeastern Italy). The first exploration revealed that the cave preserved important Mesolithic findings. Consequently, the entrance was closed again by a door that inhibits air flow (DALMERI, 1985).

The cave is cut in the dolomitized limestones of the Calcari Grigi Formation (Lias) and consists of a single downdipping gallery, 2 to 5 m wide, up to 4 m high and 72 m long, which developed along a NW trending subvertical fault 20 m below the surface. The original syngenetic morphology of the cave is now blurred by collapse phenomena, and the whole floor is covered by angular blocks, partially coated by flowstones.

Present-day environmental setting

The baseline for past climate interpretation is the present climatic and environmental setting. Climate in Valsugana Valley is of temperate humid, sub-continental type. Mean annual precipitation rate varies between 1000 and 1500 mm and shows a bimodal distribution, with a maximum in May-June and a secondary maximum in October-November. Snowfalls occur from December to March, and snowmelt takes place between March and the first half of April (BORSATO, 1995). The vegetation above the cave consists of a C_3 association with *Fagus*, *Carpinus*, and subordinate *Larix decidua* and *Abies alba*, this latter being indicative of humid and relatively warm conditions.

The cave has several drips, with low (from 0.1 to 2 ml/minute) to medium discharges (up to 50 ml/minute) feeding small, muddy concretional pools. Pools show seasonal water level fluctuations: in summer some are dry, in autumn and spring all pools fill up and several overflow

Palaeoanthropological data

The floor of the first chamber is a 45 m^2 Mesolithic paleosurface with bones of *Ibex* and red deer showing butchering marks. A camp fireplace was located at the southwest wall. The fireplace was subsequently coated by a thin flowstone. A ^{14}C analysis on charcoals yielded a date of 8140 ± 80 years BP (uncalibrated) (AWSIUK *et al.*, 1994), which sets the time span of human frequentation. The cave entrance at that time was larger than present, and was blocked by a landslide immediately after human occupation (DALMERI, 1985, AWSIUK *et al.*, 1994). Apparently, this was not the cause for the abandonment of the site. In fact, all hunting activity on the area ceased at about 8,000 years B.P., when all the high mountain sites were abandoned for the valley bottoms. Hunters returned to dwell onto the plateaus from about 5,000 to 2,800 years B.P..

The general desertion of high-mountain sites in the whole Trentino-Alto Adige region about 8,000 years ago poses the question whether this phenomenon was related to the cultural evolution or to climatic changes, or to a combination of both.

3. Methods

The two-year monitoring of environmental parameters and chemico-physical characteristics of dripwater in the first chamber indicates that dripwater has a constant temperature of 6.5 +/- 0.05°C (BORSATO, this congress), and that the relative humidity is at saturation state, i.e. there is no evaporation. These are necessary prerequisites for calcite to precipitate in isotopic equilibrium (HENDY, 1971).

A 368 mm long, cone-shaped, active stalagmite (ER 76) was removed from this chamber. ER76 was sliced along the axis and mapped to allow for precise correlation of sample location for all methods. In the axial part stable isotope samples were drilled at 2mm-interval; textures were identified through thin section series, and their changes recorded in a textural log; and dating was performed by U/Th-TIMS on five samples selected on the basis of textural changes.

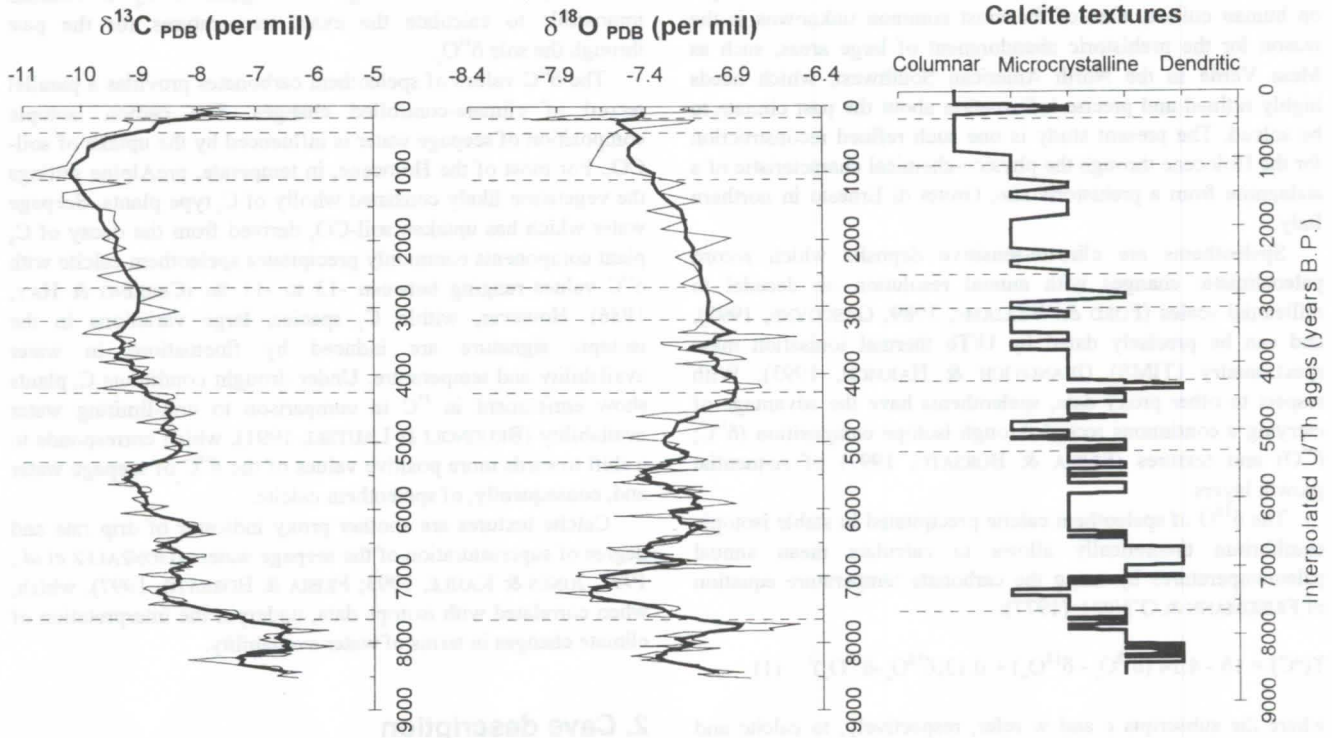

Figure 1 : the time series $\delta^{13}C$, $\delta^{18}O$ and textures for ER76 stalagmite plotted against time (U/Th interpolated ages). Nine episodes were defined on the basis of shift in $\delta^{13}C$ record accompanied by covariant $\delta^{18}O$ fluctuations . Dashed lines identify the limit of each climatic episode. Textural changes aided in the recognition of dry vs. humid conditions (cf. Table 1).

4. Results

The stalagmite commenced to grow at 8,581 +/- 150 years B.P., i.e. when the cave was still open and hunters frequented it. ER76 grew, without depositional gaps to the present. However, it has frequent textural changes with a trend from dominant disequilibrium (dendritic) to equilibrium (columnar) fabrics (FRISIA, 1996; FRISIA & BORSATO, 1997) toward the top. The synthesis of the analytical study is reported in Figure 1, which correlates stable isotope and texture trends vs. time. The climatic episodes are individuated by rapid shifts in the $\delta^{13}C$ record accompanied by covariant $\delta^{18}O$ fluctuations. The limit of the climatic episodes were set at the middle of the $\delta^{13}C$ slope for each major shift.

5. Discussion

The $\delta^{18}O$ values of calcite depend on both temperature and original composition of rainwater, and, consequently, its interpretation cannot be unequivocal. On the opposite, calcite $\delta^{13}C$ depends directly on the vegetation type and soil turnover at the surface, whereby sudden shifts in $\delta^{13}C$ can be interpreted in terms of climatic changes from humid (calcite $\delta^{13}C$ = -11‰) to dry (calcite $\delta^{13}C$ = -6‰) conditions. Therefore, in ER76 sudden shifts in $\delta^{13}C$ mark real climatic changes occurred in the Holocene and identify climatic episodes, through the correlation with textural changes and $\delta^{18}O$ fluctuations, characterized by changes in temperature and water availability in the direction summarised by Table 1.

Climatic parameters	Calcite $\delta^{13}C$	Calcite $\delta^{18}O$	Textures
Cold	⇧ (*)	⇧	Dendritic to microcrystalline
Warm		⇩	Microcrystalline/Columnar
Dry	⇧		Microcrystalline to dendritic
Humid	⇩		Microcrystalline/Columnar
Evaporation	⇧	⇧	Dendritic

Table 1 : Expected stable isotopic and textural variations for Grotta di Ernesto stalagmite calcite, as a function of climatic changes during the Holocene. (*) = only in case of severe cold (i.e. mean annual temperature <2°C that present-day), toward lack of vegetation.

The followings nine episodes have thus been identified:

- **I - from the bottom (8,580 years B.P.) to 7,650 years B.P.-** This episode shows the least negative $\delta^{13}C$ and $\delta^{18}O$ values, coupled with dendritic textures. These characteristics indicate a cold, dry environment and possible evaporation related to the fact that the cave entrance was still open.
- **II - from 7,650 to 5,300 years B.P. -** This episode is warm and humid, but punctuated by cool and dry phases, the most marked of which occurred from 6,450 to 6,130 years B.P. This climatic episode shows the most negative $\delta^{18}O$ values for ER76, which probably indicate that it was the warmest period of the Holocene, i.e. the Hypsithermal.
- **III- from 5,300 to 4,260 years B.P.-** This episode is cooler and characterized by dry conditions, with decreasing temperatures toward its end. It correlates well with the decrease of *Abies* in the area.
- **IV- from 4,260 to 3,200 years B.P.-** This period is cold and dry, with dryness decreasing towards younger ages, as indicated by the slope of the $\delta^{13}C$ curve (to negative values).
- **V- from 3,200 to 2,700 years B.P.-** This is a relatively cool and dry episode, as indicated by the presence of microcrystalline to dendritic textures and by a shift of $\delta^{13}C$ towards more positive values.
- **VI- from 2,700 to 1,100 B.P.-** This time span was characterized by humid conditions and a progressive increase of both temperature and rainfall.
- **VII- from 1,100 to 400 B.P. (900 to 1600 A.D.) -** This is a warm and humid period, which corresponds very well to the historical Medieval warm phase.
- **VIII- from 400 to 150 B.P. (1600 to 1850 A.D.)-** This time interval records a dramatic cooling, marked by a sudden negative shift of $\delta^{18}O$, which correlates with a shift towards more positive values of $\delta^{13}C$. The time span corresponds well with the Little Ice Age. The strong $\delta^{13}C$ shift may identify either a stress in the vegetation caused by cold/dry climate or extensive woodcutting above the cave for heating.
- **IX - from 150 B.P. to present-day-** This episode marks the recovery of warm and relatively humid conditions after the Little Ice Age (LIA) deterioration. It correlates well with the recovery of *Abies* and of present-day climate.

The ER76 record indicates that Mesolithic hunters frequented Grotta di Ernesto in a dry episode, when mean temperatures were about 1°C lower than at present (Fig. 2). They abandoned the high sites during the hypsithermal, when the climate was warmer and more humid. It is probable that the deciduous forest line shifted upwards and colonised the ecological niches of *Ibex* and red deer, which need open spaces and were the game of the Mesolithic hunters. This hypothesis is supported by the warm and humid (*Abies alba* etc.) pollen associations ascribed to the Hypsithermal, from a peat-bog 200 m above Grotta di Ernesto (MARTELLO, 1993). It is also probable that increased humidity made inhospitable the rock shelters of the plateau.

From the $\delta^{18}O$ values we infer (cf. Fig.2) that the hypsithermal had mean annual temperatures about 2°C higher than today. This inference is supported by the 1.5°C increase calculated for the mid-Holocene warm period in the Alps by using pollen data (BURGA & OROMBELLI, 1996).

The ER76 isotope curve shifts allow to set the end of the Hypsithermal at about 5,300 years B.P. This limit is consistent with the onset of the Alpine neoglaciation as recorded by the Iceman of Hauslabjoch (3,250m a.s.l.). The Iceman's death occurred at 5,300 to 5,050 ^{14}C cal. years B.P. and corresponds to a sudden cooling as indicated by both the conditions of the mummy and its immediate burial under snow and ice (Baroni, 1996). Therefore, we can set with confidence the end of the Hypsithermal in the Alps at 5,300 yr B.P. Hunters returned on the *plateaux* in Episode III, the subsequent cool and dry phase.

As for historic times, ER76 records high temperatures for the Late Middle Ages and sets the beginning of the LIA at the year 1,600, which corresponds to the 1594 to 1608 severely cold winters historically recorded in Trentino.

6. Conclusions

The climatic record extracted from ER76 gives useful indications to interpret cultural changes during prehistorical times. In particular, it appears probable that mesolithic hunting was related to cool and dry conditions, when game (*Ibex*, red deer) was bountiful and shelters were hospitable. Climate-related changes in vegetation associations explain major carbon isotope trends in ER76, which correlate well with pollen data from the same area. Therefore, $\delta^{13}C$ appears to be a most reliable paleoclimatic indicator in Alpine speleothems, although useful information can be extracted from $\delta^{18}O$, when confronted with the other proxy data.

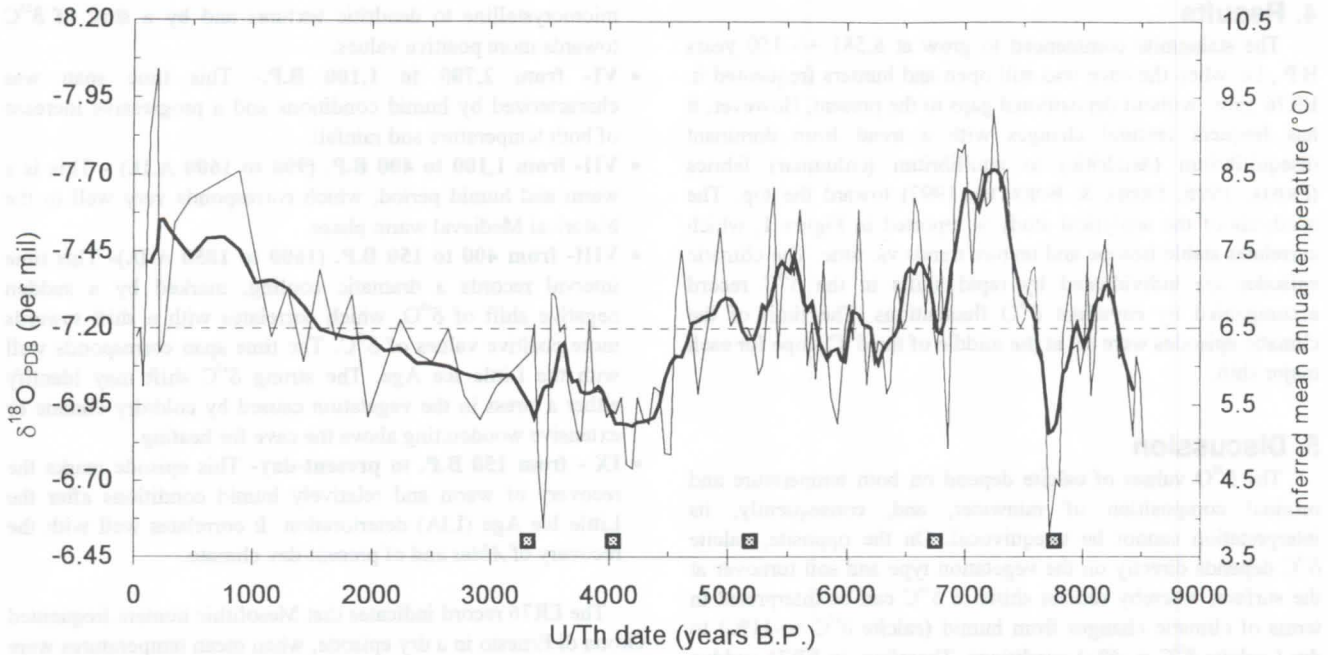

Fig. 2 : The $\delta^{18}O$ trend against time for ER76 stalagmite. Thin line: original data (mean sampling interval = 60 years). Bold line, running mean each 6 analyses (about 360 year). Full squares: U/Th dated intervals. The dashed line connects the $\delta^{18}O$ composition of ER76 tip with the present-day dripwater temperature (6.5°C). The paleotemperature fluctuations have been inferred by assuming that a 1‰ positive shift in the $\delta^{18}O$ value corresponds to a temperature decrease of 4°C according to Equation (1). The total range of temperature fluctuation for the Holocene is probably overestimated because it does not account for possible changes in the original seepage water $\delta^{18}O$ signal. Grey squares identify U/Th dated intervals.

Acknowledgements

This work is part of the E.U. project: "Holocene-Late Pleistocene high resolution climate reconstruction from continental carbonates", contract EV5V CT94-0509.

References

AWSIUK, R., BARTOLOMEI, G., CATTANI, L., CAVALLO, C., DALMERI, G., D'ERRICO, F., GIACOBINI, G., GIROD, A., HERCMAN, H., JARDON-GINER, P., NISBET, R., PAZDUR, M.P., PERESANI, M., & RIEDEL, A. 1994. La Grotta di Ernesto (Trento): frequentazioni umana e paleoambiente. *Preistoria Alpina* 27 (1991): 23-42.

BARONI, C. 1996. The Iceman and the beginning of Neoglaciation in the Alps. In: (EVANS, S.P., FRISIA, S., BORSATO, A., CITA, M.B., LANZINGER, M., RAVAZZI, C. & SALA, B., eds.): *Late-Glacial and Early Holocene Climatic and Environmental Changes in Italy, Conference Abstracts*, Trento: 5-6.

BORSATO, A. 1995. Ambiente di precipitazione e analisi microstratigrafiche di speleotemi in grotte delle Dolomiti di Brenta e Valsugana (Trento): interpretazioni genetiche e implicazioni paleoclimatiche. Unpublished Ph.D. Thesis, Milano: 175 p.

BRUGNOLI, E. & LAUTERI, M. 1991. Effects of salinity on stomatal conductance, photosynthetic capacity and carbon isotope discrimination of salt tolerant (*Gossypium hirsutum* L.) and salt sensitive (*Phaseolus vulgaris* L.) C3 non halophytes. *Plant Physiology* 95: 628-635.

CERLING, T.E. & HAY, R.L. 1986. An isotopic study of paleosol carbonates from Olduvai Gorge. *Quat. Res.* 25, 63-78.

DALMERI, G. 1985. La Grotta di Ernesto: un insediamento preistorico di grande interesse per la conoscenza del Paleolitico finale nell'area trentino-veneta (Colle dei Meneghini-Val d'Antenne, Trentino sud-orientale). *Natura Alpina* 36, (2-3), 31- 40.

FORD, D.C. & WILLIAMS, P.W. 1989. Karst geomorphology and hydrology.. Unwin Hyman, London: 601 p

FRIEDMAN, I. & O'NEILL, J.R. 1977. Compilation of stable isotope fractionation factors of geochemical interest. In: (Fleischer, E.M. ed.): Data of geochemistry. Washington DC, US Govern. Printing Office.

FRISIA, S., 1996. TEM and SEM investigation of speleothem carbonates: another key to the interpretation of environmental parameters. In: (Lauritzen S.-E. ed.): Climate Change: The Karst Record. KWI Spec. Publ. 2, Bergen: 33-34.

FRISIA, S. & BORSATO, A. 1997. Speleothem textures and microstructures: growth mechanisms and their environmental significance. *Boreas* (in press).

GASCOYNE, M. 1992. Paleoclimate determination from cave calcite deposits. *Quaternary Science Reviews* 11: 609-632.

GONZALEZ, L.A., CARPENTER, S.J. & LOHMANN, K.C. 1992. Inorganic calcite morphology: roles of fluid chemistry and fluid flow. *Jour. Sedim. Petrol.* 62: 383-399.

HENDY, C.H. 1971. The isotopic composition of speleothems - I. The calculations of the effects of different modes of formation on the isotopic composition of speleothems and their applicability as paleoclimatic indicators. *Geoc. Cosmoc. Acta* 35: 801-824.

IVANOVICH, M. & HARMON, R.S. (eds.) 1993. Uranium series disequilibrium. Applications to environmental problems, 2° ed., Clarendon Press, Oxford: 728 p.

JONES B., & KAHLE C.F., 1993. Morphology, relationship, and origin of fiber and dendrite calcite crystals. *Journ. Sedim. Petrol.* 63: 1018-1031.

MARTELLO, G.V. 1993. Gli Ambienti dell'Altopiano dei Sette Comuni: evoluzione recente e correlazione con le attività antropiche. *Acta Geologica* 70: 135-152.

Environmental controls of origin of the annually varved calcite speleothems

Michal Gradziński, Mariusz Rospondek, Joachim Szulc
Institute of Geological Sciences, Jagiellonian University, Oleandry Str. 2a, 30-063 Cracow, Poland

Abstracts

Rhythmically laminated calcite speleothems have been studied in terms of the basic environmental factors controlling their growth mechanisms. The laminated microfacies occur in speleothems of different ages and various topographical and geological settings.

Rhythmical lamination depends on alternation of white, pure calcitic layer and brownish calcite layer composing clastic and organic components. The alternation reflects seasonal changes in composition of percolating solutions. The rhythmically laminated calcite precipitates from very thin (> 1 mm) water film enriched in organo-clastic impurities during wet season (summer mostly in the studied caves) while the solution stays pure during dry (mostly cold) season.

Precise paleoenvironmental analysis is however more complex and needs regard on topographic setting (high vs. low topography), climatic controls and geographical position of the studied site.

Introduction

Last decade brought significant progress in study of speleothems as a possible tool of paleoenvironmental reconstructions. One of the most attractive type of speleothems is the rhythmically laminated calcite, found in speleothems of different age and sites (BAKER *et al.*, 1993, 1996; SHOPOV *et al.*, 1994, 1996; GENTY *et al.*, 1995, 1996; GENTY & QUINIFF, 1996). In contrast however to a wide employment of the laminated speleothems in paleoclimatic reconstructions, their growth controls are poor recognized. In order to check the effects of environmental controls (e.g. cave altitude and depth, hydrological and (micro)climatic regime, vegetation cover, age of speleothems etc.) we examined speleothem sections from several caves of Poland and Slovakia.

Research objectives, strategy and methods

Speleothems from 15 caves from Poland and Slovakia have been chosen for detailed sedimentological and geochemical analyses. Altitude of the explored caves ranges between 250 and 1400 m a.s.l. and the samples were collected in sites situated from 20 m to 150 m beneath the surface level. The profiles have been studied in terms of the microfacies variability and growth dynamics. In the present paper we discuss only the rhythmically laminated speleothems of ages between 20kA to >350 kA collected in 5 caves (Figure 1).

Figure 1 : Position of investigated caves: 1 - Wierna cave, 2 - Naciekowa cave, 3 - Psia cave, 4 - Lodova cave, 5 - Zvoniva cave

Petrographical and UV luminiscence observations were carried out on the standard thin sections of calcite speleothems. The same specimens were examined by SEM method accompanied with microprobe analysator.

A set of samples for geochemical analyses was selected based on microscopy. About 20 g of the crushed samples were treated repeatedly with acetate buffer at about 80°C until carbonates were removed. Insoluble residuum was washed with water, centrifuged, dried and weighted. Powder X-ray diffractometry (XRD) was performed on the so prepared material with a TUR M-62 diffractometer equipped with a horizontal goniometer HZG-4B. Cu-K_a radiation (Ni-filtered) was used. Elemental composition was analysed with AAS (Table 1).

Results

The rhythmical lamination is an intrinsic feature of various types of speleothems; stalactites, stalagmites and flowstone covers on cave walls. Rhythmical laminated microfacies (RLM) occurs as one of several microfacies (mf.) types building the speleothem sequences (DZIADZIO *et al.*, 1993; GRADZIŃSKI *et al.*, 1996). RLM is particularly common feature of spelean columnar calcite. Other microfacies types of speleothems e.g. botryoidal or blocky mf. are lacking of lamination.

The rhythmical lamination depends on alternation of white and dark laminae. Thickness of the laminae ranges from several microns to 1 mm. The thicker laminae are visible with naked eye whereas the thinner ones are detectable only under microscopic study. Some of the discrete ultra-thin laminae are discernible when one use other methods e.g. fluorescence phenomenon. White laminae are built by almost pure calcite while the dark laminae display higher contribution of clastic and organic components.

RLM are composed of extremely pure calcite. Acetate buffer insoluble residua compose of ~0.6% by wt. of these speleothems. Only the sample from Zvoniva cave (Slovakian Karst) contains 3.6% by wt. of other minerals. Amounts of hydrochloric acid insolubles varies from 0.08% to 0.32% by wt. Amounts of the residua after HCl treatment are listed in Table 1.

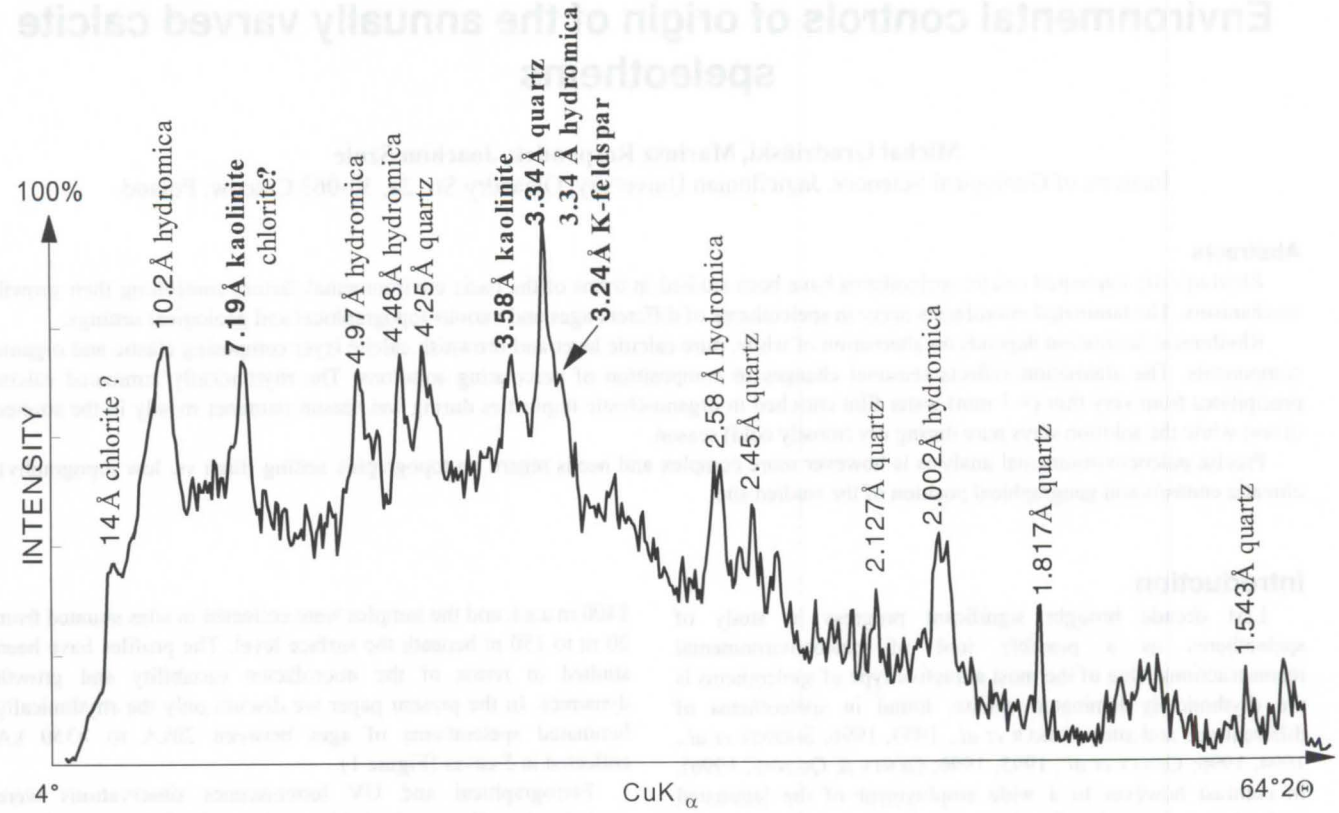

Figure 2 : Diffractogram of the residuum from Psia cave with mineral identified; kaolinite was tentatively identified, chlorite may account for most of reflections indicated for kaolinite as well

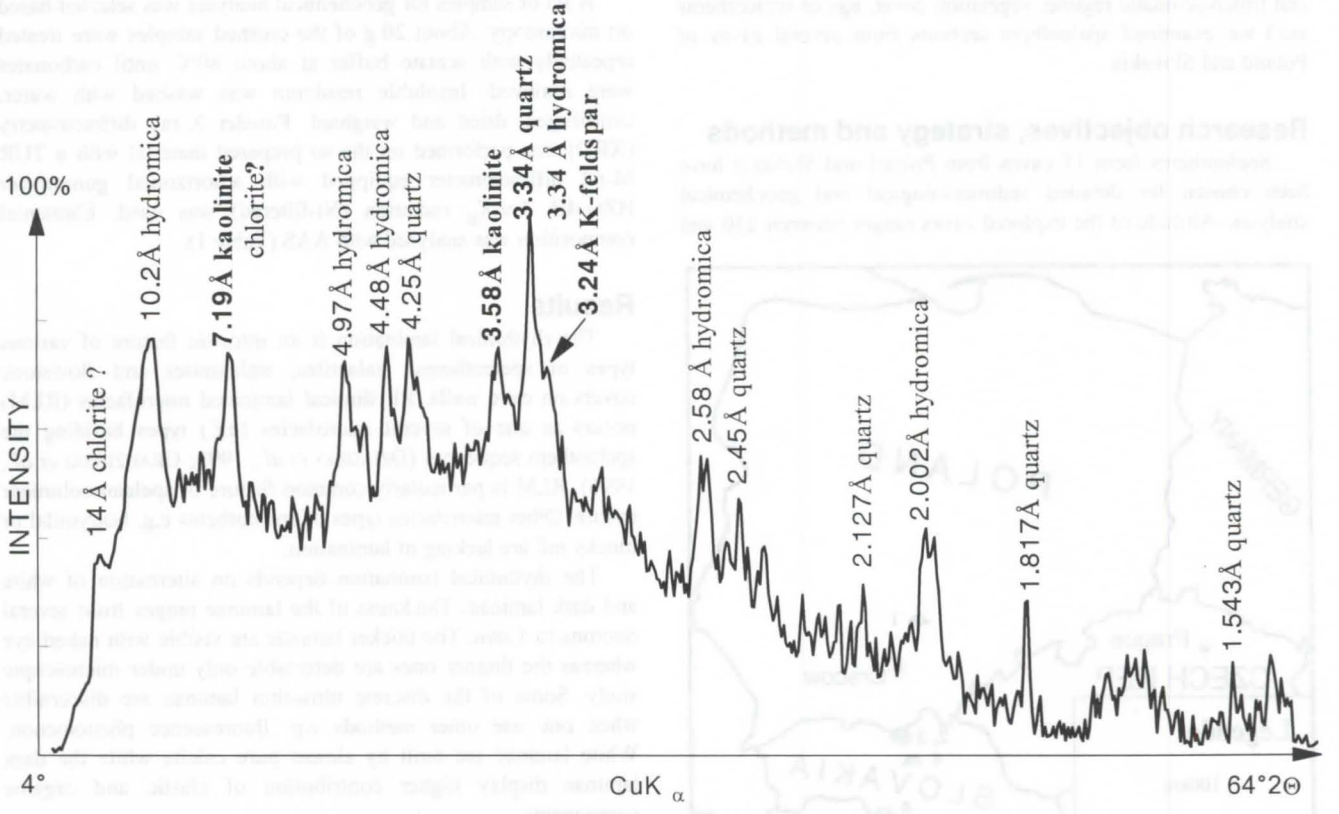

Figure 3 : Diffractogram of the residuum from Zvoniva cave with mineral identified

Mineral phases encountered in acetate buffer insoluble residua vary much from one site investigated to another. For example the residuum from Zvoniva cave, consists of kaolinite (base peak 7.19Å; 3.48Å), quartz (base peaks 3.34Å; 4.25Å), hydroxylapatite (base peak 2.82Å; 2.71Å) and traces of mica or illite. High base ground in the diffractogram is due to dispersed iron oxides which dye red the residuum (Figure 2). In Psia cave the residuum consists of hydromicas (base beak 10.2Å; 4.97Å), kaolinite, quartz and small amount of K-feldspar (base peak 3.24Å) (Figure 3).

Table 1 : Results of chemical analysis of investigated samples

	HCl soluble [by weight]						HCl insoluble [by weight]						
samples	Ca [%]	Mg [ppm]	Fe [ppm]	Mn [ppm]	Sr [ppm]	P [ppm]	residuum [%]	Mg [ppm]	Fe [ppm]	Mn [ppm]	Al [ppm]	Si [ppm]	P [ppm]
Lodova cave	39.4	1300	50	-	41	35	0.08	7	5	-	485	320	-
Wierna cave	39.8	172	80	-	-	177	0.08	-	3	-	825	400	30
Naciekowa cave	39.5	1600	250	-	-	26	0.25	26	5	-	-	916	700
Psia cave	39.6	1400	700	-	-	122	0.32	44	150	-	1120	1500	-

The longest, found continuos sequence of rhythmic laminae is estimated as much as ca. 2500 white-dark couplets. Lamination displays lateral variation and changes from flat morphology to small domal forms. This variation depends on contribution of clastic coarser material and inclusions iconcorporated within the calcite.

Discussion

Nature and origin of lamination

As suggest the thickness, composition of the laminae and scarcity of erosional and depositional breaks within RLM, this microfacies originated in thin water film under stable hydroclimatical regime.

The lamination reflects changes of precipites and depends essentially on a non-carbonate contribution within spelean carbonates. The most common white-dark coupled band may be attributed to seasonal changes during the year. White, pure calcite precipitates from solution free of other components while the coloured laminae originated in water, rich detrital and organic components.

We interpret the white lamina as dryer-season increment and the darker one as deposited during wet period. Further interpretation could be more difficult since there are several possible hydrodynamic controls of such seasonality. For example the white laminae originate during the winter, in caves situated in lowland setting of the temperate climatic zone where, in turn, the summer rainfall promotes growth of the dark

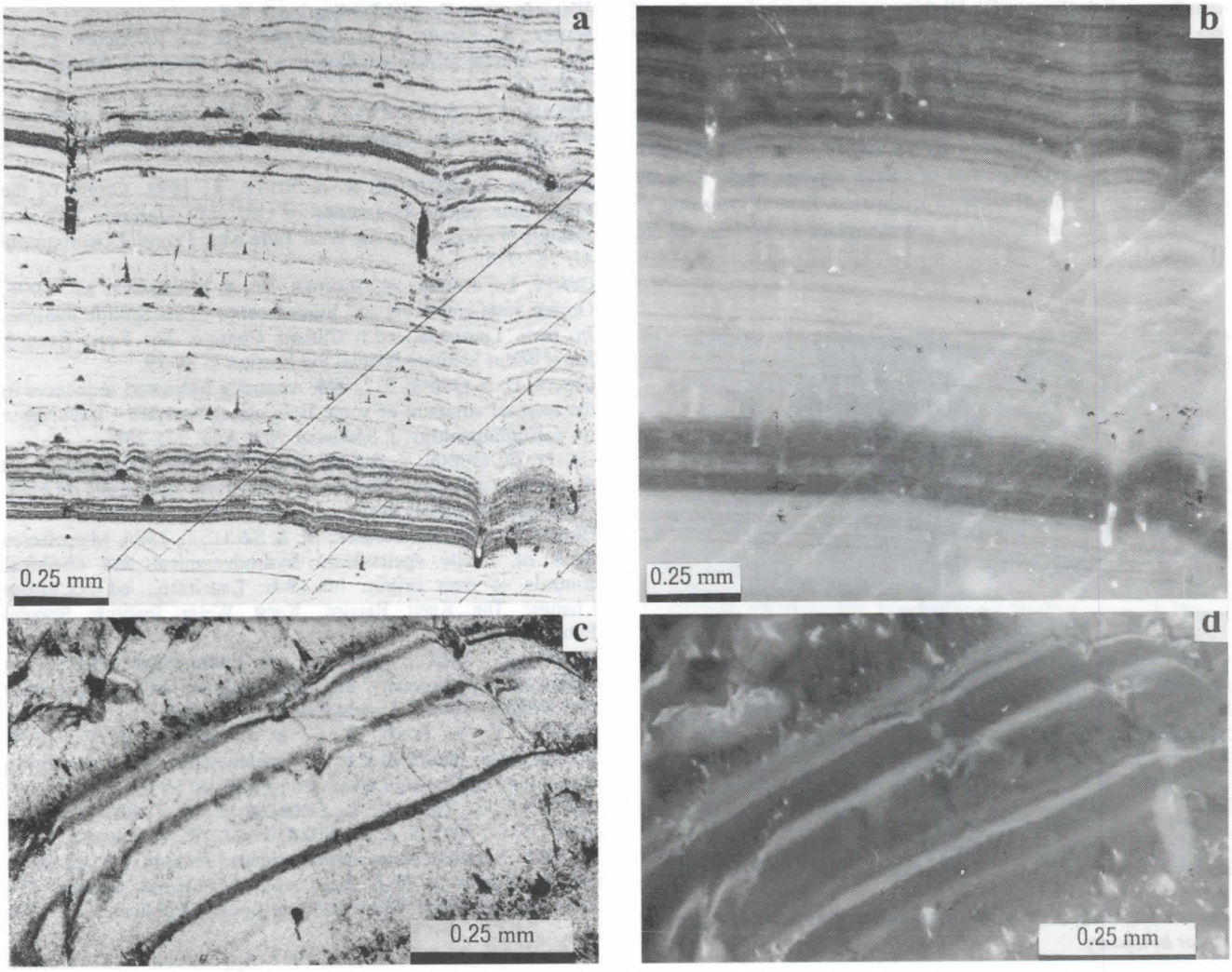

Figure 4 a-d : "Normal" (a,b) and "reverse" (c-d) luminiscence of brown laminae from RLM. Thin section of speleothem sequence from Zvoniva Cave (Slovakia).Left photos (a, c) - transmitted light, right photos (b, d) -UV luminiscence

laminae. On the other hand, the dark laminae could form during wet winter months in the Mediterranean whereas the white calcite precipites during summertime. Regarding of the possible effects of the low - vs. high-relief topography of the studied. objectives, the interpretation becomes even more complex.

Lamination as a tool of paleoclimatic reconstruction and its limitations

Annually stratified bands have been recognized as the most common climatic rhythm recorded in the laminated speleothems. Some go even further and try to find finer cycles, up to diurnal growth of speleothems (SHOPOV *et al.*, 1994, 1996). Most of the so far interpreted laminated fabrics were being studied in terms of luminescence microscopy. The luminescence has been always assumed as evoked by humic and fulvic activators, encompassed in the dark laminae. We have found however that the lamination could result both from the organic as well as inorganic contaminations in the calcite. Commonest inorganic components found in dark laminae are clay minerals, siliciclastic ultra fine grains (quartz, micas) and amorphous ferrioxides (Figures 2, 3). It is noteworthy that some of these impurities (e.g. kaolinite) could give luminescence effect similar to fulvic/humic acids (GRANT, 1962; TEICHMÜLLER & WOLF, 1977; DRAVIS & YUREVICZ, 1985). Moreover, in some cases the dark laminae are high fluorescent and in some other cases, the white laminae show higher luminescence as the darker ones (cf. GENTY & QUINIF, 1996; GENTY *et al.*, 1996). We have found this phenomenon in one thin section (Figure 4)! All this suggests that interpretation of the laminated microfacies, based on luminescence microscopy may give very equivocal results.

Optical microscopy observations show that the only one rhythm enabling further reasonable interpretations is the annual alternance. The lower-order cyclicity may be misinterpreted since the crystallographic properties of calcite crystals might strongly obliterate the visible features of lamination. Lateral vanishing or deformation of the laminae is commonplace in spelean calcite (Figure 5).

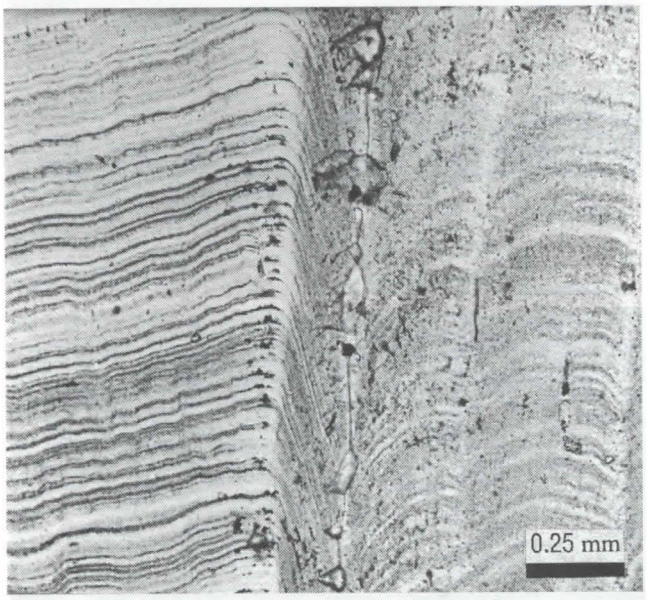

Figure 5 : Vanishing of the lamination following the growth sector boundary

The other important cause of uncertain interpretation of the high-frequency cyclicity is an information noise obtained for the rhythms shorter that the annual one. On the other hand, the cycles longer then some thousands years could be significantly influenced by local factors. Transformations of plant cover, surface morphology or tectonic motion could substantially affect discharge of cave water and finally overshadow the climatic records.

Conclusions

1. Rhythmically laminated microfacies occur in various types of speleothems formed in different geographical, topographical and climatic settings.
2. Phenomenon of cyclical lamination depends on periodical changes in non-carbonate (clastic and organic) contribution in spelean calcite
3. Climatic, annual rhythm of the growth is the most common and obvious cycle in the RLM.
4. Lower-and higher order of cyclicity might be modified or obliterated by other environmental factors

Acknowledgements

This study was supported by KBN (State Commitee for Scientific Research) grant no. 0586/P04/95/09.

References

BAKER, A., BURNES, W.L. & SMART, P.L., 1996. Luminescence and discharge in stalagmite drip waters, Bristol, England. In: (S-E. Lauritzen, ed.): Climate Change: The Karst Record. Karst Water Institute Special Publication 2: 4-6.

BAKER, A., SMART, P. L., EDWARDS, R. L., RICHARDS, D. A., 1993. Annual growth banding in a cave stalagmite. *Nature* 364: 518-520.

DREVIS, J. J. & YUREWICZ, D. A. 1985: Enhanced carbonate petrography using fluorescence microscopy. *J.Sediment. Petrol.* 55: 795-804.

DZIADZIO, P., RÓZNIAK, R. & SZULC, J., 1993. Origin of the Pleistocene calcite flowstones of two cave (Jaskinia Psia and Jaskinia Naciekowa) in the West Tatra Mts. *Przegl'd Geologiczny* 41: 767-775.

GENTY, D., BAKER, A., BARNES, W. & MASSAULT, M., 1996. Growth rate, grey level and luminescence of stalagmitic laminae. In: (S-E. Lauritzen,, ed.): Climate Change: The Karst Record. Karst Water Institute Special Publication 2: 36-39.

GENTY, D. & QUINIF, Y., 1996. Annually laminated sequences in the internal structure of some Belgium stalagmites - importance for paleoclimatology. *J. Sediment. Res.* A66: 275-288.

GENTY, D., QUINIF, Y. & DEFLANDRE, G., 1995. Microsequences de lamines annuelles dans deux stalagmites du massif de Han-Sur-Lesse (Belgique). *Speleochronos* 6: 9-22.

GRADZIŃSKI, M., ROSPONDEK, M. & SZULC, J., 1996. Microfacies types of calcite speleothem: hydrodynamical and chemical controls of their origin. In: (S-E. Lauritzen,, ed.): Climate Change: The Karst Record. Karst Water Institute Special Publication 2: 45.

GRANT, J., 1962. Application of fluorescence analysis in sedimentary petrography. In: (H.B. Milner, ed.): Sedimentary Petrography, Allen & Unwin, London: 433-462.

SHOPOV, Y. Y. FORD, D. C. & SCHWARTZ, H. P., 1994. Luminescent microbanding in speleothems: High-resolution chronology and paleoclimate. *Geology* 22: 407-410.

SHOPOV, Y. Y., TSANKOV, L., GEORGIEV, L. N., DAMYANOVA, A., FORD, D. C., YONGE, C. J., MACDONALD, W. & KROUSE, H. P. R., 1996. Speleothems as natural climatic stations with annual to daily resolution. In: (S-E. Lauritzen,, ed.): Climate Change: The Karst Record. Karst Water Institute Special Publication 2: 150-151.

TEICHMÜLLER, M & WOLF, M., 1977. Application of fluorescence microscopy in coal petrology and oil exploration. *J. Microscopy* 109: 49-73.

The antiquity of the famous Demianowska Caves (Slovakia)

H. Hercamn, P. Bella, M. Gradziński, J. Glazek, S.E. Lauritzen

1. Institute of Geological Sciences, Polish Academy of Sciences, ul.Twarda 51/55, Warszawa, Poland
2. Slovakian Karst Museum, Skolska 4, Liptovsky Mikulas, Slovakia
3. Institute of Geological Sciences, Jagielonian University, ul. Oleandry 2a, Kraków, Poland
4. Institute of Geology, Adam Mickiewicz University, ul. Maków Polnych 16, Poznan, Poland
5. Institute of Geology, Bergen University, Allegtn. 41, 5000 Bergen, Norway

Abstract

In a lot of books, Droppa's scheme of Demianovska Karst System development was used as an example of multilevel karst system which may be correlated with a river tarrases on the surface. We have collected samples from the Lodova Cave, which belongs to the IV level of Droppa's scheme. Basing on the dating results we can distinguish 4 periods of speleothems deposition: older then 350 ka; 140-190 ka; 70-108 ka; younger then 6 ka. The age of the oldest speleothems in this part of Lodova Cave allow us to estimate minimum age of Lodova Cave. Contemporary we will be able to estimate the age of IV level of Demianovska Karst System developped by Droppa. The 234U/238U method (RUBE method, IVANOVICH & HARMON, 1992) was used for estimation of the age for the oldest flowstones from Lodova Cave. 234U/238U age of the basal part of the oldest flowstone from Lodova Cave showed that 700 ka ago Lodova Cave was dry and speleothems deposition was possible. It means that the IV level of Demianowska System is much older then Droppa sugested basing on correlations with surface sediments.

Introduction

The Demianovska Valley's Karst System (DROPPA, 1957) is one of the most famous of the World. In a lot of books Droppa's scheme of its development is used as a example of multilevel Karst System which may be correlated with river tarraces on the surface. Until present no systematic work with radiometric dating of the speleothems from this system was done. Dating of speleothems from the Lodova Cave gave us the first oportunity to make a time scale for Droppa's scheme (DROPPA, 1963, 1964, 1970, 1972). We have collected 7 samples of speleothems from „Zruseny Dom" in the Lodova Cave. This passage belongs to the IV level of Droppa's scheme.

Method

Standard radiometric dating procedure of $^{230}Th/^{234}U$ method were used (IVANIVICH & HARMON, 1992). Samples of 15-30 g were dissolved in c.a. 6 M nitric acid. Uranium and Thorium fractions were separated by chromatography method. ^{234}U, ^{238}U, ^{230}Th and ^{232}Th activities were measured by using isotope dillution with $^{228}Th/^{232}U$ spike. All measurements were done with alfa spectrometry. The ages were calculated by standard algoritm (IVANOVICH & HARMON, 1992) using program ''Age04'' (LAURITZEN, 1981). Reported errors are 1 sigma.

Results

Basing on the dating results we can distinguish 4 periods of speleothems deposition (Fig. 1).

1. Older then 350 ka.
2. 140-190 ka. It may be correlated with the warm interstadials within ^{18}O stage 6.
3. 70-108 ka which correlate with ^{18}O stage 5. More precisly it may be correlated with substage 5c and 5a.
4. Younger then 6 ka which correlated with ^{18}O stage 1.

The age of the oldest speleothems in this part of Lodova Cave is the most interesting. This age allow us to estimate the minimum age of Lodova Cave. Contemporary we will be able to estimate the age of IV level of Demianovska Valley Karst System developed by Droppa. The $^{234}U/^{238}U$ method was used for estimation of the age for the oldest flowstones from Lodova Cave (Jlod 4, >350ka from $^{230}Th/^{234}U$ method). Calculated initial $^{234}U/^{238}U$ ratios for the younger samples were used for estimation of initial $^{234}U/^{238}U$ ratio in the flowstone Jlod 4 (RUBE method, IVANOVICH & HARMON, 1992). We used the mean value of all the calculated initial $^{234}U/^{238}U$ ratios and obtained estimator of initial $^{234}U/^{238}U$ ratio in the sample Jlod 4 equal 2.62±0.38. Results of $^{234}U/^{238}U$ dating of sample Jlod 4 are presented in the table 1.

We can estimate that the period of deposition of the oldest speleothems in Lodova Cave was between 400 and 700 ka. It may be correlated with the ^{18}O stages 11-14. The calcite from the flowstone Jlod 4 and c.a. 8 cm of sediments covered by this flowstone have normal magnecity what confirm that they are younger then Brunhes/Matuyama boundary.

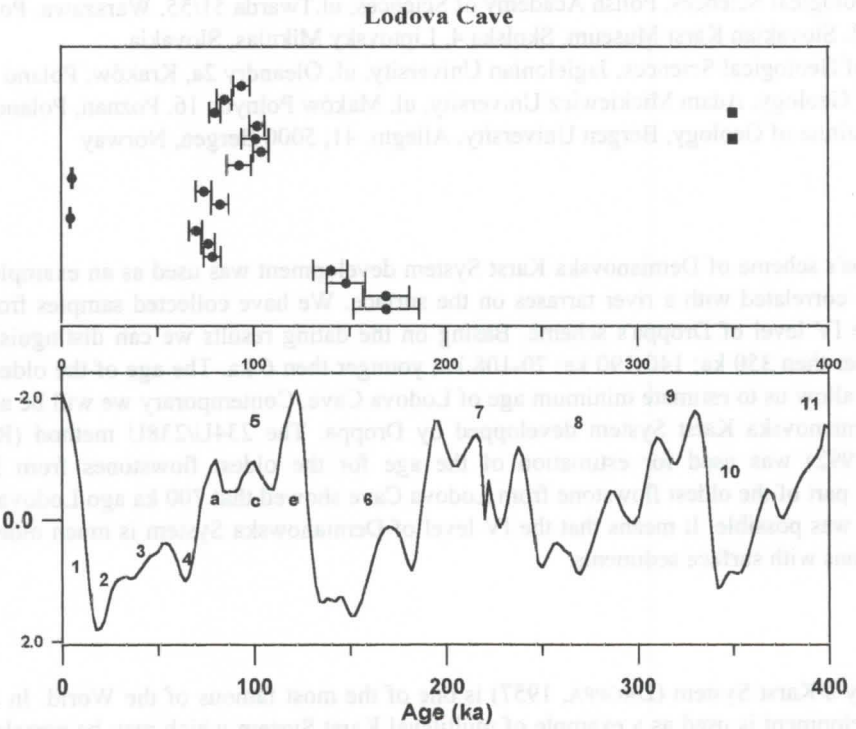

Fig. 1. U-series dating results and theirs correlation with oxygen record

Sample	$^{234}U/^{238}U$ age [ka]
Jlod 4/1 - bottom	685^{+60}_{-40}
Jlod 4/2- top	410^{+73}_{-46}

Table 1. Uranium-Uranium dating results of the oldesst flowstone from Lodova Cave

Basing on the oldest data from Lodova Cave we can make a first test of Droppa's scheme. In the Droppa's scheme Lodova Cave is the part of IV level of Demianovska Karst System. He suggested for this level the Mindel Age (DROPPA, 1970, 1972). The age of the oldest speleothems from Lodova Cave show that 600 ka ago this cave was dry and the speleothems deposition was possible. It means that the IV level of Demianovska Karst System is much older then Droppa sugested basing on correlations with surface sediments.

References

DROPPA A. 1957. Demanovske jaskyne. Krasove javy Demanovskej doliny. SAV. Bratislava. pp. 289.

DROPPA A. 1963. Paralelizacia riecnych teras a horizontalnych jaskyn. Geolog. prace GUDS. c. 64: 93-96.

DROPPA A. 1966. Correlation of some horizontal caves with river terraces. Studies in Speleology. vol. 1: 186-192.

DROPPA A. 1970. Vyskum riecnych teras v zatopovej oblasti Liptovska Mara. Vlast. zbornik Liptov. I: 7-34.

DROPPA A. 1972. Geomorfologicke pomery Demanovskej Doliny. Slov. Kras. X: 9-46.

IVANOVICH, M. & R. S. HARMON. 1982. Uranium Series Disequilibrium. Applications to environmental problems.Clarendon, Oxford, pp. 571.

LAURITZEN S. E. 1981. "Age4U2U". Program for reading ADCAM energy spectra, integration peak-correction and calculation of ^{230}Thorium/ ^{234}Uranium ages. Computer Program Turbo Pascal Code, 5,000 lines, Department of Geology, Bergen.

Speleothem growth frequencies (PDF) as a climate record: problem of significance

Helena Hercman
Institute of Geological Sciences, Polish Academy of Sciences, ul. Twarda 51/55, 01-116 Warszawa, Poland

Speleothems provide a sensitive tool for studies of past climatic changes as the periods of their growth coincide with relatively warm and humid episodes, while breaks in calcite deposition correspond to cool phases. It means that even the presence or absence of the speleothems is the source of the paleoclimatic data. The growth of individual speleothems may be affected by local factors. On the other hand, the collective properties of speleothems growth may cancel out local effects. If we have an enough large sample, the distribution of the speleothems ages through time should aproximate the volume of calcite deposited through time. It was noted quite early that speleothems deposition, at least in upper-mid latitudes, is discontinuous in time clustering into distinct groups that correlate broadly with known warm and humid periods of the Upper Pleistocene. This discontinuity of the speleothem record has been explained by climatic control.

Probability density functions (PDF) for speleothem growth are calculated from the scewed PDF for each date, using the original $^{230}Th/^{234}U$ and $^{234}U/^{238}U$ ratios with the corresponding analytical errors. Filters may be used to screen out dates with low precision. As a result we obtain a continuous record which aproximate speleothem growth frequencies.

If we want to use PDF as a climatic record we should try to answer some questions. Maybe it is not a paleoclimatic record. Maybe it is only the record of sample collection. We can test it by random elimination of a part of our original data. If the positions of the peaks are stable, PDF is more than record of sample collection.

The most important question, and the most difficult too, is about the significance of the record. Which peaks are significant?

P. Smart and his team in an article about North-West European PDF used Monte-Carlo experiment for the estimation of the peaks significance. They generated 100 times a set of random data which had uniform distribution through time and quantity and accuracy of data similar for their original data. For all data sets they constructed PDF and as an estimator of significance bands for their original PDF they used borders of 95% of the range of the experimental PDFs changes. The peaks which are above and minimas which are below these bands are significant. In fact this test may be only used as a test if distribution which is represented by our PDF is not a uniform distribution. It doesn't tell us anything about significance of the individual piks.

In all regional age frequency distributions of speleothems the Holocene signal dominates and frequency decreases with time. This is due to two effects. First, Holocene speleothems dominate in caves. Second, speleothems tend to be destroyed over time, and therefore, older specimens are rarer than younger ones. Then maybe we should use in our Monte Carlo experiment random data with a different distribution through time than uniform, for example exponential distribution. But the result will be the same. We can only tell that our distribution is different then exponential.

A little more information can be obtained from bootstraping of our data. The bootstrap is a data-based simulation method. If we assume that our PDF is a reflection of paleoclimatic conditions we can investigate how big will be the differences between the diffrent estimations. We replace our original data set by another data set, which have the same quantity of data, and construct the PDF for these data. We repeat this procedure a large number of times, say 500 or 1000. Then basing on the 500 (1000) PDFs we can estimate a confidence band for our original PDF.

Another source of information is the analysis of subpopulations in PDF record. P. Smart and his team used a simple algoritm for estimation of subpopulation parameters. The same algoritms may be used for estimation of the quantity of subpopulations too. If we try to estimate the parameters of subpopulations for a different quantity of maxima (1, 2, 3 ... n) we can find the best solution: the quantity of subpopulations which give us the best fitting.

The next source of information is multicorrelation between a PDF record and the other paleoclimatic records. The result of these analyses may be used as a base for modeling of influence of different climatic factors on the PDF record.

All these calculations are in progress and the final results will be presented on the Congres sessions.

A Long Interglacial and Interstadial Record in the North American Mid-Continent from Vadose and Phreatic Speleothems, Jewel Cave and Wind Cave, South Dakota, U.S.A.

Derek Ford, Henry Schwarcz, Hilary Stuart-Williams and Nicola Swinburne,
Geography and Geology, McMaster University, Hamilton, ON L8S 4K1 and
Joyce Lundberg, Geography, Carleton University, Ottawa, ON K1S 5B6

Geographic location

Jewel Cave and Wind Cave are located in the Black Hills, an isolated domal structure in the centre of North America. The region was not glaciated but experienced cold winters. The modern climate is at the sub-humid/semi-arid transition with grasslands above Wind Cave (m above sea level) and open pine forest at Jewel Cave (m asl).

Speleogenesis

Jewel Cave and Wind Cave are multi-storey, rectilinear dissolutional maze caves formed by thermal waters rising through Mississipian (Lower Carboniferous) limestones and dolomites in the Black Hills, a domal structure in South Dakota. The caves are now drained and relict. Jewel Cave is encrusted with 6-15 cms of euhedral calcite spar precipitated from the thermal waters. Wind Cave has much tinner crusts, including its celebrated «boxwork», and calcite raft deposits indicating paleo-watertable levels. Vadose precipitates such as stalactites and stalagmites, are spare in both caves. Isotope records in sample precipitates have been studied intensively for their paleoclimate records.

The thermal water calcites

U series and palaeomagnetic measurements have established that the great spar sheets of Jewel Cave are older than 2 million years and therefore not suitable for Quaternary paleoclimate studies. In Wind Cave the thickest sample, WCMAJ, is only 2.4 cms. Eight U series age determinations by thermal ionisation mass spectrometry (TIMS) that it great from 330 to 160 ka BP, when the water table fell below its position. $\delta^{18}O$ and $\delta^{13}C$ profiles display two distinct halve: (i) 160-225 ka, where O and C are negatively correlated and there id 3‰ variation in ^{18}O record the climate of Isotope Stage 67. (i) between 225 and 325 ka BP both isotope signals are heavier and uniform. In contrast, the U content and $^{234}U/^{238}J$ ratios display a clear glacial-interglacial cycle over this time interval. The homogenising of the ^{18}O and ^{13}C signals suggest an unknown geothermal effect which erases the paleoprecipitation signal. Core must be taken when interpreting paleoclimate records in thermal water calciates.

Vadose calcite

In Jewel Cave sample JC11 is a vadose calciate flowstone 12 cm thick, displaying strong colour banding. From twelve TIMS U series dates, the upper 4 cms grew at intervals between 92±1 and 470±50 ka BP. Eight 10-point growth layer analyses of O and C ratios were made to check for isotope kinetic fractionation effects. Four different profiles have been measured between 92 and 240 ka, with a highest resolution of 300-500 years. Marine isotope Termination II is signalled by ^{18}O increase of 3.0‰ between 131 and 129 ka. Isotope stage 5e lasted from 129 to 119 ka. At our scale of resolution, it contains four or more excursions of 0.5‰. Growth in the previous interglacial (equivalent to marine isotope Stage 7) displays abrupt shifts of up to 4‰ in the ^{18}O signal; peaks occur at ~210, ~192 and ~178 ka BP. All growth censed during the coldest parts of the glacial stades. Between 300 and 470 ka BP, $\delta^{18}O$ interglacial peaks are also in good agreement with the SPECMAP isotope records from deep ocean cores; indicating that thin speleothem in the heart of the continent is recording global climate change in the same manner.

The lower 8 cms of the sample are > 500 ka in age. They display the same patterns of colour banding growth hiatuses and stable isotope cycles as occur in the younger calcite. We are attempting to date these patterns by RUBE and U/Pb techniques.

Precise measurement of luminescence banding profiles in speleothems for paleoclimatic interpretation

William B. White
Department of Geosciences and Materials Research Laboratory
The Pennsylvania State University University Park, PA 16802 USA

Abstract

It is demonstrated that the microfocus Raman spectrometer is an ideal instrument for the measurement of luminescence banding in speleothems. The excitation source is an argon ion laser. The selected laser line is brought into a microscope through a beam-splitter and brought to a focus on the microscope stage with a spatial resolution of 2 - 3 micrometers. Luminescence radiation from the illuminated area is collected by the microscope, transmitted through the beam splitter to the entrance slit of a 0.75-meter focal length double monochromator. Luminescent intensity is measured with a photomultiplier interfaced with a computer for data processing and analysis. The luminescence wavelength can be set to any desired value and intensity measured as a function of traverse distance by moving the specimen with a precision x-y translator on the microscope stage. Complete spectra for each band can also be obtained. Records obtained with this device are suitable for input to mathematical processing such as spectral analysis and Fourier transforms.

1. Introduction

There is a long and rather complicated history that has led over a period of more than 20 years to a realization that the well-known luminescence of speleothems may contain a useful and very high resolution paleoclimatic record. A starting point is the report by GASCOYNE (1977) at the Sheffield International Congress that he could find no correlation between the color of speleothems and the iron content. GASCOYNE proposed that the pigmenting materials were organic molecules incorporated within the structure. WHITE (1981) by reflectance spectroscopy was able to support GASCOYNE'S conjecture. Later LAURITZEN *et al.* (1986) actually extracted the organic component and showed that it was a mixture of humic and fulvic acids. It was shown, as expected, that the blue-white luminescence of speleothems was also due to incorporated organic molecules, predominately fulvic acid (WHITE, 1986; WHITE AND BRENNAN, 1989).

Independently and in about the same time frame, YAVOR SHOPOV began reporting on his observations of high resolution luminescence banding within the speleothem structure. This was a new idea; previous workers had focused their attention on the bulk properties of speleothems. Shopov showed that the interesting and useful information was contained in the spatial distribution of the organic constituents.

With these observations in hand, many investigators have converged on this problem (SHOPOV *et al.*, 1994; BAKER *et al.*, 1993; BAKER *et al.*, 1995). Spatial transects along the axis of stalagmites of the alternating bands of bright luminescence could be combined with U/Th dating profiles to show that the width of the individual bands indeed represented one year of growth. Twenty years after GASCOYNE'S initial observations, it seems quite clear that the flowstone and stalagmite record does indeed have the potential of being a paleoclimate record of great value. The objective of the present paper is to develop a methodology for obtaining a more quantitative record of the luminescence banding and one that would be suitable for more advanced forms of mathematical analysis.

2. Instrumentation

The proposal is to make use of a microfocus Raman spectrometer as a device for obtaining high quality records both from spatial resolution and in terms of spectroscopic accuracy. The work of SHOPOV *et al.* (1994), BAKER *et al.* (1993), and BAKER AND SMART (1995) shows that the width of the luminescence bands is on the order of a few tens of micrometers. This means that the measurement device should have a spatial resolution of a few micrometers or about one tenth of the width of a band so that the luminescence profiles of individual growth bands may be observed.

Figure 1 illustrates the optics of microfocus Raman spectrometer. The excitation source is an argon ion laser. The beam passes through a Pellin-Broca prism to filter extraneous plasma lines, through some focusing optics, and then is brought into an optical microscope. It then passes through a beam splitter which transmits about 10% of the beam intensity down the optical path to the microscope objective. The beam emerges from the microscope objective and is brought to a focus on the sample with a focal spot 1 - 2 micrometers in diameter. The luminescent radiation emitted from the a 1 - 2 micrometer volume of the sample is collected by the objective lens and brought up through the microscope to the beam splitter which is so arranged that 90% of the luminescent light travels to the entrance slit of the monochromator. The dispersing optics in this instrument consists of two tandem 0.75-meter focal length Czerny-Turner mounted grating monochromators which provides a wavelength resolution of 0.05 nm. The monochromator system provides considerably better resolution than is required for the broad emission from fulvic acids. The light exits the monochromator through a slit and then is focused on a photomultiplier which converts it into an electrical signal which passes through some interface electronics to a computer. The computer also controls the wavelength drive system so that data points can be collected by counting light intensity at wavelength intervals as small as 0.1 nm. This allows the collection of data with very high accuracy in both wavelength and intensity. The data are also in digital form suitable for further manipulation.

The existing optical system provides high spectroscopic accuracy. The additional modification that must be made is a translation stage on the microscope with the ability to control position of a slice of speleothem with an accuracy comparable to the existing spatial resolution of the microscope - a few micrometers. This can be provided by a mechanical translator system with a precision worm drive. Data can be taken point by point by advancing a micrometer screw on the translator or as the next step, replacing the hand adjustment with a stepper motor controlled by the computer. With this arrangement the instrument can be used in either a wavelength mode where the beam is

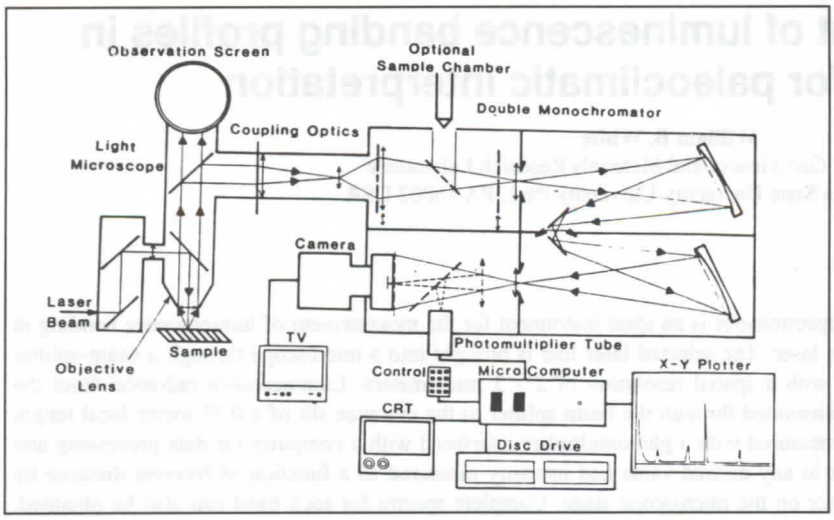

Figure 1. Optics of microfocus Raman spectrometer.

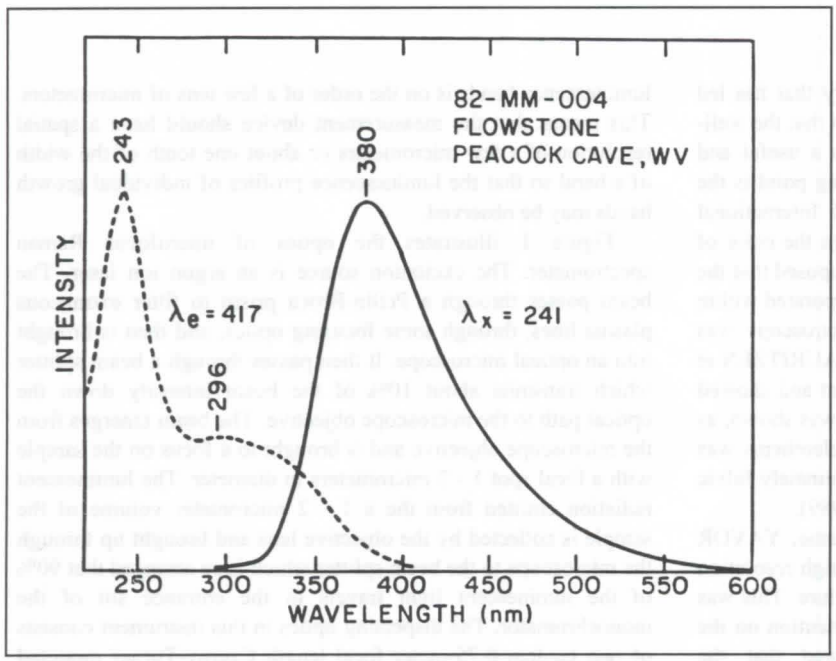

Figure 2. Emission and excitation spectra of specimen 82-MM-004, a flowstone sample from Peacock Cave, West Virginia, USA.

focused on a specific luminescence band and entire spectrum scanned or one can set the monochromator at the emission wavelength of interest and then translate the specimen to map the intensity of luminescence as a function of a x-coordinate along the translation direction.

The advantage of this type of instrumentation is in its great flexibility. It's disadvantage is that it is not convenient to use with very large specimens so that if one wished to measure the luminescence profile along a 2-meter segment of broom-handle stalagmite, it would be rather difficult.

3. Luminescence Spectroscopy

As observed visually or recorded on photographic film, typical speleothem luminescence consists of a bluish white to greenish white emission sometimes extending to the orange-yellow region of the spectrum. When examined in detail, there is much more to speleothem luminescence than alternating bands of bright and dim emission. The luminescence spectrum of a typical speleothem consists of two parts (Fig. 2). The emission spectrum is obtained by illuminating the sample with ultraviolet light of a specified wavelength and measuring the wavelength distribution of the emitted radiation. The excitation spectrum is measured by tracking the intensity of the luminescence as a function of the wavelength of the ultraviolet used to excite the luminescence. The brightest and most efficient luminescence is therefore obtained when the sample is illuminated with 243 nm UV with a secondary excitation at 296 nm. In this specimen there is a single emission band peaking at 380 nm. The spectral line shapes are approximately gaussian.

The argon ion laser has lines at 457, 488 and 514.5 nm all of which lie at wavelengths greater than the wavelengths of the excitation bands. However, the laser is highly intense and sufficient luminescence for measurement can be obtained by exciting into the long wavelength tail of the excitation band. The laser lines are also at longer wavelengths than the emission band and so cannot excite the main portion of this band. The emission observed from Ar-ion laser excitation will be due to a different set of luminophors than those excited by UV radiation. This is a difficulty that could be resolved by using a UV laser as an excitation source.

Chromatographic sepa- ration of the organic constituents of dissolved speleothems (WHITE, SMAILER, AND BRENNAN, unpublished data) show that the luminescent species in

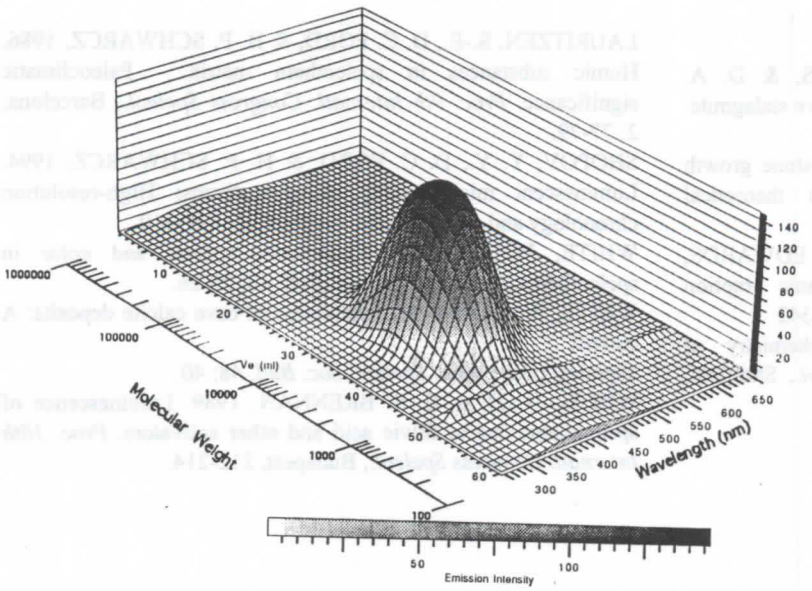

Figure 3. Three-dimensional plot of luminescence intensity as a function of both emission wavelength and molecular weight. Each tick mark on the V_e (elutriated volume) scale represents a separate chromatographic cut and a separately measured emission spectrum.

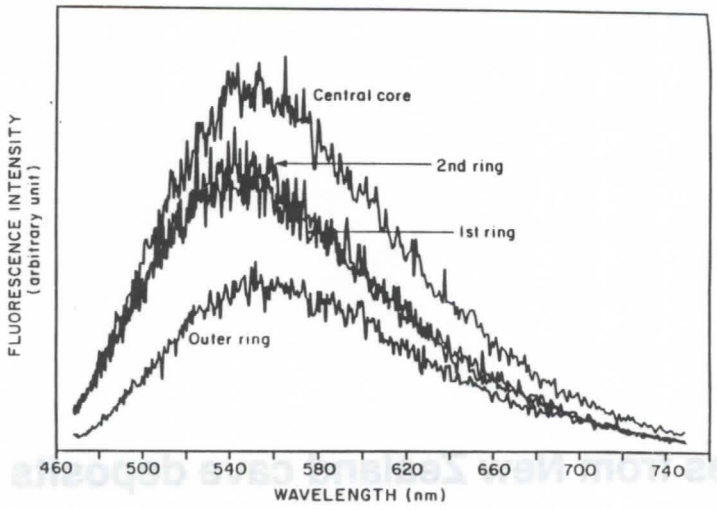

Figure 4 . Laser excited (457.9 nm line) emission spectra from individual growth bands in stalactite 88-MM-004.

speleothems consists of a mixture of molecules each of which has its own characteristic emission and excitation spectrum. As a result, the emission peak changes with wavelength of excitation. For the specific specimen used as an illustration, the main UV excited emission band has its peak intensity for the molecular weight fraction in the range of 5000 - 10,000 daltons (Fig. 3).

The emission bands excited by the 457.9 nm line of the Ar-ion laser in the microfocus spectrometer (Fig. 4) occur in the range of 550 - 560 nm, much greater wavelength than the UV-excited band shown in Fig. 2. The bands are broad but there are measurable shifts in the band positions. Fig.. 4 shows a sequence of spectra obtained from a sequence of luminescence bands in the same samples used for previous spectra. There is some variability in the spectra from one band to another but because the bands are very broad, there is a great deal of overlap. Because of the 1 - 2 micrometer spatial resolution of the laser spot, the luminescence banding can be mapped at any chosen emission wavelength.

4. Conclusions

The microfocus Raman spectrometer is shown to be a useful device for the accurate mapping of the distribution of speleothem luminescence. The spatial resolution is a few micrometers, smaller than the annual growth bands. The emission wavelength to be mapped is an adjustable variable. The instrumentation and technique could be easily extended to the use of a tunable UV laser as a source, thus adding the excitation wavelength as an additional adjustable variable.

Acknowledgment

This work was supported by a grant from the Petroleum Research Fund administered by the American Chemical Society.

References

BAKER, A., P. L. SMART, R. L. EDWARDS, & D. A. RICHARDS, 1993. Annual growth banding in a cave stalagmite. *Nature* 364: 518-520.

BAKER, A. & P. L. SMART. 1995. Recent flowstone growth rates: Field measurements in comparison to theoretical predictions. *Chem. Geol.* 122: 121-128.

BAKER, A., P. L. SMART, W. L. BARNES, R. L. EDWARDS, & A. FARRANT, A. 1995. The Hekla 3 volcanic eruption recorded in a Scottish speleothem. *Holocene* 5: 336-342.

GASCOYNE, M. 1977. Trace element geochemistry of speleothems. *Proc. 7th Internatl. Congress Speleol.*, Sheffield, 205-208.

LAURITZEN, S.-E., D. C. FORD, & H. P. SCHWARCZ, 1986. Humic substances in speleothem matrix - Paleoclimatic significance. *Proc. 9th Internatl. Congress Speleol.*, Barcelona, 2: 77-79.

SHOPOV, Y. Y., D. C. FORD, & H. P. SCHWARCZ. 1994. Luminescent microbanding in speleothems: High-resolution chronology and paleoclimate. *Geology* 22: 407-410.

WHITE, W. B. 1981. Reflectance spectra and color in speleothems. *Natl. Speleol. Soc. Bull.* 43: 20-26.

WHITE, W. B. 1986. Luminescence of cave calcite deposits: A current
appraisal (abs.). *Natl. Speleol. Soc. Bull.* 48: 40.

WHITE, W. B. & E. S. BRENNAN. 1989. Luminescence of speleothems due to fulvic acid and other activators. *Proc. 10th Internatl. Congress Speleol.*, Budapest, 212-214.

Evidence of glacial advances from New Zealand cave deposits

Paul W. Williams
Department of Geography, University of Auckland, Auckland, New Zealand

Abstract

Caves overrun by glaciers are known to accumulate dateable evidence of past glacial and interglacial events. Results are reported from investigations of Aurora Cave in Fiordland, southern New Zealand, and from other caves. Aurora Cave is situated in the side of a glacial trough. The cave commenced to form before 230 ka B.P. Sequences of glacifluvial sediments interbedded with speleothems are evidence of the number and timing of glacial advances and the status of intervals between them. Twenty-six uranium series dates on speleothems underpin a chronology of seven glacial advances in the last 230 ka, with the peak of the last main glacial advance at ca. 19 ka BP. With five advances in the Last Glacial, it is more complex than previously recognised in New Zealand. Comparison of the evidence fom caves with that recorded in deep sea sediments 300 km offshore from DSDP Site 594 reveals little matching. The results from caves support polar cap ice-core evidence for abrupt climate changes, but do not support synchroneity of onshore/offshore events.

L'oxygène et le carbone dans les concrétions nous informent-ils sur les climats passés?

par Sophie Verheyden
Aspirant du fonds National Belge de la recherche Scientifique (NFWO),
Vrije Universiteit Brussel, WE-CHRO, Pleinlaan 2, 1050 Brussel, België
sverheyd@vnet3.vub.ac.be
E. Keppens,
Vrije Universiteit Brussel,
Y. Quinif,
Faculté polytechnique de Mons.
Guy Deflandre

Abstract: Does the oxygen and carbon isotope record in speleothems register climate?
Stable isotopes of oxygen and carbon in speleothems theoretically are related to respectively the surface temperature and the vegetation present during calcite precipitation. In fact, this relationship seems more complex. The study of recent calcite and seepage water, as well as in situ measurements of climatic parameters suggest that other processes e.g. evaporation, degassing, interaction of the host rock,... affect dramatically the oxygen and carbon isotopic composition of the speleothems.

Résumé
Théoriquement l'oxygène et le carbone dans les concrétions nous informent sur respectivement la température de surface et la végétation présente lors de la précipitation de la calcite. En pratique, ces relations paraissent plus complexes. L'étude de concrétions récentes et de l'eau d'infiltration, ainsi que des mesures de paramètres climatiques dans les grottes belges remettent en question la relation théorique entre le climat et l'oxygène et le carbone dans les concrétions. Cette étude montre que des processus plus locaux comme l'évaporation, le dégazage, l'intéraction de la roche environnante,... peuvent influencer de façon dramatique le signal isotopique de l'oxygène et du carbone dans les concrétions.

1. Introduction

Cette étude fait partie du projet européen "A high resolution reconstruction of terrestrial palaeoclimate from continental carbonates" qui a pour but de retracer le climat Holocène (10000 – 0 ans BP) grace à l'étude de l'oxygène et du carbone dans les concrétions de divers sites européens. Nous présentons ici les résultats du site belge.

La grotte du Père Noël fait partie du système de Han-sur-Lesse comprenant entre autres la grotte de Han et le Père Noël. Elles sont situées dans la bande de calcaire Givetien, la Calestienne, qui traverse la Belgique d'Est en Ouest (fig. 1). On y trouve la plupart des phénomènes karstiques belges. Le Père Noël est le résultat d'un recoupement de méandre de la Lesse à travers le Massif de Boine (QUINIF, 1977). De nos jours cette cavité est entièrement fossile et un important concrétionnement s'est mis en place depuis plus de 100000 ans. Une stalagmite de 65cm de long a été prélevée afin d'étudier les changements de composition isotopique le long de l'axe longitudinal (fig. 2). La datation U/Th indique que la concrétion s'est déposée entre 13000 et 2000 ans BP (Before Present). Elle couvre donc en partie le Tardi-glaciaire et l'Holocène.

2. Les isotopes stables dans les études du climat passé

Dans la nature, il existe trois oxygènes de masses différentes: un oxygéne de masse 16 (^{16}O) (c.à.d. 16 fois la masse de l'hydrogène), un oxygène de masse 17 (^{17}O) et un oxygéne de masse 18 (^{18}O). Ce sont les isotopes de l'oxygène. Aucun de ces éléments n'est radioactif, ils sont donc tous stables. Le carbone compte deux isotopes stables, ^{12}C et ^{13}C et un radioactif, le ^{14}C. Ces isotopes sont présents en certaines proportions (on mesure généralement le rapport $^{18}O/^{16}O$ et $^{13}C/^{12}C$) . Chaque processus physique (comme l'évaporation) ou chimique (comme la précipitation de la calcite) change la proportion des isotopes. Pour faciliter les calculs on emploie les notations $\delta^{18}O$ et $\delta^{13}C$ (exprimés en ‰). Ils traduisent la différence entre le $^{18}O/^{16}O$ de la matière étudiée et une matière de réference. La matière de réference (ref) dans le cas de la calcite est le PDB, le "Pee-Dee Belemnite", un fossile de la Formation de Pee-Dee en Caroline du Sud. Plus les δ sont elevés plus il y a d'isotopes 'lourds' (c.a.d. ^{18}O ou ^{13}C) dans la calcite (c) (HOEFS, 1997).

$$\delta^{18}Oc = [(^{18}O/^{16}O)c - (^{18}O/^{16}O)ref]*1000/(^{18}O/^{16}O)ref$$

Grace à l'étude des isotopes de l'oxygène dans les dépots marins et les glaces polaires, nous connaissons bien les grandes variations climatiques à l'échelle mondiale. Ces études nous ont fait mieux comprendre les cycles froid-chaud ou glaciaire-interglaciaire. L' analyse de l'oxygène dans les tourbières et dans les dépots lacustres, ainsi que dans les concrétions nous informent sur le climat continental plus local et à plus petite échelle de temps (cycles annuels ou saisonniers).

3. Le $\delta^{18}O$ et le $\delta^{13}C$ dans les concrétions

Pour bien comprendre le mécanisme des isotopes stables dans les concrétions, rappelons-nous la formation d'une concrétion. L'eau de pluie percole dans le sol et se charge de CO_2 qui est originaire de la respiration des plantes. Ensuite l'eau s'infiltre dans les interstices du calcaire sous-jacent et dissout le $CaCO_3$. Rencontrant un vide, l'eau dégaze du CO_2 et précipite de la calcite.

Théoriquement le rapport de l'**oxygène** dans la calcite ($CaC\underline{O}_3$) dépendra de la **température** à laquelle la calcite s'est déposée et de la composition isotopique initiale de l'eau d'où la calcite précipite. Dans les deux cas le $\delta^{18}O$ est directement lié à la température de surface:

- dans les grottes belges, qui sont peu profondes la température en grotte est une moyenne annuelle de la température de surface (WIGLEY ET BROWN, 1976).

- la composition isotopique de l'eau de percolation est comparable à celle de l'eau de pluie. La composition de l'eau de pluie est en relation directe avec la température de surface (DANSGAARD, 1964).

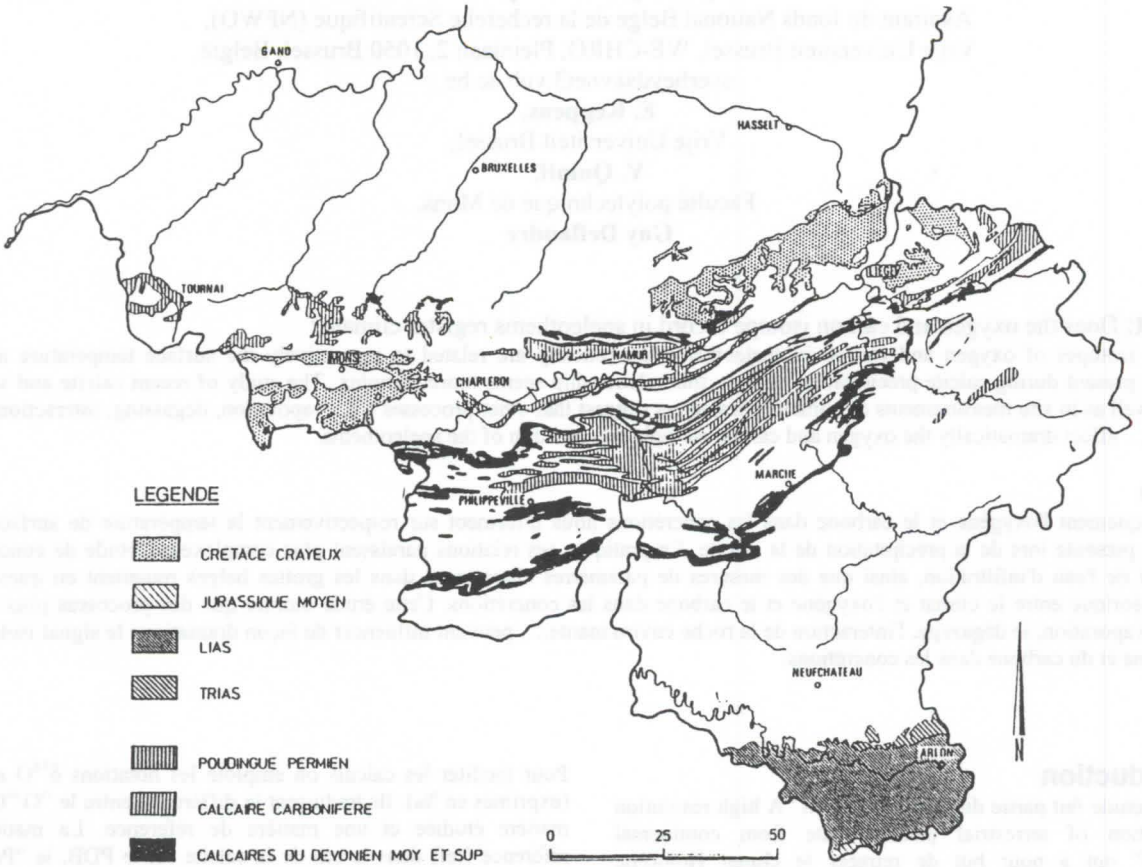

Fig. 1: Les formations carbonatées de la Belgique. Han-sur-Lesse se trouve dans la Calestienne (flèche). D'après C. EK, 1976.

On peut donc, en analysant le $\delta^{18}O$ dans la concrétion, retrouver la température qui regnait en surface lors de la précipitation de la calcite.

Le rapport du **carbone** dans la concrétion ($CaCO_3$) dépend beaucoup moins de la température mais est directement lié au type de **végétation** présent à la surface lors de la précipitation de la calcite. Selon le cycle de photosynthèse utilisé, les plantes ont un $\delta^{13}C$ différent. Le cycle Calvin est utilisé par les plantes dites C_3 (dans un premier temps elles produisent une molecule à trois atomes de carbone). En Belgique, toutes les plantes appartiennent à ce groupe, sauf le maïs. Le cycle Hatch-Slack est utilisé par les plantes dites C_4. Ces plantes vivent dans des régions arides et chaudes, les herbes de savannes sont souvent des plantes C_4. Le $\delta^{13}C$ de la calcite sera différent selon le type de plantes présent en surface lors de la précipitation de la calcite (CERLING, 1984).

Il y a néanmoins une condition pour pouvoir utiliser ces équations théoriques: c'est l'équilibre isotopique. Si la calcite se dépose de façon lente et sans perturbations les changements isotopiques sont connus grace à des expérimentations en laboratoire et on peut donc retrouver la température en faisant les mesures de $\delta^{18}O$. Si la précipitation est perturbée par un dégazage trop rapide ou de l'évaporation, ces relations théoriques ne sont plus valables (HENDY, 1971).

4. La courbe paléoclimatique

Une mesure de $\delta^{18}O$ et $\delta^{13}C$ a été faite tout les 5 mm le long de l'axe longitudinale de la stalagmite (fig. 3). La courbe d'oxygène ($\delta^{18}O$) ainsi obtenue devrait donc théoriquement retracer les changements de température entre 13000 et 2000 ans BP. La courbe de carbone devrait nous indiquer le type de végétation présent durant cette période.

Une rapide observation de ces courbes (fig. 4) montre des variations dans le $\delta^{18}O$ et le $\delta^{13}C$ tout au long du Tardi-glaciaire et de l'Holocène. Ceux-ci pourraient être en relation avec des changements climatiques. Les variations sont néanmoins les mêmes pour le $\delta^{18}O$ et le $\delta^{13}C$. Il y a donc co-variation. Cela suggère qu'un seul paramètre est à l'origine des variations et que ceux-ci ne traduisent donc pas des changements de températures ou de végétation. De plus les variations importantes du $\delta^{13}C$ sont très inattendues, puisque la Belgique n'a pas connue de plantes C_4 durant cette période (sauf le maïs dans les régions cultivées). Finalement, des mesures de $\delta^{18}O$ et $\delta^{13}C$ le long d'une même lamine de croissance montrent que la majeure partie de la stalagmite a été déposée en non-équilibre isotopique (HENDY, 1971).

Fig. 2: La atalagmite prelevée dans la grotte du Père Noël à Han-sur-Lesse est environ 65cm de long.

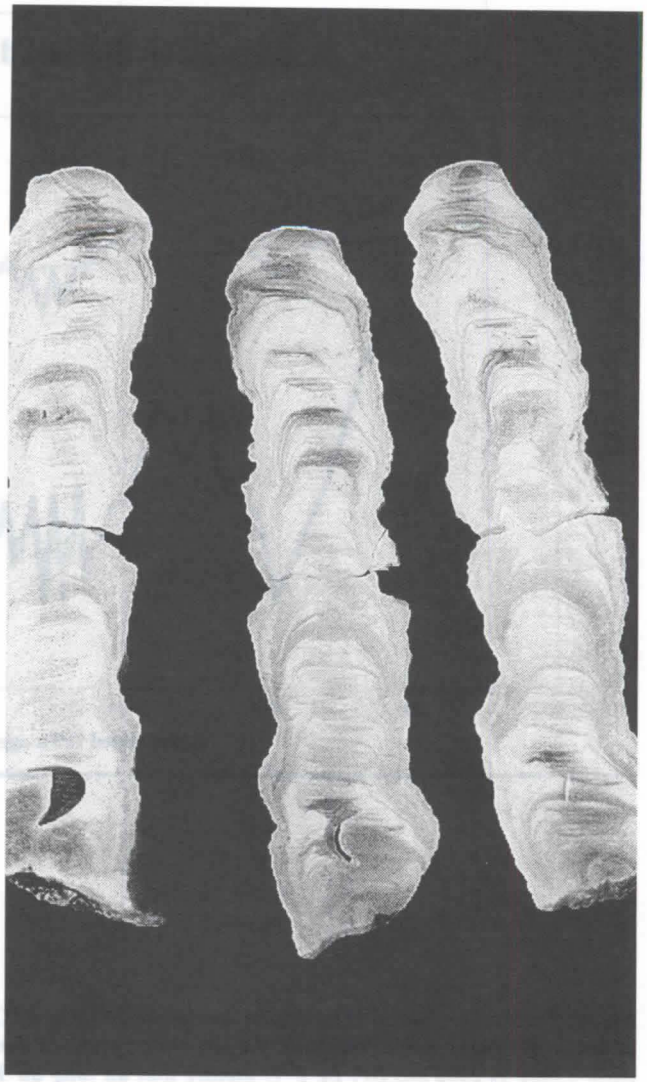

Fig. 3: La stalagmite de la grotte du Père Noël à Han-sur-Lesse en Belgique est sciée afin d'obtenir une tranche du milieu de la stalagmite. Un échantillon est prélevé tout les 5mm le long de l'axe longitudinal de la concrétion afin d'étudier les changements de la composition isotopique ($\delta^{18}O$ et $\delta^{13}C$) de la concrétion.

Les premiers résultats d'une étude in-situ mettent en relation un $\delta^{18}O$ et $\delta^{13}C$ élevé avec un débit de percolation lent. Le signal isotopique de l'eau de percolation reste toutefois inchangé par rapport au signal isotopique de l'eau de pluie. La perturbation se situe donc pendant la précipitation de la calcite. Une évaporation accrue de l'eau ($H_2\underline{O}$) pendant la précipitation de la calcite entrainera une augmentation du $\delta^{13}C$ de la calcite, mais aussi une augmentation du $\delta^{13}C$. En effet, une évaporation de l'eau va de pair avec un dégazage de $\underline{C}O_2$ plus rapide, ce qui entraine une augmentation du $\delta^{13}C$ de la calcite. Puisqu'il y a perturbation de l'équilibre isotopique, les équations théoriques ne peuvent pas être employées dans ce cas-ci. On peut toutefois supposer que pendant les périodes plus humides, le $\delta^{18}O$ ainsi que le $\delta^{13}C$ diminuent alors que pendant les périodes plus sèches, avec une évaporation plus importante, ils augmentent. Donc, si la stalagmite ne peut pas nous fournir des indications sur les changements de température et de végétation, elle peut quand même nous fournir des indications sur la pluviométrie dans le passé.

A grande échelle pourtant on peut supposer que ces perturbations ont moins d'effet puisque on considère la moyenne de longues périodes. Ainsi le $\delta^{18}O$ augmente de 1‰ tout au long de la croissance de la stalagmite. En tenant compte du changement plus ou moins connu du $\delta^{18}O$ de l'eau de pluie durant cette période on peut estimer un changement de température de 5 à 6°C entre 13000 et 2000 ans BP.

5. Conclusion

Les études de la composition isotopique de l'oxygène et du carbone d'une stalagmite Holocène belge montre que dans ce cas, les changements de $\delta^{18}O$ et $\delta^{13}C$ ne retracent pas les changements de température et de végétation comme théoriquement attendu. Des mesures in situ laissent toutefois supposer que les changements de $\delta^{18}O$ et $\delta^{13}C$ peuvent être mis en relation avec des changements de pluviometrie. A long terme, la courbe de $\delta^{18}O$ suggère quand même une augmentation de la température de 5 à 6°C entre 13000 et 2000 ans BP.

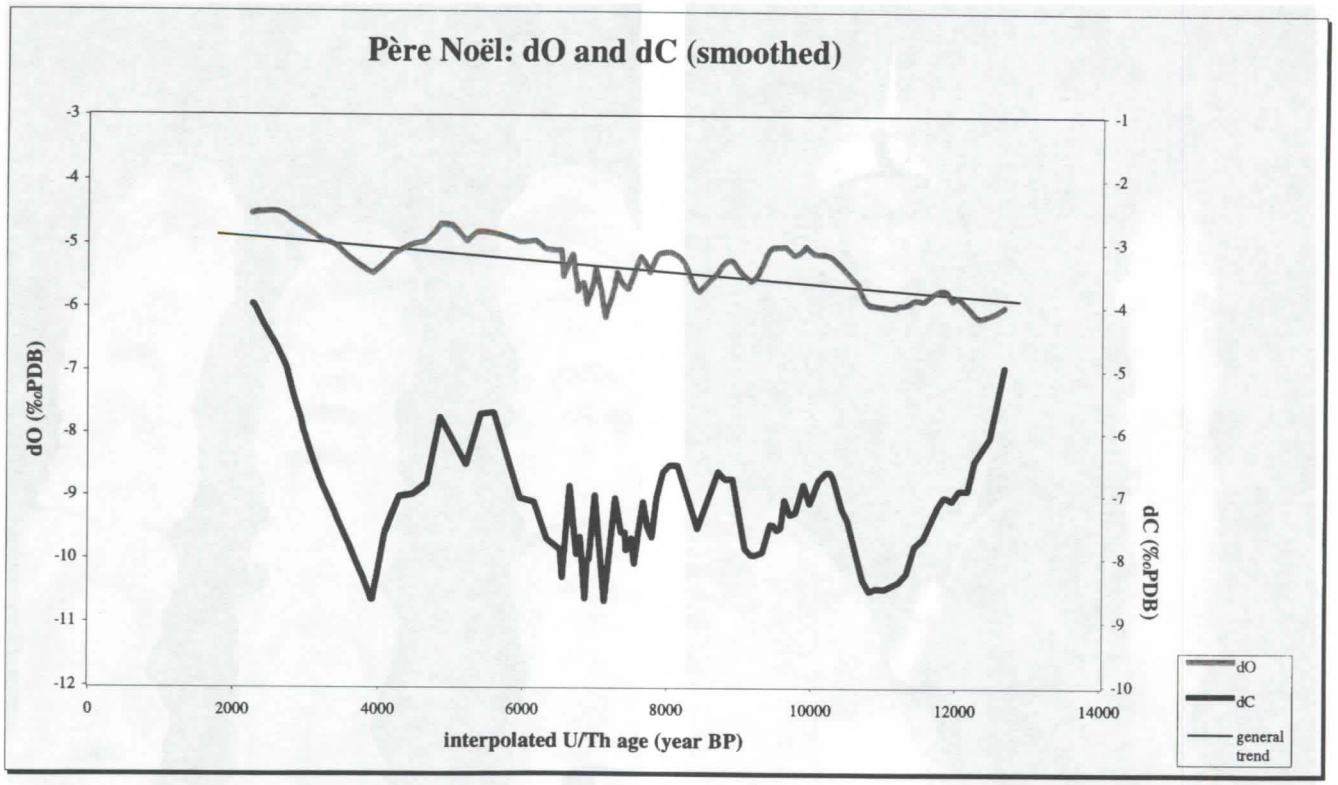

Fig. 4: En représentant la composition isotopique ($\delta^{18}O$ et $\delta^{13}C$) d'une stalagmite en fonction de l'age de chaque échantillon, on obtient une courbe paléoclimatique. La stalagmite prélevée dans la grotte du Père Noël à Han-sur-Lesse, Belgique s'est déposée entre 13000 et 2000 ans BP. Le $\delta^{18}O$ montre tout au long du Tardi-glaciaire et de l'Holocène des variations importantes. A plus long terme, une augmentation du $\delta^{18}O$ d'environ 1‰ est observée. Le $\delta^{13}C$ montre également des variations considérables durant la croissance de la stalagmite, mais pas de changement à long terme.

Je remercie vivement les grottes de Han pour l'accès au site, Dominique Genty, Yves Quinif et Eddy Keppens pour l'aide précieuse dans ce travaille, ainsi que ma famille et tous les copains pour les coups de pouce.

Les datations U/Th par spectrométrie de masse sont réalisées par F. Mc Dermott, University College Dublin. Les mesures du $\delta^{18}O$ de l'eau sont réalisées par A. Longinelli, Universita di Trieste. Ce travail a pu être réalisé grace à la Communauté européenne, projet EV5V-CT91-0509.

Références

CERLING TH.E. 1984. The stable isotopic composition of modern soil carbonate and its relationship to climate. Earth & Planetary Letters 71, 229-240.

EK C. 1976. Les phénomènes karstiques, 137-157, in Géomorphologie de la Belgique. Hommage au Prof. P. Macar, ouvrage coordonné par A. Pissart, Liège, 224p.

DANSGAARD W. 1964. Stable isotopes in precipitation. Tellus 16, 436-468

HENDY C.H. 1971. The isotopic geochemistery of speleothems. The calculation of the effects of different modes of formation on the isotopic composition of speleothems and their applicability as paleoclimatic indicators. Geochimica et Cosmochimica acta, 35, 801-824.

HOEFS, J. 1997. Stable isotopes geochemistry, 4th ed. Springer, Berlin, 241p.

QUINIF Y. 1977. Essai d'étude synthétique des cavites karstiques de Belgique. Revue Belge de Géographie 101, fasc.1 à 3, 115-173.

WIGLEY T.M.L., BROWN M.C., 1976. in: The Science of Speleology, eds. Ford & Cullingford, Academic Press, N.Y, 329-358.

Paleoclimate of the quaternary processes in the western karst of Cuba: preliminary results

Jesús M. Pajón M.
Instituto de Geofísica y Astronomía, Calle 212 # 2906, e/ 29 y 31
La Coronela, La Lisa, Ciudad de La Habana, Cuba. CP: 13 600, FAX: (537) 33.94.97

Abstract

The main goal of this research project, is to obtain quantitative assesments about the paleoclimatic evolution and the Quaternary processes of Cuba during the last one million years as a contribution to the scientific understanding of global climatic changes in the world, especially in the Caribbean region. It is impossible to understand the impact of human activity on world climate and the environment without knowledge about the natural trends in planetary evolution. In this respect, the study of the actual climate is not enough for such an evaluation and prognosis.

The fact that, most of the paleoclimatic investigations have been conducted in countries from temperate or mid latitude zones in the northern hemisphere, with only few and non integrated studies from tropical areas, is one important reason to develop such research.

At present, our Project includes:

- A Paleoclimatic Data Base System of the Cuban Quaternary.
- GIS of the Cuban Paleoclimate in key sectors of Western Cuba.
- Characterization of the Cavernary levels of the Western Karst of Cuba, and their relation with sea level flucuations during the Quaternary.
- Study of paleotemperatures, paleorainfall and paleosalinity in the Western Karst of Cuba, during the last 125,000 years and application to the models of climatic forecast.
- Knowledge of the Cuban Climate in the present millenium.
- Map of the Carbon reserves in the soils of Cuba, for the last 3,000 years.

The experimental areas of the Project consist of: two karstic cavernary systems (including up to 8 cavern levels and 40 km of underground galleries), one lake in a sedimentation basin and the Marine Terraces System in the North-Western Coastal Area of Cuba.

Very important quantitative estimations can be obtained from these studies for Cuba and the Caribbean, with incidence in the planing of a sostenaible development of the society and the preservation of the environment and the biodiversity, taking account the prognostic of the tendencies in the temperatures and the sea level changes, of great importance for the development and protection of the marine and terrestrial ecosystems, and the constructive and touristic development, specially in the coastal areas.

Resumen

El principal objetivo de este Proyecto es, obtener una valoración cuantitativa de la Evolución Paleoclimática y los Procesos Cuaternarios en Cuba durante el último millón de años, como una contribución al conocimiento de los Cambios Climáticos en el planeta y especialmente en la región del Caribe. Es imposible evaluar la Actividad e Impacto del hombre en el clima mundial y en el medio ambiente, sin un conocimiento acerca de las tendencias naturales debido a la evolución planetaria, y en este aspecto, el estudio del clima actual, resulta insuficiente para tal evaluación y pronóstico.

El hecho que la mayoría de las investigaciones paleoclimáticas han sido desarrolladas en países de zonas templadas o latitudes medias, en el hemisferio norte, con solo pocos estudios integrados en áreas tropicales, constituye otro importante aspecto que apunta a la necesidad de desarrollar tales investigaciones.

Actualmente, el presente proyecto incluye:

- Un Sistema de Base de Datos Paleoclimáticos del Cuaternario Cubano.
- SIG del Paleoclima Cubano en Sectores Llaves de Cuba Occidental.
- Caracterización de los Niveles de Cavernamiento del Karst Occidental de Cuba, y su relación con los Cambios del Nivel del Mar, durante el Cuaternario.
- Estudio de las Paleotemperaturas, Paleoprecipitaciones y Paleosalinidad en el Karst Occidental de Cuba, durante los últimos 125 000 años. Aplicación a los Modelos de Pronóstico Climático.
- Conocimiento del Clima de Cuba en el presente milenio.
- Mapa de las Reservas de Carbono en los suelos de Cuba, para 3000 y 0 años.

Las áreas experimentales del Proyecto son: Dos Sistemas Cavernarios Kársticos (con 8 niveles de cavernamiento y 40 km de galerías subterráneas); Un Lago en una Cuenca de Sedimentación y el Sistema de Terrazas Marinas en la Costa Noroccidental de Cuba.

Importantes estimaciones cuantitativas pudieran derivarse de tales estudios para Cuba y el Caribe, con gran incidencia en la planificación de un desarrollo sostenible de la sociedad y la preservación del Medio Ambiente y la Biodiversidad, pudiendo destacarse el pronóstico de las tendencias de las temperaturas y las variaciones del nivel del mar, de gran importancia para el desarrollo y protección de los ecosistemas marinos y terrestres y el desarrollo turístico y constructivo, especialmente en las zonas costeras.

General Comments

The importance of carrying this investigation in Cuba, is given by several reasons. One of them, is its geographical position between the north American continent and the tropics, specially those island from the Greater and Smaller Antilles, giving an exceptional opportunity to study the influence of continental glaciations on tropical and subtropical territories. Thus, the paleoclimatic information obtained in Cuba will be of regional relevance. Another reason is that, practically all the observed geomorphology in Cuba, was modeled during the Quaternary period in which the variations in the general sea level, temperature, humidity and rainfall have played a mayor role in landscape genesis and evolution. The results obtained will contribute to the understanding of the relations between climate, environment, landscape and time.

Moreover, in Cuba there are many different geological and geomorphologic features, amenable to be used as targets for paleoclimatic studies, as there are hundreds of kilometers of coast with limestone marine terraces at different levels, a shallow and extensive submarine platform covered with different generation of fossil and active coral reefs, and different geological formations of quaternary limestone, among others. Another peculiarity seldomly found in other countries in the world is the existence of underground ancient fluvial caves, excavated at different levels over the actual valleys, corresponding to the local base variations, due to the changes of the general sea level, motivated by the advances and recessions of the glaciers in the continents. These caves represents fragments of ancients river courses with their bed load sediments perfectly preserved in many places, interlayered also with carbonate cave sediments of chemical origin (stalagmites, sinters, etc.) which enables their dating using isotope and paleomagnetic methods, as well as their characterization from the temperature point of view. From another hand, the study of both the granulometric spectrum of the bed load sediments and coarse materials (pebbles, etc.), as well as the study of the scalloped cave conduits allows estimations of water discharges, runoff and other parameters of those ancient river, and since their basin are well bounded, paleoprecipitations can be also estimated. All these sources of evidences are located either just in the same or places not far from each other (remember also that Cuba is not a big country), so that the multivariate characterization of well dated epochs from the near geological past is possible.

Therefore, there are suitable conditions for field and laboratory investigations with a complex of quantitative methods oriented to different branches of geochemistry, geophysics, geology and geography as geochronology, atmospheric sciences, geomorphology, hydrogeology and others, which can be integrated in order to characterize the paleoclimates of the Cuban territory during different periods along the Quaternary. This characterization will involve paleotemperatures, paleorainfalls, paleosalinities and perhaps other parameters. This information, together with isotope and paleomagnetic dating will depict more precisely the regional trends on climatic changes, at least for the Cuban territory and its surroundings, as a contribution to the study and understanding of one of the most challenging and important problems of modern science, with a great impact in modern society long term development planing and environment preservation.

Some preliminary results:

The Paleoclimatic Data Base Systems of the Cuban Quaternary consist in an interdisciplinary network of information about Geochemistry of Sediments and Waters; Paleomagnetism and Magnetic Susceptibility; Stable Isotope Geochemistry and Isotopic Dating; Sea Level Changes and Neotectonic Movement; Paleorainfall, Paleotemperatures and Paleosalinity; Historic and Present Climatology; Geology, Geomorphology, Speleology and Hidrogeology; Cavernary and Marine Terrace Levels. All this information is connected to GIS according the specific experimental area, in order to obtain an integrate and interconnected evaluation.

The Majaguas-Cantera Cavernary Systems in the Western Karst of Cuba, show a development of eight underground levels from + 50 to + 290 m a.s.l. There are two active levels (+ 70 m a.s.l.), one seasonal level (+ 80 to + 90 m a.s.l.), one episodical level (+ 90 to + 110 m a.s.l.) and five merofossil levels (+ 120 to + 290 m a.s.l.) (MOLERIO, 1992, FLORES, 1995). These cavernary levels and the karstification processes, are related with the regional phenomena of the glacioeustatic changes of the sea level during the Quaternary period, as a consequence of the climatic changes.

The table 1 show a good correlation between the cavernary levels of the Sumidero Underground System (ACEVEDO, 1971) and the kaolinite contents of the quaternary sediments deposited inside the caves (PAJÓN, 1983). FAGUNDO et al. (1984) calculated from a multiple regression equation of absorbance relations in the infrared spectra.

The paleoflow, paleodrainage and paleorainfall values was calculate for the Sumidero Region in the Cuyaguateje Basin River, from the scallops analysis in a fluvial fossil gallery of the Perfecto Cave (VALDÉS, 1974). The paleorainfall value of 1410 mm suggest that the climate of the region during the hydrological behavior of Perfecto Cave (Illinois age-Cuban pluvial Illinois) was more wet that today (700 mm).

	Epoch of Speleogenesis	Cavernary Level	Absolute Altitude (m)	Kaolinite Content (%)
PLEISTOCENE	Pre-Quaternary (Pliocene)	Cima	195-250	-
	Nebraska Q_I	Soterráneos Cave	170-195	51-53
	Kansas Q_{II}	Pío Domingo Cave	130-180	35-43
	Illinois Q_{III}	Perfecto Cave	100-138	17-22
	Wisconsin early (Iowa) Q^{I}_{IV}	Clara Cave	85-132	7
	Wisconsin late Q^{II}_{IV}	Sumidero	80-130	6
	Holoceno			

Table 1.- Correlation between the cavernary levels in the Sumidero Underground System and the kaolinite content of the Quaternary sediments inside the caves. Western Tropical Karst of Cuba.

$K(\%) = 7{,}7882\ A_3/A_4 + 46{,}7491\ A_5/A_6 - 25{,}7192$

Where: $A_3 = A(925\ cm^{-1})$, $A_4 = A(808\pm3\ cm^{-1})$, $A_5 = A(1040\ cm^{-1})$, $A_6 = A(1117\pm3\ cm^{-1})$

Considering the carbonate, siliceous and gypsum relicts, as well as other geographical index, ORTEGA & ARCIA (1982), proposed a paleorainfall map for Cuba in the last glacial (Wisconsin or Wurm), suggesting an arid climate in that period.

On the base of the coastal eolic formations of the Pleistocene in the western of Cuba, SHANZER et al. (1975) considered that the arid climates coincided with the glaciations.

KARTASHOV & MAYO (1976) establish that in the Cuban Pleistocene, took place alternate climatical oscillation of pluvial and arid phases. MAYO (1970) established a correlation between pluvial and glacial advance.

Based in the weathering profiles of Guane and Guevara Quaternary Formations, KARTASHOV et al. (1981) suggest the division of the Cuban Pleistocene in two stages: a lower wet stage and an upper dry stage.

Using the Gates climatological model and the probable level of the periglacial zone, ORTEGA (1983) proposed a paleotemperature map on the base of the paleosea mean temperature.

Respect to the historical times, the records of rainfall between 1871 and 1984 in Santiago de Cuba station, show a significative increase, and a decrease between 1750 and 1871. Respect the temperature, there is an increment of 0,5°C from the XIX century and 0,2-0,3 in the last 40 years, in the Casablanca Station of Havana City (CELEIRO, 1996).

About the sea level changes, the Siboney Station (eastern of Cuba), remark a quantitative increase of 2,9 mm/year during 30 years of records (HERNANDEZ, pers. comm.).

Acknowledgements

I would like to express my greatitude to my colleague and friend Lic. Ismael Hernández for very hepful discussions and the composition of this paper.

Bibliography

ACEVEDO G. M. 1971. Geomorfología de Sumidero y sus inmediaciones, Sierra de los Órganos, Pinar del Río, Cuba. Rev. Tec. Vol. IX, No. 3-4, (1971), pp. 33-54.

CELEIRO M. 1996. Conocimiento del Clima de Cuba en el presente milenio. (En prensa).

FAGUNDO J.R., VALDÉS J.J., PAJÓN J.M. 1984. Estudio de los Sedimentos Cuaternarios de la Cuenca del río Cuyaguateje, mediante Espectroscopia Infrarroja y Difracción de Rayos X. Rev. Vol. Hid. 63. Año XXI (1984). 53-61 pp.

FLORES V.E. 1995. Niveles de cavernamiento y fluctuaciones glacioeustáticas cuaternarias de Cuba Occidental. Cong. Int. LV Aniv. de la SEC (En prensa).

KARTASHOV I.P. & MAYO. 1976. Esquema estratigráfico y división del sistema cuaternario de Cuba [en ruso]. En sedimentación y formación del relieve de Cuba en el Cuaternario, Nauka, Moscú, pp. 5-33.

KARTASHOV I.P., CHERNYAJOVSKI A.G., PEÑALVER L. 1981. El Antropógeno en Cuba [en ruso], Nauka, Moscú, 147 pp.

MAYO N.A. 1970. Depósitos pleistocénicos de los cauces abandonados de la Sierra de los Órganos: Evidencias de períodos pluviales. ACC. Ser. Esp. y Cars. 7, p. 88-89.

MOLERIO L.L. 1992. Distribución del cavernamiento en las Sierras del Pesquero, San Carlos, Resolladero y Mesa, Pinar del Río, Cuba. II Cong. Esp. Lat. y el Caribe, Pinar del Río, Cuba, 19-20 pp.

ORTEGA S.F. & ARCIA M.I. 1982. Determinación de las lluvias en Cuba durante la Glaciación de Wisconsin, mediante los relictos edáficos. Ciencia de la Tierra y el Espacio, No. 4, pp. 85-104.

ORTEGA S.F. 1983. Una hipótesis sobre el clima de Cuba durante la Glaciación de Wisconsin. Ciencias de la Tierra y el Espacio. No. 7, pp. 57-68.

PAJÓN J.M. 1983. Distribución de los Sedimentos Cuaternarios en las Cavernas del Karst de la Sierra de San Carlos, Sierra de los Órganos, Pinar del Río, Cuba. (Manuscrito Inédito, Archivo del GEM de la SEC).

SHANZER E.V., PETROV O.M., FRANCO G.L. 1975. Sobre las formaciones costeras del Holoceno en Cuba. Las terrazas pleistocénicas de la Región Habana-Matanzas y los sedimentos asociados a ellas. ACC. Serie Geográfica, No. 21, pp. 3-26.

VALDÉS J.J. 1974. Nuevo elemento para el estudio cuantitativo de los carsos obtenidos mediante el análisis dimensional y su utilidad en el cálculo de paleoprocesos geohidrológicos. Rev. Tec. Vol. XI, No. 3, Mayo-Junio/1974, pp. 23-32.

Excentriques Capillaries, Do They Carry Paleoclimatic Information?

Stephan Kempe & Jens Hartmann
Techn. Univer. Darmstadt, Geol.-Paleontol. Inst., Schnittspahnstr. 9, D - 64287 Darmstadt, Germany

Abstract

Excentriques (Helictites) are one of the most intriguing speleothems. They grow seemingly unimpeded by gravity. Apparently several different forms exist. We have investigated the capillaries of monocrystalline clear calcitic excentriques collected from caves in the Winterberg limestone quarry, Harz, Germany, in 1972. We inspected the capillaries both visually and by casting them with epoxy and dissolving the calcite in dilute HCl. The capillaries casts were then investigated by scanning electron microscopy. Even though all of the crystals are from the same cave, the capillaries show various patterns. Some show crystal faces, others are rather smooth and still others have a clearly beaded morphology. It was this beaded morphology which led Kempe and Sand Spaeth (1977) to hypothesize that the individual knots are annual growth increments. We now test this hypothesis by measuring bead sizes and we will try to link these records with recent meteorological data on temperature, precipitation and potential evaporation from the Harz region.

Zusammenfassung

Excentriques (Helictiten) gehören zu den merkwürdigsten Speläothemen. Sie wachsen scheinbar unbeeinflußt von der Gravitation. Offenbar gibt es verschiedene Formen. Wir haben die Kapillaren von monokristallinen, klaren, calcitischen Excentriques untersucht, die von einer Aufsammlung aus Steinbruchshöhlen des Winterberges, Harz, Deutschland, aus dem Jahr 1972 stammen untersucht. Die Kapillaren wurden mit Epoxydharz ausgegossen und der Kristall mit verdünnter HCl aufgelöst. Die Kapillarausgüsse wurden anschließend mit dem Elektronenmikroskop untersucht. Obwohl alle Kristalle aus der selben Höhle stammen, zeigen die Kapillaren ganz unterschiedliche Muster. Einige bilden Kristallflächen ab, andere sind glatt und wiederum andere haben eine Perlschnur-Morphologie. Diese Perlschnur-Morphologie ließ Kempe & Spaeth (1977) vermuten, daß die individuellen Knoten jährlichen Zuwachs repräsentieren. Wir testen jetzt diese Hypothese, indem wir die Knotengröße vermessen und versuchen, sie mit den rezenten Wetteraufzeichnungen über Temperatur, Niederschlag und potentieller Evaporation aus der Harz Region zu korrelieren.

References

KEMPE, S. & C. SPAETH (1977): Excentriques: Their capillaries and growth rates. - Proc. 7th Intern. Spel. Congr. Sheffield, U.K.: 259-262.

Paleoclimatic reconstruction and timing of sea level rise at the end of the Penultimate Glaciation, from detailed stable isotopic study and TIMS dating of submerged Bahamian speleothem

Joyce Lundberg
Dept. of Geography, Carleton University, Ottawa,
Ontario, K1S 5B6, Canada

Abstract

TIMS U-Th dating of a Bahamian stalagmite from -45 m ASL yielded a (preliminary) date for sea level rise at the end of the Penultimate Glaciation, past -45 m, at ≈131 ka. Sea level rise from -45 m ASL to the Last Interglacial high stand of +6 m ASL (≈130 ka) must have occurred in a short time frame of perhaps 1 kyr. The stable isotope record from this sample, of higher resolution than most other proxy records, reveals high frequency spikes and troughs that mimic the GRIP ice core record. Two preliminary dates place the isotopic curve almost exactly coincidental with GRIP, and almost mid-way between the orbitally-tuned marine foraminiferal record and DH11, the Devil's Hole calcite vein from Nevada.

Introduction

A stalagmite recovered from 45 m below present sea level in a blue hole on Andros Island, Bahamas, has been U-Th dated by thermal ionization mass spectrometry. The cave was air-filled during glacial low sea levels and stalagmites grew. Calcite deposition was stopped by rapid sea level rise at the end of the penultimate glacial (Termination II). The sample was then subject to dissolution giving it a broadly cuspate and asymmetric form (Figure 1). After this some boring of the outer surfaces by marine sponges occurred and the sample was encased in 1-5 cm of marine packstone.

A similar sample was dated by alpha counting in the 1970s (GASCOYNEet al 1979). Those dates were unreliable for two reasons: the first is that the large samples size required for alpha counting reduces the resolution attainable; the second is that the sponge borings on the outer layers introduced a younger aragonitic component. Only the dates on the inner material can be considered reliable (within the large error inherent to the alpha counting system) and these dates are not of great interest.

Materials and Methods

For this study the stalagmite (78032) was sampled from close to the core out to the youngest layer still present at the tip of a dissolution cusp. Samples for oxygen and carbon stable isotope analysis were taken approximately every millimeter using a binocular microscope to choose sites free from sponge borings. Uranium content is ≈0.2 ppm; for each date 0.2 g material was obtained (enough for 1-2 repeats) by drilling a slice parallel to the growth layers, then splitting this into 1 mm thin cleavage fragments. Each fragment was examined under binocular microscope and any boring sponge holes were drilled out. Most of the holes were empty but some had a reddish filling of younger material. Any slice with more than about 20% borings was rejected. Chemical purification of the dissolved samples was by ferric hydroxide co-precipitation of uranium and thorium and separation on anion exchange columns. Oxygen and carbon isotopic ratios were measured on a VG Isogas SIRA mass spectrometer in McMaster University, Canada. Uranium and thorium isotopic ratios were measured on a Finnigan-Mat 262 thermal ionization mass spectrometer in The University of Bergen, Norway. Dates were calculated using $^{230}Th/^{238}U$ and $^{230}Th/^{234}U$ ratios.

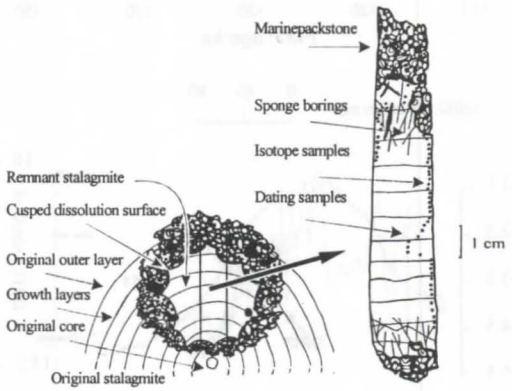

Figure 1: Sample 78032: to the left is the original speleothem cross section and the calcite remaining after dissolution and marine packstone deposition; to the right is the sampled slab showing isotope sampling holes and slices cut for dating.

Results and discussion

Date of sea level rise :

Preliminary test dates gave 142 ±7 ka close to the core and 132 ±3.6 ka on an outer layer; these results place the Termination II sea level rise past -45 m ASL a thousand years or so after 132 ka. TIMS dates on Atlantic coral reefs from isotope substage 5e extend back to ≈130-131 ka (eg, BARD *et al.* 1990; CHEN *et al.* 1991; GALLUP *et al.* 1994). Thus there is a narrow window between ≈131 ka and ≈130-131 ka when sea level rose rapidly from -45 m to +6 m ASL.

Stable Isotope Profile:

The high resolution stable isotope record (≈6 points per kyr) is shown in Figure 2, the heavy line for the two-point running mean and the lighter line for the raw data. The resolution of this record for this time period is rivalled by few other proxy paleoclimatic records. Moreover, this significant interval, from the full glacial (isotope stage 6) through the dramatic climatic changes of Termination II, is covered by few other terrestrial records with such a fine time and signal resolution. Several features are apparent:
(i) as might be expected for this oceanic site, $d^{18}O$ is dominated by the meteoric signal, with a positive relationship of $d^{18}O$ and temperature;

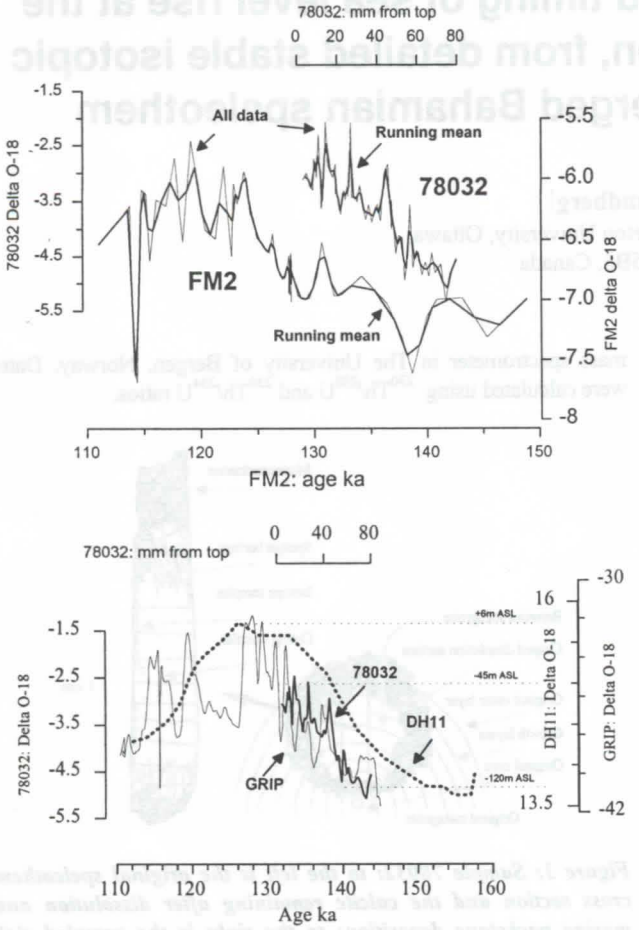

Figure 2: $d^{18}O$ values for 78032 compared with FM2, a Norwegain stalagmite (the upper graph) and with the GRIP ice core and DH11 calcite vein from Devil's Hole, Nevada (the lower graph).

(ii) there is a double warming reminiscent of the end of the last glaciation (the Younger Dryas stage of Termination I): this two step deglaciation has also been documented but with much lower precision from pollen diagrams, speleothem, ocean foraminifera, and pedostratigraphy by SEIDENKRANTZ et al (1996);
(iii) in spite of being in a tropical oceanic environment where climatic changes might be well moderated, the record is spikey, showing rapid oscillations of climate rather than a steady progression;
(iv) the range in $d^{18}O$ is high at ≈3‰: if the range in the ocean foraminiferal $d^{18}O$ is ≈2 ‰ then the extra ≈1 ‰ can be assumed to represent temperature dependent fractionation in the cave.

In Figure 2, 78032 is first compared with FM2 (LAURITZEN 1995), another high resolution speleothem $d^{18}O$ record from this time period, but from Northern Norway, at the extreme north of the Atlantic and in an area close to the Fennoscandian ice sheet and sensitive to climatic changes. 78032 actually shows a greater overall range than does FM2. Note that the isotopic signal of FM2 during the period of very rapid growth at the end of Termination II is inhibited because the sea water $d^{18}O$ is changing rapidly (see LAURITZEN 1995). The peaks and troughs for the two records can be tentatively correlated but 78032 seems to pre-date FM2 by ≈3 kyr. However, this discrepancy is probably not real: the seven alpha counted dates on FM2 have 2s errors of 8-17 kyr. In addition, the dates on FM2 can be shifted back by at least 2000 years by correlating the very cold spike at ≈114 ka in FM2 with the spike in the GRIP ice core record (DANSGAARD et al 1993, GRIP MEMBERS 1993) at ≈116 ka.

In the lower graph of Figure 2, 78032 is positioned in relation to sea level and age. It is superimposed on the GRIP record and DH11, the calcite vein from Nevada (WINOGRAD et al 1992). The coincidence of 78032 and GRIP is remarkable, as is the extent of the offset of DH11.

Conclusion

The isotopic record of 78032 during Tremination II shows rapid oscillations similar to those shown by the GRIP ice core. Overall there is a marked two-step pattern similar to that of Termination I. In terms of timing, 78032 correlates well with the GRIP record and with FM2, post-dates DH11 by ≈5 kyr, and predates the orbitally-tuned SPECMAP marine record (and thus the insolation record) by ≈4 kyr (MARTINSON et al 1987). Until further dating confirms the position of 78032, more detailed discussion is premature.

References

BARD, E., HAMELIN, B. & FAIRBANKS, R.G. 1990. U-Th ages pbtained by mass spectrometry in corals from Barbados: Sea level during the past 130,000 years. *Nature* 346: 456-458.

CHEN, J.H., CURRAN, H.A., WHITE, B. & WASSERBURG, G.J. 1991. Precise chronology of the last interglacial perios: ^{234}U-^{230}Th data from fossil coral reefs in the Bahamas. *Geological Society of America Bulletin* 103: 82-97.

DANSGAARD, W., & ten others 1993. Evidence for general instability of past climate from a 250-kyr ice-core record. *Nature* 364; 218-220.

GALLUP, C.D., EDWARDS, R.L. & JOHNSON, R.G. 1994. The timing of high sea levels over the past 200,000 years. *Science* 263: 796-800.

GASCOYNE, M., BENJAMIN, G.J., SCHWARCZ, H.P, & FORD, D.C. 1979. Sea-level lowering during the Illinoian glaciation: evidence from a Bahamas "Blue Hole". *Science* 205: 806-808.

GRIP MEMBERS, 1993. Climate instability during the last interglacial period recorded in the GRIP ice core. *Nature* 364: 203-207.

LAURITZEN, S-E, 1995 High resolution Paleotemperature Proxy Record for the Last Interglacial based on Norwegian Speleothems. *Quaternary Research* 4:, 133-146.

MARTINSON, D.G., PISIAS, N.G., HAYS, J.D., IMBRIE, J., MOORE, T.C. & SHACKLETON, N.J. 1987. Age dating and the orbital theory of the Ice Ages: development of a high-resolution 0 to 300,000 yr chronostratigraphy. *Quaternary Research* 27: 1 - 29.

SEIDENKRANTZ, M-S. & nine others 1996. Two-step deglaciation at the oxygen istotope stage 6/5e transition: the Zeifen-Kattegat Climate Oscillation. *Quaternary Science Reviews* 15: 63-75.

WINOGRAD, I.J., COPLEN, T.B., KLANDWEHR, J.M., RIGGS, A.C., LUDWIG, K.R., SZABO, B.J., KOLESAR, P..T., & REVESZ, K.M. 1992. Continuous 500,000 year climate record from vein calcite in Devil's Hole, Nevada. *Science* 258: 255-260.

Speleothem records of environmental changes in the past - potential in comparison with the other paleoenvironmental archives and related UIS international programs

by Y.Y.Shopov
Section Speleology & Faculty of Physics, University of Sofia,
James Baucher 5, Sofia 1126, Bulgaria.
E-mail: YYShopov@Phys.Uni-Sofia.Bulg

Abstract

Potential, resolution and limitation of high resolution speleothem records of Paleotemperature, Paleosoils, Paleoseismics, Past Precipitations, Rock displacement, Solar Insolation, Geomagnetic field, Plants Populations, Chemical Pollutions, Air Composition, Sea Level advances, Advances of Hydrothermal Waters, Cosmic Rays Flux variations, Cosmogenic Isotopes production and Supernova Eruptions in the Past are discussed (table 1). An international working group on "Speleothem Records of Environmental Changes in the Past" of the Commission on Physical Chemistry and Hydrogeology of Karst of International Union of Speleology is dedicated to study these records. It is coordinated by Y.Shopov and has different topic leaders (table 1).

Potential of speleothem records of environmental changes in the past is compared with other paleoenvironmental archives. It is demonstrated, that speleothems are the best paleoenvironmental archives of many properties of the environment.

Highest resolution of speleothem records (6 hours) is higher than that achieved from any other paleoenvironmental record.

Table 1. Speleothem Records of Environmental Changes in the Past

	Type of the Process Method	Obtainable information leader; best time resolution	Time range [a]
I	Changes beyond the	Solar System	
1	Past Supernova eruptions	primary cosmic ray flux variations in the past beyond the Solar System, Past Supernova eruptions Y.Shopov (Bulg); 20a	0- 10000
II	Changes within the Solar	System	
1	Cosmic Rays Flux Variations; Cosmogenic Isotopes Variations	cosmic rays flux and solar activity in the past D.Lal (USA); 20a	0- 40000
2	Solar Insolation; Laser Luminescent Microzonal Analysis (LLMZA)	Quantitative reconstructions of Solar activity variations in the past, speleothem growth interruptions, volcanic eruptions Y.Shopov (Bulg); 6hours	unlimited
III	Global Earth Processes		
1	Paleomagnetism; Magnetometry of speleothems	paleomagnetism, rock orientation changes in the past; less than 50 a A.Latham, R.Gilson (UK)	unlimited
2	Geomagnetic dipole intensity; LLMZA	quantitative reconstructions of Geomagnetic dipole intensity, solar wind flux at Earths magnetosphere in the Past Y.Shopov (Bulg); 40a	unlimited
IV	Regional Processes		
1	Paleoclimate and Paleotemperature in calcite speleothems; stable isotopes	Paleotemperature, possible plant population, precipitations and climatic cycles in the past; D.Ford, C.Yonge (Can), T.Arakawa (Jap); 25a	unlimited

2	Past Precipitations; annual growth rate observed by LLMZA	quantitative reconstructions of past annual rainfall, past floods, cycles of draughts and floods Y.Shopov (Bulg); 1a	unlimited
3	Past Paleotemperature; LLMZA	quantitative reconstructions of air paleotemperature during speleothem growth, temperature cycles, glaciations etc. Y.Shopov (Bulg); 6 hours	unlimited
4	Paleotemperature in speleothem ice; Stable isotopes	air paleotemperature, air CO_2, air isotope composition in the past C.Yonge, W.MacDonald (Can); 25a	unlimited
5	Paleotectonics and Paleoseismics; Orientation of speleothem growth	paleoseismics, rock displacements and bending P.Forti (It), N.Nori (Jap); <100a ?	unlimited
V	Local Processes		
1	Pollen analysis	plants population and paleoclimatic changes G.Brook (USA); <10a ?	unlimited
2	Soil type variations; Luminescent spectra analysis	soil and plants population variations W.White (USA); 1a	unlimited
3	Chemical microanalysis; Laser emission spectral analysis	chemical pollutions ?; 1a?	unlimited
4	Dating of sea levels; U/Th dating	sea level variations J.Lundberg (Can); 100a	0-500000
5	Luminescent records of hydrothermal activity; Time resolved photo-graphy of phosphore-scence	advances of hydrothermal waters, estimations of their temperature, mixing of surface and hydrothermal waters, uplift of bedrocks Y.Shopov, L. Tsankov (Bulg); 1a	unlimited

Speleothems as natural climatic stations with annual to dayly resolution

by Y.Y.Shopov, L.Tsankov, L.N.Georgiev, A.Damyanova, Y. Damyanov
Section Speleology & Faculty of Physics, University of Sofia,
James Baucher 5, Sofia 1126, Bulgaria.
E-mail: YYShopov@Phys.Uni-Sofia.BG;
D.C. Ford
Geography Dept., McMaster University,
Hamilton, Ontario, L8S 1K4, Canada;
C.J.Yonge, W. MacDonald, H.P.R.Krouse
Dept. of Physics, University of Calgary, Calgary, Alberta, Canada

Abstract

Calcite speleothem luminescence depends exponentially upon soil temperatures that are determined primarily by solar infrared radiation in the case when that cave is covered only by grass or upon air temperatures in case that cave is covered by forest or bush. In the first case, microzonality of luminescence of speleothems can be used as an indirect Solar Insolation (SI) index, but in the second - as an paleotemperature proxy. So, in dependence on the cave site we may speak about "solar sensitive" and "temperature sensitive" Paleoluminescence speleothem records like in tree ring records, but in our case record may depend either only on temperature or on solar irradiation:

- In case of Cold Water cave, Iowa, US we obtained high correlation coefficient of 0.9 between the luminescence record and Solar Luminosity Sunspot index (fig.1) and reconstructed sunspot numbers since 1000 AD with precision within the experimental error of their measurements;

- in case of Rats Nest cave, Alberta, Canada we measured correlation coefficient of 0.67 between luminescence intensity and air temperatures record for the last 100 years (fig.2) and reconstructed annual air temperatures for last 1500 years at the cave site with estimated error of 0.35 ^{0}C, while the error of the direct measurements is 0.1 ^{0}C.

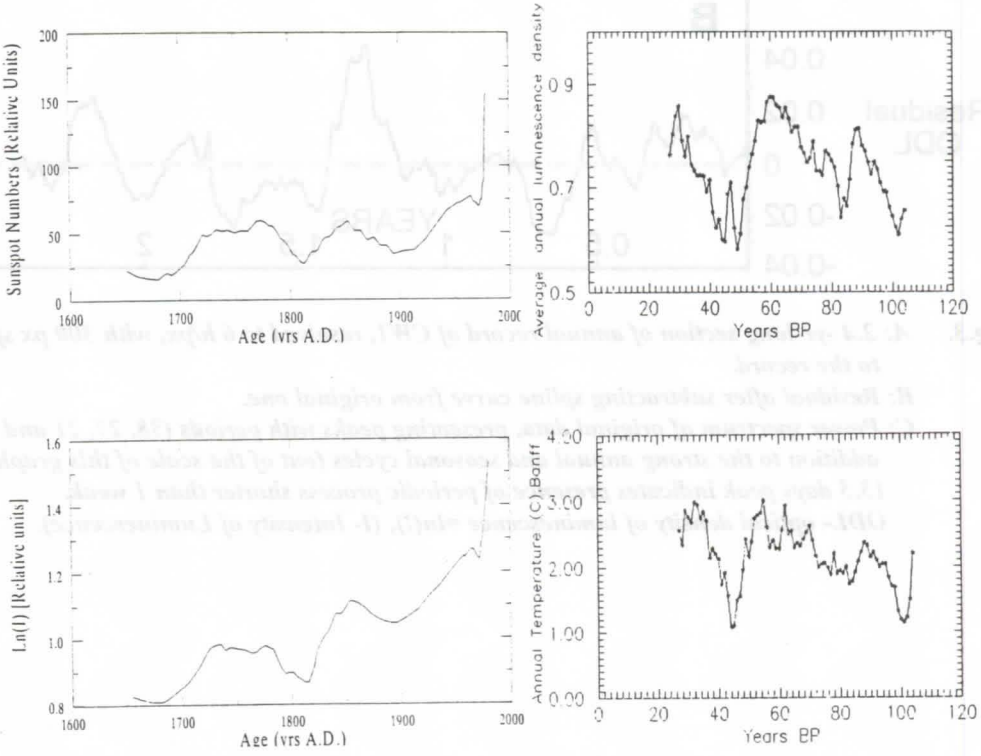

Fig.1. (left up) Twenty year average sunspot records since 1700 AD
(left down) Optical density of luminescence of a speleothem from Coldwater Cave, Iowa (USA).

Fig.2. (right up) Average annual luminescence density of a speleothem from Rats Nest Cave (Canada)
(right down) Annual temperature, Banff , Alberta (Canada).

Intensity of luminescence was not dependent on actual precipitations and sunspot numbers (zero correlation). Speleothem growth rate variations represent mainly rainfall variations. Speleothem luminescence visualizes annual microbanding we used to derive proxy records of annual precipitations for the cave site. In case of Rats Nest Cave, Alberta, Canada we reconstructed annual precipitations for last 280 years at the cave site with estimated error of 80 mm/year. By comparison of luminescent records with other solar proxy records we obtained a reconstruction of growth rates and precipitations in Bosnek karst region near Duhlata Cave, Bulgaria, for the last 50000 years, and for the last 6400 years (with averaged time step of 41 years) for Iowa, near Cold Water Cave, US. Achieved time step of 6 hours (fig. 3) in speleothem luminescence records allows resolution of several days in some best speleothem samples. Annual luminescence microbanding was used very successfully for relative and absolute dating of speleothems by Autocalibration dating. This dating method appear to be more precise than TAMS ^{14}C and AMS U/Th dating for relative dating of short time intervals and only dating method for speleothems with little uranium, younger than 2000 years.

It is demonstrated, that speleothems can be used as natural climatic stations with annual resolution for purposes of climatology and agrometeorology for a time span far exceeding all historic records.

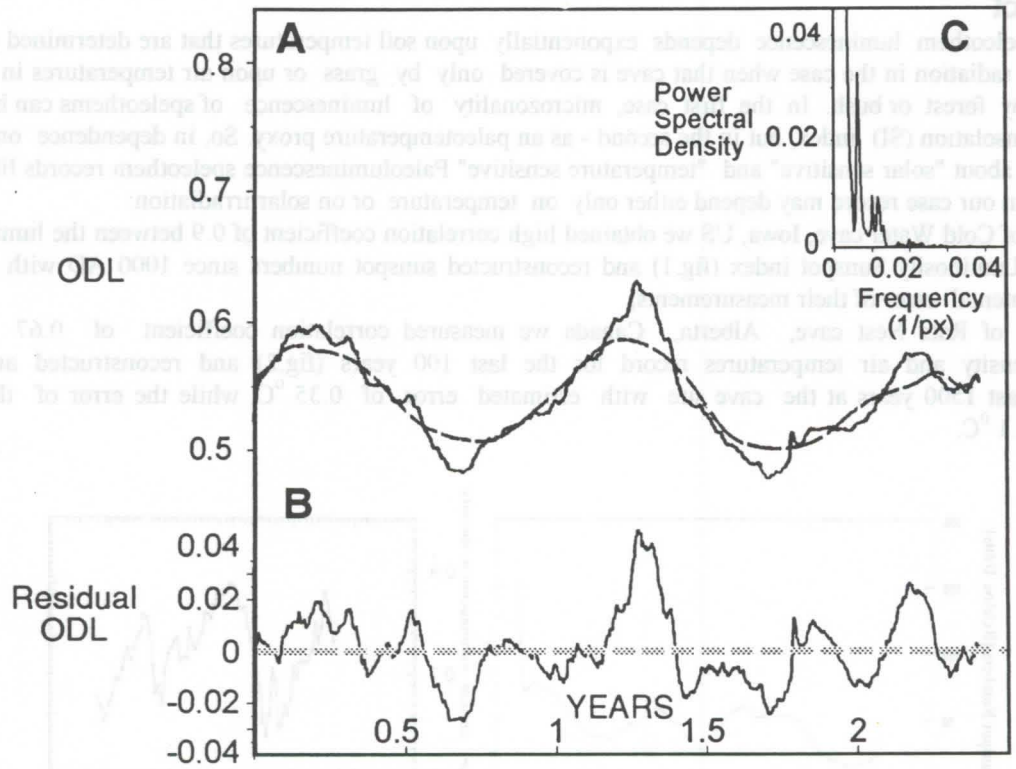

Fig.3. A: 2.4 -yr-long section of annual record of CW1, resolved to 6 h/px, with 300 px spline curve fitted to the record.
B: Residual after subtracting spline curve from original one.
C: Power spectrum of original data, presenting peaks with periods (38, 27, 21 and 13.5 days) in addition to the strong annual and seasonal cycles (out of the scale of this graph). Presence of 13.5 days peak indicates presence of periodic process shorter than 1 weak.
ODL- optical density of luminescence =ln(I), (I- Intensity of Luminescence).

Speleothem luminescence proxy records of annual rainfall in the past: Evidences for "The Deluge" in speleothems

by **Y.Y.Shopov, L.T.Tsankov, L.N.Georgiev, A.Damyanova, Y. Damyanov, E. Marinova**
Section Speleology & Faculty of Physics, University of Sofia, James Baucher 5, Sofia 1126, Bulgaria.
E-mail: YYShopov@Phys.Uni-Sofia.BG
D.C. Ford
Geography Dept., McMaster University, Hamilton, Ontario, L8S 1K4, Canada
C.J.Yonge, W. MacDonald, H.P.R.Krouse
Dept. of Physics, University of Calgary, Calgary, Alberta, Canada

Abstract

A good correlation between the growth rate of the cave speleothems and the annual precipitations at the cave site has been demonstrated. Extrapolating the results back in time we obtained a quantitative reconstruction of the annual precipitations for the last 280 years at the Rast Nest Cave site (Alberta, Canada).

Measuring another sample (from Duhlata Cave, Bulgaria) we found an enormously high growth rate at 5500 years B.C. Its possible connection with the Bible Flood is discussed.

1. Method

Speleothem growth rate variations represent mainly rainfall variations (Shopov et al.1992, 1994). Speleothem luminescence visualizes annual microbanding (Shopov et al. 1991). We used it to derive proxy records of annual precipitations around the cave site by measuring the distance between all adjacent annual maxima of the intensity of luminescence. The resultant growth rates correlate with the actual annual precipitation (summed from August to August).

2. Quantitative reconstructions of annual precipitations in the past

We studied the top of a 35 mm long stalagmite from Rats Nest cave (RNC), Alberta, Canada. We obtained reasonably good correlation (correlation coefficient of 0,57) between the annual precipitations (recorded at the closest weather station - Banff, located in the same valley, 50 km northern of the cave) and the annual growth rate of the speleothem (Fig. 1). We used obtained regression coefficients to reconstruct annual precipitations for the last 280 years at the cave site. The estimated statistical error is 80 mm/ year. Annual speleothem growth rate was independent on the intensity of luminescence, on annual temperature and on solar luminosity for the same time span (zero correlation).

3. Evidences for the Bible Flood

By "tuning" the time scale of a luminescent record with a geomagnetic dipole intensity record (Mazaud et al., 1991) we obtained a reconstruction of growth rates and precipitations in Bosnek karst region near Duhlata cave (DC), Bulgaria for the last 50000 years (Fig.2). This record shows a very prominent peak at 5500 years B.C., when the annual growth rate was over 53 times higher than today. Considering that cave site is located in the region of the oldest civilizations (Mediterranean basin) this event can be related to the Bible "Deluge". The age of the recorded event is about the age of "The Creation of the World". The duration of the recorded event is of 120 years, because of the low resolution of the record. In case that the real flood happened for a short time span it suggests enormous high rainfall. Present day precipitation at the cave site is 650 mm/yr. This speleothem was dated with 8 TAMS ^{14}C dates.

Such event is described in the Bible, Greek mythology and the Sumerian epic Gilgamesh (compiled during 3-rd millennium B.C. on the base of more ancient legends). At that time human civilization had been concentrated around the Black and Mediterranean sea, therefore the Flood hited also recent Bulgarian lands. Such immemorial precipitation probably would lead to some temporary rising of the Black Sea level. Such rising at 5500 B.C. with 150 meters (which had flooded 60000 square miles) was recently suggested by an international team of scientists, lead by Dr.William Rayn and Walter Pittman from Columbia University, Palisades, New York (their results are still presented only in a press-conference, see J. Wilford, 1996). The Black Sea level rising itself cannot be undoubtedly related to the Flood, but combined with the never seen (during the human civilization) precipitations at that time definitely lead to the conclusion,

that this phenomenon is namely the Bible Flood.

Here we suggest a hypotesis for one possible mechanism of the Flood, consisting of the following:- It is known, that the Ocean level rised from 10000 years to the time of the Flood as a result of the glaciers melting. Black Sea had been isolated from the Ocean and it's level had been much lower. In one moment the narrow band of land between the Mediterranean and Black Sea had broken down like a dam wall. This had resulted in flowing of giant masses of sea water into the Black Sea basin. When it reached the opposite cost, then a giant wave had been formed (which probably was incomparably bigger that biggest tsunami known so far). This wave had destroyed everything on lands around the Black Sea even beyond the regions flooded by the sea level rise. The never seen precipitations at that time had contributed to the rising of the sea level and maybe caused the final rising, which had turned the Mediterranean Sea over the edge to flood the Black Sea region. Further studies of the Mediterranean sea level during the Flood and data for precipitations from stalagmites taken from other caves in the region are necessary to prove this hypothesis.

The mechanism of generation of such an enormously high rainfall is even more interesting. To generate such a rainfall is necessary to have much stronger than usual water evaporation. It is very unlikely to be due to much warmer climate for several years. At the same time few percent higher than normal solar radiation will produce much higher evaporation (without significant rise of the air temperature). Such higher solar radiation can be produced by an extraordinary solar eruption, or (perhaps more likely) by explosion of a comet or asteroide in the Solar atmosphere. Such explosion (like Tungussian meteorite) can cause a major mixing of parts of Solar shells and appearance of warmer Solar matter from the depth to Solar surface. Probably several years would be necessary for recovery of the Sun from similar catastrophic event.

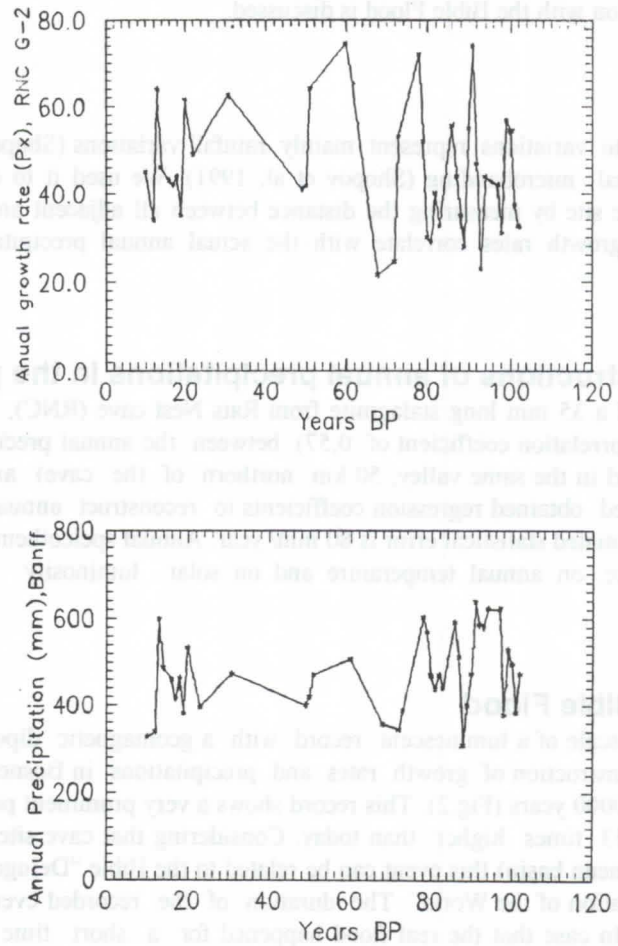

Fig.1 (Up) Annual growth rate of a stalagmite from RNC, Alberta, Canada
(Down) Annual precipitations (from August to August) for Banff station, 50 km north of the cave

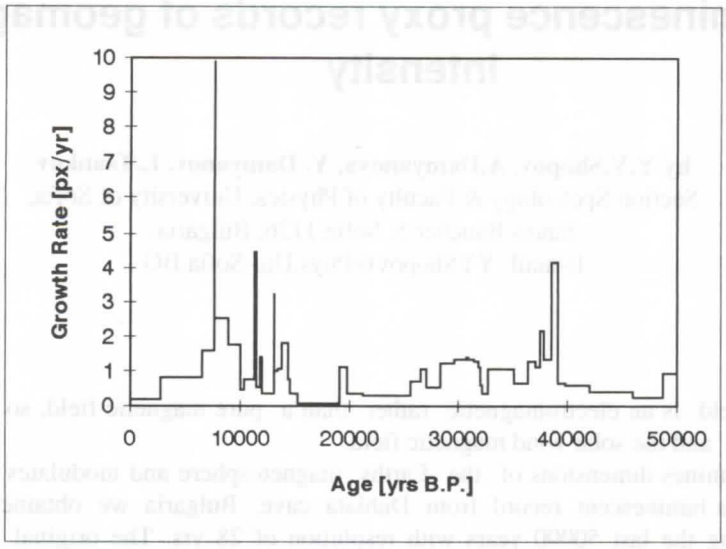

Fig.2. Reconstruction of growth rates (proxy of precipitations) of a flowstone from DC, Bulgaria for the last 50000 years.

4. Conclusion

The Bible Flood (catastrophic rainfall) as recorded in a speleothem, had probably happened 5500 years B.C., causing Black Sea level rise. It is probably due to higher water evaporation caused by higher solar radiation resulting from a catastrophic event on the Sun.

References

MAZAUD A., et al.1991:Geophys. Res. Lett., 18, No. 10: 1885-1888.
SHOPOV Y.Y., et al, 1991:IGCP299 Newsletter, 3: 52-58.
SHOPOV Y.Y., et al. 1992: GSA Abstr., 24, No.7: A268
SHOPOV Y.Y. et al., 1994: Geology, 22, 407-410.
STUIVER M. & KRA R.1986:Radiocarbon, Calibration issue, 28.
WILFORD J. 1996: Black Sea Rising: Was it the Flood? Int. Herald Tribune (19. 12. 1996)

Speleothem luminescence proxy records of geomagnetic field intensity

by Y.Y.Shopov, A.Damyanova, Y. Damyanov, L.Tsankov
Section Speleology & Faculty of Physics, University of Sofia,
James Baucher 5, Sofia 1126, Bulgaria.
E-mail: YYShopov@Phys.Uni-Sofia.BG

Abstract

The geomagnetic field is an electromagnetic rather than a pure magnetic field, so it depends on the far stronger solar magnetic field and the solar wind magnetic field.

The solar wind determines dimensions of the Earths magnetosphere and modulates the intensity of the geomagnetic dipole. Using a luminescent record from Duhlata cave, Bulgaria we obtained a reconstruction of the geomagnetic dipole during the last 50000 years with resolution of 28 yrs. The original luminescent record exhibited a correlation coefficient of 0.78 with an independent record of variations of intensity of the geomagnetic dipole for the same time span (Fig.1.).

Observed dependencies of the geomagnetic dipole intensity on the orbital variations and solar luminosity variations correlates excellently with the established theoretical equations.

Obtained reconstruction of the geomagnetic field is of vital importance for calibration of cosmogenic isotope (^{14}C, etc.) dating techniques.

NASA used a record of luminescence of a flowstone from Duhlata cave, Bulgaria to establish a standard record of variations of Solar Irradiance ("Solar constant") for the last 10000 years by calibration of the luminescence record with satellite measurements.

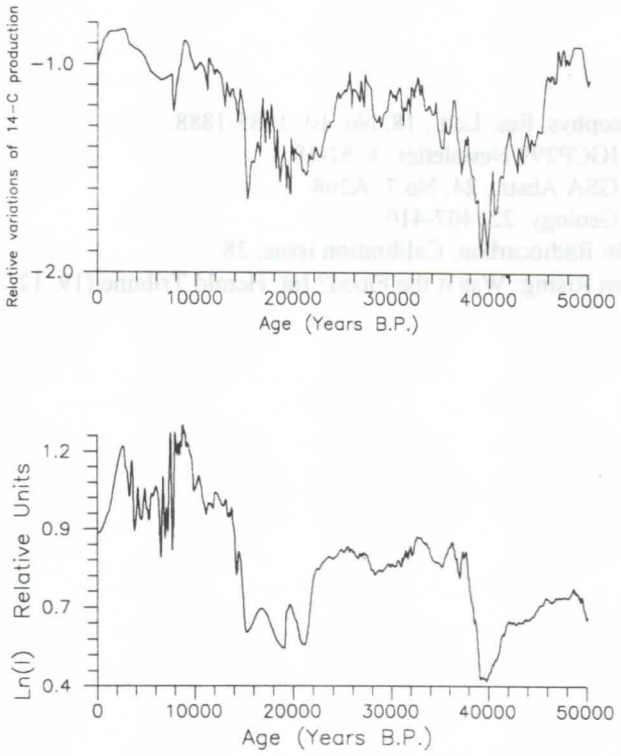

Fig.1.(up) Optical density of luminescence of a cave flowstone
(down) Past variations of intensity of the geomagnetic dipole expressed by inverted production of ^{14}C (MAZAUD et al, 1991)

Speleothem records of processes beyond the solar system (Supernova eruptions)

by **Y.Y.Shopov, A.Damyanova, Y. Damyanov, L.Tsankov,**
Departments of General Physics, Astronomy and Nuclear Physics,
Faculty of Physics, University of Sofia,
James Baucher 5, Sofia 1126, Bulgaria.
E-mail: YYShopov@Phys.Uni-Sofia.BG;
C.J.Yonge, J. Bland
Dept. of Physics, University of Calgary, Calgary, Alberta, Canada
D.C. Ford
Geography Dept., McMaster University, Hamilton, Ontario, L8S 1K4, Canada

Abstract

We used the standard Calibration ^{14}C record (Stuiver et al., 1987) to derive a proxy record of Cosmic Rays Flux. This ^{14}C record represents the Cosmic Ray Flux (CRF) and modulation of the CRF by the solar wind.

A striking correlation (with a correlation coefficient of 0.8) was demonstrated between the calibration residual delta ^{14}C record and a LLMZA speleothem record. Using a luminescent record from Duhlata cave, Bulgaria we obtained a reconstruction of the solar modulation of the CRF during the last 50000 years with time resolution of 28 yrs.

Luminescence microzonality was used to reconstruct Galactic Cosmic Rays Flux (beyond the Solar System) during the last 6500 years with 20 yr resolution by subtracting of an inverted luminescent solar activity record (sample from Cold Water cave, Iowa) from the residual ^{14}C record. Last result (fig.1) presents a picture of past Supernova explosions in our Galaxy. It is a quantitative confirmation of recent views on origin of Cosmic Rays from superposition of Supernova explosions in our Galaxy and agrees with astrophysical observations. It completely disapproves the hypothesis of origin of a significant part of Cosmic Rays Flux from relic rays of the Big Bang.

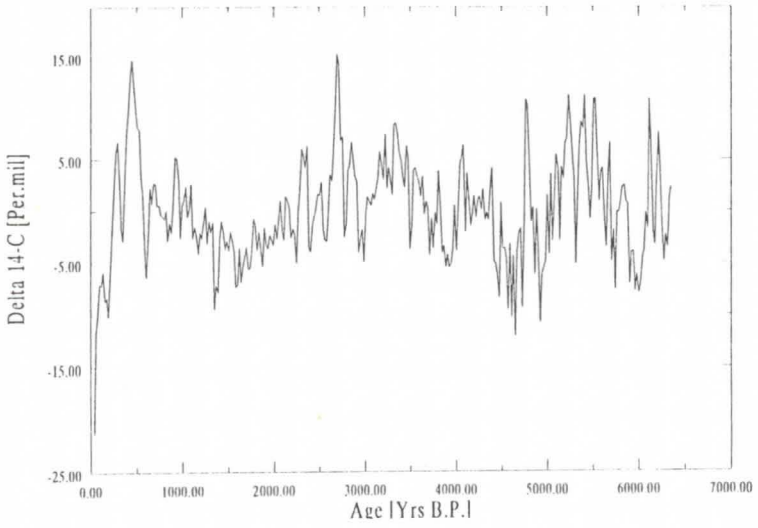

Fig.1. Relative variations of the primary cosmic rays flux, expressed by cosmogenic ^{14}C variations.

Development of cave passages according to geological structure; Example from Jama pod Peèno rebrijo, Slovenia

Stanka Šebela,
Karst Research Institute ZRC SAZU, Titov trg 2, 6230 Postojna, Slovenia

Abstract

About 1,8 km east from the entrance of Postojnska jama lies 203 metres long cave Jama pod Peèno rebrijo. The cave has two passages with two vertical entrance shafts. Northern passage phreatically developed in two layers of Upper Cretaceous limestone. Tectonic uplifting of the region caused that the cave lost its hydrological functions but a part of the cave kept primary phreatical shape.

1. Introduction

Under top of hill Peèna reber (763 m a.s.l.) above Postojna (Fig. 1) lies 203 m long cave (Reg. No. 1577).

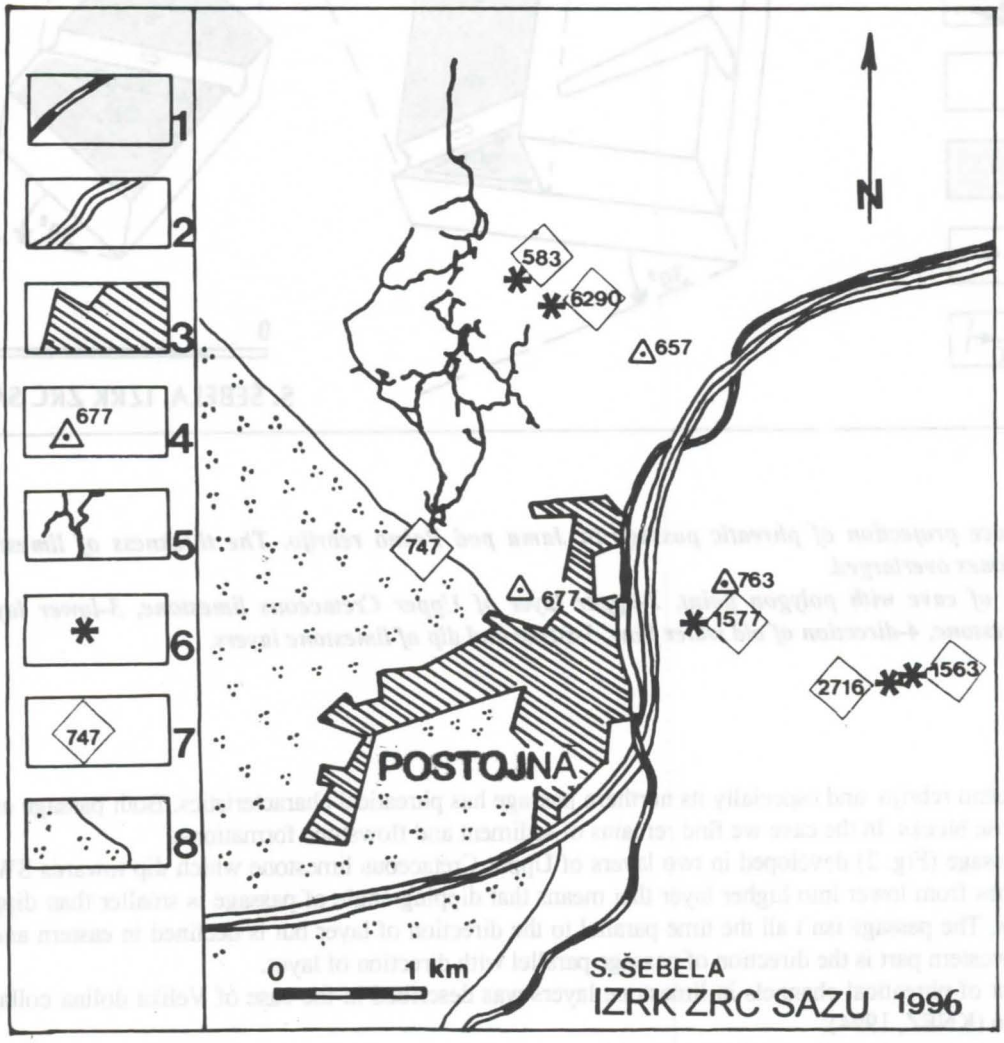

Figure 1 : The location of Jama pod Peèno rebrijo according to Postojnska jama and surrounding caves. 1-railway, 2-highway, 3-town, 4-above sea level in metres, 5-ground plan of cave, 6-cave entrance, 7-Register number of the cave, 8-Eocene flysch and Upper Cretaceous limestone.

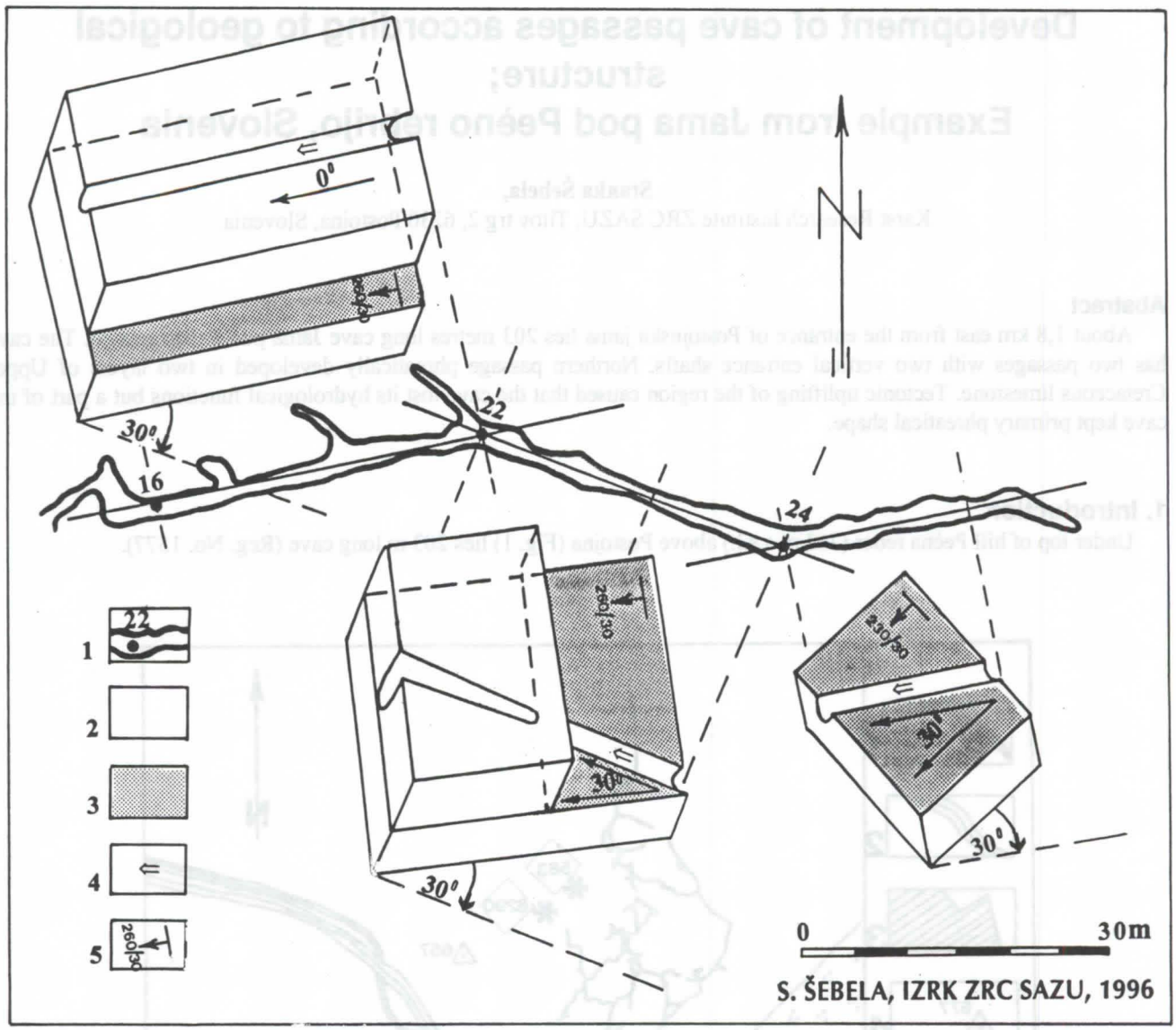

Figure 2 : Space projection of phreatic passage in Jama pod Peèno rebrijo. The thickness of limestone in block diagrams is 3 times overlarged.
1-ground plan of cave with polygon point, 2-upper layer of Upper Cretaceous limestone, 3-lower layer of Upper Cretaceous limestone, 4-direction of old water flow, 5-strike and dip of limestone layers.

Jama pod Peèno rebrijo and especially its northern passage has phreatical characteristics. Both passage ends are today closed by collapse blocks. In the cave we find remains of sediment and flowstone formations.

Northern passage (Fig. 2) developed in two layers of Upper Cretaceous limestone which dip towards SW. 120 metres long passage goes from lower into higher layer that means that dipping angle of passage is smaller than dipping angle of limestone layers. The passage isn't all the time parallel to the direction of layer but is declined in eastern and middle part for 30°. Just in western part is the direction of passage parallel with direction of layer.

Development of phreatical channels in limestone layers was described in the case of Velika dolina collapse doline in Škocjanske jame (KNEZ, 1994).

In our example first phase in development of Jama pod Peèno rebrijo is phreatical formation in strata plane with divergences 0-30° from the direction of strata plane. Dinaric tectonic activity with principal directions of faulting NW-SE and NE-SW affected the western part of the cave, which is today closed with collapse blocks. Fault zone in which entrance shaft developed is just outer part of wider fault zone.

The cave has two passages with two vertical entrances. Shaft in southern passage is 11,5 m deep and 1x1 m wide. Principal shaft entrance (647 m a.s.l. and 12,5 m deep) is accesible by badly preserved steps.

The vicinity of Postojnska jama was being explored in the 19th century already with a desire to find new parts of the cave (BERTARELLI *et al.*, 1926).

According to CAVE REGISTER in vicinity of Postojnska jama there are more 10 caves, some are not longer than 2 m and others are longer than 100 m.

Table 1 shows basic data of bigger caves near Postojnska jama.

NAME OF THE CAVE	REG. NO.	VG-REG .NO.	LONGER (m)	DEEP (m)	a.s.l. of the entrance (m)	type of the cave
Postojnska jama	747	108	19.555	115	511	ponor horizontal cave
Zguba jama	6290	563	122	4	561	horizontal cave
Jama na poti	583	2436	65	32,5	570	horizontal cave
Jama pod Peèno rebrijo	1577	-	203	38	647	horizontal cave
Javorniško brezno I.	1563	1945	20	86	725	shaft
Jama pod Volèjim vrhom	2716	1946	50	133,5	715	shaft

Table 1 : List of the biggest caves near Postojna (after CAVE REGISTER IZRK ZRC SAZU).

2. Geological conditions in Jama pod Peèno rebrijo

The cave developed in Upper Cretaceous limestone (BUSER *et al.*, 1967). Northern passage (Fig. 2) rises from the entrance shaft to the end for 38 m. We can observe one limestone layer which is very rich with rudist remaines. The passage leaves this layer east from point 16 (Fig. 2). The direction of strata in eastern part of the passage is 230/30 and in other parts 260/30. The passage dips from east towards west what is also concordant with directions of water flow shown by rocky relief. Southern passage is almost horizontal in Dinaric direction (NW-SE).

The northern passage is much more characteristically developed in strata plane than the southern one. The northern passage developed in two principal directions (Fig.2).

From point 24 to east there is first direction of cave passage (260°) which declines from direction of strata plane for 30° towards W.

Second direction of passage (290°) is between points 22 and 24. It declines from direction of strata plane for 30° towards W.

The third direction of passage has the same direction as the eastern part of passage (260°), but passage is parallel to direction of strata plane.

Tectonically crushed zones are badly expressed in northern passage being usually transverse to the passage direction.

The most expressed fault zone lies west from point 16 (Fig. 2). Its geological elements are 70/70-80. Inside this fault zone we observe 3 chimneys, one in northern passage and two others in a southern one.

Second intensive fault zone crosses entrance shaft (10 metres west from point 16) which developed between two tectonic systems. The geological elements of the stronger are 20-30/50 and of the weaker 120/30.

In northern passage we find rests of flysch sediment which completely filled the cave. In some parts flowstone is deposited over sediments. In later periods sediments and flowstone were eroded. Through almost all northern passage we observe 1,5 dm wide channel on the ceiling. It partly disappears only in chambers where stronger tectonical zones occur. Paragenetical channel probably developed after filling with sediments.

3. Conclusions

The entrance of cave Jama pod Peèno rebrijo (Reg. No. 1577) lies 647 m a.s.l. To the SE there are two shafts, Javorniško brezno I (Reg. No. 1563) which is 86 m deep and 20 m long and Jama pod Volèjim vrhom (Reg. No. 2716) 133,5 m deep and 50 m long (Fig. 1).

NE from Postojnska jama there is the entrance to 122 m long Zguba jama, Reg. No. 6290, 561 m a.s.l. (ŠEBELA, 1994).

Genetical relation between morphologically similar Jama pod Peèno rebrijo and Zguba jamo in air distance of 2 km has sense if we describe mechanics of movements of crossdinaric (NE-SW) Postojnska vrata fault zone, which lies between these two caves.

With activity or reactivity of "Postojnska vrata" fault zone (NE-SW) hydrodinamical conditions changed changing also activity of Jama pod Peèno rebrijo. It was filled with sediments and later sediments were removed. With tectonic uplifting of the region the cave lost its function of water channel for ever, but a part of the cave kept primary phreatical shape.

In the vicinity of Postojna entrances of todays water active caves as Postojnska jama and Lekinka are located in the contact of Eocene Flysch and Upper Cretaceous limestone.

References

BERTARELLI, L.V. & BOEGAN, E., 1926. Duemila grotte. Milano, 494 p.

BUSER, S., GRAD, K. & PLENIÈAR, M., 1967. Osnovna geološka karta SFRJ Postojna 1:100.000. Zvezni geološki zavod, Beograd.

CAVE REGISTER IZRK ZRC SAZU

KNEZ, M., 1994. Phreatic channels in Velika dolina, Škocjanske jame (Škocjanske jame caves, Slovenia). *Acta carsologica* 23, Proceedings of 1st international karstological school "Classical Karst", Lipica, September 20-23, 1993, Ljubljana, 63-72.

ŠEBELA, S., 1994. The caves Jama na poti and Zguba jama. *Acta carsologica* 23, International round table "E.A. Martel et le karst slovene", Postojna, 12-13 november 1993, Ljubljana, 233-243.

Genesis of Jozsefhegy hydrothermal cave, Budapest

by Szabolcs Leel-Ossy

More than 100 caves and cave-indications are known from the Triassic and Eocene carbonatic sequences of the Rozsadomb region, Buda Hills, Budapest. Most of these caves are characterised by the absence of any natural outlet. Therefore, their discovery, mainly in the 20th century, was accidental or a result of systematic research or due to the creation of artifical outcrops. One third of the caves are merely indications, another 30 percent have the size of tens of metres, while the rest exceeds the extent of several tens of metres.

Only the large cave systems of Szepvolgy and the Jozsef, Matyas, Ferenc and Szemlo Hills have the dimension of km's. Studying the geological setting of the area and the main features of the formation of the caves we can predict that substantial parts of the system are still undiscovered. Most of the indications can be found in Buda Marl, while the galleries and levels of the larger caves are situated in Szepvolgy Limestone. The currently known cavern-system, with a total length of 30 km, can be regarded as the fossile source level of the present-day thermal springs at the foot of the Buda Hills. Their origin is interpreted as a result of mixed corrosion along tectonic fractures at the level of carstic water. The radiometric age of the syngenetic minerals gave good constraints on the time of the cave-formation.

The internal size of the caves of Rozsadomb changes drastically. frequently, corridors and halls with a size of ten or hundred metres can be found. The walls of the galleries are often adorned by spherical niches. More than a dozen species of minerals were reported from these caves. Especially the variety and mass of carbonates (mainly calcite) and sulphates (mostly gypsum) are remarkable.

On the base of dating (carried out in Bergen, in the laboratory of Stein-Erik Lauritzen) the Jozsefhegy Cave is very young. The age of the system is maximum 400.000-500.000 years. A few crystals are syngenetic with the cave-system, but a lot of crystals (for example aragonite crystals) are much younger, and there are some recent crystals, too (for example gypsum needles).

Cave patterns north of the Planinsko polje (Slovenia)

France Šušteršič
University of Ljubljana, Department of Geology, SI-1000 Ljubljana, Aškerčeva 12, Slovenia

Abstract
Detailed study of cave patterns in the area of the Planinsko polje (Slovenia) revealed that rather than in levels, the caves are organized in flow corridors and tiers. The primary tubes are formed along a small number of bedding planes, predominantly on upper or lower sides of the dolomite packs. Though joints are abundant in some cases it is evident that many a passage was at least incepted before jointing. The absence of typical epiphreatic details indicates that transition from completely phreatic to pure vadose was fast.

Preface
The area of the classical karst in Slovenia is best considered as a triangle with vertices that just encompass the cities of Ljubljana, Rijeka and Gorica/Gorizia. Within the classical triangle, the sinking Ljubljanica river is the backbone of the catchment that drains towards the Danube.

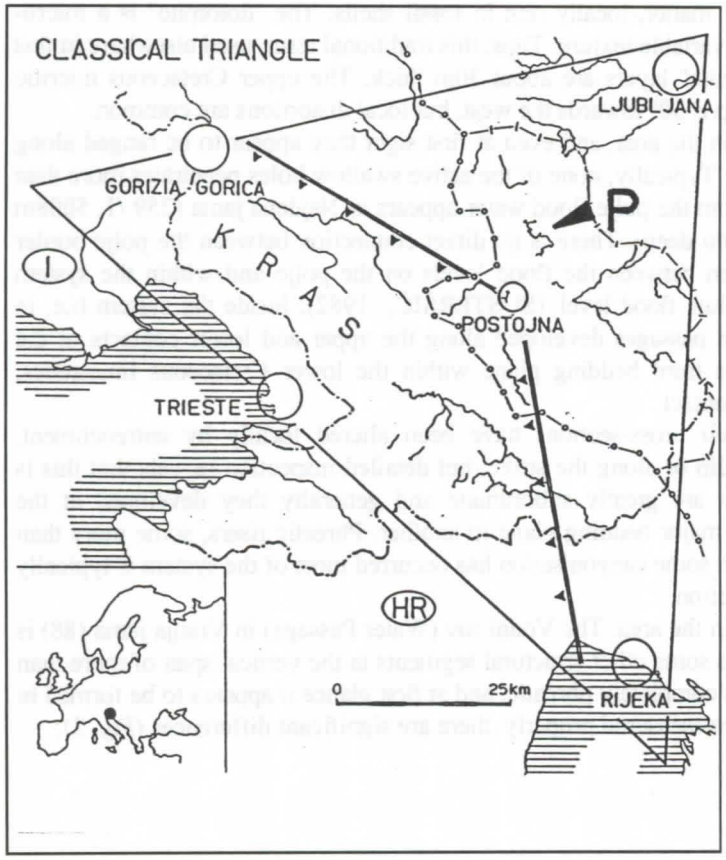

Fig 1: The classical triangle: P - Planinsko polje

It is widely known as a string of surface and underground stream segments, the latter emerging into karst poljes. It might be expected that caves in this area must be fundamentally of more or less epiphreatic origin, with their development bound intimately to the formation of the poljes and the presumed river terraces on their margins (GOSPODARIČ & HABIČ, 1979). During the last century and a half, extensive speleological and geomorphological work was carried out and the great amount of information that was gathered did not confirm it but, on the contrary, made it hardly acceptable. It was not until the nineteen-nineties that studies founded upon other paradigms began to appear (BRENČIČ, 1992; ŠEBELA, 1994; ŠUŠTERŠIČ, 1994, in press). This paper deals with a relatively small sector of the Ljubljanica catchment area (Fig. 1), north and north-east of the Planinsko polje. It appears that the FORD & EWERS' (1978) four-state cave genesis model offers a framework within which the conditions of the Ljubljanica River can be presented better than in any earlier model. Thus their terminology is used extensively in this paper, as are more recent improvements (in the author's opinion) suggested by WORTHINGTON (1991) and LOWE (1992).

The Ljubljanica catchment area
The calculated size of the Ljubljanica drainage basin is 1779 km^2 and about 1100 km^2 of this are composed of karstic rocks. The location of the water divide is approximate, and at several boundaries bifurcations have been proved by water tracing. According to studies during the complex water tracing experiments of the nineteen-seventies, the catchment area of the Vrhnika springs, where the main river definitively leaves karst terrain, covers 1108.78 km^2.
The karstic rocks in are generally micritic, locally oolitic limestones and dominantly late-diagenetic dolomites, mostly of Mesozoic age. They were formed on the Dinaric platform by continuous sedimentation under very uniform shallow sea

conditions that were responsible for their extremely high purity, with generally <5%, but as low as 0.1% insoluble residue. The total thickness of the carbonate sequence is 6850m within the considered area (ČAR, 1996). Among non-karstic rocks, only early Tertiary flysch, which was deposited directly upon the carbonate sequence, has a significant role. Younger sediments are absent, suggesting that the final emergence happened at the end of the Tertiary.
Structurally, the whole of the Ljubljanica basin belongs to the Adriatic sub-plate. The area is composed of a number of nappes (PLACER, 1982; PREMRU, 1983) that were overthrust in a NE-SW direction as a result of the collision of the Adriatic sub-plate with the European continent. Gradual change of direction of the movements brought about the formation of the Idria dextral strike-slip fault, which runs through the area in a NW-SE direction.
The surface between the Planinsko polje (445m) and the Ljubljansko Barje (Ljubljana Marsh, 294m), where the karst waters finally appear on the surface, is typically karstic. More recent research (HABIO, 1981; OUOTEROIO, 1987) has proved that the relief is essentially tectonic.
The difference between the caves that have formed as system drains and the vadose caves is very clear. On the basis of observations made predominantly by cavers, it appears that nearly a half of the caves explored within the Ljubljanica catchment area are of phreatic origin. In the following text these will be referred to as "horizontal" caves, though generally they are not horizontal in the true sense of the word.

The situation north of the Planinsko polje

The area about 1km north of the main ponors of the Planinsko polje is built up of alternations of lower Cretaceous limestone with two intercalations of "dolomite", all overlain by upper Cretaceous limestone. The lower Cretaceous limestone (90-95% CaCO3) is micritic, rich in organic matter, locally rich in fossil shells. The "dolomite" is a micro-sparry dolomitized limestone (90-95% CaCO3) of quite variable texture. Thus, this traditional term, used elsewhere in this chapter, is in fact not strictly appropriate. Both "dolomite" layers are about 30m thick. The upper Cretaceous micritic limestone is very pure (95-99% CaCO3). The general dip is 30° towards the west, but local distortions are common.
A number of fragments of horizontal caves are known in the area, and even at first sight they appear to be ranged along the lower and upper contacts of both dolomite packages. Typically, none of the active swallow holes penetrates more than some 100m from the polje. Some hundreds of metres from the polje flood water appears in Najdena jama (259 /1, 5008m long, 121m deep), and Vranja jama (88, 326m long, 90m deep). There is no direct connection between the polje border and inland caves, as a vertical difference of about 20m between the flood levels on the polje and within the system remains more or less unchanged regardless of the absolute flood level (ŠUŠTERŠIČ, 1982). Inside the system (i.e. in Najdena jama), it is evident that about 3km of its main passages developed along the upper and lower contacts of the stratigraphically higher dolomite package, and along a third bedding plane within the lower Cretaceous limestones, parallel with and about 5m beneath the lower dolomite contact.
The primary tubes are lenticular to ellipsoid but their cross-sections have been altered locally by entrenchment. Apparently the passages are orientated either down/up dip or along the strike, but detailed inspection reveals that this is only an approximation. Passages, formed along joints are greatly subordinate and generally they developed at the locations of breakthrough that provided links from one major bedding plane to another. Phreatic risers, some more than 50m (downstream) upwards, are not uncommon. Though some canyonisation has occurred most of the system is typically phreatic, with no features suggestive of water table formation.
Many of these statements also hold true for other caves in the area. The Vodni rov (Water Passage) in Vranja jama (88) is of special interest. It was formed along the same plane as some other structural segments in the vertical span of more than 100m and a horizontal distance over of 500m. Its form is completely phreatic, and at first glance it appears to be formed in the dip direction (ŠUŠTERŠIČ, 1994,a). However, when measured properly, there are significant differences (Fig. 2).

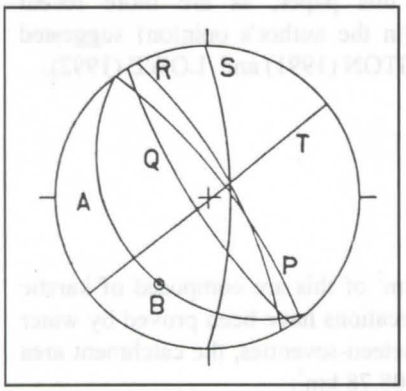

Fig. 2: Structures controlling the Water passage in Vranja jama. A - bedding plane; B - passage axis; P,Q,R,S - joints, secondarly penetrated by water; T - downdip joint, untouched by channel formation.

Although the original plane is dissected by several joints and laminated zones, they did not serve as initial structures, but water evidently penetrated into them after the main passage had been formed. Thus, though the channel was formed along the bedding plane, it does not appear to have been influenced by any of the numerous geological structures or orientations that now affect the bedding plane. Consequently, the passage must have begun to form before the structures were imposed. This is best explained by LOWE's (1992) theory of speleo-inception before orogeny.
In Najdena jama, passages are penetrable (by scuba diving) down to a level of 388.5m, while the highest known position in system is at 531.8m. They display phreatic or secondary features, and are almost always found on the upper or lower contacts of the "dolomite" layer. A number of fragments that exist on intermediate levels generally follow the same bedding planes. The most convincing interpretation of these observations is provided by WORTHINGTON'S (1991) findings, viewing all the caves in the area as representing fragments of a single tier. Similar geological conditions and speleological effects are found along an older dolomite layer, lying about 2km to the east and stratigraphically 500m lower.

Situation at the Laški Ravnik

The Laški Ravnik lies about 3km north-east of the Planinsko polje. The area is generally flat and extremely rich in solution dolines (ŠUŠTERŠIČ, 1994,b). Some main streams of the underground Ljubljanica must flow beneath the area, though no active stream cave has yet been found among a number of short fragments of evidently phreatic origin. A bed of coarse-grained secondary dolomite with a general dip of 2520 / 320 occurs on the junction between Jurassic and Cretaceous limestones. Around this outcrop, at Javorjev Grič, an area of about 1km^2 was mapped geologically and geomorphologically at 1:5000 scale. Special care was taken to observe and record all detectable originally underground karst phenomena that now appear at the surface due to denudation (Fig. 3).

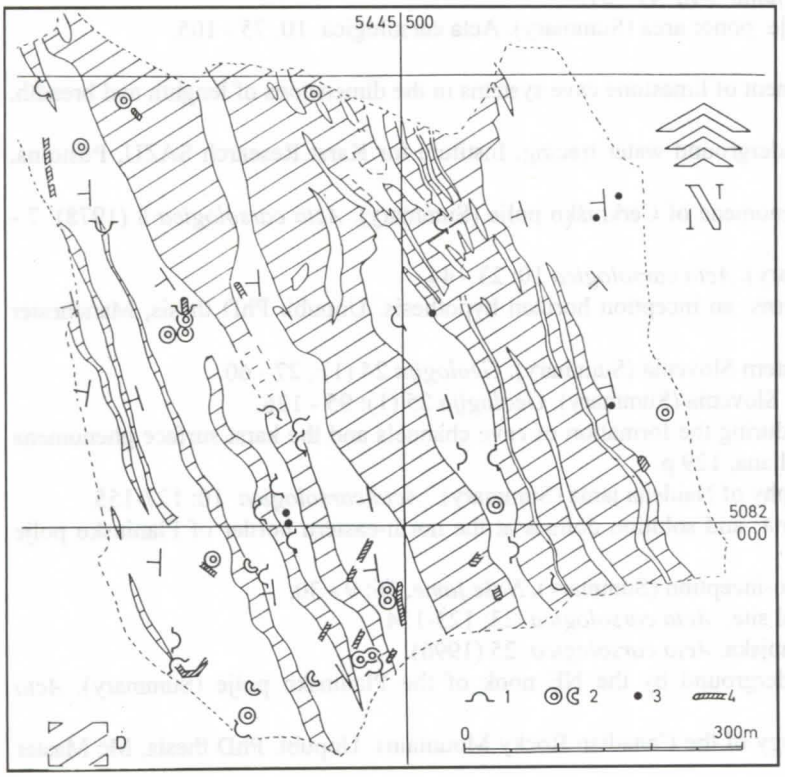

During the field work it became more evident that there is not a single dolomite package, but an interfingering of wider or narrower dolomite/limestone stripes (Fig. 3). Among the superficial karst phenomena, and true vertical (vadose) shafts being omitted, four types of underground ones were recorded (numbered as in Fig. 3):
1. Openings of phreatic tubes, not higher or larger than 0.5m. All of them become choked after some metres.
2. Small collapsed features (<3m), evidently continuing to a choked tube.
3. Segments of (sub-)vertical tubes, formed under phreatic conditions.
4. Denuded cave passages, filled with loam and other sediments.

Fig. 3: Situation at Javorjev Gric. D - dolomite; numeration - see the text!

Detailed inspection of the figure reveals that despite the area being strongly reworked by denudation it was possible to observe that most traces of phreatic tubes lie close to either the upper or lower limestone/dolomite contact. At some locations this correlation is clearly visible to the naked eye in the field..
It appears that around Javorjev Grič an earlier sector of an abandoned tier is exposed. Again, the limestone/dolomite contact was the most prone to channel formation. In the NW quadrant a concentration of features lies directly within the extrapolation of a presently non-existent continuation of a dolomite stripe what hints that the driving mechanism of inception might be recalcitisation of the dolomite.

Conclusions

Horizontal caves appear in well-expressed clusters, up to several kilometres in length, a few kilometres in width, and some hundreds of metres in depth. This pattern fits the notion of flow corridors within a single tier, as defined by WORTHINGTON (1991). Caves within a given tier were formed under phreatic conditions and reworked in vadose ones (in the hydrogeological sense). This means either that the change from the primary to the present hydrological conditions was relative fast, or that activity within the system was suspended during the transition.

Though the preserved phreatic passages are numerous where studied in detail, they are concentrated along a small number of bedding planes. In some cases it is evident that their directions do not follow any current structural framework, and that any penetration into joints was secondary. These relatively few bedding planes play the exact role of inception horizons, as defined by LOWE (o.c.).

Joints and smaller faults are really important only as master structures to guide the formation of phreatic jumps within a tier. This probably means that they play an important role during the adaptation phase of a tier. More highly tectonically disrupted zones define areas of significant cavern collapse, or local slab spalling, during the subsequent decay of the cave.

Thus, the general scheme of a cave corridor (trans)formation is:

1: initiation along bedding planes;

2: reorganisation, penetration into joints;

3: expansion by collapse of crushed zones of faults.

References

Archives of the Speleological association of Slovenia and the Karst research institute, ZRC SAZU, Postojna.

BRENČIČ, M. 1992. Koželevc (Summary[2]). *Naše jame* 34:, 41 - 51.

ČAR, J., 1982: Geologic setting of the Planina polje ponor area (Summary). Acta carsologica 10, 75 - 105.

ČAR, J. 1996: Personal communication.

FORD, D.C. & EWERS, R.O, 1978. The development of limestone cave systems in the dimensions of lenghth and breadth. *Canadian journal of earth science* 15: 1783 -1798.

GOSPODARIČ, R. & Habič, P. (eds.), 1976. Underground water tracing. Institute for Karst Research SAZU, Postojna, 309 p.

GOSPODARIČ, R. & HABIČ, P. 1979. Karst phenomena of Cerkniško polje (Summary). *Acta carsologica* 8 (1978): 7 - 162.

HABIČ, P. 1981. Karst relief and tectonics (Summary). *Acta carsologica* 10: 23 - 44.

LOWE, D. J., 1992: The origin of limestone caverns: an inception horizon hypothesis. Unpubl. PhD thesis, Manchester Polytechnic, 512 p.

PLACER, L. 1981. Geologic structure of southwestern Slovenia (Summary). *Geologija* 24 (1):, 27 - 60.

PREMRU, U. 1982. Geologic structure of southern Slovenia (Summary). *Geologija* 25 (1): 95 - 126.

ŠEBELA, S. 1994. The role of tectonic structures during the formation of cave channels and the karst surface phenomena (Abstract). Unpubl. PhD thesis, University of Ljubljana, 129 p.

ŠUŠTERŠIČ, F., 1982.: Morphology and hydrography of Najdena jama (Summary). *Acta carsologica* 10: 127-155.

ŠUŠTERŠIČ, F. 1987. The small scale surface karst and solution dolines at the north-eastern border of Planinsko polje (Summary). *Acta carsologica* 16: 51-82.

ŠUŠTERŠIČ, F. 1994, a. The Kloka cave and speleo-inception (Summary). *Naše jame*, 36: 9 - 30.

ŠUŠTERŠIČ, F. 1994, b. Classic dolines of classical site. *Acta carsologica* 23: 123-154.

ŠUŠTERŠIČ, F. in press. Caves and Poljes of Notranjska. *Acta carsologica* 25 (1996).

ŠUŠTERŠIČ, F. & Puc, M. 1970. The karst underground by the NE nook of the Planinsko polje (Summary). *Acta carsologica* 5: 205 - 270.

WORTHINGTON, S.R.H. 1991.: Karst hydrogeology of the Canadian Rocky Mountains. Unpubl. PhD thesis, Mc Master University, 227 p.

FOOTNOTES

[1] Numeration according to the central register of caves of Slovenia, maintained by the Speleological association of Slovenia and the Karst research institute, ZRC SAZU, Postojna.

[2] The titles of summaries/abstracts (if they exist) are given just to show the english reader the contents of the original texts, which are, however, considered in the whole.

Lithological control of speleogenesis in the Pre-Carpathian Region

Igor Turchinov
Lviv Geology Survey Expedition, ul.Turgeneva 33, UA-290018 Lviv, Ukraine

Abstract

The influence of lithological features of the Badenian (Middle Miocene) gypsum upon the speleogenesis in these rocks in the Pre-Carpathian region is shown on the examples of Optimisticheskaya and Dzhurinskaya caves (Western Ukraine) and Skorochitska cave (Southern Poland). In the regions of each of these caves gypsum is characterized by specific lithological and textural peculiarities which have controlled development of speleo-initiating jointing, space location of cave passages, morphology of cavities and planned structure of cave maze networks.

1. Introduction

Sulphate sediments of the Middle Badenian (Middle Miocene) evaporite formation stretch as the belt of 40-60 km in width along the northern and northern-eastern borders of the Carpathians (fig. 1). Extensive development of gypsum karst is connected with these rocks. In the region the five largest in the world gypsum maze caves are located (Optimisticheskaya - 192 km, Ozernaya - 111km, Zolushka - 89 km, Mlynki - 24 km, Kristalnaya - 22 km).

Karst development in general, and speleogenesis particularly, are controlled by numerous factors (tectonic, lithological, hydrogeological, etc.). In the Pre-Carpathian region lithological factor takes an important place in the control of karst processes. The influence of lithological and textural peculiarities of the Miocene gypsum upon the speleogenesis in these rocks is shown on the examples of Optimisticheskaya and Dzhurinskaya caves (Western Ukraine) and Skorochitska cave (Southern Poland). In the regions of each of these caves gypsum is characterized by peculiarities, which have determined features of speleogenesis.

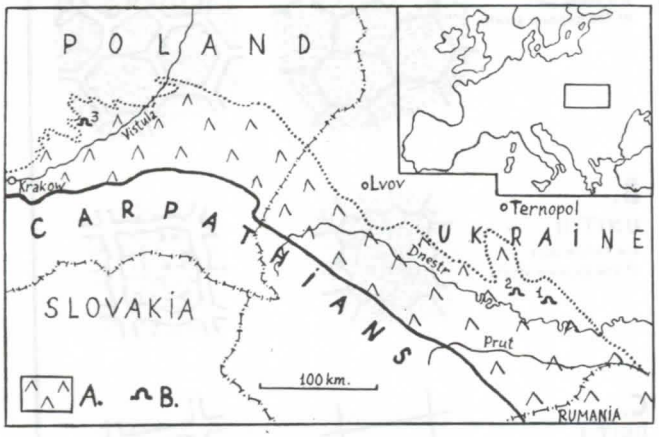

Figure1 : Location of studied area. A - sulphate facies, B - investigated caves (1 - Optimisticheskaya, 2 - Dzhurinskaya, 3 - Skorochitska)

2. Lithological peculiarities of the Middle Badenian gypsum

In the Pre-Carpathian region the gypsum stratum of 10-60 m in thickness is characterized by clear vertical structural and textural differentiation, which reflects conditions of sedimentation and diagenesis of sulphate sediments (fig. 2).

In the region of Optimisticheskaya cave the gypsum stratum of 18-22 m thickness has a three-unit composition (fig. 2A). Fine-grained gypsum with stromatolitic texture occurs in the lower part of the stratum (unit I). The middle part of the stratum (unit II) is characterized by concentric occurence of fine-grained and coarse-crystalline gypsum, which form dome-like structures of 0,5-3 m in diameter. Coarse-crystalline gypsum is composed of tabular crystals of 10-15 cm in size.

The upper part of the gypsum stratum (unit III) is separated from the middle part by a thin (1-30 cm< normally 5-10 cm) layer of bentonitic clays, and is built by giantocrystalline sabre-

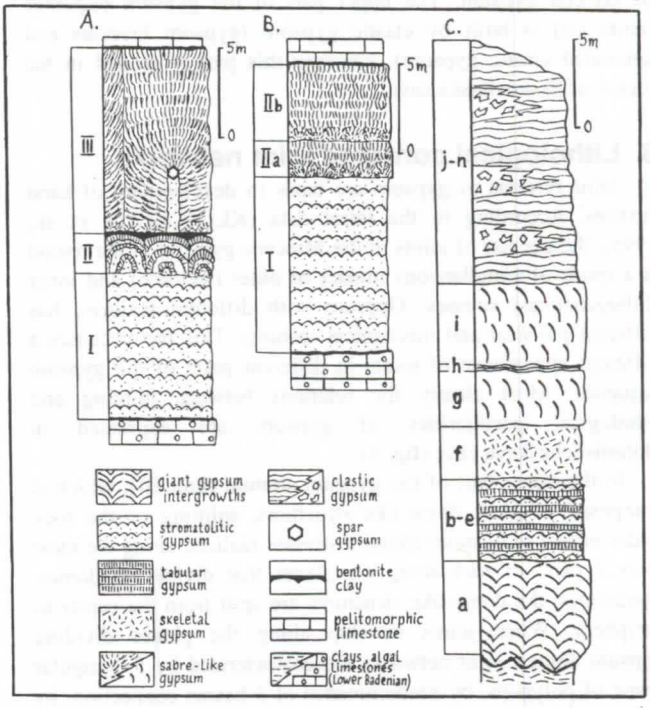

Figure 2 : Sequences of the Middle Badenian gypsum. A- in the region of Optimisticheskaya cave, B- in the region of Dzhurinskaya cave, C- typical Badenian gypsum sequence in the Southern Poland (Borkow Quarry) (PERYT & JASIONOWSKI, 1994)

like gypsum. The most distinctive feature of this part is an occurence of giant vertically elongated dome-like structures up to 10 m in diameter (normally 4-6 m) (KLIMCHOUK et al. 1995; TURCHINOV, ANDREICHOUK, 1995). The core part of the domes is built by fine-grained gypsum and has a shape elongation in the vertical direction. The transverse size of the core parts is normally 10-50 cm, and the height is 2-5 m. In the very top part of the core a monocrystal of spar gypsum occurs. Peripheral part of the dome is composed of upward-curved and splitting sabre-like gypsum crystals of 0,2-1,5 m in length. In the near-core part of the dome sabre-like crystals are cemented by fine-grained gypsum.The dome-like structures are divided by the boundaries, which create a polygonal network in the plan view.

In the region of Dzurinskaya cave (fig. 2B) fine-grained stromatolitic gypsum also occurs in the lower part of the gypsum stratum (unit I). The upper part (unit II) is built by sabre-like gypsum which forms two sub-units (IIa and Iib). Both of these sub-units have small dome-like structures of 0,1-1 m in diameter in their bottom. The length of the sabre-like crystals is 15-50 cm.

In the Western Ukraine the gypsum stratum is overlain by the Middle Badenian pelitomorphic limestones of 0,2-1,5 m in thickness.

In the Southern Poland the gypsum stratum has a complicated sequence (fig. 2C). Giant gypsum crystalline intergrowths (up to 4 m high) occur at the base of the sequence (unit a). They are overlain by bedded tabular coarse-crystalline gypsum with intercalations of alabastrine and stromatolitic gypsum (units b-e), followed by skeletal gypsum (unit f, composed of chaotically oriented tabular crystals) which pass upwards into sabre-like gypsum (units g-i) (KASPRZYK, 1993). Sometimes, the gently-sloping domes up to 12 m in diameter and 4 m in height occur in the sabre-like gypsum. Core parts of these domes are composed of skeletal gypsum. The upper part of the gypsum sequence (units j-n) is built by clastic gypsum (gypsum breccias and laminated clastic gypsum), however this part is eroded in the region of Skorochitska cave.

3. Lithological conrol of joint networks

Joint systems in gypsum are basis to development of karst cavities. According to the latest data (KLIMCHOUK et al., 1995), the genesis of joints in the Miocene gypsum in the region is a result of simultaneous impact of outer (tectonic) and inner (lithogenetical) stresses. Gypsum with different textures, has different physical and mechanical features. This factor causes a different appearance of joints in different parts of the gypsum sequence. Most clearly the relations between jointing and lithological peculiarities of gypsum are expressed in Optimisticheskaya cave (fig. 3).

In the upper part of the gypsum stratum (unit III), which is composed of giant dome-like structures, splitting of the rock under influence of outer tectonic stresses realized along the most relaxed parts of rock-along the planes that divide the domes. Sometimes, the dome-like structures are split from the center to periphery. When joints develop along the planes dividing gypsum domes, joint networks are characterized by 5-6-angular shape of polygons, by predominance of 3-beams connection, by absence of clearly expressed main orientations (fig. 3A).

In the middle part of the stratum (unit II) the rock also splits along the planes, which divide small dome-like structures occuring here, so that joints formed attain zigzag-like confuguration. The orientation of such joints is approximated by a sraight line corresponding to the axis of a passage (fig. 3B). The cave maze in this part is characterized by quadrangular shape of polygons.

In the lower part of the stratum homogeneous fine-grained gypsum is characterized by isotropy of physical and mechanical features. Here, the speleo-initiating jointing is characterized by clearly expressed main directions (with 2 main and 1-2 minor peaks on the diagram), by quadrangular shape of polygons and predominance of 4-beams intersections of joints (fig. 3C).

4. Lithological control of space position of carst cavities and their morphology

Optimisticheskaya cave

In the lower part of the gypsum stratum (unit I) the cave passages normally have rhomb-like cross sections (fig. 4A, 10). Combinations of two rhombus occur frequently (4A, 11). Such sections form due to episodes of prolonged stay of water table at a certain position, within the stage of dewatering of the gypsum stratum. Fissure-like passages (4A, 12) are less frequent here. Wide and low passages with plane ceiling occur along the contact of the gypsum stratum with the underlying formations (4A, 13).

Cavities of quadrangular shape with plane ceiling (4A, 8; 9) are common in the middle part of the stratum (unit II). Its ceiling is controlled by the bottom of the unit III. Contact surface between the units II and III is an important factor in the control of space position of cave maze networks. Verteba cave, the greater part of Ozernaya cave and many regions of Optimisticheskaya cave are timed to this contact.

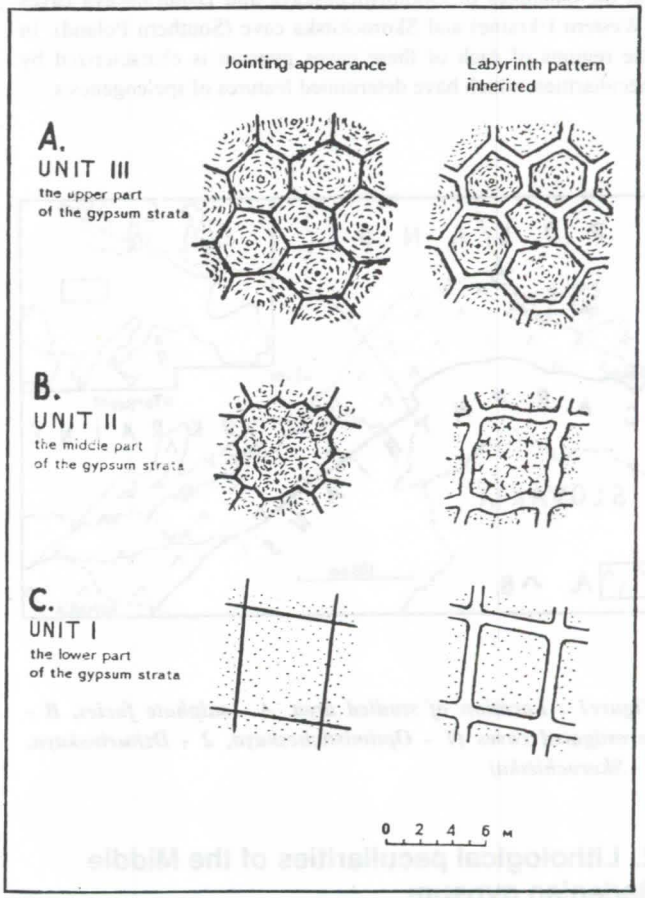

Figure 3 : Peculiarities of joint networks in different intervals of the gypsum stratum in Optimisticheskaya cave

In the upper part of the stratum (unit III) passages most commonly occur along joints along the planes dividing the dome-like structures. Such passages usually have fissure-like and triangular section (4A, 7), less frequently-rhomb-like section (4A, 1). Sometimes cave passage developed along joints radially splitting domes (4A, 6). There are also cavities developed along surfaces dividing concenters of the structures (4A, 2). Dome-like cavitites of 2-5 m in diameter (4A, 3) are common in the upper part of the stratum. These cavities have been formed by the select dissolution of fine-grained gypsum in the core and near-core parts of the dome-like structures. Some of the galleries and halls in Optimisticheskaya cave are a combination of these dome-like cavities and other speleoforms.

Cavities developed along joints dissecting the whole gypsum stratum, have more complicated morphology (4A, 14) and are represented by combinations of several speleoforms described above.

Dzhurinskaya cave

Space position of passages and galleries of this cave is controlled by the surface between the units and sub-units of the gypsum sequence (fig. 4B). Cave passages are developed commonly in the upper part of the stratum and are characterized by plane ceilings. Morphology of the passages is determined by textural peculiarities of gypsum (subhorizontal bedding of layers of sabre-like gypsum). In the lower part of the stratum cave passages seldom occur and have fissure-like cross section.

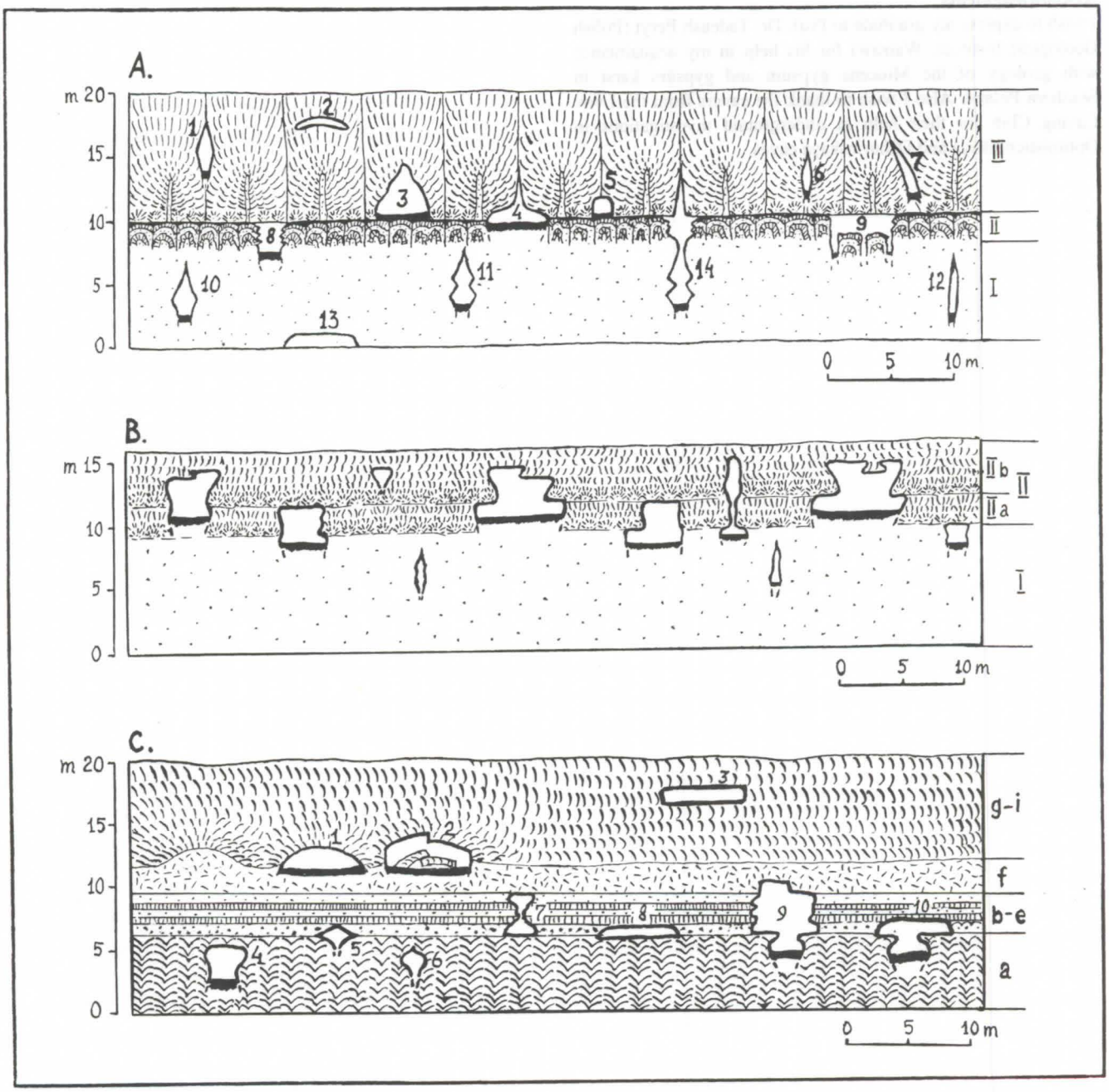

Figure 4 : Peculiarities of space location and morphology of karst cavities (in the vertical section). A - Optimisticheskaya cave, B - Dzhurinskaya cave, C - Skorochitska cave. Numbers are referred to in the text

Skorochitska cave

This cave is a canal of the underground flow, opening most ancient cavities. Localization of karst cavities is controlled by the borders between the units of the gypsum sequence (fig. 4C). Cave passages are developed along the borders between the units **a** and **b** (4C, 5; 8; 10), **e** and **f** (4C, 7; 9), **f** and **g** (4C, 1; 2). Within the units **f** and **g** original dome-like cavities (4C, 1) have been formed as a result of the dissolution of the core parts of gypsum domes. Their morphology may be complicated by collapsed gypsum blocks (4C, 2). Within the sabre-like gypsum, wide and low galleries (4C, 3) occur along the bedding planes. Within the units **b-e**, morphology of cavities is complicated by ridges and cornices, which have been formed due to the selective dissolution of fine-grained gypsum. Karst cavities developed in giant gypsum intergrowths (unit **a**) have original arched shapes (4C, 4; 6).

Acknowledgments

I wish to express my gratitude to Prof. Dr. Tadeush Peryt (Polish Geological Institute, Warsaw) for his help in my acquaintance with geology of the Miocene gypsum and gypsum karst in Southern Poland. Also I wish to thank the cavers from the Lvov Caving Club for their help in underground investigations in Optimisticheskaya and Dzhurinskaya caves.

References

KASPRZYK A. 1993. Lithofacies and sedimentation of the Badenian (Middle Miocene) gypsum in the Northern part of the Carpathian foredeep, Southern Poland. Annales Societatis Geologorum Polonide, vol.63: 33-84.

KLIMCHOUK A.B., ANDREICHOUK V.N. & TURCHINOV I.I. 1995. Structural prerequisites of speleogenesis in gypsum in the Western Ukraine. Ukrainian Speleological Association, Kiev, 104 p.

PERYT T.M. & JASIONOVSKI M. 1994. In situ formed and redeposited gypsum breccias in the Middle Miocene Badenian of southern Poland. Sedimentary Geology, 94 : 153-163.

TURCHINOV I.I. & ANDREICHOUK V.N. 1995. Dome-like structures in the Middle Miocene Badenian gypsum of the Dnestr River region (Western Ukraine). Przeglad Geologiczny, vol. 43, nr. 5 : 403-405.

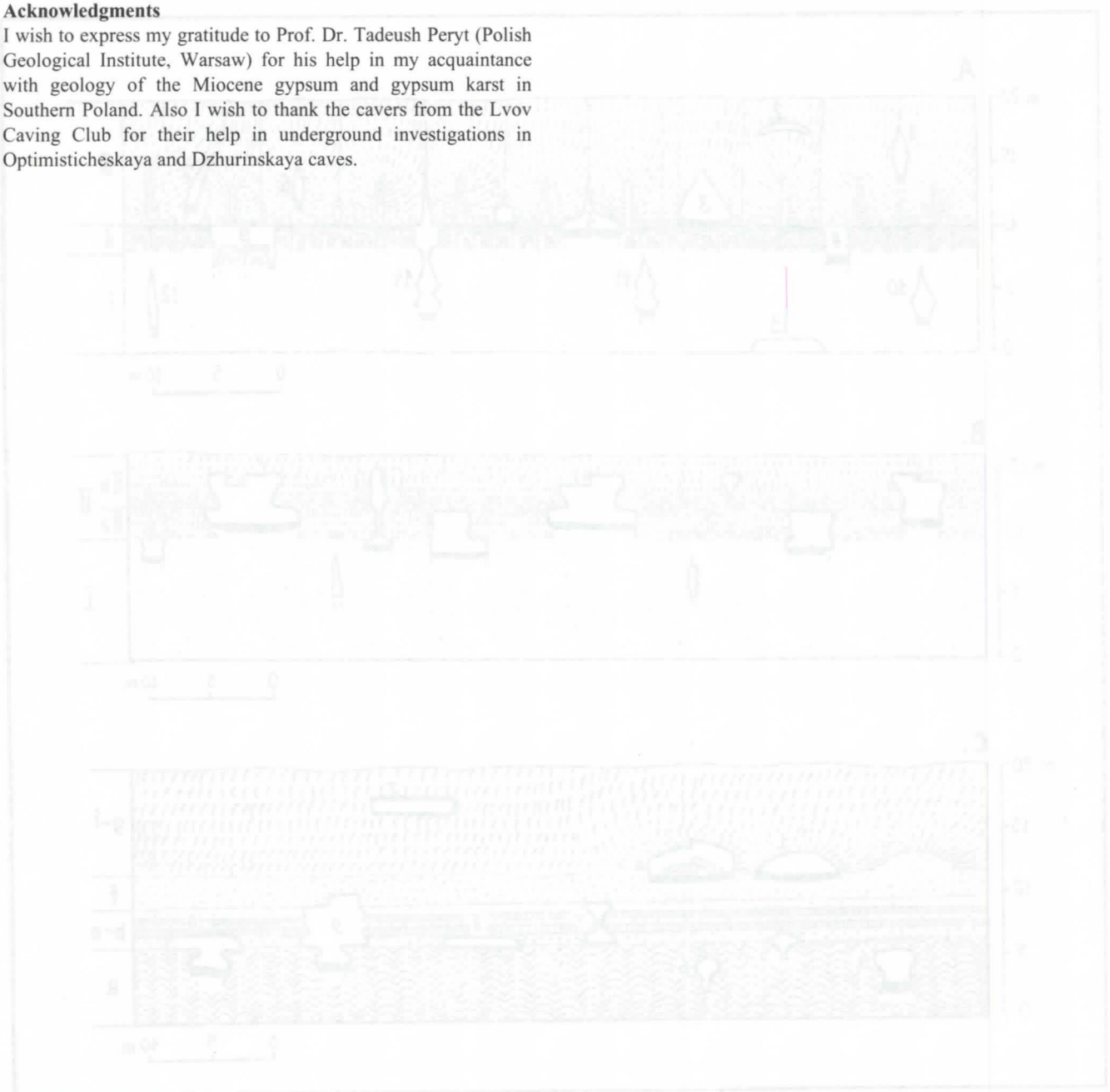

The Karst in the area of Matumbi Hills
(Kilwa district,Tanzania)
Hydrogeological characteristics and relationships between morpho-structures and tectonic phases

by Rosario Ruggieri
(Centro Ibleo di Ricerche Speleo-Idrogeologiche di Ragusa, via Carducci 165, 97100 Ragusa, Italy)

Abstract

Following the first German-Turkish expedition performed in 1994 in the area of the Matumbi Hills of Tanzania, during which 5,390 m of the Nandembo system was surveyed, in september 1995 a new Italian-German expedition carried out both further exploration of new caves and a series of geomorphological and hydrochemical researches.

With this exploration the Nandembo karst system became the thirteenth longest explored cave in Africa; other caves were surveyd in the eastern sector of Mbinga Hills, and all the geological, hydrogeological and geomorphological observations, the latter on the intraformational paleo-karst forms, allowed a relational hypotesis to formulate between the speleogenetical evolution of the explored cave system and the tectonic phases which occured in the area of Matumbi Hills in the infra-middle Jurassic and post-Callovian age.

Riassunto

Facendo seguito ad una prima spedizione tedesco-turca realizzata nel 1994 nell'area delle Matumbi Hils della Tanzania, durante la quale furono rilevati circa 5,390 m del sistema Nandembo, nel settembre del 1995 una nuova spedizione italo-tedesca effettua nella stessa area ulteriori esplorazioni di nuove cavità ed esegue nel contempo una serie di rilevamenti idrochimici e geomorfologici.

A seguito di tali esplorazioni il sistema Nandembo, con l'aggiunta del Ramo Sicilia, raggiunge i 7,510 m divenendo la tredicesima grotta più lunga d'Africa; ulteriori cavità vengono, inoltre, rilevate nel settore occidentale delle Mbinga Hills, mentre l'insieme delle osservazioni geologiche, idrogeologiche e, in particolar modo, quelle geomorfologiche sulle paleo-forme intraformazionali riscontrate, consentono di formulare una ipotesi relazionale fra l'evoluzione speleogenetica che ha caratterizzato i sistemi carsici esplorati e le vicende tettoniche, legate alle fasi di emersione, verificatesi nell'area delle Matumbi Hills in età infra-medio Giurassica e post-Calloviano.

1. Introduction

In 1994 a German Turkish expedition surveyed 5,390 m of caves in the Matumbi Hills in the Kilwa District of Tanzania. In order to continue the explorations a second expedition was carried out in September 1995 by CIRS of Ragusa with some german researches of the previous expedition. The principle objectives of the expedition was that to find in the Matumbi Hills as many caves as possible, with the aim to obtain a general view both of the morpho-structural and hydrogeological characteristics of the karst area.

The area of research, included in the maps to scale 1:50.000 Kipatimu, Sheet 239/4, and Kandawale, Sheet 255/2, is characterized by a monotonous pattern of hills, with elevation between 400 m and 570 m a.s.l., long and narrow with sides meeting to the bottom of the valley with gradients both steep around 30 ° and more gently sloping around 10 °. The superficial water flow is generated througt a hydrographyc network noticeably dendritic belonging to the basin of the Mtunbei river.

2. Geology and stratigraphic series

In the area the Jurassic sediments of the *Matumbi series* outcrop (STOCKLEY, 1943). This layers, outcroping on most of the Matumbi hills, are made up by two Formations: *Kipatimu beds* and *Mtumbei beds*. The litologic terms of the *Kipatimu beds* are made up of a series of pink-buff sandstones, from massiv to flaggy, and red, grey-green, and green blue mudstones. The sandstones form the great part of the outcropping in the area, while the presence of the mudstone is shown by the outcropping of clay colured soils. The age of the *Kipatimu beds* dates from medium Jurassic (Bathonian-Callovian) to the upper Jurassic and probably extend to the lower Cretaceous, while the thickness of the series has been estimated to be about 300 m. The underlying series called the *Mtumbei beds* is made up of oolitic limestones, hard and well bedded, from shallow sea, with interbedding of sandstones and calcareous sandstones, going toward the bottom becoming sandstones. The estimated thickness is about 150 m. The age of the *Mtumbei Formation* has been calculated, based on its fossil content, to be between the Bathonian and the Bajocian.

Morpho-structural elements

The trend of the relief shows, in the research area, the presence of a gentle anticline with an axis having a NE-SW stricke, approximately parallel to the superficial waterdivide described before, and reaching an elevation of about 700 m a.s.l. to the south west of Nwenge. In the southern sector the above mentioned structure is delimited, instead, by a fault escarpment with direction from NW-SE to WNW-SSE. The sides of the anticline are lowered by a system of faults, with a NE-SW direction, parallel to the direction of the main superficial hydrical flow. A second system of faults, approximately perpendicular to the first, with a NW-SE direction, complete the morpho-structural context of the area from which is put in evidence a general control carried out by the tectonic on the evolution of the relief, both the make up of the hydrographical network and the morphology of the outcropping.

3. A general description of the principle caves surveyed

Mpatawa cave

The Mpatawa cave is mainly made up of a large gallery 1,160 m long, with a stream flowing along its length. The cave is entered from a collapsed doline, after a steep descend, amongst rocks of various dimensions, and a low passage. The gallery, whose dimensions are about 20 x 20 m, has along the first tract corroded calcitic deposits and clastic rocks due to collapse. After about 350 m a big deposit of flowstone obstructs the middle section of the gallery and it is possible to by-pass this through a narrow conduit in the lower part of the deposit, which leads to the underlyng stream.

The above mentioned flowstone deposits shows in the upper part some big basins, and in the lower part, where the stream flows, on the ceiling, small domes, clustered together. Proceding along the stream, the gallery curves toward NE, due to a tectonic structure, then it starts a thick layer of deposits of sand and red clay.

Finaly, after a further tract of 500 m, the gallery becomes lower following the dip of the strata, until it assumes the configuration of a low flat conduit, where the water prevents further advance.

The cave runs from west to east towards the Nandembo system from which it is only 500 m and for this reason it appears probable that the two system are hydrologically linked.

Namaingo cave

The Namaingo cave, which drains the large spring of Kihangambembe, is made up of a fossil sector of 495 m and from a main gallery, along which a stream flows, and of a labyrinthine system of passages and small chambers which together form a system of 2390 m. The river after 450 m from the entrance becames a syphon, as the ceiling lowers following the dip of the layers. Along the course of the river the cave shows an ample section like a "nave" of a church with roof channels both of conical shape and with a flat base in the layer of calcareous sandstone. On the walls of the gallery morphologies of corrosion type "bear scratch" are seen and forms of corrosion type scallops. An interesting corroded surfaces, covered by a layer of siltstone, are present on th bed of a calcareous bank in a fossil sector of the cave. In this last sector, near ther ceiling, on a sandy limestone layers, small elliptical paleo-karst conduits are present.

The Namaingo cave is developed in Jurassic limestone and drains the water of infiltration of a sector of the Matumbi Hills with a main system of tectonic structures NNW-SSE and a secondary system NNEE-SSW.

The Nandembo system

The Nandembo system, surveyed for a total length of 7510 m, resulted in being made up of a main gallery, along which a stream flows from NNW to SSE, and a tributary system located in the left sector.

This last system is made up of the large Nangoma cave, the Nakitara cave and from the "Sicily inlet". In the whole system there are several macro and micro morphologies coming from the alternate karstic cycles of erosion and corrosion linked to the tectonic evolution of the area. In particular in the main gallery, along the stream, large channels are present on the ceiling with vertical walls and the upper side being flat corresponding to the calcareous sandstones layers. Still on the ceiling meandering channels, due to the erosion of the rising water level, are present. The main gallery shows elliptical tracts formed along the bedding planes, and higher tracts formed along the fractures with a direction N 170°-180°.

In the Nakitara cave a first fossil level is present partially filled by clasty and sandy deposits. This level is connected to a lower meandering system of conduits, periodically active, formed by the erosion of the rising water during the overflood phases. On the entrance of the Nakitara cave a system of fractures were surveyed showing a direction of N 70°-80°, with spacing of 2-3 m and with an interlayer extension of 2.5 m. These fractures, which appeared to be interrrupted in corresponding to the sandstone strata, are present in the layers with a dip direction of N 345° and dip of 8°. A second system of fractures intersects the first system with an angle of 90° and together forms the network of phreatic conduits, now fossil, in the initial part of the cave.

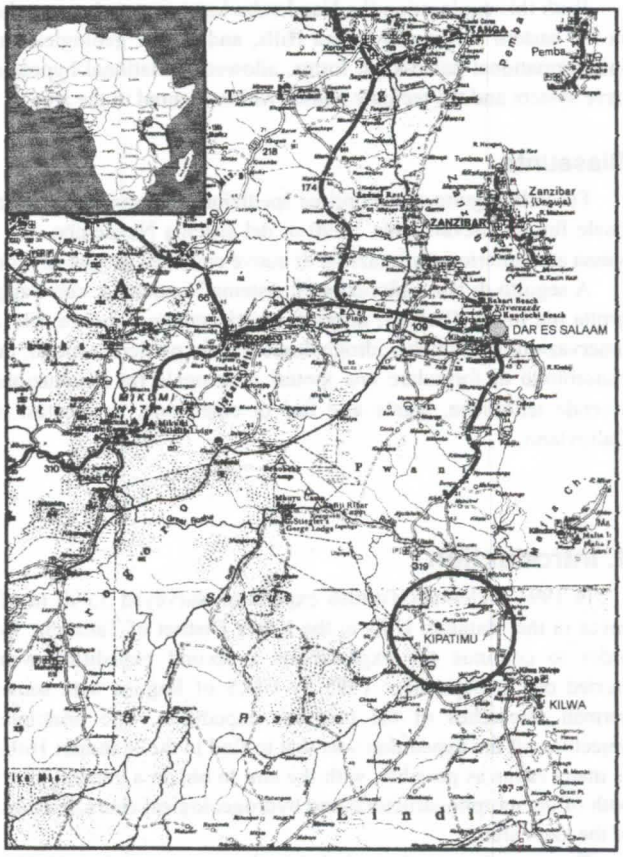

Fig. 1 Area of research in the Matumbi Hills

The Sicily Inlet

The Sicily inlet, with a length of 1,700 m, is made up of a main conduit with a stream, of a secondary fossil system located in an upper level and lastly of a fossil conduit which joins with the Nakitara cave. In this sector the cave shows a gallery with a "bell" shape and continues with a series of conduits having both "domes" and "bell" sections.

Following up this first fossil conduit, the section becomes narrower due to the raising of the floor caused by the deposits of sand. On the walls of the lower conduit, which resulted as being a "ceiling channel", particular morphologies of corrosion are present with the shape of a "scoop" , "semi-domes" and "bear scratches".

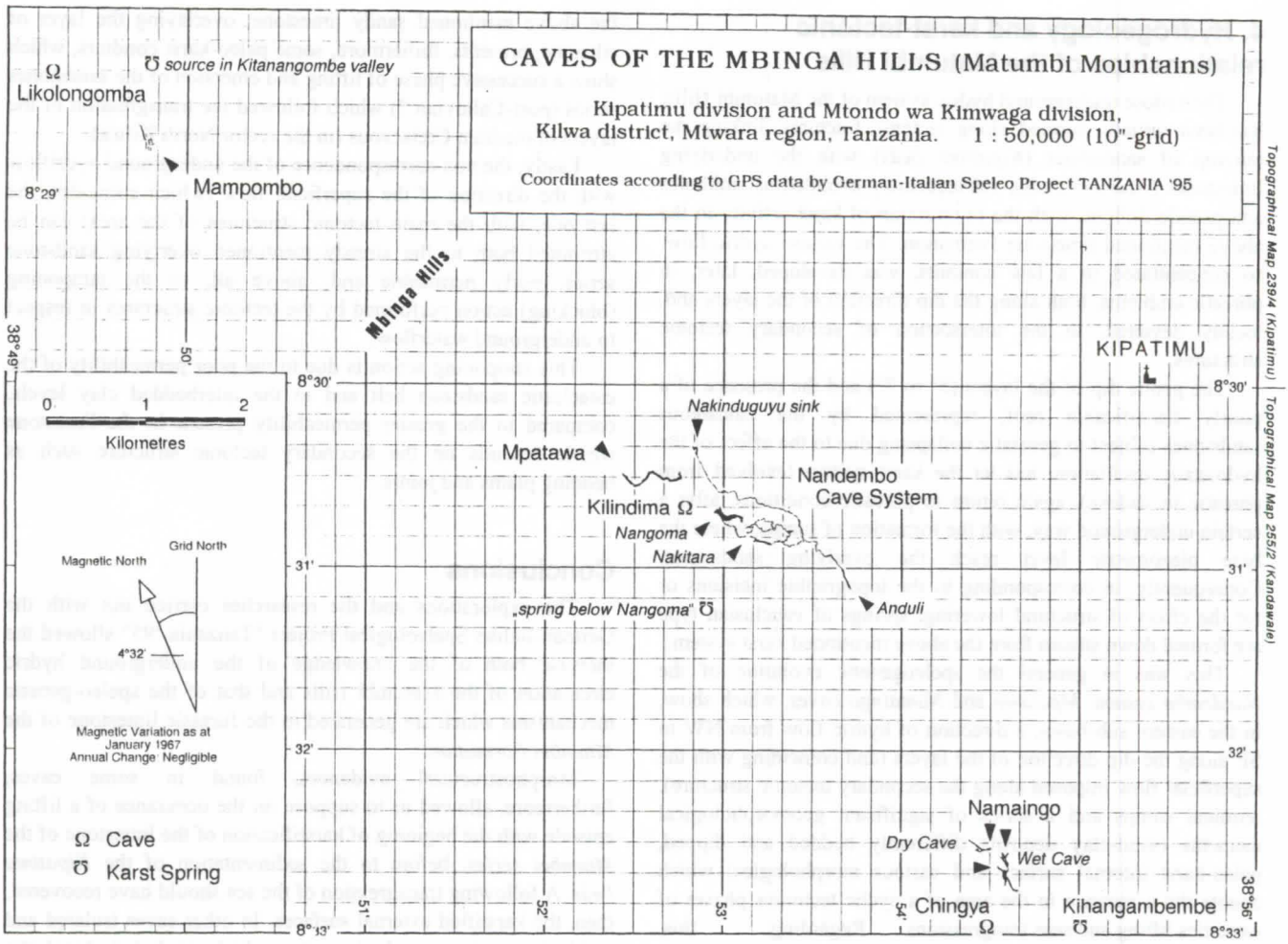

The main branch, along the stream, develops mainly from west to east with a series of galleries, on the interlayer fractures, having a direction at right angles to each other.

Along the stream, both eroded deposits of sand and silt are present and flowstone deposits which, further, have obstructed most of the gallery forming small waterfalls. This active tract so becomes impassable for excessive narrowing of the section due to the calcitic deposits and, downstream, to the final presence of a syphon.

Lastly in the fossil sector, situated in the upper level, both morphologies of vadose erosion of the floor and sections of the ceiling with a "bell" shape are present. This level in some tracts is characterized by eroded sandy deposits, with pieces of mica (the gold gallery), while in others tracts, on the walls small calcitic inflorescences shine. These small crystals have grown under a fine layer of clay deposited on the walls. This fossil branch, which connects again with the active gallery, further becomes impassable as the section narrows due to detritic deposits.

Karst genetic model of the Nandembo system

All the geomorphological and hydrogeological observations taken in the Nandembo system allowed the formulation of the following speleogenetic model.

In a first phase, coinciding with the lifting of the Matumbi Hills, a primitive net of hydric drainage begins to develop in the *Matumbi bed* Formation, corresponding to the sector of the future Nangoma cave.

A following phase of tectonic instabillity, with a probably lifting of the area, might have provocated, with the opening of new fractures, the capture of the hydric flow, its transfer to a lower level and the consequent progressive fossilization of the down stream cave. This rejuvenation which is linked to the initial development of the Nakitara cave and the successive one of the Sicily inlet, determines the drainage of the Nangoma hydric flow towards the main Nandembo system which is forming.

The successive collapsing of the Nangoma system determines the separation of the Nangoma-Nakitara circuit and the progressive fossilization of the Nakitara. The hydric flow in this phase will be further progressively absorved by the karst circuit of the Sicily inlet.

A new phase of fossilization to be linked to a marine transgression, productes in the whole system further modifications, such as the filling of some galleries and the formation of channels on the roof, both in the Sicily inlet and in the sector of the main Nandembo system.

Lastly the present phase is characterized by erosion/ corrosion, with vadose flow regime, both along the main stream and along the stream of the "Sicily inlet". This regime is provocating a further lowering of the karst corrosion level in the system, while the water oscillations, which originates in the flooding phase, are shaping the meandering morphologies along the fractures, present on the roof.

4. Hydrogeology and karst-tectonic relationships of the Matumbi Hills

The vadose underground hydric system of the Matumbi Hills, has been initially formed along tectonic fractures, linking the outcrop of sandstones (*Kipatimu beds*) with the underlying limestones (*Ntumbei beds*), subsequentely evoluted as sinkholes and pseudo-dolines, with the progression of karst activity in the above mentioned limestone Formation. The vadose hydric flow, so concentrated in a few conduits, was developed, later, in phreatic ambients, both along the dip direction of the layers and, locally deviated, to the intersection of secondary tectonic structures.

The gentle dip of the layers (5° to 7°) and the presence of a poorly karstificable roof, represented by the calcareous sandstones subject to geostatic collapsing due to the effect of the hydrostatic oscillation, has let the karst system (evolved from phreatic to vadose), again return to phreatic conditions, after a certain underground way, with the formation of sumps, where the base piezometric level reach the overlying sandstones. Consequently, in corresponding to the topographic incisions or for the effect of structural lowering, springs of vauclusian type are formed down stream from the above mentioned karst system.

This was in general the speleogenetic evolution of the *Nandembo system, Mpatawa* and *Namaingo caves*, which show, in the eastern sub-basin, a direction of hydric flow from NW to SE along the dip direction of the layers (and coinciding with the superficial flow imposed along the secondary tectonic structure), terminal sumps and a series of significant geomorphological elements (sand-clay deposits differently bedded and dipped, paleo-karst internal surface and various morphologies) which denote the accurance in the area of a cyclic tectonics phases of isostatics lifting and seas trangressions. Regarding this, according MOORE (1961), the movement of lifting of the Matumbi Hills, associated to a system of faults with a NNE-SSW and NW-SE direction, should have started in the premium Jurassic age and to have continued, in an intermittant way, up to recent times. This lifting, futhermore, could have been more intense in the western sector of the Matumbi Hills which shows more elevation component from the eastern sector.

The soils of the medium and Lower Cretaceous, along the escarpement between Migaregere and Nantumbili, overlie the Jurassic sandstone with a low discontinuity which denotes, furthermore, a phase of emersion of the Matumbi series, followed by a transgression of the sea.

Furthermore, the evidence of structural lifting of the infra-medium Jurassic age, which has emerged the limstone of the *Mtumbei Formation*, has been noted in the Namaingo cave where is visible a paleo-karst surface overlaid by a siltstone layer.

The siltstone, which covers in an irregular way the underlaying karstified surfaces, shows a lentilform thickness from half meters to three meters, and could signal the starting of the sedimentation of the *Kipatimu Formation*. In the same cave the above mentioned sandy limestone, overlaying the layer of siltstone, presents, furhermore, some paleo-karst conduits, which show a successive phase of lifting and emersion of the sandstones series (post-Callovian ?) which followed the transgression of the layers of medium Cretaceous (in the sector North Kilwa).

Lastly, the non correspondence of the underground hydriflow with the direction of the superficial flow (which coincides, the last one, with the main tectonic structures of the area) can be attributed both to the already mentioned overlying sandstone series, porly permeable and, above all, to the tamponing (blocking) action performed by the tectonic structures in respect to underground waterflow.

This tamponing action is due to the poor permeability of the cataclastic sandstone belt and to the interbedded clay levels, compared to the greater permeability present in the limestone which depends on the secondary tectonic structure such as bedding plains and joints.

Conclusions

The explorations and the researches carried out with the German-Italian Speleological Project "Tanzania '95" allowed the increase both of the knowledge of the underground hydric circulation of the Matumbi Hills and that of the speleo-genetic mechanisms which are generated in the Jurassic limestone of the *Mtumbei Formation*.

Morphostructural evidences, found in some caves, furthermore, allowed us to suppose on the occurance of a lifting episode with the begining of karstification of the limestone of the *Mtumbei series*, before to the sedimentation of the *Kipatimu beds*. A following transgression of the sea should have recovered, then, the karstified external surfaces. In other caves isolated and residual conglomerated deposits, which included bioclastic elements, were found and they could be associated to the above mentioned sea transgression that must have filled evolved karstic systems.

The possibility to undertake in the future other studies, both on the cave deposits with eventual spectrometric dating determination, and on the numerous and various morphologies, would surely allow the adding of new and important elements to the already outlined hydro-karst system of the Matumbi Hills.

Bibliografia

LAUMANNS, M. & RUGGIERI, R. (1996): Caves of the Matumbi Hills. - The International Caver (16) 1996. Aven Inter. Publications, Swindon, England.

MOORE, W.R. (1974): Geological notes on quarter degree sheets 256/256E, Kilwa, and 255, Njinjo, southern region. - Rec.Geol.Survey Tanganyca, Vol. IX - 31; Dar es Sdalaam.

STOCKLEY, G.M. (1943): The geology of the Rufiji district, including a portion of northern Kilwa district (Matumbi Hills). - Tanganyka Notes and Records, 16, Dar es Salaam.

Structures hiérarchiques dans le karst de la St Baume (Bas du Rhin, Var, France)

Martin Ph.
Université d'Artois, UFR Hist-Géo, 9 rue du Temple, BP 665, 62030 Arras cedex et
URA 903 du CNRS, Université de Provence, Institut de géographie, 29 av r. Schuman, 13621 Aix en Provence.

Abstract

On the St Baume 180 caves are opened. The deepest is the cave of Petit Saint Cassien (-321 m; 9,3km). The position and the difference in level D (gap between the highest and the lowest points) of every cave are used to check the organisation of this karst on all the montain. If the Pt St Cassien is excluded, we show : $C=287*10^{(-0,017\ D)}$. C is the number of caves whose the difference in level is inferior to D. Zipf - Mandelbrot's pattern is fitted to the distribution of the number of caves by 10 m classes. The frequencies F<0.1 is fitted to a power law (slope = g = 2,22; fractal dimension = 1/g). An additional parameter β alowes modeling all the distribution. β must translate the state of epikarst. β = 1,36. A power law allowes modeling the variation of the specific difference of level (Ds in m/km2; sum of the D of the caves which open in a disc with radius R, divided by the value of the area of the disc) according to the radius of the disc. Around the Pt St Cassien : $Ds = 221\ R^{-1,6}$. This pattern is also validated around others big caves but with shorter radius. Therefore to scale of the mountain karstification corresponds to fitted together hierarchical structures.

Résumé

Sur la Sainte Baume la karstification est développée : 180 cavités dont l'aven du Petit Saint Cassien (-321 m, 9,3 km). La position et la dénivellation D (écart entre le point le plus haut et le plus bas) de chaque cavité sont utilisées pour vérifier que ce karst est organisé à l'échelle du massif. Si on exclut le Pt St Cassien, on montre que : $C = 287 * 10^{(-0,017\ D)}$. C est le nombre de cavités d'une dénivellation inférieure à D. Le modèle de Zipf - Mandelbrot est ajusté à la distribution du nombre de cavités par classes de 10 m. Les fréquences F < 0.1 correspondent à une loi de puissance de pente g = 2,22 et la dimension fractale : 1/g. Un paramètre supplémentaire β permet de modéliser l'ensemble de la distribution. β doit quantifier l'état de l'épikarst. β = 1,36. Une loi de puissance modélise la variation de la dénivellation spécifique (Ds en m/km^2 : somme des D des cavités qui s'ouvrent dans un disque de rayon R, divisée par la valeur de la surface du disque) en fonction du rayon du disque. Autour du Petit St Cassien : $Ds = 221\ R^{-1,6}$. Ce modèle est aussi validé autour d'autres avens importants mais pour des rayons plus courts. A l'échelle du massif la karstification correspond donc à des structures hiérarchiques emboîtées.

1. Introduction

La karstification est un processus de redistribution spatiale de bicarbonates pour l'essentiel. Cette action de mobilisation puis de dépôt s'effectue aussi bien à l'intérieur du karst que entre un karst et son environnement. Cette dynamique permet d'agréger, à l'intérieur du karst, des volumes emplis d'air et/ou d'eau, dont la succession constitue le cavernement. Pour partie celui-ci est connu grâce à des inventaires réalisés par des spéléologues.

Les morphologues ont essayé, essentiellement pour des formes de surface, de découvrir des règles traduisant l'organisation spatiale des formes. Ces règles établies empiriquement par HORTON (1945) par exemple sont aujourd'hui mieux comprises car englobées dans la géométrie fractale (MANDELBROT, 1995). Ce type d'approche est encore peu fréquent dans les karsts, tant pour les formes de surface (MARTIN, 1995) que pour les formes de l'endokarst (CURL, 1966, 1986; MARTIN, 1996).

La St Baume a bénéficié de recherches spéléologiques très intenses, au moins depuis la 2ème guerre mondiale. Ces travaux ont abouti à la publication d'un inventaire des cavités très complet (C.A.F. & S.C.M., 1987 a, b). Les données utilisées en sont issues et ont été complétées (FRANCO, 1994). Sur la St Baume s'ouvrent 185 cavités (fig.1) de 0 à 321 m de dénivellation (D) qui correspond à la valeur absolue de l'écart entre la cote minimale et la cote maximale mesurées par rapport à l'entrée. Cette donnée est relativement sûre car les cotes sont généralement mesurées avec précision. Elle nous renseigne sur les épaisseurs de roches carbonatées affectées par la karstification. Nous faisons l'hypothèse que ces données sont représentatives de la karstification du massif.

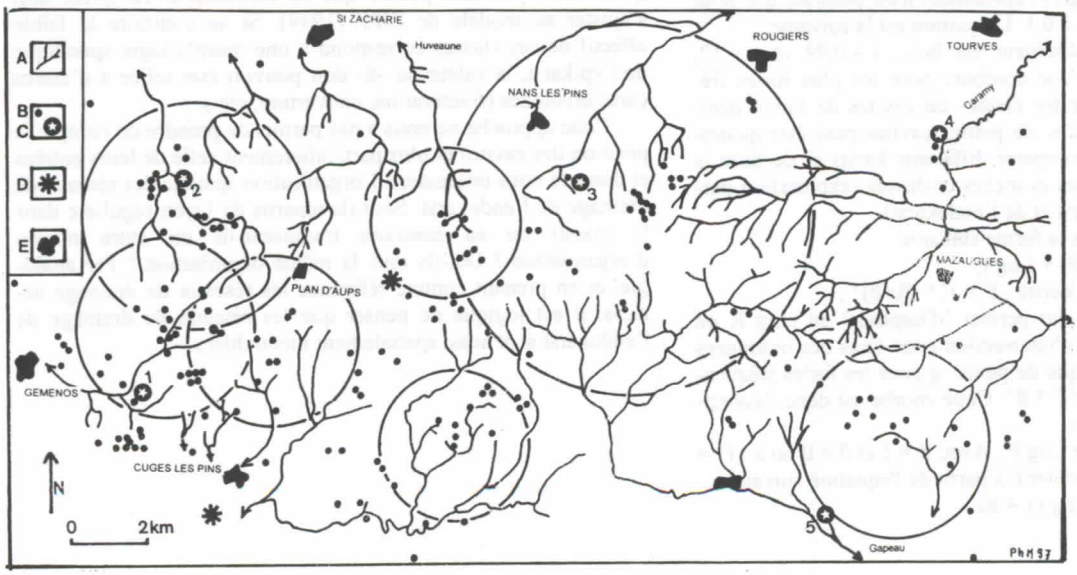

Figure 1 : Carte du massif de la Sainte Baume
A talweg
B entrée de cavité
C source principale
D poljè
E village.

2. Nombre de cavités et dénivellation

Les distributions d'objets géographiques classés en fonction de leur taille sont hyperboliques comme par exemple la surface de lacs ou d'îles, la longueur des cours d'eau (KORCAK, 1940 ; FRECHET, 1941). Elles suivent la loi de Pareto : si N est le nombre d'observations où la variable envisagée est supérieure à un nombre X, et A et B 2 constantes positives : $N = A / X^B$ et donc : $N = A X^{-B}$ ou encore $A = N X^B$; B étant l'exposant de Paréto.

Les cavités ont été classées dans un ordre décroissant, puis affectées d'un rang. La totalité de cette distribution ne s'ajuste pas à la loi de Pareto et donc au modèle bilogarithmique rang / taille de ZIPF (1949).

Cette distribution peut être par contre ajustée à un modèle exponentiel à condition d'exclure l'aven du Petit Saint Cassien ; cavité la plus profonde. Pour cela nous l'avons divisée en 13 classes de 10 m et nous avons déterminé le nombre de cavités entrant dans chacune des classes. En effectuant successivement la somme des effectifs de chacune de ces classes nous établissons la relation : $C = 287 * 10^{(-0,017\ D)}$ avec : r = 0,99 ; n = 13; D étant la dénivellation et C le nombre de cavités d'une dénivellation inférieure à D. Ce type de relation a déjà été mis en évidence pour la fréquence des dolines classées par taille (WHITE & WHITE, 1987). Ce type de distribution exponentielle traduit le caractère aléatoire de l'occurence des événements.

La dénivellation du Petit St Cassien (321 m) est proche de la différence d'altitude entre l'entrée de l'aven et le seuil de débordement de la Foux de Nans; source la plus importante et la plus proche (MARTIN, 1991). Je pense que cet aven, et son long réseau (9,3 km), correspond à une phase plus profonde et peut-être plus récente de karstification. Il convient donc de le réintégrer dans la distribution quitte à faire évoluer le modèle de référence.

Le modèle de ZIPF (1949) étendu par MANDELBROT (1953, 1995) dérive de la théorie de la gestion de l'information à l'intérieur d'un système complexe (FRONTIER & PICHOD-VIALE, 1991). Cette loi correspond, par exemple pour une langue vivante, à une optimisation des signaux. Par analogie nous pouvons penser que sa vérification sur une distribution de dénivellations de cavités correspond à une optimisation des investigations spéléologiques et/ou à une optimisation des morphologies nécessaires au transit des précipitations.

Si l'on ordonne les classes de dénivellation par ordre de fréquence d'apparition décroissante (F) et si l'on porte le logarithme de cette fréquence en fonction du logarithme du rang (R), nous obtenons un alignement de points qui permet d'ajuster une droite. L'équation est donc de la forme :

$\text{Log } F = -g * \text{Log } R + k$; g est la pente; k est une constante. Puisque lorsque R = 1, $\text{Log } F^1 = k$, on peut écrire :

$\text{Log } F^R = -g * \text{Log } R + \text{Log } F^1$ et donc : $F^R = F^1 * R^{-g}$.

Pour la St Baume (fig.1) l'ajustement n'est possible que pour les fréquences inférieures à 0,1. L'équation est la suivante:

$F = 2,07 * R^{-2,22}$. L'ajustement est bon : r = 0,99 et n = 12, mais la figure 1 montre une courbure pour les plus fortes fréquences, c'est-à-dire pour les classes de cavités de faible dénivellation. Ce relatif manque de petites cavités peut être quantifiée. Cela permettra de comparer différents karsts et de faire la part entre les 2 hypothèses avancées ci-dessus (exploration partielle et/ou état de l'épikarst et de l'endokarst).

Le modèle prend alors la forme suivante :

$\text{Log } f^R = -g * \text{Log}(R+ß) + \text{Log } f_0$.

Ce que l'on peut aussi écrire : $f^R = f^0 * (R+ß)^{-g}$;

-ß- est un paramètre qui permet "d'imposer" au rang R un décalage. $-f^0-$ est le point d'intersection entre l'axe des ordonnées et l'extrapolation de la droite de pente -g pour les fortes fréquences. Pour R = 1 on a : $f^1 = f^0 * ß^{-g}$. Cette courbe est donc l'asymptote de la droite d'équation :

$\text{Log } F_R = -g * \text{Log } R + \text{Log } F_1$. Avec R = 1 et ß = 0 on a : $F^1 = f^0$. Nous pouvons ainsi calculer ß à partir de l'équation suivante :

$\text{Log } f^0 - \text{Log } f^1 = g * \text{Log } (1 + ß)$.

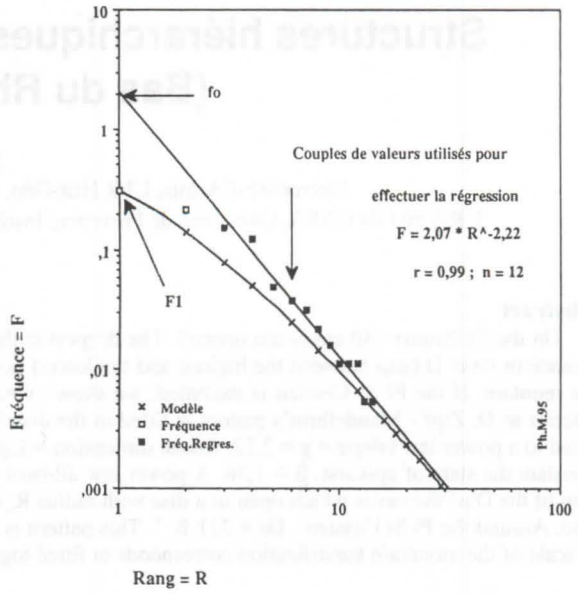

Figure 2 : Ajustement du modèle de Zipf - Mandelbrot à la distribution des dénivellations mesurées dans les cavités de la St Baume.

Pour la Sainte Baume en remplaçant les termes par les valeurs nous obtenons :

Log 2,07 - Log 0,308 = 2,22 * Log (1 + ß) soit :

0,8274 / 2,22 = Log (1 + ß) => 2,3589 = 1 + ß et donc ß = 1,36. L'ajustement du modèle à la distribution est assez bon : r = 0,95 et n = 14.

-ß- qualifie aussi bien le niveau des investigations spéléologiques que l'état de l'épikarst. Il permettra de comparer des karsts très différents de façon à voir s'il est influencé par la manière dont l'eau entre sous terre.

$-f^0-$ ne caractérise pas la courbe il est seulement choisi de telle sorte que la somme infinie $\sum(f^R)$ soit égale à 1.

-g- permet d'apprécier la diversité de la distribution. Une forte pente correspond à des effectifs réduits pour de faibles profondeurs et donc à des effectifs relativement importants pour de fortes profondeurs, et inversement. 1/g étant une dimension fractale (D_f), nous avons : $D_f = 1 / 2,22 = 0,45$.

Cette distribution de dénivellations s'ajuste donc à un modèle hiérarchique révélant une certaine organisation à l'échelle du massif. Si les faibles effectifs des classes regroupant les petites cavités traduisent un manque dans les investigations spéléologiques, nous pouvons penser que la distribution complète doit s'ajuster au modèle de ZIPF (1949). Si au contraire le faible effectif de ces classes correspond à une morphologie spécifique de l'épikarst, la valeur de -ß- doit pouvoir être reliée à d'autres caractéristiques (fracturation, couverture, etc.).

Cette approche ne nous a pas permis de prendre en compte la position des cavités et plus particulièrement celle de leurs entrées et donc de nous intéresser à l'organisation spatiale des réseaux de drainage de l'endokarst. Sont-ils répartis de façon régulière dans le massif ou au contraire traduisent-ils un autre niveau d'organisation ? Ont-ils tous la même organisation ? Par analogie, et en prenant comme référence les réseaux de drainage aériens, il est logique de penser que les réseaux de drainage de l'endokarst sont aussi spatialement hiérarchisés.

3. Répartition spatiale des dénivellations

La carte (fig.1) montre qu'à l'ouest s'ouvre un nombre plus important de cavités qu'à l'est. Les gradients altitudinaux y sont plus forts (Pic de Bertagne 1042 m; source de Saint Pons 320 m) qu'à l'est (Mourré d'Agnis 919 m; source de la Figuière 305 m). Localement nous observons des regroupements d'entrées de cavités, et dans tous les secteurs du massif, une cavité plus importante est entourée d'autres moins profondes. La répartition du cavernement n'est pas égale. Ceci est conforme à la division en sous bassins du massif établie par l'analyse du fonctionnement (MARTIN, 1991). Ce drainage dans l'endokarst est-il localement organisé ?

Nous faisons l'hypothèse qu'à l'échelle de la dizaine de km^2, se sont développés des réseaux correspondant à une structure arborescente semblable à celle que nous observons en surface (MARTIN, 1995) mais qui est, dans le cas du karst, développée dans les 3 dimensions. Une source en constituant l'extrémité aval ; des avens et des galeries en étant les entrées et les branches. Si l'analogie évoquée ci-dessus est correcte, cela implique qu'à toutes les échelles se répètent des formes semblables. Les réseaux explorés ne sont que ceux qui sont de taille suffisante pour permettre le passage des spéléologues, mais ils ne doivent pas avoir une forme différente de ceux, beaucoup plus étroits, qui resteront à tout jamais inexplorables, ou de ceux qui n'ont pas encore été découverts. Je pense donc que les données acquises sur les réseaux connus sont représentatives de l'ensemble de la structure karstique tout comme les connaissances acquises sur le réseau d'un sous bassin sont représentatives, avec certaines limites, de l'ensemble du réseau d'un bassin versant.

La cavité présentant localement la plus forte dénivellation sera considérée comme étant le drain principal avec lequel les autres cavités confluent car je considère que la découverte est plus facile, pour les spéléologues, lorsque la karstification a été plus importante. La karstification est elle d'autant plus importante que le drain est plus ancien et qu'il draine vers lui un maximum de débits. Cela a pu être établi par traçage pour l'aven du Grand Clapier et l'aven du Petit Saint Cassien mais cela reste une information exceptionnelle sur ce massif. Par contre de telles confluences sont souvent révélées au fur et à mesure que les travaux spéléologiques progressent. Il arrive toutefois qu'assez souvent un rétrécissement rende impossible la poursuite de la progression du spéléologue jusqu'au site de confluence. Ces secteurs étroits semblent aller de pair d'une part avec une diminution croissante des possibilités de mise en solution de la roche avec l'augmentation de la profondeur ou plus exactement avec l'augmentation du temps de séjour de l'eau chargée d'acide carbonique (pCO_2), mais aussi d'autre part avec les caractéristiques des connexions préexistentes entre les discontinuités initiales (fracture, joint de stratification, etc.) à l'origine du réseau. Ceci n'exclut pas en outre des possibilités locales de comblement (concrétion, remplissage, etc.). Dans tous les cas, l'absence de confluences établies par exploration ne signifie nullement l'absence de réseau unitaire.

D'après les lois de HORTON (1945) si l'organisation du drainage superficiel est de forme arborescente, nous devons observer que la longueur cumulée du réseau augmente au fur et à mesure que nous intégrons des drains d'ordre inférieur. Expérimentalement il est possible de montrer que la croissance d'un réseau de drainage s'effectue jusqu'à ce qu'il emplisse l'espace du bassin versant à l'exception des surfaces de concentration de l'eau en amont de chaque talweg initial. Nous pouvons donc établir la surface drainée par chaque ordre dont la somme est égale à la surface du bassin versant.

La longueur cumulée spécifique qui est le rapport entre la longueur cumulée des talwegs par la surface cumulée drainée par ces talwegs, augmente donc elle aussi avec l'intégration de talwegs d'ordres inférieurs. Ces considérations peuvent être résumées dans un chiffre qui est la dimension fractale du réseau. Par exemple le réseau de drainage aérien du Caramy, à l'est de la St Baume, a une dimension fractale de 1,52 (MARTIN, 1996).

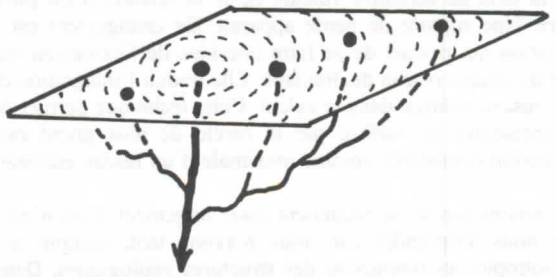

Figure 3 : Schématisation d'un réseau et méthode employée.

Dans notre approche nous ne pouvons disposer des mêmes informations pour résumer en un chiffre la qualité du réseau de drainage en raison de la méconnaissance de la totalité du réseau dans laquelle nous sommes.

Nous allons donc utiliser une autre approche et comparer les dénivellations cumulées des cavités à une surface de référence ou plus exactement établir la relation qui existe entre la variation des dénivellations cumulées spécifiques de cavités s'ouvrant dans un disque et le rayon de ce disque. Cette relation doit s'exprimer par un alignement de points en coordonnées bilogarithmiques si elle traduit une organisation fractale du réseau.

Nous pouvons vérifier cela en considérant la surface topographique comme un plan tangent au réseau qui supporte les entrées (fig.3). En prenant comme point de départ l'entrée de la principale cavité d'un secteur du massif, nous avons dessiné une série de disques concentriques dont les diamètres étaient augmentés successivement d'un km (JULIEN,1992; BONNEFOY, 1993). Nous avons calculé pour chacun d'eux la dénivellation cumulée des cavités qui y débutent. Ces dénivellations cumulées ont ensuite chacune été divisées par la surface correspondante du disque. Le résultat est une dénivellation spécifique (Ds) en m/km^2. Pour chaque secteur nous avons ensuite établi une relation bilogarithmique de la forme : $Ds = a\ R^{-b}$ entre la dénivellation spécifique et la valeur du rayon (R) en km de chacun des disques. Si le drainage s'éffectuait par des drains sub-parallèles indépendants et au moins aussi importants, nous observerions soit une valeur identique de la dénivellation spécifique quelle que soit la surface considérée - et donc l'exposant -b- tendrait vers zéro -, soit une croissance de Ds en fonction de R. -b- traduit donc la hiérarchisation du réseau. Plus la valeur de -b- est importante et plus le réseau est hiérarchisé, plus celui-ci empli l'espace de l'endokarst.

Le graphique ainsi établi (fig.4) montre un très bon alignement des points comme en atteste les coefficients de corrélation linéaire calculés (tabl.1).

-b- prend des valeurs comprises entre -1,62 et -1,04. Que le secteur où se développe l'aven le plus important soit affecté de la valeur de -b- la plus forte paraît tout à fait logique tout comme la très faible valeur de -b- pour le secteur de l'extrémité ouest de la haute chaîne où l'Escandaou, cavité en forme de mono puits, est toujours apparu comme une paléo forme déconnectée des dynamiques actuelles même si cet aven est parcouru par un filet d'eau (COULIER, 1985). La plus forte dénivellation moyenne (Dc / Nb C) par cavité a d'ailleurs été calculée pour le secteur de l'Escandaou.

-a- exprime l'importance des dénivellations cumulées (Dc) avec : $Dc = 3{,}2\ a^{1.14}$; $r = 0{,}993$; $n = 7$. Une relation peut être établie entre -a- et la valeur maximale de R : $a = -75{,}5 + 408{,}5\ \log Rmax$; $r = 0{,}92$; $n = 7$. Dc croit en fonction du nombre de cavités tout comme -a-.

Aucune relation n'a pu être établie entre l'altitude de l'entrée de la cavité constituant le centre des disques et les caractéristiques de ces réseaux. Sachant que les sources qui sont leur exutoires supposés sont situées en périphérie du massif à des altitudes voisines, il ne semble donc pas que la hauteur de chute soit un facteur déterminant dans la constitution de ces réseaux.

Au delà de certaines valeurs de R la relation n'est plus linéaire. Une rupture de pente apparaît. Ce changement est une indication qui permet de se faire une idée de l'extension maximale de chaque réseau de drainage. Elle traduit l'intégration d'un autre réseau contigu dans le calcul. Cette technique permet donc de représenter en surface par le cercle de plus grand rayon, l'extension considérée comme maximale d'un réseau endokarstique.

Certains cercles se recoupent assez largement. Cela n'est pas pour nous surprendre car nous n'avons tenu compte ni de l'anisotropie des réseaux ni des structures géologiques. Dans le cas des Encanaux, du Pin de Simon et de l'Escandaou se dessine une large bande à l'intersection des 3 cercles qui est exempte de cavité. Il nous paraît logique que la limite entre ces 3 réseaux passe à ce niveau. Dans le cas de Castelette nous savons que cette cavité est morphologiquement en rapport avec le poljè parfois fonctionnel du Plan d'Aups (MARTIN, 1991). Plusieurs tentatives de traçage effectuées dans les ponors se sont soldées par des échecs. L'extension, aussi loin vers l'ouest, du cercle circonscrivant une aire en rapport avec le Pt St Cassien nous conduit à penser que le drainage du poljé pourrait bien se faire vers cet aven.

A l'échelle du massif, ces relations bilogarithmiques traduisent donc l'existence de structures de drainage dans l'endokarst,

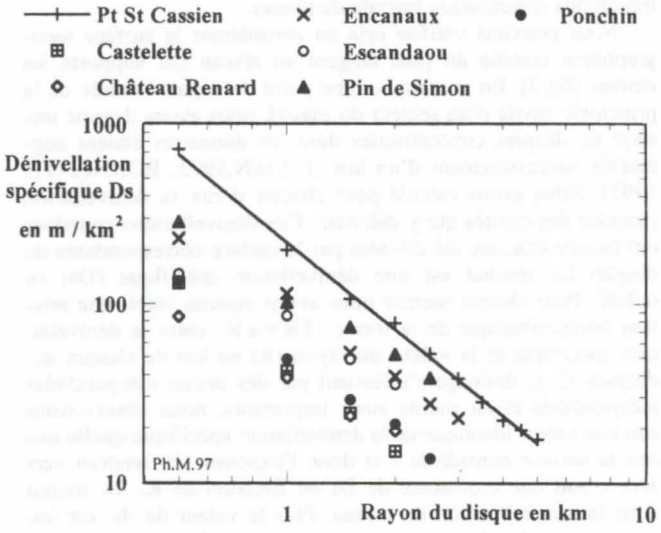

Figure 4 : Relations bilogarithmiques entre la dénivellation spécifique Ds et la valeur du rayon R des disques pour 7 secteurs de la St Baume.

hiérarchisées, plus ou moins développées et emboitées. Le type de fonction nous conduit à penser que cette organisation résulte de processus déterministes générant une morphologie fractale (LAVERTY, 1987).

4. Conclusion

Cette approche reste imparfaite sur plusieurs points. Il ne nous a pas été possible de tenir compte du cheminement des cavités à travers la masse carbonatée tout comme de l'ampleur réelle des vides induits par la karstification. Il conviendra donc de poursuivre cette recherche en essayant de rapporter les volumes dûs à la karstification à un volume de référence comme une demi-sphère. Nous ne disposons pas, pour l'instant, d'une mesure de l'ampleur des vides mais nous pouvons imaginer les déterminer à partir d'une approche fractale de chacune des cavités (SUSTERSIC, 1983, CURL, 1986). Par la suite il sera nécessaire de tenir compte de la position dans l'espace des réseaux karstiques.

Cavité = C	Modèle bilogarithmique a	b	Rmax km	Coef. Cor.	Alti. de C en m	Nb. C sur R max	Dc en km	Dc / Nb C
Pt St Cassien	221	-1,62	5,0	0,999	740	36	1361	38
Castelette	44	-1,55	2,0	0,999	600	11	187	17
Chateau R.	39	-1,10	2,0	0,999	545	10	243	24
Encanaux	98	-1,34	3,0	0,994	433	25	644	26
Escandaou	76	-1,04	2,0	0,991	892	11	445	40
Pin de Simon	117	-1,21	2,5	0,996	540	26	755	20
Ponchin	51	-1,39	2,5	0,999	745	11	265	24

Tableau 1 : Modélisation de la décroissance des dénivellations spécifiques cumulées autour des principales cavités de la St Baume - Dc = Dénivellation cumulée.

Références

BONNEFOY, J. L. 1993. Fréquentation des commerces et services. *Mappe monde* n°4, p.40-41.

CLUB ALPIN FRANCAIS, & SPELEO CLUB DE MARSEILLE, 1987 a-b. La St Baume souterraine. Tome I, 2 éd., les B. du Rh., 110 p. et Tome II, le Var. 217 p.

COULIER, C. 1985. Hydrogéologie karstique de la Sainte Baume occidentale, B. du Rh., Var; Fr. Thèse de 3 cycle, Université de Provence Aix-Marseille I, 400 p.

CURL, R.L. 1966. Caves as a measure of karst. *J. Geol.*, vol.74, n°5, part.2, p.798-830.

CURL, R.L. 1986. Fractal dimensions and geometries of caves. *Mathematical Geology*, vol.18, n°8, p.765-783.

FRANCO, A. 1994. Cavités du Var de plus de 100 m de dénivelé. *Spélunca bulletin* n°53, p.13.

FRECHET, M. 1941. Sur la loi de répartition de certaines grandeurs géographiques. *J. Soc. Stat. Paris*, vol.82, p.114-122.

FRONTIER, S. & PICHOD-VIALE, D. 1991. Ecosystèmes. Structure - fonctionnement - évolution. Masson éditeur, Paris, 392 p.

HORTON, R.E. 1945. Erosional development of streams and their drainage basins : hydrophysical approach to quantitative morphology. *Bulletin of the Geological Society of America*, 56, p.275-370.

JULIEN, R. 1992. The application of fractals colloïdal aggregation. *Croatica chemica acta* n°2, p.215-235.

KORCAK, J. 1940. Deux types fondamentaux de distributions statistiques. *Bulletin de l'Institut International de Statistique*, vol.30, p.295-299.

LAVERTY, M. 1987. Fractals in karst. *Earth surface processes and landforms*, vol.12, p.475-480.

MANDELBROT, B. 1953. Contribution à la théorie mathématique des communications. Thèse Université de Paris, Publ. Inst. Stat. Univ. Paris, 2, 121 p.

MANDELBROT, B. 1995. Les objets fractals, 4 éd. Editions Flammarion, Coll. Champ n°301, 208 p.

MARTIN, Ph. 1991. Hydrogéomorphologie des géosystèmes karstiques des versants N et W de la St Baume (B. du Rh., Var; Fr). Thèse Université d'Aix - Marseille II, 326 p.

MARTIN, Ph. 1995. Les formes fluviatiles du massif de la St Baume (B. du Rh, Var; Fr). *Theoretical and applied karstology*, vol.8, p.103-115.

MARTIN, Ph.1996. De l'organisation des formes superficielles et souterraines du massif karstique de la St Baume (B. du Rh, Var; Fr). *Ukpic* n°8, Univ. de Fribourg, Suisse, M. Monbaron et S. Fierz éditeurs, p.45-64.

SUSTERSIC, F. 1983. Determination of unknown cave passages length by means of fractal analysis. New trends in speleology, Jancarik A. éditeur, Dobrihovice, p.61-62.

WHITE, W.B. & WHITE, E.L. 1987. Ordered and stochastic arrangements within regional sinkole populations. in proceeding of 2nd multidisciplinary conference on sinkholes and environmental impacts of karst, Orlando, Floride; sous la direction de Beck B.F. et Wilson W.L. A.A.Balkema éditeur, p.85-90.

ZIPF, G.K. 1949. Human behavior and principe of least-effort, Cambridge, MA : Addison-Wesley.

A comparison of the orientation of cave passages and surface tributary valleys in the karst of southwestern Wisconsin, U.S.A.

by Craig A. Terlau and Michael J. Day
Department of Geography, University of Wisconsin-Milwaukee, Milwaukee, Wisconsin 53201, U.S.A.

Abstract

It has been suggested independently that regional structure, in the form of bedrock fractures, exerts a control over the orientation both of cave passages and surface tributary valleys. If this is so, then these features in a given area might be expected to have statistically similar orientation data sets. This hypothesis was tested by comparing orientation data for adjacent cave passages and tributary valleys in the karst of southwestern Wisconsin.

Cave passage orientation data was derived from published maps of 21 caves in Richland County, Wisconsin. Orientation data for adjacent tributary surface valleys was derived from 1:24,000 U.S. Geological Survey maps using computer-assisted techniques.

Rose diagrams generated from the data sets suggested visually a close relationship between cave passage and tributary valley orientations. Of 20 Kolmogorov-Smirnov tests, in only four cases were cave and valley orientation data sets dissimilar at an alpha level of 0.1. In 80% of cases there was a strong relationship between cave and valley orientations, suggesting that the orientation of these features in the southwestern Wisconsin karst may indeed be influenced by a common set of bedrock fractures.

Zusammenfassung: Vergleich der Richtungen von Höhlengängen und oberflächlichen Talformen im Karstgebiet im südwestlichen Wisconsin, USA.

Es wurde verschiedentlich postuliert, dass regionalgeologische Strukturen, nämlich Klüfte, einen Einfluss auf die Orientierung sowohl von Höhlengängen als auch von kleineren Talformen auf der Oberfläche (Trockentäler) haben. Wenn dem so ist, müssen solche Formen in einem gegebenen Gebiet statistisch ähnliche Richtungen aufweisen. Diese Hypothese wurde an Hand von Vergleichen der Richtungen von Höhlengängen und von oberirdischen Seitentälern im Karstgebiet im südwestlichen Wisconsin geprüft.

Die Daten zu den Gangrichtungen wurde den Plänen von 21 Höhlen in Richland County entnommen, jene der im gleichen Gebiet vorhandenen Oberflächen-Seitentäler aus den topographischen Karten U.S.G.S. 1:24'000 mittels computerunterstützten Techniken.

Auf diesen beiden Datenpaketen basierende Rosetten-Diagramme zeigen visuell starke Richtungskonvergenzen zwischen Höhlengängen und Oberflächentälern. Dies wurde mit 20 statistischen Vergleichen erhärtet: Es gab nur 4 Fälle, in denen Höhlen- und Talorientierung mit einer Irrtumswahrscheinlichkeit von 0.1 voneinander abwichen. Also deuten 80% der Fälle darauf hin, dass die Orientierung dieser Formen im südwestlichen Karstgebiet von Wisconsin durch gemeinsame Grundgesteinsfrakturen beeinflusst wird.

1. Introduction

Karst caves usually form through dissolutional enlargement of fractures within carbonate bedrock (TRUDGIL, 1985). These fractures, however, do not occur randomly, rather they are the result of directional stresses placed upon the rock. Studies of bedrock fracture orientations show that they occur in preferred directions (PARIZEK, 1976). Thus, if fractures are the dominant directional control mechanism in the formation of a particular cave, the straight sections of cave passage would be expected to have orientations similar to those of local fractures.

Dry valleys are other karst landforms which can develop along existing bedrock fractures. Drainage waters will follow the hydraulic gradient, but may find the path of least resistance along surface fractures for at least part of their course. A valley which is cut into bedrock should appear linear along sections where surface fractures were utilized (PARIZEK, 1976), these linear sections of valleys may be expected to have an orientational distribution similar to that of local fractures. If both caves and linear valleys in an area have developed under the influence of the same structural control, data sets of their orientations should be statistically similar.

The purpose of this paper is to examine the orientational relationship between linear sections of cave passage and linear tributary valleys, and to measure the extent of this relationship. Based on theory, bedrock fractures exert significant control over the development of linear sections of both caves and tributary valleys. The hypothesis being tested is that their orientational distributions are similar. Further, this relationship is expected to occur locally.

The valleys to be measured for orientation are those occurring in the areas immediately adjacent to each cave location. These valleys have been chosen for the following reasons: 1) because of their proximity, the valleys and the caves are likely to have developed along the same fractures (LAPOINTE & HUDSON, 1985), 2) the scale of the caves and the tributary valleys is similar, 3) the caves and tributary valleys occur at similar stratigraphic levels, and 4) the valleys are cut into bedrock and have little superficial cover.

2. Previous Studies of Cave Passage Orientations

There have been many previous studies involving comparison of cave passage orientations with orientations of other types of features, although few comparing cave passage and dry valley orientations. For a survey of such studies, see TERLAU (1995).

3. Bedrock Geology of Richland County

In Richland County the interfluves are capped by lower Ordovician limestones and dolostones of the Prairie du Chien group. The main valleys are cut into the underlying Jordan sandstone formation. Beds dip gently to the southwest at about one degree (HEYL et al, 1959). Very gentle folding can be observed where beds are exposed.

The Oneota formation of the Prairie du Chien group is the major cave forming member north of the Wisconsin river (DAY, 1986). It attains a thickness of about 50m (HEYL et al, 1959).

Vertical fractures cut through the Jordan sandstone and the Prairie du Chien dolostone. Single vertical joints are traceable for up to a mile and cut as much as 100m of beds (HEYL et al, 1959). The Upper Mississippi Valley has repeatedly experienced regional stresses although record of orogenic events during the Paleozoic and Mesozoic is incomplete and interpretation is speculative. Fracturing of the bedrock has been attributed to regional Paleozoic orogenic stresses (Dutch, 1981), to post-depositional shrinkage (LEITH, 1932), and to glacial crustal bending (MCGINNIS, 1969).

4. Karst and Caves of Richland County

Richland County consists of a karstic upland dissected by fluvial drainage and with a local relief of about 100m. The karst is developed on the ridges, which are narrow, gently curved on top and steep-sided. Cliffs and bedrock outcrops are common. Karst features of Richland County include over 50 sinkholes, over 600 springs, thousands of dry valleys and 44 caves (DAY et al, 1989).

In the absence of accurate dating, the age of the caves in southwestern Wisconsin is unknown (DAY, 1986a, b). Development commenced sometime between the Cretaceous and the Pleistocene, an earlier date being suggested by the fact that the caves were well integrated with the pre-Pleistocene drainage system.

There are 44 known caves in Richland County, with a total of 2100m of passage. The caves are small in both passage dimension and length (DAY, 1986a,b). They are relatively inactive and show limited signs of current dissolutional activity. Their ridgetop position places them well above the present day water table and gives the caves a limited catchment area.

Of the 44 known caves in Richland County, 23 (52%) are formed in the Prairie du Chien dolostone, and 21 (48%) are sandstone caves. Cave lengths are from 3m to 335m. Of the caves 25m or more in total length, 93% are formed in dolostone. The mean length of caves in dolostone is 100m .

Natural cave entrances occur where sinkhole collapses break through to the ceiling of the cave and as outcrop entrances where downcutting of valleys has intersected the cave passage. While Richland County has 44 known caves which have connections to the surface, doubtless there are many others that do not. One way of approximating the number of caves with no surface connection is to place known caves into classes according to their number of entrances. Of 40 of the 44 caves in Richland County, there is only one cave with three entrances, there are three caves with two entrances, and there are 36 caves with one entrance. "Statistical distribution functions and geologic reasoning agree that a substantial class of caves with no entrances should exist." (WHITE, 1988 p.61). Furthermore the class sizes of caves according to their number of entrances is suggested to follow Poisson distribution (WHITE, 1988). Applying a likelihood function to the cave entrance data from Richland County, there are likely some 187 caves with no entrance (TERLAU, 1995).

The caves of Richland County are not regularly distributed throughout the county, but occur in clusters, reflecting outcrops of the Praire du Chien Dolostone. Nearest- neighbor analysis (EBDON, 1981) resulted in a calculated value c of -2.096, and a 98% probability that the distribution of caves in the study area is significantly clustered (TERLAU, 1995). Cave clusters were identified by locating groups of points which are reflexive in that all points in the group have their nearest-neighbor within the group, and that each point within the group has a nearest-neighbor distance below the value for all points in the sample area. In Richland County, seven groups of caves fit this criteria.

5. Methodology

All linear measurements in the orientation analysis are in English units, since these are common to the USGS topographic sheets and the 21 existing cave maps which could be located. These maps are to British Cave Research Association grade 3 to 7 (ELLIS, 1984). "Caves of Richland County, Wisconsin" (PETERSON, 1968) was the source for 12 of these maps. Nine other published cave maps were obtained from sources listed by TERLAU (1995).

Cave Passage Orientations

For this study, orientation lines were drawn to parallel the walls of straight sections of passage, and to parallel linear passage features where straight sections do not exist. Sections of the caves which could not be interpreted as linear were not measured. The existing cave maps were scanned 1:1 as 600 dot per inch PICT files.

Adobe Photoshop, a graphics program which performs plotting of lines and measuring of angles, was used to obtain cave passage orientations. The angle of the line being drawn is displayed in an information box. Measurements had a high level of precision; the repeatability of measurements taken from cave maps was found to be between 0.1° and 0.5° depending on the length of the feature being paralleled. For full details of the measurement techniques, see TERLAU (1995).

Linear Valley Orientations

20 USGS 1:24,000 topographic sheets provided full coverage of Richland County. Caves in which passage orientations were measured were located and marked on the topographic sheets. The portions of the topographic sheets showing the cave location and the interfluvial ridge associated with the cave were scanned 1:1 as 600 dot per inch gray-scale PICT images. The mean area scanned from the topographic maps was 3.87 square miles. Five of the scanned map sections contained more than one cave, therefore the mean map area per cave used for analysis was 2.71 square miles.

Linear tributary valleys were identified on the maps by contour analysis (TERLAU, 1995). Map measurements were found to be statistically similar to field measurements using a paired t-test. Adobe Photoshop was used to plot lines showing the trend of linear valleys and measure their orientation. Repeatability of measurements was found to be generally between 0.5° and 2.0°, varying with the length of the valley being measured; longer valleys could be remeasured with greater precision than short valleys. A minimum of four contours had to define a linear valley in order for it to be included in the data. The contour interval on the maps is 20

feet. The data collected from linear tributary valley orientations is shown in full by TERLAU (1995).

Data Comparisons

As stated in the hypothesis, it was expected that cave passage orientations will be distributionally similar to the orientations of nearby linear tributary valleys. This relationship was tested by comparing visual representations of the data distributions, and by using statistical techniques. Selected comparisons were made using the original data sets, combined data sets and data subsets (TERLAU, 1995).

Of the 12 scanned map sections used to measure valley orientations, 7 contained only one cave, and 5 contained multiple caves. For the cases in which there is one cave to a map section, comparisons were made between the cave data and the valley data from the corresponding map sheet. How data comparisons were made for map sections containing multiple caves was decided on a case-by-case basis (TERLAU, 1995). A program in True BASIC programming language produced rose diagrams with class intervals of 10°. The data were plotted according to frequency of occurrence in each of the classes. 20 data comparisons were performed (TERLAU, 1995).

Statistical Comparison of the Data Sets:

A Kolmogorov-Smirnov two-sided, two-sample test was used to compare the data sets. The test analyzes the amount of agreement between the distribution functions of two independent data samples to determine if the two samples were drawn from the same population (or populations with identical distributions), or were drawn from populations with different distributions. The test is non-parametric, making it useful when no assumptions can be made about the distribution of values in the population from which the samples were taken. The distributions of data used in this study are likely to be multi-modal. The K-S test can be applied to data without grouping them into classes, and also has the advantage of allowing samples of unequal size to be compared.

6. Results

Kolmogorov-Smirnov Analysis

The 20 Kolmogorov-Smirnov tests comparing cave data to valley data, led to a rejection of the null hypothesis in 4 cases. Therefore, 4 out of 20, or 20% of the tests showed the distribution of the sample values of cave passage orientations to be significantly different than those of linear valley orientations at alpha = 0.1. This implies a strong relationship between the orientations of caves and valleys in the remaining 80% of the cases. Full results of the analysis are presented by TERLAU (1995).

Rose Diagram Analysis

Rose diagrams were generated to visually represent the distribution of values in the cave and valley data sets. An attempt was made to quantify the similarity of class distributions shown in the rose diagrams (TERLAU, 1995). In 11 out of 20, or 55% of the valley roses, more than half the classes corresponded to the cave roses. In visual comparison, there were eight instances where there appeared to be a strong relationship between cave orientations and valley orientations. Although comparing data sets using rose diagrams is subjective, 40% of the cave rose diagrams exhibit large classes which correspond with valley rose diagrams. The rose diagrams generated from the combined cave data and combined valley data showed considerable scatter in the distributions. Prominent orientations did emerge from the plots of these large data sets, however. The cave passage orientations showed a peak in the distribution centered at 20° and a second overall trend centered at 95°. The valley orientations had peaks in the distribution centered at 0°, 65°, 110° and 145°. The plots of these two distributions are dissimilar which confirms results of the Kolmogorov-Smirnov analysis. The rose diagram generated from the fracture data had far less scatter than the plots of combined cave or combined valley data. Peaks in this distribution occurred at 5°, 35°, 75° and 145°. The distribution roughly correlates with plots of the combined cave data, again supporting the results of the Kolmogorov-Smirnov analysis.

7. Analysis and Conclusions

In assessing the results, it is important to consider the stress and erosional history of the study area. The bedrock in which the caves and valleys have developed has been subjected to repeated stresses resulting in fracturing. Initial fracturing may have occurred as a result of shrinkage, and orogenic events during the Paleozoic resulted in further fracturing. Caves developed prior to the Pleistocene, but valley incision by meltwater was particularly acute during the Pleistocene, and glaciation then again exerted stresses resulting in additional fracturing. Hence fractures produced by glacial stresses may have influenced linear valley formation but not prior cave formation. "When the jointing pattern present in a rock mass originates from multiple fracturing episodes, the first set of joints may be spatially less variable. Subsequent stress relief leading to new fracturing may be strongly influenced by these pre-existing fractures so that they terminate against the original joints and consequently exhibit more irregular frequencies and orientations and locations." (LAPOINTE & HUDSON, 1985). The main valleys of Richland County may have developed along fractures which were produced by orogenic stresses during the Paleozoic. In the pre-glacial drainage network, the caves may have been integrated with these stream valleys. Glacial stressing during the Pleistocene may have further fractured the rock mass producing new fracture sets which terminated against existing fractures as described by LAPOINTE & HUDSON (1985). Tributary valleys of the present day ridge-and-ravine drainage network developed having available all the fractures that were present when the caves formed, plus the new fractures produced by glacial crustal bending.

The overall agreement between cave and valley orientations when compared locally was found to be 80% based on the statistical analyses. This is a significant trend which suggests that both caves and valleys developed utilizing fractures with orientations that were locally homogeneous. While it is likely that additional fractures were available to control valley formation, the 80% overall agreement between cave and valleys orientations suggests that these additional fractures were either of a different scale than those which controlled the features observed in this study, or these new fractures paralleled existing fractures.. However, the orientations of cave passages for the entire county were found to be statistically dissimilar to the orientations of linear valleys for the entire county. This suggests that the orientations of fractures of the scale which controlled the development of cave passages and tributary valleys are locally inhomogeneous.

References

DAY, M.J. 1986a. Caves in Southwestern Wisconsin, U.S.A. Proceedings 8th International Speleological Congress, 155-157.

DAY, M.J. 1986b. Caves in the Driftless Area of Southwestern Wisconsin. The Wisconsin Geographer 2, 42-51.

DAY, M.J., REEDER, P.P., & OH, J.W. 1989. Dolostone Karst in Southwestern Wisconsin. The Wisconsin Geographer 5, 29-40.

DUTCH, S.I. 1981. Lineaments and faults of Wisconsin, Minnesota and the Western part of the Upper Peninsula of Michigan. U.S. Geological Survey Open File Report 81-977, 29pp.

EBDON, D. 1981. Statistics in Geography. Oxford, England. Basil Blackwell, 195pp.

ELLIS, B.M. 1984. Surveying a Cave. In: Caving Practice and Equipment. ed., Judson, D. David & Charles Publishers, Newton Abbot 169ff

HARDER, E.C. 1906. The joint system in the rocks of southwestern Wisconsin and its relation to the drainage network. Univ. Wis., Bull. (sci. ser. 3), No.5, 207-246.

HEYL, A.V., AGNEW, A.F., LYONS, E.F. & BEHR, C.H. 1959. The geology of the upper Mississippi Valley zinc-lead district. U.S. Geological Survey Prof. Paper 309, 310pp.

LAPOINTE, P.R. & HUDSON, J. 1985. Characterization and interpretation of rock mass joint patterns. Special Paper 199, Geological Society of America, 37pp.

LEITH, C.K. 1932. Structures of the Wisconsin and Tri-State lead and zinc deposits. Econ. Geology 27(5), 405-418.

MCGINNIS, L.D. 1968. Glacial crustal bending. G.S.A., Bull. 79(6), 769-776.

PARIZEK, R.R. 1976. On the nature and significance of fracture traces and lineaments in carbonates and other terraines. Karst Hydrology and Water Resources, Water Resources Publications, 62pp.

PETERSON, G.M. 1968. The caves of Richland County, Wisconsin. The Wisconsin Speleologist 7(3), 78-109.

TERLAU, C.A. 1995. An analysis of cave and valley orientations in Richland County, Wisconsin. MS Thesis, University of Wisconsin-Milwaukee, 162p.

TRUDGILL, S. 1985. Limestone Geomorphology. Longman, London and New York, 196pp.

WHITE, W.B. 1988. Geomorphology and Hydrology of Karst Terrains. Oxford University Press, New York and Oxford, 464pp.

Labyrinthes et Sieben Hengste

par Alex Hof
Ch. du Lazé B, CH-1806 St-Légier

Abstract

By caving in Sieben Hengste, we find many labyrinths. The author discerns any types of labyrinths and explains her genesis. Her exploration necessitates perseverance and systematic when we want understand. Good luck when you explore it.

Résumé

En explorant aux Sieben Hengste, on rencontre de nombreux labyrinthes. L'auteur différencie quelques types de labyrinthes et explique leur singulière formation. Leur exploration demande de la persévérance et de la systématique si on veut les comprendre. L'auteur encourage les spéléologues qui se lancent dans une pareille aventure.

1. Introduction

En explorant la région Sieben Hengste-Hohgant, cette zone karstique des préalpes suisses bien connue pour le grand Réseau qu'elle contient, on rajoute inlassablement des conduits dans un enchevêtrement parfois déjà complexe. La contemplation de certaines zones du plan d'ensemble souterrain donne l'impression de grands labyrinthes. En fait, comment définir un labyrinthe?

2. Définition du labyrinthe

Parmi quelques définitions du mot labyrinthe proposées par des dictionnaires, retenons en deux qui s'appliquent bien à la spéléologie:

- réseau compliqué de galeries dont on a peine à sortir;
- nchevêtrement, complication inextricable.

Le terme évocateur labyrinthe convient donc bien. Cependant, il vaut la peine d'établir quelques distinctions.

3. Les pseudo-labyrinthes

En examinant des plans, certaines zones ressemblent à de touffus labyrinthes. Par contre vu de sous-terre, on ne partage pas cette impression. On parcourt des galeries avec des carrefours espacés. On n'a pas conscience de galeries proches, mais sans connexions pénétrables. Il peut aussi s'agir de plusieurs étages sans liens directs, dont les galeries ne s'enchevêtrent que sur le plan complet par additions des différents étages.

Dans ces cas, il ne s'agit pas de véritables labyrinthes. Une conjonction de facteurs favorables à la formation de galeries provoque une concentration de conduits d'âge et de morphologie divers. Citons en particulier la tectonique, l'abaissement par étapes du niveau phréatique, la présence de plusieurs horizons imperméables, etc. Pour plus de détails on consultera HOF (1995).

Dans la région Sieben Hengste - Hohgant, les exemples de pseudo-labyrinthes sont très nombreux. Citons le cas extrême du Blatersystem, découvert sous deux étages connus dont l'un était auparavant considéré comme le niveau de base. Par endroit, l'étage du Blatersystem, pourtant pas bien épais, se subdivise en trois niveaux, dont deux séparés par moins de deux mètres de roche. Heureusement, un atroce jeune méandre jonctionne ces deux niveaux de galeries phréatiques anciennes qui se croisent. Sans lui nous aurions douté longtemps de l'exactitude de notre topographie.

Pour détecter les pseudo-labyrinthes, il faut abandonner la division par cavité selon des critères de pénétration humaine. Seuls des plans d'ensemble de toutes les cavités placées dans un même système de coordonnées révèlent toute leur étendue.

Aux Sieben Hengste, ces pseudo-labyrinthes vont encore s'étendre et s'étoffer. Au-dessus de certaines zones déjà complexes la prospection systématique n'est pas encore faite. Sous-terre l'exploration devient aussi systématique et amène des découvertes même à des endroits du plan où il n'y a plus de place pour tirer un trait.

Zone de pseudo-labyrinthe du Réseau

4. Les enchevêtrements de puits

Un seul ruisseau rencontrant une zone favorable de fractures peut déjà créer des puits parallèles par capture de plus en plus précoce. Ajoutez-y un deuxième, voire un troisième écoulement pour développer une intéressante densité de puits. Intercalez maintenant quelques couches moins solubles pas trop inclinées ou, mieux encore, des joints marneux. Ainsi vous créerez des lucarnes ou des galeries de liaisons à plusieurs niveaux. Arrosez le tout pendant de nombreux siècles d'une eau bien acide. Voilà la recette qui vous donnera un joli labyrinthe tridimensionnel.

Nous avons appliqué cette recette aux Puits Johny, mais nous ne disposions que de deux écoulements. Le nombre de puits n'est donc pas très grand. Par contre, nous avons bien réussi leurs connexions et, en soignant particulièrement la qualité de l'eau, nous avons tout-de-même obtenu deux P96, un P80, un P35 et une demi-douzaine d'autres plus petits.

Au Gouffre de la Pentcôte, nous avons traversé au plus vite un intéressant entrelac de puits. Quel courageux topographe osera se lancer à les relever systématiquement?

5. Les labyrinthes classiques

Un vrai labyrinthe se perçoit déjà sous terre. Les carrefours se suivent et se ressemblent. L'explorateur retrouve difficilement son chemin.

Plusieurs modes de formation expliquent le développement de labyrinthes. Distinguons d'abord entrre ceux creusés en régime noyé et ceux résultant d'écoulements vadoses. La première catégorie se subdivise selon la vitesse du courant et la chronologie.

5.1 Les labyrinthes locaux

Parmi les plus beaux labyrinthes, on trouve ceux creusés par un écoulement lent et noyé. Cet écoulement rencontre des fractures ou un joint interstrate proposant de nombreuses amorces pour la formation de galeries. La corrosion joue un rôle prépondérant. Souvent, il n'en résulte pas un labyrinthe, mais une grande fissure ou un large laminoir. La présence de sédiments insolubles favorise le développement du dédale en bouchant les amorces peu ouvertes et en concentrant la dissolution de la roche. Ces labyrinthes peuvent être très denses, mais restent plutôt locaux. Les divers conduits sont à peu près contemporains.

Le Réseau recèle des exemples caractéristiques basés sur un joint initiateur. Au départ, un large laminoir se creuse. Ensuite, du sable se dépose au sol et le protège de la corrosion. Celle-ci s'exerce alors au plafond, ce qui donne une série de jolis profils en forme de chapeau.

Labyrinthe local dans le Gouffre de la Pentecôte

5.2 Les labyrinthes étendus

Un écoulement noyé rapide peut aussi former un labyrinthe, mais la genèse est différente. En effet, la présence de plusieurs amorces de galeries proches ne suffit pas. Dès que l'une est exploitée et que sa section augmente, elle absorbe rapidement la grosse majorité de l'écoulement, car la résistance à l'écoulement diminue fortement. Pour qu'un labyrinthe se forme, il faut que le premier conduit fasse des détours. L'eau cherche toujours la voie de la moindre résistance. Si elle trouve de nouvelles amorces plus directes qui s'ouvrent lentement par corrosion, le cheminement plus court compense en partie la faible section. L'écoulement s'y engouffre progressivement, l'agrandit rapidement par érosion et délaisse finalement le premier conduit. La répétition de ce phénomène finit par créer un labyrinthe. Ce type de labyrinthe se distingue du précédent par son étendue plus importante et la possibilité d'établir un classement chronologique des conduits. Citons un exemple de ce type dans le Réseau: les Catacombes.

Lors de l'abaissement d'un niveau phréatique, un collecteur perd son eau, tandis qu'un nouveau se développe plus bas. Ce phénomène se déroule souvent progressivement. Des soutirages capturent l'eau de l'ancien collecteur en plusieurs endroits, avec une tendance d'évolution d'aval en amont. On voit même parfois la direction d'écoulement de certains tronçons du vieux collecteur s'inverser. Ces soutirages se rassemblent pour former le nouveau collecteur. La zone de rassemblement donne quelques fois d'intéressants labyrinthes. Les soutirages de l'AKG en constituent un bel exemple.

5.3 Les labyrinthes par écoulement gravifique

Pour obtenir un labyrinthe avec un écoulement gravifique, il faut une fracturation très favorable et des horizons moins perméables suffisament mais pas trop inclinés. Un réseau de fractures dont les directions principales sont bien différentes de la ligne de plus forte pente de l'horizon peu perméable permet un enfouissement progressif de l'écoulement par le phénomène de captures successives. On obtient dans le cas idéal une disposition des galeries en grille. L'exemple le plus connu de la région est certainement la Seefeldhöhle ou Tropfsteinhöhle.

6. Remarques sur la classification

Ce texte schématise quelques modes de formation de labyrinthes. La réalité se révèle parfois plus complexe. Un labyrinthe peut évoluer d'un type vers un autre. Des labyrinthes différents peuvent se recouper. La décomposition en phénomène de base permet de s'y retrouver et de comprendre la genèse.

7. Inconvénients et avantages des labyrinthes

L'exploration des labyrinthes demande énormément de patience et de persévérance. Ne pas s'embrouiller sous-terre n'est pas le plus difficile. Trouver un volontaire pour venir les topographier exige une grande persuasion. Quand on lit ensuite dans le regard du volontaire qui tente de repérer le résultat de son travail sur le plan d'ensemble, on comprend rapidement qu'il faut rechercher une nouvelle victime pour la prochaine fois. Sa propre motivation prend aussi de sérieux coups lors de la mise au net. La superposition de plusieurs niveaux est un casse-tête. Et qui n'a pas eu envie de se jeter par la fenêtre en tentant de figurer d'innombrables liaisons sur une coupe développée? Remarquons que, par précaution, l'auteur habite un rez-de-chaussée.

Même un spéléologue ne saurait voir tout en noir. Parfois les pseudos ou les vrais labyrinthes livrent de pratiques raccourcis. Quel plaisir quand on réussit à traverser un dédale en évitant tous les pièges. Quelle satisfaction aussi quand on commence à comprendre leur formation. On échafaude des hypothèses et on se réjouit d'aller les vérifier sur place. On devine où il faut insister pour trouver une suite. Démêler un écheveau de conduits est bien plus passionant et concret que n'importe quel jeu.

8. Conclusions

Lâchez vos casse-têtes chinois. Arrêtez de jouer aux labyrinthes sur votre ordinateur. Allez plutôt explorer les dédales aux Sieben Hengste ou ailleurs!

Référence

HOF, A. 1997. Pourquoi tant de galeries sous les Sieben Hengste? Actes du 10e congrès national de spéléologie, Breitenbach 1995; à paraître.

Classification and some morphometric features of salt caves

Amos Frumkin
Cave Research Section, Department of Geography, The Hebrew University of Jerusalem, 91905, Israel
Fax: 972-25820549 Email: msamos@pluto.mscc.huji.ac.il

Abstract

General morphologic features of salt caves are presented in numeric form and used for classification and presentation of cave types. Comparison with surface streams is attempted through the Horton Laws.

1. Introduction

Salt caves display a rather simple type of karstification, with physical dissolution of halite. Known caves are of vadose origin, with multilevel branchwork passages. Here some morphologic features of salt caves are discussed, as a basis for numeric classification that may help analyze the caves and compare them with other types of karst systems.

Salt caves are best preserved in arid environments, because under more humid conditions the entire salt outcrop tends to be dissolved. Mount Sedom salt diapir (ZAK, 1967) at the south-western edge of the Dead Sea has experienced semi-arid to hyper-arid climate during the Holocene (FRUMKIN *et al.*, 1991). Since being exposed at the Early Holocene (FRUMKIN, 1996a), salt has been dissolved by runoff collected from small catchments over a relatively insoluble caprock and captured into fissures. Vadose caves, the largest known in salt, have developed as soon as the rock salt was uplifted above the Dead Sea base level. A detailed study of subaerial catchments was performed in order to detect the caves through which the runoff is drained towards base level. An active channel along each cave carries floodwater during short intense rainfall events, lasting typically several hours each year. In spite of the short rainfall duration, downcutting of cave channels is rapid (FRUMKIN and FORD, 1995), exceeding the rising rate of the diapir and Dead Sea level fluctuations (FRUMKIN, 1996b).

2. General morphological features

Fig. 1 is a Zipf Plot showing caves with an active traversible channel longer than 10 m (cf. FORD & WILLIAMS, 1989 p.245). Each cave is represented by its active channel length (as opposed to total surveyed length which includes inactive passages), and by its rank in the channel length list. Caves exceeding 50 m in length are ordered along a straight line, indicating that the entire population of these longer caves was included in the study. The inclusion of all longer caves is also indicated by air-photo field study: large caves associated with large catchments could not have been overlooked. However, caves shorter than 50 m deviate from the straight line (Fig. 1), suggesting that some shorter caves may have been overlooked and not included in the study.

A single active salt cave stream passage is referred to as a conduit. Examining the entire length of a conduit from sink point to outlet, it consists of (some or all of) the following five morphological elements (Fig. 2): (A) stream sink; (B) sub-horizontal passage in caprock; (C) vertical shaft; (D) sub-horizontal rock salt passage; (E) open outlet.

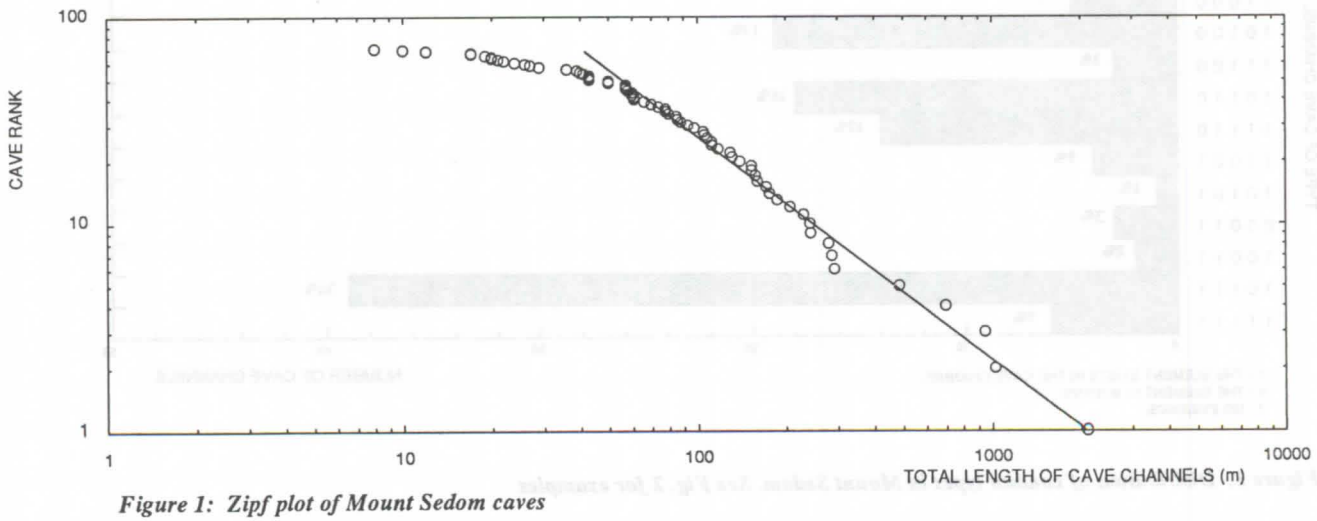

Figure 1: Zipf plot of Mount Sedom caves

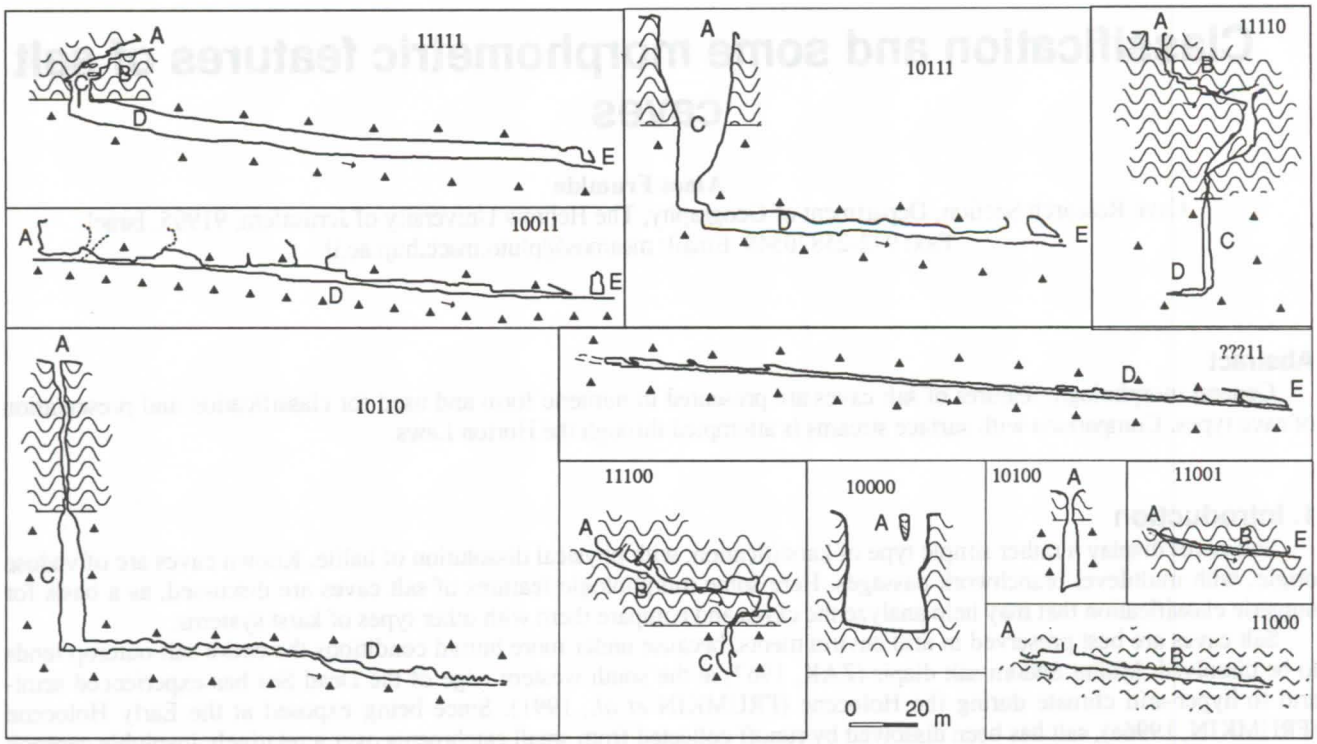

Figure 2: Examples of different types of cave conduit profiles in Mount Sedom. Black triangles indicate rock salt. Curly lines indicate caprock. The 5 digit numbers indicate the existence of the following features: (A) stream sink; (B) sub-horizontal passage in caprock; (C) vertical shaft; (D) sub-horizontal rock salt passage; (E) open outlet.

A binary system was adopted in order to classify the conduits according to the existence of the elements. Five attributes were assigned to each conduit, representing the five elements. Each attribute may receive one of the following values: 1=the morphological element exists; 0=the morphological element is missing; ?=no evidence indicating if the element exists or not; #=an attribute used only for discussion purposes in this text, for eliminating irrelevant elements (either existing or non-existing).

Examples of profiles of each conduit type are shown in Fig. 2. The distribution of the morphological types is given in Fig. 3.

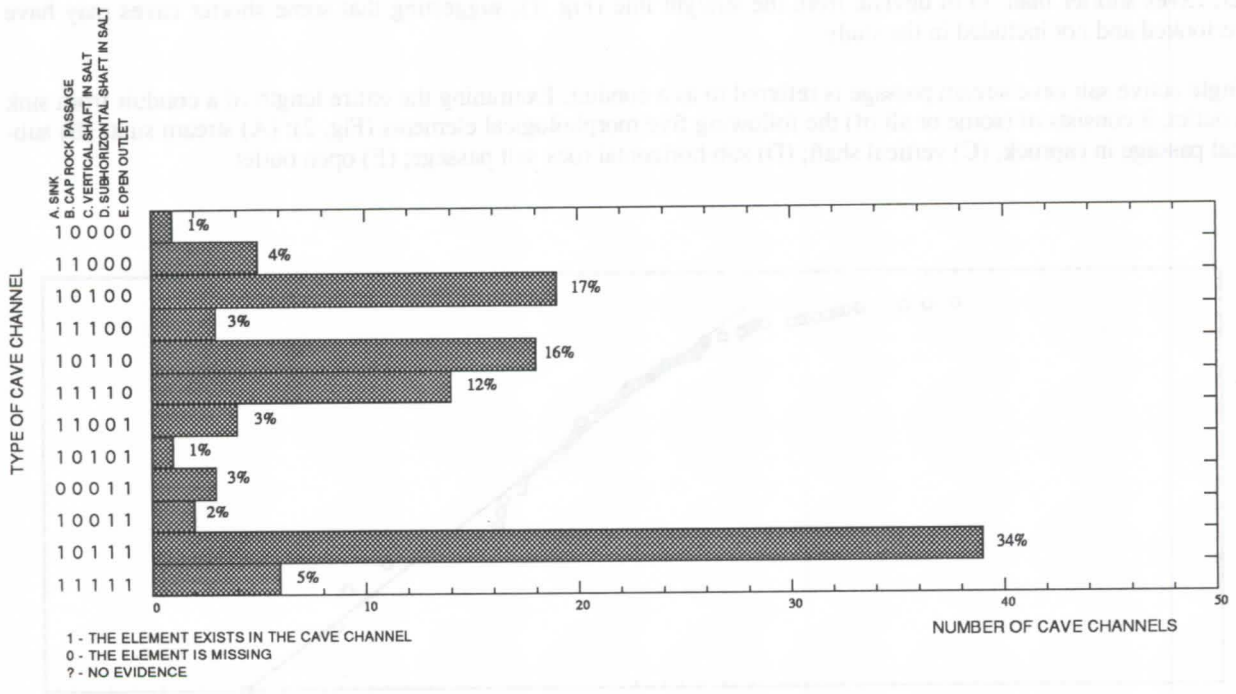

Figure 3. Distribution of conduit types in Mount Sedom. See Fig. 2 for examples

Most studied conduits (72%) include a sub-horizontal rock salt passage (###1#). The larger caves in Mount Sedom are included in this group. About a half (48%) of the studied conduits have an open outlet (####1). One third (34%) of the studied conduits consist of all morphological elements except a caprock passage (10111). One quarter (25%) of the studied caves have no salt passage and no open outlet (###00). These usually drain a small subaerial catchment, and their underground length is often limited to less than a few m. Some 28% of the conduits have developed a salt passage, but no open outlet was found (1#110). These caves, often located in the central portions of the mountain, are accessed through their sinks, and are referred to as 'inlet' caves. Inlet caves appear to terminate several m up to tens of m above the apparent water table (FRUMKIN, 1994b). Flood waters flowing into these caves partly evaporate and partly infiltrate into their alluviated floors (FRUMKIN, 1994a).

3. Horton Laws in salt caves

Some conduits join underground to form branchwork caves with several tributaries. Each tributary drains a subaerial catchment through a single active stream sink. The underground drainage system is organized in a similar way to surface drainage systems, so the HORTON (1945) stream order system may be used for the underground network, defined in the following way: a first order conduit begins at a sink where a surface stream is captured to the subsurface; two first order conduits join underground to form a second order conduit; two second order conduits join underground to form a third order conduit. A cave order equals the highest order of its conduits.

Fifty eight first order caves, eight second order caves, and one third order cave were studied. For each cave order, the following features are shown in Fig. 4: (A) number of caves; (B) mean number of tributaries per cave; (C) mean conduit length; (D) mean catchment area. All features seem to increase exponentially with cave order (straight lines on the logarithmic scale of Fig. 4). This trend is comparable with the HORTON (1945) laws for subaerial streams, in spite of structural and lithologic controls which are more dominant in caves than in subaerial streams (FORD et al., 1988).

Karst regions with a larger number of caves may yield a better evaluation of the applicability of Horton laws. The definition of stream order is more complicated in autogenic karst with many small tributaries. Autogenic cave streams may gain further recharge along their underground flow course, while the Sedom cave streams have an allogenic nature, where (almost all) discharge enters each conduit through a single input. Autogenic caves appear more likely to obey Horton Laws which were originally proposed for surface drainage with spatial contribution of precipitation. The Horton Laws certainly do not apply to maze or distributary cave systems, where different methods should be sought.

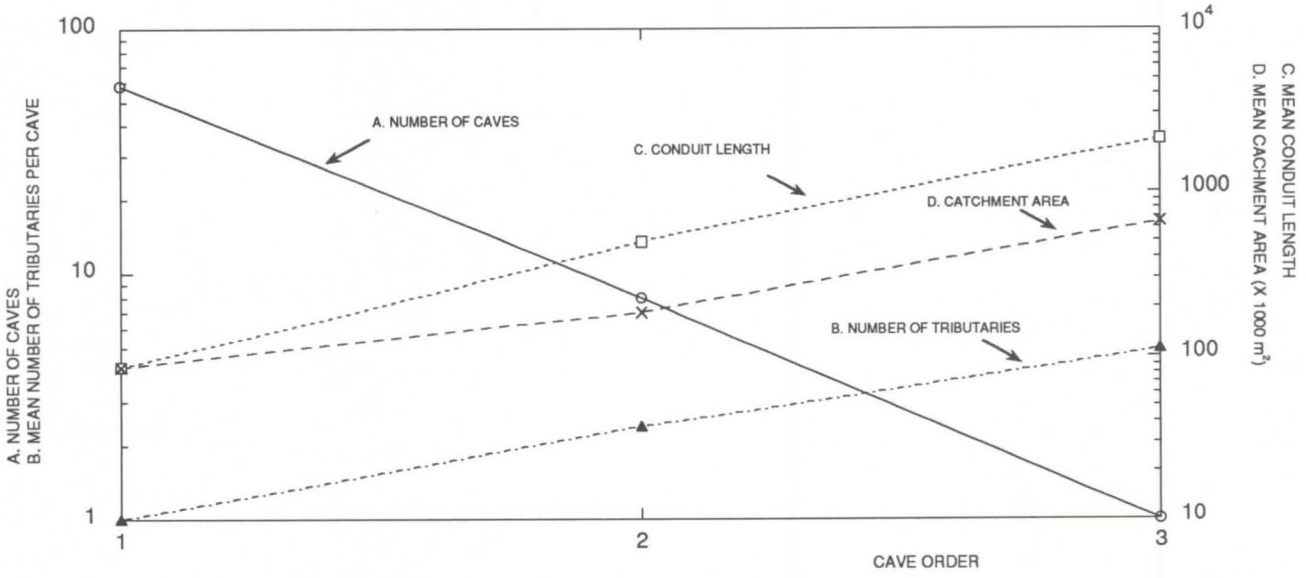

Figure 4. Morphometric features of Mount Sedom caves versus cave order

References

FORD, D. C., PALMER, A. N. & WHITE, W. B., 1988. Landform development; Karst, in: (Back, W., Rosenshein, J. S. and Seaber, P. R., eds.), The geology of North America. Geological Society of America, 401-412.

FORD, D. C. & WILLIAMS, P. W., 1989. Karst geomorphology and hydrology. Unwin Hyman, London, 601 p.

FRUMKIN, A., 1994a. Hydrology and denudation rates of halite karst. *Journal of Hydrology*, 162: 171-189.

FRUMKIN, A., 1994b. Morphology and development of salt caves. *Bulletin of the National Speleological Society*, 56 : 82-95.

FRUMKIN, A., 1996a. Determining the exposure age of a karst landscape. *Quaternary Research*, 46: 99-106.

FRUMKIN, A., 1996b. Uplift rate relative to base level of a salt diapir (Dead Sea, Israel), as indicated by cave levels, in: (Alsop, I., Blundell, D. and Davison, eds.), Salt Tectonics, Special Publication no. 100. Geological Society, London, pp. 41-47.

FRUMKIN, A. & FORD, D. C., 1995. Rapid entrenchment of stream profiles in the salt caves of Mount Sedom, Israel. *Earth Surface Processes and Landforms*, 20 : 139-152.

FRUMKIN, A., MAGARITZ, M., CARMI, I. & ZAK, I., 1991. The Holocene climatic record of the salt caves of Mount Sedom, Israel. *The Holocene*, 1 (3): 191-200.

HORTON, R. E., 1945. Erosional development of streams and their drainage basins. *Bulletin of the Geological Society of America*, 56 : 275-370.

ZAK, I., 1967. The geology of Mount Sedom. PhD (in Hebrew, English abstract), The Hebrew University, Jerusalem, 207 p.

A karstic system in a semiallochtonous gypsum unit: the Legnanone caves (Marecchia valley, Italy): preliminary geological and hydrogeological features

Daniele Farina, Gallerini Giuliano
Geoinfo, Via Marco Polo 9, 61100 Pesaro, Italy

Abstract

The Rio Strazzano basin, developed on gypsum outcrops of upper Miocenic age, shows interesting geomorphological and hydrogeological features, due to the presence of a small, yet well developed karstic system, the Legnanone caves.
The caves basically represent the underground path of the Strazzano creek, which sinks below surface in the mid -lower part of the valley, and gushes out again near the confluence with the Marecchia river. Geological, geophysical, hydrometric and hydrochemical data have been collected, in order to characterize the basic hydrogeology of the karstic system and to suggest some hypothesis on its evolution .

Geological - structural setting and geophysical informations

Rio Strazzano is a small tributary stream of the Marecchia river (Marche - Romagna regions). Its basin is characterized by a quite large outcrop of detritic" balatino" gypsum of upper Miocenic age ("Gessi" formation), underlain by a clayey formation (Casa i Gessi fm.), with lateral etheropical lenses of conglomerate, belonging to the Acquaviva formation. The latter was origined by the erosion of a carbonatic platform (S. Marino/ M. Fumaiolo fms., lower Miocene) and of the eocenic marly calcareous Flysch (M. Morello fm.). The mid - upper Miocenic sequence was formed on the large Val Marecchia allochtonous sheet represented by a highly tectonized melange-like, mostly clayey unit (Argille Scagliose s.l. / Sillano fm.) of Cretaceous - Eocenic age, including the former S. Marino and M.Morello formations. The sheet moved eastward starting from middle Miocene to lower Pliocene, forming a series of "piggy - back" sedimentary basins where the particular Rio Strazzano sequence was deposited. After the sedimentation of the Pliocenic marine clays (Argille Plioceniche fm.) topping the Gessi fm., a new major tectonic phase caused the complete imbrication of the former structures and the faulting of the relatively more rigid gypsum layer (see cross-section A-A´, taken from CONTI, 1989).

The microcristalline gypsum, derived from the erosion of primary selenitic cristals, forms massive strata (5 - 10 m thick), with local marly- bituminous intercalations (BERTOLAMI, M. ROSSI, A.,1991). The total thickness of the evaporites exceeds 60 m, gradually decreasing toward the front of the thrusted unit. This trend, detected by means of Vertical Electrical Soundings, could also outline the limits of the gypsum outcrop to the N.E. part of the Rio Strazzano watershed; besides, the geoelectrical survey showed the presence of more resistive layers inside the conductive substratum, interpreted as conglomerate lenses within the clayey Casa i Gessi formation.

Geomorphological and hydrogeological features

The Rio Strazzano basin shows interesting geomorphological and hydrogeological features, that can be summarized as follows:

- the typical asymmetrical section of the Rio Strazzano valley;
- the presence of sparse water springs gushing out the Acquaviva conglomerates and /or S. Marino - M.Fumaiolo fractured biocalcarenites in the upper part of the valley (S. Igne, Passo della Biforca sites), drained into the Rio Strazzano;
- the karstic sink situated in the mid - lower part of the valley, where the Rio Strazzano is swallowed into the Legnanone caves;
- the "dead" course of the Rio Strazzano, situated downhill the sink, which remains dry most of the year;
- a widespread system of dolinas (absorbing pits), where a large part of the precipitations is absorbed underground;
- the main entrance of the Legnanone caves, representing the resurgence of the Rio Strazzano, situated approximately 300 m uphill the confluence into the Marecchia river.

The sink of the Rio Strazzano is a narrow tunnel - like a grotto with a partially collapsed ceiling, locally comunicating with the outside. The sink occurs near a fractured and faulted zone in the mid - lower part of the valley. The "dead" course of the Rio Strazzano is characterized by a quite narrow path locally showing canyon - like features. Its bottom shows several cracks and holes, expecially on the left hydrographic side; a major sump shows seasonally fluctuating water levels. The dolinas are often aligned along major tectonic discontinuities and are normally covered with silty soil af various thickness (SOCIETÀ GEOLOGICA ITALIANA, 1992).

The Legnanone caves, which are being explored by the S. Marino Speleological Group, show at least two different levels, with the lowest one still active. The main path stretches approximately 600 m. and is characterized by frequent "pockets" of debris (boulders, sand and silt) carried by the stream inside the cave and deposited along its banks (AA.VV., 1993). Some other finer sediments seem to have penetrated from the ceiling and deposited in a cascade - like fashion at the

end of the upper level grotto. Part of the ceiling and walls are unstable and subject to rock falls. The lower level main grotto is situated 10 to 20 m above the base of the gypsum formation, underlain by the "Casa i Gessi" clays.

Hydrometric and hydrochemical data

During this preliminary study water discharge has been measured, both in the rainy and in the dry season, at both ends of the grotto. During the winter season there is no significant difference of discharge between up-hill and down-hill the cave. The yeld varies from approximately 20 l/sec. to 100 l/sec or more, right after heavy rains. During the summer base-flow the creek is almost dry (0.2 - 0.4 l /sec. up-hill, 0.1 or less at the main lower entrance). The water chemistry is of the calcium - sulphate type, with mid - salinity values (0.8 - 1.3 gr/liter) with an increasing trend during the rainy season.

Discussion

The Legnanone caves show an intimate relationship with the surface hydrology of the Strazzano creek, due to the basin's evolution during the recent Quaternary. The interpretation of all preliminary data suggests that a deep karstification of the gypsum outcrop developed as the base-level of the Marecchia - Strazzano hydrographic system kept lowering as a result of the recent uplift of the region (see the suspended alluvial terraces on the Marecchia river's bank).

The erosion of the clayey Pliocenic cover, proceeding from N-E to S-W, exposed increasing surfaces of the gypsum layer to the meteoric dissolution, causing the formation of the surficial karst forms and, particularly, the demolition of the cavities previously formed by the course of the ancient Strazzano creek: the canyon - like features of the "dead" valley , in fact, suggest that it possibly derives from the collapse of the former grottoes as linear karstification kept migrating toward the S-W.The wide fluctuation of yeld, the moderate salinity of the waters and the presence of the debris fillings inside the grotto suggest that most of the karstification process nowadays is still originated by the action of running waters.

The completion of the study should verify the formation of deeper lateral caves within the gypsum S-W- dipping monocline, topped by the Pliocenic clays. Such study should extend the use of the geoelectrical survey to model the buried geometry of the gypsum layer and should carry on extensive differential flow measurements to detect possible losses of waters seeping through major faults to a lower discharge site.

References

AA. VV. 1993. Quaderni del Circondario di Rimini n.3 - La riserva naturale di Onferno - a cura di L.Casini: 9 - 16

BERTOLAMI, M.; ROSSI, A. 1991. La petrografia della grotta di Onferno e delle aree limitrofe "Naturalia Faventina" Boll. Mus. Civ. Sc. Nat. Faenza

CONTI, S. 1989. Geologia dell'Appennino marchigiano - romagnolo tra le valli del Savio e del Foglia. Boll. Soc. Geol. It. Vol.108: 435 - 490.

SOCIETA' GEOLOGICA ITALIANA. 1992. Guide Geologiche Regionali n.4 - Appennino Tosco - Emiliano: 48 - 51, 70 - 71, 89 - 90, 295 - 298

Aknowledgement

Thanks to Stefano De Angelis for the CAD drawings.

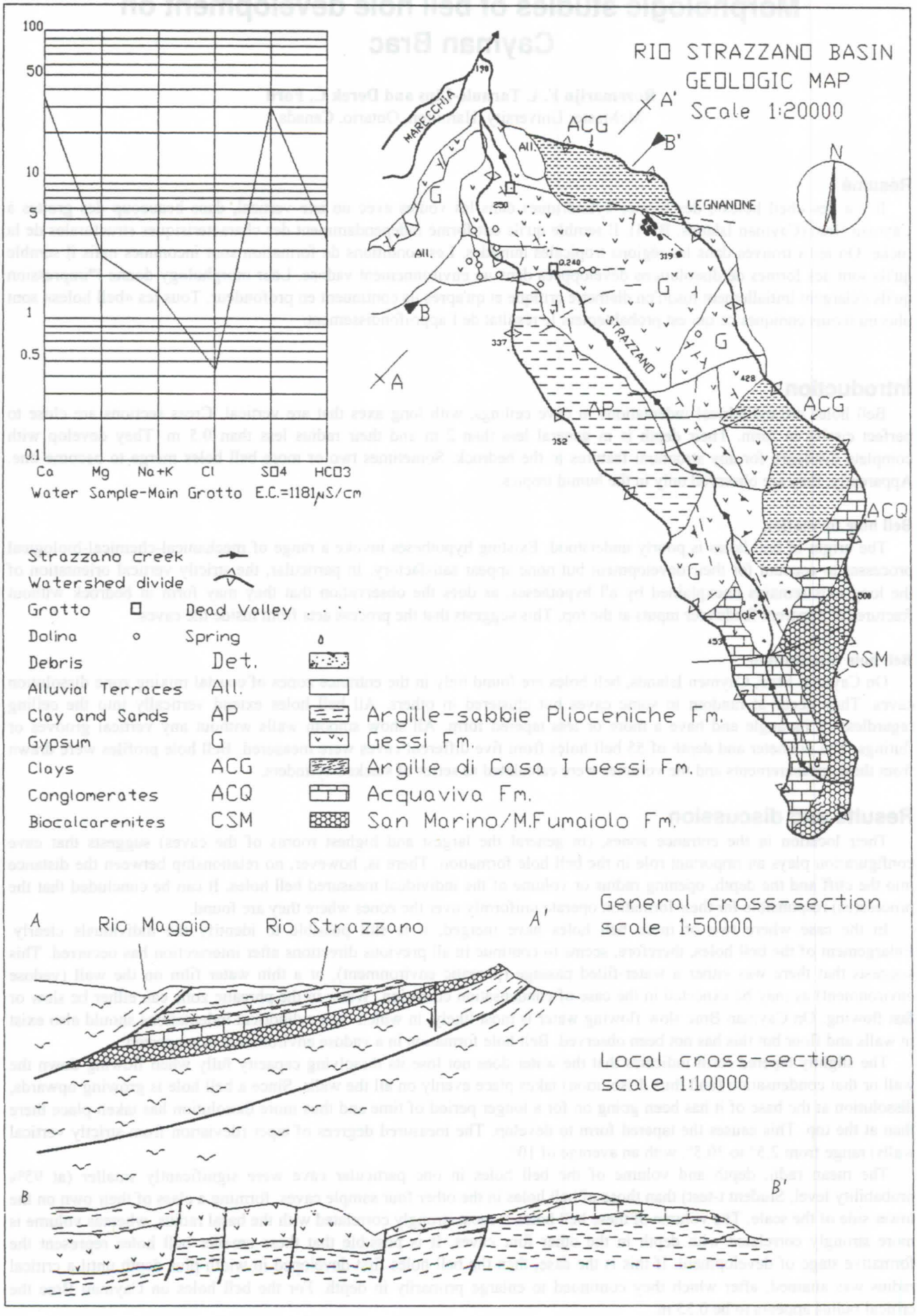
100
50
10
5
1
0.5
0.1
Ca
Mg
Na+K
Cl
SO4
HCO3
Water Sample-Main Grotto E.C.=1181 μS/cm
RIO STRAZZANO BASIN
GEOLOGIC MAP
Scale 1:20000
N
MARECCHIA
LEGNANONE
STRAZZANO
All.
G
AP
ACG
ACQ
CSM
Det.
A
A'
B
B'
Strazzano creek
Watershed divide
Grotto
Dead Valley
Dolina
Spring
Debris
Alluvial Terraces
Clay and Sands
Gypsum
Clays
Conglomerates
Biocalcarenites
Argille-sabbie Plioceniche Fm.
Gessi Fm.
Argille di Casa I Gessi Fm.
Acquaviva Fm.
San Marino/M.Fumaiolo Fm.
Rio Maggio
Rio Strazzano
General cross-section
scale 1:50000
Local cross-section
scale 1:10000

Morphologic studies of bell hole development on Cayman Brac

Rozemarijn F.A. Tarhule-Lips and Derek C. Ford
McMaster University, Hamilton, Ontario, Canada

Résumé

Il y a des «bell holes», des formes cylindriques dans les voûtes avec un axe vertical, dans beaucoup des grottes à Cayman Brac (Cayman Islands, BWI). Il semble qu'ils ont formé independamment des characterisiques structurales de la roche. On les a trouvés dans les régions tropicales humides. Les conditions de formation sont inconnues mais il semble qu'ils sont des formes de dissolutions developpées dans un environnement vadose. Leur morphology donne l'impression qu'ils s'élargent initiallement jusqu'un diametre critique et qu'aprês ils continuent en profondeur. Tous les «bell holes» sont plus ou moins coniques ce qui est probablement le résultat de l`approfondissement.

Introduction

Bell holes are cylindrical indentations in cave ceilings, with long axes that are vertical. Cross sections are close to perfect circles in form. Their depth is in general less than 2 m and their radius less than 0.5 m. They develop with complete disregard for any structural features in the bedrock. Sometimes two or more bell holes merge to become one. Apparently, they are observed only in the humid tropics.

Bell hole formation

The origin of bell holes is poorly understood. Existing hypotheses invoke a range of mechanical-chemical-biological processes to account for their development but none appear satisfactory. In particular, the strictly vertical orientation of the long axis remains unexplained by all hypotheses, as does the observation that they may form in bedrock without fractures or apparent feedwater inputs at the top. This suggests that the process acts from inside the caves.

Bell hole distribution

On Cayman Brac, Caymen Islands, bell holes are found only in the entrance zones of coastal mixing zone dissolution caves. They occur at random in some caves but clustered in others. All bell holes extend vertically into the ceiling regardless of its angle and have a more or less tapered form. All show smooth walls without any vertical grooves or flutings. The diameter and depth of 55 bell holes from five different caves were measured. Bell hole profiles were drawn from these measurements and the volumes were calculated as series of stacked cylinders.

Results and discussion

Their location in the entrance zones, (in general the largest and highest rooms of the caves) suggests that cave configuration plays an important role in the bell hole formation. There is, however, no relationship between the distance into the cliff and the depth, opening radius or volume of the individual measured bell holes. It can be concluded that the process(es) responsible for their formation operate uniformly over the zones where they are found.

In the case where two or more bell holes have merged, it is still possible to identify the individuals clearly. Enlargement of the bell holes, therefore, seems to continue in all previous directions after intersection has occurred. This suggests that there was either a water-filled passage (phreatic environment), or a thin water film on the wall (vadose environment) as may be expected in the case of condensation corrosion. Water in the phreatic zone can either be slow or fast flowing. On Cayman Brac slow flowing water is most likely, in which case cylindrical indentations should also exist in walls and floor but this has not been observed. Bell hole formation in a vadose environment is suggested.

The slightly tapered form indicates that the water does not lose its dissolving capacity fully when flowing down the wall or that condensation (and thus dissolution) takes place evenly on all the walls. Since a bell hole is growing upwards, dissolution at the base of it has been going on for a longer period of time and thus more dissolution has taken place there than at the top. This causes the tapered form to develop. The measured degrees of taper (deviation from strictly vertical walls) range from 2.5° to 30.5°, with an average of 10°.

The mean radii, depth and volume of the bell holes in one particular cave were significantly smaller (at 95% probability level, Student t-test) than those of bell holes in the other four sample caves, forming a class of their own on the lower side of the scale. The volume of these bell holes is most strongly correlated with the basal radius, whereas volume is more strongly correlated with depth in the other four caves. It is possible that these smaller bell holes represent the formative stage of development. If this is the case, then the bell holes first developed in width plus depth until a critical radius was attained, after which they continued to enlarge primarily in depth. For the bell holes on Cayman Brac the critical radius appears to be 0.35 m.

Some types of Speleogenesis and Speleohydrogeology in Dinaric Karst area (Croatia, Europe)

Prof. dr. Mladen GARASIC [1,2,3]

[1] Hrvatsko speleolosko drustvo (HSD), Nova Ves 66, HRV-10000 Zagreb, CROATIA
[2] Drustvo za istrazivanja i snimanja krskih fenomena (DISKF), Alfireviceva 13, HRV-10000 Zagreb, CROATIA
[3] Institut gradevinarstva Hrvatske (IGH), Rakusina 1, HRV-10000 Zagreb, CROATIA

Till the end the year 1996 in Croatian karst there are more than 7750 caves and pits known. They are mostly located in Dinaric karst located in the western and the southern parts of Croatia. Dinaric karst is one of the best-known typical karst area in the world. Different types of karstification processes have been observed in speleological features (caves, pits, estavelas, vruljas, ponors, etc.) of Croatia in many localities. It is most marked in the Mesozoic rocks of the carbonate facies. These rocks are mostly limestones, dolomitic limestones, lime dolomites of the Triassic, Jurassic and Cretaceous with all their varieties, from both lithologic and stratigraphic aspects. Among over 7750 speleological features that have been explored to date, about 78% are vertical structures (pits), 21% are horizontal structures (caves), while the remaining 1% are combined speleological structures. The main types of karstification processes are: gravitational karstification, inverse karstification, complex karstification, secondary and tertiary sedimentation, etc. Depending on the intensity of these processes, many special types of speleogenesis and speleohydrogeology are observed there. The results obtained by trial borings in the Adriatic karst of Croatia show that karstification processes occur even at depths of over 4 km. It should be noted that the thickness of the Mesozoic rocks found in this area amounts to 8 kilometres. In Dinaric karst area there are two pits deeper than 1000 meters; the most vertical cave in the world - Lukina jama, 1392 m in depth, and Slovacka jama, 1017 m in depth. Gravitational karstification is present in these pits located only 10 kilometres from the Adriatic Sea. Therefore, it is to be expected that speleogenesis, as a part of the process of karstification, is also very intensive in this area. According to speleogenesis, features are classified into several groups (abrasial, tectonic, erosional, corrosional, polygenetic, etc.). The process of karstification can be best observed in the subsurface where speleogenesis is one of its most intensive mode of activity. The observed regularities in speleomorphology (of the whole speleological features or of only some of their elements) undoubtedly confirm hydrogeological elements that were present (paleohydrogeology) only at a certain time of speleogenesis or are also active today. Modern hydrogeology of karst is impossible without a good knowledge of the type of speleogenesis and the degree of karstification of the areas explored.

1. Introduction

The Croatian karst is surely one of the best known "locus typicus" areas of the typical karst in the world. Subsurface forms of karst are represented, among other things, by more than 7750 speleological structures having different morphological and morphogenetic properties and hydrogeological functions (GARASIC, 1986). Therefore, it is important to become aware of comprehend the laws of speleogenesis in this very area where karstification intensity is very high as they can be applied in a large number of other karst areas in the world .

Out of a great number of speleological structures that are known in Croatia, for special research on speleogenesis in the process of karstification, 46 were selected. They are formed in rocks which differ in their litostratigraphic, tectonic and hydrogeological properties. In addition, the speleological structures selected are of different stages of speleogenesis (the initial, main and fossil stages) differing in their morphological types (simple, branched, level, knee-like and systems) and in their hydrogeological functions (springs, ponors, estavelas, percolating structures, vruljas, etc.). The classification of all the speleological structures was carried out according to the adopted categorisation (GARASIC, 1991).

The measurements of absolute neotectonic displacements in speleological structures were made over the period of between 1980 and 1996. Geomechanical properties of the rocks in which speleological structures researched into had been formed were tested in the laboratory.

All the geospeleological researches in speleological structures were carried out in co-operation with the members of the Croatian Speleological Association (CSA) and the Society for Research, Surveying and Photographing of the Karst Phenomena (DISKF) of Zagreb.

This paper deals only with speleology within the context of karst hydrogeology and the process of karstification, although the results of research lasting for several years are more comprehensive and numerous.

2. A brief survey of the past research

Almost every description of a cave or a pit includes the description of a part of speleogenesis. However, the aim of most authors or papers was not to research into speleogenesis in particular, but it was only mentioned incidentally. Therefore, only important papers that served as a basis for this paper are mentioned.

Tectogenesis of Panjkova and Muskinja cave in Kordun were written about by GARASIC (1984a), and the speleogenesis of structures in Istria was described by BOZICEVIC (1985). The morphogenetic approach and classification of speleological structures in the Croatian karst with regard to morphology and hydrogeology were dealt with by GARASIC (1986, 1991,1993). Based on a great number of speleologic structures in the Western Carpathians, BELLA (1994) showed genetic types of caves that could be partially applied in the Croatian karst. Speleogenesis of some big and small speleologic structures of Lika, Gorski kotar, Hrvatsko Zagorje and Istria was treated by MALEZ (1966), while the structures of the Krka National Park was researched into by Lukic. The neotectonic approach was given and the measuring of absolute displacements was made by GARASIC (1981, 1984b, 1989).

Special researches on a role of the karstification process in speleogenesis were done in 58 caverns on the route of the Karlovac - Rijeka highway, viz. on the sections from Ostrovica to Kupjak and in tunnels Hrasten, Tuhobic, Vrata, Sljeme, Sopac, and Vrsek in Gorski kotar .

3. General forms of speleogenesis in Croatian karst

In speleogenesis there are three basic and a few special stages of the formation of speleological structures. The basic stages are the following:

1. Early (initial) stage (Phase I);
2. Main stage (Phase II); and
3. Late (fossil) stage (Phase III).

In the Croatian karst all three stages of development have been observed. The ratio of the main stage and the late stage is about 3:1 (according to the number of structures). The early (initial) stage of development of the speleological structures is present in every place where karstification is underway, but due to the narrowness (small width) of fissures and initial joints, the direct observation of this stage of the formation of speleological structures is not possible.

Based on the results of researches and analyses of a large number of caves and pits, it can be concluded that in Croatia most of them have not gone through all three development stages yet. This can be explained primarily by geological, hydrogeological and climatic factors; for example the structures located in high mountain-ranges have not by the process of gravitational karstification yet "reached" the less permeable or impermeable rock base. A very fine example is found in several very deep pits in Biokovo (the area surrounding Lokvica and Ladena) that do not retain water in lakes or siphons even at depths bellow 500 meters, but water flows away deeper down through narrow fissures or sumps (Skolska pit, Vilimova pit, Pit on Kamenita Vrata, etc.).

A very special example is a deep pit Lukina jama, in Mt. Velebit in which a permanent ground water flow appears as deep as under 1200 meters (BOZIC, 1995). The depth of this pit is 1392 meters, which is the proof of high intensity and deep karstification. Neotectonic and hydrogeological researches into this pit are underway, and it is expected that important results will be obtained.

3.1 Tectospeleogenese

A predisposition to **tectonic** displacements of the areas in which speleological structures develop is crucial for speleogenesis. (HERAK, 1984; GARASIC, 1984,a). For example, it has been observed that karstification in horizontal or slightly inclined layers progresses more slowly than in steep or vertical layers. Such a process can be monitored in Volarica pit (vertical and very steep layers) and in Kojina pit (horizontal layers) which is a few meters away from Volarica pit. It is a question of Senonian limestones K_2^3, of the same thickness and composition. In Volarica Pit, karstification is quick (more intensive) and consequently speleogenesis has reached the depth of 118 meters, and cave channels (chambers) are bigger; in Kojina jama, after the vertical entrance to the structure follows the horizontal extension of the structure of about 60 meters in depth and about 750 meters in width. In places of Kojina jama in which vertical layers are present again, karstification is more intensive and reaches deeper (105 meters). Volarica pit and Kojina pit are located in the region of Kordun, near a small town of Furjan, on Masvina Hill near Rakovica. Even more interesting conclusions can be made from the results of systematic research into all caverns in the tunnels on the route of the Karlovac - Rijeka highway, where intensities of karstification, and morphological and hydrological data have been monitored and compared regularly. In some tunnels tectonics played a crucial role in speleogenesis. Similar results were obtained in localities in Mt. Dinara and Mt. Velebit (Hajducki kukovi, Lomska duliba).

The largest number of speleological features in the main stage of development (Phase II) was registered in the near vicinity of karst poljes and uvalas. These structures have, even today, a role of periodic or continuous springs, ponors, or estavelas, and the presence of water in them has a very important role in this stage of speleogenesis. In this paper only some less known caves along margins of the karst fields are given (GARASIC & CVIJANOVIC, 1986). These are the following: Vranova cave (Pisacusa, Lika), Bunjakova cave (Debelo brdo, Korenica, Lika), Vrsina cave near Ondic (Lika), Duman cave (Canak, Lika), Cave near Krcevine (Smiljan, Lika), Ostrovica cave (Licki Osik, Lika), Cave in Plesa (Dreznica, Gorski kotar), Crnacka cave (Jezerane, Lika), etc.

In the Croatian karst there are less than 3% of speleological structures that were formed by tectogenesis, i.e. without a significant influence of ground water. They are located in high mountains, such as Velebit and Dinara (Mala cave near Tulove grede on Mt. Velebit, Jama near Plazonica, Unista on Mt. Dinara). They are present on the top of anticlines where water had, in later stage, a minor role in speleogenesis. Examples of such structures are narrow tectonic pits, such as for example Cirova pit on Zavizan (Velebit), which is as deep as 69 meters, but very narrow. These are mostly structures developed in solid and massive dolomites.

3.2 Hydrospeleogenese

Hydrospeleogenesis is always a complex process in which water has a decisive role. In Croatia there are as much as 4% of structures formed by an **abrasive** effect of water along coasts and river and lake banks. The largest number of abrasion structures are found in breccia-like materials (about 71%), but they also occur quite often in limestones (about 25%). The main characteristic of the structures developed by abrasion process that played the predominant role is as follows as a rule they are always horizontal or very slightly inclined; they are small in size; their rocks are smooth; etc. They are also called abries or semi-caves. There are recent abrasion structures and paleo-abrasion speleologicical structures. Some speleologicical features along the Adriatic Sea, today submerged by the sea, were developed by abrasion between 100000 and 300000 years ago (MALEZ, 1966; MALEZ & BOZICEVIC, 1965), which means that they are relatively younger of more recent origin. There is no doubt that they had developed in our area even before Quartenary, but they collapsed (Phase III of speleogenesis) because it was the question of the rocks of relatively low strength and carrying capacity. When, in addition to that, chemical reactions occurred due to the effect of sea water, the process of collapsing was still more intensive. However, there are some examples of abrasion caves that are much older (Palaeogene, Neogene), e.g. near Nerezisce on the island of Brac. Here are some examples of the abrasion caves: Crvena cave on the Island of Murter (Jezera), Cave at Ivan Dolac (the island of Hvar), Strasna pec cave (Savar, the island of Dugi otok), Raca spilja (the island of Lastovo), Modra spilja (the island of Bisevo), Przinova polaca cave (the island of Sipun), Popovska cave (Baska, the island of Krk), etc.

Erosion and corrosion effects (mechanical speleogenesis and chemical speleogenesis) occur together in the forming of speleological structures (BÖGLI, 1964). In the Croatian karst, about 93% of the structures developed, to a varying extent, by the influence of erosion and corrosion has been registered so far. In some structures, cave scallops have been also noticed, which indicates the intensive process of subsurface karstification. The examples are: Pit under Debela glava (Blagaj, Kordun), Bozica pit (Masvina, Kordun), Ponor on Grgin brijeg (Jadovno, Velebit), Stanina pit (Moravice, Gorski kotar), Podublog pit (Krnica, Istria), etc. In some caves and pits some other forms of the erosion and corrosion effects of water in the cave channels have been developed as well. The examples of erosion pots in Veternica (Medvednica, Zagreb), Dulin ponor cave (Ogulin, Korski kotar), Medvedica cave (Ogulin, Gorski kotar), Jopiceva cave (Brebornica, Kordun) or the polished rocks in Novokracina cave (Rupa, Istria), Ponor at Bunjevac (Velebit), Cave near Pavlinovici (Zupa, Vrgorac) clearly demonstrate the intensity of chemical or mechanical effects. A good example of an abrasion structure is Cavle cave in the canyon of the Zrmanja river.

Limestones of different textures and ages react differently on erosion and corrosion on the ground surface; thus it can be presumed that the situation is similar in the subsurface.

In addition to all the above mentioned factors, in the Phase II of speleology a neotectonic activity is very important too; namely, it has been noticed that tectonics is still active in some speleological features even today. Measurements show that rock movements in the speleological structures located in neotectonic zones can be significant, for example in a big cave system of Muskinja and

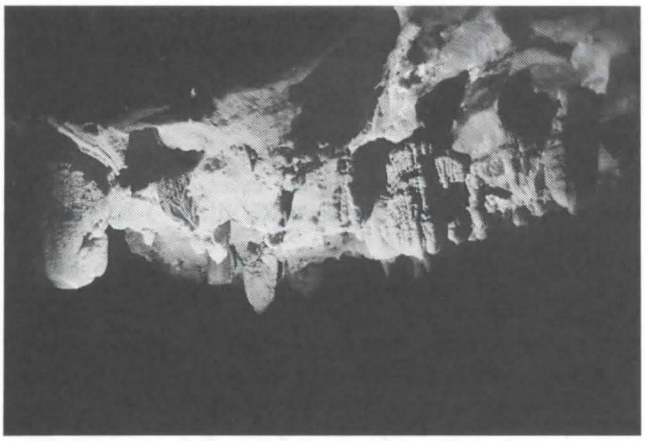

Fig 1. - Relictes in Inverse karstification (photo: dr..M. Garasic)

Pankova cave in Kordun, or in the pit Ledenica in Lomska duliba (Velebit).

Morphogenesis of speleological features in the Croatian karst is closely connected with lithostratigraphic and tectonic factors of surroundings in which they are formed, and with abrasion, erosion and corrosion effects of water as well. The neotectonic activity has even more favourable effect on karstification of the ground, and it also accelerates this process.

Morphology, length, depth, orientation, inclination and other characteristics of a cave or a pit depend on the factors of speleogenesis. In Cretaceous limestones of the Central and Inner karst zones, according to hydrogeologic karst zoning (HERAK, BAHUN & MAGDALENIC, 1969), speleological feature of the so-called polygenetic type were developed, i.e. the ones developed by the primary effects of tectonics, abrasion, erosion and corrosion. The examples are: Mijatova pit at Matesko selo in Kordun (GARASIC, 1976), Upper Cerovacka cave at Gracac in Lika, Gospodska cave near the source of the Cetina river in Dalmatia. In the Outer (Adriatic) karst belt along the coast, abrasion together with tectonics is crucial for speleogenesis, e.g. Borina cave (the island of Prvic) Pit near Jajce (the island of Zirje), Banova Ljut cave(Dubrovnik), Vela cave (Vela Luka, the island of Korcula). The Adriatic islands and the mountains by the Adriatic are most effected by erosion and corrosion, along with intensive tectonics. In terms of morphogenesis, Jurassic limestones and lime dolomites are carriers of speleogenesis accompanied by intensive tectonics and by the strong influence of erosion and corrosion. The examples are: Livnjak pit (Jasenak, Gorski kotar), Pit on Kozica (Zrnici, Gorski kotar), Janusinka pit (Dreznica, Gorski kotar), Briscinka (Biokovo), Radekina pit (Bijele stijene, Gorski kotar), Samara pit (Samarske stijene, Gorski kotar). It is in Jurassic limestones that the most interesting forms of corrosion in subsurface have been observed. Karstification have been monitored in tunnels (Gorski kotar), in fissures and caverns of all possible sizes. Measurements of the intensity of karstification in the rocks of tunnels are proportional also to the strength of speleogenesis in the same lithostratigraphic surroundings. Paleogen sediments were, in terms of speleogenesis, exposed to the influence of tectonics, abrasion, erosion and corrosion to an equal degree. The examples of big subsurface hollows in the area of Crnopac (Gracac, Lika) in which the intensity of karstification is very high , or of Golubinka Pit (Posedarje, Ravni kotari) in which a fossil phase of speleogenesis (Phase III) occurs in a part of it are very interesting.

The monitoring and measuring of the neotectonic activities in caves and pits helped a following conclusion to be made, in areas of the relative ascending of blocks (e.g. Pit on Jatarina, North Velebit) cave channels get relatively deeper (karstification is more intensive), while in the areas of neotectonic descending (e.g. Crno vrelo near Kordunski Ljeskovac in Kordun) channels are constantly filled with water, and the effect of corrosion becomes dominant.

4. Karstification processes

Karstification processes in the speleological features of the Croatian karst progress in two basic directions. The first, and more frequent, gravitationally towards the deeper layers, and the second, relatively less frequent, inversely, i.e. towards the surface. The examples of inverse karstification have been found in Istria (MAUCCI, 1952; BOZICEVIC, 1985), but also in the areas of Kordun, Lika, and Gorski kotar.

4.1 Gravitational karstification

Gravitational or surface karstification is always influenced by gravitational water, i.e. precipitation. It is very easily observed. It is very well developed in Jurassic and Cretaceous carbonate sediments. Tectonic fracturing is favourable for its development.

4.2 Inverse karstification

Inverse karstification is observable only in the subsurface and results from hydrogeologicical conditions (changes in the level of ground water, its constant presence in the subsurface during the Phase I and Phase II of speleogenesis, etc.), lithostratigraphic factors (it is frequent in soluble strata, in **Promina and Jelar** lime breccias sediments, in fine grains breccias, etc.), and neotectonic ascending of blocks. In the zones of neotectonic ascending it is unfailingly present, and its intensity is proportional to the intensity of ascending. In the zones of air cushions, on the ceilings of caves, a strong effect of inverse karstification has been noticed (Figure 1); for example Rudnica cave (Kamenica, Kordun), Vrelo cave (Fuzine, Gorski kotar). The intensity of the inverse karstification compared to the gravitational karstification is less dependent on tectonic fracture, and more on special hydrogeological conditions (GARASIC, 1993).

4.3 Ccomplex karstification

In the Croatian karst yet another karstification process, the so-called complex karstification (GARASIC, 1995) has been found too. This is the process which also requires, in addition to the conditions mentioned above, special conditions in speleogenesis that will influence the morphology of speleologicical features. These conditions are, for example, a smaller depth to the impermeable bedding in karst (the area of Kordun, Gorski kotar, etc.), the occurrence of lenses of various rocks within carbonate complexes - such as cherts within limestones or flysh materials between a carbonate series, etc. (the regions of Istria, Mt. Velebit, Mt. Mosor, etc.). For these reasons there are also formed speleological features where karstification has been developed in various directions (Figure 2), for example close to flysh or cherts or close to watertight bedding. In these cases such speleological structures suddenly change the morphological type, inclination, and shape of cave channels (pits become caves, and caves become pits; narrow channels become wide, and wide channels become completely narrow; etc.).

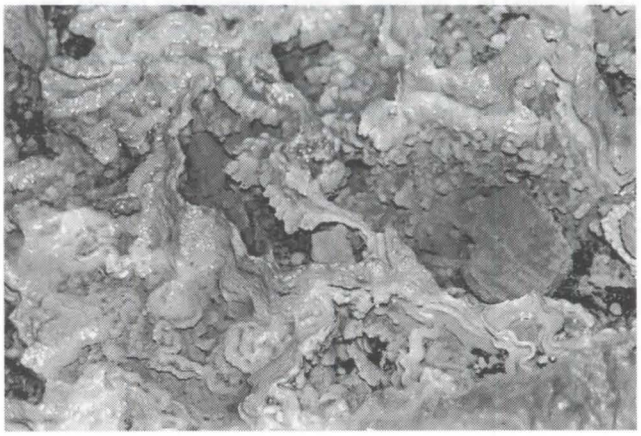

Fig.2.-Results of Complex karstification (photo: dr.M. Garasic)

5. Classification of caves and pits according to speleogenesis

Speleological features in Croatia can be classified in several groups. Basically there are **sinspeleogenetic** and **epispeleogenetic** features. The sinspeleogenetic features have been developed during the formation of matrices. There are not very frequent. They are formed by travertine barriers and falls on karst rivers and lakes (on Plitvice Lakes, by the Krka river, etc.). The epispeleogenetic features were developed by the effects of various processes in rock karstification, such as abrasion, erosion, corrosion, collapsing, tectonics, etc. Most often it is the question of **polyspeleogenetic** features. Nevertheless, only some types of caves and pits (epispeleogenetic) differing by genesis will be mentioned in these paper. These types are the following: **corrosional; corrosional and collapsing; fluvio karstic; fluvio karstic and collapsing; fluvio karstic, corrosional and collapsing; tectonic (faulted), fluvio karstic (fluvial) and collapsing; tectonic and corrosional; tectonic, corrosional and collapsing; erosional; erosional and corrosional; erosional and fluvio karstic; sedimentic; abrasial; cryogenic** (only a few structures), **vulcanogenic** (only one structure in Croatia), structures formed by the influence of plants from the ground surface, etc. A classification in phreatic structures and vadose structures, etc. has been also made.

6. Conclusion

Based on a great number of the speleological structures explored in the Croatian karst (more than 7750), their documentation, speleological surveying, hydrogeological observations and neotectonic measurements of absolute displacements in them, conclusions about the modes and types of speleogenesis, which is a part of a complex process of karstification, have been made. The influence of tectonics (initial joints, fissures, faults, folds, layers, nappes, etc.) together with litostratigraphic, hydrogeologic and climatic conditions have developed speleogenesis in several types of karstification. Gravitational or surface karstification is most frequent (above 80%); next in frequency is inverse karstification (about 19%); and complex karstification is identifiable (about 1%) too. Inverse and complex karstification can be studied into exclusively in the underground channels and chambers. Special attention has been given to researches into the karstification process in 46 caves and pits, and caverns in tunnels (Gorski kotar). In term of speleogenesis, caves and pits in Croatia can be classified into two basic groups - sinspeleogenetic and epispeleogenetic structures. Sinspeleogenetic structures were developed during the formation of matrix rocks, and epispeleogenetic structures were developed by subsequent processes of tectonics, abrasion, erosion, corrosion, collapsing, sedimentation, etc. Vulcanogenic structures have been classified separately as they do not belong to the karst area.

It can be concluded that a great number of speleological structures in the Croatian karst has different types of speleogenesis, which resulted in a diversity in speleomorphology (simple, knee-like, level, branched structures and systems) in the present stage of speleogenesis (Phase I, II or III), and in hydrogeological function of caves and pits (ponors - sinkholes, springs, estavelas, vruljas, percolating caves, and dry features).

Further researches into speleogenesis will result in new knowledge of the most intensive today's geological process - karstification.

References

BELLA, P.(1994): Genetic types caves spaces the West Carpathians. Slovensky kras, vol.XXXII, pp. 3-20, Liptovski Mikulasi.

BÖGLI, A. (1964): Die Kalkkorrosion, das zentrale Problem der Verkarstung. Steir. Beitr. Hydrogeol., vol.64, pp. 75-90, Graz.

BOZICEVIC, S. (1985): Morfogeneza speleoloskih pojava Istre i njihova zavisnost o geoloskim i hidrogeoloskim uvjetima. Disertacija, str. 1-166, Sveuciliste u Zagrebu.

BOZIC, V. (1995): L'expedition speleologique "Lukina jama 94". Regards, Bulletin de l'Union Belge de Speleologie, no 20, pp.2-6, Liege.

GARASIC, M. (1981): Neotectonics in Some of the Speleological Objects in Yugoslavia. Proceedings of 8 th International Congress of Speleology, Bowling Green, str. 148-149, fot. 3, sl. 1, USA.

GARASIC, M. (1986): Hidrogeologija i morfogeneza speleoloskih objekata s vodom u krsu Hrvatske. Disertacija. Zajednicki studij geologije PM i RGN fakulteta Sveucilista u Zagrebu, str. 1-155, sl. 53, Zagreb.

GARASIC, M. & CVIJANOVIC, D. (1986): Speleological phenomena and seismic activity in Dinaric karst area in Yugoslavia. 9. Congresso International de Espeleologia. Communicacions Barcelona, vol. 1, str. 94-97, fot. 2, sl. 8, Barcelona. Espagna.

GARASIC, M. (1989): New conception of the morphogenesis and hydrogeology of the speleological objects in karst area in Croatia (Yugoslavia). 10. International Congress of Speleology, Procceedings, vol. 1, str. 234-236, sl. 8, Budapest, Hungary.

GARASIC, M. (1991): Morphological and Hydrogeological Classification of Speleological structures (Caves and Pits) in the Croatian Karst area. Geoloski vjesnik, vol. 44, str. 289-300, fot. 3, sl. 4, Zagreb.

GARASIC, M. (1993): The Karstification processes and Hydrogeological features of the Mesozoic rocks in the Karst of Croatia (Europe). Proceedings of the XI International Congress of Speleology XI International Congress of Speleology, pp. 1-4, Beijing, China.

HERAK, M.(1984): Tektonski okvir speleogeneze. Deveti jug. speleo. kong., Karlovac, str. 111-130, Zagreb.

HERAK, M., BAHUN, S. & MAGDALENIC, A. (1969): Pozitivni i negativni utjecaju na razvoj krsa u Hrvatskoj. Krs Jugoslavije, vol. 6, str. 45-78, JAZU, Zagreb.

MALEZ, M. & BOZICEVIC, S. (1965): The Medvjedja pecina (Bear Cave) on Losinj Island, a rare Case of Submerged Cave. Problems of the Speleological Research, pp. 211-216, Prague.

MAUCCI, W. (1952): L' ipotesi dell "Erosione inversa. Bolletino dellea Societa Adriatico di Scienze Naturali, vol. XLVI, Trieste.

Origin and Development of Caves in the Devonian Massive Limestones of the Rheinisches Schiefergebirge (Germany)

by Stefan Niggemann
Institut für Geologie, Ruhr-Universität Bochum, Universitätsstr. 150, D-44780 Bochum, Germany

Abstract

Several hundred caves are located in the massive, Middle Devonian limestones of the Sauerland, Eifel and Westerwald. Twenty seven of these caves reach 500 m in length, and two of them reach even 5000 m. The Grünerbach Valley (Iserlohn, Sauerland) serves as a model of the progressive development of cave levels. The Rheinisches Schiefergebirge has been subject of continued elevation since the Pliocene, with valley entrenchments and formation of river terraces predominantly controlled by climatic factors. Interglacial phases of stagnation resulted in the development of horizontal cave tunnels extending over 2 km. The indirect correlation of cave levels with the river terraces enables determination of the minimum age of the caves and the estimation of their real age, which is believed to be some 400,000 to 500,000 years.

Zusammenfassung

Mitteldevonische Massenkalke enthalten im Sauerland, der Eifel und dem Westerwald mehrere hundert Höhlen. Insgesamt sind 27 Groß- und zwei Riesenhöhlen bekannt. Am Beispiel des Grünerbachtales (Iserlohn, Sauerland) wird die schrittweise Entwicklung übereinanderliegender Gangsysteme dargestellt. Im Zuge der seit dem Jungtertiär anhaltenden Hebung des Rheinischen Schiefergebirges kam es zur klimagesteuerten Eintiefung der Täler und Bildung von Flußterrassen. Stagnationsphasen während der Warmzeiten führten zur Herausbildung von horizontalen Tunnelgängen, die sich 2 km lang über mehrere Höhlensysteme verfolgen lassen. Eine indirekte Korrelation von Höhlenniveaus und Flußterrassen erlaubt eine Bestimmung des Mindest- und Abschätzung des Bildungsalters der Höhlen auf etwa 400.000 bis 500.000 Jahre.

1. Introduction

Devonian massive limestones of the Rheinisches Schiefergebirge contain some of Germany's biggest cave-systems. Twenty-seven of these caves reach 500 m in length, and two of them reach even 5000 m. Striking of these massive limestones is WSW/ENE following the Schiefergebirge's folding structure. Valleys of allogenic rivers cut up these small karstic areas. The cave systems with a maximum horizontal range of 400 m are characterized by high gallery density and distinctive gallery levels. This article presents a preliminary study of speleogenesis and cave development based on detailed research in recently discovered caves of the Schiefergebirge and literature information.

2. Evolution of the landscape

In the study area the origin of caves is closely connected with the Neogene to Pleistocene history of the landscape. Depression areas of massive limestones are mostly intercalated with siliciclastic rock series.

A peneplain with 20 to 50 m thick tropic weathering layers encompassed the Schiefergebirge in the Paleogen. A climatic change beginning in the Oligocene led to the selective deepening of the limestone areas within the peneplain. These depressions were used by rivers as discharge conduits (indicated by gravel deposits; SCHMIDT, 1975). The corrosive deepening of the limestone surface and formation of a "Karstrandebene" was the result of thorough wetting below the valley flat (MORELL, 1993).

In the Miocene/Pliocene the elevation of the Schiefergebirge set in with beginning erosion of weathering layers that were sometimes preserved in dolines, karstic pockets, etc. The cyclic climatic changes and continuous elevation caused valley formation in the Pleistocene. There is a simple succession of terracing and linear valley cutting (SCHREINER, 1992): 1) Interglacial stagnation without substantial erosion and only little accumulation. 2) Early glacial erosion with maximum valley entrenchment. 3) Full glacial deposition because the resulting gravel detritus cannot be transported any more.

Table 1 shows the river terraces and their supposed chronological range for the Ruhr and the tributary rivers of the Northern Rheinisches Schiefergebirge.

3. Examined caves

Detailed mapping and research have been performed in caves of the Iserlohner Kalksenke ("limestone depression"). In a 3 km long section of the Grünerbach Valley there are known 16 km of cave galleries of which the Dechen-, Knitter-, Hüttenbläserschacht-, B7- and Bunker-Emst caves comprise some 13 km. Comprehensive treatises of this karstic area can be found by HAMMERSCHMIDT et al. (1995) and NIGGEMANN (1995). The biggest cave system of the Hönne Valley (Friedrich Cave, 1300 m length, and Feldhof Cave, 200 m) is in Balve (KOLARIK & HAMMERSCHMIDT, 1987).

With a total estimated length of 7 km the Attendorner Tropfsteinhöhle (Atta Cave) in the Bigge Valley (50 km S' of Iserlohn) is the biggest cave of the Rheinisches Schiefergebirge (HAMMERSCHMIDT, 1995).

Series	Pleistocene classification	Terrace	Height above valley flat [m]
Holo-cene	Postglacial	River marsh soil	1-2
	Weichsel-glac.	Lower terrace	-4 m (below flat)
Late Pleist.	Eem-Interglac.	----	----
	Saale-Glacial		
	Warthe-Stade	----	----
	Main-Interst.	----	----
Middle Pleist.	Drenthe-Stade	Low. Middle-Terr.	8-13
	Holstein-Interglac.	----	----
	Elster-Glacial	High. Middle-Terr.	17-23
Early Pleist.	Cromer-Complex	Low. Main-Terr.	32-40
		High. Main-Terr.	43-53
Earliest Pleist.	Menap-Complex - Tegelen-Complex	Drüfel-Terrace	63-74

Table 1: Classification of river terraces (Lenne River) after VON KAMP (1972) and correlation with the chronology of Ruhr river terraces of the geological map 4510 Witten (JANSEN, 1980).

4. Morphology and sedimentology

The cave galleries mostly follow NNW/SSE striking transverse joints or WSW/ENE striking joints of bedding. Deviations arise in the case of gently dipping folding structures. At least two levels of main galleries (fossil "collecteurs") can be distinguished even in different cave systems of the same area. The tubular main galleries are considerably filled with clastic loose sediments, so the original volume is mostly unknown. Galleries of one level also show similar morphological and sedimentological features. All morphological indications (corrosive forms like anastomoses, dissolution pockets, etc.) prove a phreatic origin of caves by corrosion.

Different generations of speleothems can be distinguished in the upper cave level situated 20 to 30 m above the valley flat: An old generation includes bulky, big and often brown coloured speleothems with a rough, warty or nodular surface. The recent, mostly active speleothems are often white coloured, fragile and have a smooth surface. Stalactites, in particular, show transitions. Speleothems of the lower cave level (5 to 10 m above the valley flat) are totally part of the young generation.

The qualitative and quantitative abundance of speleothems in the upper cave level indicate a long growth period and thus a higher maximum age of speleothems (and of cave galleries) than in the lower level. HENNIG (1979) reported maximum speleothem ages of 285,000 to 340,000 years ($^{230}Th/^{234}U$ method) for the Schledde Cave in Iserlohn belonging to the upper level. In the Dechenhöhle for the same level HAUSMANN (1986) determined maximum Th/U ages of 244,000 (+83,000, -45,500) years. HOMANN (1979) mentioned maximum ^{14}C ages of 9,035 (± 175) years from Knitterhöhle belonging mainly to the lower level. Speleothems from the lower level are smaller and less widespread, explaining the muddy character of the galleries (muddy level).

In the caves from the Grünerbach Valley granulometrical and mineralogical composition of the cave clay is similar. It could be shown that the origin of the cave clay is polygenetic (Tertiary fluvial deposits, Pliocene to early Pleistocene terra fusca, Pleistocene loess, gravels and slope wash alluvium). Bones of *Stephanorhinus kirchbergensis, Ursus spelaeus,* etc. are evidential of the Pleistocene age of cave clay, a fact that is also supported by a high content of silt material derived from loess. On the Pleistocene surface a mixing of different clastic sediments seems to have occurred, which were brought in the caves by sinking rivers and/or by sliding at valley slopes.

The sedimentary and morphological research mentioned above only refers to the Grünerbach Valley caves but a similar trend can be seen in other caves (e.g. Friedrich Cave, Atta Cave and caves near Warstein). A differentiation between an upper and a lower level seems to exist in many caves of the Schiefergebirge.

5. Origin and development of the caves

The direction of cave galleries follows the parting plane system just as the hydraulic gradient. There is no evidence for any stratigraphical or facial control of cave development.

Due to low hydraulic gradients the extended genesis of main galleries could not begin before the Drüfel terrace level which is thought to be some 500,000 to 700,000 years old. Both cave levels are indirectly related to younger river terraces (upper level - lower main terrace; lower level - lower middle terrace). The accumulation of terraces took place in late glacial phases. Stagnation (no considerable accumulation or downcutting) has characterized the following interglacial phase. Stagnation phases concerning constant heights of aquifer surfaces are essential for the developing of horizontal cave passages with big gallery cross sections (PALMER, 1987). So these main galleries have developed in such long, stagnant interglacial phases by slowly streaming karstic ground water that was and still is flowing towards the bigger rivers (e.g. Lenne, Bigge) below the surface. Figure 1 shows the development of caves situated in the Grünerbach Valley. The phreatic development of meter-sized tubular cave galleries can only last 10,000 years after the initial phase (DREYBRODT, 1990).

The relief of the groundwater table is determined by the resistance of fluid flow which is low for high density of parting planes. This is demonstrated by the four-state-model (FORD & EWERS, 1978). State 1 is represented by a high resistance of fluid flow, whereas state 4 stands for low resistance (water table caves). Most caves of the Schiefergebirge belong to state 3 or 4 as can be recognized by high parting plane density and existence of cave levels. The development of caves took place in the epiphreatic zone. The vadose flowing of these water table caves occurred in a late stage because of decreasing water quantity or decreasing resistance of fluid flow as a result of increasing gallery cross sections.

The 4-phases-epiphreatic model of DAVIES (1960) can help to illustrate the cave development. 1) Deep phreatic random origin of solution pipes, pockets, etc. caused by local groundwater flow-conditions. 2) Merging and mature development of these solution structures along the epiphreatic zone during a stagnant head of the groundwater which is referred to river terraces. 3) Partial filling of caves by clastic sediments within the phreatic zone. 4) Draining of the cave caused by valley downcutting; speleothem genesis; destruction of the cave by breakdown processes.

Due to the lack of datable terrace sediments outside the caves, an absolute chronological classification of cave development phases is difficult. However, figure 2 shows first results. The lower cave level belongs to the Drenthe stadial lower middle

terrace and is of Eemian age, which is based on sinter datations with maximum holocene ages (HOMANN, 1979). Also, there is no proof for Warthe stadial river terraces. The upper cave level which is correlated to the lower main terrace of Cromer age developed in a younger interglacial period of the Cromer complex because speleothems of Holstein age are found within the galleries. The active level of the Knitterhöhle comprising a small undergound brook marks the actual water table and is correlated to the lower terrace of Weichselian age. So cave development continues under Holocene conditions.

The bulky character of speleothems within the upper cave level is caused by stronger quantities of precipitation within the Holstein and Eem interglacials which therefore increase the growth rate of speleothems. Distinctive speleothem forms like disques or cave blisters originated by capillary water were found only in the upper level. Obviously and for the same reason the hydrostatic pressure on flat sinter formations (walls, ceiling) was higher than today. This pressure is thought to control the growth of capillary sinter. Furthermore, higher dripping rates in the cave cause larger quantities of aerosol water. This is represented by many occurences of subaerial corralloids and rough surfaces of sinter formations in the upper cave level.

In the northern Rheinisches Schiefergebirge, the beginning of extended horizontal cave level development can be appointed to 400,000 to 500,000 years. Certainly, the real beginning of speleogenesis (random deep phreatic solution pockets) can be older. DREYBRODT (1990) has calculated ages between 0.4 and 2.5 million years for different karstic systems of the Schwäbische Alb. The results of this study are in agreement with other German karstic areas.

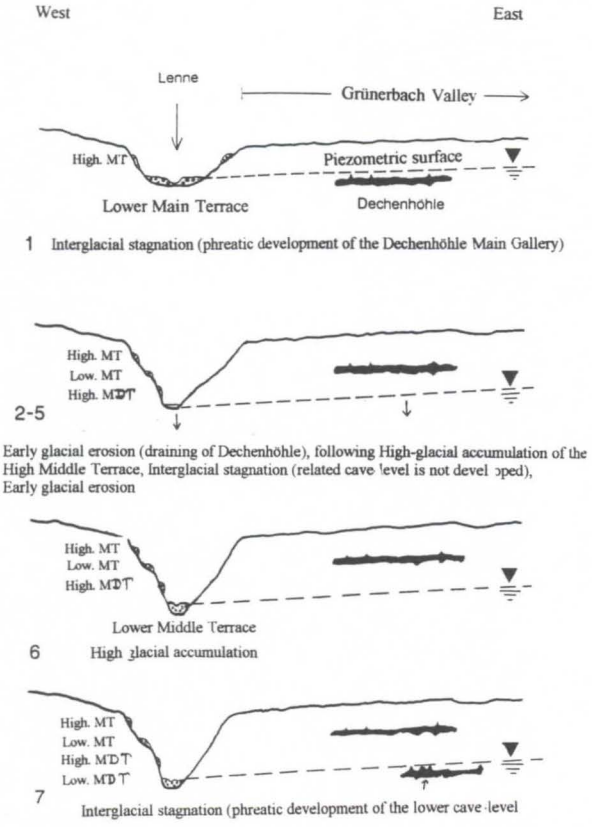

Fig. 1: Model representing the development of cave levels and river terraces in the Grünerbach Valley.

Acknowledgement

This study is part of a thesis realized at the Institute of geology at the Ruhr University Bochum. I wish to thank Prof. Richter and Dr. Brix for instruction and discussion. Furthermore, I thank all members of the Speläogruppe Letmathe, especially Elmar Hammerschmidt, for practical support in the caves.

References

DAVIES, W.E. 1960. Origin of caves in folded limestone. *NSS Bull.*, 22: 5-18.

DREYBRODT, W. 1990. Ein Modell der Entwicklung von Karst unter Berücksichtigung der Lösungskinetik auf Kalkstein: Anwendung auf die Verkarstung in der Schwäbischen Alb. *Laichinger Höhlenfreund*, 25 (2): 47-83.

FORD, D.C. & EWERS, R.O. 1978. The development of limestone cave systems in the dimensions of length and breadth. *Can. J. Earth Sci.*, 15: 1783-1798.

HAMMERSCHMIDT, E. 1996. Die neuen Teile der Attendorner Tropfsteinhöhle. In: (Ahrweiler, R.): Die Höhlen der Attendorn-Elsper Doppelmulde. *Karst u. Höhle*, 1991/92: 29-36.

HAMMERSCHMIDT, E., NIGGEMANN, S., GREBE, W., OELZE, R., BRIX, M.R. & RICHTER, D.K. 1995: Höhlen in Iserlohn. *Schriften z. Karst- und Höhlenk. in Westf.*, 1: 154 S.

HAUSMANN, R. 1986. Allgemeiner Kommentar zu den Ergebnissen der Uran- und Thorium-Isotopenanalysen. Unveröff. Manuskript; Köln.

HENNIG, G. 1979. Beiträge zur Th-230/U-234-Altersbestimmung von Höhlensintern sowie ein Vergleich der erzielten Ergebnisse mit denen anderer Absolutdatierungsmethoden. Diss. Univ. Köln: 171 S.

HOMANN, W. 1979. Zum Wachstum holozäner Großstalagmiten in der Knitterhöhle bei Letmathe/Sauerland und zur Methodik der Sinter-Probenentnahme durch Kernbohrungen. *Dortmunder Beitr. z. Landeskunde*. 13: 45-63.

JANSEN, F. 1980. Geologische Karte von Nordrhein-Westfalen 1:25.000. Erläuterungen zu Blatt 4510 Witten: 176 S.

KOLARIK, T. & HAMMERSCHMIDT, E. 1987. Die Friedrichshöhle im Hönnetal. *Mitt. u. Ber. Speläogr. Letmathe*, 4 (2): 26-31.

MORELL, U. 1993. Das Massenkalkgebiet der Hönne - eine Karstlandschaft. *Antiberg*, 52/53: 66 S.

NIGGEMANN, S. 1995. Geologische Kartierung der Dechenhöhle und ihrer Umgebung im Massenkalk bei Iserlohn. Diplom-Kartierung Ruhr-Universität Bochum: 128 S. (unveröff.)

PALMER, A.N. 1987. Cave levels and their interpretation. *NSS Bull.*, 49: 50-66.

SCHMIDT, K.H. 1975. Geomorphologische Untersuchungen in Karstgebieten des Bergisch-Sauerländischen Gebirges. *Bochumer Geogr. Arb.*, 22: 156 S.

SCHREINER, A. 1992. Einführung in die Quartärgeologie. Schweizerbart'sche Verlagsbuchhandlung, Stuttgart: 257 S.

VON KAMP, H. 1972. Geologische Karte von Nordrhein-Westfalen 1:25.000. Erläuterungen zu Blatt 4611 Hohenlimburg: 182 S.

WINOGRAD, I.J., COPLEN, T.B., LANDWEHR, J.M., RIGGS, A.C., LUDWIG, K.R., Szabo, B.J., Kolesar, P.T. & Revesz, K.M. 1992. Continous 500,000-year climate record from vein calcite in Devils Hole, Nevada. *Science*, 258: 255-260.

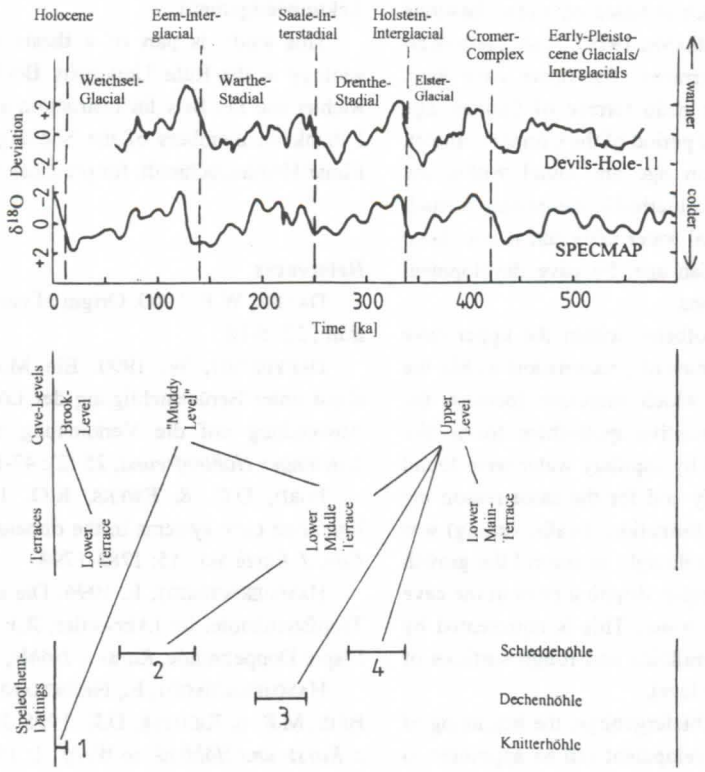

Fig. 2: Dated sediments, cave levels and chronological position of caves in the Grünerbach Valley (Pleistocene climate record after WINOGRAD et al., 1992). 1= Slim, active and mostly white speleothems with smooth surfaces. 2-4= Bulky, big and often brown-coloured speleothems with rough, warty or nodular surfaces.

Mechanics of cave breakdown: Relative importance of shear strength and fracture toughness

Elizabeth L. White and William B. White
Environmental Resources Research Institute and Department of Geosciences
The Pennsylvania State University, University Park, PA 16802 USA

Zusammenfassung

Einsturz einer Höhlendecke ist ein Problem von Brechmechanismen. Vorhandene Modelle für Einstürze sind auf der Theorie von festen und überhängenden Balken begründet, mit der Schubkraft des Daches als hauptsächlicher Parameter. Die Entstehung von gewölbten Dachprofilen vergrössert die mechanische Stärke. Breite (20-25 m), flache Decken in den Höhlen der Isla de Mona (Puerto Rico) ist grösser als die Stabilitätsgrenzen, die auf zerbrechlichen Modellen begründet sind. Man muss die Brech-zähe in Bilanz nehmen neben der Schubkraft, um angemessener weise die Stabilität der Höhlendecken zu modellieren.

Abstract

Breakdown of cave roofs is essentially a problem in fracture mechanics. Existing models for breakdown are based on the theory of fixed and cantilever beams with the shear strength of the roof rock as the material parameter. Development of arched roof profiles increases the overall mechanical strength. Wide (20 - 25 m), flat ceilings in the caves of Isla de Mona (Puerto Rico) exceed stability limits based on the brittle fracture model. It is necessary to take account of the fracture toughness in addition to shear strength in order to adequately model the stability of cave ceilings.

The Breakdown Problem

The detailed mechanics of roof failure are based on a model proposed by DAVIES (1951) who treated breakdown as a process of brittle fracture of either fixed or cantilever beams. The analysis was simply a balance between the gravitational load and the shear strength of the bedrock leading to a very simple equation for cave roof stability

$$t_c = \rho\lambda^2/2S \qquad t_c = 3\rho\lambda^2/2S \qquad [1]$$

Fixed Beam Cantilever Beam

where tc is the critical thickness for beam instability, ρ = density of bedrock, λ = beam length (equivalent to width of passage), and S = flexural stress in the extreme fiber. In this model, cave passages would be stable against breakdown until geological processes modified the parameters in the equations [1] and produced conditions of instability. WHITE and WHITE (1969) identified seven geological processes that would destabilize cave passages and produce breakdown.

Evidence Against the Fixed Beam Model

The fixed beam model implies a completely elastic response of the ceiling beds. It does not allow for inelastic deformation and long term creep that could lead to bed failure in the absence of any geologic changes. In the Mammoth Cave System (Kentucky, USA) there have been three documented roof failures in the present Century. As part of their investigation of breakdown in the 1960s WHITE and WHITE (1969) prepared a high precision topographic map of a plastically-deformed sagging bed in Pohl Avenue in the Unknown Cave portion of the System. That bed collapsed in the 1970s. Clearly, creep and plastic deformation play a role in breakdown collapse.

There are also examples of cave ceilings that are stable when the fixed beam model predicts they should be unstable. The best examples known to the authors are the caves of Isla de Mona, a 6-km diameter limestone island located between Puerto Rico and the Dominican Republic. The Isla de Mona caves are characterized by wide chambers, typically 1 - 5 m high but as much as 20 - 25 m wide. The ceilings are typically flat, often punctured by skylights, and rarely having a domal shape to provide mechanical stability. Yet breakdown in these chambers is relatively sparse. These chambers would not be mechanically stable according to the fixed beam model.

Fracture Mechanics Modeling of Cave Breakdown

The basis for a more comprehensive model was proposed by THARP (1995). Materials break through a mechanism of crack propagation. Microcracking, which allows for inelastic deformation and features within the material that inhibit crack propagation, can greatly increase the resistance to fracture. In addition to the shear strength, a critical parameter is the fracture toughness, K1c.

The Paleozoic limestones which contain most of the caves of Eastern United States are dense, fine-grained rock. Coarse fracturing occurs as joints and bedding plane partings, but within the rock mass there is little to inhibit crack propagation and these rocks are subject to brittle fracture. It is for this reason that the fixed beam model has worked so well. However, microcracking is possible leading to creep and ultimate failure as in the Mammoth Cave examples.

The Miocene limestones of Isla de Mona have never been deeply buried. They are porous, and contain an interconnected arrangement of small vugs. Propagating cracks are blocked by the vugs and pore spaces. Although the Isla de Mona rocks are softer than the Paleozoic limestones, they have a much higher toughness. As a result, the Isla de Mona cave chambers are stable with greater roof spans than would be expected from the fixed beam model

References

DAVIES, W. E. 1951. Mechanics of cavern breakdown. National Speleol. Soc. Bull. 13: 36-43.

THARP, T. M. 1995. Design against collapse of karst caverns. In (B.F. Beck, ed.): Karst Geohazards. A.A. Balkema, Rotterdam: 397-406.

WHITE, E. L. & W. B. WHITE. 1969. Process of cavern breakdown. National Speleol. Soc. Bull. 31: 83-96.

Phreatic Channels in Velika dolina Collapse Doline (Skocjanske jame Caves, Slovenia)

Martin Knez
Institute for Karst Research ZRC SAZU, SI-6230 Postojna, Slovenia

Abstract

Collapse doline might be an efficient spot to observe and to study phreatic channels. Question, which I wanted to answer during the research was originated from collapse doline *Velika dolina* which represents one of biggest collapses in Skocjanske jame Cave system. After visual observation one can easily notice that underground karstification do not appear displaced in disorder in rocky walls but is gathered along small number of bedding-planes which author calls *main* bedding-planes (Figs. 1, 2).

Because similar evidences noticed some other researchers in Slovene karst region, too (SUSTERSIC, 1994), there raised a suspicion: Is it possible to find in this facts widder lawfulness and where are the roots for it.

Main working method was microscoping over 300 thin-sections and there done over 10.000 mesurements presented in numeric form.

We did not find the concordance between the inception reasons (for instance "trans-bedding contrast", low grade of organic substances in the rock, reduction environment in the sediment, the influence of strong acids, others) and the actual state in Velika Dolina collapse doline (EWERS, 1966; RAUCH & WHITE, 1970; FORD & EWERS, 1978; WORTHINGTON, 1991; LOWE, 1992). Primary phreatic channels are concentrated along only three "formative" bedding-planes among 62 observed; less than along 5% of all bedding-planes (KNEZ, 1996). This concordance cannot be only apparent. But, it was clearly evidenced that the inception, although the rock was very pure, was concentrated on few bedding-planes only.

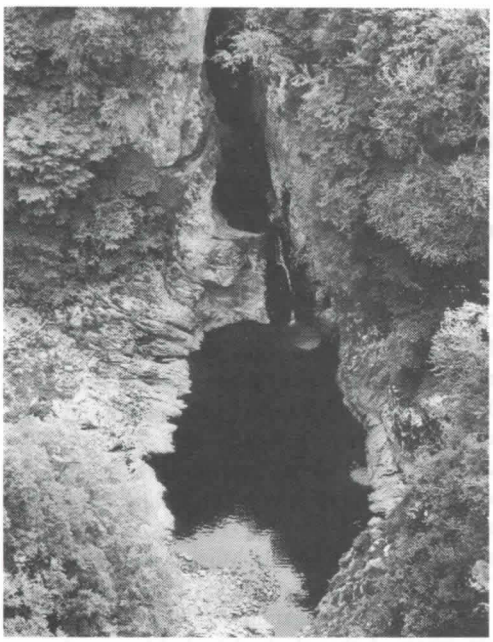

Figure 1. View of Velika dolina collapse doline (Skocjanske jame Caves).

Figure 2. Bedding-planes in Velika dolina collapse doline.

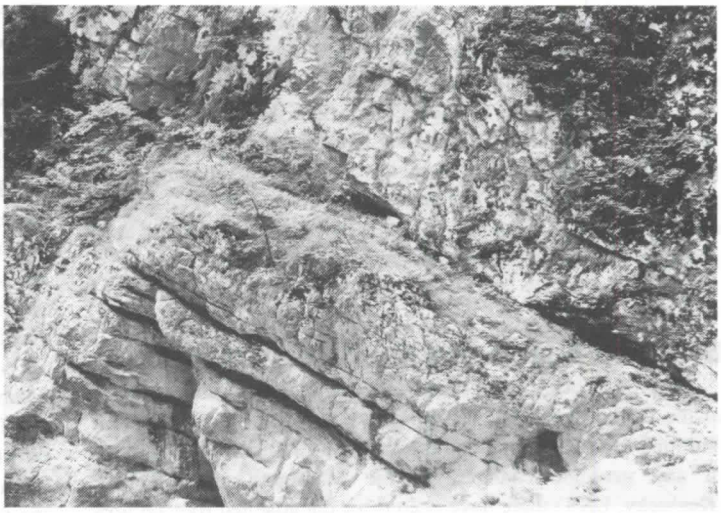

References

EWERS, R. O. 1966. Bedding-plane Anastomoses and Their Relation to Cavern Passages. Bull. Nat. Spel. Soc., 28, 3, 133-140, Arlington.

FORD, D. C. & EWERS, R. O. 1978. The development of limestone cave systems in the dimensions of lenght and depth. Canadian Journal of Earth Sciences, 15, 11, 1783-1798.

KNEZ, M. 1996. Vpliv lezik na razvoj kraskih jam. (Primer Velike doline, Skocjanske jame). Znanstvenoraziskovalni center SAZU, 14, 186 str., Ljubljana.

LOWE, D. J. 1992. The origin of limestone caverns: an inception horizon hypotesis. Unpublished PhD thesis, XIX+512 str., Manchester Polytechnic, Manchester.

RAUCH, H. W. & WHITE, W. B. 1970. Lithologic Controls on the Development of Solution Porosity in Carbonate Aquifers. Water Resources Research, 6, 4, 1175-1192, Pennsylvania State University, Pennsylvania.

SUSTERSIC, F., 1994, Jama Kloka in začetje. Nase jame, 36, 9-30, Ljubljana.

WORTHINGTON, S. R. H. 1991. Karst hydrogeology of Canadian Rocky Mountains. Unpublished PhD thesis, XVII + 227 str., McMaster University Hamilton, Hamilton.

Artesian speleogenetic setting

Alexander Klimchouk
Institute of Geological Sciences, National Academy of Sciences, P.O.Box 224/8, Kiev-30, 252030, Ukraine

Abstract

The traditional paradigm of karstology is based largely on the concepts of unconfined or "open" karst. Widely accepted definitions of the term "karst" have a largely geomorphological meaning, and formally have left no space for deep-seated artesian karst that is not manifested at the surface. Here the problem of artesian speleogenesis is overviewed and a new approach is developed based on the non-classical concept of artesian flow. Major features of artesian speleogenetic settings and artesian cave systems are summarised. Artesian speleogenetic settings have a number of peculiarities that distinguish them from traditionally defined phreatic conditions in unconfined karst. The questions of hydrodynamics, dissolution mechanisms, development of conduit systems, cave morphology, and sediments.

1. Introduction: Artesian karst-a conceptual problem

The origin of the term ***karst*** and the history of karstological studies led to karst being most commonly treated as a specific ***landscape or terrain,*** with distinctive hydrology and landforms (e.g. JENNINGS, 1985; WHITE, 1988; FORD & WILLIAMS, 1989). Most karst/speleogenetic theories are concerned with unconfined karst settings and ultimately imply close hydrological and morphogenetic relationships between the surface and subsurface. Strictly, such definitions, and the whole traditional karst paradigm, either ignore deep-seated karst that has no apparent relationship with the visible landscape, or treat such features as palaeokarst. Some authors distinguish the special category of ***intrastratal karst,*** formed within already buried rocks, where karstification is younger than the cover (QUINLAN, 1978; PALMER & PALMER, 1989; BOSAK, FORD & GLAZEK, 1989). The latter authors emphasise that there is abundant modern (active) intrastratal karstification in progress. Confined, or artesian, karst falls within this category, but the whole concept of intra-stratal karst, as well as of artesian karst, does not seem to be an essential part of the traditional karstological paradigm.

A term "karst" is also used to describe particular landforms and subsurface features produced by a specific set of processes in which dissolution is the main one, initiating or triggering other processes such as erosion, collapse and subsidence, (QUINLAN, 1978; MILANOVIC, 1981; BONACCI, 1987; JAMES & CHOQUETTE, 1988). This allows reference to deep-seated dissolution features as karst, but does not resolve the general conceptual problem.

A wider approach, long accepted in the Soviet Union, was that karst was regarded as a process, or a combination of process and resulting phenomena. In western literature, Huntoon (1995) discussed a need for a process-oriented definition of karst that emphasizes its hydrological function and geohydrological uniqueness, rather then its ambiguous morphological character. Karst is defined as a geological environment containing soluble rocks, with a permeability structure dominated by interconnected conduits dissolved from the host rock, organised to facilitate fluid circulation in a downgradient direction, and wherein the permeability structure evolved as a consequence of dissolution by the fluid (p.343). This definition, which is sufficiently broad to encompass circulation systems in the unsaturated zone, as well as in unconfined and confined aquifer system, is adopted here.

Specific works on artesian speleogenesis are scarce. FORD (1988) distinguished artesian caves as a type, referring to maze examples. However, the common view is that "true" artesian conditions, with lateral basinal flow from distant recharge areas through separated aquifers, offer limited hydrodynamic and chemical potential for speleogenesis. Examples of karst in deep-seated artesian settings are commonly treated as palaeokarst.

Adoption of the non-classical concept of hydrodynamics of artesian basins, which implies hydraulic continuity in basins and close cross-formation communication between aquifers, has allowed new conceptual models concerning artesian speleogenesis to originate during the last decade. Further development of these ideas allows abundant provings of deep-seated intra-stratal karst occurring under present artesian conditions, to be treated as a modern (active) phenomenon.

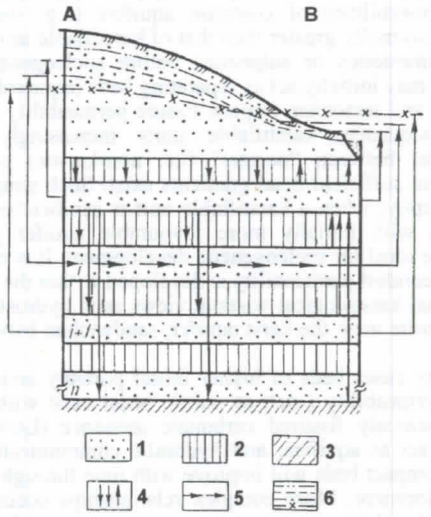

Figure 1: Flow pattern in the multi-storey artesian system (From Shestopalov, 1989). 1 = aquifers, 2-3 = aquitards, 4-5 = flow directions, 6 = potentiometric surfaces of aquifers. A = area of descending circulation, and B = area of ascending circulation.

2. Concepts of artesian flow

The classic concept of artesian flow implies that recharge occurs only on limited areas where aquifers crop out at the surface (usually at basin margins) and that groundwater flows laterally through separate aquifers in the confined area. This brings about a major problem in interpreting artesian speleogenesis. With a large distance and travel time through a karst unit, water should not be capable of further dissolution in the confined flow area. The origin of maze caves is most commonly attributed to artesian settings, but strong arguments developed from hydrodynamic (PALMER, 1975) and kinetic (PALMER, 1991) considerations questioned the possibility of maze caves origin if lateral artesian flow is implied through a karst rock unit. There is a common view that "true" artesian conditions (in the sense of the classical concept) offer limited hydrodynamic and chemical potential for karstification. Numerous existing provings of karst cavernosity in deep-seated artesian settings are commonly treated as palaeokarst.

The new approach to the problem is based upon non-classical concepts of artesian basin hydrodynamics, developed within mainstream hydrogeology in recent decades from aquifer and well hydraulics data (on a local scale), and from basin hydraulics and water resources evaluations (on a regional scale). Hydraulic continuity in basins and close cross-formational communication between aquifers are implied (e.g. MJATIEV, 1947; SHESTOPALOV, 1981, 1989; TOTH, 1995; figure 1). According to these views, recharge to, and discharge from, a given aquifer (or vertical groundwater exchange in a system) may take place across dividing beds throughout the whole confined flow area. It is controlled by the head relationships in a system (which are, in turn, controlled to a significant degree by surface topography; figure 2) and by the presence of areas (zones) of enhanced permeability in dividing beds (facial "windows", zones of enhanced fissuring, fault zones, etc.). The most important speleogenetic implication of this concept is that a karst rock unit can receive

areally dispersed aggressive recharge from adjacent formations (KLIMCHOUK, 1994).

Adoption of the non-classical concept of artesian basin hydrodynamics allowed new speleogenetic interpretations to emerge. It provides an explanation of the artesian origin of some of the world's largest cave systems, in South Dakota and in the Western Ukraine (FORD, 1989; KLIMCHOUK, 1990, 1992, 1994), and suggests some approach to the problem (KLIMCHOUK, 1994).

3. Major features of artesian speleogenetic settings

Hydrogeological structure

In a typical basin, aquifers are separated from each other and from any upper unconfined aquifer by poorely permeabile beds. Initial permeabilities of common aquifers (e.g. some clastic rocks) are normally greater then that of karstifiable units (such as massive limestones or sulphates) before speleogenesis. Thus, karst units may initially act as separating beds (aquitards). As late diagenesis and tectonism impose fissure permeability on a sedimentary sequence, karstifiable units increasingly transmit groundwater between "normal" (i.e. non-karstic) aquifers in zones where sufficient head gradients exist. Such simplified hydrostratigraphy, when a karstifiable unit is sandwiched between formations with initially more favourable aquifer properties, seems to be ideal for speleogenetic development. It is noteworthy that when conduit permeability is developed within the karst unit, conventional karstological wisdom views such hydrostratigraphy in the opposite way: the karst aquifer, sandwiched between aquitards.

In many cases beds of higher initial porosity and relatively diffused permeability (such as oolitic beds) exist within a massive and scarcely fissured carbonate sequence (LOWE, 1992). They will act as aquifers, and hydraulic communication across dividing compact beds will improve with time through speleogenetic development. More complex relationships occur in thick, lithologically inhomogeneous sequences, composed, for instance, of intercalated carbonate, sulphate and clastic beds with contrasting permeabilities. In artesian settings the inversion of hydrogeological functions of different beds in a sequence during the speleogenetic evolution of karstifiable beds is quite common (KLIMCHOUK, 1992, 1994; LOWE, 1992). This reflects the generally underestimated fact that karst permeability changes through time, while the permeability of non-karstic beds is a relatively static property.

On the local scale, the actual flow paths through a karstifiable unit are strongly guided by the initial fissure configuration.

Regional and local hydrodynamics

Artesian basins vary considerably in size, configuration and hydrogeological structure. Regions with substantial local topography and a stratified sedimentary cover (such as high-relief platforms and foreland basins) are characterised by complex flow architecture. Besides marginal recharge areas and lateral flow components, this architecture includes: laterally alternating recharge and discharge areas (areas of correspondingly descending and ascending cross communication) occurring through the whole region of confined flow; superimposition of recharge-discharge regimes for particular aquifers in a system, and flow systems at different scales (SHESTOPALOV, 1981, 1989; TOTH, 1995).

Groundwater circulation in a basin tends to adjust to configurations of maximum and minimum fluid potentials. The latter may be due to compression, compaction, dilatation, thermal effects, chemical processes, etc, although hydraulic head gradients become the increasingly prevailing driving force once the subsidence trend of tectonic movement has had reversed. In a typical basin, stratigraphically lower (older) aquiferous formations crop out at successively higher elevations along the basin margins, imposing greater heads.Hence, the regional flow system is normally characterised by an increase in head with depth, so that ascending cross-formational communication predominates through the confined flow area. However, local topographic highs superimpose local flow patterns (recharge/ descending communication), encompassing mainly the upper part of the hydrogeological sequence. Ascending cross-formational hydraulic communication is the most common pattern to favour speleogenesis in artesian settings (figure 2).

In the interior parts of a basin, lateral circulation in an aquifer is normally slow. Communication across confining beds occurs even more slowly, commonly measurable only on the time-scales of centuries or millennia. However, considering the geologically lengthy time-scales of basinal development, such movement may account for initiation of proto-conduits, or for speleo-inception in the context described by LOWE (1992). Conduit development occurs later, when uplift and geomorphic differentiation cause substantial activation of groundwater circulation.

In favourable areas, where upward head gradients are maximised (topographic-potentiometric lows - deeply incised valleys) and coincide with zones of greatest permeability in confining beds, particularly in the uppermost one (fault zones, fault-cored anticlines, structural "windows", etc.), groundwater circulation can be active enough to account for the full development of cave systems. The type of cave pattern depends largely upon the existing structural features. Rectilinear fissure caves and small mazes with fissure-like ascending pits (eastern Missouri, BROD, 1964), or without such pits (Black Sea basin, south Ukraine) can develop, as can extensive multi-storey mazes such as Wind and Jewel Caves in the Black Hills (FORD, 1989), the great gypsum mazes of the Western Ukraine (KLIMCHOUK, 1990, 1992) and Botovskaya Cave, Siberia (FILIPPOV, 1994). Multi-storey mazes form when fissures are distributed uniformly in the lateral direction and organised in extensive superimposed networks confined to specific horizons (KLIMCHOUK, 1994; KLIMCHOUK ET AL., 1995).

Maze patterns are quite characteristic, although not confined, to artesian speleogenesis. The diagnostic feature is uniform passage size and morphology at a given locality, regardless of the pattern type. The fundamental reason is that artesian speleogenesis is largely discharge-controlled, and no considerable increase in discharge occurs as an initial fissure widens by dissolution. The simplest architecture that can be considered is that of two "normal" (non-karstic) aquifers separated by a carbonate unit with fissure permeability, with the whole system confined by an upper, non-karstifiable, aquitard. In this case upward circulation and slow discharge from the system through the upper confining bed will converge towards an incising valley (figure 2).

According to PALMER's (1984) theoretical consideration, non-uniform enlargement of passages occurs at the early (laminar flow) stage when the rate at which any route enlarges depends upon the amount of flow rather than solution kinetics (discharge-controlled development). Enlargement rates increase if a passage increases its discharge, either by capturing water from neighbouring passages or by enlarging its primary catchment area. This explains competitive development of flow routes and the importance of initial differences in hydraulic efficiency in determining successful conduits in unconfined karsts. At the next (solution kinetics-controlled) stage, the enlargement rate approaches a constant value, at which successful conduits continue to develop.

In the artesian settings specified above the amount of upward flow is governed not by available recharge to the karstifiable unit (which is essentially uniform to all fissures contacting the lower aquifer) but by constrained discharge through the upper confining bed. Even a small dissolutional enlargement of the initial network in the karst unit will rapidly minimise the head difference in both adjoining aquifers. After that the flow rate will be governed solely by the upper confining bed's transmissivity, which is roughly constant and normally relatively low, unless the confinement is fully breached by an incising valley. Thus, the enlargement rate for all fissures (conduits) in the network will also be constant through most of the artesian stage, regardless of their initial dimensions.

Superimposed upon the general background of ascending circulation in areas of potentiometric lows, local convection cells may develop. These are driven by density gradients imposed by thermal or chemical contrasts between the bulk water in the aquifer and recharge water from the underlying formation. This activity may cause pronounced medium-scale effects in an already formed system (such as the growth of ceiling cupolas, half-tubes, etc) but can hardly account for the development of an entire cave system on its own.

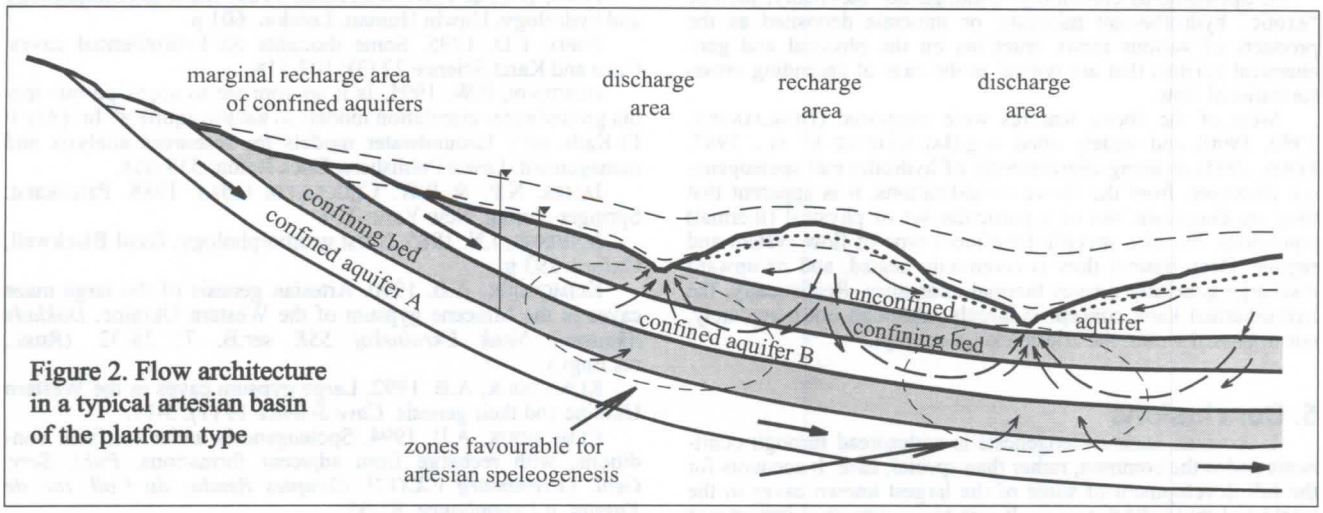

Figure 2. Flow architecture in a typical artesian basin of the platform type

Solutional potential of groundwaters in artesian settings

The concept of cross-formational communication has important implications when considering potential for dissolution. Recharge from an adjacent non-soluble formation can be highly aggressive with respect to a karstifiable rock. This is most evident in the case of simple dissociation of gypsum, but holds true for carbonate karst in shallow artesian settings, where soil-generated CO_2 is delivered by water from "classic" marginal recharge areas through non-carbonate aquifers. Waters in deep-seated horizons often have high concentrations of CO_2 derived from degradation of hydrocarbons or from other sources.

During the last decade it has been increasingly recognised that, in addition to the bicarbonate dissolutional mechanism, a number of redox reactions, particularly those involving sulphur compounds and sulphuric acid, may contribute to carbonate dissolution (FORD & WILLIAMS, 1989). Some of the related reactions generate CO_2, leading to doubled solvency. Reactions involving strong acids are believed to be particularly important during the early stages of speleogenesis (WORTHINGTON, 1992; LOWE & GUNN, 1995), which, in the light of the above consideration, commonly occur under artesian conditions. Cross-formational hydraulic communication is of paramount importance. It allows the involvement of different chemical mechanisms, as well as reinforcing mixing corrosion effects, as it causes migration of various reactants and reaction products between horizons, bringing contrasting geochemical environments and waters of contrasting chemistries into interaction (KLIMCHOUK, 1996). More extreme thermobaric conditions occurring in deep settings further increase the range of possible speleogenetic effects. Moreover, some still more exotic, as yet poorly understood, effects may have a role in speleogenesis. For instance, radiolysis of underground waters produces free H^+ and highly reactive oxidising agents (VOVK, 1979). This and related effects await further evaluation.

Stages of artesian speleogenesis

(1) During continuing subsidence and burial groundwater circulation in a basin is driven mainly by pressure heads developed by compaction and dehydration of sediments. Some speleoinception effects may operate at this stage.

(2) As the tectonic regime reverses between subsidence and uplift, and geomorphic development locally exposes basinal formations, fluid flow becomes increasingly driven by hydraulic head gradients. Speleogenetic initiation occurs widely during this stage, even in deep-seated horizons; in favourable conditions true conduits can develop. Flow is slow, especially if a cross-formational component is involved, and elapsed time spans are commonly large.

(3) As continuing uplift brings artesian aquifers closer to the denudation surface, circulation in the entire system and the cross-formational flow component are increasingly activated. The full development of cave systems occurs in a pattern of upward cross-formational communication in zones of potentiometric lows - where valleys incise into the upper confining bed. Deposition of fine clastic sediments, re-distributed from occasional cavern breakdown, may begin at this stage.

(4) Breaching of artesian confinement at local discharge areas dramatically increases upward flow through the system and enhances cave development along preferred routes. This is the last stage of artesian speleogenesis.

Ongoing entrenchment of major valleys and areal disintegration of the capping aquitard lead to radical re-organisation of recharge-discharge configurations and inversion of flow patterns; artesian cave systems become relict. A number of speleogenetic and karst morphogenetic models address these open karst settings, but commonly they fail to explain relict artesian systems adequately. These models interpret the superimposed cave development in terms of phreatic/water table/vadose flow conditions and tend to overlook the possibility that previous artesian history could have influenced such development. The inception horizon concept of Lowe (1992), although not directly refferring to confined settings, provided an important step towards the recognition of processes operating deep within rock sequences during a more extensive geological history.

The succession of stages outlined above applies only to a given formation. On the regional (basinal) scale, situations representing different stages may occur simultaneously in different formations, at different depths or in different parts of a basin.

4. Major features of artesian speleogenesis

These can be summarised as follows:

1. The imposition of basic cave system frameworks show no genetic relationship to modern landscapes. However, in the context of palaeo-geomorphology, active and significant cave growth is normally induced by and converges towards valleys incising into an upper aquitard.

2. Caves patterns are guided by fissuring, and passages within a given series (storey) are quite uniform in size and morphology. Two- or three-dimensional (multi-storey) rectilinear mazes are typical, although neither confined to nor diagnostic of artesian speleogenesis.

3. Ceiling cupolas or half-tubes originated by the action of convection circulation cells or currents are common medium-scale morphological features.

4. Clastic cave sediments are represented mainly by fine clays and silts. These can be partly autochthonous (comprising insoluble residues). However, they are mainly allochthonous, intruded into artesian systems from overlying formations only during the late stages (stages 3-4). Breakdown processes are induced by a decrease of hydrostatic pressure, and increasing flow velocities allow some transport and re-distribution of clastic material. However, gradient fields in the aquifer remain much more uniform, and the energy of water flows remains much lower than in unconfined settings, so that sediments display fine-grain composition. Whereas sediments in unconfined phreatic and, especially, vadose caves are characterised by great structural and lithological variation over short distances, and by rapid facies changes, artesian caves normally contain sediments that are much more uniform, and display similar facies even on a regional scale.

5. Speleothems commonly, although not inevitably, include "exotic" hydrothermal minerals, or minerals deposited as the products of various redox reactions on the physical and geochemical barriers that are typical in the case of ascending cross-formational flow.

Most of the above features were suggested (DUBLJANSKY, 1980, 1990) and widely cited (e.g.BAKALOWICZ ET AL., 1987, FORD, 1995) as being characteristic of hydrothermal speleogenesis. However, from the above considerations, it is apparent that they are diagnostic not of a particular set of physical (thermal) conditions, but of a specific (confined) type of flow system and regime. Deep basinal flow is commonly heated, and its upward discharge generally creates thermal anomalies. Realistically, the hydrothermal karst concept is largely, although not completely, encompassed within the artesian karst concept.

5. Conclusions

1. Artesian karst/speleogenesis is widespread through continents and is the common, rather than special, case. It accounts for the full development of some of the largest known caves in the world and many shorter caves. It also has an immense importance in speleo-inception. By far the greatest part of presently unconfined karst rocks experienced more or less prolonged episodes of basinal development before undergoing major uplift. Thus, artesian karstification almost inevitably precedes unconfined karst development.

2. Adoption of the non-classical concept of artesian flow in karst hydrogeology gives a wider perspective for development of the theory of artesian karst/speleogenesis. The latter is adequate to explain the hydraulic and chemical mechanisms involved. There are also numerous provings of modern deep-seated intrastratal karst, and major features of known relict artesian cave systems.

3. Artesian speleogenesis occurs in different lithologies. It involves various dissolution mechanisms that operate under different physical parameters, although resulting in similar cave features. This indicates clearly that the main factor responsible for the genetic specifics of this kind of speleogenesis is the type of flow system, not a single chemical or physical peculiarity of the genetic environment.

4. Recognition of the scale and importance of artesian karst/speleogenesis and of hydraulic continuity and cross-formational communications between aquifers in artesian basins, is indispensable for the correct interpretation of speleogenetic processes (evolution of karst aquifers) and the resultant phenomena, regional karst water resource evaluations, and the genesis of some karst-related mineral deposits. It has numerous other theoretical and practical implications, and ultimately requires in replacement of the traditional karstological paradigm, which is based largely upon concepts of unconfined karst.

References

BAKALOWICZ, M.J. et. al. 1987 Thermal genesis of dissolution caves in the Black Hills, South Dakota. Bull. Geol. Soc. Amer., 99: 729-738

BONACCI, O. 1987. Karst hydrology, with special reference to the Dinaric Karst. Springer-Verlag, New York: 184.

BOSAK, P., FORD, D.C. & J. GLAZEK, 1989. Terminology. In: (P.Bosak, D.Ford, J.Glazek & I.Horacek, eds.): Paleokarst: a systematic and regional review. Academia, Praha: 25-32.

BRODT, L.G., 1964. Artesian origin of fissure caves in Missouri. *NSS Bulletin* 26 (3): 83-114.

DUBLJANSKY, Y.V. 1990. Regularities of the formation and modelling of hydrothermal karst. Nauka, Novosibirsk: 150 p.

DUBLJANSKY, W.N. 1980. Hydrothermal karst in the Alpine folded belt of southern parts of the USSR. *Kras i Speleologia* .3 (12): 18-36.

FILIPPOV, A.G. 1994. Botovskaya cave in the East Siberia. Problems of Physical Speleology. Moscow: MFTI Publ. 102-110. (Russ., res.engl.).

FORD, D.C. 1988. Characteristics of dissolutional cave systems in carbonate rocks. In: (N.P. James & P.W. Choquette, eds.): Paleokarst. Springer-Verlag, New York: 24-57.

FORD, D.C. 1989. Features of the genesis of Jewel Cave and Wind Cave, Black Hills, South Dakota. *NSS Bulletin* 51: 100-110.

FORD, D.C. & P.W. WILLIAMS. 1989. Karst geomorphology and hydrology. Unwin Human, London. 601 p.

FORD, T.D. 1995. Some thoughts on hydrothermal caves. Cave and Karst Science 22 (3): 107-118.

HUNTOON, P.W. 1995. Is it appropriate to apply porous media groundwater circulation models to karstic aquifers? In: (Aly I. El-Kadi, ed.): Groundwater models for resources analysis and management. Lewis Publishers, Boca Raton: 339-358.

JAMES, N.P. & P.W. CHOQUETTE (eds.). 1988. Paleokarst. Springer-Verlag, New York: 416.

JENNINGS, J.N. 1985. Karst geomorphology. Basil Blackwell, Oxford: 293 p.

KLIMCHOUK, A.B. 1990. Artesian genesis of the large maze caves in the Miocene gypsum of the Western Ukraine. *Doklady Akademii Nauk Ukrainskoj SSR* ser.B, 7: 28-32. (Russ., res.Engl.).

KLIMCHOUK, A.B. 1992. Large gypsum caves in the Western Ukraine and their genesis. *Cave Science* 19 (1): 3-11.

KLIMCHOUK, A.B. 1994. Speleogenesis under confined conditions, with recharge from adjacent formations. *Publ. Serv. Geol. Luxembourg v.XXVII. Comptes Rendus du Coll. Int. de Karstol. a Luxembourg:* 85-95.

KLIMCHOUK, A.B. 1996. The role of karst in the genesis of sulfur deposits, Pre-Carpathian region, Ukraine. *Environmental Geology* 28 (3).

KLIMCHOUK, A.B., V.N.ANDREJCHOUK, & I.I.TURCHINOV 1995. The structural prerequisites of speleogenesis in gypsum in the Western Ukraine. Ukr.Speleol.Assoc., Kiev: 106 p.

LOWE, D.J. 1992. The origin of limestone caverns: an inception horizon hypothesis. Ph.D. Thesis, Manchester Metropolitan University.

LOWE, D.J. & J. GUNN. 1995. The role of strong acid in speleo-inception and subsequent cavern development. In: (I.Barany-Kevel, ed): Environmental effects on karst terrains. *Acta Geographica*, vol.XXXIV. Szeged, Hungaria: 33-60.

MILANOVIC, P.T. 1981. Karst hydrology. Water Resources Publications, Littleton, CO: 434 p.

MJATIEV, A.N. 1947. Confined complex of underground waters and wells. *Izvestija AN SSSR, otd. tekhnich. nauk*, 9: 33-47 (russ.).

PALMER, A.N. 1975. The origin of maze caves. *NSS Bulletin* 37 (3): 56-76.

PALMER, A.N. 1984. Geomorphic interpretation of karst features. In: (R.G. LaFleur, ed.): Groundwater as a geomorphic agent. Allen & Unwin, Boston: 173-209.

PALMER, A.N. 1991. Origin and morphology of limestone caves. *Geol. Soc. Am. Bull.* 103: 1-21.

PALMER, M.V. & A.N. PALMER, 1989. Paleokarst of the United States. In: (P.Bosak, D.Ford, J.Glazek & I.Horacek, eds.): Paleokarst: a systematic and regional review. Academia, Praha: 337-365.

QUINLAN, J.F. 1978. Types of karst, with emphasis on cover beds in their classification and development. Ph.D.Thesis, Univ. of Texas at Austin.

SHESTOPALOV, V.M. 1981. Natural resources of underground water of platform artesian basins of the Ukraine. Nauk. Dumka, Kiev: 195 p. (russ.).

SHESTOPALOV, V.M., ed. 1989. Water exchange in hydrogeological structures of the Ukraine. Water exchange under natural conditions. Naukova dumka, Kiev: 288 p. (russ.).

TOTH, J. 1995. Hydraulic continuity in large sedimentary basins. *Hydrogeology Journal* 3 (4): 4-15.

VOVK, I.F., 1979. Radiolysis of underground waters and its geochemical role. Nedra, Moscow: 231 p. (Russ.).

WHITE, W.B. 1988. Geomorphology and hydrology of karst terraines. Oxford University Press, Oxford: 464 p.

WORTHINGTON, S.R.H. 1992. Karst hydrogeology of the Canadian Rocky Mountains. Ph.D. Thesis, McMaster University.

Speleogenetic effects of water density differences

Alexander Klimchouk
Institute of Geological Sciences, National Academy of Sciences, P.O.Box 224/8, Kiev-30, 252030, Ukraine

Abstract

High solubility of some karst rocks, particularly salt and gypsum, leads to a significant increase in the density of dissolving water. This can be up to 30% for salt and 0.1% for gypsum, as compared to aggressive water entering a karst system. Gravitational separation of water may be well expressed as density stratification or as circulation cells and distinct buoyant currents. Such phenomena may occur in a single cave pool, or at aquifer scale. The most pronounced speleogenetic effects occur when aggressive water recharges a gypsum stratum continuously from an underlying formation under sluggish artesian flow conditions. In this case dissolution by natural convection flow may affect the cave system layout. More localised effects include the formation of dissolution notches, bevels and facets (due to density stratification), and formation of ceiling half-tubes, pockets, cupolas,and domepits (by buoyant currents) in confined settings.

1. Introduction

As a karst rock is dissolved and the solute content of the dissolving water increases, the solution increases in density. The greater the solubility of a rock, the greater the density differences that may develop within an aquifer or water body, especially if there is a continuous or frequent pulse supply of contrasting relatively fresh water. This causes gravitational separation and convectional circulation of water, which are most pronounced under sluggish laminar flow conditions with continuous fresh water recharge.

CURL (1966) provided a theoretical analysis of cave conduit enlargement by natural convection in a limestone aquifer, depicting transition conditions determining the prevalence of natural convection or forced flow regimes. He found that, with sufficiently slow water circulation, convection caused by density differences may be the primary flow mode for limestone removal. This is made possible by even extremely small compositional differences. Supposed morphological effects include the upward enlargement of anastomoses above bedding planes, development of vertical asymmetry of conduits, and upward growth of dome-like ceiling features.

This paper discusses hydrological settings and types of water density difference phenomena, as well as the resulting morphological effects.

2. Water density stratification and local convection cells

In shallow phreatic and water-table aquifers with sluggish flow, or in standing water bodies such as perched cave lakes, marked water density stratification can develop. To maintain or reinforce such stratification, continuous or periodic inflow of relatively "fresh" water is needed. This may enter from above (vadose percolation), from the side (e.g. from sinking streams) or from a basal non-karstic aquifer (upward recharge). In all cases, less dense fresh water will tend to occupy the uppermost available position, forming a more or less distinct layer. The hydrochemical stratification phenomenon is particularly pronounced, and has been well documented, in gypsum caves.

In passages that originated (or significantly modified) at a shallow depth below the water-table, flat ceilings ("Laugdecke" in German) or bevels are common. They are formed by dissolution in the uppermost, aggressive, layer of water, where a pattern of small up- and downwelling convection cells ("salt-fingers") operates due to small density differences (KEMPE, 1972; KEMPE ET AL., 1975; figure 1-A). Such flat ceilings are best displayed in gypsum caves in Germany, but also occur in the Western Ukraine, the Urals and Siberia. Flat ceilings, combined with inclined facets, are typical for many German caves, producing cross-section in the form of a tip-down triangle. This reflects dissolutional widening in low-energy shallow phreatic or artesian conditions, with successive fast draining, and without any significant morphological modification under water-table conditions. However, field observations from caves elsewhere than Germany suggest that not only flat ceilings, but also ceilings with cupola-like forms and gothic arch shapes can form under the same conditions (figure 1-C).

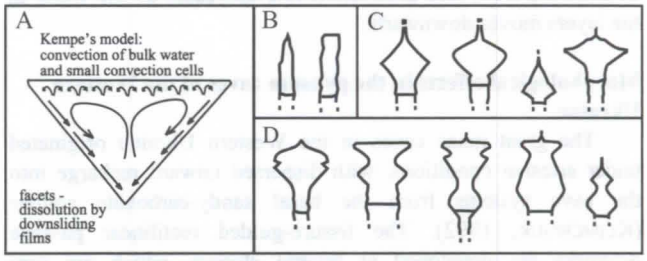

Figure 1. Wall notching and wall facet formation by dissolution caused by natural convection. A = Kempe's model; B,C,D = typical passage cross-sections from the gypsum caves of the Western Ukraine, showing varieties of morphological modification.

In England, distinct water stratification has commonly been observed by divers in phreatic passages in the limestone caves of the Yorkshire Dales (CORDINGLEY, 1991). Brown "peaty" water is frequently seen occupying the upper part of the water body, whilst nearer the floor the water is virtually transparent. The interface between the two layers is commonly well defined. A possible explanation of the phenomenon is that relatively fresh (less dense) peat-stained water replaces most of the water in phreatic passages during a flood and is then trapped in the higher levels as denser autogenic percolation water accounts for an increasing percentage of flow in passages during a drought. Differential dissolution is believed to account for the formation of ceiling solution domes. It is also hypothesised that horizontal wall notches can be formed due to water stratification under phreatic conditions, instead of being formed at a water-table, as traditionally believed. Such notches have been observed in

phreatic passages that have never been drained (CORDINGLEY, 1991).

Hydrochemical stratification of water is well documented where water bodies with an open surface occur in gypsum caves, either as aquifer "windows or as perched pools. In the partly drained Miocene gypsum aquifer of the Western Ukraine (cave lakes with sluggish flow in Optimisticheskaya Cave) a distinct density stratification develops, with solute content rising downward from 1.1-1.3 to 2.0-2.5g l^{-1} within a depth of 25-30cm. Subsequently, SI_g increases from -0.4 almost to saturation value, and dissolution rates (measured from tablet experiments) decrease from -6.4 to -7.2mg day cm^{-2} in the uppermost layer to -0.08 to -0.06mg day cm^{-2} at depths below 15cm (KLIMCHOUK & AKSEM, 1988). This leads to the formation of recent water level notches in walls. Horizontal notching due to chemical stratification of water, with higher dissolution rates in the uppermost layer, is a common morphological effect for caves in all major karstifiable lithologies (FORD & WILLIAMS, 1989), although it is best displayed in salts (FRUMKIN, 1994) and gypsum.

The typical morphological elements of notches are steep inwardly inclined sidewalls, or facets ("Facetten" in German), described from gypsum caves in Germany (BIESE, 1931; PFEIFFER & HAHN, 1972) and the Urals (LUKIN, 1967), and explained as being formed due to conduit-scale convection circulation. Formation of facets in gypsum was studied in detail and modelled theoretically by KEMPE (1972) and KEMPE ET AL (1975). Dissolution causes layers of water adjacent to the walls to become denser than the bulk water in the upper horizon, so that films of water "slide" downwards along the walls (figure 1-A). Examples of such 1-3mm-thick currents descending the walls were measured at 3-30cm min-1 in a cave pool by KEMPE ET AL (1975). The inclined plane of a facet forms because solute content increases and dissolution rate decreases as the water in the layers moves downward.

Morphological effects in the gypsum caves of the Western Ukraine

The great maze caves in the Western Ukraine originated under artesian conditions, with dispersed upward recharge into the cave systems from the basal sandy-carbonate aquifer (KLIMCHOUK, 1992). The fissure-guided rectilinear passage networks are developed at several storeys, which are pre-determined by the multi-storey occurrence of fissure networks (KLIMCHOUK, 1994; KLIMCHOUK ET AL., 1995). The multi-storey structure and different location of artesian cave systems in relation to modern, deeply entrenched, valleys, combined with differential regional uplift rates, caused a variety of draining (dewatering) histories, and hence a varying degree of water-table modification of passage morphology. Passages with different degrees of modification may occur at different levels, or in different areas of a single cave system.

Artesian conduits that have experienced virtually no modification normally display fissure- and cleft-like morphologies (figure 1-B). Less commonly they are tubular in shape. Many passages have one "level" of notching, with inwardly inclined sidewalls; ceilings may be of different shapes (figure 1-C). Such formed under shallow artesian conditions, with dissolution by natural convection operating, and passed quickly to the fully drained state, so that no true water-table notching developed. When more then one level of horizontal notching occur in the walls (figure 1-D), the additional notches signify more or less stabilized palaeo-positions of the water-table. They can be traced continuously across large distances within a given series of a labyrinth.

3. Buoyant currents from basal recharge under artesian settings

Cave development in artesian settings is commonly associated with recharge from an underlying aquifer (KLIMCHOUK, in press). Local hydraulics and details of the speleogenetic development are well illustrated by the gypsum caves of the Western Ukraine, although their features are neither unique to the region nor to gypsum.

Head gradients are directed upwards, but flow is slow due to the high resistance of the upper aquitard, and of the karstifiable unit itself during the early stages of speleogenetic development. As water in the underlying aquifer is less dense than water already within a karst system, it tends to move upwards by natural convection, so that forced flow and natural convection coincide.

When forced flow through the karst system is negligible due to poor vertical connectivity and the high resistance of flow paths, the natural convection regime predominates and "closed" cells develop. After dissolving some material and increasing in density, the water returns downwards into the underlying aquifer and outflows laterally with the regional flow. Conduits at the bottom of the gypsum stratum and along the lowermost available fissures grow by upward stoping due to natural convection dissolution. Solution cupolas and domepits develop along vertical fissures and propagate upwards to, or even beyond, the edge of the fissure plane. In this way, connections can be established from two or more neighbouring domepits with open and interconnected fissures of the next higher storey of fissures. Thus, backward circulation loops can be extended through two storeys, continuing the speleogenetic development. As buoyant currents of aggressive recharge always tend to occupy the uppermost available space in a developing conduit system, further upward propagation of dissolutional forms driven by natural convection will proceed, and eventually lead to establishment of direct hydraulic connection with the overlying aquifer.

When the high resistance to flow between the lower and upper aquifers is destroyed, the equipotential field is drastically re-organised and forced convection flow becomes predominant. Because high conductivity is now established through the gypsum stratum, the head gradient between the two aquifers is minimised. Flow remains small and slow due to the remaining relatively high resistivity of the upper aquitard. But, the flow pattern changes from backward loops and "closed" cells to an unlooped ascending system. Natural convection still contributes to the overall flow, and gravitational separation of buoyant currents becomes perhaps even more distinct, as the general flow component pattern is now unlooped.

The most common morphological effect of buoyant currents is the formation of keyhole cross-sections or distinct ceiling half-tubes. Keyhole passages are usually assumed to be associated with vadose incision into the bottom of phreatic passages; half-tubes are widely believed to originate from dissolution by surviving flow through a passage that has become choked with sediment (FORD & WILLIAMS, 1989). However, half-tubes are acknowledged as being controversial. It is suggested here that both features can be formed in artesian caves when natural buoyant convection currents are established within an unlooped and generally ascending bulk water flow, as described above, although other interpretations such as noted above, are not excluded. Both types of feature are widespread in the gypsum caves of the Western Ukraine.

In the most complete cases, these features can be traced through two, or even three, storeys of passages. When a fissure receives recharge from below, the less dense aggressive water

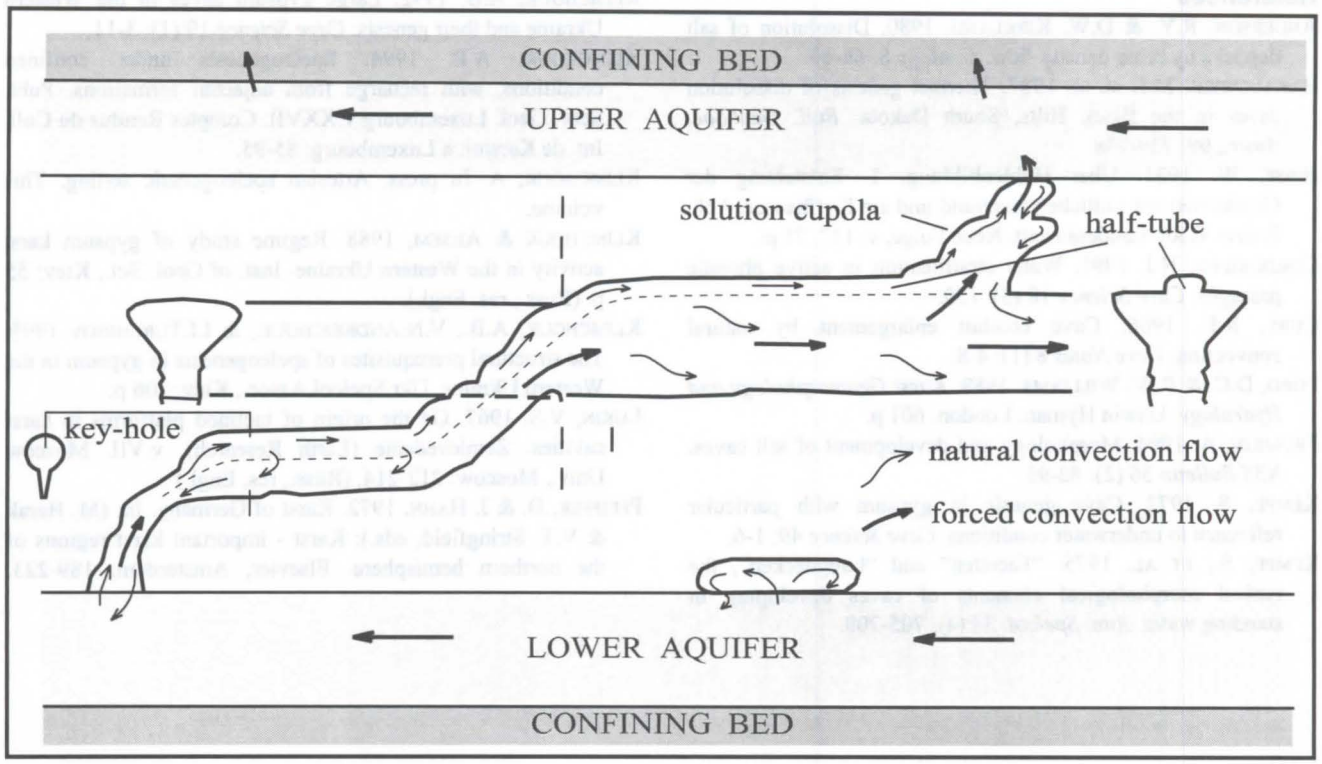

Figure 2. The formation of upward solution forms by buoyant currents. The diagram shows schematically the relationship between lines of natural convection flow and forced flow on the mature stage of artesian speleogenesis, when conduit connection has already been established through the gypsum, but the forced flow is still slow due to the major constraint of the upper aquitard.

tends to occupy the uppermost available space and flows towards the nearest connection with the upper conduit. The rounded sections of keyhole passages are formed in this way (figure 2). The tube climbs the wall where the lower passage joins the upper one, and continues as a ceiling half-tube in the upper passage. Half-tubes normally end in a domepit open to the next higher passage or at the bottom of the overlying aquifer. Though most convincingly displayed in the gypsum caves of the Western Ukraine, the suggested mechanism is likely to have broad applications.

When continuous aggressive recharge takes place under artesian conditions, circulation cells driven by the density gradients may develop at aquifer scale within salt deposits (ANDERSON AND KIRKLAND, 1980).

The density gradients that give rise to natural convection circulation, can also be developed or reinforced by chemical mechanisms, by thermal differences or by suspended load injection. Ascending flow due to thermal convection circulation is believed to contribute to the development of maze caves in the Black Hills (BAKALOWICZ ET AL., 1987). In particular, natural convection accounts for the upward dissolution of the cupola-like ceiling forms typical of the highest parts of the multi-storey Wind Cave and Jewel Cave systems. Suspended load injected into the cave systems of the Western Ukraine due to occasional breakdown during the last stage of artesian speleogenesis is likely to have reinforced the density gradients between the bulk water in passages and buoyant ascending currents as described above.

4. Conclusions

1. When continuous or periodic recharge of "fresh" water occurs, rock dissolution sets up density gradients, which cause gravitational separation (stratification) of water and drive natural convection circulation. The phenomenon may operate at local scale or at aquifer scale, and may be expressed as looped circulation cells or unlooped directional currents. Because dissolution always leads to density increase, gravitational separation of water and natural convection due to this effect are inherently involved in, and affect the process of, speleogenesis. Their importance is relatively high in sluggish flow conditions (particularly in artesian settings) and relatively low to negligible in cases of high flow velocity. The phenomenon is more pronounced and more important in gypsum and salt karsts, and in cases where fresh recharge occurs from below. Natural convection may also be caused by thermal anomalies.

2. Density stratification and natural convection circulation (currents) cause differential dissolution and related morphological effects in caves. The formation of flat ceilings, cupolas and domepits, ceiling half-tubes, keyhole profiles, inwardly inclined sidewalls and horizontal notches can be explained in this way.

3. Natural convection circulation and dissolution by buoyant currents may not only modify passage morphology, but may play an important role in building up the whole patterns of artesian cave systems during the early stages of ascending artesian speleogenesis. They cause upward stoping of dissolutional forms before the initial flow paths through a karstifiable unit are hydraulically interconnected and/or where they are highly resistant to through flow between the input and output boundaries (between the upper and lower aquifers).

References

ANDERSON, R.Y. & D.W. KIRKLAND. 1980. Dissolution of salt deposits by brine density flow. *Geology* 8: 66-69.

BAKALOWICZ, M.J. et. al. 1987. Thermal genesis of dissolution caves in the Black Hills, South Dakota. *Bull. Geol.Soc. Amer.*, 99: 729-738

BIESE, W. 1931. Uber Hohlenbildung, 1. Entstehung der Gipshohlen am sudlichen Harzrand und am Kyffhauser. Abh. Preuss. Geol. Landesanstalt, Neue Folge, v. 137, 71 p.

CORDINGLEY, N.J. 1991. Water stratification in active phreatic passages. *Cave Science* 18 (3): 159.

CURL, R.L. 1966. Cave conduit enlargement by natural convection. *Cave Notes* 8 (1): 4-8.

FORD, D.C. & P.W. WILLIAMS. 1989. *Karst Geomorphology and Hydrology*. Unwin Hyman, London. 601 p.

FRUMKIN, A. 1994. Morphology and development of salt caves. *NSS Bulletin* 56 (2): 82-95.

KEMPE, S. 1972. Cave genesis in gypsum with particular reference to underwater conditions. *Cave Science* 49: 1-6.

KEMPE, S., ET AL. 1975. "Facetten" and "Laugdecken", the typical morphological elements of caves developing in standing water. *Ann. Speleol.* 30 (4): 705-708.

KLIMCHOUK, A.B. 1992. Large gypsum caves in the Western Ukraine and their genesis. *Cave Science* 19 (1): 3-11.

KLIMCHOUK, A.B. 1994. Speleogenesis under confined conditions, with recharge from adjacent formations. Publ. Serv. Geol. Luxembourg v.XXVII. Comptes Rendus du Coll. Int. de Karstol. a Luxembourg: 85-95.

KLIMCHOUK, A. In press. Artesian speleogenetic setting. This volume.

KLIMCHOUK & AKSEM, 1988. Regime study of gypsum karst activity in the Western Ukraine. Inst. of Geol. Sci., Kiev: 55 p. (Russ., res. Engl.).

KLIMCHOUK, A.B., V.N.ANDREJCHOUK, & I.I.TURCHINOV 1995. The structural prerequisites of speleogenesis in gypsum in the Western Ukraine. Ukr.Speleol.Assoc., Kiev: 106 p.

LUKIN, V.S. 1967. On the origin of inclined platforms in karst cavities. Zemlevedenie (Earth Research), v.VII. Moscow Univ., Moscow: 212-214. (Russ., res. Engl.)

PFEIFFER, D. & J. HAHN. 1972. Karst of Germany. In: (M. Herak & V.T. Stringfield, eds.): Karst - important karst regions of the northern hemisphere. Elsevier, Amsterdam: 189-223.

Le rôle de la zone épinoyée dans la spéléogenèse

par Philippe AUDRA
Groupe de valorisation de l'environnement (GVE), URA D1476 du CNRS,
Université de Nice-Sophia-Antipolis, 98 boulevard Edouard Herriot, BP 209, 06204 Nice Cédex.
& Cagep (URA 903), Aix-en-Provence.

Résumé

Lors des crues, le niveau de la zone noyée est susceptible de présenter d'importantes variations. Des exemples actuels montrent que l'ampleur verticale de la zone épinoyée peut atteindre plusieurs centaines de mètres. C'est dans la zone épinoyée que se cumulent les processus mécaniques et chimiques. La concentration de conduits de grande taille en est la marque. Ces processus permettent notamment de comprendre l'origine de formes qui ne pouvaient s'expliquer par un creusement noyé, comme les tubes inclinés sur de grandes dénivellations. On insiste sur la pertinence de la conception du drainage de la zone noyée, par des conduits localisés dans la zone épinoyée. Les grands karsts noyés (Vaucluse...) pourraient s'expliquer par un noyage postérieur à leur genèse.

Abstract : the epiphreatic zone part in the speleogenesis.

During floodings, the phreatic zone can undergo important level variations. Some contemporary examples show that the vertical extension of the epiphreatic zone can reach several hundred of metres. Mechanical and chemical processes cumulate in this zone, marked by a concentration of large galleries. These processes allow to understand the origin of some forms which could not be explained by a phreatic evolution, such as large sloped tubes. The phreatic zone drainage by conduits located in the epiphreatic zone seems to be the most adjusted conception. Large phreatic karsts (Vaucluse...) could be explained by water-table rises occuring after their genesis.

1. L'ampleur des mises en charge dans la zone épinoyée

La mise en charge des parties basses de certains réseaux karstiques est un fait connu de longue date. L'exemple le plus célèbre est celui de la grotte de la Luire (Drôme, France), où l'eau remonte de 450 m avant de "crever" par le porche. Grâce à l'avancée des connaissances liées aux explorations spéléologiques (LISMONDE & al.), les exemples de mises en charge sur plusieurs dizaines de mètres de hauteur sont innombrables, ceux dépassant 100 m ne sont pas rares (fig. 1).

Cavité	Mise en charge
Grotte de la Luire (Drôme)	451 m
Perte du Calavon (Alpes Hte. Prov.)	263 m
Puits des Bans (Hautes-Alpes)	217 m
Réseau Fanges-Paradet (Pyr. orient.)	170 m
Hölloch (Schwytz)	170 m
Réseau des Siebenhengste (Bern)	150 m
Réseau du Revest (Alpes maritimes)	145 m
Trou qui Souffle (Isère)	120 m
Trou du Renard (Pyrénées atlantiques)	120 m
Aven Souffleur (Vaucluse)	120 m
Fontaine de Crèvecœur (Htes-Alpes)	100 m

Figure 1 : quelques exemples de mise en charge dépassant 100 m de hauteur.

Cette portion du karst soumise à des noyages et dénoyages successifs en fonction des variations de niveau de la zone noyée est appelée "zone épinoyée".

2. Des origines climatiques, structurales et spéléogénétiques

Ces variations de niveau de la zone épinoyée sont liées à l'arrivée brutale d'importants volumes d'eau, dépassant la capacité d'évacuation des galeries. Ces conduits de taille insuffisante fonctionnent comme un diaphragme. Ils provoquent une mise en charge à l'amont de l'obstacle. On observe alors une remontée dans les conduits verticaux qui fonctionnent en cheminée d'équilibre et des circulations noyées dans les conduits horizontaux qui deviennent temporairement actifs.

De tels phénomènes sont liés d'une part à un contexte climatique favorisant des écoulements très contrastés et d'autre part à l'existence de secteurs de faible transmissivité à l'aval des réseaux.

Les types de climats particulièrement favorables sont ceux où l'écart entre les écoulements de crue et d'étiage est important. C'est le cas des régions de montagne, où une grande partie de l'écoulement se produit durant la brève période de fonte des neiges. Les régions méditerranéennes et tropicales sont également connues pour la brutalité et la concentration des épisodes pluvieux. Néanmoins, des crues brutales sont possibles dans tous les types de zones climatiques, car des moyennes très pondérées peuvent masquer des épisodes exceptionnels.

La présence de zones de conduits à faible perméabilité à l'aval des réseaux karstiques peut avoir plusieurs origines, qui peuvent d'ailleurs se combiner (fig. 2) :

- quand les couches calcaires plongent à l'aval en-dessous du niveau de base local constitué de roches imperméables on a affaire à un karst barré. Parfois, le barrage est constitué de roches peu perméables ou légèrement fissurées (calcaires marneux, dolomies, grès...), où des circulations aquifères existent cependant (fig. 2-A). Il s'agit dans ce cas de karst "semi-barré", d'origine structurale (AUDRA, 1994).
- quand on observe un étagement des conduits lié à un enfoncement saccadé du niveau de base, bien souvent le réseau inférieur le plus récent, où s'effectuent les circulations pérennes, est peu évolué, avec des conduits de petite taille, parfois impénétrables (fig. 2-B). L'origine est ici spéléogénétique.

Dans les deux cas, le karst adopte deux types de comportements hydrodynamiques en fonction de son état de charge. A l'étiage, les écoulements transitent au travers des fissures et des conduits de faible débit. L'eau ressort au contact du niveau de base local, par une source généralement impénétrable. En crue, l'eau excédentaire ne peut franchir les secteurs peu transmissifs et envahit la zone épinoyée. Elle franchit l'obstacle par des conduits supérieurs et sort au niveau d'un trop-plein perché au-dessus du niveau de base dont les galeries sont généralement vastes et pénétrables.

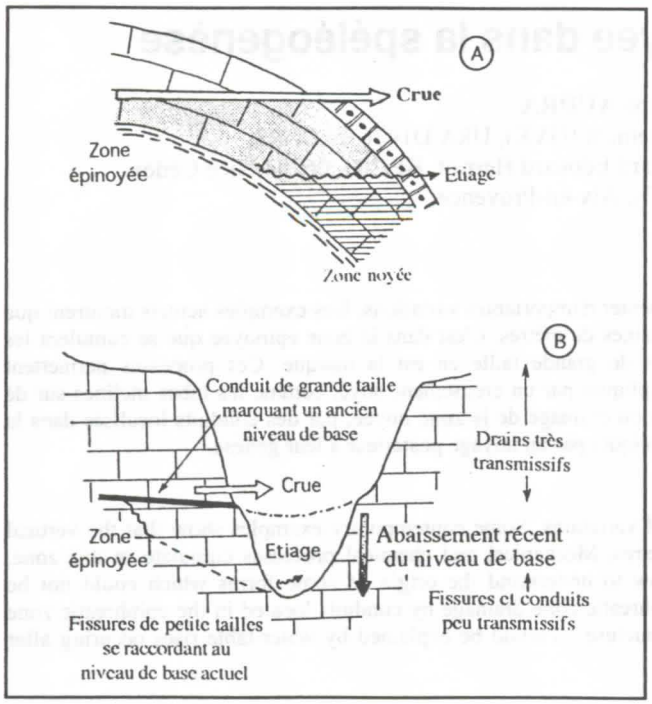

Figure 2 : zones épinoyées liées à un karst semi-barré (A) ou à une adaptation récente à l'abaissement du niveau de base (B).

Du point de vue morphologique, les deux types de conduits s'opposent radicalement. Les réseaux inférieurs sont constitués de fissures à peine élargies, bien souvent impénétrables et noyées. Les réseaux supérieurs localisés dans la zone épinoyée présentent quant à eux des puits et des galeries horizontales ou inclinées de belle taille en forme de tubes. Ces réseaux sont fréquemment tapissés d'argiles de décantation, abandonnées durant la phase de décrue.

3. Conséquences sur le fonctionnement de la zone épinoyée et son rôle spéléogénétique

Tout d'abord, cette zone est soumise à des variations de pression hydrostatique considérables dont les effets mécaniques sont incontestables, ainsi qu'à des circulations temporaires extrêmement abondantes. La corrosion s'effectue non seulement pendant la phase de crue où circulent des eaux agressives largement renouvelées, mais elle se poursuit en plus après le dénoyage, grâce au film d'eau recouvrant les parois, au contact avec une atmosphère relativement riche en gaz carbonique. C'est le "creusement dans la zone inondable", particulièrement efficace (CHOPPY, 1994). L'exceptionnelle concentration de conduits de grande taille dans la zone épinoyée en est la traduction.

Tous ces réseaux présentent des sections tubulaires organisées par les crues en labyrinthe anastomosés (PALMER, 1991). Ceux-ci sont disposés selon un plan horizontal, soit pour des causes structurales (utilisation des joints de stratification plats), soit au toit de la zone noyée, auquel cas les conduits sont indifférents à la trame structurale. Il s'agit des water table caves des anglo-saxons (FORD & WILLIAMS, 1989). Les conduits peuvent également s'agencer selon les discontinuités structurales en toboggans fortement inclinés, reliés par des puits verticaux ou des galeries horizontales, leur section étant toujours tubulaire. Ils forment ainsi de grandes boucles en montagnes russes dont l'ampleur dépend de la hauteur de la zone épinoyée et peut atteindre jusqu'à 250 m (fig. 3) ; ce sont les loop caves[1].

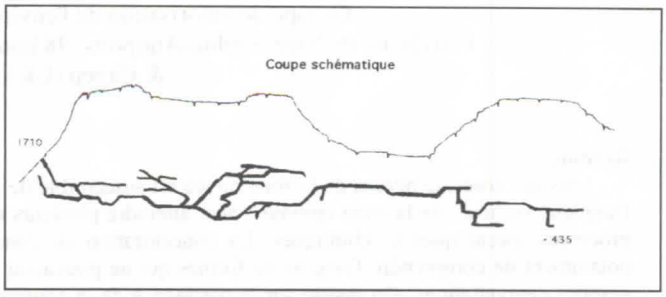

Figure 3 : le réseau de la Tantalhöhle (Salzbourg, Autriche) présente des tubes en montagnes russes dont les boucles atteignant plusieurs centaines de mètres d'ampleur correspondent à une ancienne zone épinoyée (topographie d'après COURBON & CHABERT, 1986).

Ainsi peut s'expliquer l'origine de ces tubes inclinés sur plusieurs centaines de mètres de dénivellation, caractéristiques de la base des réseaux de montagne. Ils ne peuvent en effet qu'être liés aux mises en charge de la zone épinoyée durant les crues et ne peuvent en aucun cas s'accorder avec une zone noyée dont le niveau serait stable et largement perché au-dessus du niveau de base, celle-ci ne pouvant se maintenir sans se vidanger rapidement à l'extérieur.

Ces phénomènes de mise en charge impliquent donc l'existence de circulations temporairement noyées bien au-dessus du niveau de base lors des périodes de crues. Autrement dit, il est nécessaire d'être prudent, surtout dans les karsts de montagne, lorsque l'on considère, comme c'est fréquemment le cas, d'anciens niveaux de galeries en tube comme étant des marqueurs altitudinaux de niveaux de base passés. Ils peuvent être en effet considérés comme tels, à la précaution près que le niveau de base pouvait se situer en-dessous des galeries, et parfois plusieurs centaines de mètres plus bas.

4. Vers une remise en cause du creusement noyé profond ?

Il est manifeste qu'il est difficile de théoriser sur la spéléogenèse profonde, sachant d'une part que l'on ne possède guère de données vérifiables sur les phases initiales de karstification et en particulier sur la genèse des proto-conduits et d'autre part que la connaissance des zones noyées, bien qu'ayant récemment fait d'immenses avancées grâce à la spéléo-plongée, reste encore bien insuffisante. Néanmoins, certains faits d'observation s'intègrent mal à la théorie du creusement noyé profond et impliquent, sinon une révision complète, tout au moins certaines remises en cause.

Depuis DAVIS (1931) et BRETZ (1942), cette théorie admettait qu'en l'absence d'écran imperméable à la base de l'aquifère (autrement dit dans le cas des karsts barrés), que les circulations s'enfonçaient profondément dans la zone noyée, pour remonter à la surface au contact du mur imperméable sous la forme d'une émergence vauclusienne (fig. 4-A) (on exclut le cas particulier des aquifères artésiens où les circulations sont contraintes par la structure à un cheminement profond). Ainsi expliquait-t-on l'origine des karsts profondément noyés, drainés par des

[1] FORD attribue leur genèse à un creusement toujours noyé. Selon cet auteur, la différence entre les *water table caves* et les *loop caves* serait liée à une fracturation décroissante. A notre avis, la différenciation provient en fait des variations du gradient hydraulique et de l'ampleur de la zone épinoyée (voir aussi CHOPPY, 1994).

émergences remontantes dont la fontaine de Vaucluse est l'exemple le plus marquant. Paradoxalement, on utilisait simultanément les anciens réseaux horizontaux comme indicateurs de positions de niveaux de base passés, sous-entendant implicitement que les circulations suivaient le toit de la zone noyée sans s'enfoncer en profondeur !

Or, il est désormais admis que la structuration du drainage karstique hiérarchisé dans le milieu calcaire hétérogène s'effectue sous le contrôle du gradient hydraulique, qui tend à générer des drains où les pertes de charge sont minimales (SWINNERTON, 1932 ; PALMER, 1991). Autrement dit, le "chemin de drainage" (CHOPPY, 1994) tend à se rapprocher de la ligne droite, en direction du point d'émergence. Ainsi, dans la zone vadose, les circulations s'enfoncent verticalement sous l'influence de la seule gravité. Arrivées au niveau de la zone noyée, elles prennent alors la direction de l'émergence selon une pente faible. La ligne droite étant le plus court chemin, le conduit principal suivra le toit de la zone noyée (water-table cave), ou se développera dans la zone épinoyée, lorsqu'elle existe, puisqu'elle offre la moindre résistance aux circulations, de la faible l'importance des cavités (fig. 4-B). L'utilisation des discontinuités structurales favorise l'apparition de tubes en montagnes russes (loop cave). Dans ce cas, les circulations noyées profondes sont négligeables et ne peuvent donner naissance à des conduits suffisamment importants pour concurrencer ceux de la zone épinoyée.

Les réseaux noyés profonds, pour lesquels il est nécessaire de fournir une explication cohérente, auraient dans ce cas une origine distincte (on ne prend pas ici en considération les karsts hydrothermaux dont l'énergie de provenance endogène suffit à expliquer leur existence). Cette origine pourrait très bien se trouver dans leur genèse. Ces karstifications profondes se seraient développées lors de périodes d'abaissement du niveau de base, puis elles auraient été noyées suite à une remontée du niveau de base. Les réseaux créés à grande profondeur, puis noyés, seraient toujours fonctionnels, car ils offrent les meilleures facilités de circulation du fait de leur antériorité.

De telles oscillations du niveau de base se sont effectivement produites durant le Quaternaire sous l'effet des glaciations, ainsi qu'au Messinien lors de l'assèchement partiel de la Méditerranée. Les karsts littoraux, ainsi que ceux situés à proximité des fleuves ayant profondément surcreusé leur lit parfois très en amont sur plusieurs centaines de kilomètres durant les épisodes régressifs, ont connu une telle évolution. Des concrétions actuellement noyées à plus de 100 m de profondeur attestent de la réalité de cet ennoyage (goul de la Tannerie au bord du Rhône en Ardèche - ANDRÈS & LISMONDE, 1995).

Ce modèle suggère l'abandon d'anciennes théories, en minorant l'ampleur de la karstification noyée profonde, au profit d'un drainage localisé au toit de la zone noyée et en particulier dans la zone épinoyée, car il s'accorde mieux avec les observations accumulées par les progrès récents des explorations. Il constitue un cadre de réflexion susceptible de mieux comprendre la réalité de ces phénomènes majeurs qui conditionnent toute l'organisation des réseaux que nous étudions.

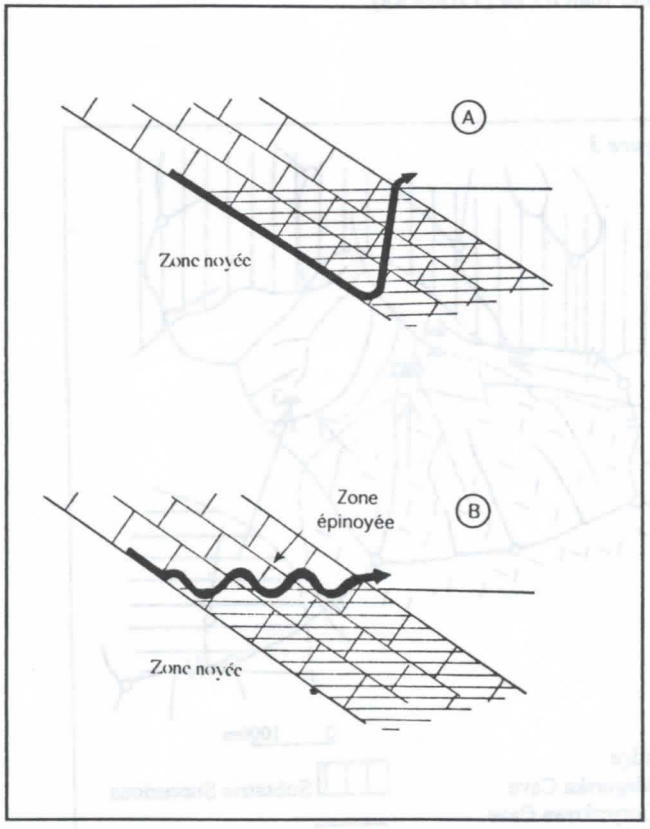

Figure 4 : disposition des conduits de drainage de la zone noyée. A) modèle critiqué, avec un creusement noyé profond et une émergence vauclusienne.
B) modèle avec un creusement au toit de la zone noyée, dans la zone épinoyée, avec des conduits en montagne russes. Les circulations noyées profondes sont marginales

Références

ANDRÈS, D. & LISMONDE, B. 1995. *Bertrand Léger, spéléonaute.* Groupe spéléo de La Tronche & Comité départemental de spéléologie, Grenoble, 126 p.

AUDRA, Ph. 1994. *Karsts alpins. Genèse de grands réseaux souterrains. Exemples : le Tennengebirge (Autriche), l'Ile de Crémieu, la Chartreuse et le Vercors (France). Karstologia Mémoires*, n° 5. Thèse à l'Université J. Fourier - Grenoble I. Fédération française de spéléologie, Paris & Association française de karstologie, Bordeaux, 280 p.

BRETZ, J. H. 1942. Vadose and phreatic features of limestone caverns. *The Journal of geology*. 50, 6 : 675-811.

CHOPPY, J. 1994. La première karstification ; *Synthèses spéléologiques et karstiques*. Choppy, Paris, 72 p.

COURBON, P. & CHABERT, Cl. 1986. *Atlas des grandes cavités mondiales*. Fédération française de spéléologie, Paris & Union internationale de spéléologie : 255 p.

DAVIS, W. M. 1931. L'origine des cavernes calcaires. *Science*. 73, 327-331.

FORD, D. & WILLIAMS, P. 1989 : *Karst geomorphology and hydrology*. Unwin Hyman, Londres : 601 p.

LISMONDE, B. & LES SPÉLÉOS GRENOBLOIS DU CAF, 1995. La crue du 18 mai 1994 au Trou qui Souffle (Vercors). *Karstologia*, 25. Fédération française de spéléologie, Paris & Association française de karstologie, Bordeaux, p. 1-12.

PALMER, A. N. 1991. Origin and morphology of limestone caves. *Geological society of American bulletin*. 103 : 1-25.

SWINNERTON, A. C. 1932. Origin of limestone caverns. *Bulletin of the geological society of America*. 43 : 663-694.

Reconstruction of paleocurrents in caves of the Bystra Valley (Tatra Mountains, Poland), on the basis of scallops and deposits analyses

Ditta Kicinska
Hydroconsult, ul. Ratajcaka 10/12, 61 - 815 Poznan
Insitute of Geology, Adam Mickiewicz University, ul. Maków Polnych 16, 61 - 686 Poznán, Poland

Abstract

Tatra Mountains are the highest and northernmost massif in the West Carpathian system (fig. 1). The central and southern parts of the Tatra Mountains are built of Paleozoic crystalline rocks. The northern slope of the massif consists of Mesozoic sedimentary rocks. Among them several overthrusted tectonic units are distinguished (which are again distinguished into shallower Hightatric Succesions and deeper Subtatric Succesions).

The Bystra Valley is the easternmost valley of the West Tatra Mountains. The karst catchment area of the Bystra Stream is considerably greater than the surface catchment of the Bystra Valley. It resulted from underground water flows, which created cave systems. The underground flows of big karst springs in the valley are supposed to come from the area lying east of the valley built up of granitoids rocks and from the west of the valley where sedimentary rocks dominate. The Southern border of the valley is built up of metamorphic rocks injected by granitoids and overthrusted over a sedimentary sequence.

The analyses of paleocurrent directions were made in bigger horizontally developed caves (Magurska 1200 m of length, Goryczkowa 312 m, Kalacka 360 m) lying 50-150 m over the present valley bottom.

The analyses of scallops asymetry and deposits (heavy minerals, roundness grades, grain size) in these caves were made in order to reconstruct the direction of paleocurrents. Variability of the mineral-petrographic composition and observations of scallops enable to distinguish two opposite directions of underground flows in these caves (fig. 2 and 3). The development of underground flows is much more complicated than it was supposed so far.

The analyses of paleocurrents and isotopic dating of speleothems with U/Th method showed that the earlier directions are older than 210 ka (+16/-14 ka) and the younger ones are older than 89 ka (+10/-9 ka).

This work was supported by grant KBN 0888/P2/94 06.

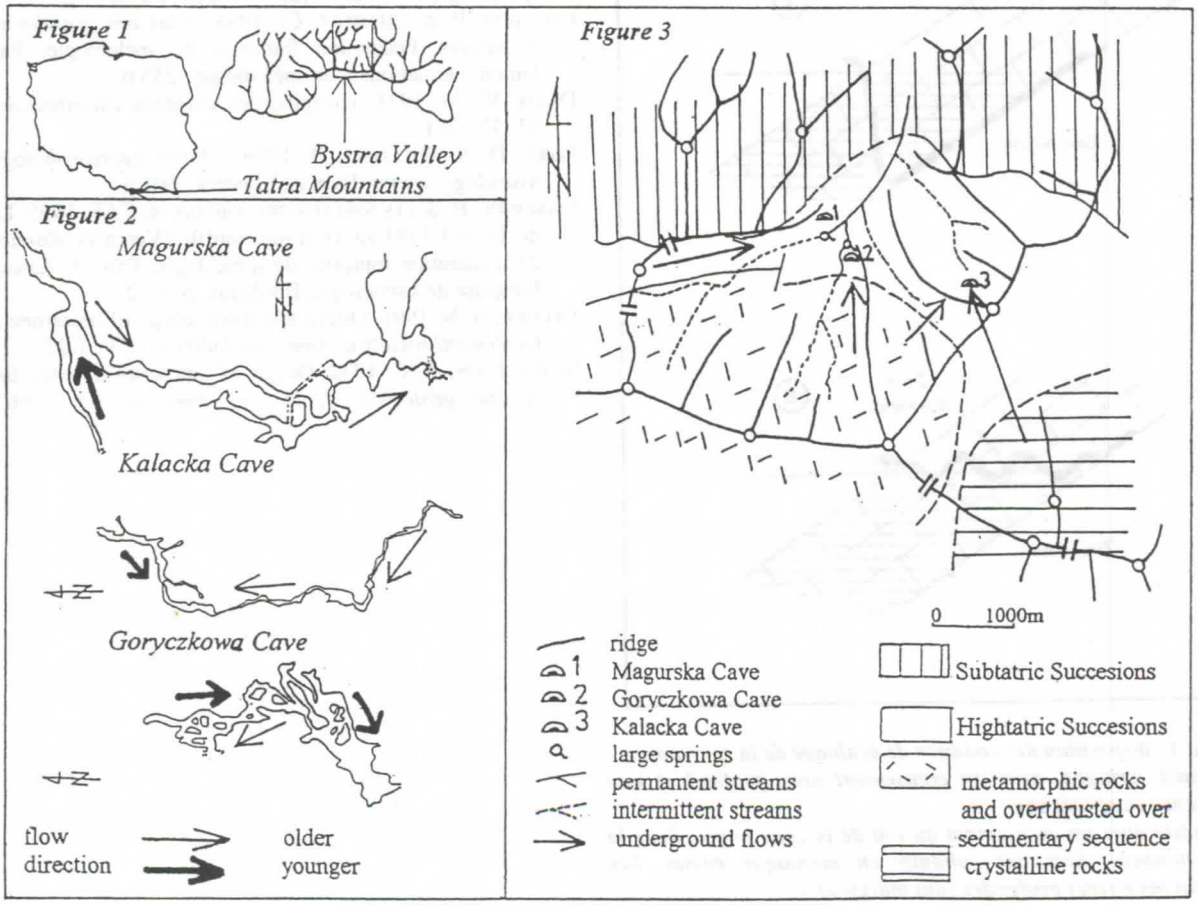

Hypothèse sur la genèse d'un siphon

par J. Foltete
Diren de Franche-Comté, 5, Rue du Général Sarrail 25014 Besançon

Abstract
Mechanical assumptions on waterflows in a limestone massif try to explain the genesis of siphons in the underground networks. This paper trends to make them complete when groundig them on tectonical and hydraulical data.

Résumé
Des hypothèses mécaniques sur les écoulements dans les massifs calcaires contribuent à expliquer la genèse des siphons dans les réseaux souterrains. La présente note vise à les compléter en s'appuyant sur les données de la tectonique et de l'hydraulique.

Introduction

De nombreuse rivières souterraines voient leur cours emprunter un tracé en siphon juste à l'amont de leur émergence et cela dans une zone où précisément existent souvent des galeries superposées, nombreuses, plus ou moins anastomosées et colmatées, témoins de circulations anciennes.

La présence d'un siphon est, en spéléologie, un phénomène suffisamment général pour que l'on se pose la question de sa genèse : Pourquoi en effet l'eau des massifs calcaires ne descend elle pas tranquillement, ou par chutes successives, jusqu'au niveau de l'émergence, pourquoi l'existence de cette section en conduite forcée juste avant la sortie à l'air libre?

Les explications mécaniques du phénomène, s'appuyant sur les bilans énergétiques des écoulements, ne répondent que partiellement aux questions posées; d'autres explications se trouvent dans la connaissance de la structure du massif mais cela revient à l'étude d'un cas d'espèce à partir de relevés géologiques et la transposition à d'autres systèmes n'est pas généralisable.

Une hypothèse ancienne

P. Pétrequin s'est beaucoup interrogé sur cette question, notamment à l'occasion de ses sorties et publications sur le Verneau*; il avance l'hypothèse de la détente des calcaires en bordure des vallées. Très succinctement, on peut résumer cette hypothèse comme suit : Parallèlement à la vallée, la bordure du plateau est affectée par des "plans de détente "du calcaire qui entraînent par "appel au vide" une fissuration transversale au réseau karstique; ces plans affectent le plateau sur une frange de quelques dizaines à quelques centaines de mètres.

On peut concevoir en effet que dans une vallée où l'érosion a fait disparaître une grande épaisseur de sédiment, des réajustements isostatiques ou liés à la décompression du sédiment, entraînent des mouvements qui sont à l'origine des ruptures en bordures; l'interface alors se traduit par un plan vertical, parallèle à la vallée, limitant deux domaines; ce plan correspond à une surface de "décohésion" de "microfissuration" de la roche et peut être multiple comme cela apparaît dans ce schéma que l'on doit à Pétrequin.

Chacun a pu vérifier la justesse de ce schéma au cours d'expéditions spéléologiques ou de relevé de fissuration. Cette hypothèse est compatible avec l'idée d'un effet qui se propage à partir du bord de la vallée vers l'intérieur du plateau au fur et à mesure de l'élargissement de celle-ci. Dans ce cas, les panneaux effondrés, en bordure de falaise, ne sont que des réajustements d'équilibre dans la morphologie actuelle.

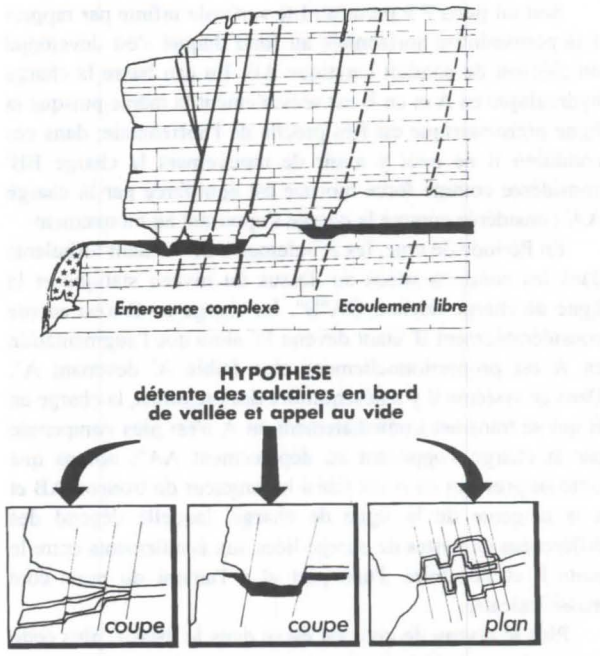

P. Pétrequin, 1980

Autre hypothèse

Soit un plateau tel que l'a imaginé P. Pétrequin limité par une vallée; en bordure de celle-ci et parallèlement à son axe de développement, la détente des calcaires a occasionné des plans de microfissuration; dans ces plans verticaux la porosité est plus importante que dans le reste du massif entraînant une meilleure perméabilité verticale.

Si en outre quelque accident tectonique vertical, incident sur la vallée, recoupe les plans précédents on remarquera que les conditions sont réunies pour la constitution d'un axe préférentiel de fissuration à l'intersection des deux plans verticaux, véritable "puits potentiel" à l'intérieur du massif. En cas de développement d'un karst à partir de l'accident tectonique précédent le "puits potentiel" est appelé à jouer un rôle particulier dans l'apparition du siphon.

L'eau de pluie tombant sur le massif s'infiltre lentement dans les microfissures sous l'effet combiné de la pesanteur et des forces capillaires opposées. Si ce cheminement croise un segment plus perméable -joint de stratification, plan de fissuration- et que ce segment conduise à une zone de libre écoulement, l'eau empruntera ce parcours dès que la pression dans le massif sera suffisante, soit au moment de l'averse. Au voisinage du niveau de base, la présence permanente de l'eau améliore la dissolution, par augmentation du temps de contact

et le processus de creusement d'abri sous roche ou de vasque, embryon de réseau, pourra s'enclencher. A l'intérieur du massif, dans un "puits potentiel" la karstification se développe avec la même logique de descente vers le niveau de base.

En fond de puits, là où la dissolution est la plus importante, l'absence de soutirage par le fond peut ralentir l'évacuation des produits de dissolution qui se fera néanmoins par diffusion dans la colonne d'eau puis renouvellement lors de la montée de l'averse. Si, au cours de sa descente, la karstification rencontre un plan horizontal plus fissuré, pourront se créer des conditions favorables à l'utilisation du cheminement hydraulique le plus économe en perte de charge (voir schéma). L'agrandissement du schéma illustre les conditions dans lesquelles le "cheminement hydraulique minimum" pourra entrer en fonctionnement et être à l'origine d'un écoulement en siphon.

Soit un puits P à perméabilité verticale infinie par rapport à la perméabilité horizontale au fond duquel s'est développé un élément de conduit karstique AB. En eau basse la charge hydraulique en A et en B est sensiblement la même puisque la ligne piézomètrique est très proche de l'horizontale; dans ces condition il ne peut y avoir de mouvement la charge BB' considérée comme force motrice est équilibrée par la charge AA' considérée comme la charge s'opposant au mouvement.

En Période de crue, les écoulements deviennent turbulents dans les conduits situés au dessus du niveau statique et la ligne de charge devient OA"B". La charge en B s'est accrue considérablement B' étant devenu B" alors que l'augmentation en A est proportionnellement plus faible A' devenant A". Dans ce système il y a déséquilibre des pressions, la charge en B qui se transmet immédiatement en A n'est plus compensée par la charge s'opposant au déplacement AA"; notons que cette surpression en A est liée à la longueur du tronçon AB et à la tangente de la ligne de charge, laquelle dépend des différences de pertes de charge liées aux écoulements entre le puits P et l'exutoire d'une part et à l'amont du puits côté massif calcaire.

Plus le niveau de crue est élevé dans le massif, plus cette surpression est importante et pour un niveau de rupture suffisant les écoulements se feront dans les microfissures entre A et O

Ainsi les conditions pour la création d'un siphon sont :

- L'existence de puits verticaux liés à l'intersection de deux plans de microfissuration permettant une circulation de haut en bas plus facile dans le massif;
- Une dissolution maximale sous le niveau de base par augmentation du temps de contact et une évacuation des produits de dissolution à la montée des eaux;
- L'existence de zone à meilleure perméabilité horizontale, joint de stratification par exemple, permettant, par leur karstification, la création de segments économes en perte de charge.

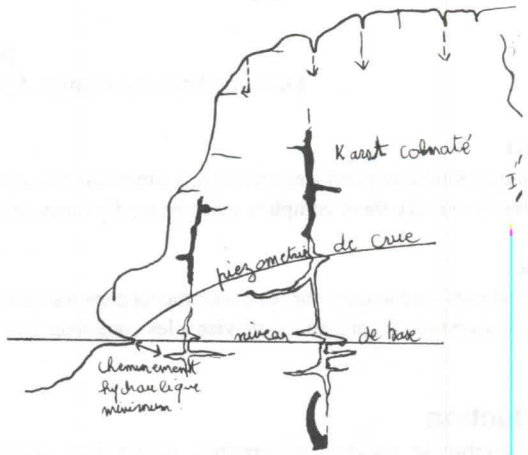

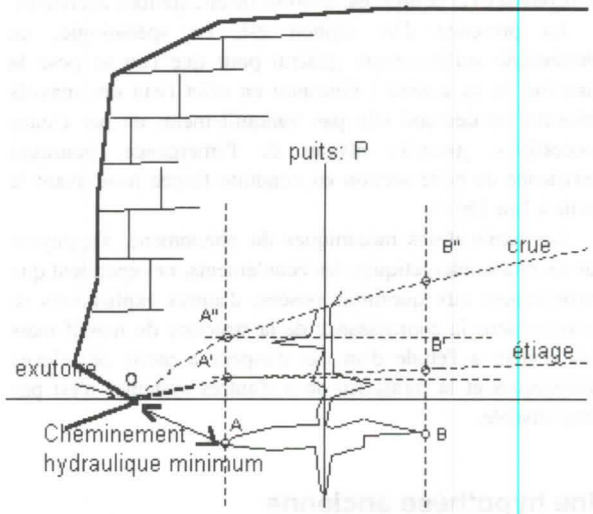

Dans cette hypothèse, il est admis que la première fissure horizontale rencontrée sous le niveau de base sera karstifiée et se développera en raison de la présence permanente d'eau, limitant d'autres développements à un niveau inférieur, et que l'extension vers l'intérieur du massif est limitée par l'absence de plan de décompression dès que l'on se situe au delà de la frange de terrain affecté par la détente du calcaire.

Références

AUCANT, Y., C. SCHMITT & J.P.URLACHER. 1985. Le Verneau souterrain, Ed. SHAG

Hydrologie du système karstique du Rupt du Puits (Lorraine/Champagne, France) : Fonctionnement du siphon aval

par Stéphane Jaillet,
Laboratoire de Géographie Physique Appliquée - Université Michel de Montaigne Bordeaux 3 - 33 405 Talence - France
avec l'aide du Laboratoire de Géographie Physique de l'Université de Metz - Ile du Saulcy - 57 045 Metz Cedex 1 - France.

Abstract
Under the lowland plateaus located at the border line between Champagne and Lorraine, we find a covered karst called the "Rupt du Puits", wich is an affluent of the river Saulx. The subterranean main river arm alternately flows under and overground. Downstream, a 450 m siphon runs into two points of emergences : a permanent one saturing at a flow of about 300 to 400 l/s, and a temporary one getting active when the permanent one reaches a flow of 200 l/s. Globally the siphon's feeding pattern is complex. Infiltrating water via the main river arm feeds the springs, though it does not contribute by more than two thirds to their flow. When reflecting on the origins of the hydrous complement, we are led to believe that it might be provided by other phenomena, in particular by the Saulx itself. Both the morphological aspects and the varuous measuring campaigns carried through seem to be indicative of a karstic type water circulation beaneath base level adding to the downstream water flow.
Key-words : karst system, siphon, water bearing bed/river communication, emergence, Rupt du Puits, Barrois, Lorraine.

Résumé
Au contact de la Champagne et de la Lorraine se développe un karst couvert de bas plateau : le Rupt du Puits, affluent de la Saulx. Le collecteur souterrain présente une alternance de zones tantôt noyées tantôt à surface libre. Le siphon aval, long de 450 m débouche sur deux émergences : l'une pérenne saturant vers 300 à 400 l/s et l'autre temporaire se déclenchant quand la pérenne est à 200 l/s. Son alimentation est complexe. L'infiltration rejoint, via le collecteur, la zone des émergences mais ne participe qu'auxx 2/3 de leur débit. La recherche d'un complément hydrique pousse à supposer une alimentation par d'autres drains et par la Saulx elle-même. Les données morphologiques et les différentes campagnes de mesures tendent à mettre en évidence une circulation karstique, fonctionnant sous niveau de base et participant à l'alimentation du siphon aval.
Mots-clés : système karstique, siphon, échange nappe/rivière, émergence, Rupt du Puits, Barrois, Lorraine.

1. Un karst couvert de Bas-Plateau

Un pays de contact

Entre Lorraine et Champagne, dans la partie est du Bassin Parisien, se développe le karst couvert du Rupt du Puits. Plus important système karstique souterrain connu du nord de la France, c'est aujourd'hui plus de 21 km de conduits qui ont été reconnus. Le plus important réseau de ce système développe à lui seul 11 800 m et fut reconnu en grande partie en exploration post-siphon au début des années 70 avant que ne soit percé un forage d'accès de 47 m qui permet aujourd'hui de prendre pied directement dans la rivière souterraine. Cette unité hydrogéologique (mise en évidence par de nombreux traçages) assure, en forêt de Trois Fontaines, la transition entre deux ensembles morphostructuraux. A l'Ouest, c'est le Perthois et le Vallage où les dépôts argilo-sableux du Crétacé déterminent un paysage de plaine à topographie molle.

Ils recouvrent, en discordance, vers l'Est les plateaux calcaires du Barrois. Armés par les dépôts carbonatés du Portlandien, ces derniers offrent un paysage plus sec où les rivières (la Saulx et l'Ornain) ont incisé des vallées sur une centaine de mètres de profondeur (Fig. 1).

C'est dans ce contexte que se développe donc le collecteur souterrain du Rupt du Puits. Le drain principal, long de 7 km, est connu sur plus de 80% de son parcours. C'est une succession de zones noyées et de zone à surface libre. De l'amont vers l'aval, la Dorma, la Béva et la rivière souterraine du Rupt de Puits zone trois secteurs où l'écoulement rapide, exondé, tranche avec les zones noyées qui les séparent (Fig. 2). Le dernier siphon, le plus à l'aval présente une diffluence. Une première branche (la plus au nord) rejoint l'émergence pérenne du Rupt de Frainiau. La seconde (la plus au sud) file vers la vasque temporaire du Rupt du Puits. Cette dernière, légèrement perchée, fait office de trop plein de la première. C'est cette vasque, qui, plongée dans les années 60 - 70, permit la découverte des réseaux donnant son nom à tout le système. Nous ne nous intéresserons dans le présent article qu'au fonctionnement d'une de ces zones noyées : le siphon aval.

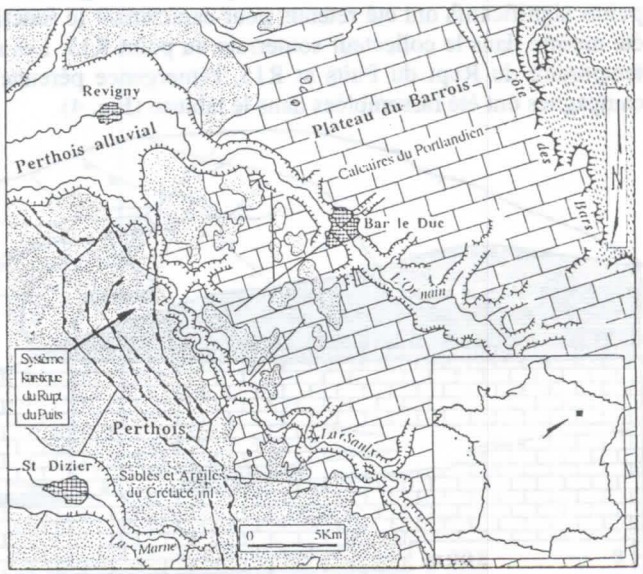

Figure 1 : Situation du karst du Rupt du Puits au contact du Barrois calcaire et du Perthois argilo-sableux.

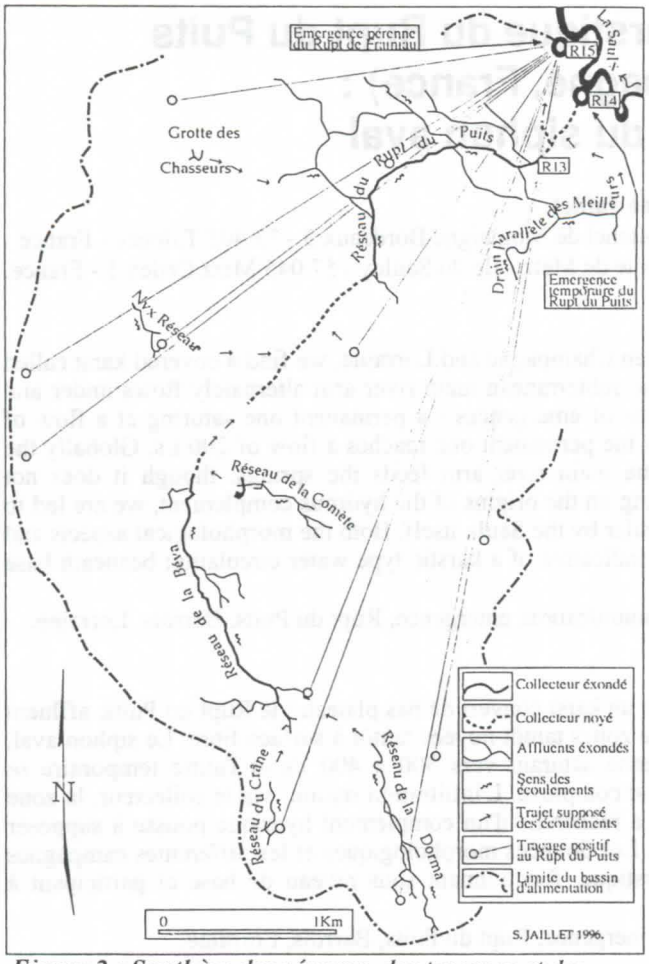

Figure 2 : Synthèse des réseaux, des traçages et des limites du bassin d'alimentation du Rupt du Puits

Le siphon aval

Les premières plongées dans le siphon aval du Rupt du Puits sont l'oeuvre de Bertrand LEGER. Après la lecture d'un article de DESCAVES publié en 1962 dans Spélunca, il se rend à la fin des années 60 à Robert Espagne, dans la Meuse, puis au bord de la vasque et pénètre dans la galerie noyée. Plusieurs plongées seront nécessaires pour le franchir et c'est finalement une équipe de jeunes meusiens qui le 16 novembre 1971 passe le siphon (LUCION, in JAILLET, 1994).

Il a été décrit comme suit. C'est une galerie, d'abord étroite et ébouleuse qui adopte ensuite une section plus régulière (3 à 4 m de large pour 2 à 3 m de haut). Trois cloches franchies à 97, 188 et 256 m, et l'écoulement jusqu'alors temporaire devient pérenne. A cet endroit, la fameuse diffluence permet aux écoulements de filer au Nord vers le Rupt de Frainiau. Les tentatives de plongées vers cette branche n'ont rien donné. Un fort remplissage occupe le fond de la galerie qui, devenant de plus en plus basse devient infranchissable. Côté Rupt de Frainiau (l'émergence pérenne), les tentatives de plongées n'ont de même rien donné. Un amas de blocs barre effectivement l'accès. De la vasque du Rupt du Puits au collecteur souterrain, c'est 445 m de siphon qui ont donc été franchit. C'est à l'époque un véritable exploit et le Rupt du Puits restera un temps le plus long réseau au monde exploré derrière siphon. Depuis que le forage d'accès au collecteur du Rupt du Puits a été creusé en 1975, il semble que plus aucun plongeurs n'ait franchi le siphon (Fig. 3). Nous avons en projet de faire revisiter ce siphon pour en obtenir un levé morphologique le plus précis possible.

En attendant, c'est comme une boite noire que nous avons décidé d'aborder le fonctionnement de ce sous-système du système karstique du Rupt du Puits.

C'est à dire en analysant ce qui y entre et ce qui en sort. Pour cela plusieurs mesures de débits, conductivités, températures et quelques analyses physico-chimiques complémentaires ont été mises en place (DEVOS *et al.*, 1996). Ces mesures se répartissent dans l'année de façon hétérogène, mais touchent différentes situations hydrologiques.

2. Dix campagnes de mesures de débits sur le siphon aval du Rupt du Puits

A dix reprises, nous avons pu mener des campagnes de mesures sur le siphon aval du Rupt du Puits. Chacun de ces points de jaugeage a été mesuré à la perche à intégration de mesure de débits, tant sous terre qu'aux émergences. Trois points significatifs ont été retenus pour caractériser le fonctionnement du système siphon aval. L'entrée dans le système a été mesuré dans le collecteur souterrain au point R13. Les sorties du système sont les deux émergences : R14, la vasque temporaire du Rupt du Puits et R15, l'émergence pérenne du Rupt de Frainiau. Les valeurs obtenues lors de ces dix campagnes ont été rassemblées dans le tableau (Fig. 4).

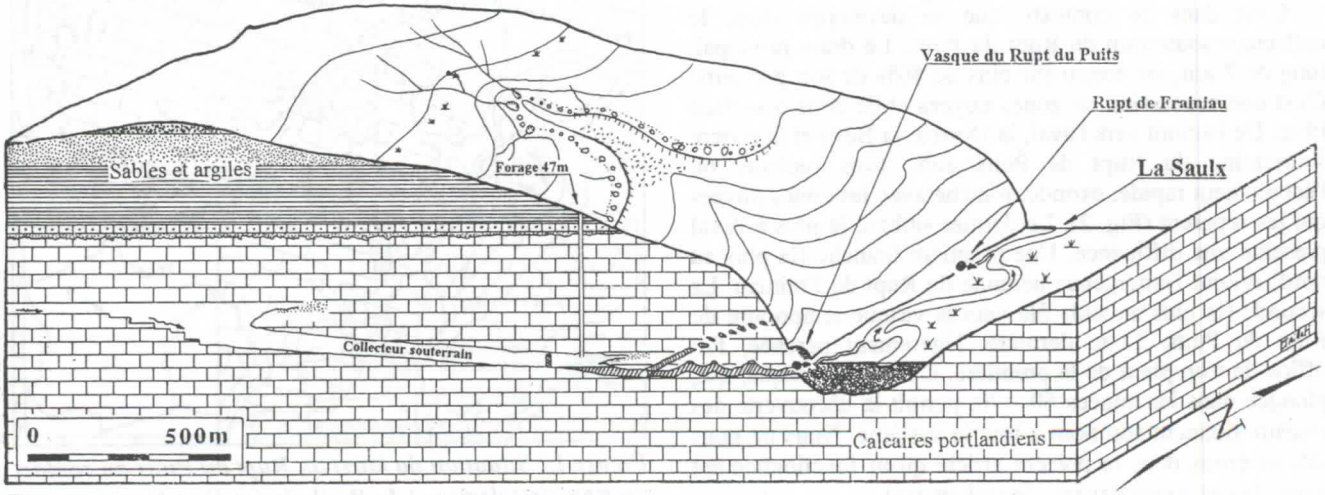

Figure 3 : Bloc diagramme du site du réseau du Rupt du Puits.

Figure 3 : Bloc diagramme du site du réseau du Rupt du Puits.

Campagnes de mesures	Collecteur R 13 enl/s	Vasque RdP R 14 en l/s	R. Frainiau R 15 en l/s	Total Emergences	Apport siphon (l/s))	% par rapport au collecteur	situation hydrologique
22-Fév-95	139	0,39	232	232,39	93,39	67,19	Hautes eaux
23-Fév-95	224	72	272	344	120	53,57	Hautes eaux
24-Fév-95	1029	1271	451	1722	693	67,35	Crue hivernale
9-Déc-95	19	0	15	15	-4	-21,05	Étiage (R15 douteux)
25-Fév-96	316	171	219	390	74	23,42	Fonte nivale (petite crue)
26-Fév-96	200	2,2	224	226,2	26,2	13,10	Fonte nivale (décrue)
21-Mar-96	26	0	52	52	26	100,00	Étiage hivernal
7-Avr-96	22	0	38	38	16	72,73	Étiage hivernal
7-Déc-96	186	99	185	284	98	52,69	Décrue
8-Déc-96	167	20	141	161	-6	-3,59	Décrue

Figure 4 : Débits (en l/s) en R13 (collecteur à l'amont du siphon) et aux deux émergences (R14 et R15) et apport calculé du siphon à partir de ces débits, lors de dix campagnes.

Il apparaît que dans tout les cas (sauf un), le débit aux émergences est supérieur à celui du collecteur souterrain. Le rapport moyen entre l'entrée dans le système (le collecteur R13) et la sortie du système (les émergences R14 + R15) est de 1,6. Selon la situation hydrologique, l'importance relative des deux émergences varie, exprimant la très grande variabilité des débits que peut supporter l'émergence temporaire (ici 0 à 1271 l/s) à la différence de l'émergence pérenne (15 à 451 l/s) (JAILLET, 1996).

Le cas du 9 décembre 1995 est intéressant à plus d'un titre. C'est la campagne d'étiage la plus basse. Sous terre, le débit est de 19 l/s. L'émergence temporaire ne coule pas tandis qu'au Rupt de Frainiau (l'émergence pérenne), il coule 15 l/s. C'est le seul cas de déficit. Il est très tentant de mettre ce déficit en rapport avec une perte de débit dans le conduit souterrain à la faveur d'une émergence sous-alluviale aujourd'hui inconnue. L'existence d'autres émergences sous-alluviales mise en évidence par traçage colorimètrique (Vieux Jeand'Heurs, Usine de Beurey sur Saulx) accrédite cette hypothèse. Cependant, il est bon de noter les conditions de mesures médiocres qui règnent à l'émergence du Rupt de Frainiau (R15) : section large, eau profonde, fond vaseux et surtout vitesse d'écoulement très lente. Une erreur de quelques litres secondes dans la mesure modifie de manière considérable le résultat. On se gardera donc de toutes conclusions hâtives tant que d'autres mesures n'auront pas permis de confirmer ce fait. Les campagnes ont alors été classées selon les débits en R13 et représentées dans le graphique suivant.

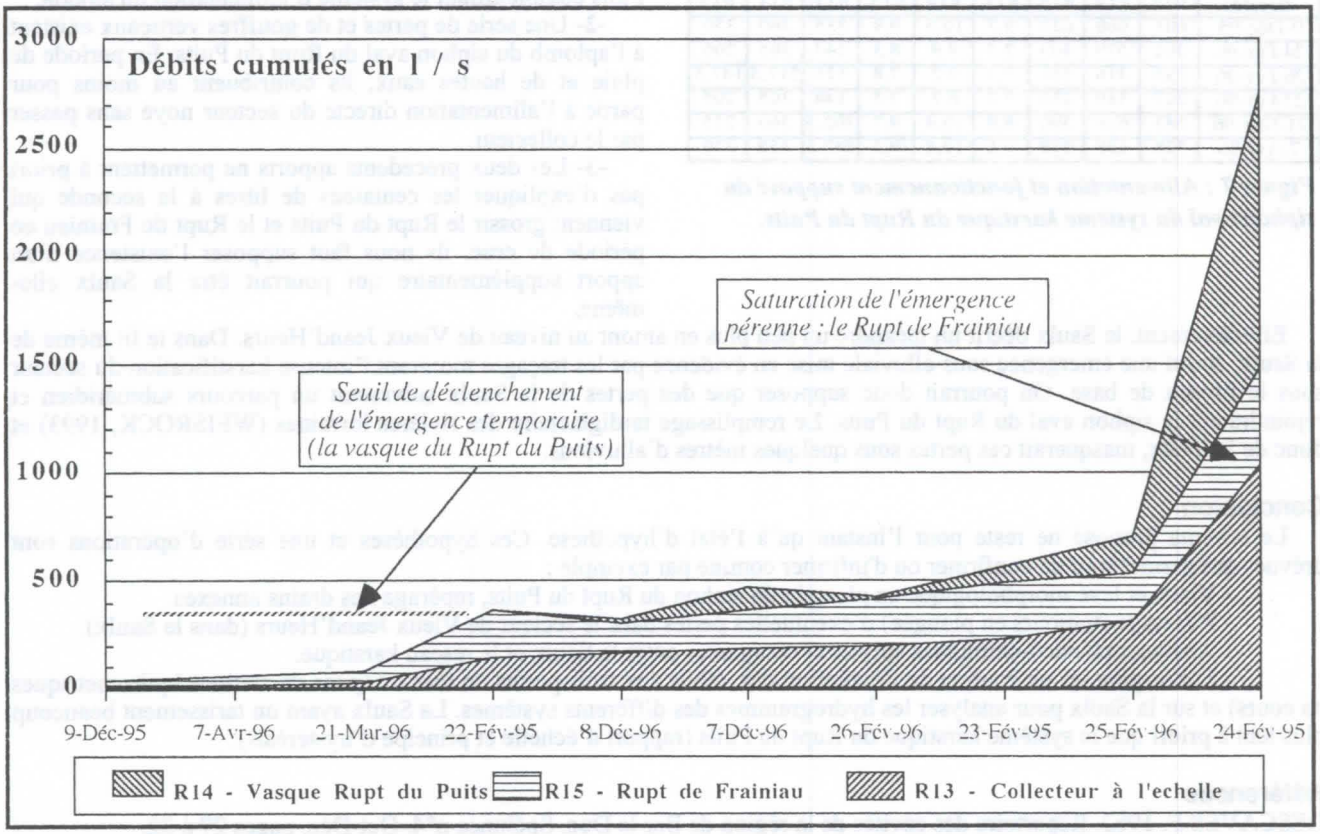

Figure 5 : Représentation graphique des dix campagnes de mesures de débits aux trois points caractéristiques du siphon aval du Rupt du Puits.

Sur les quatre premières campagnes (Fig. 5), quand le débit, augmente sous terre (au collecteur), il augmente (toute proportion gardée) à l'émergence pérenne : le Rupt de Frainiau. La vasque (temporaire) du Rupt du Puits elle, ne coule toujours pas. A partir d'un certain débit que nous qualifierons de débit seuil, la vasque s'amorce et se met à couler. A

partir des campagnes de mesures dont nous disposons, il semble raisonnable de penser que ce débit seuil se situe entre 210 et 230 l/s. Si le débit au collecteur continue d'augmenter, la vasque temporaire du Rupt du Puits prend le relais et son débit augmente dans des proportions bien plus importantes que le Rupt de Frainiau qui voit son débit continuer de croître mais semble vite saturer.

Les mesures de conductivités, de températures et les différentes analyses physico-chimiques réalisées sur les trois points caractéristiques du siphon aval du Rupt du Puits permettent de préciser la nature de ces écoulements souterrains (Fig. 6). On constate ainsi que quelle que soit la situation hydrologique, la conductivité, la température et la dureté totale des émergences sont supérieures aux valeurs du collecteur souterrain. Systématiquement, la vasque temporaire du Rupt du Puits est la plus chargée, et la plus chaude. Certes, durant son parcours noyé, l'eau continue à se charger, mais les 450 m de parcours souterrain ne suffisent pas à expliquer une telle variation du chimisme.

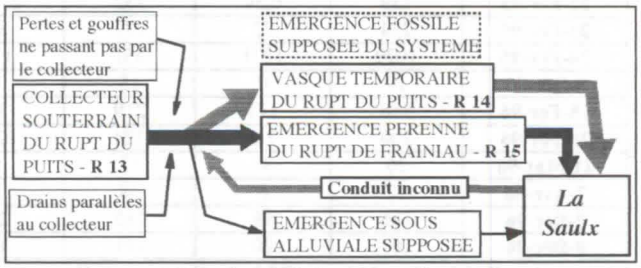

Figure 6 : Conductivités, températures et duretés totales lors de quelques campagnes.

Ainsi lors de la campagne du 24 février 1996, la charge dissoute en carbonates double en moins de 500 m de parcours souterrain noyé et ceci pour une vitesse de transit de l'ordre de 3 à 6 heures. Comme pour les débits, le chimisme montre un apport d'eau complémentaire dont il nous faut trouver l'origine.

3. Vers un schéma de fonctionnement du siphon

A partir de ce constat, il convient de tenter de déterminer la nature des apports qui permettent d'expliquer l'augmentation de débit et la variation de chimisme dans le siphon aval du Rupt du Puits (Fig. 7). Ils peuvent selon nous être de trois types :

-1- Une série de drains parallèles au collecteur du Rupt du Puits rejoignent le système dans le siphon aval. L'un au moins est assez bien connu, c'est le drain parallèle des Meilleurs.
Une coloration dans cette galerie a permis de montrer son appartenance au système.

Campagne de mesures	Conductivités en uS / cm			Températures °C			Duretés mg/l eq. Ca		
	R13	R14	R15	R13	R14	R15	R13	R14	R15
9-Déc-95	601	660	622	9,7	10,5	9,9	335	360	350
24-Fév-96	262	579	409	7,5	9,9	8,3	144	305	205
26-Fév-96	235	416	251	7,5	9,2	7,8	125	217,5	147,5
27-Fév-96	227	339	235	7,2	8,7	7,5	144	305	205
21-Mar-96	543	636	590	8,8	10,4	9,7	302,5	360	275
7-Avr-96	528	638	578	9,1	10,4	9,7	287,5	355	320

Figure 7 : Alimentation et fonctionnement supposé du siphon aval du système karstique du Rupt du Puits.

A partir d'un certain débit, ce drain se met de même à déborder et rejoint le collecteur souterrain du Rupt du Puits complexifiant le système d'alimentation du siphon.

-2- Une série de pertes et de gouffres verticaux existent à l'aplomb du siphon aval du Rupt du Puits. En période de pluie et de hautes eaux, ils contribuent au moins pour partie à l'alimentation directe du secteur noyé sans passer par le collecteur.

-3- Les deux précédents apports ne permettent à priori pas d'expliquer les centaines de litres à la seconde qui viennent grossir le Rupt du Puits et le Rupt de Frainiau en période de crue. ils nous faut supposer l'existence d'un apport supplémentaire qui pourrait être la Saulx elle-même.

Effectivement, la Saulx décrit un méandre un peu plus en amont au niveau de Vieux Jeand'Heurs. Dans le lit même de la Saulx, sourd une émergence sous-alluviale mise en évidence par les traçages montrant l'intense karstification du secteur sous le niveau de base. On pourrait donc supposer que des pertes de la Saulx suivraient un parcours subméridien et rejoindraient le siphon aval du Rupt du Puits. Le remplissage tardiglaciaire des rivières lorraines (WEISROCK, 1993) et donc de la Saulx, masquerait ces pertes sous quelques mètres d'alluvions.

Conclusion

Le schéma proposé ne reste pour l'instant qu'à l'état d'hypothèse. Ces hypothèses et une série d'opérations sont prévues qui permettront de confirmer ou d'infirmer comme par exemple :

- Visite et levé morphologique en plongée du siphon du Rupt du Puits, repérage des drains annexes.
- Repérage (toujours en plongée) d'éventuelles pertes dans le secteur de Vieux Jeand'Heurs (dans la Saulx).
- Analyses physico-chimiques suivies et comparées entre la Saulx et le réseau karstique.
- Suivis poussés en continu de l'évolution des débits aux trois points de mesure (pose de stations hydrométriques en cours) et sur la Saulx pour analyser les hydrogrammes des différents systèmes. La Saulx ayant un tarissement beaucoup plus lent à priori que le système karstique du Rupt du Puits (rapport d'échelle et principe d'hystérésis).

Références

DESCAVES F. 1962. Répertoire des cavités de la région de Bar le Duc. Spélunca n°4. Oct-Déc. pages 27 à 32.
DEVOS A. DEPAQUIS J.P. HERBILLON C. JAILLET S. 1996. Une campagne de mesures de débits au Rupt du Puits. Écho des cavernes meusiennes n°4. CDS 55. Bar le Duc.
JAILLET S. 1994. Une classique revisitée: L'aventure du Rupt du Puits. Spéléo n°18, la spéléo grand format. page 3 à 6.
JAILLET S. 1996. Dynamique des karsts couverts de bas-plateaux : L'exemple du Rupt du Puits. Morphologie, Hydrologie, Indicateurs de l'environnement. D.E.A. Université Michel de Montaigne Bordeaux III. 151 p.
WEISROCK A. 1993. Le remplissage tardiglaciaire et holocène des vallées lorraines. L'eau, la terre et les hommes : au fil de l'eau, hommage à R. FRECAUT. Presses universitaires de Nancy, page 303 à 309.

The Role of Groundwater in the Genesis of Resava Cave

by Danica Vasileva
Federal Hydrometeorological Institute, Birčaninova 6, 11000 Belgrade, Yugoslavia

Abstract

Resava Cave is situated in the northern marginal part of the Divljakovac Polje in the eastern part of Yugoslavia. One of the region's most beautiful caves (also called the Resava Jewel) or was created by a long geological history of primarily groundwater activity. The cave is impressive and rich in sinter decorations such as stalagmites and stalactites.

The genesis of Resava Cave is very complex and its generation was determined by many factors, primarily by tectonic and hydrogeological ones.

Water impacts on the cave's genesis have been connected with Alpine orogenesis. In the geological past, a stream flowed through the Divljakovac Polje. At that time, the river bed was at the cave entrance level and water was discharged in part and infiltrated into minor and major fissures, resulting in mechanical and chemical processes in the carbonate rocks which created the cave and its present appearance.

Résumé

La Caverne Resava est située au nord bord du champ calcaire Divljakovac à la part orientale de Yougoslavie.

Une de la plus belle caverne (appelée aussi la Caverne Gemme) était crée pendant une longue histoire géologique avec des eaux, en premier lieu, des eaux souterraines. La caverne semble impressive, rich avec les ornaments des concrétions calcaires comme des stalactites et des stalagmites.

La genèse de la Caverne Resava est très complexe et sa forme est définie par beaucoup de facteurs, premièrement tectoniques et hydrogéologiques.

Le but de ce travail est une représentation de la rôle des eaux souterraines sur la genèse de la Caverne Resava.

L'action des eaux souterraines sur la création de la caverne était en liaison avec Orogenèse alpine dramatique. Dans le passé géologique un cours d'eau était écoulé en traversant le champ de Divljakovac. Autrefois, le fond du lit était au niveau avec l'entrée de la caverne et une part d'eau était débordée et pénétrée à travers les crevasses moins grandes et plus grandes, faisant au long de sa route des procès mécanique et chimique dans le roches calcaires ce pourquoi on est crée la forme de la caverne avec le temps.

1. Introduction

The aim of this paper is to attempt to explain the genesis of Resava Cave as the result of complex geologic factors, and especially by groundwater activity. The geology, tectonic development, geomorphological features surrounding the cave were presented by YUGOSLAV COMMITTEE FOR INTERNATIONAL HYDROLOGICAL DECADE (1976) and by CIRIC (1996). A general review of the cave's genesis relative to Balkan tectonism was given by VASILEVA (1995)

2. A general review

The recent "static" phase of the Resava Cave's genesis has been preceded by sedimentation of limestone and intensive tectonic development which continued for a long time on the Balkan Peninsula. The large carbonate masses were deposited from Middle Triassic to Upper Cretaceous Time, beginning approximately 235 million years ago (Table 1).

Carbonate rocks of the Tertiary age occur sporadically cover smaller surfaces.

Intensive tectonic deformation of carbonate rocks related to Alpine orogenesis, began during movements that created the chain of mountains such as the Alps, Carpatho-Balkanian Arc, Caucasus and some mountains in Asia.

During that period of time, the majority of the initial conditions were created, such as faults, fissures and cracks.

MESOZOIC			CENOZOIC		PERIOD
T	J	Cr	Tc	Q	
280	195	137	67	1.5	Age [Million years]
CARBONATE ROCKS					Sedimentation
ALPINE OROGENESIS			Neotectonic		Tectonic
PRE-PHASE (Sedimentation) and TECTONIC PHASE (Dynamic Development)			Recent phase ("Static")		Cave's Genesis

Table 1: Chronological review of carbonate sedimentation, tectonic and cave's genesis on the Balkan Peninsula

Alpine orogenesis continued for about 150 million years from the Middle Jurassic. During the Middle Oligocene, this stage calmed but the tectonic activity continued by neotectonic development of terrain which is present today. The main stage of the cave's formation by groundwater activity was related to the late Tertiary and beginning of Quaternary, when the majority of territory was covered by water. In the Quaternary, during the major climatic changes, water played an essential role in genesis of underground karst forms.

3. Position, geological composition and tectonic development of the terrain

The Resava Cave is situated about 140km to the south-east of Belgrade (Figure 1) in the valley of the Divljakovac River, a southern tributary of the Resava River. The cave entrance is 483m.a.s.l. The cave was discovered more than three decades ago and was opened in 1972 for tourist visits.

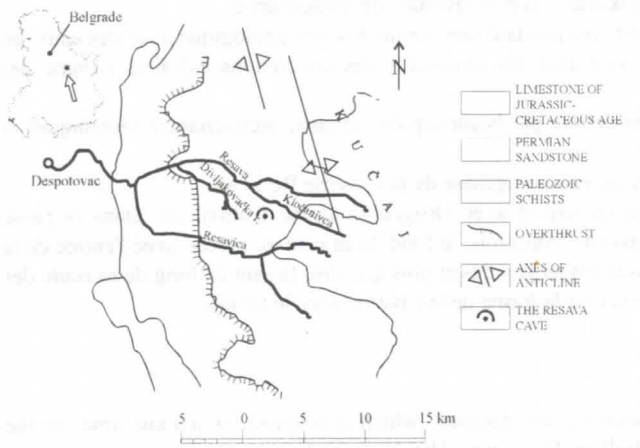

Figure 1: Position and geological composition of Resava Cave surroundings (Source: YUGOSLAV COMMITTEE FOR INTERNATIONAL HYDROLOGICAL DECADE, 1976)

The geological composition surrounding Resava Cave (Figure 1) is complex (ANTONIJEVIĆ *et al.*, 1962; BOGDANOVIĆ, 1968) The limestone rocks of Jurassic-Cretaceous age extend as a belt of 10km width between Permian sandstone in the west and Paleozoic schist in the east. The complex geological composition of terrain is a consequence of tumultuous geological past (CIRIC, 1996).

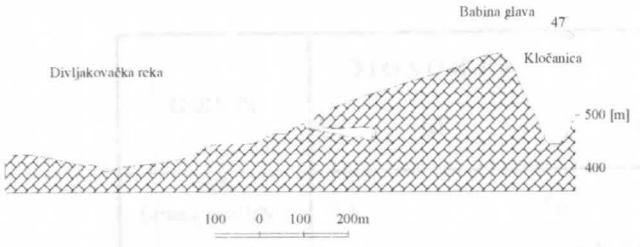

Figure 2: Position of Resava Cave in the limestone of Kučaj's anticline

The main stages of Resava Cave's development can be involved in the scheme mentioned above. The Permian sandstone in the west was dragged on the Mesozoic limestone as an overthrust, probably at the beginning of Tertiary. During the Alpine orogene stage, the limestone of Jurassic-Cretaceous age was folded with the axes generally oriented north-south. Resava Cave is situated in the western slopes of Ku~aj's anticline (Figure 2).

By folding of carbonate rocks in Alpine orogenesis, faults and fissures were created, predominant directions of the future groundwater flows and underground karst development.

4. Geomorphological features of Resava Cave

From the geomorphologic point of view, Resava Cave is a very complex karst phenomenon. The ground plan of the cave is an irregular shape (Figure 3). This dry cave is a former ponor, consisting of halls, canals and crevices situated at two levels. The difference between the highest (482.6) and the lowest elevation (453.7) is 28.9m.

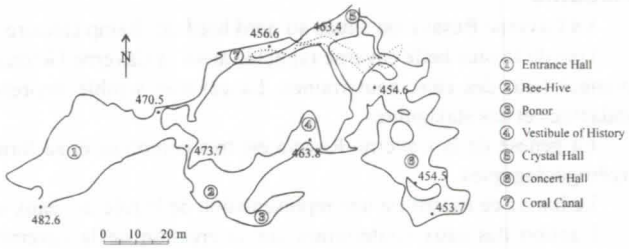

Figure 3: The ground plan of Resava Cave (Source: LAZAREVIĆ, 1991)

The entrance of the cave leads to the Entrance Hall, which has approximately 630m^2 of the floor area, and reaches ceiling heights of 2-3m. From there, the path leads southern and down into the Bee-Hive, which is 4-5m high and divides into Ponor to the south and to the Vestibule of History to the north which is 7-8m high. The path continues north for 20m along a dug passage and enters the Crystal Hall which is rich in stalactites, and reaches ceiling heights of about 4m. The Crystal Hall has three exits: one leads into narrow canal that heads west for about 25m and opens 3m above the Coral Canal. The second exit is situated to the north-east with a network of canals and ponors heading different directions. The final exit leads downstairs (through a dug canal) for a length of 10m into the Concert Hall. The Concert Hall has 850m^2 of floor area, reaches a height of about 20m, and is rich in sinter decorations. A ponor existed at the bottom of the Concert Hall which was filled when the cave was prepared for tourist visits.

From here the path leads gradually up to the Coral Canal and afterwards, to the Entrance Hall where the trail finishes with a length of 402m through the cave.

Geomorphologic features of the cave, relate to groundwater flow movements and water action in its mechanical and chemical formation.

5. Groundwater impact to Resava Cave genesis

The rivers Resava and Resavica flow through the investigated terrain and meet at Despotovac (Figure 1). Resava Cave is situated between the southern tributaries of Resava: Kločanica River and Divljakovačka River (Figure 2).

By the end of the Tertiary and beginning of the Quaternary, large quantities of water penetrated this area and flowed into the

Morava Neogene Basin. At that time, groundwater created the majority of underground karst phenomena.

Divljakovačka River played an essential role in the creation of Resava Cave. At that time this river flowed widely through the valley and its level was above or at the entrance level (Figure 2) where water directly infiltrated into faults, fissures, cracks and crevices.

The width of infiltrated water flow was probably not less than the 20m width of the Entrance Hall. The head of a water was not less than 2-3m. The velocity of water was not enough to mechanically erode the carbonate rocks in height, but lateral water power was strong.

At the bottom of the Entrance Hall, groundwater reached a certain velocity and divided into two directions: to the southeast the Bee-Hive, to the east the Coral Canal. The larger quantity of groundwater flowed southeast, judging by the dimension of the Bee-Hive, and drained out through the Ponor partly. With increased velocity, water flowed into the Vestibule of History and cut a canal afterwards with a height of about 7-8m. By increasing its velocity and power, the groundwater flow fell into the Concert Hall. The groundwater flow descended the Coral Canal with a rapid acceleration along the steep slope of the canal, and drained out to the beginning of the Concert Hall. At the same time, the water flow infiltrated into the system of canals in the Crystal Canal, from where it drained partly through 25m long canal and fell in the Coral Canal from the height of 3m. The other part of the groundwater flow caused by the steep slope, entered the Concert Hall, joining the above mentioned water flows and with greater mechanical power, dug a cavity of large dimension (25x34x20m), and afterwards disappeared at to unknown depths through the ponor at the bottom of the hall, probably to the south-east direction.

In final stage of cave formation, the rivers cut into carbonate rocks and descended down gradually to the river bed (about 80m), so it remained out of the river range. Except the temporary floods, the cave has become dry with permanent moist walls, by which calmer process of cave formation has continued.

The chemical impact of water on genesis of Resava Cave related, not only to dissolving of carbonate rocks, but also in its sedimentation in the form of cave ornaments such as stalactites, stalagmites, and columns (MIJATOVIĆ, 1984). The sinter decorations were generated during favourable conditions: a necessary concentration of calcium carbonate in the water, the favourable temperature for its sedimentation, also the absence of mechanical destruction, such as cave floods and collapse of ceilings caused by earthquake.

There are no cave ornaments in the Entrance Hall because it has been exposed to external climatic variations which did not allow creation of appropriate conditions.

The Crystal Hall is very rich in sinter decorations, there are, especially, numerous small stalactites. There are, also, the decorations in the Bee-Hive, Vestibule of History, and Coral Canal. In the Concert Hall are an abundance of stalactites and stalagmites, and the two massive columns. One is at the beginning of the hall and is 10m in diameter. The other is at the bottom of the hall and has an irregular shape of 5-15m in diameter. Judging by the dimensions of these columns, the time of their creation is very long and entered Upper Tertiary. That means the cave, with its system of canals and halls, was also created during the Tertiary.

Resava Cave had not been researched paleontological during its discovery. During preparation of the cave for visits, any remains of the flora and fauna were probably eliminated.

The clayey and muddy traces founded on the walls and decorations testify that the cave floods temporarily. The important problem of adequate illumination of the cave has been solved professionaly (LAZAREVIĆ, 1991), by which the natural conditions have been protected

6. Discussion

In previous researches of Resava Cave's genesis, there is no evidence of the cave's age as underground karst phenomenon, the age of the oldest ornaments, and nor an age of possible remains of flora and fauna.

Therefore, an obligation remains to establish the ages mentioned above and, also, the geomorphologic features of the cave area by which the data of Resava Cave's genesis would be complete. Thus, the role of groundwater in Resava Cave's genesis will become more clear.

Conclusion

A general summary of cave's genesis as a result of the complex geological-tectonic development on the Balkan Peninsula has been presented in this paper.

The sedimentation of carbonate rocks began 235 million years ago, from Middle Triassic to Upper Cretaceous, and the duration of intensive tectonic development as a consequence of Alpine orogenesis was for 150 million years from Middle Jurassic to Middle Oligocene as a pre-phase to the recent "static" genesis of the cave.

The genesis of Resava Cave, as a result of numerous factors, primarily of hydrogeological one, has been presented.

The Divljakovačka river played an important role in the Resava Cave's creation. At that time, the river bed was at the cave entrance level and river water was discharged into faults, fissures, cracks and crevices, resulting in mechanical and chemical erosion of the carbonate rocks. The analysis of groundwater flow on cave development has been done indirectly using the cave's geomorphologic features.

It is believed that the cave with its system of canals and halls was created during the Tertiary.

Resava Cave is rich in stalactites, stalagmites and columns. The columns have a large thickness which gives an evidence of their long period of generation, that probably entered the Upper Tertiary. Nevertheless, for more exactly determination of Resava Cave's age and the role of groundwater in its formation, data obtained by laboratory analysis are necessary.

Acknowledgement

I would like to express my appreciation to the Federal Hydrometeorological Institute in Belgrade for its support and also to Mr. Dejan Lekić, B.Sc. for graphical description. Special thanks are due to Dr. Radenko Lazarević for important oral information.

References

ANTONIJEVIĆ, I. & R. MILOŠAKOVIĆ. 1962. Geological column of Kučaj. Geozavod (Yugoslavia). *Vesnik* XX, Belgrade: 93-102.

BOGDANOVIĆ, P. 1968. Stratigraphy of Upper Cretaceous of Eastern Serbia. Geozavod (Yugoslavia). *Vesnik* XXVI, Belgrade: 71-90.

CIRIC, B. 1996. Geology of Serbia. Geokarta (Yugoslavia), Belgrade: 273.

VASILEVA, D. 1965. Impressions from scientific excursion: Resava Cave - Devil's Town. Lecture. Belgrade: 1-8.

LAZAREVIĆ, R. 1991. Results of microclimatic measurements in the Resava Cave. Institute for Protection of Nature, (Yugoslavia). *Protection of Nature* 43-44, Belgrade: 57-79.

MIJATOVIĆ, B. 1984. Hydrogeology of the Dinaric Karst. Verlag Heinz Heise GmbH, Germany. International Contributions to Hydrogeology, Vol. 4, IAH: 255.

YUGOSLAV COMMITTEE FOR INTERNATIONAL HYDROLOGICAL DECADE. 1976. Hydrogeological Map, scale 1:500000, Belgrade.

Bell hole morphometry of a flank margin cave and possible genetic models: Lighthouse Cave, San Salvador, The Bahamas

Stein-Erik Lauritzen[1]
Joyce Lundberg[2]
John E. Mylroie[3] **& Toby Dogwiler**[3]

[1]Department of Geology, University of Bergen, Allégaten 41. N-5007 Bergen, Norway, stein.lauritzen@geol .uib.no
[2]Department of Geography, Carleton University, Ottawa, Canada KlS 5B6, jlundber@ccs. carleton.ca
[3]Department of geosciences, Mississippi State University, Mississippi State, MS 39762 USA, MYLROIE@Geosci.msstate.edu

Lighthouse cave is a large flank-margin cave that is developed within eolian calcarenites of pre-last Interglacial age, whilst most of the speleogenesis might have taken place within a time window of about 15 ka during Oxygen Isotope stage 5 (MYLROIE & CAREW). The cave ceiling displays a vast amount of bell-holes. Bell holes are vertical, cylindrical to paraboloidal holes that may penetrate up to several meters into the host rock, in most cases without evidence for any pre-existing guiding void or fracture. Morphologically, they are superimposed onto the primary (phreatic) cave ceiling. They may occur isolated, but are most often clustered in groups that, at high density, display polygonal packing patterns. In the main chamber of the cave, 30 bellholes were measured and accurately located relative to each other. Due to the distribution over the sloping ceiling of the cave, there appear to be no level (watertable) control in their distribution. Almost without exception, each bellhole is paired by a floor counterpart (bell-pit) that is slightly wider and shallower, and aligned vertically beneath. The shape characteristics of the bell holes, their relation to corresponding floor cavities (bell pits) and their relation to corroded calcite speleothems and evaporite crusts is suggestible of a vadose origin rather than a phreatic, convection-cell type of formation mechanism. This will be discussed towards various genetic modes and mathematical models for bellhole development.

Cave development along the water table in Cobre System (Sierra de Peñalabra, Cantabrian Mountains, N Spain)

by Carlos Rossi (1), Alfonso Muñoz (2) and Adriano Cortel

(1) Dpt. de Petrología y Geoquímica, Facultad de CC Geológicas, Universidad Complutense, 28040 Madrid, Spain. (2) Dpt. de Geodinámica, Facultad de CC Geológicas, Universidad Complutense, 28040 Madrid, Spain.

Abstract

Cobre Cave System (CCS), with 10.6 km of surveyed passage, is developed in a 150-m-thick sequence of Carboniferous limestones dipping 45-60º against the valley slope. CCS has a multi-story structure, with abundant relict levels at different elevations in 225 m of vertical range. Drainage at the modern level is mainly strike-oriented and occurs along two types of passages: (1) a low-gradient canyon in equilibrium with the water table, (2) a system of phreatic tubes upstream. Six sumps are known in this area that have water at the same elevation and are thus exposures of the water table. Along the strike, the water-table gradient is very low (1.4%), having only minor steps caused by faults. Profiles perpendicular to bedding reveal a more steeper gradient (4.6%) as a result the lower hydraulic conductivity in this direction. The low-gradient canyon has several levels of notches with corrosion bevels (flat solutional roofs regardless of geologic structure) above the modern channel. They can be correlated along great distances and represent paleo-water tables. The canyon may be a 50-m-high, single conduit, but it usually splits into several relict, beveled canyons with separate phreatic roofs, low-gradient floors and whose elevation ranges do not overlap. The existence of correlatable, beveled canyons in nearly all the vertical range of the CCS indicates a long history of base level changes characterized by periods of static base level interrupted by episodic downcutting.

1. Introduction

The recognition of fossilized paleo-water table surfaces in multiphase caves can serve not only to study base level evolution but also to understand the present-day hydrology of the system. In addition, the knowledge of the geometry and gradient of the present water table will help to validate the paleo-water-table definition. Several morphologic criteria have been developed to define paleo-water tables inside multiphase cave systems, such as the piezometric limit concept (PALMER, 1987-1989), the distribution of isolated vadose trenches in the upper parts of phreatic loops (e.g. SMART & CHRISTOPHER, 1989) or the presence of extensive beveled corrosion notches (FORD & WILLIAMS, 1989; FRUMKIN, 1995).

Cobre System is a multiphase cave, 10.6 km long, developed in steeply dipping Carboniferous limestones. The downstream part of the lowest active level consists of a subhorizontal river passage that extends for 1.7 km to the spring and is apparently adjusted to the present base level of the system. This disposition suggests that the river passage could reflect the water table of a true phreatic zone. If this phreatic zone really exists downdip the limestone, and a water table control for the low-gradient river could be demonstrated, then projected elevations of the stream will show the topography and gradients of the water table surface, and eventually the influence of local geological structures, lithology and recent base level evolution on this geometry. All these data will be crucial for the definition and correlation of water-table-controlled, relict features inside the system, which represents an ideal site for this kind of study, as: (1) the steeply dipping nature of the beds allows easy discrimination between lithologic and water-table controls upon passage development, (2) there is an exceptional development of beveled notches of great lateral extent that can mark paleo-water levels very precisely and (3) the system show a well-developed multi-story structure, with abundant relict vadose, phreatic and water table passages, over 225 m of vertical range above the present active level.

The aim of this article is to discuss the possible water-table control for the low-gradient river, and eventually the precise geometry and controls of this water table. As accurate elevation data is essential for this analysis, a specific survey have been carried out along the lowest active level of the cave, with a mean vertical error estimated in 0.1% of surveyed length. Elevations of the water surface, passage floors, notches and corrosion bevels have been measured in every survey station of the main passage (128 stations). All these features were correlated in situ and mapped in profiles. A 3D frame of the survey of the whole cave system as well as some selected projected profiles have been produced and analyzed with CAD software. In these profiles the survey line of the river passage has been transformed to represent the low water level of the stream.

2. Geological and hydrological setting

Cobre Cave System (CCS) is located in the Sierra of Peñalabra, in the central part of the Cantabrian Mountains (Province of Palencia, N Spain). The cave is developed in a 150-m-thick sequence of Carboniferous limestones (the Agujas Limestone Member) sandwiched between impervious siliciclastic turbidites of the Vañes and Covarrés Formations (VAN DE GRAAF, 1971). These formations crop out in the south-western flank of the Sierra, where they show an overturned dip of 45-60º against the slope (Fig. 1). This structural pattern locates the position of the karst base level just at the outcrop of the lower contact between limestones and turbidites, i.e., at the intersection of this lithologic boundary with the topographic surface. The karst base level is thus stratigraphically perched above the regional base level, which is located 100-500 m bellow at the Pisuerga river valley, built in non-karstifiable rocks.

The outcrop of the lower limestone-turbidite boundary along the Sierra is marked by several permanent karst springs, each one being the outlet of a separate cave system. The karst is thus divided into several blocks, separated by major faults and/or transverse valleys incised into the limestone. Each block drains preferentially along the strike, discharging at a spring located at the lowest outcrop point of the limestone. Cobre cave entrance represents one of this springs, draining a major limestone block

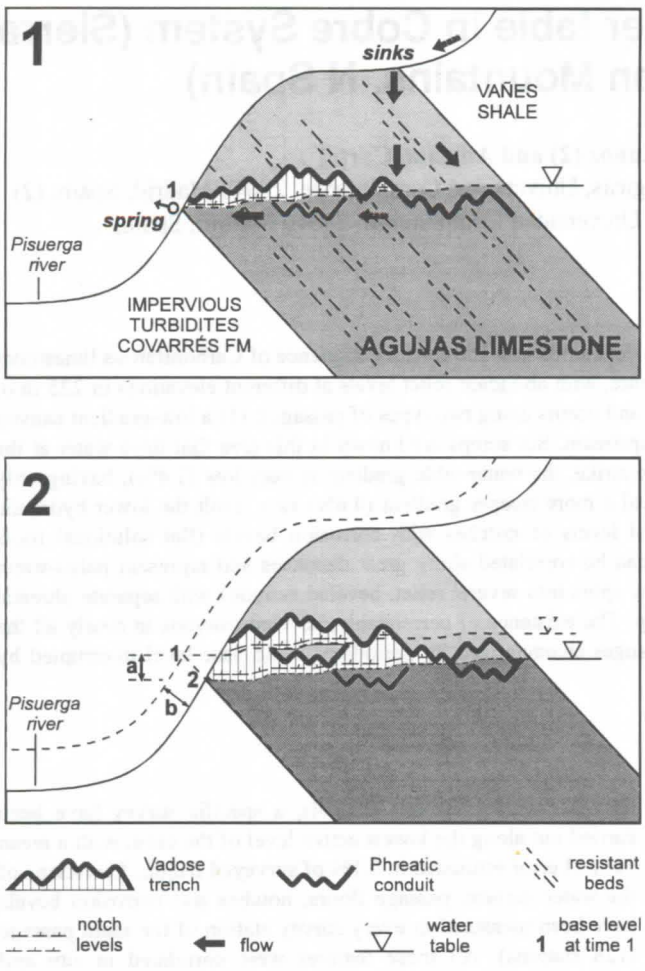

Fig. 1: Schematic vertical section of CCS in the dip direction, showing the response of the cave system to a base-level lowering (of "a" magnitude) caused by an erosive slope retreat (of "b" magnitude).

at the south-western corner of the Sierra and giving access to nearly 10 km of surveyed passage.

The Agujas limestone, whose outcrops range in altitude from 1600 to 1900 m asl. in the CCS area, is overlain by unconformable Triassic Buntsandstein facies (sandstones, shales and conglomerates), which form the summits of the Sierra at 2100-2300 m asl. As the limestone crop out in only a narrow strip, sinking surficial streams originated in the Buntsandstein highlands provide most of the recharge for the karst aquifers in the underlying limestone.

A significant part of the allogenic recharge to the CCS occurs via two major penetrable sinks: the *Torcón* (explored for 0.9 km and 140 m in depth) and *Sel* (explored for 0.7 km and 115 m in depth) sinks, both connected hydrologically, but not yet physically, with the main cave. The streams that sink in Torcón and Sel drain the Covarrés Cirque and the Sel de la Fuente valley, two major forms of glacial origin, built essentially in insoluble Buntsandstein, and partially filled with Pleistocene moraine deposits (HERNÁNDEZ-PACHECO, 1944). Torcón, as other sinks or paleo-sinks explored along the system, are partial to entirely filled by till; wedged boulders of limestone and Buntsandstein conglomerates that can reach several meters in diameter can be found deep into the cave system, occasionally sealing some inlet passages.

3. Description of the cave system and its hydrology

CCS is comprised of three different sectors (Fig. 2) in terms of morphology, hydrology and relative age: (1) the low-gradient Apia canyon; (2) the Sifones-Sel-Torcón branch; (3) the south-eastern branch.

(1) The Apia canyon is a low-gradient river passage in the downstream part of the system. The active channel is excavated in the limestone bedrock and shows relatively little clastic bed load. Although the canyon may be a 50-m-high, single conduit guided by a mayor phreatic tube, it usually splits into several relict canyons with separate phreatic roofs, low-gradient floors and whose elevation ranges do not overlap. Along its entire elevation range, the canyon and its sub-canyons develop extensive and correlatable levels of corrosion notches.

(2) The Sifones-Sel-Torcón branch is a mixture of looping phreatic tubes and active vadose conduits, which transmit to the Apia river most of the allogenic water from the Torcón and Sel sinks. The entrance series of Torcón and Sel consist of active vadose shafts and high-gradient active canyons whose water finally disappears in impenetrable fissures. These canyons intersect a system of relict phreatic tubes that loop at elevations between 95 and 81 m above the spring level (abbreviated as a.s.). In both caves, narrow vadose canyons are found again below this depth, giving access to another system of looping tubes in the range of 62-44 m a.s. and ending in a stagnant sump at the lowest point. An obviously equivalent and nearby tube system is accessible from the upstream end of the Apia canyon in Cobre Cave. This tube system, known as the Sifones series, is developed in the same elevation range of Sel-Torcón lowest tube system, and contains exclusively phreatic tubes that form remarkable loops of 25 m of maximum amplitude. Five sumps are known in this area, all having water at near the same elevation (43-45 m a.s). The more north-westerly of these sumps supply most of the flow of the low-gradient Apia river, whose floor is also coincident in elevation with the water levels in the sumps upstream. The water in the other sumps are apparently stagnant, but their water levels fluctuate seasonally at least 1 m.

(3) The south-eastern branch, that will not be discussed in this paper, consists of a series of upper level relict conduits (the oldest passages in the CCS) partially captured by modern small streams infiltrated from the moraine deposits that cover the limestone in this area. The vadose streams of this branch join directly the Apia river through the Mareo meander or become lost in impenetrable fissures towards the active Sifones-Sel-Torcón branch.

4. Profiles and gradient of the river passage

The Apia river extends for 1.7 km, from the active sump that supplies its water to the spring at the Cobre entrance. The difference in elevation between the spring and the water-supplier sump is 44 m, which gives a mean gradient of 2.5%. Seen in extended profiles (Fig. 3), the gradient is not uniform along the river passage, which can be subdivided for this purpose into two separate sectors: the downstream quarter (450 m of passage), with a mean gradient of 4.6%, and the remaining 1630 m upstream, with a remarkably less steeper mean gradient of 1.4%. Once again, along each sector the gradient is not uniform. The shorter and steeper downstream quarter comprises several lower-gradient segments separated by short ramps whose location is controlled by dolomite zones concordant to the bedding (see further details in ROSSI & MUÑOZ, 1993). Upstream, the

remaining main portion or the river passage shows an almost uniform gradient, near to the mean value of 1.4%, only interrupted by minor steps of decimetric magnitude associated to mineralized faults.

If the survey of the river surface is analyzed on projected profiles, it becomes evident that the gradient threshold correlates with a significant change in passage structural orientation: (1) the downstream quarter of the river is broadly oriented parallel to the dip direction of the bedding, and in this sector the cave rapidly penetrates most of the stratigraphic section of the Agujas limestone following a series of faults. (2) Upsteam, the main portion or the river passage follow either faults or bedding planes (both steeply dipping), but in this case there is a clear general tendency to drain along the strike of the limestone.

5. Morphology of the active channel

Close to the active channel, the lowest portion of the Apia canyon contains three extensive levels of solutional sub-horizontal notches along the walls (Fig. 3). These notches extend several meters into the rock, are typically 1 m deep and show remarkably flat solutional roofs that bevel the dipping strata (corrosion bevels, according to FORD & WILLIAMS, 1989, nomenclature). These beveled notches are partly filled with fining-upwards sand and gravel sequences capped by flowstone.

In the downstream quarter of the Apia canyon, the present stream occupies an incised trench under the lowest notch. The depth of the trench under this notch is maximum near to the entrance (about 6 m), decreasing rapidly and progressively in the upstream direction. 560 m away from the entrance this trench disappears, and the underground river is at the level of the lowest notch. This lowest notch, which develop a very sharp bevel, can reach 20 m in width near the entrance, but progressively reduces upstream until vanishing as a notch approximately 1 km away from the spring. The second notch is composed of two sub-notches with corresponding bevels located at constant relative elevations of 1 and 2 m, respectively, above the bevel of the lowest notch. This composite notch, especially the upper sub-notch, can be correlated along the entire Apia river. This notch is however interrupted when the phreatic roof descends to its level or just below, representing paleo-sump sections that represent de facto piezometric limits (sensu PALMER, 1987), which demonstrates the strong water-table control in notch origin

6. Discussion

The interpretation of the Apia river in CCS as an exposure of the water table is supported by (1) the low-gradient and perennial character of the stream, (2) the upstream origin of the water supply, directly from flooded phreatic conduits, (3) the coincidence in elevation between the sumps of the Sifones-Sel-Torcón branch upstream and the water level in the Apia river downstream and (4) the broad parallelism between the profile of the present stream in Apia canyon and of those of the recent beveled notches, interpreted in turn as stable water-table features. The peculiar structural pattern of the limestone, steeply dipping against valley slope and with underlying impervious rocks, favors water impoundment and thus produces a phreatic zone downdip the limestone. The lowest outcrop point of the limestone-turbidite contact controls the vertical position of the spring, which in turn controls the elevation of the water table at the output of the aquifer.

Water table geometry

If the water table is defined by the level of the active passage floor in the low-gradient river and by sump levels in the phreatic segments upstream (in the Sifones-Sel-Torcón branch), then their projected profile will show the topography of the present water table surface. Along the strike, the water-table gradient is very low (1.4%), having minor steps caused by faults that give a smooth, stair-like geometry to the water table. Profiles in the dip direction of the bedding, reveal a more steeper gradient of the water table (above 4º). This geometry is caused by the lower hydraulic conductivity in the dip direction, as the flow has to cut across the bedding; moreover, the limestone has several chert-rich beds that act as minor hydrologic barriers. Along the strike, the hydraulic conductivity is enhanced as underground drainage is favored by the bedding planes and abundant faults parallel to bedding. The topography of the stable paleo-water tables deduced from projected profiles of the beveled notches is roughly the same (with the above-expressed exceptions), which strongly supports this interpretation of the water table geometry.

Present development of active phreatic conduits

As the existence of a phreatic zone requires effective porosity below the water table, and the Agujas limestone itself lacks intrinsic porosity, the phreatic development must be achieved via solution conduits, open fractures or both. Upstream of the Apia canyon, in the Sifones sector, perhaps most of the flow occurs through active phreatic conduits that transmit to the Apia river the allogenic recharge that enters via the Torcón and Sel sinks. The existence of a well integrated tube system in this area is suggested by: (1) the water of Apia river is supplied by a flooded rising phreatic tube; (2) the Sifones sector (and also most of the lower sections of Sel and Torcón) consists almost exclusively of dry looping phreatic tubes, generated when the water table was higher: a similar system could be active today in the same sector below the water table (3) several stagnant sumps with equivalent water levels are known in this area, which suggest the existence of an active system of liked tubes in which a steady phreatic flow is taking place today.

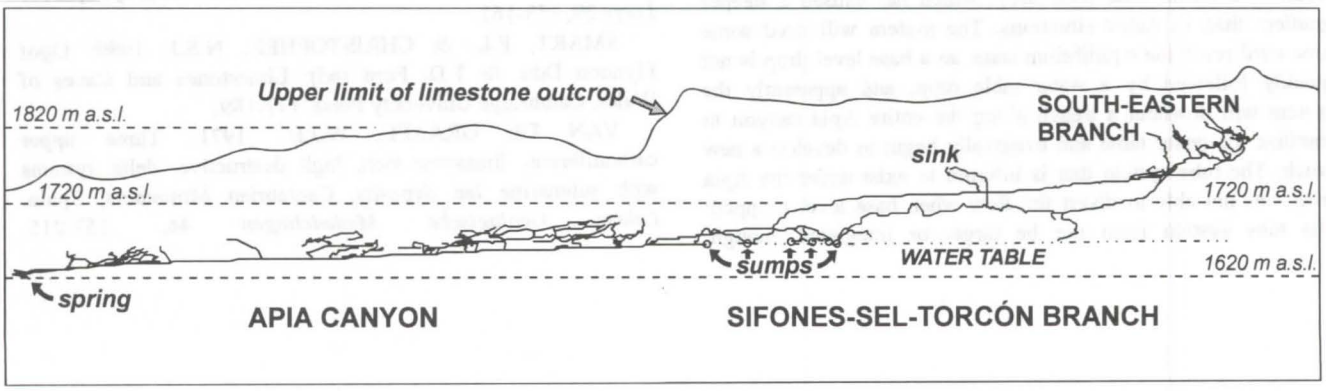

Fig. 2: Profile view of the the survey frame of Cobre Cave System along the strike of the limestone.

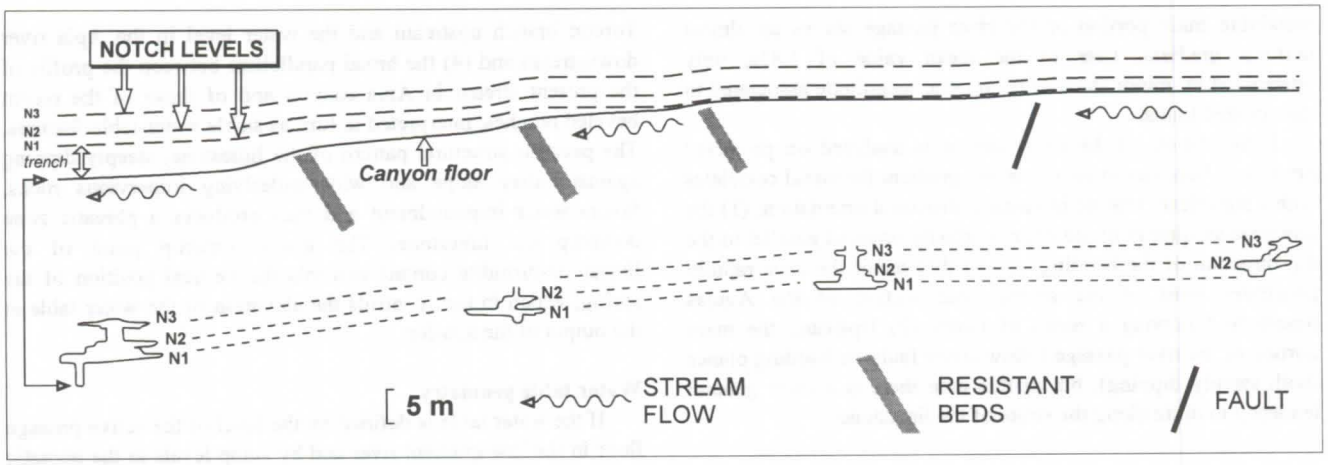

Fig. 3: Schematic extended profile of the Apia Canyon (above) and correlation of some representative cross-sections of the lower part of the canyon (below). Horizontal scale arbitrary.

The existence of phreatic conduits below the level of the stream in the Apia canyon is more difficult to prove, as no undoubted tubes have been detected under the shallow water. Nevertheless, along the whole height of the canyon there are abundant relict phreatic tubes that can be linked physically to former canyon levels and notches, distributed in an elevation range of 50 m above the stream. These relict levels and their associated tubes will not be discussed in this paper, but work in progress (ROSSI, CORTEL & KELLER, in prep.) suggests that the relict low-gradient canyon levels and stories are absolutely analogous in morphology and long profiles to the modern channel. The invariable presence of looping phreatic tubes under every relict level of the Apia canyon strongly suggest that similar phreatic conduits could be active actually under the stream level.

Evolution of the water table after a recent base level fall

The comparison of the active stream profile of Apia canyon and the profiles of the recent notches indicates that the river is actually downcutting: the trench under the lowest notch decrease progressively in the upstream direction, disappearance 0.5 km away from the entrance. From this point to its upstream end, the underground river is still at the level of the latest notch. This incision seems to be actually in progress, and it is expected that in some time in the future it will extend upstream to the limit of the active canyon. The disapparition of the lowest notch 1 km away from the spring suggests that this notch was not fully developed when a base level drop aborted it and caused its incision. The second notch, however, can be correlated along the entire Apia river, which indicate that this second notch had thus enough stable time to develop.

The present water table is thus relatively unequilibrated as a result of a recent base level drop, which has caused a steeper gradient than in stable situations. The system will need some time until reach the equilibrium state, so a base level drop is not quickly followed by a water table drop, and apparently the system will downcut a trench along the entire Apia canyon to stabilize the water table and eventually begin to develop a new notch. The tube system that is inferred to exist under the Apia river was not able to divert the flow when base level dropped: this tube system must not be large- or integrated enough. Furthermore, as seen in the relict tube systems above in the canyon, the tubes under the river passage tend to be relatively short diversions that rejoin the low-gradient passage. Consequently, as the tube has to divert the water towards the same passage, the water level in the stream will not drop.

Acknowledgments

O. Bernaldo, F.L. Quintanilla, A. Marcos, E. González and A. González contributed to the production of the high-precision survey of the Apia river. This paper is a contribution to the IGPG project 379. The cooperation of the Consejería de Medio Ambiente y Ordenación del Territorio (Junta de Castilla y León) is also gratefully acknowledged.

References

FORD, D.C. & WILLIAMS, P.W. 1989: *Karst geomorphology and Hydrology*. Unwin Hyman, London: 601 p.

FRUMKIN, A. 1995: Morphology and development of salt caves. *National Speleological Society Bulletin*. 56, 82-95.

HERNANDEZ-PACHECO, F. 1944: Fisiografía, geología y glaciarismo cuaternario de las montañas de Reinosa. *Memorias Real Academia de Ciencias de Madrid, Sec. Ciencias Naturales*, 10.

PALMER, A.N. 1987: Cave level and their interpretation. *National Speleological Society Bulletin* 49 (2): 50-66.

PALMER, A.N. 1989: Geomorphic history of the Mammoth Cave System. *En:* WHITE, W.B. y WHITE E.L. (Eds.): *Karst Hydrology (Concepts from Mammoth Cave area)*, 317-337.

ROSSI, C. & MUÑOZ, A. 1993: Geometry of piezometric surfaces in a perched karst: Redondo Valley, Cantabrian Mountains, N Spain. *Bulletin de la Société Géographique de Liège* 29, 153-161.

SMART, P.L. & CHRISTOPHER, N.S.J. 1989: Ogof Flynnon Ddu. *In* T.D. Ford (ed): Limestones and Caves of Wales. Cambridge University Press. 177-189.

VAN DE GRAAFF, W.J.E., 1971: Three upper carboniferous, limestone rich, high destructive, delta systems with submarine fan deposits, Cantabrian Mountains, Spain. *Leidse Geologische Mededelingen* 46, 157-215.

Multiple paleo-water tables in Agujas Cave System (Sierra de Peñalabra, Cantabrian Mountains, N Spain): Criteria for recognition and model for vertical evolution

by Carlos Rossi (*), Adriano Cortel and Rocío Arcenegui

(*) Dpt. de Petrología y Geoquímica, Facultad de CC Geológicas, Universidad Complutense, 28040 Madrid, Spain.

Abstract

Agujas System, a multi-phase cave with 9 km of passages, is developed in a 350-m-thick sequence of Carboniferous limestones dipping 50º to NE. Ten distinct levels of abandoned sub-horizontal water-table trunks are known, each confined in a specific elevation range covering together 300 m of depth. The present base level drainage must be about 100 m below the lowest abandoned trunk, but to date exploration has failed to find access to the lower levels. The relict trunks are wide meandering canyons, 20-40 m high, with low-gradient floors and extensive levels of notches with corrosion bevels. These notches become wider near the base of the canyons, extending as far as tens of meters into the rock. Looping phreatic tubes develop just below the canyons, emerging from the floor of a given notch. The extensive notches that bevel dipping strata, their low-gradient character and the multiple vadose-phreatic transitions at their bases, demonstrate that the beveled canyons are relict water-table trunks. They represent an exceptionally complete record of paleo-water tables that can be restored in geometry and evolution. Extended periods of constant base level were followed by abrupt drops (15-60m) producing a new canyon at a lower elevation. Canyon downcutting is very rapid first, but later decelerates and reaches equilibrium creating wide notches at the water table and phreatic tubes below.

1. Introduction

Agujas Cave System (ACS), with 9 km of surveyed passage, has a complex multi-story structure developed in more than 300 m of vertical relief. Looping phreatic tubes and vadose high-gradient canyons and shafts are present in the entire elevation range. Nevertheless, most of the explored passages are low-gradient, water-table trunks, which are found almost in every part and at every elevation. This assemblage of relict conduits contains an exceptionally complete record of fossilized, stable paleo-water tables that can be defined by separate criteria and traced along large areas of the system.

The aim of this article is to describe the general characteristics of the relict trunks and to show the relationships between these trunks and the genetically-linked systems of phreatic tubes. Based on high-quality survey information and detailed morphological observations, we will support a water-table origin for the trunks and discuss the water table evolution during trunk formation and also at the scale of the whole cave system.

ACS, whose explored conduits range in altitude from 1650 to 1950 m a.s.l., is located in the Sierra of Peñalabra, in the central part of the Cantabrian Mountains (Province of Palencia, N Spain). The cave is developed the Upper Carboniferous Agujas Limestone (VAN DE GRAAF, 1971), which exceeds 350 m in thickness in the ACS area. In the southern flank of the Sierra, the Agujas limestone has an overturned dip of 50º against the slope, and is sandwiched between conformable impervious turbidites. This structural pattern favors the development of a true phreatic zone downdip the limestone and places the karst base level (the springs) at the outcrop of the lower boundary between limestones and turbidites. The geometry and gradient of the water table in an equivalent and nearby karst aquifer is discussed in detail in ROSSI, MUÑOZ & CORTEL (this volume), where the reader can find additional data of the Peñalabra karst.

2. The cave levels

Ten distinct levels of relict low-gradient canyons are known in ACS to date. These canyons are distributed in more than 300 m of vertical relief, each canyon being confined in a specific elevation range (Figs. 1 and 2).

The relict canyons are 20- to 40-m-high meandering passages, with low-gradient floors and guided by looping phreatic tubes (Fig. 3). They all show extensive levels of subhorizontal corrosion notches with bevels (flat roofs regardless of geologic structure). These notches are usually restricted to the lower parts of the canyons, becoming progressively wider (as far as tens of meters) towards their bases. The exploration of these beveled meandering canyons is not an easy job: the notches may be wide but are usually less than 1 m deep and separated by narrow trench intervals; frequently, the canyons are interrupted by breakdown (induced by notching) or by flowstone blockages; the canyons have a pronounced sinuosity and meanders overlap at different levels, creating complicated labyrinths where the explorer has to check regularly the paleo-flow from the scallops to avoid becoming lost. The guiding phreatic tube at the roof (devoid of meanders, notches and usually of breakdown) often represents an alternative and easier route, except where the trench under the tube is too wide or where a younger vadose capture has widened the canyon walls.

Systems of linked looping phreatic tubes can be found in the vertical space between each couple of successive low-gradient canyons. Each tube system develop below the floor of the upper canyon and the roof of the subsequent canyon. These tubes are usually accessible from the floor of a notch in the lower part of the canyon. Parts of these phreatic systems become the guiding tubes (the roofs) of the following canyon underneath. So, it seems that each canyon has associated a system of genetically-related phreatic tubes just below its floor and usually above the following trunk. Occasionally, some major tubes contain steep-to-vertical segments that descend 80 m or more below the floor level of the parent trunk, covering the depth range of several trunks.

There are some differences in the style of the trunk-tube systems between the upper, middle and lower parts of the explored cave system:

(1) The two uppermost, and therefore oldest, relict trunks are characterized by the scarcity of notches except in the base of the canyon, where they acquire an exceptional development: here, two or three closely-spaced notches show remarkably sharp bevels that can reach as far as 30 m in width, the maximum observed in ACS. Below both canyons there are extensive systems of looping phreatic tubes with multiple connections to the notches of the canyon floor and even with some maze sections. The loops of these tubes are usually restricted to a

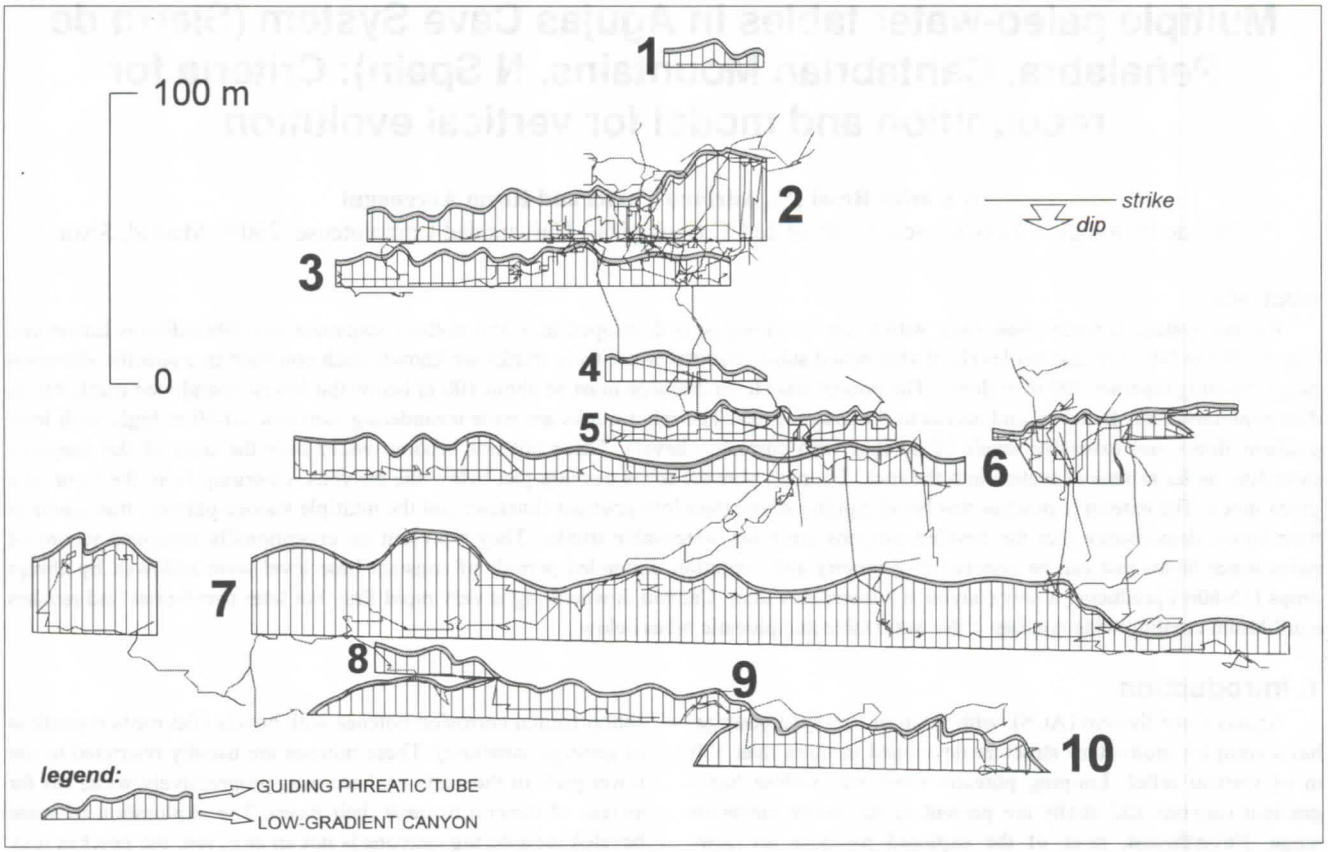

Fig. 1: Profile view of the Agujas Cave system along the strike of the bedding. A schematic representation of the low-gradient canyons is superimposed over over the survey frame.

vertical range of a few tens of meters below the parent notch, but they can exceptionally reach maximum vertical ranges of 50 and 80 m, respectively, below the trunks. Most of these tubes remains undisturbed but some have been captured by younger vadose streams, that have cut narrow trenches in their floors.

(2) The five levels of subhorizontal canyons situated at intermediate elevations inside ACS are characterized by the abundance of beveled notches along most of their vertical sections. The upper part of these canyons, close to the guiding tube, usually consists of a notch-free incised interval. The five canyons cover together about 150 m of vertical amplitude, each canyon being typically 20-30 m high. The canyons of this part of ACS are well interconnected by major shafts, many of them active. With almost 2 km of surveyed passage, the topographically-lower of these five canyons is now the best known of ACS.

(3) The two topographically lowest levels of ACS are poorly developed and also still poorly explored. Both are relatively narrow and show very few notches. The explored horizontal segments of these canyons frequently grade to phreatic conduits below the level of their floors. The present base level drainage must be about 100 m below the lowest known low-gradient canyon, but to date exploration has failed to find access to the lower levels.

The systems of relict low-gradient trunks and phreatic tubes may be affected by younger vadose captures that cut trenches in their floors. These trenches are narrow, with high-gradient floors, devoid of horizontal notching and usually linked to vertical shafts in both the upstream and downstream directions. Some of these vadose captures are relict features but many are active: small streams of aggressive water can be followed occasionally for more than 150 m in depth, creating shafts as far as 80 m deep and using parts of relict trunks and tubes, with or without trench development in them.

3. Discussion and conclusions

Origin of the low-gradient relict canyons

The beveled low-gradient canyons represent relict water-table trunks, as demonstrated by: (1) the low-gradient character of the canyon floors, which transect steeply-dipping beds, cherty intervals and faults; (2) the presence of extensive levels of subhorizontal notches that bevel dipping strata (3) the abundant transitions to phreatic tubes at the canyon floors. Furthermore, the deduced paleo-water tables show a general gradient towards the SW, i.e., towards the present base level. Along the strike the paleo-water-table gradients are usually very low, being remarkably higher in the dip direction, as expected by the lower hydraulic conductivity in this direction.

Each relict canyon represents a period characterized by low rates of lowering of the water table (and thus of the base level). At the floor of the canyons, extended periods of constant base level are recorded, which allowed the formation of extensive corrosion notches at the water table and contemporaneous phreatic systems below the water table.

The highly stable periods recorded at the canyon floors were followed by abrupt base level drops (15-60m), deep enough to cause the abandonment of the passage. Immediately after the drop, the flow was diverted to lower phreatic conduits that were rapidly downcut, producing a new canyon at a lower elevation. The downcutting of this new canyon is very rapid first, but later decelerates and reaches equilibrium again, creating wide notches at the water table and phreatic tubes below. This sequence of events repeated at least ten times, producing an exceptionally complete record of paleo-water tables that can be restored in geometry and evolution.

Each relict trunk shows a characteristic cross section in terms of relative elevation and relative width of the notches and trenches. This canyon "fingerprint" seems to be correlatable along the explored length of each trunk. The vertical sequence of canyon fingerprints may be representative of the whole system and thus offer a basis for correlation with nearby systems. Further exploration is needed, however, to link the known sequence with the lowest active level of the cave (the most obvious datum for correlation) and to clarify this sequence which at present shows some considerable gaps.

Coexistence of water-table passages with deep phreatic loops

The coexistence of water-table canyons and contemporaneous deep phreatic loops is a remarkable feature of ACS. In systems of low water-table relief such as ACS, the relatively low hydraulic head (the height of the water table above the spring) reduces the possibility of deep phreatic circulation and favors the development of water table passages. Moreover, in tightly folded rocks where fissure frequency is high, such as the Agujas Limestone, water table caves are favored (FORD & WILLIAMS, 1989). These and other factors, such as the aggressiveness of the allogenic water or the siliciclastic (highly abrasive) composition of the abundant allogenic sediments carried by the cave streams, have possibly contributed to the predominance of water-table canyons in ACS.

Nevertheless, abundant phreatic tubes, some of them deep, were generated under the water-table canyons, apparently at the same time, as the former are physically connected to the floors of the later. The reason of this exceptional phreatic circulation under a low-relief water table must be the relatively high vertical hydraulic conductivity of the phreatic zone downdip the limestone: as the strata dip quite steeply, bedding planes tend to entrain groundwater to great depth. Other factor that could have favored deep phreatic circulation is the relatively high residence times of the water table in the same stable position (inferred by the well-developed beveled notches) coupled with the high erosive power of the allogenic water and sediments.

Significance

The record of paleo-water tables, and thus of base level evolution, is exceptionally complete in ACS and represents a substantial vertical range (300 m) that further exploration will extend. This complete record could be the reflect of (1) an exceptionally long history of evolution or (2) a highly-sensitive system to water table fossilization or (3) both factors.

Paleo-water tables are relatively easy to define and trace along the system. The combined presence of extensive sub-horizontal beveled notches and of vadose-phreatic morphological transitions (piezometric limits) at the same elevation are relatively conclusive criteria for paleo-water table definition. The levels to which vadose trenches are graded represent an additional criterion for paleo-water table definition, but it should be carefuly employed to avoid consideration of trenches caused by younger captures. Moreover, the paleo-water tables defined exhibit a low gradient towards the base level, cutting through structures and steeply-dipping strata, which strongly supports their interpretation as water-table features.

Acknowledgments

ACS were discovered in 1993 and is actually being explored and mapped by a team of independent cavers which, besides the authors, includes the following: R.L. Anzuola, A. Ortiz Salinas, A. González and B. Rojo, with the aid of C. Gibson, R. Close, F.L. Quintanilla, A. Marcos, J. Matas, P. Gómez, E. Pérez, P. Keller and J. Borneman. This paper is a contribution to the IGPG project 379. The cooperation of the Consejería de Medio Ambiente y Ordenación del Territorio (Junta de Castilla y León) is gratefully acknowledged.

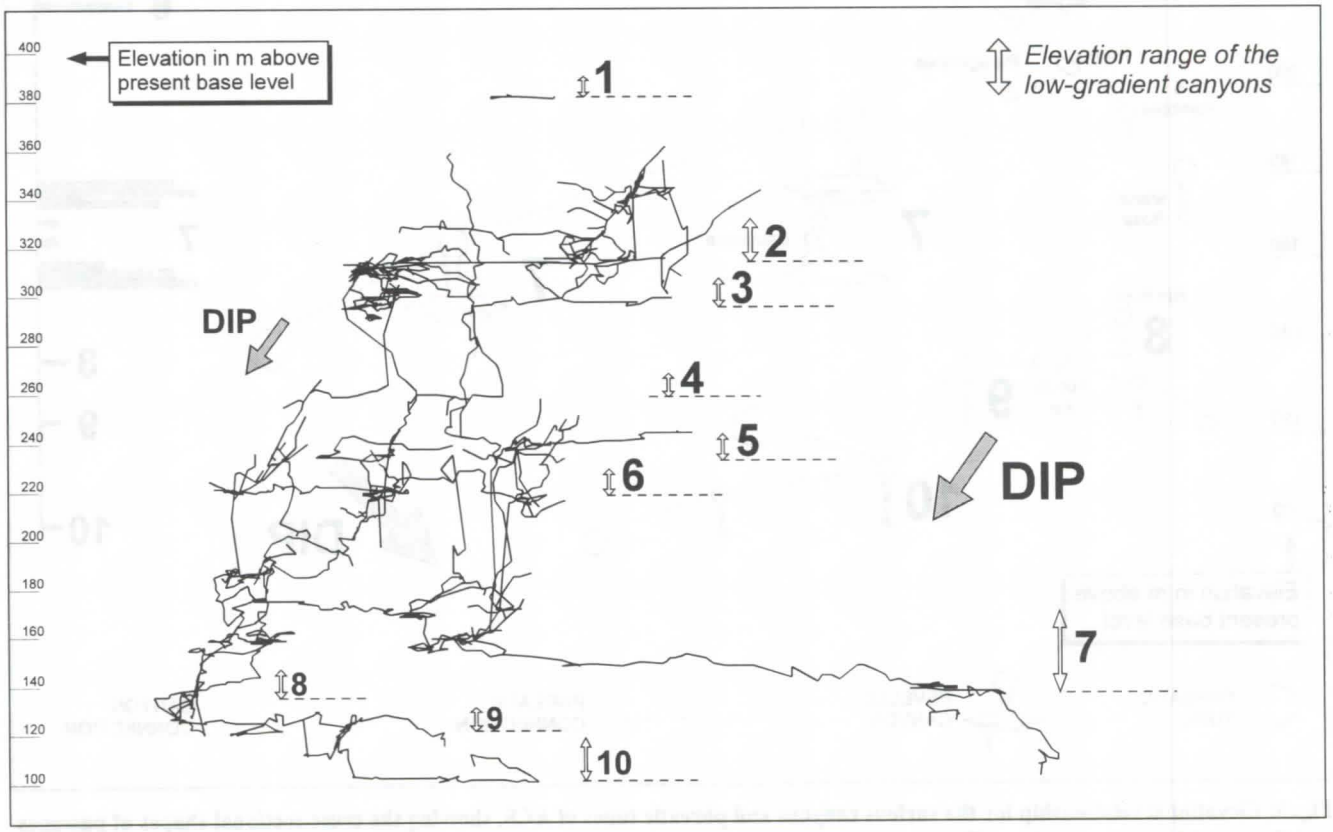

Fig. 2: Profile view of the the survey frame of Agujas Cave System in the dip direction of the limestone, showing the elevation range of the low-gradient canyons.

References

FORD, D.C. & WILLIAMS, P.W. 1989: *Karst geomorphology and Hydrology*. Unwin Hyman, London: 601 p.

VAN DE GRAAFF, W.J.E., 1971: Three upper carboniferous, limestone rich, high destructive, delta systems with submarine fan deposits, Cantabrian Mountains, Spain. *Leidse Geologische Mededelingen* 46, 157-215.

ROSSI, C. MUÑOZ, A. & CORTEL, A. (this volume): Cave development along the water table in the Cobre System (Sierra de Peñalabra, Cantabrian Mountains, N Spain).

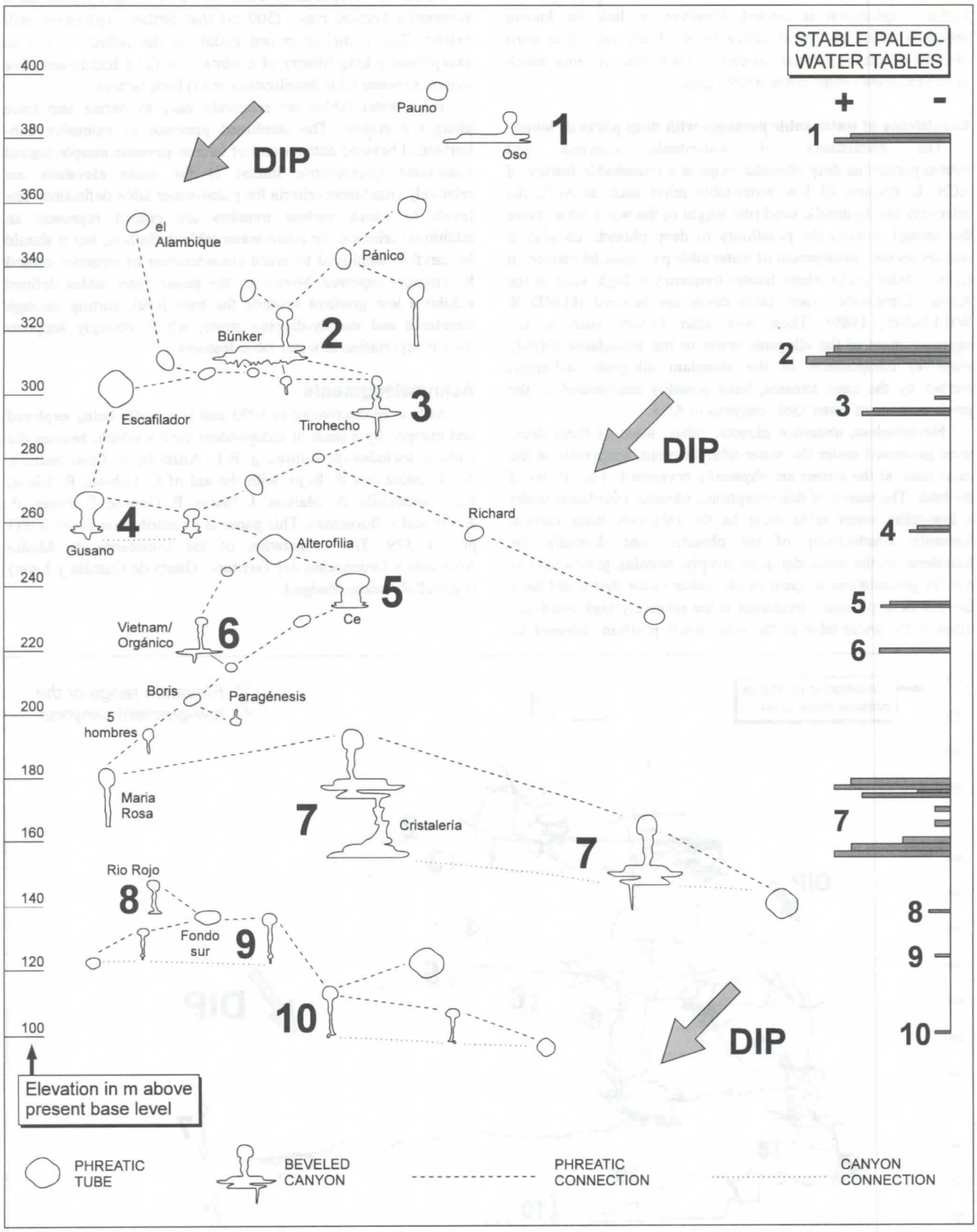

Fig. 3: Elevational relationship for the various canyons and phreatic tubes of ACS, showing the cross-sectional shapes of passages and the transitions between them. The diagram to the right is a schematic plot of the relative importance of each period of water-table stability, deduced from the amplitude and persistence of the beveled notches and from the relative importance of associated phreatic development below.

La corrosione di placchette calcaree ad opera di acque sulfuree: dati sperimentali in ambiente ipogeo

Sandro Galdenzi[1], Marco Menichetti[2] e Paolo Forti[3]
[1]Istituto Italiano di Speleologia, sede di Frasassi - v.le Verdi,10 60035 Jesi Italia
[2]Centro Escursionistico Naturalistico Speleologico - Loc. Calcinaro 7/A 06021 Costacciaro Italia
[3]Istituto Italiano di Speleologia - via Zamboni, 67 40127 Bologna Italia

Abstract

Sulphuric water corrosion on limestone in cave environment was measured through limestone tablets placed inside the Frasassi Caves. The room where the experience took place is interested by phreatic sulphuric water flow and shows many corrosion features and gypsum deposits due to mineralized water reaction with limestone walls.

Some tablets were placed in the groundwater and others exposed to H_2S vapours in the cave atmosphere; the experiment had a term of five years, and half of the tablets were weighed after two and half years. The surface corrosion resulted very evident in every tablet, and the weight loss reached values spreading from 15 to 20 mg/cm^2/y; the limestone surface was covered by a thin layer of organic matter, which surely plays an important role in H_2S oxidation and in limestone corrosion.

In the groundwater the tablet surface was uniformly corroded; the weight loss resulted the same in the two different measurement stations and it remained constant during the whole period. The tablets placed in the cave atmosphere were wholly covered with replacement gypsum, deriving from H_2S oxidation and reaction with limestone; the tablet surface - under gypsum cover - was deeply and quite irregularly corroded; the weight loss shows an increasing velocity in time and reached the highest values, but it changes owing to the location of each tablet.

Introduzione

Negli ultimi anni è stato fortemente rivalutato il ruolo delle azioni speleogenetiche non collegate alla presenza di CO_2 nelle acque carsiche: in diverse aree geografiche sono state segnalate importanti grotte la cui origine è stata imputata a fenomeni di ossidazione dell'H_2S circolante entro i massicci carsificati (EGEMEIER, 1981; HILL, 1987; GALDENZI & MENICHETTI, 1995), mentre è stato ridiscusso il ruolo dei fenomeni di ossidoriduzione dello zolfo (FORTI, 1988). La presente ricerca si proponeva appunto di verificare l'esistenza in grotta di azioni corrosive dovute alle acque sulfuree e di quantificarne l'intensità.

Aspetti morfologici

Le Grotte di Frasassi (Appennino Centrale) rappresentano il miglior esempio presente in Italia di grotte originate per effetto della circolazione di acque sulfuree all'interno di un massiccio calcareo (GALDENZI, 1990); esse sono costituite da un reticolo molto ramificato, a tratti labirintico, di gallerie e sale disposte su più livelli sub-orizzontali, originati in conseguenza dell'approfondimento dell'idrografia superficiale. L'evoluzione della grotta è stata piuttosto rapida, ed i più antichi speleotemi trovati non superano i 200.000 anni di età (TADDEUCCI *et al.*, 1992). I livelli inferiori della grotta raggiungono la falda freatica, e qui possono essere effettuate interessanti osservazioni sui presenti processi morfogenetici. La speleogenesi è collegata principalmente all'ossidazione dell'H_2S nella parte superiore della falda freatica o nell'atmosfera, secondo reazioni, probabilmente catalizzate da batteri, del tipo:

$$H_2S + 2\,O_2 + CaCO_3 + H_2O \leftrightarrows CaSO_4\,2H_2O + CO_2$$

Una caratteristica della grotta è costituita dalla presenza di depositi gessosi, in tutti i livelli, testimonianza della passata circolazione delle acque sulfuree. Il gesso risulta attualmente in formazione solo in ambiente aerato, dove le esalazioni di H_2S vengono a reagire con l'ossigeno atmosferico e con le pareti calcaree. Situazioni morfologiche favorevoli risultano le località in cui acque sulfuree risalgono da condotti con lunghi tratti sommersi. Le pareti direttamente esposte ai vapori sono interamente ricoperte da gesso, che si presenta per lo più in forma microcristallina, bianco, molle e lattiginoso; nelle zone limitrofe il fenomeno si attenua e sulle pareti possono comparire grumi gessosi più isolati (Fig. 1); queste azioni possono tuttavia rimanere attive anche a oltre 50 m di distanza dalle acque sulfuree, secondo la locale circolazione dell'aria. La formazione del gesso è limitata agli ambienti aerati, mentre sottofalda esso viene disciolto ed asportato. Le pareti calcaree in cui si è avuta la formazione di gesso risultano interessate da alveoli e fossette, di dimensioni centimetriche, ben evidenti dove il gesso è stato dilavato dalle acque percolanti (Fig. 2).

Le zone soggette alla circolazione di acque sulfuree sono estremamente ricche di materiale organico, presente in piccoli accumoli sapropelitici in falda o nelle diffuse vermicolazioni. Molto comuni anche organismi superiori, più abbondanti che nel resto della grotta.

Le modalità dell'esperimento

La misura dell'entità della corrosione in aree carsiche è stata oggetto di numerose ricerche condotte con differenti metodologie. La misura della perdita di peso di placchette calcaree esposte agli agenti atmosferici (TRUDGILL, 1975) è

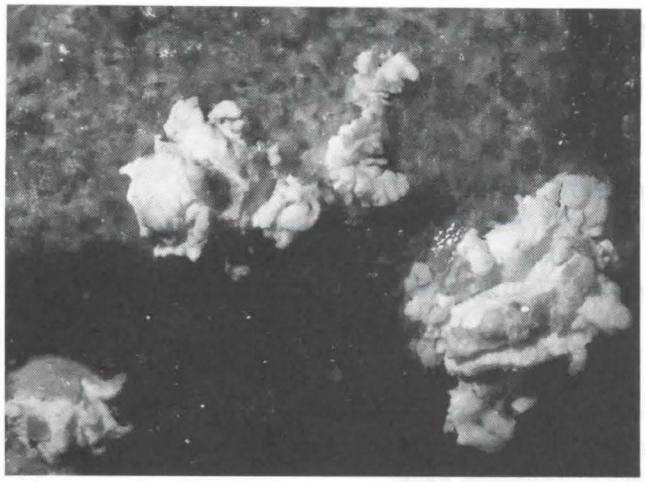

Fig. 1 : gesso in formazione sulle pareti calcaree

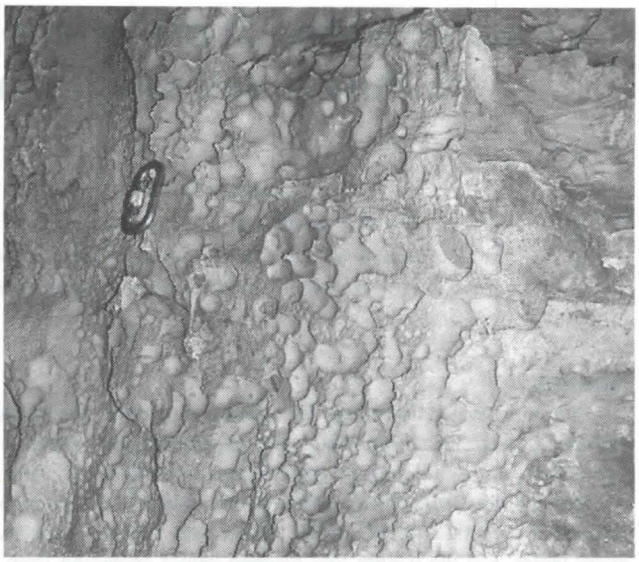

Fig. 2 : morfologie corrosive sulla parete calcarea evidenziate dal dilavamento del gesso

sembrato un metodo idoneo ad essere impiegato anche in grotta, in condizioni ambientali difficili, per verificare l'esistenza di azioni corrosive dovute alla circolazione di acque sulfuree, e per quantificarne l'intensità. L'esperimento si è protratto per 5 anni, ed a metà periodo è stata effettuata una prima serie di misure (GALDENZI & MENICHETTI, 1994). Un altro vantaggio legato all'impiego di questa metodologia è costituito dalla disponibilità di una ricca documentazione sui risultati conseguiti in precedenti esperienze condotte in superficie (GAMS, 1985; STEFANINI *et al.*, 1985).

La stazione sperimentale è stata installata nel Crepaccio Sulfureo della Grotta del Fiume; l'intensa circolazione di acque sulfuree, l'esistenza di un ampia interfaccia tra la falda freatica sulfurea e l'atmosfera della grotta, la diffusa formazione di gesso sulle pareti hanno infatti consentito di riconoscere condizioni ottimali. Nel sito prescelto sono state realizzate tre stazioni di misura appendendo le placchette con filo di nylon (Fig. 3); nelle stazioni subacquee sono state collocate almeno 2 placchette, mentre in ognuna delle 2 stazioni aerate sono state appese 4 placchette. Un'altra placchetta è stata seppellita sotto gesso molle in formazione.

Le placchette, dalle dimensioni di circa cm 8 x 4 x 1, sono state levigate e misurate per calcolarne la superficie laterale. Il peso è stato determinato con precisione di 0.1 mg, previo essiccamento in condizioni standard a 110 °C. Esse sono state realizzate con Calcare Maiolica (Cretacico inferiore), litotipo affiorante nell'area: si tratta di calcare micritico assai puro, privo di impurità e di strutture interne che avrebbero potuto complicare le operazioni di preparazione e misura delle placchette stesse.

Le placchette sono state posizionate nel marzo 1990 e in ciascuna stazione sono state prelevate metà delle placchette dopo due anni e mezzo, nel settembre 1992. Le rimanenti sono state ritirate nel marzo 1995, dopo 5 anni di

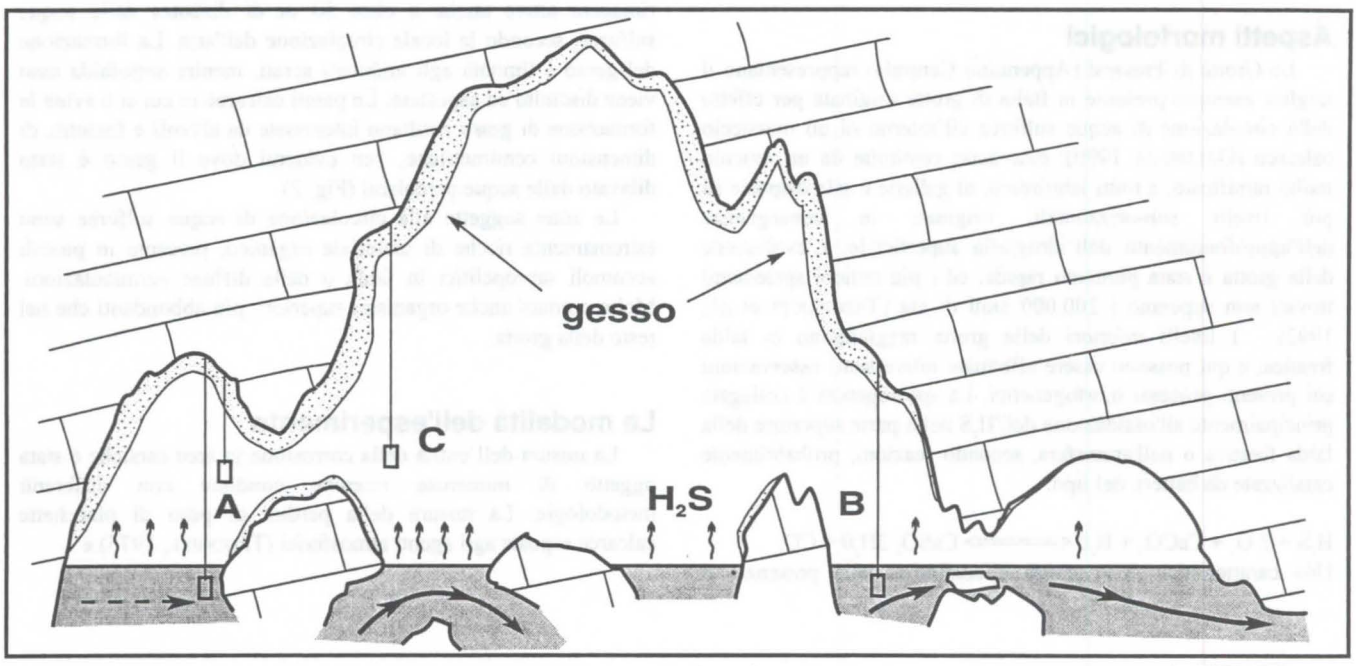

Fig. 3 : Grotta del Fiume, ramo sulfureo - schema sito sperimentale

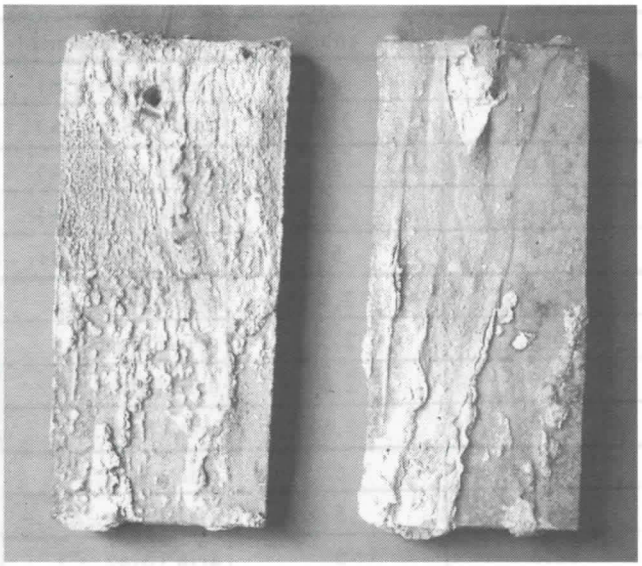

Fig. 4 : Placchette esposte per 5 anni ai vapori di H_2S, con gesso di neoformazione

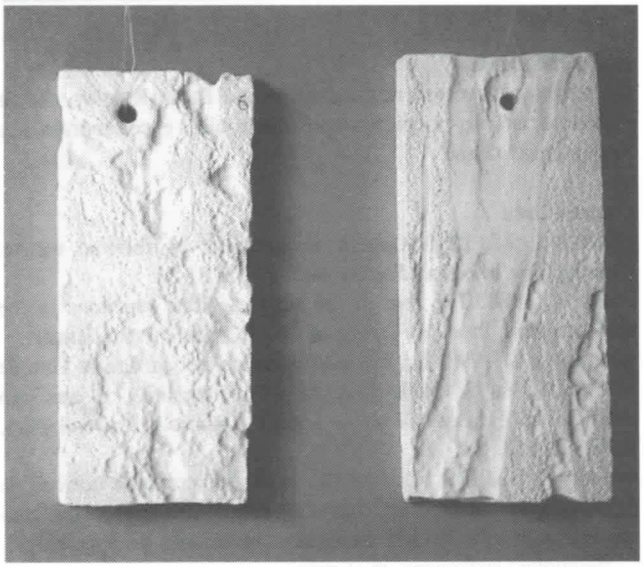

Fig. 5 : Superficie delle placchette dopo il lavaggio del gesso di neoformazione

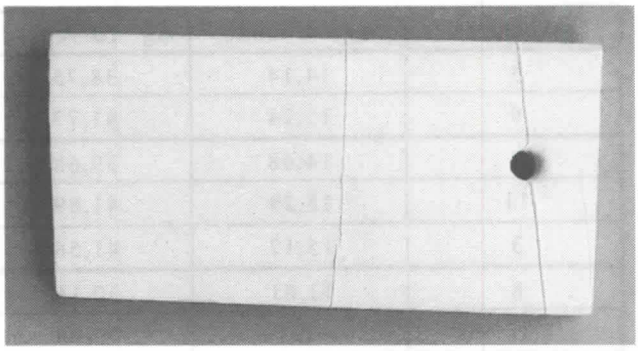

Fig. 6 : Placcchetta dopo 5 anni di immersione in acque sulfuree; notare le vene di calcite in rilievo

esposizione; una placchetta è andata perduta per la rottura del filo, fortemente indebolito dalle esalazioni sulfuree.

Le placchette esposte all'aria erano interessate dalla formazione di gesso già sei mesi dopo l'inizio dell'esperienza; al momento del recupero era presente uno spessore variabile di gesso, sia in forma bianca, microcristallina, che in forma cristallina, generalmente in superficie o dove il fenomeno era meno sviluppato (Fig. 4). Prima di pesare le placchette è stato necessario disciogliere il gesso in acqua distillata saturata con polvere di calcare, fino a scoprire la superficie calcarea, che appare corrosa in maniera molto eterogenea, con "cariature" profonde alcuni millimetri (Fig. 5). Le placchette erano rivestite da patine scure, costituite da materia organica, interposte tra calcare e gesso.

Le placchette lasciate in falda erano invece coperte da uno spesso strato di materia organica, in cui prosperavano anche vermi, in corso di studio. La superficie calcarea è uniformemente corrosa, priva di gesso, con vene di calcite spatica in rilievo per corrosione differenziale (Fig. 6). La presenza di evidenti filamenti di materia organica sulla superficie calcarea delle placchette è poi stata confermata dalle osservazioni al microscopio elettronico (Fig. 7).

Risultati dell'esperimento

I risultati delle misure relative alla perdita di peso, riportati in tabella 1 secondo diverse unità di misura già utilizzate in bibliografia, abbinati alle dirette osservazioni effettuate, consentono di trarre alcune significative conclusioni.

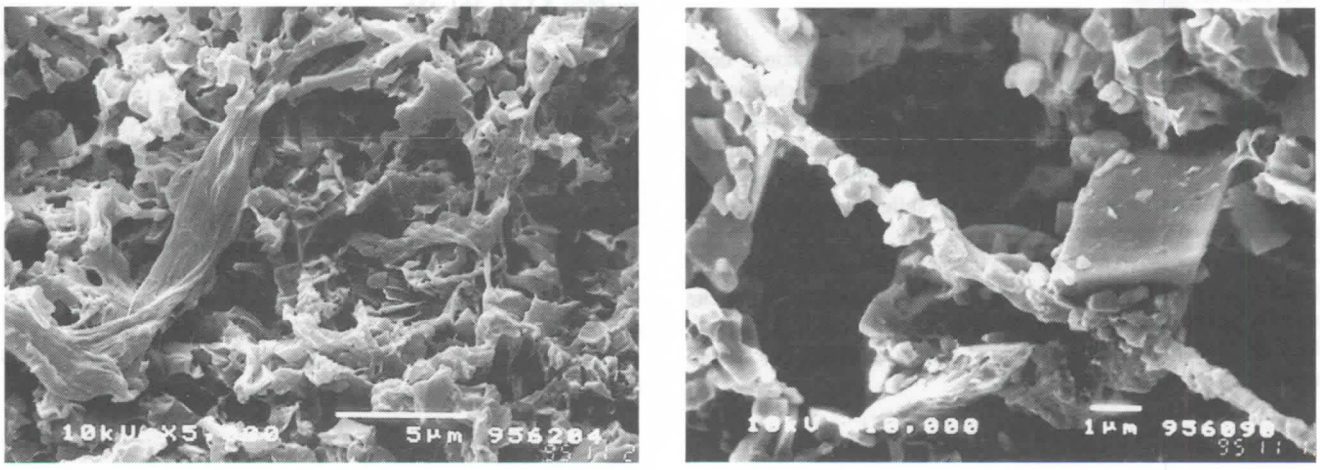

Fig. 7: superficie delle placchette al microcoscopio elettronico (notare la presenza di filamenti di materia organica) in falda (a sinistra) - nell'atmosfera della grotta (a destra)

Placchetta	mg/cm^2/anno	mg · 10^{-3}/cm^2/di	mm/1000 anni	anni	Posizionamento
5	14,14	38,75	55,6	2,5	falda (Staz. B)
9	15,24	41,77	59,9	2,5	falda (Staz. A)
7	14,48	39,68	56,9	5	falda (Staz. A)
11	15,29	41,89	60,1	5	falda (Staz. A)
3	15,17	41,56	59,7	5	falda (Staz. B)
8	11,01	30,16	43,3	2,5	aria (Staz. A)
10	6,97	19,09	27,4	2,5	aria (Staz. A)
13	8,59	23,55	33,8	2,5	aria (Staz. C)
14	16,27	44,56	64,0	2,5	aria (Staz. C)
1	17,46	47,82	68,7	5	aria (Staz. A)
12	13,89	38,06	54,6	5	aria (Staz. A)
2	21,56	59,12	84,8	5	aria (Staz. C)
15	17,6	48,23	69,2	2,5	in gesso

Tab. 1- risultati prove di corrosione delle acque sulfuree sulle placchette calcaree

- Le placchette ubicate sottofalda presentano un uniforme grado di corrosione, intorno ai 15 mg/cm^2/anno, indipendentemente dalla stazione in cui sono collocati; la perdita di peso per quelle esposte ai vapori di H_2S risulta invece molto più variabile, in conformità a quanto riconoscibile anche macroscopicamente.
- La velocità dei flussi freatici (maggiore nella stazione B che in A) non ha influenzato i risultati per le placchette ubicate in falda. Al contrario nell'atmosfera i risultati variano in funzione del tipo di circolazione idrica; nella stazione C, ubicata allo sbocco di un canale sommerso con scorrimento rapido ed abbondanti esalazioni i valori risultano più elevati.
- Il grado di corrosione in ambiente freatico è rimasto costante anche in rapporto al tempo di esposizione; le placchette esposte ai vapori di H_2S hanno subito azioni corrosive di intensità crescente nel tempo; i valori medi calcolati su base annua per le placchette dopo 5 anni di esposizione risultano pari a circa il 160% di quelli calcolati dopo 2,5 anni. In termini reali la perdita di peso per le placchette esposte 5 anni è risultata in media di 88,2 mg/cm^2, contro i 26.8 mg/cm^2 delle placchette prelevate dopo 2,5 anni; ipotizzando che anche le placchette esposte per 5 anni abbiano subito nel primo periodo una perdita di peso media pari a 26,8 mg/cm^2, risulta che nella seconda frazione dell'esperimento la corrosione è stata di 61.4 mg/cm^2, cioè oltre due volte maggiore.

I presenti dati indicano che le reazioni di ossidoriduzione dello zolfo in atmosfera si sono attivate più lentamente che non in falda, verosimilmente per i tempi più lunghi necessari allo sviluppo di consistenti colonie batteriche sulle placchette esposte all'aria. Gli alti valori misurati per la placchetta collocata entro gesso di neoformazione già esistente sulle pareti della grotta concordano con questa interpretazione.
- Le azioni corrosive in atmosfera ad opera di vapori di H_2S sono risultate più rapide che non in falda; è bene tuttavia ricordare che questi fenomeni hanno una elevata intensità solo in ristrette località, prossime alle polle di acqua sulfurea, e calano rapidamente allontanandosi da esse.

Ringraziamenti
Un sentito e doveroso ringraziamento ad ELISA ROMINI, che ha realizzato le foto al microscopio elettronico e collaborato alla loro interpretazione.

Opere Citate

EGEMEIER, S.J. 1981. Cavern development by thermal waters. *National Speleological Society Bulletin* 43: 31-51.
FORTI, P. 1988. The role of the sulfide-sulfate reactions in the speleogenesis. Proc. 1st Congr. of FEALC, Ouro Preto, Brasil.
GALDENZI, S. 1990. Un modello genetico per la Grotta Grande del Vento. In: (S. Galdenzi & M. Menichetti ed.): Il carsismo della Gola di Frasassi. *Memorie Istituto Italiano di Speleologia* s. II, 4: 123-142.
GALDENZI, S. & M. MENICHETTI. 1994. Misure sulla corrosione di placchette calcaree ad opera di acque sulfuree: primi dati sperimentali. Atti XXVII Congresso Nazionale di Speleologia. Castelnuovo Garfagnana, in stampa.
GALDENZI, S. & M. MENICHETTI. 1995. Occurrence of hypogenic caves in a karst region: examples in Central Italy. *Environmental Geology* 26: 39-47.
GAMS, I. 1985. International comparative measurement of surface solution by means of standard limestone tablets. *Razprave iv. razreda* XXVI: 361-386.
HILL, C.A. 1987. Geology of Carlsbad Caverns and other caves of the Guadalupe Mountains, New Mexico and Texas. *New Mexico Bureau Mines & Miner. Resources Bull.* 117: 150 p.
STEFANINI, S.; ULCIGRAI, F.; FORTI, F. & F. CUCCHI. 1985. Resultats experimentaux sur la degradation des principaux lithotypes du karst de Trieste. Actes XVI Congr. Nat. de Spel. (Nancy - Metz, 1985). *Spelunca Memories* 14: 91-94.
TADDEUCCI, A.; TUCCIMEI, P. & M. VOLTAGGIO. 1992. Studio geocronologico del complesso carsico "Grotta del Fiume-Grotta Grande del Vento" (Gola di Frasassi, AN) e indicazioni paleoambientali. *Il Quaternario* (5) 2: 213-222.
TRUDGILL, S.T. 1975. Measurement of erosional weight loss of rock tablets. *Brit. Geomorph. Res. Group. Tech. Bull.* 17: 13-19.

Caves climatic systems

Bulat R. Mavlyudov
Institute of Geography Russian Academy of Sciences Staromonetny per. 29, Moscow 109017 Russia

Abstract

Cave climate is not homogeneous. It is possible to choose three basic caves climatic systems in dependence on cave morphology and ventilation (for caves without water): of horizontal caves (with entrances at different levels), of inclined descending and ascending caves. In caves of each climatic system there are from 3 to 5 climatic zones. Size and completeness of collection of climatic zones depends on outside climate and cavern morphological peculiarities. Climate of caverns with complex morphology will have combinations of basic climatic systems. Cave climatic system can be complicated by accumulation of perennial snow and ice or by flowing water or completely disturbed by them.

1. Introduction

Investigations of last years shows that we can't compare small caves climate with large caves climate. There are many caverns with very big length and big difference between entrances and its lowest parts. Some of these caverns dissect a few surface climatic belts. Climate of such caverns have big unhomogeneous. In some cases we need to say about microclimate of different parts of caverns. If we carefully consider climatic structure even of not very big cave we understand that it is not very simple. Traditional point of view on cave microclimate not allow us to do climatic description for big quantity of big caverns. In this report we discuss common principles of caves climatic structures (caves climatic systems) for caverns with different morphology and size.

2. Factors that define cave climate

They are:

- climate of area where the cave is situated;
- cavern morphology that determines system of air circulation in it;
- geothermal conditions of the rock massif where cave is situated;
- system of water streams flows in caverns;
- quantity of precipitation that penetrate in caves (first of all snow).

We shall discuss influence of these factors on climatic conditions in caverns in brief.

Air temperature and humidity, wind velocity and direction, atmospheric pressure will be more important factors of external climate, that have influence on cave climate. The warmer external climate will be the higher cave temperature will be. There are mean year air temperatures (MYAT) up to 12°C in caves of south slope of the Big Caucasus (TINTILOZOV, 1976). In the middle Ural cave MYAT is about 5-6°C. There is lower value of air humidity in the caves in the dry regions but in the wet regions humidity of cave air is higher. Strong summer wind that blows in the entrance of small cave can be the reason of cave climate similar to external. Sudden change of atmospheric pressure leads to appearance of air flow in or out of the cave.

Air movement is the more significant agent for transmission of external climate influence inside the caves. In is possible to choose two main mechanisms of air movement inside the caves (MAKSIMOVICH, 1963):

1) There is chimney effect of air movement in caverns with some (two or more) entrances at different altitudes. The reason of it lays in difference of air columns weights near entrances. There are air movement from lower entrance to upper in winter and from upper to lower in summer (LISTOV, 1885). Air flow in the cave changes its direction when surface air temperature will be equal to one in the middle part of the cave (neutral zone, DUBLJANSKI, 1977).

2) In inclined caverns air moves because of difference of air density in different parts of the cave. Cold external air in winter ejects more warm cave air in inclined descending caves. Warm more light air in summer ejects more cold cave air in inclined ascending caves (MAKSIMOVICH, 1963). Air movement stops in both cases when external and cave temperatures will be equal. The air movement in caves can occur also when wind blow in cave entrances, when moving water takes air with it, when external atmospheric pressure suddenly changes.

Temperature of rock massif where cave is situated also has big influence on cave climate. External climate is transmitted inside the caves by cave wind. It is superimposed on the climate that rock define in the cave. Water streams also have influence on the rock temperature around the cave. We can read in scientific literature two main opinions about temperature inside the caves: 1) MYAT in neutral zone in caves is equal to external MYAT (PULINA, 1974) and 2) cave MYAT not depends on external MYAT; it is determined by cave morphology and peculiarity of air changing with the surface (DUBLJANSKI & LOMAEV, 1980). We can't agree with second opinion because of it is well known that cave temperature decrease with elevation (MAKSIMOVICH, 1963).

However we can observe equal values of cave MYAT and external MYAT not everywhere. From hydrogeothermy we know that rock temperature at the neutral layer of the earth (layer with minimum year amplitude of temperature oscillation) have value on some degrees higher of MYAT (FROLOV, 1976). This layer usually situates on depth about 15-20 m lower day surface. For the area of the former USSR temperature difference changes from 2 to 6°C. Rock temperature increases with depth on 1 degree on each 30-40 m. If we shall imagine closed cavern that haven't contact with day surface air temperature will be equal to the rock temperature in it. The dipper cave will be the higher temperature will be in it. We can expect that temperature in deepest parts of real caves (without water) will be almost equal to surrounding rock temperature. Investigations in some caves show that MYAT in their neutral zones are lower the rock temperature. For example, this difference in the Kungur Cave is about 1,0°C and in the Cave Sumgan-Kutuk (the Ural) is about 1,5°C.

Caves usually situate in regions with not equal difference between external MYAT and rock temperature of neutral layer. Caves locate also at different depths from day surface. Therefore it is difficult to expect equal regularities between external and cave temperatures. For example, MYAT in caves neutral zones in Carpatians and Podolia is almost equal to theoretical value of

rock temperature. It exceeds external MYAT on 3.7°C. This difference in the Kungur Cave consist about 3°C for ventilated parts and 4°C for not ventilated parts of the cave. In caves and mines of the Pamirs this difference is about 7°C.

There are regularities of regional changing of cave MYAT in their neutral zones. Some empirical equations for calculation of thermal conditions in the caves were received on basis of statistical analysis of cave temperatures data. For North America equation is next (MOORE & SILLIAN, 1978): $\mathbf{T_c = 38 - 0.6L - 0.002h}$, and for Europe it is (CHOPPY, 1977): $\mathbf{T_c = 54.3 - 0.9L - 0.006h}$, where L is geographical latitude, degrees; h is elevation, metros. If we shall base on previous discussion it is possible to suppose that such equations have only estimative character.

The fact that MYAT in big quantity of large caves are higher than external MYAT allows to say that mean year heat and moisture flows have constant direction oriented outside from these caves.

Since heat capacity of water is approximately in 30 times higher than one of air it is possible to say that influence of water on cave climate is more intensive than influence of air on it. In many European caves in low mountain relief influence of water lead to equality of external and cave MYAT. On the contrary, in high mountains it is typical for caves with flowing melt water that caves MYAT are lower than external ones. The supply of caves by thermal water leads to exceeding cave MYAT above external one. Seasonal water inputs into caves (floods) lead to warming of cold zones in some parts of the caves and colding of warm zones in another.

Snow is accumulated in some caves. Snow is one of sources of coldness in the caves. Rain as a rule warms cave climate.

Now we shall consider climatic systems of typical caverns (without water): "horizontal" (the caves with some entrances at different elevations) and inclined (bag type) caves with one entrance. We can divide second type into two groups: caves with entrances in its upper end and caves with entrances in its lower end. Climate of caves with other morphology we can ascribe to one of main types or their combinations.

3. Horizontal caves

We can divide horizontal caves into 5 climatic zones (beginning from lower entrance): 1. Lower transitional zone (LTZ); 2. Cold temperature anomaly zone (A-); 3. Constant temperature zone (neutral zone) (CTZ); 4. Warm temperature anomaly zone (A+); 5. Upper transitional zone (UTZ). The fist who said about zones A+ and A- in caves was Russian scientist V.S. LUKIN, 1965. Presence of zones A- and A+ in such caves come in contradiction with conception of existence of equalizing zone between external climate and cave conditions of V.N. DUBLJANSKI, 1977 and others.

Lower transitional zone (LTZ) LTZ situates near lower cave entrance. During the cold period of year (between two changings of air movement direction) external climate have influence on LTZ by air flow into the cave, by solar radiation and outside wind. Air temperatures in LTZ in spring and autumn are positive, in winter they are negative and almost equal to external temperature. In summer air temperature in LTZ is alittle above zero because of air moves here through cold zone A-. Size of LTZ is different in all caves and depends on dimensions of caves channels, intensity of air circulation, entrance orientation, directions of main winds in surrounding area, quantity of snow at entrance of cave. Big part of year external air humidity is higher than caves one. I.e. moisture flow has direction into the cave and only in first part of winter it has direction from the cave. There are typical values of MYAT: $T_s > T_1$ and humidity: $E_s > E_1$. Its means that during the year LTZ receives more coldness than warmth, and mean year moisture flow have direction into the cave.

Cold temperature anomaly zone (A-) Zone A- has influence of LTZ during the winter and influence of CTZ in summer. Boundary between zones A- and CTZ lay on the line with year temperature oscillations about 0.5°C. Air temperature in zone A- changes from the lowest value at the boundary with LTZ ($T_2 < T_s < T_3$) to temperature at boundary with CTZ ($T_s < T_2 = T_3$). Coldness flow in zone A- from LTZ in winter is not compensated by heat flow from LTZ and CTZ in summer. It lead to cooling of zone A- to MYAT below external MYAT. Since in winter absolute air humidity grows from boundary with LTZ to boundary with CTZ, the moisture flow has direction contrary to air flow (Fig 1a).

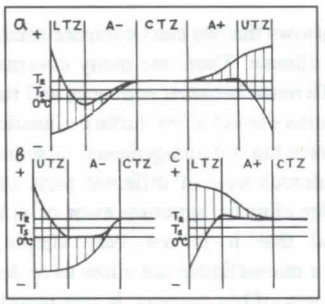

Fig. 1.

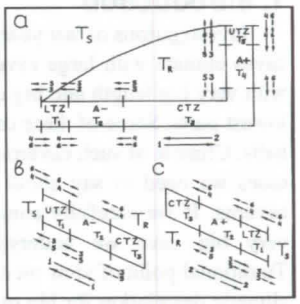

Fig. 2.

Fig. 1. Structure of climatic zones of horizontal (a), inclined descending (b), inclined ascending caves (c). Air circulation in winter (1), in summer (2); heat flows: in winter (3), in summer (4); moisture flows: in winter (5), in summer (6).

Fig. 2. Amplitudes of temperature oscillations in horizontal (a), inclined descending (b) and inclined ascending (c) caves.

During the year moisture flow in zone A- has transit orientation to the lower cave entrance. It is possible to see changing of air temperature in zone A- on Fig. 2. The zone A- length depends on diameter of cave channel, wind velocity in channel and distance between two entrances.

Zone of constant temperature (neutral zone) (CTZ) CTZ exist in central parts of caves. The reasons why temperature in CTZ can differ from rock temperatures we discussed earlier. This zone length depends on common length of cave and distance between entrances. When we move further from channels with air circulation (in maze caves) air temperature and humidity will increase alittle and amplitudes of their year oscillations are decrease. As we can see on Fig. 1a the moisture flow direction is constant from boundary with zone A+ to boundary with zone A- during the year and not depends on direction of air circulation.

Warm temperature anomaly zone (A+) Upper entrances in horizontal caves often exist as fissures and narrow pits. Since people can't go through them, there is almost no observations in them. The inner boundary of zone A+ situates on the line with amplitude of year air temperatures oscillations about 0.5°C ($T_R > T_4 = T_3$) and outer boundary is on maximum value of cave MIAT ($T_4 > T_R > T_3$). Moisture flow on the boundary with CTZ has direction inside cave in all seasons of year (fig. 1a). On the boundary with UTZ moisture flow in winter has direction out of cave but in summer it has direction inside cave. MYAT in zone

A+ are above rock temperature. It connects with situation when heat flow from boundary with UTZ in summer not compensates heat flow from CTZ in winter. The zone A+ length depends on fissures and pits width. This length, as a rule, is smaller than one of zone A-. Since maximum amplitude of rock massif cooling is measured from T_3 (but not from external MIAT) on absolute value it is higher than maximum rock massif warming in summer (Fig. 2). Because of it duration of periods of cave warming and cooling are different (also as caves wind velocities in summer and winter). For example, in the Kungur Cave duration of winter air circulation consists about 200 days (from 1969 to 1993) and duration of summer air circulation consists about 150 days (DOROFEEV & MAVLYUDOV, 1993). Melting and condense water from UTZ has influence on climate of zone A+ in winter. Flow of warm wet air from zone A+ through UTZ in atmosphere gives white jets in hard frost (they are like a smoke column). Warm wet air have contact with rock and snow. As a result melt water penetrate into UTZ and A+. Water move down and is warmed from air and rock. In summer warm wet air from surface through UTZ moves into zone A+ where it has contact with more cold walls. In result of condensation of vapor the additional heat penetrates in the cave.

Upper transitional zone (UTZ) UTZ is the equalizing zone between zone A+ and external climate. Situation in UTZ is similar to one in LTZ with difference that it has contact with not A- but with A+. There are only some measurements of temperature of air that flow out from UTZ in autumn and winter. Temperature 6.8°C was in October 1986 in air flow from Kungur Cave when external air temperature was 0.3°C. In February 1987 temperature of air flow from the cave was about 4.5°C. In Bzybskij Ridge (the Caucasus) in January 1980 temperature of air flow from the rock under snow cover consists 2.2°C at elevation 2000 m. At the upper part of mountain Razvalka in the North Caucasus temperature of air flows from rocks consisted 6°C but mean winter temperature was about 2.7°C (LUKIN, 1990). Cooling of UTZ is possible in winter by falling and blown snow. We can see moisture and heat flows on Fig. 1a.

Next expressions are truth for winter: $T_s<T_2<T_3<T_4>T_s$ and $E_s<E_2<E_3<E_4>E_s$, and for summer: $T_s>T_2<T_3<T_4<T_s$ and $E_s>E_2<E_3<E_4<E_s$. It is possible to observe all collection of zones in the caves where distance between entrances is large. If we take the cave with lesser length it lead to decreasing on CTZ. If difference of height between entrances will be lesser it lead to decreasing of length of zones A+ and A-. It occur because of decreasing intensity of air circulation and warm and cold inputs in cavern. It is possible complete elimination of CTZ and part or complete superposition of zones A+ and A- in the caves with small length. Decreasing of accessible for people parts of the caves by narrowness of its galleries lead to situation when we can see only separate parts of climatic systems. Sometimes we can see caves that have only A+ or A- zones. Small caves in gypsum mountain in town Iletsk (the Ural) (LISTOV, 1885) and mine gallery of mount Razvalka (LUKIN, 1990) can be examples of cold caverns. Pits in the Crimea and Caucasus that form in cracks along escapes can be example of warm caverns. Cave MYAT exceed external MYAT on 2°C in such pits in the Crimea (DUBLJANSKI, 1977).

4. Inclined caves

Nature of air movement in the inclined cave connects with air thermocirculation: cold hard air moves down the slope along floor of gallery and more warm and more light air moves up the slope along roof of gallery. In inclined descending caves cold external air eject warm cave air in winter, but in summer more light warm air can't penetrate in cold cavern. In inclined ascending caves warm external air eject more cold cave air in summer, but in winter cold hard air can't penetrate in warm cavern.

4a. Inclined descending caves (IDC) There are three climatic zones in this caves with big length (Fig. 1b): (UTZ), (A-), (CTZ).

Upper transitional zone UTZ includes upper part of cave near it entrance (pit or doline). Climate of UTZ is similar to external because of influence of wind. In winter T_1 and E_1 are almost equal with external. In summer T_1 in upper part of UTZ can be higher than external on the sunny places. The lower boundary of UTZ is situated on the line with minimum MYAT. Usually the size of UTZ is not very large. In some caves with wide entrance wind influence can penetrate to considerable depth. For example in the Cave Bolshoj Buzluk in Crimea this depth reach 40 m from surface. In summer moisture flow has direction in the cave in winter it has direction from the cave. If cave entrance has south orientation the sun can illuminate UTZ and even A- zone for some time.

Cold temperature anomaly zone (A-) Air movement depends on: difference external temperature and temperature in lower part of cave slope and difference of height between entrance and the end of zone A-. The more difference of temperatures is the bigger air movement velocity is at a floor of gallery. The dipper inclined gallery will be the bigger air movement velocity will be. Decreasing difference of temperature leads to reduction of air changing between surface and cave. In zone A- we can see increasing of T_2 from entrance inside cavern. Any increasing of external temperature T_s and strong wind can block the cave, i. e. stagnant zone or local whirlwind appear in UTZ that block penetration of external air in the cave. If temperature difference between upper and lower parts of zone A- will be sufficiently large local circle air movement occur. It will not connect with surface (local whirlwind). If height of gallery is not big but length of it is sufficiently large the air circle movement can divided into two or more whirlwinds. In difference from horizontal caves where we can observe almost constant air movement in zone A- (in winter in one direction, in summer in another) in IDC air movement is possible only in winter when $T_s < T_2$ (i.e. it occur not more than 2/3 of winter duration). There is moisture flow in winter from CTZ through zone A- and UTZ to the surface. In summer moisture flow has direction from surface into the cave to zone A- and also from CTZ to zone A- . Inner boundary of zone A- lays on the line with amplitude of air temperature oscillation about 0.5°C.

Constant temperature zone (CTZ)

Amplitude of year oscillations of air temperatures in this zone is not more than 0.5°C. There is no air circulation in CTZ. Far from entrance air temperature is almost equal to rock temperature.

There are all three zones in large IDC. But only two or one climatic zones can exist in more small caverns. Zone A- has small size or completely absent if cave entrance has small dimensions and/or if in winter it is closed by snow.

4b. Inclined ascending caves (IAC) The structure of climatic zones of IAC (Fig. 1c) is similar to so of IDC: LTZ, A+, CTZ. Zone A+ forming by warm light summer air that penetrate in it. Moisture flow in the cave in winter has direction from zone A+ to CTZ and through LTZ to the surface. In summer moisture flow has direction from surface through LTZ and zone A+ to CTZ. In spring air begins flow in the cave when $T_s>T_2$. In autumn air circulation is ended when $T_2>T_s$.

5. Vertical caverns

Pits is IDC but with almost vertical incidence. Air movement, T and E in them are similar to ones in IDC. Cold air usually penetrates in pits though center of shaft and more warm air lifts at perimeter of it. However if pit cross sections on different depths are not equal replacing of cold air stream occurs to one of pit wall. Snow accumulates in pits in winter. Snow in pit can melt or not in dependence from pit depth, degree of its cooling, quantity of falling and blown snow in it, quantity of heat that penetrate in pit with rain. Snow is additional source of pits cooling. The more snow gets into pit the more long time snow remains in it. Big quantity of snow in pits guarantees conservation of zero temperatures in pits during all warm period of year. Very big depth of pits is not favorable for snow conservation in them because snow gets in warm part of zone A- and melts quickly. In the dry dip caverns T3 can grow with depth in accordance with geothermal step of that area.

6. Caves with water

Water streams have big influence on caves climate. The more water gets into the cavern the more homogeneous cave climate becomes. All before mention climatic zones can disappear because water flows warm caverns in winter and cool them in summer. Through cave with constant big water flow will contain CTZ and seasonal small UTZ and LTZ. Caverns lost all or part of cold accumulated in winter if they have small constant or episodic water flows in summer. In these caves zone A- will be almost similar to LTZ.

Water in vertical caverns with big depth has especially big influence on caves climate. Melt water strong cools caverns and difference (T_s - T_c) becomes considerable. So in the shaft Kujbyshevskaja (the Caucasus) at the depth 800 m from surface cave temperature is about 2°C (DUBLJANSKI & KIKNADZE, 1984) (external MYAT at this elevation is about 7°C). In the shaft Snezhnaja (the Caucasus) temperatures are: T_c=4.5°C at depth 700 m (T_s=6°C) and T_c=6.2°C at depth 1370 m (T_s=10°C). In the spring Mchishta where shaft Snezhnaja has discharge water temperature is about 10°C (T_s=14°C). It is possible to calculate changing T_c with depth (i.e. vertical temperature gradient - VTG) for CTZ in climatic system of shaft Snezhnaja. It consists about 0.25°C on each 100 m of depth (let's compare it with VTG of Carpatians caves - 0.4°C/100m and VTG of free atmosphere - 0.6°C/100m).

Peculiarity of climatic systems in big vertical caverns consists in air movement in them. It depends on: difference of altitudes between entrances, capacity of water to take air with it, inversion of climatic zones in caverns when there is zone A- (because of snow) near upper entrance of "horizontal" cavern, but at lower entrance exists more warm zone. Sometimes descending air movement in upper part of cave system will be in opposition to ascending air movement from lower entrance in summer. Increasing of T_c in CTZ with depth leads to arising of ascending air movement under roofs of galleries (even when lower entrance is absent). As a whole climatic systems of large complex caves still wait their investigators.

7. Conclusion

Cave climatic systems is not something constant. Changing of external climate has influence on caves climate. First of all length of zones A+ and A- changes from it. External climate warming leads to decreasing or decay of zones A- in some caves. Calculations using mathematical model of air circulation in the Kungur Cave show that decreasing of external MYAT on 1°C lead to increasing of length of zone A- in the cave on 20-30 m (MAVLYUDOV, 1985).

But not only natural changing have influence on cave climate. Anthropogenic factors have big influence on it in last years. Next factors have influence on air circulation in the caves: placing of entrance doors, changing of cross sections of caves galleries, changing of groundwater levels. It leads to changing of cave climate and first of all dimensions of zones A- and A+.

Since there are not regular meteorological measurements in majority of russian caves observations of dimensions of zones with ice can be good indicators of natural or anthropogenic changing of cave climate.

We discussed climatic systems of main morphological types of caves only in common features. More detail study of them still wait own investigators.

References

CHOPPY, J. 1977. La temperature des cavites en fonction de la latitude et de l'altitude. Spelunca, 3: 117-118.

DOROFEEV, E.P. & B.R. MAVLYUDOV. 1993. Dynamic of Kungur Cave glaciation. Peschery, Perm, 23-24:131-140 (in russian).

DUBLJANSKI, V.N. 1977. Karst caves and shafts of the Mountain Crimea. Nauka, Leningrad, 182 p. (in russian).

DUBLJANSKI, V.N. & A.A. LOMAEV. 1980. Karst caves of the Ukraine. Naukova Dumka, Kiev, 180 p. (in russian).

DUBLJANSKI, V.N. & T.Z. KIKNADZE. 1984. Karst hydrogeology of Alpine folding area of the south USSR. Nauka, Moscow, 128 p. (in russian).

LISTOV, Yu. 1885. Caves-glaciers. Data for geology of Russia. Sankt-Peterburg, v.12: 105-280 (in russian).

LUKIN V.S. 1965. Temperature anomalies in caves of the Preduralje and critical analisys of underground cold theories. Peschery, Perm, 5(6): 164-172 (in russian).

LUKIN V.S. 1990. Temperature anomalies of the mount Razvalka near town Zheleznovodsk. In: Problems of geometeorology and winter cold accumulation. Sverdlovsk: 50-53 (in russian).

MAVLYUDOV, B.R. 1985. Geographical regularities of caves with ice. Data of Glaciological Studies, Moscow, 54: 193-200 (in russian, english summary).

MAVLYUDOV, B.R. 1987. Cave glaciation of the Pamirs. Data glaciological Studies, Moscow, 59:173-179 (in russian, english summary).

MAVLYUDOV, B.R. 1988. Cave glaciation of the Ural. Data glaciological studies, Moscow, 61:123-129 (in russian, englih summary).

MAKSIMOVICH, G.A. 1963. Bases of kastology. 1. Perm knizh. izd., Perm, 445 p. (in russian).

MOORE, G.W. & F.S.C. Sillian. 1978. Speleology. Study of caves. Zephyrus Press Inc., Teaneck, 150 p.

PULINA, M. 1974. Denudacja chemiczna na obrazach krasu weglanowego. PAN, Warszawa, 159 p.

TINTILOZOV, Z.K. 1976. Karst caves of the Georgia. Metsniereba, Tbilisi, 275 p. (in russian).

FROLOV, N.M. 1976. Hydrogeothermy. Nedra, Moscow, 280 p. (in russian).

Some concepts about heat transfer in karstic systems

by Pierre-Yves Jeannin[1,2], Rudolf Liedl[2] & Martin Sauter[2]

[1]Center of Hydrogeology, University of Neuchâtel, Rue Emile-Argand 11, CH-2007 Neuchâtel, Switzerland

[2]Applied Geology, University of Tuebingen, Sigwartstraße 10, D-72076 Tuebingen, Germany

Abstract

The conceptual model of heat transfer in karst systems presented here is based on the existing models for the saturated zone and on a simple air flow model for the unsaturated zone. It is in good agreement with the fields observations. As a first approximation, it can be used to interpret the temperature responses of karst springs. The *shape* of the temperature pulses provides information about the *geometry of the conduit network* within the saturated zone. The *amplitude* of the temperature pulses provides informations about water *flow velocities* in the unsaturated zone. The *positive/negative temperature pulses* («warm floods» in summer and «cold floods» in winter) provide information about the *depth of the phreatic zone* below the ground surface.

Résumé

Le présent modèle conceptuel des transferts de chaleur dans les systèmes karstiques se base, pour la zone saturée, sur les modèles existants et, pour la zone non saturée, sur un nouveau modèle simple des circulations d'air. Ce mdoèle est conforme aux observations de terrain. En première approximation, il peut être utilisé pour interpréter la réponse thermique des sources karstiques. La *forme des impulsions* de température fournit des informations sur la *géométrie du réseau de conduits karstiques* dans la zone saturée. *L'amplitude des impulsions* de température donne des informations surtout sur la *vitesse verticale de l'eau* dans la zone non saturée. L'existence *d'impulsions positives ou négatives* de la température à la source donne des informations sur la *profondeur de la zone saturée* sous la surface du bassin versant.

1. Introduction

Temperature records of karst-spring waters can easily be measured with a high degree of precision. Until recently, interpretations of this parameter have been restricted due to the absence of a physical concept of heat transfer in karst.

BENDERITTER *et al.* (1993) present a first theoretical concept and model for heat flow processes in carbonate systems. This model considers a single karst conduit which transmits waters rapidely to the spring and exchanges heat with the rock matrix. Results show that temperature pulses are only slightly modified by the flow through the conduit.

RENNER (1996) has developed a similar approach for modelling heat transfer in the saturated zone (flooded conduits). He also observed that temperature pulses due to recharge events can propagate far across the saturated zone before they dissipate; the shape of the pulse is modified along the underground travel depending on the geometry of the conduit-network (LIEDL *et al.* 1997). Such a model allows the evaluation of the effect of different geometrical characteristics of the conduit network on spring temperature. Applied to a real karst system, volume, surface and openings of conduits could be estimated. It is pointed out that the sensitivity of temperature responses on geometrical parameters of the conduit network is very high. Nevertheless, in this model, the shape of the input temperature pulse is considered as a calibrating parameter.

Heat processes within the *saturated* zone appear to be well described by the models above. However, there is still no approach which allows the physical modelling of the heat transfer processes in the karst *unsaturated* zone.

The aim of this paper is to present an overview of some general concepts and physical background which can be applied to model heat transfer in karst systems.

2. The conceptual model

Basic simplifications

Several different assumptions have to be made in order to be able to calculate heat flow transfer in karst systems:

1) Conduits are considered as a network of one-dimensional pipes (no change in fluid velocity at right angle to the flow).

2) Flow velocity within the matrix is low, i.e. it can be neglected; heat transfer in the matrix can then be described by conduction only.

3) Conduit walls have simple geometry (circular or rectangular cross-sections).

These assumptions apply to both the unsaturated zone and the saturated zone. The phases that have to be considered are rock and water in the saturated zone, and rock, air and water in the unsaturated zone.

Other models can be considered depending on the aims of the studies. Our model gives a first global approximation of the heat transfer within complete karst systems. It is not the aim of the study to explain local microclimates in caves.

Boundary conditions

Two types of boundary conditions are considered (figure 1).

1) *The deep geothermal heat* is coming from sources deeper than the karst system. In continental lithosphere geothermal heat flow ranges between 40 and 70 kW/km^2 depending on the position on the Earth surface. The heat results of radioactive decay within the continental crust and of temperature gradient between crust and mantle. This implies that steady state conditions prevail independently from surface features like karst systems. Here we assume that geothermal heat flow is equal to 60 kW/km^2.

It can be demonstrated that geothermal heat flow is very low with respect to water flow through most karst systems. In temperate areas, the specific discharge of karst springs ranges between 1 and 100 l/s/km^2, corresponding to $3.15 \cdot 10^4$ to $3.15 \cdot 10^6$ m^3/km^2/y. On the one hand, the geothermal energy is $1.9 \cdot 10^9$ J per year and per km^2; on the other hand, the energy needed to heat 1 m^3 of water by 1°C is $4.19 \cdot 10^6$ J, meaning that the geothermal heat flow can heat approximately 453 m^3 of water by 1°C per year. Applied to a karst specific discharge this flux can heat karst waters by less than 0.1°C/y. Similar values stem from BOEGLI (1980) and MATHEY (1974).

The consequence of this low heat flow is that the lower limit of karst systems can be considered as a «no heat flow boundary» as well as a «constant heat flow boundary». The model results will hardly be affected by the geothermal flow.

mass conservation:

$$-\frac{\partial}{\partial t}\int_{\Omega}\rho \cdot d\Omega + \int_{\Sigma}\rho \cdot \vec{v} \cdot \vec{n} \cdot d\Sigma = 0 \qquad (6)$$

with $v=v_{fl}$, n is a normal vector to Σ, Σ is the wall surface of the conduit segment and Ω its volume.

momentum conservation:

$$\frac{\partial}{\partial t}\int_{\Omega}\rho \cdot \vec{v} \cdot d\Omega + \int_{\Sigma}(\rho \cdot v \cdot \vec{v}) \cdot \vec{n} \cdot d\Sigma - \int_{\Sigma}\bar{\tau} \cdot \vec{n} \cdot d\Sigma - \int_{\Omega}\rho \cdot g \cdot d\Omega = 0 \qquad (7)$$

with g=gravitational acceleration and τ =viscosity stress tensor.

energy conservation (see equ. 11 for Q_ψ):

$$\frac{\partial}{\partial t}\int_{\Omega}\rho \cdot (U + \frac{v^2}{2}) \cdot d\Omega - \int_{\Sigma}\vec{v} \cdot (\bar{\tau} \cdot \vec{n}) \cdot d\Sigma - \int_{\Omega}\rho \cdot \vec{v} \cdot g \cdot d\Omega - \int_{\Sigma}\vec{\Phi} \cdot \vec{n} \cdot d\Sigma - \int_{\Omega}Q_{\psi} \cdot d\Omega = 0 \qquad (8)$$

perfect gas equation:

$$P = \rho \cdot R \cdot T \qquad (9)$$

with R=gas constant.

internal energy equation:

$$U = \frac{5}{2} \cdot R \cdot T \qquad (10)$$

Such a problem has to be solved numerically.

Φ and Q_ψ in equ. 8 can be considered as boundary conditions of the conduit system. Meanwhile, to solve the problem correctly, one has to consider conduit and matrix as a system, meaning that Φ has to be calculated using equ. 1. The full system is then made up of six nonlinear equations. This is a very complicated problem to be solved by computer programs.

A further problem is introduced by air humidity (Ψ). Humid air contains more energy than dry air at the same temperature. This is due to the energy needed to evaporate the amount of water enclosed in the air. It can easily be shown that a normal atmospheric vertical temperature gradient for dry air is 9.76°C/km, and only 5.1°C/km for humid (saturated) air (see ROEDEL 1994). Air within karst conduits is almost saturated, but atmospheric air, entering the conduits is usually unsaturated. This has to be introduced into equation 8 in the last term:

$$Q_{\psi} = -L_w \cdot d\psi_{wsat} \qquad (11)$$

It becomes apparent that equation 5 is a special case of equation 8, except for the hydrodynamical dispersion which is not considered within equation 8.

First results and comparison with field data

So far, the conceptual model described above has not been coded into a computer program. However, two parts have been modelled separately: the phreatic zone (RENNER 1996) and the unsaturated zone in a simplified manner (only air circulation using equations 6 to 10).

Results from the unsaturated zone model show that air temperature is mainly influenced by three factors: the elevation, the humidity (term 5 in equ. 8) and the heat exchanges between phases (term 4 in equ. 8). Flow velocity or cross-sectional variations have only a limited effect on the air temperature.

Heat exchange between air and cave walls

A change in Φ value (energy) in term 4 of equation 8 induces a direct effect on temperature of the air. This shows that the air temperature is strongly influenced by the heat exchange with the walls (and/or water). WIGLEY & BROWN (1971) have shown that air temperature equilibrates with walls (and/or water) over a short distance in flow direction, the distance being dependent on the flow velocity and the contact surface between air and walls (and/or water). It can be observed at the cave entrances that the distance, along which temperature significantly varies along the year, is generally quite short. It is known as the «heterothermic zone». This zone seldomly extends over more than 50 to 100 meters. If the air flow is very high and the passages very wide, the equilibration distance can reach about 500 meters. Fields observations demonstrate that this principle can also be applied to water temperature, but so far, a theoretical approach of this process is still lacking. Evaporation/condensation processes may play an important role.

Vertical air temperature gradients and humidity

Vertical gradients found by our model are 9.76°C/km for dry air. Humid air gradients are calculated introducing equation 11 in term 5 of equation 8. The calculated value is then 4.80°C/km what is not exactly the value expected from the literature (5.10°C/km). This might be due to different physical constants used in both calculations.

Temperatures have been measured in more than 50 vertical caves around the world. Gradients ranges between 2 and 5°C/km, most of them being very close to 5°C/km (figure 2).

Lower gradients observed can generally be related to local conditions like the presence of snow in cave entrances (shafts) which normally cools the cave down for some hundreds of meters. In this case, the heat exchange with the conduit's wall (the snow) is not equal to zero (Φ in equation 8), but is highly negative. In such cave sections, this effect leads to cooler air temperatures than the expected outside mean annual temperature, but this leads also to lower vertical gradients (less than 5°C/km). If conduits are vertical, cave temperature can be affected down to 200 or possibly 300 meters. Such a case has been observed by JEANNIN (1990).

Heat exchanges within the phreatic zone

Within the phreatic zone, heat exchange between water and solid rock is of the same type as for air and solid rock. However, with water having a larger heat capacity, any disequilibrium between water and rock temperature tends to extend over much larger distances (kilometers).

BENDERITTER *et al.* and RENNER's models are capable of simulating pretty well the observed temperature variations at springs. However, in both models, temperature of water entering the phreatic zone, which depends on the processes described above within the unsaturated zone, is a calibrating parameter. The model presented here provide independent information on this input temperature.

Temperature of water entering the phreatic zone

In both saturated models the input records were different: RENNER used only «cold» inputs and BENDERITTER «cold» in winter and «warm» in summer. In fact these different inputs are in agreement with our conceptual model.

Our model assumes that temperature of air and water depends on the season down to a depth of about 50 m, possibly 100 m below the surface (heterothermic zone). In the catchment studied by BENDERITTER the water table is approximately 10 meters below the surface. Therefore, it has to be expected that spring water temperature are season dependent.

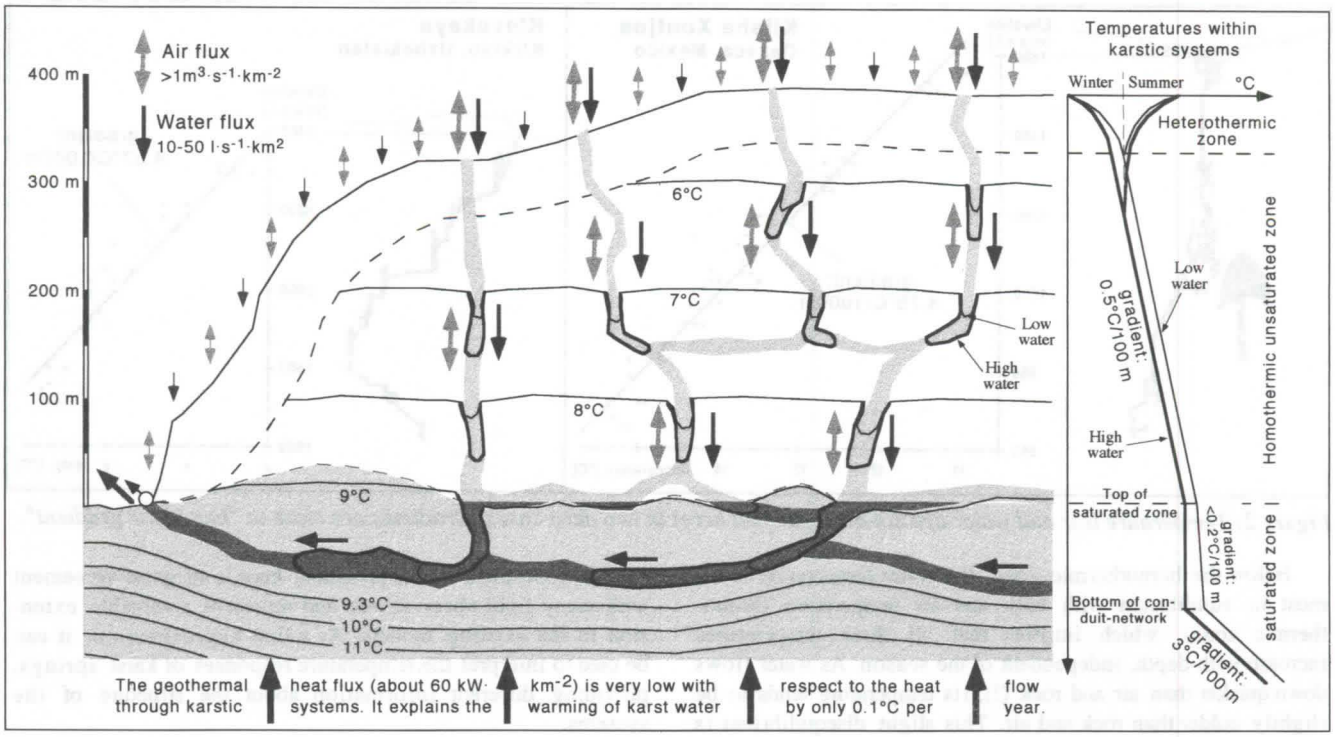

Figure 1: Conceptual model of water temperature distribution in karst systems. Air and water temperatures are generally almost equilibrated.

2) *The atmosphere* exchanges air and water with the karst system. Air and water temperature of the atmosphere, as well as water quantity mainly depend on meteorological processes. Fortunately they can easily be measured.

Processes

There are different types of heat transfer mechanisms within the karst systems: heat conduction (mainly within the rock), heat convection in water, heat convection in air, heat exchanges (between the three phases), evaporation and condensation, etc. Without having a physical model of each process, it is difficult to evaluate their respective importance.

Heat conduction in the matrix rock

It can be demonstrated that this process is of importance only if the respective phase is immobile, i.e. in the solid rock phase. In fluids, heat conduction is normally low compared to heat convection. Heat conduction in the rock can be described by the following equation:

$$\frac{\partial T_m}{\partial t} = \alpha \frac{\partial^2 T_m}{\partial z^2} = \alpha \cdot div(\lambda_m \cdot \overrightarrow{grad}\, T_m) \qquad (1)$$

where α is the thermic conductivity of the rock material and λ_m is the heat conductivity of the solid rock:

$$\alpha = \frac{\lambda_m}{\rho \cdot c} \qquad (2)$$

where ρ is the density and c the heat capacity of the rock. The heat flux Φ across a surface A is:

$$\Phi = -A \cdot \lambda_m \cdot \overrightarrow{grad}\, T_m \qquad (3)$$

Equation 1 gives the relation between the variation of temperature in time at one point ($\partial T/\partial t$) and the variation of temperature in space ($\alpha \cdot div(\Phi)$). Assuming a geometry for the conduits, heat fluxes across conduit walls can be calculated for a given temperature distribution in conduit and matrix rock. Carslaw & Jaeger (1959) provide different analytical solutions for these calculations.

Heat convection

This type of heat flux describes the heat transferred by fluid flow. It depends mainly on the fluid velocity v_{fl}. The velocity is not constant across the section of a conduit, we therefore have to account for hydrodynamic dispersion (D). We can then assume one dimensional conduit flow (in the direction of the conduit length), but with a dispersion D_x describing the effects of a 3-dimensional velocity field. The equation is :

$$\frac{\partial T}{\partial t} = -v_{fl} \frac{\partial T}{\partial x} + D_x \frac{\partial^2 T}{\partial x^2} \qquad (4)$$

This equation describes the heat transfer along an isolated conduit with a constant cross-section. The variations in cross-section can also account for changes in D_x.

Coupling conduction and convection

Equation 4 describes heat transfer along an isolated conduit. If we assume that there are heat exchanges between fluid in the conduit and matrix, we obtain the following coupled equation:

$$\frac{\partial T}{\partial t} = -v_{fl} \frac{\partial T}{\partial x} + D_x \frac{\partial^2 T}{\partial x^2} + \frac{\lambda_m}{V_{fl} \rho_{fl} c_{fl}} A \frac{\partial T_m}{\partial z} \qquad (5)$$

where v_{fl} is the water velocity, ρ_{fl} is the water density, c_{fl} is the water heat capacity, A is the contact surface between rock and water, and z is a direction perpendicular to x.

Analytical solutions of this equation have been developed for simple geometries (Carslaw & Jaeger 1959). In a simplified form (dispersion term neglected) and coupled to a water flow model through pipes, analytical solutions of equ. 5 have been used by Benderitter *et al.* (1993) and Renner (1996) to calculate heat transfer within the phreatic zone of karst systems. Numerical solutions have been used as well.

Problems related to air circulation

Basically equation 5 is valid for any fluid. The first problem with air is the calculation of v_{fl}. With air being compressible, v_{fl} is a function of four variables: head difference ΔH, pressure P, air temperature T and air density ρ. In total there are five unknowns implying that five equations have to be solved:

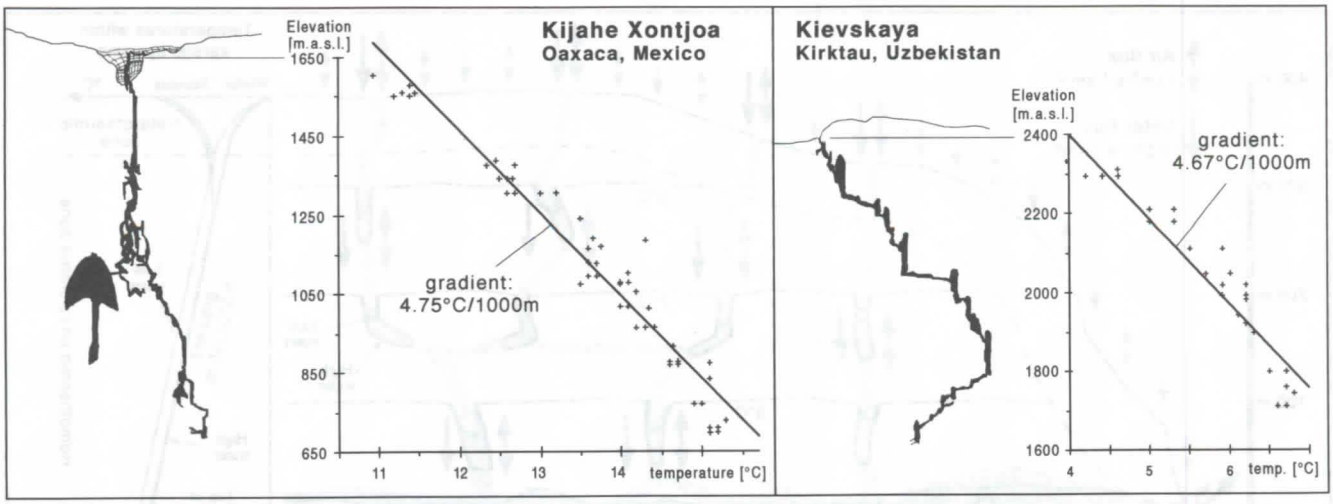

Figure 2: Temperaure (air and water are not distinguished here) in two deep caves. Gradients are close to "humid air gradient".

Below the homothermic zone, the water temperature is almost in equilibrium with rock and air temperature (homothermic zone), which implies that all three temperatures increase with depth, independent of the season. As water flows down quicker than air and rock (!), its temperature tends to be slightly colder than rock and air. This slight disequilibrium is a function of the vertical flow velocity of the water. In the catchment studied by RENNER the water table is about 100 to 150 meters below ground surface. The phreatic conduits are located within the homothermic zone. The more rapid the water flows down, the colder it reaches the phreatic zone.

A further example illustrating the « almost exclusive » relation between flow velocity (or discharge) and water temperature within the homothermic unsaturated zone has been described by JEANNIN (1990): water temperature has been measured in a cave at a depth of 200 meters, once in summer during a summer storm flood (warm infiltration) and a second time in early spring (April) during snowmelt. The discharge in summer was about twice the one in spring. The water temperature of the river was about 0.3 °C higher in April than in summer.

Conclusion

The conceptual model presented here assumes that the karst systems can be considered as composed of three main zones: the *heterothermic zone* close to the surface, the *unsaturated homothermic zone* and the *phreatic zone*. In each zone, air water and rock temperature tend to equilibrium. Heat exchange between air, water and walls is therefore the dominant process acting in all three zones. Meanwhile, temperature in each zone appears to depend on different dominating factors.

Air, water and rock temperature in the heterothermic zone are mainly influenced by the outside temperature.

In the homothermic unsaturated zone the mean air, rock and water temperature seem to depend almost exclusively on the air temperature defining a vertical gradient of about 5°C per 1000 m of elevation. Temporal variations can be induced by slight disequilibrium of water temperature with respect to rock and air due to velocity of water. Water is then slightly colder than rock and air, implying that the quicker the water flows down, the colder it reaches the phreatic zone. Our model implies therefore that average air discharge through karst systems are much higher than average water discharge.

In the saturated zone, water and rock temperature are hardly affected by geothermal heat flux. Heat pulses flow through the saturated zone almost conservatively. The shape of the pulses are somewhat changed, mainly as a results of the geometry of the conduit system in the saturated zone.

The conceptual model presented here is in good agreement with many field observations and represent a valuable extension to the existing models. As a first approximation, it can be used to interpret the temperature responses of karst springs, providing different information about the structure of the systems:

1) The *shape of the temperature pulses* provides information about the *geometry of the conduit network* within the saturated zone (see RENNER, 1996 or LIEDL *et al.*, 1997 for more details);

2) The *amplitude of the temperature pulses* provides information about the importance of the unsaturated zone and mainly about *flow velocities* in it.

3) The *positive/negative temperature pulses* («warm floods» in summer and «cold floods» in winter) provide information about the *depth of the phreatic zone* below the ground surface. If the top of the phreatic zone is located within the heterothermic zone (probably less than 50 meters below ground), positive (in summer) and negative (in winter) pulses will be observed. If the saturated zone is located in the homothermic zone, negative pulses will be observed all along the year. This can be slightly modified by the presence of large concentrated infiltrations (large sinks) which may make the heterothermic zone deeper.

References

BENDERITTER, Y.; ROY, B. & A. TABBAGH 1993. Flow characterization through heat transfer evidence in a carbonate fractured medium: first approach. *Water Res. Res., 29 (11): 3741-3747.*

BOEGLI, A. 1980. : Karst Hydrology and Physical Speleology. Springer Verlag, New York, 284 p.

CARSLAW, H. S. & J. C. JAEGER 1959. Conduction of heat in solids. 2nd ed., Oxford University Press, London, 510 p.

JEANNIN, P.-Y. 1990. Températures dans la zone vadose du karst. – *Bull. du Centre d'hydrogéologie de l'Univ. Neuchâtel, No 9, 1990: 89-102.*

LIEDL, R.; RENNER, S. & M. SAUTER 1997. Obtaining information on fracture geometry from heat flow data. *This issue.*

MATHEY, B. 1974. Gradient géothermique et hydraulique souterraine dans un aquifère karstique (Bassin de la source de l'Areuse / NE). – *Bull. Soc. neuch. Sci. nat., Tome 97: 301-314.*

RENNER, S. 1996. Wärmetransport in Einzelklüften und Kluftaquiferen - Untersuchungen und Modellrechnungen am Beispiel eines Karstaquifers. *PhD Thesis, Tübinger Geowiss. Arbeiten C30, 89 p.*

ROEDEL, W. 1994. Physik unserer Umwelt: die Atmosphäre. Springer Verlag, Berlin: 467 p.

WIGLEY, T. M. L. & M. C. BROWN 1971. Geophysical applications of heat and mass transfer in turbulent pipe flow. *Boundary-Layer Meteorology, D. Reidel Publ., Dordrecht (Holland), 1.: 300-320.*

Hyperthermic caves of the United States

by Willlam R. Halliday
Hawaii Speleological Survey of the National Speleological Society
P.o. Box 1526, Hilo, Hawaii, U.S.A. 96721

Abstract

In the United States, hyperthermic caves exist in a variety of environments: hot spring terraces, craters of dormant volcanoes, karsts in thermal areas, and others. Those in craters are of two types. One consists of ablation caves between firn or ice and the crater wall. The other includes a variety of hollow volcanic features discussed in a companion paper. Air temperatures are as high as 62°C in a cave in a 1919 lava flow on the floor of Kilauea crater. Relative humidity is near 100% and steam currents are common in these caves. New techniques have permitted limited exploration and study of caves with air temperatures as high as 51°C. Constant temperature monitoring and maintenance of escape routes is essential.

1. Introduction

In various parts of the U.S.A. the temperature of some caves is influenced by warm or hot springs, cooling dikes or sills, diffuse areas of volcanic heat, or localized fumaroles. The two most celebrated hyperthermal caves are karstic solution caves: Warm River Cave, VA (DOUGLAS, 1964) and Lower Kane Cave, WY (HILL et al, 1976). Newly studied caves in Kilauea Crater, HI have much higher temperatures and much greater variety of climatic conditions.

2. Hyperthermic karstic solution caves

Air and water temperatures in Warm River Cave reach at least 28°C. A warm stream enters a small terminal passage and equilibrates its air. In less constricted areas, the air temperature is essentially normothermic. This is a well-known thermal area including the famous resorts of Hot and Warm Springs, VA.

Lower Kane Cave contains a seasonal resurgence of a thermal stream. In winter, the stream disappears and fumarolic gases enter the cave at the resurgence point. Summer air and water temperatures are about 27°C. A dry, detached upper level passage is less hyperthermic. Other hyperthermic karstic solution caves exist in Wyoming (HILL et al, 1976), in addition to what may be dissolution caves in hot spring terraces.

3. Hyperthermic travertine caves

Some travertine caves are formed by deposition from thermal waters, and some dissolution occurs within travertine terraces. Residual heat causes elevated temperatures in various caves in the terraces of Mammoth Hot Springs, Yellowstone National Park, WY and elsewhere. Steam emerges from the mouths of some of these caves. With about 100 m of dendritic passages, Ron's Secret Cave, WA is an example of mildly hyperthermic caves formed by travertine deposition by a small spring at a temperature of less than 25°C (HALLIDAY, 1982).

4. Geothermal ablation caves

Geothermal ablation caves form at the interface of volcanic "hot spots" and glacial ice or firn. Two of the five or six recorded caves of this type are in Washington state. Large, complex examples exist along the inner crater walls of Mount Rainier and Mount Baker (KIVER, 1971, 1975a, 1975b; HALLIDAY, 1978, 1980; HALLIDAY & COUGHLIN 1970). The morphology of these caves and their climatic conditions change rapidly with snowpack and variations in volcanic activity. An old photograph shows the former existence of a similar cave high on the north slope of Mount St. Helens, WA at the site of the first phase of the 1980 eruptions. In the summer of 1975 only a patch of bare rock marked its former location. In these caves flakefall and other special hazards of glacier caves are added to those of hyperthermic caves per se (HALLIDAY, 1974).

5. Hyperthermic lava tube and other caves in pahoehoe basalt

After the primary heat of their speleogenetic processes is dissipated, lava tube and related caves of pahoehoe basalt flows in Hawaii normally become normothermic within weeks or months. A few are affected by continued or renewed volcanic activity, or by slower cooling at depth. An example of the latter is a rift tube cave extending lateral to the bottom of Mauna Ulu crater. This crater was active in 1972-76. In 1981 a residual temperature of 207°C existed in a fissure

intersecting the cave (FAVRE, 1995). Steamy lava tube caves with temperatures over 50°C exist in and near the Puhimau steam vent field near the crater of Kilauea volcano. These have not been studied.

Three lava tube caves located between the East Rift Zone of Kilauea volcano and the coastline are hyperthermic. Best known is Hot Tub Cave, where a bather died -- almost certainly of hyperthermia. Its bottom is a long, narrow pool with a temperature said to vary with rainfall. Before the entrance was obstructed to prevent additional deaths, I estimated the air and water temperatures as about 38°C. Farther east are two other small lava tube caves with localized hyperthermic sections, in a group of seven nearly parallel caves, perhaps remnants of a braided system. Except for ceiling drip, all are dry. The westernmost of the group has a 20 meter section where the dripping water is hot and the air temperature consistently measures about 34 C. A cutaround crawlway in another cave about 200 m farther east is estimated to have a localized air temperature of about 30°C but has not been studied. Hot Tub Cave is about 4 km from the East Rift Zone and its hot water probably is the result of localized heating of ground water by residual heat of a 1950 eruption. The cause of the localized thermal zones of the other caves are less clear. Possibly small dikes extended from the rift zone to their vicinity in 1950. Solar radiation is not a localized factor.

6. Hyperthermic caves in Kilauoa crater, Hawaii

The principal studies of hyperthermic caves in Hawaii have been on the floor of Kilauea crater. The last eruption in this crater was in 1982 but the Postal Rift lava flow of 1919 has been steaming since its deposition. All the hyperthermic caves known in this crater are in this flow, but not all its caves are hyperthermic.

These steamy, hyperthermic caves include small lava tube caves (three in the Postal Rift System and others), boundary ridge caves of lava rises and other structures (WALKER, 1991) hollow tumuli, and others discussed in my companion paper. Measured air temperatures are as high as 62°C. Many have humidity approximating 100 %. In some, steam currents are constant or intermittent. Their elevated temperatures may be due to residual 1919 heat, to independent shallow magma bodies, or both.

Using ordinary caving clothing and low tech thermometric equipment, we have developed successful techniques for brief exploration and study of caves with air temperatures as high as 51°C. Our worst consequences have been faces reddened for a few hours (we plan to test face masks and shields soon). Despite the common presence of sweet-tasting fumes (probably hydrated sulfates), we have had no respiratory difficulties. Above 38°C we have found light cotton clothing helpful in avoiding steam burns. At lower temperatures clothing seems to be optional.

Especially important is constant monitoring of air temperature. In some caves it has shown microclimates where we can crawl or stoop beneath steam currents or pockets of very hot air. We use an inexpensive "Radio Shack" digital thermometer with a response time of 15 seconds and a remote sensor. At all times we expect sudden changes in air flow and temperature, and we are constantly aware of quick, safe escape routes.

Our learning period was lengthy and we urge similar caution for others working in hot caves. Increasingly, we are using sublingual digital thermometers as part of our learning. On one occasion we found hyperthermia of 4°C in a caver after 5 minutes in a cave at 46°C. This correlated with perceptible deterioration of physical and mental performance, lasting a few hours. Evidently there is considerable variation in tolerance to these conditions.

References

DOUGLAS, H. H. 1964. Caves of Virginia. Falls Church, VA. Virginia Cave Survey. p. 81.

FAVRE, G. 1993. Some observations on Hawaiian pit craters and relations with lava tubes. In: Proceedings of the 3rd International Symposium on Vulcanospeleology, Bend, Oregon, 1982. p. 37.

HALLIDAY, W. R. 1974. American caves and caving. New York, Harper and Row, p. 58. (Aiso Barnes and Noble edition-, 1982, p. 58)

HALLIDAY, W. R. 1978. Geothermal week in Washington. Cascade Caver, 17:13, March-April.

HALLIDAY, W. R. 1980. Mt. Baker crater caves. Cascade Caver 19:55, May.

HALLIDAY, W. R. 1982. Ron's Secret Cave, Snohomish County, WA.

Cascade Caver, 21:18, April-May.

HALLIDAY, W. R. & CHARLES L, COUGHLIN 1970. A preliminary reconnaissance of the Summit Steam Caves of Mount Rainier. Washington Speleological Survey Bulletin 7 (Western Speleological Survey Serial #42.)

HILL, C., W. SUTHERLAND & L. TIERNEY. 1976. Caves of Wyoming. Geological Survey of Wyoming Bulletin 54, p. 89.

KIVER, E. P. 1971. Summit firn caves of Mount Rainier. Science, 173:320, 23 July.

KIVER, E. P. 1975a. Firn caves in the volcanic craters of Mount Rainier, Washington. Nat. Speleol. Soc. Bull. 37:45, July.

KIVER, E.E P. 1975b. The first exploration of Mount Baker ice caves. Explorers Journal 53:84, June.

WALKER, G. P. L. 1991. Structure, and origin by injection of lava under surface crust, of tumuli, "lava rises", "lava rise pits", and "lava inflation clefts" in Hawaii. Bull. Volcanol. 53:546.

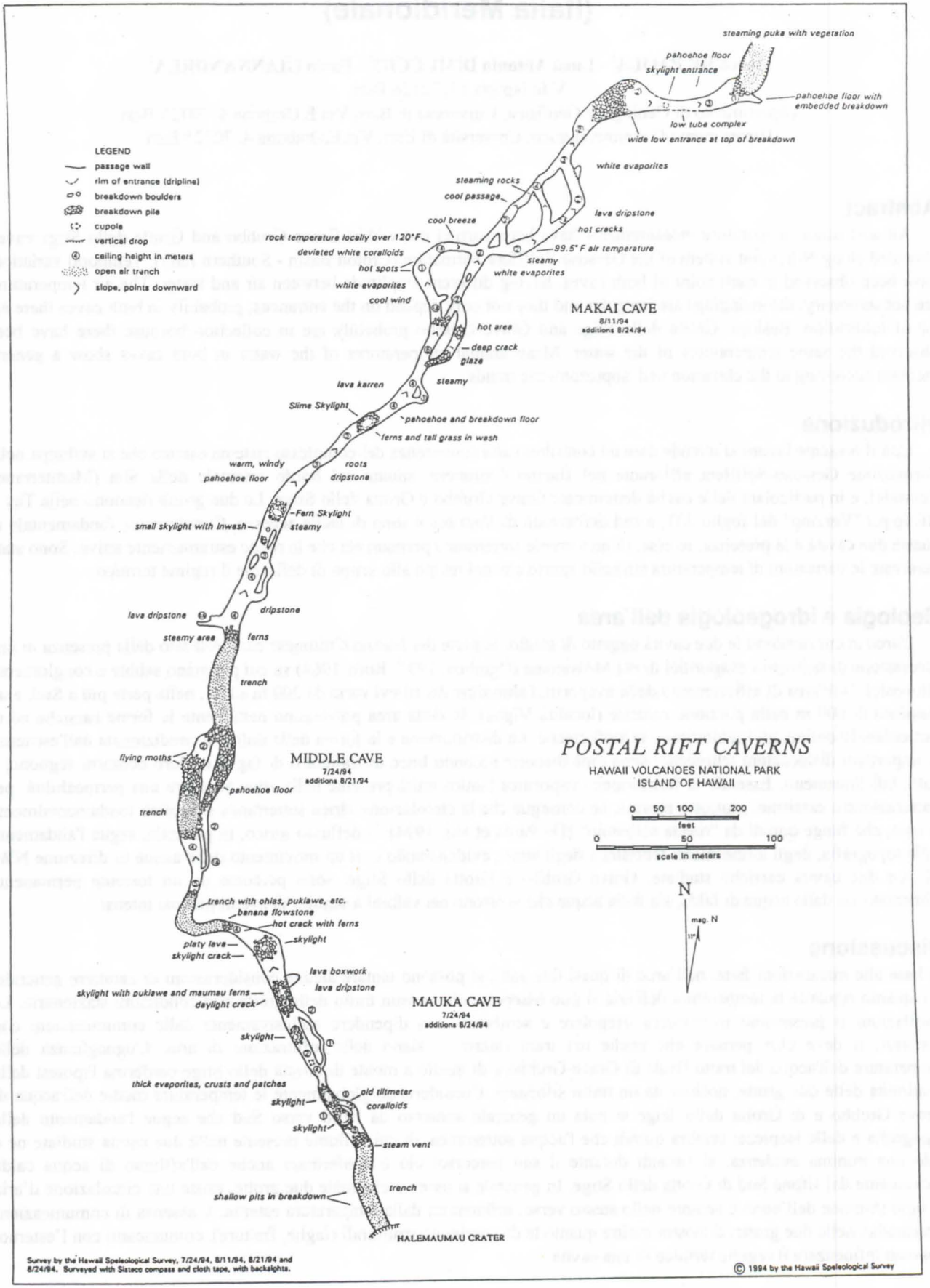
steaming puka with vegetation
pahoehoe floor
skylight entrance
pahoehoe floor with embedded breakdown
low tube complex
wide low entrance at top of breakdown
white evaporites
steaming rocks
cool passage
lava dripstone
hot cracks
cool breeze
rock temperature locally over 120°F
deviated white coralloids
99.5° F air temperature
steamy
hot spots
white evaporites
white evaporites
cool wind
MAKAI CAVE
8/11/94
additions 8/24/94
hot area
deep crack
glaze
steamy
lava karren
Slime Skylight
pahoehoe and breakdown floor
ferns and tall grass in wash
warm, windy
pahoehoe floor
roots
dripstone
Fern Skylight
steamy
small skylight with inwash
lava dripstone
dripstone
steamy area
ferns
trench
flying moths
MIDDLE CAVE
7/24/94
additions 8/21/94
pahoehoe floor
trench
trench with ohias, pukiawe, etc.
banana flowstone
hot crack with ferns
skylight
platy lava
skylight crack
lava boxwork
lava dripstone
skylight with pukiawe and maumau ferns
daylight crack
MAUKA CAVE
7/24/94
additions 8/24/94
skylight
thick evaporites, crusts and patches
old tiltmeter
coralloids
skylight
skylight
steam vent
trench
shallow pits in breakdown
HALEMAUMAU CRATER
LEGEND
passage wall
rim of entrance (dripline)
breakdown boulders
breakdown pile
cupola
vertical drop
ceiling height in meters
open air trench
slope, points downward
POSTAL RIFT CAVERNS
HAWAII VOLCANOES NATIONAL PARK
ISLAND OF HAWAII
0 50 100 200
feet
0 50 100
scale in meters
N
mag. N
11°
Survey by the Hawaii Speleological Survey, 7/24/94, 8/11/94, 8/21/94 and 8/24/94. Surveyed with Sistece compass and cloth tape, with backsights.
© 1994 by the Hawaii Speleological Survey

Misure di temperatura in due cavità carsiche nella formazione Gessoso-Solfifera dell'alto Crotonese (Italia Meridionale)

Marco DE PAOLA[1] - Luca Antonio DIMUCCIO[2] - Paolo GIANNANDREA[3]

[1] V.le Japigia 84, 70126 Bari.

[2] Dipartimento di Geologia e Geofisica, Università di Bari, Via E.Orabona 4, 70125 Bari.

[3] Dipartimento Geomineralogico, Università di Bari, Via E.Orabona 4, 70125 Bari.

Abstract

Air and water temperature measurements have been carried out within Grave Grubbo and Grotta dello Stige caves, alineated along N-S, karst system of the Gessoso-Solfifera Formation (Croton Basin - Southern Italy). Temporal variations have been observed in each point of both caves, having different amplitude between air and water. The air temperatures are not stationary; the swingings are irregular and they not only depend on the entrances; probabily in both caves there are air of infiltration. Besides, Grotta dello Stige and Grave Grubbo probabily are in collection because there have been observed the same temperatures of the water. Mean annual temperatures of the water in both caves show a general increase according to the elevation and isopiezometric trends.

Introduzione

Con il presente lavoro si intende dare un contributo alla conoscenza del complesso sistema carsico che si sviluppa nella Formazione Gessoso-Solfifera affiorante nel Bacino Crotonese, situato sul bordo orientale della Sila (Mediterraneo Centrale), e in particolare delle cavità denominate Grave Grubbo e Grotta dello Stige. Le due grotte ricadono nella Tav. I NE (p.p.) "Verzino" del foglio 237, a sud dell'abitato di Verzino, e sono di facile accesso. Caratteristica fondamentale di queste due cavità è la presenza, in esse, di un torrente sotterraneo permanente che le rende estremamente attive. Sono state osservate le variazioni di temperatura sia nello spazio che nel tempo allo scopo di definirne il regime termico.

Geologia e idrogeologia dell'area

L'area in cui ricadono le due cavità oggetto di studio, fa parte del Bacino Crotonese caratterizzato dalla presenza di una successione di sedimenti evaporitici di età Messiniana (Ogniben, 1957; Roda 1964) su cui poggiano sabbie e conglomerati Pliocenici. Nell'area di affioramento delle evaporiti, l'altitudine dei rilievi varia da 200 m s.l.m., nella parte più a Sud, a un massimo di 600 m nella porzione centrale (località Vigne). In detta area prevalgono nettamente le forme carsiche ed in particolare le doline, gli inghiottitoi e le valli cieche. La distribuzione e la forma delle doline è condizionata dall'esistenza di importanti dislocazioni tettoniche: sono cioè disposte secondo linee di frattura o di faglia e i loro contorni seguono, a tratti, tali lineamenti. Essendo la formazione evaporitica l'unica unità presente nella zona ad avere una permeabilità, per fratturazione e carsismo, piuttosto elevata, ne consegue che la circolazione idrica sotterranea si esplica fondamentalmente in essa, che funge quindi da "roccia serbatoio" (De Paola et alii, 1994); il deflusso idrico, in generale, segue l'andamento della topografia, degli allineamenti tettonici e degli strati, evidenziando così un movimento delle acque in direzione NW-SE. Le due cavità carsiche studiate, Grave Grubbo e Grotta dello Stige, sono percorse da un torrente permanente alimentato sia dalle acque di falda, sia dalle acque che scorrono nei valloni a seguito di eventi piovosi intensi.

Discussione

In base alle misurazioni fatte, nell'arco di quasi due anni, si possono tentare alcune considerazioni di carattere generale. Per quanto riguarda la temperatura dell'aria si può osservare che nessun tratto delle grotte è in condizioni stazionarie. Le oscillazioni si presentano in maniera irregolare e sembrano non dipendere esclusivamente dalle comunicazioni con l'esterno; si deve cioè pensare che anche nei tratti interni ci siano delle infiltrazioni di aria. L'uguaglianza delle temperature dell'acqua del tratto finale di Grave Grubbo e di quello a monte di Grotta dello Stige conferma l'ipotesi della continuità delle due grotte, occluse da un tratto sifonante. Considerando globalmente le temperature medie dell'acqua di Grave Grubbo e di Grotta dello Stige si nota un generale aumento da Nord verso Sud che segue l'andamento della topografia e delle isopieze: sembra quindi che l'acqua sotterranea, di cui il fiume presente nelle due cavità studiate ne è solo una minima evidenza, si riscaldi durante il suo percorso: ciò è confermato anche dall'afflusso di acqua calda proveniente dal sifone Sud di Grotta dello Stige. In generale si osserva che nelle due grotte, esiste una circolazione d'aria in ogni stagione dell'anno e sempre nello stesso verso, influenzata dalla temperatura esterna. L'assenza di comunicazioni intermedie, nelle due grotte, dimostra inoltre quanto le discontinuità strutturali (faglie, fratture), comunicanti con l'esterno, possano influenzare il regime termico di una cavità.

Monitoring results in "Grotta Grande del Vento" (Frasassi, Ancona, Italy) and its visitors' capacity

Arrigo A. Cigna
Società Speleologica Italiana, Fraz. Tuffo, I-14023 Cocconato AT, Italy

Abstract

The "Grotta Grande del Vento" is the Italian show cave with the highest number of visitors. For many years a monitoring network for the survey of some climatological parameters was been in operation. Now the results obtained for the period 1991-1993 by such a monitoring network are here reported and examined. The influence of the tourists flow in the cave on air temperature and carbon dioxide concentration of the cave atmosphere is investigated and an evaluation of the visitors' capacity is estimated.

Riassunto [Risultati del monitoraggio nella Grotta Grande del Vento (Frasassi, Ancona, Italia) e la sua capacità ricettiva]

La Grotta Grande del Vento è la grotta turistica italiana con il maggior numero di visitatori. Da parecchi anni è in funzione un sistema di monitoraggio di alcuni parametri climatologici. In questo lavoro vengono riportati i risultati ottenuti nel periodo 1991-1993 dalla sopra citata rete di monitoraggio e ne viene fatto un esame critico. E' stata inoltre studiata l'influenza del flusso turistico sulla temperatura dell'aria e sulla concentrazione dell'anidride carbonica nell'atmosfera della grotta e, su questa base, è sta fatta una stima della capacità ricettiva della grotta stessa.

1. Introduction

The Grotta Grande del Vento is one of the most relevant Italian show caves both for the number of visitors and its intrinsic characteristcs. Together with the Grotta del Fiume, they form a karst system about 20 km long with an abundant cave fauna and many cave minerals. In fact the genesis of the system is due to the combined action of thermal water, rich in H_2S, and karst water (CIGNA 1993).

Just after the cave was discovered in 1971 air temperature within the cave was measured at different instances. Since September 1974 the cave was opened to tourists who could reach a trail of 850 metres through an artificial tunnel.

In 1982 a first automatic network consisting of two stations for the measurement of temperature, humidity, air velocity and CO_2 concentration in air along the tourist trail was set up. The system was rather unreliable and in 1989 it was replaced by a new network with six station. The set-up of this network required a rather long time on account of troubles due to sensors and to storms resulting in frequent failures (BERTOLANI et al. 1991). On October 1993 a lightning badly injured the system and up to now (December 1996) the monitoring was interrupted. It is hoped that the operation of a more modern and reliable monitoring system should possibly start in 1997.

In this paper the results obtained in the period 1991-1993 are reported and examined with the aim of investigating the influence of the tourists flow in the cave on air temperature and carbon dioxide concentration of the cave atmosphere. In addition the visitors' capacity is estimated and the propagation of the seasonal thermal wave in different points of the cave is also studied.

2. The data set

As it was reported previuously, the automatic monitoring network gave a number of wrong results and had some period of failure. Therefore it was necessary to "clean" the original values from those which were unmistakable wrong. Fortunately the wrong values were easily identifiable and therefore the cleaning did not introduce subjective modifications to the data set.

The stations taken into consideration are reported in Table 1. In addition some spot measurements of air temperature obtained in the period 1972-1978 were also considered to evaluate the trend of the air temperature in the last twenty years since the management of the show cave.

Table 1: Location of sampling points

Station	Distance from the entrance (m)	Parameter
Outside	-	Air temperature
Ancona Hall	350	Air temperature
Sala dei Duecento	400	CO_2 concentration
Lake Smeraldo	500	Air temperature
L'Orsa	585	Water temperature
Cannella	655	Air temperature

3. Air and water temperature trend

Long term

The plots of the air temperature data over a period of 21 years which are available for two stations (Ancona Hall and Cannella) show an average increase of about 0.0345 _C per year. This trend has been calculated for the Cannella values which are less influenced by the seasonal thermal wave (Fig. 1). Then, the air temperature in the period 1972-1993 is given by the equation:

$$T = T_0 + 0.0345\ n$$

where: T_0 = 13.16_C (air temperature at Jan. 1972)
n = number of years from 1972

It is interesting to observe that the air temperature calculated by this equation and extrapolated to Jan. 1996 has a good agreement with the experimental measurements.

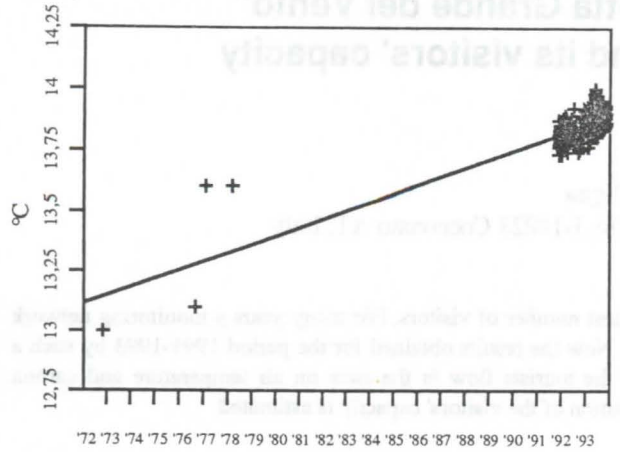

Figure 1 : Best fit of the air temperature in the period 1972-1993 for the "Cannella" station.

But the accuracy and precision of the early measurements performed in the 70's is rather uncertain on account of possible systematic errors in the calibration of the thermometers used at that time and the influence of the seasonal thermal wave which cannot be taken into due account because of the paucity of data.

Short term

The analysis of the three years (1991-1993) here considered gives results which are much more consistent (on the short term) on account of a much larger number of measurements and an intrinsic consistency of the data which were obtained by the same sensors throughout the whole period.

The average increase of the air temperature is reported in Table 2

Table 2 : Average increase of air temperature in the period 1991-1993.

Station	Distance from the entrance (m)	Increase _C/year
Ancona Hall	350	0.189
Lake Smeraldo	500	0.222
Cannella	655	0.042

These results show a correlation between the tourists flow and the increase of the air temperature inside the show cave. Such an effect is quite larger for the first two stations which are closer to the tourist trail, while for the last station (Cannella) which is beyond such trail, the value of the increase is about 5 times lower and rather close to the value measured over a period of 21 years.

Seasonal thermal wave

The air temperature outside the cave has obviously a seasonal variation which is found also inside the cave with a delay depending on the position and local characteristics. The sinusoidal best fit of the data available for the period 1991-1993 is given by the equations reported in Table 3.

It must be emphasized that the water temperature measured in a lake at "L'Orsa" was around 14.5_C during 1991 and decreased in an interval of three months to a value around 13.2_C (Fig. 2). Unfortunately it is not possible to ascertain if this pattern is due to a real change
in the water circulation or to a breakdown of the monitoring network. For this reason the sinusoidal best fit of the water temperatures of "L'Orsa" was carried out for the interval 1992-1993 only.

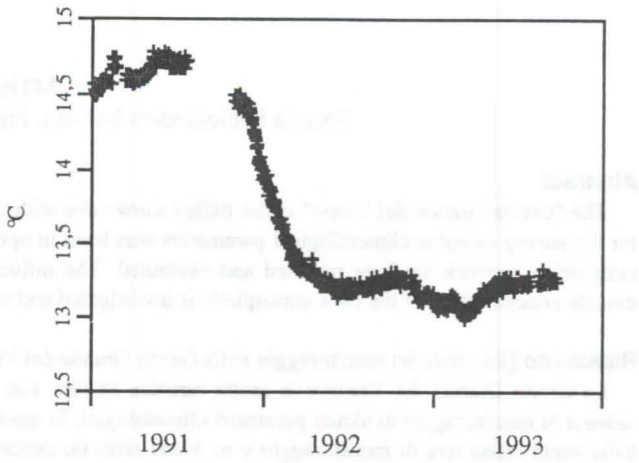

Figure 2 : Water temperature measured at "L'Orsa" station.

The propagation of the thermal wave from outside as detected from the measurements performed in the "Grotta Grande del Vento" cannot be through the rock because both the attenuation and the delay would have been much greater (CIGNA 1978).

A careful examination of the data reported in Table 3 shows that the air temperature inside the cave is slightly less than the temperature outside. The attenuation factor of the wave amplitude is between 25 and 50 for the stations close to the tourist trail, decreasing to 675 for the station (Cannella) beyond such a trail. In Fig. 3 and 4 the sinusoidal best fit of the air temperature measurements carried out outside the cave and in the Ancona Hall sare reported.

Table 3 : Sinusoidal best fit of temperature values.

Station	Equation
Outside	T(_C) = 14.23 - 9.45 sin [2π (d +57)]
Ancona Hall	T(_C) = 13.73 - 0.192 sin [2π (d +27)]
Lake Smeraldo	T(_C) = 13.51 - 0.302 sin [2π (d +33)]
L'Orsa (water)	T(_C) = 13.19 - 0.386 sin [2π (d +57)]
Cannella	T(_C) = 13.84 - 0.014 sin [2π (d+125)]

The dates of the first maximum of the sinusoidal best fit applied to the temperature values measured in the different stations is reported in Table 4.

The delay with respect to the maximum of the thermal wave of the outside air emperature is an evaluation of the speed of propagation of the thermal wave itself. For the stations "Ancona Hall" and "Lake Smeraldo" there is a delay of about one month and there is no correlation with the distance from the entrance. Therefore, it can be inferred that the heat transport is due to the tourist flow.

Table 4 : Dates of the first maximum of the sinusoidal best fit.

Station	Distance from the entrance (m)	Date (days since Jan.1st,91)	Delay (days)
Outside	-	216	0
Ancona Hall	350	247	31
Lake Smeraldo	500	241	25
L'Orsa	585	217	1
Cannella	655	510	294

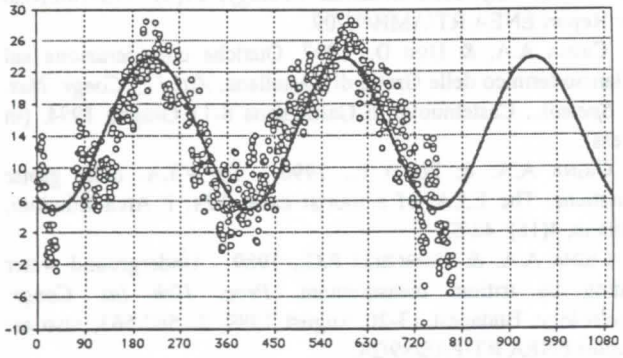

Figure 3 : Sinusoidal best fit of the air temperature measurements carried out outside the cave. Air temperature (_C) is reported on the Y-axis and the days since Jan. 1st, 1991 are reported on the X-axis.

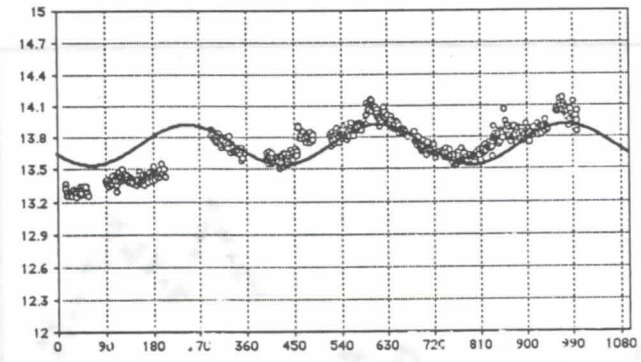

Figure 4 : Sinusoidal best fit of the air temperature measurements carried out in the Ancona Hall. Air temperature (_C) is reported on the Y-axis and the days since Jan. 1st, 1991 are reported on the X-axis. It is also evident the long term increase of about 0.189 _C/year.

Obviously, such a flow operates according two mechanisms: first, each person releases a given amount of heat to the cave environment, resulting in the positive trend of the temperature reported in the previous two sub-chapters; second, the tourist flow causes a slow air circulation resulting in a delayed and subdued thermal wave along the show cave.

Beyond the part visited by tourists, the thermal wave propagates much slowlier as it was found for the station "Cannella" reached by the wave nearly 10 months later.

The water temperature as measured at "L'Orsa" appears to be synchronous with the temperature outside. But it is also possible that the delay corresponds to whole number of years. In fact, the age of the water of some lakes in the same part of the cave was found to be around some years (CIGNA & GIORCELLI 1989).

4. CO_2 concentration

In February 1993 a sensor for CO_2 was included in the monitoring network and its concentration was recorded hourly in the "Sala dei Duecento". The daily average values available are here reported.

As it can be seen in Fig. 5 the CO_2 concentration is influenced by two different factors. One is of a nautural origin and it is responsible of the main mean term variations, the other is due to the breathing of the visitors and results in the peaks synchronous with the sundays and the holidays periods. E.g., the peak in April corresponds to Easter; the short peak at the end of February seems to be not related to a higher flow of visitors and therefore it could be due to a natural source.

In 1983 some measurements of the CO_2 concentration had already been carried out in the same station. Unfortunately the instrument was not fit to operate in a cave environment and after some month it was no longer recording. Nevertheless the data obtained at the time gave a first idea on the existence of two sources (natural and anthropogenic) as it was pointed out by CASTELLANI (1988) who suggested that there might be a natural reservoir of CO_2 elsewhere in the cave that was contributing to the build-up (CIGNA, 1993).

The new set of data obtained at the end of 1993 confirm the previous hypothesis. While the contribution of visitors to the CO_2 concentration in show caves has been studied rather extensively (e.g.: VILLAR et al. 1986) the mechanism and, more in general, the processes by which CO_2 is naturally released in a cave environment are still unexplained.

Obviously, some hypothesis on possible sources connected with the seasonal cycle of vegetation and/or a contribution from thermal water circulation can be formulated. Nevertheless, this problem should be investigated with great attention because the identification of the processes involved could greatly contribute to the knowledge of the cycle of CO_2 in caves and, perhaps, to some details concerning the speleogenesis.

5. Conclusion

The results reported here suggest some further actions in different fields. With reference to the protection of the cave environment, the temperature trend in the tourist section of the cave clearly points out that the present flow rate in the cave is slightly above the visitors' capacity of the cave itself (CIGNA 1989; CIGNA & FORTI 1990). The pattern of the CO_2 concentration in the cave atmosphere seems to confirm a total recovery of the natural conditions throughout the years.

Therefore the overall effect due the visitors is probably only on the heat balance of the cave environment. An evaluation of the "static"heat balance of the cave has been made by MENICHETTI (1997); it would be rather interesting to develop an appropriate model to take into account the seasonal effect of the outside temperature as has been carried out recently for the Castellana caves (CIGNA & DINI 1997).

In any case, for the managemnt of the Grotta Grande del Vento, it would be convenient to take into account the effect of the visitors flow on the air temperature of the cave. In particular, a decrease of the thermal impact could be achieved through a

reduction of the heat released by both the electrical lighting and the tourists.

A better choice of the lamps installed in the cave (with a higher efficiency of light output) and a decrease ot the lighting time (if compatible with the needs of the show cave) could be beneficial.

A decrease of the number of visitors would be not acceptable from an economical point of view of the show cave management. Therefore the only possibility to decrease the heat released by the persons would the the reduction of time they spend into the cave. Such a result would be achieved by the opening of another tunnel to avoid the return through the same pathway covered when entering.

The excavation of a new tunnel had already been considered in the past also for safety reasons: therefore a design already exists and the requirements to avoid changes in the air circulation inside the cave have been defined. Then it would be really worthwhile to take into account the opportunity to have another artificial access to the show cave.

Acknowledgements

I express my gratitude to my colleagues who contributed to this work and, in particular, to M. Menichetti who provided the data obtained by the automatic monitoring network and to F.G. Giorcelli who prepared some programmes for the elaboration and the calculation of the sinusoidal best fit of the values and assisted me with great patience during the development of thie whole work.

References

BERTOLANI M., CIGNA A.A., MACCIÒ S., MORBIDELLI L., SIGHINOLFI G.P., 1991 - The karst system "Grotta Grande del Vento - Grotta del Fiume" and the conservation of its environment. In: SAURO U., BONDESAN A. & MENEGHEL M, (Eds.) Proc. Int. Conf. on Environmental Karst Areas (Italy, 15-27 Sept.,1991). *Quad. Dip. Geografia, Univ. Padova,* 13, 1991: 289-298; also as: Report ENEA RT/AMB/92/19.

CASTELLANI V., 1988 - Frasassi e speleo-monitoraggio. *Speleologia* **9**(18): 33-35.

CIGNA A.A., 1978 - Meteorologia ipogea. In: Società Speleologica Italiana - *Manuale di speleologia.*, Longanesi, Milano: 341/367.

CIGNA A.A., 1989 - La capacità ricettiva delle grotte turistiche quale parametro per la salvaguardia dell'ambiente sotterraneo. Il caso delle Grotte di Castellana. *Atti XV Congr. Naz. Speleol.,* Gruppo Puglia Grotte - Amm. Comunale Castellana Grotte: 999/1012.

CIGNA A.A. 1993. Environmental management of tourist caves. The examples of Grotta di Castellana and Grotta Grande del Vento, Italy. *Environmental Geology,* 21(3): 173-180.Also as: Report ENEA RT/AMB/93/09.

CIGNA A.A. & DINI D., 1997. Qualche considerazione sul bilancio termico delle Grotte di Castellana. *Atti 17_ Congr. Naz. di Speleol..,* Castelnuovo di Garfagnana 8-11 Giugno 1994, (in press).

CIGNA A.A. & FORTI P., 1990 - La V.I.A. delle grotte turistiche. The E.I.A. of a tourist cave. *VIA*, l' Arca Edizioni, Milano, 4(16): 42/53.

CIGNA A.A. & GIORCELLI F.G., 1989 - Underground water dating by tritium measurement. *Proc. 10th Int. Congr. Speleology,* Budapest 13-20 August 1989, 2: 562/563; also as: Report ENEA RT/PAS/89/24.

MENICHETTI M., 1997. Bilancio energetico di una grande grotta turistica: la Grotta Grande del Vento a Frasassi (An). *Proc. Int. Symp. Show Caves and Environmental Monitoring,* Frabosa Soprana 24-26 March 1995, (in press).

VILLAR E., FERNANDEZ P.L., GUTIERREZ I., QUINDOS L.S. & Soto J., 1986 - Influence of visitors on carbon dioxide concentrations in Altamira Cave. *Cave Science*, **13**(1): 21-23.

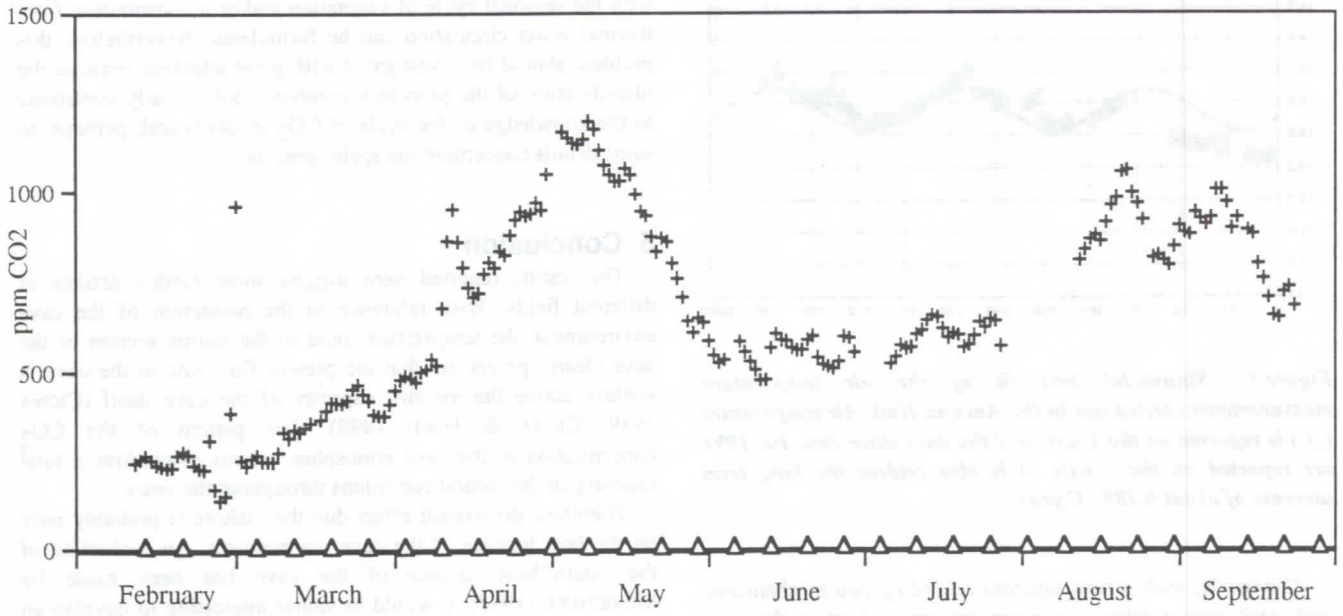

Figure 5 : CO_2 concentration in air measured at the station "Sala dei Duecento" in 1993. The triangles correspond to Sundays.

Temperature Anomalies Formation and Secular Instability Research of Ice of Atmospheric Origin in the Karst Caves of North Albanian Alps

Alexey Stoev
Astronomical Observatory and Planetarium, 62 Tsar Ivan Shishman Str., 6000 Stara Zagora, Bulgaria
Penka Muglova
Solar-Terrestrial Influences Laboratory, 6000 Stara Zagora, Bulgaria
Dimitar Stoev
Sarnena Gora Touristic Society, 6000 Stara Zagora, Bulgaria

Abstract

The negative temperature anomalies in the karst caves of North Albanian Alps are a widespread phenomenon. The anomalies represent a decrease of the average anomalous temperature of the air and the main rock, in the cave entrances, in comparison with caves' deeper parts, in the presence of a lot of ice there.

The difference in air exchange between caves with a different morphology and altitude is examined in the paper. An analysis of the temperature regime of thirty-eight caves has been made. The interaction between ice formations and karst massif geothermal field is shown. Three types of caves has been determined:

1)warm caves with cold entrances and steady ice accumulations;

2)completely warm caves;

3)cold caves with significant seasonal changes of the air flow in their entrances.

The influence of snowfalls' quantitative balance on caves' temperature regime is investigated. The combination of three heat bearers: ground atmospheric air, the karst massif and the falling water on it and within it forms a relatively stable temperature, providing constant seasonal course of the temperature in the caves.

It is shown that the microclimatic regime in caves, as a whole, is not determined by their origin, but depends on two factors: the angle of the negative bias of the caves, from the entrance to the bottom (depth of the karst massif) and the surface of the entrance aperture cross-cut-section. It has been found that the accumulation of cold increases with the increasing of the two factors. If the negative slope has a greater angle, and the entrance opening is comparatively small the cave is classified as "cold ".

More than 40% from the investigated caves are glacial. The ice accumulates in the spring, when a big part of the incoming waters freezes over the supercooled walls of the karst massif. Another way of prolonged ice supply forming is due to the infiltration humidity, carried up from the bottom to the cave surface, during the winter - spring period.

The negative temperature anomalies' formation in the karst caves of North Albanian Alps is determined by their peculiarities as physico-geographical objects. They are interesting to study due to their situation in the caves and in the karst massif, availability to express contrasts in the microclimate of the whole cave, and due to original processes of atmospheric circulation inside and outside the caves combined with the specificity of hydrological processes (HOTI MAHIR, 1990).

Temperature anomalies could be defined as a result of microclimatic processes in the caves that cause a decrease of the mean annual temperature of the air and the main rock, in the cave entrances, in comparison with caves' deeper parts. Most of the caves in this region of the Albanian Alps are cold during the whole year because of the constant mean day-time temperature in the interval of -1÷4°C, as well as of the existence of great amount of ice, firn and snow in the entrance cliffs and halls. The basic factors that influence such temperature anomalies' formation are:

1. Caves' morphology.
2. Peculiarities of the local relief.
3. Temperature regime of the underground waters.
4. Their thermal regime which depends on the character and intensity of the air exchange.

The caves are grouped in a zone placed north-west of Shcoder, in the region of the high-mountain village of Drugomiri, at 800 to 2000m altitude. The mean annual air temperature is in the region of 8 to 12°C and the mean annual rainfall is in the interval of 1600 to 3000mm. The rainfall minimum occurs during the summer and the depth of the maximum seasonal freezing is nearly 120cm. The climate is subtropical and Mediterranean and it is cool and damp in the mountainous massif covered with limestone (STOEV, 1996).

The karst massif temperature is in the dynamic interval from 2.6 to 7.8°C in the shade during the summer (SAVELEV, 1985). The rock temperature in the stratum is a constant temperature of 2.6°C, and its temperature in the first level carrying water is 2.2°C. A field work on defining basic microclimatic elements' regime and the cave typology has been done as follows:

- depending on the snow-ice stock;
- depending on the temperature of zones with constant temperature (ZCT);
- determining of speleoatmosphere humidity;
- determining of the dynamics of the air exchange;
- determining of the dynamics of the water flowing from the glacier or the snowdrift.

Applying classical methods of microclimate investigation in the caves from the region, data for the basic microclimatic parameters have been obtained. Comparatively low air temperatures in the interval of -0.8 to +4.4°C have been registered. These temperatures as well as the availability of snow and ice mass of many years determine the examined caves as ice-caves. The zone of thermostatic air begins from the place of the first snow accumulation which imbalances the microclimate of the caves and they become colder than the others at the same sea level and climatic zone (SHVETSOV & KOVALKOV, 1986). In ZCT the relative humidity is 60 to 80% and in most of the caves the flowing and dropping water is too little. Shift-flowing draughts with high velocities are not typical of the air exchange in caves. The standard equalization of both cave barometric pressure and that one of the outside ground air layer creates weak draughts outside and inside without anomalies of the velocity or their direction. Taking into account that the caves in the region are developed mainly in zones of vertical-going down, passing and horizontal circulation of the underground waters, it is natural to associate part of the air exchange with karst massif clefts connected with the surface. Velocities of the order of 0.005 to 0.020m/s were registered. The air quantity coming in the caves from the plateau is $30m^3/h$ for isostatic caves and 20 to $25m^3/h$ for dynamic ones.

The analysis of the collected material connected with microclimatic studying permits making of following conclusions:

1. Formation of karst, caves and cave systems contributes to accumulation of cold air masses. This determines the caves investigated as cold and some of them as icy caves.
2. Only the following basic conditions are completed the cold generation. Ice formation and its long period preserving in the caves from the region are possible because of:
   a) considerable height difference of the local relief forms;
   b) bag form of the karst systems or siphon available;
   c) good cleft net with guaranteed opening on the surface;
   d) the bottom of the cave is screened by alluvial material -clay and rubble.
3. The sharp temperature boundary between cold and warm air masses which is on the way of infiltration waters contribute to detaining and piling up incoming water in hard state.
4. Preserving ice during summer is favoured by the northern slope, the slow melting of the large volume snow stoppers and cold air standstill in the clefts and negative relief forms.
5. The diurnal temperature amplitude becomes quiet at a depth of 35 to 36m from the surface.
6. Ice formations are localized at the cave entrances and on the walls and bottoms of the large vertical caves.
7. The cave ice is polygenetic. At the entrances the ice tongues, firn cones and gaskets are mainly of atmospheric origin and are formed after making tight snow masses entering from the surface. In the inner parts icy stalactites, stalagmites, columns, and icy "armours" have mainly hydrogen origin due to both infiltration of atmospheric rainfalls through the cleft net of the karst massif and freezing of the condensation water.
8. The snow, firn and ice accumulation are favoured by the large initial precipices (>20m). The age of blocks of snow and ice could be estimated using measurements about their annual layers (SHUMSKI, 1955). In a section of a block from K25 cave nearly 356 layers has been registered. For K25A cave they are 286. Probably this stratification shows limited age of the blocks - about 400 years.
9. The optimal water flow supplying levels carrying water is formed from the melting ice and the process of condensation in cave volume.

References

HOTI, M. 1990. Particularites de la depression de mbishkodra et son region collineen,Tirana, *Studime gjeographice*, 4: 159-172

RJEVSKI, V. & G. NOVIK.1978.Osnovi fizikii gornih porod, Moskva, Nedra

SAVELEV, V.1985. Metodi izucheniya merzlih porod I ldov, Moskva, Nedra

SHUMSKI, P. 1955. Osnovi strukturnogo ledovedeniya, Moskva, (AN SSSR ed.)

SHVETSOV, p. & V. KOVALSKI. 1986. Fizicheskaya geokriologiya, Moskva, Nauka

STOEV, A. 1996. Microclimatic parameters of the karst caves from the region of the village Drugomiri, North Albanian Alps, Annual reports of the National speleoexpeditions in Albania 1994-1996, Bulgarian Federation of Speleology

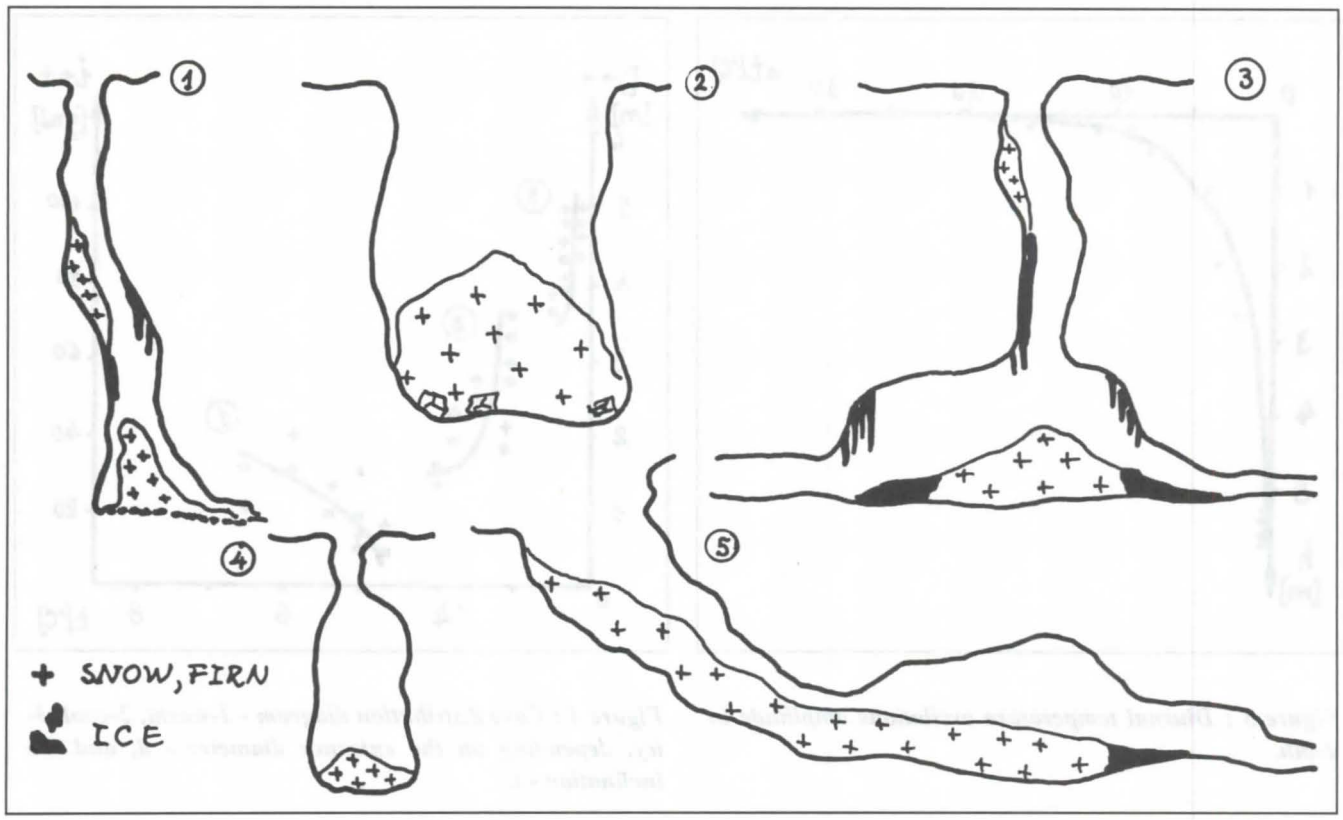

Figure 1 : Morphological typologies of snow-ice accumulations.

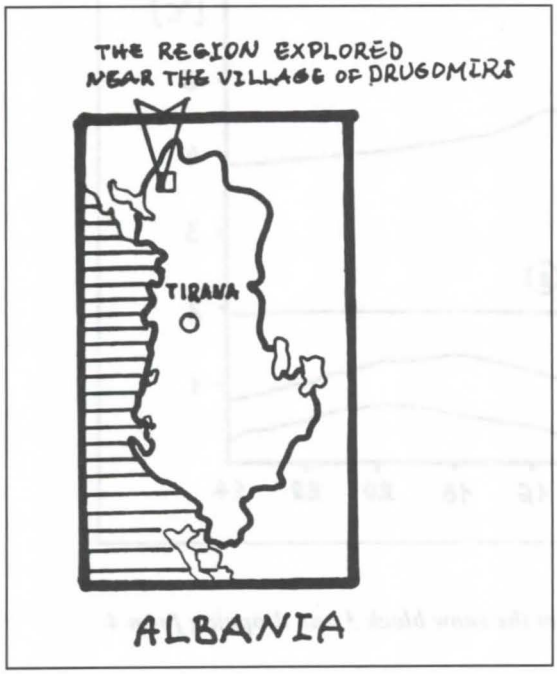

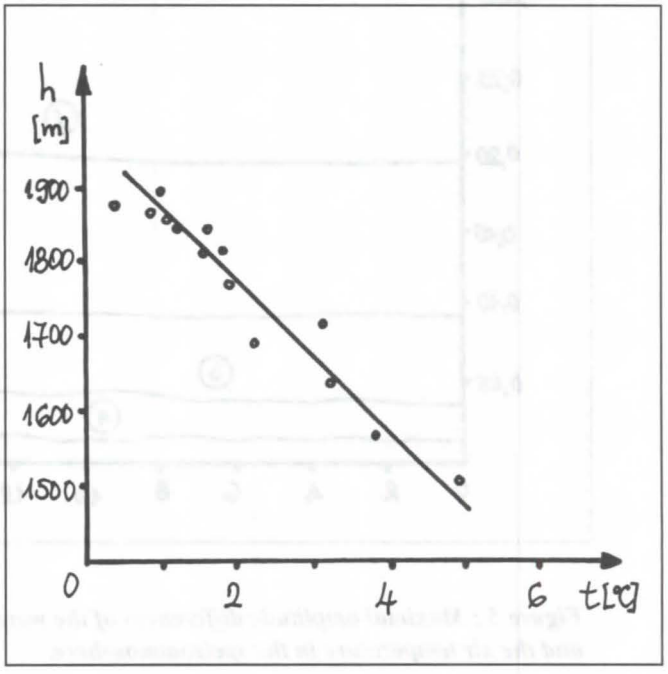

Figure 2 : Air temperature in the zone of constant temperatures depending on the altitude of the entrances.

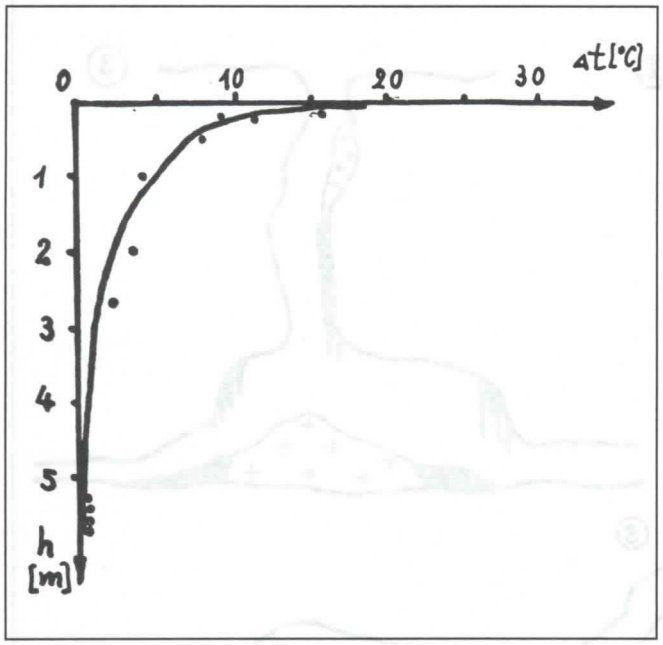

Figure 3 : Diurnal temperature oscilations amplitude in depth.

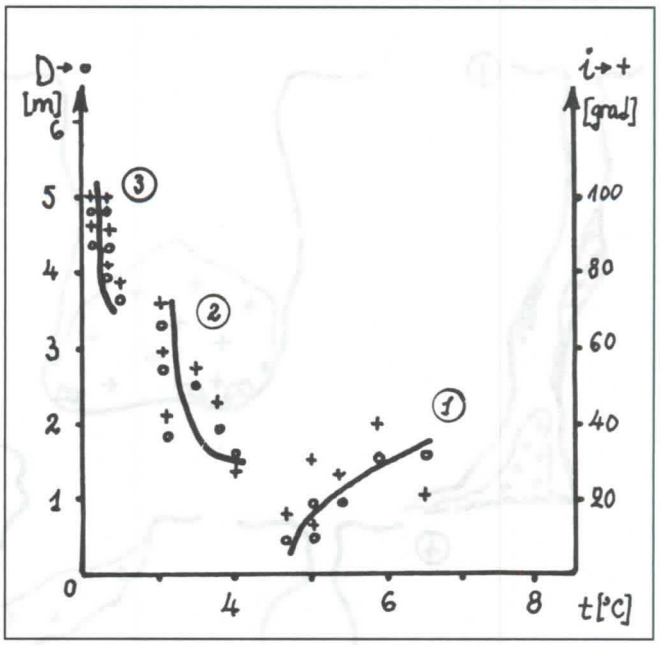

Figure 4 : Cave distribution diagram - 1-warm, 2-cool, 3-icy, depending on the entrance diameter - d, and the inclination - i.

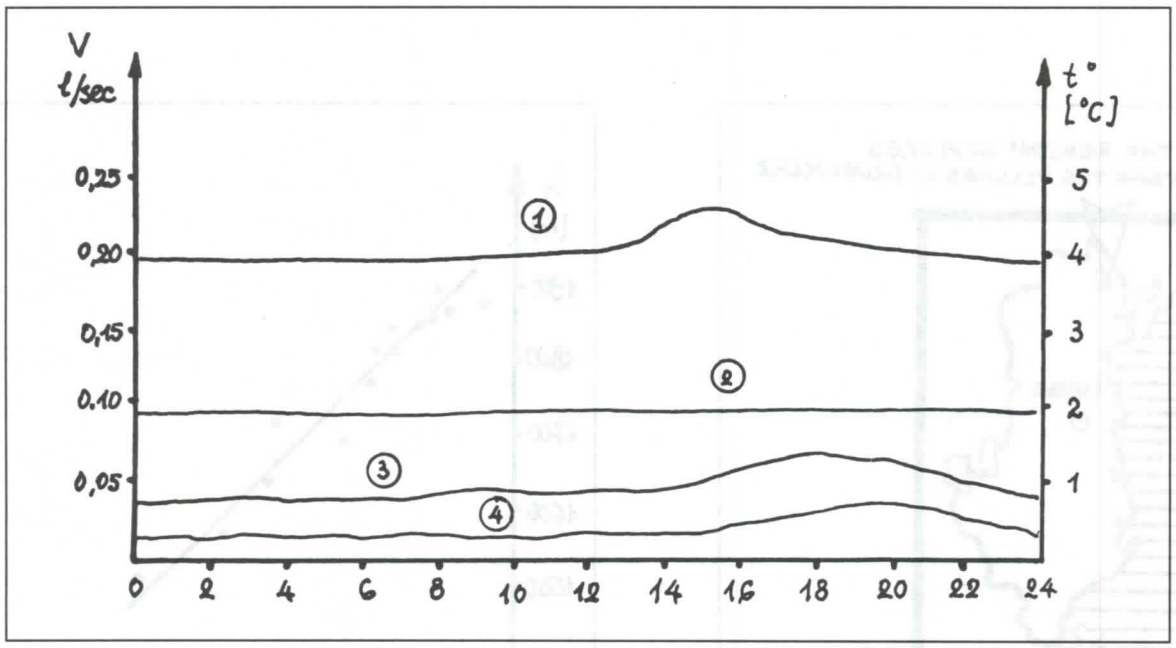

Figure 5 : Maximal amplitude differences of the water stock from the snow block 3 and dropping form 4 and the air temperature in the speleoatmosphere.

CO_2 - Gehalte von Luft und Wasser im vadosen Karst und in der Bodenauflage

von Eberhard Pechhold
Am Ring 73, 71642 Ludwigsburg, Deutschland

Abstract

The CO_2 available in the soil plays the most important part in determining where and to what extent corrosion of carbonate rock takes place. The CO_2 content of the soil air is a dynamic equilibrium between biological CO_2 production and CO_2 losses by physical and chemical processes. The CO_2 concentration, and thus the corrosion, in particular areas of karst rock is reduced mainly by convection-induced ventilation of the rock and the overlying soil. By the lower CO_2 concentration measured below sloping soil surfaces, the formation of dome reliefs on carbonate rock can be explained as a natural consequence of physicochemical processes without assuming any special conditions.

Zusammenfassung

Das im Boden verfügbare CO_2 bestimmt, wo und in welchem Ausmaß Korrosion des Karbonatgesteins stattfindet. Der CO_2-Gehalt der Bodenluft ergibt sich als dynamisches Gleichgewicht zwischen biologischer CO_2-Produktion und CO_2-Verlusten durch physikalische und chemische Vorgänge. So setzt vor allem eine konvektionsbedingte Ventilation des Karstgesteins und des aufliegenden Bodens die CO_2-Konzentration und damit die Korrosion im Gestein herab. Mit der durch Messungen belegten niedrigeren CO_2 - Konzentration unter geneigt gelagerten Bodenflächen läßt sich die Entstehung von Kuppenreliefs als natürliche Folge physikalisch-chemischer Vorgänge erklären, ohne besondere Entstehungsbedingungen vorauszusetzen.

Luftströmungen im Karst

Neben Einflußgrößen wie Temperatur, Niederschlagsmenge und Art und Dichte der Vegetation, die in erster Linie die CO_2 - Produktionsrate bestimmen, kommt der den Karst durchströmenden Luft eine besondere Bedeutung beim Verkarstungsprozeß zu: Wie das Wasser die Hohlräume des Karstgesteins und die diesem aufliegende Bodenschicht durchdringt und dort die für die Korrosion des Karbonatgesteins maßgebende CO_2-Konzentration beeinflußt, so tut dies auch die atmosphärische Luft. Während Wasser dabei der Schwerkraft nach, immer in derselben Richtung strömt, folgt die Luft einem zeitlich veränderlichen Druckgefälle, das ihre jeweilige Strömungsrichtung und -intensität bestimmt. Meist wird dieses Druckgefälle durch einen temperaturbedingten Dichteunterschied zwischen Karstluft und Außenluft hervorgerufen. Die zwischen unterschiedlich hoch gelegenen Ein- und Austrittsstellen im Karst sich ausbildenden Luftströmungen, die sich z.B. in Höhlen als Höhlenwind bemerkbar machen können, sind somit Konvektionsströme. Luftströmungen im Karst können aber auch andere Ursachen haben. Beispielsweise können, vor allem in der Nähe größerer Karsthohlräume, wetterbedingte Luftdruckschwankungen zu temporären Luftströmungen Anlaß geben. Auch Wind kann, da er zwischen Luv- und Leehängen der Karstoberfläche erhebliche Druckunterschiede erzeugt, Luftströmungen im darunterliegenden Karst hervorrufen. Die Wege, die Luftströme im Karst nehmen, können beliebig lang und kompliziert sein und, im Gegensatz zu Wasserwegen im vadosen Bereich, vertikale Strecken beider Richtungen einschließen, beispielsweise von einer Karsthochfläche hinab auf den Karstwasserspiegel und wieder hinauf zur Karsthochfläche führen.

Während man die Wirkungen des Wassers im Karst intensiv erforscht hat und noch erforscht, wurde der den Karst durchströmenden Luft, abgesehen von der Wetterführung in begehbaren Höhlen, die gelegentlich zur Entdeckung neuer Höhlenteile führt, nur recht wenig Aufmerksamkeit geschenkt.

Es gab zwar frühzeitig Ansätze, den Einfluß von Luftströmungen bei der Karstbildung mitzubetrachten – beispielsweise sah Alfred Bögli Ventilation durch Klüfte als eine mögliche Ursache für die Entstehung unterschiedlich kalkgesättigter Wässer an (BÖGLI, 1969) – , jedoch wurden diese nicht konsequent weiterverfolgt, um Art und Ausmaß der Wirkung von Luftströmungen auf das CO_2-Angebot und damit auf die Karstbildung zu bestimmen. Ein Grund dafür liegt sicher in den meßtechnischen Schwierigkeiten, die man hat, Karstluft nachzuweisen, insbesondere dann, wenn es sich um schwache oder fein verteilt durch Klüfte und Bodenauflage dringende Luftströmungen handelt.

Messtechnische Erfassung von Karstluftströmen

Eine Möglichkeit, Karstluft von gewöhnlicher atmosphärischer Luft zu unterscheiden und als solche zu identifizieren, bietet die Messung ihres CO_2-Gehaltes , der meist erheblich über dem der atmosphärischen Luft liegt. Jedoch ist die Beurteilung von Luft allein nach ihrem CO_2- Gehalt schwierig. Da ständig neues CO_2 durch biologische Prozesse entsteht, an die Atmosphäre entweicht, durch Korrosion von Karbonatgestein verbraucht oder durch Wasser zugeführt oder abtransportiert wird, schwankt der CO_2-Gehalt örtlich und zeitlich stark und ist von vielen Einflußgrößen abhängig. Dennoch läßt sich nach genügend langer Beobachtung, häufigen Messungen und deren statistischer Auswertung Luft, die durch die Bodenauflage in das Karstgestein eingedrungen ist oder Kontakt mit Karstwasser hatte, von Luft unterscheiden, die durch ein offenes Kluftsystem herangeführt wurde oder nur eine Schotterhalde unterquert hat.

Wichtiger noch als Art und Herkunft der Luft festzustellen ist es, Aus- und Eintrittsstellen von Luftströmen zu finden und diese beispielsweise Besonderheiten der Karstoberfläche zuzuordnen, um hieraus Auswirkungen der Karstdurchlüftung auf die Korrosion der Gesteinsoberfläche und ihre Bedeutung für das Karstrelief erkennen und abschätzen zu können.

Besonders interessant sind hierbei Stellen, an denen Luft auf einer größeren Fläche, fein verteilt durch die Bodenauflage hindurchtritt und dabei den CO_2 -Gehalt der Bodenluft verändert. Derartige Bodenflächen lassen sich im Gelände optisch meist

nicht erkennen. Man kann hier nur, auf den Zufall hoffend, stationäre Bodenluftsonden ausbringen und die CO_2 -Konzentration der Bodenluft, die mit der der Karstluft vergleichbar ist, über einen längeren Zeitraum hinweg messen. Wechsel der Strömungsrichtung, wie sie bei Konvektionsströmungen bei einer Umkehr des Temperaturgefälles zwischen Außenluft und Karstluft auftreten, zeichnen sich im CO_2 -Verlauf ab und erlauben es, ventilierte Bereiche der Karstoberfläche als solche zu identifizieren. Zum Nachweis von in der Nähe von Karstquellen liegenden Lufteintritten kann ergänzend zur CO_2 -Messung in der Bodenluft das physikalisch gelöste CO_2 (sogenannte freie Kohlensäure) in dem mit der Karstluft in Kontakt befindlichen Wasser bestimmt werden.

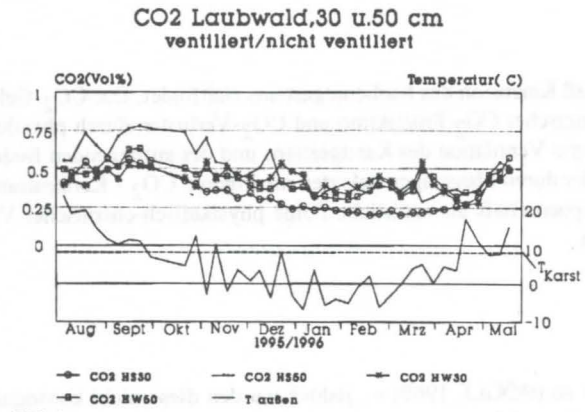

FIG.1

Fig. 1 zeigt z.B. den Verlauf der CO_2 -Konzentration der Bodenluft in jeweils 30 und 50 cm Tiefe im Laubwald (Schwäbische Alb, 750 m NN). Während ein erstes Sondenpaar (HS 30, HS 50) in nicht von Karstluft durchsetztem Boden das ganze Jahr über die übliche Zunahme der CO_2 - Konzentration mit der Tiefe zeigt, kehrt sich bei einem zweiten, etwa 1 km von dem ersten Sondenpaar entfernt ausgebrachten Sondenpaar (HW 30, HW 50) dieser Gradient um, sobald im Winter die Außentemperatur die Temperatur des Karstgesteins unterschreitet und dadurch eine Ventilation des Bodens aus dem Karstuntergrund heraus in Gang setzt. Die aus dem Karst aufsteigende Luft enthält hier relativ wenig CO_2 ,was auf eine kurze, hindernisarme Zuführungsstrecke und fehlenden Kontakt mit Karstwasser schließen läßt.

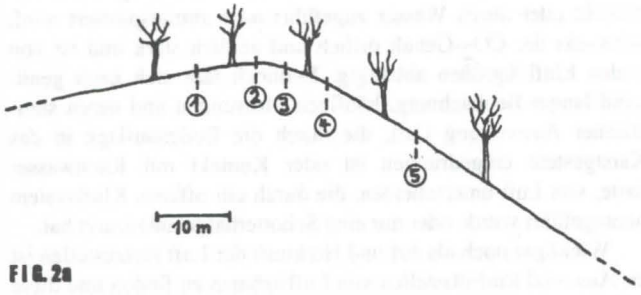

FIG.2a

Fig. 2 zeigt CO_2 -Gehalte der Bodenluft in 20 cm Tiefe im Bereich einer in Fig. 2a skizzierten Karstkuppe. Wie die Werte der Sonden WK1 und WK2 in den Wintermonaten erkennen lassen, bildet sich hier eine Karstluftströmung zur Kuppenspitze hin aus, die die CO_2 -Konzentrationen der Bodenluft im Bereich der Kuppenspitze weit über Sommerwerte hinaus ansteigen lassen. Die wie in einem Kamin zur Kuppenspitze aufsteigende Karstluft enthält hier mehr CO_2 als die Bodenluft, was auf fein

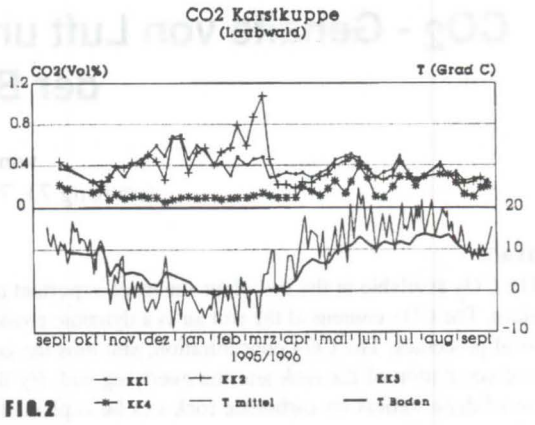

FIG.2

verteiltes Eindringen in den Karst durch die Bodenauflage hindurch schließen läßt. Kontakt mit Karstwasser ist hier nicht anzunehmen, da der Verlauf des CO_2-Gehaltes des Wassers des das Gebiet entwässernden Siebenbrunnens (Fig. 7) darauf keinen Hinweis gibt.

Nachdem sich die Richtung der Karstluftströmung mit dem Temperaturgradienten zwischen Karstluft und Außenluft grundsätzlich umkehrt, darf davon ausgegangen werden, daß im Sommer, der für die Korrosion des Karbonatgesteins besonders wichtigen Jahreszeit mit hoher CO_2 - Produktionsrate und hohen Niederschlägen, sowohl an dem im Zusammenhang mit Fig. 1 erwähnten zweiten Sondenpaar als auch im Bereich der in Fig. 2a wiedergegebenen Karstkuppe CO_2 - arme Außenluft in den Karst eindringt und dabei die CO_2 - Konzentration der Bodenluft herabsetzt.

Zur CO_2-Messung in Luft gibt es heute genau und schnell arbeitende Meßgeräte. Ich verwende z.B. ein von der Firma Dräger AG entwickeltes, nach einem optischen Verfahren (Infrarotabsorption) arbeitendes Gerät (Typbezeichnung: Multiwarn P - CO_2), das die Luft mittels einer kleinen Pumpe ansaugt und schon nach wenigen Sekunden einen sehr genauen Wert anzeigt. Mittels eines selbst gebauten Zusatzes läßt sich das Gerät auch zur Vor-Ort-Messung des im Wasser physikalisch gelösten CO_2 einsetzen.

Auswirkung von Luftströmungen im Karst auf die Karstbildung

Aufgrund von über sechs Jahren Mess- und Beobachtungstätigkeit bin ich heute der Ansicht, daß alle wichtigen Einflüsse, welche die im Karst strömende Luft auf die Karstbildung ausübt, letztendlich auf ihrer Fähigkeit beruhen, gasförmiges CO_2 zu transportieren. CO_2 -Transport beeinflußt die Karstbildung wiederum dort am stärksten, wo durch ihn hohe CO_2 - Konzentrationen, die hohe Korrosionsraten im Karbonatgestein verursachen können, herabgesetzt werden, wie dies zum Beispiel in einer dem Karstgestein aufliegenden, porösen Bodenschicht, durch die hindurch CO_2 -arme Außenluft in den Karst eintritt , der Fall ist. Durchsickerndes Niederschlagswasser nimmt in einer solchen Bodenschicht weniger CO_2 auf und kann entsprechend weniger Karbonatgestein lösen. Die Durchlüftung des Bodens bewirkt damit hier eine gewisse Abtragungsresistenz des darunterliegenden Karstgesteins im Vergleich zu benachbarten, nicht oder weniger gut durchlüfteten Bereichen und, über längere Zeit hinweg, ein Herausheben des durchlüfteten Bereichs über seine Umgebung, also die Entstehung einer Kuppe. Daß durch strömende Luft zumindest zeitweilig auch CO_2 in Karstbereiche mit ursprünglich niedriger CO_2 -Konzentration transportiert wird

und dort zu erhöhter Korrosion führen kann, zeigt das oben im Zusammenhang mit Fig. 2 beschriebene Beispiel für die Zeit der Wintermonate.

Herabsetzung der CO2- Konzentration durch Konvektion im Hangboden

Bei der großen Anzahl von CO_2 -Messungen in der Bodenluft, die ich zunächst mit Hilfe einer unmittelbar vor der Messung in den Boden getriebenen Sonde, bald jedoch mit stationär eingesetzten Sonden in verschiedensten Böden durchführte, fiel mir bald auf, daß sich in stärker geneigt gelagerten Böden, z.B.an Talhängen, grundsätzlich ein Durchlüftungseffekt zeigt, der die CO_2 -Konzentration der Luft dort stärker herabsetzt als in entsprechenden, eben gelagerten Böden und nicht überall durch in den Boden ausmündende Karstspalten hervorgerufen sein kann. Nach genauerer Untersuchung dieser Erscheinung ergab sich als einzig sinnvolle Erklärung hierfür eine Eigenbelüftung des Hangbodens durch Konvektion infolge eines Temperaturunterschiedes zwischen Bodenluft und Außenluft.

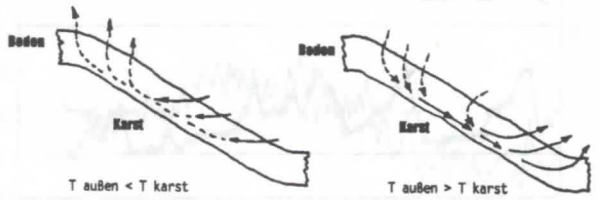

FIG. 3

Dank der Neigung der Bodenschicht, die den Aus -und Eintritt von Luft auf unterschiedlicher Höhe ermöglicht, kommt hier, wie in Fig. 3 schematisch dargestellt, eine Bodenluftströmung nach demselben Prinzip wie die konvektionsbedingte Karstventilation im Großen in Gang : Ist die Außenluft kälter als die Luft innerhalb des Hangbodens, so steigt wärmere und infolgedessen leichtere, CO_2-haltige Bodenluft innerhalb der porösen Bodenschicht nach oben und saugt kältere, CO_2 -arme Außenluft von der Seite her nach. Ist die Außenluft wärmer, so sinkt kältere Bodenluft in der Bodenschicht nach unten und saugt wärmere, CO_2 -arme Außenluft von der Seite her nach. In beiden Situationen wird Bodenluft durch CO_2 -arme Außenluft ersetzt und die CO_2 -Konzentration im Hangboden gegenüber der CO_2 - Konzentration in vergleichbaren eben gelagerten Böden, in denen sich wegen der fehlenden Neigung keine Konvektion ausbilden kann, herabgesetzt.

In manchen Hangböden bilden sich offenbar durch Aneinanderkoppeln einzelner Konvektionszellen ausgedehnte Bodenluftströmungen aus, die dazu führen, daß im Bereich des Hangfußes bei gegenüber der Bodenluft kälterer Außenluft (z.B.im Winter) extrem niedrige CO_2 -Konzentrationen, bei wärmerer Außenluft (z.B.im Sommer) dagegen CO_2 -Konzentrationen, die mit denen der Bodenluft ebener Böden vergleichbar sind, in der Bodenluft gemessen werden . Umgekehrt werden am oberen Hangende bei kälterer Außenluft vergleichsweise hohe und bei wärmerer Außenluft niedrige CO_2 -Konzentrationen der Bodenluft beobachtet.

Fig. 4 zeigt den Verlauf der CO_2-Konzentration der Bodenluft an 30 und 50 cm tiefen Sonden im Laubwald, im Fußbereich eines mit 30-Grad geneigten Hanges und in fast ebenem Boden.

Eine von mir aufgrund der Meßergebnisse eines Jahres vorgenommene Abschätzung der durch die Bodenluftkonvektion an diesem Hang zu erwartenden Korrosionsminderung ergab knapp

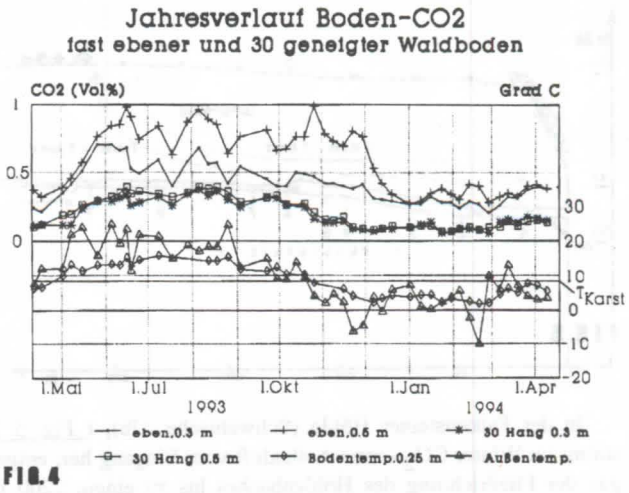

FIG. 4

25%, bezogen auf die Korrosion unter dem entsprechenden, eben gelagerten Boden (Pechhold 1996).

Es ist klar, daß eine solche Korrosionsminderung unter Hangböden im bedeckten Karst eine beachtliche Abtragungsresistenz geneigter Flächen gegenüber ebenen Flächen schafft, die sich im Relief der jeweiligen Karstoberfläche dokumentieren muß. Über längere Zeit betrachtet nimmt bei Abtragung einer Karstfläche- sofern sich die Klimabedingungen nicht wesentlich ändern und Erosionseinflüsse nicht überhandnehmen - der Anteil der abtragungsresistenteren geneigten Flächen gegenüber dem der ebenen Flächen zu, bis schließlich nur noch geneigte Flächen vorhanden sind und sich die gesamte Karstlandschaft aus kegeligen oder satteldachförmigen Vollformen zusammensetzt. Da die Bodenluftkonvektion in Hangböden mit deren Schräglage zunimmt, neigen die Hangflächen darüberhinaus zur Versteilerung bis es zum Abrutschen der Bodenauflage und zur Ausbildung nackter Felsflanken kommt, die nur noch in ihrem Fußbereich einer höheren Korrosion durch Kontakt mit Bodenschichten ausgesetzt sind und sich dadurch zu senkrechten oder sogar überhängenden Steilwänden weiterentwickeln können.

Beeinflussung des Karstwassers durch Luftströmung im vadosen Bereich

Hohe CO_2 -Konzentrationen herrschen meist auch im Karstwasser, in dem sich in wenig durchlüfteten Bereichen der vadosen Zone das physikalisch gelöste CO_2 nahezu im Gleichgewicht mit dem CO_2 - Gehalt der umgebenden Luft befindet. Da vor allem rasch fließendes oder fallendes Wasser CO_2 sehr schnell mit der Umgebungsluft austauscht, entzieht über die Wasseroberfläche streichende oder Tropfwasserzonen durchströmende, CO_2 - arme Luft dem Wasser schnell einen großen Teil des gelösten CO_2 , sodaß zuvor kalkaggressives Wasser nicht mehr korrodierend wirkt, in manchen Fällen sogar Kalk ablagert.

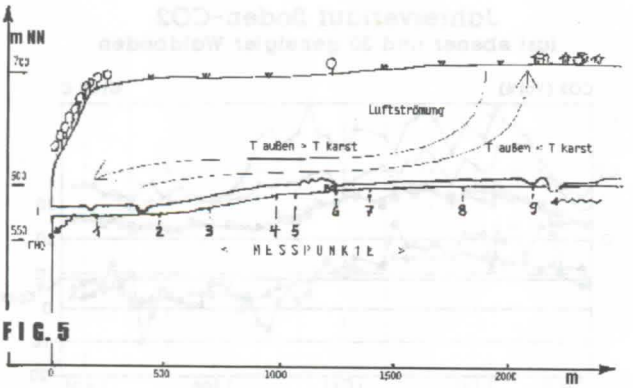

FIG. 5

In der Falkensteiner Höhle (Schwäbische Alb), (Fig. 5), strömt im Winter CO_2 -arme Außenluft vom Eingang her, entgegen der Fließrichtung des Höhlenbaches bis zu einem 2200 m vom Eingang entfernten Siphon . Sie verläßt das Höhlensystem fein verteilt durch die etwa 100 m mächtige Höhlenüberdeckung. Im Sommer dringt umgekehrt CO_2 - arme Außenluft durch die Höhlenüberdeckung in die Höhle ein und strömt in Fließrichtung des Höhlenbaches zum Eingang.

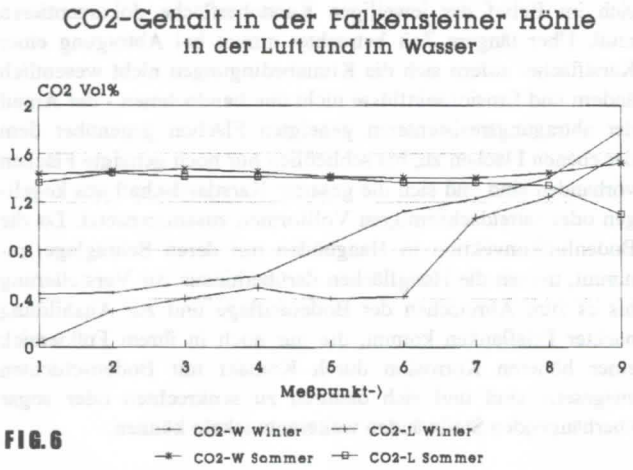

FIG. 6

Fig. 6 zeigt an neun Meßpunkten in der Höhle gemessene CO_2 - Gehalte der Höhlenluft (CO2-L) und des Höhlenbachwassers (CO2-W) im Winter und im Sommer. Vor allem im Winter ist das Höhlenbachwasser, das den größten Teil seines CO2 an die entgegenströmende Luft abgibt, im vorderen Teil der Höhle stark kalkübersättigt, was zu Kalkablagerungen im Höhlenbach auf den ersten 1000 m der Höhlenstrecke geführt hat. Der relativ niedrige CO_2 - Gehalt der von oben her zuströmenden Luft unmittelbar vor dem Siphon (Meßpunkt 9) , im Sommer, nimmt höhlenauswärts rasch einen höheren Wert an, was hier klar auf Kosten des CO_2 -Gehaltes des Höhlenbachwassers erfolgt. Hochwässer können durch Bildung eines zusätzlichen Siphons etwa 400 m innerhalb der Höhle die Luftströmung unterbinden, was sich, insbesondere im Winter, durch starke Anstiege im CO_2 - Gehalt des Höhlenbachwassers bemerkbar macht und in der CO_2 - Konzentration der Elsach-Hangquelle (s. Fig. 7) , an der das Höhlenbachwasser der Falkensteiner Höhle ins Freie tritt, deutlich wird.

Die in der Falkensteiner Höhle nachweisbare Wirkung strömender Luft auf das Karstwasser kann die Karstbildung prinzipiell überall im vadosen Karst beeinflussen. Da das Wasser der vadosen Karstzone oft in phreatische Bereiche abfließt, kann eine Durchlüftung der vadosen Zone nicht nur dort selbst, sondern bis weit in die phreatische Zone hinein Korrosion herabsetzen und damit auch dort auf die Karstbildung einwirken.

Bei Quellen im seichten Karst und im Grenzbereich zum tiefen Karst ist ein sicheres Indiz für den Kontakt mit Karstluft ein Rückgang des physikalisch gelösten CO_2 mit der Schüttung. Durch Öffnen von Siphonen und Freiwerden von dicht über dem Wasserspiegel gelegenen luftwegsamen Räumen infolge des sinkenden Wasserspiegels wird nämlich der Kontakt zwischen Wasser und Karstluft und damit der CO_2 -Austritt in die über das Wasser streichende Luft verbessert. Zusätzlich werden bei weniger Wasser und einer eher zunehmenden Menge zugeführter, CO_2 -ärmerer Luft sowohl das den CO_2 -Austritt bewirkende CO_2 -Konzentrationsgefälle zwischen Wasser und Luft vergrößert als auch, infolge verringerter Fließgeschwindigkeit, die Kontaktzeit zwischen Wasser und Luft verlängert und damit die CO_2 -Abgabe aus dem Wasser weiter verstärkt.

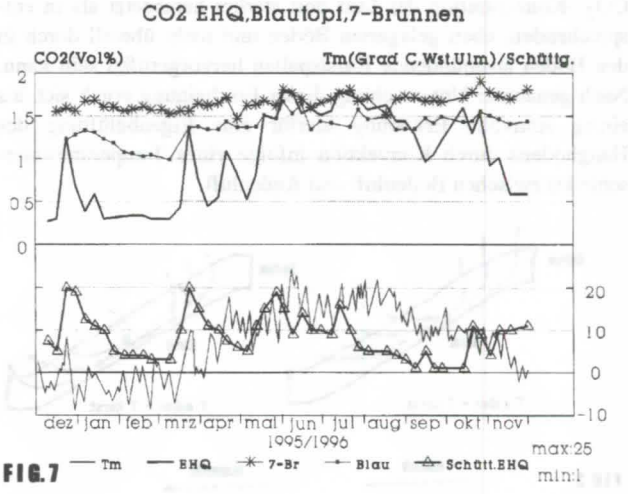

FIG. 7

Fig. 7 zeigt neben dem Verlauf der Schüttung und des physikalisch gelösten CO_2 der o. g. Elsach-Hangquelle (EHQ) auch den Verlauf des CO_2 -Gehalts des Blautopfs (Schwäb.Alb) und des oben erwähnten Siebenbrunnens, einer aus dem phreatischen Karstbereich entspringenden Quelle in der mittleren Schwäbischen Alb. Aus dem Rückgang des CO_2 - Gehaltes des Blautopfwassers während der niederschlagsarmen Zeit von Januar bis Mitte März 1996 läßt sich hier z. B. schließen, daß auch der aus dem phreatischen Karstbereich austretende Blautopf von Karstluft beeinflußtes Wasser aus dem vadosen Karstbereich enthält.

Schriftenverzeichnis

BÖGLI, A. 1969. CO_2 - Gehalte der Luft in alpinen Karstböden und Höhlen. - V. Int. Kongr. Späologie Stuttgart, Abh., 2: 28/2 - 28/9, 4 Tab.; Stuttgart.

PECHHOLD, E. 1996. Die Rolle der Gesteins - und Bodenbewetterung beim Verkarstungsprozeß am Beispiel der Schwäbischen Alb. - Laichinger Höhlenfreund, 31, (1): 25 - 38, 10 Abb., 1 Tab. ; Laichingen.

Daily atmospheric variation within caves in southwestern Wisconsin, U.S.A.

by Robert J. Mueller and Michael J. Day
Department of Geography, University of Wisconsin-Milwaukee, Milwaukee, Wisconsin 53201, U.S.A.

Abstract

Although the general body of theory holds that typical cave atmospheres are relatively stable, with predictable temperatures reflecting the mean annual surface temperature, and consistently high relative humidities, this may not be the case where short, shallow, ridgetop caves in fractured rocks, particularly caves with multiple entrances, permit considerable air exchange between the cave passages and the surface.

Caves in southwestern Wisconsin are typically short (less than 300m) and shallow (less than 10m). Most are in ridgetop locations and have entrances in sinkhole bases or quarry faces. Most have single entrances, but several have multiple entrances, some natural, others excavated. The Ordovician limestones and dolostones in which many of the caves are developed are typically thin-bedded and intensely fractured.

Over a two week period from May 26 through June 8, 1990 daily measurements were made of temperature and relative humidity at seven stations within John Gray Cave, a single sinkhole entrance ridgetop cave in Richland County. The cave is 232m long, composed of an entrance lobby beneath the sinkhole and three radiating passages 49m, 72m and 111m in length.

Mean annual temperature in southwestern Wisconsin is about 10 degrees C. During the study period mean external temperature was 19.0 degrees C, ranging from 10.0 to 23.9 degrees C. Lobby temperatures were similar, ranging from 12.5 to 23.3 degrees C, with a mean of 18.6 degrees C. Temperatures in the three passages varied less, but with ranges of 6.2 to 8.4 degrees C around station means between 14.1 and 16.4 degrees C. External relative humidity ranged from 32.0 to 90.0%, with a mean of 58.9%. Mean lobby RH was 52.2%, ranging from 41.0 to 69.2%. RH in the three passages ranged from 38.9 to 65.6%, with station means between 47.0 and 52.9%.

The temperature data, considerably different from the mean annual surface temperature and with daily variations reflecting external temperature changes during the study period, coupled with the low and variable relative humidities within the cave, indicate a dynamic cave atmosphere suggestive of considerable air exchange with the surface.

Zusammenfassung

Es wird in der Literatur allgemein dargelegt, dass die typische Atmosphäre in Höhlen relativ stabil ist. Dies mit voraussagbarer, der Oberflächendurchschnittstemperatur entsprechender Höhlentemperatur und konsistent hoher relativer Luftfeuchtigkeit. Dies erscheint jedoch nicht der Fall zu sein in kurzen, niedrigen Höhlen, die im oberflächennahen, frakturierten Gestein gelegen sind, vor allem wenn sie mehrere Eingänge besitzen, welche beträchtlichen Luftaustausch zwischen Aussenoberfläche und Höhle zulassen.

Höhlen im südwestlichen Wisconsin sind überwiegend kurz (weniger als 300m) und niedrig (weniger als 10m). Die Mehrzahl ist oberflächennah und besitzt Eingänge durch Schlucklöcher bzw. Dolinen oder Steinbruchaufschlüsse. Die meisten Höhlen haben nur einen Eingang, einige jedoch besitzen mehrere entweder natürliche oder durch Steinbrucharbeiten verursachte Eingänge. Die Kalk- und Dolomitgesteine im Ordovizium, in denen sich viele der Höhlen gebildet haben, sind typischerweise dünnschichtig und intensiv frakturiert.

Wahrend einer zweiwöchigen Untersuchungszeit vom 26. Mai bis 8. Juni 1990 wurden täglich Temperatur und relative Luftfeuchtigkeit an sieben Messstationen in der John Gray Höhle aufgenommen. Diese Höhle besitzt einen einzigen Eingang (Doline) und ist auf einer Erhöhung im Richland County gelegen. Die Höhle ist 232m lang und besteht aus einer Eingangshalle unterhalb der Doline und drei davon wegführenden Gängen mit jeweils 49m, 72m und 111m Länge.

Die Jahresdurchschnittstemperatur im südwestlichen Wisconsin ist ca. 10 Grad C. Während der Untersuchungszeit betrug die durchschnittliche Aussentemperatur 19.0 Grad C mit Schwankungen zwischen 10.0 und 23.9 Grad C. Temperaturen in der Eingangshalle waren ähnlich, mit Schwankungen zwishen 12.5 und 23.3 Grad C (Durchschnitt 18.6 Grad C). Die Temperatur in den drei Gangen variierte etwas weniger, jedoch immerhin zwischen jeweils 6.2 bis 8.4 Grad C um die Messungsstationsdurchschnittswerte von 14.1 bis 16.4 Grad C. Die relative Aussenluftfeuchtigkeit variierte von 32.0 bis 90.0% mit einem Durchschnitt von 58.9%. Die durchschnittliche relative Luftfeuchtigkeit in der Eingangshalle betrug 52.2% und variierte zwischen 41.0 und 69.2%. Die relative Luftfeuchtigkeit in den 3 Gängen variierte zwischen 38.9 und 65.6% (Stationsmittel zwischen 47.0 und 52.9%).

Die Temperaturen der Höhle wichen demnach beträchtlich von der durchschnittlichen jährlichen Oberflächentemperatur ab. Sie zeigten dazu noch tägliche Schwankungen auf, welche mit den Schwankungen der Aussentemperaturen während der Untersuchungszeit korrespondierten. Zusammen mit der niedrigen und variablen relativen Luftfeuchtigkeit in der Höhle zeigen die Daten eine dynamische Höhlenatmosphäre auf, was auf einen beträchtlichen Luftaustausch zwischen Höhle und Oberfläche hindeutet.

1. Introduction

The general body of theory, as presented in both introductory and advanced texts (e.g. MOORE & SULLIVAN, 1978; WIGLEY & BROWN, 1976) indicates that typical cave atmospheres are relatively stable, with predictable temperatures reflecting mean annual surface temperatures, and consistently high relative humidities. Conversely, detailed studies have shown that at least some cave atmospheres are more variable, particularly in short caves, near entrances, and in caves with more than a single entrance (DAVIES, 1960; CROPLEY, 1965; ATKINSON ET AL, 1983; NEPSTAD & PISAROWICZ, 1989; TRAPASSO & KELETSKY, 1994).

On the basis of these previous studies, it is hypothesized here that cave atmospheric variability is particularly pronounced in the karst of southwestern Wisconsin, where the caves are typically short, shallow, in ridgetop locations, and developed in thin bedded and intensely fractured carbonate rocks. Under such conditions, it is anticipated that there is considerable exchange of air between the caves and the surface, resulting in cave atmospheric variability reflecting changing surface weather conditions.

2. Caves in southwestern Wisconsin

The karst of southwestern Wisconsin is developed in the Ordovician-age Prairie du Chien and Platteville-Galena Formations, and constitutes part of the upper Mississippi Valley karst, which is essentially coincident with the unglaciated Driftless Area of the upper Midwest. The carbonate rocks outcrop typically at or near the summits of interfluvial ridges, and karst landforms, with the exception of springs, occur in disjunct ridgetop clusters.

The karst includes a wide array of dry valleys, sinkholes, caves and springs (DAY et al, 1989). North of the Wisconsin River most caves are developed in the Oneota dolostone, which attains a maximum thickness of about 30m. South of the river caves are developed in the Platteville-Galena limestones and dolostones, which attain a total thickness in excess of 100m. The carbonate rocks are variably bedded, and Paleozoic tectonic stresses have resulted in intense regional and local fracturing, accentuated near the surface by dissolution and by Pleistocene periglacial conditions.

Although there are more than 200 caves in southwestern Wisconsin, most are less than 300m in total length, and none exceeds 1000m (DAY, 1986a,b). Dimensions are constrained by the slow dissolution rate of the dolostones, limited ridgetop catchment areas, thin bedding (typically less than 0.5m), and the dismemberment of formerly more extensive systems by valley incision. Most caves are shallow, typically at depths of 10m or less, and rarely exceeding a depth of 25m (DAY et al, 1989).

3. Hypotheses and methodology

The research reported here represents a portion of a larger study of cave atmospheric conditions in southwestern Wisconsin. The larger study involves longer time periods and several caves, and is as yet incomplete (Mueller, in progress).

This report deals only with the results obtained from a single cave (John Gray Cave, in Richland County, Wisconsin) over a fourteen day period, from May 26 through June 8, during the summer of 1990.

John Gray Cave is representative of caves formed north of the Wisconsin River in the Prairie du Chien Formation.

Located on a ridgetop, it has a single sinkhole entrance leading to an entrance lobby and three radiating passages, which are essentially the remnants of phreatic tubes, 49m (passage A), 72m (passage B) and 111m (passage C) in length (ALEXANDER, 1980). All three passages are less than 10 m below the surface of the ridgetop.

Based on the general body of theory , on the size and topographic location of the caves in southwestern Wisconsin, and on the seasonal surface atmospheric situation, the following four hypotheses are tested here: a) the cave air temperature is relatively constant, reflecting mean annual surface temperature, b) the relative humidity of the cave air is consistent and high, c) the air temperature decreases with distance into the cave, and d) the relative humidity increases with distance into the cave.

Between May 26 and June 8, 1990 temperature and relative humidity were measured daily at seven stations within the cave between 08.30 and 13.00 hours. Station L1 was in the entrance lobby, adjacent to the talus pile beneath the sinkhole entrance; stations A1 and A2 were 5m and 20m respectively into passage A; stations B1 and B2 were 10m and 55m respectively into passage B; and stations C1 and C2 were 20m and 25m respectively into passage C.

Temperature and relative humidity were measured at between 12 and 15 centimeters above lobby and passage floors using a Pacer Industries digital hygrothermometer with a resolution of 0.1 % RH and 0.1 degrees C. Reading accuracy is estimated conservatively to be within 1.0% RH and 0.5 degrees C. Surface temperatures and relative humidities were also measured with the same hygrothermometer, and were consistent with data for the same time periods obtained from an independent National Meteorological Service weather station at the Tri-County airport, located at Lone Rock, Wisconsin, 32km from the cave.

4. Results

Mean surface temperature during the fourteen day monitoring period was 19.0 degrees C, ranging from a low of 10.0 degrees C to a high of 23.9 degrees C. Temperatures in the entrance lobby corresponded generally with the surface temperatures, with a mean of 18.6 degrees C and a range of 11.2 degrees C, from 12.5 degrees C to 23.3 degrees C. Six of the fourteen lobby temperature readings were above those of the surface, seven were below, and one was the same.

Temperatures within the three passages followed generally the same trends as the surface and the lobby, varying in similar patterns on a daily basis, but with lower temperature means and smaller ranges (Table 1; Figure 1). Temperatures generally decreased with increasing distance into all three passages, and passage temperatures in general were lower than those in the lobby. Passage A, the shortest, was consistently the warmest, and passage C, the longest, was consistently the coolest (Table 1; Figure 1).

Table 1. Passage temperatures.

Station	Mean	Minimum/Maximum	Range
A1	16.4	12.2 / 18.9	6.7
A2	15.8	11.9 / 18.1	6.2
B1	15.4	10.2 / 17.8	7.5
B2	14.9	9.3 / 17.9	8.2
C1	14.6	8.8 / 17.3	8.4
C2	14.1	8.8 / 17.1	8.3

Surface relative humidities varied considerably, ranging 58%, from 32.0% to 90.0%, with a mean of 58.9%. Relative humidities within the entrance lobby were similar, but muted, with a range of 27.2%, from 41.0% to 69.2%, and a mean of 52.2%. Six of the fourteen lobby RH readings were above those of the surface, seven were below, and one was the same.

Relative humidities within the three passages followed generally the same trends as the surface and the lobby, varying in similar patterns on a daily basis, but with generally lower means and smaller ranges (Table 2; Figure 2). Relative humidities generally increased with increasing distance into the three passages, although passage
humidities in general were lower than those in the entrance lobby. Passage C, the longest, had the highest RH readings consistently, whilst passage A, the shortest, had the lowest.

Table 2. Passage relative humidities.

Station	Mean	Minimum/Maximum	Range
A1	47.0	39.6 / 56.7	17.1
A2	48.1	40.0 / 58.1	18.1
B1	48.9	38.9 / 60.0	21.1
B2	50.2	41.0 / 61.3	20.3
C1	51.5	40.7 / 64.8	24.1
C2	52.9	41.1 / 65.6	24.5

5. Conclusions

Analysis of the results demonstrates clearly that both temperature and relative humidity in John Gray Cave throughout the fourteen day study period fluctuate considerably and mimic changes in surface atmospheric conditions. This points unequivocally to a dynamic cave microclimatology linked to external stimuli via air exchange between the cave and the surface.

Of the four hypotheses only the third is supported solidly by the data, and the fourth to a lesser degree. Cave air temperatures generally are not constant, and do not reflect the mean annual surface temperature. Likewise, the relative humidity of the cave air is variable and often falls below 50%. Cave air temperatures do generally decrease with distance in to the cave, and relative humidities tend to increase, although not consistently.

Variations in cave air temperature are particularly clear reflections of surface air temperature changes. This is especially the case in the entrance lobby where the temperature range (11.2 degrees C) is similar to that at the surface (13.9 degrees C). Lobby temperatures were generally lower than surface temperatures, but in six instances the lobby was warmer than the surface, perhaps resulting from retention of heat in the rock walls.

Air temperatures within the three passages were generally lower than those at the surface or in the lobby, and they varied less, although still by between 6.2 and 8.4 degrees C. As expected, temperatures within the longest passage were the lowest, although this passage demonstrated conversely the greatest temperature range.

Relative humidities within the cave demonstrated essentially similar patterns, with lobby RH clearly related to surface conditions, and passage air RH showing similar but depressed fluctuations. Cave air RH was always less than 70%, while surface RH ranged up to 90%.

Although the results are suggestive of considerable air exchange between the surface and the cave, no measurements have yet been made of air movement either within the cave itself or through the entrance. Equipment available during this study was unable to detect air movement of less than 0.2 meters per second, and monitoring of cave air flows remains a project for the future.

References

ATKINSON, T.C., SMART, P.L. and WIGLEY, T.M.L. 1983. Climate and natural radon levels in Castleguard Cave, Columbia Icefields, Alberta, Canada. Arctic and Alpine Research 15: 487-502.

ALEXANDER, E.C. (Ed) 1980. An Introduction to Caves of Minnesota, Iowa and Wisconsin. N.S.S., Huntsville, 190 p.

CROPLEY, J.B. 1965. Influence of surface conditions on temperatures in large cave systems. Bulletin National Speleological Society 27: 1-9.

DAY, M.J. 1986a. Caves in southwestern Wisconsin, U.S.A. Proceedings 9th International Congress of Speleology, Volume 1: 155-157.

DAY, M.J. 1986b. Cave studies in southwestern Wisconsin: Implications and importance. The Wisconsin Speleologist 19(3): 1-21.

DAVIES, W.E. 1960. Meteorological observations in Martens Cave, West Virginia. Bulletin National Speleological Society 27: 1-9.

MOORE, G.W. and SULLIVAN, G.N. 1978. Speleology: The Study of Caves. Cave Books, St. Louis, 150p.

NEPSTAD, J and PISAROWICZ, J. 1989. Wind Cave, South Dakota: Temperature and humidity variations. Bulletin National Speleological Society 41: 125-128.

TRAPASSO, L.M. and KALETSKY, K. 1994. Food preparation activities and the microclimate within Mammoth Cave, Kentucky. Bulletin National Speleological Society 56: 64-69.

WIGLEY, T.M.L. and BROWN, M.C. 1976. The physics of caves. In: The Science of Speleology, ed. T.D. Ford and C.H.D. Cullingford: 329-358. Academic Press, London.

Overview of cave minerals onthogeny

Vladimir A. Maltsev
VNIIGEOSYSTEM institute. Moscow 121351, Yartsevskaya ul., 15-21, Russia

Abstract

The onthogenetic approach in mineralogy, mostly developed in the former USSR, covers the part of the earth science, connecting mineralogy and crystallography. The subject of study within this approach is the minor mineral bodies hierarchy, their structures and textures, and the genetic controls for the separate features of the structures and textures. Onthogenetic tools, including the concept of characteristic symmetry, Curie symmetry principle, conception of mineral bodies with strict or partial interactivity, allow precise reconstruction of the genetic mechanisms for the minor mineral bodies. Caves, with their "clear-case" crystallization environments and almost unlimited space for free crystallization, allow to study the higher levels of the minor mineral bodies hierarchy, than are displayed in other geologic sites. The knowledge, received from this, may in its turn be applied to other cases, where the mechanisms are the same, but are not so clear, and thus significantly enriching the general knowledge of mineralogy.

Introduction

Onthogeny of minerals is one of the main parts of the mineralogical science in the former USSR, and is almost not studied abroad. Onthogenetic tools are rather important in studying speleothems. Expecially cave environments (crystallization in empty space) display higher organized objects, than other geologic environments, thus requesting more powerful tools for their study.

Basic concepts

The subject of the onthogenetic approach is the minor mineral bodies hierarchy, the minor mineral bodies interactions, and the connection between minor mineral bodies and their parent morphogenetic environments. A "minor mineral body" is a term, separating the mineral bodies that are to be studied by means of mineralogy (starting with individual crystals, and raising to approximately veins), from the mineral bodies, that must be studied by means of petrography (these are rocks). In cave environments minor mineral bodies include objects, starting with individual crystals, and raising up to whole speleothem ensembles, reflecting a whole cycle of the cave development history.

Standard hierarchy

In "usual" (non-cave) mineralogy the mineral bodies hierarchy is defined as following. According to DYMKOV [1991], the term "mineral" is wide, and joins together mineral species, mineral variety, mineral individual, mineral aggregate. Zhabin [1979] and Godovikov [1989] enchanted the list, and now it's as below (excluding species and varieties, that have strictly the same sense that in Western science).

- 1-st order mineral individuals. These are simply crystals.
- 2-nd order individuals. These are objects, having an internal structure, but still no texture. They grow from a single crystal nucleo during a single-act crystallization process, and may appear as skeleton crystals, or splitted crystals. Skeleton crystals appear in environments with high oversaturations and poor feeding or poor mixing as a result of a disbalance between the rapid growth possibility and too poor supply for this [GRIGORJEV, ZHABIN 1975]. This leads to rapid growth on edges and tips, without massive growth on faces. Splitted crystals appear as a result of mechanical or chemical admixtures in the parent solution, and, due to the splitting grade, may appear as partly faced cheaf-like crystals, or spherolites, or spherocrystals (top splitting grade with complete disappearance of any boundaries between sub-individuals, and appearance of curved crystal faces and spherical cleavage). In Western science skeleton crystals are usually taken together with dendrites, and spherolites - together with radial-fibrous aggregates. This is unlikely, because both dendrites and radial-fibrous aggregates belong to higher hierarchy levels, grow from multiple nucleos, and display selection between individuals.
- aggregates. These are minor mineral bodies, displaying some regular co-growth of multiple mineral aggregates. On this organization level [MALTSEV et. al. 1995] some kind of selection (competition) between individuals is necessary, defining the texture of the aggregate. Some explorers even take the terms "aggregates" and "textures" as synonyms, but this is truth only when considering the lowest level of texture. By definition, texture is a set of geometric variations of the structures of mineral individuals and aggregates in the complete space of synchronous crystallization [STEPANOV 1973], and therefore may apply to co-growths of aggregates. The same kind of aggregate may be built from different individuals. For example, popcorn and frostwork appear as the same aggregate - crystallictite [SLETOV 1985], built from spheroidolites in the first case, or crystals in the second.
- higher organized minor mineral bodies. usually, they need not to be classified. Outside caves the synchronously generated minor mineral bodies, having through structure or through texture, and raising higher than aggregates are only veins or unique phenomenas. Others convert into rocks, losing through structure and texture.

Hierarchy enhancement for caves

Caves (or separate rooms) by definition are "complete space of synchronous crystallization", and all the sinter has through texture, therefore matches the definition of a minor mineral body. In spite of this, several organization levels can be observed clearly higher, than aggregates. They can be observed in almost all the caves, and so are to be classified.

It's not enough to simply add some levels. Firstly, one must define the boundary between aggregates and higher-organized mineral bodies correctly, because currently it is not clear.

Here we'll consider as aggregates only minor mineral bodies, having a mono-mineral composition, and built from homogenous individuals.

1. The first enhancement is needed on the individuals level. In caves we meet mineral individuals, having both features of skeleton growth and splitted growth, even other kinds of abnormal growth, at the same time. These are selenite needles [MALTSEV 1996], nests [MALTSEV 1997a], etc. They are rare

enough not to be classified, but usual enough to define a group of "complicated individuals".

2. Multi-aggregates [MALTSEV 1995]. If an aggregate is something monomineral, mostly built from homogeneous individuals (both except the case of changing the environment between crystallization acts), multi-aggregate may consist of several minerals, of several kinds of individuals, even may be an intergrowth of several aggregates, but they are always generated by the same crystallization environment. To understand the necessity of this conception, let's discuss two examples. In many caves we can see the following sequence: calcite corallites, aragonite crystallictites, hydromagnesite efflorescences. This sequence can be seen in each single bush or branch, and all three phases are simultaneous and singenetic. The capillary solution film, while moving along the multi-aggregate and evaporating, gets enriched in magnesium, controlling mineral changes. The magnesium even goes into a cycle, being dissolved in the root part, where the solution is undersaturated in magnesium (drawing). Even more - different minerals in the same state of the crystallization environment grow into different individuals and aggregates - the crystals splitting grade is very different. This regular singenetic intergrowth of different minerals in different aggregates is what we call a multi-aggregate. One can note, that this example shows a phenomena, which is interesting for general mineralogy. It is possible to have a complete picture of sequential crystallization (even without appearance of induction surfaces) in a synchronous case. Another example is the syngenetic intergrowth of calcite druses and grainy calcite, described by DYMKOV & SLETOV [1981]. An interesting analogy is that the multi-aggregates conception seems like an onthogenetic reflection of the paragenesis conception (first observed by Stepanov [unpublished lectures], that described paragenetic sets of aggregates, that cover a half of possible multi-aggregates types), appearing, as a rule, only in karstotypic [MOROSHKIN, 1986] surroundings.

Multi-aggregates appear as the last hierarchy level, where a through structure may be observed. On the upper levels we can only speak about texture. Also, multi-aggregates, as it can be seen from the first example, appear to be the first level, where we must speak not only about synchronous crystallization, but synchronous crystallization and re-crystallization.

3. Crusts. The term was first suggested by STEPANOV [1971], then concreted by several authors [MALTSEV, 1993, MOROSHKIN, 1976, 1986]. Now it is understood as a union of aggregates and multi-aggregates, generated within the same crystallization environment, not only locally in the cave.

Good examples of crusts are the stalactite-stalagmite crust (union of products of gravitation-controlled dripping and flows), the corallite crust (joining all the subaerial popcorn and frostwork, generated by capillary films evaporation), the antholite crust (joining all the efflorescences, generated from the inside-pores solutions evaporation).

On all the preceding levels, starting from individuals, the hierarchy can break. Individuals, not joining into aggregates, are possible (calcite spherolites inclusions in gypsum crystals from Podolian caves [TURCHINOV 1993], selenite needles [MALTSEV 1996]). Aggregates, not joining into crusts, are even more usual (helictites).

4. The last hierarchy level appear in mineral ensembles. This concept, making a difference to previous ones, is not strictly determined, and it is not even transitive. The idea of such conception was first suggested by STEPANOV [unpublished lectures], but its final sense was concreted only in [MALTSEV 1995]. It can be understood as some generalization of the mineral association conception. As is shown in [MAXIMOVICH 1961, STEPANOV 1971a], crystallization processes in each cave element change, due to microclimate changes, in linear or cyclic manner. Crystallization environments also change, generating new types of individuals, new types of aggregates and multi-aggregates, new types of crusts, they dissolve existing ones. Such sequences are mostly different in different caves and cave groups. We'll call a mineral ensemble the sequence of sets of mineral individuals, aggregates, multi-aggregates, and crusts, generated on the monotone part (to general inundation) of the last crystallization cycle, that is defining the "mineralogical landscape" of a cave element.

The most important thing that we can get from this conception, is to make the interaction between cave mineralogists and normal cavers when exploring a large cave much more simple. The idea is that in a cave, in a group of caves, even on a whole karst massif, we can find not only finite, but the very small quantity of ensembles. For example, in very variable Kugitangtou caves - 8 [MALTSEV 1993]. And in each ensemble a diagnostics set of 2-5 aggregates and multi-aggregates can be easily found. So, we have a compact convolution of mineralogical information, easy to be used by normal cavers, and informative enough for a mineralogist. It carries almost full description of the last crystallization cycle in an explored cave element, and some part of its modern geological history.

5. Non-mineralogical formations. Understanding some logical impropertness, we'll continue considering them as minor mineral bodies, studied via means of mineralogy, residual formations like "gypsum flour" [ANDREICHOUK 1992], or "sulfide mirrors" [MALTSEV 1993], coming from dissolution or sublimation of speleothems. These formations are really rocks and theoretically are to be studied by means of petrography, but there are few of them, and the cumulative effect of this error is not significant. Moreover, really being rocks, they still join into the above described hierarchy approximately on the level of multi-aggregates, appearing as elements of crusts and ensembles.

Morphogenetic environments

The morphogenetic environment concept (or crystallization environment) [STEPANOV 1971a, MOROSHKIN 1986] is the main tool, used in the onthogenetic approach. Each individual, aggregate, or multi-aggregate is a product of some morphogenetic environment, and the central problem in genetic modelling is the problem of understanding, which environments, and in which sequence produced the mineral object that is studied.

It's evident, that properties of the morphogenetic environments may be decoded from the mineral bodies features, but it is not very evident, in what manner. For example, the shape of individuals give only restricted information on the environment - only the information on the crystallization kinetics. It's theoretically impossible [STEPANOV, 1973] to decode even the phase conditions of the environment from only the shape. Individuals and aggregates structure give a bit more information, but also a poor one. The bigger part of the genetic information, allowing the real decoding of genesis may be read from high-level object's texture, mostly through the characteristic symmetry tool.

Characteristic symmetry

By definition, characteristic symmetry of some class of objects, or some media, or some process (not a certain object), is a maximum possible symmetry, compatible with existence of this class, media, or process [ZHABIN 1979]. Characteristic symmetry is usually referred through some geometrical body, having such symmetry. The most used kinds are cylindrical symmetry, cone

symmetry, spherical symmetry. Another useful concept is dissymmetry, that is defined as some symmetry element, missing to raise some phenomena to the next level of characteristic symmetry. We can find an illustration to this when comparing a cave pearl and a stalagmite. They display the same kind of an aggregate (druse of spherolites), having spherical symmetry in their texture. But in the stalagmite case we have a linear dissymmetry, caused by the gravitation control. It's very important, that the main symmetry and the dissymetry appear on different examination levels, in spite of that their causes exist simultaneously. This means, that the texture symmetry features raise the contrast between effects, caused by different properties of the morphogenetic environment, and that's the usual thing.

Usage of the characteristic symmetry concept comes through the universal Curie symmetry principle: "If some cause has some consequence, then the consequence's characteristic symmetry (dissymetry) is a projection of the cause's characteristic symmetry (dissymmetry)" [STEPANOV 1970]. When applied to the minor mineral bodies genesis, this mostly gives a one-to-one connection between the texture features and the mass-transportation physics in the crystallization environment. For example, solution flows have spherical mass-transportation physics on lower levels, overlapped by dissymetries on upper levels. Thin film evaporation has cone symmetry of mass-transportation, aerosol precipitation - cylindrical one, etc.

In reality not only the mass-transportation physics are important. If we take a usual ice hoarfrost, on the bushes level we'll see the cone texture symmetry, caused by a thin film of evaporation processes, and not an inverse cone symmetry, that must appear within sublimation environments. The reason of this is simple. Ice has low thermal conductivity, vapors condensation frees a lot of energy, and so does crystallization. Therefore, cristallisation is possible. So, the areas of preferable condensation become forbidden for crystallization (no heat removal). Only the areas of extra heat removal may appear as crystallization areas, and these are areas of higher evaporation. Some of the latest studies by other authors also show, that here we deal with a more complicated process, than a direct crystallization from vapors. For example, PARUNGO [1983] speaks about "quasi-liquid phase" on the surface of growing hoarfrost. So, the mass-transportation physics here is based not by the basic properties of the environment, but by the energy-transportation physics in it. On the higher level (crusts) of the same hoarfrost we'll see the inverse cone symmetry, and air flow geometry controlled dissymetries.

If we consider the physics of the symmetry features projection, we must note, that there are only two mechanisms for this - the nucleation mechanism, and the individuals selection (competitions) mechanism. The first one defines the low-level features, the second one - high-level ones. The selection may be fortuitous, or geometric (both with aligning to the substrate surface, and both appearing only in spherical symmetry), or driven by the mass-transportation (energy-transportation) physics (for lower symmetry classes, with aligning to some definite direction, or locally defined directions). A good example of fortuitous selection is seen in druses of spherolites, geometric - in druses of crystals, definitely directed - in soda-straws, locally defined - in frostworks and popcorns.

The high contrast and hierarchical construction of the symmetry and dissymmetry features in the mineral bodies texture allows clear decoding of the morphogenetic environment properties in most of the cases, like shown in the example with the hoarfrost.

Interactive aggregates and multi-aggregates

Not all the mineral aggregates and multi-aggregates are passive products of some crystallization environment. Some of them may create the crystallization environment themselves, or significantly modify the parent environment. The grade of this effect can be different. The most clear case is shown by the helictites, described in [SLETOV, 1985]. Several parallel spherolite bunches, growing together, in some chemical starting conditions leave a channel between them. At this moment the aggregate goes out of the controls of the parent environment (that can be both gravitational or capillary), creating the special environment with capillary channel, taking the solution from the parent environment and feeding a very local capillary film spot at the end. This makes spherolites grow only in sharp sectors, and this, together with differently located zones of main CO_2 loss and of the final evaporation, keeps the aggregate together. We'll call such aggregates and multi-aggregates strictly interactive, and will note, that they never belong to some crust.

For strictly interactive aggregates and multi-aggregates their definition using structure and texture is not complete. We must speak about a new property - behavior while interacting with obstacles. For the aragonite helictites from Khaidarkan [SLETOV 1985], four types of behavior are found :

a) breaking (when perpendicular contact);

b) reflection;

c) rounding;

d) building together with further movement along the obstacle surface. Growing apart again is also typical.

Some multi-aggregates don't create their own environment, but modify the parent one. So, the multi-aggregate, already discussed as an example (called multi-corallite), creates itself the disymmetry of magnesium mass-transportation in the capillary film, that controls its differences from a regular corallite. Their behavior is complicated enough, not the same as behavior of normal corallites - the internal magnesium cycle is much more sensitive to the closeness of obstacle than growth itself, so some elements of reflection are always seen. Such aggregates and multi-aggregates are restrictedly interactive, and usually belong to some crust.

Some features of interactivity (less grade) may be found also for almost any dendritic aggregate and multi-aggregate.

The interactivity and behavior concepts have some historic roots. STEPANOV [1971b] noted, that the shapes of some complicated speleothems (corallites, etc.) have a property of high individuality, known before only for organisms. Now we use the term "behavior" in the same sense as for organisms, as a product of interaction with the environment - also in the same sense as for organisms.

Discussion

The two rather important concepts in the cave minerals onthogeny, both settled by Stepanov, but never published, currently became the central points of modern studies. These are the concept of the hybride textures, and the usually underestimated role of re-crystallization.

It was shown above, that the minor mineral bodies texture sharpens the contrast between the effects, caused by different properties of the morphogenetic environment. With this, a minor mineral body may be produced by two environments with different physics at the same time. This leads to their appearance of hybride textures, possessing symmetry features of both environments on the same hierarchy level. Consequently this results in contiguous rows of formations. For example, these are contiguous lines between shields and helictites [SLETOV 1985],

stalactites and frostwork [MALTSEV 1997b], etc. Some of these lines are usually interpreted as re-crystallized sequential growth [MAXIMOVICH 1961], but the author couldn't find any evidences of this. On the opposite, active growth of such hybride formations is usually seen.

With this, the role of re-crystallization in the speleothems growth is much greater, than is usually considered. On high hierarchy levels interactions between the minor mineral bodies and the parent environments become strong, and the re-crystallization is one of the main physical mechanisms for these interactions. We can take a usual carbonate soda-straw as a good example of this [MALTSEV 1997b]. The zone of active growth is controlled by hydrodynamic effects while dripping. This causes strikes of supersaturation (through CO_2 loss) without re-mixing of the solution (on corresponding speed). This are conditions for the skeleton crystals growth, and in reality each soda-straw has a crown of skeleton crystals on the tip. The pressure pulsation inside the channel, caused by the came dripping, is the condition for rapid re-crystallization. And while any re-crystallization process, poorly balanced individuals, like skeleton crystals, re-crystallize first [MOROSHKIN 1976]. And this is the real reason of why soda-straws are monocrystalline.

For a lot of other formations [MALTSEV 1989, 1993] re-crystallization also plays the leading role, as a necessary result of self-organization of complicated systems.

References

V.N.ANDREICHOUCK 1992. A genetic classifications of karst cave sediments and deposits (in Russian)//In book: Studies of Ural caves, Perm, p.95-98.

A.A.GODOVIKOV, O.I.RYPENEN, V.I.STEPANOV 1989. Spherolites, spherocrystals, spheroidolites, corespherolites (in Russian) // Novye Dannye o Mineralakh (New Data on Minerals), vol. 36, Moscow, "Nauka", p.82-89.

D.P.GRIGORJEV, A.G.ZHABIN 1975. Onthogeny of Minerals. Individuals (in Russian). Moscow.

JU.M.DYMKOV 1991. Current problems of minerals onthogeny (in Russian). Moscow, "Nauka".

V.A.Maltsev 1989. The influence of season changes of the cave microclimate to the gypsum genesis//Proc.10th Int.Cong.Spel.Vol. III.Budapest, p.813-814

V.A.MALTSEV 1993. Minerals of the Cupp-Coutunn cave system, Southeast Turkmenistan // World of Stones, No.2, Moscow, p.5-30.

V.A.MALTSEV 1996. Sulfate filamentary crystals and their aggregates: Proc. Univ. Bristol Spelaeol. Soc., 20(3), pp 171-185.

V.A.MALTSEV., 1997a. Gypsum nests from caves - complex mineral individuals: Litologiya i Poleznye Iskopaemye, 1987, no.2. In Russian.

V.A.Maltsev, 1997b, Once more on stalactites with "internal" and "external" feeding: Natl. Speleol. Soc. Bull., in press.

V.A. MALTSEV, V.V.KORSHUNOV, A.A.SEMIKOLENNYKH 1995. Scientific report on the field studies in Kugitangtou caves on March 1995: Dep. RSIC N003-B95, 90p. In Russian.

G.A.MAXIMOVICH 1961. The genetic row of cave flowstone formatoins (carbonate speleolithogenesis)//Peshchsery, No.5(6). In Russian

V.V.MOROSHKIN 1976. On genesis of crystallictite type of aggregates (in Russian). // Novye Dannye o Mineralakh SSSR (New Data on Minerals in USSR), vol. 25, Moscow, "Nauka", p.82-89.

V.V.MOROSHKIN 1986. Karstotypic mineralisation (in Russian). // Mineralogicheskiy Journal, Kiev, vol.8, No.5, p.10-20.

F.P.PARUNGO 1983. Ice crystals growth at (-8+/-2)C//Journ. Research Athmos. Vol.17.No 2, 139-156

V.A.SLETOV 1985. On onthogeny of crystallictite and helictite aggregates of calcite and aragonite from the caves of Southern Fergana (in Russian) // Novye Dannye o Mineralakh (New Data on Minerals), vol. 32, Moscow, "Nauka", p.119-127.

V.I.STEPANOV 1970. On genesis of so-named "collomorphous" mineral aggregates (in Russian) // In book: Ontogenetic methods of minerals studying. Moscow, "Nauka", p. 198-206

V.I.STEPANOV 1971a. Crystallisation processes periodity in karst caves (in Russian) . Trudy mineralogicheskogo muzeja imeny Fersmana. Moscow, 1971, No.20., p.161-171

V.I.STEPANOV. 1971b, Studies of Khaidarkan caves, both hydrothermal and cold; *in* Velikii, A. S., Volgin, V. J., Ivanov, V. S., and Stepanov, V. I. (eds.), Structural features and genetic sequences for some central Asian Hg-Sb depositions: Unpub. Rept., IMGRE All-Russian Geol. Found., p. 184-220. In Russian.

V.I.STEPANOV 1973. On aims and methods when studying crystallisation sequences in ore mineral aggregates (in Russian) //In book: Issledovaniya v oblasty prikladnoy mineralogii i kristallohimii. Moscow, IMGRE, p.3-10.

I.I.TURCHINOV 1993. Secondary mineral formations op the West Ukrainian gypsum caves (in Russian) // Svet, No.3(9).

A.G.ZHABIN 1979. Onthogeny of Minerals. Aggregates (in Russian). Moscow.

Pyrocoproite (Mg $(K,Na)_2$ P_2O_7, monoclinic), a new mineral from Arnhem Cave (Namibia), derived from bat guano combustion

By Jacques E.J. Martini
Council for Geoscience, Private Bag X112, Pretoria, 001, South Africa

Abstract

The author describes a pyrophosphate mineral defined by chemical analyses, X-ray diffraction patterns, cell parameters, measured and calculated densities, and optical characteristics. It forms tiny crystals in slag produced by spontaneous combustion of bat guano in the deep part of a cave about 2000 years ago. Comparison is made with other minerals described elsewhere in the world and also derived from fire.

Résumé

L'auteur décrit un nouveau minéral, un pyrophosphate, qui est défini par des analyses chimiques, des diagrammes de diffraction X, la maille élémentaire, les densités mesurées et calculées, et les propriétés optiques. Il forme des cristaux microscopiques dans des scories produites par la combustion spontanée de guano de chauve-souris, dans la partie profonde d'une grotte il y a environ 2000 ans. Le minéral est comparé avec d'autres espèces décrites ailleurs, lesquelles sont aussi dérivées de la combustion de matière organique.

1. Introduction

During the course of a speleological investigation conducted by the South West African Karst Research Organisation in 1991, Arnhem Cave, situated 150 km east of Windhoek, was studied for mineralogy.

The author collected a white, porous and friable slag forming a thin layer in a profile of the cave soil. It resulted from the melting of ashes during bat guano combustion about 2000 years ago and the fire is believed to have been spontaneous (MARTINI 1994b). Spontaneous ignition of bat guano became recently less hypothetical after the observation of active burning in a pothole of Martinique Island (Mouret 1996). Two main mineral phases were identified (MARTINI 1994a) in this slag: pyrophosphite (K_2Ca P_2O_7, monoclinic $P2_1/m$) and arnhemite ($(K,Na)_4$ Mg_2 $(P_2O_7)_2 \cdot 5H_2O$) . Pyrophosphite derived from the melting of orthophosphates containing the cations H^+ or NH_4^+ beside K^+ and Ca^{2+}. During the process of combustion, the oxides of the two former elements were lost as volatiles and the orthophosphate anion was depleted of half an oxygen, thus producing pyrophosphates. Arnhemite is a hydrous pyrophosphate and was thought to have been derived by hydration of an anhydrous precursor (MARTINI 1994a). A suitable primary phase was found in the same cave in the course of a more thorough sampling in 1995 and is the aim of the paper.

2. Description

Physical properties. In the slag, the mineral forms grains a few 10 microns across, without definite crystalline outline, always corroded and partly replaced by arnhemite. It is colourless. The hardness could not be measured on account of small grain size. No cleavage was observed.

The density could not be measured easily by „float and sink" in a mixture of tetrabromoethane and acetone due to the small grain size and intimate association with arnhemite, which is lighter (2.35 g/cm^3). Nevertheless, at density 2.96 g/cm^3 only a few particles sank and this figure represents the density of the mineral free of impurities. This value is consistent with the density calculated after the unit cell (2.98 g/cm^3).

Optical properties. The mineral is transparent, has a relatively high refringence, but a very weak birefringence: $\alpha = 1.558$, $\beta = ?$, $\gamma = 1.560$. No additional data could be obtained due to the small size of the grains and their impure nature.

Chemical data. Eight chemical analyses were carried out by means of an electron microprobe and gave the average values presented at table 1. They yield the empirical formula, based on O=7:

$(K_{1.55}, Na_{0.38})_{1.93}$ $(Mg_{0.96}, Ca_{0.06})_{1.02}$ $P_{2.007}$ O_7

or ideally:

$(K, Na)_2$ Mg P_2 O_7

The mineral is insoluble in water, but readily soluble in strong acids. Pyrocoproite appears to hydrate more easily than pyrophosphite: among eight studied samples, in only one pyrocoproite was not completely altered into arnhemite; this was the sample used for this study. In contrast, pyrophosphite was always present.

Table 1

	1	2	3
Na_2O	4.44	1.92	2.51
K_2O	27.13	29.26	28.20
MgO	14.44	12.26	14.35
CaO	1.21	2.95	1.42
P_2O_5	53.09	53.28	53.87
TOTAL	100.31%	99.67%	100.35%

1. Pyrocoproite from Arnhem Cave, average of 8 analyses from the sample containing the anhydrous phase.
2. Pyrocoproite from oven melted arnhemite, from cave; average of 5 analyses.
3. Synthetic pyrocoproite, average of 2 analyses.

Crystallography. The X-ray diffraction powder pattern could be indexed by analogy with the pyrophosphite pattern, which shows comparable reflections, but shifted towards larger spacings (table 2). Pyrocoproite is therefore its isomorphic magnesium equivalent. The cell parametres are:

a=9.410, b=5.424, c=12.540 Å, β=104.35°, Z=4.

By analogy with synthetic potassium-calcium pyrophosphate (BROWN *et al* 1963), the space group is $P2_1/m$.

Table 2: Diffraction powder patterns: reflections relative intensities, observed and calculated d values, Miller indices.

PYROCOPROITE ($(K, Na)_2 Mg P_2 O_7$)				PYROPHOSPHITE ($K_2 Ca P_2 O_7$)			
I/I_{100}	d_{obs}	d_{calc}	hkl	I/I_{100}	d_{obs}	d_{calc}	hkl
63	4.55	4.549	$11\bar{1}$	2	6.77	6.779	101
40	4.18	4.177	$20\bar{2}$	23	4.73	4.731	$11\bar{1}$
14	3.488	3.491	112	32	4.32	4.321	$20\bar{2}$
17	3.268	3.269	$11\bar{3}$	2	3.614	3.621	112
29	3.119	3.123	$10\bar{4}$	17	3.386	3.388	$11\bar{3}$
46	3.040	3.037	004	4	3.242	3.247	$30\bar{1}$
94	2.882	2.878; 2.882	$20\bar{4}$; 113	33	3.137	3.138	004
100	2.714	2.715	$31\bar{1}$	64	2.987	2.985	113
6	2.411	2.409	114	36	2.974	2.975	$20\bar{4}$
29	2.277	2.275	$22\bar{2}$	100	2.821	2.816	311
40	2.091	2.089; 2.088	222; $40\bar{4}$	2	2.497	2.494	114
9	2.021	2.025; 2.022	006; $31\bar{5}$	7	2.365	2.365	$22\bar{2}$
17	1.976	1.974; 1.979	$22\bar{4}$; 402	3	2.250	2.253	$30\bar{5}$
6	1.697	1.700	206	19	2.174	2.171	222
9	1.656	1.654	$13\bar{3}$	10	2.163	2.161	$40\bar{4}$
14	1.623	1.623	026; 315; $31\bar{7}$	3	2.093	2.092; 2.093	006; $31\bar{5}$
11	1.598	1.596; 1.597	133; $42\bar{2}$	5	2.049	2.048; 2.049	402; $22\bar{4}$
9	1.567	1.566	$33\bar{1}$	3	1.982	1.982;1.981; 1.982	$21\bar{6}$; 124; $40\bar{5}$
				2	1.759	1.758	206
				3	1.721	1.722	$13\bar{3}$
				3	1.685	1.687	107
				5	1.660	1.661; 1.658	133; 422
				5	1.631	1.630	$33\bar{1}$

Name and type material. The name is derived from its genesis by combustion of guano. Type material is deposited at the Geological Survey of Namibia, in Windhoek.

3. Synthesis and genesis

A concentrate of arnhemite from material collected in 1991 was melted at 700° and produced a slag of pyrocoproite, which yielded a X-ray diffraction pattern close to the natural mineral but with slightly smaller cell parametres: a=9.371, b=5.419, c=12.519 Å, β=104.48°. Microprobe analyses (table 1) indicate a lower Na content, but higher Ca.

In an attempt to synthetise pure $K_2Mg P_2O_7$, an equimolar mixture of $K_2 H PO_4$ and $Mg(NH_4) PO_4 \cdot 6H_2O$ was melted at 1100°C. Pyrophosphates formed, but did not combine into pyrocoproite. The experiment was repeated with the addition of some $CaHPO_4 \cdot 2H_2O$ and $Na_4 P_2O_7 \cdot 10H_2O$. Slag formed, which after X-ray diffraction and microprobe analyses was found to consist of xenomorphic pyrophosphite and pyrocoproite, with euhedral K-Mg orthophosphate. The chemical analysis of synthetic pyrocoproite is given in table 1. The X-ray diffraction pattern could not be distinguished from the one of natural material. The success of the synthesis with Na and Ca added, suggests that the presence of these elements favour the formation of pyrocoproite. In particular Na pyrophosphate considerably lowers the temperature of fusion.

During the combustion of bat guano, the process of formation of pyrocoproite may have been comparable with the laboratory experiments. The starting material may have contained archerite ($KH_2 PO_4$), biphosphammite ($(NH_4) H_2PO_4$), dittmarite ($Mg(NH_4) PO4 \cdot H_2O$), stercorite ($Na (NH_4)(HPO_4) \cdot 4 H_2O$), mundrabillaite and swaknoite (both $Ca (NH_4)_2 (HPO_4)_2 \cdot H_2O$), which may have been molten into a pyrophosphate slag. All these minerals have been identified in the cave, associated with bat guano (MARTINI 1993).

4. The status of pyrocoproite as a mineral species

It is relevant to briefly review the definition of a mineral species. Indeed, since the majority of the mineralogists are involved with hard rocks only, to them this occurrence would seem odd and therefore they may question the validity of pyrocoproite as a mineral species.

Minerals are defined as natural compounds or elements, implying that chemicals manufactured by man are excluded. The boundary between minerals and artifacts, however, is not sharp: there is a transition zone of minerals, which formed by natural processes, but more or less with man's aid. Although these border minerals are not accepted by everybody as genuine species, they have been established by usage; they are listed in textbooks, like for instance: LACROIX (1913), PALACHE *et al.*

(1944) and CAIRNCROSS & DIXON (1995). Some of them, like romarchite (ORGAN & MANDARINO, 1970) have even been accepted by the International Commission for New Minerals.

These border minerals can be classified in three categories. The first one comprises minerals forming by a natural process, but from artificial material, like for instance the minerals resulting from weathering of artifacts (metal tools, slag) in archaeological sites. Romarchite (SnO) is an example. The second category includes the species resulting from a material and a process, which are both natural, but could not have formed without human intervention. They comprise the numerous minerals forming in the mines. An example is goslarite (ref. in PALACHE *et al.* 1944), which was first described in a mine, where it resulted from a natural oxidation of ore, but was deposited in an artificial cavity.

The third category are the minerals due to combustion of natural material in a natural environment, but the fire may be natural or artificial. To the contrary of the first and second categories, it is generally not possible to ascertain if there was a human imput or not from the mineralogical associations or from the environment context alone. An example of such minerals is fairchildite (MILTON & AXELROD, 1947), resulting from forest fire. Pyrocoproite is to be classified in this third category, which is the least marked by the influence of man, if there is any.

Acknowledgements

Mrs E. Hattingh of the Council for Geoscience, in Pretoria, performed the microprobe analyses. Mr J.C.E. Marais assisted the author with the sampling and Mr J. Bekker, the owner of Arnhem Cave, kindly gave permission to enter and investigate the cave.

References

BROWN E.H., LEHR J.R., SMITH J.P. AND FRAZIER A.W. 1963. Preparation and characterization of some calcium pyrophosphates. *Agricultural Food Chem.* 11: 214-222.

CAIRNCROSS B. AND DIXON R. 1995. Minerals of South Africa. Geol. Soc. South Africa, 290p.

LACROIX A. 1913. Minéralogie de la France et ses colonies, 5 vol., Blanchard, Paris.

MARTINI J.E.J. 1993. A concise review of the cave mineralogy of Southern Africa. Proc. XIth UIS Int. Congr. Speleo, Beijing 1993: 72-75.

----------1994a. Two new minerals originated from bat guano combustion in Arnhem Cave, Namibia. *Bull. South Afr. Speleo. Ass.* 33: 66-69.

---------- 1994b. The combustion of bat guano, a poorly known phenomenon. *Ibidem*, 70-72.

MILTON C, AND AXELROD J. 1947. Fused wood-ash stone: fairchildite (n.sp) K_2CO_3. $CaCO_3$, bütschliite (n.sp) $3K_2CO_3$. $2Ca\ CO_3$. $6H_2O$ and calcite $CaCO_3$, their es- sential constituents. *Amer. Miner.* 32: 607-624.

MOURET C. 1996. Echo des profondeurs - Antilles. Spelunca, no 64, 203.

ORGAN R.M. AND MANDARINO J.A. 1970. Romarchite and hydroromarchite, two new stannous minerals. *Can. Miner.* 10: p 916.

PALACHE C., BERMAN H. AND FRONDEL C. 1944. Dana's system of mineralogy, vol. 2, Wiley, New York, 1124p.

The Classification of Cave Minerals and Speleothems

By Carol A. Hill and Paolo Forti

Abstract

The classification scheme of Hill and Forti, as used in the new second edition of Cave Minerals of the World, is presented as a "practical" solution to the problem of classification of cave minerals and speleothems. Classification of cave minerals is by crystal class following nomenclature approved by the International Mineralogical Association. These classes of minerals include the native elements, sulfides, oxides-hydroxides, halides, arsenates, borates, carbonates, nitrates, phosphates, silicates, sulfates, and vanadates. No attempt is made to classify cave minerals by origin as was done in the first edition. Minerals in the outside world are not classified by origin due to the complexity of depositional environments (i.e., a mineral may form by a number of mechanisms in a variety of different settings), and for the same reason cave minerals should not be classified according to origin.

In the past, classification of speleothems has been by (1) morphology, (2) origin, or (3) crystallography (fabric). All three approaches have their problems. The compromise approach of Hill and Forti is based primarily on morphology (i.e., the shapes one sees), plus whatever is known about origin and crystallography. In the second edition of Cave Minerals of the World speleothems are divided into "official" types and subtypes and "unofficial" varieties. A speleothem type is defined as a group or category of speleothems sharing one or more morphological characteristics and having a common origin different from other speleothem types (e.g., speleothem type = cave raft). A speleothem subtype is defined as a speleothem which has a structural identity similar to the type, but which has an origin different enough from the type so as to produce a deviant morphology with additional structural elements (e.g., speleothem subtype = cave cone, of type raft). A speleothem variety is defined as a slightly variant morphology produced by differences in water flow, mineral composition, color, crystallinity or other factors. Speleothem varieties exist for both types and subtypes (e.g., "snowflakes" = variety of type raft; "volcano cone" = variety of subtype cone).

It is proposed that in the future new speleothem types, subtypes, and names be officially approved by a UIS Commission of cave mineralogists.

Crystallographical observations on calcite rafts from three Romanian caves

Iosif Viehmann[1] Lucretia Ghergari[2] Bogdan Petroniu Onac[2]

[1] Speleological Institute "Emil Racovita", Clinicilor 5, 3400 Cluj, Romania

[2] "Babes-Bolyai" University, Deptartment of Mineralogy, Kogalniceanu 1, 3400 Cluj, Romania

Abstract

The paper presents the crystallographical, morphological and mineralogical observations made on seventeen samples of calcite rafts collected from three Romanian caves (Hoanca Apei, Stanu Ciutii and Ciungi). The two sides of the rafts exhibit different morphologies; the upper side is smooth while the underwater side is rough. The 35 m^3 of "cornflakes-like" deposit (crumbed calcite rafts) and the filling-drainage mechanism of the pools from Hoanca Apei represent a unique case for the Romanian karst.

1. Introduction

The paper emphasises the mineralogical and crystallographical features of the calcite rafts discovered in 1987 in three pools and an artificial excavation (Ana's hole) in Hoanca Apei Cave (Bihor Mts.). The observations were compared with those made on similar speleothems from Stanu Ciutii (Padurea Craiului Mts.) and Ciungi (Somesan Plateau) caves. In Romania such speleothems were previously described from caves at Sura Mare (LASCU, pers. comm.), Humpleu, Piatra Altarului (FRATILA, 1996), Ponoras, Batranului, Osoi (ONAC, 1996). The calcite raft problem was world-wide treated (generally or in detail) by SALZER (1942), BLACK (1953), POMAR et al. (1975, 1976), HILLI & FORTI (1986), VIEHMANN (1992), FORTI & CHIESI (1995).

The pools from Hoanca Apei are located in a 15 per 9 m room (Sala Plutelor), at the far end of an upward side passage, 220 m behind the cave entrance. These hollow basins (down to 45 cm) are placed on an important deposit that consists of millions of crumbed calcite rafts. The excavation done to a depth of 165 cm in the center of the room, revealed that the crumbed calcite rafts sediment has a thickness of 90 cm. The rest of the deposit consist of moonmilk that subsequently was formed from accumulated calcite rafts. In the eastern part of this room there is a small spring having usually a discharge of 8 cm^3/s. After heavy rains, the discharge increase considerably so that the whole room is flooded. The pools have been found to be temporarily emptied or filled up with water.

2. Experiments

Two types of experiments were periodically carried out in the last 10 years: chromatic marking of the calcite rafts and tests concerning filling-drainage mechanism of the pools. The two experiments proved that the calcite rafts lying on the bottom of an empty pool are brought back to the surface by a water that moves per ascensum within the pool (VIEHMANN, 1992). In Ana's hole, the water filling process lasted about 90 days, which gives an average value of 1.8 cm in 24 hours. In parallel with these experiments we measured the carbon dioxide concentration in the air with a Draeger device (type WG-2M) and the water temperature in the spring, pools and cave atmosphere. While the carbon dioxide concentration have shown similar values everywhere in the cave, the temperature increased from 7.1°C in the spring to 7.4°C in the pools and to 7.8°C in the cave atmosphere. The relative humidity measured within the cave was 89%.

The surface of most of these rafts range between 1.2 and 3.4 cm^2. However, the largest calcite raft floating in one of the pools could reach, before breaking into pieces, reached a remarkable area of 600 cm^2. BLACK (1953) has described aragonite rafts in Carlsbad Caverns having more than 900 cm^2.

Following our calculation the calcite rafts deposit in Hoanca Apei Cave reaches 35 m^3.

3. Mineralogical, morphological, and crystallographical observations

Thirteen samples were collected in Hoanca Apei Cave as following: 9 samples (4-12) collected from different depths of the calcite rafts deposit (4, 8, 12, 16, 20, 24, 28, 32 and 36 cm), 2 thin rafts formed in Ana's hole (sample 3 collected in 1995 and sample 13 collected in 1996), and 2 samples from the other two pools located in Sala Plutelor (sample 1 and 2). Three samples were collected from the Stanu Ciutii Cave; one from the water surface (sample 14), another sample from the bottom of the same pool (sample 15) and the third one from the bottom of a dried pool. Only one sample was collected from Ciungi Cave (sample 17).

The analyses made on these calcite rafts samples consist of observations with scanning electron microscope (SEM), transmission polarizing microscope and binocular. Several X-ray diffractions were carried-out in order to test the mineralogical composition. With respect to the shape and size of the crystals that build the calcite raft, our samples can be ascribed to the following 3 groups:

1) Calcite rafts made of large, well developed crystals (> 100 mm). This type was observed in Stanu Ciutii, Ciungi and below 15 cm in the calcite rafts deposit from Hoanca Apei Cave.

2) Calcite rafts consisting of medium size crystals (10-100 mm) with many structural defects (imperfections) (e.g., natural pools from Hoanca Apei Cave and above 15 cm in the calcite rafts deposit from the same cave).

3). Calcite rafts composed of small crystals having many structural defects (Ana's hole).

Mineralogical composition

Optical properties and X-ray analyses showed the presence of calcite as main mineral in all samples tested. The white rafts made up of almost transparent crystals, entirely consist of calcite while the brown ones are impregnated with clay minerals. The diffraction patterns obtained of the rafts collected in the artificial pool from Hoanca Apei (sample 3, first collection) show 3 peaks of low intensity (3.24-15; 4.25-1; 1.81-1) that were ascribed to

quartz. Under the microscope this mineral cannot be seen due to the small grain size. In the sample 13 recently collected, the quartz is missing.

Morphology of the rafts

The two sides of the rafts exhibit different morphologies. The upper side is smooth and has a granular structure, punched from place to place (small holes) (Fig. 2a). If the upper side was corroded than the crystals are clearly outlined (Fig. 2b). The crystals are mostly skeletic (hopper morphology) and grow with their c-axis at various angles against the water surface. The underwater side is rough due to some prismatic crystals that grow perpendicular and at various angles against the raft surface (Fig. 2c, d). Other crystals develop around isolated crystals, resulting finally in radial shaped groups.

On the upper side of some calcite rafts, in small holes between the crystals, we found a fine yellowish silky powder (sample 17 from Ciungi and samples 1 and 13 from Hoanca Apei). This powder consists of threadshaped calcite crystals having almost similar sizes (Fig. 1e). This type of crystals is characteristic for moonmilk deposits.

The maximum thickness of the calcite rafts measured in Hoanca Apei was 0.288 mm, while the rafts that repeatedly sink and float are between 0.067 and 0.21 mm.

Crystal morphology

The crystals have different sizes depending on the location and differs even in the same cave as a matter of presence or absence of the impurities. The calcite impregnated with clay minerals always forms small crystals whereas the pure ones are larger. Sometimes the calcite crystals are covered by a thin layer of cryptocrystalline calcite (sample 17, Ciungi).

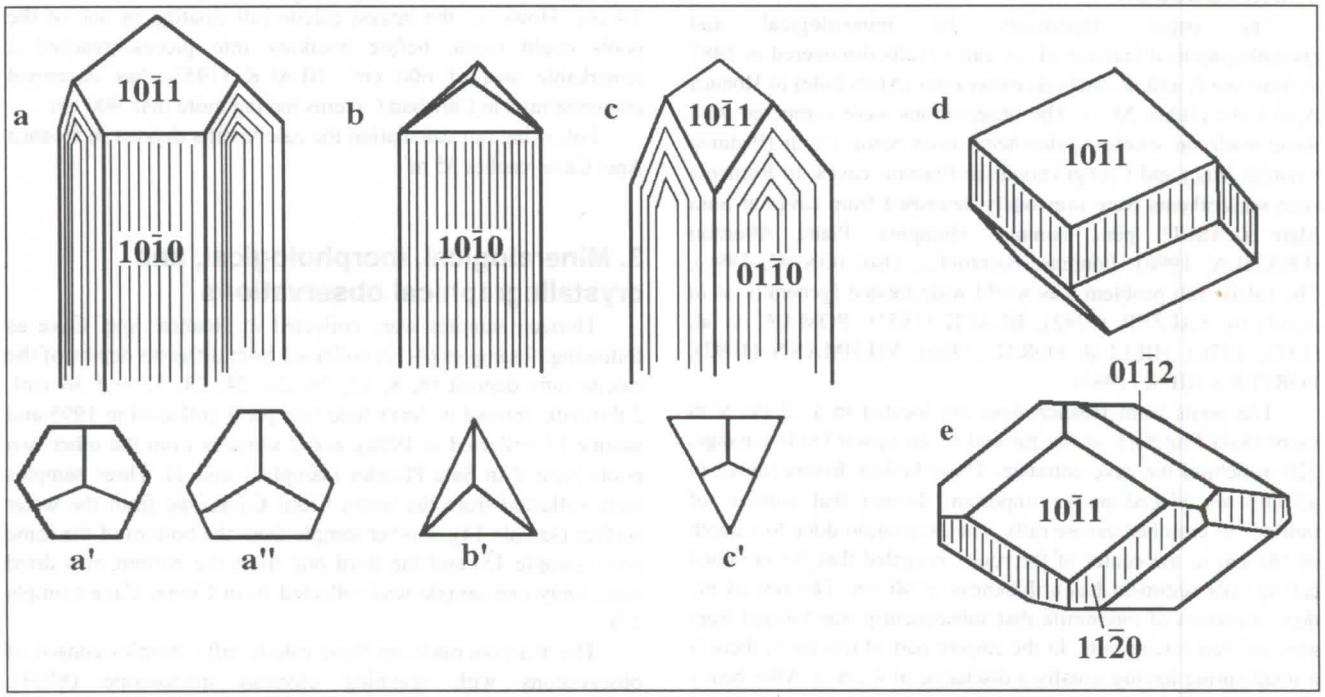

Figure 1: The habit of crystals that composed the calcite rafts

The calcite rafts samples framed into the first group consist mostly of euhedral crystals limited by well developed crystallographic faces. The crystals have prismatic habit the most common crystallographical forms being the first order hexagonal prism {10$\bar{1}$0} that usually shows striations along it. Another frequent form is the positive rhombohedron with smooth faces. The prismatic crystals differ as the sixth prism faces have various degrees of development. Hexagonal prisms with equal developed faces are rare (Figs. 1a, a'). As a rule, three of the faces are better developed when compared to the other three, that are smaller (sample 14, 16 and less 15 from Stanu Ciutii, 17 from Ciungi) (Figs. 2d, 1a"). The unequal growth of the faces leads to the development of two types of trigonal prisms: positive {10$\bar{1}$0} (samples 15, 16 from Stanu Ciutii, 17 from Ciungi) (Figs. 1b, b') and negative {01$\bar{1}$0} (sample 15-Stanu Ciutii) (Figs. 2c, d and 2c, c'). Sometimes a steep rhombohedron {40$\bar{4}$1} or {04$\bar{4}$1} forms (sample 14-Stanu Ciutii). When the calcite crystals grow parallel to the (10$\bar{1}$0) face a tabular-prismatic habit can be recognized. Among other crystals with different combinations of crystallographic forms, we want to mention: the {10$\bar{1}$1} rhombohedron as a dominant form (Fig. 1e) associated with second order hexagonal prism {11$\bar{2}$0} (subordinate) and the {10$\bar{1}$1} and

{01$\bar{1}$2} rhombohedrons together with second order hexagonal prism {11$\bar{2}$0}(Fig. 1f). Crystals on which both types of prisms (first and second order) can be distinguished are rare. Faces that belong to the second order prism show vertical striations due to alternating growth of the {10$\bar{1}$0} and {0110} faces. (sample 15, 16 from Stanu Ciutii). A second generation of crystals represented by first order prism and positive scalenohedron {54$\bar{9}$1}, fill the holes left between the other crystals.

Skeletal habit is a typical feature of the crystals that build up calcite rafts framed by us to the 2nd and 3rd group. The crystals may form parallel growth of tabular crystals developed parallel to the prism face {01$\bar{1}$0} or prismatic crystals with triangular habit due to the presence of the negative prism (Figs. 2c, f). The prisms tip is either a corrosion surface

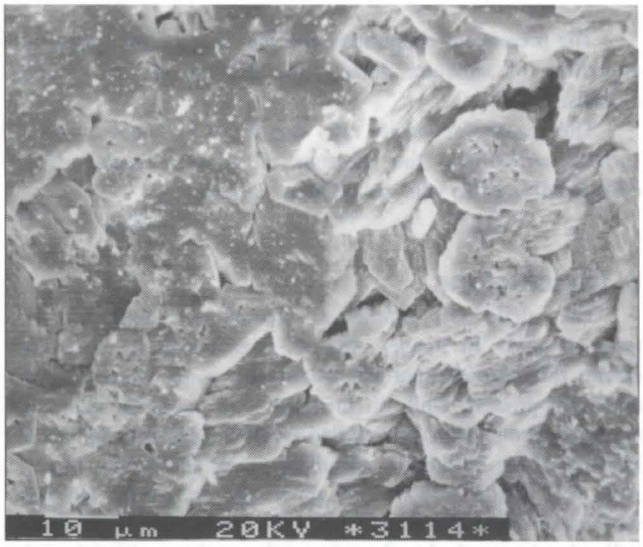

1a

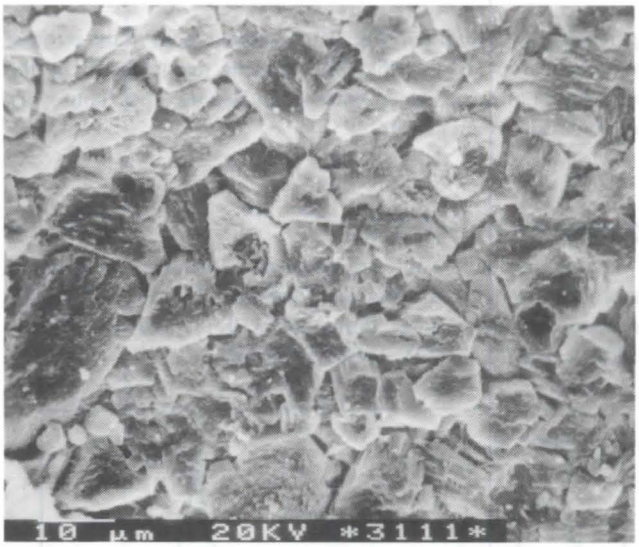

1b

1c

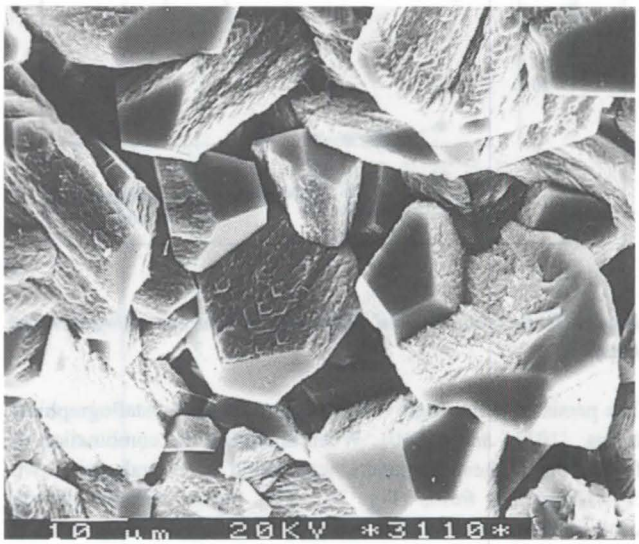

1d

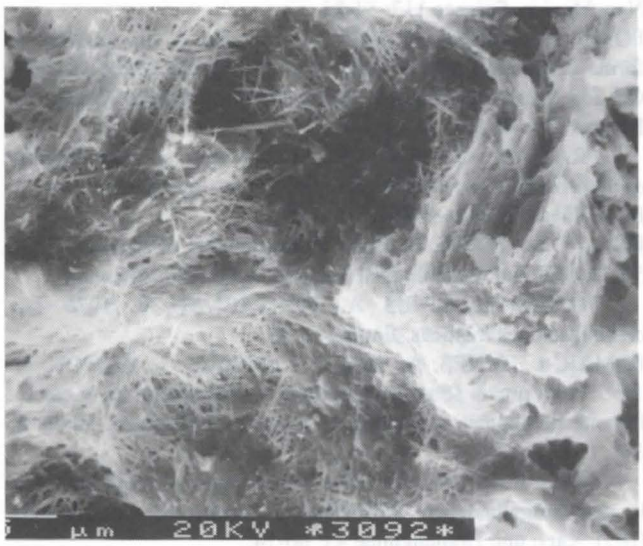

1e

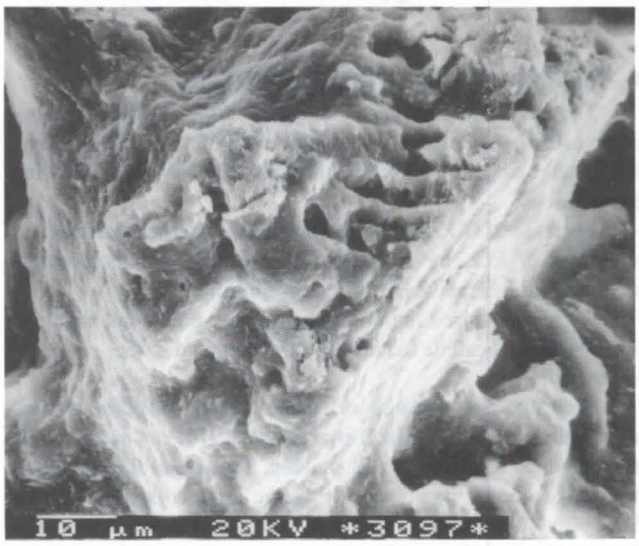

1f

Figure 2: Calcite rafts from Hoanca Apei Cave. SEM: upper side of the raft: a) (sample 12); b) (sample 11); underwater side of the raft: c) corroded crystals (sample 4); d) (sample 11); e) threadshaped calcite, grown between the crystals (sample 1); f) corroded calcite prisms (sample 4).

generated by dissolution (Fig. 2f) or smooth faces of the positive rhombohedron {10$\bar{1}$1} (Fig. 2d). Calcite rafts affected by the dissolution processes were remarked in Hoanca Apei (both types of pools) and Ciungi caves.

3. Statistical remarks

The statistical results are based on determinations made on more than 100 crystals from all 17 calcite raft samples. The most common crystallographic forms are: {10$\bar{1}$1}, {10$\bar{1}$0}, {11$\bar{2}$0}, {40$\bar{4}$1}, {04$\bar{4}$1}, {01$\bar{1}$2}, {54$\bar{9}$1} (Fig. 3a).

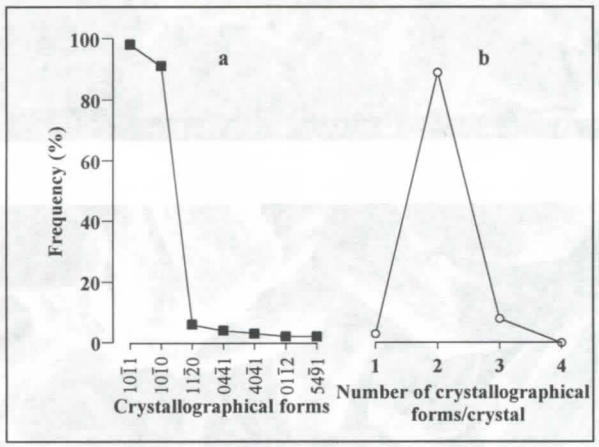

Figure 3: Persistance and frequency of the crystallographical forms

The persistence has high values for two of the crystallographical forms: {1011} and {1010}. When analysing the combination of forms, the highest frequency was found at crystals with two crystallographic forms (Fig. 3b). This means that the growth conditions are similar even when the floating-drying process is periodically resumed. Three types of contact twins were identified. Their twinning planes are (1010), (0112) and (0221).

4. The genesis of the calcite rafts

The most important factor in calcite rafts genesis, as in any other calcite speleothem is the supersaturation of the solution. This state can be achieved through one of the following processes:

- the decrease of CO_2 partial pressure at the water-air interface;
- the loss of CO_2, by diffusion into open air will increase the solution fluidity, speeding up the crystallisation;
- the increase of the solution temperature in pools will diminish the solubility of calcite bicarbonate and carbon dioxide.
- evaporation;

Very fine clay minerals or calcite crystals particles, as well as organic material (POMAR *et al.*, 1975, 1976) can act as nuclei around which calcite rafts will develop. The size of the crystals is directly related to the number of nuclei; large crystals will grow from pure solution, whereas an impure solution will encourage the growth of small crystals.

The presence of impurities and the CO_2 release lead to the apparition of structure defects, parallel growth and skeletal crystals.

The reason for calcite rafts floating was found to be the surface tension and the presence of skeletal crystals which contain holes, filled with gas, in between them.

5. Conclusions

The calcite rafts samples we studied were formed in two types of pools. In Hoanca Apei all three basins lie on a huge calcite rafts deposit and are filled with water through a per ascensum process, while in the other two caves the pools are typical rimstone dams being filled by flowing or seeping waters. Because of the different mechanisms the calcite rafts in Hoanca Apei will periodically be brought to the surface of the pool, whereas in Stanu Ciutii and Ciungi the calcite rafts once formed will either be attached to the sides of the pools or will sink under their own weight.

Both sides of the rafts consist of calcite crystals that grow perpendicular and at various angles against the raft surface. The differences between the two sides are just morphologically ones; the upper side is smooth while the underwater side is rough. The dissolution process that affected the calcite rafts from Hoanca Apei and Ciungi is due to the aggressive waters which enter the cave after havy rains. If in Ciungi, only the upper side of the rafts show corroded crystals, in Hoanca Apei both sides exhibit this phenomenon. The explanation of this peculiar situation is that when the room become flooded, the aggressive water affects the upper side of the rafts but when the pools are filled up per ascensum, only the crystals from the underwater side will be corroded.

The 35 m^3 deposit of "cornflakes-like" (crumbed calcite rafts) and the filling-drainage mechanism of the pools from Hoanca Apei represents a unique case for the Romanian karst.

References

BLACK, D. M. 1953. Aragonite rafts in Carlsbad Caverns, New Mexico. Science 117: 84-85.

FORTI, P., CHIESI, M. 1995. A proposito di una particolare forma di calcite flottante osservata nella Grotta Grave Grubbo-CB 258 (Verzino, Calabria). Atti e Memorie Comm. Grotte "E. Boegan" 32: 43-53.

FRATILA, G. R. 1996. Mineralogia si cristalografia speleotemelor din pesterile bazinului Somesului Cald, pp. 48-49. B.Sc. Thesis. "Babes-Bolyai" University.

HILL, C. A., FORTI, P. 1986. Cave minerals of the world, pp. 52-53. National Speleological Society, Huntsville, Alabama.

POMAR, L., GINÉS, A., FONTARNAU, R. 1976. Las cristalizaciones freaticas. Endis 3: 3-25.

POMAR, L., GINÉS, A., GINES, J., MOYA, G., RAMON, G. 1975. Nota previa sobre la petrologia y mineralogia de la calcita flotante de algunas cavidades del Levante Mallorquin. Endis 2: 3-5.

SALZER, H. 1942. Über das Vorkommen von Kalkhäutchen in dem aufgellassenen Gipsbergwerk "Seegrotte" bei Mödling (ND). Karst und Höhlenkünde 43: 66-74.

VIEHMANN, I. 1992. Experimental methods in studying the cave rafts. Theor. Appl. Karstol. 5: 213-215.

Mineralogy of crusts and efflorescences from Humpleu cave system

Lucretia Ghergari, Bogdan Petroniu Onac, Gheorghe Fratila
"Babes-Bolyai" University, Department of Mineralogy, Kogalniceanu 1, 3400 Cluj, Romania

Abstract

The paper presents the results of a mineralogic and crystallographic study done on crusts and efflorescences collected from Humpleu cave system. Besides calcite, aragonite and gypsum, a rich association of phosphates (hydroxyapatite, carbonatehydroxyapatite, brushite, collophane), also the presence of amorphous silica (opal) are highlighted. Our results rely on observations made with scanning electron microscope, transmission polarising microscopy, thermal and spectral analyses and X-ray diffraction.

Introduction

Humpleu cave system is composed of Pestera Mare din Valea Firii cave and Avenul din Poienita pothole and it is located in the NW part of Apuseni Mountains, on Firii Valley, left side tributary of Somesul Cald River. Humpleu cave system is one of the most spectacular endokarst phenomena of Romania by the giant dimensions of the passages and because of the abundance and variety of speleothems (GHERGARI *et al.*, 1992; ONAC, 1992; PAPIU *et al.*, 1993).

Humpleu cave system was carved in Cretaceous limestones. It developed on three levels, the lowermost active, an intermediary fossil level, less developed, and the superior fossil level, made of large halls and passages (e. g. Giants' Hall, 500x120x30 m or Gabor Halasi Hall, 310x103x35 m). The passages explored and surveyed until now have a development of 37,100 m on a vertical extent of 314 m.

The mineralogical study carried out in Humpleu cave system is focused on small dimesion minerals that form deposits such as crusts, singular crystals or crystal groups. The samples collected for mineralogical and crystallographical analyses come from several sectors of the cave, exclusively from fossil passages (fig. 1). The deposits are carbonatic, gypsiferous and phosphatic.

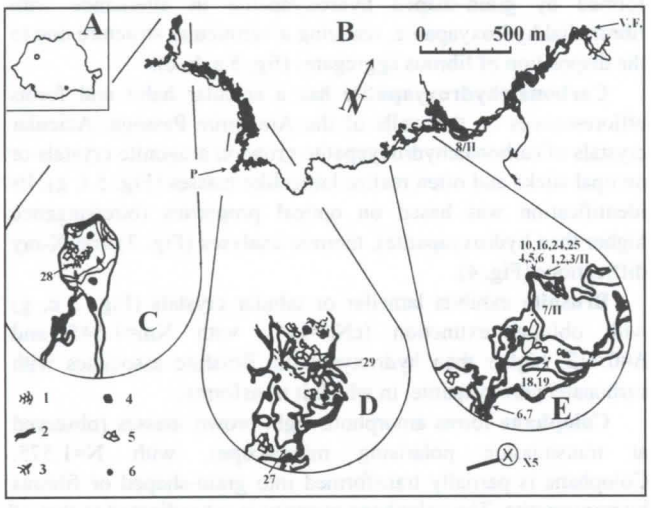

Figure 1. Map of Humpleu cave system with the location of sampling sites: A. Geographical position of Humpleu cave system; B. Plan of Humpleu cave system; C. Amphitheatre Hall; D. High Hall and the beginning of Giants' Hall; E. Lake Hall, Grenoblese Hall and Aragonite Passage; 1. gours; 2. Active passage; 3. level curves; 4. shaft; 5. blocks; 6. stalagmitic dome; •- sampling site.

The methods of analysis that we used were: transmission polarising microscopy on thin sections and in immersion, morphologic observations by means of electron microscopy (SEM), X-ray diffractions, thermal and spectral analyses.

Calcite deposits

The chemical phenomena that affect carbonate rocks in cave environment can be of two types:

-integral dissolution of carbonate rocks by water seeping through, which forms a solution of $Ca(HCO_3)_2$ solution, that represents the source of speleothems;

-partial dissolution of carbonate rocks by imbibition, forming a calcitic or dolomitic powder that fits in the granulometric sorts of lutite, silt and arenite, depending on the grain size of the weathered carbonate rocks.

The studied deposits are of the second type and appear in ventilated areas of the fossil passages, where speleothems are lacking. The weathering crust (samples 6_1, 29_1) is formed by a calcite powder made of grains between 0.0015 and 0.008 mm in diameter, rarely larger (sample 29_1). In the microgranular mass small fragments of micritic limestone appear, proving the origin of the weathered rock. Sometimes, sub-rounded grains of quartz and zircon can be found.

In the powdery calcitic mass there are two processes of speleal genesis to be remarked (sample 6_1):

- forming of acicular calcite crystals, developed parallel to the 'c' crystallographic axis, similar to the one that is composed of moonmilk;
- forming of some small columnar calcite crystals (0.02x0.04 - 0.05x0.2 mm), having both endings well developed (Fig. 2).

Crystallographical forms identified on the columnar calcite crystals are hexagonal prisms of Ist. order $\{10\bar{1}0\}$ and IInd order $\{11\bar{2}0\}$ (rarely together), the positive rombohedron $\{10\bar{1}1\}$ as dominant forms with high persistence; sometimes negative rombohedron $\{02\bar{2}1\}$ substitutes the positive one $\{10\bar{1}1\}$, the latter having a lower persistence; the rombohedrons $\{04\bar{4}1\}$, $\{40\bar{4}1\}$, $\{01\bar{1}2\}$ and the scalenohedron $\{21\bar{3}1\}$ have subordinate developments (Fig. 2).

Dehydrated moonmilk crusts appear on the floor of Amphitheatre Hall (sample 28), in Giants Hall and in Charontese Hall. The morphology of the skeletal calcite crystals that appear in this deposit corresponds to that of moonmilk described by GHERGARI *et al.* (1993, fig. 4e, fig. 14 respectively) as being a calcite paramorphosis after polysyntetic twinned aragonite; small rombic plates are twinned alternantly after face (110), the twinned complex developing in the [111] direction.

Coral-like deposits composed of groups of columnar calcite crystals disposed radial or divergent; the crystals that form groups have dimensions between 0.03 and 0.2 mm (samples 18_1, 19) contain zoned liquid inclusions on the crystallographic faces and exhibit the same crystallographic forms as those formed in the weathering crust (sample 6_1). The shape of these aggregates and the radial disposal of the crystals that usually surround other crystals or some micritic limestone lithoclasts made us suppose their forming in a weathering crust consisting of a deposit of microgranular calcite that was subsequently washed away.

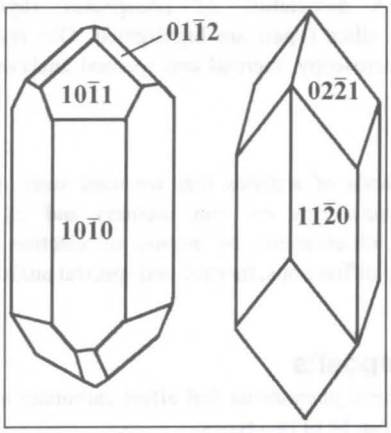

Figure 2. Crystallographical forms identified on calcite columnar crystals.

Gypsum deposits

Gypsum forms thin crusts (1-2 mm thick) that cover small surfaces (1-3 m^2) on the northern wall of the Aragonite passage (samples 3_2, 10_1) and on the sides of the fallen blocks from the same passage.

Gypsum appears as fibrous aggregates with their elongation disposed perpendicular to the wall. Crystals can reach 2-3 cm in length. From our observations on cristals' morphology, we mention:

-the change of direction of crystals' elongation as an effect of the change of calcium sulphate solutions concentration;
-bending of fibrous crystals, generating microanthodites;
-presence of some well developed idiomorphous crystals;
-corrosions due to dissolution.

In addition to the gypsum, we identified browny grain-shaped hydroxyapatite in small quantities, small calcite and aragonite crystals and sometimes subrounded quartz grains included in gypsum crystals, pyrite in sample 3 and limonite as impregnations in gypsum or in aggregates (sample 10_1).

Phosphate deposits (phosphorite)

Phosphorite found in Humpleu cave system exhibits distinct structural forms, as following:

1. Browny crusts with colomorphous aspect, smooth on the upper side and partially covered by a calcite powder, and rough on the lower side (Fig. 5 d, e). Crusts of this type were observed as spots in two different sites:
- on the western wall of Lake Hall, at some 25 cm above the floor; the spots have maximum 30 cm in diameter (sample 7_1);
- on the walls of Aragonite Passage and accidentally on the floor (sample 25_1).

2. White powdery crusts, frequently with stratified texture (Fig. 5 a), observed on the floor and on the fallen blocks in Aragonite Passage (samples 16_1, 1_2), in Grenoblese Hall and in Charontese Hall (sample 8_2).

3. Acicular carbonatehydroxyapatite in association with aragonite, opal (silica), brushite (Fig. 5 f, g), on the walls of the Aragonite Passage to the height of 2.5-3 m (samples 5_2, 24_1).

From the mineralogical viewpoint, phosphorite is constituted of hydroxyapatite (main constituent), carbonatehydroxyapatite, brushite, colophane, associated to aragonite, calcite, opal, iron and manganese oxides.

The identification of these minerals was based on optical properties studied by polarising microscopy (Fig. 5 a, b, c), crystal morphology (SEM) (Fig. 5 d, e, f, g), thermal analyses (Fig. 3), X-ray diffractometry (Fig. 4) and spectral analyses.

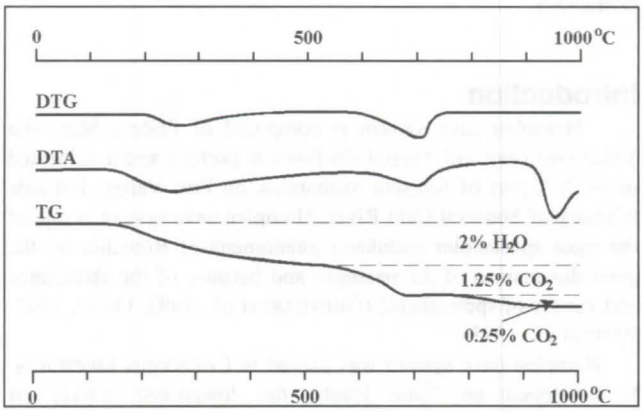

Figure 3. Thermal analysis of sample 24_1.

Hydroxyapatite is usually granular - showing no crystallographic forms - or fibrous, but sometimes tabular (pseudomorphosis after brushite) or short prismatic. Grain-shaped hydroxyapatite aggregates associated to collophane (partially transformed into a granular or fibrous mass) form, colomorphous crusts (Fig. 5 d, e) or irregular masses that preserve the organic structure that generated them. Granular aggregates of hydroxyapatite from the lower side of the crusts contain tiny calcite crystals. The white powdery crusts are formed by grain-shaped hydroxyapatite in alternance with fibroradial hydroxyapatite, realizing a vermicular structure due to the disposition of fibrous aggregates (fig. 5 a, b, c).

Carbonatehydroxyapatite has a acicular habit and forms efflorescences on the walls of the Aragonite Passage. Acicular crystals of carbonatehydroxyapatite grow on aragonite crystals or on opal sticks and often realize latticelike masses (Fig. 5 f, g). Its identification was based on optical properties (birefringence higher than hydroxyapatite), thermic analyses (Fig. 3) and X-ray diffractions (Fig. 4).

Brushite exhibits lamellar or tabular crystals (Fig. 5 c, g) with oblique extinction (cNp=14°), with Nm=1.545 and Δ=0.012, higher than hydroxyapatite. Brushite associates with carbonatehydroxyapatite, in which it transforms.

Colophane forms amorphous light-brown masses (observed at transmission polarising microscope), with N=1.575. Colophane is partially transformed into grain-shaped or fibrous hydroxyapatite. The colophane quantity is subordinated to that of hydroxyapatite.

Aragonite realizes acicular crystals, some of these constituted of two individuals twinned after (010) face (Fig. 5 f, g). A part of the aragonite crystals are mantled with amorphous silica (opal) with N=1.531. The presence of silica was distinguished by optical analyses and confirmed by spectral analyses.

3a

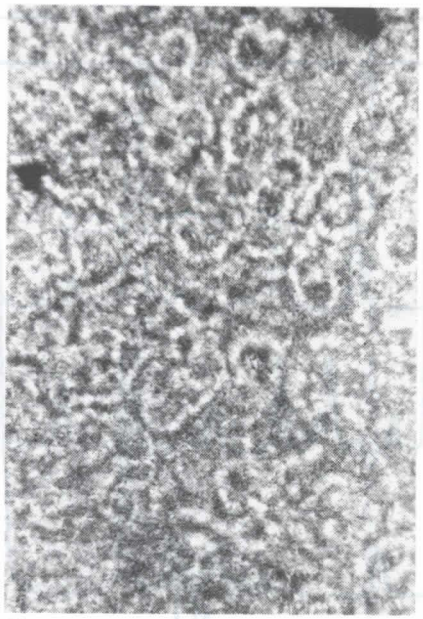

3b

3c

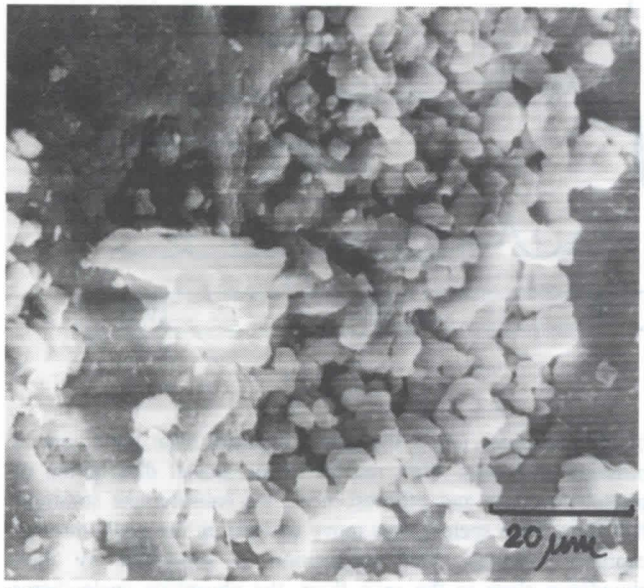

3d

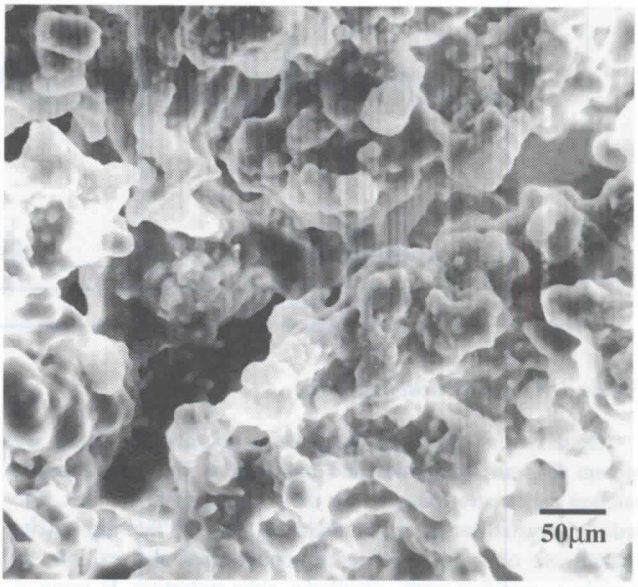

3e

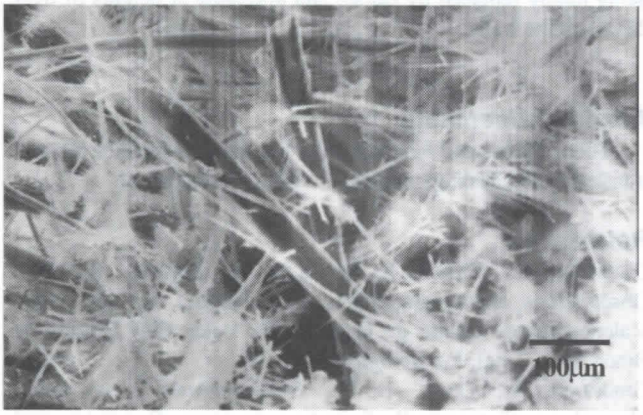

3f

3g

Figure 3. a): White powdery phosporite crust with banded texture. Granular hydroxyapatite impregnated with manganese oxides (sample 16_1, exterior zone); 1N, 165X; b): Hydroxyapatite with vermicular structure (sample 16_1, interior zone); 1N, 330X; c): Fibro-radiar hydroxyapatite and tabular brushite; the latter substitutes rhombohedral calcite crystals (sample 16_1, interior zone); 1N, 330X; d): SEM. Phosphorite crust with colomorphous aspect (dark grey) covered by calcite crystals (sample 7_1, upper side); e): SEM. Hydroxyapatite as tabular crystals, granular and with colomorphous aspect (sample 7_1, lower side; f): SEM. Aragonite crystals (black) covered by acicular carbonatehydroxyapatite (white) (sample 24_1); g): SEM. Aragonite crystals coated in silica (opal), tabular brushite crystals and acicular crystals of carbonatehydroxyapatite.

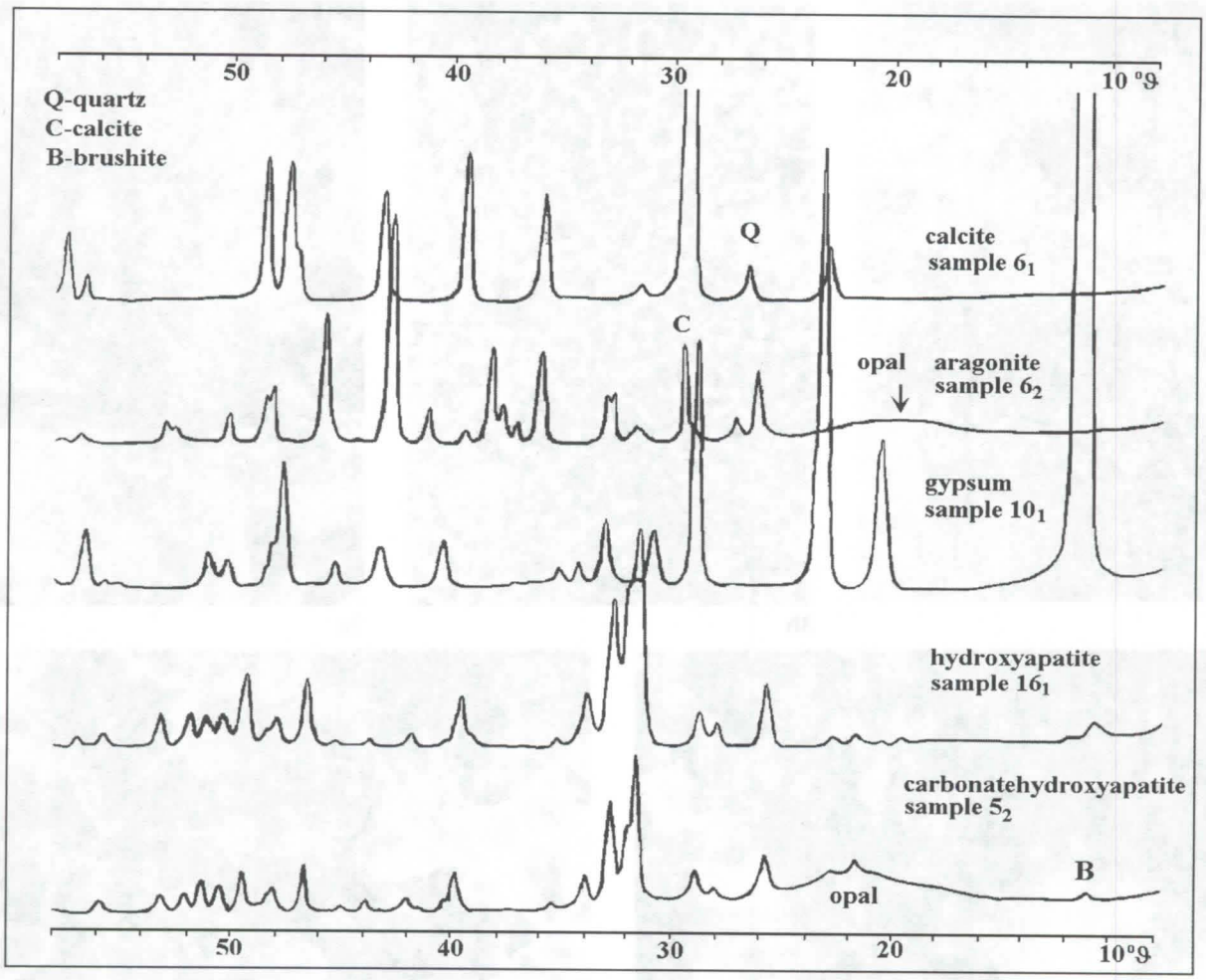

Figure 4. X-ray diffraction spectra.

Opal covers aragonite and calcite crystals (the latter are present in small quantities and represent a first generation of calcium carbonate, followed by the forming of aragonite). The order of crystallisation can be deduced from the fact that calcite crystals are often included in aragonite. Opal also exhibits as straight or ramified empty capillaries alike stalactites. In some of these voids appear carbonate remnants resulted from a corroded acicular aragonite crystal. We consider as possible the forming of fine channels inside the opal sticks as a result of dissolution of acicular aragonite crystals.

Iron oxides and hydroxides sometimes impregnate hydroxyapatite aggregates on restricted areas, giving them a browny-reddish colour.

Manganese oxides appear as films in hydroxyapatite powdery crusts at certain levels or as dendrites on their surface (Fig. 5 a).

Conclusions

The crusts and efflorescences from Humpleu cave system form extremely interesting associations. It is composed of calcite, aragonite, hydroxyapatite, carbonatehydroxyapatite, brushite, collophane, gypsum and opal. Iron and manganese oxides and hydroxides have also been identified. On the basis of our observation, we deduced the presence of several crystallogenetic stages: acicular and columnar calcite, as well as aragonite crystals were formed at first. The 2nd stage corresponds to the deposition of silica (opal), that coated the crystals of the first stage, being followed by the deposition of the phosphate minerals. The source of the phosphate ion is the guano deposits from the floors of passages and halls. With respect to the spatial distribution of phosphate crusts and efflorescences, we consider the solutions that form these speleothems move upward on the walls through capillary channels. Our supposition is supported by their abundance close to the cave floor, the phosphate speleothems being totally replaced by calcite and aragonite at heights of over 25 cm on the walls.

Acknowledgements

Tudor Tamas and Ferenc Forray are thanked for their help in translating and desktop publishing of the present paper.

References

GHERGARI, L., MARZA, I., BODOLEA, A., SCHIIAU, S. 1992. Observations cristallographiques et genetiques sur les mega-scalenoedres de calcite de la grotte de Valea Firii (Monts de Bihor, Roumanie). *Karstologia* 20: 49-53.

GHERGARI, L., ONAC, B. P., SANTAMARIAN , A. 1993. Mineralogy of moonmilk formation in some Romanian and Norwegian caves. *Theor. Appl. Karstol.* 6: 107-120

ONAC, B. P. 1992. Mineralogy of the Apuseni Mountains caves. *Theor. Appl. Karstol.* 5: 193-201

PAPIU, F., SELISCAN, D., LONDON, J. C. 1993. La Pestera Mare din Valea Firii. *Regards* 12: 1-4.

Deposition of black manganese and iron-rich sediments in Vântului Cave (Romania)

Bogdan Petroniu Onac[1] Magne Tysseland[2] Monica Bengeanu[3] Angelica Hofenpradli[4]

[1] Babes-Bolyai University, Dept. of Mineralogy, Kogalniceanu 1, 3400 Cluj, Romania
[2] University of Bergen, Dept. of Geology, Allégt. 41, 5007 Bergen, Norway
[3] Mining Research and Design Institute, T. Vladimirescu 15-17, 3400 Cluj, Romania
[4] Babes-Bolyai University, Dept. of Biology, Kogalniceanu 1, 3400 Cluj, Romania

Abstract

Mineralogical and geochemical characteristics of the black sediment coatings covering both sandy alluvium and submerged boulders in an underground stream, Vântului Cave, Romania, are discussed. An enrichment was observed in manganese and iron towards the upper part of the sediment-water interface where the overlying water supplies oxygen. The black sediments appear to be mainly composed of poorly-crystallized manganese oxides and hydroxides (pyrolusite, romanechite, todorokite, rhodochrosite) as well as goethite and kaolinite. Scanning electon microscope performed on the black earthy sediments show the material to build up botryoidal-like aggregates. Manganese may migrate in slightly acidic waters as humates or as metallo-organic complexes and is introduced into cave by stream water. Acid mine waters (with elevated levels of dissolved Fe, Al and SO_4 ions), which drained into the cave stream, are the most probable source of iron. Genetically, the black sediments from Vântului Cave seems to be deposited in a pH/*E*h controlled environment. Microorganisms may aid in the deposition of these manganese and iron minerals.

Introduction

A number of manganese oxidation states exist, but only two (Mn^{2+} and Mn^{4+}) are common in nature. These often occur together in the same mineral or in closely intergrown aggregates, giving a continuous series of net oxidation states. While the mineralogy of iron is relatively simple, the mineralogy of manganese is complex. Not only are a large number of manganese phases found, but they are difficult to characterized because of poor crystallinity, fine grain size, and intimate intergrowths. The geochemistry of both manganese and iron in cave environments is governed by oxidation and reduction reactions.

Manganese and iron oxidation differ in their pH dependence: iron oxide forms at an appreciable rate of pH's above 6, while the equivalent rate for Mn oxides is not reached until pH = 8.5 (STUMM & MORGAN, 1981). Thus in cave water (pH = 6-8), there will be a tendency for iron to be the first precipitate, but for manganese to remain longer in solution, even when thermodynamic considerations suggest that both should precipitate at the same time. So the catalytic effects of oxide surfaces (MAYNARD, 1983) as well as an possible enzymatic microbial environment are especially important in the deposition of iron-manganese oxides (CRERAR *et al.*, 1972; COMAN, 1979; MARSHALL, 1979; GRADZINSKI *et al.*, 1995).

Manganese and iron oxide and/or hydroxide minerals in caves have been found either covering cave walls, stream clasts and other speleothems, or as black sedimentary deposits (HILL & FORTI, 1986). Detailed morphological, mineralogical and genetical studies on these oxides in the cave environment have been done by CRABTREE (1962), COMAN (1979), MOORE (1981), GASCOINE (1982), HILL (1982), WHITE *et al.* (1982), KASHIMA (1983), PECK (1986), COLEMAN & RAISWELL (1993), GRADZINSKI *et al.* (1995), and ONAC (1996).

Geological and speleological setting

Karst near Suncuius, northwestern part of Padurea Craiului Mountains, Romania (Fig. 1), is mostly developed in Lower and Middle Triassic limestones and dolomites. Vântului Cave is located 2.5 km upstream from Suncuius. It has a total length of about 45 km, and is the longest cave system in Romania. The cave is developed on four levels, the lowest one having an active stream (SZILAGY *et al.*, 1979). Tracer dye labeling has showed that the recharge area of the underground flow to Vântului Cave is linked to the diffuse losses in the Recea Mining Brook Basin (ORASEANU & GASPAR, 1980-1981). Deciduous forests cover the entire basin, encouraging formation of organic acids derived from the abundant decomposing vegetation.

There is evidence that mining activities in the area have had a great impact on the cave environment as the acid-mine waters (rich in iron, aluminium and silica) drain into the cave via underground flow. Furthermore, some of the mining galleries have intercepted voids, fissures or even large passages directly connected with the cave network, and most of these gaps were used as storage for barren gangue. The mine water which fluxed these waste rocks, enabled the deposition of few unsual cave minerals (e.g., allophane and saponite) as they reacted with the limestone bedrock or floor clay.

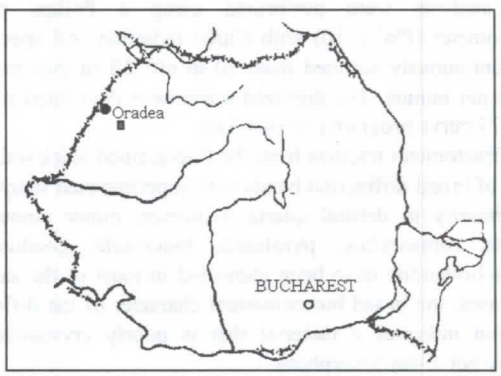

Figure 1. Map of Romania showing the karstic area around the village of Suncuius.

Location and occurrence of the black sediments

The underground stream bed in Vântului Cave is covered by black jelly-like sediments. The thickness of these sediments alters as the distance from the sediment-water interface increased. The submerged boulders and cobbles can show layers up to 2.5-3 cm thick while the sandy alluvium is covered with only 2 to 3 mm of this material. The cave walls alongside the stream are covered with black coatings of the same material, up to the highest level reached by the water.

During 1987 and 1989, once a month, in parallel with some climatic measurements, observations and sampling of the black sediments were done. In order to establish the coating rate, as well as to document the occurrence of these black precipitates, both natural and artificial substrates were put under observations, as has been described by CARPENTER & HAYES (1980). Submerged cobbles, and boulders are referred to as "natural" substrates. At the side of each observed natural substrate we emplaced, at different height, unglazed ceramic tiles (8 by 8 cm) referred to as "artificial" substrates. After four months, a continuous black film was observed on all artificial substrates located in the upper part of the water column. After a two-year period the coatings that formed on them reached 2 to 2.4 cm in thickness. The tiles lying on the stream bed or just above the sediment-water interface showed only isolated spots, and at the end of the experiment they were covered by a sub-millimetric black layer.

At the time of black sediment sampling, direct measurements of the pH and *E*h were performed. We found the pH to vary down stream (on about 2 km) from 5.1 to 8, while the *E*h values decrease from 0.83 to 0.11 volts as we move vertically down the water column in one sampling location (Fig. 3).

Analytical methods

X-ray fluorescence analyses

Major elements have been analyzed by X-ray fluorescence (XRF), in a Philips PW 1404 spectrometer, using glass beads prepared according to the method of NORRISH & HUTTON (1969). Twenty-five international standards were used, refined by least squares' procedures, using Philips model PW 1492 software for calibration.

Twelve samples collected from three different locations have given the following mean values (wt. %): SiO_2 = 28.35, MnO = 27.32, Al_2O_3 = 19.8, Fe_2O_3 = 4.02, CaO = 3.99, K_2O = 1.32, MgO = 0.74, TiO_2 = 0.5, Ni = 0.45, Ba = 0.36, S = 0.29.

X-ray Diffraction analyses

X-ray analysis were performed using a Philips powder diffractometer (PW 1710) with Cu$K\alpha$ radiation. All speciments were continuously scanned from 10 to 60° 2ϑ in increments of 0.5° 2ϑ per minute. The digitized scans were then fitted with the PW-1877 curve program (version 3.6).

Diffractometer tracings from the fine-grained black sediments consist of broad diffraction bands with superimposed sharp peaks due primarily to detrital quartz. However, minor amounts of kaolinite, romanechite, pyrolusite, todorokite, goethite and possible hollandite have been identified in most of the samples. In all cases, the broad but consistent character of the diffraction maximum indicates a material that is poorly crystallized but certainly not X-ray amorphous.

After heating the initial samples to 1000°C and performing a new series of X-ray diffraction measurements, the spectra were better resolved. They showed sharp peaks due to Mn-Al-Fe rich spinels, pyrolusite, hausmanite, hematite and quartz. This mineral association revealed that the initial black sediments are composed of amorphous aluminium and silica jelly-like material and poorly crystallized oxides and hydroxides of manganese and iron.

Thermal analyses

Simultaneous differential thermal and thermogravimetric analysis (DTA, TGA) were performed with a MOM 1200Q instrument operated at a heating rate of 10°C per minute in air with 40-50 mg of dry (over P_2O_5) sample and hematite as an inert reference material. Weight loss after static heating to 1000°C was around 20%.

Thermal decomposition of the black sediments produce a low-temperature endotherm at 220°C followed by two other weak endotherms at 550°C and 720°C. The first two effects are associated with a weight loss of 14% that derives from the expulsion of water from amorphous gels and kaolinite. The final endotherm at 720°C can be attributed to decomposition of rhodochrosite. Volatilization of resulted CO_2 produces a weight loss of 4 to 6%.

Infrared spectroscopic analysis

The sample for the infrared measurements was prepared by mixing the finely ground sample with KBr powder (approximately 5% w/w). The infrared spectroscopic analysis was performed by using a Nicolet 800 FT-IR device equipped with DTGS (Deuterated try glycyne sulphate) detector and a Spectra-Tech diffuse reflectance accessory.

Romanechite has sharp absorption peaks at 460, 523 and 580 cm^{-1}. Kaolinite shows three absorption bands of strong to medium intensity, which include peaks at 435, 538 and 690 cm^{-1}. Pyrolusite, goethite and rhodochrosite show single bands at 410, 671 and 727 cm^{-1} respectively. Single weak broad band characteristics of Si-O-Al and of Al-OH were also obtained.

Scanning electron microscope analyses (SEM)

Further investigations on the black sediments from Vântului Cave were made with a JEOL JSM6400 scanning electron microscope. SEM analyses showed a homogeneous mass made up of welded botryoidal-like agglomerates that proved to consist mainly of manganese and iron. These agglomerates are covered by clusters of thin platy crystals (Fig. 2). The diffraction pattern produced by these crystals is characteristic for phyllosilicates with pseudo-hexagonal symmetry (kaolinite).

Results and discussion

Mode of deposition

Two characteristic features distinguish the zone of the sediment-water interface: active solids and biological activity. Sediment particles in the upper part of the sediment column remain in contact with the sediments below it: residence times of the overlying water are generally much longer than the settling times. The activity of bacteria is primarily confined to the upper part of the water-sediment interface, where the exchange with the overlying water supplies oxygen (CRERAR *et al.*, 1972). Therefore, the biological activity, the chemical reactions involving organic matter and minerals, and the faster inorganic reactions of certain mineral phases make the sediment-water interface a distinct zone where special conditions for deposition exist. In this zone, black sediment will accumulate until a steady-state balance is reached between the deposition of the black sediment coatings and the physical or chemical processes that remove these coatings. The sharp line of demarcation at the sediment-water interface on both blocks and tiles suggests a

Figure 2. Botryoidal shaped agglomerates covered by clusters of thin platy crystals (see text for details).

chemical effect. *E*h, in particular, decreases abruptly in the lower part of the water column from 0.83 to 0.11 as already mentioned (Fig. 3). At low *E*h values, the predicted pH level necessary to precipitate either iron or manganese is much higher than at more positive *E*h values (COLLINS & BUOL, 1970). Under these conditions, manganese-iron precipitates are probably very unstable, and therefore the accretion rate in this part will be very reduced.

During our observations, intervals of a partial coating - partial removal process were remarked. Periods of heavy rain when the underground flow became faster and turbulent, and also dilute the acid mine waters seem to control the deposition-removal process, being in our opinion responsible for the constant thickness of the black sediments throughout the years.

Accretion rate for the black sediments appear to increase with distance above the sediment-water interface. Coatings covering the alluvium are very thin, probably due to the low *E*h existent in that part of the water column. Annual accretion rate as we measured on the artificial substrates have the following values ($\mu g\ cm^{-2}\ yr^{-1}$): at the sediment level the rate was 15, in the sediment-water interface, and above it we found 137, 211, 253 (Fig. 2).

Source of manganese and iron

A substantial amount of manganese may be released in the weathering zone by simple accumulation and decay of plants, and soluble and insoluble metallo-organic complexes of manganese may form through surface adsorption, ion exchange, chelation and formation of protective colloids (CRERAR *et al.*, 1972). Manganese appears only as a trace element in the Ladinian limestone in which Vântului Cave is formed. Owing to this, the main source of manganese might be the one suggested by CRERAR *et al.* (1972).

Sources for iron in the vicinity of Vântului Cave are easy to determine. Both refractory clays and the rocks in which these are to be found (sandstone, microconglomerates) are rich in pyrite and marcasite. The percolating waters are charged with iron, as indicated by the presence of millimetric crusts made up of goethite at many places in the cave. However, the most important source for iron seems to be the acid mine drainage that pollutes the underground stream.

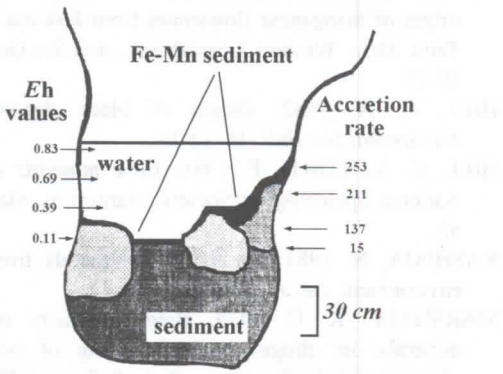

Figure 3. Cross-section of the stream bed showing the depositional environment for manganese and iron sediments, the accretion rate and Eh values at different depths.

Conclusions

The various analyses, to which the black sediments were subjected, suggest they are composed of amorphous aluminium and silica jelly-like material and poorly crystallized oxides and hydroxides of manganese and iron. Among the minerals ascribed to the later group are: romanechite, todorokite, pyrolusite, rhodochrosite, goethite and possible hollandite.

The mechanism we suggest for the deposition of the black coatings in Vântului Cave is one controlled by *E*h, pH. Precipitation of manganese and iron, and also their separation by precipitation of iron-hydroxide in a lower *E*h-pH with retention in solution of manganese-hydroxide (until a substantial rise in alkalinity or oxygenation of the solution), seems to be a valid mechanism in this peculiar case. The role played by microorganisms is not exactly known, but is to be considered as potential factor in manganese and iron deposition.

Acknowledgements

The authors gratefully acknowledge the infrared analysis provided by Dr. Alfred Antony Christy. Ing. Egil Erichsen helped with the SEM photos. Lorin Suflarszky provided assistance in the collection of cave samples. Part of this analytic work was done at the Department of Geology, University of Bergen when one of the authors (Onac) had a scholarship provided by Dr. Stein-Erik Lauritzen.

References

CARPENTER, R. H., HAYES, W. B. 1980. Annual accretion of Fe-Mn-Oxides and certain associated metals in a stream environment. *Chem. Geol.* 29: 249-259.

COLEMAN, M. L., RAISWELL, R. 1993. Microbial mineralization of organic matter: mechanisms of self-organization and inferred rates of precipitation of diagenetic minerals. *Phil. Trans. R. Soc. Lond.* 344: 69-87.

COLLINS, J. F., BUOL, S. W. 1970. Effects of fluctuations in the Eh-pH environment on iron and/or manganese equilibria. *Soil Science* 110 (2): 111-118.

CRABTREE, P. W. 1962. Bog ore from Black Reef Cave. *Cave Science* 4 (32): 360-361.

CRERAR, D. A., CORMICK, R. K., BARNES, H. L. 1972. Organic controls on sedimentary geochemistry of manganese. *Acta Miner. Petrogr. Szeged* 20: 217-226.

GASCOINE, W. 1982. The formation of black deposits in some caves of south east Wales. *Cave Science* 9 (3): 167-175.

GRADZINSKI, M., BANAS, M., UCHMAN, A. 1995. Biogenic origin of manganese flowstones from Jaskinia Czarna Cave, Tatra Mts., Western Carpathians. *Ann.Soc.Geol.Polon.* 65: 19-27.

HILL, C. A. 1982. Origin of black deposits in cave. *Nat.Speleol.Soc.Bull.* 44: 15-19.

HILL, C. A., FORTI, P. 1986. *Cave minerals of the world*, National Speleological Society, Huntsville, Alabama pp. 79-85..

KASHIMA, N. 1983. On the Wad-minerals from the cavern environment. *Int. J. Speleol.* 13: 67-72.

MARSHALL, K. C. 1979. Biogeochemistry of manganese minerals. In: *Biogeochemical cycling of mineral-forming elements* (Ed. by Trudinger, P. A. & Swaine, D. J.), pp. 253-292. Elsevier, Amsterdam.

MAYNARD, J. B. 1983. *Geochemistry of sedimentary ore deposits*. Springer-Verlag, Berlin. 305 pp.

MOORE, G. W. 1981. Manganese deposition in limestone caves. *Proc. 8th Int. Congr. Speleol.*, Bowling Green I & II: 642-644.

NORRISH, K., HUTTON, J. T. 1969. X-ray spectrographic method for the analysis of a wide range of geological samples. *Geochimica and Cosmochimica Acta* 33: 431-453.

ONAC, B. P. 1996. Mineralogy of speleothems from caves in the Padurea Craiului Mountains (Romania), and their palaeoclimatic significance. *Cave and Karst Science* 23 (3): 109-124.

ORASEANU, I GASPAR, E. 1980-1981. Cercetari cu trasori radioactivi privind stabilirea zonei de alimentare a cursului subteran din pestera Vantului (Muntii Padurea Craiului). *Nymphaea* VIII-IX: 379-386.

PECK, S. B. 1986. Bacterial deposition of iron and manganese oxides in North American caves. *Nat.Speleol.Soc.Bull.* 48 (1): 26-30.

STUMM, W., MORGAN, J. J. 1981. *Aquatic chemistry*. J. Wiley & Sons, New York. 2nd ed.

SZILAGY, A., KOMIVES, E., NAGY, I., VARGA, A., KEREKES, K. 1979. Pestera Vintului. *Trav.Inst.Speol."Emile Racovitza"* XVIII: 259-266.

WHITE, W. B., SCHEETZ B. E., CHESS, C. A. 1982. The mineralogy of black manganese minerals from caves. *Geol* 10 (1): 43.

Cave minerals of the Western Ukraine

Igor Turchinov
Lviv Geology Survey Expedition, ul.Turgeneva 33, UA-290018 Lviv, Ukraine

Abstract

Giant maze cave systems in the Miocene gypsum in the Western Ukraine are characterized by abundance and variety of secondary mineral forms. Original geological, physical and chemical conditions have determined a wide derelopment of mineral formation processes here. Minerals forming in the gypsum caves of the Western Ukraine belong to the classes of sulphates (gypsum, celestite), carbonates (calcite, rhodochrosite), silicates (chalcedony), oxides and hydroxides (iron and manganese minerals, ise), and are represented by various speleothems. Some of them have a certain scientific value.

1. Introduction

Giant maze cave systems in the Badenian (Middle Miocene) gypsum are characterized by abundance and variety of secondary mineral forms. Original geological, physical and chemical conditions (air temperature +8,2-10,5 °C, air humidity 96-100%, CO_2 concentration 0,1-4,8%, radon concentration up to 23700 Bc/m^3) have determined a wide development of mineral formation processes here.

Secondary minerals in the caves of the region belong to the classes of sulphates, carbonates, silicates, oxides and hydroxides. Genetic classification of cave minerals of the Western Ukraine is given in table 1, conditions of mineral formation are reflected at fig. 1.

Many of speleothems in the caves of the Western Ukraine are well known and described, therefore a great attention in this paper will be given to speleothems. which either have a rare spreading or have not analogous aggregates in other caves.

2. Sulphates

Gypsum

Gypsum speleothems have a most spreading in the caves of the region. They are characterized by the variety of morphology and genesis. Prismatic, rod-like and tabular euhedral crystals occur most frequently These speleothems were born and grew in thin capillar water films on the walls and ceilings of the caves. Commonly, the length of gypsum crystals is 2-10 cm, however some crystals and crystalline aggregates have length up 70-120 cm.

Speleothems which form through the evaporation of interstitial seeping water also occur frequenty. There are parallel-fibrous aggregates, cave flowers, gypsum needles. In the caves of the region gypsum needles have length up to 18-27 cm and width 1-3 mm. They grow at the soil-air boundary after the evaporation of solutions seeping through the cave soil.

Some of the gypsum speleothems (concretions, roses, twins) grow in the subsurface part of cave soil after the evaporation of solutions ascending through the soil capillaries. Gypsum twins have length 7-15 cm and width 1-3 cm. They are analogous to "eroded crystals" from the gypsum caves of Italy (HILL & FORTI, 1986).

Recently characterized (KLIMCHOUK et al., 1994; TURCHINOV, 1994) a group of gypsum speleothems of aerosol origin includes "gypsum snow", frost-like acicular crystals and gypsum rims. :Gypsum snow" is represented by accumulations of small acicular gypsum crystals on the floor of cave passages. These crystals have no attachment with substratum. It is assumed that origin and initial growth of "gypsum snow" take place in the cave air. The settling of these components takes plase after increasing their weight in the process of their growth. Components of "gypsum snow" settle along the axis of air flow, therefore accumulations of "gypsum snow" have a stretch form. Aggregates of frost-like acicular crystals on the walls of caves and gypsum rims are formed after settling of hydroaerosol drops and following crystallisation of gypsum. Sometimes clusters of frost-like crystals occur in shape of horizontal strips of 3-7 cm in width (fig. 2). This fact testifies to the united level of transfer of aerosols in conditions of quiet laminar air flows.

It is assumed, that formation of aerosols in the gypsum caves of the Western Ukraine is determined by the enhanced radioactivity and ionization of the cave air (KLIMCHOUK et al., 1994).

Celestite

Small (1-3 cm) acicular crystuals of celestite have been discovered in Kristalnaya cave in assotiation with gypsum crystals (LAZARENKO & SREBRODOLSKY, 1969). Genesis of celestite is due to strontium which is present in the Miocene gypsum (up to 3-5%).

3. Carbonates

Calcite

Calcite is a main carbonate mineral in the gypsum caves of the Western Ukraine. Formation of calcite speleothems is due to the infiltration into caves of calcium bicarbonate solutions formed through the dissolution of limestones and marls which overlie the gypsum stratum.

Many of the carbonate speleothems are represented by well known aggregates (stalactites, stalagmites, crusts, flowstones, draperies, conulites), therefore their detailed description does not adduce in this paper.

Forms, called by pseudohelictites have been found in Mlynki and Optimisticheskaya caves. Ihere are aggregates of three curved-facet crystals of 1-3 cm in length, growing on the surface of calcite crusts or stalactites. These aggregates grow in conditions of thin capillar film and their shape is determined by speed of growth of separate cryctals.

Non-described in other caves speleothems have been discovered in Dzhurinskaya, Optimisticheskaya, lynki, Slavka caves. There are calcite spherolites of 0,2

Table 1. Genetic classification of cave minerals of the Western Ukraine (numbers in brackets - see fig. 1)

Classes	Sulphates		Carbonates		Silicates	Oxides and hydroxides	
Minerals Genesis	Gypsum	Celestite	Calcite	Rhodochrosite	Quartz (chalcedony)	Iron and manganese minerals	Ice
Crystallization from free flowing water after CO_2 Loss: A. Central canal			stalactites(13) helictites (14)				
B. Dripping water			stalagmites(15) conulites(16)				
C. Intensive infiltration			crusts (17) flowstones (18) draperies (19)	in composition of the calcite crusts (28)			
Evaporation of thin film of water	Euhedral crystals (1)	Euhedral crystals (12)	pseudohelictites (20),crystals (21) spherolites (22)				
Evaporation of seeping inter-stitial water	parallel-fibrous aggregates (2) cave flowers (3) needles (4)						
Crystallization in cave soil	concretions(5) roses (6) twins (7)						
Crystallization from vein water	parallel-fibrous gypsum (8)		boxwork (23)				
Subaqueous crystallization			rafts (24) and their deposits(25) gours (26) cave pearls (27)				
Crystallization from aerosols: A.Crystallizati-on in cave air	"gypsum snow" (9)						
B. Crystallizati-on after setting of aerosols	frost-like acicular crystals (10) rims (11)						
Crystallization of gels					crusts (29) boxwork (30)		
Biochemical precipitation						powder-like deposits (31)	
Freezing crystallization							stalacti-tes (32) stalag-mites (33)

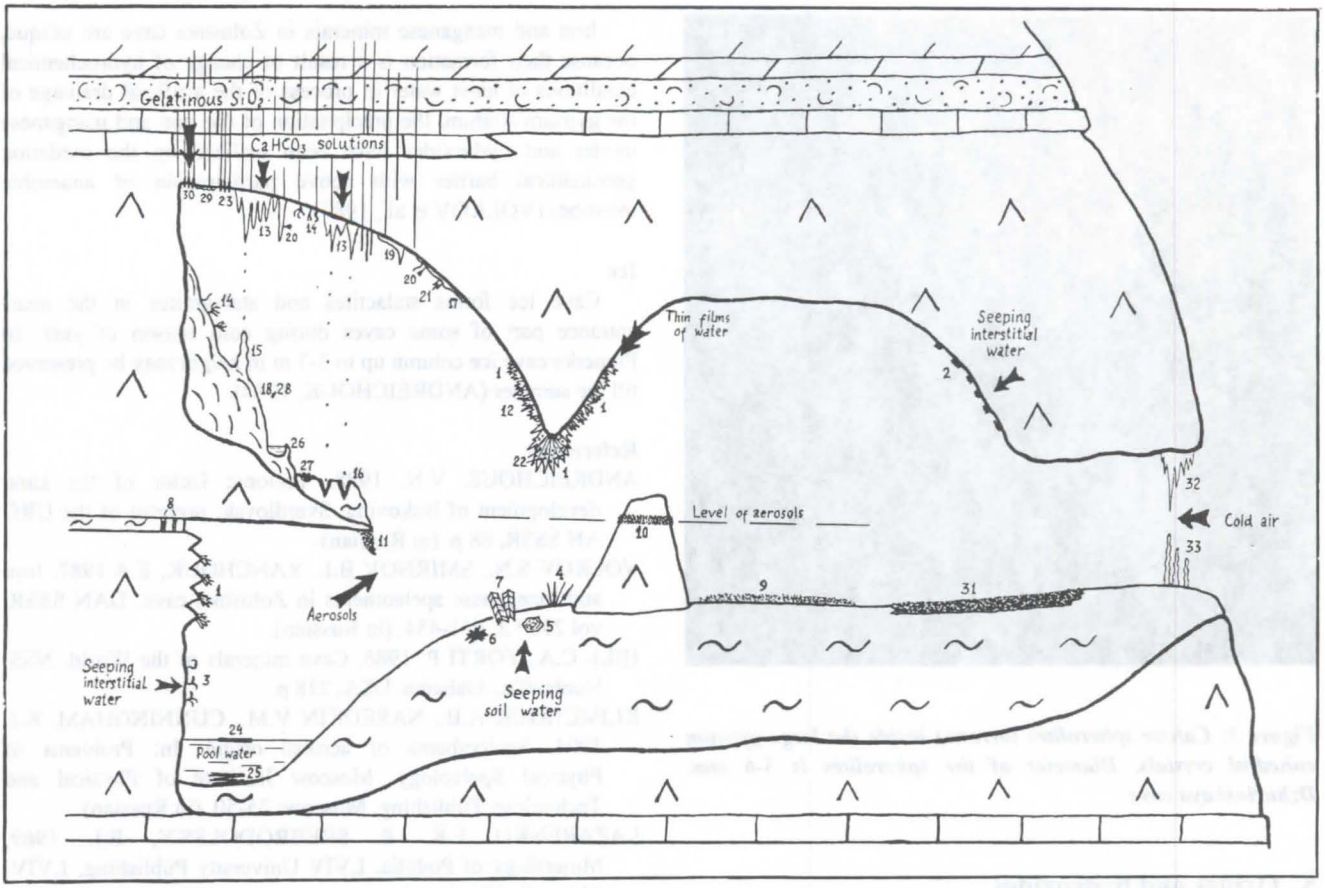

Figure 1: Conditions of mineral formation in the gypsum caves of the Western Ukraine

to 5-6 mm in diameter which are concluded inside the large transparent gypsum euhedral crystals (fig. 3). The growth of these spherolites took place simultaneously with the growth of the gypsum crystals. Diffused in primary gypsum calcium carbonate was a source of the matter to the growth of the spherolites (TURCHINOV, 1993).

Calcite boxwork forms in the zones of jointing through the near-cavity crystallization of calcite in joints and the following dissolution of gypsum.

Some of the calcite speleothems form in the subaqueous environment or on the water surface. Calcite rafts up to 1-1,5 mm in thickness form on the surface of some underground pools. Floating rafts continue to grow until they sink from their own weight, and accumulations of rafts up to 20 cm in thickness form on the bottom of pools.

Cave pearls up to 15 mm in diameter have been investigated in Ozernaya cave.

Rhodochrosite

This mineral has been found by X-ray difraction study in the calcite crust in Optimisticheskaya cave. The genesis of rhodochrosite is due to the dissolution and redeposition of primary rhodochrosite from the upper Badenian marls which overlain the gypsum stratum.

4. Silicates

Quartz (Chalcedony)

In the gypsum caves of the Western Ukraine the class of silicates is represented by chalcedony - a fibrous variety of quartz. Mineral occurs as thin (up to 2-3 mm) white or yellow crusts in the zones of jointing. The genesis of the chalcedony crusts is due to the epigenetic transformations of the Upper Badenian tuffites, bedding over gypsum. Gelatinous silicic acid, forming through the montmorillonitization of volcanic ash, infiltrated to the cave and crystallized here (TURCHINOV, 1993).

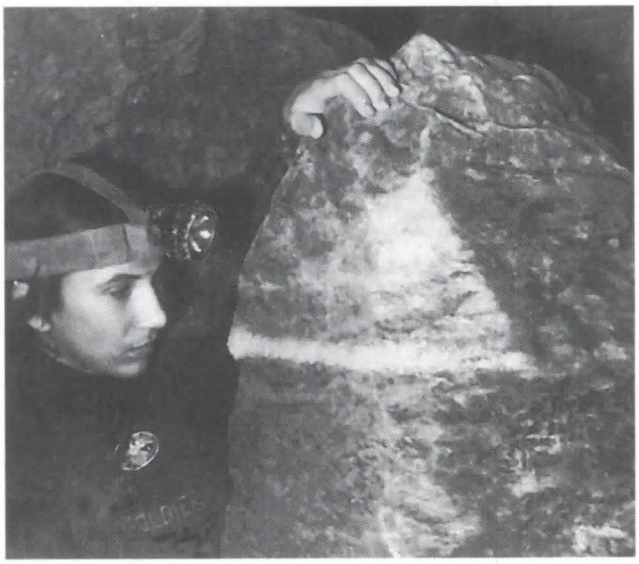

Figure 2: Horizontal strip of the frost-like acicular crystals of aerosol origin, Optimisticheskaya cave

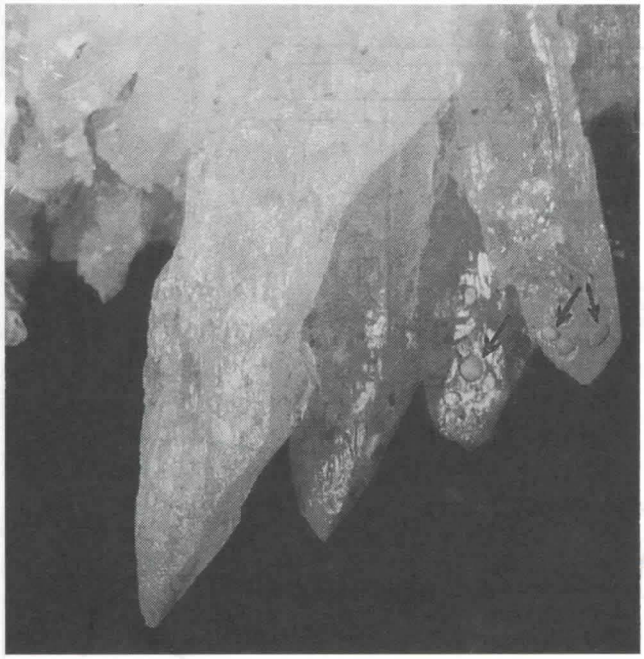

Figure 3: Calcite spherolites (arrows) inside the large gypsum euhedral crystals. Diameter of the spherolites is 5-6 mm. Dzhurinskaya cave

5. Oxides and hydroxides

Iron and manganese oxides and hydroxides

Iron and manganese minerals have a greater occurence in Zolushka cave. Here they form powder-like deposits up to 30-40 cm in thickness. Stalactite-like and stalagmite-like aggregates occur less frequently. Manganese minerals are represented by birnessite and asbolan (Co-and Ni-containing wad) (VOLKOV et al., 1987). Iron hydroxides occur in amorphous phase FeOOH * nH_2O.

Iron and manganese minerals in Zolushka cave are unique, because their formation is a result of change of hydrochemical conditions of karst water in process of the artificial drainage of the gypsum stratum. Ihe precipitation of the iron and manganese oxides and hydroxides have been realized on the oxidation geochemical barrier with active participation of anaerobic microbes (VOLKOV et al., 1987).

Ice

Cave ice forms stalactites and stalagmites in the near-entrance part of some caves during cold season of year. In Pionerka cave ice column up to 3-7 m in height may be preserved till the summer (ANDREICHOUK, 1988).

References

ANDREICHOUK V.N. 1988. Tectonic factor of the karst development of Bukovina. Sverdlovsk: preprint of the URO AN SSSR, 68 p. (in Russian).

VOLKOV S.N., SMIRNOV B.I., YANCHOUK, E.A.1987. Iron and manganese speleothems in Zolushka cave. DAN SSSR, vol 292 ' 2: 451-454. (in Russian).

HILL C.A., FORTI P. 1986. Cave minerals of the World. NSS, Huntsville, Alabama, USA, 238 p.

KLIMCHOUK A.B., NASEDKIN V.M., CUNNINGHAM, K.I. 1994. Speleothems of aerosol origin. In: Problems of Physical Speleology. Moscow Institute of Physical and Technology Publishing, Moscow: 25-50. (in Russian).

LAZARENKO E.K. & SREBRODOLSKY, B.I. 1969. Mineralogy of Podolia. LVIV University Publishing, LVIV, 346 p. (in Ukrainian).

TURCHINOV I.I. 1993. Secondary mineral formations in the gypsum caves of the Western Ukraine. Svet (The Newsletter of the Kiev Karst & Speleological Center) n.3 (9): 29-37. (in Russian).

TURCHINOV I.I. 1994. Aerosol formation of minerals in the gypsum caves of the Western Ukraine. In: Problems of Physical Speleology. Moscow Institute of Physics and Technology Publishing, Moscow: 51-63 (in Russian).

Venezuelan cave minerals: a short overview

by Franco Urbani

Universidad Central de Venezuela, Escuela de Geología, Minas y Geofísica, Caracas 1053 & Sociedad Venezolana de Espeleología, Apartado 47334, Caracas 1041A, Venezuela &.. Email: furbani@reacciun.ve

Abstract

A list of Venezuelan cave minerals and their localities is given together with a short statement of the main features of some of the occurrences and its possible origin.

Resumen

Se presenta una lista de los minerales secundarios identificados en cavidades venezolanas. Adicionalmente a la localidad, se presenta un breve enunciado de las características de alguno de los yacimientos y su posible origen.

1. Introduction

Since the very early descriptions of Venezuelan caves, speleothemes are mentioned as it happens in the 1678 description of El Guácharo Cave entrance in eastern Venezuela by the missionary Francisco de Tauste. But apart from such type of descriptions by many further visitors, the first mineralogical work of Venezuelan speleothems is that of WHITE *et al.* (1963) describing several types of calcite speleothems. They also were the first to identify gypsum in several types of occurrences. In this note a list of venezuelan cave minerals is presented with some brief remarks about the occurrence and the possible origin of some selected ones.

2. Cave Minerals

A. Carbonates

Aragonite $CaCO_3$

- *Cueva de Baruta* (Mi.11), Caracas, Miranda. URBANI (1967, 1968). This 200 m long "crystal cave" or geode was opened in January 1956 during quarry work in dolomitic marble and very soon vandalized. Aragonite was abundant as anthodites with needles as long as 5 cm, some transformed to dolomite, showing high Sr content. It is possible that this element promoted its crystallization.
- *Cueva La Guairita 2* (Mi.16), Caracas, Miranda.
- *Cueva Cantera Sur de Baruta* (Mi.28), Caracas, Miranda.
- *Cueva Ricardo Zuloaga* (Mi.42), Miranda. URBANI *et al.* (1995). As needle-like crystals associated with sepiolite in a cauliflower shaped assemblage.
- *Cueva de Iglesitas* (Mi.50), Caracas, Miranda.
- *Cueva La Peonia* (La.2), Lara.
- *Cueva de Tiburcio*, Yaracuy.

Azurite $Cu_3(CO_3)_2(OH)_2$

- *Cueva de Baruta* (Mi.11), Miranda.

Calcite $CaCO_3$

As the most common cave mineral it presents a wide variety of shapes, like stalactites, stalagmites, coatings and crusts, conulites, coralloids, cups, draperies, flowstone, helictites, moonmilk, cave pearls, rafts, rimstone dams (gours), cave clouds, shelfstone, cave shields and spar.

- *Cueva del Guácharo* (Mo.1), Monagas. This cave shows the greater variety of calcite speleothems from Venezuela, like stalactites, stalagmites, draperies, flowstones, rimstone dams, helictites, cave pearls, spar and cups. Monocrystalline stalactites and helictites were studied by WHITE *et al.* (1963). Some orange to red colored stalactites were studied by WHITE (1981) finding that the colour is due to organic compounds. Stalactites with concentric layers of calcite and detrital clay formed by periodical flooding and small stalactites with coralloid tips were reported by URBANI (1973).
- *Cueva Alfredo Jahn* (Mi.35), Miranda.
- *Cueva Quebrada Marasmita* (Mi.6), Miranda.
- *Cueva de la Discordia 1* (Fa.34), Falcón.
- *Cuevas de la Gruta* (Mi.12) and *Refugio* (Mi.30), Miranda.
- *Cueva del Cerro Autana* (Am.11), Amazonas.
- *Cueva de Baruta* (Mi.11), Miranda.
- *Cueva Walter Dupouy* (Mi.2), Miranda.
- *Cueva del cañón de Sorotamia* (Zu.72), Río Socuy. Zulia.
- *Cueva Los Encantos*, Zulia.

Calcite, var Lublinite $CaCO_3$

- *Cueva La Milagrosa* (Mo.22), Monagas. URBANI (1977b).

Dolomite $CaMg(CO_3)_2$

- *Cueva de Baruta* (Mi.11), Caracas, Miranda. URBANI (1967, 1968). Appear as elongated 1-2 cm long "fingers". In thin sections it shows concentric structures with aragonite in its center (about 5% of the total sample). Other specimens did not have aragonite. The insoluble residue of these speleothems is opal. It is believed that dolomite was formed by transformation of aragonite under the influence of seeping water with high magnesium content coming from the dolomitic marble bedrock.
- *Haitón de Sabana Grande* (Fa.52), San Luis, Falcón. URBANI (1977a).

Magnesite $MgCO_3$

- *Cueva Quebrada Ocumarito*, Distrito Federal. This is a 10 m long cave developed along a fault zone in serpentinite bedrock. The crusts may vary from a few millimeters up to 6 cm thickness.

Malachite $Cu_2CO_3(OH)_2$

- *Cueva de Baruta* (Mi.11), Caracas, Miranda.

B. Halides

Halite NaCl

- *Cueva Alfredo Jahn* (Mi.35), Birongo, Miranda. FORTI & URBANI (1996).

C. Nitrates

Nitrammite NH_4NO_3

- *Sima Aonda Superior* (Bo.54), Auyán-tepui, Bolívar. FORTI (1994). Forms a very small patch in a well-aerated and protected niche on the wall of this quartzite cave. The components are believed to come from the decaying organic matter of the surface.

Sveite $KAl_7(NO_3)_4Cl_2(OH)_{16}.8H_2O$

- *Cueva del Cerro Autana* (Am.11), Amazonas. MARTINI (1980); MARTINI & URBANI (1984). This is the first new mineral for science discovered in a Venezuelan cave. It occurs in a quartzite cave where it forms crusts and efflorescences in the walls in patches of about 1 cm thickness and up to a few square meters extent. It is clearly seen that the forming solutions seeped from the bedding planes. It is believed that the K, NO_3 and Cl

come from the organic matter at the top of the mountain, while Al and K are due to weathering of the trace amounts of plagioclase and micas disseminated in the rock. Its formation requires the evaporation of large amounts of the very diluted water.

D. Oxides and hydroxides

Goethite αFeO(OH)

• *Cuevas del Cerro María Luisa* and *Conejero*, Bolívar. The caves are developed underneath the lateritic iron crust shielding the upper part of some hills. Goethite is present as centimeter long stalactites, stalagmites, flowstones and coatings.

• *Sima de la Lluvia de Sarisariñama* (Bo.3), Bolívar. URBANI *et al.* (1976). Present as coatings and stalagmites including what seems to be the largest known goethite stalagmite in the world with about 3 m height and 1 m diameter.

• *Sima Aonda 3*, Auyán-tepui, Bolívar.

Ice H_2O

• *Cuevas de los glaciares de Timoncitos y del pico Bompland*, Mérida. PÉREZ (1978). As numerous icicles in small glacier caves.

Lithiophorite (Al,Li)$MnO_2(OH)_2$

• *Sima Menor de Sarisariñama o Martel* (Bo.2), Bolívar. URBANI *et al.* (1976). Appears in wrinkled and earthy stalactites up to 15 cm long and 20 cm in diameter at its base.

Maghemite ? αFe_2O_3

• *Cueva La Milagrosa* (Mo.22), Monagas. URBANI (1977b). Appears as crusts of up to 4 mm thickness covering the limestone walls with a shiny and botryoidal shape and near bat guano deposits.

Mn-Fe (Amorphous oxides-hydroxides)

• *Cueva El Santuario*, Trujillo. BUZIO & FORTI (1994). Forms black pisolites in a nest of more than a hundred of them, mainly of 3-5 mm in diameter but one reached 3 cm.
• *Cueva Alfredo Jahn* (Mi.35), Miranda.
• *Cueva El Samán* (Zu.30), Zulia.
• *Cueva Los Encantos*, Fundo Los Encantos, Zulia.
• *Sumidero Los Cantos* (Zu.70), Fundo Los Encantos, Zulia.
• *Cueva La Peonía* (La.2), Lara.

E. Phosphates

Brushite $CaHPO_4.2H_2O$

• *Cueva del Indio* (Mi.24), Miranda. FORTI *et al.* (1996). Identified in a light orange powdery and very light material produced by decomposition of bat guano.
• *Cueva de San Sebastián o de la Caridad* (Ar.3), Aragua.
• *Cueva Ricardo Zuloaga* (Mi.42), Miranda.

Carbonate-apatite $Ca_5(PO_4, CO_3)_3$

• *Cueva del Indio* (Mi.24), Miranda.

Carbonate-fluor-apatite $Ca_5(PO_4,CO_3)_3F$

• *Cueva del Indio* (Mi.24), Miranda.

Carbonate-hydroxyl-apatite $Ca_5(PO_4,CO_3)_3(OH)$

• *Cueva del Indio* (Mi.24), Miranda.
• *Cueva de Los Laureles* (Zu.31), Zulia.
• *Cueva de Pardillal* (Ar.15), Aragua.

Chlor-apatite $Ca_5(PO_4)_3Cl$

• *Cueva del Indio* (Mi.24), Miranda.
• *Cueva de Los Laureles* (Zu.31), Zulia.

Evansite $Al_3(PO_4)(OH)_6.6H_2O$ (?) Amorphous

• *Cueva de Urutany 1 and 2* (Bo.4,.5), Bolívar. Appears as rough stalagmites (the largest is 60 cm high and 40 cm diameter in its base) and also as coatings and flowstones on the walls of these quartzite caves. Color is yellow, yellowish brown and reddish with concentric layering and flaky appearance. It is very soft and when dried it breaks at touch. A partial chemical analysis of this material gave SiO_2 11.0%, Al_2O_3 10.7%, P_2O_5 4.9%, Na_2O 0.6%, H_2O 22.2% and minor amounts of Fe_2O_3 and K_2O. The remainder, to 100%, is organic matter. Due to the amorphous nature of the mineral its identification is not sure and probably the high silica and organic matter content may be explained by the presence of **allophane** and **pigotite**. The caves are under a jungle with thick organic soil and contain colonies of bats what partially explain the presence of P and organic components while Al and Si may be provided by the weathering of quartzite.

• *Cueva de Aguapira 9* (Bo.17), Aguapira, Bolívar.

Fluor-apatite $Ca_5(PO_4)_3F$

• *Sumidero Los Cantos* (Zu.70), Zulia. Appears as ½ cm thick light brown crust protruding 1-2 cm from the limestone bedrock wall. Found on the ceiling of the cave in a place that remains as an air-bag at moments of water flood. Appears at the would-be air-water interface. The sample also contains quartz and illite.
• *Cueva del Indio* (Mi.24), Miranda.
• *Cueva de Pardillal* (Ar.15), Aragua.

Hydroxyl-apatite $Ca_5(PO_4)_3(OH)$

• *Cueva del Guácharo* (Mo.1), Monagas. This was the first Venezuelan cave locality where a phosphate was identified. It appears as coatings on calcite flowstones and limestone bedrock in some minor passages that have active bat colonies. The crusts are black to dark brown of up to 6 mm thickness but usually they are at the scale of 1-3 mm.

• *Cueva El Samán* (Zu.30), Zulia. In one of the farthest passages of this cave, the largest in Venezuela, there is an irregular black to very dark brown mass of up to 5 cm thickness and covering about 0.5m². The XRD pattern is that of a Mn-Fe rich amorphous mineral but with all the major hydroxy-apatite peaks. EDX analyses show the presence of Mn, Fe, Ca, Al, P and Si.

• *Cueva Los Laureles* (Zu.31), Zulia. Appears as dark brown to black 1-3 mm thick crusts on the limestone bedrock. EDX analysis shows that the external surface is rich in Mn and Fe, but inside only Ca and P were detected steming from hydroxyl-apatite.
• *Cueva del Indio* (Mi.24), Miranda.
• *Cueva Ricardo Zuloaga* (Mi.42), Miranda. URBANI (1996a).
• *Cueva La Torre* and *Narices del Diablo*, Guanape, Anzoátegui.
• *Cueva del Riito*, La Aguadita, Churuguara, Falcón.
• *Cueva de Lizardo o La Cuevita* (Fa.26), Falcón.
• *Cueva de San Sebastián o la Caridad* (Ar.3), Aragua.
• *Cueva de Pararille*, Churuguara, Falcón.
• *Cueva de Pardillal* (Ar.15), Aragua.
• *Cueva de Iglesitas* (Mi.50), Miranda.

Leucophosphite $KFe_2(PO_4)_2(OH).2H_2O$

• *Cueva de los Culones de Caoma* (DF.10), Distrito Federal. URBANI *et al.* (1995a). This is a 30 m long cave in weathered garnet amphibolite. Leucophosphite is found as roughly 0.1 mm sized rounded nodules concentrically interlayered with opal in coralloid fingers. Under the binocular microscope the mineral shows bright yellowish to red colours.

Whitlockite $Ca_9(Mg,Fe)H(PO_4)_7$

• *Cueva Ricardo Zuloaga* (Mi.42), Miranda.
• *Cueva de Pardillal* (Ar.15), Aragua.
• *Cueva de Lizardo o La Cuevita* (Fa.26), Falcón.

F. Silicates

Allophane (amorphous hydrous aluminum silicate). See comments under Evansite.

Chalcedony SiO_2

• *Cueva Cerro Autana* (Am.11), Amazonas. URBANI (1976). Observed on some coralloid opal speleothems in which under thin sections the chalcedony (crystallized fibrous quartz) is seen intermixed with opal and minor calcite layers. The speleothems are active.

Opal-A $SiO_2.nH_2O$

- *Cueva de Baruta* (Mi.11), Miranda. URBANI (1967). Found as an insoluble residue of dolomite speleothems.
- *Sima de la Lluvia de Sarisariñama* (Bo.3), Bolívar. Shows a wide variety of coralloid and cauliflower forms of up to several square meters of coverage. Also as metric flowstones mainly covered with coralloid surfaces. The most spectacular forms are soda-straws and stalactites of as much as 35 cm length with a diameter of 2.5 cm at the upper part. This stalactitic opal is translucent and glassy in comparison with the usual darker and grayish coralloids. Under scanning electron microscope (SEM) all samples show filament structures suggesting an origin induced by biogenic activity.
- *Cueva de los Culones de Caoma* (DF.10), DF. URBANI *et al.* (1995). Found as ½-1½ cm long coralloids in this cave. Developed in weathered garnet-amphibolite, it is associated with leucophosphite.
- *Most caves in sandstones of the Tertiary Mirador Formation, Páramo del Tamá and Fila de Capote*, Táchira, Apure: Cueva del Loto (Ap.1) and others.
- *In all caves explored in the Precambrian quartzites of the Roraima Group* (Kukenán, Chimantá, Urutany, Aguapira, Tramen, Roraima, Yuruaní, Auyán-tepui. Bolívar and Amazonas). As coralloid speleothems. Under SEM all samples viewed (including one from Cueva El Loto, see previous locality) show numerous organic structures, usually filament-shaped, suggesting a biogenic induced origin. At the caves of the Aonda Platform coralloids are always found near the entrances in the penumbra zone with algae covering parts of the bedrock. Those coralloids are the ones that show more abundant filamentous structures under SEM, but they also occur in samples from deeper inside the caves (URBANI, 1996b).
- *Sima Mayor de Sarisariñama o Humboldt* (Bo.1), Bolívar.
- *Sima Menor de Sarisariñama o Martel* (Bo.2), Bolívar.
- *Cueva del Cerro Autana* (Am.11), Amazonas.
- *Cueva El Abismo* (Bo.7), Bolívar.
- *Sima Aonda Superior* (Bo.54), Bolívar. FORTI, 1994

Palygorskite $(Mg,Al)_2SiO_4O_{10}(OH).4H_2O$

- *Cueva Las Úrsulas* (Mi.47), Miranda. URBANI (1975). As 1 mm thick leathery sheets on the walls and fractures of this cave developed along the joints in quartz-mica-albite-schists. The sheets are light brown but also reddish due to iron-oxide staining. They are flexible and associated with minor amounts of calcite.

Sepiolite $Mg_4Si_6O_{15}(OH)_2.6H_2O$

- *Cueva Ricardo Zuloaga* (Mi.42), Miranda. URBANI *et al.* (1995). The mineral is cauliflower-shaped and is deposited along a 1 m long fracture at the ceiling. It is about 3 cm wide and 1-1½ cm thick. It is soft, wet and plastic. By XRD it appears with low-crystallinity. EDX analysis shows the presence of Si, Ca and Mg and the sample heated to 1200°C transforms to diopside (Ca, Mg-pyroxene). Ranging out from the moist to drier and older parts of the occurrence sepiolite becomes more crystalline and an increasing amount of aragonite appears.

G. Sulfates

Ammonium-jarosite $(NH_4)Fe_3(OH)_3(SO_4)_2$

- *Cueva Alfredo Jahn* (Mi.35), Miranda. FORTI & URBANI (1996). This mineral appears in light-blue spots on the calcitic marble wallrock of the Chaguaramo Saloon with millimetric thickness and mixed with hydroxyl-apatite. It is believed that the ammonium required is supplied by the organic matter carried by the water inside the cave from the tropical forest outside.

Bassanite $CaSO_4.½H_2O$

- *Cueva de San Sebastián o la Caridad* (Ar.3), Aragua. Found on shale fragments from a collapse inside this cave which formed in Paleocene limestones. Appears as white to slightly brown efflorescences of up to 3 mm thickness, soft and dusty, no traces of gypsum were found. This section of the cave is very dry and shows temperatures up to 28°C. The finding and analysis took place in 1983 but in 1996 only gypsum was found in the same spot, suggesting that bassanite formed directly in this dry environment and latter hydrated to gypsum.

Epsomite $MgSO_4.7H_2O$

- *Cueva El Ermitaño* (La.1), Lara. URBANI (1974). Appears as 2 cm thick crusts of massive epsomite with coarsely fibrous nature and transparent crystals. The external part is covered by a white powdery mineral identified as hexahydrite.
- *Cueva de la cantera Sur de Baruta* (Mi.28), Miranda.

Gypsum $CaSO_4.2H_2O$

- *Cueva del Guácharo* (Mo.1), Monagas. First identified by WHITE *et al.* (1963), it appears in a wide variety of occurrences of white to transparent crystals forming flowers, frostworks, needle-like crystals, cotton surfaces, cockscomb stalagmites, crusts on walls and ceilings making up sparkling passages, and "hair" hanging more than 3 m that can be moved by air blown onto them.
- *Cueva del Indio* (Mi.24), Miranda. FORTI *et al.* (1996). Here two types of occurrences are found, one as very rare crusts 1-2 cm thick of almost transparent fibers, the other and more common appears as a white to yellowish powdery material associated with brushite and minerals of the apatite group, both inside a decomposed bat guano deposit.
- *Cueva La Peonía* (La.2), Lara.
- *Cueva del Peñón del Diablo* (DF.12), Distrito Federal.
- *Cueva El Ermitaño* (La.1), Lara.
- *Cueva La Milagrosa* (Mo.22), Monagas.
- *Cueva Ricardo Zuloaga* (Mi.42), Miranda.
- *Cueva de San Sebastián o la Caridad* (Ar.3), Aragua.
- *Haitón de Sabana Grande* (Fa.52), Falcón.
- *Sima Mayor de Sarisariñama or Humboldt* (Bo.1), Bolívar.
- *Sima Aonda Superior* (Bo.54), Bolívar.
- *Gruta de los Morrocoyes*, Aragua de Maturín, Monagas.
- *Cueva de Iglesitas* (Mi.50), Caracas, Miranda.
- *Cueva de Pardillal* (Ar.15), Aragua.

Hexahydrite $MgSO_4.6H_2O$

- *Cueva El Ermitaño* (La.1), Lara. URBANI, 1974. As an *in situ* dehydration product of epsomite in this very dry cave.
- *Gruta de los Morrocoyes*, Aragua de Maturín, Monagas.

Koktaite $(NH_4)_2Ca(SO_4)_2.H_2O$

- *Cueva Alfredo Jahn* (Mi.35), Miranda. FORTI & URBANI (1996). Appears mixed with hydroxyl-apatite and halite in pale-gray spots on the marble bedrock.

H. Arseniates

Mangano-berzelite $(Na,Ca)_2(Mg,Mn)_2(AsO_4)_3$

- *Cueva Alfredo Jahn*, Miranda. FORTI & URBANI (1996). This is the first report of this mineral in a cave environment and is found in red to reddish-brown 1-2 mm thick crusts on the limestone bedrock under the influence of an active stream. It is associated with amorphous Fe-Mn oxide-hydroxides. Up to date the provenance of arsenic is unknown.

I. Organic minerals

Pigotite. See comments under Evansite.

J. Related forms

Mud and sand formations

- *Cueva del Guácharo* (Mo.1), Monagas. "Mud and sand castle" stalagmites have been observed in the Gran Salón del Derrumbe.
- *Cueva de Baruta* (Mi.11), Miranda.

Clay vermiculations

- *Cueva del Pio* (Mi.22), Miranda. F. URBANI (in HEDGES, 1993:4). It had the best hieroglyphic type vermiculations observed in Venezuela, now completely vanished due to touching by thousand of persons that visit the cave annually.
- *Sima del Naranjo* (Mo.41), Monagas.

- *Cueva Ricardo Zuloaga* (Mi.42), Miranda.

Rootsicles

- *Cueva de La Guairita 2* (Mi.16), Miranda.

Carbide related formations

- *Cueva de la Brújula* (Mi.1), Miranda. In a 1965 excursion calcium carbide was dumped on the floor of the innermost part of the cave, in 1995 on such dump two irregular 1½ cm high vertical calcite fingers 3-6 mm in diameter were observed. Under SEM the surface appears like a smooth polygonal pavement, while at a broken surface it looks like dogtooth spar crystals of micrometer size.

Guano-fire materials

- *Sima Fumarola de la isla de Monos* (An.5), Anzoátegui. GALÁN & GALÁN (1983). The combustion activity started in 1977 with emission of "smoke" at the upper entrance of the cave and mainly visible during the rainy season. A year later when the cave was explored at a depth of ½ m inside the former bat guano deposit the temperature was still higher than 100°C. The material was analyzed chemically but no mineralogical work was done.
- *Cueva del Peñón de las Guacas o de los Carraos* (Mi.14), Miranda.

K. Minerals in artificial cavities

Calcite, Chalcanthite, Epsomite, Fe rich (amorphous oxide-hydroxides), Goethite, Gypsum, Malachite, Melanterite, Mn rich (amorphous oxide-hydroxides), Rozenite and Siderotile.

3. Acknowledgements

To Paolo Forti, Carol A. Hill and Jacques Martini for their constant help and advice on cave mineralogy. To Wilmer Pérez, Carlos Galán, Joris Lagarde, Francisco Herrera, and the many others who collected minerals for study and/or accompanied the author in the cave trips. Very specially to Rafael Carreño who in the past few years has been my main supplier of the interesting but non-atractive "cave crusts".

4. References

BUZIO A. & P. FORTI. 1994. Las pisolitas negras de la cueva El Santuario, Santa Ana, estado Trujillo, Venezuela. *Bol. Soc. Venezolana Espeleol.*, (28):13-15.

FORTI P. 1994. Los depósitos químicos de la Sima Aonda Superior y de otras cavidades del Auyán-tepui, Venezuela. *Bol. Soc. Venezolana Espeleol.*, (28):1-4.

-----, A. ROSSI & F. URBANI. 1996. I fosfati della Cueva del Indio (Caracas, Venezuela). *Atti 17th Cong. Naz. Spel.*, Castelnuovo, Garfagnana, 1994, in press.

----- & F. URBANI. 1996. I nuovi minerali di grotta scoperti nella Cueva Alfredo Jahn (Venezuela). *Ibidem.*

GALAN C. & A. GALAN. 1983. Notas sobre la Sima fumarola de isla de Monos, N.E. de Venezuela. *Bol. Soc. Venezolana Espeleol.*, (20):3-9.

HEDGES J. 1993. A review on vermiculations. *Bol. Soc. Venezolana Espeleol.*, (27):2-6.

MARTINI J. 1980. Sveite, a new mineral from Autana Cave, Territorio Federal Amazonas, Venezuela. *Transactions Geological Society South Africa*, 83:239-241.

----- & F. URBANI. 1984. Sveita, un nuevo mineral de la cueva del Cerro Autana (Am.11), Territorio Federal Amazonas, Venezuela. *Bol. Soc. Venezolana Espeleol.*, (21):13-16.

PÉREZ F. 1978. Cuevas de hielo en el Parque Nacional 'Sierra Nevada', estado Mérida. *Bol. Soc. Venezolana Espeleol.*, 9(17): 104-106.

URBANI F. 1967. Venezuelan Cave Minerals. *Association William Pengelly Cave Research Centre, News* (London), (9):6-7. Reprinted in: *El Guácharo*, (5):15, 1968.

----- 1968. Calcite, aragonite and dolomite speleothems of the Baruta Cave, Venezuela (Abstract). *Geological Society of America, Annual Meeting*, New Orleans. *Abstracts with Program*. p. 226-227. Reprinted in: *El Guácharo*, 1(4):31; *The New York Caver*, 1(5):87.

----- 1973. Notas preliminares sobre varios tipos de espeleotemas localizadas en cuevas venezolanas. *El Guácharo*, 6(3-4):86-97.

----- 1974. Epsomita y hexahidrita en cuevas Venezolanas. *Bol. Soc. Venezolana Espeleologia*, 5(1):5-18.

----- 1975. Palygorskita en la cueva Las Úrsulas (Mi.47), Edo. Miranda. *Bol. Soc. Venezolana Espeleol.*, 6(11):5-12.

----- 1976. Opalo, calcedonia y calcita en la cueva del Cerro Autana (Am.11), Territorio Federal Amazonas, Venezuela. *Bol. Soc. Venezolana Espeleol.*, 7(14):129-145.

----- 1977a. Notas sobre algunas muestras de leche de luna de cuevas de Venezuela. *Bol. Soc. Venezolana Espeleol.*, 8(16):109-115.

----- 1977b. Espeleotemas de calcita (Lublinita), yeso y materiales de Guano, Cueva La Milagrosa, Monagas, Venezuela. *Bol. Soc. Venezolana Espeleol.*, 8(15):5-15

------ 1996a. El efecto del guano de murciélago en la radioactividad gamma ambiental de la cueva Ricardo Zuloaga, Miranda (Abstract). *XLVI Conv. Anual AsoVAC, Barquisimeto. Acta Cient. Venezez.*, 47(supl. 1):

----- 1996b. Espeleotemas de ópalo de origen biogénico en cavidades desarrolladas en rocas silíceas, Bolívar y Apure (Abstract). *XLVI Conv. Anual AsoVAC, Barquisimeto. Acta Cient. Venezez.*, 47(supl. 1):

-----, D. SOTO & E. DELGADO. 1995. Una ocurrencia de sepiolita y aragonito en la Cueva Ricardo Zuloaga, Peñón de las Guacas, Miranda (Abstract). *XLV Conv. Anual AsoVAC, USB. Acta Cient. Venez.*, 46(supl. 1):68-69.

-----, P. ZAWIDSKY & B. KOISAR. 1976. Observaciones geológicas de la meseta de Sarisariñama, Estado Bolívar. *Bol. Informativo Asociación Venezolana Geologia, Mineria y Petróleo*, 19(2):77-86.

WHITE W. B. 1981. Reflectance spectra and color in speleothems. *National Speleological Society Bulletin*, 44:90-97.

-----, J. F. HAMAN & G. L. JEFFERSON. 1963. Note on the mineralogy of Cueva del Guácharo. *Bol. Soc. Venezolana Ciencias Naturales*, 25(106):155-162.

Aragonite precipitation at Grotte de Clamouse (Herault, France): role of magnesium and drip rate

Silvia Frisia[1], Andrea Borsato[1], Ian J. Fairchild[2] and Antonio Longinelli[3]

[1]Museo Tridentino di Scienze Naturali, via Calepina 14, 38100 Trento, Italy; [2]Deptartment of Earth Sciences, Keele University, Staffordshire, ST5 5BG, U.K; [3]Dipartimento Scienze della Terra, Università di Trieste, Italy.

Abstract

Recent stalagmites and stalactites within Grotte de Clamouse (Southern France) are composed of both calcite and aragonite. Analyses of precipitating waters allowed us to relate the formation of aragonite to fluid with Mg/Ca ratio higher than 0.6, and to extremely low drip rates (less than one drop per hour). This last factor enhances degassing effects and subsequently increases the supersaturation state of the solution. Both the high magnesium content and the increased supersaturation favour the precipitation of the calcium carbonate metastable phase. Low drip rate is commonly related to a decrease in water availability within the karst system, i.e. to generalised dry conditions. In this perspective, aragonite is a good indicator of aridity.

Riassunto

La formazione di aragonite, la fase metastabile del carbonato di calcio, nelle stalagmiti della Grotte de Clamouse (Francia meridionale) è legata ad un rapporto Mg/Ca nelle acque di percolazione superiore a 0.6, abbinato a un gocciolamento molto lento (meno di una goccia per ora). Questo fatto promuove il degassamento facendo aumentare la sovrassaturazione dell'acqua. Sia l'elevato rapporto Mg/Ca, sia l'aumento della sovrassaturazione favoriscono la precipitazione dell'aragonite. Gocciolamenti molto lenti sono generalmente connessi alla diminuzione del volume d'acqua nell'acquifero, quindi a condizioni climatiche più secche. In quest'ottica l'aragonite si può ritenere un buon indicatore di aridità.

1. Introduction

In general, the precipitation of aragonite, the unstable $CaCO_3$ polymorph, both in the marine and continental environments appears to be related to kinetic factors and temperature (BERNER, 1975; MORSE & MACKENZIE, 1990). A most important inhibitor in the precipitation kinetics of calcite is the high Mg^{2+} concentration in the solution, whereby an elevated Mg/Ca ratio of the parent fluid favors the nucleation and growth of aragonite (MUCCI & MORSE, 1983; GONZALEZ & LOHMANN, 1987). As for temperature, above 25°C aragonite precipitation rates are much faster than those of calcite, except for very low saturation states (BURTON & WALTER, 1987).

Formation of aragonite at surface temperatures in continental settings is relatively common in caves (CABROL, 1978; GONZALEZ & LOHMANN, 1987; BAR-MATTHEWS *et al.*, 1991; RAILSBACK *et al.*, 1994) and subglacial deposits (FRISIA & BORSATO, 1994) in dolomitic terrains. Although aragonite may precipitate in low temperature caves (4° to 7° C; CABROL, 1978; HARMON *et al.*, 1983), massive aragonite formation is typical of warmer caves (T° > 12°C) such as those in southwestern U.S.A. (MURRAY, 1954), southern France (CABROL, 1978; CABROL & COUDRAY, 1982), southern Spain (CARRASCO CANTOS ed., 1993).

Recently, the presence of aragonite in speleothems has been related to a combination of increase in Mg concentration, evaporation, decrease in drip rate, and increase in temperature (RAILSBACK *et al.*, 1994). All these factors commonly combine in dry seasons or in dry and warm years.

At Grotte de Clamouse, both acicular and massive aragonite occur (FRISIA & BORSATO, 1997a). At present, massive aragonite forms only tiny stalagmites, whereas in the past it gave rise to huge speleothems. Furthermore, many acicular aragonite is being weathered or replaced by calcite.

In this study we present the results of our investigation at Grotte de Clamouse about the possible physico-chemical parameters that favour both the precipitation and preservation of the unstable $CaCO_3$ polymorph.

2. Present-day environmental setting

The Grotte-exurgence de Clamouse (Latitude 43°42'33" N, Longitude 3°36'50" E, elevation 75 m a.s.l.) is located 30 km west of Montpellier (Herault, southern France), on the right bank of the Herault River, 3 km south of the village of Saint Guilhem-le-Désert and opens at the southern margin of Causse de la Selle, a series of low-elevation calcareous reliefs.

The cave exhibits about 3,500 m of explored galleries arranged in three different levels (CHOPPY & DUBOIS, 1974). The non-touristic part of the upper level consists of a large WSW-trending subhorizontal gallery (mean diameter about 10 m), about 800 m long (*Grande Galerie*), which developed about 100 m below the surface.

Most of the cave is cut in Middle Jurassic (Bathonian) variably dedolomitized oolitic dolostones with high intercrystalline porosity. Speleothems are most abundant and spectacular, in passages cut in coarsely crystalline, polymodal, calcian (54 to 56 % $CaCO_3$) dolomite. The wealth of speleothems in these galleries may relate to the hydrological properties of the porous dolomite, such as storage of waters during floods and release of these waters during droughts. The dolomite-rich passages are also those which host aragonite speleothems.

On dolomite bedrock soils are shallow and rendzina-like. The present-day vegetation, typically mediterranean, is a *Garrigue* with *Quercus coccifera*, *Erica multiflora*, thyme, rosemary, lavander and juniper. This association is typical of calcareous substrate in arid (xerophile) regions.

Present-day climate in the area is sub-humid mediterranean, characterized by strong seasonal contrasts which increase from the coast (Montpellier) to the foothills which are subjected to alternating periods of drought and floods. The records from Aniane stations (68 m a.s.l., 3 km SE from the cave), show a mean annual precipitation of 791 mm/year, and a mean annual temperature of 14.1°C. The most striking feature in the climate of the Herault province is the summer dryness, which, when coupled with high evapotranspiration, yields a high water deficit during June, July and August.

3. Methods

The first part of the *Grande Galerie*, between the *Salle des Cloches* and the *Balcon,* is richly decorated by both aragonite and calcite speleothems, and identifies a stable environment which is not disturbed by touristic visits. Therefore, it is a suitable study reach to investigate the spelean environment.

In order to understand the present-day conditions underpinning the formation of massive aragonite (i.e. aragonite stalagmites) we analysed the chemistry and measured the drip-rate of several stalactite drips feeding both calcite (stalactites D1, C2, C12 and C16) and aragonite (stalactite D6) speleothems from June '95 to November '96.

The water chemistry was subsequently compared with the chemistry (isotope, major and trace element composition) of the precipitating carbonates. In all cases, dripwater was sampled just below the stalagmite tip, before any calcium carbonate precipitation occurred at the stalagmite tip.

At the same time, one soda straw drip from *Salle des Cloches* was monitored for conductivity and temperature. During the whole 1995-1996 period, conductivity fluctuated between 335 and 390 µS/cm (referred to 20°C), whereas temperature remained remarkably stable at 14.5 (+/-0.02)°C. Relative humidity is almost at saturation state (from 97.5 to 99%), and the *Salle* is not subjected to measurable air flow.

Stalactites were collected and observed by scanning electron microscopy to detect crystal habit and ongoing replacement phenomena. Mineralogy was determined by X-ray diffraction on powder. Major and trace elements were measured by inductively coupled plasma atomic absorption spectrometry at University of Birmingham; carbonate stable isotopes were analysed by mass spectrometry at Università di Trieste.

4. Results

The drip rates of the four low discharge soda straws (D6, C16, D1 and C12) had a constant discharge of 0.00034, 0.0065, 0.053, and 0.03 ml/minute respectively and did not seem to be influenced by the rainfall pattern. On the contrary, the fast dripping cone stalactite C2, had a mean discharge of 1.29 ml/minute, with fluctuation between 1 and 5.2 ml/minute which depended on the time elapsed from a major rainfall event.

The comparison between Mg/Ca ratio and drip rates throughout the year (Fig. 1) indicates that the Mg/Ca ratio remains fairly constant for drips from 10 to 0.01 ml/minute. For lower drip rates, the Mg/Ca ratio increases up to a maximum of 0.8 recorded by the D6 stalactite, which feeds an aragonite stalagmite. Therefore, at Grotte de Clamouse, the calcite and aragonite field can be identified by two boundaries: i) drip rates lower than 0.003; ii) Mg/Ca ratios higher than 0.62.

The comparison of Mg/Ca and Sr/Ca ratios in both waters and carbonates (Fig. 2) reflects the weathering of the host rock and the residence time of the water which reaches the stalactites feeding both calcite and aragonite. The strong covariation of Sr and Mg of different cave waters is readily explained by the progressive precipitation of calcite with much lower Sr/Ca and Mg/Ca than the parent waters, leaving the waters with enhanced Sr/Ca and Mg/Ca. Waters precipitating aragonite are at the upper end of this trend. Different cave rooms show strong Mg/Ca-Sr/Ca variations, but are offset in Mg, reflecting varying dolomite contents of the overlying aquifer.

Another factor affecting chemistry is the residence time of water in the system. Many karst systems have both dolomite and calcite present along the water flowpath, but the kinetics of the dolomite component dissolution are significantly slower than that of the calcite component (see FAIRCHILD *et al.*, 1996).

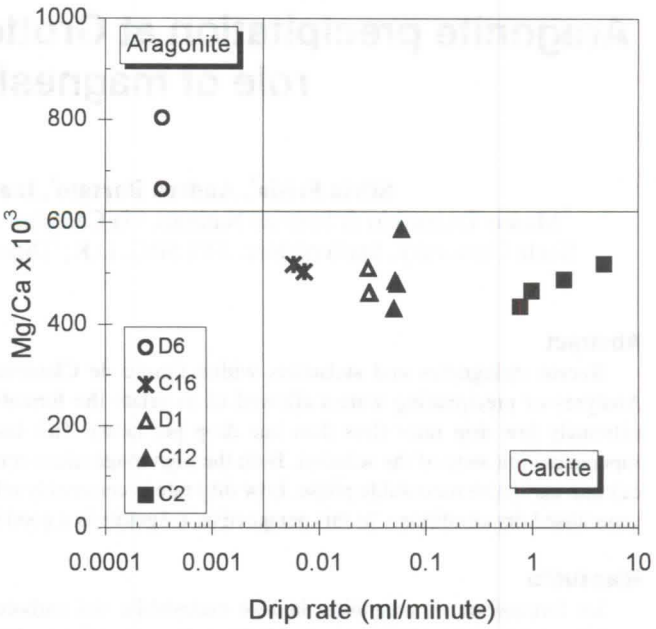

Fig. 1: Drip rates and Mg/Ca molar ratio from five stalactites feeding active calcite (C2, C12 C16, and D1) and aragonite (D6) stalagmites in Salle des Cloches (samples "C") and the Balcon (samples "D"). The vertical and horizontal lines define the stability fields for Grotte de Clamouse calcite and aragonite (see text for details).

Given a long residence time of water in contact with carbonate minerals, the solution should become enriched in solutes and Mg/Ca should rise because of enhanced dolomite dissolution. This should occur even if the waters rapidly reach equilibrium with calcite because the solution will still be undersaturated for dolomite (ATKINSON, 1983). Therefore, even at a given point with a fixed ratio of calcite to dolomite along the flowpath, higher Mg/Ca ratio in Grotte de Clamouse seepage waters would be expected if the residence time of water in the dolomite host rock was prolonged. In this case, the host rock calcites have less Sr than the dolomites, so that differential dissolution of calcite and dolomite also gives rise to Mg-Sr covariations.

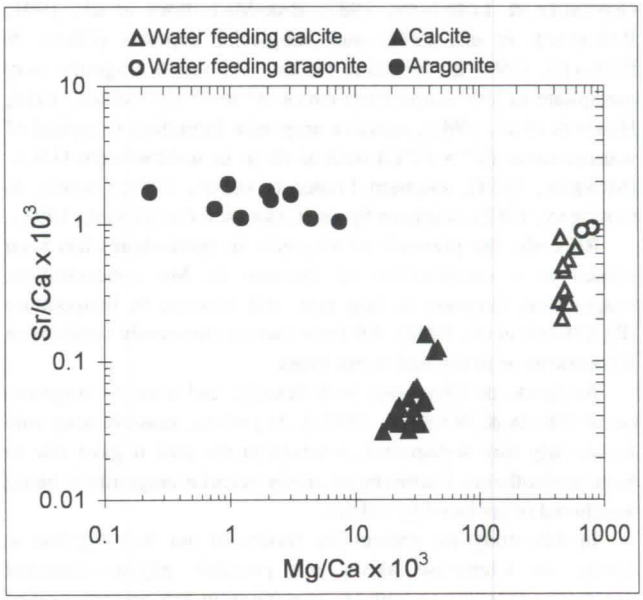

Fig. 2: Crossplot of Sr/Ca and Mg/Ca ratios of stalactite dripwaters and the associated carbonates.

As for the $CaCO_3$ precipitates, the aragonites exhibit Sr-enriched Mg-depleted chemistry, as expected from their partition coefficients (MORSE & MACKENZIE, 1990). The fact that aragonites show similar Sr/Ca ratios to water around the top of the Sr-Mg covariation (open circles in Fig. 2) implies, given the partition coefficient of around 1 for Sr in aragonite, that they formed from such end-member waters.

The stable isotope composition of calcite and aragonite informs on the precipitation mechanisms. In fact, fluid degassing results in enrichment in $\delta^{13}C$, whereas evaporation results in increase in $\delta^{18}O$. When these two mechanisms combine, there is a covariant increase of both (GONZALEZ & LOHMANN, 1987; BORSATO *et al.* 1996). The slope of the regression line depends on which of the two mechanisms is dominant. The stable isotope composition of aragonite is enriched with respect to calcite in both $\delta^{13}C$ and $\delta^{18}O$ (Fig. 3). This enrichment is, in two samples, of up to 9‰ for $\delta^{13}C$, and up to 2.5‰ for $\delta^{18}O$, values that greatly exceeds the expected $\delta^{13}C$ and $\delta^{18}O$ enrichment factor for aragonite with respect to calcite (TARUTANI *et al.*, 1969; MORSE & MACKENZIE, 1990). Consequently, for aragonite precipitation to occur, degassing must be prolonged and possibly accompanied by evaporation.

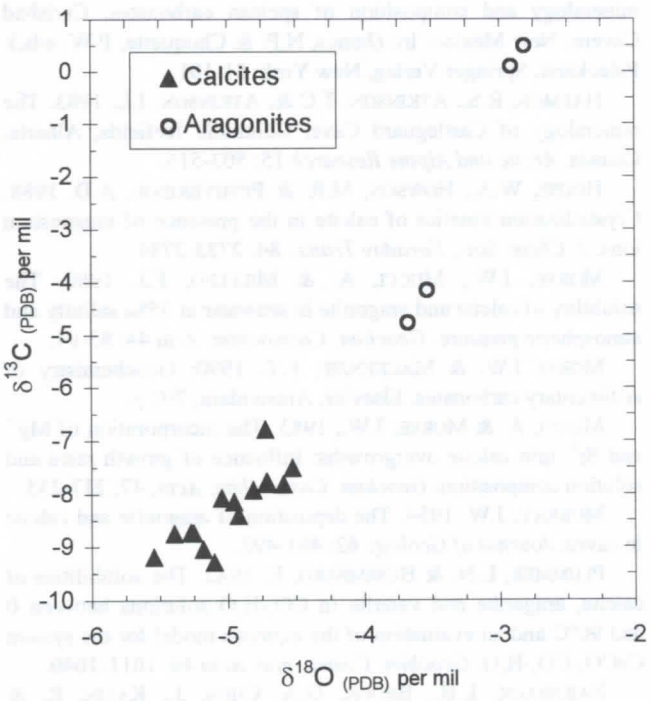

Fig. 3: Stable isotopic composition of modern stalagmites and stalactites. The aragonite samples are strongly enriched in $\delta^{13}C$ with respect to $\delta^{18}O$. This fact testifies to the prevalence of degassing on evaporation effect (see text).

5. Discussion

At Grotte de Clamouse, massive aragonite forms for drip rates lower than 0.003 ml/min and Mg/Ca ratios higher than 0.62. Temperature does not seem to play a role in controlling aragonite and calcite precipitation, as both polymorphs form in the same passage. Although the role of temperature was assessed by experiments carried out at fixed intervals, i.e. 5°C, 25°C and 37°C (BURTON & WALTER, 1987), by extrapolation of the experimental datasets for 5° and 25°C it results that above about 12°C aragonite has a precipitation rate higher than calcite. It is worth mentioning that these precipitation rates are partially controlled by the carbonate ion concentration only at very low saturation state, i.e. within the range of cave dripwaters in temperate settings.

It is, therefore, probable that the interval between 12° to 15°C identifies the "activation temperature" zone for the precipitation of aragonite. Within this interval, the controlling factors on the precipitation of one or the other of the two polymorphs can be related both to kinetic effects and to thermodynamic equilibrium. In fact, it should be emphasized that an equilibrium can be established between a metastable phase and its environment because of kinetic reasons, given the fact that the Gibbs free energies of formation for calcite and aragonite differ only by -1 kJ/mole (PLUMMER & BUSEMBERG, 1982; MORSE *et al.*, 1980). This small free energy difference is sufficient for aragonite and calcite to coexist. Consequently, given the same temperature of formation, and the small energy difference which would allow aragonite to precipitate in the same environmental conditions as calcite, we are now confronted with the understanding of the possible mechanisms influencing aragonite nucleation and growth at Clamouse. Our analytical results suggest the following effects:

1) ***Increasing concentration of Mg in the solution*** actually favours aragonite formation. This datum supports experimental studies which indicate that Mg^{2+} inhibits calcite nucleation and growth as a result of either crystal poisoning or difficulties in rapid dehydration of the Mg^{2+} ion. In other words, the presence of magnesium, which is adsorbed by calcite and much less by aragonite, directly affects calcite growth rate by the two aforementioned mechanisms, and, therefore, indirectly favours the formation of aragonite. However, the Mg/Ca ratios in Clamouse waters are not high in absolute terms, and are lower than those responsible for the precipitation of moderate to high-Mg calcites elsewhere in the field and by experiment in low ionic strength solutions (HOUSE *et al.*, 1988; CIDU *et al.*, 1989). Consequently, we believe that the high Mg/Ca ratio of the parent fluid is not necessarily the major cause of aragonite precipitation at Clamouse. This inference is supported by recent experiments on the controls of $CaCO_3$ polymorphism which indicate that extraneous ions, such as magnesium, are not required to induce calcite or aragonite to form *in vitro*, and polymorph formation could be a function of the structure of the nucleation sites (FALINI *et al.*, 1996).

2) ***Dramatic decrease in drip rate and related degassing.*** Stalactites feeding aragonite stalagmites yield one drop each hour or less. Therefore, each drop has sufficient time to degas completely, as indicated by the heavier $\delta^{13}C$ values. Progressive degassing increases the pH of the drip water and, consequently, the carbonate ion concentration (CO_3^{2-}) and the degree of supersaturation with respect to calcite. Although the supersaturation of both calcite and aragonite is increased, the effect is greater on aragonite because it is a more soluble phase.

3) ***Evaporation*** effects. Evaporation has been inferred on the basis of the observed $\delta^{18}O$ enrichment. However, the study reach is protected from air currents and the relative humidity is about 99% throughout the year. This would make evaporation difficult. An alternative hypothesis is that the oxygen isotope enrichment is also related to kinetic effects. Unfortunately, no data are available as yet on the complexity of kinetic fractionation during diffusion of ions across the crystal surface for oxygen isotopes. Following the model proposed by Turner (1982), it is possible that kinetic effects on oxygen isotope fractionation are twice that of carbon isotope fractionation. Consequently, at the present state

of knowledge it cannot be stated that evaporation has a major role in aragonite formation.

6. Conclusions

Aragonite formation at Clamouse is probably related to the combination of high Mg/Ca ratio and slow, prolonged degassing due to low drip rate. Of the two, degassing may actually control which polymorph precipitates from the solution at the temperature of the cave. The prolonged residence time of the water in the aquifer is the consequence of slow drip rate and causes the increase of Mg/Ca ratio in dripwater. At present, this happens in only few places and, in fact, most of the aragonite is being replaced by calcite under conditions of higher drip rates (FRISIA, 1996; FRISIA & BORSATO, 1997b). Therefore, the present can be considered as a relatively humid, "calcite" period in contrast to the time when aragonite was ubiquitous in the galleries cut in dolomite of the cave. The past precipitation of massive aragonite throughout most of Clamouse should, consequently, be related to dramatic decreases in drip rates in most of the passages. This phenomenon occurs when water availability at a regional scale decreases, so we can confidently relate aragonite to relatively more arid time spans. Therefore, the presence of aragonite in speleothems can be used as a reliable paleoaridity indicator.

Acknowledgements: This work is part of the CEC project contract EV5V CT94-0509. The authors wish to thank Paul Dubois and Jacques Choppy for their enthusiasm about our work, and E.M. Selmo for stable isotope laboratory work.

References

ATKINSON, T.C. 1983. Growth mechanisms of speleothems in Castleguard Cave, Columbia Icefield, Alberta, Canada. *Artic and Alpine Research* 15: 523-536.

BAR-MATTHEWS, M., MATTHEWS, A. & AYALON, A. 1991. Environmental controls of speleothem mineralogy in a karstic dolomitic terrain (Soreq Cave, Israel). *Journal of Geology* 99: 187-207.

BERNER, R.A. 1975. The role of magnesium in the crystal growth of aragonite and calcite from seawater. *Geochim. Cosmochim. Acta* 39: 489-504.

BORSATO, A., SPIRO, B., LONGINELLI, A. & HEATON, T. 1996. Isotopic composition of present-day alpine speleothems from Trentino (NW Italy): a key for palaeoclimatic interpretations in ancient speleothems. In: (Lauritzen, S.E.,ed.): *Climate Change:- The Karst Record* KWI Spec. Publ 2, Bergen: 16-17.

BURTON, E.A. & WALTER, L.M. 1987. Relative precipitation rates of aragonite and Mg calcite from seawater: Temperature or carbonate ion control? *Geology* 15: 111-114.

CABROL,P. 1978. Contribution à l'etude du concretionnement carbonaté des grottes du sud de la France, Morphologie, Genese et Diagenese. C.E.R.G.A. Memoires, XII, Montpellier, 275 p.

CABROL, P. & COUDRAY, J. 1982. Climatic fluctuations influence in the genesis and diagenesis of carbonate speleothems in southwestern France. *Nat. Spel. Soc. Bulletin* 44: 112-117.

CARRASCO CANTOS, F.(ed.) 1993. Geologia de la Cueva de Nerja, *Trabajos Sobre la Cueva de Nerja* 3, Màlaga, 354 p.

CHOPPY, J. & DUBOIS, P. 1974. La Grotte de Clamouse. *Saint Guilhem le Desert et sa region*, Millau: 34-45.

CIDU, R., FANFANI, L., ZUDDAS, P. & ZUDDAS, P.P. 1989. Travertines: Distribution coefficients of divalent cations between calcites and depositing waters. In: (Miiles, D.L. ed.): Water-Rock Interaction WRI-6, Proceedings of the 6th International Symposium on water-Rock Interaction, Malvern. A. A. Balkema, Rotterdam: 163-166.

FAIRCHILD, I.J., TOOTH, A.F., HUANG, Y., BORSATO, A., FRISIA, S. & MCDERMOTT, F. 1996. Spatial and temporal variations in water and stalactite chemistry in currently active caves: a precursor to interpretations of past climate. In: (Bottrell, S.,ed.) : *Proceedings of the fourth International Symposium on the Geochemistry of the Earth's Surface, Ilkley, Yorkshire, July 1996* . University of Leeds: 229-233.

FALINI, G., ALBECK, S., WEINER, S. & ADDADI, L. 1996. Control of Aragonite or Calcite Polymorphism by Mollusk Shell Macromolecules. *Science* 271: 67-69.

FRISIA, S. 1996. Petrographic evidences of diagenesis in speleothems: some examples. *Speleochronos* 7: 21-30.

FRISIA, S. & BORSATO, A. 1994. Composizione, precipitazione e dissoluzione di carbonati subglaciali nelle Dolomiti di Brenta. *Acta Geologica* 69 (1992): 37-50.

FRISIA, S. & BORSATO, A. 1997a. Les concretions d'aragonite de la Grotte de Clamouse. In: (Dubois P. & Choppy J., eds.): *Clamouse, 50 ans apres la decouverte*, Monpellier, (in press)

FRISIA, S. & BORSATO, A. 1997b. Speleothem textures and microstructures: growth mechanisms and their environmental significance. *Zeitschrift fuer Geomorphologie* (in press).

GONZALES, L.A. & LOHMANN, K.C. 1987. Controls on mineralogy and composition of spelean carbonates: Carlsbad Cavern, New Mexico. In: (James, N.P. & Choquette, P.W. eds.): Paleokarst, Springer Verlag, New York: 81-101.

HARMON, R.S,. ATKINSON, T.C &. ATKINSON, J.L. 1983. The mineralogy of Castleguard Cave, Columbia Icefields, Alberta, Canada. *Arctic and Alpine Research* 15: 503-516.

HOUSE, W.A., HOWSON, M.R. & PETHYBRIDGE, A.D. 1988. Crystallization kinetics of calcite in the presence of magnesium ions. *J. Chem. Soc., Faraday Trans.*. 84: 2723-2734.

MORSE, J.W., MUCCI, A. & MILLERO, F.J. 1980. The solubility of calcite and aragonite in seawater at 35‰ salinity and atmospheric pressure. *Geochim. Cosmochim. Acta* 44: 85-94.

MORSE J.W. & MACKENZIE, F.T. 1990: Geochemistry of sedimentary carbonates. Elsevier, Amsterdam, 707 p.

MUCCI, A. & MORSE, J.W., 1983. The incorporation of Mg^{2+} and Sr^{2+} into calcite overgrowths: influence of growth rates and solution composition. *Geochim. Cosmochim. Acta*, 47: 217-233.

MURRAY, J.W. 1954. The deposition of aragonite and calcite in caves. *Journal of Geology* 62: 481-492.

PLUMMER, L.N. & BUSEMBERG, E. 1982. The solubilities of calcite, aragonite and vaterite in CO_2-H_2O solutions between 0 and 90°C and an evaluation of the aqueous model for the system $CaCO_3$-CO_2-H_2O. *Geochim. Cosmochim. Acta* 46: 1011-1040.

RAILSBACK, L.B., BROOK, G.A, CHEN, J., KALIN, R. & FLEISHER, C.J. 1994. Environmental controls on the petrology of a Late Holocene speleothem from Botswana with annual layers of aragonite and calcite. *Jour. Sedim. Res.* A64:147-155.

TARUTANI, T., CLAYTON, R.N. & MAYEDA, T.K. 1969. The effects of polymorphism and magnesium substitution on oxygen isotope fractionation between calcium carbonate and water. *Geochim. Cosmochim. Acta* 33: 987-996.

TURNER, J.V. 1982. Kinetic fractionation of carbon-13 during calcium carbonate precipitation. *Geochim. Cosmochim. Acta* 46: 1183-1191.

Aragonitic/Calcitic Coralloids in Carbonate Caves: Evidence for Solutions of Different Mg Influence

by Stefan Niggemann, Dirk Habermann, Rainer Oelze und Detlev K. Richter
Institut für Geologie, Ruhr Universität Bochum, Universitätsstr. 150, 44780 Bochum, Germany

Abstract

Cave coralloids formed under subaerial conditions are precipitations from aerosolian waters with different contributions of capillary supplied aqueous solutions. Samples from limestone caves in the Sauerland, dolostone caves in the Eifel (both in Germany) as well as from rock niches of South Tyrolian dolostone areas (Italy) were examined using SEM, cathodoluminescence and X ray diffraction. The coralloids contain a µm scale lamination. The Mg content of the coralloid calcite shows a positive correlation with the Mg content of the host rock. In addition to high Mg calcite, aragonite and hydrated carbonates are common mineral phases in caves within more strongly dolomitised host rocks. The mineralization of aragonite and magnesian calcite is due to precipitation from the remaining solutions with higher Mg concentrations. Higher temperatures near the entrance of the caves produce an additional effect.

Zusammenfassung

Subaerische Koralloide (Knöpfchensinter etc.) in Höhlen sind Aerosolbildungen mit unterschiedlich starker Beteiligung kapillarer Zulieferung wäßriger Lösungen. Koralloidproben aus Kalkhöhlen des Sauerlandes und Dolomithöhlen der Eifel sowie Felsnischen im Dolomitgestein Südtirols wurden rasterelektronen- und kathodolumineszenzmikroskopisch sowie röntgendiffraktometrisch untersucht. Die Koralloide weisen einen intensiven Lagenbau im µm-Bereich auf. Der Gehalt an Mol-%-$MgCO_3$ im Calcit der Koralloide ist positiv korreliert mit dem pauschalen Mg-Gehalt des Wirtsgesteins. In Höhlen mit stärkerer Dolomitbetonung treten zusätzlich zu Höchst-Mg-Calciten Aragonit und wasserhaltige Karbonate als Mineralphasen auf. Die Mineralisation von Aragonit und Mg-reichen Calciten wird bei den Speläothemen auf eine Bildung aus Restlösungen zurückgeführt. Lokal stellen höhere Temperaturen in eingangsnahen Höhlenpassagen einen Zusatzeffekt dar.

1. Introduction

Small and breakable subaerial speleothems – with the exception of helictites or anthodites – are called subaerial coralloids. They are precipitations from aerosolian waters with different contributions of capillary aqueous solutions. Consequently, the origin of coralloids is influenced by the host rock composition and weathering. Figure 1 shows a formation model.

Our study refers to speleothems from caves in limestone areas of the Sauerland and in dolomitic areas of the Eifel and of South Tyrol (see Fig. 2).

2. Methods

SEM examinations of the surfaces of coralloids and fractures were performed using a Cambridge Stereoscan 250 MK 3.

The mineralogy of phases were determined using a Philips X ray goniometer PW 1050/25 at 40 kV and 35 mA with a 2200 W "Langfeinfokus" CuKα tube and a Ni filter respectively an AMR Monochromator. Ca and Mg concentrations were determined routinely. A linear shift of $d_{(104)}$ between 3,035 Å (calcite), 2,886 Å (dolomite) and 2,742 Å (magnesite) under admixture of an internal quartz standard was assumed (FeO<0,5 Weight.-%; FÜCHTBAUER & RICHTER, 1988: 242).

For CL investigations a "hot" cathode luminescence microscope HC1-LM was used. CL spectra were recorded with a digitally controlled EG & G spectrograph attached to a nitrogen-cooled CCD camera (see NEUSER et al., 1996 for further details).

C and O isotope ratios were determined using a Finnigan MAT 251 gas mass spectrometer with "triple collector". Data were corrected to reaction temperatures of 25 °C and calibrated against PDB (see BRUCKSCHEN et al., 1995).

3. Formation and composition

Morphology

The mm^3 to cm^3 sized coralloids are mostly spherical or mushroom-like projections (Fig. 3) in areas of caves and niches which had strong draughts. Central deepenings and rimmed edges are frequent features on the coralloid tops. Lichen or ledge-like formations are also widespread.

The surface of the coralloids from the Sauerland caves is often formed by relatively smooth faces. These planes seem to be cut and are independent from crystal faces. Crystal faces are only developed in lateral notches between individual crystals. They are steep rhomboedric in the case of calcite and prismatic in aragonite. The crystals often contain recesses, a fact that can be explained by temporal corrosion or by fast, skeletal growth.

Even in the µm-scale the surfaces of the coralloids from the Munterlei Plateau (3), and particularly those from the Grauner Walls (4), are irregular. When thin sections of coralloids were observed petrographically, it was evident that the outer laminations were cryptocrystalline. This formation is probably caused by a change of fast crystal growth at high nucleation rates (constructive phase) and corrosion (destructive phase). The occurrence of pollen shows that organic material was important.

Internal structure

The coralloids examined display a strong, µm-scaled lamination structure. The lamination in the coarser crystalline, pure calcitic coralloids from the Ostenberghöhle (1) is characterized by changes in the abundance of inclusions. This lamination is independent of the crystallographic orientation and reproduces a smooth but curved surface in accordance with the morphology of the coralloids. The inclusion tracks reflect former adhesive water stages ("meniscus outlines"), a fact that is typical for subaerial speleothems (e.g. MERGNER et al., 1992). These authors report the possibility that this intracrystalline inclusion arrangement can be confused with an "in situ" calcitization of aragonite.

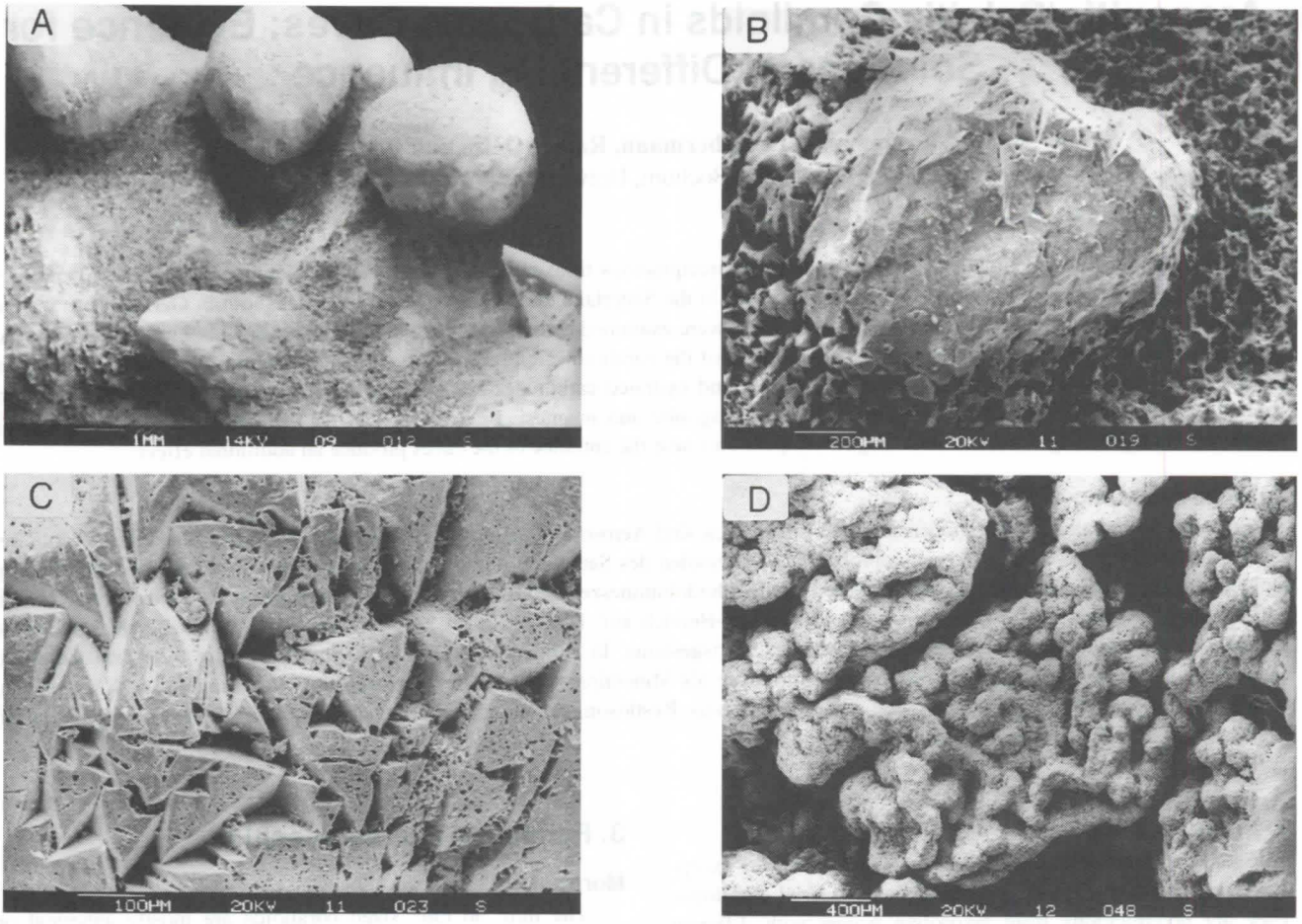

Figure 3: SEM- photographs of coralloids. A: Coralloid aggregate from the Ostenberghöhle (1). B: Single coralloid from (1). C: Surface of the coralloid (1) showing intracrystalline hollow structures. D: Lichen-like coralloid from the Grauner Walls (4).

the host rock. So we believe that there is a detrital origin for dolomite particles found within the speleothems (cf. cathodoluminescence).

Cathodoluminescence

The cathodoluminescence characteristics of water-free carbonate phases combined with high resolution spectral analyses yields the following additional information on the mineralization of coralloids (cf. Fig. 5):

a. Independent of the Mg content, the calcites show a blue ("intrinsic") luminescence likely produced by structural crystal imperfections and not by activator elements like Mn^{2+} or REE^{3+}. The emission spectra of the intrinsic CL are characterized by 5 maxima of the wide band with wave lengths between 400 nm and 660 nm. Due to the general origin of speleothems from meteoric waters with oxidizing conditions an intrinsic CL characteristic should be expected (but see b-d).

b. Thin laminae of the calcitic parts are orientated parallel to the growth front of the coralloids. These layers are independent of the orientation of the calcite crystals reflecting a growth limitation by adhesive water. Free calcite growth could not be seen on the coralloids. The laminae luminesce dull orange. Emission spectra of these zones show a maximum of the wide bands at ~605 nm proving the fitting of Mn^{2+} in the Ca position of the calcite. With increasing Mg content of the calcite the wide band maximum shifts to higher wave lengths up to 630 nm (cf. HABERMANN et al., 1996).

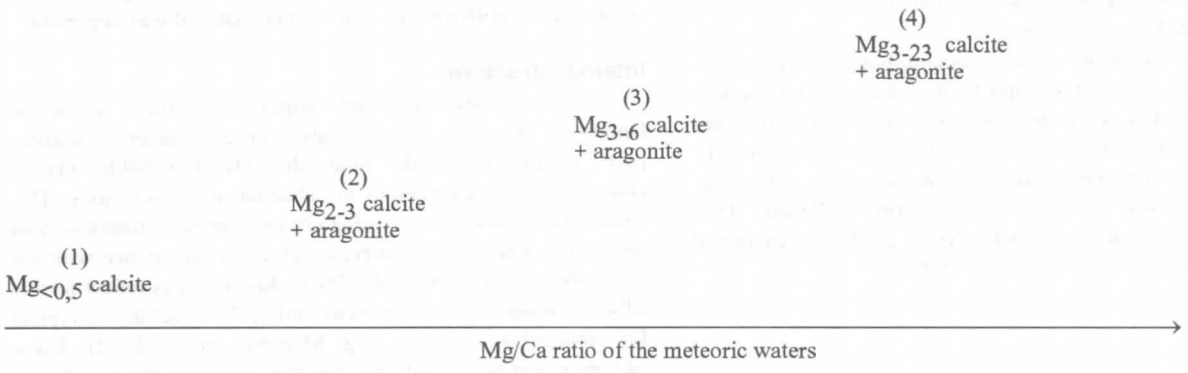

Figure 4: Chemical composition of aragonite and calcite in the examined coralloids (localities 1 to 4). Mg values represent the range of the measured data.

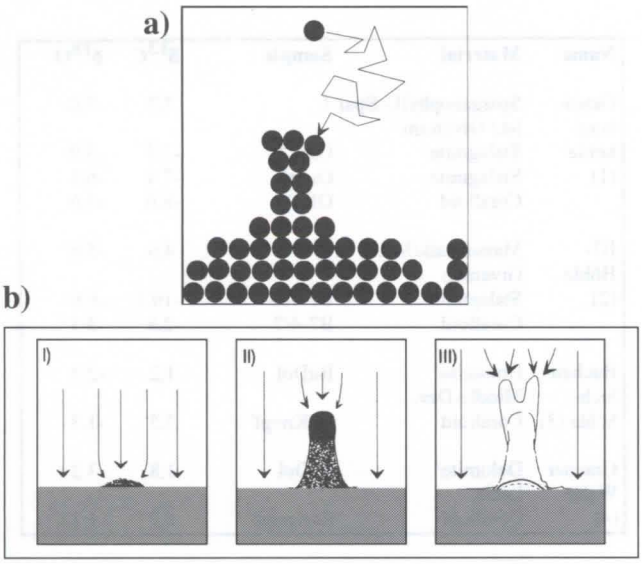

Figure 1: Model explaining the growth of subaerial coralloids with diffusion limited deposition of aerosolian particles (OELZE, 1993). These particles, moving irregularly on random tracks (a), more probably hit a projection than a depression (b). Thus, projections develop to coralloids (I to III).

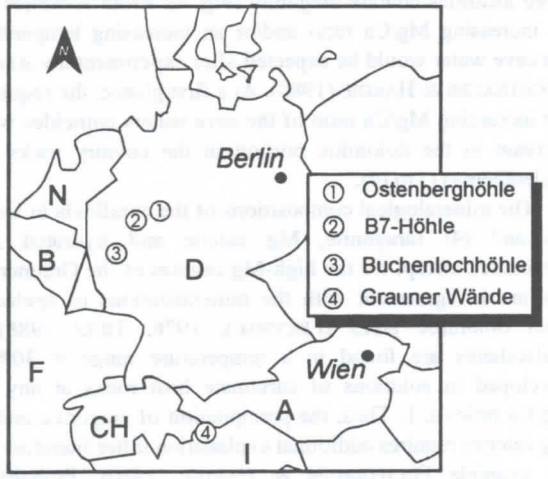

Figure 2: Locations of the four coralloid occurrences.
1= Ostenberghöhle near Bestwig (Sparganophyllum Limestone, Givetium), 2 = B7-Höhle near Iserlohn (Givetian Massive Limestone and hydrothermal dolomites), 3 = Buchenlochhöhle at Munterlei Plateau, Gerolstein (Devonian dolomites), 4 = Rock niche at Grauner Walls, South Tyrol (Ladinian dolomites).

As a rule, fine crystalline calcitic and coarser crystalline aragonitic layers can be distinguished microscopically in coralloids from the B7-Höhle (2) and from the Munterlei Plateau (3). The aragonitic layers are mainly composed of fans of varying thicknesses. In transmitted light, a light-dark change, reflecting differences in crystal growth, can be observed. This feature exists even in calcite internal parts and is reminiscent of stromatolites.

Coralloids from the Grauner Walls (4) are fine crystalline ("cryptocrystalline" - Ø <10 µm) and a layered structure was only rarely observed. The formation of these coralloids is reminiscent of the "cauliflower" structures seen in dolomitic caves of the Fränkische Alb (South Germany) described by FISCHBECK & MÜLLER (1971).

Mineralogical and chemical composition

The coralloids from the Ostenberghöhle (1) are exclusively composed of calcite. The $d_{(104)}$ data of 3,035 - 3,032 Å show very low Mg contents (≤ 1 mole-% $MgCO_3$, Fig. 4) and thus a nearly stoichiometric composition. Finding relatively pure calcite phases was not unexpected as the Sparganophyllum Limestone host rock comprised of calcite of nearly stoichiometric composition. This statement is compatible with molar Mg/Ca-ratios of 0,07 to 0,14 determined in cave water by OELZE (1993).

The $d_{(104)}$ data of coralloid calcite from the B7-Höhle (2; 3,033 - 3,023 Å) are shifted towards increased mole-% $MgCO_3$ (0,7 - 4,0; Fig. 4). In these samples aragonite is found among calcite. The Mg calcite as well as the aragonite are not compatible with the Iserlohn Massive Limestone composed of nearly stoichiometric calcite. The speleothem composition results from hydrothermal dolomitization zones developed in the sampling area. Hence, in comparison with pure limestone areas the Mg/Ca ratios of cave waters are increased so that Mg containing calcite and aragonite can develop (cf. FÜCHTBAUER & RICHTER, 1988). But molar Mg/Ca ratios of cave waters distinctly remain < 1 in calcite/dolomite mixed rocks. So coralloids from the B-7-Höhle probably precipitated from remaining concentrated solutions (see chap. 3).

Calcite, aragonite and hydrated Ca/Mg carbonates can be determined by X-ray diffraction of coralloid samples from the Buchenlochhöhle (3). The $d_{(104)}$ values of the main calcite phases correspond with $Mg_{2,3\text{-}7,1}$-calcites (Fig. 4). In contrast to pure calcite phases, an increasing peak asymmetry towards lower d values demonstrates a more Mg-rich calcite in the Buchenlochhöhle samples. Thus, in one sample this Mg-richer calcite phase exists beside the calcite phase of the higher intensity. This is also expressed in the width at quarter height (= peak sharpness) of the $d_{(104)}$ reflexes. These amount to about 5 mm for calcites of stoichiometric composition with width at half height of an external driven quartzite standard -$d_{(100)}$ quartz- of 3,1 ± 0,1 mm (after RICHTER, 1984: 21). In contrast, the width at quarter height of the $d_{(104)}$ calcites of coralloids from the Buchenlochhöhle reach a maximum value of 10 mm.

The Mg/Ca content of coralloids from the Munterlei Plateau match the mineralogical composition of speleothems from dolomitic caves of the Fränkische Alb (cf. TIETZ, 1988). Only the high Mg calcites need an additional explanation because they are not recorded as discrete phases. Possibly, on hot summer days the draughty cave galleries near the entrances of the Munterlei Plateau undergo an exchange of cold air inside with warm air outside, so that secondary calcite phases with higher Mg contents may develop.

The Mg contents of coralloids from the Grauner Walls (4) vary widely between 3 and 24 mole-% $MgCO_3$ (Fig. 4). There are accumulations of discrete phases for $Mg_{3\text{-}7}$ and $Mg_{15\text{-}22}$ calcites with two maximum peaks in the same sample. Beside the Mg-calcitic phases changing contents of secondary aragonite, monohydrocalcite, nesquehonite and hydromagnesite can be found. Some samples also contain a dolomitic phase with 49-51 mole-% $MgCO_3$.

Except for the highest Mg calcite the mineralogical composition of the South Tyrolian coralloids coincides with the mineralogical composition of speleothems from dolomitic caves of the Fränkische Alb reported by FISCHBECK & MÜLLER (1971) und TIETZ (1988). Probably the Mg richer calcites are caused by stronger weathering of the niches above the Reschen Lake and by temporary higher temperatures (i.e. hot summer days). The latter effect corresponds with the synthesis of Mg calcite described by FÜCHTBAUER & HARDIE (1980). The stoichiometric dolomite of the coralloids are in accordance with the dolomite composition of

c. The calcitic coralloids of the Ostenberghöhle (1) contain thin, pale-blue to violet zones. The emission spectra of these zones show typical narrow bands indicating the occurrence of Sm^{3+} (peaks at 562, 598/604, 652, 662 and 708 nm), Tb^{3+} (peak at ~545 nm) and Dy^{3+} (peaks at 486, 580, 672 and 761 nm; RICHTER et al., 1995). The latter authors explain this effect with the influence of weathering solutions derived from adjoining siliciclastic rocks.d. The aragonite crystals are green luminescing with a maximum of the wide bands at ~560 nm (Mn^{2+} in tetraedric coordination). This green luminescence is more or less near to a dark green-blue colour ("intrinsic" CL) due to the very low Mn contents in speleothems (see a.). As it is very difficult to distinguish pure carbonates based solely on their visual CL characteristics the use of high resolution spectral analyses is helpful as it enables you to detect minor traces of Mn in the lattice. Furthermore, the maxima of the wide bands are at different positions (520 nm for calcite, 560 nm for aragonite).

e. Irregularly formed dolomitic crystals or aggregates are embedded in the layer structure of the coralloids from the Buchenlochhöhle (3) and the Grauner Walls (4). In the first case the aggregates emit an orange luminescence produced by Mn^{2+} cations present within the dolomite structure (Mg layer and Ca layer). The red luminescing parts of the coralloids from the Grauner Walls (4) indicate the sole fitting of Mn^{2+} in the Mg position of the dolomite lattice (cf. HABERMANN et al., 1996). The CL characteristics of the dolomitic parts within the coralloids in both cases correspond with the characteristics of the dolomitic host rock. The dolomites are thus most probably of detrital origin (cf. mineral phases).

Stable isotopes

The isotopic composition of stalagmites from caves of the Sauerland are typical of meteoric calcites ($\delta^{18}O$-values of -5,9 to -6,1 and $\delta^{13}C$ values of -7,3 to -10,1 (Table 1 - cf. ALLAN & MATTHEWS, 1982). The isotopic data of the coralloids from the Ostenberghöhle (1) are within the range of the data of the stalagmites described above. In the case of the coralloids of the B7-Höhle (2), however, slightly heavier $\delta^{18}O$ and $\delta^{13}C$ values were obtained (Table 1). Finally, the isotopic compositions of coralloids from the Buchenlochhöhle (3) and the Grauner Walls (4) are significantly heavier.

The recorded trend is preserved even in consideration of somewhat higher temperatures of formation or of the partially Mg calcitic or aragonitic composition (different fractionation factors) of the coralloids from the Grauner Walls (4). In our opinion the increasingly (locality 1 to 4) heavier isotopic composition of the coralloids reflects the increasing importance of previously concentrated solutions from which the coralloids have precipated.

4. Summary and discussion

The analyses underline the importance of adhesive water films in the growth of coralloids. The existence of Mn containing calcite layers on surfaces exposed to the cave is remarkable. Meteoric cave seepage waters normally indicate oxidizing conditions. Obviously, speleothems temporarily precipitate under oxidizing and reducing micro environments. This could also be shown for speleothems from other localities in very different climatic zones (e.g. in flowstones of Hydra Island/Greece).

Name	Material	Sample	$\delta^{13}C$	$\delta^{18}O$
Ostenberghöhle (1)	Sparganophyll.- lst./ Givetium	Spar 1	3,7	-7,0
	Stalagmite	OeStA	-7,3	-5,9
	Stalagmite	OeStB	-7,4	-6,1
	Coralloid	OB 9	-8,6	-5,6
B7-Höhle (2)	Massenkalk/MK 1 Givetium		4,6	-5,8
	Stalagmite	B7-100	-10,1	-6,0
	Coralloid	B7-4/7	-2,8	-5,3
Buchenlochhöhle (3)	Dolomite/ Middle-Dev. Coralloid	BuDol	1,2	-2,3
		BuKnopf	5,5	-1,3
Grauner Walls (4)	Dolomite/ Ladin	ReDol	1,8	-3,2
	Coralloid	ReKnopf	8,7	-1,3

Table 1: $\delta^{13}C$ and $\delta^{18}O$ composition of speleothems and host rocks from the four localities.

A comparison of the examined localities showed the Mg content within the calcite gradually increased from the Ostenberghöhle (1) via the B7-Höhle (2) and the Buchenlochhöhle (3) to the Grauner Walls (4). In addition, the speleothems from the latter three localities contain aragonite (Fig. 4). From localities 1 to 4 an increasing Mg/Ca ratio and/or an increasing temperature of the cave water would be expected after experimentally studies by FÜCHTBAUER & HARDIE (1980). At a first glance, the requirement for increasing Mg/Ca ratio of the cave waters coincides with the increase in the dolomitic portion in the country rocks of the speleothems (1) to (4).

The mineralogical compositions of the coralloids in localities (3) and (4) (aragonite, Mg calcite and hydrated Mg/Ca carbonate), except for the high-Mg calcites of the Grauner Walls (4), are in agreement with the mineralizations of speleothems from dolomitic areas (FISCHBECK 1976, TIETZ 1988). Our speleothems are found in a temperature range < 30°C and developed in solutions of carbonate host rocks at any molar Mg/Ca ratios ≤ 1. Thus, the precipitation of aragonite and high-Mg calcites requires additional explanation (after literature study, for example FÜCHTBAUER & HARDIE, 1980). Probably, the crystallization developed from the remaining more concentrated solutions with increased Mg/Ca ratios. These solutions originated from seeping waters after previous precipitation of calcite. The chemical composition of the aragonitic coralloids from the B7-Höhle (2) supports this explanation due to abnormally strong draught in this locality (full year temperature ~ 10°C). In this respect, it is worth to note the decrease in crystal size from (1) to (4) coeval with an increase in draught. This possibly reflects an increase in the concentration of the solution from which the coralloids were precipitated (cf. C/O-isotopes). This is in agreement with the observation of special aragonite-rich coralloids from localities (3) and (4). Temporarily higher temperatures (hot summer days) may exert an additional effect.

The REE contents of the speleothems from the Ostenberghöhle (1) can be explained by the existence of nearby siliciclastic sediments in the catchment area of the meteoric waters. Of course, crystallization of these phases should also reflect previously concentrated solutions because the REE layers can mostly be observed in speleothems precipitated under subaerial conditions.

Detrital material (e.g. pollen and host rock detritus) is of secondary importance in all examined coralloids.

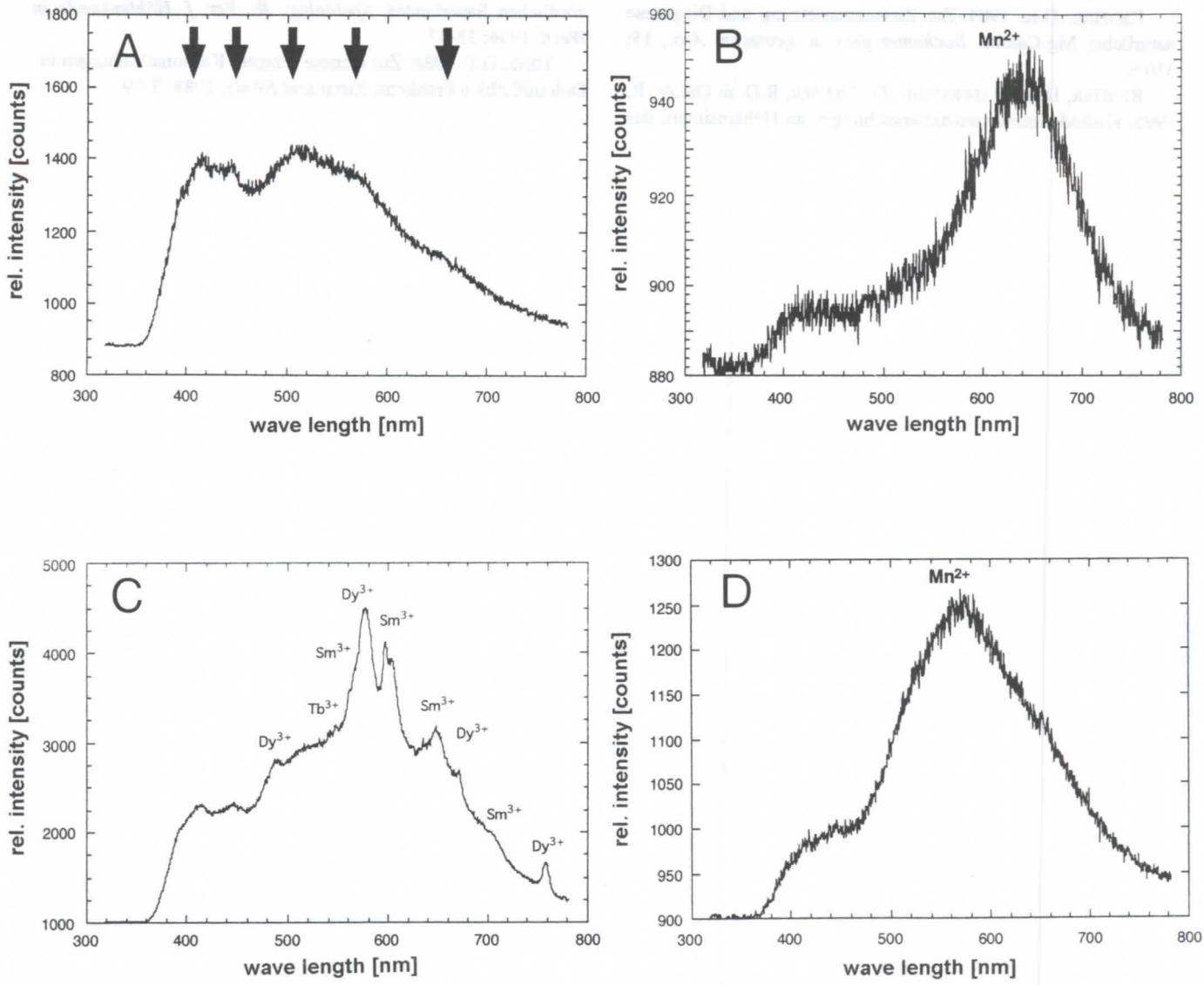

Figure 5: CL spectra of different carbonate layers. A: Blue ("intrinsic") CL of calcite. B: Orange CL of calcite. C: Dull blue to violet CL of calcite. D: Green CL of aragonite.

Acknowledgement

For technical assistance we are grateful to K. Aschenbrenner and M. Oly (Geol. Institute, Ruhr-University Bochum). Further thanks are due to F. Bruhn and G. Carden (also Bochum) for editing our English.

References

ALLAN, J.R. & MATTHEWS, R.K. 1982. Isotope signatures associated with early meteoric diagenesis. *Sedimentology.* 29: 797-817.

BRUCKSCHEN, P., BRUHN, F. & RICHTER, D.K. 1995. Geochemische Variationen in Karbonatzementen als Dokument der Beckenevolution. Eine Fallstudie aus dem Trochitenkalk Nordwestdeutschlands. *Z. dt. geol. Ges.* 146: 355-371.

FISCHBECK, R. 1976. Mineralogie und Geochemie carbonatischer Ablagerungen in europäischen Höhlen – ein Beitrag zur Bildung und Diagenese von Speläothemen. *N. Jb. Miner. Abh.* 126: 269-291.

FISCHBECK, R. & MÜLLER, G. 1971. Monohydrocalcite, Hydromagnesite, Nesquehonite, Dolomite, Aragonite and Calcite in Speleothems of the Fränkische Schweiz, Western Germany. *Contr. Mineral. and Petrol.* 33: 87-92.

FÜCHTBAUER, H. & HARDIE, L.A. 1980. Comparison of experimental and natural magnesian calcites. *Internat. Assoc. Sedimentol. 1st. Europ. Mtg., Abstr., Bochum:* 167-169.

FÜCHTBAUER, H. & RICHTER, D.K. 1988. Karbonatgesteine. – In: (Füchtbauer, H. (Hrsg.): Sedimente und Sedimentgesteine. Schweizerbart, Stuttgart: 233-434.

HABERMANN, D., NEUSER, R.D. & RICHTER, D.K. 1996: Hochauflösende Spektralanalyse der Kathodolumineszenz (KL) von Dolomit und Calcit: Beispiele der Mn- un SEE-aktivierten KL in Karbonatsedimenten. – *Zbl. Geol. Paläont. Teil I,* 1995 (1/2): 145-157.

MERGNER, W., BRIX, M.R., HAGEMANN, P., OELZE, R. & RICHTER, D.K. 1992. Sinterbecken im Malachitdom mit wasserspiegelparallelen Carbonatkrusten. – In: (Geologisches Landesamt NRW): Der Malachitdom. Ein Beispiel interdisziplinärer Höhlenforschung im Sauerland. GLA Krefeld: 151-173.

NEUSER, R., BRUHN, F., GÖTZE, J., HABERMANN, D. & RICHTER, D.K. 1996. Kathodolumineszenz: Methodik und Anwendung. *Zbl. Geol. Paläont. Teil 1,* 1995(1/2): 287-306.

OELZE, R. 1993. Zur Sedimentologie der Ostenberghöhle bei Bestwig/NRW. Diplomarbeit, Ruhr-Universität Bochum: 133 S.

RICHTER, D.K. 1984. Zur Zusammensetzung und Diagenese natürlicher Mg-Calcite. *Bochumer geol. u. geotechn. Arb.*, 15: 310 S.

RICHTER, D.K., HABERMANN, D., NEUSER, R.D. & OELZE, R. 1995. Kathodolumineszenzuntersuchungen an Höhlensintern des nördlichen Sauerlandes. *Speläolog. Jb. Ver. f. Höhlenkunde in Westf.* 1994: 33-37.

TIETZ, G.F. 1988. Zur Genese rezenter Karbonatbildungen in Dolomithöhlen Frankens. *Karst und Höhle*, 1988: 7-79.

Characterisation of speleothem crystalline fabrics by spectroscopic and digital image processing methods (Choranche, Vercors, France)

Yves Perrette[1], Dominique Genty[2], Jean-Luc Destombes[3], Jean-Jacques Delannoy[1] and Yves Quinif[4]

1) Institut de Géographie Alpine, URA CNRS 903, Université Joseph Fourier, 17 rue Maurice Gignoux, 38031-Grenoble, France. 2) Laboratoire d'Hydrologie et de Géochimie Isotopique, URA CNRS 723, Université de Paris-Sud, 91405-Orsay Cedex, France. 3) Laboratoire de Spectroscopie Hertzienne, URA CNRS 249, Centre d'Etudes et de Recherches Lasers et Applications, Université des Sciences et Technologies de Lille, 59655-Villeneuve d'Ascq cedex, France. 4) Centre d'Etude et de Recherches Appliquées au Karst, Faculté Polytechnique de Mons, 9 rue de Houdain, 7000-Mons, Belgique.

Abstract

For many years, the interest of speleothems in the search for palaeoenvironmental informations has been noticed. Since the beginning of the 90's, some new methods have been developed to systematize the study of their internal structure and it has been shown that the crystalline fabrics and the porosity variations can be read as palaeoenvironmental data. In this work, grey levels profiles, reflectance measurements (l = 635 and 457.9 nm), laser induced fluorescence (excitation at 457.9 nm ; observation at l > 550 nm) and Raman spectroscopy have been used to study a well laminated part of a stalagmite extracted from the Coufin-Chevaline cave (Choranche, Vercors, France). Merits and limits of each method are evaluated and organised for a precise stratigraphic study of the sample in order to reveal environmental informations.

Résumé

Depuis de nombreuses années, il est apparu que les spéléothèmes peuvent enregistrer des informations relatives aux paléoclimats. Depuis le début des années 90, un certain nombre de méthodes nouvelles ont été développées pour systématiser l'étude de leur structure interne, afin de mieux appréhender les informations environnementales qu'ils contiennent. Dans ce travail, des mesures de profil de niveaux de gris, de réflectance (λ = 635 and 457.9 nm) et de fluorescence induite par laser (excitation à 457.9 nm ; observation à λ > 550 nm) ainsi que quelques mesures en spectrométrie Raman ont été effectuées sur une portion bien laminée d'un échantillon stalagmitique prélevé dans le réseau de Coufin-Chevaline (Vercors, France). Les apports et les limites de ces méthodes sont décrits en vue d'une étude stratigraphique fine de l'échantillon pouvant conduire à l'acquisition d'un certain nombre d'informations environnementales.

1. Introduction

Since the 80's, the study of speleothems has been included in the karstologic studies and they are usually used to date karst landforms and sediments. Particular climatic contexts can be inferred from their absence/presence since their growth is clearly dependent on the interactions between climatic and bio-pedologic conditions (MAIRE, 1990 ; BAKER *et al.*, 1995 ; and references therein). Since the beginning of the 90's, the internal structure of speleothems is also actively studied (WHITE & BRENNAN, 1989 ; KASHIWAYA *et al.*, 1991 ; GASCOYNE, 1992 ; SHOPOV *et al.*, 1994 ; SZABO *et al.*, 1994 ; GOEDE, 1994 ; BAKER *et al.*, 1993 ; GENTY & QUINIF, 1996) : existence of hiatus and discontinuities gives evidence of great tectonic events (MORINAGA *et al.*, 1994 ; BINI & QUINIF, 1996) ; precise knowledge of the calcite crystallisation conditions allow us to use the crystalline fabric in the search for palaeoenvironmental changes (DREYBRODT, 1981 ; BAR-MATTEWS *et al.*, 1991 ; DICKSON, 1993 ; QUINIF *et al.*, 1994 ; GENTY & QUINIF, 1996 ; and references therein) ; spectroscopic evidence provides informations on the organic matter content (WHITE, 1981 ; ROUSSEAU, 1992 ; LAURITZEN, 1996 ; and references therein), etc ....

In this work four different methods have been used to study a well laminated stalagmite extracted from the Coufin-Chevaline cave (Choranche, Vercors, France) : visual observation, digital image processing, reflectance measurement using lasers, laser-induced fluorescence and Raman spectroscopy. Their combination allowed us to increase the quality of the collected informations. In a first part, we shortly describe these methods. Comparison between them is given in a second part before including each one in a methodological way for a precise stratigraphic analysis where they appear as efficient tools.

2. Description of the methods

Stratigraphic analysis

This method aims at describing the main characteristics of the crystalline facies evolution. To carry out such a description, it is necessary to choose a spatial, and then a temporal, resolution according to the purpose of the study. At this resolution, different aspects of the speleothem internal structure will appear. Current knowledge on the development of active modern speleothems allow us to distinguish several features :

- global crystalline structure (banded, laminated, stromatolitic, ...)
- crystalline fabrics (palisadic, columnar, acicular, ...) and crystalline macroscopic colour and opacity
- intra- or inter-crystalline inclusions

These characteristics of the speleothem internal structure help to reveal different types in the crystal growth processes. This visual study consists in an observation of the sample with naked eyes and with binoculars (x 4 to x 40). The time resolution obtained should permit to distinguish facies evolutions due to global or local environmental changes.

Grey level study by digital image processing

This fast method has been described previously (GENTY, 1992 ; GENTY & QUINIF, 1996). It mainly consists in digitally processing an image of a vertical cut made parallel to the growth axis of the speleothem. The vertical section is polished and the sample is placed under a video bench. Specific programs permit a wide range of digital processings including mask filtering, histogram analysis, smoothing, cross correlation of grey-level profiles. In this way, it has been established that speleothems are composed, partly or totally, of couplets of white-porous laminae (WPL) and dark-compact laminae (DCL) of submillimetre dimensions, which are characterised by a different pore density (GENTY & QUINIF, 1996).

The interest of this method is double : counting the laminae, and then determining the precise age of the sample, is greatly facilitated ; determining the thickness of each lamina is also very easy and allows a precise study of the speleothem growth rate to be made. Digital processing also reveals discontinuities in the sample colour which depends on the crystalline properties of the calcite, but also on the polished surface state. The brightness of the surface then provides informations on the crystalline fabric evolution. Grey-level study of speleothem internal structure has already permitted to demonstrate the annual character of lamina couplets due to water excess variations, and to establish a correlation between the WPL growth and water excess periods (GENTY & QUINIF, 1996).

Reflectance measurement

When white light falls on a surface, part of it penetrates in the material where it is finally absorbed if the sample thickness is sufficient, another part is diffused at the surface or in the bulk, and a last part is reflected at the surface (specular reflection). Light absorption depends on the wavelength and on the composition and concentration of the chemical compounds in the sample. Diffusion is closely related to the physical state of the sample (porosity, crystalline fabrics, inclusions, ...) but depends also on the wavelength. Specular reflection clearly depends on the state of the polished surface.

In a real sample, all these processes contribute to its macroscopic colour which is complementary to the colours absorbed by the sample. Unusual colours of speleothems (blue, green, pink, yellow, red, ...) are generally attributed to the presence of metal oxides with concentration in the percent range (WHITE, 1981). On the contrary, more classical colours (brown, beige, milky yellow, ...) have been attributed to organic macro-molecules like humic or fulvic acids dissolved by the seepage water in the pedologic part of the karst (GASCOYNE, 1977 ; WHITE, 1981 ; WHITE & BRENNAN, 1989 ; SHOPOV *et al.*, 1994 ; BAKER *et al.*, 1993 ; GENTY & QUINIF, 1996). To a certain extent, using a monochromatic light from a laser should allow to favour one of the physical processes described above.

The experimental set-up is very simple : an elongated laser beam (4000x50 µm) with its great axis parallel to the laminae illuminates the sample perpendicularly to its polished surface. Using an elongated beam leads to an averaging in the direction parallel to the laminae making the method less sensitive to the microscopic surface defaults. An integrating sphere is used to collect all the light re-emitted by the sample. Detection is achieved by solid state photo-diodes . Two laser wavelengths have been used : λ = 635 nm (HeNe laser with a power P = 2 mW) and λ = 457.9 nm (Ar^+ laser, P = 20 mW). Samples were attached to a translation stage drived by a PC which is also used for data acquisitions. Experimental results have shown that diffusion is the main physical process at work in the calcite samples studied here and that selective absorption by organic molecules cannot be evidenced, probably because of their low concentration. In these conditions, reflectance measurements are expected to be very similar to the grey-level measurements, which has been confirmed by the present work (see *infra*).

Laser induced fluorescence measurements

When excited by UV light, most organic molecules and especially fulvic/humic acids are characterised by an intense light emission in the visible part of the electromagnetic spectrum, the intensity of which depends on the molecular concentration(YANG & ZHANG, 1995). This fluorescence has been extensively used to characterise the speleothems laminae (BAKER *et al.*, 1993 ; SHOPOV *et al.*, 1994 ; GENTY & QUINIF, 1996) by assuming it is due to these organic macro-molecules which are swept along by the seepage water and trapped in the calcite during the crystallisation process (GASCOYNE, 1977 ; WHITE, 1981 ; WHITE & BRENNAN, 1989). In these works, excitation was done in the UV around 330 nm, and the fluorescence was detected through a filter centred at about 450 nm.

According to the laser equipment available, our measurements were made by exciting the sample at λ = 457.9 nm (Ar^+ laser P = 30 mW) and the fluorescence was detected through a low pass filter with a cut-off wavelength of 550 nm. As in the reflectance measurements, emitted light was collected by an integrating sphere and detected using photo-diodes. It is then easy to change from reflectance to fluorescence measurements by just inserting the low-pass filter. Reflectance and fluorescence scans are then made over exactly the same path on the sample, with the same spatial resolution. Most of the samples showed a strong fluorescence with spectra similar to those observed on commercial humic acids.

Raman spectroscopy

Contrary to the fluorescence experiments which show very wide, structure-less bands, Raman spectroscopy is potentially much more selective since it is based on the vibrational bands which characterise each type of chemical bonds. This technique is extensively used in chemical characterisation of organic molecules, and has been recently applied to the study of humic acids (YANG *et al.*, 1994). Experiments were carried out using the Raman Micro-Probe of the Laboratoire de Spectroscopie Infrarouge et Raman (CNRS and University of Lille). Attempts to detect vibrational bands of humic acids failed, probably because of low concentrations and of a diffuse repartition of the molecules in the samples. Also, relatively intense fluorescence background prevented the use of the full sensitivity of the spectrometer.

In fact, Raman micro-spectrometry is much better adapted to the characterisation of very small grains of a given material embedded in a matrix. In this work, this technique has been used only to identify inclusions observed during the microscopic investigations. In this way, we identified several inclusions like iron oxide, clay, quartz and rutile particles. Raman spectrometry also unambiguously demonstrated the presence of abundant charcoal particles.

Figure 1 : Comparison of the measure obtained by the application of the four methods over the summital part of the sample 5531a, from the top to the back (left to right), 0 to 6 cm (source : authors)

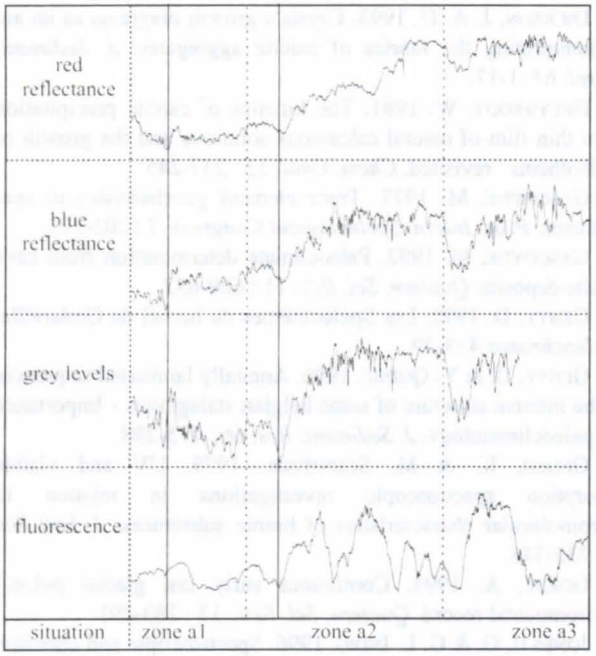

Figure 2 : Comparison of the measure obtained by the application of the four methods over the summital part of the sample 5531a, from the top to the back (left to right), zoom between the continuous line (fig. : 1). (source : authors)

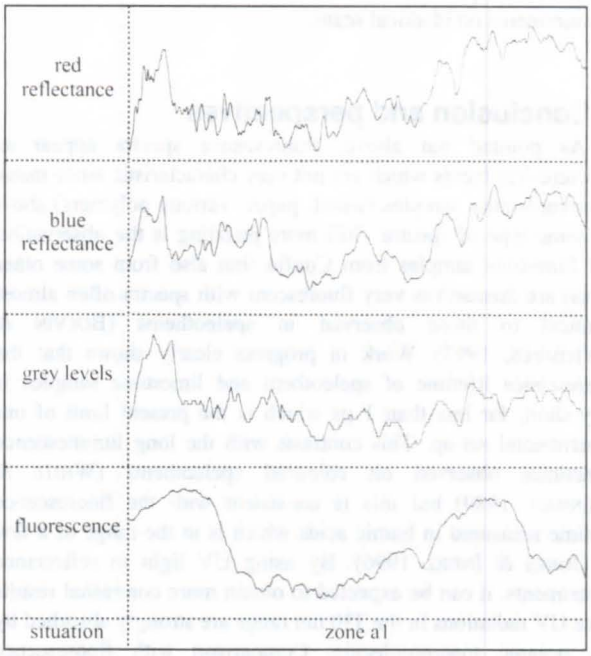

3. Comparison of the methods

Presentation of the sample

The methods shortly described above have been applied in the study of a stalagmite sample extracted from the Cathedral Room of the Coufin-Chevaline cave (Choranche, Vercors, France). A drilling was made vertically in an active « tam-tam » stalagmite and the study of the core was made partly within the framework of an integrated french-belgian program (PERRETTE, 1996). In particular, the well laminated upper part which covers historical times has been studied and is described in more details in the communication « Enregistrement de l'activité charbonnière dans les spéléothèmes de Choranche » by PERRETTE *et al.* (1997) at this Congress. Owing to the active character of the stalagmite, a relative chronology has been established.

The speleothem section studied in this work is mainly composed of compact palisadic crystals and only crystal size and coalescence vary. From top to bottom (figure 1), we observe a 1.5 cm thick zone of very pure white calcite dominated by DCLs (zone a1), which overlays a grey layer which has a thickness of about 2 cm. This zone a2 contains many charcoal inclusions and is characterised by crystal facets more visible and less coalescence. Below, a 2.2 cm layer has a milky aspect and is dominated by well marked WPLs (zone a3). Some detritic layers are also observed and are associated with lamina undulations. Owing to the various facies observed, this core was choosen for the comparison of the methods.

Results

Comparison between the results obtained by the different methods are presented on figure 1. Figure 2 gives a more detailed view of the zone a1 at higher spatial resolution.

From figure 1 it is clear that there is a strong correlation between the reflectance results and the grey level ones, especially in the blue. As the grey level method records the macroscopic colour of calcite, the signal is maximum in the charcoal zone a2. If the blue reflectance appears very similar, this does not seem to be true for the red reflectance which shows a more gradual increase. This can be interpreted as a change in the crystalline structure, progressively going from compact palisadic crystals to crystals with moderate coalescence. Similarly, the compact, coalescent and palisadic milky zone a3 contrasts with the less coalescent zone a2. This is also interpreted as an evolution in the crystalline structure.

Humic/fulvic acids can also play a role in the interpretation of the red/blue difference because of the very important red/blue differential absorption observed in these molecules (GHOSH & SCHNITZER, 1979). However, in that case, the fluorescence intensity which is directly related to the molecular concentration, should also show a strong correlation with the blue reflectance. This is clearly not the case even if there are some similarities between them in the zone a1. Although the measurements are made at the same spatial resolution, fluorescence results do not show the numerous alternations observed in reflectance and in grey levels which are associated to visual laminae. Fluorescence seems to give more global results and this again rises the question of the relation between organic matter and visual laminae.

4. Discussion

During this comparison, several tests were also made in order to set limits in the applicability of the laser methods which are still under development. They showed that laser measurements are sensitive to surface state quality, as are the grey level ones. For example, all methods revealed oscillations which were due to a step growth of the columnar crystals.

Nevertheless, all these methods are clearly complementary. From a methodological point of view, they can be organised as different tools to be used within an unique approach of the internal structure of speleothems. The first, visual, level is relieved by image processing and its statistical possibilities. Laser methods can go farther in the study by allowing the description of the crystalline structure which is often difficult at visual level.

Redundancy between reflectance and grey levels results actually leads to a link between visual and spectroscopic approaches. This has been made possible by the similitude between reflectance and fluorescence protocols which allows us to make the measurements on identical scans.

5. Conclusion and perspectives

As pointed out above, fluorescence spectra appear as structure-less bands which are not very characteristic since many macromolecular samples (wood, paper, various polymers) show the same type of spectra. Still more puzzling is the observation that limestone samples from Coufin (but also from some other caves) are themselves very fluorescent with spectra often almost identical to those observed in speleothems (BOLVIN & DESTOMBES, 1997). Work in progress clearly shows that the fluorescence lifetime of speleothem and limestone samples is very short, far less than 1 µs which is the present limit of our experimental set-up. This contrasts with the long luminescence sometimes observed on coloured speleothems (WHITE & BRENNAN. 1989) but this is consistent with the fluorescence lifetime measured in humic acids which is in the range of a few ns (JONES & INDIG. 1996). By using UV light in reflectance experiments, it can be expected to obtain more contrasted results since UV radiations in the 330 nm range are strongly absorbed by any organic macromolecule. Comparison with fluorescence results will be then of great interest. Studies using Raman spectrometry should also be developed in two directions : toward the *in situ* detection of humic/fulvic acids by using an excitation in the near IR where the intrinsic fluorescence background of the sample is much weaker, and also toward the study of the crystalline state and porosity of the calcite samples by quantifying the Raman spectrum of the calcite itself.

Nevertheless, the preliminary results presented here confirm that the information content of speleothems is very rich and that the « speleothem tool » can be used in palaeoenvironmental studies provided a clear methodological approach is used. This should allow us to compare speleothem informations coming from different parts of a given karstic system and then from different systems. However these results also rise again the question of the relation between organic matter and visual laminae.

Acknowledgements : The Centre d'Etudes et de Recherches Lasers et Applications (CERLA) is supported by the Ministère chargé de la Recherche, the Région Nord/Pas de Calais and the Fonds Européens de Développement Economique des Régions. We wish to gratefully acknowledge Gilbert Mantovani for his constant interest and encouragement in developing scientific works in the Coufin cave. Many thanks are also due to all the guides of this cave for their constant availability. Raman experiments were carried out at the Laboratoire de Spectroscopie Infrarouge et Raman (CNRS and University of Lille) and were made possible by the kindness of C. Bremard and J. Laureyns who are deeply acknowledged, as is Laurent Paccou who set up the reflectance experiment.

References

BAKER, A., SMART, P. L. & A. RICHARDS. 1993. Annual growth bandings in a cave stalagmite. *Nature*, 272 : 24-28.

BAKER, A., SMART, P. L. & R. L. EDWARDS. 1995. Paleoclimate implications of mass spectrometric dating of a british flowstone. *Geology* 23 : 309-312.

BAR-MATTEWS, M., MATTEWS, A. & A. AYALON. Environmental controls of speleothem mineralogy in a karstic dolomitic terrain (Soreq Cave, Israel). *J. Geol.* 99 :189-207.

BOLVIN, H. & J. L. DESTOMBES. 1997. Work in progress.

DICKSON, J. A. D. 1993. Crystals growth diagrams as an aid to interpreting the fabrics of calcite aggregates. *J. Sediment. Petrol.* 63 :1-17.

DREYBRODT, W. 1981. The kinetics of calcite precipitation from thin film of natural calcareous solutions and the growth of speleothems : revisited. *Chem. Geol.* 32 : 237-245.

GASCOYNE, M. 1977. Trace element geochemistry in speleothems. *Proc. Intern. Speleological Congress*. 7 : 205-208.

GASCOYNE, M. 1992. Paleoclimate determination from cave calcite deposits. *Quatern. Sci. Rev.* 11 : 609-632.

GENTY, D. 1992. Les Spéléothèmes du tunnel de Godarville. *Speleochronos* 4 :3-29.

GENTY, D. & Y. QUINIF. 1996. Annually laminated sequences in the internal structure of some belgian stalagmites - Importance for paleoclimatology. *J. Sediment. Res.* 66 : 275-288.

GHOSH, K. & M. SCHNITZER. 1979. UV and visible absorption spectroscopic investigations in relation to maromolecular characteristics of humic substances. *J. Soil Sci.* 30 :735-745.

GOEDE, A. 1994. Continuous early last glacial palaeoenvironmental record. *Quatern. Sci. Rev.* 13 : 283-291.

JONES II, G. & G. L. INDIG. 1996. Spectroscopic and chemical binding properties of humic acids in water. *New J. Chem.* 20 : 221-232.

KASHIWAYA, K., ATKINSON, T. C. & P. L. SMART. 1991. Periodic variations in late pleistocene speleothem abundance in Britain. *Quatern. Res.* 35 : 190-196.

LAURITZEN, S. E. 1996. Climate Change : the Karst Record. Extended abstracts of the Bergen Conference, August 1-4th, 1996, University of Bergen, Norway.

MAIRE, R. 1990. La haute montagne calcaire. Thèse de Doctorat d'Etat., Université de Bordeaux. Karstologia Mémoires, vol. 3, 731 p.

PERRETTE, Y. 1996. Contribution des spéléothèmes à la connaissance paléoenvironnementale. Mémoire de Maîtrise, Université Joseph Fourier, Grenoble, 188 p.

QUINIF, Y., GENTY, D. & R. MAIRE. 1994. Les spéléothèmes : un outil performant pour les études paléoclimatiques. *Soc. Géol. France, Bull.* 165 : 603-612.

ROUSSEAU, L. 1992. Etude physico-chimique des planchers stalagmitiques du Pléistocène moyen.. Thèse de Doctorat, Institut de Paléontologie Humaine, Muséum d'Histoire Naturelle, Paris.

SHOPOV, Y. Y., FORD, D.C. & H. P. SCHWARCZ. 1994. Luminescent microbanding in speleothems : high-resolution chronology and paleoclimate. *Geology* 22 : 407-410.

SZABO, B. J., KOLESAR, P. T., RIGGS, A. C., WINOGRAD, I. J. & K. R. LUDWIG. 1994. Paleoclimatic inferences from a 120000-yr calcite record of water-table in Browns room of Devil's Hole, Nevada. *Quatern. Res.* 41 : 59-69.

WHITE, W. B. 1981. Reflectance spectra and color in speleothems. *NSS Bulletin* 43 : 20-26.

WHITE, W. & E. S. BRENNAN. 1989. Luminescence of speleothems due to fulvic and other activators. *Proc. Intern. Speleological Congress*. 10 :212-214.

YANG, Y.-H., LI, B.-N. & Z.-Y. TAO. Characterization of humic substances by laser Raman spectroscopy. *Spectrosc. Lett.* 27 : 649-660.

YANG, Y-H. & D.-H. ZHANG. 1995. Concentration effect on the fluorescence spectra of humic substances. *Commun. Soil Sci. Anal.* 26 : 2333-2349.

Studies of speleothem dissolution on Cayman Brac and Isla de Mona

Rozemarijn F.A. Tarhule-Lips and Derek C. Ford
McMaster University, Hamilton, Ontario, Canada

Résumé

Des périods de cessation de croissance ou dissolution des concrétions ont eu lieu dans le passé et ont lieu à présent. On est en train de dater ces périods avec la méthode U-séries TIMS (Thermal Ionisation Mass Spectrometry) pour que l'on peut déterminer quand elles eu lieu et ce qui peut être responsable. Cette information, combiné avec des données sur la micro-climatologie et des conditions chimiques de l'eau présentes, peut contribuer à la reconstruction de l'histoire géologique Quaternaire de la Caribique.

Les temps de présence des hiatus de croissance dans des concrétions différentes ne coincident pas nécessairement. Ceci suggère que ce qui est responsable pour l'inhibition de croissance ou carrément l'erosion n'est pas une phénomène régionale mais plutôt une phénomène locale déterminé par des conditions particulière de grottes et pas par des conditions climatiques régionales. Des fluctuations climatiques glaciales et interglaciales n'ont probablement joué qu'une rôle secondaire dans le développement des concrétions. Il y a deux causes possibles pour la cessation de croissance ou dissolution: submersion de la grotte ou corrosion par de l'eau de condensation agressive. Le dernière cause semble être le plus probable dans la plupart des cas.

Introduction

Speleothem growth and dissolution are being studied in caves on Cayman Brac, Cayman Islands, and on Isla de Mona, Puerto Rico. These are two small islands bounded by cliffs containing relict mixing zone caves. At present, the majority of speleothems in the caves are dry and show signs of dissolution. Comparable dry and/or dissolving periods also existed in the past and are represented as growth hiatuses in the calcite. In an earlier study on Cayman Brac some of these hiatuses were dated by alpha-spectrometry. They were found to occur at >350 ka, around 200 ka (oxygen isotope substage 7) and between 75 ka and 20 ka (oxygen isotope substage 3 and 4). However, not all the samples showed the hiatuses at the same time.

One of the objectives of this study is to date speleothems by U-series TIMS (Thermal Ionisation Mass Spectrometry) to better pinpoint when these hiatal episodes occurred and what the possible cause(s) were. At the same time, field experiments are being carried out to establish what the present microclimatic and water chemical conditions are in the caves. This might help to explain why speleothem growth is presently occurring only in certain areas in given caves and what may have occurred in the past. This information may contribute towards a reconstruction of the Quaternary geologic history of the Caribbean.

Preliminary results

Growth hiatuses in different speleothem samples are not necessarily coincident in time. This suggests that whatever was responsible for the inhibition of growth or the outright erosion is not a regional but a local phenomenon that has more to do with particular cave conditions than with the regional climatic conditions. It is inferred that the glacial and interglacial fluctuations of climate have played a secondary (if any) role in the deposition of the speleothems.

Of the two possible causes for growth cessation/dissolution, i.e. flooding of the cave or corrosion by aggressive condensation water, the latter appears to be the more probable in most cases, because all sample caves are above sea level and have been there for at least the past 125 000 years.

Condensation in the cave air was induced with the help of plastic bottles filled with ice. The condensation water was collected and analysed. Its chemical composition lay between that of local rainwater and speleothem drip water. It is, in general, undersaturated with respect to calcite and dolomite but its aggressiveness can vary with time and space within the same cave and between caves.

In several caves gypsum tablets of known weight were suspended for a little more than one year. At the end of the period the tablets were weighed again and dissolution rates were calculated. The surface retreat rate was found to vary between 0 and 0.5 mm/yr, indicating that dissolution in the caves is taking place at present.

Conclusion

Both in the past and at present, we find periods of speleothem growth, cessation and/or dissolution. Dating of the timing of (some of) these periods is under way. However, it is clear that a simple relationship between growth cessation/dissolution and glacial/interglacial periods can not be established. Instead it seems that cave configuration and cave microclimatology play important roles, encouraging processes like condensation corrosion to occur.

Chemical Differences Between Light and Dark Coloured Speleothem

P.E. van Beynen, D.C. Ford and H.P. Schwarcz
School of Geography and Geology, McMaster University, Hamilton, Ontario L8S 4K1, Canada

Abstract
Twelve speleothem, six light coloured, six dark, were analyzed for their fluorescence and organic characteristics. It became apparent that fluorescence is caused by fulvic acid, with humic acid having a much lower influence. While darker specimens contained higher concentrations of organic substances, this does not necessarily lead to higher fluorescence. Humin is also a possible contributor to fluorescence. Gel chromatography of the fulvic acid and NMR work still has to be concluded.

Rationale
Annual laminae have been discovered in speleothem, and each band has a section of light and dark calcite. The main technique for quantifying this variability in the calcite is the use of luminescence microscopy. However, this microscopic scale makes analysis of the bands impossible. The only available avenue is to ascertain the chemical differences on a larger scale, i.e. square centimetres of light and dark speleothem. Of importance is the discovery of the cause of fluorescence and the characterization of these fluorophores.

Methods
Samples were selected for their uniformity of colour and results of preliminary studies. Their locations stretch across North America and extend to Wales and Australia. The variable organic concentrations between light and dark specimens could be obtained by taking dissolved organic carbon measurements and comparing these to the fluorescence of each sample. Fluorescence spectroscopy of solid and dissolved speleothem should provide some indication of what substance is causing fluorescence. Dissolved samples were firstly separated into humic acid (HA) and fulvic acid (FA). These spectra can be compared to known fluorophores, both organic and ionic. Further identification of the FA fraction will be undertaken using gel chromatography. Measures of the molecular weight of these compounds are ascertained through ultrafiltration. NMR could provide clues as to the functional groups present.

Results
Preliminary results have shown that darker speleothem have higher concentrations of organic matter, shown both in the DOC and precipitate in the dissolved speleothem. Spectroscopic analysis revealed spectra indicative of fulvic acid, especially in the lighter specimens. However, darker speleothem provided an additional problem of not allowing incoming light to penetrate the speleothem due to the high concentrations of organics which could produce an extinction effect. Whether this is a function of the power of the light source has yet to be determined. Rare earth elements may be present, including Europium, Dysprosium, Uranium and Lead. This has yet to be confirmed with ion probe analysis of the solid speleothem. Changes in the spectra with different excitation wavelengths suggests more than one humic substance is contributing to fluorescence. It is hoped that gel chromatography will give further clarification. Spectroscopically the precipitate produced similar spectra to the solid speleothem, suggesting not only FA contributes to fluorescence. Humin could be a possible contributor as could humic acid. Humic acid was investigated spectroscopically, but it's fluorescence intensities were very low compared to that of FA, though it's contribution did increase for darker speleothem.

Conclusions
With the advent of new technology it may be possible to analyze annual bands of calcite, but presently much larger samples and extrapolation of results are required. Fluorescence appears to be caused by organic substances, predominantly FA, and occurs in higher concentrations in darker speleothem. The type of organics has important implications the wavelength of excitation used to generate fluorescence. Additional information will be soon available about the character of the FA and the possible contribution of rare earth elements.

Ribbon Helictites from Jenolan Caves, NSW Australia

by Jill Rowling,
2 Derribong Place, Thornleigh, NSW Australia 2120

Abstract
An interesting form of helictite has been found at Jenolan Caves. Ribbon helictites are characterised by their flat, thin, ribbon-like appearance together with an opaque white central canal (diameter around 0.2 mm). Cleavage planes and crystal orientation have been examined and growth mechanisms suggested. Laser Raman spectroscopy showed the material to be calcite. Ribbon helictites are associated with areas of cave fill which has reacted chemically with the limestone. The speleothem may be a previously undescribed variety of helictite.

Zusammenfassung
Eine interessante Form von Heliktiten wurde in den Jenolan Höhlen gefunden. Charakteristisch für Band-Heliktiten ist die flache, dünne und bandähnliche Erscheinungsform, zusammen mit dem opaken Mittelkanal (ca. 0,2 mm Durchmesser). Die Spaltebene und Kristallausrichtung wurden untersucht und ein Wachstumsmechanismus ausgearbeitet. Mittels Laser Raman Spektroskopie konnte das Material als Kalzit identifiziert werden. Band-Heliktiten werden in Zusammenhang mit Oberflächen von Höhlenfüllungen, die chemisch mit Kalkstein reagiert haben. Dieses Sintergebilde könnte eine bisher unbeschriebene Art von Heliktit sein.

1. Introduction
Jenolan caves are famous throughout the world for their beauty and variety of speleothems, so it is surprising that the caves should be the home of a possibly new type of helictite, previously undescribed in the most commonly referenced book on cave minerals (HILL AND FORTI, 1986) and apparently not described in the speleological literature. The ribbon helictites were first found by the author in June, 1994, in Jubilee Cave, one of the northern show caves and shortly afterwards in Orient Cave, one of the southern show caves. A report was forwarded to the Jenolan Caves Reserve Trust (J. ROWLING, 1994). Subsequent trips to the Jubilee Cave revealed that the ribbon helictites were relatively common in sections of that cave. An article was prepared for the Journal of the Sydney Speleological Society (J. ROWLING, 1995) to show other cavers what these helictites looked like. In August 1995, permission was obtained from the Jenolan Caves Reserve Trust to remove samples for analysis. A total of 6 helictites were taken without having to damage any of the exhibits. These were initially analysed using Laser Raman Spectroscopy, UV light and a hand lens, and another report was forwarded to the Jenolan Caves Reserve Trust (J. ROWLING, 1995). This paper summarises the earlier work and introduces new discoveries regarding ribbon helictites.

2. Environment
At Jenolan, Ribbon helictites are associated with areas of cave fill which has reacted chemically with the silurian limestone bedrock. This fill is typically composed of rounded pebbles (shale, quartz porphyry) together with red and yellow muds. The muds may be chemical reaction products (limonite, etc) from reactions between oxidising pyrite in the cave fill and the limestone. In some areas of the Jubilee cave, near to where ribbon helictites are found, there are small deposits of gypsum on the floor. Surface coatings (secondary carbonate deposits) in areas with ribbon helictites vary from sugary (large rhombic- or scalenohedral- terminated crystals) to smooth. Both the Jubilee and Orient caves are deep within the tourist caves complex. The humidity is very high (typically around 98% RH), the temperature is around 13°C and the CO_2 level is only mildly raised (typ. 0.7%). Air movement is very little.

3. General Appearance
A generalised ribbon helictite is shown in fig. 1. Ribbon helictites are usually attached to the cave wall by a stem in which a very small canal may be seen. The stem is usually perpendicular to the cave wall. After a few millimetres, the helictite develops a flat ribbon, oriented parallel to the stem but apparently growing outwards, perpendicular to the stem. A central canal is visible in the stem and ribbon as an opaque white stripe. At the end of the ribbon is presumably the growing tip. Fig. 2 is a sketch of the 6 samples from Jubilee Cave. Only samples 'a', 'b' and 'd' had their stems intact; the stems of 'a' and 'd' were later broken. The longest ribbon helictite seen in Jubilee Cave is about 120 mm long, about 5 mm wide and about 2 mm thick.

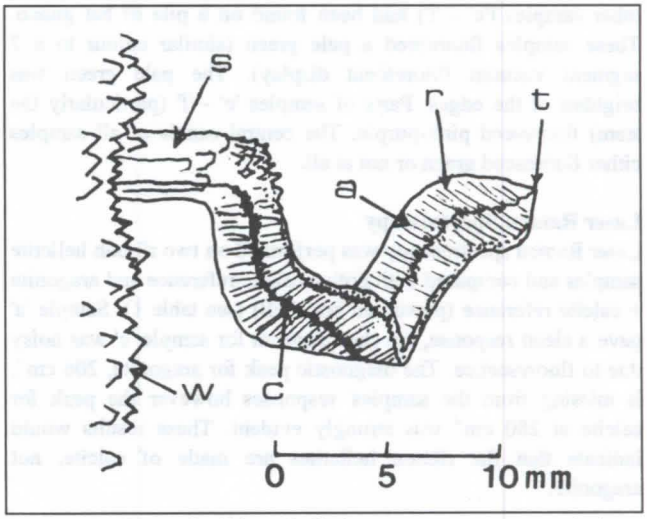

Figure 1: General ribbon helictite. s = stem, a = striations (parallel to c axis), r = ribbon, t = tip, c = central canal, w = wall of cave.

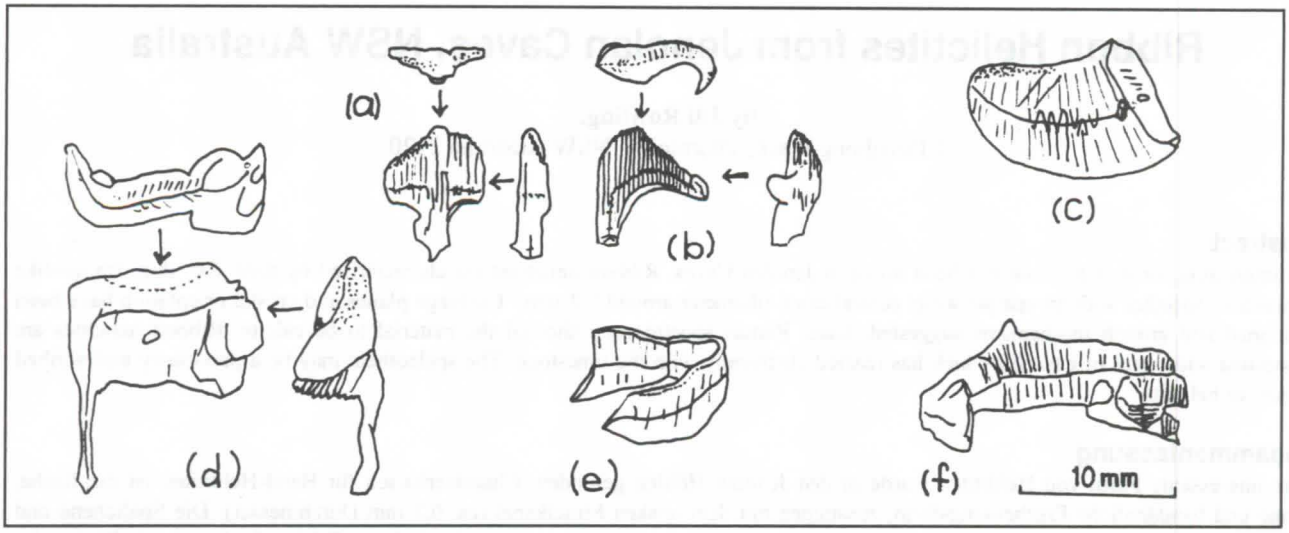

Figure 2. The 6 samples, 'a' - 'f'. Various views.

4. Tests Performed

Initial Tests

In order to determine the composition of the ribbon helictites, some simple initial tests were performed. Hardness: harder than fingernail, softer than steel, therefore not gypsum or quartz. Taste: none, therefore not guano-based (salt, nitre, etc). Colour: transparent. Lustre: glassy. Cleavage: at least one perfect. Crystal shape: roughly flattened hexagonal prisms with scalenohedral or blade-like terminations, a little like aragonite.

Phosphorescence and Fluorescence

Ribbon helictite sample 'a' exhibited phosphorescence when a photographic flash gun was used. Persistence time was about 0.3 seconds. All the ribbon helictite samples fluoresced when exposed to long wave UV light from a 15 watt tube source. Samples 'a' and 'b' fluoresced pink-purple; these were from a relatively clean part of the cave (not in bat guano or mud). The other samples ('c' - 'f') had been found on a pile of bat guano. These samples fluoresced a pale green (similar colour to a 7 segment vacuum fluorescent display). The pale green was brightest at the edges. Parts of samples 'c' - 'f' (particularly the stem) fluoresced pink-purple. The central canals of all samples either fluoresced green or not at all.

Laser Raman Spectroscopy

Laser Raman spectroscopy was performed on two ribbon helictite samples and compared with both a calcite reference and aragonite + calcite reference (powdered sea shell) (see table 1). Sample 'a' gave a clean response, but the spectrum for sample 'c' was noisy due to fluorescence. The diagnostic peak for aragonite, 206 cm^{-1}, is missing from the samples' responses however the peak for calcite at 280 cm^{-1} was strongly evident. These results would indicate that the ribbon helictites are made of calcite, not aragonite.

Infra Red Spectroscopy & SEM/EDX

A small piece of broken stem from sample 'a' was recently (1996) analysed using an IR spectrophotometer and SEM/EDX (energy dispersive analysis by X-rays using a scanning electron microscope). The crystal terminations were observed to be as per fig. 3 (most common form) (P. MAYNARD, pers. comm).

IR results:	Structure:	Calcite (not aragonite)
	Anions:	CO_3^{2-} 100%
SEM/EDX results:	Cations:	Ca 99.5 atomic %
		Fe 0.5 atomic %

It was unknown whether the Fe was part of the crystal structure, or an inclusion, or a surface contaminant.

Sample Description	Wave numbers (cm^{-1})
Calcite sample	1088, 714.5, 283.6, 158.4
Published data for Calcite	1086, 712.0, 280.0, 153.0
Aragonite + calcite sample	1084.6, 701.6, 278.6, 204.6, 152.0
Published data for Aragonite	1085.0, 702.0, 270.0, 206.0, 189.0, 177.0, 151.0, 112.0
Sample 'a'	1082.9, 709.7, 279.8, 152.6
Sample 'c' (noisy)	1088.1, 714.5, 284.2, 157.8

Table 1. Laser Raman Spectroscopy results. Only important peaks have been listed.

5. Under the microscope

Crystal form

The terminals of individual crystals were studied on ribbon helictite samples 'a', 'b' and 'd'. Fig. 3 illustrates some of these forms. The long crystals are irregularly hexagonal in cross section, many being terminated by scalenohedrons or blades.

The Stem

Samples 'a', 'b' and 'd' had their stems intact and could be examined. Each had a white line running down the stem. In the case of samples 'b' and 'd', the line ended at a small hole, visible in the broken stem. In sample 'a', there were two white lines which appeared to define the boundaries of individual crystals. A hole was not visible. Fig. 4 shows the broken stem of sample 'd'. Also visible in this view are some of the cleavage planes. The stem appears to be composed of a bundle of separate crystals, aligned with their c axes (optical axis) parallel to the stem as shown.

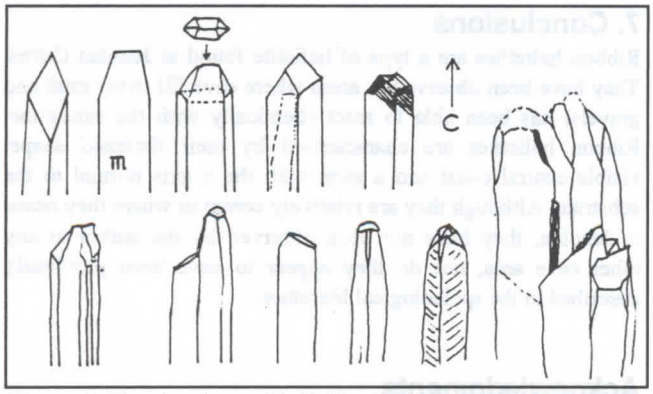

Figure 3. Terminations of individual calcite crystals as seen on ribbon helictites. Termination 'm' is the most common form seen. Arrow indicates c axis.

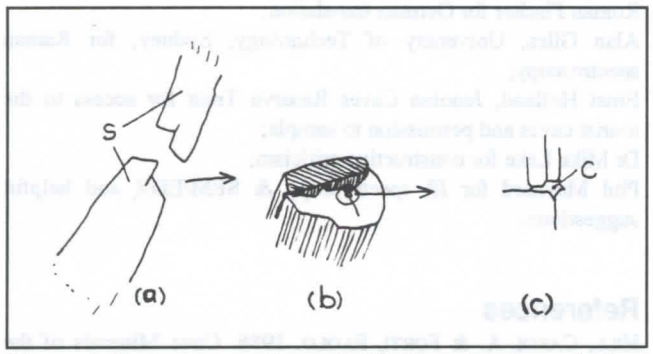

Figure 4. Broken stem of sample 'd'. View (a) shows broken stem s. View (b) is a close-up of the break showing cleavage planes and small hole (circled). View (c) is a close up of the hole showing the central canal c as an interstitial site between crystals.

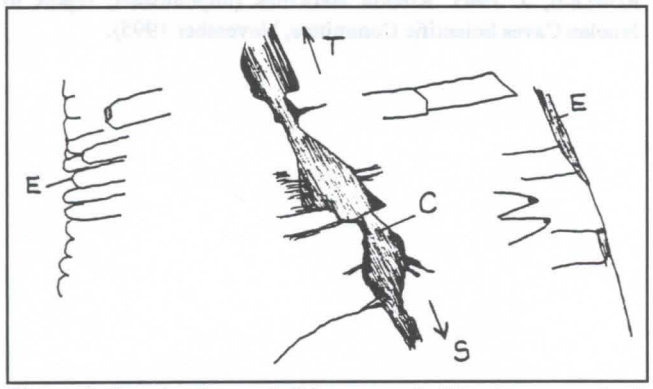

Figure 5. Sketch of part of ribbon, sample 'b' using transmitted polarised light. Edges of ribbon, E, exhibit both smooth and rough crystal terminations. Only some surface crystals are shown. Central canal, C, is irregular and appears to delineate crystal faces. Direction T is toward the tip; S is toward the stem.

The central canal

The central canal was visible in all samples. Samples 'c' and 'd' had broken sections where the central canal could be inspected. The canal diameter of sample 'c' was about 0.2 mm diameter, measured by comparison with a graticule. The canal in sample 'd' was roughly circular and lined with drusy crystal. In all samples, the average diameter of the central canal seemed to decrease at the tip and stem. Assuming that the helictites grow from the tip, this implies that the average canal diameter of the ribbon increases with age of an active ribbon helictite. Fig. 5 is a sketch of the central canal of sample 'b'. The central canal here appears as a set of concentric cones, possibly defined by crystal boundaries. The shape of the canal may be due to dissolution (P. MAYNARD, pers. comm).

The tip (growing point?)

The small hole at the tip of sample 'b' was irregular in shape and may have been damaged. The surrounding material had a glassy lustre. No canals at the tips of sample 'a' could be seen at the surface, however the canal appeared to get very close to the tip - see fig. 6.

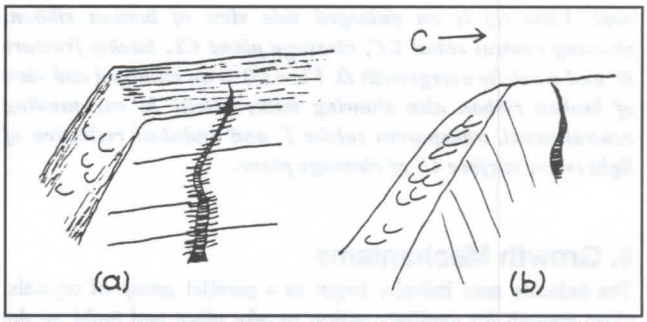

Figure 6. Sketches of the tips of sample 'a'. (a) Using transmitted polarised light, the striations are visible and parallel to the c axis; (b) using reflected polarised light, cleavage lines are visible on the surface. The central canal gets close to the tip, but no hole at the tip could be seen.

The ribbon

The ribbon seems to be formed from close spaced crystal aggregates with their c axes aligned in the same direction as the stem. The c axis and striations (see figs. 1 and 2) lie parallel to the long flat side. The long edges of the ribbon vary from smooth to angular and sharply defined. They may correspond to crystal faces. On some ribbon helictites, these edges are rough due to the steep scalenohedral crystal terminations, but on others, they may be smooth and glassy. Some of the long crystals superficially resemble aragonite, however the cleavage is of the calcite type. Using polarised light, the flat face of sample 'a' was examined for optical extinction. This sample has two ribbons. Each ribbon exhibited complete extinction, however, the angle at which this occurred was different for each ribbon. Looking down the c axis of samples 'a' and 'c', it was observed that the crystals offset. The direction of offset varies with individual helictites.

Ovals and other bizarre growths

Many ribbon helictites have an oval shaped side growth that is attached to the ribbon. Fig. 7 shows an oval on sample 'd'. In the field, ovals have been seen on several ribbon helictites. They do not seem to be connected to the central canal, rather they appear to be part of the ribbon surface. The c axis of crystals comprising these growths does not seem to be related to that of the ribbon. They may represent twinning at the ribbon surface. Sample 'f' exhibited a small ribbon growing from the main ribbon (see fig. 2, sample 'f').

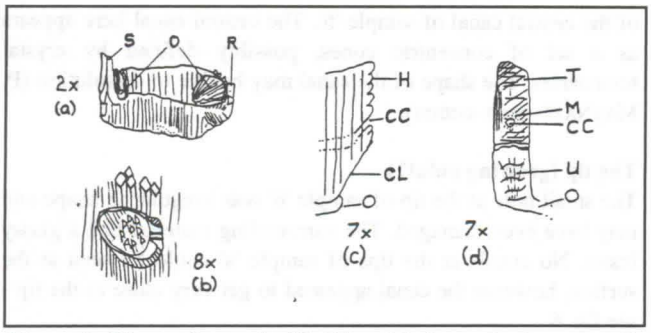

Figure 7. Views of sample 'd'. View (a) shows broken stem S, and broken ribbon R with two ovals O. View (b) shows detail of oval. View (c) is an enlarged side view of broken ribbon, showing central canal CC, cleavage plane CL, hackly fracture H, and a calcite overgrowth O. View (d) is an enlarged end view of broken ribbon also showing milky calcite M surrounding central canal, transparent calcite T, and undulose reflection of light (wavy surface U) of cleavage plane.

6. Growth Mechanisms

The helictite may initially begin as a parallel group of crystals, close enough for capillary action to take place and build up the stem. Alternatively, they may begin as fine, straight spicular helictites. A mechanism for initiation of ribbon growth is yet to be determined, however it must explain how the central canal alters its direction from normal to the substrate, to parallel to the substrate. It must also explain why the c axis of most of the helictite's crystals remain parallel to the stem, unlike most helictites in which the c axis is radial to the central canal. Calcite dissolves or deposits preferentially along the c axis. In ribbon crystals, the c axis is normal to the central canal. The average diameter of the central canal may be larger along the ribbon than at the stem due to this preferential dissolution. The diameter of the canal at the tip may be small as this may be where calcite is being initially deposited. The various smooth and rough faces of ribbons indicate there may be more than one mechanism involved in the formation of ribbon helictites.

7. Conclusions

Ribbon helictites are a type of helictite found at Jenolan Caves. They have been observed in areas where cave fill (river mud and gravels) has been able to react chemically with the limestone. Ribbon helictites are characterised by their flattened shape, visible central canal and a stem with the c axis normal to the substrate. Although they are relatively common where they occur at Jenolan, they have not been observed by the author at any other cave area, nor do they appear to have been previously described in the speleological literature.

Acknowledgments

The author is extremely grateful for the assistance of the following people:
Tony Allan, University of Technology, Sydney, for access to the microscope and useful books on mineralogy;
Roman Fischer for German translation;
Alan Giles, University of Technology, Sydney, for Raman spectroscopy;
Ernst Holland, Jenolan Caves Reserve Trust for access to the tourist caves and permission to sample;
Dr Mike Lake for constructive criticism;
Phil Maynard for IR spectroscopy & SEM/EDX and helpful suggestions.

References

HILL, CAROL A. & FORTI, PAOLO. 1986. Cave Minerals of the World. National Speleological Society: Huntsville. 238 p.
ROWLING, J. Investigation of Speleothems at Jenolan. (unpublished; report to Jenolan Caves Reserve Trust, June 1994).
ROWLING, J. 1995. Ribbon Helictites: A New Type of Speleothem? *Journal of the Sydney Speleological Society*, 39 (7): 152
ROWLING, J. 1995. Ribbon Helictites (unpublished; report to Jenolan Caves Scientific Committee, November 1995).

Stalactites, crystlactites, corlactites, tuflactites - 4 types of "stalactite-like" formations, generated from crystallization environments with different physical properties

Vladimir A. Maltsev
VNIIGEOSYSTEM institute. Moscow 121351, Yartsevskaya ul., 15-21, Russia

Abstract

The most usual speleothems – stalactites – appear to be a mixture of at least 4 types, having unsimilar structure and texture, which seems to be controlled by different crystallization physics. It was first suggested by STEPANOV 1973 to call them "stalactites", "tuflactites", "crystlactites", "corlactites", etc., but the definitions were based on their textures only, without analyzing structures and growth kinetics. Recent studies of stalactites crystallization physics have shown strict boundaries for the 4 main types listed above, and allowed to formulate definitions for these formations. All 4 terms apply to minor mineral bodies with gravitational dissymetry in their texture, forming in subaerial conditions out of dripping solutions. Among them, the term "stalactites" must be used for the formations whose crystallization is controlled by hydrodynamic effects; "crystlactites" and "corlactites" - for the formations whose crystallization is controlled by evaporation, The "crystlactites" are built of crystals, the "corlactites" of spheroidolites; "tuflactites" - for the gravitation-controlled tufa formations. In most of the cases crystallization of the "tuflactites" is related to P-T barriers.

Introduction

In the early 70-th STEPANOV (1971, unprinted lectures in 1973) suggested an onthogeny-based classification of speleothems. One of the central points was a concept of the network of contiguous genetic lines, connecting different speleothems through hybridization of their textures.

Let's see closely the formation from the fig. 1. It has properties of both a stalactite with a drapery (general geometry, orientations of crystals, etc.), and of a frostwork bush (lack of channels, faced surfaces, surface brakes on flow lines, etc.). In Stepanov's classification this is a crystlactite - a hybride formation on the connection line between stalactites and frostworks. There were suggested also names for some other "around-stalactites" connection lines, leading to popcorns (corlactites), to helictites (helilactites), etc. A separate place is taken by the concept of tuflactites - stalactite-like carbonate formations of rapid growth. They are not points on some connection lines, but separate speleothems, that have non-regular tufa structure, so being not mineral aggregates, but more likely tufa facies.

The studies by the author have shown, that some of these formations are really hybride formations as, for example, helilactites (on the fig. 2 one of such formations is shown), but some of them appear as separate aggregates with definite growth

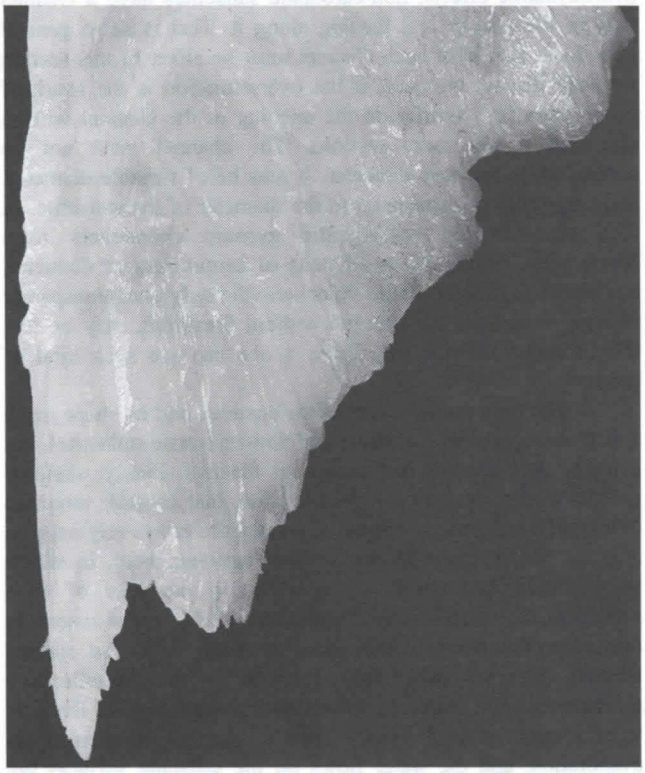

Figure 1. Calcite crystlactite, 8 cm long, from the Navstrechu Cave, Khaidarkan mines, Kirgizstan.

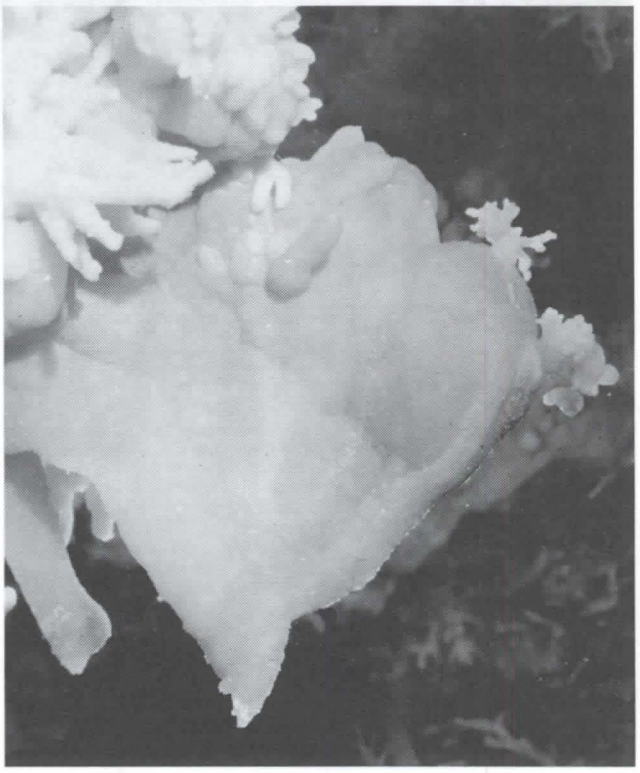

Figure 2. Double-hybride formation 40 cm long, with it's texture, mixed from stalactite, shield and helictite. Cupp-Coutunn cave, Turkmenistan.

mechanisms. They really have hybride textures, but there are no any contiguous rows between them. These are real stalactites, crystlactites, and tuflactites. Corlactites are the same type of mineral aggregate as crystlactites, and their growth is controlled by the same mechanism, but they differ in the mineral individual type (crystals vs. spheroidolites). This strongly affects their morphology. Therefore, it seems to be reasonable to keep different terms.

Regular stalactites

On contrary to the wide-spread understanding (HILL & FORTI, 1986), regular calcite stalactites have the mechanism of oversaturating of the solution. This process is more complicated, than simple disbalance between CO_2 contents in the air and in the seeping water. MALTSEV 1997 has shown, that in the regular case for soda-straws the initial disbalance is absent. The oversaturation appears only on the soda-straw's tip as a result of hydrodynamic strikes while the disconnection of drops. This mechanism defines the structure, that can be seen on the figure 3. The explosive CO_2 loss in solutions happens from mechanic impacts. Therefore, any hydrostatic pressure jump strongly disbalances the solution-air system. Time intervals of impacts are too short for mixing of the solution. These two conditions together allow crystals to grow on edges or tips, but forbid massive growth on faces, and this results in skeletization of the crystals (ZHABIN, 1979). Inside the drop these crystals are immediately dissolved again, but along the contact with the air they survive. On the photo, one can see this "crown" of skeleton crystals. Skeleton crystals are poorly balanced formations. Therefore, the pulsations of the pressure inside the channel re-crystallize this crown into a monocrystal. The phases of this process may also be seen from the photo.

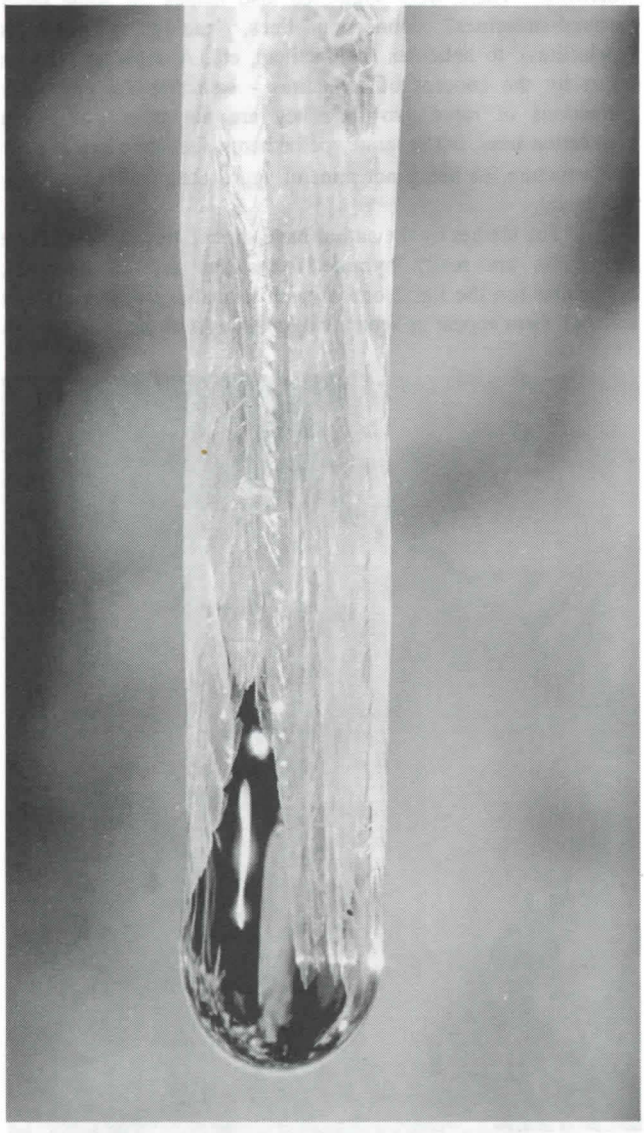

Figure 3. Calcite soda-straw. There can be seen the "crown" of skeleton crystal, and its sequential re-crystallization into a monocrystalline tube.

The described mechanism has two interesting consequences. The first is that the channel in regular stalactites is secondary. It is not a feeding channel, but a result of the crystallization physics. The cone stalactites are not soda-straws with later overgrowth, but are simply stalactites with initially oversaturated feeding. The extra calcite is crystallized on the side surfaces, and the crystallization on the tip is just the same as for soda-straws.

The second consequence is much more important. The pressure impacts while drop disconnection is significant for the carbonates only. Solubility of usual salts, not needing to lose carbondioxide for their crystallization, may not significantly change. Therefore, non-carbonate formations must have some principally different crystallization mechanisms, and their structure must be very different. This concept matches general observations. Non-carbonate stalactites of usual shape are rare. For example, gypsum stalactites usually appear as chandeliers, and gypsum "soda-straw-like" stalactites were reported only several times. Unfortunately without good photos, allowing to see their structure.

Non-carbonate crystlactites and corlactites

In contrary to regular carbonate stalactites, whose channel alway is a result of their crystallization through hydrodynamic effects, non-carbonate stalactites have a channel only in the case of real feeding along it. That is not a general case. Let's see, what such channel must be alike. In this section we shall discuss the case, if the oversaturation is the result of evaporation (P-T barrier on the opening of the channel will be discussed in the next section). The channel must not be controlled by the drop diameter. It may be of variable diameter, and may roughly correspond to the diameter of the stalactite. In fact, channels in the gigantic gypsum chandeliers from Kugitangtou caves may reach tens of centimeters in diameter, and channels in small halite stalactites (the only ones transparent enough to observe the channel without breaking), may be less than 1 mm wide. On the figure 4 one can see such kind of channel.

Not only the existence of the channel, and its shape make a difference between carbonate and non-carbonate stalactites, but a lot of their textural and structural features. Firstly, skeleton growth with permanent re-crystallization, that controls structure of a regular stalactite, is absent. A crystlactite grows originally as a group of crystals with competition between them, in which usually only one survives. Secondly, in the case of cone stalactites, the sharp contrast between core and crust is absent. In this case, the overgrowing crust, growing from the surface feeding, does not differ from the core in the crystallization mechanisms, and therefore, grows as a continuation of the core without any textural break. Thirdly. As the mechanism is evaporation, and the water flows on the stalactite surfaces are usually slow and thin, the crystallization partly depends on the surface geometry, enforcing on the points with high surface curvature (MOROSHKIN, 1976). This provides partial conic

characteristics symmetry of the aggregate's texture (usual growth from water flows, losing CO_2, has spherical characteristics symmetry). Therefore, we definitely receive a real hybride texture between frostworks and stalactites, with no possibility of separating them on any organization level, as it was proposed by Stepanov.

Corlactites appear in very similar cases, but only if the chemical or mechanical admixtures in the solution makes the crystals grow splitted. All the considerations on the channel geometry remain the same, but the considerations about their surface overgrowth change. Splitted crystals, especially if they are splitted to high grades (spherolites or spherocrystals), do not have sharp tips and edges. This spreads the surface flow more regularly, so the hybridization of texture is incomplete. At the hybridization grade, where the cone symmetry is still hardly noticeable, separation of texture proceeds, and we can observe isolated popcorn bushes, mounted into an almost inaffected druse of spherolites.

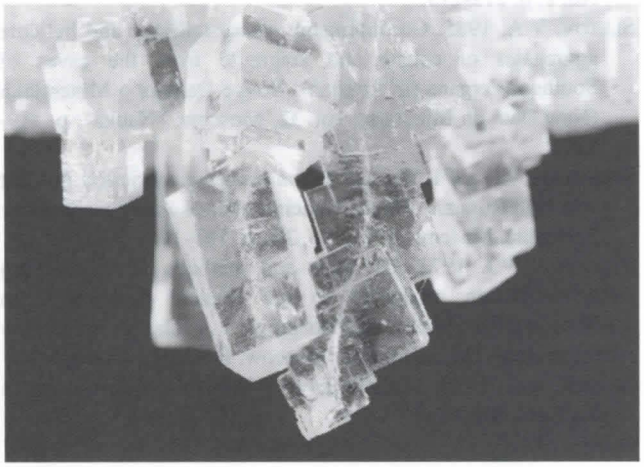

Figure 4. Halite crystlactite, 3 cm long. Small cave, intersected by Ingurotzlow mines, Poland.

Carbonate crystlactites and corlactites.

The previous chapter shows the impossibility of real stalactite appearance in the non-carbonate case. But this does not mean, that corlactites and crystlactites are absolutely impossible in the carbonate case.

Corlactites and crystlactites are possible in the carbonate case if the growth is so slow, that the quantity of material, crystallizing in the hanging drop between the dripping moments, becomes compatible with the quantity of material, precipitated during the one-drop impact. These are very rare conditions for calcite, usually found only in deep isolated caves, that are sometimes intersected by mines, like the cave, where the crystallictite from fig. 1 grew. But these are not very rare conditions for aragonite in the case, when its growth is provided by the presence of the Mg ion. The CO_2 contents regulates the general carbonate solubility. If we consider the Mg ion separately, its solubility depends more on the evaporation. According to that, almost always aragonite crystals in regular conditions appear splitted. Finds of aragonite corlactites are more usual. The fig. 5 demonstrates the growth zone of such formation.

In the carbonate case of crystlactites and corlactites we can clearly recognize, that though they have a real hybride texture, they can't be considered as points on the contiguous rows, connecting parent aggregates. The classifying feature - existence of the re-crystallized central tube, heaving a break to the overgrowths - appears step-wise. Therefore, we deal with row frostworks - crystlactites and popcorn - corlactites. Both of them have no connection to real stalactites.

Tuflactites

Contrary to real stalactites, crystlactites and corlactites, tuflactites are not some regular-crystalline formations. They were separated from other formations on the very first stage of applying onthogenetic approach to the cave mineralogy (STEPANOV, 1971). By Stepanov's definition, tuflactites are stalactite-like formations, growing from very strong water flows. In these conditions the main mechanism for the solution oversaturating is again mechanical - turbulence of the flow. This leads to the spatial nucleation, not allowing crystals to start the competition and to form any kind of a regular aggregate. Tuflactites may have an internal channel or not. But in any case, they do not have a monocrystalline core, and their structure though concentric-zonal, is not radial-fibrous. If the channel exists, it has irregular geometry. The characteristic symmetry of texture is spherical. In reality they are the most noticeable kind of stalactite-like formations in every wet cave, but are rarely studied - studies concentrate on smaller speleothems, that are usually regular.

This definition covers only a part of the stalactite-like speleothems, specified by lack of regular crystalline structure. The conditions of spatial nucleation appear on P-T steps on the feeding channels openings. This can be seen in a lot of ore mines, where tuflactites grow in mines themselves. Sharp P-T barriers, appearing between feeding fractures and mine galleries even lead

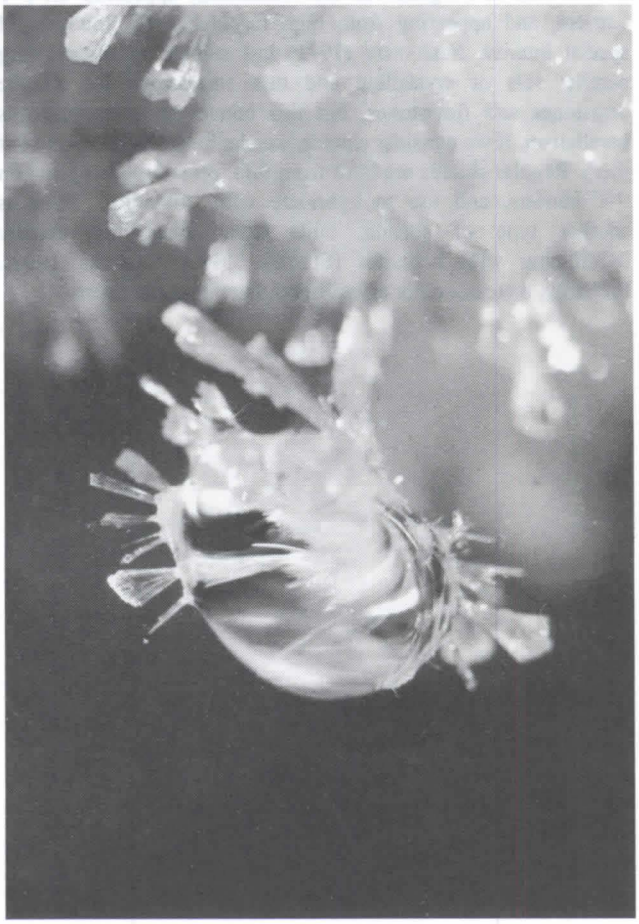

Figure 5. The growth zone of an aragonite corlactite. Cupp-Coutunn cave, Turkmenistan.

to appearance of thin, soda-straw-like formations, but microcrystalline and high-porous. The author observed such formations in Khaidarkan and Kadamjai mines in Kirgizstan. Similar formations, not only carbonate ones, are also reported from cavities in iron deposits. For example, PLAVSHUDIN (1973) describes cryptomelane tubular stalactites from Nikopol'skoye deposition, providing the photos, where the core is definitely an irregularly microcrystalline.

Tuflactites as corlactites and crystlactites, do not make up any contiguous connection rows to any of the formations discussed above. Due to the variations of conditions, they may be mixed with any other layer (mostly with regular stalactites).

Discussion

This study illustrates a rather important effect. A good onthogenetic study, like the one of Stepanov, based only on description of structures and textures of aggregates without any theoretical modelling (STEPANOV, 1973), gives very precise results. The stalactite type classification was received from such study, and it matches the crystallization physics perfectly. Furthermore, this physics modelling disproved part of the general ideas.

Probably, it is interesting to continue the modelling with some neighboring types of speleothems. Firstly, the stalactite-like formations are not only those, growing from solutions in subaerial conditions. For example, icicles (growing from melts) show a texture very similar to real stalactites (MAKKONEN, 1988), and the reasons of this remain unstudied. Another example - subaquaeous pseudostalactites, that partly match tuflactites (also P-T barrier), and partly do not.

The convergence of the formations, appearing on P-T barriers, and appearing from high turbulence of flows, is of special interest. STEPANOV (1971) has shown non-hybridizing parallel sets of crystalline and tufa formations for all the dripstones and flowstones, but this convergence extends this parallelism. If we consider shields, we shall also see two kinds of them. Regular shields are built from tufa, probably also grow on P-T barriers, and use to hybridize with tuflactites. There is another type of shields, built from spherolites, usually hybridizing with helictites (SLETOV, 1985; CABROL, 1997). Probably, there are other crystalline/tufa twin speleothems.

References

CABROL, P. 1997. Blue Cave. In: HILL & FORTI, Cave minerals of the world, 2-nd edition. NSS, in press.

HILL, C. & FORTI, P. 1986. Cave minerals of the world, NSS, 238p.

MAKKONEN B.A. 1988. A model of icicle growth. Journal of Glaciology, vol. 34, No. 116, pp. 64-70.

MALTSEV, V.A. 1997, Once more on stalactites with "internal" and "external" feeding: National Speleol. Soc. Bull., in press.

MOROSHKIN, V.V. 1976. On genesis of crystallictite type of aggregates (in Russian). Novye Dannye o Mineralakh SSSR (New Data on Minerals in USSR), vol. 25, Moscow, "Nauka", p.82-89.

PARUNGO, F.P. 1983. Ice crystals growth at -8+/-2°C. Journ. Research Athmos. Vol. 17.No. 2, 139-156

PLAVSHUDIN, V.G. 1973. Cryptomelane stalactites from the Nikopol'skoye deposition. Zapiski Vsesouznogo Mineralogicheskogo obschestva, Leningrad, 1973, vol. 102, No. 2, p. 213-215.

SLETOV, V.A. 1985. On onthogeny of crystallictite and helictite aggregates of calcite and aragonite from the caves of Southern Fergana (in Russian). Novye Dannye o Mineralakh (New Data on Minerals), vol. 32, Moscow, "Nauka", p. 119-127.

STEPANOV, V.I. 1971. Crystallisation processes periodity in karst caves (in Russian) . Trudy mineralogicheskogo muzeja imeny Fersmana. Moscow, 1971, No. 20., p. 161-171

STEPANOV, V.I. 1973. On aims and methods when studying crystallisation sequences in ore mineral aggregates (in Russian). In book: Issledovaniya v oblasty prikladnoy mineralogii i kristallohimii. Moscow, IMGRE, p. 3-10.

ZHABIN, A.G. 1979. Onth/1ogeny of Minerals. Aggregates (in Russian). Moscow.

Cave Popcorn - an Aerosol Speleothem?

Yuri V. Dublyansky(*) and Serguei E. Pashenko(**)

(*) Institute of Mineralogy and Petrography, Russian Academy of Sciences, Siberian Branch, 3 University Avenue, 630090, Novosibirsk, RUSSIA. (**) Institute of Chemical Kinetics and Combustion, Russian Academy of Sciences, Siberian Branch, 3 Institutskaya Str., 630090, Novosibirsk, RUSSIA

Abstract

Nodular coralloids, "cave popcorn", are often reported from hypogene caves. In Hungarian hydrothermal caves, cave popcorn display regular distribution on cave walls. In caves composed of a multitude of spherical cupolas, 0.5 to 3.0 m in diameter, it lines m 0 the lower halves of each cupola. In large cave rooms it forms slightly undulating "popcorn lines" 1.5 to 2.0 m below ceiling. Individual nodules exhibit growth layers which are thicker at the nodules' tips and become thinner or even disappear at their "stems."

Speleothemic material gets into the cave air during the process of evaporation in hypogene caves during the stage of partial dewatering. Convection, condensation, chemical reactions (including redox- and radiochemical ones) readily occur in the cave atmosphere at that stage. Aerosols nucleated in the cave atmosphere migrate and settle down under combined action of convective air currents, Brownian diffusion, and gravitation. Geometry of popcorn deposition zones is governed by cave morphology, as well as by the dimensions of aerosol particles. Monte-Carlo modeling suggests that distributions of popcorn similar to those observed in Hungarian caves is predictable if the speleothemic material was supplied by aerosols.

1. Introduction: speleothems of aerosol origin

A number of speleothem types have been proposed as having an aerosol origin. CSER & MAUCHA (1968) made the first attempt to substantiate an aerosol origin for needlelike "helictites" (hoarfrost) not possessing capillary canals in some Hungarian caves. According to these authors, such crystal deposition resulted from an electrostatic effect where supersaturated and charged hydroaerosol droplets were deposited at the tips of the frostwork at the highest potential-gradient points. HALBICHOVA & JANCARIK (1983) described "aerosol sinter" in the Konepruske caves, Czechoslovakia, which sinter occurred in thin layers in the proximity of a cave entrance through which air is flowing. It was suggested that calcite aerosol particles act as condensation nuclei for moisture so that, when the air impacts a cave wall, the calcite is deposited as a thin film coating the wall. Gypsum crystals located on cave walls at passage intersections, "snow" (or "frost") on the floor, rims, and hollow stalagmites were considered by KLIMCHOUK *et al.* (1995) to be of aerosol origin.

The aerosol hypothesis for speleothem growth has been criticized by MALTSEV (1994). In the second edition of their book "Cave Minerals of the World," HILL & FORTI (*in press*) introduced a Special Topic Section entitled "Aerosols: are they a mechanism of speleothem growth?" (authored by CIGNA & HILL), where the comprehensive overview of the problem is given. It is emphasized that the aerosol hypothesis has neither been proved nor disproved, and that the major problem with this hypothesis is the poor understanding of the physics of aerosols in cave atmospheres.

Below, we hypothesize the possibility for cave popcorn to be formed from the moisture of the cave air with aerosol mass transfer being crucial to the process.

2. Cave popcorn

Popcorn is a nodular coralloid, growing roughly perpendicularly to the substratum. Individual nodules are often thinner at their "stems" and form larger rounded tips 0.3-0.8 cm in diameter. The typical size of individual nodules is 1-5 cm. Nodules often grow separately, close to each other; in other instances individual nodules merge at the advanced stages of growth. They also may branch and form bush-like aggregates with extremely variable morphology.

3. Growth from cave air: supporting evidence

Our hypothesis is based on the three observed features: (1) close relation between popcorn and hypogene caves; (2) regular distribution of popcorn on the cave walls; and (3) characteristic pattern of growth layers in individual nodules of popcorn.

Popcorn and hypogene caves

Cave popcorn is most often reported from hypogene caves. For instance, the two sites where it is most abundant and where it was studied in considerable detail are hypogene Carlsbad Cavern in New Mexico, USA and numerous hydrothermal caves in Hungary. At the beginning of this century the cave popcorn was even regarded to be evidence for a hydrothermal origin for the caves of Budapest (TAKÁCS-BOLNER & KRAUS, 1989).

Distribution of popcorn on the cave walls

Our observations in Hungarian caves have shown that distribution of cave popcorn on the cave walls exhibits the following regularities (figure 1). In "classic" multi-cuspate bush-like hydrothermal caves, such as Bátori Cave, popcorn occupies the lower halves of each spherical cupola (the latter being 0.5 to 3.0 m in diameter). Thickness of popcorn lining (which is, the

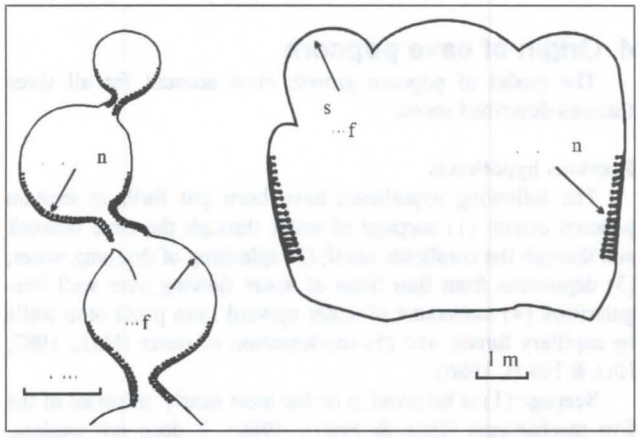

Figure 1 : Distribution of cave popcorn on the walls in Hungarian caves (schematized). Left - multi-cuspate bush-like hydrothermal cave Bátori; Right - large room in Foldvari Aladar Cave

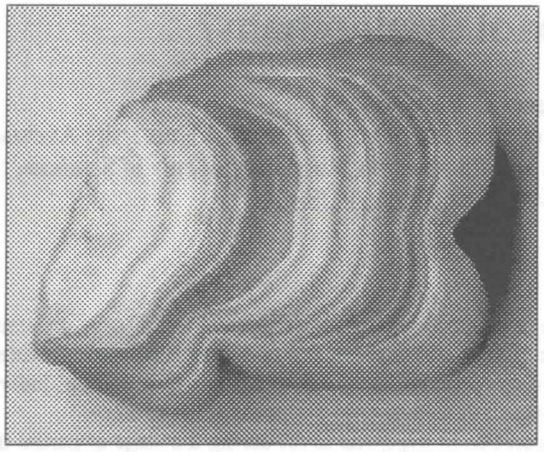

Figure 2 : Cross section of the cave popcorn nodule in its original growth position. Note the disappearance of growth layers towards nodules' "stem" (left).

length of individual nodules) increase in each lining zone downwards. Such pattern repeatedly occur in each cupola, so that the popcorn-lined and the solutionally-carved parts of the cave alternate within a 0,5-1,0 m distance.

In cave rooms 3-5 m high and tens of meters long/wide, as in the Foldvari Aladar Cave, popcorn forms nearly a horizontal (slightly undulating) line on the wall some 1.5-2.0 m below the ceiling. Again, the thickness of popcorn lining increases downwards from 0.5-1.0 cm at the upper limit of the "popcorn line" to 5-6 cm at its bottom.

Fragments of the "popcorn line" were observed in some passages of the network maze of the Szemlo-hegyi Cave. The "line" is also documented in Carlsbad Cavern, New Mexico, USA (HILL, 1987). Overall distribution of popcorn on the walls in different (hypogene) caves does not show any relation to the bedrock lithology.

Growth layers in popcorn nodules

Being cut across the axis of growth, individual nodules exhibit concentric growth rings. Along the growth axis, the layers are thicker at nodules' tips; some growth layers are present only at the tips and gradually disappear closer to the "stems" of the nodules (figure 2). The growth layers in Hungarian cave popcorn are composed of rhombohedral crystals 40-80 μm; there occur sporadic micritic layers 80-100 μm thick (NÁDOR, 1993).

4. Origin of cave popcorn

The model of popcorn growth must account for all three features described above.

Previous hypotheses

The following hypotheses have been put forth to explain popcorn origin: (1) seepage of water through the cave bedrock and through the coralloids itself; (2) splashing of dripping water; (3) deposition from thin films of water flowing over wall irregularities; (4) movement of water upward from pools onto walls by capillary forces; and (5) condensation of water (HILL, 1987; HILL & FORTI, 1986).

Seepage (1) is believed to be the most nearly universal of the five mechanisms (HILL & FORTI, 1986). It does not explain, however, regular distribution of popcorn on the cave walls: the popcorn occurs in caves developed in different rocks; it lines bedrock and older speleothems cutting across lithologies and does not show any relation to the character of the substratum.

Deposition from splashing water (2) is feasible; however, the largest amounts of popcorn form in cave settings where the presence of dripping water is not possible (e.g., figure 1). The splash aerosol droplets are comparatively large (1-100 μm), and according to aerosol mechanics they must settle down within 0,1-10,0 m distance from the drip point (assuming the air velocity does not exceed 10 cm/s). Hence, this mechanism cannot account for extensive popcorn deposits covering hundreds of square meters of the cave walls (unless unrealistically high number and regular distribution of drip points across the cave is assumed).

Deposition from gravitation-driven or capillary films (3 and 4) does not account neither for the characteristic morphology of individual nodules, nor for the uneven distribution of growth layers in nodules, nor for the regular distribution of popcorn on the cave walls.

Of the five mechanisms suggested, only condensation (5) relates deposition of popcorn to the cave atmosphere. We suggest the precipitation of hydroaerosols as another mechanism, complementary to condensation.

Deposition by aerosol mechanism: a new hypothesis

To allow growth of speleothems from an aerosol phase it is necessary for aerosols to carry speleothemic material. We suggest that this material gets into the cave atmosphere when mineralized water evaporates. The process is governed by thermodynamic properties of the cave water and atmosphere, such as temperature and saturation pressure of dissolved species. By way of example: extensive studies of the chemistry of aerosols collected above the oceans, carried out in 1950s, have shown that the concentrations of major elements in aerosols correspond to those of oceanic water (AEROSOLS AND CLIMATE, 1991)

Apparently, hypogene caves upon their partial dewatering, represent the most favorable setting for dynamic processes in the cave atmosphere above the water table. Intensive evaporation and thermal convection occur above the surface of hot water, which contains elevated amounts of dissolved solids and gases. Vertical temperature gradients in such caves are often high, so the rising of moist warm air to the upper cooler parts of the cave leads to condensation, which may happen on the cave walls, but also in the air, resulting in the nucleation of aerosols. High thermal gradients, however are not a strictly necessary prerequisite. Nucleation of aerosols may take place even in nearly isothermal environments on local thermodynamic fluctuations.

H_2S degassed from water into the cave air may oxidize upon contact with outside air, forming aggressive H_2SO_4. Radioactivity in hypogene caves might be elevated due to emanation of radon and lack of ventilation, which promotes radiochemical reactions in the air (e.g., conversion of H_2S to H_2SO_4) and creates chemically active hydroaerosols.

Summarizing, the hypogene caves upon their incomplete dewatering represent a most favorable setting for the appearance and active migration of hydroaerosols with enhanced chemical aggressiveness. We suggest that comparatively fast growth of cave popcorn occurs during the stage of partial draining of hypogene caves and slows down or ceases when the cave acquires a "normal" ventilated regime.

A site where very fast (artificially enhanced) growth of popcorn can be observed is the Reczk mine in Hungary. There, at depth exceeding 1 km, the high-pressure warm mineralized waters seep out of fissures and form aerosols. The latter are transported by air currents created by mining ventilation. Popcorn grows at intersections of mining galleries; individual nodules reach size of 2-3 cm within a 2-3-year time span.

It should be emphasized that the above outlined mechanism of generation of autochthonous hydroaerosols carrying speleo-

themic material is applicable to all hypogene caves - not only those where the cave popcorn occurs. For popcorn to be formed, some additional requirements have to be met. We believe, that one of these requirements is relatively low thermal gradients, and thus, low velocities of convective air movement, which allows for aerosol precipitation in accordance with aerosol mechanics.

We suggest that the two mechanisms, inherent to hypogene setting and aerosol systems, air convection and aerosol precipitation, govern the distribution of popcorn on the cave walls. BADINO (1995) has shown that when an aerosol droplet is transported downwards by air flow (which is expected for the convective-cell pattern of air movement), it is compelled to evaporate, and when its size falls below the limit corresponding to its inside vapor overpressure, the droplet disappears, and the surrounding air equilibrates to a higher vapor pressure. If air becomes oversaturated, the droplets condense on the lower parts of cave walls. If these droplets contain dissolved salts, deposition of aerosol particulate matter may occur.

In those settings where convection is slow or non-existent, the aerosols are deposited according to the aerosol mechanics. It will be shown in the following sections that deposition of aerosol particles on the walls will be zoned.

Once the liquid aerosol particle hits the wall or the surface of a growing popcorn nodule, it may merge with other droplets to form a thin film of water. Subsequent migration and deposition of speleothemic material occur with and within this film (capillary movement, diffusion, chemical reactions). Because the "source" of aerosols (and of speleothemic material) is the bulk of the cave air, the tips of growing nodules are more accessible than deep "tunnels" between nodules. Hence, the supply of water and solute will be more intensive at the tips, which may account for the thicker growth layers, observed there.

Precipitation of dissolved material from thin films may occur due to loss of CO_2 or due to evaporation. Isotopic values $\delta^{13}C$ and $\delta^{18}O$ of popcorn samples from Carlsbad Cavern plot along the line which was interpreted by HILL (1987) as the "evaporation trend." Analysis of published (NÁDOR, 1993) and our original data have shown, however, that Hungarian popcorn does not exhibit such a pattern. Our detailed studies revealed significant variations (up to 3-4 permil) in stable isotopic properties within individual nodules. Apparently, there must exist more than one mechanism of calcite deposition in popcorn layers.

5. Hydroaerosols and speleothemic material in the cave air

The water in the cave air may exist in gaseous (vapor) and particulate (aerosol) form, the latter, most probably, being formed through homogeneous and heterogeneous condensation, developing due to fluctuations in cave temperature and humidity. The sizes of aerosol particles occurring in the cave air may vary from ~$5 \cdot 10^{-7}$ cm (several molecules) to ~0.01 cm (such particles contain up to 10^{16} molecules). Particles falling in the size range from $0.5 \cdot 10^{-7}$ to $5.0 \cdot 10^{-7}$ cm are often called "clusters" to emphasize their unusual properties. Within this size range there occur a sharp change in many properties of the matter (optical spectra, energetic levels, thermodynamic constants, etc.) from the molecular level to a level of solids.

Chemical analyses of water condensed from cave air on the chemically non-reactive surfaces often yield significant concentrations of Ca, Mg, HCO_3, and SO_4 (tens to hundreds of mg/l; MAIS & PAVUZA, 1994). Concentrations measured in cave condensate often appear to exceed those of the atmospheric precipitation in the region (Roosamarijn TARHULE-LIPS, *pers. com.*).

Condensation of the moisture contained in the cave air may occur onto cave walls and clastic sediments. Beside that, the moisture can condense in the air, sometimes forming fog (JAMESON, 1995). Presence of solid aerosol particles in the cave air promotes condensation and formation of hydroaerosols, because they serve as condensation nuclei. Our studies in the Kungur Cave in the Urals, Russia have shown that solid aerosol particles, brought into the caves by inward air circulation, acquire a water coat within a few hours (PASHENKO *et al.*, 1993; 1996).

6. Precipitation of aerosol particles inside caves - theoretical consideration

Let aerosols of different radii r form uniformly within a closed sphere or cube having dimension R. There is no air movement in the cavity. Particles precipitate on the cave surface due to: (1) Brownian diffusion (coefficient of diffusion D) and (2) gravitational sedimentation (velocity V_g). Distribution of the precipitation on the cave walls needs to be determined. The boundary condition is the immediate precipitation of a particle upon its contact with the wall. The latter is typical of particles with $r < 10$ μm; larger particles cannot be formed by the mechanism of homogeneous nucleation and consequent coagulation.

The characteristic time of the diffusion wandering before a particle hits the wall is $T_d = R^2/D$, whereas the time of particle sedimentation is $T_s = R/V_g$. Let us introduce a dimensionless number: $CAV(r) = T_d/T_s = RV_g(r)/D(r)$. This number characterizes the leading mechanism of particle movement: when CAV is small, diffusion prevails and sedimentation can be neglected; conversely, when CAV is large, diffusion can be neglected. It is to be noted that in a cave of a given size, the CAV depends only on the size of particles r.

Differential equation describing diffusion and sedimentation of particles is difficult to solve analytically. Introduction of the parameter CAV allowed us to obtain numeric solution by the Monte-Carlo method (direct modeling of particle precipitation process). The results are shown in figure 3.

In a spherical cavity at CAV=0.1 (small particles, diffusion), aerosols precipitate uniformly on the entire cave surface. At CAV=5 (large particles, sedimentation), precipitation occurs in the lower quarter of the sphere. Curves for intermediate CAV's intersect at approximately 1/3 of the cave height, which means that 4-6 % of particles of any size, precipitate at such height.

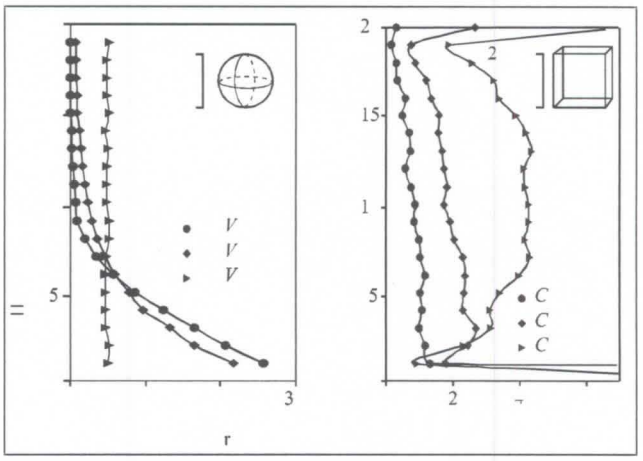

Figure 3 : Precipitation of aerosol particles on the surface of cave - a Monte-Carlo modeling. Left - spherical cave; right - cubic cave. See text for details.

In a cubic cavity at CAV=0.1, about 35% of particles precipitate on the floor and ceiling; at CAV=1 this number reaches 65% and 85% for CAV=5. So, only precipitation on the vertical walls is shown in the figure 3. Unlike in spheres, the curves of precipitation density have maxima. It is most prominent at CAV=0.1 and disappears at CAV>1. This means that if cave aerosol is composed of small particles, its deposition on the cave wall will not be uniform, and it will form a horizontal "line."

As it is seen from figure 3, the calculated distributions of aerosol precipitation on the cave walls are similar to that observed in natural caves.

7. Discussion

In constructing the model of cave popcorn growth with an aerosol supply of dissolved speleothemic material, we used the following line of reasoning: (1) speleothemic material is present in the cave air (as it is implied by chemical composition of condensate); (2) this material and water can reside in the cave air in form of a gas (vapor), molecular clusters, and aerosols; (3) the migration and sedimentation of each form obey physical laws (gas dynamics and aerosol mechanics); (4) characteristic distribution of cave popcorn on the cave walls, as well as peculiar form of popcorn nodules and the details of growth layering may be accounted for by intrinsic features of the aerosol system (precipitation of particles under action of gravitation and Brownian diffusion).

Our numeric estimations made for Hungarian caves have shown that the size of aerosol particles taking part in formation of cave popcorn must have been 0.01 to 0.02 μm. The characteristic time of popcorn growth is estimated as 3 to 30 thousand years, which is in agreement with geologically young ages obtained for popcorn samples from Carlsbad Cavern (33 to 45 thousand years; HILL, 1987)

Acknowledgments

We are thankful to Dr. Gabor Szunyogh for field assistance and fruitful discussions. Logistical support of the staff of Hungarian Speleological Institute (K. Szekely, K. Takács-Bolner, and S. Kraus) is appreciated. Special thanks to Carol Hill for discussion and editorial help.

References

AEROSOLS AND CLIMATE. 1991. /K.Y. Kondratiev, Ed. Leningrad: Gidrometeoizdat. 541 p. (*In Russian*)

BADINO, G. 1995. Fisica del clima sotterraneo. Memorie dell' Istituto Italiano di Speleologia. Serie II, v. 7. 138 p.

CSER, F. & L. MAUCHA. 1968. Contribution to the origin of "excentric" concretions. *Karszt és Barlangkutatas.* 5: 83-100.

GADOROS, M. & F. CSER. 1986. Aerosols in Caves - Theoretical Consideration. *9th Int. Congr. Speleol.* 90-92.

HALBICHOVA, I. & A. JANCARIK. 1983. Aerosol sinter and cave development. *Proc. of Int. Conf. "New trends in speleology"* Czechoslovakia. 8-10.

HILL, C. 1987. Geology of Carlsbad Cavern and other caves in the Guadalupe Mountains, New Mexico and Texas. *New Mexico Bureau of Mines & Mineral Resources Bull.* 117: 151 p.

HILL, C. & P. FORTI. 1986. Cave Minerals of the World. NSS, Hunstville. 238 p.

HILL, C. & P. FORTI. 1997. Cave Minerals of the World. Second Edition. (*in press*)

JAMESON, R. 1995. Condensation, Condensation Corrosion, and Associated Features in Snedegars and Greenville Saltpeter Caves. Underground in the Appalachians. A Guidebook for the 1995 NSS Convention. Blacksburg, Virginia. 122-125

KLIMCHOUK, A., V. NASEDKIN & K. CUNNINGHAM. 1995. Speleothems of Aerosol Origin: *NSS Bulletin*. 57: 31-42.

MAIS, K. & R. PAVUZA. 1994. Preliminary climatological observations in alpine caves of Austria. *Publ. Serv. Geol. Luxembourg,* 27: 165-171.

MALTSEV, V. 1994. On the aerosol origin of cave mineral aggregates: critical review of existing hypotheses. *Problems of Physical Speleology* (Moscow). 89-99. (*In Russian*)

NÁDOR, A. 1993. Mineralogy and stable isotope geochemistry of spelean carbonates from hydrothermal caves: *Conference "Karst and Cave Research Activities of Educational and Research Institutions in Hungary"*, Jósvafö, Hungary. 23-29.

PASHENKO, S., Y. DUBLYANSKY, & V. ANDREICHUK. 1993. Aerosol studies in Kungur Ice Cave. *11th Int. Congr. Speleol.* 190-192.

PASHENKO, S., Y. DUBLYANSKY, V. ANDREICHUK, & E. PASHENKO. 1996. Transformation of fractal atmospheric aerosol moving through natural cave. *J.Aerosol Sci.* 27, Suppl. 1: S127-S128.

TAKÁCS-BOLNER, K. & S. KRAUS. 1989. The results of research into caves of thermal water origin. *Karszt és Barlang*, Special Issue:31-38.

Microbial agents of moonmilk calcification

Michal Gradziński*, Joachim Szulc*, Boleslaw Smyk**

* Institute of Geological Science, Jagiellonian University, Oleandry Str. 2a, 30-063 Cracow, Poland

** Department of Microbiology, Agricultural University, Mickiewicza Str. 24/28, Cracow, Poland

Abstract

Moonmilk deposits from several caves from southern Poland (the Cracow-Wieluń Upland, the Tatra Mts.) have been studied. Two morphological types of moonmilk - furry and felt - have been distinguished. The former develop exceptional in shallow zone of the caves. The differentiation of moonmilk depends of the type of water supply. Both types occur primary as wet substance but during diagenesis become dry, porous and dusty.

Detailed microscopic observations display that moonmilk is organo-mineral mat built up by microorganisms (bacteria and fungi) as well as low-Mg calcite crystals. The growth of crystals is owing to biomineralization processes (both intra- and extracellular). High contents of organic matter and recognizing several species of microorganisms in wet moonmilk deposits strongly support the above conclusion. Diagenetic processes blur the former microbial structures, and therefore in dry moonmilk they are difficult to recognize.

Introduction

Moonmilk speleothems are common cave deposits, which differ from other autochthonous spelean sediments with massive and porous fabrics, soft and pasty consistency and very high contents of the water. Ageing, the moonmilk becomes dry, more rigid and compact, by secondary cementation, nevertheless the external morphology stays unchanged.

The moonmilk attracted man's interest for a long time. First, written records are by Georg Agricola, which described in 16th Century such speleothems from cave Mondmilchloch in Pilatus Mount (Switzerland). First scientific hypotheses on moonmilk origin, are known from 18th century (cf. BERNASCONI, 1961; FISCHER, 1988).

More recent, petrographical and microbiological studies revealed relationship between moonmilk and host rock mineralogies (POBEQUIN, 1960; BROUGHTON, 1971; FISCHBECK & MÜLLER,1971; HARMON *et al.*, 1983) and needle fibre calcite crystals as main components of the moonmilk (GRADZIŃSKI & RADOMSKI, 1957; HARMAN & DERCO, 1976; STOOPS, 1976). Due to a common presence of living microbes (HØEG, 1946; CAUMARTIN & RENAULT, 1958; MASON-WILIAMS, 1959, 1961; DANIELLI & EDINGTON, 1983) or their mineral replicas (SCHNEIDER, 1977; JONES & MOTYKA, 1987; JONES & MACDONALD, 1989) the moonmilk has been regared either as microbially precipited authochtonous carbonates or as microbially desintegrated remnants of the host rocks.

This paper presents some results of our studies on the origin of the moonmilk deposits as resulted from microbially controlled calcification

Materials and methods

Fresh, soft moonmilk specimens have been collected in several caves of the Cracow - Wieluń Upland (e.g. Zlodziejska, Zegar) and the Tatra Mts. (e.g. Szczelina Chocholowska, Naciekowa, Kozia, Magurska) (S. Poland) (Figure 1) differing in altitude (from 250 to 1800 m. a.s.l.), microclimate and vegetation cover.

In 24 hours after collecting, the samples were examined by means of a scanning electron microscopy and by *in vitro* culture. These investigations have been supplemented by chemical analyses of water and organic contents and mineralogical composition. In order to check postdepositional changes in the moonmilk deposits, the older, inactive moonmilk speleothems were examined by means of the same geochemical methods.

Figure 1 : Study area map

Results

Types of moonmilk speleothems

We have discriminated two types of moonmilk speleothems: the **furry and felt moonmilk,** which differ in several morphological and geochemical characteristics (Table 1). The furry moonmilk cover, up to 40 cm thick, occurs in shallow zone of caves (2-15 m beneath the surface) while the thinner (up to 10 cm) felt moonmilk has been also found in deeper caves (Figures 2, 3). Felt moonmilk are always covered with thin water film, dripping slowly down. Furry moonmilk accumulates a capillary and condensed vapour water. All the studied samples are built by low magnesiam calcite.

	furry moonmilk	felt moonmilk
H_2O contents [% by wt.]	71-75	92-96
$CaCO_3$ contents [% by wt. in dry mass]	88-94	69-74
organic matter contents [% by wt. in dry mass]	0.3-2.4	0.8-4.0

Table 1 : Basic geochemical charcteristics of fresh moonmilk

Internal fabrics of the moonmilk

Fresh moonmilk deposits consist of micritic irregular grains, needle fibre calcite crystals, fine-grained clastics, calcified microbe replicas and densely packed, interwoven cells of living microbes. The last-named form structural framework, which bound the mineral components of the moonmilk. This organo-mineral mats is fixed by sticky, exopolymeral mucus, which isolates the microbes from external environment (Figures 4, 5). In the aged, consolidated moonmilk the crystalline components dominate and the microbial replicas are sporadic.

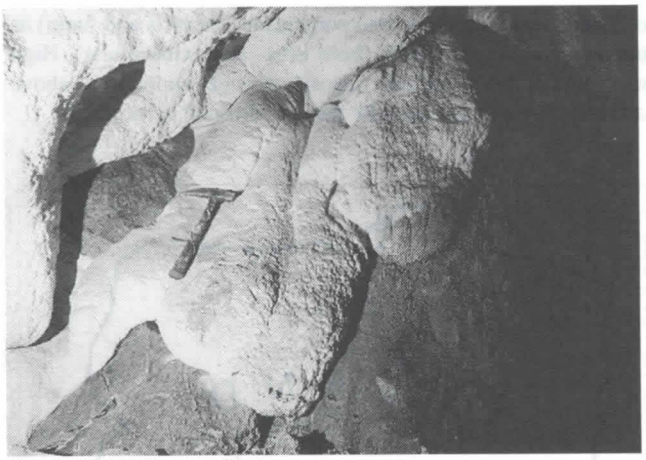

Figure 2 : General view of the furry moonmilk. Szczelina Chocholowska cave

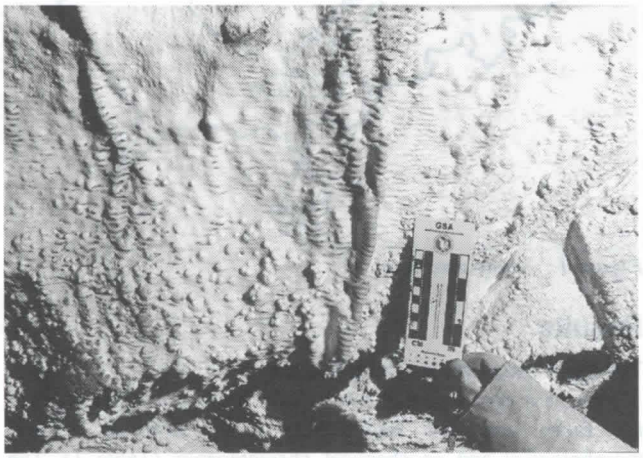

Figure 3 : General view of the felt moonmilk. Szczelina Chocholowska cave

The mentioned two types of moonmilk comprise the same components, however their proportion and arrangement are different. The furry moonmilk displays very high growth porosity and well developed needle fibrous calcite, growing freely within the pores (Figure 6). The felt moonmilk lacks of larger pores and the fabrics are composed of micritic agglomerates bound together by the mucus (Figure 4). As a rule, the felt moonmilk comprises substantial amount of mineral detritus forming faintly stratified laminae, laid paralelly to speleothem surface.

Microbial assemblage of the moonmilk mat

In vitro culture of the collected samples revealed numerous genera of bacteria and fungi forming the microbial mat of moonmilk deposits (i.e. *Arthrobacter crystallopoietes*, *Bacillus alcalophilus*, *Selibetria stellata*, *Xanthobacter autotrophicus*). The so called "knallgas-bacteria", belonging to the chemoautho-lithotrophes, seem to play decisive role in calcification processes. Other genera (e.g. the alcalophilic chemoheterotrophes) support the mineralisation processes.

Origin of the moonmilk speleothems

Microbial calcification

Mineral replicas of microbes constructing the moonmilk mat, show full-relief morphology and similar parameters as the living organisms (Figure 5, 6). This indicates physiologically-controlled calcification of the bacteria cells (cf. JONES & KAHLE, 1985) induced by autolytical mineralisation of microbial cell (SZULC & SMYK, 1994). Very extensive binding of the calcium in carbonate phase, might be related to Ca-detoxification of the microbial colonies by mass growth of the cells, known also from other environments (SIMKISS, 1977; KAZMIERCZAK *et al.*, 1986; SZULC & SMYK, 1994).

Beside the cellular calcification, the microbial mat, is intensively cemented by extracellular precipitation of $CaCO_3$. This process is mediated by knallgas-bacteria, which assimilate CO_2 and drive the pH of the mat toward value > 9 (cf. ARAGNO & SCHLEGEL, 1992).

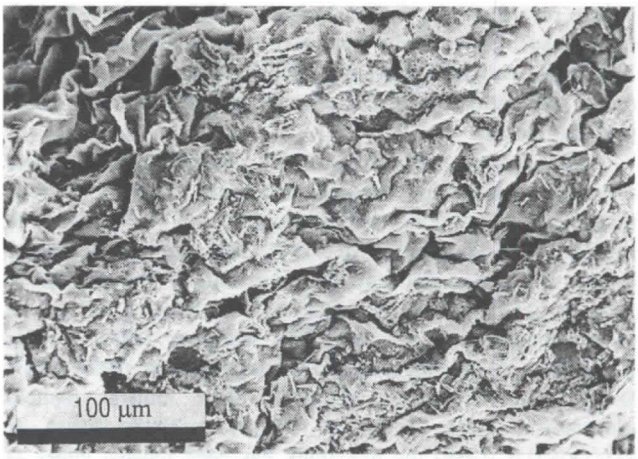

Figure 4 : SEM view of the microbial felt moonmilk mat (folded due to SEM procedure)

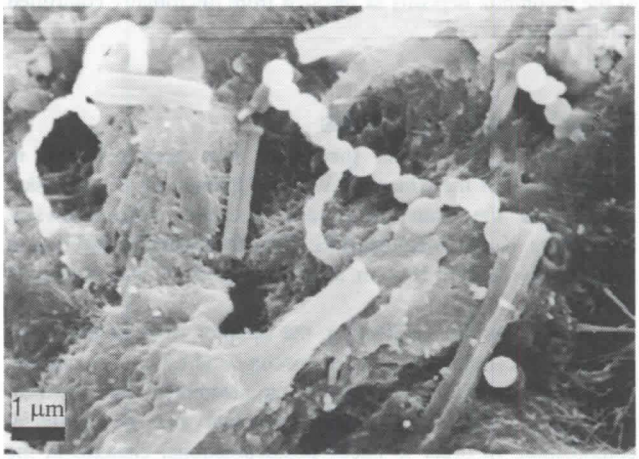

Figure 5 : Close up of the Figure 4. Note the globular bacteria chains and the interwoven, partly calcified, filamentous bacteria in the background

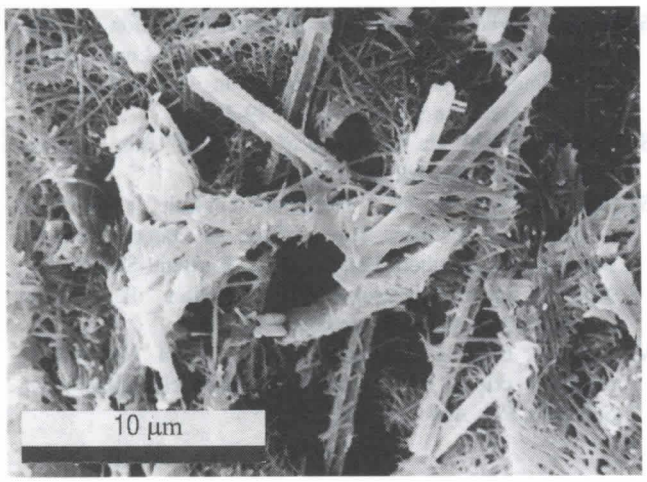

Figure 6 : Filamentous bacterial mat (furry moonmilk) and incipient, needle fibrous crystals of calcite

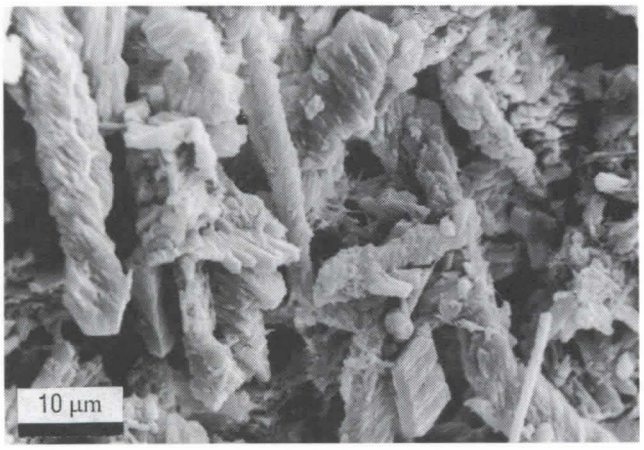

Figure 7 : Typical habit of aged, inactive furry moonmilk fabrics. See text for further explanations

Diagenetic processes

During early diagenesis the filamentous cells serve as crystallisation seeds of the needle fibre calcite (VERRECCHIA & VERRECCHIA, 1994; GRADZIŃSKI, 1995) grouped in characteristc *en echelon* rows (Figure 7). The globular and rod-shaped cells arise the micritic agglomerates of calcite (Figure 5). The described process leads finally to obliteration of primary habit of the moonmilk fabrics.

Controls of the moonmilk type variations

As shown above the calcification proceeds in the same manner in the both types of moonmilk deposits. The described differences depend on hydrodynamic factors influencing microbial mat. The dripping water makes the microbial mat more denser and produces the compact, felt type of the moonmilk. Moreover, the frequent changes of the water chemistry, involves increased production of the buffer mucus, which farther consolidates the moonmilk structures. These processes are absent in the furry moonmilk, supported by condensed vapour water.

Conclusions

1. Moonmilk speleothems are mineral-organic mat composed of living microbes, mineralised microbial cells and extracellular cement calcite.
2. Mineralisation of the moonmilk mat proceeds as direct, physiologically-controlled calcification of bacteria cells and by microbially-mediated extracelullar cementation, resulted from alkalisation of the mat microenvironment.
3. Chemically controlled, later diagenesis obliterates primary fabrics of the moonmilk mat.
4. The distinguished furry and felt moonmilk types are resulted from different hydrodynamic controls.

Acknowledgements

This study was supported by KBN (State Commitee for Scientific Research) grant no. 0057/P2/93/05 to M.G.

References

ARAGNO, M. & SCHLEGEL, H. G., 1992. The mesophylic hydrogen - oxidizing (knallgas) bacteria. In: (Ballows, A., Truper, H. G., Dworkin, M., Harder, W., Schleifer, H. G. eds.): The Prokaryotes. A Handbook on the Biology of Bacteria: Ecophysiology, Isolation, Identification, Applications. Springer Verlag, Berlin: 344-384.

BERENSCONI, R., 1961. L'évolution physico-chimique du mondmilch. *Rassegna Spel. Ital., Mem.* 5 (2): 75-100.

BROUGHTON., P. L., 1971. Secondary mineralization in the cavern environment. *Stud. Speleol.*, 2: 191-207.

CAUMARTIN, V. & RENAULT, P., 1958. La corrosion biochimique dans un résau karstique et la genèse du mondmilch. *Notes Biospéleol.* 13: 87-109.

DANIELLI, H. M. C. & EDINGTON, M. A., 1983. Bacterial calcification in limestone caves. *Geomicrobiology J.* 3: 1-16.

FISCHBECK, R. & MÜLLER, G., 1971. Monohydrocalcite, hydromagnesite, nesquehonite, dolomite, aragonite and calcite in speleothems of the Frankische Schweitz, Western Germany. *Contr. Mineral. Petrol.* 33: 87-92.

FISCHER, H., 1988. Etymology, terminology and an attempt of definition of mondmilch. *Nat. Speleol. Soc. Bull.* 50: 54-58.

GRADZIŃSKI, M., 1995. Bacterial origin of needle-fibre calcite. *Terra Nova* 7, Abstracts Supplement 1: 235.

GRADZIŃSKI, R. & RADOMSKI, A., 1957. Cavern deposits of "rock milk" in the Szczelina Chocholowska Cave. *Rocz. Pol. Tow. Gol.* 26: 63-90.

HARMAN, M. & DERCO, J., 1976. Problems of mineralogy and genetics in soft sinters in the Slovak caves. *Slovensky Kras* 14: 61-81.

HARMON, R. S., ATKINSON, T. C., ATKINSON, J. L., 1983. The mineralogy of Castelguard Cave, Columbia Icefield, Alberta, Canada. *Arctic Alpine Res.* 15: 503-516.

HØEG, O. A., 1946. Cyanophyce and bacteria in calcareous sediments in the interior of limestone caves in Nord-Rana, Norway. *Nytt Mag. Naturvid.* 85: 99-104.

JONES, B. & KAHLE, C. F., 1985. Lichen and algae: agents of biodiagenesis of karst breccia from Grand Cayman Island. *Can. Soc. Petrol. Geol. Bull.* 33: 446-461.

JONES, B. & MACDONALD, R. W., 1989. Micro-organisms and crystal fabrics in cave pisoliths from Grand Cayman, British West Indies. *J. Sediment. Petrol.* 59: 387-396.

JONES, B. & MOTYKA, A., 1987. Biogenic structures and micrite in stalagmites from Grand Cayman Island, British West Indies. *Can. J. Earth Sci.* 24: 1402-1411.

KAZMIERCZAK, J., DEGENS, E. T. & ITTEKOT, V., 1986. Cellular response to Ca^{++} stressand its geological implications. *Acta Paleont. Pol.* 30: 115-126.

MASON-WILLIAMS, A., 1959. The formation and deposition of moonmilk. *Trans. Cave. Res. Group Great Brit.* 5: 135-139.

MASON-WILLIAMS, A., 1961. Biological asopects of calcite deposition. *Rassegna Spel. Ital., Mem.* 5 (2): 235-238.

POBEQUIN, T., 1960. Sur l'existance de giobertite a de dolomite dans des concretions du type "mondmilch". *Compt. Rend. Ac. Sci. Paris* 250: 2389-2391.

SCHNEIDER, K., 1977. Carbonate construction and decomposition by ephilitic and endolithic micro-organisms in salt and freshwater. In: (E. Flügel, ed.): Fossil Algae. Springer Verlag, Berlin: 248-260.

SIMKISS, K., 1977. Biomineralization and detoxification. *Calcified Tissue Res.* 24: 199-200.

SIMKISS, K., 1986. The processes of biomineralization in lower plant and animals - an overwiev. In. (B. S. C. Leadbether & R. Riding, eds.): Biomineralization in Lower Plant and Animals. *Sys. Assoc. Spec. Vol.* 30: 19-37.

STOOPS, G.J., 1976. On the nature of "lublinite" from Hollanta (Turkey). *Am. Mineral.* 61: 172.

SZULC, J. & SMYK, B., 1994. Bacterially controled calcification of freshwater *Schizotrix*-Stromatolites: an example from the Pieniny Mts., Southern Poland. In: (J. Bertrand-Sarfati & C. Monty, eds.): Phanerozoic Stromatolites II. Kluwer Academic Publishers, Dordrecht: 31-51.

VERRECCHIA, E. P. & VERRECCHIA, K. E., 1994. Needle-fibre calcite: a critical review and a proposed classification. *J. Sediment. Res.* A64: 650-664.

Classification of Shields in Shihua Cave, Beijing

SONG Linhua

Group of Karstology and Speleology, Institute of Geography, Chinese Academy of Sciences, Beijing 100101, China

Abstract

Shihua cave, 50 km to the southwest of Beijing, is located in the transition zone from Yanshan Mountain and Beijing Plane. It developed in the Ordovician limestone and dolo-limestone. The Middle Ordovician limestones are overlain by carboniferous sediments with coal. The acid groundwater from the carboniferous sediments is benefit to the development of cave systems in the limestone.

The Shihua cave has 6 levels with a total length of 2900 m. The sixth level is developed under the groundwater table. In summer, the fifth level is seasonally filled with water.

The first and second levels of the cave system have been public since 1984. The first level is characterized by the presence of speleothems and moonmilk. The second level includes two parts, the first presents speleothems, flowstones, helictites and moonmilk, the second is predominated by small dropstones, helictites and flowstones.

There are over 1000 shields and larger or smaller plates in Shihua cave. According to their dipping, they may be classified as vertical plates like the stone walls, horizontal plates with some basket and declined plates. Based on the position against the root base, they may include cave roof shields, cave wall shields, shields parasitized on stalactites, stalagmites, columns even flowstone and plates. According to the plate structure, they may be drawn as monoplates, twin plates, x-plates and network plates. They may be divided into board plates, hair-brush plates, basket shields, mosquito-net shields and column shields. Referring to the relation between the plates and the features below them, most of the shields grow along fine fissures in the dolomitic rocks.

Shields have been reported from many countries from tropical to temperate climatic zones. HILL & FORTI (1986) described the shields as «oval or circular speleothems consisting of two spherical, parallel plates or discs, each about a centimeter thick, which are separated by a medial crack». Based on this definition, the shields broadly developed in Banqi Water Cave in the Northeastern China, Shihua cave near Beijing, Yaolin cave and Linqi Cave in the eastern China, Yilin cave in Guangxi, and Swallow cave, Jiuxian cave and Alugu cave in Yunnan. Shihua cave is an important museum of cave shields in China, not only from the number, but also from the form, size, structure and their growing base. The author describes the possible classification of shields in Shihua cave.

The Shihua cave is one of the largest and most wonderful show caves in Northern China. The magnificent and spectacular carbonatic sceneries are mainly distributed in the narrow passages with multiple levels. It is becoming the main tourist cave in Beijing area, which attracted 400,000 visitors in 1995. The shields are the main attraction in the Shihua cave.

Introduction

The Shihua cave is located between Yanshan Mountain and Beijing Plane, 50 km to the southwest of Beijing and 26 km to the southwest of Zhoukoudan Beijing Man cave. It is in the temperate climatic zone, with an annual average temperature of 11°C, and precipitations of 620 mm. The rain water mainly falls from June to September. It is dry in winter and spring. The evaporation reaches up to 1477 mm annually.

The Shihua cave develop in the middle Ordovician limestone and dolo-limestone with dense fractures directed N30-70° E and N0-60° W and dipping at 40-90°. The carboniferous sediments with coal are laid on the limestone. The acid groundwater from the carboniferous sediments is benefit to the development of the cave systems and fissures in the limestone. The surface water from the coal piles flows into the limestone through the solutional fissures and sinkholes. The cave passages and speleothems develop along the faults and fractures.

The red soil and weathering materials cover the limestone and fill the fissures. They formed during the subtropical and humid climatic conditions of the Tertiary. During the Yanshan Tectonic Movement, which uplifted the Taihang Mountain and caused the descending of the North China plane and the deposition of Cenozoic formations, 6 levels of cave system developed. In Shihua cave area, many other cave systems such as Yinhu cave, Kongshui cave, Qingfeng cave-Bailong cave, Maxian cave, Caoyang cave, Suanluo cave and Baiyin cave are developed.

Brief description of Shihua Cave

The Shihua cave system consists of 6 levels with a total length of 2900 m (LI, 1993). The first five levels are dry, the sixth is located in the groundwater. Vertical shafts connect the upper and lower passages. During the rain season, the fifth level also acts as a flood course. The basic features of the passages are as follows:

The first level consists of three large chambers with a total length of 348 m, the width varies from 1.5 m to 10 m. The average height is 24.8 m, at an average elevation of 250 m a.s.l. The main speleothems are dropstones such as stalactites, stalagmites, columns, rocky fall, and shields in different dimensions. The most famous are the vertical shields named as the jaw wall, the twin shields as the fairy net, and the maze-structure shields.

The second level has 8 chambers and the floor elevation varies from 170 m to 218 m, with a mean value of 202 m a.s.l. The largest chamber – Central Chamber – is 42 m high and 23 m wide with a curtain made of a serious boards about 2 m wide, 20-30 cm thick and 10-15 m high, columns about 30 m high. The western branch is a treasure palace with white helictites, rocky ear called as the silver flag, and moonmilk river. It may be divided into two passages, the upper is the exit and lower is the declinal passage with helictites and micro-stalactites.

The third level is 560 m long, the elevation of its floor is 155 m above the sea level. The length of the largest chamber is 160 m. It is characterized by white helictites and a floor covered by the crust of calcareous deposits.

The fourth level is 60 m long and dips along the passage with the flowstone.

The fifth level is 560 m long and develops at an altitude of 120 m above the sea level. Cave pearls and fine sand occur in the passage. In Summer, it is flooded.

The sixth level develops under the groundwater table.

The shields and plates are deposited in the first and second level. The big shields appear in the first level and upper and middle parts of the second level, The small appear in the lower branch of the second level. The micro-size shields are related to the helictites.

The classification of the shields

In 1995, Dr. Peter Habic and I roughly surveyed the shields in the first and second level of Shihua cave system during his visit. There are about 1200 shields and plates larger or smaller, in which, almost 300 shields and plates with a diameter more than 0.30 m, most of them in the range of 1-2 m. The shields occur at different dipping angles, on different bases and in different organizations and structures.

According to the dipping of the shields, they may be classified as vertical plates (Fig. 1), horizontal plates (Fig. 2) and decline plates (Fig. 3). Most of them are dipping with 30-45°.

Based on the growing base, they may include: (1) the cave ceiling shields growing from the cave ceiling, the shields generally grow from fissures at an angle less than 40° with the ceiling. (2) cave wall shields growing from fissures of the limestone wall (Fig. 4). They form vertical shields, declinal shields and horizontal shields. (3) shields growing on stalactites, stalagmites, columns and even one flowstones, shields or plates (Fig. 5).

From the structure of the shields or plates, they may be divided into monoshields or plates (complete shields). Twin shields share a joint part (Fig. 6), generally taking an angle of 120-150°. Most of them form a shield column and mosquito net. The x-shields and network plates which usually are microshields growing from the dense joints.

Also – according to the relations of the plates with the features below the plates – they can be divided into board plates without any dropstones, hair-brush plates with a lot of small pipes hanging, basket shields, mosquito-net shields, and column shields. The mosquito-net shields with twin shields in Linqi cave, Zhejiang Province, reach a height of 14 m and a diameter of 0.7-1 m (ZHOU, 1992). Some shields take beautiful forms such as the stone fungus and butterfly shields (Fig. 7).

References

CAROL A. HILL & PAOLO FORTI, 1986. Cave Minerals of the World. National Speleological Society. 238p.

LI TIYIN, 1993. The exploitation and conservation of Stone Flower Cave, Beijing. Proceedings of the XI International Congress of Speleology, August, 1993, Beijing. 163-165.

ZHOU XUANSEN, 1992. The Cave Tourist Culture in Zhejiang Province. Hangzhou University Publisher. 183p.

This project is financed by the National Natural Science Foundation of China, No.49471008.

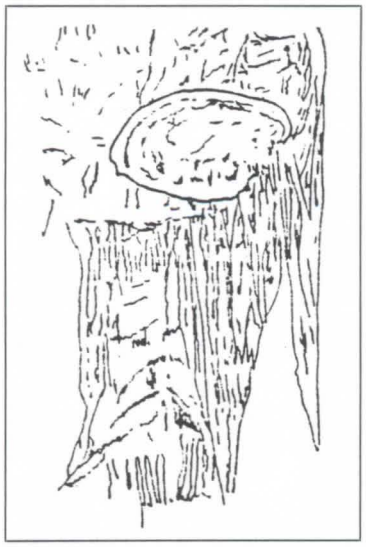

Fig. 1: The ear-shape shield from the column in Shihua cave.

Fig. 2: The monoshield.

Fig. 3: Horizontal shields and declinal shield

Fig. 4: The dragon month shield from the cave wall.

Fig. 5: Nearly horizontal bridge shield.

Fig. 6: The shell shields.

Fig. 7: The stone fungus (a) and butterfly shields (b) in Shihua cave.

Swiss Speleological Society (SSS/SGH)

Proceedings of the 12th International Congress of Speleology

Volume 1

Symposium 8

Karst Geomorphology

La Chaux-de-Fonds, Switzerland, 10-17.08.1997

Swiss Speleological Society (SSS/SCH)

Proceedings of the 12th International Congress of Speleology

Volume 1

Symposium 8

Karst Geomorphology

La Chaux-de-Fonds, Switzerland, 10-17.08.1997

Geomorphology of limestone pavements of some British, Irish and Swiss sites

Helen S. Goldie and Nicholas J. Cox
Department of Geography, University of Durham, U.K.

Abstract

This paper presents and analyses morphometric data for limestone pavements in Britain, Eire and Switzerland. It outlines methods for measurement and analysis and compares and contrasts the morphometry of these landforms, considering variations at and between sites, and identifying explanatory factors. All the pavements are in hard, compact, mechanically competent and relatively pure limestones, with variable texture. Ages vary from Lower Cretaceous and Upper Jurassic in the Alps to Cambrian in Scotland, but are mostly Carboniferous. Altitudes range from near sea-level in some of the Irish and Cumbrian sites to nearly 3000 m in Switzerland.

Previous literature

There is considerable literature on limestone pavements, but major morphometric comparisons are still lacking. GOLDIE (1973, 1976, 1981) compares some of the present sites. There was substantial work on the general geomorphology and geology of these landforms in the 1950s and 1960s (e.g. MOISLEY, 1953; SCHWARZACHER, 1958; SWEETING, 1966; WILLIAMS, 1966; CLAYTON, 1966; DOUGHTY, 1968): Alpine sites were specifically discussed by CORBEL (1957) and BÖGLI (1960), among others. Recent glaciological discussions include SHARP et al. (1989) and research on smaller-scale forms is exemplified in a recent symposium (FORNOS and GINES, 1996).

Data sampling and field methods

Field sampling was carried out to measure sizes of blocks (clints) and fissures (grikes) on as wide a variety of pavement outcrops as possible. The field procedure was as follows: at each site a 10 m by 10 m sampling square of pavement was delimited and marked with a tape. Five points within this square were chosen with random numbers. Clint length and width and grike depth and width nearest to each point were measured (Figure 1). Length was taken along the longest axis with width perpendicular to that. Clint measurements were made with a surveying tape and grike measurements with a graduated auger or a tape. If there were exceptional features or blockage at the chosen grike sampling point, measurements were made nearby. Grike orientations and rock dip were measured as well. Rock samples were collected from sample squares. Pavement character, details of the surface, nature of solution features and extent and nature of soil and vegetation were noted.

Site descriptions

1. Switzerland: Two Alpine areas were sampled: the Lapis de Tsanfleuron, at Sanetschpass near Sion and Glattalp, above Muotathal near Schwyz. The Lapis de Tsanfleuron consists of very pure Schrattenkalk. Karst features extend from 2000 to 3000 m. Although the area is still partially glaciated, the Glacier de Tsanfleuron has shrunk since the late 18th century (CORBEL, 1957). A continental climate prevails, with annual precipitation below 2000 mm, soils are thin and vegetation sparse. The Glattalp pavements are on the Quintnerkalk. The area has probably been ice-free for 10,000 years (CORBEL, 1957). The climate is wetter and milder than Sanetsch with over 2000 mm precipitation, (altitude 1850 m). Soil and vegetation are very sparse.

2. Yorkshire: Pavement outcrops were sampled at Ingleborough, Malham and Wharfedale (Figure 2). All sites are in Carboniferous Great Scar Limestone, except Oughtershaw Side, which is in Yoredale Main Limestone. The area is described in detail in WALTHAM et al. (1996). Massive limestones give a succession of low escarpments supporting pavements. Possible pavement development is limited by the dip of 3-5 degrees to east and north, where the limestone becomes overlain. Devensian glaciers scoured the area and pavements have developed on the resultant surfaces. The climate is damp, cool, temperate upland. Annual precipitation ranges between 1000 and 1500 mm. Highly varied pavements are found in all the sample areas. Glacial drift causes patchy outcrops. Pavement outcrops in Wharfedale follow the valley sides, and are limited by overlying beds.

3. Ireland: Extensive limestone pavements outcrop on Arainn, Aran Islands, Co. Galway and on Burren, Co. Clare (Figure 2). The Burren sites extend from sea-level to 300 m and those on Arainn up to 120 m. On Burren, general relief and pavement form are influenced by gentle folding and both areas have a southerly dip of 2-5 degrees. There is evidence of faulting. The pavements are in well-jointed, well-bedded Carboniferous Limestone, similar to those of N.W. England. Both areas have been glacially scoured, by ice from the north-east. Thin glacial deposits are found and both areas are relatively bare.

4. Cumbria: Carboniferous Limestone outcrops in Cumbria are small but scattered (Figure 2). Lithology is similar throughout the region, although thickness varies. Morecambe Bay, Farleton Knott and Orton-Asby were sampled. Farleton Knott has extensive pavement on which varied forms are found, influenced by folding and fracturing (MOSELEY, 1973). Hutton Roof Crags is steeply sloping with excellent Rinnenkarren. The low sites near Morecambe Bay are well vegetated, the higher sites less so. The Orton-Asby escarpment lies between 290 and 350 m and gentle folding influences pavement form (GOLDIE, 1993, 1995). Erosion by Lake District and local Howgill Fell ice, as evidenced by erratics, may not have been very vigorous. Numerous small pavements occur around Morecambe Bay: Hampsfield Fell, Great Urswick, Birkrigg Common and Gaitbarrows.

5. Wales: Pavements are in either heavily weathered limestone, as at Cader Fawr, or very laminated limestone (THOMAS, 1959). North Wales outcrops are more massive (e.g. Eyarth Rocks, Great Orme, Din Lligwy). Frost action is significant in such conditions. There has also been some human damage.

6. Scotland: Limestone pavement occurs on Dalradian Limestone, on both Skye and the mainland. On Skye undamaged

massive pavement was sampled on outcrops just above sea-level, near Torrin by Loch Slappin, and in Strath Suardal, south-west of Broadford. These sites are largely intact.

Analysis of morphometric data

All the data sets were compared and frequency distributions of clint length, clint width, grike width and grike depth were analysed in detail. In interpreting the results it is important to note that the sample size varies from 10 for Scottish sites to 510 for Burren (Table 1).

The histograms of the total data set (Figure 3) show that all the variables are highly skewed. This is typical of morphometric properties which have physical lower limits close to zero but no definite physical upper limits. The histograms are all drawn with horizontal scale the range of the variable and 50 classes: this brings out a contrast between clint length, clint width and grike width on the one hand and grike depth on the other. Grike depth has a distribution made approximately symmetrical by transformations close to the square or cube root, whereas the other three are more skewed in distribution and would require a transformation closer to the logarithm. In fact, they are close to lognormal in shape, while grike depth is more like a gamma distribution. For simplicity, however, all have been logged for several graphical analyses.

Clint length: Mean clint lengths of 4.49 m for Glattalp and 4.04 m for Sanetsch compared with 5.09 m on Burren and 4.75 m on Arainn (Table 1). Thus Burren has the longest clints overall. These results contrast with means below 3 m in Wharfedale, Wales and the Malham area. Ingleborough, Cumbria and Scotland by comparison have mean clint lengths between 3 and 4 m. The mean for the whole data set is 4.13 m. Arainn has the greatest dispersion of values around the mean with a standard deviation of 8.36 m, closely followed by Burren with 7.27 m and then Glattalp with 7.16 m. The Wharfedale clint length data have the smallest dispersion of values with a standard deviation of 0.91 m. The greatest range of values is found on Burren with a minimum clint length measured of 0.23 m and a maximum of 88 m. The narrowest range of values was found in Wharfedale where the respective figures are 0.56 m and 4.27 m. These characteristics emphasise the similarity of the distributions for Arainn, Burren and Cumbria and suggest some similarity between Glattalp and Sanetsch and to a lesser degree Ingleborough. The Wharfedale and Malham data sets also have features in common.

Clint width: The clint width data show somewhat different features (Table 1). The highest mean width is on Arainn at 1.92 m, closely followed by the Scottish sites with a mean width of 1.88 m. The latter set of sites, having a mean length of 3.09 m, clearly have squarer clints than the Arainn set. The area with the longest clints, Burren, has the third widest, with a mean width of 1.66 m. Thus this set is more elongated still than Arainn and Scotland. The most elongated clints are at Glattalp. At the lower end of the scale the lowest mean width is in Wharfedale with 0.84 m, closely followed by Malham with 0.88 m, although both sites are less square than Scotland. The greatest dispersion around the mean is in the Arainn data and the least dispersion in Wharfedale. Arainn also provides the greatest range of values, with a minimum of 0.02 m and a maximum of 25 m. The Malham sample has the narrowest range of width values, from 0.23 m to 2.59 m. It emphasises similarities between various pairs of sites, namely Burren and Cumbria, Ingleborough and Sanetsch, and Malham and Wharfedale.

The scatter plot of clint length against clint width (Figure 4) for the N.W. England sites is useful for demonstrating varying degrees of elongation of the clints. Logarithmic scales are used to accommodate the great variations in size, allowing particular ratios of clint length to clint width to be shown by parallel lines. The lowest line on the plot shows equal length and width (square clints) and is a limit: width cannot exceed length. Above that line of equality, parallels show ratios of 2, 5 and 10. Cumbria (C) clearly has many large clints, several of which are also considerably elongated. Wharfedale (W) has some clints 10 times as long as wide, although these are fairly small. Ingleborough (I) has a few very elongated mid-sized clints, while Cumbria has both mid-sized and large elongated clints. These results indicate a dominant joint set which may reflect structural controls in the areas concerned. The scatter plot of clint length against clint width for the Irish and Swiss sites was prepared separately for clarity (Figure 5). Numerous sites on Burren and Arainn have both large and small clints which are very elongated. Glattalp has one extremely elongated clint.

Grike width: Glattalp has the largest mean grike width at 28.9 cm, compared with 26.2 cm in Scotland. The Arainn pavements have the narrowest grikes with a mean grike width of 9.6 cm. The Welsh sites average 12.9 cm and the next widest are on Burren, at 14.3 cm, then Cumbria at 16.7 cm. Malham, Wharfedale and Sanetsch all have values around 18 cm, while Ingleborough has mean 19.1 cm. Scotland has the highest dispersion followed by Glattalp, although Cumbria's range of values is the greatest, 2-140 cm. The narrowest range is at the Scottish sites, 6-59 cm.

Grike depth: Mean grike depths range from 42.6 cm in Wales to 103.9 cm on Ingleborough. The Scottish mean is slightly greater than in Wales, while Arainn and Sanetsch have similar values, 62.1 and 63.1 cm. Wharfedale averages 74.6 cm, just a little less than Glattalp at 79.7 cm. Burren and Cumbria have similar mean grike depths (87.9, 88.7 cm). The greatest range of depths was found at the Cumbrian sites, 12-274 cm. The Welsh sites had the most limited range, 4-95 cm: it was also the only area to have no grikes measured over 1 m.

Limestone character

Thin sections were taken of limestones in most sample areas and examined for sparry calcite, quartz content and other characteristics. Influence of these lithological factors on pavement forms was discussed by SWEETING (1966) and GOLDIE (1976). This paper extends discussion to other areas. Nearly all the limestones are the same basic type, biosparites and sparry limestones, with variations in freshness, texture, fossil content, sparry calcite content and additional minerals. Limestones vary more at Sanetsch than within any other comparable area sampled. Sparry calcite contents of 35-90% are found. Quartz content ranges 1-10%. Fossil content is highly variable. This contrasts markedly with Glattalp, where all six sections were very dark, fine-textured biomicrites with only moderate fossil content, sparry calcite content is about 5%. Quartz is present in all the Glattalp samples up to about 1%.

By comparison the Northern England thin sections vary much less being predominantly medium-textured, with sparry calcite and quartz varying from 50 to 80% and 0 to 1% respectively. Many are altered, cracked and iron-stained. All samples are fossiliferous. Cumbria varied less than Yorkshire: 50- 5% sparry calcite and less fossiliferous and less quartzitic. Burren sections contained 45-80% sparry calcite, mostly 55-70%. Arainn samples are similar but less sparitic, 45-55%. They are medium to coarse-textured: quartz was detectable in some up to 3%. Most samples contained some shaly partings. Several show alteration and iron stain and most are highly fossiliferous.

GOLDIE (1976) could not demonstrate a clear influence of sparry calcite content on clint size. This study still does not reveal a close relationship between morphometry and sparriness of limestone. Structural and other factors appear to be more important and within-sample variation is considerable. Close fractures in fault zones are the cause of some of the lower clint widths and lengths (eg the Clouds, Cumbria; Blue Scar, Wharfedale).

Discussion

Processes involved in the development of the basic pavement form may affect their morphometry. Glaciation has been stressed as the main stripping agent producing this surface, but survival of elements of landforms from before the Last Glaciation may explain some larger negative landforms, especially where glaciation may have been less severe than hitherto assumed, for example the northwestern corner of the Yorkshire Dales. BURGESS and MITCHELL (1992-3) and VINCENT (1995) consider palaeokarstic origins for aspects of pavement form. Numerous factors influence limestone pavements and their development (e.g. SWEETING, 1966; WILLIAMS, 1966; GOLDIE, 1976). The factors being emphasised here relate to the limestones themselves and the differing effects of glaciation. Varying effects of human occupation both directly and indirectly through soil and vegetation cover also need consideration.

Sanetsch is the only sample area currently near a glacier and its mounding is distinctive. The other sites are largely more flat-bedded. At Sanetsch, observations suggested distance from the glacier possibly influences clint size. GOLDIE's (1976) data suggest a trend to greater dissection away from the glacier. Duration of pavement exposure to subaerial denudation and solution under soil and vegetation influence pavement morphometry, although not as strongly as might be expected. The area immediately by the glacier is where SHARP et al. (1989) demonstrated the role of subglacial drainage in producing surface forms. Away from the ice-covered area the mounded topography, type of limestone bedding and jointing density must play a part in interfering with the influence of duration of exposure from beneath ice. Over time solutional erosion becomes more important and the effects of subglacial drainage less.

Pavement slope is quite variable so morphometric data were considered in relation to slope. No very strong connection was revealed although for Sanetsch the largest clint length mean was obtained on gentle rather than on very gentle slopes. Elsewhere, slope is clearly a cause of variety of arrangement of features for example at The Clouds, Hutton Roof and Farleton Fell (Cumbria).

Conclusion

This work has established morphometric characteristics of several limestone pavements in differing environments. Numerous controlling factors can be identified, including topographic slope, bedrock dip, closeness of fractures and varying durations of solution, under soil cover or subaerially. Varying degrees of runnel development, with enlargement of fissures, and physical weathering, produce a gradual breakdown of the clints. All these ultimate and intermediate factors combine in complex ways to produce huge morphological variety on pavements. It is thus perhaps surprising that there is considerable similarity in their morphometry. Some of the differences may be explained by time available for the forms to develop since glaciation. Limestone properties do not appear to account for much variation. Glaciation did not always leave smooth plane surfaces in which fissures were enlarged and on which runnels developed. Further work is needed before the morphometric differences can be fully explained.

References

BÖGLI, A. 1960. Kalklösung und Karrenbildung. Z. f. Geomorph. Supp. 2: 4-21.

BURGESS, A.C. & MITCHELL, M. 1992-3. Origin of limestone pavements. Proc. Cumb. Geol. Soc. 5(4): 405-413.

CLAYTON, K.M. 1966. The origin of the landforms of the Malham area. Field Studies 2(3): 359-384.

CORBEL, J. 1957. Karst Haut-Alpins. Rev. géog. de Lyon 32: 135-158.

DOUGHTY, P.S. 1968. Joint densities and their relation to lithology in the Great Scar Limestone. Proc. Yorks. Geol. Soc. 36: 479-512.

FORNOS, J.J. and GINES, A. 1996. Karren Landforms. Univ. de les Illes Balears, Palma. 450p.

GOLDIE, H.S. 1973. The Limestone pavements of Craven. Trans. Cave Res. Gp. G.B. 15(3): 175-190.

GOLDIE, H.S. 1976. Limestone pavements, with special reference to N.W. England. Unpublished D.Phil. thesis, Oxford University.

GOLDIE, H.S. 1981. Morphometry of the limestone pavements of Farleton Knott (Cumbria, England). Trans. Cave Res. Assoc. 8(4): 207-224.

GOLDIE, H.S. 1987. Human impact on limestone pavements in the British Isles. In: (J. Kunaver, ed.): Karst and man. Department of Geography, University E. Kardelj of Ljubljana: 179-199.

GOLDIE, H.S. 1993. The legal protection of limestone pavements in Great Britain. Environ. Geol. 21: 160-166.

GOLDIE, H.S. 1995. Major protected sites of limestone pavement in Great Britain. In: (I. Barany-Kevei, ed.): Environmental effects on karst terrains. Special Issue of Acta Geographica Szegediensis: 61-92.

MOISLEY, H.A. 1953. Some karstic features in the Malham Tarn district. Rep. Council for Promotion of Field Studies: 33-42.

MOSELEY, F. 1973. Orientations and origins of joints, faults and folds in the Carboniferous Limestone of North-west England. Trans. Cave Res. Gp. G.B. 15(2): 99-106.

SCHWARZACHER, W. 1958. Stratification of the Great Scar limestone in the Settle district of Yorkshire. Liverpool and Manchester Geol. Journal 2(1): 124-142.

SHARP, M., CAMPBELL-GEMMELL, J. & TISON, J-L. 1989. Structure and stability of the former subglacial drainage system of the Glacier de Tsanfleuron, Switzerland. Earth Surface Processes and Landforms 14: 119-134.

SWEETING, M.M. 1966. The weathering of limestones, with particular reference to the Carboniferous limestones of Northern England. In: (G.H. Dury, ed.): Essays in geomorphology. Heinemann, London: 177-210.

THOMAS, T.M. 1959. The geomorphology of Brecknock. Brycheiniog 5: 129-136.

VINCENT, P.J. 1995. Limestone pavements in the British Isles: a review. Geog. Journ. 161: 265-274.

WALTHAM, A.C., SIMMS, M.J., FARRANT, A.R. & GOLDIE, H.S. 1996. Karst and caves of Great Britain. Chapman & Hall, London. 358p.

WILLIAMS, P.W. 1966. Limestone pavements with special reference to Western Ireland. Trans. Inst. Brit. Geog. 40: 155-172.

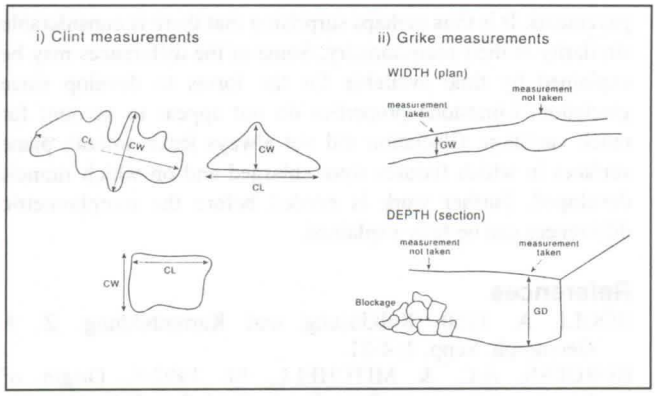

Fig. 1

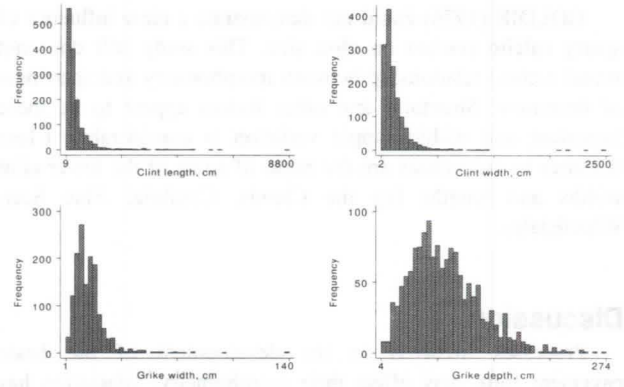

Fig. 3

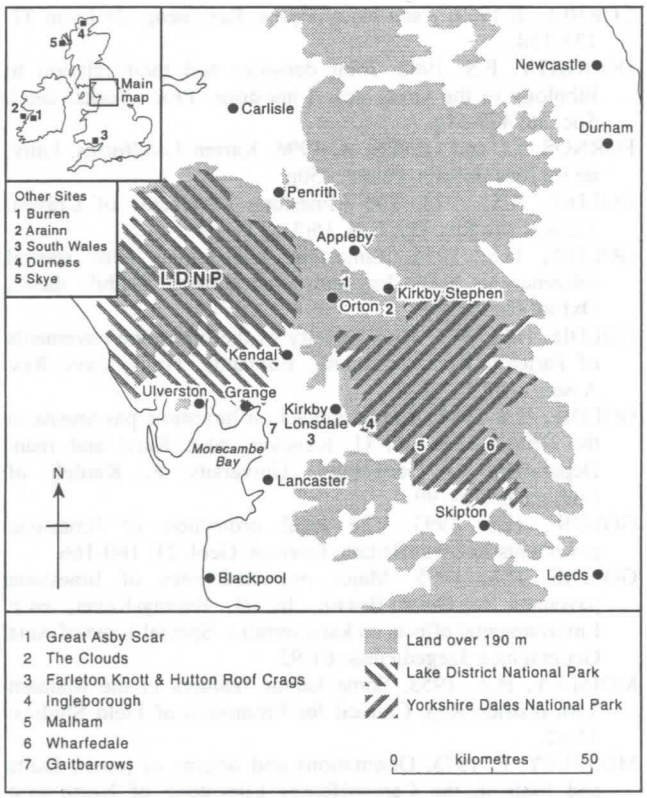

Fig. 2: Localisation Map

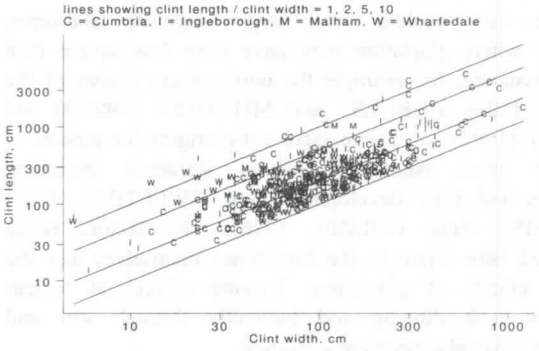

Fig. 4

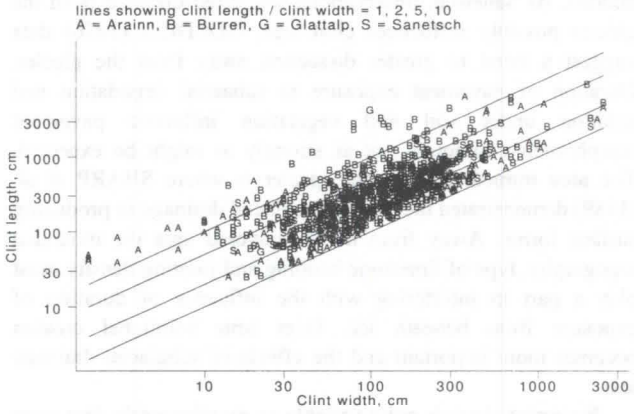

Fig. 5

	n	mean	SD	min	max
Clint length (cm)					
Cumbria	250	368.08	595.91	30	4600
Burren	510	508.84	727.20	23	8800
Arainn	200	475.43	836.23	23	6000
Glattalp	29	448.62	715.91	50	4000
Sanetsch	100	404.15	403.57	52	2400
Ingleborough	138	337.24	325.69	13	2182
Malham	35	235.20	209.29	56	975
Wharfedale	70	181.04	90.54	56	427
Wales	85	226.28	346.33	9	2700
Scotland	10	309.30	315.39	32	1018
Clint width (cm)					
Cumbria	250	142.32	146.46	13	1200
Burren	510	165.63	210.18	10	2500
Arainn	200	192.12	295.66	2	2500
Glattalp	29	104.69	66.81	15	260
Sanetsch	100	147.03	224.52	10	2100
Ingleborough	138	139.30	118.09	5	823
Malham	35	88.40	49.71	23	25
Wharfedale	70	83.51	45.04	5	229
Wales	85	95.55	135.28	4	1200
Scotland	10	188.10	225.88	20	717
Grike width (cm)					
Cumbria	250	16.73	10.64	2	140
Burren	510	14.26	7.69	1	71
Arainn	200	9.56	7.66	1	100
Glattalp	29	28.93	15.92	10	80
Sanetsch	100	17.99	14.22	5	140
Ingleborough	138	19.05	10.13	1	56
Malham	35	17.66	14.18	2	61
Wharfedale	70	17.77	13.90	1	76
Wales	85	12.92	9.36	1	46
Scotland	10	26.20	20.15	6	59
Grike depth (cm)					
Cumbria	250	88.67	45.61	12	274
Burren	510	87.88	41.64	8	260
Arainn	200	62.05	30.44	9	157
Glattalp	29	79.69	26.10	50	140
Sanetsch	100	63.07	30.60	20	150
Ingleborough	138	103.85	45.72	5	244
Malham	35	92.49	43.87	38	244
Wharfedale	70	74.57	28.14	15	168
Wales	85	42.58	20.15	4	95
Scotland	10	49.10	23.49	22	105

Table 1

Epikarstic features in zones affected by periglacial processes - example of the Silesian-Cracow Upland (Poland)

Andrzej Tyc
Department of Geomorphology, University of Silesia, ul. Bedzinska 60, 41-200 Sosnowiec, Poland

Abstract

Occurence of the epikarstic (subcutaneous) zone in the upper part of most carbonate massives complicates control of karst water chemistry and morphogenetic processes. The nature of the epikarstic zone, affected by strong physical weathering and periglacial processes during the late Pleistocene within Middle Triassic dolomites and limestones and Upper Jurassic limestones of the Silesian-Cracow Upland is presented. Case studies of the upper part of epikarst with nonactive patterned-grounds and polygons have been carried out in several outcrops of the area. During Pleistocene glaciations, the investigated karst area, situated close to the southern limit of ice-sheet, was strongly modelled by frost action.

Résumé

La zone épikarstique, affectant les parties supérieures de la plupart des massifs karstiques, complique le chimisme des eaux karstiques et modifie les processus morphogénétiques. Dans l'article, on présente des traits caractéristiques de l'épikarst dans les calcaires et dolomies du Triassique moyen et du Jurassique supérieur du Plateau de Silésie-Cracovie, ayant été transformé par l'intense altération physique et les processus périglaciaires, au cours du Pléistocène tardif. A cette époque, la région étudiée se trouvait dans le voisinage direct de l'étendue sud de la glaciation continentale et était fort modelée par l'action du gel. On a présenté en détail des exemples de plusieurs affleurements de la zone épikarstique.

1. Introduction

The epikarstic zone after GUNN (1986), MANGIN & BAKALOWICZ (1989), FORD & WILLIAMS (1989) and KLIMCHOUK (1995) or subcutaneous zone after WILLIAMS (1983) forms the upper layer of carbonate rocks affected by weathering processes. This layer is usually several meters thick, highly fissured and karstified. It is a transitional zone between surface or soil horizon and bulk mass of the karst rocks in the depth. WILLIAMS (1983) showed a distinct difference between the permeability of the epikarstic zone and the underlying vadose zone. This factor causes a perched aquifer to form within the epikarst. Water storaged in this aquifer and flows centripetally toward main joints in the underlying vadose zone.

As it is shown in the cited literature, this specificity of epikarst hydrology influences the morphogenetic processes in karst. Autogenic diffuse recharge in the upper part of epikarstic zone and concentration of the flow in major joints in its lower part are responsible for solution doline initiation (WILLIAMS, 1983). More complex roles of epikarst morphogenetics in karst are presented by KLIMCHOUK (1995 and earlier publications). In his opinion development of karren fields, shafts, collapse dolines and closed depressions are different stages of such morphogenesis. These forms develop as a result of intense widening of major joints, progressing downwards formation of vertical "hidden" shafts. Collapses and further development of closed depressions are results of progressive increase of shaft diameter.

Because development of the upper layer of carbonate massives is strongly controlled by weathering processes the nature of the epikarstic zone is influenced by climatic conditions much more than other zones in karst. Case studies and field observations of the epikarstic zone on the Silesian-Cracow Upland affected by periglacial processes in Pleistocene climate are presented.

2. Geological settings of the studied area

The study area for the investigations of the epikarstic zone on the Silesian-Cracow Upland covers two most important karst aquifers developed in Middle Triassic limestones and dolomites and Upper Jurassic limestones (figure 1). Field observations were conducted in several quarries within both geological formations. Epikarsts developed in Gogolian strata of the Middle Triassic excavations in vicinity of Olkusz, Tarnowskie Góry and Mikolów were investigated. Investigations of epikarst in Oxfordian limestone were carried out in quarries in vicinity of Klucze and Zawiercie.

Triassic carbonate rocks in the studied outcrops are mostly represented by pelitic, crinoide and marly limestone belonging to Gogolian strata of lower Middle Triassic (Muschelkalk). Limestones are bedded with different thickness of layers (0.05-2 m). The uppermost layer of the geological profile of the Gogolian strata is built by thin-bedded limestones with intercalations of marls. With diminishing thickness of layers decrease resistivity to physical weathering. Most karstified are thick beds of the Gogolian strata.

The complex of Upper Jurassic limestones of the investigated area is more heterogenous. The geological profile is divided into rocky, bedded and chalky limestones. There is evident difference between the mentioned rock types in the karstification degree. Most karstified and jointed are rocky limestones. They build residual hills - an important morphological feature of the E part of the Silesian-Cracow Upland, with a great number of small caves. Rocky limestones are accompanied by plate, thin-bedded and chalky limestones.

3. Fossil periglacial structures within the epikarst of the Silesian-Cracow Upland

Presented geological settings create specific and complex features in the epikarstic zone of the Silesian-Cracow Upland. As it is shown on figure 1, the investigated area is situated in a zone of direct and indirect influence of Pleistocene glaciation. Some of the studied outcrops (e.g. Mikolów, Tarnowskie Góry) are related to the limit of the Sanian and Odranian glaciations and probably, the carbonate rocks in these places were covered by glacial and fluvioglacial sediments. It is necessary to point out that all obser-

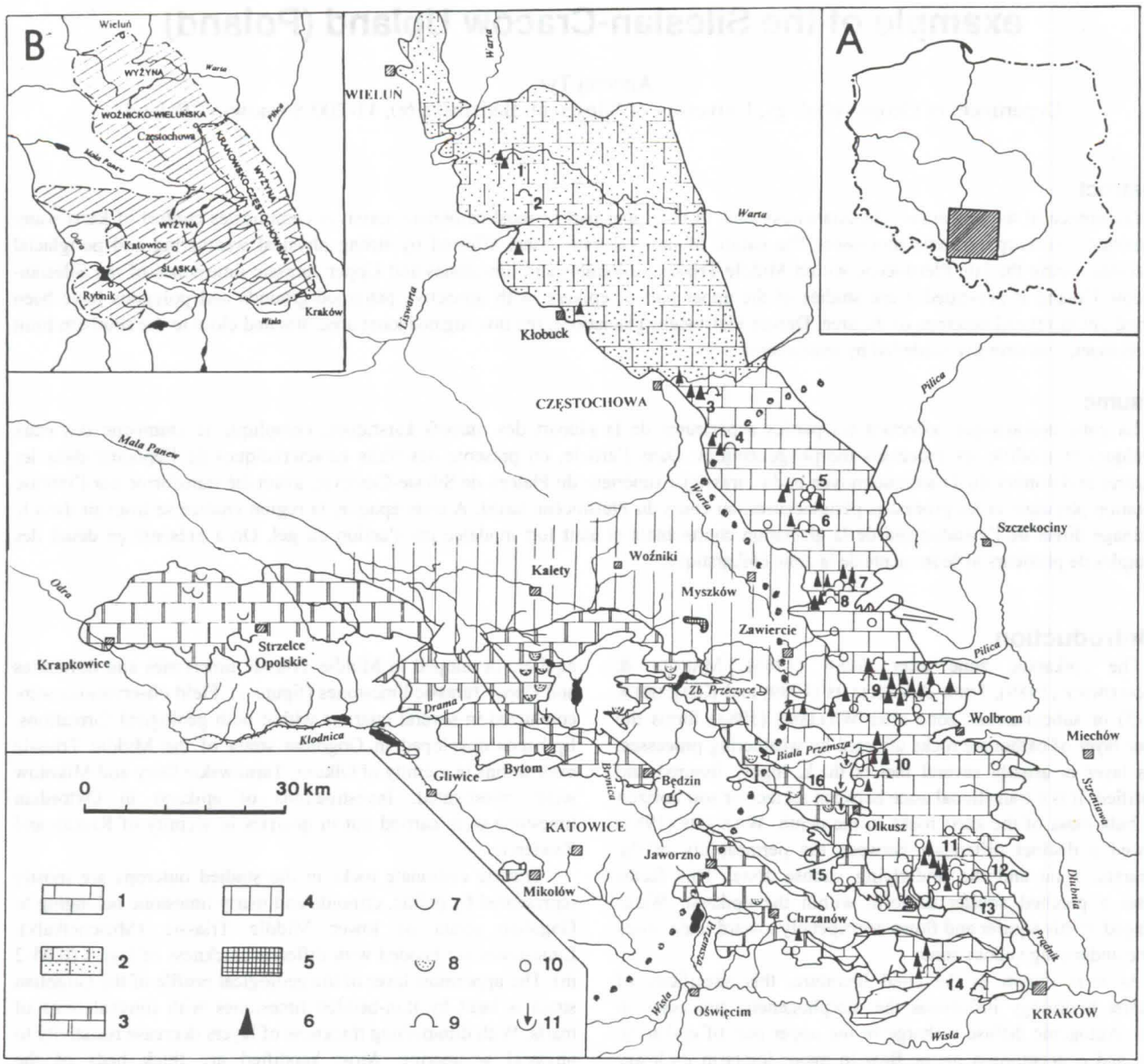

Figure 1 : Karst phenomena of the Silesian-Cracow Upland. A- location: B- geographical division; 1- karst in Upper Jurassic limestones; 2- karst in Upper Jurassic limestones covered by Quaternary sediments; 3- karst in Middle Triassic limestones and dolomites; 4- karst in Middle Triassic carbonates covered by impermeable sediments of Upper Triassic and Lower Jurassic; 5- karst in Devonian limestones; 6 residual hills; 7- complexes of dolines; 8- paleokarstic features; 9- most important caves; 10- karst springs; 11- sinkholes induced by human activity. Dotted line show southern limit of the continental glaciation in Pleistocene.

ved walls in quarries of Triassic and Jurassic limestones are devoid of sedimentary cover now (lack of Quaternary deposits). This indicates that sediments of two older Pleistocene glaciations were removed from the karst plateaus (probably during Masovien interglacial period) and the complex of carbonate rocks was transformed during Vistulian glaciation. In the polar and subpolar climate of this glaciation upper layer of fissured and karstified rocks was affected by periglacial processes. It is well visible in the studied outcrops as thick strata of limestone rubble resulted by frost action (figure 2). There are common sequences of fossil periglacial forms related to strong physical weathering and sorting. Forms of patterned-grounds - sorted stony circles, polygons and debris islands occur within the limestones of the Middle Triassic and Upper Jurassic (figure 3 and 4). Well sorted grounds are 2-4 m of diameter (TYC, 1994; 1996).

ALEXANDROWICZ (1958) has reported features of periglacial cryogenic disturbances within the upper layer of limestones of the Gogolian strata from quarries in the vicinity of Tarnowskie Góry and Mierzecice. Besides the mentioned patterned grounds he has described fold structures built by fragments of limestones inherent in nonstratified marls and sandy clay. The amplitude of the folds was ca. 0.5 m and tabular stones were composed of "synclines" and "anticlines".

In all investigated quarries of the Silesian-Cracow-Upland, the occurence of fossil periglacial forms within epikarst are related to the lithology of Middle Triassic and Upper Jurassic limestones. Patterned-grounds and other cryogenic disturbances are well defined in plate, thin-bedded limestones.

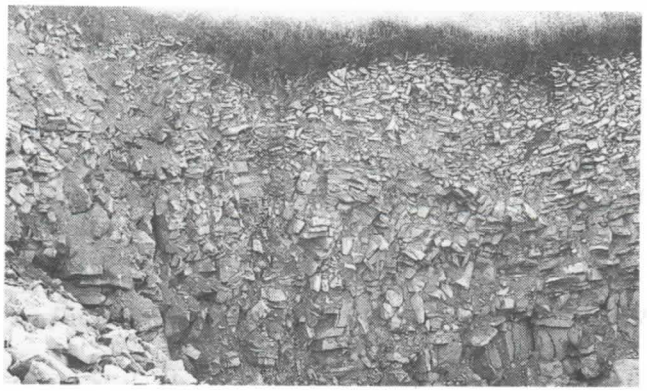

Figure 2 : Thick strata of limestone rubble in the upper part of the epikarst in Upper Jurassic limestone resulted by frost action (quarry wall in Bogucin near Olkusz).

Figure 3 : Upper layer of the epikarstic zone affected by frost action - strong physical weathering and sorting (quarry wall in Bogucin near Olkusz).

4. Morphogenetical importance of epikarstic zone affected by frost action

Fossil periglacial forms of patterned-grounds in the upper part of epikarst have significant importance for the hydrology and morphogenesis of karst of Middle Triassic and Upper Jurassic limestones of the Silesian-Cracow Upland.

First, rock layer just below soil or slope sediments shows a strong physical weathering as a result of frost action and as a consequence of sorting, tabular stones tend to be on edge with their long axis in the vertical plane parallel to the border of circles or polygons. Most of the stones dip at angles > 45° (figure 3 and 4). In effect, zones of patterned-ground within the bedded limestones are more permeable than the same limestone without influence of frost action. Stony borders of sorted circles and polygons are most permeable. These phenomena increase with the size of patterned-grounds. With increasing size of forms, the size of border stones increases as well as the depth of the physical weathering and sorting (figure 4). Another important factor controlling the hydrological significance of affected layers of rock is the connection of periglacial forms with underlying karstified limestones. From this point of view there are two groups of sorted circles and polygons: (1) small stony circles hanging within fine material, not related to rock debris and underlying rocks, (2) large and medium size stony circles and polygons connected with fissured and karstified lower part of epikarstic zone. Both are important for dispersed recharge of underlying epikarst, but only the second one plays an important role in transmission of water and pollutions to the aquifer.

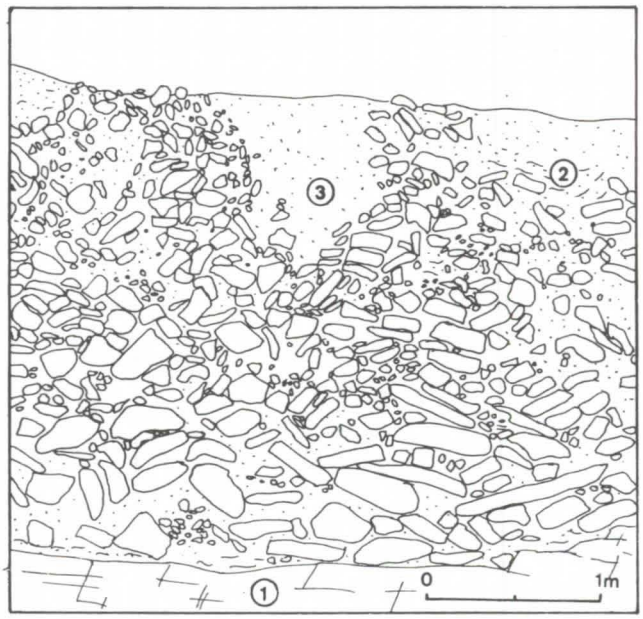

Figure 4 : Profile of the limestone rubble with fossil periglacial forms of patterned grounds (according to Tyc, 1996). 1- fissured and jointed limestone; 2- clay with sand and debris admixture; 3- sorted stony circle with fine material inside.

Secondly, sorted stony circles, polygons and debris islands of sorted commonly due to a border of stones surrounding finer material and of semi-conical shape have hydrologic and morphogenetic properties very similar to closed depressions in karst. Two most important hydrologic features of epikarst - storage, as a result of delay in trough-flow of diffusely infiltrated precipitation and flow, initially diffused and concentrated while passing from epikarstic zone to the underlying zones of the aquifer are accelerated due to horizon of patterned-grounds within the upper part of epikarst.

References

ALEXANDROWICZ, S. 1958. Periglacial structures in Triassic limestones in vicinity of Tarnowskie Góry and Mierzêcice (in Polish). *Biul. Peryglacjalny*,, 6: 117-125.

FORD, D. & P.W. WILLIAMS. 1989. Karst Geomorphology and Hydrology. Unwin Hyman, London, 601 p.

GUNN, J. 1986. Solute processes and karst landforms, [in:] S.T. Trudgill (ed.), Solute Processes, John Wiley and Sons, Chichester, pp. 363-437.

KLIMCHOUK, A. 1995. Karst Morphogenesis in the epikarstic zone. *Cave and Karst Science*, Vol. 21, No. 2: 45-50.

MANGIN, A. & M. BAKALOWICZ. 1989: Orientation s de la recherche scientifique sur le milieu karstique. Influences et perceptibles en matiere de protection. *Spelunca* 35, Protection des cavernes et du milieu karstique, Paris: 71-79.

TYC, A. 1994. Anthropogenic Impact on Karst Processes in the Olkusz-Zawiercie Karst Area (Silesian-Cracow Upland) (in Polish). PhD thesis, University of A. Mickiewicz, Poznañ.

TYC, A. 1996. The nature of epikarst and its role in dispersed pollution of carbonate aquifers. International Conference on Karst-Fractured Aquifers - Vulnerability and Sustainability. Katowice-Ustroñ, June 10-13, 1996, 270-281

WILLIAMS, P.W. 1983. The role of the subcutaneous zone in karst hydrology. *J. Hydrol.* 61, 1/3: 45-67.

Contribution à la compréhension du fonctionnement hydraulique de l'épikarst; expériences d'arrosage sur le site de Bure (Jura, Suisse)

par Vincent Puech & Pierre-Yves Jeannin
Centre d'hydrogéologie de l'Université, Rue Emile-Argand 11, CH-2007 Neuchâtel, Suisse

Abstract

In order to study the hydraulic behavior of the epikarst, we carried out several irrigation field experiments. A several tens square meters area was irrigated simulating precipitation between 8 and 20 mm/h. Simultaneously the infiltration was recorded using rain gauges at several points located in the cave below.

These experiments show that, after a dry period, the first amount of infiltrated water (about 15 mm) is absorbed and stored by the epikarst and constitute the «basis recharge of the epikarst». During this first recharge time, there is almost no reaction in the cave system. When the basis recharge of the epikarst is exceeded, the major part of the infiltration quickly flows towards the karst conduits network (more than 55% of the injected water quickly converge to the conduits). Finally, after the end of the recharge period, the so called «basis recharge» is slowly drained.

Résumé

Le comportement hydraulique de l'épikarst du plateau de Bure (Jura, Suisse) a été étudié en arrosant une surface de sol de quelques dizaines de mètres carrés avec des infiltrations d'intensités comprises entre 8 et 20 mm/h. L'effet de ces aspersions a été observé à l'aide de pluviographes installés dans une grotte sous-jacente.

Ces expériences ont permis d'observer, qu'après une période sèche, la première partie des précipitations (env. 15 mm) est absorbée et retenue dans l'épikarst et n'engendre pas, ou peu, de réaction en profondeur. Une fois que ce „stock de base" de l'épikarst est saturé, les écoulements s'organisent dans l'épikarst et une bonne partie de l'eau converge rapidement vers les drains karstiques profonds (plus de 55 % de l'eau injectée sur 30 m^2 est récupérée rapidement). Après la fin de la période de recharge, la réserve de base de l'épikarst se vidange relativement lentement (plusieurs jours).

1. Introduction et buts

La vulnérabilité des aquifères karstiques est liée aux écoulements particuliers qui caractérisent ces terrains (crues brutales et décrues rapides). En effet, la rapidité d'acheminement des eaux vers l'exutoire est un facteur défavorable puisque les processus lents d'auto-épuration et de dilution ne peuvent s'opérer.

Le transfert rapide des eaux depuis la surface jusqu'au réseau de conduits est rendu possible par l'existence d'une couche superficielle perméable appelée *épikarst.*

S'il est venu à l'esprit des hydrogéologues et des géomorphologues (MANGIN 1975, WILLIAMS 1983) de différencier la zone épikarstique du reste du massif, c'est que cette zone possède des propriétés particulières. En effet, étant par définition situé en surface, l'épikarst est soumis à une altération poussée liée à une forte dissolution (50 %, voire 80 % de la dissolution totale a lieu dans les premiers mètres de terrain), aux phénomènes de décompression de la roche à proximité de la surface, ou encore à l'action de la gélifraction, des racines, etc. L'intense fracturation et karstification qui en découlent confèrent à l'épikarst une plus grande porosité et perméabilité que le reste du massif. D'un point de vue hydraulique, il est admis depuis longtemps (MANGIN 1975) que la différence de perméabilité entre l'épikarst et les terrains sous-jacents peut entraîner la formation d'une nappe épikarstique temporaire. Ensuite, soit l'eau momentanément stockée est drainée rapidement, via les petits conduits de l'épikarst, en direction du réseau de conduits karstiques de grande perméabilité (transit rapide vers l'exutoire), soit elle s'infiltrera de manière plus diffuse dans les volumes de roche fracturée peu perméable, situés sous la zone épikarstique (temps de transfert longs).

Cet article présente les résultats obtenus sur un site expérimental du Jura suisse. Ces expériences avaient pour but de comprendre et de quantifier la réponse d'un type d'épikarst particulier à une arrivée d'eau produite par un arrosage au sol (voir aussi THIERRIN 1996 et PUECH 1996).

2. Localisation et présentation géologique

Le site choisi pour procéder aux expériences est situé sur un plateau calcaire d'une altitude moyenne de 500 m, près du village de Bure (canton du Jura, Suisse), non loin de la ville de Porrentruy. Du point de vue géologique, ce plateau appartient au Jura tabulaire. Il s'agit d'un plateau sub-tabulaire à soubassement Jurassique supérieur, incliné vers le nord et recoupé par des fractures méridiennes.

L'aquifère karstique se développe dans le Kimméridgien inférieur, dans les formations nommées : calcaire à Astartes et Natices, calcaires sublithographiques ou calcaire marneux (Séquanien inférieur dans la terminologie suisse).

Le plateau de Bure est drainé par la rivière souterraine de la Milandrine, affluent souterrain de l'Allaine. Le réseau spéléologique se développe sur une dizaine de kilomètres.

Le karst jurassien du site du Maira est presque totalement recouvert par des sols dont l'épaisseur peut varier entre quelques centimètres et plusieurs mètres. Il est donc particulièrement difficile d'observer directement l'épikarst. Divers travaux effectués sur le site (nombreux forages, géophysique, etc.) nous apprennent que l'on peut observer une extension en profondeur de l'épikarst allant jusqu'à 10 voire 20 mètres (TURBERG 1993, DA VEIGA 1995, THIERRIN 1996), la limite de l'épikarst étant considérée comme la limite inférieure de la zone intensément fracturée au sommet du substratum calcaire.

Un petit secteur du bassin de la Milandrine a été choisi pour ces expériences. Il a la particularité de se trouver 35 mètres au-dessus de la grotte de Milandre, ce qui permet d'observer directement l'arrivée des infiltrations dans la rivière souterraine. La galerie à cet endroit est située au droit d'une faille majeure qui influence la perméabilité des terrains – donc les infiltrations – jusqu'en surface. Le site étudié, c'est évident, correspond à un cas particulier. Il n'a pas la prétention d'être représentatif de l'ensemble du karst Jurassien, ni même du karst du plateau de Bure.

3. Buts et dispositif expérimental

Le premier objectif a été de mesurer **le temps de parcours** (tp) de l'eau entre la surface, au moment où l'on commence l'expérience, et la galerie, au moment où l'on y observe les premières arrivées d'eau. Le deuxième objectif était d'évaluer le taux de récupération dans la grotte de l'eau injectée en surface. Le troisième objectif était de voir si ces paramètres varient en fonction de l'intensité de l'arrosage.

Pour l'observation souterraine des infiltrations, plusieurs pluviographes ont été installés dans la galerie située sous le site d'arrosage (figure 1). Les pluviographes ont été placés sous diverses arrivées d'eau de manière à observer différents types d'écoulements : le pluviographe n°2 a été posé au milieu de la galerie au-dessous d'une cheminée karstique (écoulement rapide). Les pluviographes n°1, 3, 4 et 5 ont été placés le long des parois à divers endroits sous des concrétions ou des petites fissures.

Les arrosages ont été faits par créneau, c'est-à-dire en alternant les périodes d'arrosage à débit constant et de repos (cf. figure 2).

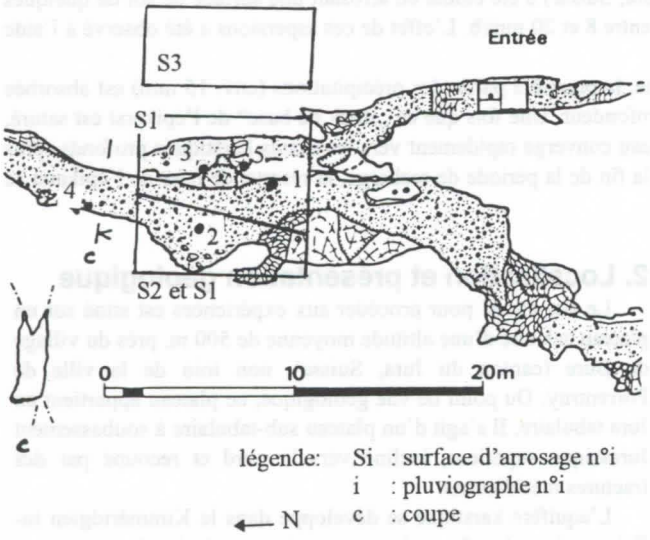

Figure 1 : Extrait de la topographie de la grotte au niveau du site d'étude.

4. Résultats et interprétation

Temps de parcours

Par hypothèse, posons que le temps de parcours (tp) correspond à la somme d'un **temps de transfert** (tT) et d'un **temps de saturation minimale** (ts) de l'épikarst. On a tp=tT+ts. Le «temps de transfert» est supposé être le temps mis par l'eau pour aller de la base de l'épikarst jusqu'aux pluviographes. Le «temps de saturation minimale» est la durée nécessaire à l'épikarst pour arriver à un degré de saturation minimal qui permet à l'eau de le traverser (c'est la somme de l'eau de rétention dans le sol ainsi qu'à la surface de la roche, et de l'eau de la nappe épikarstique temporaire).

Deux séries d'arrosages ont été effectuées pour mesurer ces différents temps.

Arrosage 1 (surface arrosée S1=70 m^2, figure 1)

La dernière précipitation avant cette expérience remonte à 16 jours, ce qui a dû permettre au stock d'humidité des sols et de l'épikarst de descendre à une valeur faible (il s'agit d'une période estivale). Quatre injections de durée et d'intensité légèrement variables sont infiltrées (figure 2).

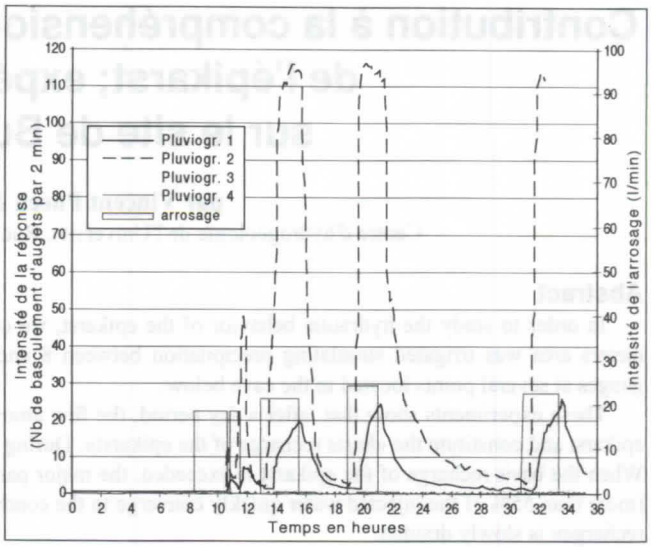

Figure 2 : Réponse des pluviographes à l'arrosage n°1

La réaction des pluviographes à la première injection est de faible amplitude et débute plus de 90 minutes après le début de l'injection. La réaction aux injections suivantes est plus rapide et de plus forte amplitude.

Considérons d'abord les variations d'amplitude. Le pluviographe n°1 n'atteint une valeur maximale de percolation que pour le quatrième créneau. Pour les autres créneaux, il arrive respectivement à 25%, 75%, 95% de cette valeur. Or, tous les créneaux d'arrosage sont d'une intensité et d'un vo-lume semblables. Ceci nous indique clairement qu'à chaque créneau d'arrosage une partie de l'eau sert à augmenter encore «le taux de saturation» de l'épikarst, c'est-à-dire que les in-filtrations en profondeur se font parallèlement à la mise en ré-serve de l'eau. On obtient un résultat similaire si l'on con-sidère le volume infiltré plutôt que l'amplitude. Une réaction semblable du pluviographe n°2 ne peut pas être exclue[1].

Considérons maintenant les temps de réaction du pluviographe qui réagit le plus rapidement aux infiltrations. Le pluviographe n°2, qui capte les infiltrations les plus rapides, réagit 90 minutes après le début de premier créneau d'injection (tp1=90 min). Ce temps de réaction diminue progressivement pour atteindre 26 minutes au quatrième créneau (tp4=26 min). En supposant que «l'état d'humidité» de l'épikarst était minimal au début du premier créneau (ts=max) et maximal au début du quatrième créneau (ts=0), nous pouvons alors estimer le temps de transfert et le temps de saturation minimal (ts) :

tT=tp4=26 minutes

ts=tp1-ts=64 minutes

Vu les conditions d'arrosage (19 l/min et 25 l/min.), ce temps de saturation correspond à un volume stocké dans l'épikarst[2] de :

Ve = 90 min * 19 l/min - 26 min*25 l/min = **1060 litres.**

La zone étudiée couvrant une superficie de 70 m^2, ce volume correspond à une précipitation de 15 mm.

La «recharge de base» de l'épikarst, qui correspond au volume minimal nécessaire avant que la capacité de drainage et de concentration de l'eau dans l'épikarst soit effective, est donc

[1] Le pluviomètre n°2 semble arriver rapidement à un régime permanent; ce n'est cependant pas le cas, on a simplement atteint les limites de mesure de l'appareil.

[2] En théorie, ce stock se situe entre le sol et la galerie, mais d'après la morphologie souterraine (calcaire massif et compact), on peut admettre que la majeure partie de ce stock se constitue à proximité de la surface.

d'environ 15 mm au niveau de la zone étudiée. Ce volume ne correspond pas à la recharge totale de l'épikarst qui, comme on l'a vu, continue d'augmenter alors que les infiltrations en profondeur sont effectives. D'après l'analyse des pluviographes et pour ces conditions d'arrosage, la recharge totale serait d'environ 2000 litres (30mm).

Le quatrième arrosage, effectué environ 10 heures après la fin du troisième, nous renseigne sur la vidange de la «recharge de base» : après environ 10 heures de repos, le temps de transfert passe à 30 minutes. C'est-à-dire seulement 4 minutes de plus que pour le 3ième créneau. On peut donc déduire que la vidange de l'eau retenue dans l'épikarst a été de l'ordre de :

30 min * 23 l/min - 26 min * 25 l/min = **40 litres**.

Il reste donc encore à peu près 1000 litres stockés après dix heures sans arrosage. Il s'agit cependant d'une période nocturne pendant laquelle l'évapotranspiration est faible.

Arrosage 2 (surface arrosée S2=30m^2, figure 1)

A part une surface d'injection plus petite que pour l'essai précédent, les conditions sont les mêmes. La figure 3 présente les résultats obtenus.

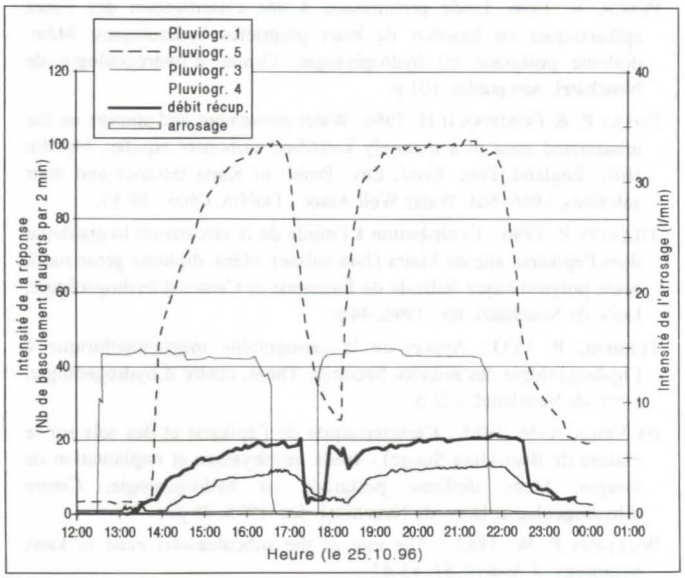

Figure 3 : Réponse des pluviographes à l'arrosage n°2

Cette expérience a été effectuée sur quatre jours et en trois créneaux d'arrosage. Le premier (non représenté) a été injecté trois jours avant les deux créneaux donnés en figure 3 (créneaux n°2 et 3). En admettant le stock nul avant le premier créneau et complet au début du troisième, on obtient :

Ve2=89*16-30*15=**970 l** (soit 30 mm sur la surface arrosée).

Le stock est donc très élevé comparativement à l'essai précédent. Mais le temps de parcours est ici estimé à partir du pluviographe n°5. Or, celui-ci a un temps de réaction légèrement plus long que le pluviographe n°2 (qui a du être enlevé), ce qui introduit une surestimation de la recharge de base. De plus, les effets de bords sont ici certainement proportionnellement plus importants. Malgré cela, on peut conclure que la réserve d'eau de la surface S1 se situe principalement dans la partie correspondant à la surface S2 (que l'on vient d'arroser). Ceci traduit le rôle important joué par les sols, car par opposition à l'autre partie où la roche est presque affleurante, la surface S2 est recouverte d'une épaisseur de sol de plus d'un mètre.

La durée de repos entre les créneaux 1 et 2 a été de 69 heures. Après **69 h**, le temps de réaction est passé de 86 à 76 minutes (débit de 15 l/min). Le „stock de base" de l'épikarst peut alors être estimé à :

89 min * 16 l/min - 76 min * 15 l/min = **300 l**.

La vidange de cette «recharge de base de l'épikarst» a donc été de 700 litres en 3 jours (les 2/3), ce qui est nettement plus élevé que l'estimation précédente qui correspondait à une période nocturne uniquement.

Les faibles temps de transfert obtenus démontrent que le site étudié présente une composante très perméable qui ne se met à fonctionner qu'après que la „recharge de base de l'épikarst" soit suffisante (après une précipitation de l'ordre de 15 à 30 mm). L'observation aux autres pluviographes et en particulier au pluviographe n°4 met également en évidence l'existence d'une composante lente correspondant à la vidange de cette „recharge de base" et alimentant les volumes de calcaires fissurés peu perméables.

Essai de récupération maximale

La composante rapide des écoulements provient essentiellement de la cheminée captée par le pluviomètre n° 2. Pour évaluer la part de la composante rapide, il a suffi de mesurer le volume total provenant de cette cheminée. Une bâche a donc été installée et le volume récupéré lors de l'arrosage n°2 (figure 3) a ainsi pu être évalué.

Pour le premier créneau, la récupération est de 1100 litres sur les 3460 injectés, soit **32 %**. La bâche ne récupérant pas la totalité des écoulements, ce taux pourrait atteindre 45% au maximum (valeur estimée).

Pour le deuxième créneau, la récupération est de 1900 litres sur les 3440 injectés, soit **55 %**. En tenant compte de la récupération incomplète dans la bâche, ce taux pourrait atteindre 80 %.

La différence entre les deux créneaux n°2 et 3 doit correspondre à la recharge du „stock de l'épikarst". Elle est comprise entre 900 et 1200 litres (selon la récupération admise dans la bâche). En ajoutant les 300 litres qui restent théoriquement dans le stock de base, on obtient le stock total (stock maximum pour cette intensité puisque l'on a atteint un régime permanent).

Il ressort de ces mesures que sur le site utilisé pour cette injection, 50 à 80 % des infiltrations peuvent circuler très rapidement vers la rivière souterraine. Ce pourcentage diminue cependant nettement pour de faibles infiltrations, lorsque le „stock de base de l'épikarst" n'est pas encore saturé.

Le deuxième créneau d'aspersion présente un régime permanent très rapidement après le début de l'injection. A ce stade, le stock de l'épikarst ne varie plus (il serait surprenant que la recharge de ce stock se fasse à un régime permanent). Il est donc probable que les 20 à 45 % restant alimentent une autre zone que celle de la galerie. Cette autre zone est peut-être constituée par les volumes de roche peu perméable. Pour comparaison, JEANNIN & GRASSO (1995) ont évalué la recharge respective des conduits karstiques et des volumes de roche peu perméable à partir d'une étude du flot de base de la rivière souterraine. Ils remarquent que plus de 21% des infiltrations alimentent les volumes de roche peu perméable, mais plus vraisemblablement environ 50%. Sachant qu'une partie du „stock de base de l'épikarst" s'ajoute au pourcentage calculé ci-dessus, les ordres de grandeurs calculés par JEANNIN & GRASSO sont tout à fait comparables à ceux obtenus dans les expériences d'aspersion présentées ici.

Variation de l'intensité d'arrosage

Le rôle joué par la saturation du „stock de base de l'épikarst" a été démontré dans les paragraphes qui précèdent. Une fois le stock saturé, le fonctionnement de l'épikarst varie-t-il en fonction

de l'intensité des infiltrations ? Sachant que la densité de fracturation et le degré de karstification décroissent rapidement en profondeur, il faut s'attendre à une saturation rapide au niveau de l'interface entre l'épikarst et la zone de roche moins perméable sous-jacente. Cette saturation devrait entraîner des écoulements hypodermiques sub-horizontaux rapides en direction du réseau karstique et la proportion du volume d'eau rechargeant la zone peu perméable devrait ainsi être d'autant plus forte que l'intensité d'arrosage est faible.

Arrosage 3 (S3=40 m^2, figures 1 et 4)

L'arrosage est effectué en trois créneaux : le premier est destiné à saturer le „stock" et les créneaux deux et trois ont des intensités respectives de 13 et 5 l/min.

La méthode d'interprétation est basée sur le rapport de l'intensité des deux réponses l'une par rapport à l'autre en comparaison avec le rapport de l'intensité des deux arrosages.

Le rapport des arrosages est de 5/13=0.38. Autrement dit, l'intensité du créneau 2 atteint 38 % de celle du premier.

Le rapport des intensités des réponses au pluviographe 1 est de 80/105=0.76, c'est-à-dire que l'amplitude de la réponse au deuxième créneau atteint 76 % de celle du premier. Au pluviographe 5, ce même rapport est de 85 %.

La répartition des infiltrations varie donc en fonction de l'intensité d'arrosage. La réponse à un faible arrosage est ici proportionnellement plus grande que celle à un arrosage intense. Il semble donc que l'on atteint rapidement les limites de drainage de l'eau en direction de la galerie où sont placés nos pluviographes. L'eau est alors poussée latéralement lorsque l'on augmente le débit (effets de bords de plus en plus importants). Relevons que l'intensité d'aspersion maximale est de 20 mm/h ce qui correspond à des événements pluviométriques exceptionnels (22 mm/h atteint le 22.09.90).

5. Conclusion

Ces expériences nous ont permis de mettre en évidence quelques particularités du fonctionnement hydraulique de l'épikarst, que l'on peut résumer en trois points :

1 - Lors d'une infiltration, les premiers apports d'eau (ici env. 15 mm) servent à reconstituer la «recharge de base» de l'épikarst (nappe épikarstique). Durant cette phase, il n'y a pas, ou peu, de réaction en profondeur. L'importance de cette recharge dépend de l'épaisseur de sol et de l'épikarst.

2 - Lorsque le «stock de base» est saturé, l'épikarst peut commencer à développer pleinement son comportement hydraulique particulier (conformément à MANGIN 1975 ou SMART & FRIEDERICH 1986). En fonction de l'intensité des infiltrations, une partie croissante de l'eau transite rapidement vers le réseau karstique profond. Des écoulements sub-horizontaux peuvent apparaître dans l'épikarst en fonction des différents gradients de perméabilité. Le stock d'eau dans l'épikarst continue cependant à augmenter jusqu'à une valeur limite. Et, si les infiltrations sont constantes, un régime permanent peut être atteint à ce stade seulement. L'eau infiltrée dans l'épikarst se répartit entre les drains karstiques (écoulement rapide), et la recharge des volumes de calcaires fissurés peu perméables.

3 - A la fin de la période de recharge, les parties perméables de l'épikarst se vidangent rapidement, alors que s'effectue un tarissement (ou plutôt un égouttement) relativement lent de l'eau de la «réserve de base» de l'épikarst. A ce stade, la distinction entre les écoulements lents dans les volumes de calcaires fissurés peu perméables entourant les conduits karstiques et l'égouttement lent du stock de base de l'épikarst ne peut pas être effectuée.

Pour tenter d'obtenir une image un peu plus représentative de différents types d'épikarsts, des essais similaires seront effectués sur d'autres secteurs du bassin versant de la Milandrine. De même, un suivi en continu de la réponse aux pluviographes face aux précipitations naturelles est actuellement en cours, et devrait apporter des informations complémentaires sur les grandes lignes du fonctionnement de l'épikarst. Cette étude montre que l'épikarst joue un rôle fondamental sur la répartition des infiltrations entre la composante rapide et la composante lente des écoulements, ce qui est très important pour l'évaluation de la vulnérabilité des aquifères karstiques.

Références

JEANNIN P.-Y. & GRASSO D. A. 1995. Recharge respective des volumes de roche peu perméable et des conduits karstiques, rôle de l'épikarst. *Bull. d'hydrogéologie de Neuchâtel, univ Neuchâtel: 95-111.*

MANGIN A. 1975. Contribution à l'étude hydrodynamique des aquifères karstiques. *Ann. Spéléologie, 29, 283-329.*

PUECH, V. 1996. Etude préliminaire à une classification des zones épikarstiques en fonction de leurs propriétés hydrauliques. Mém. diplôme postgrade en hydrogéologie, Centre d'hydrogéologie de Neuchâtel, non publié, 101 p.

SMART P. & FRIEDERICH H. 1986. Water movement and storage on the unsaturated zone of a maturely karstified carbonate aquifer, Mendip Hills, England. Proc. Conf. Env. Probl. of Karst terranes and their solutions, 1986, Nat. Water Well Assoc., Dublin, Ohio : 59-87.

THIERRIN R. 1996 : Contribution à l'étude de la circulation hydraulique dans l'épikarst, site du Maira (Jura suisse). Mém. diplôme génie rural, école polytechnique fédérale de Lausanne et Centre d'hydrogéologie, Univ. de Neuchâtel, fév. 1996, 44 p.

TURBERG P. 1993 : Apport de la cartographie magnétotellurique à l'hydrogéologie des milieux fracturés. Thèse, centre d'hydrogéologie, Univ. de Neuchâtel, 132 p.

DA VEIGA A.-M. 1995 : Caractérisation de l'épikarst et des sols sur le plateau de Bure (Jura Suisse) - étude géophysique et implantation de forages. Mém. diplôme postgrade en hydrogéologie, Centre d'hydrogéologie, Univ. de Neuchâtel, déc. 1995, 76 p.

WILLIAMS P. W. 1983 : The role of rhe subcuteanous zone in karst hydrology. *J. hydrol. 61, 45-67.*

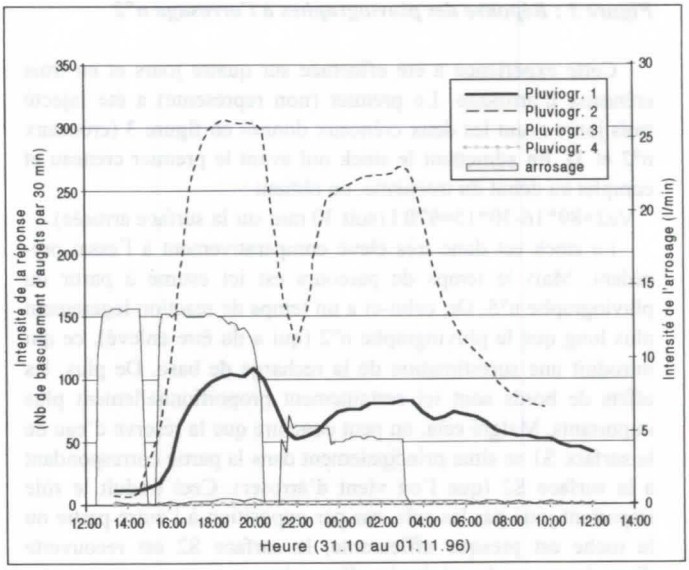

Figure 4 : Réponse des pluviographes à l'arrosage n°3

Intensité de la corrosion dans les sols du Jura Méridional (France) – Note préliminaire

A. Sbai*, M. Gaiffe**, C. Ek***, et R. Lhenaff****

*Université des Sciences et Technologies de Lille, Laboratoire de Géomorphologie, et Université de Liège, Département de Géographie physique.

** Université de Franche-Comté, Laboratoire de Pédologie, Besançon.

*** Université de Liège, département de Géographie physique.

**** Université de Savoie, Chambéry.

Abstract : Intensity of corrosion in some soils of Southern Jura (France), preliminary note

Experimental estimation of dissolution in different soils has been performed. 33 standardized limestone tablets were buried into different soil horizons and weighed regularly twice a year. The results are expressed in g/m^2/year and transformed into mm/1000 years.

We have selected three limestone types in order to compare their dissolution in different horizons. These data were used for a rough estimation of the time necessary for the formation of limestone soils, under the asumption that insoluble residue is the only source of mineral soil. About 1 million years was estimated for 89 to 112 cm of mineral soils.

Key-words : Dissolution of limestone, soils, Southern Jura, France.

Résumé

Des expériences ont été faites pour estimer l'intensité de la dissolution des calcaires dans les sols du Jura méridional. 33 plaquettes calcaires standardisées ont été déposées dans différents horizons et pesées régulièrement deux fois par an. Les résultats sont exprimés en g/m2/an puis transformés en mm/1000 ans.

Nous avons choisi trois types de calcaires pour comparer leur dissolution dans les différents horizons. Ces différentes données sont utilisées pour une estimation approximative du temps nécessaire pour la formation d'un sol sur roche calcaire en supposant que les résidus insolubles sont les seules sources des minéraux des sols. Pour 1 million d'années est estimée la formation d'un sol de 89 à 112 cm.

Mots-clés : Dissolution des calcaires, sols, Jura méridional, France.

Introduction

La formation des sols issus de roches carbonatées n'est pas suffisamment clarifiée malgré les différentes investigations. Parmi ces principaux problèmes de discussion on trouve l'origine des minéraux de ces sols. C'est évident qu'une partie des minéraux de ces sols est originaire des résidus insolubles des roches, mais des matériaux allochtones, surtout sous forme de dépôts éoliens, peuvent en faire partie (BARSHAD, J. *et al.*, 1956; WERNER, J., 1958; KHAN, R.D., 1959; CIRIC, M. et ALEKSANDROVIC, D., 1061; BOTTNER, P., 1971; MACLEOD, D.A., 1980). La relation entre ces différentes sources est très importante pour la formation des sols en régions calcaires.

Si on considère les résidus insolubles comme une source possible de la partie minérale, il faut tenir compte que la quantité de ce résidu est très faible et que la dissolution est également faible. La corrosion chimique des calcaires et des dolomies est connue comme un processus lent, mais la dimension réelle du facteur temps reste à déterminer à partir des expériences sur le terrain dans des conditions différentes. C'est la raison pour laquelle nous avons essayé d'estimer l'intensité de la dissolution des calcaires dans le sol.

De telles expériences avaient été réalisées par C. EK dans sa thèse de doctorat (1969) puis par M. KUPPER, également dans sa thèse de doctorat (1981). Mais ces expériences n'ont pas donné lieu à des publications dans des revues largement diffusées.

Méthodes et localisation des sites

Nos expériences ont été réalisées dans la région d'Izernore à 600-750 m d'altitude, ce qui peut être considéré comme représentatif du Jura externe (étage collinéen). D'autres plaquettes ont été déposées précédemment dans différents écotopes (SBAI, A., 1992).

Les températures moyennes annuelles à Izernore sont de 9° C (1973-1992) et le total pluviométrique annuel est de 1479 mm (1961-1992).

Dans chaque horizon, ont été exposées trois plaquettes de calcaires; ces plaquettes ont été pesées régulièrement deux fois par an.

Puisque les calcaires et les dolomies sont, dans la formation des sols, exposés à la dissolution, en contact du sol, nous avons choisi 5 sites et 7 profils.

Site 1 Chaîne des Bethiants, Heyriat, Mont Chakamont.

* Profil 1 : sol brun calcique superficiel sur calcaire marneux et sur colline (2 horizons).
  - A1 : 0-10 cm, agrégats avec une belle structure
  - B : 10-20 cm, sol argileux limoneux brun jaunâtre (10YR3/4), uniforme avec des gravillons, structure polyédrique
  - C : calcaire marneux.
* Profil 2 : sol brun colluvial (calcique ?) : milieu à bonne agressivité (2 horizons).
  - A1 : 0-15 cm, sol brun foncé, structure polyédrique, système racinaire, 10YR3/3
  - B : > 15 cm, sol brun, structure polyédrique
  - C : moraine.

Site 2 : Versant est de la chaîne des Berthiants

* Rendzine humifère sur moraine et sur versant (1 seul horizon)
  - A1 : 0-14 cm, sol riche en matière organique (racines) structure grumeleuse, 10YR3/3
  - A1C : 14-30 cm, zone plus riche en graviers, sol brun foncé
  - C : moraine.

Site 3: Plaine d'Izernore

* Rendzine rubéfiée sur nappe glacio-lacustre, sol calcique, fersiallitique, le fer provient des fragments du Crétacé inférieur, filtre poreux (2 horizons).
  - A1 : 0-15 cm, sol fersiallitique, structure grumeleuse, 7,5 YR3.3, beaucoup moins de cailloux par rapport à A1C
  - A1C : 15-25 cm, horizon de transition, sol très chargé en éléments grossiers (graviers)
  - C : nappe glacio-lacustre d'Izernore.

Site 4 : Versant ouest de la chaîne des Joux blanches

* Renszine colluviale sur éboulis (1 seul horizon)
  - A : 0-10 cm, sol très sableux, graveleux, 10YR3/4
  - C : éboulis.

Site 5 : Sommet de la chaîne des Joux blanches

* Profil 1 : sol brun humifère superficiel à blocs entre les lapiés, milieu acide (1 seul horizon)
  - A1 : 0-15 cm, sol brun très foncé (10YR2/2), très riche en matière organique, structure grumeleuse,
  - C : calcaire du Jurassique supérieur
* Profil 2 : sol de dépression karstique très profond (2 horizons), moins humifère que le profil précédent.
  - A1 : 0-10 cm, sol moins humifère, argileux, structure polyédrique
  - B : 10-50-100 cm ? sol argileux avec graviers
  - C : calcaire du Jurassique supérieur.

Dans chaque horizon, ont été exposées trois plaquettes de calcaires différents : calcaire oolithique du Crétacé inférieur (Valanginien, Groissiat), calcaire lithographique du Jurassique supérieur (Kimméridgien-Portlandien, Mont de Verlon, Viry) et calcaire dolomitique du Jurassique moyen (Bajocien, Bugey méridional) soit un total de 33 plaquettes. Nous avons essayé de ne pas perturber l'environnement pédologique dans lequel ont été mises ces plaquettes.

Résultats et discussion

La perte de poids des différentes plaquettes est significative dans tous les horizons. Néanmoins, on constate une différence entre les différents profils et au sein du même profil. D'un profil à l'autre, ce sont les sols sur les sommets qui marquent les fortes pertes de poids de plaquettes. Ces sols ont des teneurs en argile élevées (35 %). Ils en est de même des sols des dépressions sur les chaînes (20-30 %). Les sols sableux ou qui contiennent une proportion élevée de sable et de limons grossiers se caractérisent par des pertes de poids faibles. Ces sols ont des conditions pédoclimatiques sèches très prononcées en comparaison avec les autres sols.

Au sein du même profil, les horizons supérieurs (A) enregistrent les pertes élevées. Ce qui est normal si on considère que ces horizons contiennent une forte proportion de matière organique et par conséquent une forte production de CO_2 et d'acides organiques qui causent une forte corrosion.

Les trois types de calcaires étudiés ont des comportements qui ne diffèrent pas beaucoup. Même le calcaire dolomitique du Bajocien a des pertes de poids élevées. On a souvent pensé que les dolomies ou les calcaires dolomitiques sont moins solubles que les calcaires. Cependant, ces calcaires dolomitiques laissent sur place une pellicule blanche de dissolution au contact avec le sol.

Des corrélations ont été faites entre la dissolution d'une part et la texture et les paramètres physico-chimiques des sols d'autre part (Tabl. 1).

	Argiles	Limons	Sables	Calcimétrie	pH	CO_2	C	CEC	Ca^{++}	S
Dissolution 93-94	0,45	0,26	0,02	0,58	0,72	0,84	0,68	0,03	0,80	0,80
Dissolution 94-95	0,52	0,04	0,22	0,63	0,71	0,77	0,65	0,08	0,85	0,83

Tableau 1 : Coefficients de corrélation de la dissolution avec la texture et les paramètres physico-chimiques.

On note une forte corrélation entre la dissolution et Ca^{++}, CO_2, S, pH … La dissolution et Ca++ sont inversement corrélés. Ces différentes données peuvent être utilisées pour une estimation approximative du temps nécessaire pour le développement des sols sur calcaire, en supposant qu'ils dérivent seulement des résidus insolubles, sans dépôt de matériel allochtone, et en négligeant les variations climatiques au cours du temps qui constituent un facteur approprié à la dissolution des calcaires. Les calculs faits sous ces hypothétiques limites nous donnent simplement un ordre de grandeur. Ils montrent que le temps nécessaire pour la formation d'un sol de 90 à 110 cm par exemple dérivé de calcaires lithographique ou oolithique avec 4,9 % de fraction insoluble s'élève à 1 million d'années. Les fissures doivent augmenter la surface de dissolution et par conséquent son intensité. En effet, les calcaires du Jura méridional et surtout les calcaires du Jurassique supérieur sont très fracturés. ceci peut donc augmenter l'ordre des résultats obtenus.

En Grèce, MACLEOD, D.A. (1980), a calculé indirectement que la formation de 40 cm de sol rouge méditerranéen en Epire (Grèce), à partir des calcaires de Pantokraton qui ont 0,15 % de résidus insolubles, nécessiterait 5 millions d'années.

En Yougoslavie, au Mont Igman, CIRIC M. et SENIC P. (1985) estiment à 1,5 - 2 millions d'années la formation d'un sol de 20 cm sur des calcaires avec 0,3 % d'insolubles. Si on prend en compte que les calcaires de Pantokraton ou du Mont Igman ont un pourcentage très faible de résidu insoluble et que le climat méditerranéen est largement favorable à la dissolution des calcaires, ces calculs diffèrent de nos expériences. Ceci s'explique par la proportion de la fraction insoluble : 4,9 % contre 0,15 et 0,3 %.

Le terrain étudié a été affecté par des glaciations au cours du Pléistocène, donc dans plusieurs endroits la couverture du sol a été enlevée au lavage ou carrément érodée (SBAI, A., 1987).

Dans plusieurs endroits, on peut trouver des sols bien développés. A partie des résultats de nos expériences la proportion des minéraux dans le sol n'est pas due à l'accumulation des résidus insolubles en moins de 10.000 ans (période post-Würm), mais également à des colluvions et des dépôts allochtones.

Bibliographie

BARSHAD, J. et al. 1956. Clay Minerals in some limestone soils from Israël. *Soil Science*, 6, 423-437.

BOTTNER, P., 1971. Evolution des sols en mileiu carbonaté. *Thèse Doct. Univ. Montpellier*, 156 p.

CIRIC, M. et ALEKSANDROVIC, D;, 1951. A view on the genesis of Terra Rossa. *National Science Foundation*, Washington D.C.OTS 60-21667, 12 p.

CIRIC, M. et SENIC, P., 1985. Intensity of dissolution of limestone and dolomite in different soil media (feild experiment). *Catena*, 12, 211-214.

EK, C., 1969. *Facteurs, processus et morphologie karstiques dans les calcaires paléozoïques de la Belgique*. Thèse de doctorat, Université de Liège, 3 vol. + 2 vol. d'annexes.

JAKUCS, L., 1979. Morfogenez karstovih oblastei, Izd. *Progress*. moskva. 387 p.

KHAN, R.D., 1959. Profile distribution of sand minerals in some rendzinas, red-brown soils and Terra-Rossa. *Soil Science,* 2, 67-76.

KUPPER, M., 1981. *Les vitesses d'érosion du calcaire. Etude de processus actuels sous différents climats*. Thèse de doctorat, Université de Liège, 1 vol.

MACLEOD, D.A., 1980. The origin of the red mediterranean soils in Epirus, Greece, *Journal of Soil Sience*, 31, 125-136.

SBAI, A., 1987. Quelques aspects d'une moyenne montagne englacée. Exemple de la région d'Oyonnax (Ain, Jura méridional). *Hommes et Terres du Nord*, 3, 179-186.

SBAI, A., 1992. Premiers résultats de mesures de la corrosion dans le karst du Jura méridional (France). *Actes Seconde Rencontre d'Octobre. Chambéry*, 17-18, Octobre 1992, 74-77.

SBAI, A., 1992. Quelques expériences de mesures de la corrosion dans le karst du Jura méridional. *Conférence européene de spéléologie, Hélécine, Belgique, 20-23 août 1992. Bull. Soc. Géogr. de Liège*, Vol. 29, 1993, 145-151.

WEERNER, J., 1958. Zur Kenntnis der braunen Karbonatböden auf der schwäbischen Alb. Stuttgart, 94 p.

Carbon dioxide in soil and its drive to karst processes: A case study in transitional zone between North and South China

Zaihua Liu[1], Daoxian Yuan[1], Jingbo Zhao[2]
[1] Institute of Karst Geology, 541004 Guilin, P.R. China
[2] Xi'an College of Geology, 710054 Xi'an, P.R. China

Introduction

Zhen'an County of Shanxi Province is situated in climatically transitional zone between North and South China, where Yudong (Fish-cave) Underground Stream was formed. The mean annual air temperature here is about 11°C, and 850 mm for mean annual precipitation. The karstified rock is predominately Carboniferous-Permian limestone intercalated with coal measures. Due to the sinkholes in recharge area, Yudong Underground Stream is connected to the peak-cluster depressions, where terra rossa and loess formed. The length of the stream is about 30 km, with catchment area of 85 km^2 and flood peak discharge of about 10 m^3/s. Because of these characteristics, this area become a important site to study the karst processes.

Study method

a. CO_2 content at depth of 20cm and 50 cm in soil was measured in situ with CO_2-GASTEC meter.

b. Temperature, pH and $[HCO_3^-]$ of water from Yudong Underground Stream were measured in situ with portable pH-meter and alkalinity meter. CO_2 partial pressure in water was calculated with WATSPEC computer program, by using the field observation data.

All measurements were made once a month.

Results

Figure 1 and figure 2 show the results from this study.

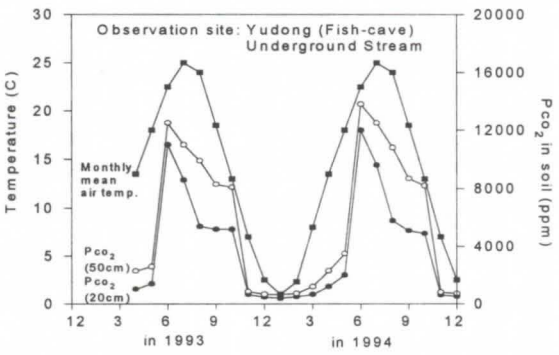

Figure 1 Seasonal change of Pco_2 in soil and its relation with air temperature

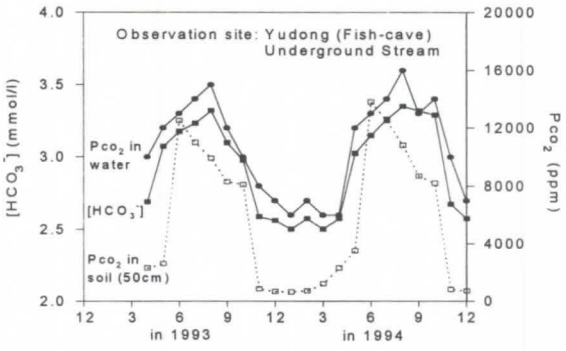

Figure 2 $[HCO_3^-]$, Pco_2 in Yudong Underground Stream water and their relation with Pco_2 in soil

Discussion and conclusion

It can be seen that CO_2 partial pressure (Pco_2) in soil changes with season remarkably, with the highest value (>10,000 ppm) in summer and the lowest value (<1,000 ppm) in winter. This may be due to the strongest biological activities in summer and the lowest biological activities in winter, and can be further evidenced by the good relation with air temperature (figure 1).

CO_2 partial pressure (Pco_2) in water is related to that in soil, which can be infered by the fact that both show the same fluctuations (figure 2). From the basic chemical principle, it can be known that high Pco_2 in water increases the dissolution rates and the solubility of limestone, due to the reaction: $CaCO_3 + CO_2 + H_2O \rightarrow Ca^{2+} + 2HCO_3^-$. This is the reason why the $[HCO_3^-]$ in water shows the same behaviour as Pco_2 in water (figure 2).

So, it is concluded that it is the CO_2 in soil that drives the karst processes under soil layer. Due to the seasonality of biological activity, CO_2 content in soil changes with season, so do the karst processes. The significance of this investigation lies not only in understanding the mechanisms of carbonate rock dissolution, but also in revealing the role of karst processes in the sink of global green-house gas, which has been given little attention in the study of global carbon cycle.

The influence of the soil air P_{CO2} on the chemical composition of karst spring water (Swabian Alb, SW Germany)

Torsten Clemens, Claudia Müller, Martin Sauter
University of Tübingen, Applied Geology, Sigwartstr. 10, D-72076 Tübingen, Germany

Abstract

The principal source of carbon dioxide, available for the dissolution of carbonate rock is found in the soil zone. However only few studies have been conducted where both, the P_{CO2} in the soil atmosphere and the chemical composition of spring water have been compared. In this study the P_{CO2} in the soil was measured at various depths beneath the surface and for different types of vegetation in a well defined holokarst groundwater catchment. Further, the chemical composition of the spring water was determined.

The results show that the spring water is always saturated with respect to calcite and that the water reaches the equilibrium concentration of calcium in the subcutaneous zone under open system conditions with respect to carbon dioxide. The CO_2 content of the spring water and of the soil decreases during the winter months. The P_{CO2} in the soil increases with depth and is dependent on the type of vegetation. The comparison of different groundwater catchments with 50 % and 20 % of agricultural land showed that the calcium content of the spring water is dependent on the vegetation in the catchment area. Therefore the determination of the denudation rate for the geological past should not be based on todays water composition affected by agricultural activity.

Zusammenfassung

Als Hauptquelle für das Kohlendioxid, ein wichtiger Faktor bei der Verkarstung von Karbonaten, werden die biologischen Abbauprozesse in der Bodenzone angenommen. Es gibt jedoch bisher wenige Arbeiten, die den Kohlendioxidgehalt in der Bodenzone und gleichzeitig die chemische Zusammensetzung von Wässern von Karstquellen untersuchten. In der vorliegenden Arbeit wurde der P_{CO2} im Boden in einem Holokarsteinzugsgebiet für verschiedene Vegetationen und Tiefen unter der Oberfläche gemessen. Weiterhin wurde die chemische Zusammensetzung des Quellwassers bestimmt.

Die Ergebnisse zeigen, daß das Quellwasser immer gesättigt in bezug auf Kalzit ist und sich im Epikarst in einem offenen System in bezug auf CO_2 entwickelte. Der Kohlendioxidgehalt des Quellwassers und der Bodenluft nimmt während des Winters ab. Der P_{CO2} im Boden nimmt mit der Tiefe zu und ist von der Art der Vegetation abhängig. Der Vergleich zweier Einzugsgebiete mit unterschiedlichen Anteilen an ackerbaulicher Nutzung (50 % gegenüber 20 %) ergab, daß der Kalziumionengehalt des Quellwassers von der Vegetation des Einzugsgebietes abhängig ist. Diese Beobachtungen führen zu dem Schluß, daß sich die Denudationsrate zu früheren Zeiten von Karstgebieten, die durch die Landwirtschaft stark verändert wurden, nicht bestimmen läßt.

Introduction

Carbonate minerals are only slightly soluble in water. The solubility of these minerals is determined by the action of the carbonic acid and therefore strongly dependent on the partial pressure of carbon dioxide (P_{CO2}). The principal source of carbon dioxide, available for the dissolution of carbonate rock has been suggested to lie in the soil zone. Therefore concentrated on the investigation of the soil parameters such as vegetation cover, grain size and pore volume on the soil air P_{CO2} (GERSTENHAUER 1972, MIOTKE 1974).

Furthermore, studies were performed showing that the seasonal variation of springwater chemistry can be used to classify carbonate springs into diffuse-flow and conduit-flow types (SHUSTER & WHITE 1971). The P_{CO2} in the spring water of the different types was examined and found that the CO_2 pressures of conduit springwaters show a regular seasonal trend whereas the CO_2 content of diffuse-flow springs is highly variable (SHUSTER & WHITE 1972). JACOBSON & LANGMUIR (1974) found in diffuse-flow spring waters only small changes in the P_{CO2} after storm events. SCANLON & THRAILKILL (1987) observed temporal variations in all Inner Bluegrass karst springs with the lowest values of P_{CO2} after snow melt in the early spring. A strong annual cycle appears in the data of karst springs in Kentucky when the data are averaged on a monthly basis (HESS & WHITE 1993).

In addition to the studies of the karst spring water mentioned above investigations were conducted inferring from the chemical composition of spring water on the soil air P_{CO2} (HARMON et al. 1975, DRAKE & WIGLEY 1975). DRAKE (1980) showed that the chemical composition of springwater was an indication whether the water evolved under open or closed system conditions with respect to CO_2.

Only few studies were performed comparing the soil air P_{CO2} with the chemical composition of karst spring water. ATKINSON (1977) suggested from a comparison of karst spring water in the Mendip Hills and soil air P_{CO2} that another source of CO_2 apart from the soil must exist.

The study presented here was carried out on the Swabian Alb. The aim of the study was to determine the source of the P_{CO2} in the water of a karst spring. Furthermore the parameters determining the CO_2 content of the water were examined.

Geographical and Geological Setting

The project area is situated on the Swabian Alb approximately 60 km south of Stuttgart, SW Germany. The Swabian Alb consists of Upper Jurassic limestones. This study was performed in the catchment of the Ach-spring which is located in the well karstified Kimmeridgian bioherm facies at an altitude of 557 m. The Ach-Spring is a conduit karst spring with a mean discharge of 590 L/s.

Methods

The catchment area of the Ach-spring was determined at 50 km^2 based on geological information and tracer tests. Boreholes for the measurement of the soil air P_{CO2} were drilled to different depths below ground for different types of vegetation. The soil air P_{CO2} was determined using a DRÄGER-multiwarn infrared-spectroscope (resolution: 0.01 Vol%).

Further, the soil profile was examined in the laboratory for different parameters, i.e. grain size distribution, percentage of organic material, calcite content and pH in order to determine the reason for the different soil air P_{CO2} beneath different types of vegetation.

The concentration of CO_2 in the water of the Ach-spring was determined using Henry's law

$$(CO_{2(aq)}) = K_H \; P_{CO2}$$

P_{CO2} was measured in the gas phase of a sample bottle after equilibration.

The pH was measured with a pH-meter and C_{HCO3} of the spring water was determined by titration directly after taking the water samples. The samples were acidified with HNO_3 and later analysed for Ca^{2+}, Mg^2 on a Perkin Elmer Model 1100 atomic adsorption spectrometer (AAS). The saturation index *SI* was calculated using

$$SI = \log [(a_{Ca}{}^{2+} \; a_{HCO3}{}^{-} \; K_2)/(a_H{}^{+} \; K_c)]$$

with the activities *a* of the species and the equilibrium constants K_2 and K_c. The temperature dependence of K_2, K_H and K_c was calculated using the equations given by PLUMMER & BUSENBERG (1982).

The first 90 m of the Wimsen-cave from which the Ach-spring emerges are accessible on a boat. Afterwards a siphon has to be dived through. The air P_{CO2} of the cave on both sides of the siphon was measured with the DRÄGER-multiwarn infrared-spectroscope to obtain a value for the P_{CO2} in the vadose zone of the aquifer.

In order to compare the effect of different vegetation covers on the composition of springwater at a catchment scale two further karst springs were examined.

Results

The temporal variations of the soil air P_{CO2} for the sites are shown in Figures 1-3.

The time series of the soil air P_{CO2} show that the soil P_{CO2} generally increases with depth. In February 1996 the curves exhibit smaller differences in the soil air P_{CO2} because the frozen soil inhibits the gas diffusion to the atmosphere. The soil air P_{CO2} decreases during the winter in all sample sites and increases again towards the spring. The strong increase in the soil air P_{CO2} at the arable site was probably due to the fertilising increasing the biological degradation processes in the soil. The lowest soil air P_{CO2} is measured at the sample site covered by beech, higher values are found beneath the fir and the highest values beneath the arable field.

The reason for the different P_{CO2} at the sample sites was found in the humus matter. Beneath the forest the humus matter consists of moder with only 5.3 % of organic matter and explains the low pH of 4.9 of the soil water, determined according to SCHEFFER & SCHACHTSCHABEL (1975). The soil beneath the field consists of mull with 8.61 % organic matter with a pH of 6.5 of the soil water. The results indicate that the conditions for the development of the edaphon are favourable beneath the field. Therefore the air P_{CO2} in the arable soil is considerably higher than in the forested stands.

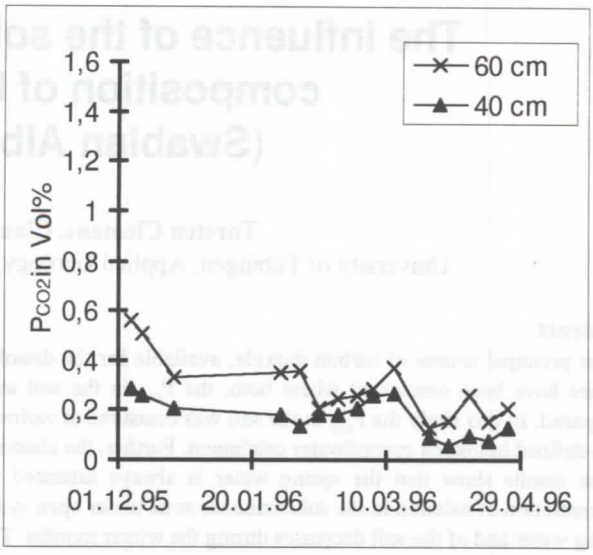

Figure 1: Soil air P_{CO2} for two different depths at the beech stand.

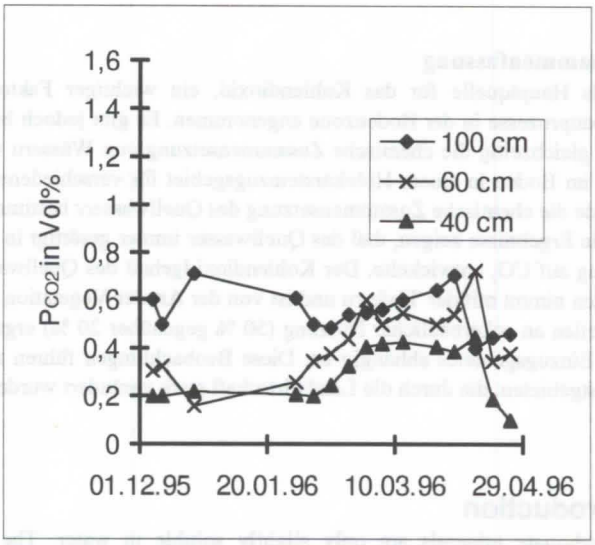

Figure 2: Soil air PCO2 for three different depths at the spruce stand.

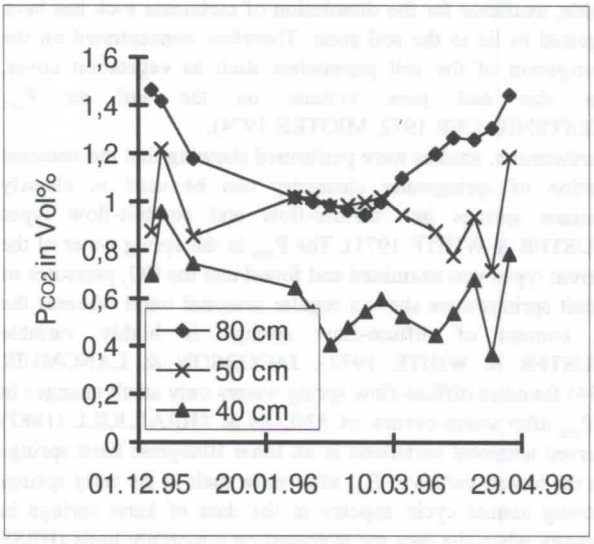

Figure 3: Soil air PCO2 for three different depths at the arable site.

The temporal variation of the P_{CO2} in the water of the Ach-spring is depicted in Figure 4. The P_{CO2} in the water of the Ach-spring decreases during the winter. The decreasing P_{CO2}

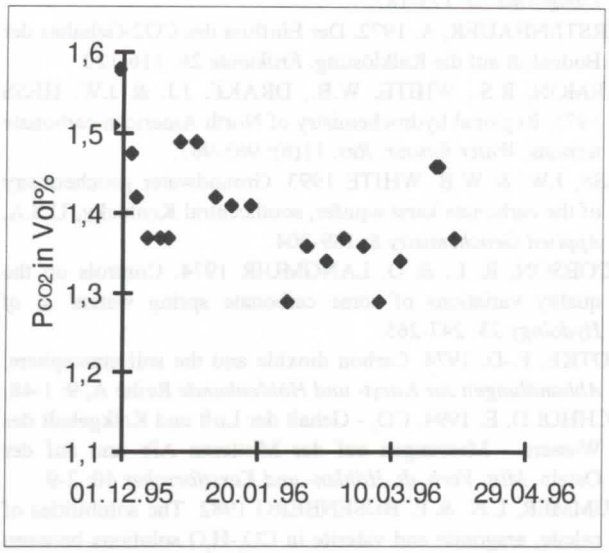

Figure 4: PCO2 in the spring water of the Ach-Spring.

content during the winter months was also measured in the Echaz-spring positioned at the northern edge of the Swabian Alb. The water of the Ach-spring was always saturated or supersaturated with respect to calcite with SI ranging from 0.02 to 0.38.

The arithmetic means of the P_{CO2} and Ca^{2+}-concentration in the water of three springs on the Swabian Alb are shown in Figure 5. The differences can be explained by the different vegetation covers of the three catchments. 60% of the catchment of the Echaz-spring, 50% of the Ach-spring catchment and only 20% of the Brenztopf catchment are arable fields.

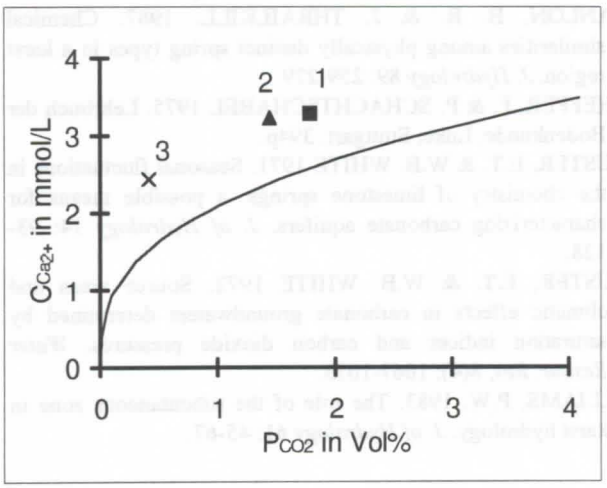

Figure 5: Arithmetic mean of the chemical composition of the water of the Echaz-spring (1), Ach-spring (2) and Brenztopf (3).

Discussion

The increase in the soil air P_{CO2} with the depth (Figure 1-3) has been found by REARDON et al. (1979) in calcareous soil in Canada and MIOTKE (1974) in soils in Germany. The reason for the increase is the production of CO_2 in the soil by the edaphon and the gaseous exchange by diffusion to the atmosphere. If the gas exchange is inhibited as in February and March 1996 (Figure 1,2) the soil air P_{CO2} at different depths approaches a more uniform value.

The soil air P_{CO2} is considerably higher in arable soils than in forest soils. Similar results were obtained by GERSTENHAUER (1972), MIOTKE (1974) and PECHHOLD (1994) in soils of the Rhein-Main-Area, Canada and the Swabian Alb. The soil examination in the laboratory shows that the soil beneath the forest has a low pH and lower organic carbon content disfavouring the growth of the edaphon as compared to arable soil.

CO_2-contents in spring water of the Ach-spring decreases during the winter months. However, the P_{CO2} in the spring water is considerably higher than the soil air P_{CO2}. Even during flood events the P_{CO2} of the spring water only decreases slightly. Therefore the water must equilibrate with the P_{CO2} of a source other than the soil air P_{CO2}. This source probably lies in the subcutaneous zone where a perched aquifer is developed (WILLIAMS 1983, SAUTER 1992). A conceptual model of the soil and subcutaneous zone is shown in Figure 5.

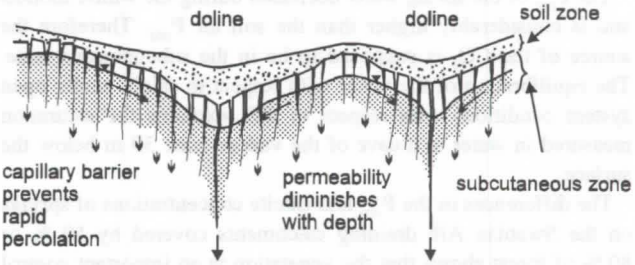

Figure 6: Conceptual model of the soil and subcutaneous zone (modified after WILLIAMS 1983).

The temperature is almost constant during the year and postulated to be between 1 °C and 2 °C lower than in the aquifer lying 200 m below (RENNER 1996). The equilibration of recharge water with calcite in the subcutaneous zone is further supported by the measurements of BEHRINGER (1987) who found that the water entering the Nebelhöhle cave (Swabian Alb) which lies 30 m below the surface is saturated with respect to calcite. ATKINSON (1977) concluded from comparing the CO_2-content of spring waters and soil air P_{CO2} in the Mendip hills that the source of CO_2 is not the soil air P_{CO2} but the "ground air" CO_2 located in the vadose zone.

The equilibration of the water with calcite in the subcutaneous zone explains the supersaturation observed in the spring water. During the flow of the water through the vadose zone, CO_2 diffuses into the cave air in the vadose zone. This assumption is supported by the measurement of the cave air P_{CO2} in a part of the cave, sealed to the atmosphere by a siphon. The P_{CO2} of the cave air was 1.6 Vol% which can only be explained by degassing of water as observed by EK & GEWELT (1985). Furthermore, the higher temperature in the aquifer leads to lower solubilities of calcite and therefore higher oversaturation of the water which equilibrated in the cooler subcutaneous zone.

The results show that the vegetation cover of a catchment has an important influence on the chemical composition of karst spring water. Therefore the ecological model of soil CO_2 production introduced by DRAKE & WIGLEY (1975) and modified by DRAKE (1980) cannot be generally applied. This model is based on the assumption that the variations in vegetation are less important because of the temporal and spatial integrating effects of groundwater recharge. This is true for anthropogenically unaffected catchments however in regions affected by agriculture this modification can overwhelm the natural climatic effect.

The results of the study presented here further indicate that the use of actual carbonate concentrations in karst spring water of the Swabian Alb in order to determine the denudation rate may not be used to calculate the denudation rate of the region in the geological past.

Conclusions

The soil air P_{CO2} was measured in sample sites at the Swabian Alb covered by different types of vegetation in different depths below the surface. These results were compared with the chemical composition of the karst spring draining the catchment.

The results show that the soil air P_{CO2} increases with depth and is considerably higher in soils covered by fields than by forest. The reason for the differences was found in laboratory investigations of the soil to be the favourable environment for the evolution of the edaphon in field soils. The increase of the P_{CO2} with the depth below the surface is caused by the diffusional exchange of the soil air with the atmosphere.

The P_{CO2} of the spring water decreases during the winter months and is considerably higher than the soil air P_{CO2}. Therefore the source of the CO_2 is supposed to be in the subcutaneous zone. The equilibration of the water with respect to calcite under open system conditions with respect to CO_2 explains the saturation measured in water in a cave of the vadose zone 30 m below the surface.

The differences in the P_{CO2} and calcite concentrations of springs on the Swabian Alb draining catchments covered by 50 % or 80 % of forest shows that the vegetation is an important control of the chemical composition of karst spring water. Therefore assumptions about the differences in the soil air P_{CO2} without taking into account the vegetation must be used with caution.

Acknowledgements

The authors want to thank Eberhard Pechhold for the fruitful discussions.

References

ATKINSON, T.C. 1977. Carbon dioxide in the atmosphere of the unsaturated zone: an important control of groundwater hardness in limestones. *J. of Hydrology* 35: 111-123.

BEHRINGER, J. 1987. Hydrogeochemische Kurz- und Langzeitstudien im Malmaquifer der mittleren Schwäbischen Alb. *Thesis. Univ. Tübingen*: 207p.

DRAKE, J.J. 1980. The effect of soil activity on the chemistry of carbonate groundwaters. *Water Resour. Res.* 16: 381-386.

DRAKE, J.J. & T.M.L. WIGLEY 1975. The effect of climate on the chemistry of carbonate groundwater. *Water Resour. Res.* 6: 985-962.

EK, C. & M. GEWELT 1985. Carbon dioxide in cave atmospheres. New results in Belgium and comparison with some other countries. *Earth Surface Processes and Landforms* 10: 173-187.

GERSTENHAUER, A. 1972. Der Einfluss des CO2-Gehaltes der Bodenluft auf die Kalklösung. *Erdkunde* 26: 116-120.

HARMON, R.S., WHITE, W.B., DRAKE, J.J. & J.W. HESS 1975. Regional hydrochemistry of North American carbonate terrains. *Water Resour. Res.* 11(6): 963-967.

HESS, J.W. & W.B. WHITE 1993. Groundwater geochemistry of the carbonate karst aquifer, southcentral Kentucky, U.S.A. *Applied Geochemistry* 8: 189-204.

JACOBSON, R. L. & D. LANGMUIR 1974. Controls on the quality variations of some carbonate spring waters. *J. of Hydology* 23: 247-265.

MIOTKE, F.-D. 1974. Carbon dioxide and the soil atmosphere. *Abhandlungen zur Karst- und Höhlenkunde* Reihe A, 9: 1-48.

PECHHOLD, E. 1994. CO_2 - Gehalt der Luft und Kalkgehalt des Wassers - Messungen auf der Mittleren Alb und auf der Ostalb. *Mitt. Verb. dt. Höhlen- und Karstforscher* 40: 2-9.

PLUMMER, L.N. & E. BUSENBERG 1982. The solubilities of calcite, aragonite and vaterite in CO_2-H_2O solutions between 0 and 90 °C, and an evaluation of the aqueous model for the system $CaCO_3$-CO_2-H_2O. *Geochim. et Cosmochim. Acta* 46: 1011-1040.

REARDON, E.J., ALLISON, G.B. & P. FRITZ 1979. Seasonal chemical and isotopic variations of soil CO_2 at Trout Creek, Ontario. *J. of Hydrology* 43: 355-371.

RENNER, S. 1996. Wärmetransport in Einzelklüften und Kluftaquiferen - Untersuchungen und Modellrechnungen am Beispiel eines Karstaquifers. *Tübinger Geowissenschaftliche Arbeiten* C 30: 89p.

SAUTER, M. 1992. Quantification and forecasting of regional groundwater flow and transport in a karst aquifer (Gallusquelle, Malm, SW. Germany). *Tübinger Geowissenschaftliche Arbeiten* C 13: 150 p.

SCANLON, B. R. & J. THRAILKILL. 1987. Chemical similarities among physically distinct spring types in a karst region. *J. Hydrology* 89: 259-279

SCHEFFER, F. & P. SCHACHTSCHABEL 1975. Lehrbuch der Bodenkunde. Enke, Stuttgart: 394p.

SHUSTER, E.T. & W.B. WHITE 1971. Seasonal fluctuations in the chemistry of limestone springs: a possible means for characterizing carbonate aquifers. *J. of Hydrology* 14: 93-128.

SHUSTER, E.T. & W.B. WHITE 1972. Source areas and climatic effects in carbonate groundwaters determined by saturation indices and carbon dioxide pressures. *Water Resour. Res,* 8(4): 1067-1073.

WILLIAMS, P.W. 1983. The role of the subcutaneous zone in karst hydrology. *J. of Hydrology* 61: 45-67.

A theoretical model for the distribution and transport of carbon dioxide in the epikarst

William B. White and Elizabeth L. White
Department of Geosciences and Environmental Resources Research Institute
The Pennsylvania State University, University Park, PA 16802 USA

Zusammenfassung

Die chemikalischen Funktionen des Epikarstes sind abhängig von der CO_2-Bildung und vom Transport, welche mit Hilfe von vier miteinander gekoppelten Prozessen modelliert werden können: (i) Geschwindigkeit der CO_2-Bildung. (ii) Infiltration des Regenwassers durch die Bodenschicht, um das Gestein zu erreichen. (iii) Lösungsgeschwindigkeit des CO_2 des versickernden Wassers. (iv) Geschwindigkeit des CO_2-Verlustes durch Diffusion aufwärts durch den Boden zur Atmosphäre. Diese vier Prozesse bestimmen den Anteil des CO_2, der das Gestein erreicht.

The Conceptual Model

The amount of CO_2 that ultimately ends up in the karst water depends on the rate of CO_2 generation, the time distribution of infiltrating water, on the kinetics of the dissolution of CO_2 in water, balanced off against the loss of CO_2 upward into the atmosphere (Fig. 1). The model for CO_2 transport in the epikarst is determined by four coupled rate equations.

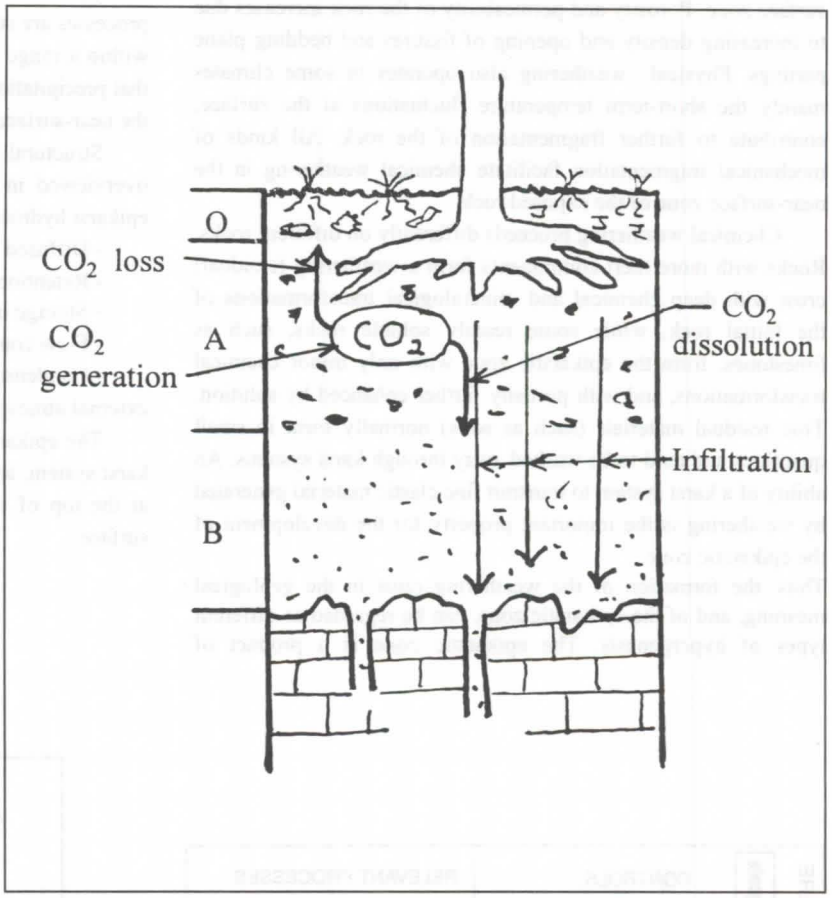

Carbon Dioxide Generation

The ultimate sources of carbon dioxide in the epikarst are exhalation from plant roots, from the decay of organic material in the soil, and from the action of microorganisms. In northern climates, CO_2 producing processes operate at a maximum rate in the summer and either slow or stop during the winter. CO_2 generation can be modeled as a time-dependent function of the soil temperature.

Infiltration Rate of Storm Water

There is a very large literature and good theoretical description and infiltration water movement in unsaturated soils. The rate of infiltration depends on storm intensity, storm spacing, and antecedent soil moisture conditions.

Dissolution Kinetics of Carbon Dioxide

The rate equation for the mass transfer of carbon dioxide from the gas phase to the infiltrating water has been worked out in laboratory experiments.

Carbon Dioxide Loss

Carbon dioxide diffuses upward through the porous soil so that some fraction of the generated CO_2 is ultimately lost to the atmosphere. This term in the overall model can be described by Fickian diffusion with a diffusivity determined by the soil porosity.

The nature and principal characteristics of epikarst

Alexander Klimchouk
Institute of Geological Sciences, National Academy of Sciences, P.O.Box 224/8, Kiev-30, 252030, Ukraine

The epikarstic zone is the uppermost zone of exposed karstified rocks whose porosity, due to fissuring and diffused karstification, is considerably enhanced compared to the bulk rock mass below.

The formation of the epikarstic zone is the result of interaction of various endogenetic and exogenetic processes (Fig.1). It is usually initiated by mechanical processes rather than dissolution. Stress-release causes fissuring to develop in the near-surface zone. Porosity and permeability of the rock increases due to increasing density and opening of fissures and bedding plane partings. Physical weathering also operates in some climates mainly the short-term temperature fluctuations at the surface, contribute to further fragmentation of the rock. All kinds of mechanical fragmentation facilitate chemical weathering in the near-surface zone of the exposed rock.

Chemical weathering proceeds differently on different rocks. Rocks with more inert components form a weathering (residual) crust with deep chemical and mineralogical transformations of the initial rock, while some readily soluble rocks, such as limestones, form the epikarstic zone with only minor chemical transformations, and with porosity further enhanced by solution. True residual materials (such as soils) normally form in small quantities and tend to be washed away through karst systems. An ability of a karst system to transmit fine clastic material generated by weathering is the important property for the development of the epikarstic zone.

Thus, the formation of the weathering crust in the geological meaning, and of the epikarstic zone, can be regarded as different types of hypergenesis. The epikarstic zone is a product of weathering processes specific to some readily soluble rocks. The development of epikarst depends on mechanical properties of the rock, initial partings structure, chemical purity, climate, the rate of uplift and denudation and the previous karstification history (the presence of inherited karst porosity formed in the internal zones of a massif before an uplift and exposure).

In some readily soluble rocks, such as gypsum, the epikarstic zone does not develop, at least in semi-arid and arid climates. The main reason is that dissolution-precipitation processes are strongly affected by changes of physical conditions within a range commonly occurring at the near-surface zone, so that precipitation/re-crystallisation results in sealing of fissures in the near-surface zone and in cementation of clasts.

Structural characteristics of the typical epikarstic zone are overviewed in the paper, as well as the principal features of epikarst hydrology (Fig.2). The latter include:

- Diffused absorption of a surface runoff;
- Retention of vertical percolation;
- Storage of groundwater;
- Flow concentration at the base of the epikarstic zone,
- Condensation of water during the air exchange between the external atmosphere and the aerated space of the vadose zone.

The epikarstic zone comprises an important subsystem of a karst system, and determines to a great extent both speleogenesis at the top of the vadose zone and karst morphogenesis at the surface.

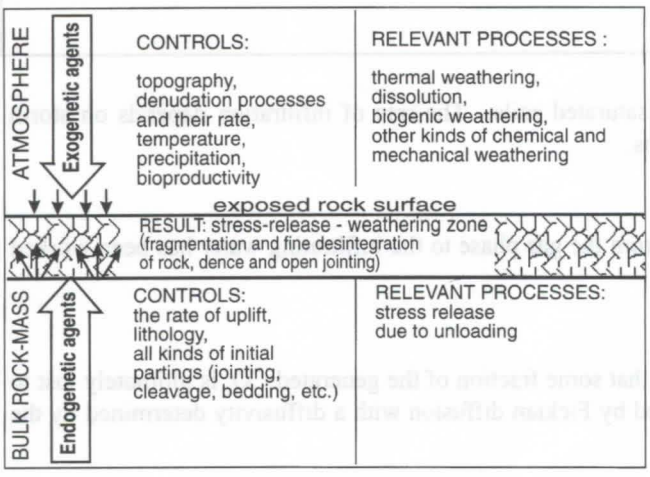

Figure 1: The processes and controls in the formation of the epikarstic zone.

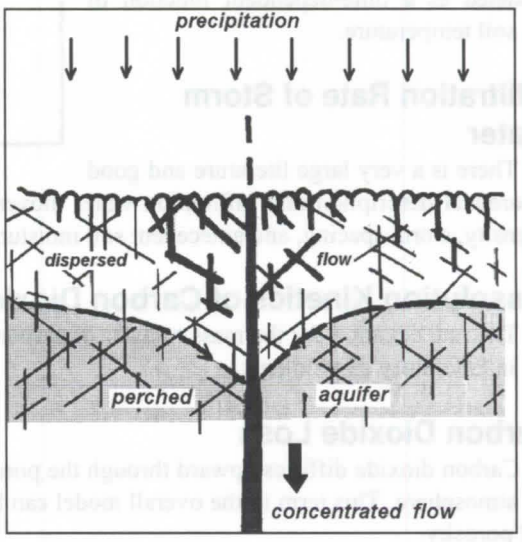

Figure 2: Retention, storage and flow concentration in the epikarstic zone.

Changes in chemical composition and physical parameters of water in an alpine karst system (Totes Gebirge, Steiermark, Austria)

Christof Harlacher, Torsten Clemens, Martin Sauter
University of Tübingen, Applied Geology, Sigwartstr. 10, D-72076 Tübingen, Germany

Abstract

The chemical composition and temperature of karst water were studied in an alpine karst system (Totes Gebirge, Austria) in order to investigate the spatial distribution of the carbonate dissolution and the role of the epikarst for the dissolution processes. Discharge, specific conductance and temperature of water were continuously monitored using data loggers in caves at different levels of the vadose zone and in groundwater emerging from a spring at the base of the plateau. Further, the chemical composition of the water was determined during peak flow and low water periods.

During low water periods, the water was saturated with respect to calcite in the whole system. Following recharge events, undersaturation was observed in the vadose zone as well as in the spring water. Therefore the enlargement of the conduits in the phreatic zone of alpine holokarst areas can only occur during recharge events whereas during low water periods dissolution only takes place in the epikarst.

Zusammenfassung

Die chemische Zusammensetzung und die Temperatur von Karstwässern wurden in einem alpinen Karstsystem untersucht (Totes Gebirge, Österreich), mit dem Ziel die räumliche Verteilung der Kalzitlösung und den Einfluß des Epikarstes für die Karbonatlösung zu ermitteln. In verschiedenen Tiefen in Höhlensystemen sowie an Karstquellen am Rand des Gebirgsstockes wurden die Schüttung, die elektrische Leitfähigkeit und die Temperatur des Wassers mit Datenloggern kontinuierlich aufgezeichnet. Des weiteren wurde die chemische Zusammensetzung des Wassers bei Trockenwetterbedingungen und bei Hochwasserereignissen bestimmt.

Bei Trockenwetter war im gesamten System das Wasser in bezug auf Kalzit gesättigt bzw. übersättigt. Nach Niederschlagsereignissen wurde Untersättigung des Wassers in der vadosen Zone und an der Quelle festgestellt. Demzufolge ist davon auszugehen, daß die Karströhren in der phreatischen Zone alpiner Holokarstgebiete nur während Niederschlagsereignissen erweitert werden, während Trockenwetterbedingungen hingegen findet die Lösung nur im Epikarst statt.

Introduction

The variation in the calcium concentration and temperature of limestone springs can be used in order to classify karst aquifers. SHUSTER & WHITE (1971) found that springs fed by open conduits respond rapidly to fluctuations in discharge, whereas springs fed by small fissures, exhibit little change in temperature or water chemistry after recharge events. The conduit-springs examined by SHUSTER & WHITE (1971) were always aggressive with respect to calcite.

JAKUCS (1959), TERNAN (1972) and JACOBSON & LANGMUIR (1974) attributed the variability in calcium hardness to differences in the recharge process. The influence of these different types of water transmission in the saturated zone and recharge on the spring hydrograph was analysed by SMART & HOBBS (1986). RENNER (1996) used water temperature data, provided by a spring in the karst of the Swabian Alb, in order to obtain information on the geometry of the conduit system.

The distribution of solutional erosion of limestone was examined by CORBEL (1959). He concluded that in alpine karst areas between 50 % and 80 % of the dissolution occurs in the endokarst. SMITH & ATKINSON (1976) propose that between 50 % and 90 % of the solutional erosion occurs close to the surface in temperate climates, however they had not enough data to determine the percentage of subsurface erosion in alpine areas. THRAILKILL & ROBL (1981) found that in limestone aquifers in Kentucky which are not overlain by other lithologies, essentially all dissolution of calcite is occurring at the soil-rock interface.

Due to the high amount of dissolution close to the surface, fissures in the uppermost zone are enlarged. As a result a zone develops which functions as a water storage. Evidence for this zone - the epikarst - is provided by BAKALOWICZ et al. (1974), MANGIN (1975), GUNN (1981), WILLIAMS (1983) and SAUTER (1992).

Continuous recordings of discharge, electrical conductance and temperature of water in karst areas are generally available only from karst springs of highlands. Data from alpine holokarst areas are scarce. Furthermore comparisons between the water chemistry and its variations in the vadose zone and in the karst springs are lacking due to the lack of accessibility of the actual feeder system in the vadose zone. In alpine karst areas the huge vadose zone, up to 1000 m deep, offers the possibility to provide data directly from the vadose feeder system.

In this paper the temporal and spatial distribution of the chemical composition and temperature of water in an alpine karst area is analysed with respect to the spatial and temporal distribution of dissolution of limestone. Data were collected at a spring at the base in the South of the Totes Gebirge plateau as well as in vertical shafts in the vadose zone of the karst area in order to obtain information about the epikarst in this alpine karst area and the temporal and spatial distribution of dissolution

Geographical and Geological Setting

The Totes Gebirge is the largest limestone plateau in Northern Limestone Alps, covering an area of approximately 500 km^2. It is situated 60 km East of Salzburg (Austria). The Totes Gebirge consists of a sequence of Triassic and Jurassic limestones and dolostones and is part of the Northern Calcareous Alps. A geologic cross section with the location of the karst spring, the vertical shafts and the water table is depicted in figure 1.

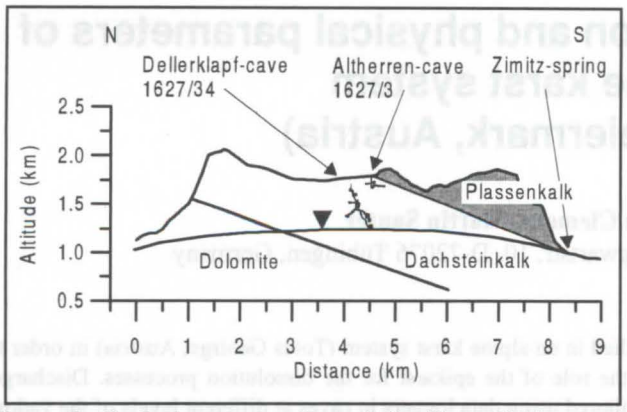

Figure 1: Geologic cross section of the Totes Gebirge and location of the vertical shafts and the karst spring.

The base of the sequence consists of 1000 m of Triassic dolostone (Hauptdolomit). It is followed by 1000 m of Triassic limestone (Dachsteinkalk). The uppermost 150 m of limestones are of Jurassic age (Plassen-Kalk) and are separated from the underlying Triassic limestones by a silicate rich layer (Oberalmer Kalk). The strata dip in SE direction with 20° to 30°.

The elevation of the plateau ranges from 1600 m to 2100 m. The plateau ends in 1000 m deep steep cliffs in the North and the South. With an average precipitation of 2200 mm/y the region is the area with highest precipitation in Austria.

The karstification of the region began during the Aquitanian (KUFFNER, 1994). As a result of the uplift of the Alps several cave levels developed. Today, the region is characterised by conduit springs at the base of the plateau and of feeder conduits in the vadose zone that could be followed down to a depth of 1000 m below the surface of the plateau.

Methods

Over a 2 ½ month period, 116 water samples were collected. Waterlevel, electric conductance and temperature of the water were monitored by automatic digital dataloggers (PHYTEC, PRODATA) with a sampling frequency of 7 to 10 minutes at the spring and in two feeder caves in the vadose zone. During some high water events in the caves the sampling frequency was reduced to one minute for better temporal resolution.

The spring is situated in the South of the plateau at 1000 m altitude. The entrances of the caves are located on the plateau on an altitude of 1790 m (1627/3 Atherren-cave) and 1700 m (1627/34 Dellerklapf-cave). The dataloggers were installed in the caves at 80 m (Atherren-cave) and 220 m (Dellerklapf-cave) below the surface.

Waterlevel was measured at a resolution of 1 mm, electric conductance at 0.1 µS/cm (WTW LA 1/T) and the water temperature at 0.01 °C. The electrical conductance values are temperature corrected for 25 °C.

During low water level and during some recharge events pH and hydrogen carbonate concentration were determined immediately after sampling. The samples were acidified with HNO_3 and later analysed for Ca^{2+}, Mg^{2+}, K^+ and Na^+ on a Perkin Elmer Model 1100 atomic adsorption spectrometer (AAS). The saturation index *SI* was calculated using

$$SI = \log [(a_{Ca}2+ \cdot a_{HCO3}- \cdot K_2)/(a_H+ \cdot K_c)]$$

equilibrium constants K_2 and K_c. The pCO_2 of the water was calculated by

$$P_{CO2} = (a_H+ \cdot a_{HCO3}-)/(K_H \cdot K_1)$$

The temperature dependence of K_1, K_2, K_H and K_c was calculated using the equations given by PLUMMER & BUSENBERG (1982).

Furthermore air P_{CO2} and air temperature were measured at different elevations in both caves with a DRÄGER-multiwarn infroredspectroscope (resolution 0.01 Vol%) and a thermometer (resolution 0.05 °C) respectively.

Results

Low water periods

During the low water period the stream in the Altherren-cave 80 m below the surface discharges only a few mL/s. Arithmetic mean values of the chemical and physical parameters of the water are given in table 1. The P_{CO2} of the cave water was 0.045 ± 0.01 Vol%.

The values in the Dellerklapf-cave 220 m below the surface are similar (table 1) to the one from the Altherren-cave.

The chemical and physical parameters of the Zimitz-spring water differ somewhat from the water in the caves. The water temperature is considerably higher and the saturation index less than in the cave water. Calcium and magnesium concentrations are comparable with the one in the cave waters.

Recharge events

On the 2nd of August 1996 a 45 minute storm provided 19.9 mm of precipitation and caused a flood event in the Altherren-cave within 15 to 25 minutes after the commencement of precipitation. The discharge of the stream increased within 2 minutes from 10 mL/s to about 5 L/s. At the same time as discharge increased, specific conductance decreased from 240 µS/cm to 122 µS/cm and temperature increased from 2.5 °C to 6.3 °C. C_{HCO3}- decreased from 2.6 mmol/L to 1.4 mmol/L, the SI dropped from +0.5 to -0.5, C_{Ca}^{2+} from 1.5 mmol/L to 0.8 mmol/L and C_{Mg}^{2+} from 0.04 mmol/L to 0.025 mmol/L (s. Figure 2).

On the 14th of August we observed in the Dellerklapf-cave the effects of a storm on the chemical and physical parameters. The changes of the parameters resembled the observations in the Altherren-cave: the discharge increased from 10 mL/s to 1.5 L/s and the specific conductance decreased from 185 to 172. The temperature increased during the flood event from 2.2 °C to 2.5°C.

The Zimitz-spring in the South of the plateau discharges about 30 L/s during dry periods. On the 4th of September a flood

	temperature in °C	specific conductance in µS/cm	$C_{Ca}2+$ in mmol/L	$C_{Mg}2+$ in mmol/L	SI	pH
Altherren-cave	2.3 ± 0.2	250 ± 18	1.4 ± 0.2	0.03 ± 0.005	0.42 ± 0.1	8.3 ± 0.2
Dellerklapf-cave	2.05 ± 0.25	180 ± 6	1.0 ± 0.1	0.08 ± 0.003	0.35 ± 0.1	8.35 ± 0.2
Zimitz-spring	4.2 ± 0.1	190 ± 5	1.3 ± 0.1	0.05 ± 0.004	-0.05 ± 0.15	

Table 1: Temperature and chemical composition of the water in the caves and at the spring for dry periods.

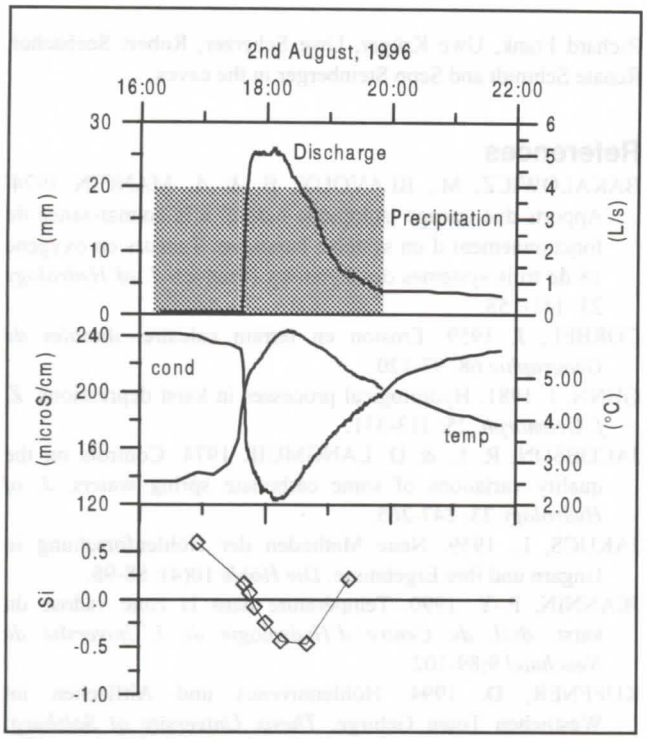

Figure 2: Discharge, electrical conductance, temperature and SI in the Altherren-cave at 80m below the surface.

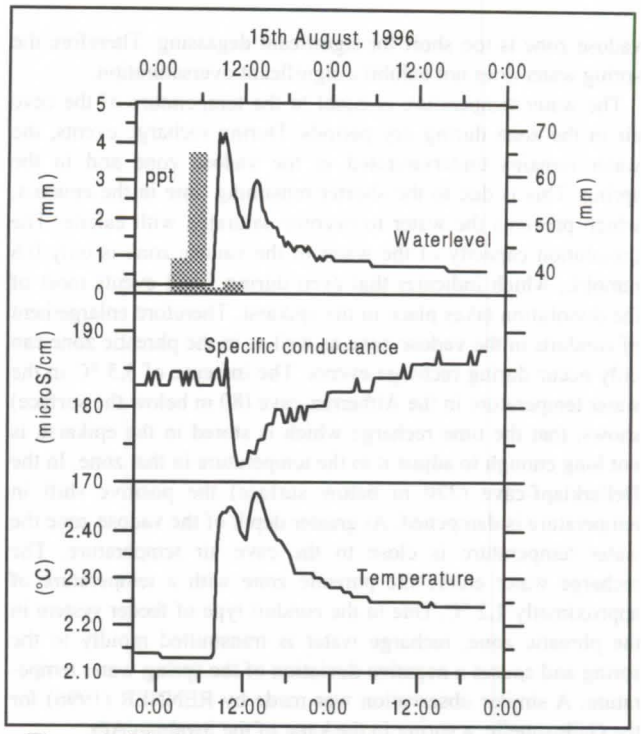

Figure 3: Discharge, electrical conductance and temperature in the Dellerklapf-cave 220 m below the surface.

was analysed. In addition to the automatically monitoring dataloggers, 23 water samples were collected over a 36 hour period. Within 30 minutes the discharge increased from about 30 L/s to 1000 L/s. As the discharge passed beyond 300 to 350 L/s, a second spring became active, 50 m higher in elevation than the observed one. The lag time between precipitation on the plateau and the response of the spring was about 3 to 4 hours. In contrast to the variation of water temperature in the cave which exhibits an increase during the recharge event, at the spring the water temperature decreased after a short positive peak. With continuing high discharge the temperature increased above the pre-event value. 30 minutes after the commencement of the flood, specific conductance decreased in two steps from 192 µS/cm to 178 µS/cm. C_{Ca}^{2+} and C_{Mg}^{2+} showed a brief rise at first but both decreased during the event. The SI decreased during the flood event to -1.2 and rised afterwards to 0 (Figure 4).

Cave air P_{CO2} and cave air temperature

The P_{CO2} in the Altherren-cave and Dellerklapf-cave does not exhibit a major variation. The P_{CO2}-values (0.02 Vol% to 0.03 Vol%) are in the range of the CO_2-concentration in the atmosphere and are only slightly elevated in those parts of the cave with little air movement (0.04 Vol%). The air temperatures in the caves are also almost constant at 2.0 ± 0.2 °C. An altitude dependent gradient in cave air temperature, as described by JEANNIN (1990) from caves in Switzerland, was not observed.

Discussion

During dry periods the water in the vadose zone is supersaturated with respect to calcite (SI = 0.35 ± 0.1). The supersaturation and the P_{CO2} of the water (0.045 Vol%) indicate that the water reaches saturation in the epikarst with the soil air P_{CO2}. In the vadose zone this water degasses during low flow conditions because the cave air P_{CO2} is significantly less (0.03 Vol%) than the soil air P_{CO2} in the epikarst. This degassing causes the observed supersaturation. In contrast to the cave stream water, the spring water is saturated (SI = 0 ± 0.15). During dry periods the spring is mainly fed by water stored in the phreatic zone. This water has reached the phreatic zone in a state of undersaturation during recharge events and becomes saturated without degassing, because the time period of flow through the

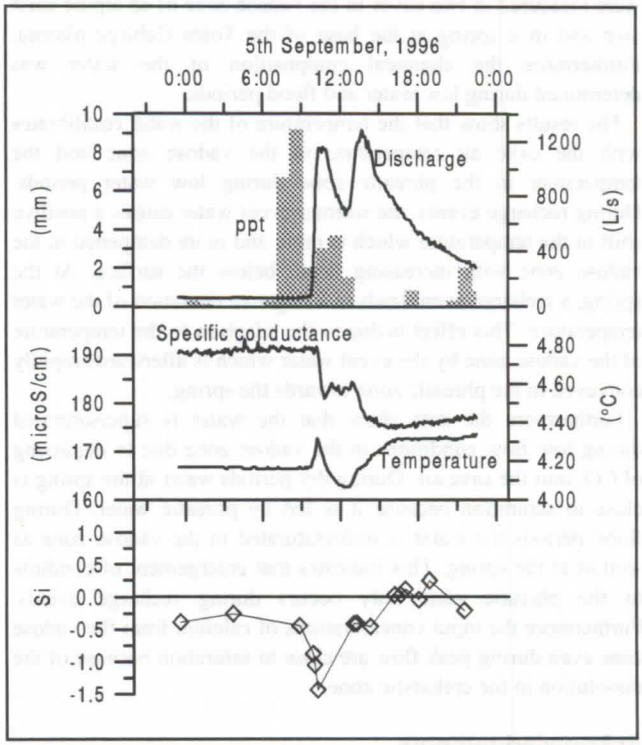

Figure 4: Discharge, electrical conductance, temperature and SI in the Zimitz-spring at the base of the plateau.

vadose zone is too short for significant degassing. Therefore the spring water does not exhibit a significant oversaturation.

The water temperature is equal to the temperature of the cave air in the zone during dry periods. During recharge events, the water remains undersaturated in the vadose zone and in the spring. This is due to the shorter remaining time in the epikarst, which prevents the water to become saturated with calcite. The dissolution capacity of the water in the vadose zone is only 0.6 mmol/L, which indicates that even during flood events most of the dissolution takes place in the epikarst. Therefore enlargement of conduits in the vadose zone as well as in the phreatic zone can only occur during recharge events. The increase of 3.5 °C in the water temperature in the Altherren-cave (80 m below the surface) shows, that the time recharge which is stored in the epikarst, is not long enough to adjust it to the temperature in that zone. In the Dellerklapf-cave (220 m below surface) the positive shift in temperature is dampened. At greater depth of the vadose zone the water temperature is close to the cave air temperature. The recharge water enters the phreatic zone with a temperature of approximatly 2.2 °C. Due to the conduit type of feeder system in the phreatic zone, recharge water is transmitted rapidly to the spring and causes a negative deviation of the spring water temperature. A similar observation was made by RENNER (1996) for the Gallusquelle, a spring in the karst of the Swabian Alb.

Before the fast recharge water reaches the Zimitz-spring, temperature rises above background levels synchroneously with a discharge increase. This rise may be caused by the recharge water of the zone close to the spring where the vadose zone is only some meters thick. Therefore the water can reach the phreatic zone without adapting to the lower temperature of the vadose zone.

Conclusions

The electric conductance, water temperature and pressure head were measured in two caves in the vadose zone of an alpine karst area and in a spring at the base of the Totes Gebirge plateau. Furthermore the chemical composition of the water was determined during low water and flood periods.

The results show that the temperature of the water equilibrates with the cave air temperature in the vadose zone and the temperature in the phreatic zone during low water periods. During recharge events, the warmer event water causes a positive shift in the temperature which is more and more dampened in the vadose zone with increasing depth below the surface. At the spring, a recharge event leads to a negative deviation of the water temperature. This effect is due to the adaption to the temperature of the vadose zone by the event water which is afterwards rapidly conveyed in the phreatic zone towards the spring.

Furthermore the data show that the water is supersaturated during low flow conditions in the vadose zone due to degassing of CO_2 into the cave air. During dry periods water at the spring is close to saturation because it is fed by phreatic water. During flood periods the water is undersaturated in the vadose zone as well as at the spring. This indicates that enlargement of conduits in the phreatic zone only occurs during recharge events. Furthermore the input concentrations of calcium from the vadose zone even during peak flow are close to saturation because of the dissolution in the epikarstic zone.

Acknowledgements

This study was supported by the German Research Foundation (DFG) as a part of the Collaborative Research Centre 275 (SFB 275). We appreciate the assistance of Heidrun André, Richard Frank, Uwe Krüger, Uwe Scherzer, Robert Seebacher, Renate Schmidt and Sepp Steinberger in the caves.

References

BAKALOWICZ, M., BLAVOUX, B. & A. MANGIN 1974. Apports due tracage isotopique naturel à la connaissance du fonctionnement d´un système karstique: Teneurs en oxygène 18 de trois systèmes des Pyrénées (France). *J. of Hydrology* 23: 141-158.

CORBEL, J. 1959. Erosion en terrain calcaire. *Annales de Géographie* 68: 97-120.

GUNN, J. 1981. Hydrological processes in karst depressions, *Z. f. Geomorph.* 25: 313-331.

JACOBSON, R. L. & D. LANGMUIR 1974. Controls on the quality variations of some carbonate spring waters. *J. of Hydrology* 23: 247-265.

JAKUCS, L. 1959. Neue Methoden der Höhlenforschung in Ungarn und ihre Ergebnisse. *Die Höhle* 10(4): 88-98.

JEANNIN, P.-Y. 1990. Température dans la zone vadose du karst. *Bull. du Centre d´Hydrologie de L´Université de Neuchatel* 9:89-102

KUFFNER, D. 1994. Höhlenniveaus und Altflächen im Westlichen Toten Gebirge. *Thesis University of Salzburg*: 269p.

MANGIN, A. 1975. Contribution à l´étude hydrodynamique des aquifères karstiques. Thesis Univ. Dijon, France, *Ann. Spéléol.* 30: 21-124.

PLUMMER, L.N. & E. BUSENBERG 1982. The solubilities of calcite, aragonite and vaterite in CO_2-H_2O solutions between 0 and 90 °C, and an evaluation of the aqueous model for the system $CaCO_3$-CO_2-H_2O. *Geochim. et Cosmochim. Acta* 46: 1011-1040.

RENNER, S. 1996. Wärmetransport in Einzelklüften und Kluftaquiferen - Untersuchungen und Modellrechnungen am Beispiel eines Karstaquifers. *Tübinger Geowissenschaftliche Arbeiten* C 30: 89p.

SAUTER, M. 1992. Quantification and forecasting of regional groundwater flow and transport in a karst aquifer (Gallusquelle, Malm, SW. Germany). *Tübinger Geowissenschaftliche Arbeiten* C 13: 150 p.

SCANLON, B. R. & J. THRAILKILL. 1987. Chemical similarities among physically distinct spring types in a karst region. *J. Hydrology* 89: 259-279

SHUSTER, E.T. & W.B. WHITE, 1971. Seasonal fluctuations in the chemistry of limestone springs: a possible means for characterizing carbonate aquifers. *J. of Hydrology* 14: 93-128.

SMART, P.L. & S.L. HOBBS 1986. Characterisation of carbonate aquifers: a conceptual base. *Proc. of the Environmental Problems in Karst Terrains and their Solutions Conference*, Bowling Green, Kentucky: 1-14.

SMITH, D.I. & T.C. ATKINSON 1976. Process, landforms and climate in limestone regions. In: *Geomorphology and Climate*, E. Derbyshire, ed., Wiley & Sons, London New York Sydney: 367-409.

TERNAN, J. L. 1972. Comments on the use of a calcium hardness variability index in the study of carbonate aquifers: with reference to the Central Pennines, England. *J. of Hydrology* 16: 317-321.

THRAILKILL. J. & T.L. ROBL 1981. Carbonate geochemistry of the vadose water recharging limestone aquifers. *J. of Hydrology* 54: 195-208.

WILLIAMS, P.W. 1983. The role of the subcutaneous zone in karst hydrology. *J. of Hydrology* 61: 45-67.

Definition and characteristics of stone forest epikarst aquifers in South China

Peter W. Huntoon
Department of Geology and Geophysics, University of Wyoming, Laramie, Wyoming 82071 U.S.A.

Abstract

Epikarsts serve as hosts for shallow, thin, largely unconfined aquifers, herein called stone forest aquifers. Stone forest aquifers are characterized by very large lateral permeabilities and small reservoir storage. These aquifers occur in lowland environments such as karst plains, valley floors and floors of karst depressions. Most of the ground water exploited from them in south China is produced from under broad karst plains and along stream valleys.

Stone forest aquifers occupy the epikarst zone where the undissolved carbonate bedrock, which is virtually impermeable, serves as a structural framework that holds saturated or partially saturated unconsolidated infills comprised of soils, dissolution residual clays and externally derived clastics sediments.

The water in the stone forest aquifers usually represents the top of a fully saturated substrate. Consequently, in lowland areas, there usually is no underlying vadose zone. Lateral circulation predominates.

Storage within the stone forest aquifers occurs within dissolution voids and dissolution-widened fractures in the carbonates, and, more importantly, in the intergranular porosity within the unconsolidated infills. Permeability through the aquifers in decreasing order of importance results from: (1) partings between the carbonates and infills, (2) interconnected dissolution cavities within the carbonate bedrock, and (3) intergranular permeability within the infills. The largest permeabilities are associated with the partings between the carbonate bedrock and the infills at the bases of the dissolution fissures which separate the stone pinnacles.

The large lateral transmissivities and poor storage characteristics of stone forest aquifers causes them to be difficult to manage. Seasonal recharge during the wet season, although it commonly fully saturates the aquifers, is quickly transmitted out of the area during the dry season. Water levels decline rapidly as the water is lost from storage and little water remains in the aquifers to sustain yields during the latter parts of the dry season.

Two common hazards plague regions underlain by stone forest aquifers: (1) sinkhole collapses and (2) leaky dams. The sinkholes usually result from collapses of the infill material into the space created by dissolution near the base of the epikarst zone. Dam failures are characterized by lateral underflow through the epikarst zone under the dam.

Stone forests

The Chinese term "stone forest" is defined in YUAN (1988) as: "a complex landscape consisting of dense rock spires having a variety of shapes separated by numerous dissolution-widened fractures (grikes). The surfaces of the spires and walls of the grikes exhibit vertical flutes (lapies). The spires are commonly about 20 m high although the highest reach 50 m. The upper surfaces of the spires are modified by dissolution by rain water." See Figure 1.

The origin of stone forests is the subject of debate with some workers claiming that stone forests develop under soils whereas others believe they are surface dissolution forms. The Chinese perspective on this debate is briefly summarized in JIANG, YUAN & HUNTOON (1993). My experience in the karst areas of southeast Asia is that most stone forests are at least partially buried by combinations of soils, dissolution residuals and externally derived clastic sediments (Figure 2). These unconsolidated materials will be collectively referred to as infills in this article. The bulk of the dissolution which gives rise to stone forests in this environment appears to take place below the infills.

I have not observed fundamental morphologic distinctions between the bare epikarst and soil-covered epikarst that I have examined in southeast Asia. In fact, as I compared profiles through both types in quarry walls, wells, and outcrops along stream channels and excavations, taxonomic distinctions between the morphologies found in different settings became even more ambiguous. This finding has been reinforced by tracing epikarst exposures from bare hill environments into quarried soil-covered zones in the adjacent plains in Guangxi and Guizhou. Little morphologic variability is evident, other than obvious dissolutional modification of the exposed spires by rainfall.

Kunming stone forest

The 912 km^2 Lunan stone forest is an archetypical example of a stone forest from which the geometric characteristics that are described herein were observed. It is located 84 km southeast of Kunming, Yunnan Province, Peoples Republic of China (LIAO & XU, 1993). This stone forest is commonly known as the Kunming stone forest by international tourists.

The Lunan stone forest is a spectacularly well developed epikarst characterized by stone pinnacles separated by dissolved fissures (Figure 1). The pinnacles reach heights of 50 m. The attribute which makes this stone forest so unique is that the infilling sediments have been almost totally removed so we can see the complete three-dimensional morphology of the dissolved carbonate bedrock.

Epikarst

Stone forests are spectacular epikarst features and as such they have a significant hydraulic function. The word "epikarst" was first employed as an adjective to qualify a class of aquifers by MANGIN (1974-75) in mountainous terrain. He defined "epikarst aquifer" to denote saturated zones within the intensely dissolved veneers on carbonate sections beneath soils and on exposed carbonate outcrops.

Mangin's usage of epikarst aquifer, as well as its use by most subsequent workers, is restricted to the saturated parts of dissolution veneers occurring on elevated outcrops which are separated from underlying aerially extensive aquifers by a vadose zone. Although there are important lateral circulation components within the elevated epikarst aquifers, they were initially conceptualized as compartmentalized collector systems which ultimately funnel water to infiltration conduits through the vadose zone (WILLIAMS, 1985). Consequently, vertical flow was emphasized over lateral circulation, particularly in alpine and

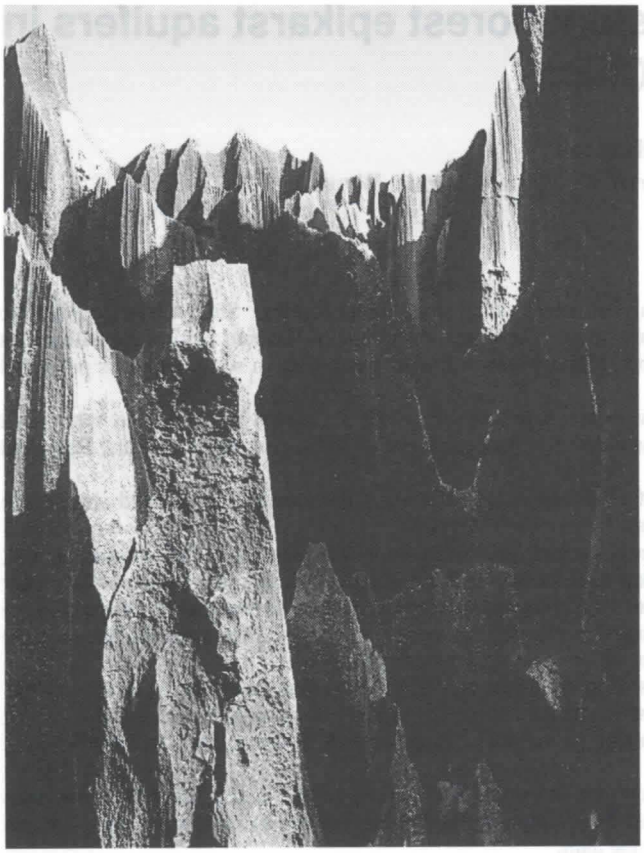

Figure 1. Stone pillars such as these serve as the framework for stone forest aquifers when infilled with sdiuments. Kunming stone forest, Yunnan Province, China.

sub-alpine areas.

Since introduction of the concept of an epikarst aquifer, epikarst has been widely adopted as a noun to denote the morphology of the highly dissolved veneer itself. This usage is adopted here.

> Epikarst is an intensely dissolved zone consisting of an intricate network of intersecting roofless dissolution-widened fissures, cavities, and tubes dissolved into the uppermost part of the carbonate bedrock. The dissolution features in the epikarst zone are organized to move infiltrating water laterally to downgradient seeps and springs or to collector structures such as shafts that conduct the water farther into the subsurface.

Lateral ground water movement predominates over vertical movement in most epikarst zones, especially in lowland environments such as the many karst plains, valley floors and floors of karst depressions found throughout southeast China and elsewhere in the world. Epikarst zones are commonly ephemerally or partially saturated (MILLS, 1989).

Stone forest aquifers and their importance

In many low-lying environments, the epikarst serves as an host for shallow, thin, largely unconfined aquifers, herein called stone forest aquifers. Stone forest aquifers are characterized by very large lateral permeabilities and small reservoir storage.

Stone forest aquifers occur in areas underlain by carbonate rocks. They occupy the epikarst zone where the undissolved carbonate bedrock, which is virtually impermeable, serves as a structural framework that holds saturated or partially saturated unconsolidated infills comprised of soils, dissolution residual clays and externally derived clastics sediments.

When I was searching for a term to describe the shallow, unconfined epikarst aquifers that serve as the primary water supplies for many towns and rural areas in south China, I wanted to find a term that also conveyed the characteristics of the highly dissolved carbonate substrate that served as a framework for such aquifers. The term "stone forest aquifer" ideally served this need because it conveys a robust visual image. Compare this to the obvious alternative - epikarst aquifer - which would mean little to most people. My choice resulted directly from a visit to the famous Lunan (Kunming) stone forest.

The term "stone forest aquifer" was also deliberately chosen to avoid having to distinguish between the saturated and unsaturated parts of the epikarst morphologic zone, and the controversies that karstologists engage in as they try to draw taxonomic distinctions between the myriad epikarst dissolutional landforms. Instead, the term stone forest aquifer focuses on commonalities in hydraulic function within the epikarst zone, and carries with it the notion of saturation which is implicit in the noun aquifer.

The total area underlain by carbonate rocks in China is 3.4×10^6 km^2. Most of these carbonates are buried by Quaternary deposits or other rocks. Carbonates crop out over 910,000 km^2 (LI and others, 1985), and, of that total, about 100,000 km^2 is tower karst in Guizhou and Yunnan provinces, and the Guangxi Autonomous Region. Owing to this vast distribution of carbonates, and the fact that stone forest aquifers provide most of the exploitable ground water in the south China karst belt, it is clear why stone forest aquifers are of such importance. Their importance is accentuated by the huge populations that depend

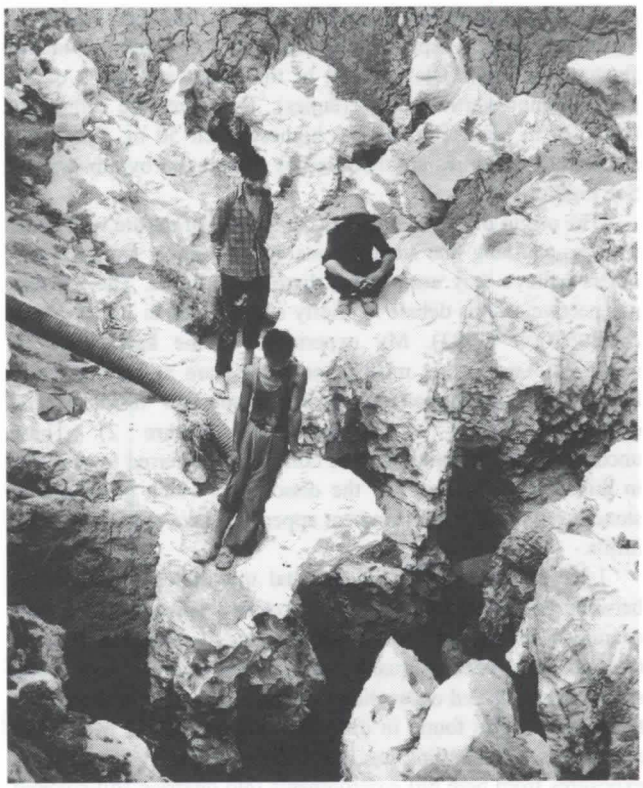

Figure 2. Laborers have started to dig into the solution cavities in a well in a stone forest aquifer after removing the overburden near Xiaopingyang, Guangxi Autonomous Region, China.

on them. Approximately 100 million Chinese live in the south China karst belt.

Aquifer properties

Stone forest aquifers occur under flat areas within the south China karst belt, including karst peneplains, river valleys, all classes of karst depressions, and various flat upland areas. Most of the exploitable ground water is produced from under broad karst plains and along stream valleys (Figure 3).

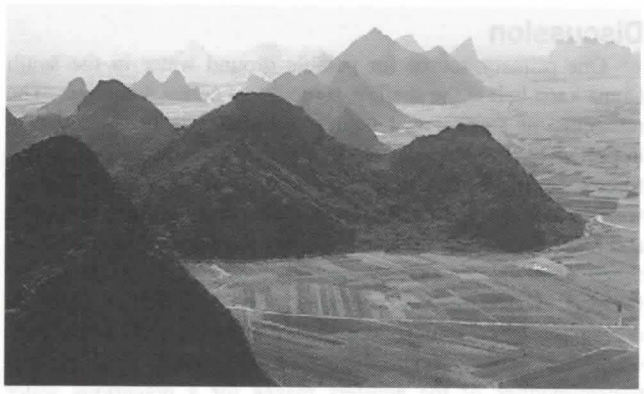

Figure 3. Stone forest aquifers underlie the karst plains shown her, Guangxi Autonomous Region, China.

The water in the stone forest aquifers usually represents the top of a fully saturated substrate. Consequently, in lowland areas, there usually is no underlying vadose zone. Lateral circulation predominates. Storage within the stone forest aquifers occurs within dissolution voids and dissolution-widened fractures in the carbonates, and, more importantly, in the intergranular porosity within the unconsolidated infills. Permeability results from, in decreasing order of importance: (1) partings between the carbonates and infills, (2) interconnected dissolution cavities within the carbonate bedrock, and (3) intergranular permeability within the infills.

In most case that I examined, the largest permeabilities were associated with the partings that develop between the carbonate bedrock and the infills. Such partings are most prevalent between the infills and bedrock at the bases of the dissolution fissures which separate the stone pinnacles. These partings tend to be laterally interconnected and highly permeable. The permeabilities of the infills are generally very small owing to the presence of clays.

Figure 4 summarizes the porosity distributions in a typical stone forest aquifer. Notice that the carbonate bedrock, which comprises the framework for the stone forest aquifer, generally has negligible permeability. The volume of limestone dissolved from the epikarst zone is a significant fraction of the total volume of rock, often being more than 80 or even 90 percent near the tops of the pinnacles. However, when the dissolved voids between the pinnacles are filled, the available ground water storage is reduced to the porosity of the infilling material represented by the left-hand curve on Figure 4.

The reservoir characteristics of stone forest aquifers are very poor. As shown on Figure 4, the saturated zone is thin, usually less than 30 m, because the porosity falls to negligible values below the base of the epikarst zone. At those depths, available

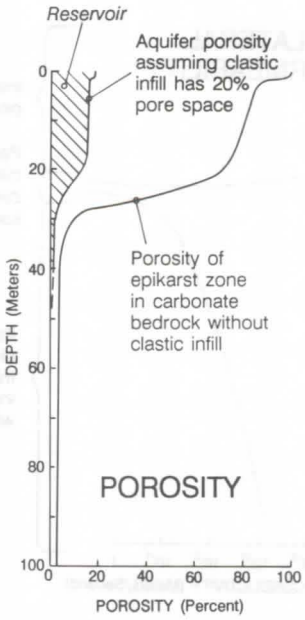

Figure 4. Porosity distributions in a typical stone forest aquifer based on oberservations from hand dug wells and quarries, Guangxi Autonomous Region, China.

porosity occurs only as dissolved openings along fractures and, rarely, as caves.

Permeabilities within stone forest aquifers are highly anisotropic and heterogeneous. In general, vertical permeabilities are small owing to the layering of the infills and the fact that many layers are clay rich. Lateral permeabilities through the clastic infills tend to be small near the surface, but reach conduit values in the interconnected separations that develop between the clastic infills and the underlying bedrock near the base of the dissolved fissures.

The lateral permeability distribution shown on Figure 5 is that observed in many hand dug wells in the south China stone forest aquifers. The highest yields typically are encountered at or very near the bases of the clastic infills. Most of the water flows into the wells from the partings between the infills and the bases of the epikarst fissures.

I interpret the development of the water-yielding partings to be direct evidence that dissolution of the carbonate bedrock is most active below the bases of the clastic infills. Commonly, the entire infill section fails when catastrophic sinkhole collapses occur in stone forest aquifers. This fact also reveals that dissolutional space is being created at the base of the epikarst zone.

The clastic infills within the stone forest aquifers can serve as effective vertical as well as lateral seals. For example, small artesian rises are often observed in wells drilled or dug into such infills, revealing the presence of vertical seals. Likewise, variable heads observed within clusters of adjacent karst windows in stone forest aquifers indicate the presence of lateral seals (HUNTOON, 1992a, p. 172-173). The compartmentalization of stone forest aquifers by lateral seals tends to be a local phenomenon.

More commonly, stone forest aquifers are characterized by excellent lateral circulation. Thus, the dominant flow direction through them is horizontal.

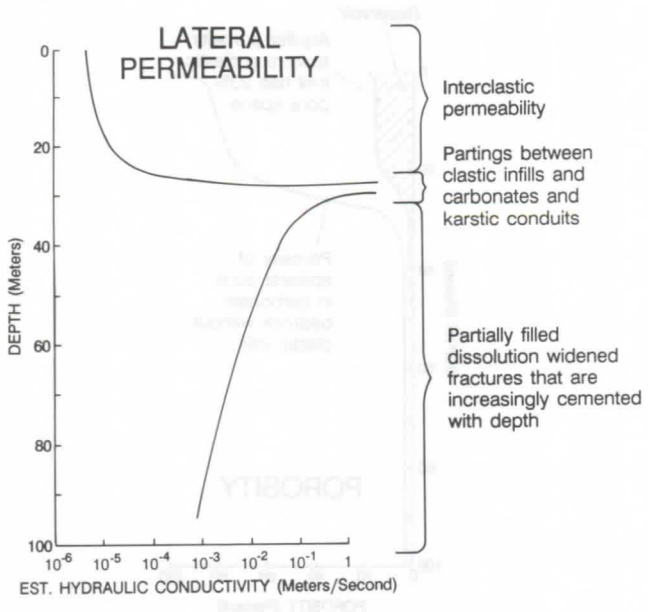

Figure 5. Idealized vertical permeability distributions in a typical stone forest aquifer based on oberservations from hand dug wells, Guangxi Autonomous Region, China.

Seasonal responses

The south China karst belt lies within the humid subtropical monsoon climatic zone. In a typical year, 70 to 75 percent of the precipitation falls during the April to August period. This produces widespread flooding of karst depressions and the stone forest aquifers become fully recharged.

Water levels fall rapidly once the rains cease. A major fraction of the water leaves in the form of lateral circulation through the basal parts of the aquifers. The interconnected separations between the clastic infills and carbonate bedrock serve as very effective drains which allow for rapid circulation to incised streams, to caves through nearby bedrock hills, or to lowland springs. Water levels drop sufficiently by October or November so that farmers must lift the water from wells and karst windows even in lowland areas which were previously flooded. By December, the bulk of the seasonal recharge has left the region and drought conditions begin to set in.

Hazards

Two common hazards plague regions underlain by stone forest aquifers: (1) sinkhole collapses and (2) leaky dams.

Ground water pumpage results in reduced pressures near the bases of the clastic infills in the stone forest aquifers. The result is failure of the infills due to the collapse of the infill material into the space created by dissolution near the base of the epikarst zone. The ground suddenly subsides between the stone pillars and ribs, often exposing the water table in the form of an artificially created karst window.

The sinkhole collapses are usually concentrated close to large capacity wells, and chains of sinkholes revealed the orientations of the most productive fissures that supplied the wells. Virtually all of the collapses that I observed in the karst plains of south China were caused by failures of the clastic infills, not collapses of caves.

Dam failures, characterized by lateral underflow through the epikarst zone under the dam, are common throughout the south China karst. The problem is circulation through the permeable stone forest aquifers, not leakage through caves. In most cases, the foundations of the leaky dams were set directly on the undisturbed land surface. A remedy is to excavate all the infill material from the epikarst zone under the dam site, and seal the dissolution fissures and tubes that are found. Complete grout curtains under the entire dam and abutments finish the job. Technical limitations and high costs of such extensive pre-dam construction work appear to preclude success in many cases.

Discussion

One primary source for potable ground water in the south China karst belt is the shallow stone forest epikarst aquifers. The reliability of stone forest aquifer supplies has been adversely impacted by massive post-1958 deforestation. Removal of the forests has significant diminished seasonal upland storage of water allowing for catastrophic flooding during the wet season and rapid streamflow recessions during the dry season. The stone forest aquifers, which rely on dry season releases from the forested uplands, now experience greatly diminished recharge during the dry season. This important hydrologic factor coupled with the poor storage characteristics and large lateral transmissivities of the aquifers makes for a precarious water supply during the latter part of the dry season. The impact on the local population is of serious concern because the south China karst belt is host to approximately 100 million people who live three crop failures away from starvation.

References

HUNTOON, P. W. 1992a. Hydrogeologic characteristics and deforestation of the stone forest karst aquifers of south China. Ground Water 30: 167-176.

HUNTOON, P. W. 1992b. Exploration and development of ground water from the stone forest karst aquifers of south China. Ground Water 30: 324-330.

JIANG ZHONGCHENG, YUAN DAOXIAN and HUNTOON, P. W. 1993. Discussion and reply, hydrogeologic characteristics and deforestation of the stone forest karst aquifers of south China. Ground Water. 31:325-327.

LIAO YIZHONG and XU GUOCAI. 1993. Characteristics of Lunan karst landform and appraisal of its tourism resources. In: (Song Linhua and Ting Huaiyuan, eds.): Karst Landscape and Cave Tourism. China Environmental Science Press (Beijing). 175-180.

LI DATONG and others. 1985. The map of soluble rock types in China (1:400,000 scale). Cartographic Publishing House, Beijing, China.

MANGIN, A. 1974-5. Contribution à l'étude hydrodynamique des aquifères karstiques. Annales de Spéléologie. 29: 3: 283-332; 29: 4: 495-601; 30:1: 21-124.

MILLS, J. P. 1989. Foreland structure and karstic ground water circulation in the eastern Gros Ventre Range, Wyoming. University of Wyoming (Laramie, USA) M. S. Thesis. 1-101.

WILLIAMS, P. W. 1985. Subcutaneous hydrology and the development of doline and cockpit karst. Zeitschrift fur Geomorphologie, N.F. 29:463-482.

YUAN DAOXIAN, chief editor. 1988. Glossary of karstology (in Chinese with English index). Geological Publishing House, Beijing, China. 1-55.

Il ruolo dello strato limite turbolento nella morfogenesi dei rillenkarren

Sergio Martini
Pian d´Ordià 190, I-19024 Varese Ligure, Italy

Abstract

Some observations on rillenkarren epigenetic morphology may show the prevailing occurrence of turbulent boundary layer property for their genesis, through minimization of the shearing stress acting on the rock wall; a "water flow-karren" interaction model is suggested and, by means of a physical quantity derived from the channels geometrical configuration and named "effective excavation factor", a procedure is formulated to account for such an hydrodynamical efficiency.

Riassunto

Alcune osservazioni relative alle morfologie epigee a campi solcati suggeriscono di poter attribuire alla loro genesi il preponderante concorso delle proprietà dello strato limite turbolento, ciò in ragione della capacità di tali superficie di minimizzare gli sforzi di attrito a parete; si propone quindi un modello di interazione "flusso idrico-karren" e si formula una procedura che ne giustifica l'efficacia idrodinamica tramite il calcolo di una grandezza fisica dipendente dalla configurazione geometrica dei solchi, detta "fattore di escavazione efficace".

Forme di dissoluzione superficiale

Le morfologie "karren" sono fortemente dipendenti dai dettagli dell'ambiente in cui hanno origine; il modello morfogenetico di queste strutture, quindi, è reso complesso dall'entità dei parametri che le controllano e dalle loro interrelazioni: lo studio teorico che propongo si limita a considerare forme risultanti da flussi di superficie scorrenti su aree in pendenza, cioè i rillenkarren. Rammento come la loro formazione sia stata sperimentata (GLEW, 1977) per mezzo di un "simulatore di pioggia" su blocchi di salgemma; dai risultati ottenuti si rileva come i rillenkarren costituiscano una morfologia stabile ripetentesi nelle rocce senza variazioni nella geometria generale: i solchi si producono nella direzione della massima pendenza e terminano quando il flusso che discende la parete "...raggiunge uno spessore critico". Lo sviluppo dei rillenkarren sembrerebbe quindi associato agli stadi incipienti del dilavamento superficiale, dove la pellicola d'acqua è sottile e la sua velocità minore. Variando la pendenza dei suoi modelli Glew ha dimostrato che la lunghezza dei solchi, dalla cresta alla linea di rottura, è funzione dell'angolo di inclinazione della superficie dilavata: questo, infatti, varia il modulo della componente gravitativa applicata alla massa fluida e quindi ne varia la velocità di scorrimento.

Il "bursting" nello strato limite turbolento

E accertato sia su base teorica che sperimentale che gli sforzi di Reynolds all'interno di correnti turbolente di parete sono preponderatamente dovuti al processo di "bursting" nello strato limite turbolento (WILLMARTH, 1977; BLACKWELDER, 1979); questo fenomeno, che è conseguenza dell'instabilità provocata dall'azione di vortici di perturbazione controrotanti (fig.1) allineati con la direzione della corrente media (COLES, 1987), consiste nell'iniezione intermittente dello strato limite di fluido a bassa velocità proveniente dal substrato viscoso prossimo alla parete e conduce quindi ad un intenso trasporto trasversale di quantità di moto che è nuovamente responsabile di un incremento delle fluttuazioni turbolente. Un punto di flesso e quindi una condizione di instabilità si produce nei profili di velocità media sotto all'azione di questi vortici che hanno origine nel processo di genesi della turbolenza ad opera di instabilità successive (STUART, 1987). Allorchè il punto di flesso si allontana dalla parete e l'azione delle forze viscose si attenua compaiono delle instabilità secondarie che innescano il bursting (LUMLEY, 1979). Si può dedurre (JANG, 1984; JANG, 1986) un modello teorico sulla genesi del "bursting" basato sull'interazione non lineare di due classi di onde di perturbazione tridimensionali: questa conduce a risonanza per una lunghezza d'onda trasversale adimensionale $\lambda^* = 90$ (le lunghezze contrassegnate con il simbolo * sono adimensionalizzate rispetto alla velocità di attrito a parete e alla viscosità cinematica); le misure sperimentali della spaziatura trasversale delle bande di fluido rallentato rispetto alla corrente media operate da diversi autori sono in perfetto accordo con tale lunghezza d'onda.

Influenza dei campi solcati sullo strato limite turbolento

Sulla base del modello di "bursting" (iniezione intermittente di strato limite di fluido a bassa velocità) ora descritto è possibile immaginare come l'esistenza di morfologie superficiali tipo rillenkarren e quindi la genesi di canalicoli concordi al flusso della corrente idrica (normalmente paralleli alla linea di massima pendenza) sulla superficie di rocce carbonatiche soggette ad intenso dilavamento costituisca una condizione di "economia" e quindi di "stabilità" del sistema, provocando una riduzione della circolazione dei vortici di perturbazione in ragione del formarsi di vortici longitudinali secondari originantisi in corrispondenza delle "creste" dei canalicoli: questo, concordemente a quanto determinato sperimentalmente, si verifica allorchè la spaziatura trasversale D* tra i canaletti del campo solcato è dell'ordine di 1/4 della lunghezza d'onda trasversale caratteristica dei vortici controrotanti (WALSH, 1982; BECHERT, 1985). La profondità adimensionale Z* dei solchi del rillenkarren dovrebbe inoltre essere dell'ordine dello spessore locale del substrato viscoso (COLES, 1987).

Un decremento nella diffusione della quantità di moto perpendicolarmente alla superficie del letto di scorrimento ed un decremento delle fluttuazioni turbolente si hanno conseguentemente alla riduzione della componente longitudinale del vettore vorticità, ma la frequenza delle iniezioni intermittenti di strato limite di fluido a bassa velocità ("bursting") rimarrebbe

inalterata (WALSH, 1984); contemporaneamente a questo "meccanismo", però, se ne verifica un secondo in grado di controllare la geometria dei campi solcati: nelle aree corrispondenti ai minimi (avvallamenti) ed ai massimi (creste) delle scanalature il flusso idrico presenta una velocità media ed un gradiente alla parete rispettivamente minore e maggiore rispetto a quelli che si avrebbero nel caso di un flusso idrico che scorra, con la medesima velocità esterna media, su di una superficie di roccia piana.

All'interno dei solchi hanno luogo riduzioni del gradiente che agiscono quindi su superfici di area ben maggiore rispetto a quelle interessate dagli incrementi del gradiente. Ne deriva in definitiva una riduzione netta del coefficiente di attrito medio alla parete, per un'entità tale da poter compensare l'incremento di superficie bagnata che la lastra rocciosa scanalata inevitabilmente comporta. Si può far rilevare come, mentre il primo modello proposto si basa su di un'analisi fenomenologica concorde all'interpretazione dei dati sperimentali, il secondo può essere descritto in forma analitica, sempre nell'ipotesi che l'altezza geometrica dei solchi sia dello stesso ordine di grandezza dello spessore del substrato viscoso, all'interno del quale la distribuzione della componente longitudinale della velocità è lineare.

Calcolo del fattore di escavazione efficace mediante trasformazioni conformi

Un buon metodo per determinare l'efficacia dei campi solcati lo si ottiene analizzando come il profilo di velocità relativo ad una superficie di roccia piana si modifica per la presenza di canalicoli e questo, limitatamente al substrato viscoso, è possibile con metodi analitici. Imponendo la condizione di una corrente stazionaria di un fluido incomprimibile, in assenza di forze di massa, l'equazione di Navier-Stokes per la componente u della valocità nella direzione del moto:

$$\frac{\partial u}{\partial t} + u\frac{\partial u}{\partial x} + v\frac{\partial u}{\partial y} + w\frac{\partial u}{\partial z} = -\frac{1}{\rho}\frac{\partial p}{\partial x} + u\left(\frac{\partial^2 u}{x^2} + \frac{\partial^2 u}{y^2} + \frac{\partial^2 u}{z^2}\right) + f_x \quad (1)$$

si riduce all'equazione di Laplace nel piano y-z:

$$\frac{\partial^2 u}{\partial y^2} + \frac{\partial^2 u}{\partial z^2} = 0 \quad (2)$$

Soluzione della (2) è il profilo di velocità lineare: $u = ky$ (3)

Caratteristico del substrato viscoso di una superficie piana. Se al posto di una superficie piana (bidimensionale) considero una superficie caratterizzata dalla presenza di solchi longitudinali (tridimensionale), introduco necessariamente la dipendenza dalla coordinata z. Occorre quindi trasformare la geometria e le proprietà della corrente fluida, note nelle condizioni di scorrimento sulla parete piana, in quelle relative al rillenkarren di geometria voluta. Nel primo caso la descrizione esaustiva si ottiene per mezzo di una griglia ortogonale in cui ogni linea orizzontale rappresenta una linea a velocità costante determinata dalla (3). Sulla superficie di un campo solcato le linee a velocità costante non sono più rettilinee ma si conformano alle nuove condizioni al contorno periodiche vincolate dalla geometria dei canalicoli: la distribuzione dei gradienti di velocità sul campo solcato è calcolabile determinando l'andamento di tali linee. Dato che per le ipotesi fatte il substrato viscoso è governato dall'equazione di Laplace (2), l'andamento delle linee a velocità costante sul rillenkarren si può ottenere, mediante generalizzazione di una metodologia proposta da BECHERT (1986), per mezzo della tecnica delle trasformazioni conformi; in questo modo: a) si ottengono soluzioni in forma chiusa; b) i punti singolari sul contorno (vincolati dalla geometria del campo solcato) risultano di agevole trattamento; c) un parametro geometrico che consente di valutare l'influenza dei solchi sul profilo di velocità (nelle immediate vicinanze della parete) detto "fattore di escavazione efficace", è ricavabile mediante espressione analitica. Tali soluzioni sono ottenibili per ogni geometria di interesse applicativo mediante algoritmi basati sulle trasformazioni di Schwarz-Christoffel e di Kutta-Joukowski. Allo scopo di ricadere in geometrie le più possibili rappresentative di situazioni "reali" ci si è limitati ad esaminare le tre configurazioni di campi solcati con canalicoli a sezione "tipo", cioè quelli che in natura sembrano poter essere soggetti a maggior generalizzazione: solchi con sezione a "setti"; solchi con sezione "concava" e solchi con sezione a "dente di sega" (MARTINI, 1997).

Confronto fra le varie geometrie dei campi solcati

L'andamento del fattore di escavazione efficace è stato calcolato, per tutte le geometrie considerate, in funzione del rapporto Z/D tra l'altezza dei solchi e la distanza intercorrente tra gli stessi. Come risulta chiaramente in figura 2, la curva della funzione Ze/D=f(Z/D) indica che le tre geometrie considerate denunciano caratteristiche più o meno identiche: l'andamento è monotono tendente ad un valore asintotico pari ad (Ze/D)max = 0,2206.

L'unica dipendenza che si rileva dalla geometria dei solchi è la rapidità con la quale si tende all'asintoto: comunque, se il rapporto Z/D non presenta valori troppo grandi solo la geometria a setti conduce ad un valore di Ze/D molto prossimo al valore asintotico; i valori del fattore di escavazione efficace corrispondente alle geometrie concava e a dente di sega sono via via minori.

Valutazione dell'efficacia dei campi solcati: confrontando i dati di resistenza superficiale ottenuti per via sperimentale (WALSH, 1982; WALSH, 1984) con il valore del fattore di escavazione efficace ottenuto analiticamente si può valutare l'efficacia che i diversi tipi di solchi presentano nella riduzione degli sforzi di attrito.

Allo scopo risulta necessario calcolare il valore del rapporto Ze/D per le varie geometrie, così da poter valutare la resistenza allo scorrimento del fluido indipendentemente da ogni "fattore di forma": i dati ottenuti per via sperimentale, infatti, vengono normalmente forniti come rapporto tra la resistenza di attrito della superficie a solchi e quella della superficie piana in funzione della spaziatura adimensionalizzata D* intercorrente tra i solchi che, essendo rappresentativi di sezioni dalla diversa geometria, non risultano direttamente confrontabili. Si tenga comunque presente che una indicazione quantitativa della riduzione di resistenza d'attrito ottenibile da un rillenkarren rispetto ad una superficie rocciosa piana si può avere solamente per mezzo di risultati sperimentali: il fattore di escavazione efficace permette di ottenere informazioni qualitative, o comunque semplicemente indicative.

Mettendo insieme i dati sperimentali con i valori del rapporto Ze/D per le diverse geometrie e prescindendo dalle alterazioni comunque presenti nelle situazioni reali, si ottiene un diagramma (fig.3) rappresentativo del "funzionamento" di vari tipi di campi solcati (cioè di vari tipi di solchi) in varie condizioni di deflusso idrico. Graficando D* in scala logaritmica, le condizioni che

comportano una diminuzione effettiva della resistenza di attrito sono ben discriminabili rispetto a quelle che ne comportano un aumento, mediante una retta nel piano (D*, Ze/D); sempre dallo stesso diagramma risaltano due regioni (A et B) in cui l'azione dei canalicoli risulta particolarmente importante nella diminuzione della resistenza: non è improbabile che queste due diverse aree siano rappresentative della diversa dipendenza che i due (diversi) meccanismi di interazione rillenkarren-strato limite presentati precedentemente hanno nei confronti della spaziatura laterale adimensionalizzata D*. Il primo meccanismo (influenza del "bursting" nello strato limite) è infatti fortemente dipendente dalla grandezza adimensionale D*: allorchè i solchi siano distanziati più di 1/4 della lunghezza d'onda trasversale dei vortici controrotanti la sua efficacia comincia a diminuire (sono proprio i vortici controrotanti, infatti, i responsabili del "bursting"). Il secondo meccanismo (riduzione media dei gradienti di velocità e quindi dello sforzo a parete), invece, non è funzione di D* ma solo dell'andamento della sezione: tanto l'area della superficie bagnata quanto la distribuzione dei gradienti di velocità, infatti, dipendono solamente dalla forma della sezione dei solchi. Tutto ciò, ovviamente, rispettate le ipotesi premesse e, in particolare, nei limiti dello spazio interno al substrato viscoso.

L'influenza del "bursting" sullo strato limite risulta allora perfettamente efficace solo nella zona A: aumentando il valore del rapporto Ze/D (aumento della superficie bagnata) la sua efficacia risulta diminuita dalla minore riduzione di resistenza consentita dal meccanismo di riduzione dei gradienti di velocità. Complessivamente, quindi, per i due meccanismi agenti contemporaneamente si ottiene l'efficacia massima per valori del fattore di escavazione efficace tra 0.16 e 0.17. E' a questo punto scontato come nell'area B risulti preponderante l'azione del meccanismo di riduzione dei gradienti di velocità (si ha infatti un minore aumento della superficie bagnata per valori ridotti del rapporto Ze/D) rispetto al meccanismo d'influenza del "bursting" sullo strato limite. Nell'area B, quindi, si hanno riduzioni della resistenza di attrito inferiori a quelle che si ottengono nell'area A, ma comunque meno dipendenti dalla grandezza D*, cioè dalle condizioni della corrente fluida.

Conclusioni

Nel caso di deflusso idrico su campo solcato (rillenkarren) il coefficiente di attrito di parete risulta influenzato dalla sinergia di due meccanismi di interazione tra correnti turbolente e solchi: 1) l'alterazione della circolazione dei vortici controrotanti responsabili del "bursting" dello strato limite è il primo meccanismo: questi è funzione della grandezza adimensionale "spaziatura laterale" D* e presenta il massimo dell'efficacia per valori di D* all'incirca inferiori a 20.2) la riduzione dei gradienti di velocità e dei gradienti alla parete è il secondo meccanismo: questi riesce parzialmente a controbilanciare l'incremento di superficie bagnata che la geometria dei campi solcati necessariamente comporta. La determinazione dei valori del fattore di escavazione efficace per varie geometrie di campi solcati e l'esame di tali dati porta ad apprezzarne la morfologia secondo un criterio di stabilità strutturale ed equilibrio energetico del sistema "flusso idrico-rillenkarren"; a tutto questo dovrà seguire un'attività sperimentale e di campagna atta a confermare o meno la validità delle ipotesi fatte sul loro meccanismo di interazione con la corrente turbolenta di parete.

Bibliografia

BECHERT, 1985: D.W. Bechert, G. Hoppe & W.E. Reif, On the drag reduction of the shark skin, AIAA-Paper 85-0546.

BECHERT, 1986: D.W. Bechert, M. Bartenwerfer, G. Hoppe & W.E. Reif, Drag reduction mechanisms derived from sharkskin, ICAS-86, 1.8.3, Londra.

COLES, 1987: D. Coles, Coherent structures in turbulent boundary layer, in "Perspectives in turbulence studies", ed. by H.U. Meier & P. Bradshaw, Springer-Verlag.

CONSTANTIN, 1988: P. Constantin & C. Foias, Navier-Stokes equations, Chicago lectures in Mathematics, The University of Chicago Press.

GLEW, 1977: J.R. Glew, Simulation of rillenkarren, Proc. 7th Internat. Congress Speleol., Sheffield, 218-219.

JANG, 1984: P.S. Jang, D.J. Benney & Y.M. Chen, Origin of streamwise vortices in turbulent boundary layer, Bull. Am. Phys. Soc., vol.29, n. 9 november 1984.

JANG, 1986: P.S. Jang, D.J. Benney & R.L. Gran, On the origin of streamwise vortices in a turbulent boundary layer, J. Fluid. Mech., vol.169.

LUMLEY, 1979: J.L. Lumley, Introduction to the Chapter II of vol.72 of Progress in Aeronautics & Astronautics, Viscous flow drag reduction, ed. by G.R. Hough.

MARTINI, 1997: S.Martini, Trasformate conformi & campi solcati, Bollettino del Gruppo Speleologico C.A.I. Genova Bolzaneto, in corso di stampa.

WALSH, 1982: M.J. Walsh, Turbolent boundary layer drag reduction using riblets, AIAA-Paper 82-0169.

WALSH, 1984: M.J. Walsh & A.M. Lindemann, Optimization and application of riblets for turbulent drag reduction, AIAA-Paper 84-0347.

WILLMARTH , 1977: W.W. WILLMARTH & T.J. BOGART, Survey and new measurements of turbulent structures near the wall, in "Structure of turbulence and drag reduction", ed. by F.N. Frenkel, M.T. Landhal & J.L. Lumley, Am. Inst. of Physics, New York.

BLACKWELDER, 1979: R.F. Blackwelder & H. Eckelmann: Streamwise vortices associated with the bursting phenomenon, J. Fluid Mech., vol.94.

Determination of the hydraulic characteristics of the epikarst - Local and regional approaches -

Martin Sauter
Applied Geology, University of Tübingen, Sigwartstrasse 10, 72076 Tübingen, Germany

Abstract

The role of the epikarst for the spatial and temporal distribution of recharge water has been recognised for some time. Further, with its position close to the surface, its high porosity and high hydraulic conductivity, as well as the considerable content in organic matter, the epikarst is regarded to dominate the release of organic contaminants in case of accidental spills. The geometry of the epikarst has been studied in several karst depressions with an integrated geophysical approach. The hydraulic properties of this important compartment of a karst system was investigated at local scale in a karst depression.

The epikarst

The epikarst can be usually described as a zone with significant fracturing, solutional enlargement of the fractures and is therefore characterised by high storage and high hydraulic conductivity. In the Swabian Alb region, SW-Germany, its thickness is estimated to vary between a few to approximately 10 m and vertical drainage is generally restricted by a less permeable base. This reduction in hydraulic conductivity is believed to be a result of the decrease in fracture apertures and due to the sealing effect of the residual products of the weathering processes. The above described structure of the epikarst explains the development of a thin saturated zone, i.e. a perched aquifer, where flow occurs laterally. The epikarst water mainly drains via solution shafts to the phreatic zone. The described structure of the epikarst explains why this zone plays a major role in the temporal and spatial distribution of groundwater recharge and with its high content in organic matter, acting as a sorbent, it is believed to be of considerable importance for the release of organic contaminants. Using geological, hydrogeological and geophysical techniques, the geometry and the characteristics of this horizon was studied in detail.

Geological investigations

In order to obtain information on the geological structure and the base of the epikarst ca. 40 small diameter boreholes were drilled using a hammer coring technique was used. Some of the boreholes were equipped as piezometers. The results of the geological investigations show that the top zone of the karst system also consists of thick unconsolidated material, which can be further differentiated geologically. These deposits are the result of the complex history and geological/geomorphological processes of the recent quaternary period (< 100000a). Therefore the concept of the epikarst needs to be modified to include the complex structure of the depression fill as well because due to its hydraulic properties it can have an important role on the temporal and spatial variation of groundwater recharge and the storage of contaminants. Figure 1 shows a geological cross-section of the unconsolidated material, covering the limestone. The thickness of this zone varies between a few decimetres and approximately 15 m, depending on the position relative to the centre of the depression. The basis consists of weathered limestone and residual loam with relatively low permeability. It is followed by a thick layer of solifluction material, which was transported during the interglacials into the topographically low areas. The centre of the depression is frequently filled with eolian sediments, e.g. loess. The solifluction material is loosely consolidated and highly porous with hydraulic conductivity of approximately 10^{-5} m/s, while the hydraulic conductivity of silty, loamy centre fill varies between 10^{-7} and 10^{-8} m/s. Therefore, only in the low conductive areas, a perched water level could be detected.

Geophysical investigations

This complex structure of the epikarstic zone requires adapted methods of investigation. Geophysical techniques had been used to delineate the boundaries of the depression, to differentiate the internal structure of the fill and to detect local perched saturated zones. However, due to this complexity, a single geophysical technique usually gives ambiguous results. DC-resistivity mapping provides a quick overview of the subsurface geology. The geoelectric properties influence the results to a lesser degree, compared to other methods. The geoelectric survey assists in designing appropriate shotpoint arrays for the seismic refraction survey. Shotpoints should be located above the topographical highs of the bedrock. With refraction seismics the structure of the boundary between bedrock and unconsolidated material can be resolved. Under favourable conditions, i.e. electrically low absorption materials, ground penetrating radar displays very good resolution for lithological and structural differences of bedrock and depression fill.

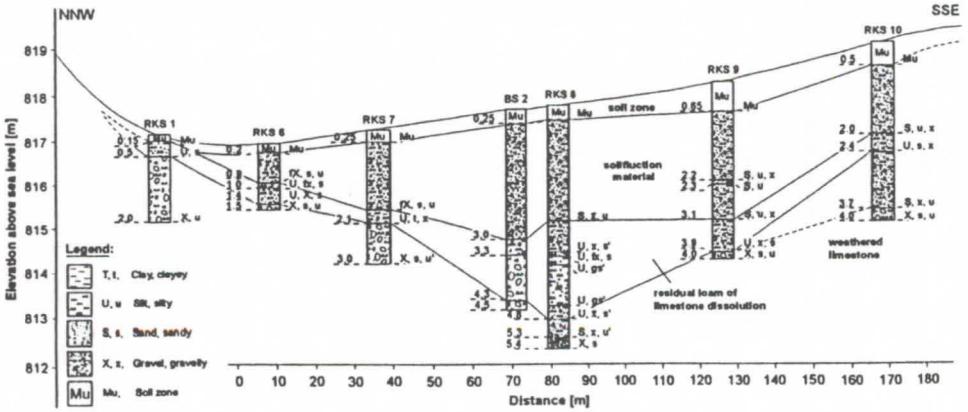

Epikarst Aquifer in Fengcong Regions, South China

SONG Linhua
Group of Karstology and Speleology, Institute of Geography, Chinese Academy of Sciences, Beijing 100101, China

Abstract

The fengcong karst landform is well developed in the slopes between Yunnan-Guizhou Plateau and Guangxi basin. The strong uplift of the region caused a deep cutting of the surface and subsurface drainage courses. Consequently, the thickness of the vadose zone ranges from some tens to several hundred meters. Even if the region is situated in the subtropical monsoon climatic zone with annual precipitations of 1000 - 2000 mm, it is very dry in winter and spring.

The underground drainage system consists of a main course and tributaries absorbing the water by the karstic fissures in this thick vadose zone. It is very difficult to locate the drainage systems. Also, it is invaluable to drill borehole for water supply for the dispersed habitants in fengcong regions. An valuable approach to solve the problems of water supply for the decentralized habitants, is to build water tanks and pools.

The surface water from the nearby hills is rich in organism and sediments. It is seriously polluted. However, the epikarst spring is a good and sufficient source for a fine quality water supply. During the raining season, it is better to diverse the epikarst spring to the water tanks and pools. The advantages of this technique are: (1) the generally high quality of the epikarst water; (2) the rather stable drains; (3) easy supply as the spring usually is at a higher position than the settlements; and (4) easy management.

It is important to improve the ecological system which controls the duration and storage of epikarst aquifer. The small springs of epikarst aquifer in the exposed karst hill only last for several months in the raining season. But in the forest covering karst hill, it lasts almost a year. To develop the epikarst water resource, the ecosystem should be improved.

Theoretical consideration

The definition and characteristics of epikarst (subcutaneous karst) aquifer have been discussed by many authors since the seventies (MANGIN, 1973-1975; GUNN, 1978, 1981, 1983; WILLIAMS, 1983, 1985; SONG, 1986; KLIMCHOUK, 1995). This paper is stressed on the development of epikarst water resource.

The joints and openings in limestone close to the surface have been strongly enlarged and widened by the physo-chemical weathering to form the fissure nets. Below the weathering zone, the density and dimensions of the fissures decrease very fast, and fissures are gradually closed with the increasing depth. The weathering residuals including debris and soil are filled into the opened fissures. The rain infiltrates into the fissures. A part of the water is stored in the fissure nets to form the epikarst aquifer while the less fractured limestone below acts as an impermeable media. Some water in the epikarst aquifer will be drained down along the main and opened fractures towards the saturated zone. The epikarst aquifer forms the hydraulic dolinal structure around the vertical fast flow channel (Fig. 1).

In some cases, the water in the epikarst aquifer is drained directly to the cave in fast flow and/or slow flow. The velocity of percolating through the limestone massif to the cave roof varies from 0.048 cm/s to 0.11 cm/s or the discharge from 1.44 l/h to 216 l/h, the minimum 0.03 l/h and maximum for the jet flow being 1620 l/h in Planina Jama (HABIC, 1979).

The epikarst may be developed both in the depression and limestone hills. The difference between the epikarst aquifers in the depression and hills are: The epikarst in the depression is shaped as the dolinal zone, the water is centralized to the vertical shaft, the vertical flow is dominant. The epikarst in the limestone hills has the shape of a convex curve with some local hydraulic dolines, which may be parallel to the hill slope. The water in the epikarst aquifer is drained in two directions, vertical to recharge the saturated zone and lateral to be drained out as the fissure spring or seasonal spring with lower discharge (Fig. 2).

In some cases, the epikarst water may represent important water resources for the local people in the dry karst areas.

Characteristics of epikarst aquifer in Fengcong regions

The fengcong karst landform is well developed on the slopes between Yunnan Plateau, Guizhou Plateau and Guangxi basin. With the strong uplift of the region, the drainage system cut down deeply, and the vadose zone got thick from some tens to several hundred meters. The descending of the drainage base stimulates an intensive vertical karstification, which created new dolines, depressions, collapses and other new features in the karstic basins, depressions, poljes, valleys even on the plateau surface to form the double structure of depressions (SONG et al., 1993). Though the fengcong regions are located in the warm and humid tropical and subtropical monsoon climatic zones with precipitations

of 1,000-2,000 mm per year, it is very dry from winter to the early summer. But even in the raining season, after some days of no rain, the rapid infiltration into the epikarst aquifer causes a lack of the surface water resource. During at least 3-6 months a year, about 10 million people are short in water supply.

50-60% of the rainwater on the karstic fengcong hills directly infiltrate into the fissures in the limestone and 30-40% of the rainwater form the surface runoff into the underground drainage system or at some places directly into the surface rivers. This means that most of the water flow into the epikarst aquifer to recharge the saturated zone and /or to discharge to the springs at suitable locations. This implies that the regime of the karstic water in the epikarst aquifer is controlled by the meteoric water. Generally, the springs flow in the raining seasons and delay about 2-3 months after the rain season. Because of the narrow limits of the collecting area, the spring discharge varies in the range of 0.10-2 l/s, most at the rates of 0.5 - 1 l/s. The epikarst aquifer water flows in a diffuse status and in full contact with the limestone. It has the time to dissolve the bedrock to become saturated in calcite (SIC) and dolomite (SID). The mineral contents in the epikarst water are very close to the one in the saturated zone and higher than the one of the underground rivers (SONG et al., 1985). As the water diffuses in the epikarst aquifer, it is very clear and good for drinking even after heavy rain.

The occurrence of epikarst water usually distribute along the faults, contacts between limestone and nonlimestone, for example the Shuidou spring with constant discharge of 0.2 l/s in the spring and 0.5 l/s in summer and autumn occurs on the contact of limestone with interbedded shales in the Zhenning limestone. The epikarst water flows out from the lateral fissures to form the temporary water «pond» as it exists in Longshi, Dahua county and at the knick point of the landform. For example, the spring of Longla in Mashan County appears at the transition from steep to gentle slope.

The development of epikarst aquifer

In the karst fengcong areas, the underground drainage systems generally are very deep and difficult to be located exactly. Therefore, it is impossible to use the water resource for water supply. Even if the ground river is found, it can not be used because of the high elevation difference of up to 100 m to 300 m. The habitants are dispersed in separate depressions and built an uniform water supply system through the karst hills, depressions and valleys. The very monogenerous karstic water-bearing bulk makes big trouble to drill boreholes for water supply.

The best way to solve the shortage of the water in fengcong areas is to develop the rainwater resources, to store rainwater in water tanks or pools. In the fengcong areas, each family builds her own water tank to store the surface runoff water. Generally, the water is charged with sediments and organism, causing a bad water quality in the tanks. Another problem is, that in general the capacity of the water tank storage is limited to 10-20 m^3.

The advantages of the epikarst aquifer are:

(1) good water quality. The rainwater infiltrates into the soil covering the limestone or filling in the fissures of the limestone mass and is filtered by the soil lays and small fractures. The sediments and organisms remain in the soil and small fractures. The epikarst water contains very few sediments and organisms, the water is good for human and animal drinking.

(2) Rather stable discharge. The surface runoff is changing quickly with the rainfall, the high flow appears just during or soon after storm and heavy rain and decreases fast with the decreasing of the rain intensity. The water tank only store the heavy rain water. The epikarst spring may flows for 2-3 months after raining season and even with low discharge the whole year. The water may be kept in the big pool or water tank net (Fig. 3). Generally, an epikarst spring with a discharge of 1 l/s may be enough for 1728 persons (water supply standard is 50 l/p.d) if the spring remains 100 days. There is a big potential of epikarst spring to solve some of the water supply problems.

(3) The water resource is easy to manage. It is very simple to get the water from the epikarst spring to the water tank or water pools. Commonly the springs distribute on the hill slope and are higher than the village. The water automatically flows into the storage or the houses. The farmers use plastic tubes of 0.5 cm in diameter to divert the water to the houses.

The individual water tanks are built for the scattered farmers. The large pool is better for the water supply for the big village as to reduce the cost. The Qibailong epikarst spring with 2-3 l/s in the rain season on the limestone hill supplies water to the water tank nets as shown in Fig. 3.

The regime of epikarst springs is controlled by ecology. For example, the epikarst spring with 0.3 l/s discharge on the karst hill in Longla village, Guangxi, dried out after deforestation in the 50's. The villagers had to fetch the water from a big spring 5 km away and with an elevation difference of about 200 m. Later, the village recognized the significance of ecology to the water supply and closed the hills 30 years ago. Now the hills are covered by the forest, the epikarst spring provides water for 125 people during the whole year.

References

GUNN, J., 1978. Karst hydrology and solution in the Waitomo District, New Zealand. PhD. Thesis, University of Auckland, Auckland.

GUNN, J., 1981. Hydrological processes in karst depressions. Z. Geomorph. 25 (3): 313-331
GUNN, J., 1983. Point recharge of limestone aquifers – a model from New Zealand karst. Journal of Hydrol., 61:19-29.
HABIC, P., KOGOVSEK, J., 1979. Percolating water karst denudation in the case of Postojnska and Planina Jama. Proceedings of the International Symposium on Karst Erosion. UIS., Aix-en-Province-Marseille-Nimes. 49-60.
KLIMCHOUK, A., 1995. Karst morphogenesis in the epikarstic zone. Cave and Karst Science, 21(2): 45-50.
MANGIN, A., 1973. Sur la dynamique des transferts en aquifer karstique. Proc. of the 6th International Congress of Speleology, Olomouc, Vol. 4: 157-162.
MANGIN, A., 1975. Contribution a líetude hydrodynamique des aquifers karstique. des thesis, Universitat of Dijon, France.
SONG LINHUA & FANG JINFU,1985. hardness of karst water on north Guizhou. Carsologica Sinica, 4: 75-83.
SONG LINHUA, 1986. Mechanism of karst depression evolution and its hydrogeological significance. Acta Geographica Sinica, 41: 41-50.
SONG LINHUA, HE YONGBIN & FENG YAN, 1993. Groundwater tracing in Wulichong drainage system, Mengzi County, Yunnan Province. In: Song Linhua and Ding Huaiyuan (Edi.), Karst Landscape and Cave Tourism. China Environmental Science Press. 104-111.
WILLIAMS, P. W., 1983. The role of the subcutaneous zone in the karst hydrology. Journal of hydrology, 61: 45-67.
WILLIAMS, P. W., 1985. Subcurtaneous hydrology and the development of doline and cockpit karst. Z. Geomorph., 29 (4): 463-82.

This project is financed by the National Natural Science Fundation of China, No.49471008.

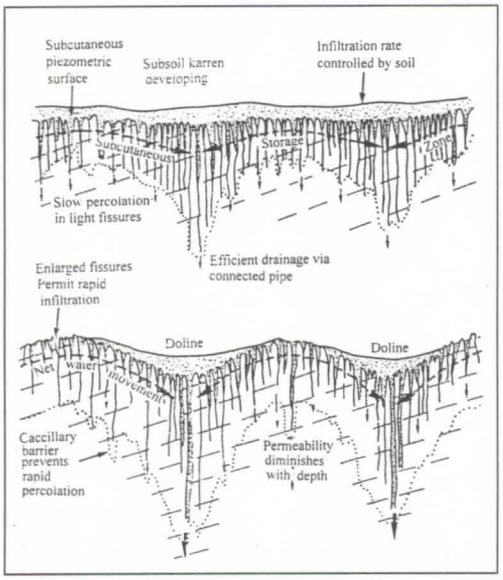

Fig. 1: The subcutaneous karst aquifer and epikarst (after WILLIAMS, 1983)

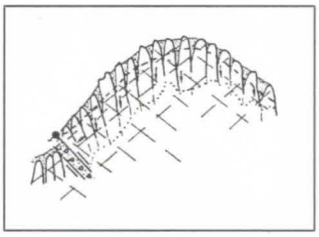

Fig. 2: The subcutaneous karst aquifer drains along the fault

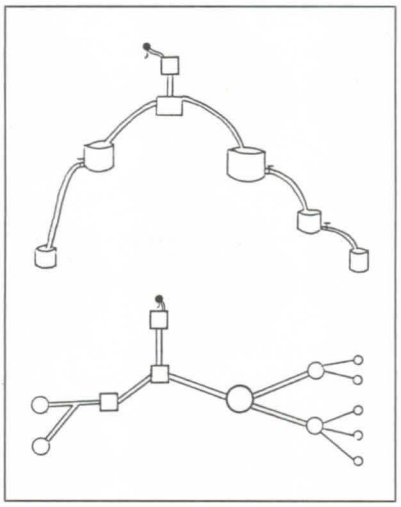

Fig. 3: The water tank nets collecting water from the epikarst karst spring

Le karst en tant que contrainte physique en aménagement du territoire. Exemple de la commune de Sprimont (Belgique)

par Camille EK et Damien CLOSSON

Résumé

La Direction de l'Aménagement du Territoire (D.G.A.T.L.P.) de la Région Wallonne (Belgique) met à jour les "plans de secteur", documents cartographiques qui planifient la gestion du sol. Les contraintes physiques sont prises en compte.

Dans ce contexte, le Département de Géographie Physique de l'Université de Liège a été chargé de réaliser entre autres, une carte des contraintes karstiques (cartes 1, 2 et 3) et un document de synthèse qui reprend l'ensemble des contraintes physiques (carte 4). Les risques d'effondrements karstiques y occupent une place importante.

Abstract: Karst, a physical constraint in land-use planning. The case of the municipality of Sprimont (Belgium)

The Head of Town and Country Planning of the Walloon Region (Belgium) updates the "planning maps", cartographic documents for the management of the country. Physical hazard and constraints are taken into account.

The Department of Physical Geography of the University of Liege was in charge, of producing a hazard map of karst (maps 1, 2 and 3) and a synthesis document which combines all the constraints (map 4). The risk of karst collapse is one of the predominant features.

Human impact on karst environment of the Silesian-Cracow Region in South Poland

Marian Pulina, Andrzej Tyc, Jacek Rozkowski
Department of Geomorphology, University of Silesia, ul. Bedzinska 60, 41-200 Sosnowiec, Poland

Abstract

The Silesian-Cracow Region a complex of carbonate and evaporite karst areas include unique in Central Europe with important paleokarst features. For many centuries this region is known as an area of lead-zinc and salt exploitation and for several decades there was groundwater pumping from karst-fissured aquifers. As a result, karst environments are under strong impact of human activity, which is a predominant factor controlling contemporary karst processes of the region. Examples of some catastrophic phenomena in karst influenced by mining (Olkusz and Wieliczka mines) and construction (artificial dam in Przeczyce) are presented.

Résumé

L'étendue du Plateau de Silésie-Cracovie englobe des régions du karst carbonaté, gypseux et salin, représentant un cas unique à l'échelle de l'Europe Centrale. Un rôle important est attribué au paléokarst du Tertiaire. La région de Silésie-Cracovie est connue depuis longtemps pour son exploitation du zinc, du plomb, du sel et depuis les dernières dizaines d'années pour celle d'importantes quantités d'eaux souterraines à partir des niveaux karstiques fissureux. Il en résulte que cette région est soumise à une forte influence de l'homme qui peut être considérée comme un facteur contrôlant le développement des phénomènes karstiques. Dans l'article, on présente des phénomènes catastrophiques dus à l'exploitation minière (région d'Olkusz et de Wieliczka) et au fonctionnement du barrage de Przeczyce.

1. Introduction

The Silesian-Cracow Region is situated in southern Poland. Several significant carbonate and gypsum-salt karstic areas occur there (figure 1). The most important of them are the karstic areas in the Middle Triassic limestones and dolomites of Silesian Upland and in the Upper Jurassic limestones of Cracow-Czestochowa Upland (GLAZEK *et al.* 1982). Geologically they belong to the Silesian-Cracow monocline. The thickness of the carbonate rock complexes reaches 400 m (in some places). The karstic areas represent polygenetic highland karst of altitude from 250 to 500 m above sea level. Karst in the Triassic carbonate rocks is covered by glacial and fluvioglacial sediments of the San and Odra glaciation in most of the area. The third interesting karstic area of Silesian-Cracow Region is situated outside of the uplands in the Tertiary salt-gypsum complex of the Wieliczka foot-hills (GLAZEK *et al.* 1982). Geologically it occurs in the Carpathian overthrust zone.

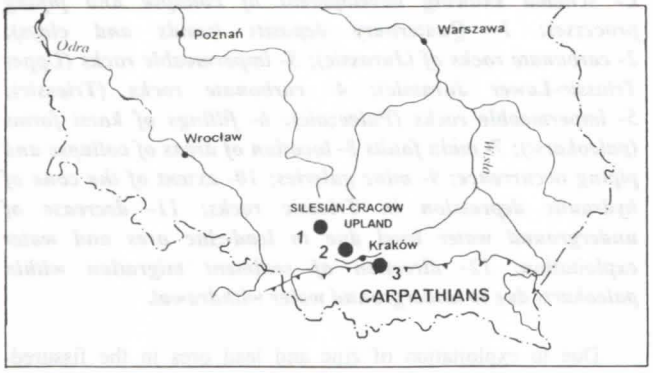

Figure 1 : Investigated karst areas of the Silesian-Cracow Region. 1- Przeczyce area; 2- Olkusz ore-bearing district; 3- Wieliczka area.

The investigated karstic areas of Silesian-Cracow Region have been under human impact for centuries because of rich deposits of silver, zinc and lead ores in Silesian Upland and rock-salt deposit in Wieliczka vicinity. The first salt mines in Wieliczka were built in the 13th century and exploitation of silver and lead ores in vicinity of Tarnowskie Gory and Olkusz took place in the medieval ages. At present, the Silesian-Cracow Region is the biggest urban-industrial agglomeration in Poland with a large water demand. The fissured-karstic aquifers in close vicinity of the Silesia and Cracow agglomerations are intensively exploited for water supply. Complexity of economical problems connected with use of the karstic areas of Silesian-Cracow Region causes big changes in the karstic environment. Such changes often implicate catastrophic phenomena with consequences much stronger than effects of natural processes. Three specific examples of influence of technical transformation on the karstic environment of the region which caused sequences of catastrophic changes in karstic water circulation are presented in this paper.

2. Influence of dam construction in Przeczyce on karstic environment

The Silesian-Cracow monocline is characteristic by some structural thresholds found on outcrops of the carbonate rocks. The threshold of limestones and dolomites of the Middle Triassic age, is the most distinct in Silesian Upland. Characteristic features of this area are gate valleys of the main rivers developed in the glacial period, of direction NE-SW. In the middle part of the above mentioned threshold, between Siewierz and Przeczyce, lies the gate section of the lower Czarna Przemsza river valley. In this valley, cut deeply in the carbonate rocks, there are big level differences. The whole area shows numerous surface karstic forms and karstic hydrography. In natural conditions the discussed fragment of the Czarna Przemsza river valley drained a Triassic aquifer with numerous karstic spring.

In the 60s in a gate part of the river an artificial large water reservoir was formed by a dam construction in Przeczyce (figure 2). From the beginning, the location of the reservoir in the karstic massif gave problems with exploitation of the reservoir and caused changes in hydrography of the area. Water damming in a zone of numerous fossil karstic forms and active water outflows caused violent changes of groundwater circulation direction. Some springs draining the Triassic aquifer located inside of the artificial reservoir have changed into sinkholes reaching the karstic massif (figure 2). As a result a zone of new springs was formed below the dam and some of them became hazardous to technical objects and buildings in Przeczyce.

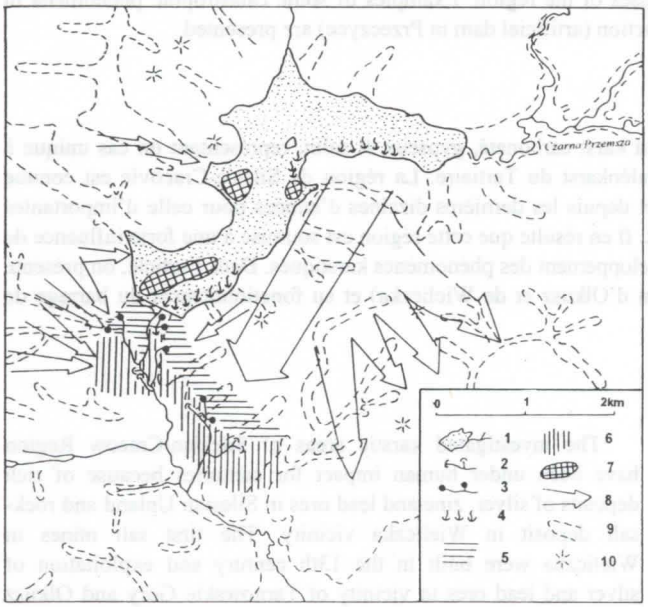

Figure 2 : Groundwater circulation in the area of the artificial dam in Przeczyce after establishment of the superficial lake (according to JANKOWSKI, 1983, modified). 1- artificial lake; 2- springs existed before construction; 3- new springs created after construction; 4- swallow holes developed on lake bottom; 5- zone of new springs; 6- zone of old springs; 7- submerged springs; 8- main directions of groundwater flow; 9- fluvial and dry valleys; 10- hills.

Detailed hydrological and hydrochemical investigations carried out in the whole area of Przeczyce reservoir impact allowed to study the influence of water damming. In the gate part of the Czarna Przemsza river there was a change of the direction of water flow into the massif (PULINA, 1974; JANKOWSKI, 1983; PULINA & TYC, 1987). As a result of damming, water reached a level of non active karstic channels. As an effect the old, well developed, underground water flow routes, cutting short the Czarna Przemsza river meander upwards dam, have been activated (figure 2).

In spite of almost 30 years which have passed from the dam construction the active processes of fossil karst exhumation take place till now. This is evidenced in new places of water escape from the reservoir and new outflows below the dam. The problems with exploitation of the reservoir still exist and constant hydrotechnical works in the basin of the reservoir are needed.

3. Karstic processes in the Triassic carbonate rocks activated by ore mining in Olkusz area

In the eastern part of Silesian Upland, in the west of Cracow, the oldest european centre of silver and lead and from the 19th century also zinc and lead ores exploitation is situated. Exploitation in past with different intensity is now succede by underground mining on the depth from some dozens to 150 m. The ore deposit is of Missisippi-Valley type and is directly connected with the karstic phenomena in carbonate rocks of the Middle Triassic. At present the deposit is exploited by three mines.

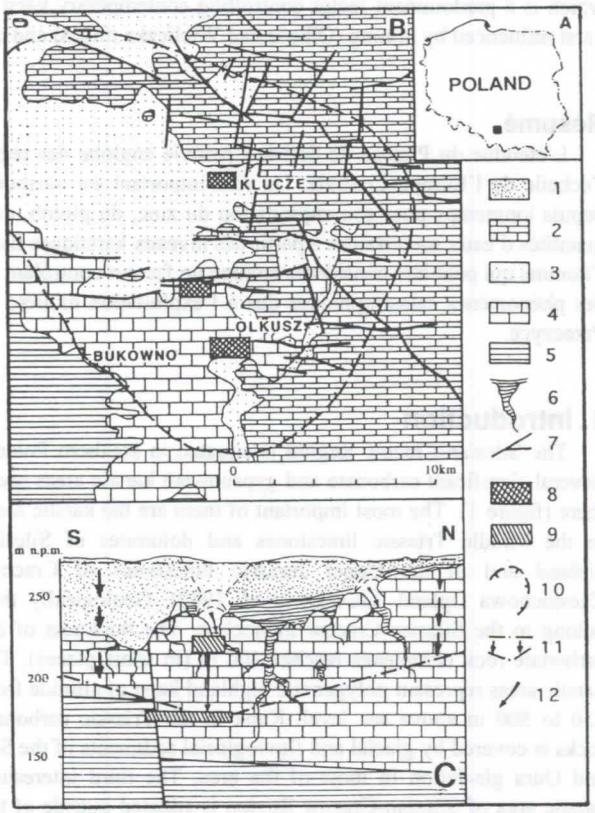

Figure 3 : Collapse and piping induced by human activity in the Olkusz lead-zinc ores exploitation district of the Silesian Upland (Poland) (according to TYC 1994, modified). A- Location of the Olkusz lead-zinc ores exploitation district. B- Geological situation (without Quaternary deposits) and C- schema showing development of collapse and piping processes: 1- Quaternary deposits (sands and clays); 2- carbonate rocks of (Jurassic); 3- impermeable rocks (Upper Triassic-Lower Jurassic); 4- carbonate rocks (Triassic); 5- impermeable rocks (Paleozoic); 6- fillings of karst forms (paleokarst); 7- main faults 8- location of areas of collapse and piping occurrence; 9- mine galeries; 10- extent of the cone of hydraulic depression in Triassic rocks; 11- decrease of underground water level due to lead-zinc ores and water exploitation; 12- direction of sediment migration within paleokarst due to underground water withdrawal.

Due to exploitation of zinc and lead ores in the fissured-karstic Triassic aquifer, 245 m^3/min of water is pumped from mine workings and together with municipal intakes - volume of about 380 m^3/min (MOTYKA, 1988). As an effect, a cone of hydraulic depression of about 350 km^2 has been developed (figure 3). An intensive artificial drainage - especially at the end

of the 70s - caused decay of some parts of the natural river network and recharged springs from the Triassic and Quaternary sediments. At the same time, changes in structure of the aquifer, in gradients of water flow as well as changes of hydrodynamic zones in the massif took place. In the Triassic carbonate series new features in form of mine workings (water galleries) became a master conduit in a functional scheme of the aquifer. A new arrangement of massif drainage hierarchy has been created in which water galleries and draining mine workings have taken over the function of the karstic channels. This is evidenced by numerous outflows from cavities and karstic channels with very high discharge rate. It should be emphasized that contemporary artificial drainage caused the connection of individual systems of deep phreatic circulation separated before by fault zones.

The advanced exhumation processes of filled karstic forms follow the processes of hydrological changes in aquifer being exploited. As a result, influx of suspended fine grained mineral matter to the workings and development of numerous sinkholes and induced sinkholes on the surface take place (TYC, 1989; 1990; 1994). Sinkholes are the most catastrophic result of exploitation in the discussed karstic area. A spatial picture of the area in which collapse sinks occur is shown in figure 3. The range of this phenomenon is closely connected with a zone of hydraulic depression impact but the origin of these forms is different (TYC, 1994). There are collapse sinks connected directly with system of ore exploitation in mine workings as well as induced forms developing outside this area. During the time period of the most intensive processing (1978-1983) the volume of sinkhole formed in the whole area of exploitation was about 990 000 m^3. The the biggest sinkhole was about 300 000 m^3. At the end of the 80s a development of new forms has been distinctly reduced (figure 3).

4. Karstic processes in gypsum-salt rocks of Wieliczka mine activated by mine workings

In a distance of about 30 km to the east from Cracow the historical salt mine Wieliczka exploitating rock salt of Tertiary age is situated. The karstic phenomena in the vicinity of Wieliczka are located within salt and sulphate rocks. In April 1992 the karstic processes were activated in the surroundings of the transverse gallery of the mine where gypsum cap was disturbed by mine workings. This cap isolated deposit from inflow of allochtonous water.

Salt deposit in Wieliczka consists of two parts: beds and blocks. Marly claystones with gypsum inserts cover it. The Tertiary clayey-marly and sandy sediments (Skawina and Chodenica beds) occur in a zone of deposit boundary in three overthrusts. Chodenica sandstones influencing water flow into Mina gallery are recharged indirectly from Quaternary deposits and/or from Tertiary sands (Bogucice sands) occuring in the further foregound of the mine (figure 4) (GARLICKI & WILK, 1993).

The aquifer being filled since the end of the last glaciation was originally in a phreatic stage with circulation lasting for centuries. The solution was close to equilibrium in moderated state of saturation of salt and sulphate rocks.

Since the start of mining exploitation the aquifer was constantly under human impact with episodes of partial drainage. Accelaration of output as well as introducing the wet exploitation in the 50s and 60s caused distinct deterioration of

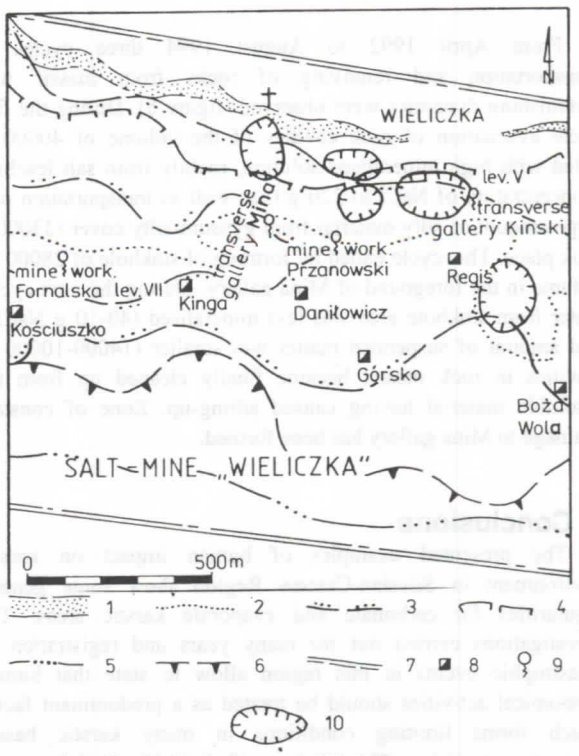

Figure 4 : Geological map of Wieliczka salt deposit area (according to SZYBIST, 1994). 1 - area of probable outcrops of Chodenica sandstones beneath Quaternary sediments, 2 - southern boundary of Chodenica sandstone beds, 3 - area of gypsum cap occuring beneath Quaternary sediments, 4 - northern boundary of salt deposit, 5 - southern boundary of salt deposit, 6 - boundary of the Carpathian overthrust, 7 - boundary of mine-field Wieliczka, 8 - shaft, 9 - the most important outflows at the northern boundary of deposit, 10 - basins without outflow

geomechanical conditions of the mine. Fissuring of the rock massif, formation of caverns in the block deposit and in the gypsum sediments were the result of uncontrolled leaching of salt lumps. Leaching of sulphate binder of Chodenica sandstones as well as high pressure of edge water caused a violent drainage of water from rock massif (up to the surface). Mina gallery became a natural water receiver after uncovering of the sandstones. A cone of depression has been formed which is not being filled at present. Water inflow through rock massif into Mina gallery has been stabilized at the volume of 150 l/min (GARLICKI *et al.*, 1996).

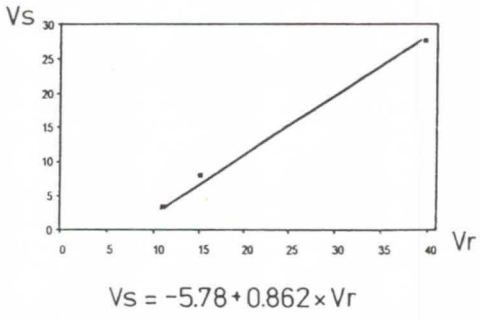

Figure 5 : Variability of total volume of rock voids (Vr, thousands of m^3) and of subsiding trough volume increase (Vs, thousands of m^3) in distinguished cycles

From April 1992 to August 1994 three cycles of transportation and removing of rocks from massif with diminishing dynamics were observed (figure 5). During the first cycle evacuation of rock cavities of the volume of 40000 m^3 filled with high mineralised solution, mainly from salt leaching (concentration of NaCl to 220 g/l) as well as transportation of a large amount of silty material from gypsum-silty cover (33000 t) took place. This cycle ended by forming of sinkhole of 28000 m^3 volume in the foregound of Mina gallery. During the next cycles water from sinkhole area was less mineralised (40-10 g NaCl/l) and amount of suspended matter was smaller (14000-10000 t). Cavities in rock massif became finally cleaned up from the insoluble material having caused silting-up. Zone of constant drainage to Mina gallery has been formed.

5. Conclusions

The presented examples of human impact on karstic environment in Silesian-Cracow Region show some general regularities for carbonate and evaporate karstic areas. The investigations carried out for many years and registration of catastrophic events in this region allow to state that human economical activities should be treated as a predominant factor which forms limiting conditions in many karstic basins contemporaneously. This is manifested by anthropogenic modification of recharge and discharge conditions depending on change of fluctuation zone of karstic water table position as well as breaking through impermeable rocks covering an aquifer.

From the examples of changes in the impact zone of Przeczyce dam and in the area of Olkusz mining it can be stated that catastrophic anthropogenic transformations can cause the activation of exhumation processes of buried routes of karstic circulation. In both cases, the contemporary „anthropogenic" circulation system in the Triassic carbonate aquifer refers to the earlier, pre-Quaternary circulation system. Damming up of water in Przeczyce reservoir in the gate part of the Czarna Przemsza river caused that surface water reached the level of non active karstic channels and activation of old sinkholes and vaucluse springs from geological times of the area took place. On the other hand the base of the artificial mining drainage in Olkusz area of zinc and lead ores exploitation is now situated beneath numerous open and filled karstic forms. It refers to pre-Quaternary circulation level in the period before burying carbonate karst by glacial and fluvioglacial sediments.

In case of Wieliczka salt mine the main process causing developoment of rock transformation is dissolution of gypsum-salt rock complex after inrush of a big volume of water. Due to the type of evaporite karst in this area the changed water circulation in massif does not use fossil courses as it happened in the areas of Olkusz and Przeczyce. New circulation courses were developed in the massif after activation of gypsum and salt dissolution processes by human activities. The reason of it was dissolution processes in evaporate karst are faster than in carbonate karst. In case of carbonate karst exhumated karst forms, which existed before, caused catastrophic scale of phenomena induced by human activity.

References

GARLICKI, A.; PULINA, M. & J. ROZKOWSKI. 1996. Influence of karst phenomena on the water threat of Wieliczka Salt Mine (in Polish). Prz. Geol. 10: 1032-1038.

GARLICKI, A. & Z. WILK. 1993. Geological and hydrogeological background of the recent water damage in Wieliczka Salt Mine (in Polish). Prz. Geol. 3: 183-192.

GLAZEK, J., GRADZINSKI, R. & M. PULINA. 1982. Karst and caves of Poland. Kras i speleologia, 4(XIII): 9-18.

JANKOWSKI, J. 1983. Chemical denudation on the basis of geographical environment of the Triassic threshold (in Polish). PhD thesis, University of Sielesia, Sosnowiec.

MOTYKA, J. 1988. Triassic carbonate sediments of Olkusz-Zawiercie ore-bearing district as an aquifer (in Polish). Scien. Bull. of Academy of Mining and Metallurgy, no. 157, Geol. Bull. 36, 109 p.

PULINA, M. & A. TYC. 1987. Guide des terrains karstiques choisis des Sudety et Haut-Plateau de Silesie-Cracovie. Uniwersytet Slaski, Sosnowiec, 101 p.

SZYBIST, A. 1994. Geological map of Wieliczka deposit region. Academy of Mining and Metallurgy, Cracow (unpublished).

TYC, A. 1994. Anthropogenic Impact on Karst Processes in the Olkusz-Zawiercie Karst Area (Silesian-Cracow Upland) (in Polish). PhD thesis, University of A. Mickiewicz, Poznań.

Environmental change and human impact on the arid karst of the Nullarbor Plain, Australia

David Gillieson
School of Geography & Oceanography, University of New South Wales,
Canberra ACT 2601, Australia.

Abstract
The arid karst of the Nullarbor Plain has considerable scientific, aesthetic and economic significance in a continent not well endowed with limestone landscapes. Unfortunately there are many problems and conflicts, many of which have arisen from uncontrolled development at the absolute limit of pastoralism. Management of increasing numbers of visitors to the caves and karst requires that resource inventories and management plans for each management unit be drawn up and used. Groundwater resources need to be evaluated, used conservatively and protected from pollution. In common with many deserts, the Nullarbor Plain has been used for weapons testing due to its remote location and low intensity land use, leaving a legacy of radionuclides.

Résumé
Le karst du domaine aride de la Nullarbor Plain a une importance scientifique, esthétique et économique considérable dans un continent où les pays calcaires sont rares. Malheureusement, il n'y a pas mal de problèmes et de conflits, dont beaucoup résultent d'un pâturage excessif jusqu'au delà des limites naturelles. Le nombre augmentant de visiteurs des cavernes et du karst demande d'établir et d'appliquer un inventaire des ressources et des plans de gestion. Les eaux souterraines doivent être évaluées, consumées économiquement et protectées contre des pollutions. Comme des autres déserts, la Nullarbor Plain a été utilisée pour tester des armes nucléaires en laissant une contamination radioactive.

1. Introduction

Australia is well known as a dry continent; this reputation can be best demonstrated by the fact that two thirds of the continent has no runoff at all. One third has less than 250 mm of rainfall and the 750 mm isohyet is rarely more than 250 kilometres inland. Much of the remainder is only seasonally or episodically moist and therefore geomorphic processes can only operate for relatively short periods. The Nullarbor Plain is Australia's largest arid karst (220,000km^2) and perhaps the most intensively studied (figure 1). The region has an arid to semi-arid climate with annual rainfall between 150 and 250mm, while annual evaporation is 1250-2500mm. The Nullarbor has no surface drainage, but relict stream channels are found on the northern and western flanks of the plain. Elsewhere the nearly flat plain has structurally aligned depressions with claypans (LOWRY & JENNINGS, 1974). These claypans act to channel the slight runoff and direct it into dolines and blowholes. Dolines are sparse, steep sided and show evidence of collapse into underlying cavities. Blowholes are very numerous, fed by deep solution pipes of complex origin. The caves are extensive, much modified by salt wedging and collapse processes, and commonly descend gently to near-static pools and lakes of brackish to saline water. A low gradient watertable underlies the plain and its depth ranges from 30m in the north to 120m in the south. The flooded tunnels of Cocklebiddy Cave are in excess of six kilometres long - only explorable by scuba diving. Withdrawal of hydrostatic support at times of lower sea level has led to collapse into these watertable caves, allowing entry into large caverns such as at Cocklebiddy, Koonalda, Abrakurrie and Weebubbie Caves. LOWRY & JENNINGS (1974) provide the definitive introduction to the geomorphology while more recent detail is given by GILLIESON & SPATE (1992).

Some solution of limestone does occur in the coastal fringe of the Nullarbor Plain and mixing corrosion may be important in this: the large caves of the Nullarbor may have been initially formed by enhanced solution at the mixing zone of fresh and saline waters (JAMES et al., 1990). The groundwater of the Eucla Basin has a high salinity (LAU et al., 1987) and some solution may also be occurring at great depth in the limestone. Inland periodic low-intensity rainfall may cause some solution on the margins of claypans, and calcretes are forming, but overall rates of solution must be very low. Of more significance are the intrusions of rain depressions of tropical origin which occur two or three times per decade. These have the capacity to dump large amounts of water on the western Nullarbor, flooding claypans and dolines, and perhaps maintaining epiphreatic passage forms in several caves such as Thampanna and Old Homestead.

2. Land degradation issues

To the Aborigines of the Mirning, Wirangu and Kokata language groups, the Nullarbor Plain was a bare, hostile environment (termed "Undiri") inhabited by malevolent subterranean spirits. These were encountered in dolines and caves, and such places are still shunned by some traditional people. The Aborigines thus avoided most of the treeless plain, although important trading and ceremonial pathways crossed it from south to north and from east to west. In 1865

Edward DeLisser explored and named the Nullarbor Plain, and by 1872 sheep were being grazed near Eucla. The Nullarbor Plain is marginal pastoral land at best; it lacks high quality water and its pastures are in poor condition, the low and erratic rainfall produces long periods of aridity, and the depressed state of the pastoral industry mitigates against technological improvements but favours overstocking with sheep. Thus stocking rates frequently exceed the carrying capacity of the native shrubs and grasses. This permits land degradation expressed as wind erosion and weed invasion, as well as native vegetation decline. The frequency of fires has also increased since European settlement: this is related to controlled burns, to sparks from trains on the Transcontinental railway, and to the increased flammability of shrubby growth promoted by sheep and rabbit grazing. Rabbits are also implicated in the decline of the bluebush *Maireana sedifolia* and the saltbush *Atriplex vesicaria*; these species, once dominant over much of the plain, have been eliminated over large areas and have been replaced by degraded grasslands. In Western Australia, rabbits are held to be the principal cause of accelerated soil loss on Nullarbor pastoral lands, and the recent spread of the Calichi virus as a biological control agent may eliminate 90% of rabbits for up to 8 years.

Anthropogenic Caesium-137 has been used extensively as a tool to measure rates and patterns of soil erosion. Fallout of this nuclide is derived from atmospheric testing of atomic weapons during and after the 1950's, with the first detectable ^{137}Cs occurring in 1958 within Australia. It's properties as a unique and discrete label of surface soil make it ideal as a tracer to test comparative rates of erosion, in which caesium measurements in erosion or deposition sites are compared to the known total or 'reference' fallout at that location (GILLIESON et al., 1996). The results of this analysis can be used to estimate net depth of soil loss (and hence tonnes/ha assuming a mean soil bulk density) from the averaged percentage depletion of soils for each paddock (Table 1). On the heavily grazed karst depressions of Mundrabilla Station the soil loss ranges from 13 - 31mm (average 21mm), and converts to a soil movement of 1.7 - 4.0 $t.ha^{-1}.y^{-1}$. This is high and consistent with other estimates of soil erosion in the Australian arid zone. In contrast, soil loss from the lightly grazed depressions of Arubiddy station ranges from 9 - 22mm (average 14mm), and this converts to a soil movement of 1.3 - 3.0 $t.\ ha^{-1}.y^{-1}$. Although these latter rates are modest, nutrient loss and soil seedbank decline can be severe as these resources are all in the top 25mm of soil. The major risk of wind erosion is normally around stock watering points or during drought conditions.

The settlement of the Nullarbor was critically dependent on water supply, and cave lakes were key resources for the pastoral industry. Direct stock access was rarely possible, so many wells and bores were sunk to intersect the groundwater. Typical of these sites is Koonalda Cave. It has unacceptable soil degradation due to runoff and siltation from its seriously overgrazed catchment, and the underground lake is seriously polluted by rafts of sheep dung and leachates from old machinery. The debris associated with underground pumping of stock water causes both visual and chemical pollution, and other stations still use bores directly into the limestone aquifer. There have been recent activities aimed at cleaning up rubbish, fencing the doline and gating the cave, and a cleanup of similar debris has also been undertaken at Weebubbie Cave. Today most travellers cross the Nullarbor at high speed on the Eyre Highway; less than 1% have the Nullarbor as a primary destination. Most casual visitors (including some divers) go to easily accessible Weebubbie and Cocklebiddy Caves, and are virtually uncontrolled in their activities. Several property owners carefully screen visitors and only allow access to accredited cavers. There is surprisingly little evidence of damage or littering at cave sites, although soil compaction around the dolines is a problem. Two commercial tour operators make regular visits to caves but seem to have a good conservation ethic. Recently a section of the entrance of Weebubbie Cave collapsed, prompting closure by the Western Australia Department of Land Administration. This may not be enforceable, and land management agencies may just have to accept that such events are a normal part of the geomorphic processes in this arid karst.

3. The legacy of weapons testing

In common with many deserts, the Nullarbor has been used for weapons testing due to its remote location and low intensity land use. Between 1953 and 1963 the U.K. Atomic Weapons Research Establishment conducted seven major trials in which nuclear devices were exploded on karst. In addition, trials were conducted to measure the dispersal of fission and activation products and their effects on biota. At four sites near Maralinga (figure 1) Plutonium isotopes (Pu^{239}, Pu^{240}, Pu^{241}) were dispersed in substantial quantities. The activity ratio of Plutonium-239 to Americium-241 is 7.4 ± 0.6, and so the activity concentration of Americium-241 can be used to estimate the Plutonium-239 activity in soil. At the Taranaki site (figure 2) a large area has soil activities in excess of $20kBq.kg^{-1}$. Most of these isotopes are relatively insoluble and are transported on the clay coatings of soil particles. Due to the higher gamma activity of the silt fraction in the soil, the concentration in inhalable dust is about $80kBq.kg^{-1}$. Although calculated dust loadings (LOKAN, 1985:59) are not significant, they assume that no dust is raised by either visitors, as a result of vegetation disturbance, or by feral animals. In addition, there is the potential for groundwater pollution by direct entry of fission products or, in the case of Am^{241}, a slightly more soluble radionuclide (JAMES, 1989). Clean-up activities and scientific investigations continue to the present. A major report (LOKAN, 1985) concludes that the regions near the ground zero of several trials have gamma radiation dose rates in excess of the maximum recommended dose rate for continuous occupancy, and that occupancy will not be safe until 2030-2050AD. Elsewhere in South Australia ALLISON et al. (1985) have investigated the rate of recharge of karst groundwater, for both exposed karst and that overlain by dunes. Recharge rates vary from 60mm yr-1 for secondary dolines to 0.06mm yr-1 for calcrete flats. Recharge rates for vegetated dunes are 0.06mm yr-1, for cleared

dunes they are 14mm yr-1. Thus the highest rates of recharge are associated with collapse dolines, where hydraulic conductivity is enhanced by fissures. This has implications for the accession of radionuclides into the Maralinga karst.

4. Discussion

The arid karsts of Australia have considerable scientific, aesthetic and economic significance in a continent not well endowed with limestone landscapes. This has been recognised by the declaration of several National Parks and equivalent reserves on arid karst, and an increasing attention to appropriate land tenure and use. Although many of the pastoralists are the second or third generation to occupy the land, their tenure is insecure and this does not promote good management. The depressed state of the pastoral industry means that most properties are under-capitalised, and there is thus considerable pressure to overstock in times of drought. Given the low stock numbers and limited number of people involved, it would be sensible to make pastoral activities secondary to conservation priorities in the arid karstlands. Yet the only viable alternative is some limited form of tourism. Management of visitors to the caves and karst requires that resource inventories and management plans for each area be drawn up and used. There is a need for a continuous ranger presence for education and land management. Some zoning and rationing of cave access may be necessary to limit the alteration of a resource which is clearly not regenerating.

References

ALLISON, G.B., STONE, W.J., & HUGHES, M.W. 1985. Recharge in karst and dune elements of a semi-arid landscape as indicated by natural isotopes and chloride. *J. Hydrol* 76: 1-25.

GILLIESON, D.S. & SPATE, A.P. 1992. The Nullarbor Karst, in Gillieson, D.S. (ed.) *Geology, climate, hydrology and karst formation: field symposium in Australia guidebook*, Spec. Publ. 4, Dept. Geogr. Oceanogr, ADFA, Canberra: 65-99.

GILLIESON, D., WALLBRINK P., MURRAY, A. & COCHRANE, A. 1996. Estimation of wind erosion using the radionuclide caesium-137 on the Nullarbor Plain karst, Australia. *Z.f.Geomorph* 105:73-90.

GRODZICKI, J. 1985. Genesis of the Nullarbor Plain caves in Southern Australia. *Z.f.Geomorph* 29: 37-49.

JAMES, J.M. 1989. Tietkens Plains karst, Maralinga, in Gillieson, D.& D. Ingle Smith (eds.), *Resource Management in Limestone Landscapes: International Perspectives*, Spec. Publ. 2, Dept. Geogr. Oceanogr., ADFA: 101-110.

JAMES, J.M., ROGERS, P. & SPATE, A.P. 1990. The role of mixing corrosion in the genesis of the caves of the Nullarbor Plain, Australia. *Proc. 10th Int. Congr. Speleol.*, Budapest: 263-265.

LAU, J.E., COMMANDER, D.P. & JACOBSON, G. 1987. *Hydrogeology of Australia*. BMR Bull. 227, Canberra, 21p.

LOKAN, K. 1985. Residual radioactive contamination at Maralinga and Emu, 1985. *Aust. Radiation Lab.Tech. Rep.* 70, 59pp.

LOWRY, D.C. & JENNINGS, J.N. 1974. The Nullarbor karst, Australia *Z.f.Geomorph.* 18: 35-81.

Table 1: Mundrabilla and Arubiddy Stations, Nullarbor Plain. Caesium-137 inventories and estimated soil loss

Mundrabilla Paddock	Mean Caesium Inventory ($Bq.m^{-2}$)	Mean % ref. inventory	Mean soil loss (mm over 30y)	Mean soil loss ($t.ha^{-1}.y^{-1}$)
No.1 bore	335.4 ± 22	74.0	20	2.6
Webbs Cave	322.6 ± 26	71.2	21	2.7
Gorringe Cave	307.3 ± 39	67.8	23	3.0
Boondara bore	316.5 ± 52	69.8	22	2.8
Uanna bore	234.4	51.7	31	4.0
Thampanna Cave	453.7 ± 13	100.1	0	0

Arubiddy Paddock	Mean Caesium Inventory ($Bq.m^{-2}$)	Mean % ref. inventory	Mean soil loss (mm over 30y)	Mean soil loss $t.ha^{-1}.y^{-1}$
Bluebush (ungrazed)	462.18 ± 48.44	105.92	0	0.0
Day's	368.46 ± 39.26	84.44	9	1.3
Dipper	292.67 ± 23.97	67.07	19	2.7
Reserve	262.34 ± 29.00	60.12	22	3.0
The Oaks	463.53 ± 32.75	77.17	7	1.4

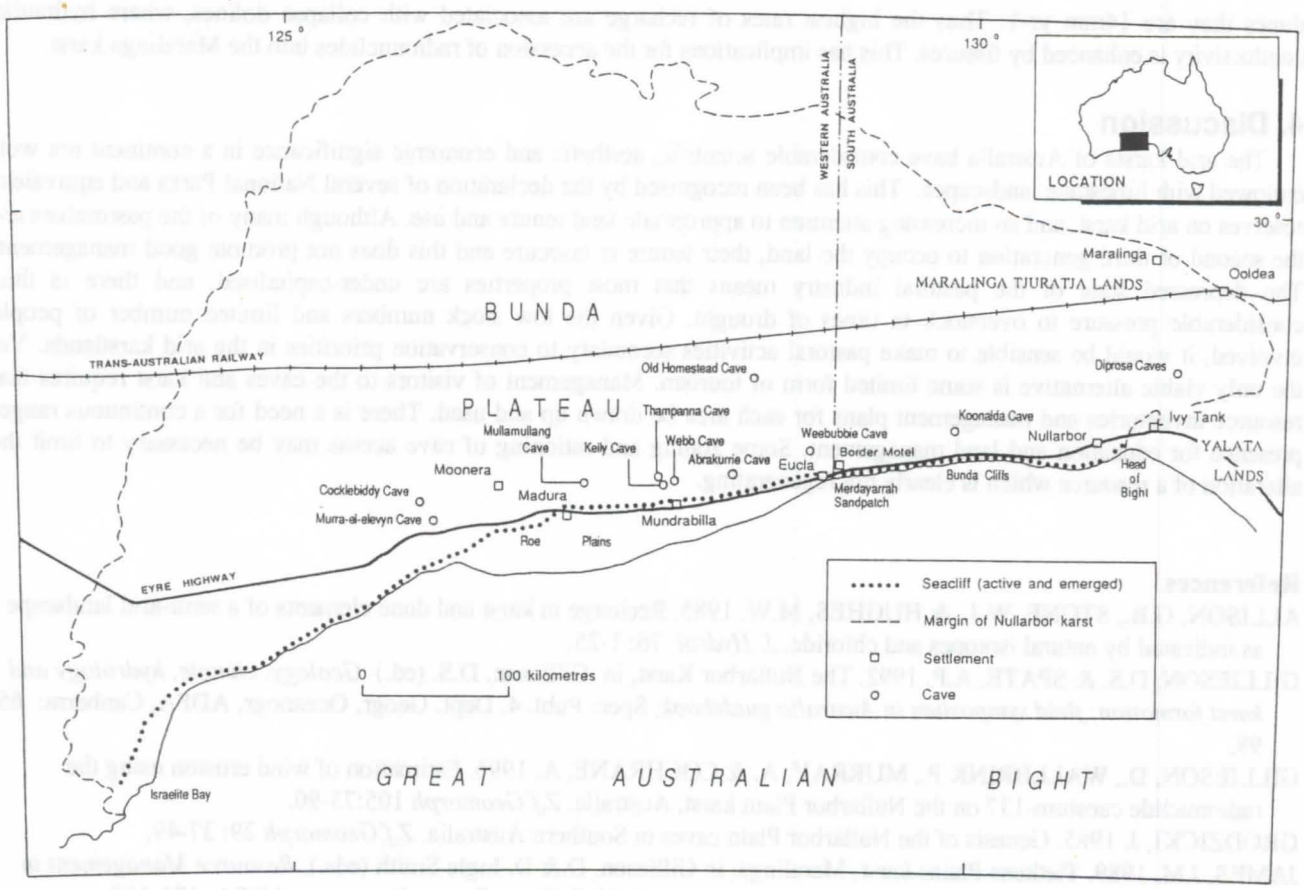

Figure 1: Principal features of the Nullarbor Plain.

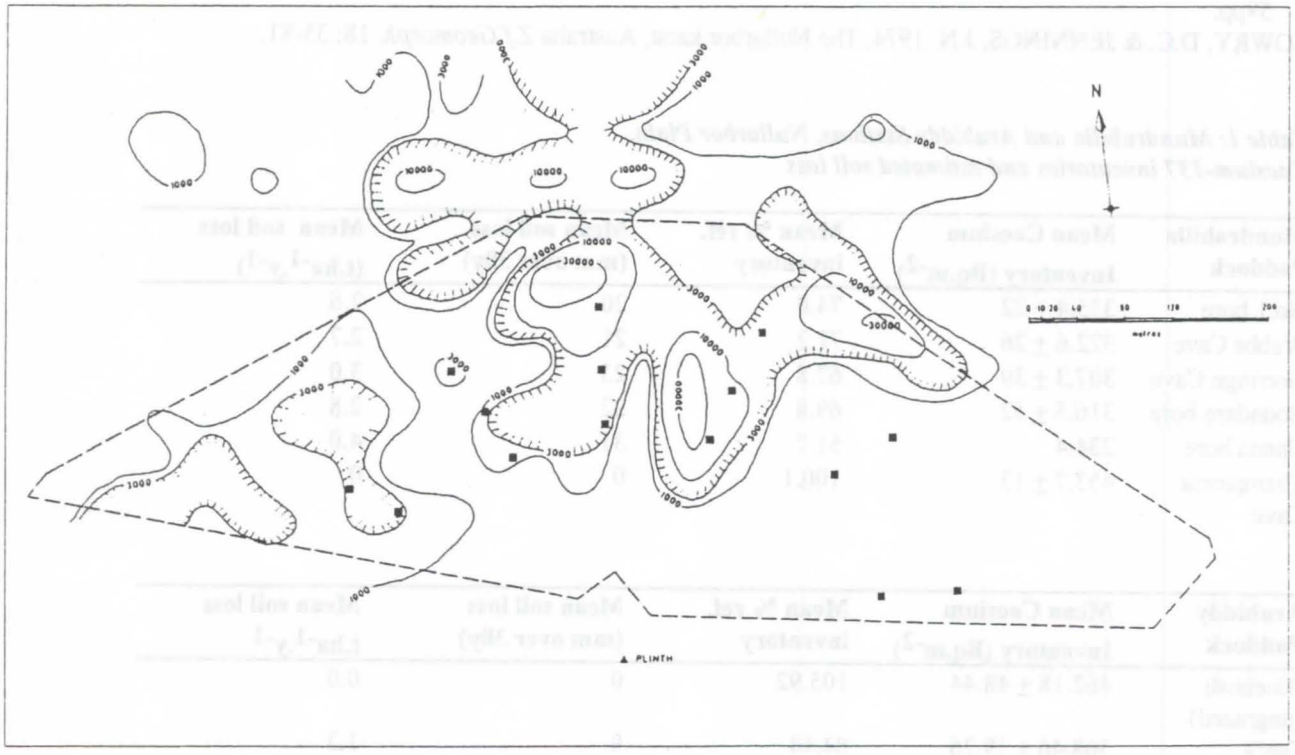

Figure 2: Activity of Americium-241 (Bq/kg) in soil for the Taranaki explosion site at Maralinga. Hatched contour corresponds to the region where soil activity of Plutonium-239 exceeds 20kBq/kg.

Les géotopes karstiques du canton de Fribourg (Suisse)

Vincent Grandgirard & Michel Spicher
Institut de Géographie, Université de Fribourg, Pérolles, CH – 1700 Fribourg, Suisse

Abstract

Within the scope of the development of a sector plan of landscapes and sites for the canton of Fribourg, our research group has established an inventory of geomorphological geotopes. This inventory takes into account more than 300 geotopes that illustrate the activity of five major geomorphological processes (fluvial, glacial, karstic, limnopaludal and slope processes).

In the canton of Fribourg, 55 karstic geotopes have been selected within the prealpine area. They consist of typical karstic landforms (such as dolines and uvalas, karren, subterranean cave systems, defiles and cluses, dry valleys) as well as landforms resulting from past or current activity of several processes (such as glacio-karstic valleys and depressions). Complexes of landforms, particularly representative of the karstic process, are also underscored.

Résumé

Dans le cadre de la réalisation du plan sectoriel des paysages et des sites du canton de Fribourg, notre groupe de recherches a élaboré un inventaire des géotopes géomorphologiques. Ce dernier recense plus de 300 objets illustrant l'activité de cinq processus majeurs (fluviatile, glaciaire, karstique, limno-palustre et gravitaire).

Au sein des Préalpes fribourgeoises, 55 géotopes karstiques ont été sélectionnés. Ces derniers consistent en formes typiques du modelé karstique (dolines et ouvalas, lapiés, réseaux de cavités souterraines, défilés et cluses , vallées sèches) ainsi qu'en formes résultant de l'activité passée ou actuelle de plusieurs processus (vallées et dépressions glacio-karstiques). Des complexes de formes, particulièrement représentatifs du processus karstique, sont également mis en évidence.

1. Introduction

Le terme «géotopes» désigne des «portions de la géosphère présentant une importance particulière pour la compréhension de l'histoire de la Terre» (GRANDGIRARD, 1996). En fonction de leurs caractéristiques, les géotopes peuvent être rangés en plusieurs types, correspondant aux différents domaines des sciences de la Terre. On peut ainsi distinguer des géotopes structuraux, minéralogiques, pétrographiques, paléontologiques, stratigraphiques, sédimentologiques, géomorphologiques, etc. Un même géotope peut appartenir à plusieurs types.

Les géotopes géomorphologiques correspondent à des formes du relief, actives ou non, qui délivrent des informations permettant de décrypter l'histoire de la Terre et/ou d'appréhender son évolution actuelle et future.

En pays calcaire, le relief est profondément marqué par l'action du processus karstique, souvent dominante. L'aménagement des régions karstiques pose de nombreux problèmes spécifiques, en particulier dans les domaines de la conservation de la nature et des paysages ainsi que de la protection des eaux souterraines. Diverses recherches appliquées, menées notamment en Belgique (DE BROYER, 1979), en Suisse (BOYER, GRANDGIRARD & MONBARON, 1995), en France (HOBLÉA, 1995) et en Slovénie (ROJSEK, 1994 et 1995), se sont efforcées d'apporter des solutions à de tels problèmes dans des circonstances particulières.

La présente communication présente les modalités de la prise en compte des phénomènes karstiques par le plan sectoriel des paysages et des sites du canton de Fribourg. Le canton de Fribourg (1670 km^2) se situe à l'W de la Suisse, à cheval sur le Plateau molassique et les Alpes (ou, plus précisément, les Préalpes). Il se caractérise par un environnement naturel riche et diversifié.

2. Le plan sectoriel des paysages et des sites

Le plan sectoriel des paysages et des sites du canton de Fribourg, en cours d'élaboration, est un instrument d'aménagement du territoire. Ce plan sectoriel procède à la sélection des sites remarquables (sites naturels, culturels et géologiques-géomorphologiques), présentant un intérêt cantonal, et définit les objectifs et principes qui régissent leur gestion (TEAM+, 1995).

En vue de leur prise en compte par ce plan sectoriel, les sites géomorphologiques d'importance cantonale ont été sélectionnés et décrits dans le cadre de la réalisation de l'inventaire des géotopes géomorphologiques du canton de Fribourg (GRANDGIRARD, 1996 & à paraître a).

3. L'inventaire des géotopes géomorphologiques

Les objectifs

L'inventaire des géotopes géomorphologiques permet de mettre en exergue les richesses géomorphologiques du canton de Fribourg. Il se présente comme un catalogue des reliefs observables sur le territoire cantonal, chaque type de relief étant illustré par un ou plusieurs exemples remarquables.

Cet inventaire sert une triple cause:

- il rend attentif à l'importance de la géomorphologie pour l'étude et la gestion du milieu naturel;
- il livre des informations détaillées sur la nature et la genèse des reliefs fribourgeois, permettant de décrire et de comprendre les paysages de ce canton;
- il fournit la liste des objets géomorphologiques de plus grande valeur, qui méritent une attention particulière.

Il est important de préciser que les objets géomorphologiques qui ne sont pas répertoriés ne sont pas pour autant dépourvus de valeur et que, pour toute action ayant des répercussions sur les reliefs et/ou leur dynamique, la composante géomorphologique doit être considérée.

La démarche

L'inventaire des géotopes géomorphologiques constitue une donnée de base pour des utilisateurs qui, le plus souvent, ne possèdent pas de compétences particulières dans le domaine des sciences de la Terre. Pour qu'il soit consulté, l'inventaire doit livrer des résultats convaincants et compréhensibles. Il doit par conséquent reposer sur une démarche clairement définie, basée sur des données scientifiques solides.

La démarche que nous avons mise au point pour la réalisation de cet inventaire se décompose en cinq étapes successives, que nous évoquons brièvement ci-dessous.

La diversité et la complexité des objets géomorphologiques est telle que la **catégorisation** de ces derniers est une étape préliminaire indispensable. Conformément au mode de catégorisation classique dans la géomorphologie contemporaine, qui range les formes du relief en fonction du (des) processus responsable(s) de leur genèse, nous classons les objets géomorphologiques en quatre catégories de complexité croissante (fig. 1): les formes isolées, les ensembles de formes, les complexes de formes et les systèmes géomorphologiques.

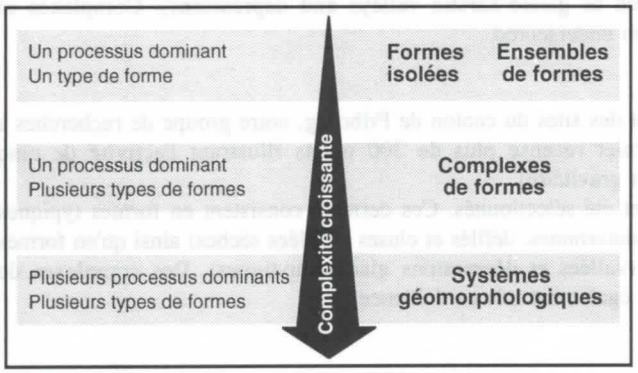

Figure 1: Les quatre catégories d'objets géomorphologiques

Il convient ensuite de procéder à l'**inventaire** aussi exhaustif que possible des objets géomorphologiques observables sur le territoire prospecté. Ces derniers sont mis en évidence par l'analyse de cartes topographiques et géologiques ainsi que de photographies aériennes, par l'étude de la littérature scientifique disponible dans le domaine des sciences de la Terre et par des reconnaissances sur le terrain. En raison de la multiplicité, de la complexité et de l'évolution des phénomènes considérés, un tel inventaire ne peut prétendre être parfaitement exhaustif.

L'**évaluation** de ces objets, à l'aide de critères judicieusement choisis, est un préalable indispensable à la sélection des géotopes géomorphologiques. Les critères utilisés pour l'évaluation des objets géomorphologiques permettent d'en apprécier la valeur scientifique, du point de vue de la géomorphologie. En fonction de leur importance dans le processus d'évaluation, nous distinguons deux types de critères: les facteurs et les indicateurs (fig. 2). Les facteurs sont les critères fondamentaux. La valeur d'un objet géomorphologique correspond à la combinaison des résultats obtenus lors de l'appréciation de chaque facteur. Les indicateurs sont des critères secondaires, à considérer lors de l'évaluation des facteurs. Un indicateur donné peut servir à l'appréciation de plusieurs facteurs.

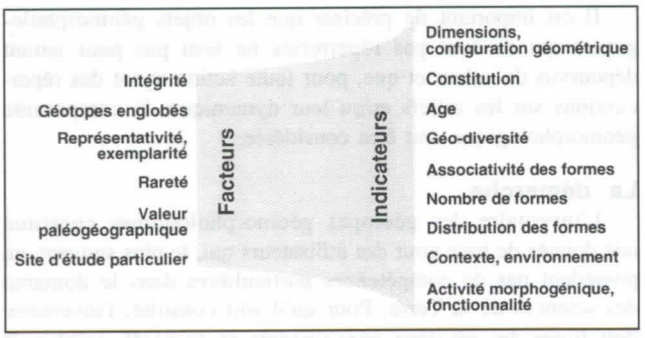

Figure 2: Les critères utilisés pour l'évaluation des objets géomorphologiques

Deux conditions fondamentales gouvernent la **sélection** des géotopes géomorphologiques: premièrement, seuls sont retenus les objets dont la valeur géomorphologique est importante (importance cantonale au moins) et deuxièmement, l'ensemble des géotopes doit être représentatif de la diversité des reliefs observables au sein du territoire cantonal.

Enfin, une **description** circonstanciée de chaque géotope est consignée dans une base de données structurée et aisément consultable. Cette dernière représente une source d'informations pour les aménagistes, les protecteurs de la nature ainsi que pour d'autres utilisateurs occasionnels. Pour chaque géotope, cette base de données fournit les informations suivantes: identification et désignation, localisation et délimitation, description géomorphologique, morphogenèse et activité actuelle, résultats de l'évaluation et sources bibliographiques.

Les résultats

L'inventaire des géotopes géomorphologiques du canton de Fribourg recense plus de 300 géotopes, représentant près de 40 types de formes et illustrant l'activité de cinq processus (fluviatile, glaciaire, karstique, limno-palustre et gravitaire).

55 géotopes karstiques ont été sélectionnés. Ils consistent en formes typiques du modelé karstique ainsi qu'en formes résultant de l'activité passée ou actuelle de plusieurs processus. Des complexes de formes, particulièrement représentatifs du processus karstique, ont également été mis en évidence.

4. Contexte géologique, hydrogéologique et géomorphologique

Les géotopes karstiques du canton se situent tous au sein de la nappe des Préalpes médianes plastiques. Cette dernière se compose d'une épaisse succession de calcaires, de marno-calcaires et de marnes principalement (fig. 3). Sa structure se caractérise par une succession assez régulière d'anticlinaux et de synclinaux dont les plans axiaux sont très inclinés. Les disharmonies de plissement y sont fréquentes, étant donné que les calcaires massifs du Malm se comportent de façon plus compétente que les autres formations rocheuses. Ces calcaires massifs sont d'ailleurs à l'origine des falaises les plus imposantes. Les décrochements observables au sein des Préalpes médianes plastiques (essentiellement dextres, ±N-S) sont contemporains du plissement (TRÜMPY, 1980).

Bien que la dissolution du gypse (fig. 3, 1) soit responsable du façonnement de dépressions karstiques, les formations triasiques (1 à 3) sont dans l'ensemble peu perméables. Les calcaires du Lias (4 à 7), peu karstifiés parce que trop siliceux, sont cependant bien fissurés et peuvent être considérés comme perméables. Les unités inférieures de la formation du Staldengraben (A et B, 8), épaisses et marneuses, se caractérisent par une perméabilité faible, qui augmente dans les unités supérieures (C et D, 9 et 10). Les phénomènes karstiques s'observent essentiellement au sein des formations des calcaires massifs du Malm (12 et 13) et des calcaires plaquetés du Crétacé inférieur (14), qui se distinguent par leur fissuration importante et leur forte perméabilité. Enfin, alors que la formation de l'Intyamon (15) et les flyschs (17) sont quasi-imperméables, les Couches rouges (16) présentent une perméabilité faible à moyenne, qui varie en fonction de l'intensité de la fissuration (MÜLLER & PLANCHEREL, 1982).

Au moment de la mise en place des Préalpes, les cours d'eau exerçaient une intense activité érosive, qui est à l'origine du décapage des flyschs de la nappe de la Simme et des formations supérieures de la nappe des Préalpes médianes (MAIRE, 1990). Dès la fin du Tertiaire, fortement influencées par les conditions lithologiques (formations rocheuses superficielles per-

méables) et structurales (plis, plongements axiaux, ensellements, décrochements, etc.), l'érosion karstique et l'érosion fluviatile ont conjugué leurs effets pour modeler les principaux traits du réseau hydrographique (BUGNON, 1988). Certains réseaux souterrains ont également été formés à cette époque (TESTAZ, 1969).

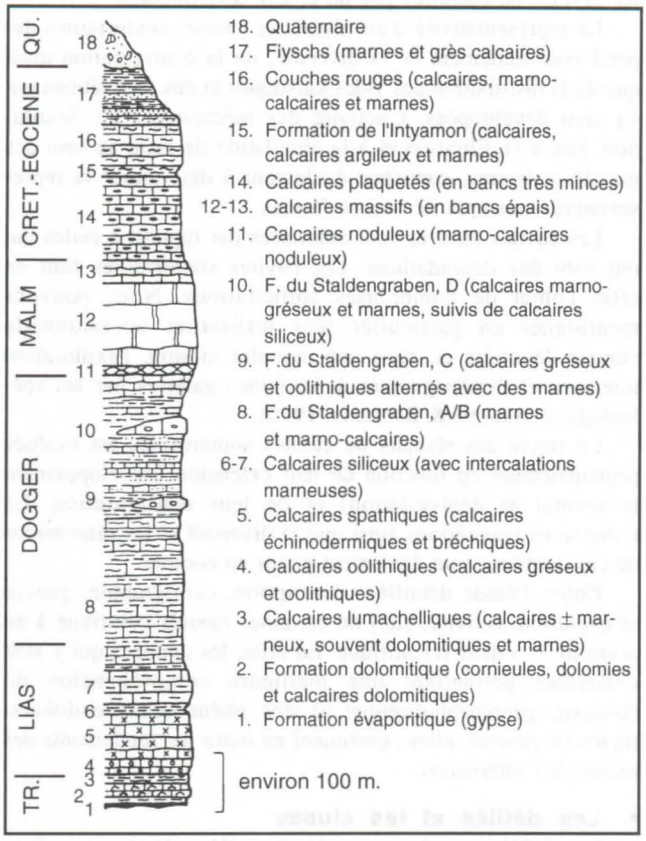

Figure 3: Lithostratigraphie des Préalpes médianes plastiques (d'après MÜLLER & PLANCHEREL, 1982; PLANCHEREL, 1979 ET WEIDMANN, 1993)

Au cours du Quaternaire, des glaciers régionaux ou locaux ont à plusieurs reprises envahi les vallées préalpines. Ces glaciers ont profondément marqué le relief des Préalpes médianes, affouillant les vallées originelles, façonnant des cirques dans les zones d'alimentation, creusant des ombilics et des vallons en auge, etc. Les reliefs les plus élevés, libres de glace, étaient soumis à l'activité des facteurs d'érosion périglaciaires (gélifraction, formation sporadique de lapiés). L'activité karstique profonde était alors entravée, tant en altitude (présence de permafrost) que dans les zones basses (couvertes de glace) (TESTAZ, 1969). Durant les périodes interglaciaires ou interstadiaires, les écoulements superficiels et souterrains ont été les principaux facteurs d'érosion. La corrosion superficielle et semi-profonde ainsi que l'érosion fluviatile ont été particulièrement virulentes durant les phases de transition climatique (fonte des glaces).

Actuellement, l'évolution géomorphologique des Préalpes médianes est en grande partie régie par l'activité des cours d'eau superficiels qui, pour la plupart, n'ont pas encore atteint leur profil d'équilibre. Les régions karstiques, qui abondent, sont le siège de nombreux phénomènes de dissolutions, qui s'exercent tant en surface qu'en profondeur. Les conditions climatiques qui y règnent (climat tempéré humide: précipitations importantes, surtout en été, couverture neigeuse de décembre à avril, restitution des eaux de fusion nivale au printemps et au début de l'été, etc.) sont favorables à la karstification (TESTAZ, 1969 & 1970). Enfin, dissolution et gélifraction combinent leurs effets pour disloquer les bancs rocheux, souvent fissurés. Ces mécanismes sont à l'origine de l'accumulation de matériaux éboulés sur les versants et au pied des parois rocheuses.

5. Les géotopes karstiques

Les 55 géotopes karstiques du canton de Fribourg se répartissent comme suit:

- six ensembles de dolines;
- deux ouvalas;
- cinq lapiés et deux ensembles de lapiés;
- neuf réseaux de cavités souterraines;
- quatre défilés (ou cluses) et deux ensembles de défilés (ou cluses);
- deux vallées sèches et un ensemble de vallées sèches;
- quatre vallées glacio-karstiques;
- neuf dépressions glacio-karstiques et trois ensembles de dépressions glacio-karstiques;
- six complexes karstiques.

Dans le cadre de l'inventaire des géotopes géomorphologiques, les phénomènes hydrogéologiques tels que sources, résurgences, pertes concentrées ou diffuses, etc. n'ont été considérés que dans la mesure où ils sont liés à des formes de terrain clairement identifiables. Suivant les propositions de spécialistes géologues et hydrogéologues, le plan sectoriel des paysages et des sites répertorie néanmoins les principales manifestations hydrogéologiques (même lorsqu'elles ne sont pas associées à des formes de terrain remarquables).

Les formes isolées et les ensembles de formes

• Les dolines

Dans les Préalpes médianes, les dolines sont fréquemment groupées en champs de dolines. En vertu de cette caractéristique essentielle, les six géotopes recensés sont des ensembles de dolines. Ces six ensembles sont répartis à la surface des formations évaporitique et dolomitique (fig. 3, 1 et 2) ainsi que des formations des calcaires massifs et plaquetés (12 à 14). Ils renferment chacun entre 8 et 103 dolines.

Les dolines sont des formes actives, dont la valeur paléogéographique est faible. De plus, les dolines des Préalpes fribourgeoises n'ont fait l'objet d'aucune étude spécifique. Les critères déterminants pour l'évaluation des ensembles de dolines sont par conséquent la représentativité-exemplarité, l'intégrité et la rareté (fig. 2).

L'exemplarité des ensembles de dolines est principalement appréciée en fonction des dimensions, de la configuration géométrique et de l'activité des formes qui les constituent. Le contexte (géologique surtout) ainsi que le nombre, la distribution et l'associativité des dolines sont également considérés. Les dolines observées illustrent plusieurs types théoriques en fonction de la lithologie sur lesquelles elles se développent. Les gypses de la formation évaporitique (1) sont favorables à la formation de très nombreuses dolines de dissolution de dimensions faibles à moyennes (quelques mètres de diamètre), présentant une forme arrondie. Ces dolines sont le plus souvent colonisées par la végétation et leur activité est restreinte. A la surface des formations des calcaires massifs et plaquetés (12 à 14), on trouve à la fois des dolines de dissolution et des dolines d'effondrement, dont l'activité est manifeste. Alors que leur forme est irrégulière, les dimensions de ces dolines sont en général assez importantes (diamètre d'une dizaine de mètres). La distribution de ces dolines est fortement conditionnée par les éléments structuraux (failles p. ex.). Enfin, les dolines associées aux lithologies de la formation dolomitique (2) ne sont pas particulièrement représentatives.

Les dolines, peu accessibles, sont en général intactes. Quelques-unes sont altérées par la constructions de routes ou de chalets. L'intégrité des ensembles de dolines peut néanmoins être qualifiée de bonne.

Bien que les dolines soient fréquentes au sein des Préalpes fribourgeoises, elles ne sont que rarement observées à la surface de la formation dolomitique (2). La rareté des ensembles de dolines a également été appréciée en fonction de deux spécificités: les ensembles présentant le plus grand nombre de formes et au sein desquels les dolines sont les mieux développées ont été valorisés.

- **Les ouvalas**

Deux ouvalas, localisés à la surface des formations des calcaires massifs et plaquetés (12 à 14), ont été répertoriés en tant que géotopes. D'autres ouvalas, de valeur moindre, ont été observés dans les formations évaporitique et dolomitique (1 et 2).

Les ouvalas sont des dépressions karstiques nées de la coalescence de plusieurs dolines. Ils peuvent par conséquent être évalués suivant les mêmes critères que ces dernières. D'une façon générale, les ouvalas sont des formes assez rares dans les Préalpes fribourgeoises. Leur représentativité-exemplarité est le critère décisif en vue de leur évaluation. Les deux géotopes sont les ouvalas les plus imposants. Ils sont intacts et aisément identifiables.

- **Les lapiés**

Les lapiés des Préalpes médianes fribourgeoises affectent essentiellement les formations des calcaires massifs et plaquetés (12 à 14). Il apparaissent plus rarement à la surface de la formation du Staldengraben (unités C et D, 9 et 10). Plus précisément, les sept géotopes recensés consistent en champs de lapiés. Deux d'entre eux se composent même de plusieurs champs de lapiés et forment, selon notre mode de catégorisation, des ensembles.

Pour l'évaluation des lapiés, les critères discriminants sont la représentativité-exemplarité et la rareté. Les autres facteurs livrent des résultats identiques pour tous les lapiés recensés.

Les champs de lapiés observés présentent une très grande variété de microformes (lapiés nus, semi-couverts et couverts, lapiés de joints de stratification, de diaclases ou de fissures, lapiés à cannelures, à rigoles, à méandres, lapiés de parois, puits de lapiés, lapiés à pierrailles, etc.). Les dimensions, la configuration géométrique, la diversité et la distribution de ces microformes ainsi que le contexte géologique et géomorphologique sont les principaux indicateurs permettant d'apprécier l'exemplarité des champs de lapiés.

Fréquemment observés au sein des Préalpes fribourgeoises, les lapiés s'étendent généralement sur des surfaces limitées. Pour cette raison, la rareté des champs de lapiés a été appréciée principalement en fonction de leur surface. Dans certains cas, la nature du substratum constitue également un indicateur permettant d'apprécier la rareté (v. ci-dessus, formation du Staldengraben, unités C et D).

En vertu de ces conceptions, les géotopes sont des champs de lapiés de grande étendue, présentant de nombreuses microformes de dissolution. Ces dernières sont aisément identifiables et illustrent clairement le contexte et les modalités de leur formation.

- **Les réseaux de cavités souterraines**

Les réseaux de cavités souterraines des Préalpes fribourgeoises sont localisées exclusivement au sein des formations des calcaires massifs et plaquetés (12 à 14); elles se développent à la faveur d'accidents tectoniques (tels que décrochements ou failles). Parmi les nombreuses cavités recensées et explorées, neuf sont considérées comme des géotopes.

L'évaluation des cavités souterraines repose sur l'analyse de leur représentativité-exemplarité, de leur intégrité, de leur rareté ainsi que de leur importance comme site d'étude particulier. La valeur paléogéographique, jugée identique pour toutes les cavités, ne constitue pas un critère discriminant.

La représentativité d'un réseau de cavités souterraines dépend essentiellement de la diversité, de la configuration ainsi que de la distribution des vides karstiques et des concrétions qui s'y sont développées. L'activité des mécanismes de dissolution, liée à l'infiltration et à la circulation de l'eau au sein des massifs calcaires, contribue également à déterminer la représentativité-exemplarité de ces formes.

Les cavités intactes sont valorisées par rapport à celles qui ont subi des dégradations. Les cavités souterraines font en effet l'objet de nombreuses sollicitations. Nous pouvons mentionner en particulier leur utilisation occasionnelle comme dépotoirs et, dans une moindre mesure, l'exploration intensive et l'aménagement de certaines galeries par les spéléologues (ARBENZ & BITTERLI, 1995).

La rareté des réseaux de cavités souterraines est évaluée principalement en fonction de leur extension (développement horizontal et dénivellation) et de leur configuration. La richesse en concrétions ainsi que la diversité et les dimensions de ces dernières sont également prises en compte.

Enfin, l'étude détaillée (description, cartographie, genèse et évolution, activité, etc.) de certaines cavités contribue à en accroître la valeur scientifique. En effet, les données qui y sont collectées permettent une meilleure compréhension du contexte géomorphologique et des phénomènes endokarstiques en général; elles constituent en outre les fondements des recherches ultérieures.

- **Les défilés et les cluses**

Les défilés sont des segments de vallées, étroits et profondément entaillés dans le substratum rocheux. Le terme de «cluses» désigne les passages qui recoupent transversalement une structure plissée. Dans les Préalpes médianes fribourgeoises, les défilés et cluses entaillent les anticlinaux et les synclinaux asymétriques qui forment les reliefs montagneux du canton. Ils traversent toutes les formations rocheuses comprises entre la formation des calcaires oolithiques et celle des calcaires plaquetés (entre 4 et 14). Quatre défilés (ou cluses) et deux ensembles de défilés (ou cluses) constituent des géotopes.

Les critères «valeur paléogéographique» et «site d'étude particulier» ne permettent pas d'opérer une sélection parmi les défilés et les cluses. Pour ces formes, les critères discriminants sont par conséquent la représentativité-exemplarité, l'intégrité et la rareté.

L'évaluation de la représentativité des défilés et cluses se fonde essentiellement sur leurs dimensions et leur configuration. Ainsi, les défilés et cluses sont jugés d'autant plus représentatifs et exemplaires que la déclivité et la dénivellation de leurs versants sont importantes.

Les dimensions des défilés et cluses les mettent à l'abri de graves altérations. L'exploitation de carrières constitue toutefois une atteinte non négligeable, qui contribue à dévaloriser certaines de ces formes.

Les principaux indicateurs pour l'estimation de la rareté sont les dimensions et le contexte géologique. Les défilés et cluses les plus rares sont ceux dont la dimension verticale (dénivellation des versants) est importante et ceux qui recoupent un grand nombre de formations géologiques. La rareté des ensembles de défilés a en outre été évaluée en fonction du nombre de formes associées.

- **Les vallées sèches**

D'après les nombreuses études géomorphologiques et géologiques consultées, la plupart des vallées des Préalpes fribourgeoises ont été soumises à l'action de glaciers locaux lors du dernier épisode glaciaire. Au sein des formations calcaires, quelques vallées ne présentent cependant aucune trace d'activité glaciaire. En l'absence d'écoulement permanents, ces vallées sont considérées comme des vallées sèches.

Deux vallées sèches isolées et un ensemble de trois vallées sèches ont été sélectionnés comme géotopes. Ils se situent au sein des formations des calcaires oolithiques (4), des calcaires siliceux (6 et 7), du Staldengraben (8 à 10), des calcaires massifs et des calcaires plaquetés (12 à 14).

Les critères discriminants en vue de l'évaluation des vallées sèches sont leur représentativité-exemplarité et leur rareté. Leur intégrité est en général bonne tandis que leur valeur paléogéographique et leur valeur en tant que sites d'étude particuliers sont faibles.

Une dénivellation importante entre le talweg et le sommet des versants facilite l'identification des vallées sèches et contribue à en accroître l'exemplarité. L'activité karstique dont elles sont le siège, qui se manifeste par l'absence d'écoulements superficiels, est également un critère essentiel pour l'évaluation de leur représentativité-exemplarité.

La rareté des vallées sèches est avant tout estimée en fonction de leur extension longitudinale, les vallées les plus longues étant les plus rares. Leur contexte géomorphologique contribue également parfois à leur rareté. Enfin, pour les ensembles de formes, le nombre de vallées englobées est un facteur de rareté déterminant.

- **Les vallées glacio-karstiques**

Les vallées glacio-karstiques sont d'anciennes vallées glaciaires, souvent suspendues, plus ou moins surcreusées, dont l'évolution récente et actuelle est régie quasi-exclusivement par le processus karstique. Dans le cadre de l'inventaire des géotopes géomorphologiques, les vallées d'origine glaciaire drainées par un cours d'eau sont considérées comme des auges glaciaires, même si elles sont le siège de phénomènes karstiques. Ces formes ne sont pas considérées dans le présent compte-rendu.

Les vallées glacio-karstiques des Préalpes fribourgeoises sont localisées dans la formation du Staldengraben (8 à 10) ainsi que dans les formations des calcaires massifs et plaquetés (12 à 14). Quatre d'entre elles sont des géotopes.

Pour l'évaluation des vallées glacio-karstiques, les critères les plus pertinents sont la représentativité-exemplarité, la rareté et la valeur en tant que site d'étude particulier. Les quelques aménagements qu'on y observe (construction de chalets, de routes ou de sentiers pédestres) ne portent pas atteinte à leurs caractéristiques géomorphologiques (morphologie et fonctionnalité). Enfin, ces vallées possèdent un certain intérêt paléogéographique (traces de l'activité glaciaire passée, témoins du retrait glaciaire et de l'évolution récente), jugé identique pour toutes les formes considérées.

L'exemplarité des vallées glacio-karstiques est appréciée en fonction de leur configuration et de leur activité actuelle. Les vallées encaissées, présentant de nombreuses formes d'origine glaciaire (cirques, ombilics et verrous, accumulations morainiques, etc.) et sièges de phénomènes attestant l'activité du processus karstique sont les plus représentatives.

La rareté des vallées glacio-karstiques s'évalue principalement en fonction de leurs dimensions. Les vallées les plus rares sont les plus longues et les plus encaissées. La richesse en formes-témoins d'origine glaciaire ainsi qu'en phénomènes karstiques contribue également à en accroître la rareté.

Certaines vallées ont été l'objet de recherches approfondies, qui leur confèrent une valeur scientifique accrue.

- **Les dépressions glacio-karstiques**

Les dépressions glacio-karstiques sont des formes polygéniques caractérisées par une dépression majeure, siège de pertes karstiques. Ces cuvettes sont le résultat d'un surcreusement glaciaire au fond d'un cirque ou d'une vallée. La dissolution nivale et la gélifraction sont les principaux mécanismes qui en régissent l'évolution actuelle.

Les dépressions glacio-karstiques abondent dans les Préalpes fribourgeoises. Elles se rencontrent dans toutes les formations géologiques, même si la lithologie est peu propice à la karstification. L'absence d'écoulements et/ou l'infiltration des eaux de surface attestent cependant l'activité karstique actuelle. Neuf dépressions glacio-karstiques et trois ensembles de dépressions sont considérés comme des géotopes.

L'exemplarité des dépressions glacio-karstiques dépend surtout de leur contexte géologique et géomorphologique, de leur configuration et de leur dynamique actuelle. Une importance particulière a été attribuée à la profondeur de ces dépressions (qui témoigne du surcreusement glaciaire et/ou de la dissolution karstique) et à l'infiltration des eaux de surface. L'évaluation de la représentativité des ensembles de formes tient également compte du nombre et de la distribution des dépressions (p. ex. au fond de cirques voisins ou d'ombilics étagés le long d'une vallée glaciaire).

Difficilement accessibles, les dépressions glacio-karstiques sont peu menacées. Bien qu'elles soient en général intactes et actives, certaines d'entre elles sont altérées par des constructions et des routes d'accès.

Les dépressions glacio-karstiques présentent le plus souvent une forme arrondie voire elliptique et sont associées à des cirques glaciaires ou à des ombilics. Certaines spécificités telles que leurs dimensions importantes (surface, profondeur) ou leur contexte (p. ex. au fond d'une vallée glaciaire, à cheval sur les bassins d'alimentation de plusieurs sources karstiques) contribuent à en accroître la rareté. La rareté des ensembles de formes est appréciée en fonction du nombre de formes associées ainsi que de la disposition de ces dernières.

L'analyse des dépressions glacio-karstiques (de leur configuration, de leur remplissage, de leur contexte et de leur dynamique) livre d'intéressantes informations concernant l'évolution morphogénique régionale depuis le dernier épisode glaciaire.

Enfin, la valeur scientifique des dépressions glacio-karstiques est renforcée par les nombreuses études dont elles ont été l'objet. En outre, l'analyse du remplissage sédimentaire progressif de ces dépressions permettrait une meilleure compréhension de leur évolution et de la morphogenèse karstique en général (TESTAZ, 1966).

Les complexes karstiques

Les complexes karstiques consistent en surfaces d'étendue variable où de nombreuses formes de dissolution superficielles et souterraines coexistent et évoluent conjointement. Dans les Préalpes fribourgeoises, six complexes karstiques sont considérés comme des géotopes. La plupart affectent les formations du Staldengraben (unités C et D, 9 et 10), des calcaires massifs et plaquetés (12 à 14) et présentent une très grande variété de formes. Un de ces complexes fait néanmoins exception: constitué de dolines et de dépressions glacio-karstiques, il se situe au sein des formations du Trias et du Lias inférieur (1 à 4).

Les complexes sont évalués d'après les mêmes critères que les formes isolées et les ensembles de formes. Le critère «géotopes englobés» s'y ajoute parfois. Les complexes kars-

tiques sont intacts et actifs (certaines formes isolées sont parfois altérées, sans que les complexes ne soient pour autant dépréciés). Tous livrent des informations intéressantes concernant l'évolution des reliefs préalpins. Pour ces complexes, les critères «intégrité» et «valeur paléogéographique» ne sont par conséquent pas discriminants.

L'appréciation de l'exemplarité-représentativité des complexes karstiques consiste à juger de leur aptitude à rendre compte de l'activité passée ou actuelle du processus karstique dans une région donnée. Elle peut se fonder sur la prise en considération de tous les indicateurs présentés sur la figure 2.

Les complexes karstiques sont d'autant plus rares que leur surface est importante et que le nombre et la diversité des formes qu'ils comprennent sont grands. La rareté de certains complexes karstiques est fonction de leur contexte géologique (v. ci-dessus).

Certains complexes karstiques ont fait l'objet d'études géologiques générales ainsi que d'analyses approfondies, portant notamment sur leurs caractéristiques hydrogéologiques ou géomorphologiques. Leur valeur en tant que sites d'étude particulier en est considérablement accrue.

Les six complexes renferment chacun entre un et cinq géotopes karstiques de complexité moindre (formes isolées et ensembles de formes). L'intérêt géomorphologique des complexes karstiques, qui constituent l'environnement de ces formes et ensembles de valeur, en est renforcé.

6. Conclusion: la gestion des géotopes karstiques

Selon le dossier d'avant-projet (TEAM+, 1995), le plan sectoriel des paysages et des sites du canton de Fribourg vise la prévention des atteintes irréversibles aux géotopes soumis à des sollicitations particulières et/ou menacés en tant qu'éléments caractéristiques du paysage. Les mesures à prendre en vue de satisfaire à cet objectif général dépendent des menaces qui pèsent sur les géotopes (GRANDGIRARD, à paraître b).

Les géotopes karstiques du canton de Fribourg sont situés dans des régions montagneuses, élevées et accidentées; ils sont globalement peu menacés. Ces géotopes sont néanmoins l'objet de dégradations, qui ne peuvent être compensées. Pour cette raison, leur gestion repose essentiellement sur des mesures de protection. Ces dernières peuvent consister en créations de réserves naturelles (cf. DE BROYER, 1979 et ROJSEK, 1995) ou en restrictions d'utilisation, notamment dans les cas de fréquentation excessive ou peu respectueuse des cavités souterraines (cf. ARBENZ & BITTERLI, 1995 et HOBLEA, 1995). Ces mesures peuvent en outre s'accompagner d'actions d'information et de mise en valeur (p. ex. création de sentiers didactiques, opérations de dépollution des dépressions et cavités contaminées), destinées à encourager la prise de conscience de la valeur du patrimoine karstique par le plus grand nombre.

En Suisse, les dispositions légales en matière d'aménagement du territoire, de protection de la nature et du paysage, de protection de l'environnement et de protection des eaux seraient en principe suffisantes pour assurer la gestion des géotopes karstique. Les faits démontrent cependant que la valeur de ce type de patrimoine n'est que rarement reconnue. L'inventaire des géotopes géomorphologiques du canton de Fribourg et le plan sectoriel des paysages et des sites constituent des instruments qui permettent à la fois de mettre en évidence la richesse des phénomènes karstiques et d'assurer leur protection de façon ciblée et efficace.

Références

ARBENZ, T. & T. BITTERLI. 1995. Cavernes – monde fragile. SSS, Granges, 15 p.

BOYER, L.; GRANDGIRARD, V. & M. MONBARON. 1995. Evaluation des vallées sèches de l'Ajoie, aspects hydrologiques et géomorphologiques. *Regio Basilensis.* 36/2: 165-173.

BUGNON, S. 1988. La vallée de la Jogne: un exemple d'influence structurale et karstique sur la morphologie et l'orientation d'une vallée des Préalpes fribourgeoises. Mémoire de dipl., Institut de Géographie, Université de Fribourg, 171 p.

DE BROYER, C. 1979. Sites karstiques et aménagement du territoire en Wallonie. *Annales de la Société Géologique de Belgique.* 102: 95-100.

GRANDGIRARD, V. 1996. Gestion du patrimoine naturel, l'inventaire des géotopes géomorphologiques du canton de Fribourg. *Ukpik, Rapports de recherche, Institut de Géographie, Fribourg.* 8: 181-195.

GRANDGIRARD, V. à paraître a. An Inventory of Geomorphological Geotopes in the Canton of Fribourg (Switzerland). *Memorie Descrittive della Carta Geologica d'Italia.*

GRANDGIRARD, V. à paraître b. Geomorphology and Management of Natural Heritage. Experiences in Switzerland and Fribourg. In: (CCEA & CSLEM, Eds): Acts of the Conference "Caring for Home Place: Protected Areas and Landscape Ecology", Regina (Canada), September 29 – October 2 1996.

HOBLEA, F. 1995. Evaluation multicritère des sites karstiques. Document inédit. Département de Géographie, Université Lumière Lyon 2, 10 p.

MAIRE, R. 1990. La haute montagne calcaire. *Karstologia-Mémoires*, 3, AFK et FFS, 731 p.

MÜLLER, I. & R. PLANCHEREL. 1982. Contribution à l'étude de l'hydrogéologie karstique du massif du Vanil Noir et de la chaîne des Gastlosen (Préalpes fribourgeoises, Suisse). *Bull. Soc. Frib. Sc. Nat.* 71(1/2): 102-132.

PLANCHEREL, R. 1979. Aspects de la déformation en grand dans les Préalpes médianes plastiques entre Rhône et Aar. Implications cinématiques et dynamiques. *Eclogae geol. Helv.* 72: 145-214.

ROJSEK, D. 1994. Inventarisation of the Natural Heritage. *Acta carsologica.* 23: 111-121.

ROJSEK, D. 1995. The Western Visoki Kras of Slovenia – A Park?. *Cave and Karst Science.* 21/3: 93-96.

TEAM+, TÜSCHER URBANISME SA. 1995. Plan sectoriel des paysages et des sites. Dossier d'avant-projet. Canton de Fribourg, OCAT, Fribourg, 43 p. + annexes.

TESTAZ, G. 1966. Les phénomènes karstiques de la nappe des Préalpes médianes romandes. *Cavernes, bull. sect. neuch. Soc. suisse Spéléo.* 10: 69-84.

TESTAZ, G. 1969. Le rôle de l'érosion karstique dans l'évolution du relief des Préalpes médianes. In: (Société suisse de Spéléologie): Actes du 3e Congrès national de spéléologie, Interlaken, 24 et 25 septembre 1967: 23-31.

TESTAZ, G. 1970. Morphologie karstique des Préalpes romandes. Mémoire de licence, Institut de Géographie de l'Université de Lausanne, 100 p.

TRÜMPY, R. 1980. Geology of Switzerland – a guide-book. Part A: An Outline of the Geology of Switzerland. Wepf & Co., Basel, 104 p.

WEIDMANN, M. 1993. Atlas géologique de la Suisse 1:25'000, Feuille 92, Châtel-St-Denis, Notice explicative. Service hydrologique et géologique national, Berne, 55 p.

Réflexion sur les facteurs contrôlant la karstification dans l'Arc alpin

par Philippe Audra
Gestion et valorisation de l'environnement (GVE), URA D1476 du CNRS, Université de Nice-Sophia-Antipolis, 98 boulevard Edouard Herriot, BP 209, 06204 NICE Cédex & CAGEP (URA 903), AIX-EN-PROVENCE.

Abstract: Consideration about mechanisms regulating the karstification in the Alpine range.

Most of the large alpine cave systems have been made up during the Neogene and have evolved during the Quaternary. Following the first neogene uplifts, extensive subhorizontal systems, sometimes layered, have occured. At the beginning of the Upper Miocene, they have been perched by the important uplift. Then, they have been cut and dryed out by vertical shafts, from plio-quaternary age. Allogenic water have extensively contributed to their elaboration. In the Tertiary, thanks to the low relief and to the weathered rock covers, the systems develop in a fluvio-karst context. In the Quaternary, glacial waters have hollowed out the alpine shafts and reactived the old perched systems. These cave systems are geodynamic and geomorphologic milestones.

Résumé

La plupart des grands réseaux alpins se sont élaborés au Néogène et ont évolué durant le Quaternaire. Dès les premières phases de surrection néogènes, de vastes complexes de galeries subhorizontales, parfois étagés, se sont mis en place. Le soulèvement important amorcé à la fin du Miocène les a perché. Ils ont alors été démantelés et asséchés par des réseaux de puits d'une grande extension verticale, d'âge plio-quaternaire. Les apports d'eaux allogènes ont largement contribué à leur formation. Au Tertiaire, grâce aux reliefs peu élevés et aux couvertures d'altérites, les réseaux s'organisent dans un contexte de fluvio-karst. Au Quaternaire, les eaux glaciaires ont creusé les gouffres et réactivé les anciens réseaux perchés. Ces réseaux sont des jalons géodynamiques et géomorphologiques.

1. Evolution des karsts alpins depuis le début du Tertiaire

Des fluvio-karsts avec un gradient modéré, jusqu'à la fin du Miocène

Durant une bonne partie du Tertiaire, les zones alpines externes, où se localisent la plupart des massifs karstiques, ne sont guère soulevées. Plateaux et basses montagnes, proches du niveau de base, n'offrent qu'un faible gradient altitudinal.

Les massifs cristallins internes et les massifs anciens dominent ces plates-formes sédimentaires. De ces amonts descendent des cours d'eau, qui couvrent les piémonts sédimentaires d'épendages détritiques : sables éocènes en périphérie des massifs anciens (Préalpes françaises), *Augensteine* oligocènes dans les Alpes calcaires du nord de l'Autriche.

Dans un contexte climatique de type tropical, ces couvertures détritiques sont soumises à une puissante altération ("sidérolithique", *Bohnerz*). Une légère surrection permet la karstification des calcaires, par crypto-corrosion sous ces couvertures détritiques (MAIRE, 1990). Il s'élabore un paysage ubiquiste de buttes karstiques : Coulmes en Vercors (DELANNOY & al., 1988), Campo dei Fiori (UGGERI, 1992), *Raxlandschaft* des Alpes calcaires autrichiennes (LANGENSCHEIDT, 1986), sommets coniques des Alpes juliennes (HABIC, 1992).

Dans la zone interne en position plus élevée, comme pour le Marguareis, l'évolution s'amorce par décapage des couvertures autochtones (flyschs), avec également une action de la crypto-corrosion au travers des calcschistes très perméables (MAIRE, 1990).

La lente surrection accroît progressivement le gradient et les cours d'eaux allogènes disparaissent au contact des calcaires, alimentant le karst profond. Poljés, vallées aveugles et pertes de rivières constituent alors un fluvio-karst.

Les réseaux souterrains sont subhorizontaux du fait du faible gradient. L'alimentation abondante par les rivières allogènes produit de vastes galeries qui s'étagent sur quelques dizaines de mètres dans les limites de la zone épinoyée : les crues brutales, liées tant au climat contrasté qu'à la présence d'un amont imperméable, n'activent que temporairement les étages supérieurs (AUDRA, 1994).

Par ailleurs, les réseaux sont également alimentés par les infiltrations descendant au travers de la zone vadose qui empruntent des conduits subverticaux de type puits-méandres ou des galeries inclinées (BINI, 1994 ; BINI & UGGERI, 1992).

Les remplissages karstiques de cette période sont très caractéristiques (AUDRA, 1995). Les dépôts détritiques proviennent du soutirage des couvertures superficielles altérées. Ils se composent d'argiles rougeâtres, de pisolites de fer issues du démantèlement d'anciennes cuirasses, de billes de quartz ainsi que de minéraux résistants (zircon, tourmaline, muscovite...). Les roches et minéraux facilement altérables (biotite, feldspaths...) sont en général inexistants. Les concrétions reflètent les conditions climatiques chaudes avec une végétation abondante, liées tant au climat d'alors qu'à l'altitude moindre des massifs, comme le montrent les mesures sur les isotopes de l'oxygène (FRISIA & al., 1994). Elles sont massives, avec des cristallisations transparentes. Cependant, la dégradation des couvertures bio-pédologiques lors des crises climatiques épisodiques, entraînant un soutirage des sols dans le karst, se traduit par des concrétions teintées de rouge.

La surrection alpine aboutit à des karsts perchés. Rôle régional de la régression messinienne

Deux phénomènes marquent la charnière Miocène-Pliocène. La régression messinienne affecte le versant méditerranéen drainé par des fleuves dépendant du bas niveau régressif (Bas-Rhône, Provence, plaine du Pô et sans doute Alpes juliennes). Le paroxysme alpin (ou phase tectonique rhodanienne) renouvelle en partie la trame structurale. Cette tectonisation est suivie d'une phase importante de soulèvement tout au long du Pliocène, qui se poursuit de manière variable selon les lieux durant le Pléistocène. C'est la période de constitution des grands réseaux souterrains que l'on connaît actuellement.

La phase rhodanienne agit de manière différente selon les régions. Dans les massifs constitués d'alternances de couches marneuses et calcaires, comme les Préalpes françaises du nord, les mouvements se traduisent par des déformations souples plissées et chevauchantes, remodelant profondément les anciennes structures géologiques. En Autriche, où les assises calcaires atteignent plus de 1 000 m d'épaisseur, les mouvements se traduisent par des rejeux cassants subverticaux. Un

soulèvement de quelques centaines de mètres accompagne cette phase de tectonisation.

De grands réseaux subhorizontaux se mettent alors en place, conformément à cette nouvelle trame structurale. Dans les Préalpes françaises, certains bénéficient d'apports fluviatiles de poljés intra-montagnards (antre de Vénus - DELANNOY, 1992) ou peut-être alpins (Chartreuse ? - HOBLÉA, à paraître) d'autres se limitent à un drainage local (grotte Vallier). En Autriche, les *Riesenhöhlen* (Eisriesenwelt, Tantalhöhle, Raucherkarhöhle...), doivent leur gigantisme aux puissants apports des grandes rivières alpines.

En surface, l'accroissement du gradient active l'érosion des couvertures qui sont piégées dans le karst. Ces altérites remaniées se mèlent, lorsque l'alimentation est également allogène, à des éléments fluviatiles beaucoup moins altérés (fragments rocheux, minéraux fragiles plus fréquents). Les concrétions massives attestent de la persistence d'un climat chaud.

Les réseaux de la génération précédente sont perchés par la surrection, disloqués par la tectonique. Amputés de leur bassin versant, ils sont déconnectés des circulations et n'ont généralement pas de lien avec les grands réseaux nouvellement créés.

Au cours du Pliocène, le soulèvement se poursuit continuellement, renforçant encore le gradient de plusieurs centaines de mètres, ce qui porte le mouvement vertical depuis la fin du Miocène à plus d'un kilomètre. Les vallées s'adaptent par un creusement en profondeur, qui s'accompagne d'un évasement des versants. Ainsi, les grands réseaux perdent leur alimentation, par diminution de leur impluvium karstique (Vallier), par disparition de l'apport allogène (Eisriesenwelt) et deviennent inactifs. Les niveaux de circulation s'enfoncent, façonnant des étages inférieurs de conduits marquant chacune des phases de répit. L'accroissement considérable du potentiel hydraulique livre un zone vadose de plus de 1 000 m de hauteur, que les infiltrations verticales vont creuser en puits et méandres, recoupant "à l'emporte-pièce" les différents niveaux horizontaux des générations précédentes. Les conduits de la zone épinoyée correspondent à de grands tubes inclinés selon le pendage (Hölloch). Du fait de l'importante surrection, les massifs calcaires ainsi que leur soubassement imperméable s'élèvent au-dessus du fond des vallées. Pour certains d'entre eux, une faible portion descend jusqu'au niveau de base où se localisent les émergences : il s'agit désormais de karsts perchés.

La régression messinienne est un événement extrêmement brutal, qui se traduit par un puissant surcreusement des vallées jusqu'à l'intérieur de l'arc alpin (1 000 m au niveau des lacs italiens). Elle se manifeste alors que la surrection rhodanienne est déjà amorcée (CLAUZON, 1996), elle va donc en accroître les effets morphologiques sur le versant méridional alpin. L'évasement des versants décapite les anciens réseaux. Un nouveau système de drainage subvertical se met en place dans la zone vadose étendue vers le bas, qui recoupe les anciens étages horizontaux. La transgression pliocène transforme en rias ces vallées, bientôt remplies de sédiments. De ce fait, une grande partie de la base du karst est ennoyée, partiellement colmatée (BINI, 1994). Seuls les drains majeurs restent fonctionnels (émergences sous-lacustres lombardes, sources vauclusiennes bordant la vallée du Rhône...).

La réactivation par les glaciers pléistocènes

A l'aube du Pléistocène, les reliefs sont pratiquement en place ; les vallées subissent un surcreusement modéré sous l'effet des glaciations. Il serait de l'ordre de 200 à 300 m à Vallier et aux Siebenhengste, où l'on retrouve des témoins des premières glaciations dominant d'autant les moraines récentes (AUDRA, 1994 ; JEANNIN, 1991). Ces dépôts prouvent la mise en place antérieure des grands réseaux. Les nouveaux développements sont généralement limités aux niveaux les plus profonds.

Par ailleurs, des karsts plus récents (Valais, Alpes internes dauphinoises, Kitzsteinhorn...) se mettent en place en fonction du décapage des couvertures, amorcé au Pliocène et poursuivi au cours du Pléistocène (MAIRE, 1990). Leur jeunesse relative se traduit par des formes et des systèmes de drainage peu évolués.

Les grands réseaux poursuivent leur étagement en suivant les variations du niveau de base, tant d'origine tectonique que glaciaire. Dans le massif du Marguareis, d'anciens conduits horizontaux surmontent de 100 à 200 m les canyons actifs (EUSEBIO & VIGNA, 1996), tandis qu'aux Siebenhengste les circulations s'enfoncent dans des niveaux inférieurs inconnus (JEANNIN, 1990).

Dans la zone vadose, les puits et méandres évoluent par érosion régressive, créant des réseaux parallèles.

Les remplissages se disposent en fonction de colmatages et de décolmatages successifs des réseaux préexistants (AUDRA, 1994 ; BINI, 1994). Dans la zone vadose, on observe des bourrages de galets morainiques provenant de pertes glaciaires, passant à des sédiments fluvio-glaciaires sablo-graveleux (HLADNIK & KRANJC, 1977). Mais la grande originalité réside dans les mises en charge considérables des réseaux, qui sont réactivés sur plusieurs centaines de mètres de hauteur. Les fusions glaciaires estivales provoquent une sédimentation varvée, caractéristique de cette zone épinoyée (AUDRA, 1995). En milieu périglaciaire, on observe des décharges de gélifracts, des laves torrentielles liées à la gélifluxion (Dachsteinhöhle) et des limons issus du remaniement des lœss (UGGERI, & al., 1990). Durant les interglaciaires, avec la reconquête de la végétation, le concrétionnement reprend, les dépôts détritiques sont cimentés en conglomérats (MAIRE & QUINIF, 1990). Les concrétions inactives localisées au-dessus de l'actuelle limite de la forêt se rattachent à d'anciens interglaciaires plus chauds que l'actuel (grotte Vallier).

On observe ainsi, en fonction de l'évolution des conditions environnementales, le passage du type fluvio-karst, fonctionnel jusqu'au début du Pliocène à des karsts perchés par la surrection au cours du Pliocène, en partie inactifs. Par la suite, les réseaux seront partiellement réactivés sous l'effet des glaciations.

2. Les facteurs de contrôle de la karstification alpine

D'une manière générale, la karstification, est contrôlée par deux paramètres fondamentaux, le gradient altitudinal qui détermine la vitesse de circulation et le volume d'eau transitant au travers du karst, responsable de l'agrandissement des conduits. Secondairement, la présence de couvertures bio-pédologiques pourra renforcer l'agressivité des eaux en les acidifiant.

Le gradient altitudinal est obtenu dès lors qu'un relief se développe au-dessus du niveau de base, généralement sous l'effet d'une surrection tectonique (une régression peut accentuer l'ampleur du gradient).

Lorsque la surrection est progressive, les réseaux s'étagent, chaque niveau nouvellement créé est alimenté par les fuites de l'ancien étage supérieur, qui va progressivement se désactiver en raison de sa situation de plus en plus perchée. C'est dans ce contexte que les karsts évoluent depuis la fin du Miocène. En conséquence, si les grands réseaux sont perchés par la surrection, ils restent néanmoins intégrés aux réseaux plus récents qui vont les recouper. Ainsi, dans la Dent de Crolles, on connaît quatre étages successifs interconnectés, dont le plus récent est bloqué sur les marnes imperméables.

En revanche, si les mouvements ont une composante tangentielle, accompagnée d'une tectonisation (plissements, chevauchements...), ou s'ils sont très rapides, les anciens réseaux sont segmentés par la tectonique et détruits par les effondrements. L'apparition d'une structure différente conditionne la naissance de réseaux adaptés au nouveau contexte, totalement distincts des réseaux antérieurs. Ainsi, les réseaux miocènes (ou plus anciens), antérieurs au paroxysme alpin, ne sont généralement pas intégrés aux grands réseaux post-miocènes

et apparaissent à l'état de vestiges fragmentés, avec des conduits colmatés par les effondrements (*Ruinenhöhlen*...).

De tels bouleversements tectoniques modifient aussi bien les structures que les grandes lignes du relief. C'est ainsi que les directions de drainage peuvent se renverser, comme pour les Alpes juliennes, qui sont drainées vers l'est en direction du bassin pannonien avant le paroxysme alpin, puis ultérieurement vers l'Adriatique, au sud-ouest (HABIC, 1992).

Les oscillations du niveau de base peuvent aussi provenir des variations climatiques. Les régressions messinienne et glacio-eustatiques ont eut un impact capital sur les karsts de la bordure méridionale des Alpes, en engendrant des circulation profondes, en-dessous du niveau de base actuel. Le surcreusement glaciaire des vallées alpines produit le même effet. A la suite de la transgression pliocène, ou lors des interglaciaires, le niveau de base remonte. Les karsts littoraux s'ennoient (Calanques provençales), l'alluvionnement exhausse les vallées alpines. De ce fait, les exutoires sont enfouis sous les sédiments, donnant des réseaux "encapuchonnés", avec une base noyée et un colmatage d'une partie des conduits. Les sous-écoulements permanents diffusent dans la nappe alluviale alors que les sources de trop-plein se disposent au niveau actuel de la vallée, comme pour les réseaux savoyards du Haut-Giffre (MAIRE, 1990). Il en résulte, en dehors des massifs perchés sur des imperméables, que la plupart des karst possèdent une base ennoyée.

Le climat joue également un rôle direct, par le contrôle qu'il exerce sur le volume des précipitations (saisons sèches et humides alternées d'ampleur variable au Tertiaire, glaciations au Quaternaire, crues saisonnières de fonte nivale pendant les interglaciaires). C'est une donnée fondamentale influant sur la vitesse de karstification propre à chaque période.

Tectonique et climat se combinent pour définir les principales caractéristiques de chaque phase, qui sont régies par deux paramètres fondamentaux : les eaux allogènes et les couvertures bio-pédologiques. Les grandes phases de spéléogenèse correspondent aux périodes où les karsts bénéficient d'un surcroît d'alimentation s'additionnant aux infiltrations locales.

Jusqu'à la fin du Miocène, c'est dans un contexte de reliefs peu soulevés que fonctionnent les fluvio-karsts, grâce à la juxtaposition de zones imperméables aux massifs calcaires. Le climat favorise le développement des altérites et de la végétation. La karstification par crypto-corrosion est extrêmement active, grâce à l'effet acidifiant des couvertures détritiques et de la végétation sur les eaux infiltrées.

La surrection pliocène interrompt ce mode de fonctionnement en perchant les karsts au-dessus des grandes circulations fluviatiles régionales. Les couvertures sont progressivement décapées, sous l'effet conjugués de la surrection et de la dégradation climatique.

Au cours du Pléistocène, les grands glaciers alpins atteignent des altitudes élevées et réactivent une partie des réseaux perchés alimentés par les eaux de fusion glaciaire. L'abrasion glaciaire achève le déblaiement des altérites, à tel point que dans nombre de massifs karstiques, les seuls témoins de ces couvertures tertiaires sont les remplissages piégés dans les anciens réseaux.

C'est ainsi que les réseaux karstiques et en particulier les niveaux étagés de conduits horizontaux, peuvent être considérés comme des indicateurs de la position d'anciens niveaux de base, qui renseignent quant à eux sur les conditions géodynamiques et paléoclimatiques d'alors.

3. Méthodes d'étude et perspectives d'avenir

Actuellement, les méthodes d'étude les plus porteuses pour la connaissance de l'évolution et du fonctionnement passé des karsts sont les suivantes :

- l'approche géomorphologique, qui consiste à repérer les emboîtement successifs des formes afin de reconstituer une chronologie relative précise des événements. Cette méthode, certes classique, n'en demeure pas moins fondamentale, les nombreuses résultats novateurs récents sont là pour le prouver.
- la spéléomorphologie, dont l'approche est indissociable de la précédente, permet, entre autres, de repérer la position des niveaux de circulation passés, en s'appuyant en particulier sur les drains horizontaux, marquant la limite zone vadose / zone noyée. Quoique de portée plus locale, elle complète les données régionales "externes", bien souvent déficientes pour les périodes anciennes.
- enfin, l'étude des remplissages karstiques renseigne sur les conditions hydrodynamiques, paléoclimatiques, permettant de reconstituer plus précisément le fonctionnement karstique propre à chaque phase. A ceci s'ajoute la possibilité de datations absolues, bien que les méthodes actuelles ne soient guère performantes au-delà du Pléistocène moyen, laissant dans l'obscurité la plus grande partie de l'histoire des karsts.

La principale difficulté réside dans l'analyse précise des fonctionnement propres à chaque phase, qui n'est réellement possible que lorsque chacune se différencie des autres par un niveau bien individualisé de conduits. Malheureusement, au Pléistocène, les variations rapides et considérables de la position du niveau de base, vont imbriquer les témoins de chaque phase qu'il sera difficile de différencier. Les secteurs où les niveaux de karstification sont bien individualisés grâce à l'existence de calcaires sur de grandes dénivellations offrent pour celà plus de potentialités, tout comme les marqueurs chronologiques bien établis : régression messinienne, paléomagnétisme pour le Pléistocène. De nouvelles méthodes comme la téphrochronologie devraient apporter de nouvelles données. Enfin, une réflexion sur la signification précise des différentes formes de conduits élaborés en zone épinoyée et noyée en tant que marqueurs de la position du niveau de base mérite d'être entreprise (cf. article du même auteur dans ces Actes).

Références

AUDRA, PH. 1994. Karsts alpins, genèse de grands réseaux souterrains. Exemples : le Tennengebirge (Autriche), l'Ile de Crémieu, la Chartreuse et le Vercors (France). *Karstologia Mémoires*. 5. Thèse de l'Université de Grenoble, 280 p.

AUDRA, PH. 1995. Signification des remplissages des karsts de montagne. *Karstologia*. 25 : 13-20.

BINI, A. 1994. Rapports entre la karstification périméditerranéenne et la crise de salinité du Messinien. L'exemple du karst lombard (Italie). *Karstologia*, 23 : 33-53.

BINI, A. & UGGERI, A. 1992. Sédimentation en milieu périglaciaire : l'exemple de la grotte Shanghai (Monte Campo dei Fiori, Varese, Lombardie, Italie). *Journées Pierre Chevalier, Grenoble*, 118-137. Spéléo-club de Paris.

CLAUZON, G. 1996. Limites de séquences et évolution géodynamique. *Géomorphologie*. 1 : 3-22.

DELANNOY, J.-J. 1992. Apport de l'endokarst dans la reconstitution morphogénique d'un karst. Exemple de l'antre de Vénus (Vercors, France). *Etudes de géographie physique, travaux de l'URA 903*. XX : 47-60.

DELANNOY, J.-J.; GUENDON, J.-L. & QUINIF, Y. 1988. Les remplissages spéléologiques : un apport à la connaissance de la karstogenèse du massif des Coulmes (Vercors, Alpes). *Colloque international de sédimentologie karstique, Han-sur-Lesse, 1987, Annales de la Société géologique de Belgique*, Liège. 111 : 21-38.

EUSEBIO A. & VIGNA B. 1996. Il fenemeno carsico nel Piemonte meridionale : evoluzione e conoscenze. *International Congress : Alpine caves ; alpine karst systems and their environnmental context, Asiago 1992* : 193-202.

FRISIA, S.; BINI, A. & QUINIF, Y. 1994. Morphologic, crystallographic and isotopic study of an ancient flowstone (grotta di Cunturines, Dolomites). Implications for paleoenvironmental reconstructions, *Spéléochronos*, 5: 3-18.

HABIC, P. 1992. Les cavités paléokarstiques dans le Karst montagnard de Slovénie. In : Karst et évolutions climatiques. Hommage à Jean Nicod. Presses universitaires de Bordeaux : 411-428.

HASEKE-KNAPCZYK, H. 1989. Der Untersberg bei Salzburg. Wagner, Innsbruck, 224 p.

HLADNIK, J. & KRANJC, A. 1977. Fluvio-glacial sediments. A contribution to speleochronology. *7th. International Speleological Congress, Sheffield* : 240-243.

JEANNIN, P.-Y. 1990. Néotectonique dans le karst du nord du lac de Thoune (Suisse). *Karstologia*. 15 : 41-54.

JEANNIN, P.-Y. 1991. Mise en évidence d'importantes glaciations anciennes par l'étude des remplissages karstiques du réseau des Siebenhengste (chaîne bordière helvétique). *Eclogæ geologicæ helvetiæ*. 84, 1 : 207-221.

LANGENSCHEIDT, E. 1986. Höhlen und ihre Sedimente in den Berchtesgadener Alpen. *Forschungsbericht*, 10. Nationalpark Berchtesgaden : 95 p.

MAIRE, R. 1990. La haute montagne calcaire. *Karstologia Mémoires*. 3. Thèse d'Etat à Nice, 731 p.

MAIRE, R. & QUINIF, Y. 1990. Les conglomérats souterrains. Morphologie, genèse et âges U / Th d'après quelques exemples alpins et pyrénéens. *Spéléochronos*. 2 : 3-11.

UGGERI, A.; BINI, A. & QUINIF, Y. 1990. Datation des sédiments de la grotte Marelli (Italie, Lombardie, Varese). *Spéléochronos*. 2 : 21-28.

UGGERI, A. 1992. Analisi geologico ambientale di un massiccio carbonatico prealpino (M. Campo dei Fiori, Varese) : geologia, geologia del Quaternario, idrogeologia. Tesi di dottorato, Milano, 153 p.

Aufbau und Speleogenese eines hochalpinen Karstsystems (Kolkbläser-Monsterhöhle-System, Steinernes Meer, Österreich; L = 43.4 km, HD = -711 m)

von Dipl. Geol. M. Denneborg
Speleologische ArbeitsGruppe Aachen (SAGA) Laatbankstraat 40 NL - 6291 ED Vaals

Zusammenfassung
Das 1982 entdeckte Kolkbläser-Monsterhöhle-System (KMS) im Steinernen Meer zeigt wesentliche Aspekte der Entstehung der hochalpinen Karstsysteme in den nördlichen Kalkalpen in Österreich. Typisch für die nördlichen Kalkalpen ist eine prinzipielle Gliederung in drei Etagen, die im wesentlichen mit den Hebungs- und Stillstandphasen der alpinen Gebirgsbildung korreliert (Ruinenhöhlenetage, Riesenhöhlenetage, Quellhöhlenetage). Im Steinernen Meer konnten bisher die oberste und unterste Etage nachgewiesen werden.

Abstract
The Kolkbläser-Monsterhöhle-System discovered in 1982, shows main aspects of the karstification of the Alpine karst systems in the Nördliche Kalkalpen of Austria. Typical for the caves of the Nördliche Kalkalpen are three main levels which correspond more or less with the uplift of the Alps (level of cave ruins, level of giant caves, level of spring caves). In the Steinernes Meer the upper and lower levels exist (resp. are discovered).

1. Einleitung

In den Höhlen der nördlichen Kalkalpen (Abb. 1) läßt sich eine generelle Gliederung in drei Etagen feststellen, die eine Korrelation mit den Hebe- und Stillstandsphasen der Alpen nahelegt (u.a. Bd. 2 SALZBURGER HÖHLENBUCH, 1977). Im Steinernen Meer finden sich ebenfalls Hinweise, die diese These stützen. Folgende Etagen werden unterschieden: Ruinenhöhlenetage (Kap. 2), Riesenhöhlenetage (Kap. 4) und Quellhöhlenetage (Kap. 5). Im Steinernen Meer finden sich ebenfalls Hinweise, die diese These stützen. Hier wurde zwischen den beiden obersten Etagen noch eine Zwischenetage (Kap. 3) festgestellt.

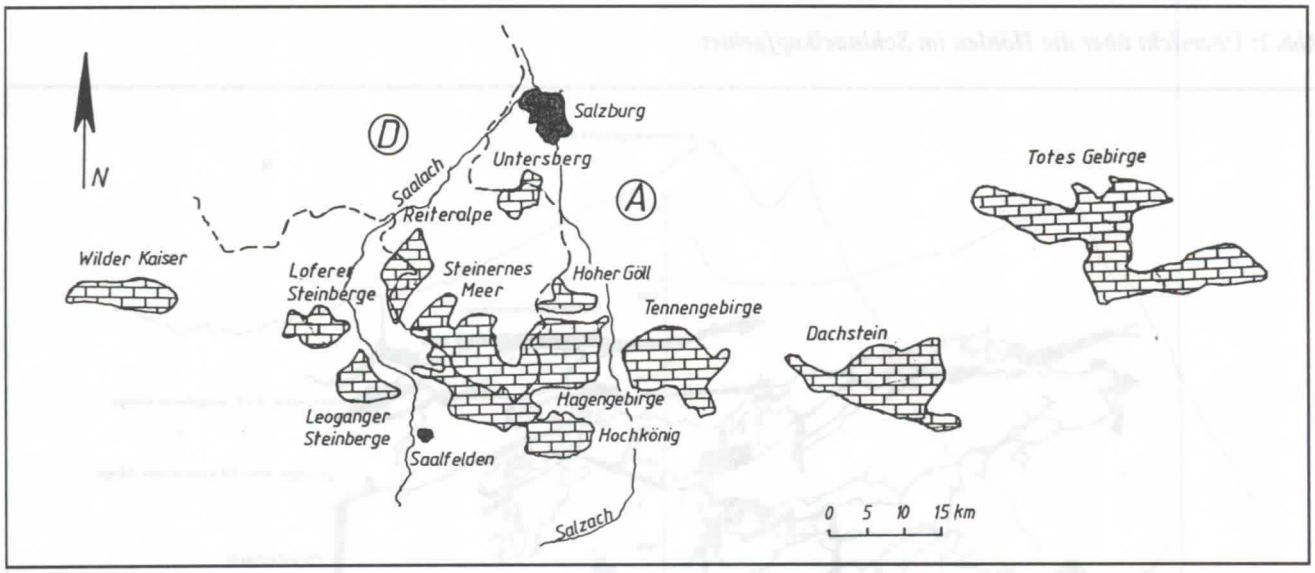

Abb. 1: Lage der nördlichen Kalkalpen

2. Ruinenhöhlenetage (2100-2250 m ü. M.)

Das Kolkbläser-Monsterhöhle-System (KMS) ist das derzeit größte bekannte Höhlensystem in der Ruinenhöhlenetage, da die Randgipfel im Steinernen Meer über 2300 m reichen und diese Gänge erhalten geblieben sind, während sie in den übrigen Kalkplateaus weitgehend erodiert wurden. Typisch sind große, horizontale und versturzgeprägte Gänge von bis zu 20 x 20 m Durchmesser. Im KMS sind drei, mehrere hundert m lange Gangstücke erhalten geblieben, die im parallelen Abstand von ca. 700 m von Süden nach Norden ziehen (*Giga, Supertramp, Vorwärts*, Abb. 2, Abb. 3). Im Süden werden die Gänge von einer hundert Meter hohen Steilwand abgeschnitten; im Norden enden sie in großen Schneekegeln. Nach schneearmen Wintern kann das KMS vom Plateau aus erreicht werden. Teilweise lassen sich die großen Gänge noch als Höhlenruinen auf dem Plateau verfolgen (*Grünschartenhöhle*, Abb. 2).

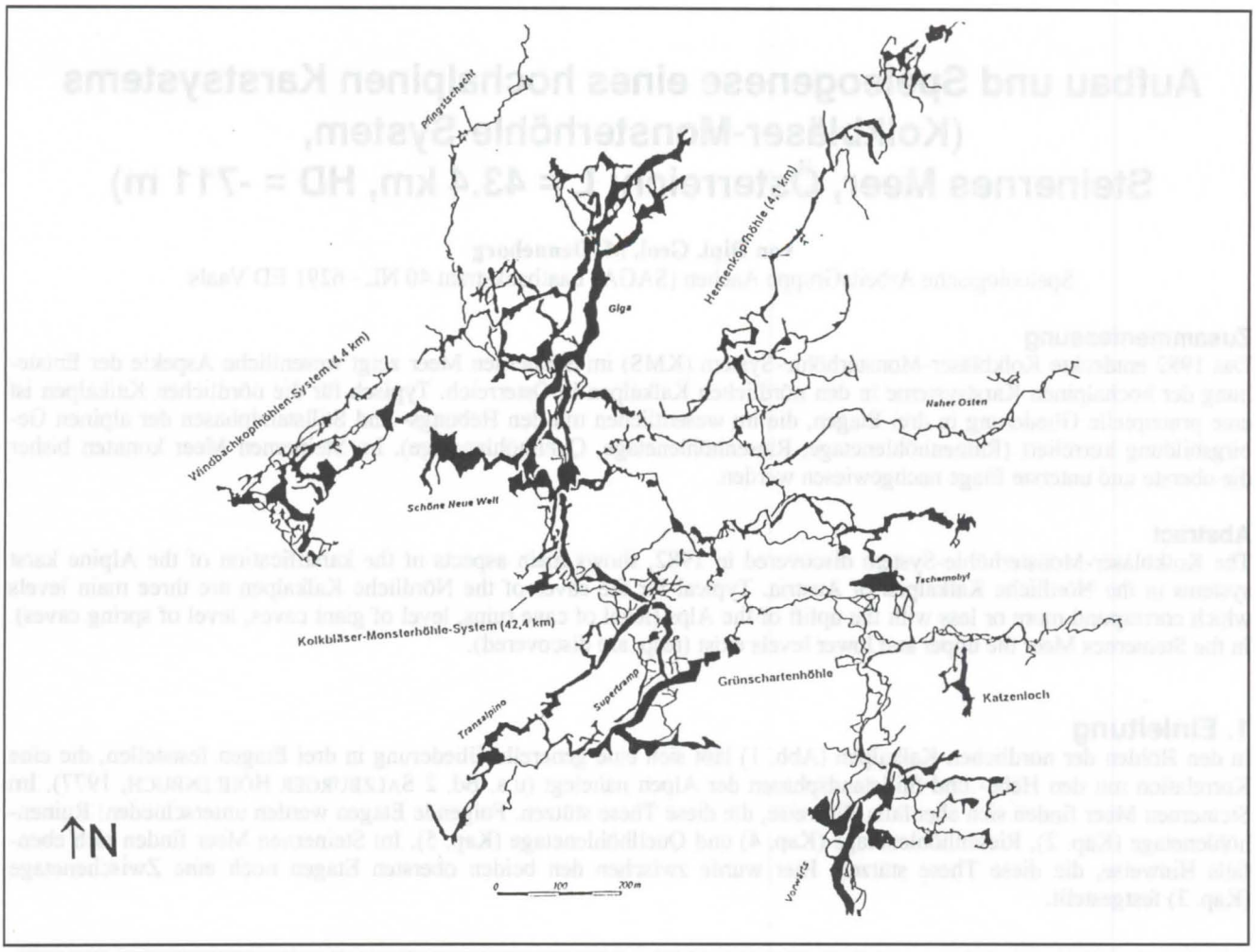

Abb.2: Übersicht über die Höhlen im Schindelkopfgebiet

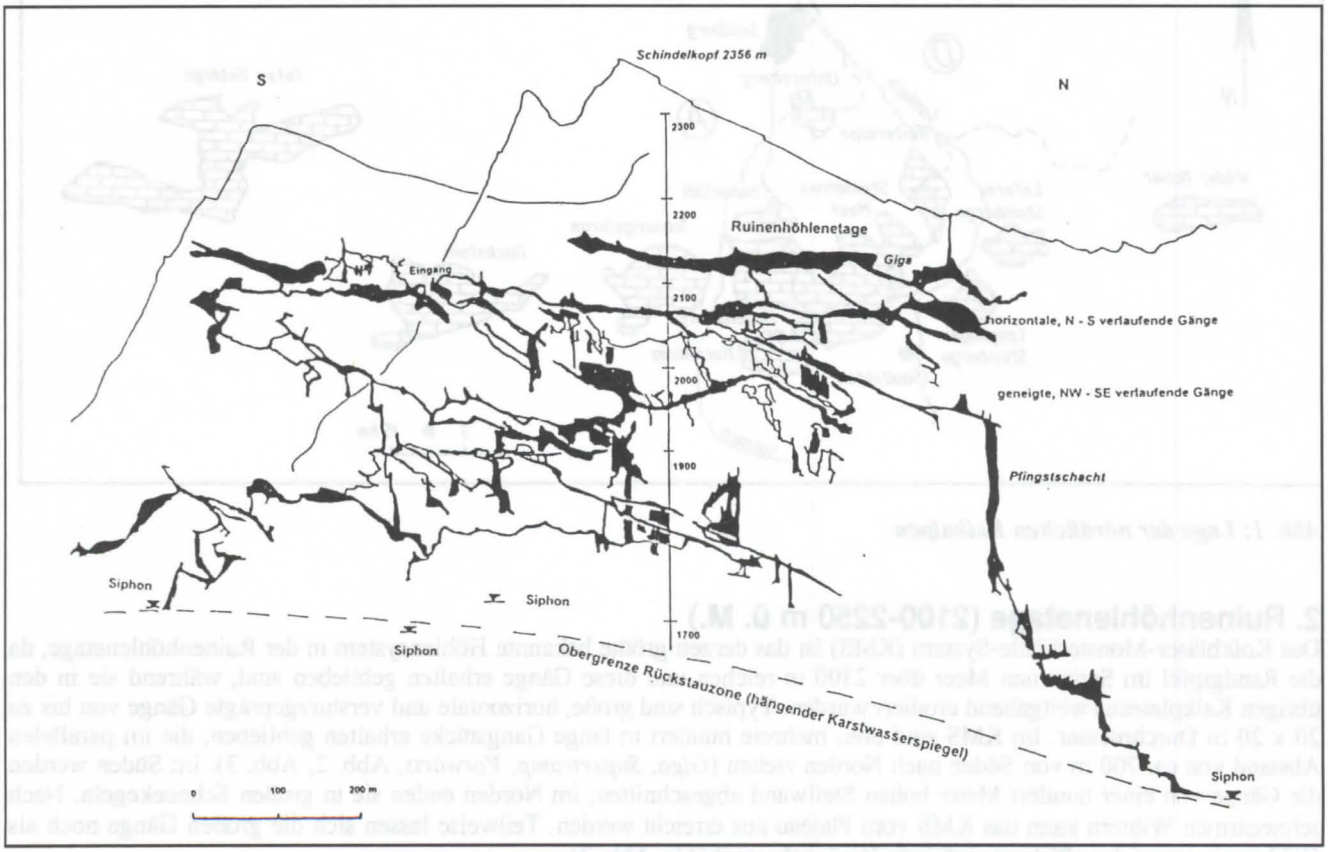

Abb. 3: Schematischer Nord-Süd Aufriss des Kolkbläser-Monsterhöhle-Systems

Die Gänge der Ruinenhöhlenetage entstanden, als vor Hebung der Alpen und vor Ausbildung der tiefen Quertäler Flüsse aus weit südlich gelegenen Einzugsgebieten außerhalb der Kalkgebiete auf ihrem Weg nach Norden in die Kalke eintraten und diese durchflossen haben (Flußhöhlen). Als Beleg finden sich Quarzgerölle, die aus den mehrere Kilometer entfernten Zentralalpen stammen (Abb. 4).

Die weitaus größten Wassermassen flossen in den mehr oder weniger horizontalen Gängen mit leichtem Gefälle nach Norden auf eine Ur-Donau (?) zu. Da für die Gangausbildung letztlich immer die Höhenlage des Vorfluterniveaus entscheidend ist, wurden die mit ca. 30 bis 40 Grad nach Norden einfallenden Schichtpakete durchschnitten, auch wenn sich die Gangausbildung lokal an den geologisch-tektonischen Gegebenheiten orientierte.

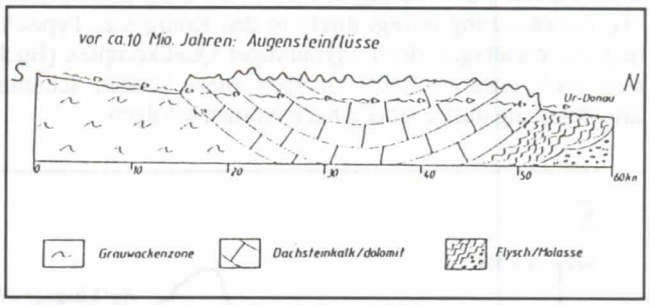

Abb. 4: Entstehung der Ruinenhöhlenetage

3. Zwischenetage im Steinernen Meer

Die bislang im KMS entdeckten Gänge unterhalb der Ruinenhöhlenetage reichen bis auf ein Niveau von ca. 1700 m; das *Pfingstschachtsystem* bis 1492 m. Sie werden zu einer Zwischenetage zusammengefaßt, zu der folgende Gangsysteme gerechnet werden:

- **horizontale, N-S gerichtete Gänge (2050-1900 m ü. M.)**
  Die Gänge unterlagern die Ruinenhöhlenetage und sind fast zeitgleich entstanden, der Durchmesser ist mit 8 bis 12 m jedoch geringer.

- **geneigte, NW-SE gerichtete Gänge (2100-1700 m ü. M.)**
  Die Gänge sind an der mit ca. 30o nach Norden einfallenden Schichtung orientiert (Durchmesser: 3 bis 8 m). Diese Gänge stellen - nach der Ruinenhöhlenetage - die spätere fossile Hauptentwässerung dar (regionale Fließsysteme) und reichen vermutlich weit nach Norden unter das Plateau. Leider endeten die Vorstöße bislang in einer ausgedehnten, min. 100 m mächtigen Lehm- und Geröllzone zwischen 1800 und 1700 m. Die Anlage der Gänge erfolgte wahrscheinlich gleichzeitig mit den horizontalen, überlagernden Gangsystemen durch tieferreichende Grundwasserzirkulationssysteme (tiefphreatisch), über die zunächst jedoch nur ein geringer Anteil der Grundwasserbewegung erfolgte. Erst bei der Heraushebung der Alpen wurden die Druckröhren ausgebildet, die noch später durch Gravitationsgerinne vados überprägt wurden (Schlüssellochprofile).

- **horizontale, E-W gerichtete Gänge (2000-1700 m ü. M.)**
  Diese Gänge sind Zubringer mit einem Durchmesser von 2 bis 5 m, die annähernd rechtwinklig (z.B. Naher Osten) auf die NW-SE gerichteten Gängen stoßen, die eine lokale Vorfluterfunktion hatten. Ergebnis ist ein spalierartiges Entwässerungsnetz. Die Höhenlage der Zubringer nimmt nach Norden hin mit den fallenden Vorflutern von ca. 2000 auf 1750 m ab.

- **Schacht- Mäandersysteme**
  Die aktiven und z.T. fossilen Schacht-Mäandersysteme verbinden die eher horizontal ausgerichteten Gänge. Bislang wurden vier schwebende Siphons mit ausgedehnten Rückstauzonen im Bereich der Kalk/Dolomitgrenze angetroffen, die auf eine - zumindest kleinräumige - Verkarstung des unterlagernden Dolomites hinweisen. Die Höhenlage der Siphons nimmt nach Norden mit der fallenden Kalk-Dolomitgrenze ab (Abb. 3).

4. Riesenhöhlenetage (1400-1600 m ü. M.)

In dieser Etage befinden sich in Österreich viele große Höhlensysteme (Tantalhöhle, Dachsteinmammuthöhle, Eisriesenwelt, etc.). Charakteristisch sind große, subhorizontale Gänge mit deutlichen Gegensteigungen und mächtigen Lehmablagerungen. Sie entstanden unter phreatischen Bedingungen. Ein Zustrom von Einzugsgebieten außerhalb der Kalkgebiete bestand wahrscheinlich immer noch.

Im Steinernen Meer ist diese Etage unseres Erachtens nicht vorhanden, da die hochanstehenden und geringer verkarstungsfähigen Dolomite am Südrand des Steinernen Meeres einen Wasserzustrom von außerhalb der Kalkgebiete verhinderten und die Verkarstung nur durch die Niederschlagswässer im Bereich der Kalke erfolgte, so daß die entsprechenden Gänge am Nordrand des Plateaus auch kleinräumiger ausgebildet sind als in der Riesenhöhlenetage.

5. Quellhöhlenetage (850-1000 m ü. M.)

Die Quellhöhlenetage weist in den nördlichen Kalkalpen sowohl aktive als auch überlagernde, ausgedehnte fossile Höhlen auf (Bergersystem, Hirlatzhöhle). Im Steinernen Meer ist die heutige Entwässerung sowohl nach Norden als auch nach Süden gerichtet. Im Norden liegt die Salzgrabenhöhle (ca. 9 km Länge) als ein fossiler Quellaustritt ca. 100 m über dem Vorflutniveau, dem Königssee (Abb. 5). Über absteigende Gänge kann der heutige Karstwasserspiegel erreicht werden. Die Entwässerung erfolgt direkt in den Königssee. Typisch sind Druckröhren ohne große Lehmablagerungen. Im Süden liegt ein ergiebiger, doch engräumiger Quellkomplex (Buchweißbachquellen) mitten im Dolomit. Die Wasserscheide ist noch nicht bekannt. Beide Quellkomplexe können Schüttungen bis zu mehreren m^3/s aufweisen. Der größte Anteil der Entwässerung dürfte jedoch nach Norden erfolgen.

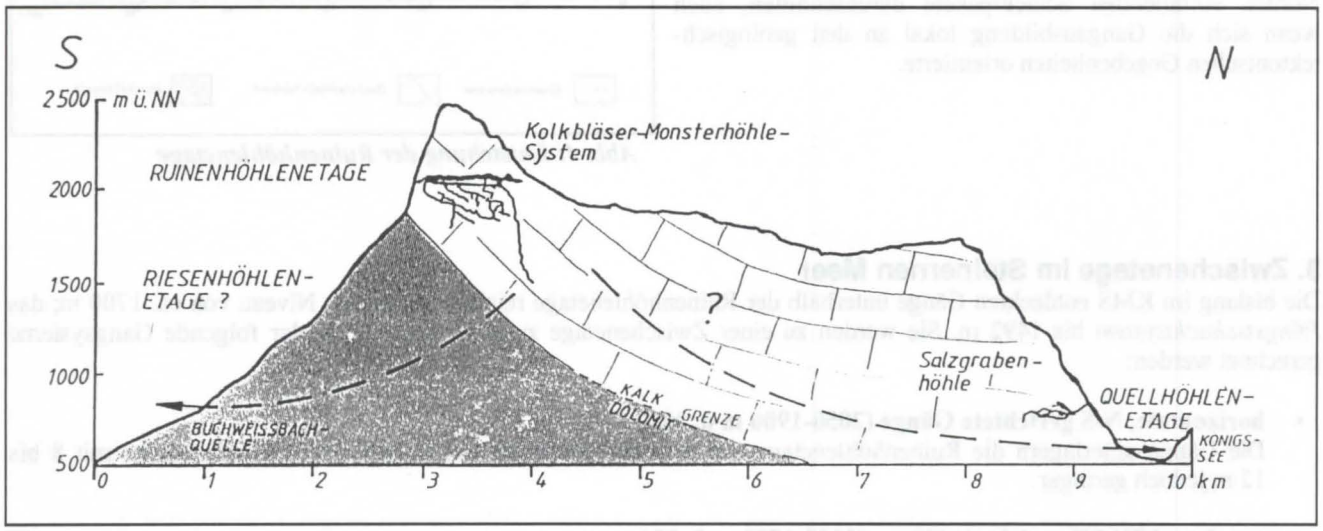

Abb. 5: Schematischer Nord-Süd Schnitt durch das Steinerne Meer

6. Schlußfolgerungen

Die bisherigen Forschungen im Steinernen Meer (und im Vergleich mit anderen Höhlensystemen) zeigen, daß die Entwicklung und der Aufbau der Höhlensysteme im wesentlichen vom Aufbau der regionalen und lokalen Grundwasserfließsysteme bestimmt wird. Hierbei spielt die Lage des Vorfluters die entscheidende Rolle. Geringe Potentialdifferenzen (Höhenunterschiede) führen zu eher horizontalen Systemen, wobei je nach Mächtigkeit des Grundwasserleiters und Aufbau der regionalen Fließsysteme bereits die tieferen Niveaus in ihrer Grundstruktur angelegt werden. Hohe Potentialdifferenzen führen zu eher vertikal entwickelten Systemen, die sich im Quellbereich durch ausgedehnte und tiefe Siphons auszeichnen (aufsteigende Grundwasserbewegung in den Aussickerungsgebieten). Modifiziert wird dieser Aufbau durch geringerdurchlässige, unterlagernde Schichten, die wie im Steinernen Meer einen Zustrom von außerhalb verhinderten und eher zur Ausbildung „collecteur" artiger Systeme führte.

Literatur

LANDESVEREIN FÜR HÖHLENKUNDE SALZBURG.1979. Salzburger Höhlenbuch, Bd. 3, Salzburg: 77-79

Karst and glaciations in the Southern pre-alpine valleys

Alfredo Bini, Paola Tognini & Luisa Zuccoli
Dipartimento di Scienze della Terra, Università di Milano, via Mangiagalli, 34, 20133- Milano, Italy
Gruppo Grotte Milano SEM - CAI, via Foscolo, 3, 20100 - Milano, Italy

Abstract

At least 13 glaciations occurred during the last 2.6 Ma in the Southern pre-alpine valleys, the glaciers being valley and warm ones. Unlike it was previously assumed till few years ago, the origin of these valleys is due to fluvial erosion related to Messinian marine regression. The valley slopes modelling is Messinian in age, too, while caves are older. The only glacier action on caves was a sediment in-filling sub-sequently eroded.

During glaciations, karst systems in these valleys could be: a) isolated, without any glacial water flowing; b) flooded, connected to the glacier water-filled zone; c) active, scoured by a stream sinking at glacier sides or in a sub-glacial position. The stream could flow to the flooded zone (b), or scour all the unflooded system long (thanks to the non-continuous arrangement of the water-filled zone) down to the resurgence zone, the latter being generally located in a sub-glacier position.

The glacier/karst system is a very dynamic one: it could get active, flooded or isolated depending on endo- and sub-glacial drainage variations.

Glaciations

As for the study of Quaternary geological and climatic events, the current trend is to reject the traditional Penck & Brückner's theory for a new construction in terms of "stratigraphycal units" instead of "glaciations" (BOWEN, 1978; SIBRAVA *et al.*, 1986; BINI, in press).

As a result, words such as Würm, Riss, etc..., are now meaningless, being the term "glaciation" assigned to a single glacier advance and recession, whose deposits are distinguishable from the ones related to other glaciations by evidence of extensive recession or of periods of warmer climate (RICHMOND, 1986). Each geological body is picked up on the basis of its sedimentological and paleontological features, and can only be arranged in a relative sequence with just a local currency, if a geochronological dating is lacking (RICHMOND & FULLERTON, 1986).

Thanks to this new conception, in the pre-alpine valleys (Fig. 1) at least 13 glaciations are singled out for the last 2.6 Ma. Each of them gets its name from the respective geological unit, and has a strictly local currency (DA ROLD, 1990; BINI, in press): glaciations thus have a different name in each valley, being the most recent of them generally referred to as LGM (Last Glacial Maximum) as for the Alps. The two oldest glaciations are Pliocenic in age, indicatively corresponding to isotope stages 96-100, while the LGM is related to isotope stage 2.

Glaciations and pre-alpine valleys

The presence of these valleys and of the lakes occupying the floor of some of them (Orta, Maggiore, Come, Iseo, Garda Lakes) (Fig.1) was traditionally related to glacial erosion. It is at present well agreed these valleys are on the contrary related to the Messinian marine regression (Miocene), their origin thus being due to fluvial erosion (BINI, 1994 for a general review). This theory is proved by the valleys continuing under the Po Plain, well South to the limit reached by glaciers, and by the spotting of relict marine lower Pliocene deposits in the valleys. As a general rule, glaciers worked on valley slopes as a re-modelling agent, but on many spots Tertiary hot-wet tropical climate features and palaeosols are well preserved, sometimes with a marine Pliocene cover.

Glaciers

The glaciers scouring alpine and pre-alpine valleys all had the same trait, being valley temperated glaciers. Their tracks and feeding areas were always the same, just like the petrological contents of the removed materials. While at the amphitheatre different glaciers of different glaciations show different extents

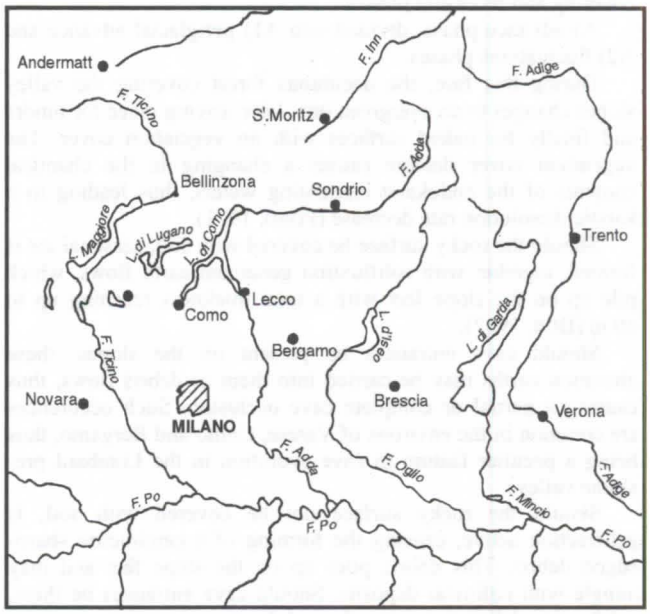

Fig. 1 - The main Lombard pre-alpine valleys

(up to 15 km South to the main lakes), on the valley slopes the altitude where we can find glacial deposits related to different glaciations is similar for all the glaciers, even if it is not possible to draw a global glacial extent limit, because of non-uniform erosion on deposits and because of post-upper Pliocene neotectonic movements. The Maximum Extention Glacier (MEG) limit in the central area of Como Lake (M. Croce di Muggio) is 1630 m a.s.l., while the LGM is 1485 m. In a Southern area, the MEG limit ranges from 1150 m (Pian del Tivano) (Fig.2) to 1310 m (Passo del Cainallo, Grigna), while the LGM limit in the same area ranges from 1000 to 1240 m a.s.l., with an altitude difference not exceeding 150 m.

Karst

The karstic evolution begins as soon as the area is lifted above sea level (upper Olig. - lower Mioc.), in a palaeogeographical environment well different from the present one, though the main valley floors were already working as a base level. During Messinian age, the excavation of deep canyons along pre-existing valleys (Fig. 2) caused a dramatic lowering of the base level, followed by a complete re-arrangement of the karstic networks, which got deeper and deeper. The Pliocene

marine transgression caused a new re-arrangement, the karst network getting mostly under sea level.

During these periods, in the region the climate was a hot-wet tropical one, characterized by a great amount of water circulating during wet season. At the same time, tectonic upliftings were at work, causing breaking up of the karst networks and a continuous re-arrangement of the underground drainage system.

Anyway, karstic networks were already well developped long before the beginning of Plio-Quaternary glaciations.

Connections of glaciers to endokarst networks

The deep pre-alpine valleys are mostly cut in limestone and dolomitic rocks containing well developped karstic networks. These networks are cut under valley slopes, while they are absent under valley floors, the latter being covered by thick Plio-Quaternary deposits.

Glaciers show different influences on karstic networks, thus working with a different effect during their advance, fluctuations, covering and recession phases.

A) advance phase, divided into A1) periglacial advance and A2) fluctuations phases.

During this fase, the deciduous forest covering the valley slopes changes to an evergreen one, later leaving place for tundra and finally for naked surfaces with no vegetation cover. The vegetation cover decline causes a changing in the chemical contents of the endokarst circulating waters, thus leading to a karstic dissolution rate decrease (FORD, 1971)

Should the rocky surface be covered with soil, seasonal ice is formed, together with solifluxtion generated earth flows, which pile up on the slope feet with a total thickness reaching up to 10 m (BINI, 1987).

Should cave entrances be present on the slopes, these alteration earths may be carried into them as debris flows, thus causing a partial or complete cave occlusion. Such occurences are common in the environs of Varese, Como and Bergamo, thus being a peculiar feature in cave evolution in the Lombard pre-alpine valleys.

Should the rocky surface not be covered with soil, is gelifraction active, causing the forming of a centimetric sharp-edged debris. This debris piles up on the slope feet and may mingle with colluvial deposits. Should cave entrances be there, gelifraction debris may enter the endokarst.

The entrance parts of many caves may moreover get turned into a "glacière" filled with snow-storing- or percolating water freezing-derived ice (dynamic and stato-dynamic "glacières"), thus undergoing a re-arrangement of their water drainage.

In the A2 phase, the advancing glacier gets closer and closer to cave entrances, though its advance is not continuous, and several fluctuations of the glacier front and related lateral tills generally occur.

Glacial debris may be injected into cave entrances (FORD & WILLIAMS, 1989), karstic springs may be filled up and debris may be carried deeper and deeper by karst circulating waters. During this phase, debris is mainly built of meltout- and flow tills: since they are generally pervious, many debris-filled spring caves are still working.

An increase in the amount of endokarst circulating water may occur, but the direct sinking of glacial streams is generally not so common an occurence, specially on valley slopes. Anyway, meltwater effects on karst networks in the pre-alpine valleys look generally very scanty, and we do not have a conspicuous evidence for either remarkable galleries enlargement or vadose entrenchment, being most underground canyons pre-glacial in origin.

B) Covering phase, till the maximum glacier expanse.

During this phase, the glacier caps the whole karstic systems and it works at its maximum erosion rate, the latter being much more remarkable on valley floors and glacial cirques than on valley slopes (FINCKH et al., 1984). Its main effect is the erasure of surface features (Ford & Willams, 1989), though many of them may nervertheless survive one or more glaciations. Underground galleries may often get unroofed, though this is a much more frequent occurence in glacial cirque areas rather than on valley slopes.

In the pre-alpine valleys, both deposition and erosion are discontinuous as for both time and space, and valley floors do not undergo entrenchment, so that base levels are not lowered any further: as valleys pre-date glaciations, glaciers effects are generally restricted to valley infilling removal (BINI et al.,1994).

During this phase, on pre-alpine valley slopes the main glacier effect is not erosion, but a spreading of a discontinuous lodgement till cover, thus making the slopes impervious and possibly closing cave entrances, springs and sinking points and therefore causing a re-arrangement of the endokarstic drainage system.

C) recession phase, divided into C1) fluctuations and C2) periglacial recession phases.

During recession phases, glaciers undergo in an inverse sense the same sequence as the A-phase, but with some remarkable differences.

1) the recession rate is higher than the advance one

2) during these phases deposition of loess is active, thus possibly improving karstic system in-filling

3) the slope re-colonization by a forest cover (previously drawn back to the central part of the Po Plain) is rather quick, so that during the earlier recession phases the glacier front should be already surrounded by forest (BINI, 1987).

Both surface tills and deposits related to glacial debris transport into endokarstic systems re-arrange both the surface and underground drainage, so that at the end of a glaciation they may not gain a complete recover, thus being very different from the pre-glacial ones (BINI, 1987).

The development of peat-bogs on glacial deposits produces acid water, possibly increasing deep endokarstic dissolution rate, while the till cover prevents limestone surfaces from being dissolved, specially if the former is carbonate in content (FORD & WILLIAMS, 1989).

During recession phases, we do not certainly observe those tremendous meltwater amounts so many authors believe in: a glacier may withdraw without any large fluctuation of its glacial front discharge, since its recession is due to a negative mass-balance.

Karstic networks lying totally above the glacial extent limit are sub-mitted to a periglacial influence all the glaciation long.

D) During post-glacial phase, karstic systems re-gain their previous role, but generally with a different arrangement of their underground drainage, because of glacial debris deposits inside of them. In addition, surface till deposits get eroded and the parent debris is carried into caves.

As a general rule limestone and dolomite slopes are not affected by tensional release collapses, unlike crystalline rock slopes.

We must emphasize a karstic system never behaves the same way during different glaciations, and the glacier influence upon it changes, too.

Formation of endokarst features

Many authors believe, or believed, the development of most surface and underground karst in the Alps is due to glaciations, being the last one held to be mostly responsible for this. In pre-alpine valleys caves we do not have evidence either of development of new caves or of remarkable changes in their features during glaciations. It is of course possible some pits or galleries could develop during this phase, but we do not observe any deep vadose canyon related to meltwater streams: if ever existing, canyons are generally found in caves above the glacial limit or in valleys where glaciers never scoured.

In the meanwhile, the spotting of boulders and peebbles trapped between roof stalactites shows several phases of galleries

infilling and eroding occured with no remarkable changing in pre-dating features, including cave decorations.

Several authors (WARWICK, 1956) deny the importance of the role played by glacier weight, which does not seem to be heavy enough to cause sub-surface karst voids collapse, particularly on valley slopes. According to these assumptions, any evidence of such collapses is not detectable in this area.

The presence of suspended karst systems do not prove a glacial origin of the valleys, since most of them pre-dates any Plio-Quaternary glaciation, as shown by calcite cave deposits older than 1,5 Ma (UGGERI, 1992).

Endokarst water circulation

The main point in the study of connections of glaciers to endokarst networks is about endokarst hydrology during glaciation phases.

A thick warmglacier does not generally has a continuous saturated zone inside, but, on the contrary, only a network of water-filled conducts, variously linked one with the others. A glacier aquifer is therefore a non homogeneous and anisotropic one: a sub-surface water table may exist, but it is generally a non continuous one, while as a rule at the glacier base, outside Röthlisberger & Nye channels only a thin water film is observed, and it is a discontinuous one, too, because of colder zones in the ice body and/or obstacles increasing pressure ice melting. Furthermore the endo-glacier aquifer structure, its water table geometry and the sub-glacier water arrangement are all dynamic features, quickly varying in time and space, often with a seasonal cycle. As a consequence, connections of endo and sub-glacier waters to endokarst ones are varying in time and space, too.

We may assume 3 possible hypotheses for water circulation in a karstic network during the maximum glacier expanse phase:

A) the karstic network is isolated and shows no glacial water circulation

B) the karstic network is completely drowned

C) the karstic network is active and scoured by waters feeding underground streams that can flow into the drowned parts or scour the whole system long to sub-glacial springs.

A) The network may get isolated by an ice stopper or by a lodgement till cover, or it may simply be in touch with parts of the glacier at present devoid of water, so that the karstic system is not scoured by any glacier water stream.

B) Karst systems in the valley slopes may have their water-filled zone in continuity to the glacier's one only provided an endo- or sub-glacier channel is by chance temporarely in direct touch with a cave entrance or a sinking point: such an occurence has very little chance on valleys slopes, being much more probable on a plateau or in a glacial cirque.

Anyway, whatever the water feeding source, if ice makes the slopes impervious and cave entrances are closed by lodgement tills, a rise in the water filled zone upper limit may occur, thus causing a flooding of the lowest parts of the systems, or even of the whole of them. Such an occurence is proved by the spotting of fine-grained deposits inside caves. Furthermore, their sedimentological analyses shows most systems underwent several repeated cycles of flooding and retreating of the floods.

C) The active parts may be restricted to the surface closer zones, or be on the contrary developped the whole system long, down to the resurgence zone, the latter being located in a sub-glacial zone or even outside the glacier covered area.

Endokarst sediments

The only way of testing the soundness of the forementioned hydraulic circulation hypothesis is to study the main characters and the spread of cave sediments, since they are the only real datum on connection of glaciers to endokarst networks.

In caves submitted to periglacial conditions all glaciations long, we can find altered earths flow deposits, sharp-edged gelifraction debris and, more seldom, alluvial deposits whose origin is not related to a glacial melt-water circulation.

In caves lower than or close to the glaciers limit we generally find large amounts of glacier-related deposits, often partly or totally occluding cave galleries. These sediments may be directly related to glaciers, i.e. carried into caves by glacial meltwaters, or be the result of surface glacial deposit erosion. They generally show 3 dominant facies: A) lacustrine deposits B) alluvial deposits and C) debris flow deposits facies.

A) Lacustrine deposits are not present in all karstic systems, and are found only at some spots, but they can be very thick and widely extended. They are built of flat-laminated carbonatic silts, indicating a deposition in very cold and thus non-aggressive waters. These lacustrine sequences often enclose alluvial deposits, such as gravels rich in exotic materials. Dendritic surge marks may show flooding and retreating phases, while the deposits sealing by calcite films suggests us the occurence of several glacial events.

The presence of lacustrine deposits is due to a total flooding of the system up to the deposits altitude. At lower altitudes only alluvial sediments are spotted, and we can therefore assume the down-laying of lacustrine deposits only occurred close to the air-water limit in a system filled with water to an altitude related to the glacier upper limit, assuming that slopes were made completely impervious.

As a general rule, such an effect is utterly discontinuous in time and space, thus causing repeated phases of flooding and of slow or sudden retreating of the floods, in an extremely dynamic situation.

B) Alluvial deposits are scattered throughout all caves at altitudes lower than the glaciers limit. They are built of fine- to coarse- grained gravels with exotic grains, and by both matrix-supported, massive, poorly bedded sands and clean, grain-supported, well bedded and sometimes imbricated gravels. The older deposits are often cemented and their spread shows that most galleries were sub-mitted to one or more infilling and eroding phases. Often it is not possible to sort glacial water alluvial deposits out of deposits having the same petrographic and granulometric features, but originated by different processes, i.e. by debris flow, glacial or alluvial-glacial deposits erosion. As a rule, the latter processes are generally younger than the maximum glacier expanse phase and are much more likely to occur than the former ones, because direct debris transport into caves by glacial streams is generally a rare occurence, specially on valley slopes.

C) Flow deposits show the same cave spread as alluvial deposits and are built of a matrix-supported diamicton with both local and exotic grains, devoid of either any bedding or sedimentary structure. Sometimes their grains are weathered and shows deposits older than the last glaciation were carried into caves from the surface. They may come directly from glaciers (flowtills) or from tills laid down during maximum expance phases and later eroded during recession and post-glacial phases.

Conclusions

The Plio-Quaternary glaciations do not seem to have affected karstic systems in the Southern pre-alpine valleys with any remarkable speleogenetic effects. Since the caves pre-date glaciations and were already well developped long before, the glaciers effects on them are generally restricted to the transport of great amounts of debris and sediments into caves.

These deposits may cause a partial or total occlusion of most galleries, thus causing a remarkable re-arrangement of the underground drainage system.

References

BINI A. 1987. L'apparato glaciale wurmiano di Como. Tesi di Dottorato di ricerca, Università degli Studi di Milano: 569 pp.

BINI A. 1994. Rapports entre la karstification périméditerranéenne et la crise de salinitè du Messinien: l'exemple du karst lombard. Karstologia 23 (1): 33-53.

BINI A., BREVIGLIERI P., FELBER M., FERLIGA C., GHEZZI E., TABACCO I. & UGGERI S. 1994. Il problema dell'origine delle valli. In: Riunione autunnale del gruppo nazionale geografia fisica e geomorfologia. CNR. Escursione sul tema: I depositi plio-quaternari e l'evoluzione del territorio varesino. Varese, 98-149.

BOWEN D.Q. 1978. Quaternary Geology. Pergamon Press.

DA ROLD O. 1990. L'apparato glaciale del Lago Maggiore, settore orientale. Tesi di Dottorato, Università degli Studi di Milano, 190 pp.

FINCKH P., KELTS K. & LAMBERT A. 1984. Seismic stratigraphy and bedrock forms in perialpine lakes. Bull. Geol. Soc. Am. 95: 1118-1128.

FORD D. 1971. Characteristics of Limestone solution in the Southern Rocky Mountains and Selkirk Mountains, Alberta and British Columbia. Canad. J. Earth Sci. 8(6): 585 -609.

FORD D. & Williams P. 1989. Karst Geomorphology and Hydrology. Unwin Hyman publ.

RICHMOND G.M. 1986. Stratigraphy and chronology of glaciations in Yellowstone National Park. In: (Sibrava V., Bowen D.Q., Richmond G.M. eds): Quaternary glaciations in the Northern Hemisphere. Report IGCP n. 24, Quaternary Science reviews 5(1-4): 83-98.

RICHMOND G.M. & FULLERTON D.S. 1986. Introduction to Quaternary glaciations in the United States of America. In: (Sibrava V., Bowen D.Q., Richmond G.M. eds): Quaternary glaciations in the Northern Hemisphere. Report IGCP n. 24, Quaternary Science reviews 5(1-4): 3-10.

SIBRAVA V., BOWEN D.Q. & RICHMOND G.M., eds 1986. Quaternary glaciations in the Northern Hemisphere. Report IGCP n. 24, Quaternary Science reviews 5(1-4).

UGGERI S. 1992. Analisi geologico-ambientale di un massiccio carbonatico prealpino (M. Campo dei Fiori, Varese): geologia, geologia del Quaternario, idrogeologia. Tesi di Dottorato, Università degli Studi di Milano, 153 pp.

WARWICH G.T. 1956. Caves and glaciation - I. Central and Southern Pennines and adjacent areas. Trans. Cave Res. Group G.B. 4(2): 127-159.

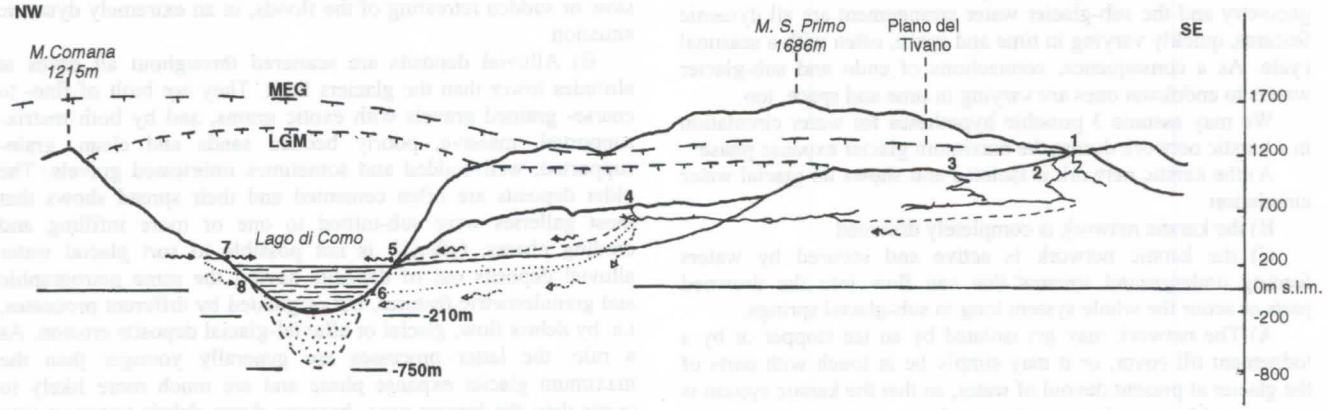

Fig. 2 - This scheme shows the altitude relationships of karstic networks with glaciers in the central area of Lake of Como.
MEG Maximun Extention Glacier limit
LGM Last Glacial Maximum limit
underground drainage directions as shown by dye-tracing
hypothetic underground drainage directions for deeper, flooded parts
1- Abisso del Cippei 2 - Grotta presso la Capanna Stoppani 3 - Bus de la Niccolina 4 - Grotta Tacchi- Grotta Zelbio system 5 - Falchi della Rupe over-flooding springs 6 - hypothetic perennial springs of the karst network of Piani del Tivano 7 - Pizzala spring- cave 8 - hypothetic perennial springs of the karst network of Piazzala
The present floor of the valley nowadays occupied by the Lake of Como is found at a depth of 410 m, that is at an altitude of - 210 m u.s.l..According to seismic data, the canyon bottom is covered with Plio-Quaternary sediments to an altitude of - 750 u.s.l.,thas is to say they are at least 540 m thick.

Entwicklungsgeschichte der Höhlen im Gebiet Hohgant–Sieben Hengste–Thunersee (Berner Oberland, Schweiz)

von Thomas Bitterli (1) und Pierre-Yves Jeannin (2)
(1) Schönaustr. 54, CH-4058 Basel
(2) Derendingerstr. 111, D-72072 Tübingen

Abstract

In this paper we present how the development of the cave systems in the region Hohgant–Sieben Hengste–Lake of Thun can be derived by using speleomorphologic observations. Several times during the course of the cave system, the karstwater table abruptly dropped for some hundred meters. These changes were normally combined with tectonic uplift and consequent deepening of the valleys. Galleries of phreatic origin partly developed close to the ancient karstwater table, however, some important draining axes were reaching 200-300 m below this level (in some extreme cases 500 m or even more).

Repeatedly, the continuously refined models of the developmental history have led to the discovery of unknown caves or cave parts; and these discoveries, in turn, contributed to the improvement of the models. One conclusion of these models is very clear: the 250 km of conduits actually known represent only a small portion of the whole extent of the cave system.

Zusammenfassung

Mit Hilfe von speläomorphologischen Beobachtungen wird versucht, die Entwicklungsabfolge der Höhlensysteme der Region Hohgant–Sieben Hengste–Thunersee aufzuzeigen. Im Verlaufe der Höhlenentwicklung lässt sich mehrmals eine sprungweise Absenkung des Karstwasserspiegels um jeweils mehrere hundert Meter nachweisen. Diese Absenkungen hängen weitgehend mit tektonischen Hebungen und Taleintiefungen zusammen. Die phreatisch entstandenen Gänge verlaufen teilweise nahe dem jeweiligen Karstwasserspiegel, einige grosse Entwässerungsachsen jedoch reichen durchwegs in Tiefen von 200-300 m (im Extremfall sogar über 500 m).

Die laufend verfeinerten Modelle zur Entwicklungsgeschichte haben wiederholt zur Entdeckung neuer Höhlenteile geführt, welche ihrerseits wieder zur Verbesserung der Modelle beitragen. Eines zeigen die Modelle jedenfalls ganz deutlich: die bekannten Gänge von gesamthaft 250 km Länge stellen lediglich einen Bruchteil des ganzen Höhlensystems dar.

Einleitung

Das Hohgant–Sieben Hengste–Höhlensystem bildet mit einer Länge von 140 km und 1340 m Tiefe eines der bedeutendsten der Welt. Die Markierversuche belegen ein gut entwickeltes Karstsystem, welches sich von den Austrittsorten beim Thunersee über 20 km weit gegen NE, entlang der nördlichen Alpenkette (Randkette) bis zur Schrattenfluh, erstreckt. Die kumulierte Länge der in diesem Gebiet bekannten Höhlen übersteigt 250 km. Versuche zur Aufgliederung der Entwicklungsgeschichte finden sich in HOF, ROUILLER & JEANNIN (1985), BITTERLI (1988) und JEANNIN (1989b, 1996).

Die Höhlensysteme zeigen einen unübersichtlichen, gebietsweise ausgesprochen labyrinthischen Charakter (siehe Fig. 1). Die heute vorliegende geometrische Anordnung lässt sich nur erklären durch die zu verschiedenen Zeitabschnitten erfolgte Ausbildung an sich unabhängiger Höhlensysteme, die mehr oder weniger zufällig miteinander verbunden sind.

Die Entwirrung solcher mehrfach vernetzter Höhlensysteme, d.h. die Erkennung der Entwicklungsabfolge und die widerspruchsfreie Zuordnung der Formen und Ablagerungen zu den erkannten Phasen, bildet eine der anspruchsvollsten Aufgaben der modernen Höhlenforschung. Da die interne Entwicklung eines Karstsystems meist eine Reaktion auf Veränderungen der Aussenwelt (z.B. Relief der Erdoberfläche, Klima, Vegetation) darstellt, kommt diesem jungen Wissenschaftszweig eine Schlüsselrolle für die noch weitgehend unbekannte geologische Geschichte der letzten paar hunderttausend bis Millionen Jahre zu. Die entsprechenden Informationen und Relikte an der Erdoberfläche sind in der Regel der Erosion zum Opfer gefallen.

Methodik

In der Erdgeschichte kennt man sowohl kontinuierliche, dynamische Prozesse als auch abrupte und katastrophale Ereignisse, wobei letztere unter Umständen tiefgreifende Auswirkungen haben können. Die Entwicklung der Karstsysteme macht hierin keine Ausnahme, zumal sie unmittelbar an Faktoren der Aussenwelt gekoppelt ist. Solche einschneidenden Ereignisse können sein:

- Tektonisch bedingte Hebungen mit gleichzeitiger Tieferlegung der Talsohlen: Absenkung der Vorflut und damit des Karstwasserspiegels.
- «Überwindung» von geologischen Barrieren innerhalb des Karstsystems: Absenkung eines lokalen, nicht an eine Talsohle gekoppelten Karstwasserspiegels.
- Tektonische Bewegungen: Eröffnung neuer Fliesswege.
- Auffüllung von Tälern infolge tektonisch bedingter Absenkung oder Gletscherbildung: Anstieg des Karstwasserspiegels.
- Erweiterung oder Verlust eines ganzen Einzugsgebietes (z.B. durch Taleintiefung): Änderungen in der Schüttung und im Fliessverhalten.
- Übergang Warmzeit zu Kaltzeit: Erosion der Böden und Einschwemmung in den Karst (erkennbar an den für Böden typischen Tonmineral-Umwandlungen).
- Übergang Kaltzeit zu Warmzeit: Schüttungszunahme mit grossen jahreszeitlichen Schwankungen, starke Erosion.

Die bisherigen Kenntnisse deuten darauf hin, dass ein Karstsystem jeweils mit geringer Verzögerung (in geologischen Zeitmassstäben gerechnet) auf wesentliche Veränderungen der Aussenwelt reagiert. Einige dieser Änderungen, welche an der Erdoberfläche über eine längere Zeit hinweg abliefen, widerspiegeln sich im Karstsystem als ausgesprochen deutliches Signal. So ist der Übergang zwischen vados und phreatisch gebildeten Gängen, welcher dem ehemaligen Karstwasserspiegel entspricht, oft gut eingrenzbar. Die vertikalen Änderungen dieser Marke erfolgten jeweils sprungweise, und zwar – im Sinne der

allgemeinen Hebungstendenz des Alpenkörpers – jeweils um mehrere hundert Meter nach unten. Die vergleichsweise kurzzeitigen eiszeitlichen Anhebungen des Karstwasserspiegels hingegen schlagen sich kaum in der Gangmorphologie (aber sehr wohl in den Sedimenten) nieder.

Dank dieser Diskretisierung sind wir überhaupt erst in der Lage, einen groben Raster der Entwicklungsgeschichte des Karstsystems zu erarbeiten. Die einzelnen, durch die beschriebenen abrupten Ereignisse abgetrennten Phasen lassen sich durch folgende Grössen charakterisieren:

- Über längere Zeit hinweg konstanter, über grösseren Bereich nachvollziehbarer Karstwasserspiegel mit geringem Gefälle: abzuleiten aus dem höchsten Verlauf zusammenhängender phreatischer Systeme (Minimalhöhe) bzw. aus dem Übergang in vadose, gleichzeitig entstandene Zubringer (absolute Höhe).
- Mächtigkeit der Hochwasserzone: sie führt zu einer gewissen «Verschmierung» der Abgrenzung zwischen phreatischen und vadosen Gangformen, allenfalls zur Vorspiegelung eines höhergelegenen Pseudo-Karstwasserspiegels. Die Hochwasserzone kann auch in einem gut entwickelten Karst durchaus eine Mächtigkeit von 100 m erreichen.
- System von subhorizontalen, phreatischen Gängen, welche sich bevorzugt knapp unter dem Karstwasserspiegel erstrecken.
- Grosse, auf bedeutende Distanzen gebündelten Entwässerungsachsen, welche bis zu einigen hundert Meter unter den Karstwasserspiegel reichen können. Solche Gänge können auf lange Strecken subhorizontal verlaufen, aber auch bedeutende vertikale Sprünge aufweisen.

Zu den Grössen, welche sich innerhalb einer Phase nur geringfügig ändern, zählen wir: geometrische Anordnung der Einzugsgebiete und Austrittsstellen, hydraulischer Gradient, Fliessrichtungen, mittlere Schüttungen, tages- und jahreszeitliche Schüttungsschwankungen. Ebenso gehören dazu die klimatischen Faktoren, welche über Ablagerung und Erosion der Höhlensedimente sowie über Sinterbildung und Korrosion entscheiden. Sedimenteinlagerung erfolgt bevorzugt während Kaltzeiten (kein schützender Boden, Moränenschutt), Sinterbildung während Warmzeiten (Böden mit CO_2-Produktion).

Im folgenden wird versucht, die einzelnen Phasen im Gebiet Hohgant–Sieben Hengste–Thunersee anhand der Entwicklung des Karstwasserspiegels zu beschreiben. Andere Ereignisse (z.B. tektonische Bewegungen, Ablagerung und Erosion von Sedimenten, Sinterbildung und Korrosion) können jeweils nur bedingt herbeigezogen werden: die Unterscheidung zwischen lokaler und regionaler Relevanz ist teilweise schwierig, und vorläufig liegen noch zu wenig Daten für eine eindeutige relative Altersfolge vor.

Die Phasen werden anhand von Typlokalitäten (Höhlenname oder Höhlenteil) benannt, wobei jeweils die zugehörige Höhe des Karstwasserspiegels beigestellt ist. Die Angabe von Höhenkoten bezieht sich jeweils auf aktuelle Höhe über Meer. Infolge seitheriger Hebungen entsprechen sie nicht der absoluten Höhe zur Entstehungszeit der Höhlengänge.

Phase «L16–P2» (mind. 1900 m)

Die Erosion hat nur einen geringen Prozentsatz der Gebietsfläche in Höhenlagen über 1800 m belassen. Gleichwohl sind in den höchstgelegenen Bereichen Überreste von grossen, phreatisch entstandenen Gängen erhalten geblieben, welche einen ehemaligen Karstwasserspiegel auf mindestens 1900 m Höhe anzeigen (Fig. 2). Sofern es sich tatsächlich um eine einzige Phase handelt, weist die phreatische Zone einen Tiefgang von mehr als 150 m auf. Zumindest im Bereich der Sieben Hengste zeichnet sich eine Entwässerung gegen NE, d.h. entgegen der heutigen Entwässerungsrichtung, ab.

Ein derart hochgelegener Karstwasserspiegel ist nur unter der Annahme eines Reliefs ohne die heutigen, über 1300 m tiefen Taleinschnitte vorstellbar. Ähnlich hochgelegene und grossräumige Fossilsysteme bestehen auf der Schrattenfluh. Es ist denkbar, dass die Karstgebiete Sieben Hengste-Hohgant-Schrattenfluh einst eine zusammenhängende Einheit bildeten.

Die Sedimentfüllungen und Sinterbildungen dieser hochgelegenen Gänge sind bislang noch kaum untersucht.

Phase «Glacière–Haglätsch» (1720 m)

Diese Phase ist im Bereich der Sieben Hengste, aber auch rund um den Hohgant (obere Anteile K2 und F1, Haglätsch und Gopital), durch ein weitumspannendes Netz von recht grossen und oft labyrinthischen Gängen mehrfach belegt (Fig. 2). Die wichtigsten, mehrere Kilometer umfassenden Hauptentwässerungsachsen belegen einen tiefreichenden Karst von mindestens 250 m unter dem Karstwasserspiegel. Oft verläuft dieser Hauptzug parallel zum Schichtstreichen und damit auch im tiefphreatischen Bereich auf weite Strecken horizontal. Dieser Hauptzug wird an diversen Orten von phreatischen Gängen überlagert, welche sich im Bereich des damaligen Karstwasserspiegels erstrecken.

Ähnlich der vorhergehenden Phase war die Entwässerung im Bereich der Sieben Hengste eindeutig nach NE, im Bereich der Haglätschhöhle demgegenüber nach E bis SW gerichtet. Somit deutet vieles auf einen dazumaligen Austritt im Bereich des heutigen Fallbachtales hin, welcher die Wässer von beiden Seiten her einzog. Wie aus der Fig. 2 leicht ersichtlich ist, sind v.a. im flächenmässig grösseren, östlichen Teileinzugsgebiet noch zahlreiche Gänge unentdeckt. Aber auch weiter im W, gegen das heutige Aaretal zu, sind in dieser Höhenlage bislang kaum Höhlen bekannt, so dass vorläufig nichts über eine gleichzeitige Entwässerung in Richtung eines möglichen Paläo-Aaretales ausgesagt werden kann (vgl. GERBER, BITTERLI, JEANNIN & MOREL 1994).

Die Gänge der Phase «Glacière–Haglätsch» zeichnen sich durch bedeutende Lehm- und Sandfüllungen aus. Detaillierte Profilaufnahmen im westlichen Teileinzugsgebiet deuten auf kaltzeitliche, phreatisch erfolgte Ablagerungen hin (JEANNIN 1989a). Darunter finden sich grosse Granitgerölle in 1700 m Höhe, welche nur mit Ferntransport durch Gletscher erklärt werden können. Da die grossen Gletschervorstösse der quartären Kaltzeiten nach bisherigen Kenntnissen nie eine Höhe von 1450 m überschritten, muss von einer präquartären Ablagerung dieser Sedimente ausgegangen werden.

Im östlichen Teileinzugsgebiet sind derartige Funde bislang ausstehend. Zumindest in der Haglätschhöhle herrschten sehr ruhige Ablagerungsbedingungen mit geringen Fliessgeschwindigkeiten vor. Auf die Austrocknung und Setzung der Sedimente, folgte eine durchdringende Versinterung, welche teilweise wieder korrodiert und von einer Mondmilchkruste überzogen wurde, und schliesslich die Ausräumung eines Grossteils der Sedimente durch in die basale Sandlage infiltrierende Wässer.

Phase «B6.5–Mäanderhöhle» (1585 m)

Der grosse Tiefgang der phreatischen Zone der Phase «Glacière–Haglätsch» macht es ausserordentlich schwierig, tiefergelegene, überschneidende Karstwasserstände zu erkennen. Dies betrifft insbesondere die beiden Phasen «B6.5–Mäanderhöhle» (135 m tiefer) und «Lausannois» (215 m tiefer), in welchen die bereits bestehenden Gänge der Phase «Glacière–Haglätsch» mitbenutzt

und zugleich neue Gänge geschaffen wurden.

Im Bereich der Sieben Hengste bestehen einige mehr oder weniger isolierte Höhlen oder Höhlenteile, welche eindeutig der Phase «B6.5–Mäanderhöhle» zugeordnet werden können (Fig. 2, vgl. BITTERLI, in Vorb.). Die Entwässerung ist wiederum gegen NE, d.h. zum Fallbachtal hin, gerichtet. Im nördlichen Teileinzugsgebiet fehlen – abgesehen von der Mäanderhöhle – entsprechende Zeugen. Für die beschränkte Verbreitung dieser Phase auf den Bereich der Sieben Hengste fehlt bislang eine befriedigende Erklärung.

Auch diese Gänge zeigen massive Sedimentfüllungen, darunter grosse Granitgerölle weit über dem bislang belegten Höchststand der quartären Gletschervorstösse (JEANNIN 1989b, 1991).

Phase «Lausannois» (1505 m)

Im NE-Teil der Sieben Hengste kann ein ehemaliger Karstwasserspiegel ziemlich genau auf 1505 m eingrenzt werden (Fig. 2, BITTERLI 1990). Die Entwässerung war stets noch gegen NE, zum Fallbachtal hin, gerichtet. Ausserhalb des Bereichs der Sieben Hengste fehlen entsprechende Hinweise auf dieses Niveau. Es stellt sich also dieselbe Frage wie bei der vorhergehende Phase «B6.5–Mäanderhöhle».

Die Sedimentuntersuchung zweier Profilschnitte (JEANNIN 1989b) ergab eine weitgehend phreatisch erfolgte, vermutlich kaltzeitliche Ablagerung bei vergleichsweise geringen Fliessgeschwindigkeiten. Die Ablagerung wird gefolgt von einer massiven Versinterung. Bei einigen dieser Tropfsteinvorkommen sind alternierend Aragonit- und Kalzitlagen ausgebildet. Die intensiv rote Einfärbung einiger Sintergebilde erfolgte demgegenüber viel später. Vermutlich im Zusammenhang mit der Ausbildung der Zubringer zum System «F1–Faustloch» wurde ein Teil der Sedimente wieder ausgeräumt.

Seit der Gangausbildung erfolgten bescheidene tektonische Bewegungen auf dextralen E–W-Horizontalverschiebungen (Grössenordnung 20-30 cm, maximale NNW–SSE-Kompressionsrichtung). Sie konnten bislang nur in Gängen nachgewiesen werden, welche nicht jünger als die Phase «Lausannois» sind. Vermutlich haben sie zum Ausbildungsmuster der nachfolgenden Phase «F1–Faustloch» beigetragen (JEANNIN 1990).

Phase «F1–Faustloch» (1440 m)

Mit der Absenkung des Karstwasserspiegels auf eine Höhenlage von 1440 m erfolgte eine völlige Umorientierung des Entwässerungssystems. Im Gegensatz zu allen vorhergegangenen Phasen war die Entwässerung des gesamten Gebietes deutlich nach SW, in Richtung des heutigen Aaretals, gerichtet (siehe Fig. 3). Die Hochwasserzone dieses bedeutenden Systems reichte wahrscheinlich einige Dutzend Meter über den Niedrigwasserstand und wies möglicherweise mit dem 60-70 m höhergelegenen fossilen Austritt der Phase «Lausannois» einen Überlauf ins Fallbachtal auf.

Die Gänge der Phase «F1–Faustloch» sind sehr ausgedehnt und grossräumig. Die diversen Zubringer aus dem vadosen Bereich tauchen mehr oder weniger der Schichtung folgend bis 200-250 m unter den vermuteten Karstwasserspiegel ab. Hier bildet sich ein eigentlicher Kollektor heraus, welcher vom F1 und K2 her nach SW zieht und damit die Zuflüsse von den Sieben Hengsten her einzieht. Erstmals in der hydrogeologischen Geschichte übernimmt nun auch die geologisch bedeutende Hohgant-Sundlauenen-Verwerfung (Sprunghöhe in diesem Bereich: 200-300 m) die Funktion einer Barriere: im Falle des K2 bildete sich daran ein immenses Labyrinth heraus. Wegen des parallel zur Verwerfung gerichteten hydraulischen Gradienten wurde sie aber nirgends überwunden.

Zu Beginn der «Zone Profonde» durchquert der grosse Kollektor eine bedeutende Verwerfung, in deren Bereich sich ein wahrhaft dreidimensionales Labyrinth herausbildete. Die Hauptachse sinkt hier in eine Tiefe von 350-400 m unter den damaligen Karstwasserspiegel ab. Unklar werden die Verhältnisse ab jenem Punkt im Faustloch, wo der grosse Gang steil abbricht, und gleichzeitig die Hohgant-Sundlauenen-Verwerfung quert. Dieser Verlauf ergäbe eine Tiefenlage der phreatischen Gänge der Phase «F1–Faustloch» von – je nach Variante – 600 m oder 850 m.

Stattdessen besteht auch die Möglichkeit, dass das Wasser durch bislang nicht bekannte Wege zum A2 aufstieg und weiterhin auf der bisherigen Seite der Hohgant-Sundlauenen-Verwerfung dem Aaretal oder Justistal (Fig. 3) zustrebte. Von diesem unterirdischen Verlauf von über 6 km Luftlinie sind nur wenige und kurze Ausschnitte bekannt.

Praktisch in sämtlichen Fossilgängen, welche mit der Achse F1–Faustloch verknüpft sind, lassen sich tektonische Bewegungen von 1-5 cm auf Schichtfugen und Klüften nachweisen, welche nach der Gangbildung erfolgt sind. Die Bewegungsrichtungen zeigen eine vertikale Kompression und eine E–W-Dehnung an (JEANNIN 1990).

Einige noch schlecht belegte Anzeichen im F1 und im Endlabyrinth des K2 deuten auf die Existenz einer jüngeren Phase mit einer Höhe des Karstwasserspiegels auf 1290-1300 m hin.

Phase «Beatushöhle–Josephine» (1120 m)

Für die weitere Absenkungsgeschichte des Karstwasserspiegels bestehen nur wenige konkrete Hinweise. Im gehobenen NW-Flügel bildet die schwer durchlässige Unterlage südwestlich des A2 eine Schwelle (Fig. 3). Sobald der Wasserspiegel unter eine Höhe von etwa 1400 m ü.M. absinkt, bewirkt diese geologische Schwelle die hydraulische Abkoppelung des quellnahen südwestlichen vom entfernten nordöstlichen Einzugsgebiet. Während sich das quellnahe Einzugsgebiet der Beatushöhle weiterhin auf dem gehobenen NW-Flügel der Hohgant-Sundlauenen-Verwerfung entwickeln konnte, mussten sich die Wässer des entfernteren Einzugsgebietes Hohgant–Sieben Hengste ihren Weg via den tieferliegenden SE-Flügel suchen, in welchem dann auf grosser Strecke gespannte Verhältnisse vorlagen.

Die grosse, durchgehende Deckenellipse der Beatushöhle belegt einen Tiefgang der phreatischen Zone von rund 400 m, wobei der Eingang vermutlich den Tiefstpunkt darstellt. Vermutlich ist der ehemalige Austritt in westlicher Richtung zu suchen.

Im Einzugsgebiet Hohgant–Sieben Hengste herrschten bergwärts der «Zone Profonde» vadose Verhältnisse. Damit erfolgte auch die Überwindung der Hohgant-Sundlauenen-Verwerfung im F1 und K2. Ein Teil dieser Wässer querte die Verwerfung möglicherweise ein zweites Mal und erreichte auf tieferem Weg die phreatische Zone der «Zone Profonde». Die Höhe des damaligen Karstwasserspiegels lässt sich im Zubringermäander zum Faustloch mit etwa 1120 m eingrenzen. Im Faustloch schliesslich bahnte sich das Wasser definitiv seinen Weg auf die Ostseite der Hohgant-Sundlauenen-Verwerfung und floss via die Josephine in den Bärenschacht. Der Tiefgang der phreatischen Zone betrug damit mindestens 350 m, der Wiederaufstieg der gespannten Wässer im Bereich des heutigen Aaretales dürfte immer noch durch 100-200 m eigentlich undurchlässigen Sandstein und Flysch (oder allenfalls durch die Lokkergesteinsfüllung des Aaretales) erfolgt sein.

Vor allem zwischen dem Faustloch und dem Bärenschacht besteht eine Zone starker Sedimentverfüllung, welche noch zu phreatischer Zeit entstanden sein dürfte. In der Beatushöhle finden sich zudem einige grössere Granitgerölle.

Phase «Dent-Tranchante–Akkordloch» (770 m)

Anzeichen für ein tieferes Niveau in der Beatushöhle bestehen erst auf 770 m. Dieselbe Höhenlage für die phreatische Zone zeichnet sich im Faustloch ab, wo der Tiefgang der phreatischen Zone mindestens 170 m ausmacht (Fig. 3).

Der Bärenschacht zeigt zwei Niveaus von Fossilgängen, welche untereinander mehrfach durch ebenfalls phreatische Rampen und Gänge verbunden sind. Die ursprüngliche Anlage des Ganggerüstes erfolgte bereits früher (v.a. Phase «Beatushöhle–Josephine»). Die Phase «Dent-Tranchante–Akkordloch» führte zur Ausbildung eines ergänzenden Ganggeflechtes rund um den Karstwasserspiegel auf 770 m.

Grosse Teile des Bärenschachtes, aber vor allem dessen fossile Austritte, sind massiv mit Sedimenten verstopft. Auch hier finden sich grosse Kristallinfragmente. Im Faustloch reichen die Ablagerungen bis zu 100 m über den damaligen Karstwasserspiegel.

Der grösste Teil der Gänge im Bärenschacht findet sich in einem tieferen Niveau, welches sich höhenmässig allerdings nicht sehr deutlich festlegen lässt (rund 680 m). Ein wesentlicher Teil davon dürfte jedenfalls bereits während früherer Phasen angelegt worden sein.

Heutige Verhältnisse (560 m)

Der heutige Karstwasserspiegel auf rund 560 m zeigt zumindest im Bärenschacht keine enormen Schwankungen. Im Faustloch sind Schwankungen von 5-10 m sehr häufig, solche von über 15 m hingegen ausgesprochen selten. Trotz dieser bescheidenen Hochwasserzone ist kein offensichtliches eigenes Niveau erkennbar; es werden durchwegs die in vorhergehenden Phasen geschaffenen Gangsysteme benutzt.

Gemäss Markierversuchen umfasst das heutige Einzugsgebiet der Quellaustritte im Thunersee zumindest einen Teil der 20 km entfernten Schrattenfluh. Die rasche Durchlaufzeit des Markierstoffes (38 h) verleitet zur Annahme eines Systems grossräumiger Gänge, womöglich sogar begleitet von fossilen Niveaus. Gleichwohl ist bis heute noch kein einziger Gang bekannt, welcher eindeutig dem Schrattenfluh-System angehört. So bleibt unklar, ab welchem Zeitpunkt sich dieses grosse Einzugsgebiet «anhängte».

Schlussfolgerungen

Die umfangreichen Forschungsresultate im Gebiet Hohgant–Sieben Hengste–Thunersee erlauben es, eine vorläufige Entwicklungsgeschichte dieses riesigen und mehrphasig entstandenen Karstsystems zusammenstellen. Auch wenn etliche Fragen offen bleiben, so übersteigt der Detaillierungsgrad dieser relativen Abfolge bei weitem die reichlich vagen und widersprüchlichen Vorstellungen der Geologen zu den frühquartären und jungtertiären Ereignisse.

Bereits anhand der vorliegenden Ergebnisse lassen sich mehrere Phasen ausscheiden, welche auch erdgeschichtlich von Bedeutung sind:

- Die ältesten Gänge (Phase «L16–P2») entsprechen einem Vorflutniveau von heute mindestens 1900 m Höhe, d.h. 1300 m über dem aktuellen Niveau. Möglicherweise umfasste das Einzugsgebiet auch die heutige Schrattenfluh.
- Die Phase «Glacière–Haglätsch» bedingte eine Höhe des Vorfluters auf rund 1720 m. Einiges deutet auf einen damaligen Austritt im Fallbachtal hin. Es ist sehr wohl vorstellbar, dass die Ur-Aare ursprünglich via das Fallbachtal ins Mittelland entwässerte (siehe Fig. 2).
- Die Bedeutung der beiden Phasen «B6.5–Mäanderhöhle» (1585 m) und «Lausannois» (1505 m) ist vorläufig unklar. Möglicherweise sind die beiden Systeme nur lokal ausgebildet. Beide Systeme entwässerten jedenfalls ins Fallbachtal, doch ist auch eine gleichzeitige Eintiefung des heutigen Aaretals denkbar. Funde von Granitgeröllen weit über dem bislang belegten Höchststand der quartären Gletschervorstösse deuten auf ein präquartäres Alter dieser und der vorhergehenden Phasen hin.
- Die vollzogene Umpolung des Karstentwässerungssystems mit der Phase «F1–Faustloch» ist eine Folge der Eintiefung des heutigen Aaretales auf rund 1400-1440 m. Das Fallbachtal hat damit seine regionale Bedeutung praktisch vollständig verloren.
- Die Phase «Josephine–Beatushöhle» geht auf eine Vorflut in der Höhenlage von 1100-1120 m zurück, welche der damaligen Sohle des Aaretals entsprach. Der problematische Aufstieg der Karstwässer östlich der Hohgant-Sundlauenen-Verwerfung (Bärenschacht) aus einer Tiefe von mindestens 350 m könnte durch eine tiefgreifende Talfüllung begünstigt worden sein.
- Die Phase «Dent-Tranchante–Akkordloch» entspricht einer Höhenlage des Aaretals von 770 m. Seither hat sich das Aaretal um weitere 200 m eingetieft, ohne eindeutige Höhlenniveaus zu schaffen.

Der Versuch, diese relative Abfolge der Höhlenentwicklung vor allem mit Hilfe der Ablagerungen und Sinterbildungen zu verfeinern, mit absoluten Datierungen zu kalibrieren und mit Ereignissen der Aussenwelt zu korrelieren, ist nicht nur für den Höhlenforscher bei seiner Suche nach Neuland von Interesse. Er bildet auch ein wesentliches Hilfsmittel zur Erarbeitung der geologischen Geschichte der letzten paar Millionen Jahre. Immerhin umfasst praktisch jede der ausscheidbaren Phasen warm- und kaltzeitliche Ablagerungen, deren wissenschaftliche Informationen sonst nirgends mehr registriert sind.

Literatur

BITTERLI, T. 1988. Das Karstsystem Sieben Hengste–Hohgant–Schrattenfluh: Versuch einer Synthese. *Stalactite:* 38 (1/2-1988): 10-22.

BITTERLI, T. 1990. Réseau des Lausannois. *Höhlenforschung in der Region Sieben Hengste–Hohgant:* No 2, 65 p.

BITTERLI, T. (in Vorb.) Das B6.5 (Sieben Hengste, BE, Schweiz). *Höhlenforschung in der Region Sieben Hengste–Hohgant (HRH):* No 4.

GERBER, M.; BITTERLI, T.; JEANNIN, P.-Y. & MOREL, Ph. 1994. A2–Loubenegg. *Höhlenforschung in der Region Sieben Hengste–Hohgant (HRH):* No 3, 63 p.

HOF, A.; ROUILLER, Ph. & JEANNIN, P.-Y. 1985. Sieben Hengste–Hohgant Höhle. *Le Trou:* no 34, 106 p.

JEANNIN, P.-Y. 1989. Remplissages karstiques du réseau des Sieben Hengste. *Travail de diplôme de 3e cycle en Hydrogéologie:* tome 2 (non publié).

JEANNIN, P.-Y. 1989. Etude géologique de la région Burst–Sieben Hengste (Chaîne bordière helvétique, canton de Berne): Apports de l'étude des cavernes à la connaissance structurale et à la mise en évidence de phases tectoniques quaternaires. *Mémoire diplôme géologie, Univ. Neuchâtel:* 122 p.

JEANNIN, P.-Y. 1990. Néotectonique dans le karst du nord du lac de Thoune (Suisse). *Eclogae geol. Helv.:* 83/2: 323-342.

JEANNIN, P.-Y. 1991. Mise en évidence d'importantes glaciations anciennes par l'étude des remplissages karstiques du Réseau des Sieben Hengste (Chaîne bordière helvétique). *Eclogae geol. Helv.:* 84/1: 207-221.

JEANNIN, P.-Y. 1996. Structure et comportement hydraulique des aquifères karstiques. *Thèse fac. Sc. Univ. Neuchâtel,* 260p.

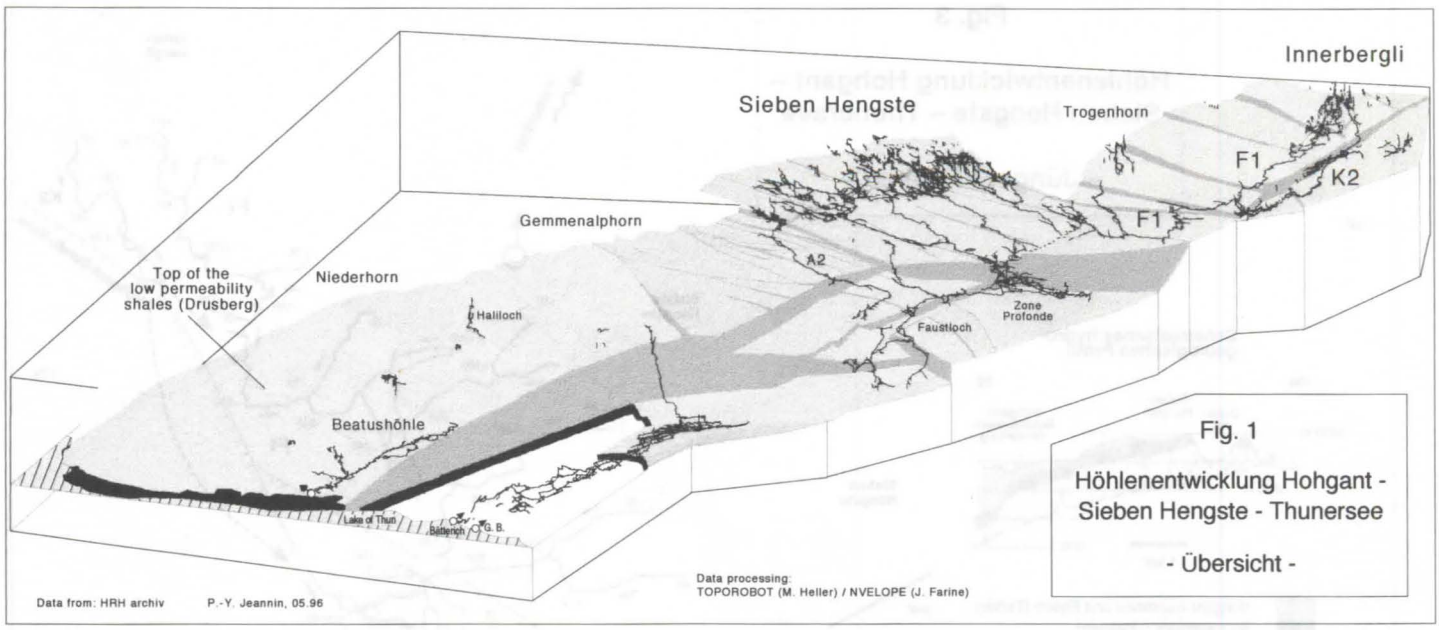

Fig. 1

Höhlenentwicklung Hohgant - Sieben Hengste - Thunersee

- Übersicht -

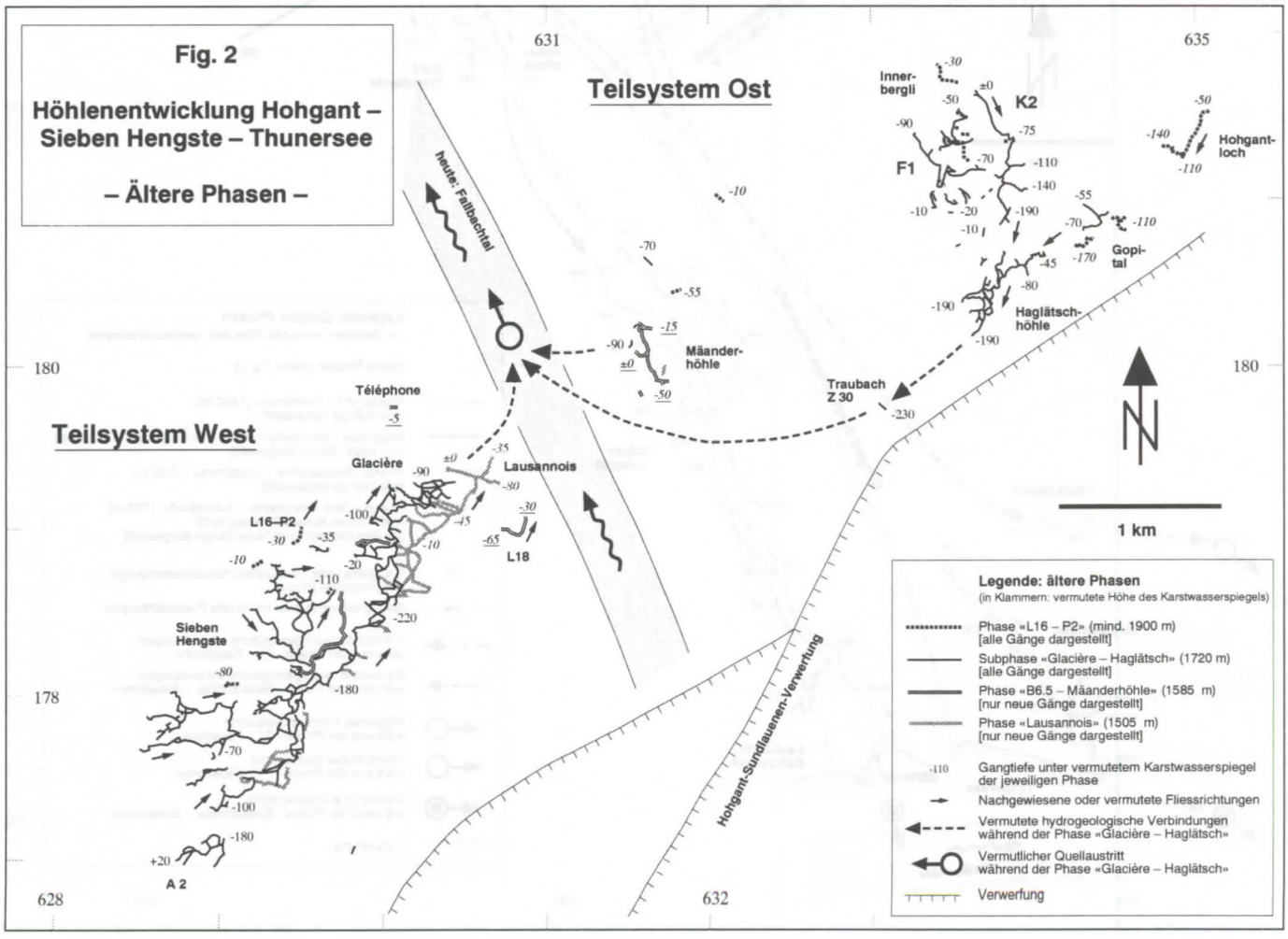

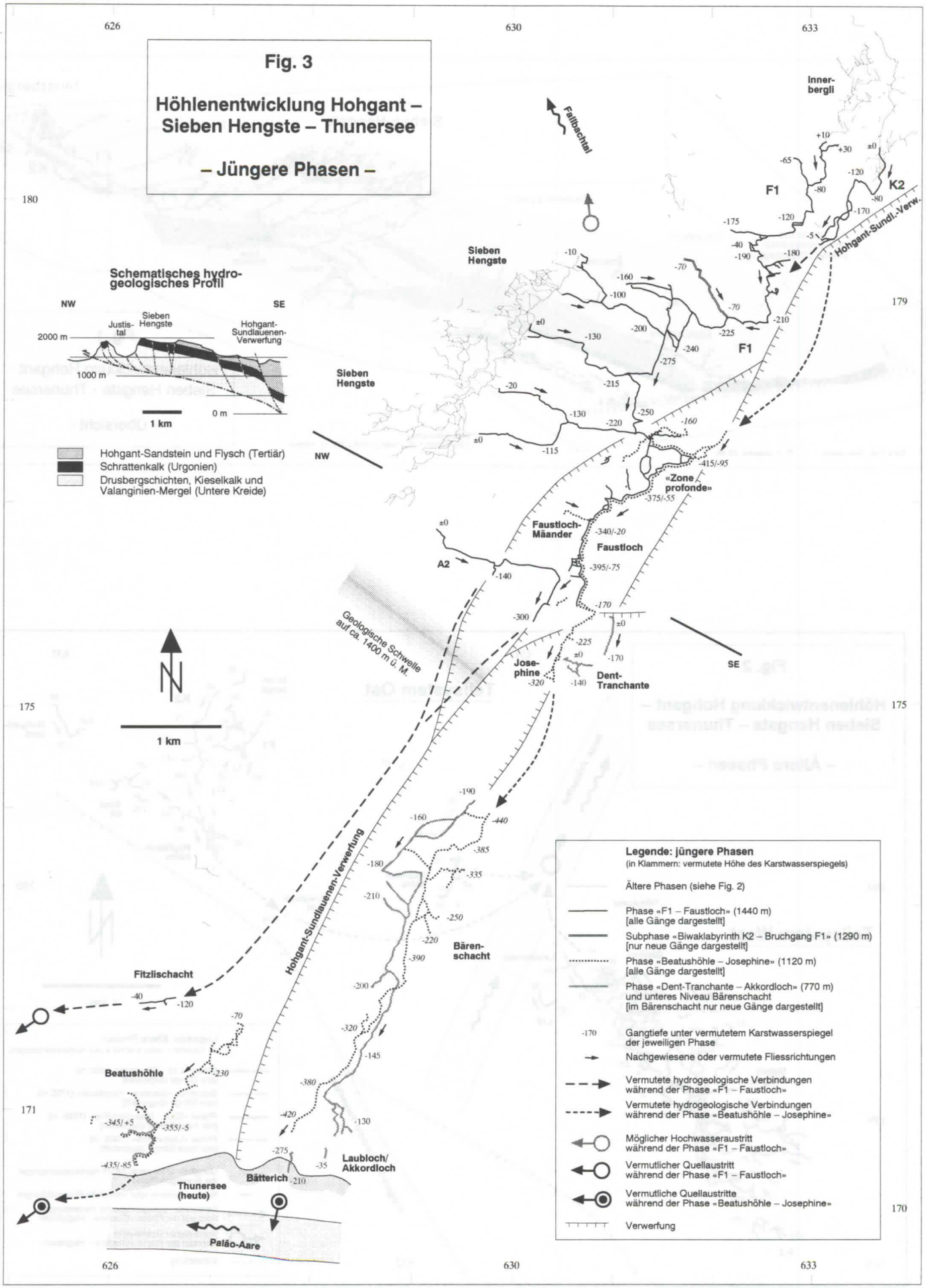
Fig. 3
Höhlenentwicklung Hohgant – Sieben Hengste – Thunersee
– Jüngere Phasen –
626
630
633
180
179
175
171
170
Innerbergli
Fallbachtal
F1
K2
Hohgant-Sundl.-Verw.
Sieben Hengste
Schematisches hydrogeologisches Profil
NW
SE
Justis-tal
Sieben Hengste
Hohgant-Sundlauenen-Verwerfung
2000 m
1000 m
0 m
1 km
Hohgant-Sandstein und Flysch (Tertiär)
Schrattenkalk (Urgonien)
Drusbergschichten, Kieselkalk und Valanginien-Mergel (Untere Kreide)
«Zone profonde»
Faustloch-Mäander
Faustloch
A2
Geologische Schwelle auf ca. 1400 m ü. M.
Josephine
Dent-Tranchante
Hohgant-Sundlauenen-Verwerfung
Bärenschacht
Fitzlischacht
Beatushöhle
Laubloch/ Akkordloch
Bätterich
Thunersee (heute)
Palä-Aare
Legende: jüngere Phasen
(in Klammern: vermutete Höhe des Karstwasserspiegels)
Ältere Phasen (siehe Fig. 2)
Phase «F1 – Faustloch» (1440 m) [alle Gänge dargestellt]
Subphase «Biwaklabyrinth K2 – Bruchgang F1» (1290 m) [nur neue Gänge dargestellt]
Phase «Beatushöhle – Josephine» (1120 m) [alle Gänge dargestellt]
Phase «Dent-Tranchante – Akkordloch» (770 m) und unteres Niveau Bärenschacht [im Bärenschacht nur neue Gänge dargestellt]
-170 Gangtiefe unter vermutetem Karstwasserspiegel der jeweiligen Phase
Nachgewiesene oder vermutete Fliessrichtungen
Vermutete hydrogeologische Verbindungen während der Phase «F1 – Faustloch»
Vermutete hydrogeologische Verbindungen während der Phase «Beatushöhle – Josephine»
Möglicher Hochwasseraustritt während der Phase «F1 – Faustloch»
Vermutlicher Quellaustritt während der Phase «F1 – Faustloch»
Vermutliche Quellaustritte während der Phase «Beatushöhle – Josephine»
Verwerfung

Le synclinal oriental de Chartreuse - facteurs influant sur la genèse des grands réseaux

par Bernard Loiseleur
Chemin de la Liasse 39, F-69570, Dardilly, France

Résumé

Le synclinal oriental de Chartreuse est formé par l'alignement des cinq massifs du Granier, de l'Alpe, du Seuil, de Bellefond et de la dent de Crolles. L'ossature en est constituée par les calcaires urgoniens particulièrement propices à la karstification superficielle et profonde. Trois d'entre eux possèdent de grands réseaux explorés, tous d'un développement supérieur à 40 km.. Les deux autres sont beaucoup moins riches en cavités explorées. La communication cherche à faire la part de chacune des raisons d'origine diverses pouvant justifier le sous-développement apparent des réseaux du Seuil et de Bellefond.

Abstract

The eastern Chartreuse syncline is a strip of five massifs : Granier, Alpe, Seuil, Bellefond and Dent de Crolles. The urgonian limestone is the main karstified level. It is covered with large clints. Deep and long caves are numerous. Three of them (Dent de Crolles, Alpe, Granier) are more than fourty kilometers long. But on Seuil and Bellefond the nerworks are rather less important. Various reasons may justify such differences. They are the object of this communication.

1. Introduction

Le synclinal oriental de Chartreuse est le composant essentiel de la Chartreuse orientale. Ses limites sont marquées à l'ouest par le chevauchement oriental de Chartreuse, qui court des Bauges au Vercors, et à l'est par le Grésivaudan et la vallée de l'Isère. Du sud au nord se succèdent les massifs de la Dent de Crolles (2,3 km^2), de Bellefond (2 km^2), du Seuil (13 km^2), de l'Alpe (10 km^2) et du Granier (2,8 km^2). Il appartient à l'ensemble cartusien qui, en limite du domaine jurassien, relève pour l'essentiel du domaine subalpin.

2. La problématique des grands réseaux

L'ensemble karstique ainsi formé renferme à ce jour trois des sept plus grands réseaux spéléologiques français et les deux plus vastes des Alpes françaises, le Trou qui souffle (Vercors) dépassant de peu le Granier :

- le réseau de l'Alpe - 60 195 mètres
- le réseau de la Dent de Crolles - 50 000 mètres
- le réseau du Granier - 39 000 mètres.

D'autres cavités non reliées aux précédentes portent le développement connu au delà de 88 km sous l'Alpe et de 55 km sous le Granier. A l'inverse, le Seuil ne renferme à ce jour que 38 km de conduits explorés dont 16 km pour le seul réseau de Malissard. Quant à Bellefond, toute cavité importante en est absente. Or le Seuil est le plus vaste massif du synclinal oriental. Quant à Bellefond, il s'agit de la continuation nord de la Dent de Crolles. La densité de galeries est de 22 000 m/km^2 sous la Dent de Crolles, de 8 800 m/km^2 sous l'Alpe et de 2 900 m/km^2 au Seuil . Elle est proche de 0 à Bellefond.

Des massifs d'aspects très semblables présentent donc d'évidentes disparités aux plans des réseaux explorés et de la répartition des cavités, alors même que les conditions climatiques et donc les conditions de karstification ont du rester homogènes à travers le temps. La problématique est d'établir si cela tient à de réelles différences structurelles, ou si cela ne résulte que d'écarts dans l'avancement des explorations, liés à des facteurs secondaires ayant limité celles-ci. Il faut noter que, en termes d'efforts spéléologiques, tous ces massifs se trouvent sur un même pied, aucun d'entre eux n'ayant fait l'objet d'un ostracisme particulier. Tout au plus, selon l'adage que le succès appelle le succès et le collecteur les spéléologues, le Seuil et Bellefond sont dans les années 90 l'objet d'une moindre attention.

3. La disposition des grands réseaux connus

Si trois grands réseaux sont connus, leur distribution spatiale est sensiblement différente.

3.1 La Dent de Crolles

Le collecteur y est reconnu sur la longueur de la gouttière synclinale. En dehors de l'exsurgence du Guiers mort, les accès préférentiels au réseau se font à partir du flanc des falaises, à l'est et à l'ouest. Mais la forme effilée du massif côté sud et la position des orifices connus ne permet pas de conclure quant à leur situation initiale, avant recul des falaises. Le Trou du Glas lui-même est une ancienne émergence et se développe parallèlement à l'axe synclinal. L'essentiel des conduits est réparti en plusieurs étages non loin de l'axe synclinal et il faut remarquer que la densité maximale, créant un véritable labyrinthe de puits et couloirs, se trouve entre le trou du Glas et le Guiers mort sur une bande d'une largeur de 400 mètres. Ce lacis se développe entre 1350 m et 1600 m d'altitude. Plus au sud, la largeur s'en réduit à 200 mètres jusqu'au double conduit grotte Chevalier - grotte Annette. Le flanc est présente peu de galeries explorées, à l'exception du gouffre Thérèse et de la galerie Spit. La galerie du solitaire, vers 1450 m, marque la limite est des galeries. Sur le plateau, en dehors des deux accès au réseau (P40, gouffre Thérèse), les gouffres sont globalement peu nombreux et peu profonds, même si, en trois points, des remontées ont permis de se rapprocher très près de la surface. Elles s'arrêtent sur le niveau à orbitolines, difficilement franchi au P40 (galerie d'York).

3.2 L'Alpe

Les réseaux de l'Alpe et du Pinet présentent un grand nombre d'entrées (35 et 13) tant à partir du flanc ouest que du plateau sommital. Le collecteur principal est reconnu sur la quasi totalité de sa longueur. L'idée généralement reçue est que le flanc est ne présente pas de cavités. En fait, il faut plutôt dire que là aussi il ne présente pas de cavités humainement reliées au réseau principal. Certes le collecteur de l'Alpe marque sensiblement la limite est du réseau, mais l'analyse statistique réalisée par le SCAL (ROMANI L., 1995) montre un flanc est riche en orifices - qui 'ne passent pas'. La falaise ouest renferme des cavités de

haut niveau (Biolet, grotte aux ours, Pinet, ...) considérées parfois comme d'anciens collecteurs antépliocènes (Biolet) en raison de leur disposition et de leur morphologie. Surtout, le volet ouest du synclinal est riche de gouffres à grand développement connectés aux deux réseaux principaux mentionnés ci-dessus. La densité globale de conduits reste très inférieure à celle rencontrée à la Dent de Crolles, en particulier du fait d'un lacis de conduit sur l'axe synclinal bien moindre.

3.3 Le Granier

Le collecteur principal a disparu avec la gouttière synclinale. Les orifices se situent dans les falaises comme sur le plateau. L'absence de collecteur explique que les cavités explorées se regroupent en plusieurs réseaux non reliés. Là aussi à l'ouest existent des grottes de haut niveau (Pincherins, Balme à Collomb, Grande ourse). La disposition générale des cavités est très semblable à celle rencontrée sur le secteur occidental de l'Alpe.

L'opposition morphologique est donc forte entre Alpe et Granier d'une part, Dent de Crolles d'autre part. La caractéristique commune est l'existence d'un réseau profond de grand développement. A l'inverse au Seuil et à Bellefond, les cavités de bordure sont absentes - hors les exsurgences (Guiers vif, Mort- Rû, Fontaine noire). En particulier, aucune cavité n'est connue en face ouest sur la longue arête des Lances de Malissard. Quelques orifices sans suites notables existent en face est sur le Seuil (Palais des choucas). L'existence d'au moins deux collecteurs parallèles alimentant l'exsurgence du Guiers vif est présumée mais reste pure hypothèse dans la mesure où le collecteur principal n'a pu être atteint ni par l'exsurgence, ni à partir du plateau. Quant à Bellefond, la disparition de l'axe synclinal a désorganisé le drainage.

4. Le contexte géomorphologique

Si, globalement, on parle du synclinal oriental de Chartreuse, dans le détail, les dispositions rencontrées varient avec les massifs comme le montrent les coupes géologiques est-ouest (GIDON M., 1990).

Le massif du Granier se présente sous la forme d'un volet synclinal penté vers l'Est avec un pendage moyen de l'ordre de 10°. Le volet oriental a disparu, l'axe synclinal n'apparaît plus au niveau de l'Urgonien mais seulement de l'Hauterivien, niveau dans lequel se situe l'exsurgence principale des Eparres.

A l'Alpe le synclinal est complet, les deux flancs symétriquement répartis autour d'une gouttière axiale coïncidant sensiblement avec la faille N-S (faille de la Gorgette) qui court depuis la Dent de Crolles. Le pendage est faible et n'atteint exceptionnellement 30° qu'au niveau de la flexure axiale dont le bord ouest est assez redressé au dessus de la faille de la Gorgette. L'axe synclinal coïncide avec l'axe géométrique du massif. L'exsurgence du Cernon s'aligne sur le décrochement de l'Alpette.

Au Seuil, le synclinal a conservé ses deux flancs, mais ceux-ci sont fortement dissymétriques et la gouttière axiale ne coïncide qu'en partie avec la faille de la Gorgette. Entre Marcieu et le cirque de St Même, celle-ci est doublée par un éventail de petites failles dont la terminaison se marque sur la faille décrochante du Fourneau. Le rejet de l'ensemble est de 100 mètres. L'axe synclinal est très décalé vers l'ouest du massif. Le pendage moyen coté ouest est de 40° au dessus d'une flexure très brutale. Quant au pendage du flanc est, il atteint 30° mais seulement sur la partie la plus élevée. Le cœur du synclinal présente un pendage inférieur à 5° ouest sur une largeur de 700 mètres. La forme de combe est donc très marquée.

A Bellefond ne subsiste que le volet oriental du synclinal. La disposition est donc exactement contraire à celle rencontrée au Granier. Encore, ce volet est il fortement entamé par les éboulements du chaos. Bellefond a du constituer le prolongement hydrologique de la Dent de Crolles avant que ne se creuse le cirque du Prayet.

Enfin, la Dent de Crolles possède une structure synclinale dont le volet occidental diminue progressivement d'amplitude du sud vers le nord pour disparaître complètement au niveau de la grotte-exsurgence du Guiers mort à l'occasion du passage du décrochement du Prayet.

Le facteur morphologique le plus favorable est donc la conjugaison entre l'axe synclinal et la faille de la Gorgette accompagnée d'un pendage modéré du volet synclinal ouest. On relève ainsi la différence entre Alpe et Seuil où le développement transversal du niveau urgonien est comparable (2500 mètres). Mais le faible pendage a clairement favorisé l'implantation de cavités bien développées sur l'Alpe. A l'inverse, au Seuil, le flanc ouest du synclinal est trop redressé pour avoir permis le développement de cavités notables. Depuis l'Alpette de la Dame (Seuil) ces différences morphologiques sont parfaitement visibles. Ce pendage des Lances de Malissard justifie également l'inexistence de cavités de haut niveau telles Glas ou Biolet liées précisément à une inclinaison assez faible pour avoir permis la constitution de cavités transverses au synclinal.

Quant à la différence de comportement spéléologique entre les flancs est et ouest du synclinal, il s'agit d'une constatation empirique pour laquelle il n'y a pas d'explication satisfaisante, si ce n'est - pure supposition - l'existence d'un paléo-versant plus développé coté ouest (flanc anticlinal disparu).

5. La stratigraphie

L'ensemble stratigraphique est, du nord au sud, très homogène. L'essentiel de l'ossature du synclinal est constitué par la masse urgonienne qui forme des remparts très élevés au dessus des vallées environnantes. Par suite du creusement progressif de celles-ci, les cinq massifs considérés sont restés suspendus en hauteur. Le niveau de basse théorique actuel est donc constitué par les marnes hauteriviennes. Ce niveau peut être traversé à l'occasion d'accidents tectoniques importants (Les Eparres, Fontaine noire, le Mort-Rû sont situées dans le Valanginien).

Au dessus de la masse urgonienne supérieure subsistent localement des lambeaux d'Aptien supérieur (lumachelles) et de Sénonien (craie marneuse). C'est le cas sur l'Alpe, dans le cœur du synclinal, et au Seuil, d'une part à l'Alpette de la Dame et, d'autre part, dans le cœur du synclinal sur la prairie de Marcieu. A l'inverse, l'Urgonien supérieur a pu disparaître en tout ou partie. C'est le cas sur la plus grande partie du Granier ainsi qu'au Seuil sur le vallon de la Rousse, sous les falaises des Roches blanches et sur les pentes est des lances de Malissard à l'aplomb du vallon de Marcieu. Il faut noter que la disparition des lumachelles sur l'axe synclinal du Seuil doit résulter d'une action érosive récente. En effet, la séquence urgonienne y est complète. Ceci laisse à penser que la couverture de lumachelles, voire de Sénonien n'y a disparu que très récemment. De la même manière, on trouve sur les crêtes du Haut du Seuil des blocs de lumachelles épars.

Les lumachelles ne constituent pas un obstacle total à la karstification. Plusieurs gouffres importants s'y ouvrent et les traversent (V92, V94 et FJS41 au Seuil, Golet du Tambourin, Source vieille, Grand Ragne sur l'Alpe entre autres). La densité de cavités y est toutefois moins élevée que dans l'Urgonien. En effet, d'une part ces zones sont occupées par des prairies qui colmatent le lapiez, et ,d'autre part, constituant des zones d'alpages, les orifices y ont souvent été obstrués volontairement.

De plus, les conduits horizontaux qui s'y développent sont souvent de petites dimensions.

Le niveau à orbitolines qui sépare Urgonien supérieur et Urgonien inférieur joue un rôle essentiel. Situé à 80 mètres du haut de l'Urgonien, il constitue un frein puissant à l'exploration spéléologique, spécialement sur le Seuil. Sur une vingtaine de mètres alternent de minces bancs calcaires et des niveaux plus marneux. Ils provoquent souvent la formation soit de vastes salles, au sol plat couvert d'éboulis infranchissables résultant d'un processus d'incasion, soit de galeries étroites comblées par les remplissages. Au Seuil, ce niveau n'est franchi aisément que dans trois cavités, le Trou des Flammes, le Trou de la Turbine et le FJS41. Partout ailleurs, le déblaiement est insuffisant pour permettre le passage du spéléologue et seuls des travaux importants ont permis de dépasser cet horizon. Ce n'est qu'à partir d'une taille suffisante des cavités que l'obstacle est surmonté. C'est précisément le cas sur l'Alpe la plupart du temps où la décompression du massif sur le flanc ouest est associée au passage d'accidents tectoniques décrochants importants.

La disparition de l'Urgonien supérieur et du niveau à orbitolines facilite la pénétration profonde des réseaux. C'est le cas au Granier où de très nombreux gouffres du plateau passent, Encore a-t-il fallu attendre la découverte des Myriades, puis, dans les années 90, le boom des explorations du au Spéléo Club de Savoie pour constater cet effet. A l'inverse, au Seuil, il n'en est rien. En effet, ce niveau est absent en plusieurs endroits, notamment les pentes des lances de Malissard au dessus du vallon de Marcieu et le versant incliné situé sous les Roches blanches. Mais les énormes éboulis qui ont résultés du glissement sur le substratum constitué par le niveau à orbitolines sont récents et n'ont pas été évacués. D'autre part, si l'on suppose sur les lances de Malissard l'existence de cavités anciennes calées sur le niveau à orbitolines la disparition de l'Urgonien supérieur a entraîné leur démantèlement pur et simple. Seul, au nord du Seuil, le trou de l'Alpe bénéficie de cette disposition pour plonger directement jusqu'à -243 m.

A l'inverse, le contact Urgonien supérieur - lumachelles a favorisé la formation de gouffres, en particulier à l'Alpe où paradoxalement cette limite paraît avoir peu fluctué dans le temps.

6. La tectonique

Elle est très comparable du nord au sud du synclinal. Les massifs sont séparés par des décrochements dextres N50 qui décalent progressivement l'axe synclinal de l'est vers l'ouest. Du nord au sud, on passe de la dominante volet ouest à la dominante volet est. Le découpage transversal des massifs résulte de fractures regroupés en plusieurs familles (GIDON M., 1990) liées à la direction de raccourcissement N100.

Une faille longitudinale N10 prenant naissance au sud de la Dent de Crolles (faille de la Gorgette) court jusqu'au Granier. Sur la dent de Crolles, elle passe à l'ouest de l'axe synclinal, puis, sur le Seuil, elle se confond d'abord avec celui-ci avant de s'en éloigner franchement à l'est. A l'occasion du décrochement de l'Alpe, elle repasse à l'ouest de l'axe synclinal.

Elle joue un rôle important au Seuil. En effet, c'est elle qui y conditionne l'existence probable de deux collecteurs parallèles. Ceci est lié à son important rejet (allant jusqu'à 100 mètres) qui décale vers le haut le compartiment occidental et met en contact les marnes hauteriviennes à l'ouest avec l'Urgonien à l'est. Il en résulte que le karst constitué par la partie orientale du massif est barré. Du habert ruiné de Marcieu au cirque de St Même, elle court plusieurs centaines de mètres à l'est de l'axe synclinal (LOISELEUR B., 1994). De plus le faisceau de failles nord-sud de faible rejet compris entre elle et l'axe synclinal gêne la concentration des écoulements s'écoulant d'est en ouest (sens du pendage). Ainsi, aucun affluent ne rejoint la rivière de Malissard en rive droite, à l'exception du Trou des Flammes. Tous ces écoulements ne convergent que sur la faille décrochante du Fourneau, très près de l'exsurgence du Guiers vif.

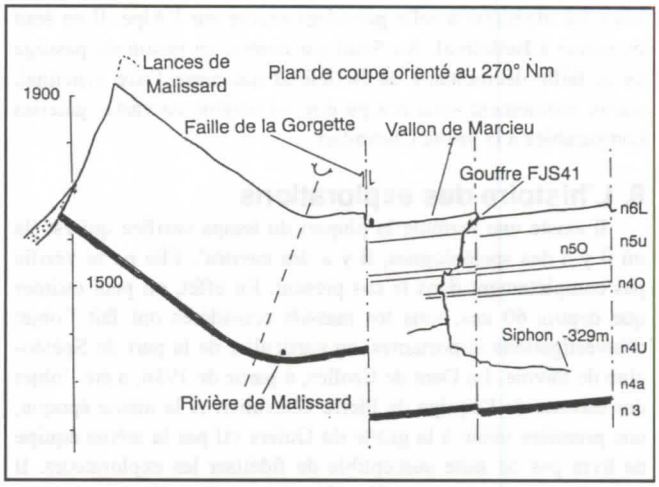

Figure 1 : Coupe transverse du massif du Seuil au niveau du gouffre FJS41. Le compartiment est est barré.

Compression et décompression des massifs ont un rôle actif. Ainsi, au Granier, volet synclinal posé sur un soubassement marneux, la décompression générale observée a pour conséquence la genèse de vides souterrains importants. Inversement, au Seuil, la compression des couches de l'Urgonien liée au très fort pendage du volet ouest contrarie la formation de cavités pénétrables. Par contre, toujours au Seuil, l'ouverture au niveau du Barrémien inférieur liée à une flexure brutale a permis au collecteur occidental de se développer pratiquement à l'aplomb des crêtes de Malissart.

7. L'évolution paléo-géographique

Il s'agit du facteur qui a le plus conditionné l'évolution ancienne et la formation des réseaux de Chartreuse. Il est en effet nécessaire de faire appel à lui pour expliquer soit les dimensions de certaines galeries (grotte Chevalier à la Dent de Crolles), soit la disposition de certaines cavités (grotte du Biolet, grotte des Pincherins), soit la densité de conduits. Il est aussi le plus difficile à maîtriser. Plusieurs théories ont été élaborées à ce sujet depuis Cl. Mugnier (MUGNIER C.,1965) qui fait appel à une karstification antépliocène, jusqu'à à Ph. Audra et F. Hobléa (AUDRA P. et al.,1993). Quant aux mécanismes et à la chronologie des mouvements ayant amené à la mise en place des reliefs actuels, ils restent malgré tout très hypothétiques et complexes compte tenu des multiples phénomènes ayant interféré entre eux depuis le Crétacé supérieur jusqu'au Pléistocène. Le point essentiel non résolu concerne l'extension ancienne des éléments manquants du synclinal et les conditions de leur disparition. M.Gidon émet à ce titre des hypothèses sur une troncature plane ayant affecté les massifs à une époque anté-miocène, et en tout cas avant la surrection finale du massif alpin. Dans ces conditions, des bassins d'alimentation auraient pu exister au sud de la Dent de Crolles - prolongation du synclinal - comme à l'ouest et au nord de l'Alpe et du Granier - flan anticlinal. A la Dent de Crolles comme à Bellefond, le volet synclinal ouest aujourd'hui disparu se développait entre les failles du col de Baure et de la Gorgette avec un pendage certainement très fort si on en juge par celui des couches

marneuses au col des Ayes (GIDON M., 1993). De plus, les failles décrochantes de Bellefond et du Prayet limitaient leur extension. En ce sens, le paléo-versant occidental de la Dent de Crolles ne pouvait être que fort réduit. Il présentait un aspect très semblable à celui des lances de Malissart. On ne rencontre d'ailleurs pas, dans le réseau de la Dent de Crolles, de vestiges de galeries provenant de l'ouest ce qui serait le cas si la situation avait été identique à celle prévalant encore sur l'Alpe. Il en était de même à Bellefond. Au Seuil par contre, en raison du passage de la faille décrochante de Bellefond qui barre l'axe synclinal, aucun écoulement axial n'a pu être à l'origine de vastes galeries comparables à la grotte Chevallier.

8. L'histoire des explorations

Il existe une formule la plupart du temps vérifiée qui est 'là où il y a des spéléologues, il y a des cavités'. Elle ne se vérifie pas complètement dans le cas présent. En effet, on peut estimer que depuis 60 ans, tous les massifs considérés ont fait l'objet d'investigations importantes, en particulier de la part du Spéléo-club de Savoie. La Dent de Crolles, à partir de 1936, a été l'objet des travaux de l'équipe de Pierre Chevalier. A la même époque, une première visite à la grotte du Guiers vif par la même équipe ne livra pas de suite susceptible de fidéliser les explorateurs. Il faut dire qu'en termes d'explorations, c'est l'existence des grandes cavités de haut niveau qui a servi de déclencheur : Trou du Glas à la Dent de Crolles, Biolet à l'Alpe, Balme à Collomb au Granier. Les explorations par le plateau ne sont venues que plus tard. Or, au Seuil en l'absence d'accès latéraux, seules les gouffres ont été susceptibles de fournir des accès au collecteur. Ce fut le cas du Gouffre cavernicole en 1981 puis du Trou des flammes, connu depuis 1973, mais pour lequel l'accès au collecteur ne fut découvert qu'en 1984.

9. Impact des glaciations

Dans toute la Chartreuse, les périodes glaciaires se sont traduite de façon homogène par la formation de glaciers locaux dont les traces subsistent en divers points. En particulier les axes synclinaux ont partout été occupés par des langues glaciaires.

10. Conclusions

Deux types de grand réseaux cohabitent. L'un privilégie le creusement à partir d'un paléo-versant ouest et nord (Alpe, Granier), l'autre, le creusement à partir d'un paléo-versant sud (Dent de Crolles). Le flanc est du synclinal est partout pauvre en cavités. Le Seuil présente la même morphologie que la Dent de Crolles mais n'a pu bénéficier de l'apports de bassins aujourd'hui disparu. Le cavernement ne peut y être que moindre. Bellefond se compare au flanc est de la Dent de Crolles. Il est peu probable qu'un réseau maillé y existe.

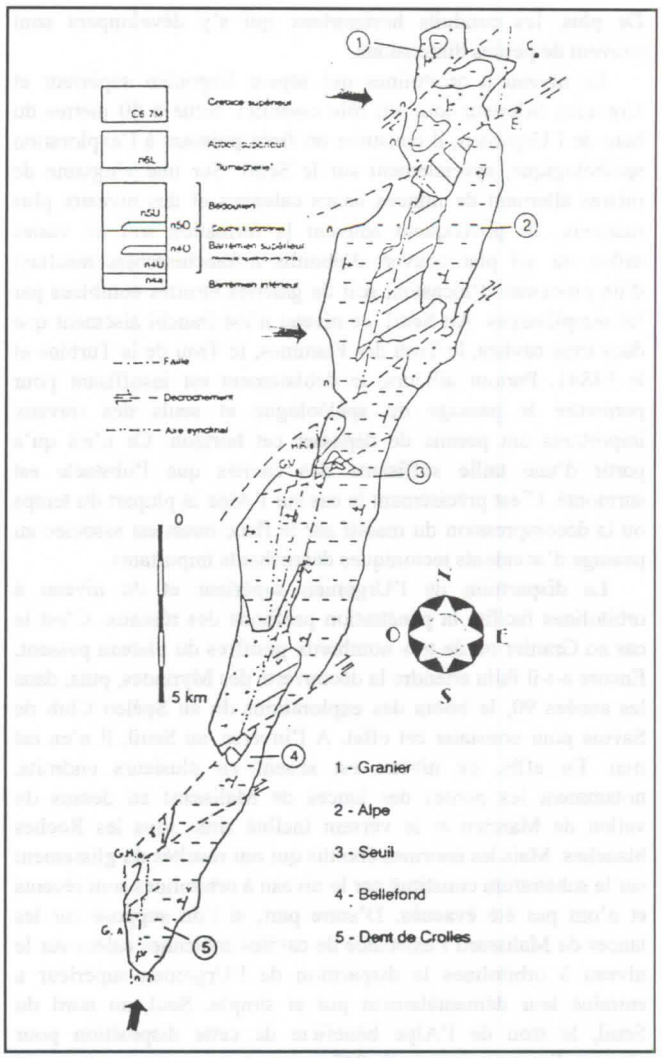

Figure 2 : Schéma général du synclinal oriental de Chartreuse.

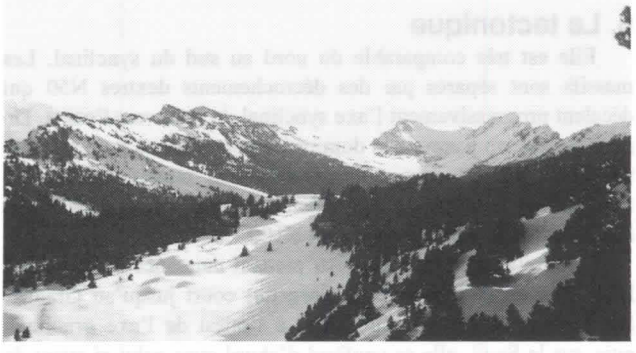

Figure 3 : Sur le synclinal oriental de Chartreuse, l'Alpe et le Seuil.

Références

AUDRA P. et al., 1993, signification paléogéographique des réseaux perchés dans les Alpes du Nord, Travaux de l'URA 903 XXII : 3-17.

GIDON M., 1990, Géologie de la Chartreuse, A la découverte du patrimoine de Chartreuse.

GIDON M., 1993, Circuit de la Dent de Crolles, A la découverte du patrimoine de Chartreuse.

LOISELEUR B., 1994, Le massif du Seuil (Chartreuse, France) organisation des réseaux souterrains, Karstologia 24 : 13-28.

MUGNIER Cl, 1965, Les karstifications antépliocènes et plioquaternaires dans les Bauges, la Chartreuse septentrionale et les chaînons jurassiens (Paris), Annales de spéléologie (Paris) 1-2 : 15-46 et 167-208.

ROMANI L, 1995 - La répartition des entrées de cavités sur le plateau de l'Alpe, Calaven 9: 173-179.

Néotectonique et spéléogenèse : application au massif pyrénéen des Arbailles (France)

par Nathalie Vanara et Richard Maire
Laboratoire de Géographie Physique Appliquée et DYMSET (CNRS),
Institut de Géographie, Université de Bordeaux III, 33405 Talence cedex, France

Abstract

In the alpine ranges, the plio-quaternary tectonics is recorded by speleogenesis steps. The Arbailles massif is a folded area of Jurassic and Lower Cretaceous limestones belonging to the north-pyrenean zone, located in an active seismic area. The plio-quaternary uplift, of 1000 m according to the altitude of the dry valleys levels, permitted the lowering of the base level and the deepening of endokarst. The cave levels indicate the steps of uplift. During Quaternary, the morphology of galleries was modified by a compressive tectonics. The recurrent faulting provoked the shearing of walls and rock falls. Speleothems recorded paleoseisms by broken stalagmite massifs. The U/Th dating of older stalagmitic generation in the lower level of Nebele cave (alt. 365 m, base level 200 m) indicates an uplift average of 0,4 mm/yr from 400 000 years.

Résumé

Dans les chaînes alpines, l'étude des étapes de la spéléogenèse permet d'estimer l'importance de la surrection plio-quaternaire. Le karst des Arbailles, unité plissée de calcaires jurassico-crétacés de la zone nord-pyrénéenne, est localisé dans un contexte sismique actif. La surrection plio-quaternaire, estimée à 1000 m d'après les niveaux étagés de vallées sèches, a permis l'étagement des réseaux souterrains. Au cours du Quaternaire, le drainage hypogé (captures) et la morphologie des conduits ont été modifiés par la surrection (tectonique compressive principalement). Le rejeu des failles a entraîné le cisaillement des parois des galeries et des chutes de blocs (trémies, chaos). Les spéléothèmes ont également enregistré des paléoséismes : massifs de stalagmites brisées, chutes de stalactites. La datation U/Th de la génération la plus ancienne de stalagmites dans la niveau inférieur du Nébélé indique un taux moyen de surrection de 0,4 mm/an depuis 400 000 ans.

1. Introduction

Le massif basque des Arbailles (165 km^2) appartient aux chaînons calcaires de la zone nord-pyrénéenne (figure 1). Il présente une surface fluvio-karstique héritée, à buttes résiduelles (1000-1250 m) façonnée dans les calcaires jurassico-crétacés et perchée à plus de 800 m au-dessus du niveau de base régional. Les étages génétiques de cavités et les rejeux de failles actives indiquent une forte activité tectonique de surrection au cours du Pléistocène. Actuellement, la zone est toujours sismiquement active. On observe une correspondance entre l'étagement des cavités et celui des principaux niveaux des vallées sèches perchées.

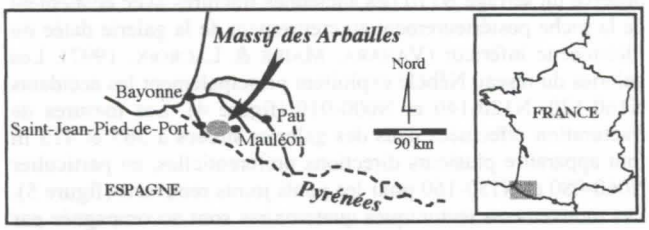

Figure 1 : Situation géographique du massif des Arbailles.

2. Les indices néotectoniques globaux : l'étagement des cavités

Les recherches spéléologiques ont permis le recensement de 600 cavités sur l'ensemble du massif (DELAITRE, 1995). 37 gouffres dépassent 100 m de dénivellation. Parmi eux 16 ont plus de 200 m de profondeur et/ou plus de 1000 m de développement.

Les types de réseaux

L'ancienneté de la karstification est attestée par l'existence de plusieurs familles de cavités. Les réseaux mis au jour, localisés sur les buttes et les versants, sont les témoins de cavités anciennes, concrétionnées, décapitées par l'érosion (Belchou, 1120 m ; Heguilloré, 990 m). Pour les réseaux souterrains, on observe deux types d'étagement :

1- Certaines galeries perchées se développent sur des niveaux lithostratigraphiques comme les calcaires marneux de l'Aptien inférieur et du Néocomien (Grande Bidouze).

2- D'autres sont des niveaux "fossiles" génétiques marqués par de grandes galeries subhorizontales creusées dans la masse des calcaires et correspondant à un ancien stationnement du niveau de base local (VANARA, 1996).

Sur la bordure E du massif, on distingue un étagement des réseaux le long de la vallée sèche d'Ithé (figure 2) : niveau de 365 m du Nébélé et niveau de 675 m d'Etxanko Zola.

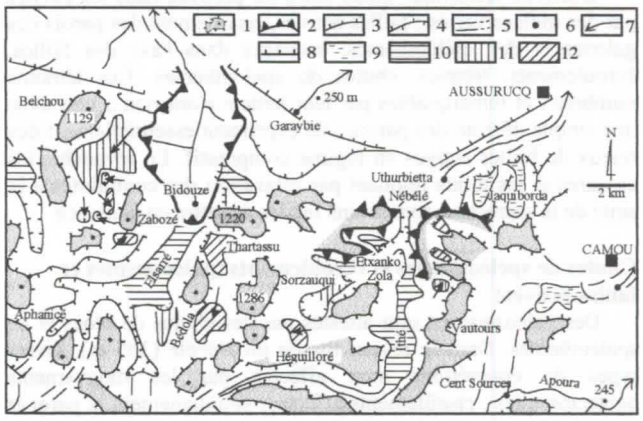

Figure 2 : Carte géomorphologique simplifiée de la partie NE du massif des Arbailles. 1- Butte résiduelle de la haute surface (>1000 m), 2- Rupture de pente avec corniche, 3- Rupture de pente convexe, 4- Crête, 5- Vallée sèche et prolongement supposé, 6- Emergence, 7- Cours d'eau, 8- Faille normale, 9- Niveau 350-400, m 10- Niveau 680-750 m, 11- Niveau 800-850 m, 12- Niveau 900-950.

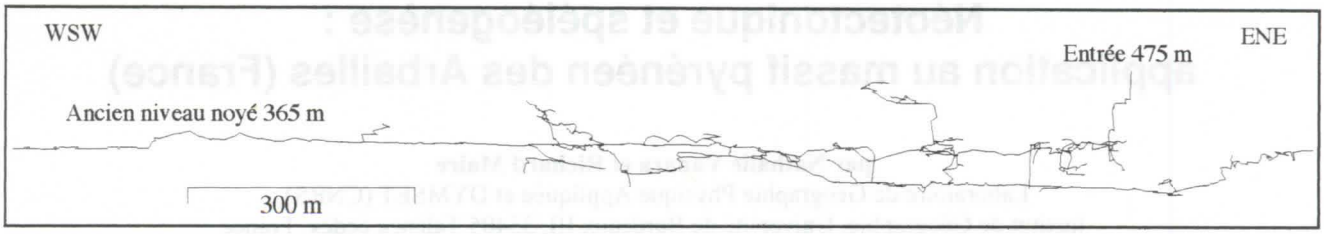

Figure 3 : Coupe projetée du réseau Nébélé (Toporobot, topographie Collectif Nébélé).

Sur le karst sommital des Arbailles, au-dessus de 1000 m, les grands gouffres à structure verticale sont également liés à la surrection du massif. Ils s'ouvrent généralement dans les calcaires marneux albiens comme le gouffre d'Aphanicé (-504 m) dont le puits de 335 m traverse les calcaires urgoniens à la faveur d'une faille majeure.

Les niveaux du Nébélé et d'Extzanko Zola

Le réseau du Nébélé (alt. 465 m, 14 km, -160 m) se développe dans les calcaires du Dogger à la base du massif. Un grand niveau de galeries sèches, localisé à 365 m d'altitude, indique un stade de creusement en régime noyé, généré par l'ancien niveau de base (figure 3). Cet étage correspond au niveau inférieur de vallée sèche situé vers 380 m (Jaquiborda) au-dessus d'Aussurucq. Un traçage à la fluorésceine prouve que les eaux du réseau du Nébélé émergent à la source d'Uthurbietta. Plus haut, le réseau d'Extzanko Zola (alt. 645 m, 4 km) est le témoin d'une ancienne émergence de la vallée d'Ithé. Le niveau fossile des "Planches à Clous" (675 m) présente un profil en "montagnes russes" typique d'un ancien niveau noyé qui émergeait à la hauteur du niveau subhorizontal de 700 m de la grande vallée sèche d'Ithé. A la suite de la surrection, la galerie des Planches à Clous s'est asséchée de même que la conduite forcée de la zone d'entrée. En surface, l'érosion régressive dans la vallée de l'Apoura est responsable de la capture de l'amont de la vallée d'Ithé et de son assèchement. La capture des eaux souterraines du réseau d'Etxanko Zola vers le nouveau niveau de base de l'Apoura (Cent Sources) s'est effectuée à la faveur du pendage général vers le S et le SW et de la fracturation NW-SE et N-S.

3. Les indices de compression récents dans les cavités

L'activité tectonique quaternaire est prouvée dans les cavités par des indices variés : failles actives, cisaillement des parois des galeries et des spéléothèmes, broyages dans l'axe des failles, écroulements, trémies, chutes de spéléothèmes. Ces témoins nombreux et remarquables par leur netteté n'ont rien à voir avec une simple détente des parois : ils expriment essentiellement des rejeux de failles actives en régime compressif. En revanche, les cassures et les joints rejouant par relaxation des contraintes à la suite de la surrection sont moins faciles à mettre en évidence.

Chutes de spéléothèmes et écroulements (paléoséismes et failles actives)

Des paléoséismes sont attestés par des chutes de blocs et de spéléothèmes. Dans le réseau fossile du Nébélé (365 m), divers types de concrétions sont affectés par les mouvements néotectoniques : cisaillements affectant simultanément la paroi et les stalagmites, stalactites cassées et plantées dans les banquettes argileuses, cimetières de stalactites et de piliers brisés. Les observations de ce type se font par dizaines. Les failles actives jouent principalement en régime compressif et induisent une fracturation secondaire oblique et/ou perpendiculaire à la direction principale : fissures irrégulières de cisaillement, réouvertures de stylolithes, de joints de fracture calcités et de joints de stratification. Les rejeux provoquent de petits décalages atteignant fréquemment 5 à 10 cm mesurables sur les coupoles de plafond, mais ils peuvent atteindre jusqu'à 1 m dans Etxanko Zola. La plupart des grands écroulements observés dans le Nébélé sont liés directement aux rejeux récents des failles. Il ne s'agit pas de vides tectoniques tels que les rampes mortes d'écailles (hypothèse actuelle pour la salle de la Verna à la Pierre Saint-Martin, BOURROUILH & *al.*, 1996).

Détermination des contraintes tectoniques récentes

Les structures compressives de la phase pyrénéenne (raccourcissement majeur N020 et secondairement N030, N160 et N110) sont profondément influencées par les dispositifs mis en place lors de la distension mésozoïque, d'où l'existence de cinq directions de fracturations privilégiées : N035-40, N080, N120, N170 et N000 (OLLIER & ROVIRA, 1983).

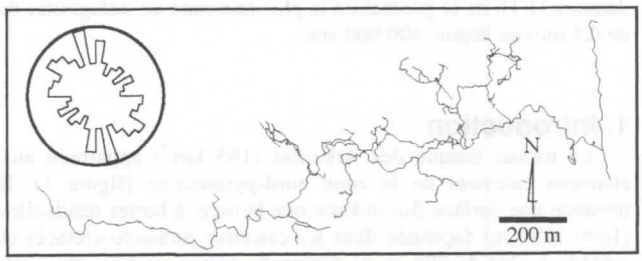

Figure 4 : Plan du réseau Nébélé (Toporobot, topographie Collectif Nébélé) et diagramme de directions des galeries de plus de 10 m de long, réseau du Nébélé (308 valeurs).

La néotectonique (Quaternaire moyen et récent) fait rejouer certaines familles de fractures. Dans le réseau d'Extanko Zola (niveau fossile de 675 m exploitant un accident N040), on observe un serrage N110 des anciennes fractures avec éclatement de la roche postérieurement au creusement de la galerie datée du Pléistocène inférieur (VANARA, MAIRE & LACROIX, 1997). Les galeries du réseau Nébélé exploitent principalement les accidents N160-170, N120-140 et N000-010 (figure 4). Les mesures de fracturation effectuées dans des galeries situées à 365 et 415 m font apparaître plusieurs directions préférentielles, en particulier N060-080 et N150-160 pour les petits joints réouverts (figure 5). Les mouvements tectoniques quaternaires sont accompagnés par des cisaillements au tracé irrégulier dont les directions sont obliques par rapport aux failles majeures.

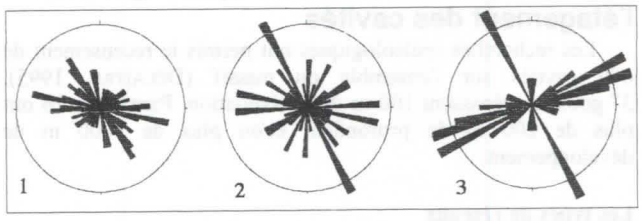

Figure 5 : Diagramme de fracturation du réseau Nébélé, 1- fissures de cisaillement et écailles (85 valeurs), 2- fractures (35 valeurs) 3- anciennes fractures réouvertes (32 valeurs). Intervalle : 5°, rayon 10 %.

4. Les étapes de la surrection

Les arguments géomorphologiques

Des paléocavités, recoupées par l'érosion, témoignent d'une karstogenèse ancienne puisque leur situation au sommet des buttes ou sur les versants, implique la disparition d'une tranche de calcaire importante. Les arguments géomorphologiques plaident en faveur d'une karstification remontant au Tertiaire supérieur. Les gros massifs stalagmitiques, constitués de calcite pure, suggèrent un environnement chaud et stable. Certains dépôts détritiques de paléocavités (Bédola) montrent un cortège minéralogique d'origine allochtone (verre, feldspath, amphibole, rutile, calcédoine, etc.). Celle-ci provient d'un ancien amont aujourd'hui déconnecté en raison de l'enfoncement des vallées périphériques consécutif à la surrection. On retrouve aussi de nombreux éléments de cuirasses ferrugineuses indiquant une genèse en zone mal drainée, dans un contexte karstique de basse altitude (VANARA, MAIRE & LACROIX, 1997).

La composante de surrection quaternaire (figure 6)

La vitesse de surrection quaternaire a été estimée par la datation U/Th de stalagmites. Ainsi le niveau du Nébélé situé à la cote 365 m est formé par des conduits dont la morphologie en "conduite forcée" indique un creusement en régime noyé. Il émergeait à l'altitude de l'ancien niveau de base. A la suite de l'approfondissement de la vallée consécutif à la surrection, la galerie s'assèche et des spéléothèmes se déposent. Or, il existe une faible latence entre l'assèchement et la précipitation de la calcite due aux eaux de percolation. En datant par la méthode U/Th la calcite de la génération de stalagmites la plus ancienne du niveau de 365 m, on date donc le début de l'assèchement et par conséquent le début de la surrection.

La génération la plus ancienne, reposant sur le plancher de la galerie, est âgée de 407 000 ans (+78 700, -46 600). Une autre famille de stalagmites scellant des remplissages argileux est datée de 95 000 ans (+3 100, -3 000). Elle se situe donc dans l'interglaciaire du stade isotopique 5 (Eémien ls) (analyses CERAK, Y. QUINIF, Mons, Belgique). On estime donc que le massif s'est soulevé de plus de 165 m en 400 000 ans environ, soit un taux de surrection de 0,4 mm/an.

La composante de surrection quaternaire serait de l'ordre de 700 m en tablant sur ce taux moyen de 0,4 mm/an. Le premier grand niveau perché de vallées sèches (Elsarré, Ithé, alt. 700 m) daterait du Pléistocène inférieur (1,3 à 1,5 Ma). Les niveaux supérieurs de vallées sèches (Sorzauqui, Thartassu) seraient à la limite Pléistocène-Pliocène (1,9 à 2,1 Ma). Par conséquent, la haute surface située entre 1000 et 1200 m d'altitude daterait du Pliocène, ce qui est confirmé par la flore tertiaire découverte dans la concrétion du Belchou. On estime donc la surrection plio-quaternaire à 1000 m au moins.

La surrection plio-quaternaire résulte de mouvements tectoniques principalement compressifs. Le niveau intermédiaire d'Ithé marque un stade d'arrêt au cours du Pléistocène qui a permis l'élaboration d'un profil en long tendu de plusieurs kilomètres, incliné à 1 ou 2°, interrompu à l'aval par une reculée ou une gorge dont l'âge est contemporain de la dernière phase de soulèvement. Ce type de niveau ne peut perdurer que dans une roche carbonatée dure et fissurée permettant un bon drainage souterrain.

Plus au sud, dans le massif de la Pierre-Saint-Martin, les spéléothèmes hérités observés à l'affleurement à plus de 2000 m ont tous plus de 400 000 ans. Comme ces derniers ne se forment pas dans l'étage supraforestier, ils sont la preuve d'un contexte climatique plus chaud et d'un soulèvement important (BINI *& al.*, 1989 ; MAIRE, 1990).

5. Conclusion

A l'Oligocène supérieur et au Miocène inférieur-moyen, le massif des Arbailles est en continuité morphologique avec les poudingues de Mendibelza au sud et les flyschs au nord. La proximité du niveau de base et le climat tropical humide sont favorables à une importante altération ferralitique. Un système fluviatile bénéficiant des amonts gréso-conglomératiques se met en place sur la couverture semi-imperméable des calcaires marneux albiens et des affleurements résiduels de flysch. A partir de la fin du Miocène supérieur, puis au Plio-Pléistocène, la chaîne pyrénéenne connaît une grande phase de surrection provoquant un étagement des cavités et des vallées sèches. Le niveau majeur de vallée sèche d'Elsarré et d'Ithé (700 m) n'a pu s'élaborer que lorsqu'il était raccordé directement, à l'aval, au niveau de base et ,à l'amont, au massif de Mendibelza (Pléistocène inférieur). Les réseaux souterrains d'Etxanko Zola et du Nébélé se sont donc formés au cours du Pléistocène inférieur et moyen après la déconnexion de ces vallées avec leur amont imperméable (tableau 1).

L'évolution morphologique des galeries indique une influence majeure des failles actives au Pléistocène : cisaillement des parois, chaos de blocs, chutes de spéléothèmes. Actuellement, l'essentiel du drainage s'effectue par des systèmes souterrains qui n'ont aucune liaison avec le paléoréseau hydrographique. La carte des séismes (magnitude ^{3} 4 depuis 1900) des Pyrénées occidentales montre une activité sismique importante au niveau de la zone nord-pyrénéenne où se situe le grand accident décrochant E-W (séisme d'Arette en 1967, magnitude 5,3) (figure 7). Une autre ligne orientée N-S, située sur un accident transverse, va de la bordure orientale des Arbailles à la vallée de Roncal en Navarre en passant par la Haute Soule. Le massif des Arbailles apparaît donc dans un contexte sismique actif et les chutes de spéléothèmes du Nébélé témoignent de paléoséismes majeurs qui se sont produits entre 400 000 ans et aujourd'hui.

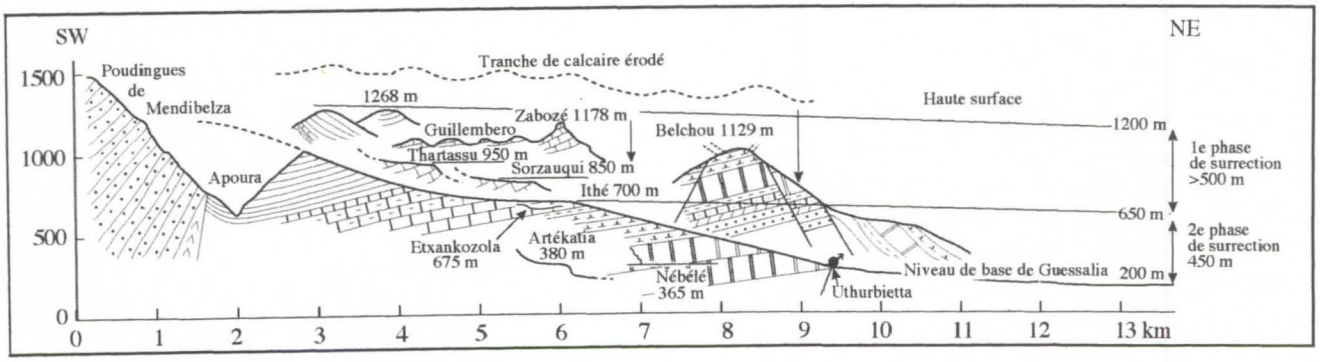

Figure 6 : Correspondance entre les stades de surrection, les niveaux de vallées sèches et les niveaux souterrains.

Le réseau de la Pierre-Saint-Martin permet des observations similaires (MAIRE, 1990). De même, des mouvements tectoniques récents ont été étudiés dans les cavités des Alpes de Lombardie en zone sismique active (BINI *et al.*, 1992)

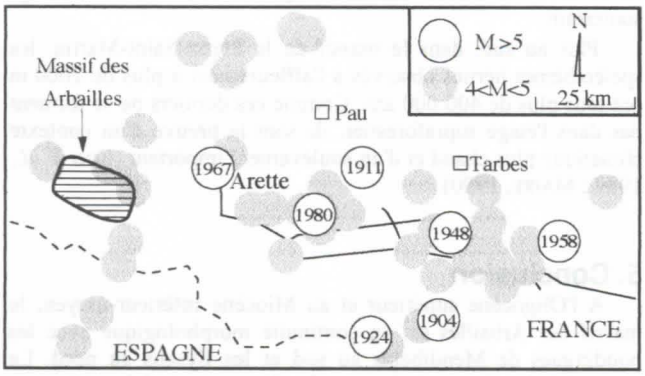

Figure 7 : Carte des séismes de magnitude ³ 4 depuis 1900 dans les Pyrénées occidentales (Massinon, 1979 ; fichier de sismicité de l'Observatoire Midi-Pyrénées , 1995, synthèse A. Souriau, modifié).

Références

BOURROUILH, R.; BAUER, J.; DELOFFRE J.; DOUAT, M.; MAIRE, R. & NURISSO, J. 1996: Inversion tectonique et rampes d'écailles : nouvelles données tectoniques et stratigraphiques fournies par le réseau karstique géant de la Pierre St-Martin, Pyrénées-Atlantiques, France. *C. R. Acad. Sc. Paris,* t. 322, Série IIa.

BINI, A.; DELANNOY, J. J.; MAIRE, R. & QUINIF, Y. 1989: Générations de cavités karstiques dans les chaînes alpines s.l. *C. R. Acad. Sc. Paris*, 309, II: 1183-1190.

BINI, A.; QUINIF, Y.; SULES, O. & UGGERI, A. 1992: Les mouvements tectoniques récents dans les grottes du Monte Campo dei Fiori (Lombardie, Italie). *Karstologia*, 19, pp. 23-30.

DELAITRE, E. 1995: Massif des Arbailles, base de données. Comité Départemental de Spéléologie des Pyrénées-Atlantiques, Pau, 375 p.

MAIRE, R. 1990: La haute montagne calcaire : karsts, cavités, remplissages, Quaternaire, paléoclimats. Thèse d'Etat, Univ. de Nice, in *Karstologia-Mémoires*, 3, 731 p.

MASSINON, B. 1979: Vue d'ensemble de la sismicité instrumentale en France de 1962 à 1976, in Vogt, J.: Les tremblements de terre en France, *BRGM* n°96.

OLLIER, G & ROVIRA, A. 1983: Etude sédimentologique et structurale de la discordance jurassico-crétacée dans le massif des Arbailles (Pays basque). ENSPM, 156 p.

QUINIF, Y.; GENTY, D. & MAIRE R. 1994: Les spéléothèmes, un outil performant pour les études paléoclimatiques. *Bull. Soc. géol. Fr.*, 165, 6: 603-612.

VANARA, N. 1996: Les cavités du massif des Arbailles. Types et indicateurs de l'évolution géomorphologique. *Upik*, Institut de Géographie, Université de Fribours, Suisse. vol. 8: 79-98.

VANARA, N.; MAIRE, R. & LACROIX, J. 1997: La surface carbonatée du massif des Arbailles (Pyrénées-Atlantiques) : un exemple de paléoréseau hydrographique néogène déconnecté par la surrection. *Bull. Soc. Géol. France* (sous presse).

Périodes et âges	Niveaux étagés (endo et exokarstiques)	Composante de surrection depuis l'Actuel
Actuel	Niveau de base régional (200 m)	Surrection en cours (zone sismique active)
Pléistocène moyen	Niveau de 365 m du Nébélé 0,4 Ma (U/Th)	>160 m (0,4 mm/an)
Pléistocène inférieur	Niveau d'Elsarré-Ithé 700 m Â 1,3-1,5 Ma	>450 m (dernière grande phase de surrection)
Pléistocène inf.-Pliocène sup.	Niveau Sorzauqui-Thartassu 850-950 m Â 1,8-2 Ma	>700 m
Pliocène	Haute surface Arbailles Sommets buttes 1100-1250 m	>1000 m
Fin Miocène	Début épirogenèse	>1300 m environ
Oligo. sup.-Miocène	Phase de stabilité et d'altération	—

Tableau 1 : Chronologie générale des évènements morpho-tectoniques sur le massif des Arbailles

Geography and Speleology

Oscarlina Aparecida Furquim Scaleante
Estação Floresta, Av. Oscar Pedroso Horta, 144 13083-510 Campinas, SP, Brazil

Abstract

Speleology as a science is still in its infancy in Brazil, not yet having achieved academic identity. In contrast to most of the sciences, however, it involves a multidisciplinary field of study combining the efforts of geologists, paleontologists, archaeologists, biologists, etc. Speleologic work requires the combined efforts of many professionals, each studying specialized aspects inside caves, but more or less independently.

It is suggested here, however, that speleological work should not be conducted as a multi-disciplinary endeavor, but rather as an inter-disciplinary one. The traditional emphasis of scientific inquiry involves a single, positivist method of investigation which leads to a fragmented view of the world and its problems, but interdisciplinarity is necessary to deal with the complexities of modern-day problems. This is where geography can be make an important contribution.

Resumo

A espeleologia é uma ciência que dá seus primeiros passos no Brasil, pois ainda não possui identidade acadêmica. Diferente das demais em decorrência do próprio contexto histórico em que nasce, trata-se de uma ciência multidisciplinar, pois congrega geólogos, paleontólogos, arqueólogos, biólogos, etc. Enfim, uma equipe de trabalhos espeleológicos só se considera completa se contar com profissionais de diversas áreas do conhecimento que adentram as cavernas, cada um estudando aquilo que lhe interessa no seu campo de estudo específico.

A proposta que se faz é que tais equipes espeleológicas, em lugar de multi, passem a ser interdisciplinares. Juntamente com esta sugestão, é apresentada a maneira pela qual a ciência geográfica pode oferecer a sua contribuição à espeleologia brasileira.

A busca da interdisciplinaridade ocorre como saída para uma séria insuficiência de procedimentos científicos para abordagem dos problemas da atualidade, ou seja, as formas de trabalho dentro das ciências estão dando mostras de esgotamento.

Essa falta de metodologia mais abrangente para estudar os diversos fenômenos se dá em virtude da formação clássica das ciências, as quais se consolidaram numa época em que a forma de produzir conhecimento obedecia aos métodos positivistas.

As raízes positivistas dificultam enormemente o chegar à interdisciplinaridade, tendo em vista o hábito de visão fragmentada que os cientistas foram adquirindo com o passar do tempo.

Porém, não havendo condições para decodificar as mensagens que atualmente se nos apresentam, vale a árdua tentativa de se revolucionar os métodos científicos que até hoje vigoram, porque eles não mais nos fornecem as respostas que prercisamos.

Em tempos de busca de aperfeiçoamento para produção de conhecimento é de fundamental importância manter contatos internacionais entre cientistas de várias áreas do saber.

Introduction

At the present time, it is extremely important to join efforts to promote the equilibrium between man and nature, both threatened with extinction if we are unable to understand and act in the face of socio-environmental dilemmas. Speleology seems to be unaware of the importance and possible contributions of geography, while geography ignores caves.

Speleology is already a multidisciplinary science combining the efforts of history, biology, archeology, paleontology, psychology, geology, etc., but it should not ignore the possible contributions of geography. Nor should geography, basically concerned with society in general (ANDRADE, 1994) as inserted in the construction of spaces, deny greater attention to speleology. The latter is a new science in Brazil, not yet having achieved academic identity, but our caves, the objective of its study, are rapidly acquiring a new status. They have been recognized by society as more than mere accidents of nature. Man finds himself more closely linked to these "geographic accidents" than ever before due to the demands of tourism, sportsmen, mining, and the damming of rivers for the generation of energy.

Geography is a science which studies nature, not in isolation, but always in conjunction with some sort of social aspect; it is a science whose principal objective is to study the society/spaces produced by man or the natural spaces which he alters, and it is relevant wherever human society exists. It is exactly this interface between society and nature which links geography to speleology, rather than the "borrowed" view of geomorphology, as "only part of geomorphological knowledge is assimilated by geography" (MARINHO, 1995).

Interdisciplinarity

The world ecological conference RIO 92 gave rise to many questions about the environment and the quality of human lives. There seems to be an ever-growing consensus that the problems facing us today must be dealt with in a more global or holistic manner, being studied from all possible angles to ensure greater possibilities for understanding and solution, thus leading to "anthropogenic alterations" rather than "anthropogenic destruction" (HELENE and BICUDO, 1994).

The best path to an understanding of unfamiliar phenomena or situations is through scientific interdisciplinarity. This interaction between various sciences integrates concepts and methods, with the common objective of a unified approach and a more complete understanding of human development within a reorganized world. Such interdisciplinarity should help provide new perspectives for accumulated knowledge and, by the reconciliation of knowledge and practice, furnish a basis not only for the confirmation of what already exists but also what is to come. This practice seeks answers to the emerging questions which have not yet been contemplated by political science, sociology, biology, or even modern scientific technologies (FREITAG et al., 1992).

Living with interdisciplinarity is a complex task because all of the present-day sciences were created as independent, compartmentalized disciplines. The positivism which reigned from the end of the 19th century until the middle of the 20th was basically responsible for this compartmentalization of scientific knowledge, and the positivist methods of description, analysis, experimentation, measurement, and rigorous control of phenomena gave rise to models of scientific procedures which accepted as science only that which could be fit into these pre-established models. But these models envision static concepts, not dynamic interaction, and this has hindered the advance of knowledge because many aspects of our reality today no longer fit into these traditional niches or approaches. We can now see that the consolidation of the sciences is necessary to provide space for the consideration of new aspects and new approaches which will lead to a more complete view of natural phenomena.

Since the knowledge available today was constructed within a methodology based on separation and specialization, extreme efforts may be required to achieve what is sought. Geography has already embarked on this path, eliminating the traditional distinction between physical geography and human geography to form a single, integrated discipline (ANDRADE, 1985; LACOSTE, 1976). In its struggle for academic legitimacy, speleology in Brazil should follow the example of geography and promote interdisciplinarity, thus fostering a more complete comprehension of the natural subterranean world and man's position in it so that the social impacts on nature can be minimized while providing maximal benefits for man. It must be remembered that a cave consists of far more than empty internal space: it involves a whole complex of interrelated systems, including the exokarstic geologic formations and the hydrologic systems which depend for their continued existence on human activities. In order to guarantee the necessary protection/conservation of that which nature has given us, it is necessary to cultivate a more global view contemplating not only natural phenomena, but a combination with nature inserted in society, so that the best means of exploitation of former can be used to help overcome the shortcomings of the latter.

Relationship between Geography and the Caves

How should geography fit into the work of the speleologists of Brazil, a third-world country with serious social problems which has wrought tremendous depredation on nature. Caves are a natural phenomena, and geography is interested in the "comprehension/ approach of social relationships as a component of the diverse scenes in which they are inserted: the presence of natural aspects is not dissociated from the play of reciprocal influences involved in the organization of society" (MENDONÇA, 1994). Such a geography should concern itself with the new socio-environmental question of the caves. If a cave is not respected, the use and occupation of the land may lead to the destruction of the forest to plant crops, the change in the course of a river for personal benefit, or the inappropriate construction of dams which flood caves and archeological sites, in addition to the rampant destruction wrought by various mining acitvities for conducted with exclusive consideration of financial profits.

Relationship beween Society and the Caves

The relationship between society and nature should be taken more seriously by speleoloigists. They need to remember that human society is linked, either directly or indirectly, with their object of study or they will see this destroyed by the action of man. Whether organizing an expedition to explore an area and draw topographical maps or making a detailed study of the fauna of a cave or some paleontological escavation of interest, the speleologist should not hold himself aloof from the inhabitants of the area. He must remember how the humble inhabitants think and live (generally in misery). It is not unusual for speleologists to stay in the homes of these local inhabitants when exploring caves, and they generally encounter a very degrading way of life: the family lives poorly, eats poorly, and often has no convenient source of fresh water. It is difficult to expect people living in such sub-human conditions to respect nature. They do not even have access to medical assistance, nor are retirement benefits available when they can no longer work. Historical conditions inherited from the period of slavery have shown that the individual does not actually own his land and is always being threatened with expulsion -- Why should one be concerned about its preservation? The Brazilian society has always been an elitist one, and marks have remained on the collective memory. The owner of the sugar mill or the coffee baron controlled the slaves, and the rich landowner often

continued the same treatment for the rural worker. Preference was given to foreign workers, and local workers were rejected as "surplus" by the large farmers because they would not accept the cruel treatment dispensed to slaves. A large segment of the population thus found itself segregated because it was neither rich nor slave.

Speleologists often encounter irreversible destruction provoked by the action of man, but much of this damage could have been avoided by a bit of local awareness. The destruction of one cave in Bonito would never have happened if the local population had realized that the speleothems were not precious stones, and the road passing directly over the Toca dos Ossos in Bahia would never have been built in such a precarious place if people had been aware of the danger of destruction.

Speleological activity cannot afford to ignore the question of the human society, since this society is moving ever closer to the caves; moreover, speleologists should be able to provide a positive impact on the local population and help promote a better way of life for the local inhabitants in the surrounding areas, thus helping prevent the destruction of these caves. These examples show how speleology and geography could benefit from a closer approximation. Not only must the actions of the local inhabitants be considered in the preservation of the caves, but the so-called ecological tourism which has been emerging in the country in the past few years has also been having an effect, and the increasing demand for energy has provoked the flooding of large areas containing caves and archeological sites. There is much for geography to do.

Conclusion

What is proposed here is a non-fragmented search for knowledge, questioning the legitimacy of the model of production and organization of scientific knowledge which produces specialists who are more and more specialized (SOUZA, 1994). It is to suggest interdisciplinarity, not a simple cooperation between specialists, each working independently, but a more complete understanding of an integrated whole which is greater than the sum of its parts.

Speleologists can leave their marks on the world by helping to improve the local conditions of life. The path of humanity in Brazil has not led to complete development and a dignified life for all, but rather progress for the privileged few. Interdisciplinarity in Brazilian speleology, rather than multidisciplinarity, should lead to greater concern about the local inhabitants, including their education, so they can take on a part of the preservation of our caves.

No single science is the owner of truth, nor is a science a static entity; all are constantly looking for new challenges, and interdisciplinarity may be a good one. In Latin America this position has special significance, due to the sub-human living conditions of the majority of the population. The speleologist traverses the country from one end to the other, meeting natives who help him in locating caves and providing shelter, but these individuals see no improvements in their lives after these visits. Speleologists come and go, but the miserable life of the community goes on. The Vale do Riberia, for example, has the largest concentration of caves in the State of São Paulo, and possibly in Brazil, but it is also one of the poorest regions of the country. Not even the rampant tourism flooding the area has been sufficient to raise the economic standards of the local population. Members of the scientific community are constantly in attendance there -- walking the trails and exploring the caves -- but then they leave. The story has been repeated for years. It is time for the speleologist to take a more active role. The place to start may easily be the inclusion of a geographer in the team.

Bibliography

ANDRADE, Manuel Correia de (ed.). Élisée Reclus - Geografia. São Paulo, SP: Editora Ática, 1985. Uma Geografia para o Século XXI. Campinas, SP: Papirus, 1994.

FREITAG, Barbara, PORTELLA, Eduardo, GUATTARI, Felix, VATTEMO, Gianni, FAURE, Guy Olivier,

JAPIASSU, Hilton, D'AMARAL, MarcioTavares, MAFFESOLI, Michel, and PASSET, René. Interdisciplinaridade. Rio de Janeiro, RJ: Edições Tempo Brasileiro, 1992.

HELENE, Elisa Marcondes, and BICUDO, Marcelo Brizza. Cenário Mundial - Sociedades Sustentáveis. São Paulo, SP: Editora Scipione, 1994.

LACOSTE, Yves, A Geografia Serve antes de mais nada para Fazer a Guerra. Campinas, SP: Papirus, 1989.

MARINHO, Eduardo Galliza do Amaral. Desenvolvimento e Natureza da Geomorfologia. Campinas, SP: Cadernos IG/Unicamp, v. 5(1), 1995.

MENDONÇA, Francisco. Geografia e Meio Ambiente. São Paulo, SP: Edições Contexto, 1994.

SOUZA, Marcelo José Lopes de. Planejamento Integrado de Desenvolvimento - Natureza, Validade e Limites. São Paulo, SP: Terra Livre 10 AGB, 1994.

Response of karst environment to acid rains (example: The Massif of Snieznik - The Sudety Mountains Polish and Czech sides)

by Piotr Glowacki & Marian Pulina

Department of Geomorphology, University of Silesia, ul. Bedzinska 60, 41-200 Sosnowiec, Poland

The aim of this speech is the presentation of hydrochemical processes occurring in the area built of carbonate rocks which is a buffer against anthropogenically transformed precipitation. The Massif of Snieznik is the area fulfilling the conditions for such an investigation. It is built of Precambrian metamorphic rocks (acid schists and gneiss as well as alkaline marbles) with numerous karst forms (Jaskinia Niedzwiedzia - Bear Cave - a natural museum and tourist attraction). The area is located in the zone of transborder flow of air masses, the most intensively transformed ones in Europe, where significant amount of contamination from the atmosphere is being removed by precipitation in the mountain regions. The massif has been being affected by acid rains for over thirty years. The authors would like to present the results of extensive, interdisciplinary investigations carried out in two hydrological years (1992, 1993), based on the results obtained from permanent monitoring stations.

The model of the hydrochemical processes in the carbonate area of the Massif of Snieznik is based on average results of numerous data presented as a balance of load in tons/km^2/year.
The model includes the following:

1. Exterior elements (precipitation waters, non-karst surface waters)
2. Karst massif with an epikarst zone and large caves in the hydrological vadose zone. Mixed waters from the border of the phreatic and vadose zones)
3. Waters flowing out of the massif.

The authors would like to emphasize significant difference between anthropogenic loads on the northern and the southern slopes of the Massif of Snieznik, e.g. NO_3^- (from 3 up to 6 t/km^2/year) with extremely acid precipitation (pH = from 3.7 to 3.3)! The karst massif with a large cave Jaskinia Niedzwiedzia was the main site of the investigation determining occurence of "acid cave rains". They are caused by waters infiltrating from the epikarst zone (mainly in the initial stage of snow melting as well as after intensive summer precipitation) and anthropogenically transformed condensation waters from cave chambers opened for tourists (contents of CO_2 in the air from 0.03 to 0.32%). Corrosion of cave deposits is the result of activity of condensation waters of low mineralization, low pH and high aggressiveness. The corrosion is less intensive in places where condensation waters are mixed with percolation ones. Intensity of corrosion depends also on intensity of the tourist traffic and the season of the year (in summer - intensive tourist traffic and low level of water). The condensation waters constitute less than twenty per cent of the total hydrological balance of the cave.

Determination of exchange balance of certain ions in karst environment is the main result of the research. They prove the important role of the karst region as a buffer for the most intensively transformed precipitation waters on the continent. Various levels of resistance to such influence were observed in particular parts of the Massif of Sniezik. The southern slopes have exceeded the level of resistance to anthropopression (no difference between surface waters from karst and non-karst springs). The northern slopes are still "fighting" and the level has not been exceeded yet even in the vicinity of Jaskinia Niedzwiedzia, where intensive, but controlled tourist traffic occurs (high pH in the karst springs when compared with the non-karst springs, the same content of nitrates in both types of waters).

This conclusion is also proved by different levels of distruction of forests on both sides of the Massif of Snieznik. The results of the investigation on the influence of anthropopression in Jaskinia Niedzwiedzia have been used to determine limits of intensity of the tourist traffic in the cave (it is open 10 months a year, 5-6 days a week and the amount of visitors is limited to 450 persons per day). It is absolutely necessary to continue further investigations to determine so called "critical loads" for various areas considering their geological structure and carrying on recultivation of the areas affected by acid rains.

References

JAHN A., KOZLOWSKI S., & PULINA M. - scientific editors (1996) The Massif of Snieznik - Changes in the natural environment. PAE, Warszawa, 320p.

JAHN A., KOZLOWSKI S., & WISZNIOWSKA T. - editors (1989) Jaskinia Niezwiedzia w Kletnie. Badania i udostepnienie. Ossolineum, Wroclaw, 367p.

KULICKI A., PIASECKI J., SOBIK M. (1994) Zakwaszenie pokrywy snieznej w Dolinie Klesnicy w Masywie Snieznika Klodzkiego. In: Prace instytutu Geograficznego. Seria C. Meteorologia i Klimatologia. Tom II Wydawnictwo Uniwersytetu Wroclawskiego, pp.107-116

La tectonique et le karst

par **Jacques Choppy**
182 rue de Vaugirard, F-75015 Paris

Abstract : Tectonics and karst

A systematic study of the role of tectonics in karst leads to contradict a few theories generally admitted.

The part played by tectonics is limited. Karst forms have no relationship with the importance of geological discontinuity surfaces (joints and bedding planes) and have much smaller dimensions. Often small fissures and bedding planes used at the beginning of the cave formation are no longer detectable.And it is wrong to say that tectonics «controls» karst.

Karstic drainage, between the sinkhole at the surface and the outlet, is controled by the «drainage route», which is characterized by a minimum pressure drop and causes a drainage concentration to its advantage. Little by little, the whole drainage forms an outlet of considerable volume.

In this perspective, faults, folds are «used» by the drainage route. Thus they can play various roles : drain, barrier, indifferent. And, according to the dip, the roles of discontinuity surfaces are varied.

At last, various underground forms as well as surface forms, can only be explained by a a slackening.

Résumé

Une étude synthétique du rôle de la tectonique dans le karst conduit à contredire plusieurs opinions généralement admises :

Le rôle de la tectonique est limité : Les formes karstiques sont sans relation avec l'importance des surfaces de discontinuité géologiques (fractures et joints de stratification), et de dimensions très inférieures. Souvent les modestes diaclases et joints de stratification utilisés au début du creusement ne sont plus décelables. Et il est faux de dire que la tectonique «commande» le karst.

Ce qui « commande » les circulations karstiques, entre le point d'absorption en surface et l'émergence, c'est le «chemin de drainage»; celui-ci est caractérisé par une perte de charge minimum, et il provoque à son profit la concentrations du drainage. De proche en proche, l'ensemble des circulations aboutit à une émergence de volume considérable.

Dans cette optique, les failles, les plis sont «utilisés» par le chemin de drainage. Ils peuvent alors jouer des rôles divers : drain, barrière, indifférent. Et, selon le pendage, le rôle des surfaces de discontinuité est divers.

Enfin, diverses formes profondes comme de surface ne peuvent guère être expliquées que par une distension.

Un travail de synthèse détaillé (CHOPPY 1990-1992) sur le rôle des facteurs tectoniques dans le karst conduit à contredire plusieurs opinions généralement admises.

1. Le rôle de la tectonique est limité

On a pu dire que la dépendance du karst à la tectonique "est loin d'être totale" (CAVAILLÉ 1962). Cette proposition est à la fois fausse et vraie.

Fausse, car il est bien difficile d'imaginer que, dans une roche très peu poreuse, une circulation karstique ait pu débuter si ce n'est dans les fractures et joints de stratification.

Mais cette proposition est vraie, car certaines formes karstiques n'ont pas de relation claire avec les structures tectoniques, ou n'en apparaissent que très localement influencées : Contrairement à ce qui est si souvent représenté sur des schémas, le croisement de deux fractures provoque rarement une amplification des vides karstiques. Quant à l'intersection d'un joint de stratification et d'une fracture, elle s'exprime souvent par la nette prépondérance de l'une des deux surfaces de discontinuité, l'autre ne faisant que de la figuration.

D'ordinaire, les directions tectoniques importantes ne sont suivies par des conduits karstiques que sur des longueurs brèves : Des gouttières synclinales sont utilisées sur des distances kilométriques, mais le trajet souterrain ne suit l'axe synclinal proprement dit que sur des longueurs plus courtes. Des circulations connues par coloration suivent la direction d'une faille sur des distances également kilométriques, mais on ne connaît pas de galerie pénétrable suivant une faille sur plus d'un kilomètre.

Cette «indifférence» pour des failles, des plis a semblé paradoxale : dans la grotte de Han (Belgique), creusée dans des strates pentées ou à l'occasion de diaclases, on observe que tous les conduits sont cependant à peu près horizontaux (MARTEL 1894). De même, dans la Bachaï di Fayes (Haute-Savoie), «bizarrement la direction générale ne suit ni le pendage, ni une fracturation précise, mais une direction intermédiaire»; de sorte que, fréquemment, «le réseau connu se développe... selon deux directions bien définies, l'une parallèle, l'autre perpendiculaire au pendage»

Et «certains éléments structuraux influençant fortement l'alignement des gouffres et des dolines en surface restent apparemment sans effet sur l'orientation des cavités karstiques en profondeur» (MARTEL 1894, 429). En surface, si les bassins fermés, les poljés sont de dimensions comparables à celles de structures tectoniques de moyenne extension et du reste orientés par elles, ce sont en fait des formes non karstiques, dont le karst a permis la conservation grâce au drainage souterrain, mais sans apporter de retouches importantes. Seuls les méga-couloirs du karst de quelques régions atteignent des longueurs kilométriques.

Il est donc faux de dire que la fracturation «commande» le développement du karst. De sorte que les corrélations statistiques entre phénomènes tectoniques observés en surface et formes karstiques ne peuvent suggérer que des présomptions, car elles ignorent les autres facteurs qui interviennent dans la karstification. Du reste les phénomènes géologiques sont souvent beaucoup plus compliqués dans l'intérieur d'un massif que ce que nous pouvons en connaître par les observations extérieures.

2. Le chemin de drainage

En fait, le karst suit une autre logique : les circulations karstiques sont «commandées» par ce qu'il faut nommer le **chemin de drainage**, qui est celui de perte de charge minimum entre un point d'absorption de l'eau en surface et l'émergence. Cette notion explique le «mépris» des circulations pour s'adapter au relief extérieur comme à certaines surfaces de discontinuité

géologiques : Celles-ci sont en fait seulement «utilisées» par le chemin de drainage :

Le chemin de drainage concentre à son profit le drainage. Cela permet de comprendre la ré-organisation des circulations karstiques en profondeur, donc l'existence d'émergences de volume considérable.

3. Utilisation des structures tectoniques

Contrairement à ce qui fut souvent admis, on observe que :

- Certains anticlinaux sont favorables aux circulations souterraines, surtout à proximité de la surface.

- Les failles jouent un rôle original, induisant des morphologies spécifiques ; le rôle individuel des diaclases est médiocre, mais leur rôle collectif est important, notamment dans la zone d'altération épikarstique.

- Des failles inverses sont effectivement utilisées par les circulations (il est vrai qu'elles ont surpris les auteurs, qui les ont donc mentionnées); à la phase de compression, une phase de distension aurait-elle succédé ? Des décrochements sont assez souvent utilisés, mais beaucoup semblent « indifférents ».

En effet, trois types de fonctionnement (drain, barrière, indifférent) sont depuis longtemps connus pour les failles. Une classification du même type s'impose pour les plis. Et une faille peut être à la fois barrière et drain. Le rôle d'une fracturation dense semble très variable, allant du drain à la barrière.

Les conduits en baïonnette et le pseudo-méandre nous introduisent dans la notion d'utilisation alternée des facteurs, qui semble fort générale ; a fortiori dans le cas de fractures conjuguées. Les utilisations complémentaires de facteurs, définissant chacun une partie de la forme, sont également fréquentes.

Dans l'utilisation de la structuration tectonique par le karst, on constate souvent que :

- Si le pendage est faible, l'organisation des drainages subhorizontaux est très dépendante des joints de stratification ; leurs ondulations et certaines fractures semblent souvent responsables de la localisation précise des écoulements. La plupart des dénivellations brutales des circulations sont liées à des fractures et surtout à des failles.

- Lorsque le pendage s'accroît, les creusements de type « monoclinal », c'est-à-dire selon la ligne de plus grande pente des surfaces de discontinuité (joints de stratification, failles et peut-être diaclases) sont responsables de la majorité des conduits pentés.

- En cas de pendage très élevé, les joints de stratification et les fractures jouent des rôles remarquablement interchangeables.

4. Rôle de la distension

La distension se rencontre logiquement dans un massif en surrection, mais on sait combien la chose est banale. Les caractéristiques des circulations karstiques correspondantes sont alors modifiées ; LISZKOWSKA, LISZKOWSKI (1995) en ont fait l'étude théorique. Inversement, c'est par la distension qu'une surrection peut intervenir dans le développement karstique.

En profondeur apparaissent des élargissements de fissures dans des localisations inconnues ailleurs (dans les banquettes résultant d'un surcreusement, par exemple), et des effondrements de plafond de faible portée. C'est alors que des fractures sont utilisées sur les longueurs les plus grandes. Certains réseaux maillés, pour le moins, semblent provoqués par une distension. Les phénomènes dits par les spéléologues "de néotectonique" sont facilités.

En surface, les localisations apparemment aléatoires des reliefs ruiniformes, des couloirs du karst, ou leur développement plus spectaculaire, trouvent dans une distension une explication vraisemblable.

Il ne faut pas confondre la distension avec une moindre compression ou un appel au vide. Et il ne faudrait pas penser (RAFFY 1977) qu'une distension est indispensable au développement des phénomènes karstiques : d'une part, les exemples vraisemblables montrent que les cas raisonnablement crédibles sont assez dispersés. Dans des zones en compression comme il en existe en Quercy, par exemple, on trouve de nombreuses cavités et dépressions karstiques. Et des exfoliations de parois de conduit à grande profondeur montrent l'existence de contraintes de compression importantes.

5. Conclusion

Le karst utilise indifféremment les déformations tectoniques, qu'elles soient minimes, invisibles à l'échelle du géologue, ou considérables.

Si le rôle des facteurs structuraux apparaît sans rapport avec leur importance géologique, c'est qu'ils sont seulement «utilisés», dans la mesure où ils «correspondent par ailleurs à une direction privilégiée de développement de la cavité» (CHOPPY 1985). La diversité de ces «utilisations» est considérable. Et il ne se dégage pas de «règle» applicable à l'ensemble des karsts ; à ce niveau, toute tentative de prévision semble vouée à l'échec.

Un aspect du facteur tectonique est néanmoins souvent ignoré : Dans la plupart des karsts de montagne, la surrection, de 100 à 1000 mm/millénaire, est souvent dix fois supérieure à la dissolution karstique (de 10 à 100 mm d'épaisseur équivalente de roche enlevée par millénaire). On conçoit alors que «le perchement relatif de la plupart des unités karstiques de montagne soit maintenu et même renforcé» (JULIAN 1992), et que certaines formes semblent liées à une distension.

Bibliographie

CAVAILLÉ A. - 1962, Le système karstique et l'évolution des grottes; *Spelunca (4) Mém. 2*, 9-28.

CHOPPY J. - 1985, Dictionnaire de spéléologie physique et karstologie; Paris, 148 p.

CHOPPY J. - 1990-1992, Les facteurs tectoniques, 4 fascicules à compte d'auteur.

CHOPPY J. - 1996, Rôle de *la distension dans le karst; Actes 6° Rencontre d'Octobre, Spéléo-Club de Paris, 24-29.*

JULIAN M. - 1992, Quelques réflexions théoriques sur le karst; in « Hommage à Jean Nicod - Karst et évolutions climatiques », Presses universitaires de Bordeaux, 31-42.

LISZKOWSKA E., LISZKOWSKI J. - 1995, Influence of vertical crustal movements on karst hydraulics and the karstification process; *Acta carsologica*, Ljubljana, XXIV, 347-54.

MARTEL E.A. - 1894, Les abîmes; Delagrave éd., Paris, 579 p.

RAFFY J. - 1977, Le karst d'Italie centrale; *Norois* n° 95 bis "spécial Karstologie", 133-147.

Monitoring tropical geosystem, underground topography and potential water resources for sustainable development using geoinformatics – Indian case study

R.B. Singh
Department of Geography, University of Delhi, Delhi-110007, India

Abstract

The advancement of geoinformatics technique provides ready access to interpret various geological, topographic or spatial data in a relational data base correlation, analysis and modelling. The emphasis is on integration of conventional land based and remotely sensed data so as to develop comprehensive data bases in a particular area which can be used for micro-level planning. The empirical analysis of ground water resources includes, i) spatial data; aquifer catchment boundry, well location; ii) parameter data relating to properties and qualities i.e. aquifer parameters, ground water quality etc.; iii) aquifer depth data; depth to water table, well hole depth, depth to water bearing information; and iv) temporal data; ground water hydrographs and land use etc. Specific research and inventory is needed for value assessment including evaluation techniques for drinking water, and irrigation. It is true that in a dynamic context, the overall interest of a country may dictate certain modifications in the existing resource utilization but it needs to be stressed that these should be introduced in such a manner that the natural endowments and recent advances in technology are kept in view. In this way, geoinformatics can play an effective role for decision support of sustainable development and management of the natural resources.

Introduction

The geosystem resources are a prime natural capital for human sustenance and regional development. The development, utilization and conservation of geosystem resources particularly hydrological input is one of the major priority sectors in the national planning process. India is endowed with not only vast and varied geosystems but also huge network of river basins. Recently India is facing the problem of distribution of water from surplus to deficit areas for utilization in various sectors. As Hydrology is concerned with the water in streams and lakes, rainfall and snowfall, snow and ice on the land, water occurring below the earth's surface in the pores of the soil and rocks (Subramanya, 1984), the application of geoinformatics becomes essential for the study of complex parameters which comes into play in the overall hydrological cycle.

Monitory of the geosystem (SINGH, 1992; SINGH & HAIGH, 1995) and its underground topography is a critical function which entails accurate information for effective implementation of resource planning. Without accurate information about various geosystem and hydrological parameters, any sort of water monitoring and management is futile. Monitoring refers to the assembling of various data sets which are coordinated and used for evaluation of the status of any geosystem. Therefore, one can ascribe the following subsystems for geosystem monitoring (SINGH, 1996) :

(i) precise and adequate resource inventory or data base,
(ii) establishment of various networks for observation and coordination of hydrological and geological events;
(iii) analyse and yield current and time series information on the status of geosystem;
(iv) test the scientific hypothesis about the interaction and functioning of geosystem and finally to predict resource potentials.

Geoinformatics technology

The generation of geoinformatics data is the foundation upon which a sound geosystem monitoring is based. Availability of authentic and reliable geosystem data also helps in processing the utilization pattern, future needs, and management strategy. The science of geoinformatics is a multi-disciplinary subject for extracting reliable georeferenced data of geosystem and the environment. This covers the data acquisition, processing, and representation of geospatial data. Under geoinformatics, the techniques relating to surveying, geodesy, photogrammetry, remote sensing, cartography, GIS and GPS, are being combined for solving local, regional, national and global problems. Geoinformatics monitor the spatial/location of objects and characteristics of natural or geosystems features and aerial coverage of the earth. The emerging advance technologies in remote sensing, i.e. Very High Resolution Satellite Images, Synthetic Aperture Radar (SAR), Airborne Remote Sensing and GPS are providing great opportunities to monitor and manage geosystem in a sustainable manner (MURAI, 1996).

New Opportunities in Application of Geoinformatics

With launching operational remote sensing satellites IRS-1A (1988) and 1B (1991) and setting up of information systems like NNRMS, NRIS, RRSSCs and NRDMS, about 350 national/regional level remote sensing application projects have been conducted in India. The successful launch of second generation and indigenously built IRS-1C satellite on 28th December, 1995 in India has provided tremendous opportunities for applying space informatics in areas of environmental monitoring and natural resources management (SINGH, 1994). Browse data for PAN and LISS - III are being generated for users.

The IRS-1C marks a major milestone in India's satellite remote sensing programme by contributing to National Natural Resources Management System with better resolution, coverage and revisit in order to provide invaluable data on environmental resources. The IRS-1C surveys the whole earth surface in just 24 days.

The IRS-1C satellite has three types of advanced imaging sensors. The Panchromatic Camera (PAN) provides very high spatial resolution data of 5.8 m and a ground swath of 70 km. The PAN camera can be steered to ± 26 degrees which in turn increases revisit capability to 5 days. Linear Imaging and Self Scanning (LISS-III) Sensor provides multispectral data collected in four

bands. The Wide Field Sensor (WiFS) collects data in two spectral bands (Table 1). All the three cameras are operating in real time over Indian ground station visibility circle two or three times a day (NRSA, 1995)

Table 1 Characteristics of IRS-1C Sensors

Sensors	Spatial Resolution (m)	Grand Swath (km)	Bands/Regions (Microns)
PAN	5.8	70	Visible Region 0.50 - 0.75
LISS-III			
Visible and Infra-red	23.5	141	0.52 - 0.59 0.62 - 0.68
Shortwave Infra-red	70.5	148	1.55 - 1.70
WiFS	188	810	Visible Region 0.62 - 0.86 Near Infra-red 0.77- 0.86

Applications of geoinformatics in ground water exploration

The application of geoinformatics promotes the appropriate use of photo-hydrogeologic, remote sensing and GIS based techniques in the identification of occurrence and availability of ground water of diverse geological environments. The image intepretation helps to detect the location of aquifers from surface features.

Linear and morphologic features indicate possible presence of ground water. Drilling and testing of sites selected by remote sensing technology have achieved 85 per cent success in crystalline hard rocks. Land forms, drainage characteristics, soil tones, outcrop types, land occurrence (Table 2).

Colour composite images prepared for temporal satellite data are exclusive images for ground water interpretations. But fracture-trace and lineament maps, palaeo-drainage and weathered zones are detected on near-infrared images and large scale air photos (SHARMA, 1996).

Ground water recharge possibilities of a granitic terrain is controlled mainly by the factors of geologic structure and surface weathering. Low sun Angle and digitally enhanced satellite imagery, and aerial photography have their proven utility in the evaluation of a site for ground water recharge. Most common use of satellite imageries is for structural interpretation and particularly lineament analysis. The small scale, large area coverage from imagery provides a synoptic coverage of spatial features whereas 3-D interpretation of topographic and morphologic features of landscape provide a detailed account of recharge and discharge situation of a granitic terrain. Fractured granite rocks normally exhibit secondary porosity only. Primary porosity is absent in them either because of their original texture or because of changes in their texture by geological processes. Secondary openings result from stresses caused by folding, faulting, fracturing or flexing. Weathering processes serve to enlarge these openings. Topography, depth of weathering, degree of jointing and climate have a large influence on the ground water potential of a granitic rock terrain (Table 3 & 4; Fig. 1) (SHARMA, 1996).

Table 2 Method for ground water exploration

Remote Sensing Data Products	Application
1. Colour composite maps	Images for aquifer mapping over granitic terrain.
2. Band 7 Landsat and IRS images	Drainage pattern, density & texture.
3. Digitally enhanced Landsat, IRS and spot images	Lineaments, fracture types & symmetry; continuous & linear stream channels, valleys, aligned pattern of ponds.
4. Image classification & density slicing	Delineates landforms.
5. Thermal infra red images	Geologic structure & water bodies.
6. GIS overlays	Homogenous unit over a granitic terrain are combined with GIS overlay analysis to produce area-wise maps of varying recharge possibilities.

This is supplemented by satellite lineament mapping. A lineament is a mappable feature of surface whose parts align in a straight or slightly curving relationship. The surface expression that makes up a lineament may be a geomorphic or tonal expression of lineaments. Lineaments which are composite comprise more than one type of feature such as combination of stream segments, straight ridge and tonal anomalies etc. Lineaments represent zones of weakness leading to greater infiltration of water underground through fractures and linear features.

Table 3 Hydrologic significance of morphologic units in Swarnamukhi sub-basin

Landform	Ground water possibility
Inselberg Area (granite ridges)	Granite-gneiss, fracture permeability high, recharge and run-off potential.
Pediment slope/ colluvial fan	Zone of infiltration & probable source of base-flow.
Pediplain or buried pediment surface	Deeply weathered surface, tributary valley bottoms and possible source of reasonable good water supply.

Table 4 Hydrologic significance of morphogeologic units in Nagari sub-basin

Landform	Ground water possibility
1. Granite hills generating area.	Less jointed granite rocks; run-off
2. Pediment slope	Pediment plain fringing and encircling granite outcrops; zone of infiltration; possible fractures revealed through pediment zone in tributary valley o Nagari are areas of infilteration.
3. Buried pediment	Deeply weathered basement, tributary valley of Goddu Vanka stream has relat ively greater possibility of obtaining moderately large ground water supplies.

Conclusion

Inspite of various research activities, there is a serious gap in knowledge, especially with regard to understanding the geosystem - hydrologic interactive processes. In such interdependent situation, multi-dimensional and long term studies are needed in order to understand macro to micro-level geosystem functioning. The comparative studies of various geosystems in different climatic conditions will help in filling the gaps and better understanding of the influence of natural processes on hydrological cycle.

A systematic, accurate and up-to-date monitoring of geosystem and underground topography are essential for water resource management and sustainable development planning. At any particular point of time, the geospheric resource planning of the country is determined by physical, economic and institutional factors taken together. The term geosystem carries different connotations and implications in systems, land evaluation and sustainable land use measuring through carrying capacity. With the help of large scale topographical maps, air photographs and remote sensing data, it is possible to identify a hierarchic system of critical geospheric units. This further needs to (i) evaluate the positive and negative aspects of capabilities and (ii) identify the gap between its present productivity and potential. This gap needs to be reduced over the years so as to achieve land use specialization and integrated land use both in physical and economic terms at micro-level. This can be achieved by developing an institutional setup equipped with modern geoinformatics techniques for continuous monitoring and modeling. Geoinformatics will be more and more advanced under the support of computer, space and multi-media technologies.

References

MURAI, S. 1996. Advanced Technologies in Geoinformatics papers presented before *International Seminar on Space Informatics for Sustainable Development*. ICIMOD, Kathmandu.

National Remote Sensing Agency (NRSA). 1996. *IRS-IC Sensors; Interface*. 7:1-8.

SHARMA, S.K. 1996. *Remote Sensing and GIS applications in Ground Water exploration*. Unpublished thesis submitted to Rajasthan University, Jaipur.

SINGH, R.B. ed. 1992. *Dynamics of Mountain Geosystems*. Ashish Publication, New Delhi.

SINGH, R.B. 1994. *Space Technology for Disaster Monitoring and Mitigation in India*. INCEDE Report, University of Tokyo.

SINGH, R.B. 1996. *Disasters, Environment and Development*. Oxford & IBH Pub., New Delhi.

SINGH, R.B. & HAIGH, M.J. eds. 1995. *Sustainable Reconstruction of Highland and Headwater Regions*. Oxford & IBH Pub., New Delhi.

SUBRAMANYA, K. 1984. *Engineering Hydrology*. Tata McGraw Hill Pub., New Delhi.

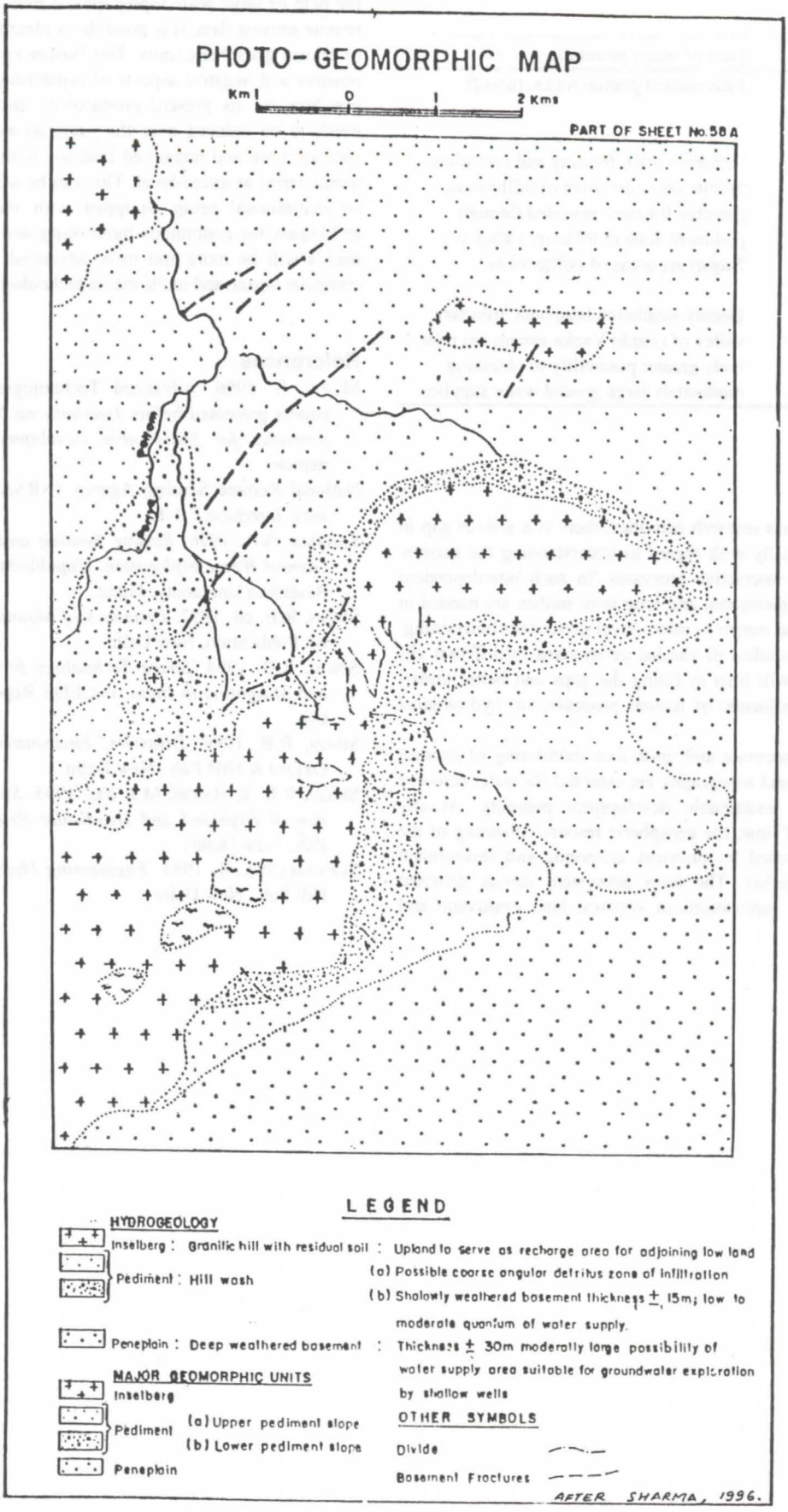

Figure 1: Photo-Geomorphic Map.

The Effects of Aridity and Topography on Limestone Cave Development

by George Veni,
George Veni and Associates, 11304 Candle Park, San Antonio, Texas 78249-4421, U.S.A.

Abstract

The effects of aridity and topography on cave development were examined by analyzing the precipitation at and geologic origins of 615 caves across the Edwards Plateau, Texas, U.S.A. Topographic slopes were also measured for the entrances of 338 of the caves. Precipitation in the study area ranges from 34-81 cm/year, and most of the caves were located in the stream-dissected and topographically diverse Plateau margin. There were insufficient data to quantify the absolute values of cave development relative to precipitation; however, vadose caves were found to increase in frequency by 0.3%/cm of mean annual precipitation, up to about 63.5 to 67.5 cm/year, and then increase with a frequency of 0.78%/cm at higher rainfalls. The abrupt gain in frequency appears to coincide with the presence of thicker and more continuous soil coverage. Analyses of topographic slopes revealed that vadose caves preferentially develop in level or near-level terrains; over 80% occur in slopes of <5%. Springs and paleosprings increase numerically relative to precipitation, and develop primarily in near-vertical or near-level terrain. Unless perched on impermeable formations, cliffside springs generally drain comparatively small drainage areas while streambed springs drain comparatively large areas. Phreatic relict caves form by hydrologic regimes which are unrelated to modern conditions; thus, they do not correlate to current climates and topographies.

Resumen

Los efectos de aridad y topografía en el desarollo de cuevas fueran examinados por la analasís de las orígines geológicas y precipitación en las alrededores de 615 cavernas en la meseta Edwards de Texas, EUA. Cuestas topográficas fueran medidas por 338 de las cuevas. Precipitación en el área de estudio llega entre 34 y 81 cm/año, y la mayoría de las cuevas se localiza en las orillas de la meseta donde se encuentra terreno mas inclinada y cortada por cañadas. No fueron datos suficientes para determinar la relación exacto entre precipitación y el desarrollo de cuevas, pero se encuentra que las cuevas vadosos incrementaron en frecuencia por 0.3%/cm de precipitación medio anual hasta aproximadamente 63.5 a 67.5 cm/año, y en seguida incrementar con una frecuencia de 0.78%/cm con mas precipitación. El precipitado ganacia en frecuencia aparece coincidir con la presencia de suelos mas gruesos y continuosos. Análisis de cuestas topográficas revelló que cuevas vadosas favoran terrenos planos o cerca de plano. Mas de 80% occuren en cuestas menos de 5%. Manatiales y paleo-manatiales incrementan numéricamente relativo al precipitación, y revellen principalmente en terrenos muy verticales o muy planos. Si no ubican arriba de formaciones inpermeables, manatiales en relices generalmente drenajen áreas relativamente pequeñas, y manatiales en arroyos drenajen áreas relativamente grandes. Cuevas freáticas y fósiles fueron formadas por condiciones hidrológicas sin relación con los del presente día, entonces no tienen correlación con climas y topografías corrientes.

1. Introduction

Limestone in arid climates is known to have poorly developed karst due to low precipitation and minimal soil development, which significantly limits carbon dioxide production needed for calcium carbonate dissolution (e.g. JENNINGS 1985; FORD & WILLIAMS, 1989). While denudation of limestone karst has been measured in different precipitation regimes, development of limestone caves as a function of precipitation has not been quantified. Similarly, the effects of topography on cave development have not been examined.

In this study I have determined the topography and mean annual precipitation at, and origin of 615 caves in a 420-km-long west to east band extending across the Edwards Plateau, Texas, U.S.A. In this region, mean precipitation ranges from 34-81 cm/year, from sub-arid to sub-humid climates, and the land surface around cave entrances slopes 0-90º from the horizontal. This range of conditions provides sufficient variation to measure the effects of aridity and topography on cave development.

2. Methodology

I examined the files of the Texas Speleological Survey for caves across the Edwards Plateau. The criteria I used for accepting a cave into the database for this study were:

1) The cave must be formed in the Edwards or equivalent limestones to minimize variations from significantly different limestone lithologies.
2) Each cave's entrance must be located with sufficient precision on 1:24,000 scale topographic maps so mean land slope at the entrance could be measured.
3) The likely origin of each cave had to be known or determinable based on personal knowledge of the site, or be morphologically or hydrologically clear from written descriptions, photographs, and/or maps.

With cave locations established, lithologies were determined from geologic maps (BARNES 1977, 1979, 1981a, 1981b, 1982, 1983), and mean annual precipitations were determined from the Climatic Atlas of Texas (LARKIN & BOMAR, 1983). Land slopes at the cave entrances were measured directly from the topographic maps and calculated in degrees slope from the horizontal plane. Generally, about a 100-m-diameter transect was measured, which easily encompassed most drainage areas flowing into Edwards Plateau cave entrances; larger and smaller areas were also measured if they better represented actual conditions. The caves located in streambeds were also noted.

Caves were classified by their origin as one of five types:

1) Phreatic relicts: hydrologically inactive caves formed during pre-existing hydrological conditions.
2) Vadose caves: hydrologically active caves, primarily sites of groundwater recharge, forming under current hydrological conditions.

3) Transitional caves: phreatic relicts which are undergoing current vadose modification into recharge sites.
4) Paleosprings: hydrologically inactive sites of groundwater discharge.
5) Springs: hydrologically active sites of groundwater discharge.

In the western portion of the Plateau, 277 collapse features were included in the study, based on geologic mapping, drilling, and research which demonstrated they are large, relict phreatic conduits (FREEMAN, 1968; VENI, 1994). Since they do not have entrances, they were not considered in the analyses of topographic slope.

The number of known caves is skewed upward toward the wetter, eastern half of the Edwards Plateau, nearer urban population centers where more exploration of the karst has occurred. Consequently, in the precipitation-based analyses below, which are affected by this non-uniform distribution, the number of caves was converted to percents of cave types to diminish explorational bias in the results. However, the analyses on topographic slope below are unaffected by regional variations in exploration, and the data's absolute numerical values are used.

One of the analyses in the following section compares the distribution of phreatic and vadose caves. The actual number of these caves is not known. However, phreatic relicts appear to have a relatively uniform distribution throughout the Plateau, and while they do not necessarily dictate vadose cave distribution, they serve in this study as a paleohydrological standard by which to measure the development of modern vadose caves.

3. Results

Figure 1 plots the percent of cave types against precipitation. Phreatic relict caves and vadose caves together account for 60-100% of the caves in each precipitation range. The percent of phreatic relicts declines markedly with increased precipitation, while vadose caves increase in relative abundance, with a good inverse correlation of R= -0.9 or an 81% interdependence. Despite fluctuations in the plot at the 45-53 and 57-65 cm/year ranges, probably due to few known caves in those areas, vadose caves increase in overall relative frequency along a regression-determined rate of 0.5%/cm of mean annual precipitation. Further, two rates appear to actually occur, one of 0.3%/cm up to about 67.5 cm/year, and 0.78%/cm at higher mean annual precipitations.

The distribution of transitional caves support the above data by generally increasing with precipitation. However, the sudden increase in transitional caves in the 59.5-67.5 cm/year range may indicate that accelerated vadose development begins at about 63.5 cm/year mean annual precipitation instead of 67.5 cm/year, as indicated by the vadose caves alone. Unfortunately, these increases in vadose and transitional cave development can only tentatively be proposed as measurable relationships since few caves are known in the 59.5-67.5 cm/year range. Meanwhile, until more caves are found and examined, it is important to note that these possible increases seem to relate to the occurrence of more continuous and thicker soils on the Edwards Plateau. Future studies should include comparisons with soil distributions, to include known distribution of paleosols which do not exceed the ages of the caves.

The relative occurrence of springs and paleosprings shows no significant change with precipitation in Figure 1, due to a proportional increase in the number of cave springs with precipitation. Springs and paleosprings generally account for about 10-20% of the caves. Where precipitation is <45 cm/year, they apparently drop to 0-2% of the total, but this is probably a misleading low value resulting from four factors:

1) insufficient exploration of probable spring areas;
2) minimal documentation of small paleospring caves;
3) nonrecognition of the greater number of springs which are only seasonally active in drier climates; and
4) deep phreatic groundwater circulation in the drier regions.

In the Edwards Plateau region, spring caves are rarely of significant size because valley incision along the Plateau margin results in their rapid abandonment in favor of lower and more hydrologically favorable discharge sites. Major spring caves, including the longest cave in Texas, occur primarily at the base of the limestone where groundwater cannot migrate through impermeable underlying units to topographically lower locations.

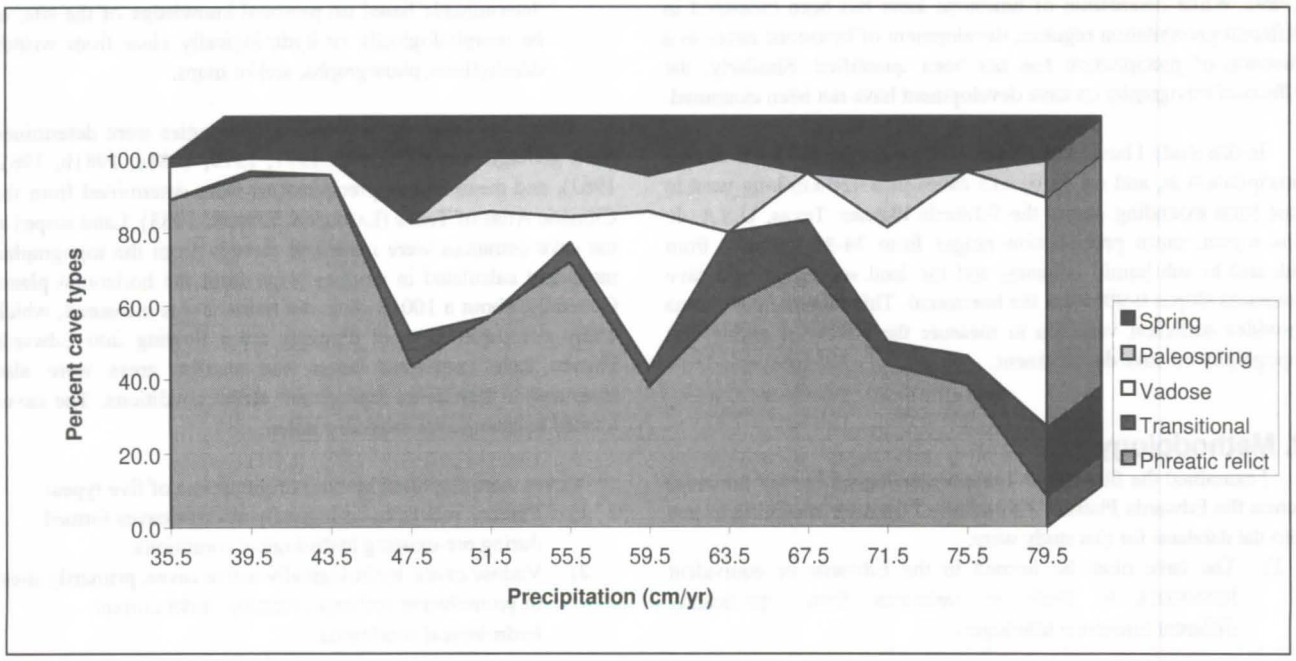

Figure 1: Variations in the percent of cave types with precipitation.

Although the precise percentages of springs and paleosprings require better definition, their generally low numbers support a model of dendritic aquifer development, where relatively few springs are fed by a relatively high number of recharge sites.

Figure 2 illustrates some effects of topography on cave development by comparing land slope at the entrances of 316 caves with the caves' speleogenetic types. Slopes in the figure range in one-degree increments from 0-16º, then in a 10-degree increment from 80-90º; data on an additional 16 caves scattered between 17-79º were too few to be significant and were excluded from the graph.

The most dramatic aspect of Figure 2 is that vadose and transitional caves preferentially develop in low gradient topography. Respectively, 87.3% and 81.6% of vadose and transitional caves occurs in slopes of 0-5º. Their declines in number with increased slopes follow exponential and near exponential functions. Although

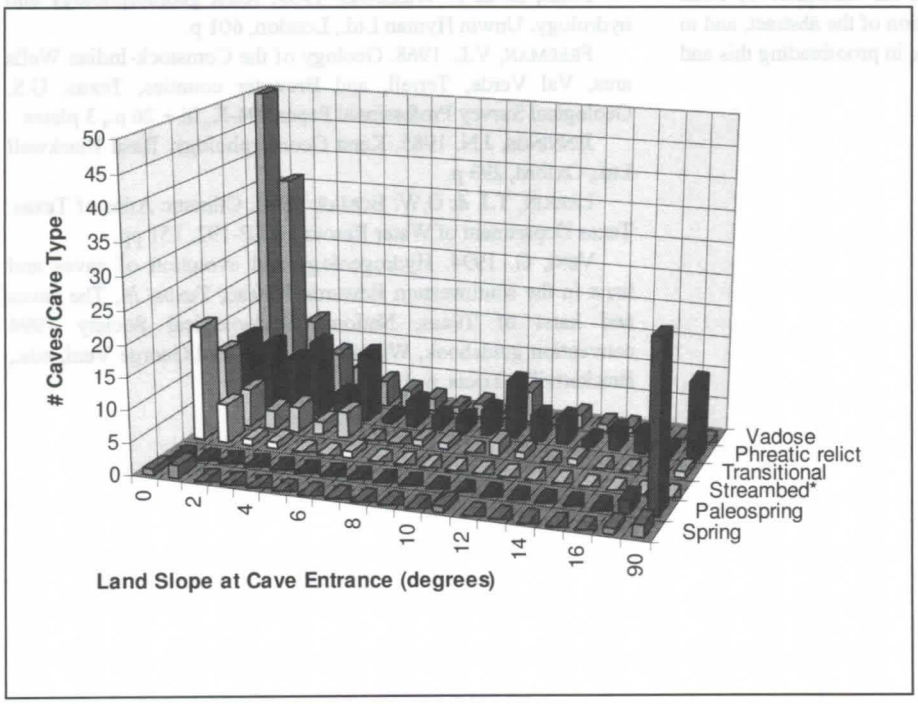

Figure 2: Variations in the number and types of caves with the topographic slope at the cave entrances (*streambed category only includes vadose and transitional caves in streams).

the Edwards Plateau might seem to have a disproportionate percentage of low gradient areas, most of the caves in this study were located in the rolling and highly stream-dissected margin of the Plateau, where a broad range of gradients occurs and level areas do not comprise the majority of the surface area. In support of the data distribution, vadose caves in hilly terrain often occur in narrow but roughly level benches between steep slopes.

Slow runoff of rainfall is the primary cause of greater vadose cave development and modification in low-slope terrains. In steep terrains, there is a much higher hydraulic inertia for rapid overland flow through open, low impedance channels rather than into the ground through fractures of far lower transmissivities. Although high secondary permeabilities could solutionally develop in the fractures and eventually form caves, channel and valley erosion is generally greater than the rate of cave development. The prevalence of vadose caves in level areas of both uplands and floodplains further indicates that the rate of sinkhole development cannot compete with the rate of erosion in steep terrains. Closer field investigations also show that vadose caves on steep slopes often form when local surfaces are relatively level, but are later intersected by retreating valley margins or deepened by continued karst development.

In contrast to steep terrains, runoff on low-slope topographies is slow or ponded. Surface water is retained on the limestone for longer periods of time, allowing greater infiltration down steep, but initially poorly permeable hydraulic gradients. However, this promotes dissolution of fractures into permeable openings which self-accelerate their growth by capturing increasing volumes of runoff through sinkhole development. This low-slope effect is not limited to upland areas, and is evident in streambeds. Of the 338 caves that were topographically analyzed, 31 (9.2%) were located in streambeds (21 vadose, 7 transitional, 1 phreatic relict, and 2 springs). Figure 2 plots the number of vadose and transitional caves in streambeds, and like their non-streambed plots, the caves' occurrence decreases at a nearly exponential rate with increasing slopes, with 64.3% occurring where the stream gradients are <1º.

Figure 2 shows that phreatic relict caves have no correlation to topographic slope. They occur in roughly equal numbers throughout most slope ranges. This is expected since they pre-date and have no hydrologic relationship to modern hydrologic conditions. In contrast, paleosprings are only known from nearly vertical slopes. Two factors contribute to this distribution. First, most paleosprings are short-lived features which drain nearby upland areas along steep hydraulic gradients to nearby valleys, and are abandoned for lower flow routes as the valleys deepen. Second, paleosprings are better preserved in cliffs; in level terrain they become sinks for water and often fill with sediment, or cannot be easily distinguished from vadose caves. Springs form predominantly in either the very steep or very flat slopes. They tend to occur in cliffs when capturing local upland drainage, and in streambeds when capturing regional drainage recharged throughout the entire valley or from larger areas.

4. Conclusions

The adage "caves are where you find them" was coined to humorously explain what was considered an inexplicable pattern of cave distribution. This study joins the growing body of knowledge which demonstrates that caves occur in predictable patterns, and it is the first to quantify some of the effects of aridity and topographic slope. While there were insufficient data to determine absolute values in quantifying the development of caves with increased precipitation, I found that vadose caves increase in relative frequency by 0.3%/cm of mean annual precipitation, up to about 63.5 to 67.5 cm/year, and then increase with a frequency of 0.78%/cm at higher rainfalls. The sudden gain in frequency

roughly correlates with the presence of thicker and more continuous soil coverage. My analyses of topographic slopes found vadose caves initially tend to develop in level or near-level terrains, with over 80% occurring in slopes of <5%. Springs and paleosprings increase numerically in proportion to precipitation, and occur mostly in either near-vertical or near-level terrain. Unless perched on impermeable formations, cliffside springs tend to drain relatively small drainage areas, while streambed springs drain relatively large areas. Phreatic relict caves were formed by hydrologic regimes which are unrelated to modern conditions, and thus do not correlate to current climates and topographies. These caves are still "where you find them," unless you can determine the conditions which created them.

Acknowledgments

I am grateful to the Texas Speleological Survey, without which this study could not have been conducted. TSS had the foresight to begin collecting cave and karst information for Texas over 36 years ago, and has kindly provided me access to its data files for this paper's analysis. I also greatly appreciate the assistance of Peter Sprouse, who provided the Spanish translation of the abstract, and to my wife Karen Veni for her eternal patience in proofreading this and all of my reports.

Bibliography

BARNES, V. 1977. Geologic Atlas of Texas, Del Rio Sheet. Bureau of Economic Geology, The University of Texas, Austin, 1 sheet.

BARNES, V. 1979. Geologic Atlas of Texas, Emory Peak - Presidio Sheet. Bureau of Economic Geology, The University of Texas, Austin, 15 p. + 1 sheet.

BARNES, V. 1981a. Geologic Atlas of Texas, Llano Sheet. Bureau of Economic Geology, The University of Texas, Austin, 15 p. + 1 sheet.

BARNES, V. 1981b. Geologic Atlas of Texas, Sonora Sheet. Bureau of Economic Geology, The University of Texas, Austin, 1 sheet.

BARNES, V. 1982. Geologic Atlas of Texas, Fort Stockton Sheet. Bureau of Economic Geology, The University of Texas, Austin, 12 p. + 1 sheet.

BARNES, V. 1983. Geologic Atlas of Texas, San Antonio Sheet. Bureau of Economic Geology, The University of Texas, Austin, 9 p. + 1 sheet.

FORD, D. & P. WILLIAMS. 1989. Karst geomorphology and hydrology. Unwin Hyman Ltd., London, 601 p.

FREEMAN, V.L. 1968. Geology of the Comstock-Indian Wells area, Val Verde, Terrell, and Brewster counties, Texas. U.S. Geological Survey Professional Paper 594-K, iii + 26 p., 3 plates

JENNINGS, J.N. 1985. Karst Geomorphology. Basil Blackwell Ltd., Oxford, 293 p.

LARKIN, T.J. & G.W. BOMAR. 1983. Climatic Atlas of Texas. Texas Department of Water Resources LP-192, 151 pp.

VENI, G. 1994. Hydrogeology and evolution of caves and karst in the southwestern Edwards Plateau, Texas. *In*, The caves and karst of Texas, National Speleological Society 1994 convention guidebook, William R. Elliott and George Veni, eds., Brackettville, Texas, p. 13-30.

Cave Rocky Relief and its Speleogenetical Significance

Tadej Slabe
Karst Research Institute, Scientific Research Centre of the Slovenian Academy of Sciences and Arts, Titov trg 2, SI-6230 POSTOJNA, Slovenia

Abstract

Cave rocky relief is an important evidence on the formation and development of karst caves and, as such an indispensable component of speleomorphogenetical studies.

1. Introduction

Factors shaping the karst underground leave the traces on the rocky perimeter of the caverns. The associated rocky features are called rocky relief. The supposition that cave relief may be an important evidence on the formation and development of karst caves was checked by a great pattern of various Slovene caves. The methodological foundations of origin and development of rocky features and their association into rocky relief are determined and at the same time the speleogenetical significance of rocky relief in selected areas of the Slovene karst is evaluated.

2. Rocky features

Rocky features (Table 1) are controlled by mutual relation of lithology, how it is fissured and bedded and by various processes that affect the rock surface. The dominant processes influencing the rocky perimeter moulding are solution of the rock, mechanical corrasion when water flow transports the load and tears protruding pieces of the rock from its surface, and weathering. The factors that decide about origin and development of typical rocky features enable the acting of processes and removal of their products. These factors act on lines, planes or points. The first is controlled by turbulent water and air flow, by percolation water, then by a smaller quantity of water flowing on rocky bottom or above fine-grained deposit. Stable factors acting on the surface are stagnant water or moisture at the contact with the fine-grained sediment. These are characterised by diffusion removal of the products of rock solution. The point factors are waterfall, water infiltrated from the fissures in the ceiling and cave drips.

Several authors have reported studies and determined of the association of scallop length and water flow velocity that forms them. I stated that the size of scallops (Figure 1) is also controlled by composition of the rock and how it is fissured, and that scallops in certain hydraulic conditions obtain a typical shape. I divided the shape of ceiling pockets and determined a decisive importance of hydraulic conditions in variously shaped passages for their origin and development. There are also various sorts of potholes of typical shapes. The pendants I divided into columns, knives and "èeri". Their origin and shape are mostly controlled by fissures in the rock and hydraulic conditions. Wall notches indicate water level, joining of passages or water flow above a deposit. Smaller amount of water incise various floor channels (Figure 2) into rocky bottom of passages.

Above-sediment rocky features are: ceiling and wall channels, anastomoses, ceiling pockets that are characteristic for the passages that were filled up by flood deposits. Experiments in plaster of Paris are useful in explaining their origin and development. At first the water flowed through a siphon below a plaster of Paris slab evenly, later drainage was taken over by single channels. A levelled network of channels developed typical of well developed anastomoses. Typical traces in epiphreatic passages which are more affected by water level oscillations than water flow are the below-sediment solution bevels, pits and points. The origin of solution bevels and their shape on the walls with different inclinations were also confirmed by laboratory experiments.

On relatively homogeneous, but grained rock prominent traces of trickling water occur. Homogeneous rocky surface are vertical and rather smooth. On inclined rocky surfaces different bevels develop. Pits are due to water dripping off the ceiling fissure and they occurred in plaster of Paris also. Below ice rock is usually smooth.

In a selected passage I measured climatic conditions, condensation moisture and studied the impacts on its walls. Abundant condensation due to distinct air current causes the origin of ceiling pockets, scallops and flutes while smaller condensation moisture dissolves rocky and flowstone surface by different degree. Also below the lichens the rocky surface in thinly etched.

3. Rocky relief

In active caves or shafts rocky relief reflects their uniform or diverse formation. Thus one may define a typical rocky relief shaped by single factors. Water flows that by various velocity and turbulence corrosionally dissolve or

Table 1: Rocky features, factors and conditions controlling their origin, and processes shaping them.

ROCKY FEATURES	THE MODE OF WATER FLOW (REMOVAL OF PRODUCTS)	FACTORS	CONDITIONS OF ORIGIN (hydrological zones)	PROCESS ON THE ROCK
	L			
large scallops, ceiling pocket			phreatic	corrosion
scallop ceiling pocket, wall notches	**turbulence**	water flow	epiphreatic	corrosion,
scallops, potholes, floor channel,			vadose	mech.act.
flutes	**I**			corrosion,
	turbulence	air flow	vadose	mech.act.
large scallops, ceiling pockets,				
channel	**N**			corrosion
	recharge	trickling water	vadose	
channels, solution niche		filtering of		corrosion,
	E of	deposit	epiphreatic	mech.act.
below sediment channel				
	small water	above deposit		corrosion
	A		epiphreatic	
		on rocky floor	phreatic	
ceiling channel, anastomosis	**quantity**		vadose	
				corrosion
floor channel	**R**			corrosion
	P			
niche, pocket		stagnant	phreatic	corrosion
niche, pocket	**L**	water	epiphreatic	corrosion
niche, wall notch			vadose	corrosion
below sediment niche, pocket	**A**	deposit	epiphreatic	corrosion
	N			
below ice notch, notche		ice cover	vadose	corrosion
	E			
biogene furrows		lichens	vadose	corrosion
	P			
floor pit		dripping	vadose	corrosion,
	O			mech.act.
ceiling pocket		filtering of a	vadose	
	I	fissure		corrosion
pothole	**N**	falling water flow	vadose	
	T			mech.act., corrosion
block breakdown chip breakdown	*	*	*	mechanical desintegration

mechanically polish rocks of different structure and differently fissured on the perimeter of passages and shape typical rocky relief in various hydrological zones. In the phreatic zone water flow is usually slower and scallops are therefore bigger; through seasonally flooded passages fast and slow water streams are flowing. On lee-ward parts in wider pasages water flow deposits fine-grained sediments below which, in dry periods, below-sediment rocky features occur. Estavellas too, have a unique rocky relief; that reflects (below sediment pits and bevels) frequent alternating of water level intheir lower parts and periodical outbreak of water out of the cave or fast water flow into the cave. Fast water flows with free surface commonly transform the riverbed in the passages only.

Rocky relief formed by trickling water is mostly controlled by composition, fissures, bedding and inclination of rock over which various amounts of water trickles.

Shape properties of passages, specially those in larger cave systems are basic for explanation of the underground karst. In the same cave several different development phases may occur. In larger caverns rocky relief is a combination of traces of past development periods and their recent formation. The traces of different development periods are preserved in old caves also. That the diversity of rocky relief is sensible is specially seen in typical caves f an aquifer. Gradual or intensive karstification of karst regions due to changed hydrological conditions is also reflected in rocky relief of caves. Water level in an aquifer lowers due to tectonic uplifting of karst terrains, due to erosional lowering of impermeable barrier that surround them and, of course, due to climatic conditions that commonly cause their frequent variations. Through passages flooded in past, today flows a fast water stream with free surface or else, the traces of water flow are old. Also less distinctive factors as is, for example, water flow above fine-grained deposits, acting on single parts of perimeter only or they are less efficient, biocorrosion, enabling preservation of old, once prevailing traces.

Rocky relief may frequently display very clear traces of the most prominent, prevailing development phases of a cave. It also offers rather complete insight into cave formation during these periods. Development phases of rocky relief usually appear in levels, and only when less efficient younger factors partly cover traces of older ones, development may be followed on the same rocky surface. However, only rocky relief is usually not sufficient to provide an entire insight into cave development. The traces of older cave formation are covered by younger processes in particular, when development periods occur at the same altitude and when karstification is not intensive. This is most commonly due to tectonic properties of aquifers and sediment deposition. Rocky relief does not give a direct temporal determination of cave development phases.

Figure 1: Scallops that were mechanically deepened

Figure 2: Floor channel

4. Conclusion

Diverse network of rocky relief may be seen by rich and heterogeneous material offered by simple outflow and throughflow karst aquifers. To simulate rocky features in plaster of Paris proved to be advantageous. This is a step forward from observations of the factors that mould a rock. The origin of rocky features is studied rather irregularly, to some of them more attention was given than to the others. Yet numerous ways for future studies are opened, as are detailed observations and comparisons of rocky features forms. The process affecting a rock may be rather reliably seen by observing the rocky surface by scanning electron microscopy.

The results of study of rocky features must be further complemented by observing other types of karst, as is thermal karst, coastal karst or karst in various rocks. The basic properties of rocky relief are presented in hydrologically differing types of passages. But rocky relief should be studied in comparison with the form of passages and various types of caves and then these results must be involved into a complete model (hydrogeological, morphogenetical) of a karst aquifer.

In short, rocky relief is important although a limited evidence of actual and previous formation of karst caves. The knowledge is an indispensable component of morphogenetical studies.

Solutionally Enlarged Glacial Striae on Ordovician Dolomites in Western Wyoming, USA

Keith E. Goggin
Dept. of Geology, University of Georgia, Athens GA, USA

Douglas M. Medville
11762 Indian Ridge Rd., Reston VA, USA

Abstract

Glaciated pavements on carbonate rocks are found in several locations on the west slope of the Teton range, Wyoming, USA, at elevations between 2800 and 3000 meters. One such surface (43 41' N. Lat., 110 54' W. Long.) , an exposure of the upper Ordovician Bighorn Dolomite, has an aerial extent of approximately 6 square kilometers. This exposure exhibits a wide range of classic karren forms (e.g., large kluftkarren, spitzkarren, trittkarren), as well as an unusual and possibly unique form, consisting of a system of subparallel furrows having both linear and lateral extents of hundreds of meters. The furrows have been observed only on the dolomite. Individual furrows vary from about 10 cm to one meter in width and depth. The furrows appear to be the product of solutional enlargement of glacial striae on the dolomite surface resulting from Pleistocene alpine valley glaciation. While the furrows are found on several stratigraphic horizons in the dolomite, lithologic changes between members exhibit no observable controls on furrow development. The furrows are observed on both horizontal and vertical rock surfaces, follow valley trends, and exhibit no relation to current drainage patterns or structural dip, all of which suggest a synglacial origin for the furrow patterns. Large kluftkarren that are parallel or subparallel to regional strike are crossed by the furrows at oblique angles. Examination of the cross-cutting relations between the furrows and the kluftkarren as well as the sizes and configuration of the furrows above and below the kluftkarren indicates that the furrows predate the kluftkarren.

Introduction: Geology and Glacial History

The area described in this paper is located in Darby Canyon, on the western side of the Teton mountain range, in western Wyoming, USA. Elevations in the area vary from 2700 meters to about 3000 meters above sea level and the study area has an aerial extent of about 6 square kilometers. Rocks of Cambrian through Mississippian age are exposed in Darby Canyon with the Ordovician Bighorn Dolomite the dominant rock type. The regional dip is to the west-northwest at 8-12 degrees. The solutionally enlarged glacial striae described below are developed exclusively on the Bighorn Dolomite.

The Bighorn Dolomite is easily identified in outcrop by its very massive nature and tendency to form cliffs having vertical extents of 150-200 meters. The Bighorn was first subdivided into three lithologic members (based on rock type) by DARTON (1906). These members consist of the basal Lander Sandstone which is overlain by the unnamed massive dolomite member and the Leigh Dolomite member. Only the top two members are present in Darby Canyon. The unnamed member consists of an extremely resistant, massive, granular dolomite and weathers with a characteristic "fretlike" texture (KEEFER and VAN LIEU, 1966). This rough, pitted weathering pattern is consistently present in all exposures and appears to be in excess of 90 meters thick locally.

The Leigh dolomite Member is a thinly bedded, light gray to white pure dolomite which weathers to a chalky white. The Leigh Member and the underlying unnamed dolomite are conformable and appear to have a gradational contact. Due to the gradational nature of this contact and the lack of detailed stratigraphic sections locally, the thickness of the Leigh Member was not determined, but appears to be about 10 meters. Based on the paleontological work of several researchers, the age of the Bighorn dolomite is considered to be Late Ordovician. KEEFER and VAN LIEU (1966) include a summary of the relevant discussions concerning the age determination of these rocks.

Three major stages of glaciation occurred during the Pleistocene in the study area: Pinedale, Bull Lake, and several pre-Bull Lake events (LOVE and REED, 1971). The peak of the Pinedale glaciation occurred about 25,000 years b.p. (GOOD and PIERCE, 1996) and is probably the event that initiated the geomorphic features described in this paper. The Bull Lake glaciation predates the Pinedale and has been dated at 140,000 years b.p. (GOOD and PIERCE, 1996). While some terminal moraines from this period remain, most of the Bull Lake features have been obscured by Pinedale glaciation. Pre-Bull Lake glaciers were present as far back as the Pliocene, with the oldest age estimates set at about 5.3 million years b.p. (LOVE and REED, 1971).

Karst features found in the study area are typical for alpine karst terranes. Cave entrances, sinking streams, and surficial karren forms are all present. The most obvious karst form consists of many large, open joints (*Bogaz*—a large, corridor-like type of kluftkarren), (SWEETING, 1972). Field measurements have shown several of these bogaz to be in excess of 30 meters in depth. Other, smaller karren forms are present as well, including rillenkarren, trittkarren, spitzkarren, rinnenkarren and solution basins. Morphologic descriptions of these forms are found in SWEETING (1972), BOGLI (1980), JENNINGS (1985), and WHITE (1987). SWEETING (1972) provides the following definition of karren, which applies to all of the above forms: "Minor solution channels on a karst surface caused by meteoric or soil water before it permeates underground. The individual channel-form depends on the nature and disposition of the rock and the solution process." The geomorphic feature described below differs from the karren features noted above in scale and origin, although they most closely resemble very long, low gradient rinnenkarren. It is possible that an example of this feature is presented in FORD and WILLIAMS (1989), p. 478, where a "glacial-moulded ridge in marble" is illustrated.

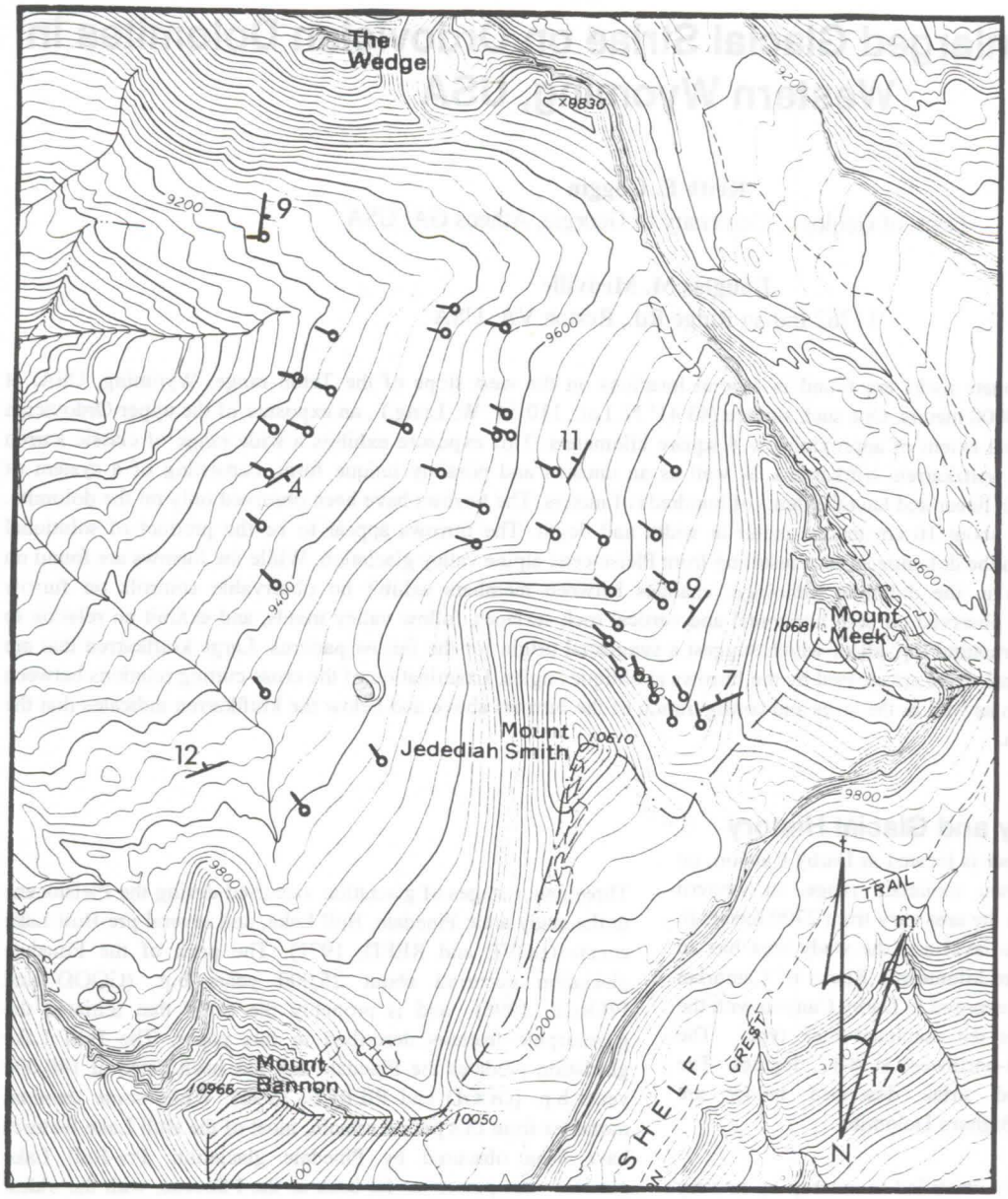

Figure 1: Study Area map showing the downslope trends of selected furrows and structural attitudes

Location and Description of the Furrows

The system of furrows observed in the study area can be followed down slope for more than 3 kilometers; from the upper terminus of Darby Canyon at an elevation of about 3000 meters to a series of cliffs terminating the Bighorn outcrop, at an elevation of 2700 meters. The aerial extent of the furrows and the measured down slope trends of selected furrows as well as the local dip are shown in Figure 1. The furrows themselves are illustrated in Figures 2 and 3. Individual furrows can be followed for distances of up to 100 meters and are generally parallel or slightly subparallel to adjacent furrows throughout their length. Locally, the furrows exhibit a somewhat chaotic pattern, apparently in response to abrupt changes in topography such as small cliffs (up to 5 meters in height) of bedrock resulting from glacial plucking.The furrows are 12 to 30 cm deep and are spaced 25 to 65 cm apart, on average although substantial differences in furrow density, width, and depth occur across the upper Darby Canyon basin. On occasion, furrows having widths and depths of up to one meter are observed. Secondary karren development, e.g., rillenkarren, is seen on furrow walls and in the rounded bases of the furrows, trittkarren have also been observed. Where solution has removed sufficient quantities of dolomite, residual furrow walls are reduced to aligned spitzkarren. In some areas, the karren and indeed the furrows themselves are no longer present as a result of local snow-melt ponding in low gradient areas.

The furrows have been observed on rocks of both the Leigh Member and the underlying, unnamed dolomite within the Bighorn. Although no detailed chemical analyses have been performed on these rocks, it appears that there are no lithologic controls on furrow formation; i.e., the directional orientation of the furrows is not controlled by joints or bedding partings. The directional orientation of the furrows varies across the structural surface represented by upper Darby Canyon. Along the canyon's northern margin the down-valley direction of the furrows is 280 to 290 degrees. In the center of the basin, two km. to the south, the down-valley direction is 320 to 330 degrees The directional orientation of the furrows appears to be controlled by the direction of movement of valley glaciation rather than by the local dip since the measured difference between furrow trends and dip direction is up to 30 degrees and the furrow trends parallel the major axes of re-entrant valleys to upper Darby Canyon as illustrated in figure 1. Also, a glacial origin may be indicated by the presence of subdued furrows on vertical rock surfaces at those locations where small escarpments, due to glacial plucking, are observed.

Furrow Size Distributions

To estimate of the distribution of furrow widths and depths, a traverse of the area containing the furrows was conducted. This traverse, at elevation 2860 meters, covered a kilometer of linear extent at a bearing of 200 degrees; about perpendicular to the furrow trend. Over this distance, 253 furrows were measured. These had a mean width of 35.6 cm and mean depth of 17.4 cm. It was observed however, that furrow density, width, and depth varied greatly as the traverse was conducted. Near the northern margin of the basin, the furrows tended to be both more shallow and narrow than in the center of the basin and accounted for a

Figure 2: View across Darby Canyon furrows

smaller percentage of the traverse distance (i.e., the furrows occupied a smaller percentage of the surface area).

The 178 furrows measured at the northern margin of the basin had a mean width of 22.9 cm (standard. deviation (sd) = 4.9 cm) while the 75 furrows measured in the center of the basin had a mean width of 65.6 cm (sd = 12.2 cm). Using a distribution-free statistical test (Kolmogov-Smirnov), it was concluded that at the .01 level of significance, the two samples of furrow width were not drawn from the same population. Similarly, mean furrow depth at the northern margin of Upper Darby Canyon was 12.4 cm (sd = 1.8 cm) while in the center of the basin the mean depth was 29.3 cm (sd = 5.2 cm) and again, it was found that the difference in the mean depth was sufficiently large to reject the hypothesis, again at the .01 level of significance, that the two furrowsamples were drawn from the same population.

It is clear that as one traverses the width of Upper Darby Canyon, furrow width and depth increase. This may be due to a greater glacial load in the center of the canyon causing deeper initiating striae to develop or to increased post-glacial seasonal snowpack and snowmelt in the canyon's center, resulting in a higher rate of corrosion of the striae in the dolomite than occurs along the canyon's northern margin. We postulate that many of the proto-furrows in the canyon's center have coalesced into the fewer, deeper furrows observed and that this accounts for the higher percentage of linear traverse distance accounted for by the furrows in the center than at the northern margin of the canyon (61.5% vs. 34.0%).

Age and Origin of the Furrows

Field observations present several lines of evidence regarding the age of the furrows with respect to other features found in the study area. For example, present surface drainage channels exist in the study area, although these are dry for much of the year. Due to the karstic nature of the study area, active surface drainage is generally limited to the spring snow melt. These channels consist of meandering trenches in the bedrock, with local shallow depressions where ponding occurs during wet periods. Though the channels were formed by corrosion of bedrock, there has been little secondary karren development on the walls of these channels. Several areas were observed in which these drainage channels cut across furrows. In many areas, the furrows show little or no relationship to present day drainage patterns. The lack of secondary karren development on the drainage channels and the presence of karren on the furrows indicates that the furrows predate the formation of the channels. The fact that the channels are dissolutional in origin suggests that the older furrows must predate these. This is consistent with the synglacial origin hypothesis noted below.

Many sub-linear, north-south trending bogaz are present in the study area. The furrows generally have a down-slope trend (to the west) in the main Darby Canyon, while they trend north to northwest in the side valleys. Close examination of the furrow and bogaz intersections shows that individual furrows do not terminate on the up-slope sides of the bogaz, but instead can be seen to cross the bogaz openings with no apparent directional deviation. This crosscutting relationship may suggest that the furrows were present before the bogaz were formed.

Origin of the Furrows

To accurately date the origin of the furrows, the chemical composition of the bedrock must be analyzed and dissolution rates calculated. Although this analysis has not been performed, field observations support the following qualitative hypothesis for furrow genesis. The evidence given above for the relative age of the furrows strongly suggests a synglacial origin for the furrows. In rocks that are more resistant to chemical weathering (such as granites), glacial striae can persist for thousands of years; however, SWEETING (1972) notes that on recent exhumed limestones in Europe, these striae are eroded away in about 10 years. The solutional enlargement of the striae found in the study area suggests that the dolomite is resistant enough to chemical erosion to retain the original striations, but sufficiently susceptible to corrosion to allow solutional enlargement of selected striae to take place. The process of preferential enlargement apparently erases striae located between the preferred striations, resulting in the large furrows visible today with occasional smaller, perched furrow remnants between these). The presence of furrows that are skewed with respect present drainage suggests that this process was initiated during glacial retreat. Subsequent furrow development most likely occurs on an annual basis, as seasonal snows melt and drain along the downslope trending furrows.

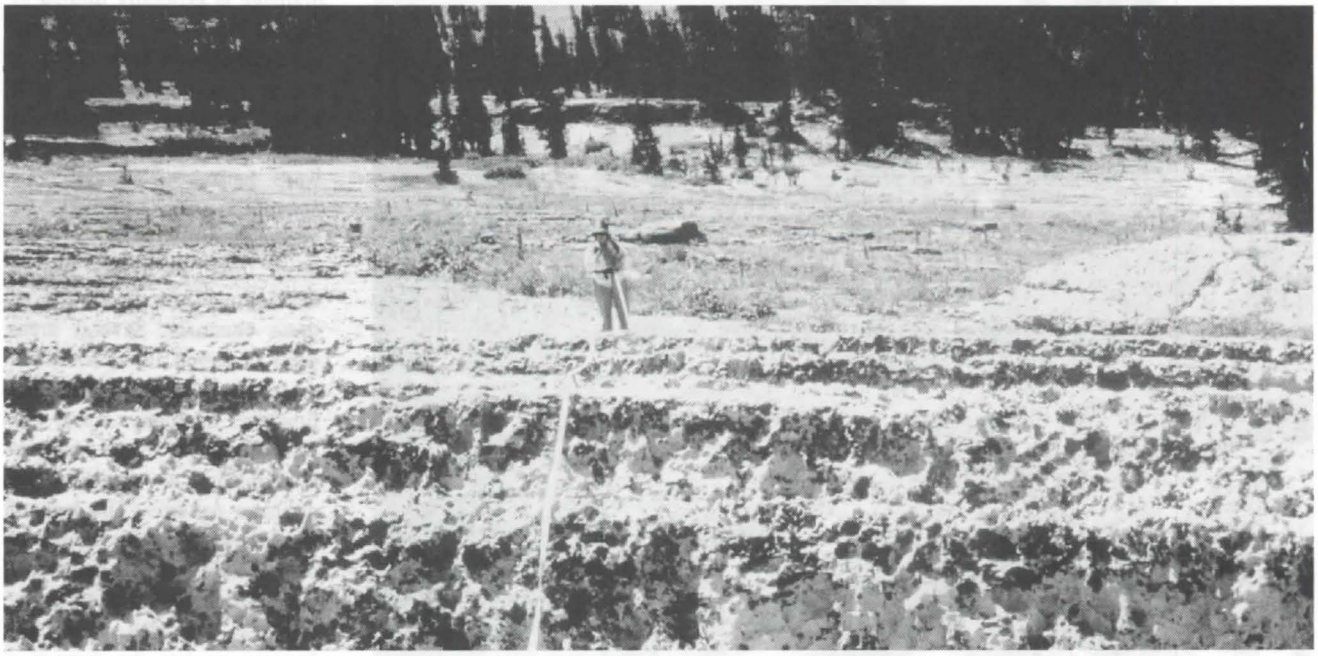

Figure 3: Darby Canyon furrows showing secondary solution on furrow walls

References

BOGLI, A. 1980. Karst Hydrology and Physical Speleology, Springer Verlang, Berlin, 270 p.

DARTON, N.H. 1904: Comparison of the Stratigraphy of the Black Hills, Bighorn Mountains, and Rocky Mountain Front Range, *Geol. Soc. Of America Bull.*, Vol. 15, p. 379-448

DARTON, N.H. 1906: Geology of the Bighorn Mountains. U.S. Geological Survey Prof. Paper 51, 129 p.

FORD, D. and P. WILLIAMS. 1989: Karst Geomorphology and Hydrology: Unwin Hyman, London, 610p.

GOOD, J.M. and K.L. PIERCE. 1996: Recent and Ongoing Geology of Grand Teton and Yellowstone National Parks, Grand Teton Natural History Association, Moose, Wyoming, 58p.

JENNINGS, J.N. 1985: Karst Geomorphology: Basil Blackwell, Oxford, 293 p.

KEEFER, W.R. and J. A. VAN LIEU. 1966: Paleozoic Formations in the Wind River Basin, Wyoming: U.S. Geol. Survey Prof. Paper 495-B, 60p.

LOVE, J.D. and J.C. REED. 1971: Creation of the Teton Landscape, the Geological Story of Grand Teton National Park: Grand Teton Natural History Association., Moose, Wyoming, 120 p.

REED, J.C. and J.D. LOVE. 1971. Preliminary Geologic Map of the Mount Bannon Quadrangle, Teton County, Wyoming: U.S. Geological Survey Open File Report 71-233.

SWEETING, M.M. 1972: Karst Landforms: MacMillan, London, 362p.

WHITE, W.B. 1987: Geomorphology and Hydrology of Karst Terrains: Oxford University Press, New York, 464p.

Simultaneous systematic evolution of Fenglin karst landforms

Zhu Xuewen
Institute of Karst Geology, Chinese Academy of Geologic Sciences;
40 Qixing Road, Guilin 541004, Guangxi, P.R.China

Abstract

The Fenglin Karst of South China is topographically divided into two very different morphologic landform types: Fengcong (peak-cluster depression, or cone karst) and Fenglin (peak-forest plain, or tower karst and using the same name as the region). Fengcong landforms seem to be in a young stage of development while Fenglin landforms are in an old stage. For a long time, it has been accepted that there is a geomorphic and evolutionary relationship between the two types. The author, from the view point of non-uniformity and differences in exchange of material and energy under various conditions within a open system, proposes a new concept of simultaneous systematic evolution of Fenglin Karst landforms, namely, the two main type landforms could develop parallely and synergetically within the same genetic system.

Introduction

Fenglin Karst, formed in widespread, exposed, thick-bedded carbonate rocks accompanied by an intense exchange of material and energy, is a kind of holokarst and is classified into two main morphologic types: Fengcong (peak-cluster depression, cone karst) and Fenglin (peak-forest plain, tower karst). Generally speaking, Fenglin Karst spreads over an area of 140,000 km^2 in Southern China. Fengcong occupies 86% of the total area while Fenglin occupies 14%. This is quite unusual in comparison with karst landforms of the same or similar type in the world.

Deduced from geomorphic cycle theory (DAVIS, 1899), academic circles have long believed that the formation and evolution of Fenglin Karst landforms followed a geomorphologic sequence model from Fengcong to Fenglin (including isolated-peak plain and residual-hill plain). Consequently, this geomorphological sequence represents an age series from young to old respectively.

In recent years, the author's research, in light of system theory, and taking such aspects as landform charateristics, mutual relationships, internal conditions and external environments into consideration, has come to the conclusion that the above mentioned sequential evolution probably is neither the only nor the main model for the formation and development of Fenglin Karst landforms.

Fenglin Karst Distribution

In China, the distributional relationship between the two main types of Fenglin Karst landforms is that the ratio of Fenglin to Fengcong increases from the Yunnan-Guizhou Plateau to the Guangxi Basin. However, if these two landform types are analyzed on the basis of a hydrologic watershed or an input-output system of material and energy, they both actually exist in the same system and usually have similar genetic and systematic relationships. Guilin Fenglin Karst, for example, has a total area of 2,400 km^2 in the upstream region above Yangshuo within the Lijiang River Basin and 52% of this region is covered by Fengcong (therefore, the Fenglin-Fengcong ratio is still less than 1). Even though isolated-peak plain is the dominant geomorphic landscape in the area between Guangdong and Guangxi Province, Fengcong landforms still accompany Fenglin. This topographic discordance within the same zone is difficult to explain using existing geomorphic cycle theory.

Research Results

In contrast to Fenglin landforms, research has shown that the Fengcong subsystem is quite stable in evolution and has a relatively high degree of order in its internal structure (i.e. cave and hydrologic systems). Studies on cave development and speleothems also indicate that Fengcong is not necessarily younger than Fenglin in evolution age, but often the contrary. Even in the same geographic region or in an hydrologically independent river basin, the internal conditions (including lithology, strata thickness and occurence, exposure and distribution relationship with the adjacent nonkarst strata, other geologic and tectonic factors, etc.) and the external environment (including climate, hydrology, base level variation, etc.), both of which control and affect the evolution of Fengcong and Fenglin landforms, are not all the same in different locations. A geomorphologic zone with a deep watertable is the best place for developing Fengcong landforms while an area with a watertable close to the surface is most suitable for the formation of a Fenglin landscape. The type of material and energy movement is definitely different during the formation process of the two type Fenglin Karst landforms. The surface topography of Fengcong is mainly formed by the vertical movement of meteoric waters, while Fenglin is the result of horizontal corrosion by surface water flow. The initial orientation of landform evolution, controlled by both internal conditions and the external environment, is largely responsible for its successive development.

In addition, research on the characteristics of cave evolution in the isolated-peak, insular-Fengcong and residual-hills of a Fenglin subsystem shows that positive reliefs over the plain give no evidence of originating from early Fengcong

landform. On the contrary, they are the result of a long term independent evolution under the condition of planation of Fenglin landforms.

Conclusions

The author therefore proposes that, in most circumstances, the formation of Fengcong and Fenglin landforms is mainly a result of different initial evolutionary orientations(Fig.1). That is to say, the two morphologic types could develop parallelly within the same system but restrain and affect eachother mutually. This is the simultaneous system evolution theory of Fenglin Karst, and its basic principle is as follows: In an input-output system (i.e. hydrologic system) , the uneven spatial distribution of the exchange of material and energy and the change in geological process due to differences in both the internal conditions and the external environment will result in a parallel development of the two types of Fenglin Karst landforms through reciprocal inhibition and depending upon and synergizing with each other. Fenglin, for instance, is most easily formed along the interface between limestone and noncarbonate rocks where the karst strata is gently dipping and underlaid by an impermeable layer, and recharged by alot of allogenic water. Fengcong will primarily develop from the initial surface funnelization of meteoric waters in an area with a deep ground water table.

The simultaneous system evolution theory of Fenglin Karst breaks the classical geomorphological cycle theory which has become a fixed model in geomorphology for over a century. The nature, character, distribution, and evolution of Fenglin Karst, in light of this theory, has pointed out a new direction for further study, and also has a great instructional significance for resource exploitation, environment conservation, and other practical activities in Fenglin Karst areas.

References

DAVIS W.M. 1899. The geographical cycle, Geog.Jour. 14.

FORD D.C. & Williams P.W. 1989. Karst geomorphology and hydrology, Unwin Hyman Ltd. London.

JENNING J.N. 1985. Karst Geomorphology, Oxford: Basil Blackwell.

SWEETING M.M. 1972. Karst landforms, London: Macmillam.

SWEETING M.M. 1990. The Guilin karst, Z.Geomorph: N.F. Suppl-Bd. 77.

ZHU XUEWEN. ZHU DEHAO. RU JINWEN. 1980. Fenglin karst landform and its development in Guilin Area, Proceedings of international exchange of geologic sciences (Vol. 5), Geological publishing house(in Chinese).

ZHU XUEWEN. WANG XUNYI. ZHU DEHAO. et al. 1988. Study on karst geomorphology and caves in Guilin, Geological publishing house (in Chinese).

ZHU XUEWEN. 1991. New considerations on characteristics and evolution of Fenglin karst, Carsologica sinica, No. 1, 2, 3. Vol.10 (in Chinese).

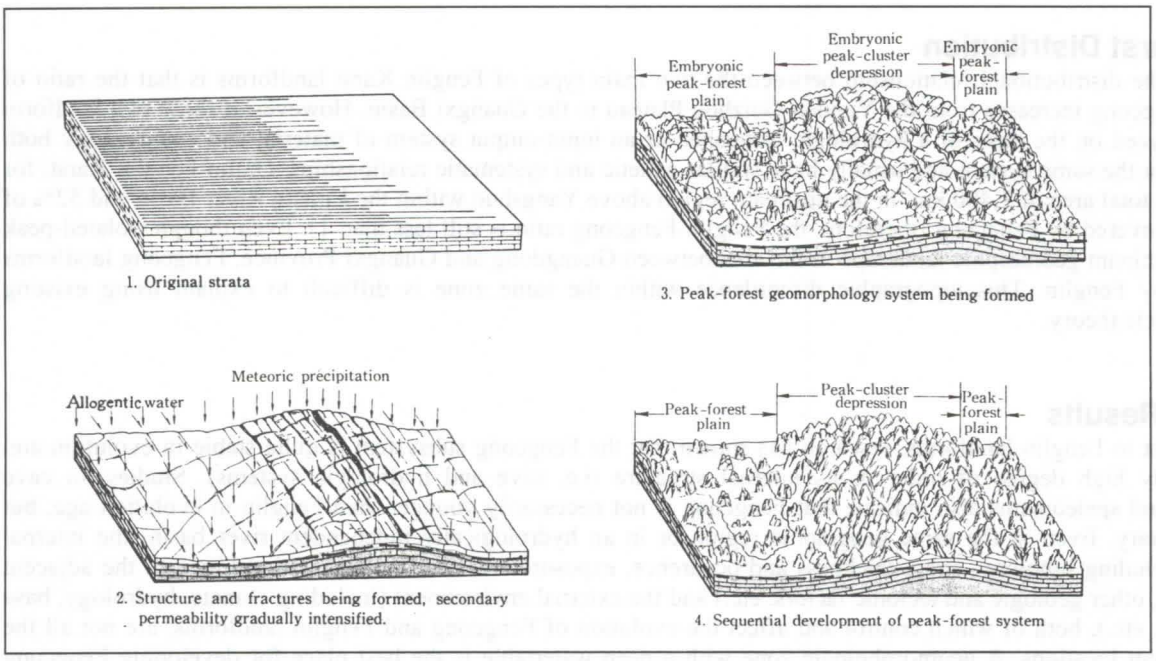

Fig. 1: Simple model showing the simultaneous systematic evolution of fenglin karst landforms.

Reconstruction of the Development of Semiblind Ponor Valleys in Moravian Karst Based on Geophysical Surveying, Czech Republic

Jaroslav Kadlec

Czech Geological Survey, 118 21 Prague, Czech Republic

Abstract

At the border between the Devonian limestones of Moravian Karst and the Lower Carboniferous non-karstic sediments deep valleys originated during the Cenozoic. These valleys are filled mostly by fluvial sediments up to 60 m thick. Measurements in a network of gravity profiles complemented by vertical electrical sounding measurements were conducted in two semiblind valleys situated on the northern rim of Moravian Karst. The geophysical data allowed to produce 3-D diagrams of valleys without sedimentary fill. Based on the shape of the valleys and the fluvial sediments of different ages preserved in the surrounding caves a reconstruction of the development of the valleys and of the genesis of cave systems in Moravian Karst during the Cenozoic is possible.

1. Introduction

The Moravian Karst area is located 200 km SE of Prague. The limestone area is bounded by faults against Lower Carboniferous non-karstic sediments in the north and in the east. Deep ponor valleys were incised by streams near this boundary during the Cenozoic and subsequently filled with fluvial sediments. In these valleys, surface streams sink under the surface and flow through cave systems more than 20 km long in total. Two ponor valleys originated at the northern margin of Moravian Karst - the Sloup Valley and the Holštejn Valley. The present surface of sediments filling these valleys lies 470 m above sea level. Boreholes drilled more than three decades ago revealed that the thickness of fluvial sediments in the valleys ranges between 25 and 58 m (DVORÁK, 1961). Reconstruction of the development of ponor valleys and cave systems in the N part of Moravian Karst is exemplified in this contribution on the Sloup Valley, which contains the Sloupsko-šošùvské Caves. The cave system includes two horizontal levels connected by several chasms. The present surface stream sinks at the upper level of caves and, vertically dropping by 70 m, flows through the lower cave level to the Amatérská Cave.

2. Shape of the ponor valleys as determined by geophysical surveying

The study was conducted using a combination of gravitational method and vertical electrical sounding. A grid of transversal and longitudinal gravity profiles complemented by vertical electrical soundings was measured in the Sloup and Holštejn valleys. Processing and evaluation of the obtained geophysical data provided an idea of the physiography of the valleys under the sedimentary fill across the individual profiles. They revealed that the shapes of both valleys are identical. 3-D images of the valleys stripped of their sedimentary fill can be modelled on the computer (Fig. 1).

The image shows what the Sloup Valley would look like after the removal of all its sediments. The valley has the highest depth in its western part (i.e., on the right in Fig. 1). A relict of a narrow, canyon-like valley is developed here with its bottom lying at 400 m above sea level. The stream which formed this blind canyon terminated by an almost 100 m high terminal wall was flowing horizontally into the Amatérská Cave. The present thickness of fluvial sediment fill reaches 70 m here. The eastern tract of the deep canyon is surrounded by a ramp-like limestone plateau, the surface of which lies 30 m above the canyon bottom. To the south, this surface gradually passes into the bottom of the narrow tract of the valley (Fig. 1). Thicknesses of fluvial sediments above the plateau and in the narrow valley range between 35 and 40 m.

3. Origin and history of the Sloup Valley

The genesis of the valley is closely linked with the surrounding cave systems which were draining the basin in different periods. It is essential to know the shapes of all parts of depressions for the reconstruction of the origin, development and filling history of the ponor valleys at the N margin of Moravian Karst. The previous authors (PANOŠ, 1961; Štelcl, 1962) did not have the necessary data at their disposal; therefore, their ideas suffered of a number of inconsistencies.

In the **Paleogene**, surface streams in the Moravian Karst area formed shallow valleys. First horizontal cave systems originated at the levels of the bottoms of these oldest valleys. The upper level of the Sloupsko-šošùvské Caves dates back to this time (e.g., HYPR, 1980). A relict of old fluvial sediments with strongly weathered greywacke pebbles is known from this cave. Above the sandy gravels, silts with an inverse paleomagnetic polarity are deposited (ŠROUBEK & DIEHL, 1995). The intensive weathering of greywacke pebbles along with the inverse values of paleomagnetic polarity from the silts indicate a considerable age for these fluvial sediments. They are most probably older than the paleomagnetic Brunhes/Matuyama boundary, i.e., they were deposited in the Lower Pleistocene or earlier. It cannot be excluded that these sediments were deposited in times when only a shallow valley existed.

The shallow valleys of Paleogene age were deepened by surface streams in Moravian Karst during the **Lower Miocene** (e.g., HYPR, 1980). Deep canyons originated whose bottoms became an erosional basis for the northern part of Moravian Karst. As a result of a relatively rapid change in gradient characteristics, the surface drainage was replaced by underground drainage and the Amatérská Cave with adjacent cave systems were formed (KADLECOVÁ & KADLEC, 1 995). Retrograde ero sion of a stream sinking in the Sloup Valley was a response to the new gradient characteristics.

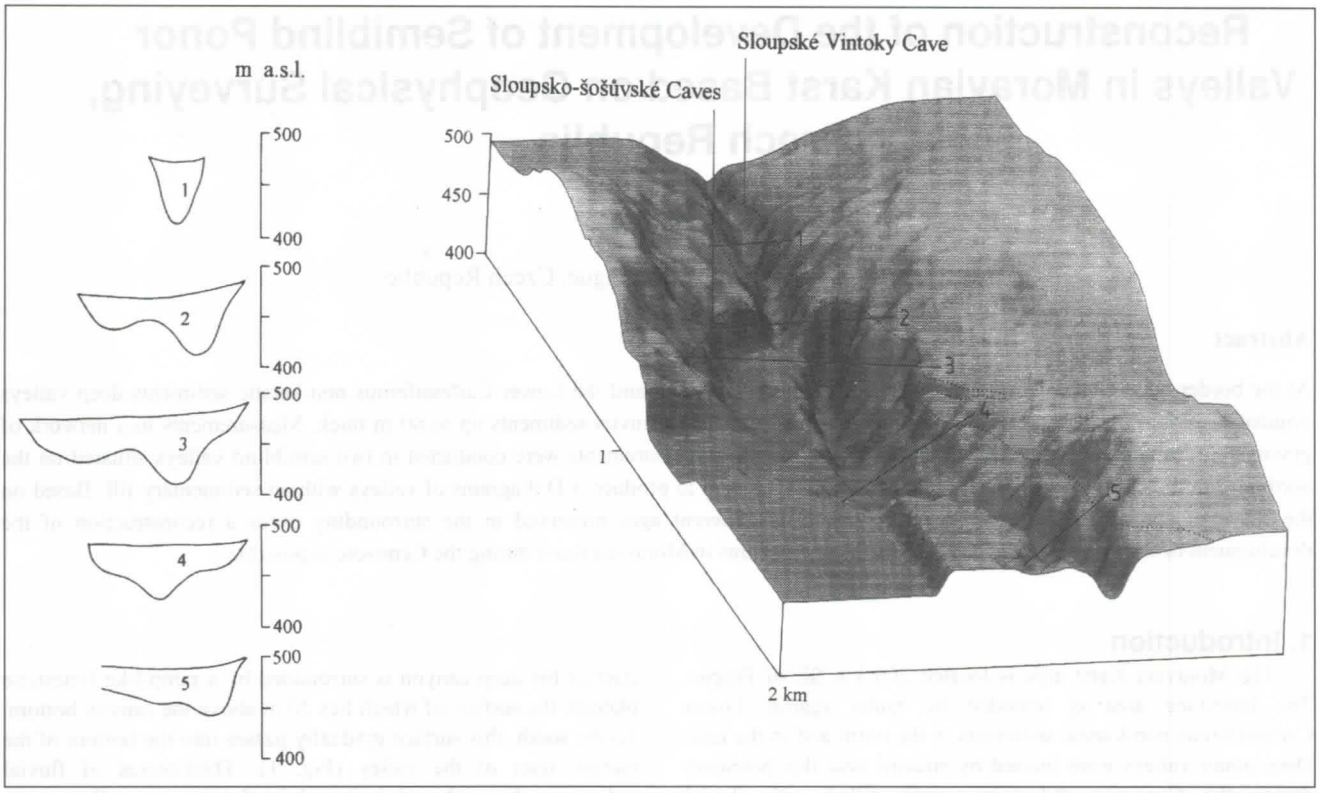

Figure 1 : The Sloup Valley stripped of its sedimentary fill; a view from the NE. Lines numbered 1 through 5 mark the locations of transversal gravity profiles, the dotted line shows the level of the present surface of the sedimentary fill in the valley. The shape of the valley at locations of transversal gravity profiles is shown on the left. 2.5 times exaggerated.

This erosion gave rise to a narrow, deep canyon at the western flank of the shallow valley. From here, water was horizontally drained by the Amatérská Cave. The upper level of the Sloupsko-šošůvské Caves got into hanging position after the incision of the deep canyon, lying some 65 m above the stream level (see Fig. 2). As a result, it could not be flown by an active stream.

In early **Middle Miocene** (during Lower Badenian), sea transgressed over the Moravian Karst and other areas on the E margin of the Bohemian Massif. The surface of the karst area was covered by marine sandy gravels and clays and all karst processes were interrupted. Also the semi-blind Sloup Valley was filled with marine sediments.

After the retreat of the sea (in late Lower Badenian), streams in Moravian Karst began to erode the marine deposits. The surface stream found its way to the original pre-Badenian cave system (the Amatérská Cave) after some time. Marine sediments were then removed from the canyon in the Sloup valley by fluvial erosion and water was again horizontally flowing to cave systems in the same manner as before the marine transgression (see Fig. 2).

The mouth of the cave system at the head of the blind canyon got blocked due to severe floodings or rockfall, which led to gradual filling of most of the canyon-like valley with fluvial sediments. In the **Pliocene**, the whole Moravian Karst area and its vicinity was getting slightly tilted towards the east as a result of doming of the Bohemian Massif. The courses of streams in the ponor valleys started to shift to the east, and a karst pediplanation process was initiated, lasting till the present (PANOŠ, 1963). The Sloup Valley was widening in the eastward direction and the limestone plateau surface originated, which is visible in the eastern part of the depression in Fig. 1. The stream was sinking by the SE valley wall thus forming the lower level of the Sloupsko-šošůvské Caves system. This level was used by the stream to flow back to the Amatérská Cave.

Climatic changes which occurred at the **Pliocene/Pleistocene** boundary had a deep influence on the processes in the Moravian Karst area. Large floodings taking place in transition periods between colder and warmer episodes were responsible for gradual filling of ponor tracts of cave systems with clastic sediments. This probably resulted also in blocking the ponors. The water then could not flow into caves but flowed through channels on the surfaces of karst canyons. This situation led to the accumulation of clastic sediments in the Sloup Valley and to its filling with fluvial deposits up to the upper cave level. After a long pause, the stream penetrated again to the upper level of the Sloupsko-šošůvské Caves (see Fig. 2). Chasms originated between the upper and lower cave levels to allow water to return to the lower drainage level (the Amatérská Cave). Through these chasms the stream dropped vertically by 70 m.

A new interruption in the drainage of the Sloupsko-šošůvské Caves occurred due to blocking of the cave corridors by clastic sediments at the **Lower/Middle Pleistocene** boundary, or possibly in the Middle Pleistocene. The stream was flowing on the surface to the southern end of the Sloup Valley where it was sinking in a cave called Sloupské Vintoky (Fig. 1). From this ponor upstream, retrograde erosion started to be effective forming a narrow part of the valley whose bottom was lying at the same altitude as the surface of the ramp-like plateau in the broad part of the valley. This narrow part got filled with fluvial sediments as early as in the Middle

Pleistocene as documented by a fossil soil sediment preserved above the fluvial fill of the narrow part of the Holštejn valley. Micromorphological study has shown that the soil sediment comes from the last interglacial (SMOLÍKOVÁ & KADLEC, 1993).

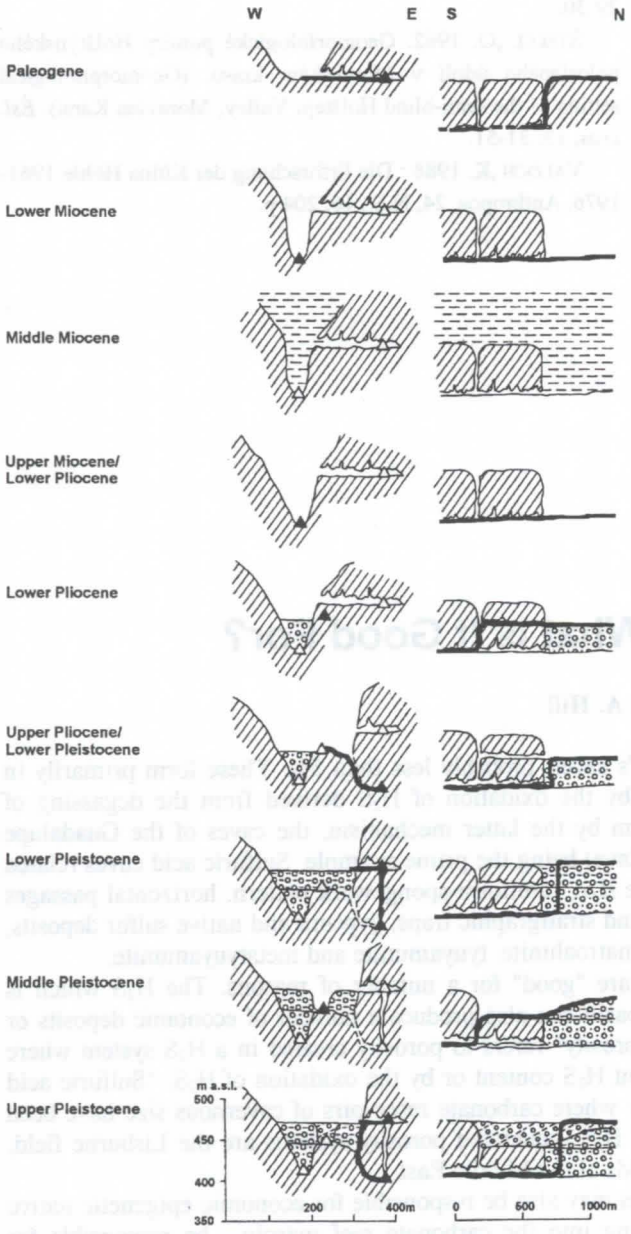

Figure 2 : Development of the Sloup Valley. Left - a vertical profile with indicated valley development at the location of transversal gravity profile 2. Right - a longitudinal vertical section across the valley from gravity profile 2 toward the S end of the valley. Small black triangle in the transversal section - active cave level, empty triangle - nonactive cave level. The course of the stream is marked by a heavy line. For other explanations see the text.

In the **Upper Pleistocene**, the surface of sediments filling the valley was lying at about the same altitude as it is today. A narrow valley in front of the Kùlna Cave - it is a part of the upper level of Sloupsko-šošùvské Caves - has been already filled with fluvial sediments which allowed the stream to flow to this cave. Fluvial sediments ranked within the last interglacial are exposed at bases of measured sections in extensive archeological excavations in the Kùlna Cave. Well-known sections with loess and debris intervals representing a complete sedimentary record of the last glacial are exposed in their hangingwall (VALOCH, 1988). During the Upper Pleistocene, the stream was flowing through the upper level of the Sloupsko-šošùvské Caves where it deposited thick accumulations of fluvial sandy gravels.

No substantial changes occurred in the Sloup Valley in the **Holocene**. The surface stream was sinking in the frontal part of the upper level of the Sloupsko-šošùvské Caves, dropped vertically by 65 metres into the lower level wherefrom it was flowing horizontally to the Amatérská Cave. This situation lasts till the present.

4. Conclusions

1. Geophysical measurements were successfully used for the determination of the topography of sediment-filled ponor valleys in Moravian Karst. Morphology of the valleys allowed to reconstruct the history of the valleys as well as of extensive cave systems in the northern Moravian Karst area.
2. The topographies of the Sloup and Holštejn valleys are identical. The valleys are the deepest in their western tracts where relicts of deep, canyon-like valleys are preserved being filled with fluvial sediments of probably Pliocene age.
3. The valleys were widened towards east and ramp-like plateaus originated in their bottoms at the Miocene/Pliocene boundary and especially during the Pliocene. The broad valley tracts upstream of the plateaus are filled with Lower Pleistocene fluvial sediments.
4. The narrow valley tracts originated in late Lower Pleistocene and in the Middle Pleistocene. They were filled with fluvial sediments of Middle Pleistocene age.
5. The presented model of the origin and filling history of the Sloup and Holštejn valleys does not necessarily imply numerous repeated periods of sediment accumulation and erosion during the Quaternary as suggested by some older studies.

Acknowledgments

The study of sediments of the Moravian Karst is supported by the Grant Agency of the Czech Republic (grant No. 205/93/0726) and U.S.-Czech Science and Technology Program (grant No. 95 051).

Geophysical measurements and data interpretation were provided by the staff of the company of G Impuls Praha s.r.o. with an unusual effort.

References

DVORÁK, J. 1961. Výsledky vrtného prùzkumu v severní èásti Morav ského krasu. (Results of drilling investigation in the northern part of Moravian Karst). Symposion o problémech pleistocénu, Anthropos, 14: 93-95.

HYPR, D. 1980. Jeskynní úrovnì v severní a støední èásti Moravského krasu. (Cave levels in the northern and central parts of Moravian Karst). *Sbor. Okr. muzea v Blansku*, 1980: 65-79.

KADLECOVÁ, R. & J. KADLEC. 1995. Vznik a stáøí Amatérské jeskynì. (Origin and age of the Amatérská Cave). *Speleo*, 20: 16-22.

PANOŠ, V. 1961. Sloupské údolí a Pustý •leb v Moravském krasu, jejich postavení v krasovém cyklu. (Sloup and Pustý •leb valleys in Moravian Karst, their position within a karst cycle): MS, PhD. Thesis, National Library Praha, 383 p.

SMOLÍKOVÁ, L. & J. KADLEC. 1993. Interglaciál v holštejnském údolí v Moravském krasu. (Interglacial in the Holštejn valley, Moravian Karst). *Vist.Èes.geol.Úst.*, 68, 4: 63-64.

ŠROUBEK, P. & J.F. DIEHL. 1995. Paleomagnetické/environmentální magnetické studium jeskynních sedimentù Moravského krasu. (Paleomagnetic/environmentally magnetic study of cave sediments, Moravian Karst) - in CÍLEK, V.ed.: Svìt v podzemí. (The Underground World): Knihov. ÈSS, 25: 29-30.

ŠTELCL ,O. 1962. Geomorfologické pomìry Holštýnského poloslepého údolí v Moravském krasu. (Geomorphological setting of the semi-blind Holštejn Valley, Moravian Karst). *Èsl. kras*, 13: 31-51.

VALOCH ,K. 1988 : Die Erforschung der Kùlna Höhle 1961-1976. Anthropos, 24, N.S., 16, 204 p.

Sulfuric Acid Karst: What is it Good For?

By Carol A. Hill

Sulfuric acid caves make up a small minority of the world's caves, probably less than 5%. These form primarily in one of two ways: by the oxidation of sulfide ore bodies, or by the oxidation of H_2S derived from the degassing of hydrocarbon basins. Only five cave systems are known to form by the latter mechanism, the caves of the Guadalupe Mountains, New Mexico (e.g., Carlsbad Cavern, Lechuguilla Cave) being the prime example. Sulfuric acid caves related to hydrocarbon basins can be recognized by their large passage size, ramiform-spongework pattern, horizontal passages connected by deep pits or fissures, location beneath structural and stratigraphic traps, gypsum and native sulfur deposits, and the sulfuric acid/ H_2S indicator minerals endellite, alunite, natroalunite, tyuyamunite and metatyuyamunite.

The mechanisms which produce sulfuric acid karst/caves are "good" for a number of reasons. The H_2S which is genetically responsible for these caves around a hydrocarbon basin can also produce a number of economic deposits or create the porosity needed for these deposits. " H_2S -related porosity" refers to porosity created in a H_2S system where dissolution can be produced by the mixing of waters of different H_2S content or by the oxidation of H_2S. "Sulfuric acid oil-field karst" refers to a specific kind of H_2S -related porosity where carbonate reservoirs of cavernous size have been dissolved by a sulfuric acid mechanism. Possible examples of H_2S -generated porosity systems are the Lisburne field, Prudhoe Bay, Alaska, and some of the extremely productive fields of the Middle East.

Hydrogen sulfide produced in association with hydrocarbons may also be responsible for economic epigenetic native sulfur deposits within a basin, or it can also - upon migrating into the carbonate reef margin - be responsible for Mississippi Valley-type lead-zinc sulfide deposits. Here, sulfide deposits can be produced in the zone of reduction, and sulfuric acid caves can be produced in the zone of oxidation. Thus, sulfuric acid caves may be exploration indicators for hydrocarbons, native sulfur, and Mississippi Valley-type ore deposits. The role of the migration of H_2S has hitherto been underestimated as a speleogenesis mechanism and in the formation of ore deposits and reservoir porosity. Speleologists in the next millenium should consider applying their knowledge of sulfuric acid karst processes to the field of economic geology.

Karst denudation in Irkutsk Region

Elena Trofimova
Institute of Geography, Siberian Branch of Russian Academy of Sciences
Ulanbatorskaya str.1, Irkutsk, 664033 Russia

Abstract

Using method of prof. M. Pulina karst denudation is tallied up for 93 river basins of Irkutsk Region. Its schematic map was created. Two big regions with karst denudation from 20 to 50 mm/1000 years and three small regions with values from 20 to 30 mm/1000 years are distinguished. Considerable values of karst denudation are explained in the context of peculiarities of karst processes in the Region.

Zusammenfassung

Mit Hilfe der Methode von Prof. M. Pulina ist die Karstdenudation von 93 Flusseinzugsgebieten von Irkutsk abgeschätzt worden. Dabei wurde eine schematische Karte der Karstdenudation erstellt. Zwei grössere Gebiete mit Karstdenudationen von 20 bis 50 mm/1000 Jahre und drei kleinere Gebiete mit solchen von 20 bis 30 mm/1000 Jahre sind speziell behandelt worden. Die bedeutende Karstdenudation wird im Kontext mit speziellen Karstprozessen in diesen Gebieten erklärt.

1. Introduction

Areas covered by karst rocks occupies about 50 % of Irkutsk Region, a total of more than 400.000 km^2. Soluble rocks are disposed in all stratigrafic stratums and geostructural elements of two main karst regions, the Siberian Platform and its mountain range. Karst is developed in carbonate and sulphate rocks and salts of Lower Cambrian, dolomites and limestones of the Ordovician, Silurian and Devonian of Platform and Precambrian rocks of mountain regions, crystalline marbles, limestones and dolomites. Depending on geological, geomorphological and hydrogeological conditions, karst occurs on the surface of the earth or revealed at depths of more than one kilometre. That is why the objective estimation of intensity of modern karst processes is really necessary for the considered area.

2. Experience of regional investigations

VOLOGODSKY (1975) was the first karstologist who systematized all information about karst phenomena in Irkutsk Region. Using the abound data of field observations he distinguished four types of areas with different intensity of karst processes: weak exhibition, weak, sometimes strong, strong and strong in separate parts.

LITVIN (1988) explored karst in researched area after VOLOGODSKY (1975). Works of LITVIN (1988) are the first attempts of regional characterisation of the karst quantitatively. He discerned four categories of areas attacked by karst in Priangarje and Pribajkalje: very poor, single manifestings of karst; poor - less than 10 %; mean - 10-25 %; high - 25-50 %. Attack of area by karst is defined as ratio of areas with relatively high concentration of surface forms and fixed underground forms (for example, caves) to all area. But the considered index doesn't depend on age and modern activity of karst. Moreover, karst forms are not the indications of modern karst processes (GAMS, 1976). It is required to choose the quantitative way of research to the intensity of karst processes.

3. Methods of explorations

Much research activities were devoted to karst denudation. There are some quantitative approaches to estimate its intensity.

Firstly, strategies of KRUBER (1915) and CORBEL (1959) and etc. Data about the content of calcium carbonate dissolved in water are used in calculations. Secondly, ways of WILLIAMS (1963) and GAMS (1969), calcium and magnesium carbonates are accounted in computations. Neglection of the content of another dissolved component is the common lack of these methods. The approach of PULINA (1968, 1992) eliminates this lack. It allows to include into the calculations the content of water dissolved components as in salts by precipitation. And nevertheless, very often scientists work with the more simple method of CORBEL (1959) only.

With the aim of a comparison of the methods of CORBEL (1959) and PULINA (1968, 1992), computations of karst denudation (we will only consider chemical part of karst denudation) were tallied up for four river basins of Irkutsk Region in relationship about which in karstological literature repeatedly was published (GVOZDETSKY, 1972; CHIKISHEV, 1973; and etc.).

River basin	Karst denudation		Type of karst
	Corbel	Pulina	
Bajronovka	6,0	6,4	carbonate
Zalari	2,2	7,2	carbonate and sulphate
Manzurka	5,7	13,4	carbonate,
Lena (head river)	7,8	16,5	sulphate and salt

Table 1
Comparative calculations of karst denudation after methods of CORBEL (1959) and PULINA (1968, 1992)

These calculations were accomplished for river basins which are distinguished by different types of karst - carbonate, sulphate and salt.

As will be apparent from table 1, strategy of CORBEL (1959) gives understated results, especially in areas with exhibitions of uncarbonate karst. That is the reason why the more complicated calculation method of PULINA (1968, 1992) will be more convenient for quantitative estimation of karst denudation in the Region.

4. Calculation of karst denudation

Leaning on the method of PULINA (1968, 1992), the calculations of karst denudation were accomplished for 93 river basins situated in different parts of Irkutsk Region, on Siberian Platform and its mountain range. With the aim to except the

influence of tranzit water's mineralization we will consider small and middle river basins only. 33 % of the rivers have the overall area less than 1000 km^2.

It was used the information about average annual mineralization as well as average annual runoff which was averaged at all period of hydrological observations. Annual mineralization was determined as averaged one in different phases of hydrological regime - winter and summer drought, rise, recession of flood and crest. The same procedure was realized for precipitation. Data about their mineralization were received from observations in meteorological stations which are disposed in different parts of area: Preobrazhenka (north part of Irkutsk Region), Boljshie Koty (west shore of lake Baikal), Khamar-Daban (western Khamar-Daban range) and Mondy (East Sayan range).

It is necessary to note that PULINA (1968) tried his method in the researched area middle of the sixties for several river valleys - see table 2. As evident from table 2, some divergences occur between data of PULINA (1968) and our calculations. These differences in values of karst denudation is possible to explain by the following.

Karst area		Karst denudation	
		Pulina (1968)	Author
South Scarp of Siberian Platform:			
River Basins:	Unga	8,1	21,8
	Osa	19,7	21,0
Sayan Scarp:			
Boljshaya Belaya basin		8,3	12,7
Western Khamar-Daban:			
	Sludyanka	61,4	27,4
	Pokhabikha	61,4	50,9

Table 2
Karst denudation in Irkutsk Region,m^3/km^2/year or mm/1000 years

In the first place, representative row of observations taking into consideration the phase of high and small water content in averaging of hydrological characters is going on for not less than 30 years in Siberia. Duration of observations of the hydrological regime of rivers, are presented in table 2, existed only for 30 in the middle of the sixties. For instance, gauging station in Unga basin was found in 1963 only. In the second place, it is possible, Pulina sampled the water for hydrochemical analysis in one, not in all, phases of hydrological regime of rivers. While, for example, for Unga basin, differences in mineralization of waters in winter drought and crest reach 2200 mg/l.

The schematic map of karst denudation was created basing on calculated data for 93 river basins (fig.). These basins are united to follow groups in value of karst denudation: 1 - less 5 mm/1000 years - 2 - 5-10; 3 - 10-15; 4 - 15-20; 5 - 20-50; 6 - more than 50 mm/1000 years.

5. Characters of regions with intensive development of karst

Maximum values of karst denudation are observed in two main regions:

First, East bordering of Siberian Platform, belt with width 40-80 km, area of spreading of carbonate and sulphate rocks of Lower Cambrian with stratums of salt. Valley of Kirenga with tributaries and valley of Chuya (right tributary of Lena) are assigned to this region. Karst denudation vary between 20 and 50 mm/1000 years.

Typical karst features such as single and group potholes (dolines), ponors, karst basins, dry valleys, estavelles, karst springs and lakes, underground cavities and caves are encounted here.

A lot of dolines are located on the basin divide between rivers Levaya Kirenga and Tongoda. The depth of potholes are changed from 1-3 to 30-40 m and the width is to 200-400 m. Some are the ponors for surface streams. Karst basins are noted in right part of catchment of river Kirenga. Collapse depressions have the sizes from few metres to 10-15 kilometres in length and from several metres to several kilometres in width. Dry valleys are revealed in basins of Handa, Okukikta and etc. Host of karst springs are disposed here, very often they have a chlorine-natrium or sulphate-hydrocarbonate content and mineralization up to 2,7 g/l. Karst lakes Blizhnee (valley of river Okunajka, length of it is 3 km) and Ploschadinskoe (left tributary of Lena, length of it is 2,5 km) are the most representative lakes occupying the karst basins. A wide known spring is situated at the left shore of river Kirenga, near village Ermaki, its mineralization is 3 g/l, discharge is 100 l/s. Few caves are discovered in valleys of Uljkan and Kirenga. Two caves in limestones are disposed near town Kirensk.

Maximum karst denudation is in basin of river Minya - 52,1 mm/1000 years. That is maximum for Irkutsk Region. Powerful karst springs of chlorine-natrium content with mineralization more than 600 mg/l and discharge 1000-1500 l/s are revealed here.

In opinion of VOLOGODSKY (1975), this area is strongly exhibited of karst processes generally. LITVIN (1988) reasons that this area is characterized by different categories of attacks by karst - from very poor with single manifestings to mean. But as for basin of Minya, he think that this basin is without significant distribution of karst (LITVIN, 1988).

Second, south shore of lake Baikal, western Khaman-Daban range (basins of Pokhabikha, Bezimyanka, Kharlakhta and etc.) - area of spreading of Archean rocks represented by carbonate rocks (marbles) in alternation with gneisses and crystalline schists. The peculiarity of karst here is the placing to tectonic crevasses and zones of faults along that the underground water leakage occurs. Maximum of karst denudation fall in Pokhabikha valley - 50,9, minimum - in Snezhnaya valley - 6,3 mm/1000 years. There are follow forms of karst manifestings: a lot of springs, dry valleys, sinking streams and its restoration, underground cavities filled by water. Karst potholes and karst basins are presented weakly. It is conceivable, that is why LITVIN (1988) interprets that the karst processes don't develop in this region. VOLOGODSKY (1975) assignes this area to one of strong karst along tectonic crevasses and zones of tectonic faults.

Modulus of springs runoff are 1,0 -1,65 l/s from 1 km^2. Distribution of springs is very irregular. Areas without it, with dry valleys and parts of loss of runoff are changed by a group characterized by seepages of underground waters. Discharges of springs reach 20 l/s, mineralization - to 500 mg/l. Multitude of sinking streams are fixed in basin of rivers Pravaya Pokhabiha - to 5 m^3/s to 1 km of river length, Sludyanka - 0,18, Uluntuj (right tributary of Sludyanka) - 0,17 (HYDRODEOLOGY, 1968). Underground cavities with waters are revealed in mountain drifts of Sludyanka deposit.

Three separate small regions with karst denudation from 20 to 30 mm/1000 years are distinguished too. Two regions are connected with impact of sulphate karst.

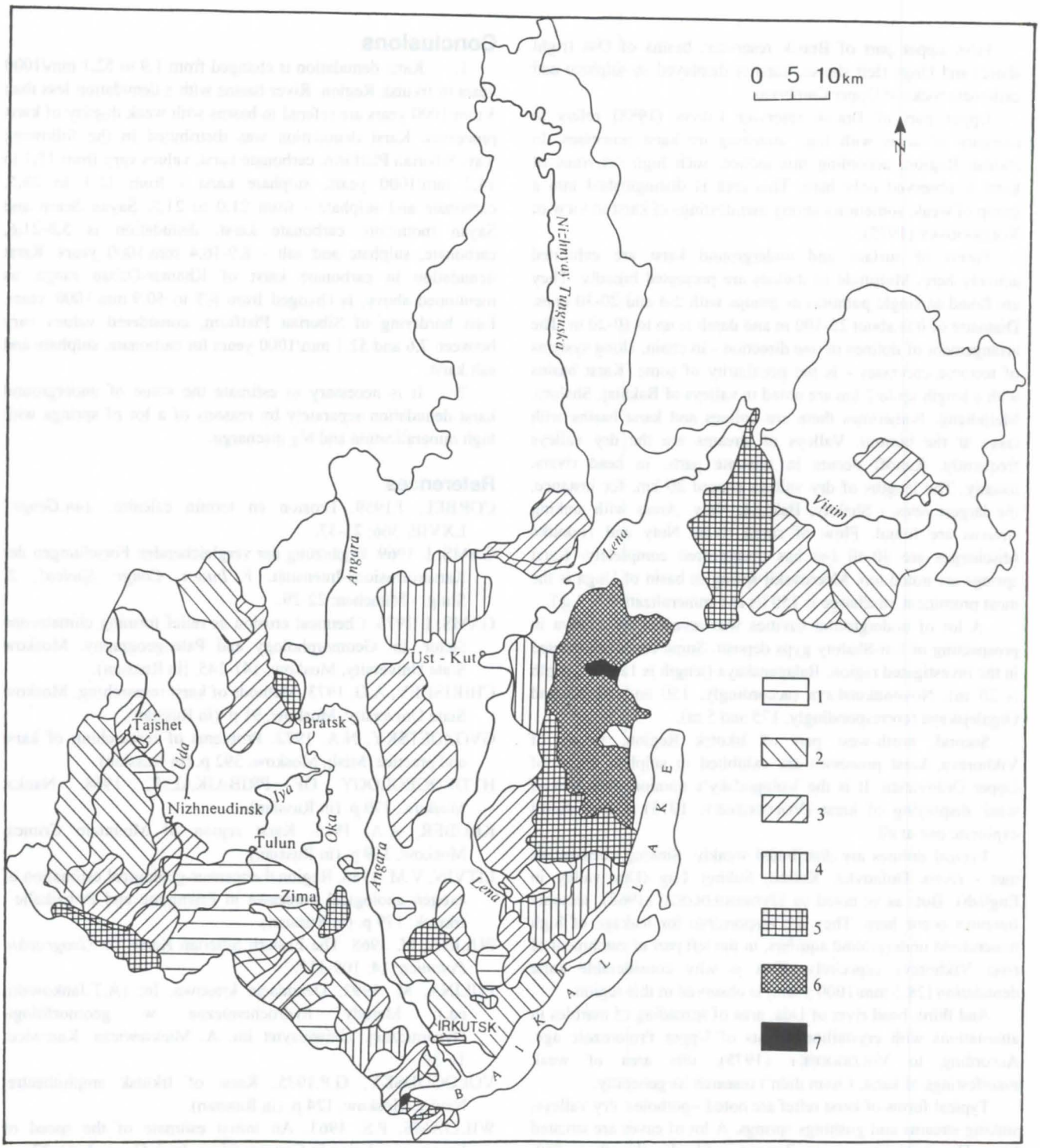

Figure: Karst denudation in Irkutsk Region:
1 - < 5 mm/ 1000 years; 2 - 5-10; 3 - 10-15; 4 - 15-20; 5 - 20-30; 6 - 30-50; 7 - > 50.

First, upper part of Bratsk reservoir, basins of Osa (right shore) and Unga (left shore), karst is displayed in sulphate and carbonate rocks of Upper Cambrian.

Upper part of Bratsk reservoir LITVIN (1988) refers to category of areas with high attacking by karst processes. In Irkutsk Region, according this author, such high activities of karst is observed only here. This area is distinguished into a group of weak, sometimes strong manifestings of karst in view of VOLOGODSKY (1975).

Forms of surface and underground karst are exhibited actively here. Multitude of dolines are presented broadly. They are found as single potholes as groups with 2-4 and 20-30 ones. Diametre of it is about 25-100 m and depth is up to 10-20 m. The arrangement of dolines in one direction - in chain, along systems of tectonic crevasses - is the peculiarity of some. Karst basins with a length up to 2 km are noted in valleys of Bakhtaj, Shaloty, Meljkhetuj. Sometimes there are dolines and karst basins with lakes at the bottom. Valleys of streams are the dry valleys frequently. Runoff occurs in separate parts, in head rivers, usually. The lengths of dry valleys exceed 20 km, for instance, the largest ones - Shaloty, Bakhtaj, Noty. Areas with sinking streams are found. Flow of small rivers Noty and Nukutka (discharges are 30-40 l/s) has disappeared completely. Karst springs are noted too. Meerovskij spring in basin of Unga is the most prominent, discharge is 150 l/s and mineralization is 5 g/l.

A lot of underground cavities was revealed by Ljvova in prospecting of Ust-Shaloty gyps deposit. Some caves are located in the investigated region: Balaganskaya (length is 1200 m, depth is 20 m), Novonukutskaya (accordingly, 150 and 10 m) and Orgalejskaya (correspondingly, 175 and 5 m).

Second, north-west part of Irkutsk Region, valley of Vikhoreva, karst processes are exhibited in sulphate rocks of Upper Ordovician. It is the Vologodsky's opinion, this area of weak displaying of karst (VOLOGODSKY, 1975). Litvin didn't explorate one at all.

Typical dolines are distributed weakly. Sinking streams are met - rivers Dolnovka, Kaltuk, Sukhoj Log (Dry valley in English). But, as is noted in HYDROGEOLOGY (1968), tectonic fractures occur here. They are responsible for leakage of high mineralised underground aquifers, in the left part of catchment of river Vikhoreva especially. That is why considerable karst denudation (28,5 mm/1000 years) is observed in this region.

And third, head river of Uda, area of spreading of marbles in alternations with crystalline schists of Upper Proterozoic age. According to VOLOGODSKY (1975), this area of weak manifestings of karst, Litvin didn't research its generally.

Typical forms of karst relief are noted - potholes, dry valleys, sinking streams and gushings springs. A lot of caves are situated here. The most known are Zimnyaya Skazka (length is 780, depth is 28 m) and Spirinskaya (correspondingly, 540 and 45 m). Mountain terrain (mean high of basin is 1760 m above Baltic sea) is the main factor in intensive development of karst here.

Conclusions

1. Karst denudation is changed from 1,9 to 52,1 mm/1000 years in Irkutsk Region. River basins with a denudation less than 5 mm/1000 years are refered to basins with weak display of karst processes. Karst denudation was distributed in the following way. Siberian Platform: carbonate karst, values vary from 12,1 to 14,2 mm/1000 years, sulphate karst - from 12,1 to 28,5, carbonate and sulphate - from 21,0 to 21,7. Sayan Scarp and Sayan mountain: carbonate karst, denudation is 5,8-21,6, carbonate, sulphate and salt - 8,9-16,4 mm/1000 years. Karst denudation in carbonate karst of Khamar-Daban range, as mentioned above, is changed from 6,3 to 50,9 mm/1000 years. East bordering of Siberian Platform, considered values vary between 7,6 and 52,1 mm/1000 years for carbonate, sulphate and salt karst.

2. It is necessary to estimate the value of underground karst denudation separately by reasons of a lot of springs with high mineralization and big discharge.

References

CORBEL, J.1959. Erosion en terrain calcaire. *Ann.Geogr.*. LXVIII, 366: 21-37.

GAMS, I. 1969. Ergänzung der vergleichenden Forschungen der Karstkorrosions-Intensität. *V Intern. Congr. Speleol.*, 2, Stutg. - München: 22-29.

GAMS, I. 1976. Chemical erosion as relief forming climatezone factor. In: Geomorphology and Paleogeography. Moskow State University, Moskow: 141-145. (in Russian).

CHIKISHEV, A.G. 1973. Methods of karst researching. Moskow State University, Moskow, 91 p. (in Russian).

GVOZDETSKY, N.A. 1972. Problems of researching of karst and practice. Mislj, Moskow, 392 p. (in Russian).

HYDROGEOLOGY OF PRIBAJKALJE, 1968. Nauka, Moskow, 170 p. (in Russian).

KRUBER, A.A. 1915. Karst region of Mountain Crimea. Moskow, 319 p. (in Russian).

LITVIN, V.M. 1988. Regional engeneer-geological estimation of exogen geological processes in Priangarje and Pribajkalje . Irkutsk, 179 p. (in Russian).

PULINA, M. 1968. The Eastern Siberian Karst. In: *Geographia Polonica*. 14: 109-117.

PULINA, M. 1992. Denudacja krasowa. In: (A.T.Jankowski, ed.): Metody hydrochemiczne w geomorfologii Dynamicznej. Uniwersytet im. A. Mickiewicza. Katowice: 16-39.

VOLOGODSKY, G.P.1975. Karst of Irkutsk amphitheatre. Nauka, Moskow, 124 p. (in Russian).

WILLIAMS, P.S. 1963. An initial estimate of the speed of limestone solution in Country Clare. *Irish.Geogr.*4: 21-27.

Karst geomorphological process and climate

Lin Junshu, Li Juzhang & Fang Jinfu
Institute of Geography, Chinese Academy of Science, Beijing 100101, China

Abstract

Studies of dissolution rates in various areas of China lead to the consideration of seven equations in order to link environmental factors to dissolution rates. The model shows that precipitation is the most important factor affecting the rate of denudation. The temperature plays an important role as well. The temperature of 15°C appears to be a threshold. Lithological and morphological factors play less important roles in the dissolution process.

Introduction

Dissolution is the main geomorphological process in karst landform development. This implies that the circulation and the chemical composition of karst groundwater have to be considered in any geomorphological study. The first methods for assessing the dissolution rates were developed during the last century (FORD *et al.* 1989, SWEETING, 1965). Today, the most common methods used to assess denudation rates are: limestone tablets, micro-erosion measurements and formulae based on water characteristics.

J. Corbel (1957, 1959) proposed one of these formulae:

$$x = 4\frac{ET}{100},\ X = 4\frac{ET}{100}\bullet\frac{1}{n}$$

where X is the value of carbonate rock solution (m^3/km^2.a, or mm/ka), E is annual runoff (dm), T is mean water hardness $CaCO_3$ or $CaCO_3 + MgCO_3$ (mg/l) and n is the proportion of carbonate rock in the catchment. Later, WILLIAMS (1968), GAMS (1967), PULINA (1971) and SMITH *et al.* (1976) derived new formulae from this one. Other approaches have been presented by DRAK & FORD (1973), WHITE (1984), PALMER (1984), etc.

The results discussed in this paper are based on measurments of water chemistry and runoff at 124 karstic springs or underground rivers in the Hongshui River Basin. From this data, the denudation rates were calculated by the means of Cobel's formula. Further observations have been carried out in this basin as in some others (Beijing, Shandong and areas of North China). Limestone tablets were used to measure the dissolution rates in a dozen of places located in the tropical karst area of South China as well as in the temperate karst area of North China. Comparative studies between these data lead to conclusions about the relations between solution process and environmental factors i.e. climate.

Solution process as a responses to multiple environmental factors

From the discharge Q and its solute content T the Corbel formula gives the total denudation rate X over the limestone part of the catchment area, namely $X = Q \cdot T$. This simple formula arbitrarily assumes a runoff coefficient of 0.25 (the proportion of the total precipitation which recharges the groundwater Q). Further, applying one single formula over the whole catchment assumes that this coefficient is the same over the whole catchment area. This cannot always be assumed. For instance, the runoff coefficient ranges between 0.3 and 0.9 in the Hongshui River Basin. The value is lower in karst areas of north China. The Corbel formula has been used here only as a quantifying tool in order to detect relationships between karst processes and environmental factors.

The solution rates depend on environmental factors, e.g. annual precipitation, temperature, lithology and morphology. These parameters have to be observed at each point in order to examine their relative importance.

A power relation could be established between most of these factors and the solution rates. This mathematical method has been used to simulate the process.

In figure 1, the positive correlation between dissolution rates and precipitations can be recognised. Similar diagrams have shown that the influence of relief and temperature are of lower importance (in the Hongshui River Basin). FANG JINGFU *et al.* (1993) and LI JUZHANG *et al.* (1994) found the following relations between the solution rate X and precipitation P, runoff E, lithology L and geomorphology G (in the Hongshui River Basin):

$$\ln(X) = -4.32 + 0.567\ln(E) + 0.807\ln(L) + 0.497\ln(G)$$

and

$$\ln(X) = 1.03\ln(P) + 0.74\ln(L) + 0.482\ln(G)$$

As the weight of each factor of this equation must depend on environmental conditions, we can express this using a variable weighting model (LI JUZHANG *et al.* 1994):

$$\ln(X) = a_P\ln(P) + a_L\ln(L) + a_G\ln(G) = \frac{(a+b+c)}{\left(\frac{a}{\ln(P)} + \frac{b}{\ln(L)} + \frac{c}{\ln(G)}\right)}$$

and so it is given by

$$\ln(X) = \frac{1}{\left(\frac{4.210}{\ln(P)} + \frac{0.829}{\ln(L)} + \frac{0.295}{\ln(G)} - 0.636\right)}$$

where a_P, a_L, a_G are respectively the factor weight for precipitation, rock solubility and landform relief. a, b and c are coefficients.

Dissolution and temperature

The effect of temperature on limestone dissolution is an important topic. Some experiments showed that at a constant partial pressure of CO_2, an increase in temperature reduces the absorbtion coefficient of CO_2, leading to a negative correlation (Smith et al. 1976; Ford et al. 1989). Other experiments showed

that the dissolution rate of carbonates correspond to the Boussinesque recession equation of CO_2, meaning that temperatures lower than 0.5°C and higher than 60°C are not favourable for dissolution (HUANG SHANGYU *et al.* 1987, 1991). In addition, some studies suggest that the kinetics of the processes are more rapid at higher temperatures. It is well known that a temperature increase of 10°C accelerates the chemical reaction by a factor of two (BÖGLI, 1980; SWEETING, 1965). Biogenic processes are influenced by temperature and might also play a certain role (JAKUCS, 1977).

Using observations of limestone tablets in natural environments from south to north China, we could simulate the relationship between observed dissolution rates X_{lw} , total precipitation during the observation period P_{ot}, annual precipitation P_{ym}, and mean annual temperature T_{am}. These simulations show that the dissolution is affected not only by precipitation but also by temperature. The relation is found to be the following:

$$\ln(X_{lw}) = -14.9 + \frac{31.9}{\left(\frac{2}{\ln(P_{ot})} + \frac{1}{\ln(P_{ym})} + \frac{0.8}{10 - \ln(20T)}\right)}$$

$$T = T_{am} - 15 \quad if \quad T_{am} > 15$$

$$T = 45 - 3T_{am} \quad if \quad T_{am} \leq 15$$

The dissolution rate for the same precipitation increases when the mean annual temperature is both lower or higher than 15°C. This value appears then to be a threshold. This shows that temperature is associated with precipitation in the dissolution process. This corresponds to the transition between temperate and subtropical areas, i.e. between the Qinling Mountain and the Huaihe River in China.

Acknowledgements

This study is a part of projects 49070012, 49271012 and 49471008 which are supported by the National Natural Science Foundation of China. We thank Prof. Zhang Yaoguang and Prof. Song Linhu of the Institute of Geography, Chinese Academy of Sciences for their many valuable comments.

References

BÖGLI, A. 1980. Karst hydrology and physical speleology, Berlin: Springer-Verlag.

FANG J., LIN J., LI J. & ZHANG Y.. 1993. Relation of solution to environment in karst area. A case study of Hongshui River Basin. *Acta Geographica Sinica, 48(2): 122-130.*

FORD, D. C. & WILLIAMS, P. W. 1989. Karst geomorphology and hydrology, London: Unwin Hyman Ltd. 96-115

HUANG S. & SONG H. 1987. The corrosion of carbonates and environment temperature. *Carsologica Sinica, 6(4): 287-296.*

JAKUCS, I. 1977. Morphogenetics of karst regions, Bristol: Adam Hilger Ltd.

LI, J.; LIN, J. & FANG J. 1994. Analysis and estimation of the karst solutional intensity. *Geographical Research, 13(3): 90-97.*

PALMER, A. N. 1984. Geomorphic interpretation of karst features. In: (R. G. Lafleur Ed.): Groundwater as a geomorphic agent. London: Allen & Unwin, 173-209.

SMITH, D. I. & ATKINSON, T. C. 1976. Process, landforms and climate in limestone regions. In: (E. Derbyshire Ed.): Geomorphology and climate. John Wiley & Sons Ltd. 367-409.

SWEETING, M. M. 1965. 1. Introduction, Denudation in limestone regions: a symposium. *The Geographical Journal, Vol. 131, Part I:34-37.*

SWEETING, M. M. 1980. Karst and climate - a review. *Z. Geomorph. N. F. Suppl.-Bd, 36(49): 203-216.*

WHITE, W. B. 1984. Rate process, chemical kinetics and karst landform development. In: (R. G. LaFleur, Ed.): Groundwater as a geomorphic agent. London: Allen & Unwin. 227-248.

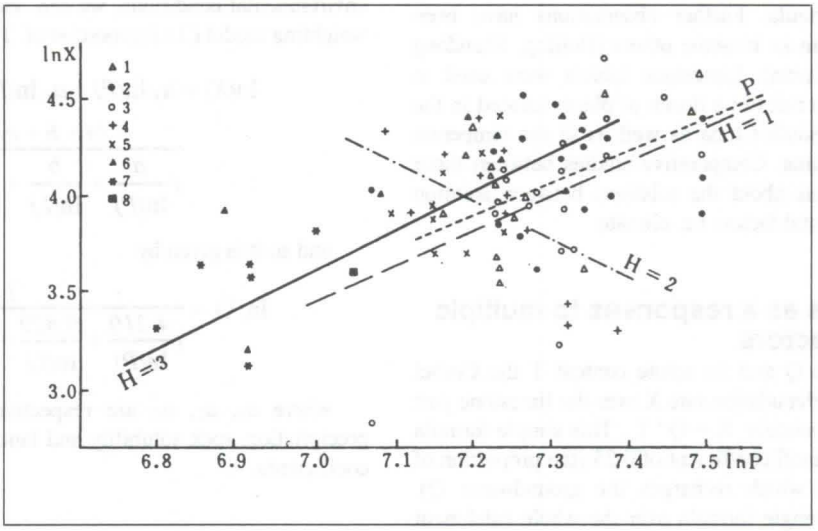

Figure 1: Relationship between solution rates and precipitations for various types of environments.
1. Plain; 2. Lower mountain of low relief; 3. Middle mountain of low relief; 4. Lower mountain of median relief; 5. Middle mountain of median relief; 6. Lower mountain of high relief; 7. Middle mountain of high relief; 8. Higher mountain of high relief.

Deep Messinian Karst in Mediterranean Area

Prof. ing. Giuliano Perna
Salita dei Molini 49 I 38050 Villazzano- Trento, Italy

Abstract

The karstic base level was lowered up to 1000 ÷ 2000 m below the actual sea level, during the dissecation of the Mediterranean Sea from Messinian Stage (Upper Miocene, 6.3 m. y.) to Zanchean Stage (Pliocene, 5.2 ÷ 5.3 m.y.).

According to this event in Mediterranean Area we may have deep karst systems and the presence of a great reserve o thermal fresh or brackish waters, in connection or not with the supply area.

Riassunto

In conseguenza del disseccamento del Mare Mediterraneo dal Messiniano (Miocene sup. 6,3 m. a.) allo Zancheano (Pliocene 5,2 ÷5,3 m. a.), il livello di base carsico si abbassò di 1000÷2000 m sotto l'attuale levello del mare.

In conseguenza può essere presente nell'area del Mediterraneo un carsismo profondo, contenente grandi riserve di acque termali dolci o salmastre, ancora o non, in connessione con l'area di ricarica.

1. Preview

During Messinian Stage (Upper Miocene Epoch 6.3 m.y.) the Mediterranean Sea was totally dissecated (fig. 1) and in consequence the erosion level of rivers and the base level of the karstic waters follows the level of the sea, 1000 ÷ 2000 meters under the actual level (CITA & CORSELLI, 1993).

According to the tectonic and stratigraphic studies, in Messinian Stage the connection between Atlantic Ocean and Mediterranean Sea (between Spain and Marocco) was closed. The Mediterranean sea is now, and was in greater measure at that time of warmer climate, deficient in the water cycle and in a short time almost totally dried. This fact is documented by the thickness and extension of the evaporites (essentially gypsum, but also kainite and halite) not only in outcrops but also on the bottom of the sea.

As a consequence of that the hydrographic network dramatically lowered, as proved by the deep canyons accompanying main rivers like the Nile and Rodan. These evidence have been discovered by geophysical research and oil drills. A large lake occupied at that age the area between Alps and Apennines in northern Italy, where the big alpine rivers merged in.

The alpine rivers were influent streams in this lake ("Padano Lake"), with big canyons, in the place were we have now the piedmonts lakes: Maggiore, Como, Garda. Also karstic base level was lowered at the new sea level (FINK, 1978).

In the Zanchean Stage (Pliocene 5.2÷5.3 m.y.) the connection between the Mediterranean Sea and Atlantic Ocean was reopened and the original level of the Mediterranean Sea was restored in a short time.

The Nile and Rodan came back to original level and the canyons were filled by sediments. Also the level of the deep karst was lifted to previous level but the karstic voids and channels of the Messinian karst non necessary were closed. This voids contain now a very big reserve of thermal waters according to geothermal gradient. In some cases we have brackish water, caused by intrusion of marine waters (fig. 2). When the tectonic and/or sedimentation have occluded the karstic outfalls in the sea, we have a resource of fresh water (fig. 3). When the karstic system is still active, we have a recharge and the resource is renovable.

2. Examples of deep Messinian karst in SW Sardinia

Since 1975, with the financial support of CEE and mines located in the Iglesiente Area (led, zinc, barite mines) and Sulcis Area (coal mines) investigations have been carried out about the hydrogeology of carbonatic rocks from Cambrian to Eocene. Direct knowledge on the karstic circulation has been acquired until a depth of 250 m below actual sea level in the Iglesiente area and until 400 m in the Sulcis zone. Indirect informations have been obtained by means of drills (depth of 1000 m) and geophysical prospecting (4000 m). A detailed study of karst passages have been enterprised for that part above sea level, showing similarities and differences with the correspective cavities present at different depth until 400 m below sea level. Detailed studies have been brought out concerning filling deposits, waters and their geochemistry.

In the mining district of Iglesiente a sea water intrusion has been observed in deep Messinian karst in Cambrian limestone formation (mineralized with Pb+Zn, fluorite, barite ores). The flow pumped out from the mining area ranges around 2000 l/s; 40% of this water is associated with the input of sea water. We have also an elevated grade of heavy metals related to residual clay in waters (Hg, Zn, Cd, Fe).

In the mining district of Sulcis the coal beds are located in the "Miliolithic limestone" formation (Eocene). The deep karst evolution on this formation stopped in the early stage and the sea water intrusion didn't appear, the flow pumped out is given by fresh water with a volume ranging around 30 l/s and 42°C (fig. 3).

3. Examples of deep Messinian karst in Venetian and Po Valleys

In the Mesozoic and Tertiary Series (essentially limestones and dolomites) of the Southern Alps are present old deep karstic systems, that feed some thermal fresh waters springs (PICCOLI et al., 1976) (fig. 4). We may remember Sirmione (Southern border of Garda Lake), Verona, Abano - Montegrotto - Battaglia Terme district, Vicenza wells and springs, Grado and Monfalcone at the eastern boundary of Venetian plain.

4. Other examples

Recently the genesis of the Movilé Cave (on the border of Black Sea, Romania) is related to Messinian stage. We have some other indications of Messinian karst in Southern Italy, Greece and Croatia - Albania. Perspective of study are present in Balearic Islands, Spain and other states of the Mediterranean area.

5. Conclusions

With the data in our possession (remote sensing by satellite and aircraft, geoelectrical profiles, deep seismic soundings, isotopic geochemistry), detailed geology and hydrogeology and comparisons with other situations it is now possible the formulation of the hypothesis about Messinian karst.

We define Messinian karst a very deep karst (1 to 2 km or more) related to the dissecation of the Mediterranean sea in Messinian stage. (PERNA, 1994) This is a depth undoubtedly superior than that connected with the vertical drop of the sea during glaciations (about 100 m). This karst may be also now in connection with upper actual karstic circulation of waters.

The hypothesis of the existence of Messinian karst must be confirmed with further examples and studies not only for scientific interest but also for practical implication related to the research of new fresh and thermal resources.

References

CITA, M.B. & C. CORSELLI 1993. Messiniano: vent'anni dopo. *Mem. Soc. Geol. It.*, 49: 145-164, Roma.

FINK, P.G. 1978. Are alpine lakes former Messinian Canyons?: *Marine Geology* 27:289-302, Amsterdam

PERNA, G. 1994. Il carsismo profondo nel Sulcis - Iglesiente (Sardegna Sud Occidentale) e nel Trentino - Veneto (Alpi orientali Italiane). "Carsismo messiniano": esempi di carsismo profondo correlati con il livello del Mediterraneo nel Messiniano. *Ann. Musei civici - Rovereto, Sez. Arch., St., Sc. nat.*, 10: 327-378.

PERNA G. 1996. Il carsismo messiniano e la circolazione profonda delle acque nel Sulcis - Iglesiente (Sardegna Sud Occidentale). *Mem. Ass. Min. Sarda,* 2: 27-38, Iglesias.

PICCOLI G., R. BELLATI, C. BINOTTI, E. DI LALLO, R SEDEA, A. DAL PRA`, R. CATALDI, G.O. GATTO, G. GHEZZI, M. MARCHETTI, G. BULGARELLI, G. SCHIESARO, C. PANICHI, E. TONGIORGI, P. BALDI, G.C. FERRARA, F. MASSARI, F. MEDIZZA, V. ILICETO, A. NORINELLI, GP. DE VECCHI, A. GREGNANIN, E.M. PICCIRILLO & G. SBETTEGA. 1976. Il sistema idrotermale Euganeo-Berico e la geologia dei Colli Euganei. *Mem. Ist. Geol., Mineral. Univ. Padova*, 30: 1-266.

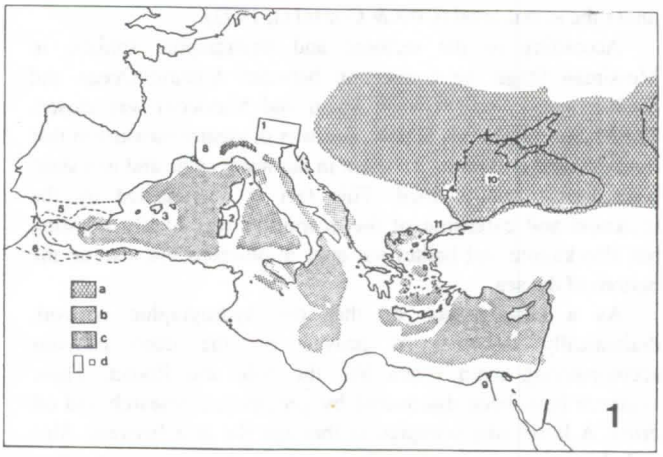

Fig. 1. Actual Mediterraneaan Sea (from CITA & CORSELLI, 1993, modified).
In the Messinian Stage the Gibraltar (7) strait was closed. With the closure of N Bethic (5) ad S Rifan (6) Straits the Mediterranean sea was isolated from Atlantic Ocean and dried almost completely. The extension of evaporites (b), Lake Padano (c) and Lake Mer (a) is indicated.
(1) Venetian Prealps, (2) Sulcis - Iglesiente (SW Sardinia), (3) Balearic Islands, (4) Movilé Cave, Rumania, (8) Rhone River, (9) Nile River, (10) Black Sea, (11) Dardanelli Strait.

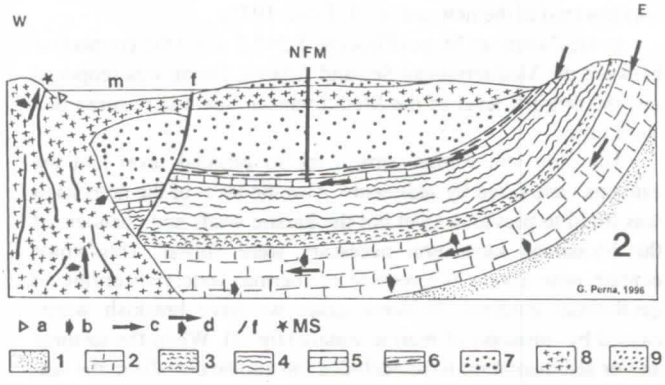

Fig. 2. In the Iglesiente Area (SW Sardinia) there are ore deposits (Pb, Zn, pyrite,barite, fluorite) in Cambrian carbonatic sequence. The same rocks are interested by policyclic karsts from Ordovician to Actual. In the Monteponi and San Giovanni mines we have brackish water circulation, while Masua and Campo Pisano present fresh waters. Seismic investigation revealed the presence of sedimetary rocks at a depth of more than -4000 m. We suppose that this complex is overtrusted and is present a second Cambric sequence: carbonatic rocks of the deeper structure are also interested by Messinian karst and are in connection with sea. The sea water mixed with fresh water (old and actual) upwell through a transversal fault present in the Monteponi sincline and mix with actual karstic water.
Hydrogeological model: (a) Sea water; (b) Thermal sea water; (c) Fresh water; (d) Brackish thermal water; (e) faults; (f) overtrust fault; (1) Pre Cambrian; (2) Lower Cambrian, Nebida Fms.(Sandstone); (3) Lower Cambrian, Gonnesa Fms. (Limestone and dolomite); (4) Middle Cambrian,Cabitza Fms. (shale); (5) Ordovician ("Puddinga"); (6) Post Messinian sediments; (7) Cixerri Fms (sandstone, shale).

Fig. 3 In the Sulcis Area, Miliolitic limestone Fms (Cenozoic) is interested by a circulation of thermal waters (42°C) in a karstic not much evoluted system. Below we have a continental Permo - Triassic impermeable series and then the karsified Cambrian carbonatic sequence. The two groundwaters are not connected. The deep thermal water circulation produce an extended thermal anomaly, tha interest all the Sulcis Area.
Hydrogeological model: (a) Sea water; (b) Thermal sea water; (c) Karsic water; (d) Brackish thermal water; (f) fault; (MS) Maladroxia Spring; (m) Sea level; (NFM) Nuraxi Figus coal mine.
(1) Lower Cambrian, Nebida. Fms. (Arenarie); (2) Lower Cambrian, Gonnesa Fms. (Karsified Limestone and dolomia); (3) Middle Cambrian, Cabitza Fms. (Shale); (4) From Permian to Ordovician (Shale, conglomerate, sandstone etc. (impermeable); (5) Cenozoic: "Miliolitico" karsified limestone, (6) Cenozoic: Limestone, marl, argillite e coal beds ("Produttivo"); (7) Middle Eocene - Lower Oligocene Cixerri Fms: Conglomerate, sandstone, shal, (8) Cenozoic Vulcanites, (9) Quaternary: Sands.

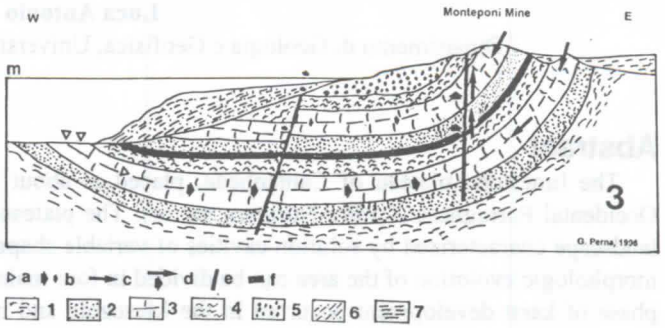

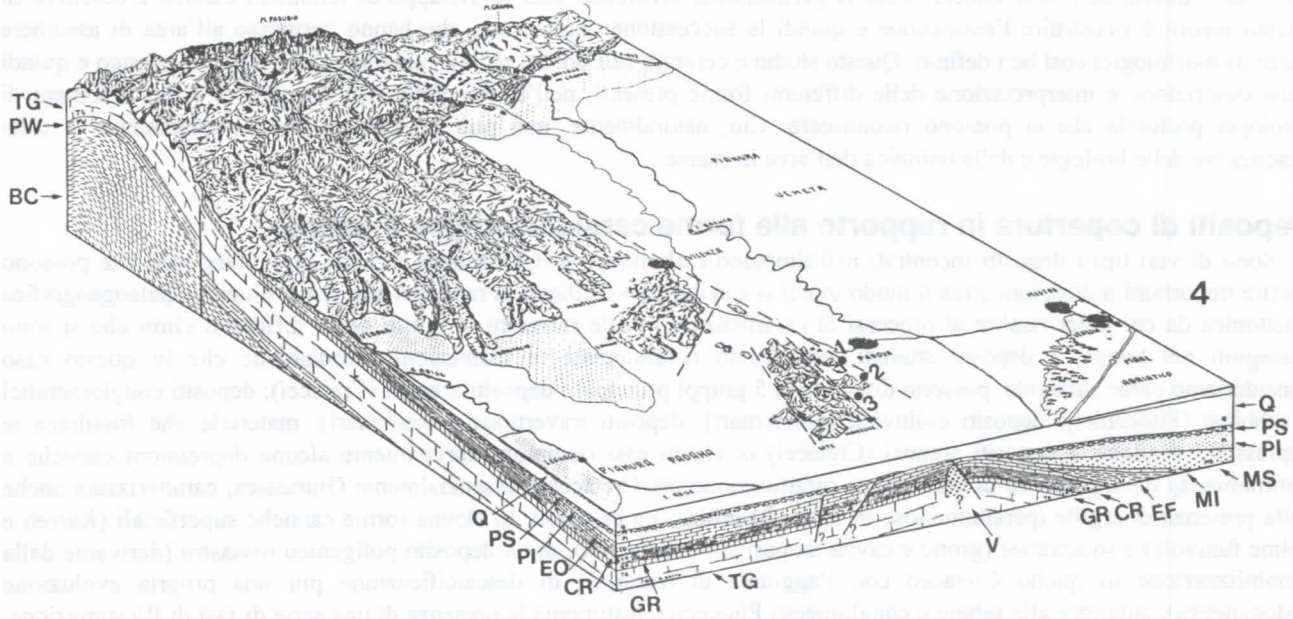

Fig. 4. Hydrogeologic scheme of the Abano, Montegrotto and Battaglia Terme hydrothermal area (From PICCOLI et al, 1976). Geologic stereogram of Western Veneto, with zones of alimentation) in Venetian Prealps) and outcrops of Thermal circuit (Euganei hills, SW of Padua).
(BC) Cristalline basament; (PW) = Permian- Werfen (sandstones, limestones, domites, gypsum); (TG) = Trias and Jurassic (Limestones and dolomites); (GR) = Jurassic (Nodular limestones of Rosso Ammonitico Frm.); (CR) = Cretaceous (Biancone limestones and Scaglia Rossa Frm.); (EO) = Eocene and Oligocene (Nummolitic limestone); (EI) = Eocene inf. e medio (flysch), (MI) = Miocene inf. (limestone and marls); (MS) = Middle and inf. Eocene (clastic facies); (PI) Inf. Pliocene (sands); (PS) Upper Pliocene (sands and clay); (Q) = Quaternary (Marine and coastals sediments and alluvium); (V) = eruptive bodies; (f) faults.
1. Abano, (2) Montegrotto; (3) Battaglia Terme.

Studio morfoevolutivo del fenomeno a carsico dell'altopiano carbonatico di Cantanhede (a NW di Coimbra - Portogallo)

Luca Antonio DIMUCCIO[1]

[1] Dipartimento di Geologia e Geofisica, Università di Bari, Via E. Orabona 4, 70125 Bari, Italia.

Abstract

The limestone plateau of Cantanhede, placed at about 130 m of altitude, is situated at the Orlo Meso-Cenozoic Occidental Portughese (Centre-Northern sector). The plateau is modelled on Jurassic limestone rocks and shows a karst landscape characterized by solution cavities of variable shapes and depth, filled with a fine well-cemented sediment. The morphologic evolution of the area can be divided in four main phases: the first one is represented by a severe and complex phase of karst development occurred in the Mesozoic and by a following burial of karst landforms; the second phase, occurred during the Tertiary, was enhanced by important erosive processes which brought to the reexhumation of karst paleolandforms with subsequent new karst development also under-cover; the third phase occurred between Quaternary and Tertiary and was characterized by transgression-regression cycles with the formation of wide flat surfaces which strongly affect the present landscape; finally, during the last phase, occurred during the Quaternary, erosion processes were responsible for the reexumation of paleokarst landforms.

Introduzione

L'altopiano di Cantanhede è un rilievo poco esteso con caratteristiche geologiche, strutturali e morfologiche ben definite ed è situato a pochi km a NW della città di Coimbra. Pecularità di quest'area è la presenza di un largo affioramento calcareo e calcareo-marnoso del Dogger su cui poggia una copertura detritica post-Giurassica. L'andamento del paesaggio è evidentemente condizionato dalla presenza degli affioramenti carbonatici, interessati da strutture tettoniche; queste ne hanno condizionato la permeabilità favorendo così lo sviluppo di fenomeni carsici. L'obiettivo di questo lavoro è ricostruire l'evoluzione e quindi la successione degli eventi che hanno permesso all'area di assumere caratteri morfologici così ben definiti. Questo studio è centrato sull'analisi della evoluzione del fenomeno carsico e quindi nella descrizione e interpretazione delle differenti forme presenti, nell'analisi della rete idrografica e dei fenomeni di idrologia profonda che si possono riconoscere. Ciò, naturalmente, non può prescindere dal riconoscimento e dalla descrizione delle litologie e della tettonica dell'area in esame.

Depositi di copertura in rapporto alle forme carsiche epigee e ipogee

Sono di vari tipi i depositi incontrati nell'altopiano carbonatico di Cantanhede, e nelle aree marginali, che possono fornire importanti indicazioni circa il modo in cui si è sviluppato il rilievo in rapporto alla sua evoluzione paleogeografica e tettonica da cui poter risalire ai processi di carsificazione e alle relazioni di questi con i differenti climi che si sono susseguiti nel tempo. I depositi studiati, escludendo naturalmente le formazioni carbonatiche che in questo caso consideriamo come substrato, possono dividersi in 5 gruppi principali: depositi arenosi (Cretacei); depositi conglomeratici e sabbiosi (Pliocenici); depositi colluviali (Quaternari); depositi travertinosi (Quaternari); materiale che fossilizza le depressioni carsiche. I depositi arenosi (Cretacei) in alcuni casi riempiono direttamente alcune depressioni carsiche a testimonianza della presenza di una fase di carsificazione pre-Cretacea o essenzialmente Giurassica, caratterizzata anche dalla presenza di argille iperallumonose in facies bauxitica. La presenza, in alcune forme carsiche superficiali (Karren e doline funivole) e sotterranee (grotte e cavità da pori sin-diagenetici), di un deposito poligenico rossastro (derivante dalla rimobilizzazione di quello Cretaceo con l'aggiunta di materiale di descalcificazione più una propria evoluzione pedogenetica), anteriore alle sabbie e conglomerati Pliocenici, testimonia la presenza di una serie di fasi di Riesumazione, Carsificazione e Interramento differenziale durante il Terziario. I travertini e la presenza di depositi derivanti dal rimaneggiamento di sabbie quaternarie (depositi colluviali) e Plioceniche, in altre forme carsiche superficiali (karren giganti), invece, testimoniano una importante carsificazione anche nel Quaternario.

Sintesi e Conclusioni

L'Altopiano Carbonatico di Cantanhede risulta modellato su rocce carbonatiche fratturate di età Giurassica interessate da imponenti forme carsiche relitte in parte sepolte (fossilizzate) da depositi terrigeni superficiali post-Giurassici. Lo studio congiunto dei depositi superficiali e l'analisi delle forme del paesaggio ha permesso di distinguere quattro fasi principali nell'evoluzione morfologica dell'area: la prima include una fase di carsificazione accentuata e complessa durante il Mesozoico; un'altra essenzialmente terziaria in cui si verificano importanti fenomeni erosivi con riesumazione di paleoforme carsiche e conseguente ripresa dei processi carsici superficiale e sotto copertura; la terza fase, verificatasi al passaggio dal Terziario al Quaternario, è marcata da ripetute ingressioni marine con il modellamento di superfici subpianeggianti determinanti per l'attuale configurazione del paesaggio; l'ultima fase è quella Quaternaria in cui si ha nuova erosione con conseguente totale o parziale riesumazione delle forme carsiche ereditate dalle fasi anteriori.

Quelques observations sur les lapiaz de Majorque

par **Jacques Choppy**
182 rue de Vaugirard, F-75015 Paris

Abstract: A few observations on the Mallorca limestone pavements

Through a detailed study of limestone pavements under very different climates, I have been able to distinguish «nival» forms and «pluvial» forms.

At Majorca the first forms are found as solution flutes (rillenkarren) and terraces. But there are also pluvial flutes, small terraces and runnels.

Of course, nival forms are fossil at Majorca, their presence being explained by the last glaciations.

Résumé

Une étude approfondie des lapiaz sous les climats les plus divers m'a permis de distinguer des formes «nivales» et des formes «pluviales».

A Majorque, on trouve les premières sous formes de cannelures et de terrasses. Mais il existe aussi des cannelures pluviales, des terrassettes et des rigoles ou «runnels».

Les formes nivales sont à Majorque évidemment fossiles ; leur existence se comprend à la lumière du développement des dernières glaciations.

Ces observations sur les lapiaz de Majorque sont l'application d'études approfondies menées dans des régions variées : notamment, dans les lapiaz haut-alpins, je fus conduit (CHOPPY 1995, 1996) à distinguer des **formes nivales**, systématiques dans des régions à enneigement prolongé et inconnues dans d'autres ; et des **formes pluviales**, que l'on trouve seulement dans les zones où la pluie tombe sur la roche nue, et pas dans celles à enneigement prolongé. Une coupure aussi nette justifie l'emploi d'expressions génétiques, indispensables pour regrouper des formes diverses ; à défaut, il faudrait du reste donner à chacune de ces formes une dénomination descriptive, nécessairement complexe.

Formes nivales

- A Majorque, même d'après photos, on est frappé par la présence généralisée de **cannelures nivales** (photo 1) ; il est évident que ce sont des formes héritées, ayant du reste continué d'évoluer, mais il est remarquable de les trouver dans les conditions géographiques actuelles.

- Les aspects de pinacles (photo 2) semblent pour une part dus à la fracturation ; ils sont sculptés de cannelures nivales, et il serait hasardeux d'en faire une forme tropicale.

- Aux formes nivales, on doit rattacher des **terrasses**, qui sont des surfaces d'égalisation interrompant la base de cannelures nivales (photo 3), et pouvant être au sommet d'autres cannelures nivales ; ces terrasses atteignent des dimensions pluri-décimétriques, plus vastes que celles connues ailleurs ; mais, ayant subi une évolution, elles ne peuvent être mises en relation avec le climat actuel.

- Aux formes nivales, on doit probablement rattacher un petit groupe de **rigoles** en demi-fuseau sur une surface en pente de 15 à 20° (photo 4).

Formes pluviales

Ces formes nivales ont presque toujours évolué :

- Le cas le plus habituel est celui où les cannelures nivales sont entaillées par des **cannelures pluviales** (photo 5) ou dégradées par une probable évolution sous couverture. Ces cannelures pluviales sont longuement étudiées dans la littérature sur Majorque, en particulier dans les communications du Symposium de 1995.

- Ailleurs, les sillons des cannelures nivales sont entaillés de **terrassettes** superposées qui ne se rencontrent qu'en climat relativement chaud, au moins méditerranéen, tandis que les crêtes séparant les cannelures nivales sont entaillées de cannelures pluviales (photo 6). Le même tableau, visible à la sierra del Endrinal (Andalousie), est représenté par DELANNOY, DIAZ DEL OLMO (1986).

- Les terrasses décrites ci-dessus sont fréquemment creusées de **kamenitzas** de petite taille (photo 7), et de **rigoles** ("runnels" de HUTCHINSON 1996 - photo 8). Ces formes sont en partie liées à des processus biologiques.

Conclusion

On peut être surpris de la place que j'accorde à des formes nivales. L'existence de telles formes n'est pourtant pas inconnue dans le domaine méditerranéen : jusqu'au niveau de la mer dans les calanques du littoral français, et à partir de 900 mètres d'altitude au Liban; dans ce pays, ces formes sont même actuellement fonctionnelles vers 1500 mètres d'altitude, car les précipitations s'y font presqu'exclusivement sous forme de neige.

Bibliographie

CHOPPY J. - 1995, Les karsts étagés ; "Les facteurs géographiques", Paris, 66 p., 66 fig.

CHOPPY J. - 1996, Les cannelures et rigoles sont des indicateurs climatiques (karst profond et karst superficiel) ; Actes du symposium "Karren Landforms", Soller 1995, Palma, 137-48.

DELANNOY J.-J., DIAZ DEL OLMO F. - 1986, La Serrania de Grazalema (Malaga, Cadiz) ; *Karstologia Mém.* 1, 45-70.

HUTCHINSON D.W. - 1996, Runnels, rinnenkarren and mäanderkarren : form, classification and relationships ; Actes du symposium "Karren Landforms", Soller 1995, Palma, 209-18.

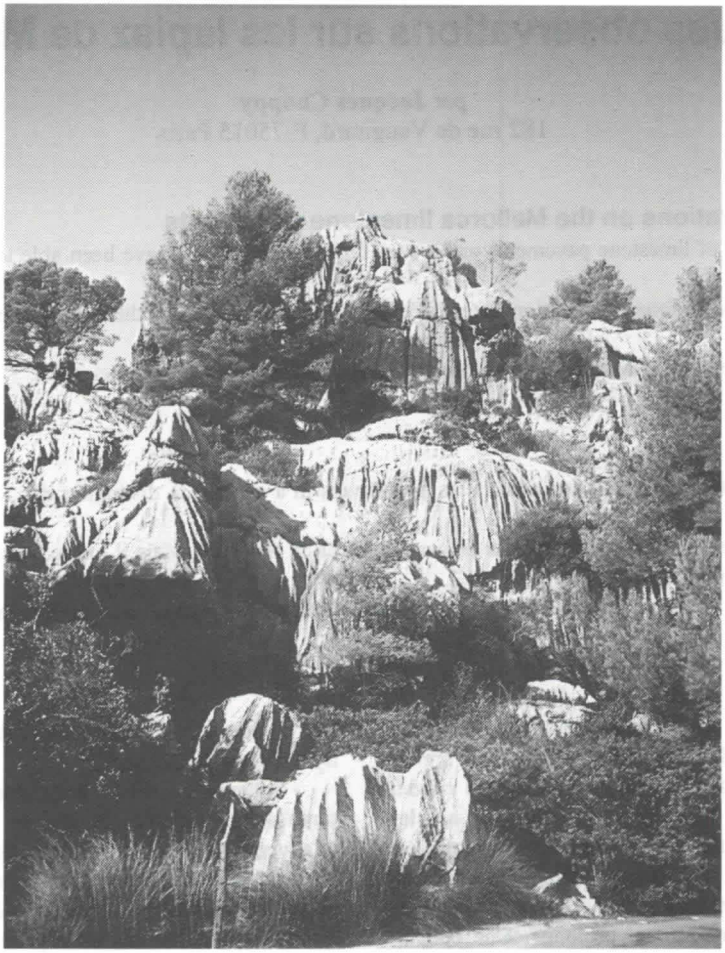

Photo 1 : cannelures nivales, c'est-à-dire sillons jointifs entaillant des parois en forte pente, de 10 à 20 centimètres de largeur en général, s'accroisant vers le bas; à Majorque, c'est seulement vu de loin que leur aspect est caractéristique

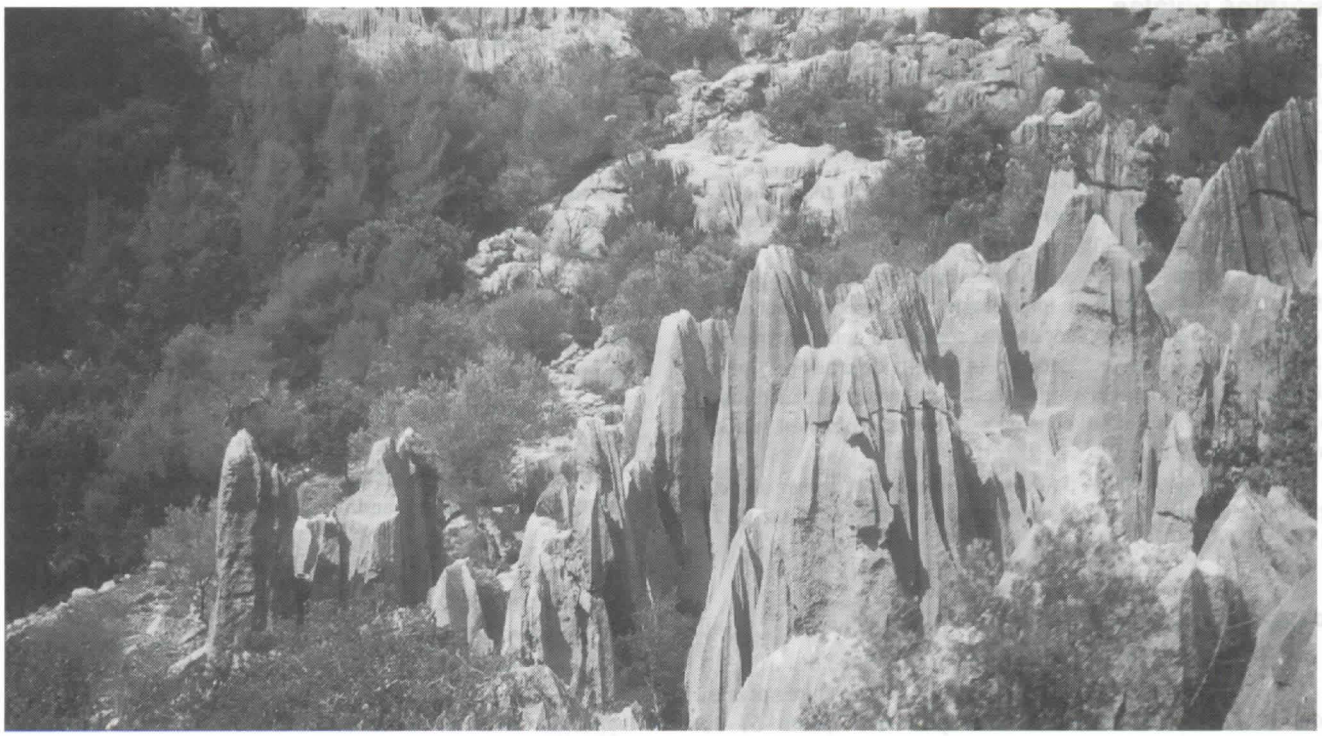

Photo 2 : pinacles

Photo 3 : terrasse; les cannelures pluviales entaillant les cannelures nivales sont bien visibles sur cette photo; la terrasse est elle-même entaillée par une corrosion sous couverture d'humus

Photo 4 : Les jambes du personnage, en haut à droite, donnent l'échelle. D'après leur largeur, il est probable qu'il s'agit ici d'anciennes rigoles nivales; les micro-baquets étagés ne sont pas rares dans ce genre de rigoles

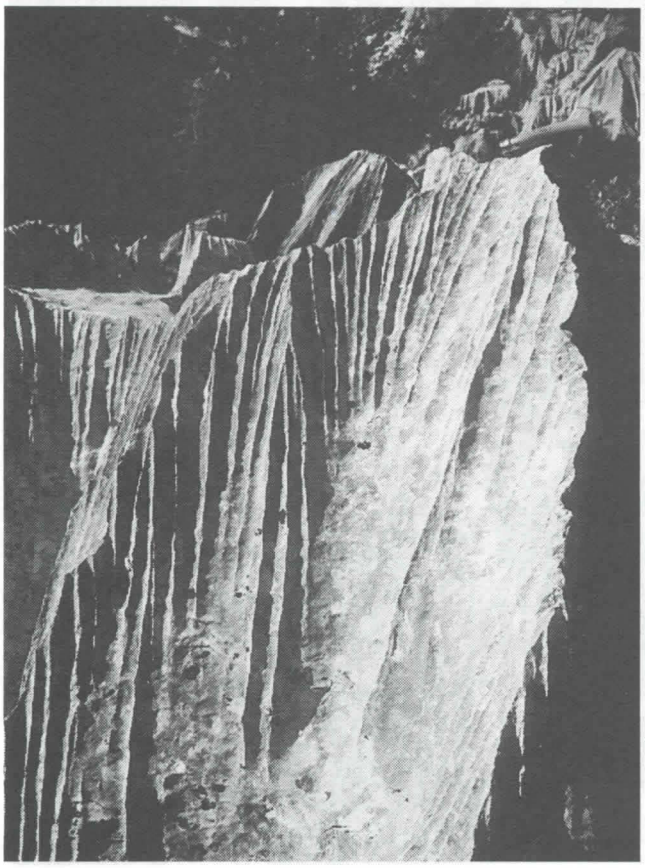

Photo 5 : cannelures nivales entaillées par des cannelures pluviales; ces dernières sont des sillons jointifs de 1 à 2 centimètres de largeur en général, s'amenuisant vers le bas; le couteau a 11 cm de long

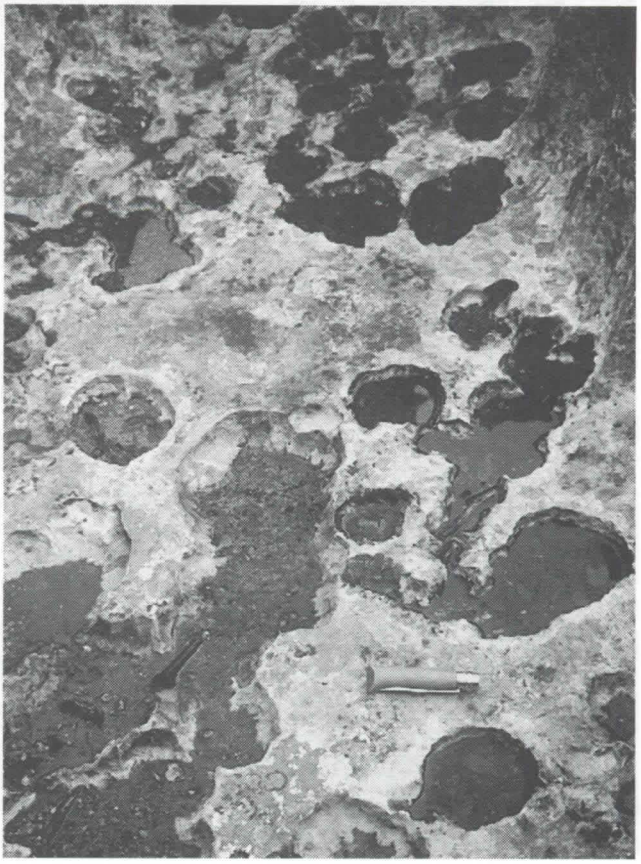

Photo 7 : terrasse entaillée de kamenitzas; même couteau

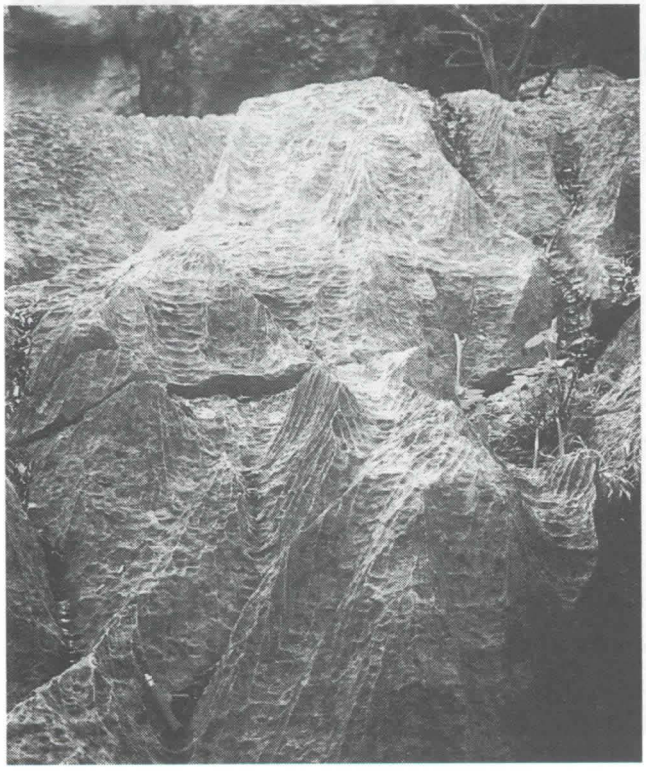

Photo 6 : cannelures nivales entaillés de terrassettes superposées; même couteau que sur la photo précédente

Photo 8 : terrasse entaillée d'une rigole; même couteau

Karst of the Tatra Mountains

by Jerzy Glazek
Institute of Geology of the A. Mickiewicz University ul. Maków Polnych 16, PL 61-606 Poznan, Poland

Abstract

The karst is developed on the N slope of the the Tatras in narrow structural belts of limestones and dolomites of the Middle Triassic and limestones of the Upper Jurassic - Lower Cretaceous. More than 800 caves are known in the Tatras. Among them 8 caves are longer than 5 km and 7 are deeper than 300 m. The bigest cave system Wielka Sniezna – Wielka Litworowa reaches 17.3 km of length and 814 m of denivelation. Their development and age are discussed.

Résumé

Le karst est développé dans le versant nord des Tatra dans les bandes structurales étroites de dolomites et calcaires du Trias moyen et de calcaires malmo-néocomiens. Il y a plus que 800 cavernes connues dans les Tatra. Parmi celles-ci, 8 cavités ont une longueur qui dépasse 5 km et 7 gouffres ont une profondeur qui dépasse 300 m. Le plus grand gouffre de ces montagnes est le système Wielka Sniezna – Wielka Litworowa qui mesure 17.3 km de longueur et 814 m de dénivélation. Le développement et l'âge de ce karst est discuté dans cet article.

Introduction

The Tatra Mts. represent little but the highest and northern most alpine massif in the whole Carpathian belt. They are latitudinally elongated and asymmetric with steep S and SE slopes and relatively smooth N and W slopes. The Tatras are c. 55 km long and 15 km wide with the highest peaks reaching 2655 m a. s. l. on the S side of the main crest elevated to 2637 m a. s. l. The total surface reaches 785 km^2, of which only 175 km^2 of the N slope belong to Poland, while over 3/4 of the area lie within Slovakia. The morphological asymmetry is caused by geological structure in which karst rocks occur on the N slope between sedimentary sequences, while the main ridge and S slope are built up of crystalline rocks. Thus over 50 % of the Tatra karst areas with nearly all biggest and deepest caves belong to Poland (Fig. 1). This part is thoroughly penetrated by cavers and investigated, as an unique high mountainous karst area in whole country. On the contrary, the Slovakian part, as remote and one of several very interesting karst areas in that country is much lesser penetrated and investigated. Thus this paper is based mainly on the observations in the Polish part of the mountains (Fig. 2).

Scarce information on caves, huge karst springs and dry valleys in the Tatra Mts. were published since 17th century. The first was a citation of shepherds opinions (J. P. HAIN 1681), that in Tatra is a cave (Magurska Cave? – g in Fig. 2) plenty of huge "dragon bones" (*Ursus spelaeus* bones). Precise hydrologic observations on Tatra karst were published by L. ZEJSZNER (1844). Description of 30 caves and sketch-maps of two of them in the Polish West Tatra were published by J. G.

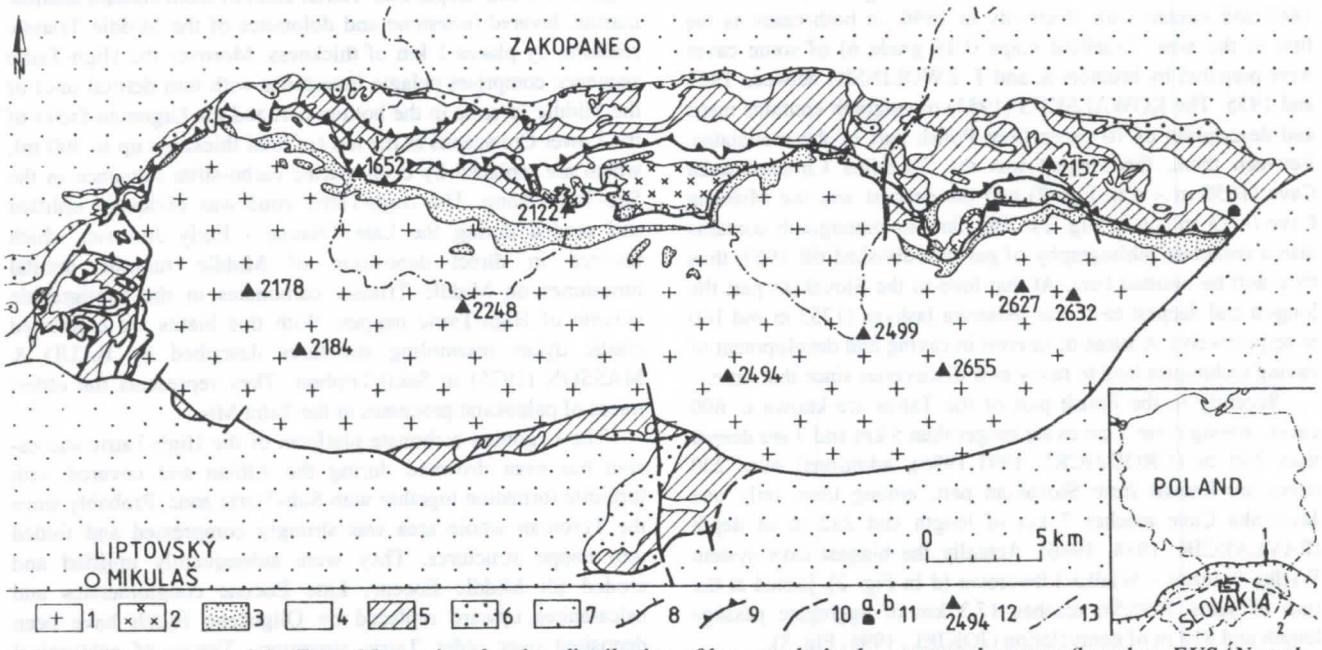

Figure 1: Sketch-map of the Tatra Mountains showing distribution of karst rocks in the structural context (based on FUSÁN et al., 1963 and MAHEL' et al., 1964): 1 - Paleozoic crystalline massif, 2 - crystalline cores of High-Tatric nappes, 3 - basal siliciclastics of High-Tatric units (Lower Triassic), 4 - carbonates (Middle Triassic - Lower Cretaceous), 5 - Mesozoic non karst deposits, 6 - Eocene basal carbonate conglomerates, 7 - Podhale flysch, 8 - overthrust of High-Tatric nappe, 9 - overthrusts of Sub-Tatric nappes,
10 - faults, 11 - Slovakian caves mentioned in the text (a - Javorinka, b - Belanska), 12 - important peaks with altitudes a. s. l. in m representing the highest points on crystalline and on carbonate rocks, 13 - state boundary. The inset shows the wider context: 1 - frontal overthrust of the External Carpathian, 2 - Pieniny Klippen Belt - the boundary of the Internal Carpathians

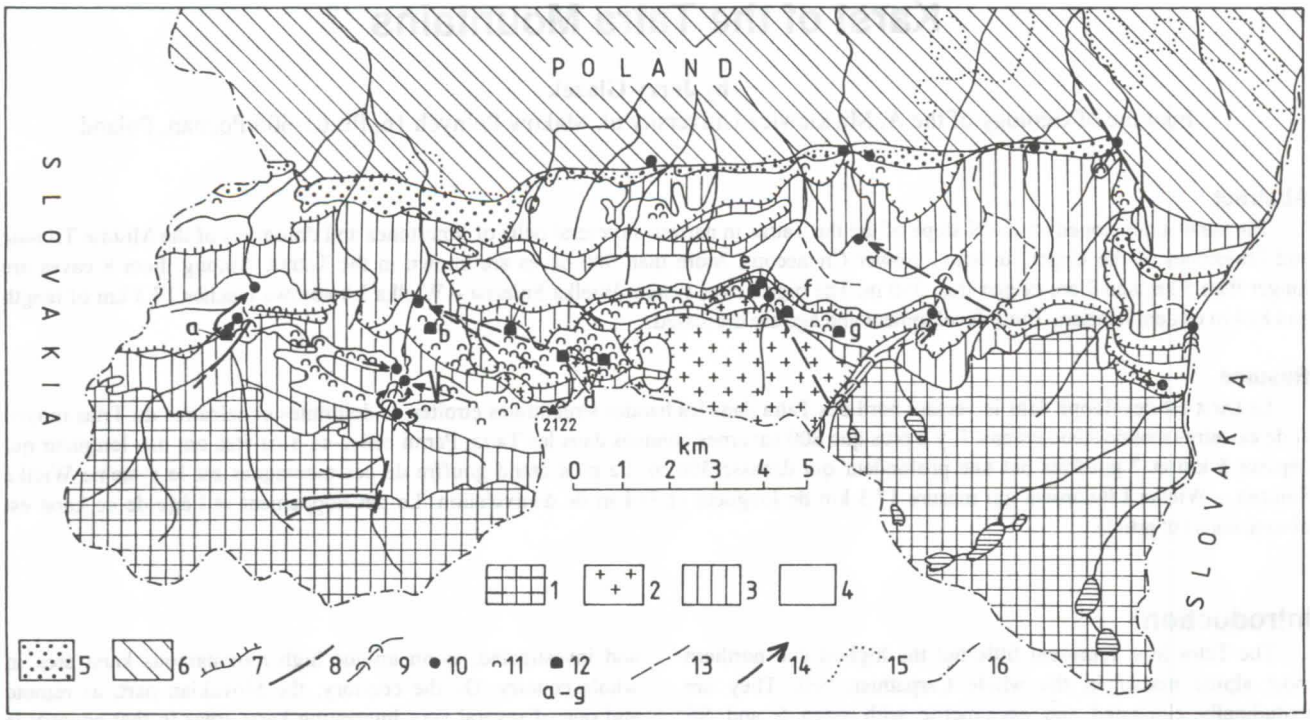

Figure 2: Karst areas in geological structure of the Polish Tatra Mountains
Rocks: Palaeozoic metamorphics and granitoids: 1 – of the Tatra crystalline core, 2 – of the overthrusted units; Mesozoic sedimentary: 3 – non karst (unsoluble or weak soluble), 4 – karst (limestones and dolomites); Tertiary sedimentary: 5 – karst (detrital carbonate), 6 – non karst (Podhale flysch). Important tectonic boundaries: 7 – overthrusts, 8 – faults. Karst features: 9 – swallets, 10 – karst springs, 11 – caves, 12 – caves mentioned in the text (a – Chocholowska Szczelina, b – Mrozna, c – Miêtusia, d – Wielka Litworowa – Wielka Sniezna, two main entrances, e – Bystrej, f – Kasprowa Niznia, g – Magurska), 13 – periodical streams, 14 – stated underground drainage conections. Boundaries of: 15 – the Tatra National Park, 16 – the states

PAWLIKOWSKI (1877). The Cave Belanska (on the eastern slope of Tatra Mts. - b in Fig. 1) plenty of speleothems was discovered in 1881 and immediately managed for tourists in 1882 and lighted with electricity in 1896, in both cases as the first in the area. Excellent maps (UIS grade 6) of some caves were prepared by brothers S. and T. ZWOLINSKI between 1923 and 1955. The KOWALSKI'S (1953) monograph contains maps and description of 70 caves from Polish part of the mountains. Between them, the longest was the Szczelina Chocholowska Cave (1650 m – a in Fig. 2) and the deepest was the Miêtusia Cave (-213 m – c in Fig. 2). This famous monograph contains also a complete bibliography of papers published till 1952, thus they will be omitted here. At that time in the Slovakian part the longest and deepest cave was Belanská Jaskyna (1752 m and 160 m respectively). A surge of interest in caving and development of caving techniques lead to many new discoveries since that time.

Recently in the Polish part of the Tatras are known c. 600 caves, among them 7 caves are longer than 5 km and 7 are deeper than 300 m (GRODZICKI, 1991-1996), additional over 200 caves are known from Slovakian part, among them only one Javorinka Cave reaches 5 km of length and 232 m of depth (PAVLARČIK, 1984, 1986). Actually the biggest cave system Wielka Sniezna – Wielka Litworowa (d in Fig. 2), joined at the turn of years 1995/96 reaches 17.3 km of aggregate passage length and 814 m of denivelation (JOKIEL, 1996; Fig. 3).

Geological setting

The karst phenomena in the Tatras occur in narrow belts of carbonate rocks directed E-W and dipping to the N. These structures represent nappe-strips (LUGEON 1903) and are complicated by transversal elevations and depressions (Fig. 1). These sedimentary rocks belong to two sequences: shallower High-Tatric and deeper Sub-Tatric. Both of them contain shallow marine, layered limestone and dolomites of the Middle Triassic reaching by places 1 km of thickness. Morover the High-Tatric sequence comprises pelagic limestones with thin detrital ones of the Middle Jurassic in the bottom part and the Urgonian facies of the Lower Cretaceous at the top (of total thickness up to 300 m), which are replaced by deep marine carbo-silite sequence in the Sub-Tatric zone. The High-Tatric zone was obliquely uplifted and eroded during the Late Triassic - Early Jurassic, which resulted in direct deposition of Middle Jurassic detrital limestones on Middle Triassic carbonates in the stratigraphic column of High-Tatric nappes. With this hiatus are connected clastic dykes resembling structures described by BAUD & MASSON (1975) in Saint-Triphon. They represents the oldest traces of paleokarst processes in the Tatra Mts.

The Urgonian carbonate platform of the High-Tatric succession has been drowned during the Albian and covered with turbidite formation together with Sub-Tatric zone. Probably since the Turonian whole area was strongly compressed and folded into nappe structures. They were subsequently uplifted and eroded till Middle Eocene. Late Eocene conglomerates and calcarenites upward replaced by Oligocene flysch have been deposited over older Tatric structures. Traces of subtropical weathering and karstification are known at the base of Eocene transgression (GLAZEK, 1989), which could be correlated with excellent contemporaneous tropical karst described in Hungary (BÁRDOSSY & KORDOS, 1989) and S Slovakia (ČINČURA, 1993).

Since the Middle Miocene the Tatras have been subject to further deformation, asymmetric uplift and erosion of *c.* 4 km

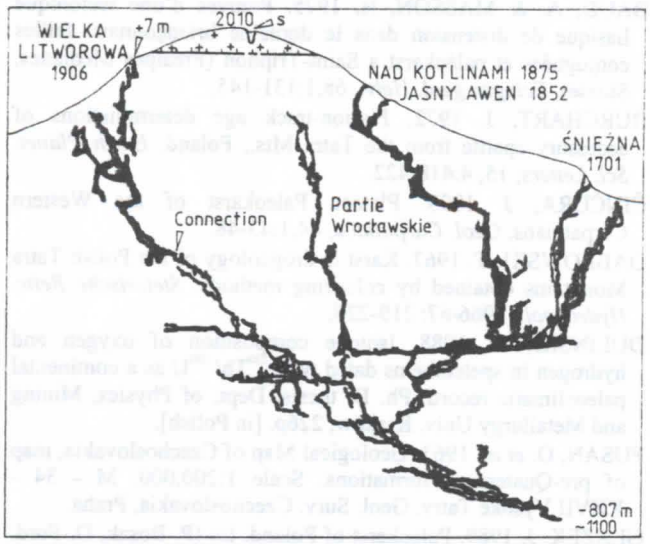

Fig. 3. East-west section of the biggest cave system in the Tatras: Wielka Sniezna – Wielka Litworowa (modified after Caving Section of Wroclaw Alpine Club, 1996). The system is developed beneath overthrusted crystalline rocks in steeply dipping limestones of High-Tatric nappe. Vertical invasion caves crosses the older horizontal cave at c. 1400 m a. s. l.
S - marked sinhole reproduced in tectonized granitoids on the top, which probably caused developement of Partie Wroclawskie. Further explorations are promising both in climbing up, as well as in diving the sump

thick sedimentary overburden (BURCHART, 1972), which finally caused the development of high mountainous karst during the Pliocene and Quaternary.

Cave systems

Among bigger karst caves multiphase cave systems dominate, some portion of them are typical vadose, the other phreatic or water-table. A storied arrangement of horizontal conduits, connected by shafts (Fig. 3) and scanty speleothems are characteristic features of Tatra caves (RUDNICKI, 1967). The spelethem deposition is restricted to the interglacial stages with climate similar to that of present day. Palaeontological materials in the cave deposits are poor and point only to the Late Pleistocene and Holocene. There are not evidences of prehistoric man inhabitance in Tatra caves. Horizontal passages of shallow phreatic or water-table character of various age have been encountered near the valley bottoms, 40-60, 80-120, 200-230 and 350-400 m above present valley bottoms. The highest horizontal passages are broader and probably Upper Miocene in age, the passages lying at relative height 200-230 m could be treated as Lower Pliocene, and those at the height 80-120 m as Late Pliocene. The cave Chocholowska Szczelina (a in Fig. 2) elevated c. 50 m exhibits speleothems of Middle Pleistocene age, about 300 ka (DULIŃSKI, 1988). While the caves Bystra and Kasprowa Nizna (cf. e and f respectively in Fig. 2) at the level of valley bottom contains vadose speleothems older than 120 ka and should be older than the Upper Pleistocene (HERCMAN, 1991).

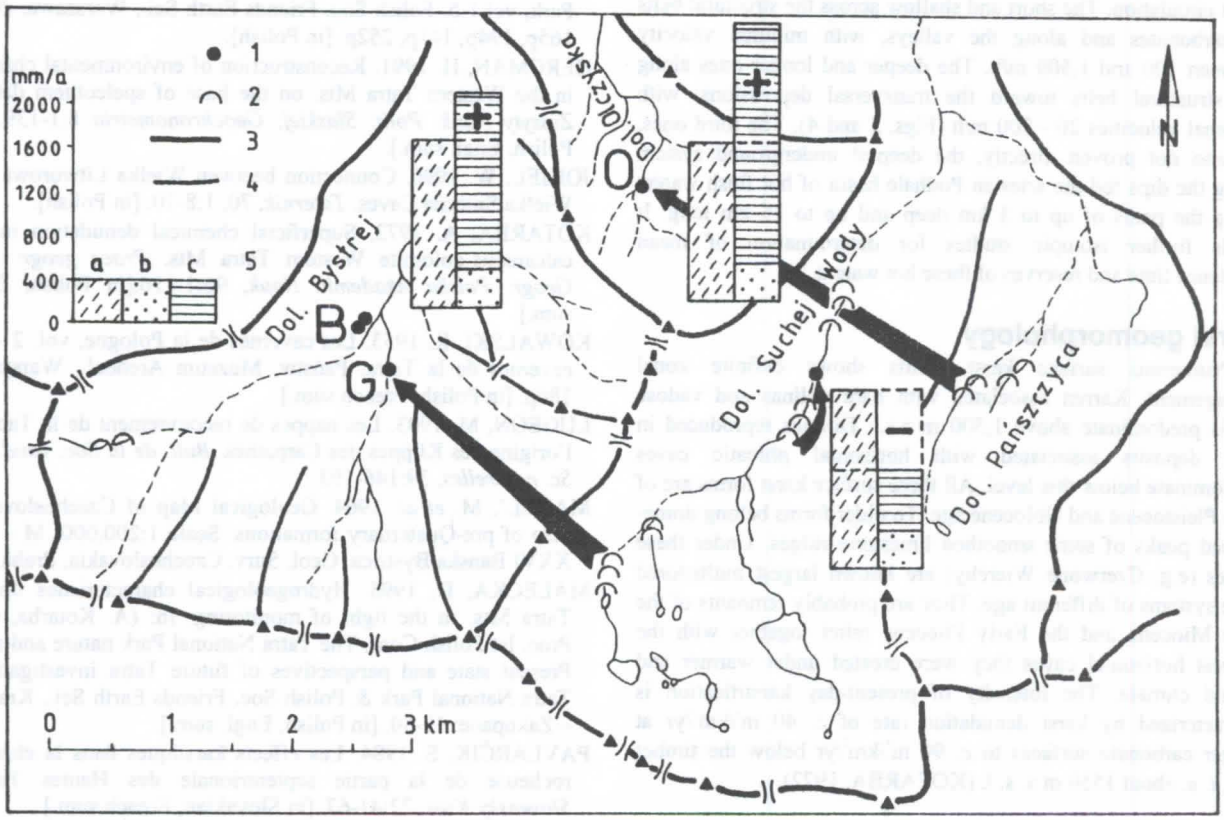

Fig. 4: Influence of karst intervalley flows on water balances of neighbouring valleys (Bystrej, Olczyska and Suchej Wody) surface catchments. Based on tracing experiments (DABROWSKI 1967) and balance calculations (MALECKA 1996)
1 – resurgences (B – Bystrej, G – Goryczkowe, O – Olczyskie), 2 – swallets, 3 – main surface watersheds, 4 – secondary watersheds, 5 – indexes of water balances: a – precipitations, b – evaporation, c – surface outflow; + and – on diagrams represent stated outflow difference from the calculated value

Thus the role of glacial overdeepening of valleys in the Tatras is negligible. Dating of cave deposits with different methods place temporal constrains of local glaciations in the Tatras. The last glaciation ceased completely speleothem deposition beetwen 23 and 10 ka. The vertical caves revealed early stages of speleogenesis and may be treated as vadose invasion caves developed by the inflow of melt waters from glaciers and snow caps covering flat ridges (fields) during deglaciation (Fig. 3), they could be treated as montainous proglacial caves (GLAZEK *et al.*, 1977).

In the Tatra Mts. only the mentioned Belanska Cave (b in Fig. 1) and Mrozna Cave (b in Fig. 2) are fully adapted for tourists, however four others in the Polish part of the mountains are partly adapted for tourists (there are marked trails, steps and chains). The Tatra Mountains on both side of state boundary are legislated as national parks, the caving there needs special permission of managments.

Karst hydrogeology

The karst areas are discharged by few springs which reach a yield of 2.0 m^3/sec. Even main streams crossing carbonate belts totally lost the water in dry years. The subsurface outflow from one valley to another one is also seen in the calculation of water balance (MALECKA, 1996) and in depth of valley incission. There due to lost of water the main, strongly glaciated Suchej Wody Valley is over 100 m less incised than lesser valleys Olczyska and Bystrej on the boundary of mountains (Fig. 4). Probably subglacial karst outflow of melt waters from hot glacier flor caused increased friction and stopped for long time glacial tongue.

Tracing of underground water paths showed three types of karst circulation. The short and shallow across the structural belts of carbonates and along the valleys, with minimal velocity between 100 and 1,500 m/h. The deeper and longer ones along the structural belts toward the transversal depressions, with minimal velocities 20 - 300 m/h (Figs. 2 and 4). The third ones, hitherto not proven directly, the deepest underground system along the dips fed the artesian Podhale basin of hot fresh waters along the paths of up to 3 km deep and up to 15 km long. It needs further isotopic studies for determination of mean residence time and reserves of these hot waters.

Karst geomorphology

Numerous surface karst forms shows definite zonal arrangement. Karren associated with bare dolinas and vadose shafts predominate above 1,500 m a.s.l. Dolinas reproduced in drift deposits associated with horizontal phreatic caves predominate below this level. All these surface karst forms are of Late Pleistocene and Holocene age. To older forms belong dome-shaped peaks of some smoothed limestone ridges. Under these ridges (e.g. Czerwone Wierchy) are known largest multistored cave systems of different age. They are probably remnants of the Late Miocene and the Early Pliocene relief together with the highest horizontal caves they were created under warmer and humid climate. The intensity of present-day karstification is characterized by karst denudation rate of *c.* 40 $m^3/km^2/yr$ at hihger carbonate surfaces to *c.* 90 $m^3/km^2/yr$ below the timber line, *i. e.* about 1550 m a. s. l. (KOTARBA, 1972).

References

BÁRDOSSY, G. & KORDOS, L. 1989. Paleokarst of Hungary. In: (P. Bosak, D. Ford, J. Glazek & I. Horaček, eds.): Paleokarst, a systematic and regional review. Elsevier & Academia, Amsterdam & Praha: 137-153.

BAUD, A. & MASSON, H. 1975. Preuves d'une tectonique liasique de distension dans le domaine briançonnais: failles conjuguées et paléokarst a Saint-Triphon (Préalpes Médianes, Suisse). *Eclogae geol. Helv.*, 68,1:131-145.

BURCHART, J. 1972. Fission-track age determinations of accessory apatite from the Tatra Mts., Poland. *Earth Planet. Sci. Letters*, 15, 4:418-422.

ČINČURA, J. 1993. Plateau Paleokarst of the Western Carpathians. *Geol. Carpathica,* 44,1:43-48.

DABROWSKI, T. 1967. Karst hydrogeology of the Polish Tatra Mountains obtained by colouring methods. *Steierische Beitr. Hydrogeol.*, 1966/67: 219-226.

DULINSKI, M. 1988. Isotope composition of oxygen and hydrogen in speleothems dated with $^{230}Th/^{234}U$ as a continental paleoclimatic record. Ph. D. thesis. Dept. of Physics, Mining and Metallurgy Univ. Kraków, 226p. [in Polish].

FUSÁN, O. *et al.* 1963. Geological Map of Czechoslovakia, map of pre-Quaternary formations. Scale 1:200,000. M - 34 - XXVII Vysoké Tatry. Geol. Surv. Czechoslovakia, Praha.

GLAZEK, J. 1989. Paleokarst of Poland. In: (P. Bosak, D. Ford, J. Glazek & I. Horaček, eds.): Paleokarst, a systematic and regional review. Elsevier & Academia, Amsterdam & Praha: 77-105.

GLAZEK, J. 1996. Karst and caves of the Polish Tatra Mountains, state of knowledge and perspectives. In: (A. Kotarba, ed.): Proc. 1st Polish Conf. The Tatra National Park. Nature and Man. Present state and perspectives of future Tatra investigations. Tatra National Park & Polish Soc. Friends Earth Sci., Kraków – Zakopane: 31-44. [in Polish, Engl. sum.].

GLAZEK, J., RUDNICKI, J. & SZYNKIEWICZ, A. 1977. Proglacial caves – a special genetic type of cave in glaciated areas. Proc. 7 Intern. Speleol. Congr. Sheffield: 215-217.

GRODZICKI, J. (ed.). 1991-1996. Caves of the Tatra National Park, vol.1-5. Polish Soc. Friends Earth Sci., Warszawa, 200p, 165p, 194p, 141p, 252p. [in Polish].

HERCMAN, H. 1991. Reconstruction of environmental changes in the Western Tatra Mts. on the base of speleothem dating. *Zeszyty Nauk. Polit. Slaskiej, Geochronometria* 8:1-139. [in Polish, Engl. sum.].

JOKIEL, W. 1996. Connection beetwen Wielka Litworowa and Wielka Sniezna Caves. *Taternik*, 70, 1:8-10. [in Polish].

KOTARBA, A. 1972. Superficial chemical denudation in the calcareous-dolomite Western Tatra Mts. *Prace geogr. Inst. Geogr. Polska Akademia Nauk*, 96:1-116.[in Polish, Engl. sum.]

KOWALSKI, K. 1953. Les cavernes de la Pologne, vol. 2 –Les cavernes de la Tatra. Pañstw. Muzeum Archeol., Warszawa, 186p. [in Polish, French sum.].

LUGEON, M. 1903. Les nappes de recouvrement de la Tatra et l'origine des Klippes des Carpathes. *Bull. de la Soc. vaud. des Sc. naturelles,* 39:146-193.

MAHEL', M. *et al.* 1964. Geological Map of Czechoslovakia, map of pre-Quaternary formations. Scale 1:200,000. M - 34 - XXVI Banska Bystrica. Geol. Surv. Czechoslovakia, Praha.

MALECKA, D. 1996. Hydrogeological characteristics on the Tatra Mts. in the light of monitoring. In: (A. Kotarba, ed.): Proc. Ist Polish Conf. The Tatra National Park nature and man. Present state and perspectives of future Tatra investigations. Tatra National Park & Polish Soc. Friends Earth Sci., Kraków – Zakopane: 19-30. [in Polish, Engl. sum.].

PAVLARČIK, S. 1984. Les effects karstiques dans la chemise rocheuse de la partie septentrionale des Hautes Tatras. *Slovensky Kras*, 22:41-67. [in Slovakian, French sum.].

PAVLARČIK, S. 1986. Underground hydrological systems of the High Tatras. *Bull. Slovak Speleol. Soc.*, 17, 1-2:48-53.

RUDNICKI, J. 1967. Genesis and age of caves of the Western Tatra Mts. *Acta Geol. Polon.*, 17, 4:521-591. [in Polish, Engl. sum.].

Karst morphology in Bazovski part of Vratsa mountain (Stara Planina, NW Bulgaria)

Konstantin Kostov
Geological Institute of Bulgarian Academy of Sciences, Acad. G.Bonchev str, Bl.24, 1113 Sofia, Bulgaria,
e-mail: kskostov@geology.acad.bg

Abstract

Vratsa mountain is situated in the West Stara Planina. The investigated karst massive takes the southeastern part of the mountain. The studied territory covers 69.7 km^2.

Zgorigrad anticline builds up the Bazovski part of Vratsa mountain and the Mid-Upper Triassic and Upper Jurassic-Lower Cretaceous carbonates are subjected to karstification. The faulting is a precondition for tectonic fracturing of high degree. The karst waters are supplied by infiltration of rains and the massive is drained entirely by the river drainage system.

The surface forms are presented by cleft, runnels and rill karren; 153 dolines of different types; 15 uvalas. The vertical caves are. prevailing among the subsurface karst forms - the most important here are Pukoya (-178m) and Yavorets (-147m).

The recent karst in Bazovski part is a result of various paleogeographical conditions during the Quaternary, accompanied by higher neotectonic activity

1. Introduction

Vratsa mountain is one of the most interesting karst massifs in Bulgaria. It is situated in West Stara Planina (Balkan) and attracts the attention with numerous karst forms and complicate orographic, lithostratigraphic and tectonic conditions on a comparatively small territory. This investigation is connected with the main morphologic characteristics of the karst from the southeastern part of the mountain, known as Bazovski part.

The studied region is clearly morphologically marked out. At northwest the Streshero part of Vratsa mountain is separated through the deep valley of Leva river. The southeastern boundary of the studied territory is the valley of Zlatitsa river. To southeast the massif is limited by the Stara Planina Iskar gorge and to northwest its boundary with the Vratsa plain is marked by the imposing cliff of Vezhdata. The noted boundaries of tectonic and erosional type enclose a territory of 69.7 km^2 (Fig. 1).

The delevelling in Bazovski part of Vratsa mountain varies from 250 m (the regional base-level of Iskar river) to 1394 m (peak of Buk). The region is named to peak of Bazova mogila (1314 m) which visually dominates over the rest of peaks.

The karst morphology and evolution of the studied area are examined by RADEV (1915), MISHEV & POPOV (1958), BENDEREV *et al.* (1979), ANGELOVA *et al.* (1995). The caves are investigated and mapped by speleoclubs "Edelweiss" and "Akademik" (Sofia) and "Veslets" (Vratsa).

2. Preconditions for karstification

Geological settings

Bazovski part of Vratsa mountain is geologically complicated - the rocks of that part are quite different by age, origin and tectonic processing. The karstification is spread over the Mid-Upper Triassic, Upper Jurassic - Lower Cretaceous carbonates on area of 55.6 km^2. The Lower Triassic clastics build up a regional impermeable horizon (Fig. 1).

The limestones in the investigated region are characterized by low contents of insoluble residue, thatswhy they are subjected to intensive karst denudation. The last one in Vratsa mountain is determined through Pulina's equation and amounts to 24 mm/1000 years - relatively great value compared to another karst areas in Bulgaria (MARCOVICZ *et al.*, 1972).

Zgorigrad anticline is the most sizable structure here. It is crossed by the Leva river valley which also marks the NW boundary of the region. The core of the anticline is constructed by Permian conglomerates, outcropped in the Leva's valley. The limbs and the crest are built up by Triassic, Jurassic and Lower Cretaceous sediments. According to TRONKOV (1965) its main strike is 120-130°. To SSW the anticline is limited by Plakalnitsa reverse-fault but to east it is cut by Kostalevo reverse-fault (Fig 1 - ①, ②).

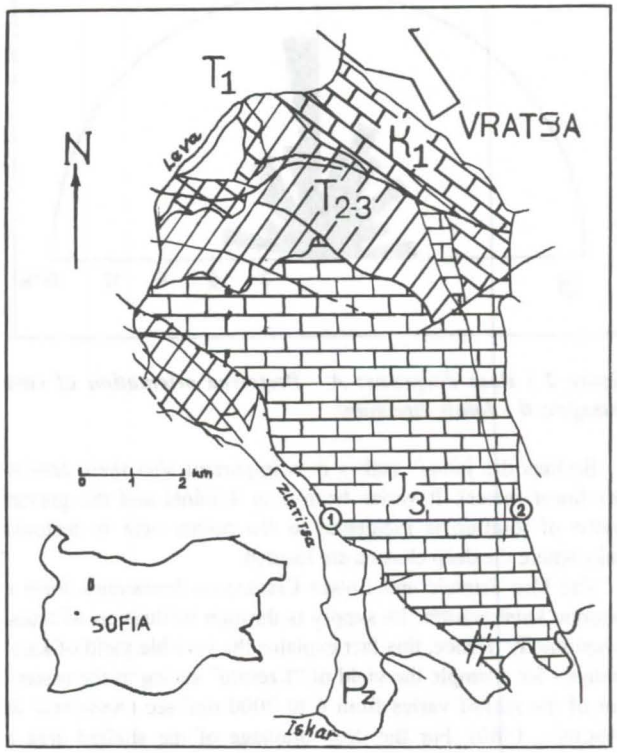

Figure 1 : Location and geological sketch of Bazovski part of Vratsa mountain: ① - Plakalnitsa reverse fault; ② - Kostalevo reverse fault.

Plakalnitsa reverse-fault is the main fault-structure in Vratsa mountain. It has a constant strike of 120° but the dip of fault-

plane varies from 42° to 50°. The vertical displacement reaches up to 2000 m at the Iskar river valley where the Paleozoic sediments lay over the Upper Triassic ones that are subjected to karstification. The strike of Kostalevo reverse-fault is 160-170° and it is clearly expressed on the surface through the "Vezhdata" cliff over 6-7 km.

These fault structures determine the high frequency of tectonic jointing. To find the connection between the orientation of karst forms and joints there were measured out the directions of the galleries of 43 caves (62 measurements). Measuring of 186 joints in 5 points of the studied area was made also. Analyzing the diagrams it is find out there is clearly expressed structural predetermination in the karst forming, i.e. there is N-S oriented maximum at the preferred directions of cave passages and it is analogous to the diaclases'configuration in Bazovski part of Vratsa mountain (Fig. 2).

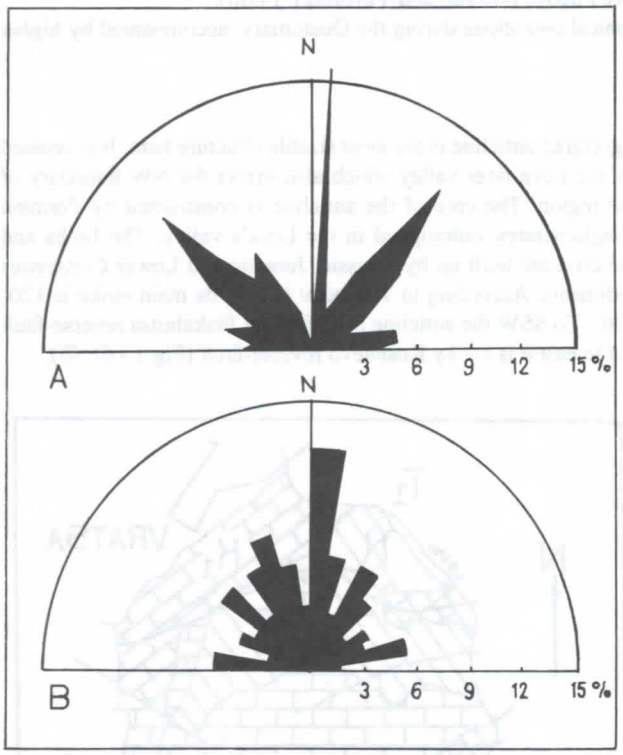

Figure 2 : Rose diagrams: A - Preferred orientation of cave passages; B - Joints directions.

Besides the joints' strikes it is important also their density (per linear meter). It varies from 4 to 9 joints and the greater degree of jointing is incidental to the points near to tectonic faults where the deep chasms are located.

The Mid-Triassic and Lower Cretaceous limestones form a common karst aquifer. Its supply is through infiltration of rains, exceptionally. Hence, this fact explains the variable yield of karst springs - for example the yield of "Ezeroto" spring in the eastern foot of the massif varies from 6 to 2000 dm^3/sec (ANTONOV & DANCHEV, 1980). For the deep drainage of the studied area a permanent water-saturated zone with complete hydraulic connection in the channel-gallery net is not formed. In the known parts of the high-situated caves and chasms subsurface streams and rivers are not established.

Geographical settings

The relief is one of the factors that act directly upon the overland flow and infiltration of surface waters, and hence the intensity of karstification. To clarify its concrete significance for Bazovski part of Vratsa mountain it is necessary to examine the orographic characteristics.

It is adapted the view that the crestal denudational plane of Vratsa mountain /at altitude of 1000-1200m in the investigated area/ is aged as Early Miocene (GALABOV, 1982, In: Geography of Bulgaria, Vol. 1). This plane has been altered by the karst processes and it is presented by residual karst heights /named "mogilas"/, divided by uvalas and dolines. The heights are defined by MISHEV & POPOV (1958) as "hums" and are examined as relict forms of tropical cone and tower karst. As far as is known in regional aspect that the "hums" are residual features in the poljes of Dinarides then their treatment as mountain morphographic unit is quite unconvincingly.

One of the basic geomorphological factors for karstification is the dip of topographical surface. Quite many authors have been worked on the relations between the spreading of karst forms and slope decline (GVOZDETSKII, 1988). For that purpose it was worked out a topoisocline model of Bazovski part of Vratsa mountain (Fig.3) The morphometrical indices of average declination of the slopes is calculated through Volkov's method as tangential function of the differences in the altitudes of the highest and lowest points in each square with known area and the distance between these points /in meters/. Map-measuring is made on topographic map scaled 1:25000 on area of 1 km^2. The density of dolines in the studied region is determined using a detailed working map of the karst forms on the same territory and scale, prepared by speleoclub "Edelweiss" - Sofia.

The most considerable average slope declines are fixed for the eastern and northern peripheral parts of the massif where the maximum of it reaches 32-40°. The areas with minimum declines are highly situated and coincide with the crest denudation plane. Comparing both two models is established that the maximum of average decline of the areas with dolines is 15-18°. The greatest depression density (18 dolines per sq.km) is fixed on area with 4.9° declination. About 70% of depressions are formed on a plane declined to 10° and this fact confirms the inverse proportion in the growth of both indices.

The average annual rainfall is 811 mm. It is interesting to find what kind of rain portions feeds the flow and therefore it is necessary to determine the evapotranspiration. Its determination is made through the Turk's equation, depending on the altitude. As initial data are used the average annual indices such as rain and temperature, obtained by the only meteorological station in the region - Vratsa. The evapotranspiration decreases proportionally to the increasing of altitude - from 507 mm (300-400 m GL - Vratsa) to 402 mm (1300-1400 m GL). Consequently, the greatest rain portions that feed the underground flow are noticed in the high areas of Bazovski part - 683 mm in the altitude range of 1300-1400 m.

Karst in the studied area is covered by thin layer of brown forest soils (in some places are missing at all), highly permeable. The flora of the region is presented mainly by herbaceous species. The higher parts are characterized by beech-trees (*Fagus sp.*) and hornbeams (*Carpinus sp.*). The enrichment of the rain-waters with CO_2 by the soils and flora is not investigated particularly for the region.

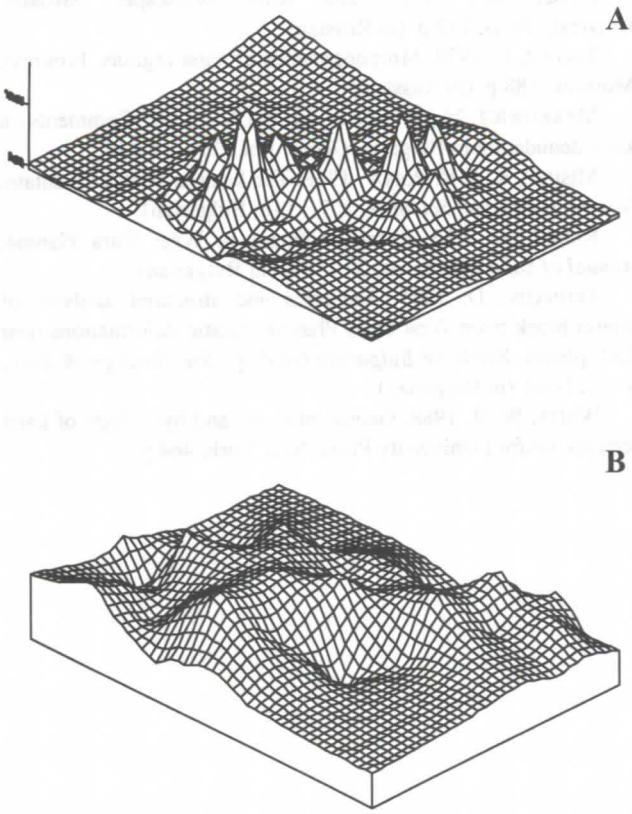

Figure 3 : Relations between dolines distribution and slope declination: A - Depression density model on the studied area from SW; B - Topoisocline model on the studied area from SW.

3. Karst landforms

Different classifications of the karst landscapes have been published based on important indications. An attempt for the karst characterization of studied territory founded on existing typology is made.

According to Quinlan (1978) /In:WHITE, 1988/ the landscapes could be defined through the dominating karst forms. In this way, the Bazovski part has some features of cockpit karst, such as high doline-area ratio and low depression density. Depending on cover the karst landscape is subsoil (covered by thin soil-herbaceous layer) and in some places - naked (denuded karst). According to the hydrographical scheme of JAKUCS (1979) the studied area is typical example for autogenous karst and after GVOZDETSKII (1988) it could be related to the mid-mountain karst.

Surface landforms

The epikarst forms on studied territory has been investigated already by RADEV (1915) whose classic work is still actual.

The Bazovski part of Vratsa mountain is distinguished for the considerable distribution by area of different karren. The cleft karren are most frequently seen and their depth varies from several centimeters to 1.5-2 m. Their dominating directions of growth are 0-20^g and 40-60^g. They form not big but difficult karren fields. There are established runnels whose depth does not exceed 0.5-0.6 m. The rills are peculiar to the steep rock slopes in the massif' periphery and to the entrances of some chasms.

The dolines are the most widespread surface karst forms in the studied area. There are 153 dolines fixed on a working map of the karst forms scaled as 1:10000 and prepared by "Edelweiss" speleoclub. The main index at the degree of surface karstification determination is the depression density - its value for the Bazovski part of Vratsa mountain is 2.75 dolines per sq. km. The relatively low density depends on the great karst area. The doline-area ratio is 0.26 and the area of individual dolines is 14.8 km^2. Their size varies from 2-3 m to 200m and they are quite morphologically divers. The soil-mantled sinkholes with slant slopes are prevailing but the collapse sinks with vertical walls are widespread also.

RADEV (1915) describes in details 15 uvalas in the studied region. Generally, it could be differentiated prolonged uvalas and funnel-shaped uvalas. Depending on the structural settings their prevailing direction of growth is N-S with maximum length to 1200-1400 m. The diameter of funnel-shaped uvalas reached up to 300 m (at depth of 150-160 m) - for example "Goliam Skravenik" in the central parts of the massif. According to the local toponymy not only in the studied area but in the whole Western Stara Planina the term "uvala" is known as "valog".

Underground landforms

There are known and mapped out about 160 caves and chasms, catalogued in Bulgarian Federation of Speleology. The small caves are prevailing. Only 21 of them have more than 50 m length and 6 caves are more than 100 m long. The longest cave in the region is Varteshkata (# 13) - 158 m. The chasms are typical for the Bazovski part. Here the most sizable are Pukoya (-178 m), Yavorets (-147 m) and Panchovi Gramadi (-102 m). The first ones are known also with their impressive pits - 140 m very steep (75-85°) passage in Pukoya and 75 m entrance pit in Yavorets.

The cave sediments are presented by gravitational and fluvial deposits and speleothems. The weathering detritus is widespread in the entrance parts of the caves. The great block breakdowns (with the size of blocks 4-5 m) are very characteristic for some caves like Varteshkata (# 13), Dedovata (-60 m) etc. The speleothems are multiple - for example in Varteshkata (# 13) there are very interesting cylindrical stalagmites up to 4.5 m high and 12-15 cm in diameter.

The mesokarst forms come in the range of 250-1250 m altitude (there are caves on the medow of Iskar river). The main base-level in Upper Pliocene and Quaternary is Iskar river and during the relatively calm tectonic periods its terraces form the Stara Planina Iskar gorge. The positive neotectonic movements determine the stages of river's incising and the forming of contemporary karst landscape in Bazovski part of Vratsa mountain. BENDEREV *et al.*(1979) and ANGELOVA *et al.*(1995) correlate the relative altitudes of caves levels and the altitude of terraces above the base-level within the boundaries of investigated area. The results obtained show that from the beginning of Early Pleistocene to the present days the Vratsa mountain has been elevated about 120-140 m. The Early Pleistocene is characterized with the most intensive karstification also.

4. Conclusion

This work examines some important aspects of karst geomorphology in a classic mountain karst region in Bulgaria. There is an optimal combination of karstification factors in Bazovski part of Vratsa mountain - such as lithological, tectonic, orographic and climatic. It should be underlined that for the accurate age determination of karst forms it is necessary to use

the methods of absolute geochronology which are principal for karst evolution reconstruction.

The neotectonic movements' indices, in some caves and chasms are very interesting about the history of recent karst and are an object of future investigation.

References

ANGELOVA, D., A. BENDEREV, G. BALTAKOV, I. ILIEVA, T. NENOV. 1995. On the karst evolution of the Stara Planina Iskar Gorge. *Rev. of the Bulg. Geol. Soc.* 56, 3: 111-124 (in Bulgarian)

ANTONOV, H. & D. DANCHEV. 1980. Underground waters in Bulgaria. Technika, Sofia, 360 p. (in Bulgarian)

BENDEREV, A., I. ZDRAVKOV, I. ILIEVA. 1979. The role of tectonic movements for karst development around Cherepish railway station. Proc. of Speleol. Conf. - Russe: 209-214 (in Bulgarian)

GEOGRAPHY OF BULGARIA, Vol. I - Physical geography. 1982. BAS, Sofia, 511 p (in Bulgarian)

GVOZDETSKII, N.A. 1988. Karst landscapes. Moskow Universty Press, 112 p. (in Russian)

JAKUCZ, L. 1979. Morphogenetics of karst regions. Progress, Moskow, 388 p. (in Russian)

MARKOWICZ, M., W. POPOV, M. PULINA. 1972. Comments on karst denudation in Bulgaria. *Geogr. Pol.*, 23: 111-139

MISHEV, K. & V. POPOV. 1958. The karst in Vratsa mountain. *Nature. Bulg.Akad.Sciences*. 1: 7-13 (in Bulgarian)

RADEV, Z. 1915. Karst landforms in West Stara Planina. *Annual of Sofia University*, X: 1-149 (in Bulgarian)

TRONKOV, D. 1965. Tectonics and structural analysis of Vratsa block from West Stara Planina. Plastic deformations near fault-planes. *Works on Bulgarian Geology. Ser. Stratigr. & Tect.*, VI: 217-251 (in Bulgarian)

WHITE, W. B. 1988. Geomorphology and hydrology of karst terrains. Oxford University Press, New York, 464 p.

Karstological Investigations in the Middle Basin of Iada Valley (Padurea Craiului Mountains, Romania)

Tudor Tamas, Matei Vremir
"Babes-Bolyai" University, Faculty of Biology-Geology, str M. Kogalniceanu, Nr. 1, R-3400, Cluj Napoca, Romania

Abstract

The Middle Basin of Iada Valley hosts some well developed and particular endokarst forms, many of which were discovered in the last years, by means of prospection or mining works. The surveys carried out in the cavities of the area, combined with altimetric measurements and observations on morphology and hydrology, revealed the presence of five well delimited karstification levels, developed on a vertical extent of 350 m.

Résumé

Le Bassin Moyen de la Vallée de Iada est une zone où les phénomènes endokarstiques sont particuliers et bien développés. Beaucoup de ces formes ont été decouvertes par prospection ou travaux miniers dans les dernières années. Les topographies effectuées, combinées avec mesures altimétriques et avec des observations morphologiques et hydrologiques, ont mis en évidence cinq niveaux de karstification bien délimités, développés sur une extension verticale de 350 m.

1. Introduction

The speleological investigations performed in the last years in the Middle Basin of Iada Valley had their result in some new discoveries of very interesting caves, studied from morphological, speleogenetic and mineralogical viewpoints (RUSU, 1988; LAURITZEN, ONAC, 1995; ONAC, 1996; ONAC, LAURITZEN, 1996; VREMIR, 1994, 1995, 1996; VREMIR, KOVACS, 1996). Some of these caves were intercepted by mining works or hydro-power tunnels (VREMIR, 1994), showing a series of voids and drainage segments whose integration in the hydrological system and even in the karst evolution of the area may be problematic.

This was the main reason for the most recent started work, the typological classification of nearly 250 caves and potholes (VREMIR, 1996), simultaneously with altimetric zoning of the most characteristic caves and radiometric analyses on speleothems (LAURITZEN, ONAC, 1995; ONAC, 1996; ONAC, LAURITZEN, 1996).

2. Geographical position

The Middle Basin of Iada Valley is situated at the Eastern limit of Padurea Craiului Mountains, the Iada being an important left side tributary to Crisul Repede river that it reaches near Bulz (Bihor county). The studied area extends on some 20 sq km, from downstream the village of Remeti to Lesu lake (fig.1b).

3. Geology

From geological standpoint, the Middle Basin of Iada Valley belongs to the Remeti Graben, one of the major tectonic features of the Padurea Craiului Mountains. The Remeti Graben consists mostly of a quasi-sedimentary series known as the *Bihor Autochtonous*. The Bihor Autochtonous consists of alternating detrital and carbonate deposits, of ages generally ranging from Upper Permian to Upper Cretaceous.

The karstifiable rocks are Middle Triassic limestones and dolomites (Anisian, Ladinian), Jurassic (Upper Sinemurian-Carixian and Upper Callovian-Tithonian) limestones and Lower Cretaceous (Neocomian-Lower Aptian) limestones (IANOVICI et al, 1976; ORASEANU, 1991). The sedimentary formations suffered evident fragmentation and folding during Laramian orogenesis (fig. 2).

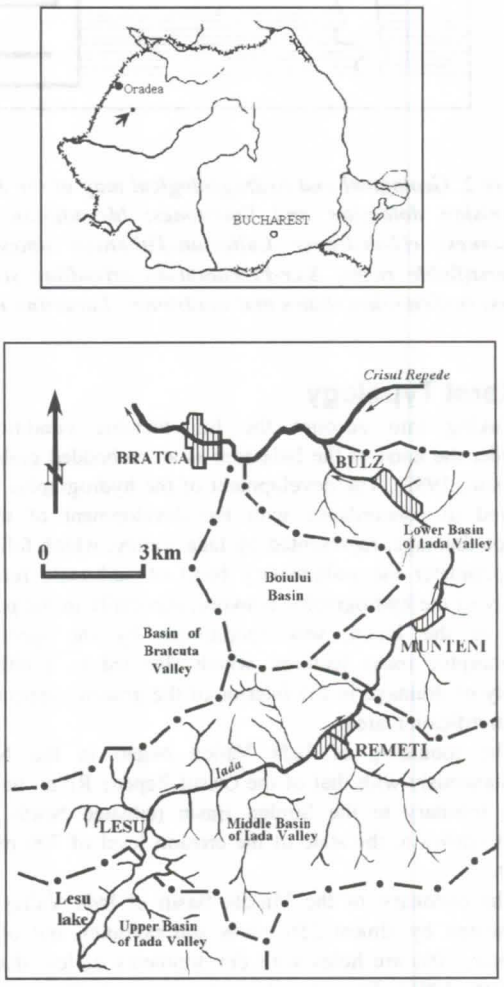

Figure 1a,b: Geographical position of the Middle Basin of Iada Valley

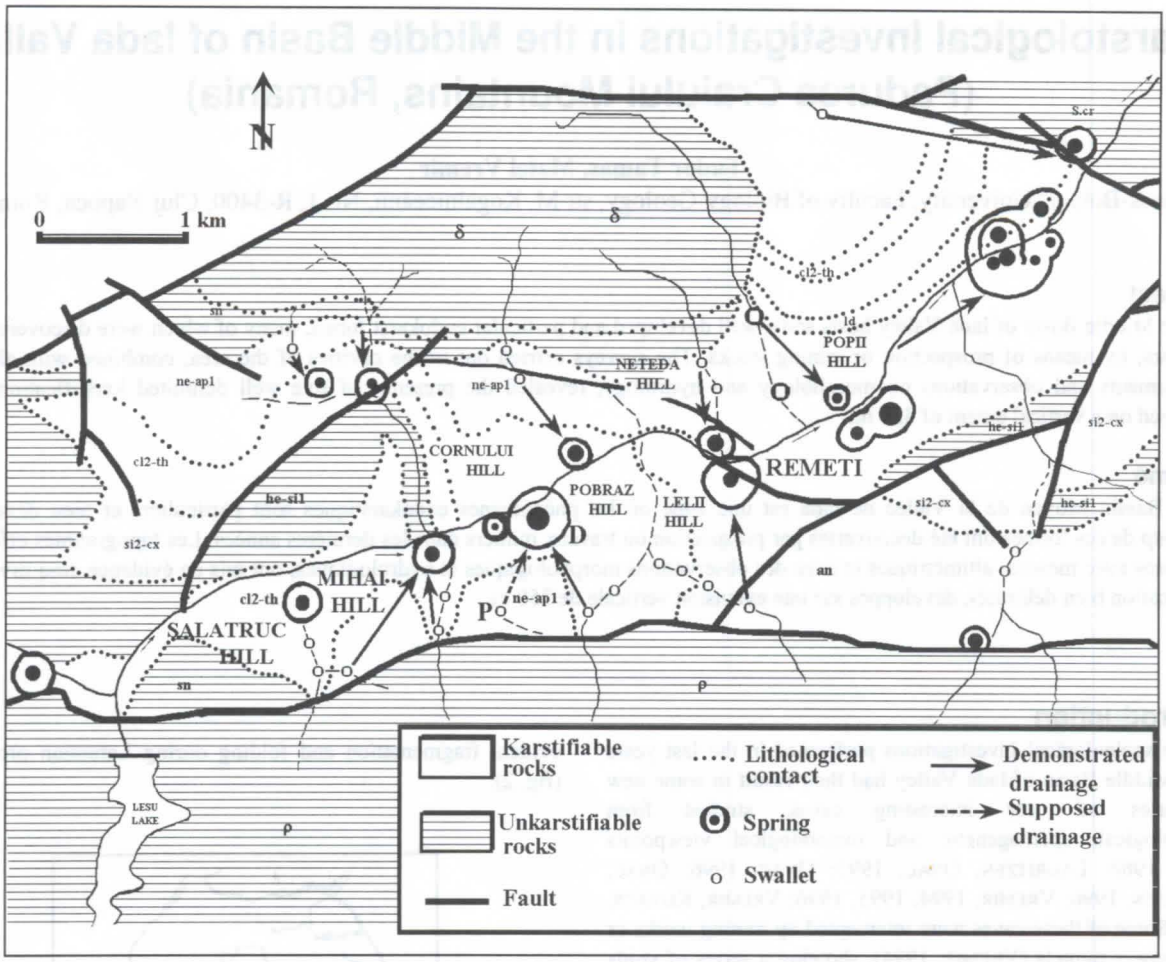

Figure 2. Geological and hydrogeological map of the Middle Basin of Iada Valley. Karstifiable rocks (Mesozoic carbonate series): an-Anisian dolomites and limestones; ld-Ladinian recifal limestones; si2-cx-Upper Sinemurian-Carixian encrinitic sandy limestones; cl2-th-Upper Callovian-Tithonian limestones; ne-ap1-Neocomian-Lower Aptian limestones with pachyodonts. Unkarstifiable rocks: S.cr-Precambrian cristalline schists; he-si1-Hettangian-Lower Sinemurian quartzitic sandstones, plastic shales; sn-Senonian shales and sandstones. Laramian magmatites: ρ-rhyolites; δ-dacites. (from ORASEANU, 1991).

4. Karst Typology

Taking into account the litho-tectonic conditions, we consider the karst of the Iada area as an embedded graben karst (BLEAHU, 1982). The development of the hydrographic network evolved in concordance with the development of the main surface drainage, represented by Iada Valley, which followed in this perimeter the sedimentary band of carbonate rocks. The density of the hydrographic network, especially in the peripheric zone of the Basin, was conditioned by the igneous and metamorphic rocks features, which also led to a rather high density of drainage in the interior of the graben, respectively in the karstification area.

The moulding of Iada Valley began in the Neogene, simultaneously with that of the Crisul Repede River, the former being tributary to the Simleu Basin (situated North of Iada Valley) down to the state of the erosion level of 700 m (RUSU, 1988).

The endokarst of the Middle Basin of Iada Valley area is represented by almost 250 caves and potholes, out of which, however, 70% are holes with developments of less than 50 m (VREMIR, 1996). From typological viewpoint (COCEAN, 1990), these are mainly subcutaneous caves or results of the drainage of the hill-slopes. The potholes represent only 9,4% of the total systems (including caves with pitch-type entrances). This fact may well be attributed to the small extent of plain, plateau-like zones. The active caves represent only 13% of the systems, but the total length of their afferent passages exceeds 56% of the totally known length.

We consider this situation typical for the graben karst, in which overlapping of the karstification levels is obvious, the succession taking place in a long period of time, simultaneously with filling processes of the fossil caves.

5. Karstification levels

We divided the Middle Basin of Iada Valley in three areas, dominated by specific litho-tectonic conditioned characters:

A. Lesului Valley Subbasin-the karstifiable rocks appear in patches, interrupted by a series of faults, with less possibilities of tracing distinct levels;

B. The middle area of the Remeti Graben-between Lesu dam and the village of Remeti. This part boasts the most typical phenomena of a very clear overlapping of the caves, exhibiting the most varied karst forms. It also has the highest density of cavities/sq km in Padurea Craiului Mountains (RUSU, 1988).

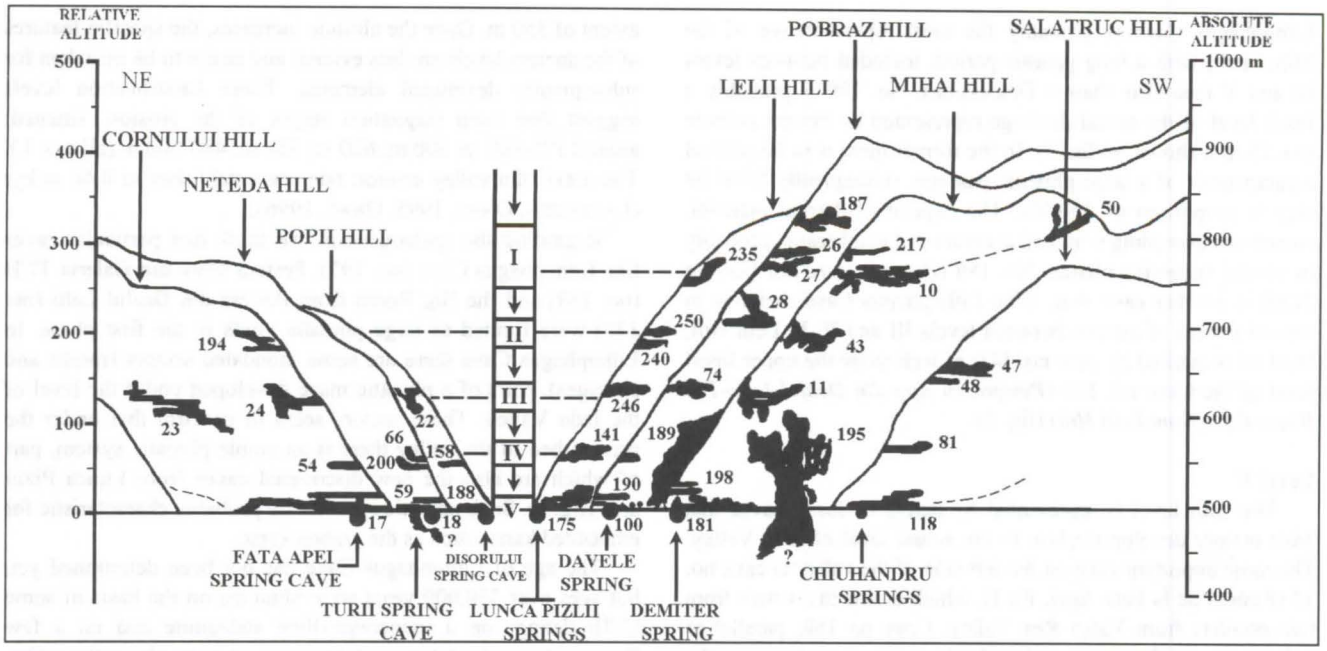

Figure 3. Perspective cross-section in the Middle Basin of Iada Valley, showing the caves and the karstification levels.

C. The subbasin of the Bisericii Valley and the perimeter downstream the village of Remeti shows the same situation as in the Lesului Valley area, but with less developed karst forms.

Most of our work was focused on the median zone of the Remeti Graben (figure 2), the area between Salatruc Hill to the West, downstream to the village of Remeti, on a 5 km long segment of Iada Valley.

We noticed the existence of 5 different karstification levels (fig. 3), developed within a vertical extent of 350 m. On both sides of the valley, at particular heights, one might observe segments of insurgent or resurgent caves, mostly opened and some partially destroyed by erosion. The filling courses being very strong, only parts of the old systems are known by intercepted segments.

Level I

The first karstification level and the eldest yet known may be followed on both hillsides of Iada Valley, in a zone situated among 250 and 300 m relative altitude (750-800 m a.s.l.). Resurgent-type (no. 26, 27, 235/3720[1]) and insurgent type caves (no. 50, 28) are characteristic for this level, as well as the segments of a cave with lateral digression (no. 10 and 217) (fig.3). The most interesting cave of this level is Pestera cu Cristale din Dealul Mihai (no 10, *Crystal Cave of Mihai Hill*), multi-levelled and with dendritic development.

On Lelii Hill, at 750 m a.s.l. and on Pobraz Hill at 770 m a.s.l. we discovered some natural arches that attest the past existence of some very impressive passages developed on the line of the initial drainages, oriented perpendicular to the main course of Iada valley.

Level II

The second level develops among heights of 680 and 700 m a.s.l.and it can be followed on both sides of the Iada Valley. On the Cornului Hill (left side) there is cave no. 194 (fig.3) (*Pestera din Mina Cornului-The Cave of Cornului Mine*), which now drains the water collected in some small depressions above the area; the fossil level of the cave has the character of a phreatic maze which in a later phase had become vadose, with great flowrate variations (fig. 3).

Some characteristic caves of this level can be found on the right slope of the valley: pothole no. 43 (Mihai Hill), 25 (Pobraz Hill), caves no. 240 and 250 (Lelii Hill) (fig. 3). All these caves developed around 700 m a. s. l.

Level III

Level III is well represented on both sides of Iada Valley, at an approximate altitude of 620 m a.s.l. In the Cornului Hill, the most important segment is cave no. 23 (*Pestera lui Rotarides, Rotarides' Cave*), a dendritic multi-level lateral digression in which vadose and phreatic phases alternate; the cave has at -50 a subfossil level that probably belongs to level IV. At the same height of about 620 m a.s.l.one can find pothole no. 24 (also on Cornului Hill) and pothole no. 22 on Popii Hill (fig. 3).

Level III is well marked on the right side of the valley by the pothole no. 11 on Mihai Hill (Iadul Alb-*The White Hell*, a two levelled cave with a pitch-type entrance) and cave no. 74 on Pobraz Hill (fig. 3).

Level IV

The fourth level develops around 550-570 m a.s.l.(50-70 m above the valley). At this level there are the resurgent caves no. 54 (Cornului Hill), no. 66 and 200 (Neteda Hill) and no. 158 on Popii Hill, all located on the left side of Iada Valley (fig. 3). The fourth level is better represented on the right side: cave no. 81 on Salatruc Hill, no. 195 (Lithophagus Cave) on Mihai Hill, and no 190 (Pestera cu Cristale din Galeria TCH-*Crystal Cave from the TCH Gallery*) and no. 189 (Pestera Mare din Galeria TCH-*The Big Cave from TCH Gallery*) on Pobraz Hill (see figure 3).

[1] Cave numbers are taken from the National Caves Inventory (GORAN, 1982), completed with later discoveries.

Lithophagus Cave is probably the most representative of the Mihai Hill, with a long genesis period, included between levels III and V (see also chapter Discussion). No. 190 is probably a fossil level of the actual drainage represented by Pobraz pothole (no. 25, not shown on fig. 3). In the former there is to be noticed a paragenesis of a large phreatic passage, subsequently filled by clay in proportion of 80-90%. The deposit of detrital material, sometimes exceeding 6 m, had accumulated epiphreatic, probably in several succesive phases. No. 189 (*Pestera Mare din Galeria TCH*) is another cave that, alike Lithophagus Cave, belongs to several phases of genesis between levels III and V. In Lelii Hill, level IV is marked by cave no. 141, as well as by the upper fossil level of the Cave no. 175 (*Pestera cu Apa din Dealul Lelii-The Water Cave from Lelii Hill*) (fig. 3).

Level V

The fifth level is represented by active or fossil caves that have mainly developed close to the actual level of Iada Valley. The most important cave on the left side of the valley is cave no. 17 (Pestera de la Fata Apei, fig.3), which drains the waters from two swallets from Valea Rea Valley. Cave no 180, parallel to Iada Valley, is also active and probably drains some losses in the riverbed.

Another active cave is no. 21 (*Pestera cu Apa de la Remeti-Water Cave from Remeti*), which communicates with Turii Spring Cave (no. 18, fig. 3). This is a complex maze that developed mainly phreatic, explored on over 750 m of partially inundated passages (GYURKA, 1990). The system drains some losses of Disorului Valley and of Iada Valley. In the southern part of this system, a descendent passage leads to a large, unexplored phreatic void, situated under the base level of Iada Valley. On Popii Hill, level V is represented by cave no. 188.

Like in the case of level IV, the right side of Iada Valley shows more specific elements, exhibited by the active caves from Salatruc Hill (no. 118), Mihai Hill (no. 181 and 195), Pobraz Hill (no. 100 and 189) and Lelii Hill (no. 175) (fig. 3).

6. Tracer tests

Most of the drainages in the Middle Basin of Iada Valley were studied by RUSU (1988) and ORASEANU (1991). It is worth mentioning the presence of some permanent losses in the Iada Valley riverbed, downstream of cave no. 18 (Turii Cave). They drain a large amount of water (average flowrate of 100-200 l/s) to the Toplet Spring, situated 600 m downstream and 15 m below, in 220 hours (ORASEANU, 1991). The flowrates at the resurgence remain almost unchanged even in prolonged dry periods, when the average flowrate of Iada Valley substantially decreases.

In November 1996, we tried a tracer test with 800 g of fluoresceine in the main cave stream of Pobraz pothole (no. 25/3720; marked "P" in figure 2). We suspected its communication with Davele karst spring(fig. 3; marked "D" in figure 2), with an average flowrate 20 l/s. The spring is situated at 700 m straight line distance and 235 m elevation range from the entrance of the pothole. The average flowrate of the main stream of Pobraz pothole was of 3 l/s (normal). However, the tracer didn't reappear in the next four days neither at Davele spring, nor at the other springs nearby (see fig. 2) and wasn't reported after.
This was the second tracer attempt in Pobraz pothole. The first one, made in october 1975, had the same result.

7. Conclusions

In the Middle Basin of Iada Valley we determined 5 different karstification levels (fig. 3), generally developed within a vertical extent of 350 m. Once the altitude increases, the specific features of the ancient levels are less evident and easier to be mistaken for subsequently developed elements. These karstification levels suggest five main stagnation stages of the erosion, situated: around 770-800 m; 700 m; 620 m; 550 m; 480-500 m (all a. s. l.). The maximum valley erosion rate was established at 0,46 m/kyr (LAURITZEN, ONAC, 1995; ONAC, 1996).

Regarding the speleogenesis, we think that particular caves like Lithophagus Cave (no. 195), Pestera Mare din Galeria TCH (no. 189) and the Big Room from Pestera din Dealul Lelii (no. 175) were formed as large phreatic voids in the first phase. In Lithophagus Cave there are some inundated sectors (rooms and passages), parts of a phreatic maze developed under the level of the Iada Valley. These sectors seem to confirm that under the present bed of the valley there is an ample phreatic system, part of which are also the new discovered caves from Lunca Pizlii area (fig. 3). Such phreatic systems are probably characteristic for embedded karsts such as the graben karst.

The age of Lithophagus Cave has not been determined yet, but ages over 350,000 years were obtained on the basis of some U-Th datings on a monocrystalline stalagmite and on a few flowstone samples taken from the cave, at 62 m above the valley (ONAC & LAURITZEN, *in press*). These ages suggest that the fossilization phase at that level has started in the Lower Riss. The proper age of the Lithophagus cave might descend to Lower Pleistocene.

References

BLEAHU, M. 1982. Relieful carstic. Ed. Albatros, Bucuresti, 295 p.

COCEAN, P. 1990. Tipuri genetice de pesteri si avene din carstul Muntilor Apuseni. *Studia Univ. "Babeº-Bolyai", Geogr., Cluj-Napoca*. 35: 19-29.

GORAN, C. 1982. Catalogul sistematic al pesterilor din Romania, Ed. CNEFS, Bucuresti, 496p.

GYURKA, Z. 1990. Noi galerii postsifon in Valea Iadului. *Speotelex*, VIII, 6 (18): 6.

IANOVICI, V., BORCOS, M., BLEAHU, M., PATRULIUS, D., LUPU, M., DIMITRESCU, L., SAVU, H. 1976. Geologia Muntilor Apuseni. Ed. Acad. R. S. R., Bucuresti, 631p.

LAURITZEN, S.E., ONAC, B. P. 1995. Uranium series dating of some speleothems fom Romania. *Theor. Appl. Karst.*, 8: 25-36.

ONAC, B. P. 1996. Mineralogy of speleothems from caves in the Padurea Craiului Mountains and their palaeoclimatic significance. *Abstract, Ph. D. Thesis, Babes-Bolyai University,* Cluj-Napoca.

ONAC, B. P., LAURITZEN, S. E. 1996. The climate of the last 150,000 years recorded in speleothems: preliminary results from NW Romania *Theor. Appl. Karst.*, 9 (*in press*).

ORASEANU, I. (1991). Hydrogeological map of the Padurea Craiului Mountains. *Theor. Appl. Karst.*, 4: 97-127.

RUSU, T. (1988). Carstul din Muntii Padurea Craiului. Ed. Dacia, Cluj-Napoca, 254 p.

VREMIR, M. 1994. Pesteri descoperite prin lucrari industriale in Bazinul mijlociu al Vaii Iadei-Muntii Padurea Craiului. *Ardealul Speologic;* 4: 30-57.

VREMIR, M. 1995. Pestera Lithophagus din Bazinul Mijlociu al Vaii Iadei. *Cercetari Speologice*. 3: 34-37.

VREMIR, M. 1996. Inventar speologic in Bazinul Mijlociu al Vaii Iadei. *Cercetari Speologice* 4: 23-27.

VREMIR, M., KOVACS, ZS. 1996. Pestera-aven din Dealul Pobraz.. *Cercetari Speologice* 4: 38-43.

Macroscopic paleokarstic features in upper cretaceous limestones of the Adriatic-Dinaric carbonate Platform (SW Slovenia)

Bojan Otoničar
Karst Research Institute ZRC SAZU, Titov trg 2, 6230 Postojna, Slovenia

Abstract

The investigated area of SW Slovenia (Matarsko Podolje) in a paleogeographical sense belongs to the Adriatic-Dinaric carbonate platform. The lower boundary of the youngest (terminal) megasequence of the platform is represented by regional disconformity that was caused by Late Cretaceous and Early Paleogene emersion of the carbonate platform. We can find evidence for emersion in surface and subsurface paleokarstic phenomena. For both paleokarstic types dissolutional morphological features, either covered or infilled by different sediments, paleosols and cements (speleothems), are characteristic. Paleokarst surface is irregular or undulated and could penetrate into underlying limestones through subcutaneous dissolutional pits and pipes. Subsurface paleokarst features are marked by different porosity types (vuggy, channel and cavern porosity). There is obvious lateral variability in development of the surface and subsurface paleokarstic features. Facies variabilities are also found in limestones below and above disconformity.

Figure 1. Geographical position of the investigated area

1. Introduction

Several workers recognised evidence for subaerial exposure of the Upper Cretaceous carbonates of the SW Slovenia (PLENIČAR et al., 1973; HAMRLA, 1986; DELVALLE & BUSER, 1988/89; DROBNE et al., 1987; KNEZ & PAVLOVEC, 1990; ŠRIBAR, 1995; JURKOVŠEK et al., 1996) and of the neighbouring areas (CUCCHI et al., 1984; CUCCHI & PUGLIESE, 1984; CUCCHI et al., 1987; RADRIZZANI et al., 1987; GUŠIĆ & JELASKA, 1990; GABRIČ et al., 1995) but these articles generally deal with chronostratigraphic gaps with brief descriptions of the paleokarst features only.

The purpose of this paper is to document the nature of the surface and subsurface paleokarst features of the Upper Cretaceous carbonates that crop out along Matarsko Podolje area in SW Slovenia (Fig. 1). These data could serve as a basis for further investigations on Upper Cretaceous and Lower Paleogene paleokarst phenomena of this and neighbouring territories. In recent years, numerous studies have focused on descriptions, classifications and interpretations of paleokarstic features of ancient carbonate platforms (JAMES & CHOQUETTE, 1988a; FRITZ et al., 1993). Similar phenomena are recently present on subaerially exposed parts of still active carbonate platforms (MYLROIE & CAREW, 1995) or below them in geologic record (JONES, 1992).

2. Stratigraphic framework

Detailed reconstruction of stratigraphic evolution of the Adriatic-Dinaric (A/D) carbonate platform (sensu GUŠIĆ & JELASKA, 1993) is beyond the scope of this report. The reader has to refer to above mentioned articles.

In a paleogeographical sense the investigated area belongs to the northern part of the A/D carbonate platform. The platform was active throughout most part of the Mesozoic and Early Paleogene. Almost all of its active life time it functioned like an isolated carbonate platform with sedimentation of the pure shallow water carbonates. Temporary interruptions by relative sea level rise produced pelagic or pelagic influenced environments. On the other hand episodes of subaerial exposure caused formation of paleosol and paleokarst features.

The depositional history of the Upper Cretaceous carbonates of the investigated area has been studied intensively for the last few years (ŠRIBAR, 1995; JURKOVŠEK et al., 1996) and it is comparable with other areas of the A/D carbonate platform (CUCCHI et al. 1987; GUŠIĆ & JELASKA, 1990). Succession was lithostratigraphically divided into several formations. Paleokarst features related to described regional disconformity are found in carbonates of rather different ages and lithology. These differences are significant on the relatively short distances. The overlying rocks are also lithologically and chronostratigraphically varied. In Matarsko Podolje area the paleokarst features are developed in Upper Coniacian limestones, but some tens km towards north the youngest rocks below the disconformity are Upper Santonian limestones. In some parts carbonates below the disconformity belong to the Upper Campanian. On the most distal northern part of the A/D carbonate platform continuous sedimentation was followed by Upper Maastrichtian hemipelagic limestone instead of subaerial exposure (ŠRIBAR, 1995). On the whole territory of the SW Slovenia shallow water carbonate sedimentation was renewed in the Middle Maastrichtian except on the NE edge of the platform and on the most southern part of the SW Slovenia (ŠRIBAR,

1995). In some, usually more southern parts of the A/D carbonate platform, we can find even Eocene limestones above this paleokarst surface. In general there is a recognisable trend of increasing of the chronostratigraphic gap from NE towards SW.

3. Paleokarst features and related sediments

Surface as well as subsurface paleokarst occur on the investigated area. Both types are marked by characteristic solution morphology and are covered or filled by different sediments, paleosols and/or cements (speleothems).

Paleokarst surface and paleosols

The term paleokarst surface represents solution that took place at the atmosphere-rock (or soil-rock) interface in surficial paleokarsts (WRIGHT, 1982). Although outcrops and geologic profiles are very limited on the investigated area it is quite easy to find paleokarstic interface in the field. Usually, there is a very obvious colour difference between the limestone below the paleokarst surface (white or light grey limestone frequently with rudists) and the limestone above it (dark grey or mottled limestone).

An irregular or undulate topography (Fig. 2) of the paleokarst surface is covered by carbonates of restricted marine or palustrine / lacustrine environments (motteled limestone, black & white pebble conglomerates), paleosol breccias (regoliths) and in some places with lenses or pockets of the "bauxitic" material. Somewhere, it is difficult to say without stratigraphic control if distinct paleokarst surface (Fig. 2) belongs to described paleokarst or it is one of better developed exposure surfaces of the overlying formations. In this case, there is no prominent facies contrast between limestones below and above paleokarst surface.

Subcutaneous dissolution pipes and pits are commonly associated with paleokarst surface (Fig. 2). Up to three meter deep and one meter wide dissolution pits are filled by few generations of breccia. Average maximum diameter is about 5 cm but they could be as big as 25 cm. These clasts are slightly rounded and are made of pedogenetically altered parent biomicritic wackestone. They "float" in tan marl, which somewhere exhibits vague lamination. Similar breccia is developed also on slightly undulated surface.

In some places paleokarst surface is expressed by complex interface between two very different lithofacies types. Because of the contrasting colours of these two lithofacies (white versus black), high irregularity of the interface and/or pedogenically altered parent limestones this contact could be expressed by mottled zone. Limestones below this zone are practically braided by dissolution pipes. Up to few dm wide pipes dipped several meters below paleokarst surface. In some places it is difficult to differentiate among subcutaneous disolution pipes, subsurface pit caves and spongework branches of a larger horizontal phreatic caves.

All voids and pits had been filled by sediments of different sources. The most characteristic type is matrix-supported chaotic breccia (sensu KERANS, 1993) that includes clasts of the host limestone (usually biomicritic wackestone), reworked "bauxitic" deposits and pedogenically altered host limestones (blackening, root casts). Some clasts are partly coated by pedogenic laminated crust (caliche). Clast size is up to 10 cm and they could be angular to rounded. Matrix is "bauxitic", usually with high carbonate content (micrite or microsparite) and exhibits pedogenic features. In the matrix we can observe laminated rhizolitic crusts, alveolar structure and different kinds of peloids (faecal pellets, "bauxitic / ferruginous" ooliths, calcrete and ferruginous nodules or rinds around clasts...).

Fossils (foraminifers, big gastropods) and particularly Microcodium fragments are very characteristic components in

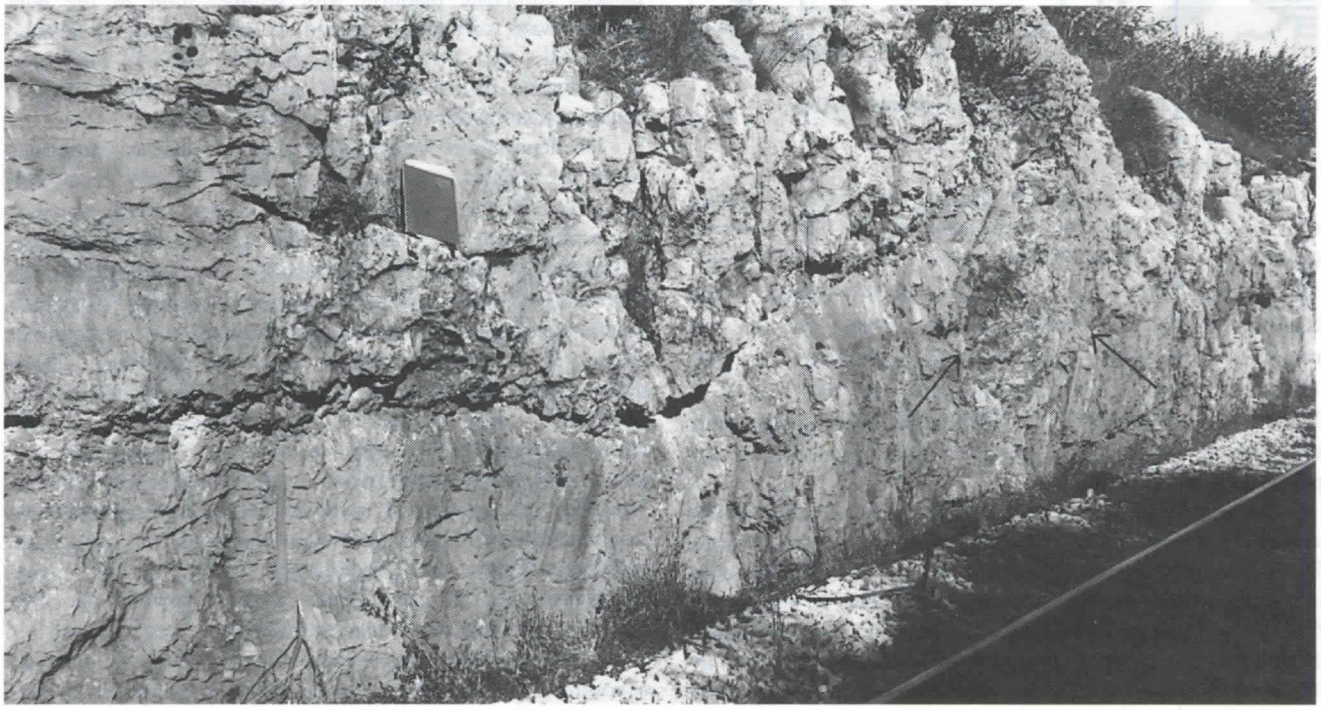

Figure 2 : Undulated paleokarst surface with dissolution pit (arrows) covered by carbonate breccia with pedogenically altered clasts. Notebook is 33 cm high.

the matrix. Pyrite framboids, often oxidised, are frequent in the matrix, clasts and host rocks. Pyrite in the soil is a characteristic product of marine hydromorphism that can occurs during initial phase of marine flooding of the exposure surface (WRIGHT, 1994). Smaler pipes are frequently infilled by sediment similar to the above described breccia matrix.

Often, it is difficult to describe infillings of the pipes and larger horizontal caves separately, because also subsurface paleokarst voids had been influenced by sediment supply from the surface via pipes and other interconnected voids (dissolutionally enlarged fenestral pores, root moulds and other pores).

Subsurface paleokarst

Subsurface paleokarst is expressed by larger phreatic horizontal caves (up to few meter high and up to few tens of meter wide / long) and smaller voids mentioned above. In some places infilled mouldic and vuggy porosity was found as well.

The shape of the caves is highly irregular and in some places they branch in smaller voids that could also be arranged in horizons. It is possible that these smaller dissolutionally enlarged voids acted as primary paths for fluid flow through carbonates, as they had already existed before major subaerial exposure like sedimentary or pedogenic voids. Only sporadic we can find regular joints. Each void is completely infilled by different sediments and cements or speleothems (Fig. 3). Sedimentation or precipitation was disrupted by periods of erosion and/or dissolution.

A variety of breccia types are common in this paleokarst. According to breccia classification of KERANS (1993) we can find all four basic breccia types. Fracture and mosaic breccias are found in some places near or on the cave wall and it seems that they have gradational contacts with the host limestone. Somewhere, fracture breccias are not in visible contact with any void. Clasts in these breccias are very angular up to 20 cm in diameter. They are composed of host rock lithology. Matrix in mosaic breccias includes red highly carbonate micritic sediments. Fracture breccias are infilled by white calcitic cement and reddish/tan laminated carbonate sediment. Matrix could exhibits geopetal fabric. Clast-supported chaotic breccias include clasts of the wall rock material and clasts of the resedimented void filling sediments. Matrix is similar to below described sediments.

Finer-grained sediments alternate with breccias and speleothems or cements. They are usually laminated. Particularly significant are red laminated micrites that alternate with thin crusts of calcitic crystals. Micritic red limestones frequently contain crystal debris that came from the disintegrated crystal rafts and other speleothems or cements. Sporadically "bauxitic / ferruginous" ooliths and clasts of the parent rock can "float" in this sediment.

Another significant finer-grained deposit exhibits very regular cyclic sedimentation. Each of the lower coarser grain laminae (2 cm thick) that exhibits gradation is covered by few very thinly-laminated and very fine-grained laminae (up to ten approximately 0,2 mm thick laminas in each cycle). Deposits of fine grained sediments on steep slopes and local slumps (in dm scale) are frequent phenomena as well.

Next significant deposits are coarse, up to 8 cm long pillar white calcite crystals often with pyramidal termination. They have the same thickness from all side of the cavities. This type of crystals was found in all profiles, usually few meter below the paleokarst surface, but they could be also truncated by it. These deposits alternate with red sediments described above. The empty space left after precipitation of coarse crystals is sometimes filled by red/tan "bauxitic" and/or black probably pedogenic sediments (fig. 3).

Smaller dissolution enlarged and mouldic pores are filled by similar deposits as larger cavities but not in such heterogeneity.

Parent biomicritic limestone is frequently reddish stained and recrystallized. Especially at the contact with infilled voids it could exhibits microsparitic belt.

Figure 3 : Smaller, probably phreatic channel filled by deposits of different composition, source and origin. Longer axis of the picture is 20 cm long.

4. Conclusions

According to characteristic paleokarst features and infilling deposits surface and subsurface paleokarst in Upper Cretaceous limestones of the SW Slovenia have been divided for the first time.

The most obvious characteristic of paleokarst features and related cover and void-filling deposits is their tremendous variety. Especially vadose voids and pits are usually infilled by "bauxitic" deposits exhibit different pedogenic features. Surface is usually covered by sediments that are typical for restricted shallow marine / lacustrine (dark grey to black with sparse ostracods, charophytes and gastropods) and palustrine environments (brownish pedogenically reworked carbonate clasts in marl, black & white conglomerates and mottled limestones).

According to morphological characteristics, horizontal character and infilling content we can say that development of larger caves was influenced by fresh or brackish water lenses. Caves were later modified and infilled under different conditions.

From this data, by previous investigations and data from other parts of the A/D carbonate platform we can conclude that described disconformity marks important change in depositional environments and it has a regional distribution. "Bauxitic" material is one of the main evidences for long duration of the subaerial exposure under warm humid climate. The minimum duration of exposure for development of oxisols that can be considered as present-day equivalents of bauxites is in the order of 10^6 years (D'ARGENIO & MINDSZENTY, 1995). We can also find out that disconformity is not synchronous everywhere on the platform and it has not lasted in an equally long time span. We can classify it like interregional paleokarst (sensu JAMES & CHOQUETTE, 1988b) with local tectonical influence that was caused by regional tectonics. The formation of the disconformity could be explained by forebulge uplift that it is associated with an early stage of the foreland basin development.

5. References

CUCCHI, F. & PUGLIESE, N. 1984. Fenomeni paleocasici al passaggio Cretacico - Terziario nel Carso Triestino. Studi Trentini di Scienze Naturali. 61: 93 - 100.

CUCCHI, F.; FORTI, F. & FORTI, P. 1984. I paleodepositi di riempimento della "Grotta dell'ultimo Dinosouro" presso Trieste. Atti a Mem. Comm. Grotte "E. Boegan", 23 p.

CUCCHI, F.; RADRIZZANI, C. P. & PUGLIESE, N. 1987. The carbonate stratigraphic sequence of the Karst of Trieste (Italy). Mem. Soc. Geol. Ital. 40: 21 - 34.

D'ARGENIO, B. & MINDSZENTY, A. 1995. Bauxites and related paleokarst: Tectonic and climatic event at regional unconformities. Eclogae geol. Helv. 88/3: 453 - 499.

DELVALLE, D. & BUSER, S. 1988/89. Macrofacies analysis of limestones from the Upper Cretaceous to the Lower Eocene of SW Slovenia (Yugoslavia). Geologija 31: 351 - 394.

DROBNE, K.; OGORELEC, B.; PLENIČAR, M.; BARATTOLO, F.; TURNŠEK, D. & ZUCCI - STOLFA, M. L. 1987. The Dolenja vas section from Cretaceous to Palaeogene in the NW Dinarides, Yugoslavia. Mem. Soc. Geol. Ital. 40: 73 - 84.

FRITZ, R. D.; WILSON, J. L. & YUREVICZ, D. A.. 1993. Paleokarst and related hydrocarbon reservoirs. SEPM Core Workshop No. 18, Tulsa.

GABRIČ, A.; GALOVIC, I.; SAKAČ, K. & HVALA, M. 1995. Mineral deposits of Istria - Some deposits of bauxite, building - stone and quartz "sand". Excursion guide-book. Firs croatian geological congress, Zagreb, 182 p.

GUŠIĆ, I. & JELASKA, V. 1990. Upper Cretaceous stratigraphy of the island of Brač. Opera Academiae scientarum et artium Slavorum meridionalium, 69, Zagreb, 160 p.

GUŠIĆ, I. & JELASKA, V. 1993. Upper Cenomanian - Lower Turonian sea-level rise and its consequences on the Adriatic - Dinaric carbonate platform. Geol. Rundschau 82: 676 - 686.

HAMRLA, M. 1986. Premogišče Sečovlje v Slovenskem primorju. Rudarsko - metalurški zbornik. 33: 151 - 168.

JAMES, N. P. & CHOQUETTE, P. W. 1988a. Paleokarst. Springer - Verlag, New York, 416 p.

JAMES, N. P. & CHOQUETTE, P. W. 1988b. Introduction. In: (N. P. James & P. W. Choquette, eds.): Paleokarst. Springer - Verlag, New York: 1 - 21.

JONES, B. 1992. Void-filling deposits in karst terrains of isolated oceanic islands: a case study from Tertiary carbonates of the Cayman Islands. Sedimentology. 39: 857 - 876.

JURKOVŠEK, B.; TOMAN, M.; OGORELEC, B.; ŠRIBAR, L.; DROBNE, K.; POLJAK, M. & ŠRIBAR, Lj. 1996. Formacijska geološka karta 1: 50.000 južnega dela Tržaško-Komenske planote. Inštitut ža geologijo, geotehniko in geofiziko, Ljubljana, 143 p.

KERANS, C. 1993. Description and interpretation of karst-related breccia fabrics, Ellenburger group, West Texas. In: (R. D. Fritz; J. L. Wilson & D. A. Yurewicz, eds.): Paleokarst and related hydrocarbon reservoirs. SEPM Core Workshop No. 18: 181 - 200.

KNEZ, M. & PAVLOVEC, R. 1990. Paleokras v starejšem paleogenu zunanjih Dinaridov. Rudarsko - metalurški zbornik. 37: 359 - 365.

MYLROIE, J..E. & CAREW, J. L.1995. Karst development on carbonate islands. In: (D. A. Budd; A. H. Saller & P. M. Harris): Unconformities and Porosity in Carbonate Strata. AAPG Memoir 63, Tulsa: 55 - 76.

PLENIČAR, M.; POLŠAK, A. & ŠIKIĆ, D. 1973. Tolmač za list Trst. Osnovna geološka karta SFRJ 1:100 000, Zvezni geološki zavod, Beograd, 68 p.

RADRIZZANI, C. P.; PUGLIESE, N. & STOCCA, G. 1987. The Cretaceous - Tertiary boundary at Monte Grisa (Karst of Trieste - Italy). Mem. Soc. Geol. Ital. 40: 53 - 66.

ŠRIBAR, L. 1995. Evolucija Gornjekredne Jadransko-Dinarske karbonatne platforme u jugozapadnoj Sloveniji. Magistrski rad, Sveučilište u Zagrebu, Prirodoslovno matematički fakultet, Zagreb, 89 p.

WRIGHT, V. P. 1982. The recognition and interpretation of paleokarsts: Two examples from the Lower Carboniferous of South Wales. Jour. Sed. Petrology. 52: 83 - 94.

WRIGHT, V. P. 1994. Paleosols in shallow marine carbonate sequences. Earth - Science Reviews. 35: 367 - 395.

Caves and karst areas in Serbia

by Predrag Djurovic,
Geographic Institute "Jovan Cvijic", Serbian Academy of Arts and Science, Djure Jaksica 9, Belgrade, Yugoslavia
and Vladimir Ljubojevic,
Student Speleologic and Alpinistic Club, Studentski trg 16, Belgrade, Yugoslavia

Abstract

Karst areas occur in Eastern and Western Serbia, represented mostly by isolated limestone areas separated by Neogene basins, rocks belonging to Tertiary volcanism and deep canyons and valleys. A great number of allogenous water courses enabled the formation of prominent karst hydrological systems, as well as springs (average maximal yield 3 - 15 m^3/s), underground courses (up to 24 km long). The surface morphology is dominate by sink holes and uvalas, while poljes as well as microkarstic features are rare. Approx. 4000 caves have been explored in Serbia so far. The length of the largest caves varies from 2000 to 7500 m, with maximal denivelation not exceeding 270 m.

Résumé

Le karst est dévelopé aussi bien dans l'Est que dans l'Ouest de la Serbie. Il est caractérisé par des superficies calcaires isolées, qui séparent les bassins néogènes, les rochers du volcanisme tertiaire ou cañons et vallées profondes. De nombreux cours d'eau allogènes ont déterminé la création d'un abondant système hydrologique en dépit du fait qu'il s'agit de régions karstiques: sources (3 - 15 m^3/s, moyenne maximum), cours d'eau souterrains (jusqu'à 24 kilomètres de longeur). La morphologie de surface est dominée par les dépressions (dolines et uvalés), tandis que les poljés ainsi que les formes microkarstiques sont rares. En Serbie, plus de 4000 grottes et gouffres ont été prospectés. Les principales grottes ont de 2000 à 7500 m de longeur, et la dénivellation maximum des gouffres y est de 150 à 270 mètres.

1. Karst extent

Karst in Serbia occurs in bordering parts of the country (fig. 1). In Eastern Serbia it belongs to Karpatho-Balkanian geotectonic unit. It is characterised by isolated limestone areas separated by Neogene basins whose sediments cover the borders of the limestone areas. Some of the limestone masses are separated by Tertiary volcanic rocks. The thickness of limestone mass is not uniform, though the average thickness is 500 m. Karst is developed on mountain plateaus of various altitudes, starting with 1500 - 1600 m asl (at Suva planina Mt.), but mostly at the altitudes 1000 to 1100 m (at Beljanica, Devica, Ozren, Tupiznica, Vidlic, Tresibaba and Kucaj Mts.), and also much lower at 500 to 700 m (on Miroc, Kalafat, Tresibaba Mts.). Karst in Serbia is mostly covered by forest and grass vegetation. Barren areas are scarce, related mainly to limestone cliffs and steep hillsides.

Karst in Western and South-western Serbia belongs to the Dinaric tectonic unit. Here as well, limestone mass is divided into larger or smaller complexes, mostly by deep canyons. Limestones are much thicker then within Karpatho-Balkanian Tectonic unit.

2. Karst hydrology

Division of limestone mass was caused by considerable presence of fluvial erosion in Serbian karst. Numerous allogenuos courses dissected, or are still dissecting the limestones. In many cases, the development of karstic processes converted the surface drainage into underground drainage systems. That way numerous systems of swallow holes and related springs were formed. Both alluvial and cavernous ponor zones and swallow holes are present, draining rivers and streams of considerable flow.

In Serbia exists a great number of karst springs. Both types of outflow (gravitational and siphonal) occur among the springs with major discharge. Springs are characterised by high discharge oscillations, many of them drying up during dry periods. During those periods, the discharge of the strongest springs is reduced to several hundreds lit/s. Compared with the average maximal discharge amounting to 10 m^3/s, during dry period reduction is several tens of times. A great number of springs is used for water supply of adjacent settlements.

Many river courses sink on the contact with limestones, reappearing again on the surface in the form of kasrt springs. The underground water connections identified so far, confirm the presence of well developed hydrological systems in the karst of Serbia.

Nr.	Name	Minimal discharge	Maximal discharge
01	Beli Drim	1.10	15.5
02	Crni Timok	0.15	16.0
03	Krupacko vrelo	0.15	10.0
04	Vrelo Mlave	0.29	14.8
05	Vrelo Vape	0.55	10.0
06	Vrelo Istok	0.80	6.5
07	Vrelo Raske	0.60	7.0
08	Krupajsko vrelo	0.30	3.0
09	Perucac	0.40	9.0
10	Zlotsko vrelo	0.15	3.0

Table 1: Major springs and their average maximal and minimal discharge (m^3/s)

Nr.	Swallow hole	altitude (m asl)	Spring	altitude (m asl)	distance (km)
11	Radmilovac	335	Pastrici	200	8.625
12	Plandiste	370	Pastrici	200	8.950
13	Povlenska reka	602	Zelenci	265	9.075
14	Povlenska reka	602	Paklja	260	9.250
15	Savina reka	1560	Istok	520	11.500
16	Suvi potok	1085	Raska	726	24.000
17	Lepenac	1132	Prizrenska Bistrica	1050	18.000
18	Busovata	1000	Veliko vrelo	410	8.825
19	Odorovacko polje	680	Gradiste	420	8.300
20	Brezovica	840	Grza	410	10.750

Table 2: Major underground courses

3. Surface karst morphology

In the surface morphology of Serbian karst, dolines and uvalas abound. Microkarstic features occur only sporadically, and poljes are rare. Dolines are of various forms and dimensions. Usually they are filled by residual material, rarely are rocky. At some areas sink holes are very numerous.

Amongst larger karst features, uvalas are the most numerous. Originated by karstification of valleys in karst, uvalas are elongated and follow ancient valley direction. They could occur by combining of dolines, but that is less frequent case. Most of the uvalas contain courses sinking underground, but there are as well dry uvalas without water flow.

4. Caves

Speleological explorations of the caves in Serbia have been carried out during the past hundred years. Though, central speleological catastre does not exist, it has been estimated that more than 4000 caves were explored. Out of that number, some ten caves have been, or are still arranged for touristic exploitation. Because of comparatively well preserved river system, taking into account dimensions, dominating cave types are: spring caves, ponor caves and tunnel river caves. The length of largest varies from 2 km to 7.5 km.

Because of comparatively small thickness of limestone mass, the denivelation in caves is small. The depth of largest caves is between 150 and 270 m.

Name	Location	altitude (m asl)	length (km)	width (km)
Recke	Beljanica	990	1.3	0.4
Busovata	Beljanica	1020	1.2	0.4
Divljakovac	Kucaj	420	2.0	1.0
Veliko Igriste	Kucaj	770	2.0	1.0
Velika Brezovica	Kucaj	835	1.5	1.0
Mala Brezovica	Kucaj	835	1.5	1.5
Odorovacko polje	Vidlic	700	10.0	3.0
Pojatiste	Vidlic	700	2.0	1.5
Radjena	Vidlic	700	1.5	0.5
Berovica	Vlaska planina	740	2.5	0.8
Dobro polje	Tara	1152	3.5	0.7
Ljuto polje	Tara	1250	2.5	1.0
Bare	Tara	1130	1.43	1.0
Kali polje	Javor	1198	2.5	0.5
Bazdar	Javor	1060	2.0	0.8
Rasno polje	Ninaja	1120	3.0	1.5
Pestersko polje	Pester	1160	13.0	8.5
Savina voda	Mokra gora	1560	2.0	1.5
Kostan polje	Ninaja	840	7.0	1.0

Table 3: Some of the largest uvalas and poljes

Nr.	Name	Length (m)
21	Bogovinska pecina	7500
22	Usacki pecinski sistem	6200
23	Cerjanska pecina	5150
24	Nemacki ponor	3700
25	Resavska pecina	2830
26	Samar	2790
27	Buronov ponor	2400
28	Rajkova pecina	2304
29	Stopica pecina	2160
30	Pogana pec	2000

Table 4: Longest caves in Serbia

Nr.	Name	Denivelation (m)
31	Dubasnica	276
32	Jama u Lanistu	272
33	Rakin ponor	256
34	Tisova jama	235
24	Nemacki ponor	210
27	Buronov ponor	187
37	Dragov ponor	183
23	Cerjanska pecina	176
39	Cvijiceva jama	171
40	Mijajlova jama	167

Table 5: Deepest caves in Serbia

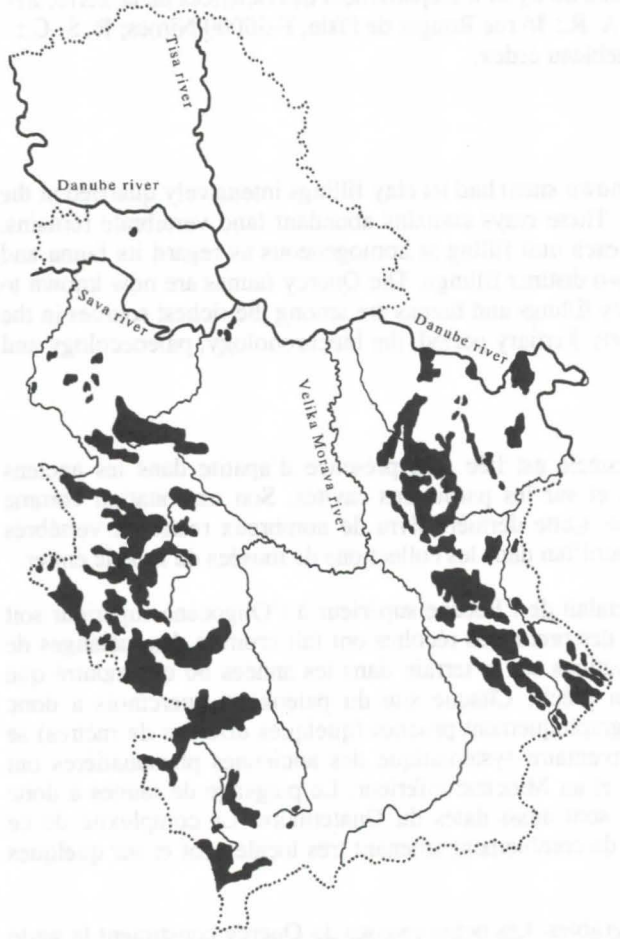

Figure 1: Extent of karst in Serbia

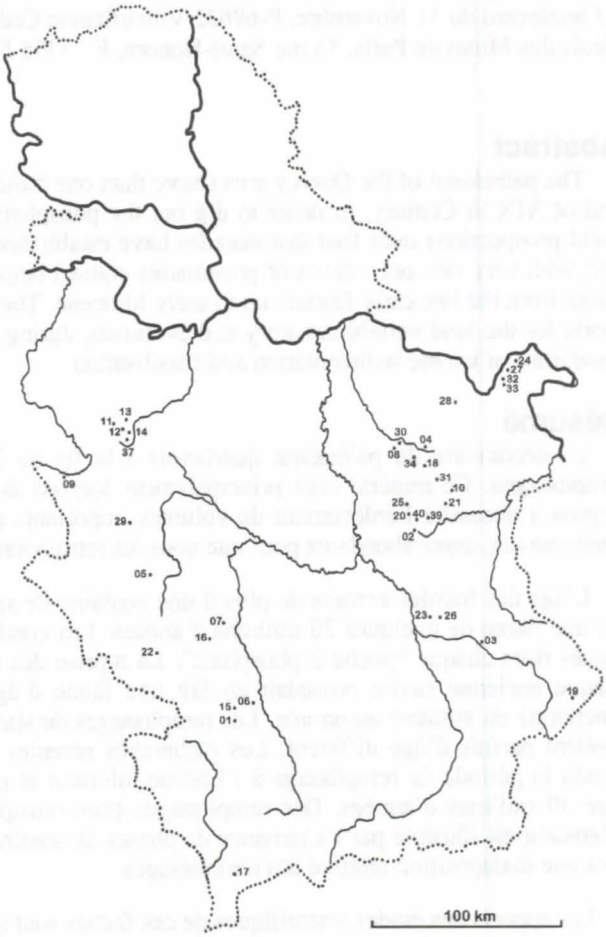

Figure 2: Locations of some karst features: major springs (1 - 10), underground water courses (11 - 20), longest caves (21 - 30), deepest caves (31 - 40)

References

MAKSIMOVIC D. 1996. Najdublji i najduzi speleoloski objekti u Jugoslaviji. Zbornik radova 3. Simpozijuma o zastiti karsta. ASAK, Beograd

GAVRILOVIC, D. 1976. Problems of karst hydrology in Yugoslavia. Memoirs of Serbian geographic society, Volume 13, Belgrade: 1 - 95

LAZAREVIC R. 1996. Valjevski kras - pecine, jame, kraska hidrologija. Srpsko geografsko drustvo, Beograd

LAZAREVIC R. 1996. Pecine i jame Zlatibora, Geologija Zlatibora. Geoinstitut, Posebno izdanje br. 18, Beograd

OCOKOLJIC M. 1994. Zakarscenost recnih slivova u Srbiji - njihov uticaj na rezim voda. Recueil des raports du comite pour le karst et la speleologie, Academie serbe des sciences et des arts, V, Belgrade

STEVANOVIC Z. 1994. The possibilities for artificial regulation of sources of karst ground water in the Carpatho Balkanides, Serbia. Recueil des rapports du comite pour le karst et la speleologie, Academie serbe des sciences et des arts, V, Belgrade

Le paléokarst polyphasé du Quercy (Sud de la France)

par J.-Y. Crochet, J.-G. Astruc, C. Blondel, L. de Bonis, C. Denys, S. Duffaud, J.-L., Hartenberger, F. Laudet, S. Legendre, B. Marandat, J.-C. Rage, J.A. Remy, B. Sigé, R. Simon-Coinçon, J. Sudre & M. Vianey-Liaud,

J.-Y. C, C. B., J.-L. H., F. L., B. M., B. S., J. S. & M. V.-L.: Laboratoire de Paléontologie, Institut des Sciences de l'Évolution, CC 064, Université de Montpellier II et E.P.H.E., Place Eugène-Bataillon, F-34095 Montpellier-cedex 5. J.-G. A.: B.R.G.M., Service géologique régional Midi-Pyrénées, 12 rue Michel Labrousse, BP 1342, F-31106 Toulouse; L. de B.: Université de Poitiers, laboratoire de Géobiologie, Biochronologie et Paléontologie humaine, 20 avenue du recteur Pineau, F-86022 Poitiers cedex; C. D.: Muséum national d'Histoire naturelle, Laboratoire des Mammifères et Oiseaux, 55 rue Buffon, F-75005 Paris; S. D. & J.-C. R.: Université deParis VI, laboratoire de Paléontologie des Vertébrés, tour 15, case 106, 4 place Jussieu, F-75252 Paris-cedex 05; S. L.: Université de Lyon I, Département des Sciences de la Terre, 27-43 boulevard du 11 Novembre, F-69622 Villeurbanne Cedex; J. A. R.: 36 rue Rouget de l'Isle, F-30000 Nîmes; R. S.-C.: École des Mines de Paris, 35 rue Saint-Honoré, F-77305 Fontainebleau cedex.

Abstract

The paleokarst of the Quercy area (more than one hundred known sites) had its clay fillings intensively quarried at the end of XIX th Century, in order to dig out the phosphatic ore. These clays contains abundant land vertebrate remains. Field prospections over four last decades have established that each unit filling is homogeneous as regard its fauna and age, with very rare occurences of presumable contact between two distinct fillings. The Quercy faunas are now known to range from the late early Eocene up to early Miocene. The Quercy fillings and faunas are among the richest sources in the world for the land vertebrates story and evolution, during the early Tertiary period, the biochronology, paleoecology and conditions of karstic sedimentation and fossilisation.

Résumé

La découverte du paléokarst quercinois à la fin du XiXè siècle est liée à la présence d'apatite dans les anciens remplissages. Ce minéral était principalement localisé au fond et sur les parois des cavités. Son exploitation comme engrais a nécessité l'enlèvement de volumes importants d'argile. Cette dernière livra de nombreux restes de vertébrés continentaux, assez abondants pour que nous les retrouvions aujourd'hui dans les collections de musées du monde entier.

L'âge des fossiles extraits de plus d'une centaine de sites s'étalait de l'Éocène supérieur à l'Oligocène supérieur soit sur une durée de quelques 20 millions d'années. Les conditions des premières récoltes ont fait croire à des mélanges de faunes dans chaque "poche à phosphate". La reprise des observations sur le terrain dans les années 60 ont montré que chaque ancienne cavité possédait en fait une faune d'âge bien précis. Chaque site du paléokarst quercinois a donc fonctionné en système autonome. Les remplissages de sites géographiquement proches (quelques dizaines de mètres) se révèlent parfois d'âge différent. Les recherches récentes et l'inventaire systématique des anciennes phosphatières ont étendu la période de remplissage à l'Éocène inférieur et moyen et au Miocène inférieur. Le piégeage de faunes a donc duré 30 millions d'années. Des remplissages (non phosphatés) sont aussi datés du Quaternaire. La complexité de ce paléokarst est illustrée par l'alternance de phases de soutirage et de comblement amenant très localement et sur quelques sites une juxtaposition relative des remplissages.

Les apports des études scientifiques de ces faunes sont considérables. Les petits causses du Quercy constituent la seule région au monde où nous pouvons suivre l'évolution et les transformations subies par les faunes continentales (vertébrés et mammifères principalement) durant une aussi longue prériode. La biochronologie et la biostratigraphie en milieu continental de l'ère tertiaire ont été renouvellées et 5 sites quercinois ont été retenus comme gisements de référence européenne au Symposium International tenu à Mayence en`1987.

En ce qui concerne la systématique, plus de 200 espèces valides de mammifères (sur 326 identifiées appartenant à 12 ordres) ont été décrites sur la base du matériel sauvé au cours de la période d'exploitation industrielle mais les localités de provenance restent inconnues. Chaque année, de nouvelles espèces sont identifiées et crées à partir du matériel récolté récemment et donc bien daté et de provenance connue.

L'étude des assemblages fauniques est rendue possible par l'établissement de listes des espèces présentes dans chaque localité. Ces assemblages sont significatifs des conditions climatiques et permettent une restitution des paysages végétaux successifs.

La taphonomie révèle les conditions de remplissage de chaque site et permet de reconstituer les différentes phases qui ont précédé le piègeage des faunes dans chaque cavité.

Le paléokarst quercinois est un véritable laboratoire de l'évolution.

Speleological Investigations in Saudi Arabia

Ralf Benischke*, Gerald Fuchs & Volker Weissensteiner****
* Inst. f. Hydrogeology & Geothermics, Joanneum Research, Elisabethstrasse 16, A-8010 Graz, Austria
**Landesverein f. Hoehlenkunde i. d. Steiermark, Brandhofgasse 18, A-8010 Graz, Austria

Abstract
Speleological investigations in the Summan Plateau (Saudi Arabia, Eastern Province, Emirate of Ma'aqla) were part of a joint project of the Austrian Academy of Sciences and the King Fahd University of Petroleum and Minerals, Dhahran, Saudi Arabia.
A short survey on earlier speleological investigations in Saudi Arabia is given, a characterization of the main topographical, geological and geomorphological features of the study area and a description of representative morphological patterns of cave development showing the distiguished morphogenetic evolution of the landscape depending on tectonic movements in the wider framework of the geological development of the Arabian Shelf Platform.

Zusammenfassung
Höhlenkundliche Untersuchungen im Summan Plateau (Saudi Arabien, Ostprovinz, Emirat Ma'aqla) waren Teil eines gemeinsamen Projektes der Österreichischen Akademie der Wissenschaften und der King Fahd University of Petroleum and Minerals, Dhahran, Saudi Arabien. Es wird ein kurzer Überblick über frühere speläologische Forschungen in Saudi Arabien gebracht, eine Charakteristik der wichtigsten topographischen, geologischen und geomorphologischen Gegebenheiten des Untersuchungsgebietes und eine Beschreibung repräsentativer morphologischer Muster der Höhlenentwicklung, die auf eine besondere Morphogenese der Landschaft in Abhängigkeit von den tektonischen Bewegungen im weiteren Rahmen der geologischen Entwicklung der Arabischen Schelfplattform hinweisen.

1. Indroduction
The project was entitled "Karst Phenomena of the Arabian Shelf Platform and their Influences on Underground Aquifers". It was thought as an extension of a preceding project named "Quaternary Period of Saudi Arabia" (AL-SAYARI & ZÖTL, 1978; JADO & ZÖTL, 1984).

The main objective of the project was to study the karst phenomena in the outcrop-area of the Paleocene Umm-er-Radhuma-formation and to point out the interrelation between karstification processes, aquifer development and groundwater recharge with respect to the geomorphologic conditions, the geologic, sedimentologic and structural prerequisites and the climatic influences. Because the primary objective was a hydrogeological one the speleological investigations had to be seen in the context of the above mentioned objectives, and included mapping and surveying of caves, their documentation and speleogenetic interpretation, structural investigations and samp ling of speleothems for dating (BENISCHKE *et al.*, 1987, 1993).

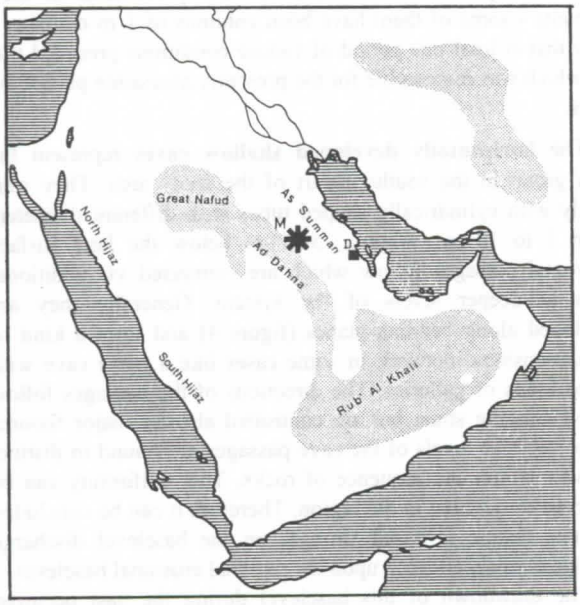

Figure 1: Generalized topographic map of the Arabian Penninsula with the study area (marked with asterisk). M= Ma'aqla, D= Dhahran.

2. Topographic Overview
The Summan Plateau starts in the North near the border to Kuwait and extends to the South over 800 km as a relatively narrow arch to the northern margin of the wide Rub' al Khali desert. To the East the plateau changes gently to the coastal plains at the Arabian (Persian) Gulf. To the West the plateau is contiguous to the parallel running dune belt of Ad Dahna, which connects the Nafud desert in the North and the Rub' al Khali in the South.

The study area (subsequently called Ma'aqla region) is situated in the As Sulb Plateau which belongs to the greater region of the Summan Plateau in northeastern Saudi Arabia.

The Ma'aqla region itself is located in the center of the Summan Plateau within a quadrangle of approx. 26°15' N and 26°45' N, and 47°00' E and 47°30' E respectively (figure 1). The main settlement is the small village of Ma'aqla which had been a fort against the aboriginal bedouine tribes during the Osmanian occupation. The base camp during the field work was Shawyah another small bedouine village situated at the margin of Ad Dahna about 37 km southeast of Ma'aqla.

3. Geological Setting
The Ma'aqla region is characterized by the Paleocene Umm-er-Radhuma-formation (= UeR). This formation consists of light, aphanitic and arenitic limestones and brown dolomites with chert nodules abundant. Within the sequence of this formation thick beds of marl-like layers offered good possibilities for karstification or erosion. In detail the genesis of these layers is uncertain but lithological and sedimentological investigations as well as the study of numerous thin-sections showed a strongly recrystallized texture, dolomitization and partly complete decalcification.

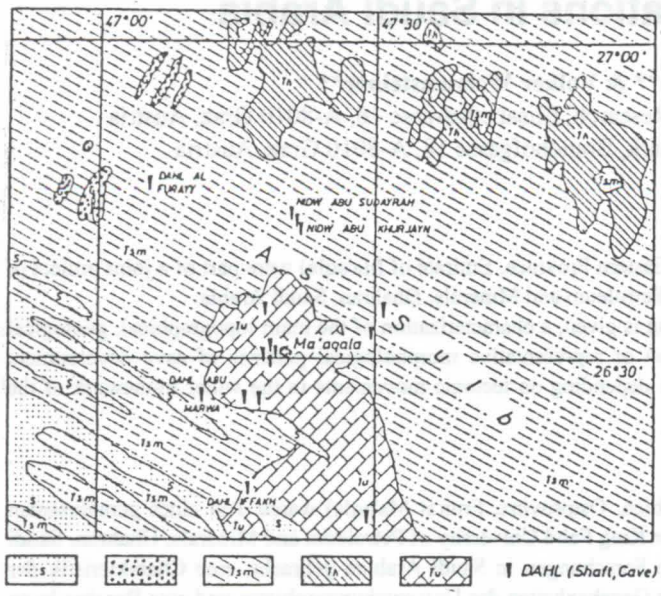

Figure 2: Generalized geological map of the Ma'aqla region. S=Aeolian sand, G=Gravel deposits from basement rocks, Tsm=Sandstone, marl, limestone (Miocene), Th=Sandy Limestone, Hadrukh-formation (Early Miocene); Tu= Umm-er-Radhuma-formation (Paleocene), from AL-SAYARI & ZÖTL (1978).

As the central part around the village of Ma'aqla is only at a few places overlain by Miocene clastic sediments (=Tsm), the eastern part towards the coast consists almost exclusively of these younger sediments. Because the clastic sediments are strongly cemented by calcium carbonate these layers have also a potential for cave development.

Generally the strata dip very gently to NE and E according to the general dipping of the entire platform. Cave development is generally controlled by tectonics but also by stratigraphy, which can clearly be shown on the cave-maps. The general direction of the cave systems is closely bound to the strata-dipping (NE or E) whereas the local direction of individual passages depend on tectonic structures such as significant joints.

4. Earlier Speleological Investigations

PHILBY (1925) gave some references on karstification, and an approximate localization of caves can be obtained from the geological map (BRAMKAMP & RAMIREZ, 1958). A detailed description of the karst and cave distribution, in particular from the Summan Plateau can be found in AL-SAYARI & ZÖTL (1978) together with first results on speleothem-dating with ^{14}C, which brought ages ranging from 30-40 ky BP.

A survey from MIDDLETON (1978) mentions the possibilities of caving in the Arabian region deduced from the distribution of karstifieable rock formations. Later on parts of the Eastern Province were explored with descents into shafts down over 75 m (DAVIS, 1983). French speleologists mapped the cave *Aiyn Hit* near Riyadh (COURBON, 1985).

A series of new and intense exploration from American speleologists brought new insights into the distribution of caves in the eastern part of Saudi Arabia, particularly into morphological details (PINT, 1985; PINT & PETERS, 1985). They surveyed 600 m of the so-called *Blowhole Cave* near Ma'aqla later named after a local guide as *Dahl Sultan*. A very detailed description about caves and karst in Saudi Arabia followed some years later (PETERS *et al.*, 1990). *Dahl Abu Hashami* a shaft cave, *Dahl Abu Marwah* a cave ruin and again *Dahl Sultan* have been explored.

5. Morphology of the Ma'aqla Caves

According to their position in the landscape we found three types of caves: cave ruins, horizontally developed caves only some meters beneath the land surface and as a third group shafts with only some smaller horizontal extensions.

The **cave ruins** consist of types, where almost all rooms and galleries have been destroyed by landerosion or consist of types where only a relatively weak influence of erosion or denudation leads to opening of cave passages to the land surface. A very impressive example is the so-called *Open-Air-Cave* (figure 3) or the *Chert Cave*. In all cases it could be observed that remnants of speleothems could be found on the surface or close to the entrance openings or cemented in duricrust. This apparently shows that an older landscape has been destroyed either by linear erosion or by denudation. Moreover the speleothems or their remnants - some of them have been columns of 1 m diameter - show that at least one period of vadose conditions preceded that one which was responsible for the presently accessible part of the caves.

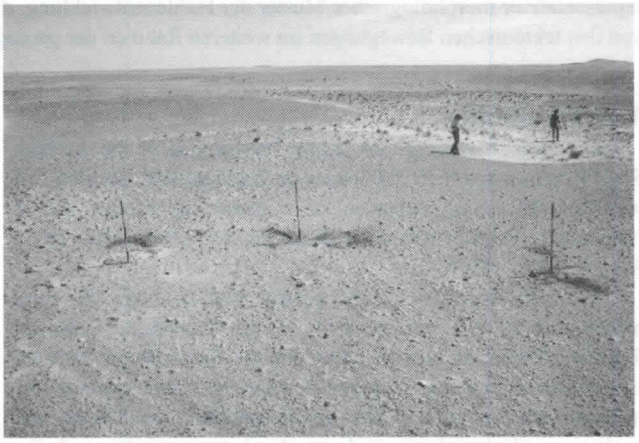

Figure 3: Example for a cave ruin with remnants of big columns of dripstone (Open-Air-Cave).

The **horizontally developed shallow caves** represent the main group in the southern part of the study area. They start mostly with cylindrically shaped tubes with different diameters (from 1 to 10 m). Approx. 5-12 m below the land surface horizontal passages follow which are connected via additional tubes to deeper levels of the system. Generally they are developed along bedding-planes (figure 4) and form a kind of two-dimensional network in some cases like a maze cave with closed loops of galleries. The directions of the passages follow the NE-dipping strata but are controlled also by major fissures and joints. The levels of the cave passages are bound to distinct intervals within the sequence of rocks. This uniformity can be observed throughout in the region. Therefore it can be concluded that this feature is based strongly on the baselevel discharge conditions in dependence upon the regional erosional baselevel.

The drawdown of this baselevel during the past occurred only within a small difference of some tens of meters, which seems to be an indication for the evolution of only a weak relief during the past. This group of caves is mainly represented by

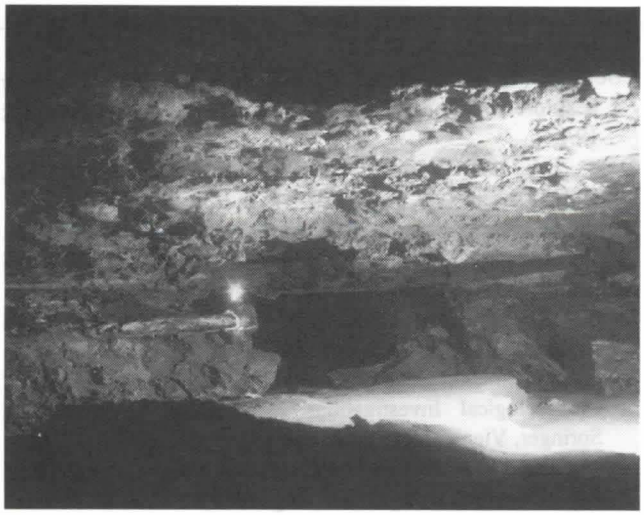

Figure 4: Bedding-plane passage in the UPM-Cave as example for the horizontally developed caves. The passage is developed in the marl-like beds, the floor is covered with spilled-in sand.

caves such as the *UPM-Cave* (668 m long), *B32-Cave* (1.1 km long) and the *Dog Cave* (360 m long).

The third group of caves is represented by mainly vertically developed caves or shafts with only some short horizontal extensions. The caves lead down to a depth approx. 45 m below the land surface. It is of interest that most of those caves are developed in their upper part in the Tsm-formation and in their lower part in the Umm-er-Radhuma-formation (figure 5). Only in the close vicinity of Ma'aqla the normally overlieing Tsm-unit is missing due to an tectonic updoming. Some of these caves have been explored by American collegues too (PETERS *et al.*, 1990) such as the *Dahl Abu Hashami* and some others.

In other regions in the North of Ma'aqla the shafts are developed in the Tsm, which is a result of a relative low position of this part of bedrock, wherein the Tsm-unit has been conservated. This process originated from a continuous development during an uplift of the Arabian Shield in the West and parallel from a gentle tilting to the East of the adjacent Shelf Platform.

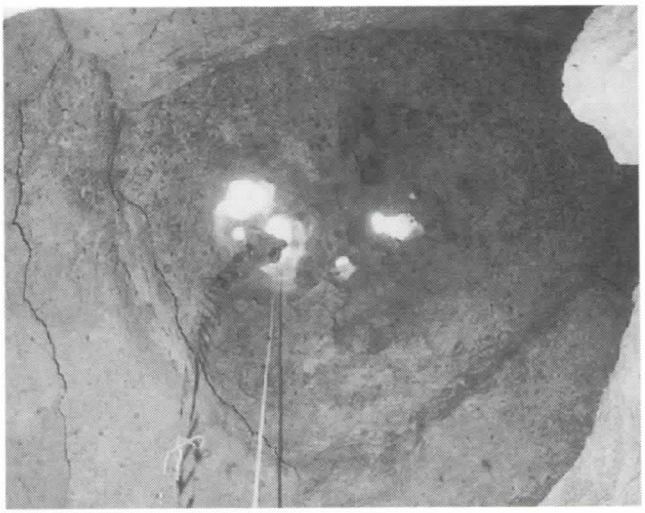

Figure 5: Typical dome-shaped shaft (Pigeon Dome) in the North of Ma'aqla. The entrance part forms a cupola with some small holes for access.

6. Speleogenesis of the Ma'aqla Caves

Lithology, (Geo)tectonics and bedding conditions are seen as more static elements in cave development, whereas climate and biological factors are considered to be the more dynamic factors. To understand the development of a landscape its morphogeny is essential for interpretation of karstification processes. All the karst phenomena including the caves are descendants of an older landscape, which in the case of the ruins had been destroyed successively either by surface denudation or by linear erosion resulting later on in wadi systems

During our investigations we have found the above mentioned three types of caves which are bound to distinct evolutional levels of the landscape. Beginning with the uppermost part the cave ruins and sometimes remnants of dripstones show very clearly that there was an old horizon of vadose galleries. During that times the other deeper situated horizons were under phreatic conditions. The process of drawdown of the baselevel and the subsequent development of cave levels was initialized by geotectonic movements (uplift of Arabian Shield) starting in the Late Mesozoic and after sedimentation of the UeR-Formation. At last this resulted in a E or NE-tilting of the Shelf Platform during the Late Eocene and the Oligocene (HÖTZL *et al.*, 1993).

Concerning the group of horizontal caves we explored a well karstified, more or less shallow horizon of bedding-plane passages covering an interval of approx. 40 m. But most of the accessible caves are developed only 10 m below the land surface. This horizon is accessible only in caves but is visible in boreholes too drilled by the ARAMCO oil company. These boreholes show another interesting feature such as two other intensively karstified but dry horizons in different depths (75-80 m and 90-100 m below the land surface). The actual water table is today in a depth of 160 m. This is considered to be the presently active phreatic level but could never be reached during the field campaign.

For a better understanding of some details of the evolutional phases in particular the question about the age of speleothems, we carried out sampling of sinter and stalagmites or stalactites. Two groups could be distinguished: an older group and a younger group. The older group is represented by bigger stalgmites and shows after Uranium-Series dating in most cases an age of more than 200 ky B.P. The younger group dated with ^{14}C respresents material with ages between Late Pleistocene and Holocene.

Another detail was the observation of reddish-brown sediment-relics consisting of quartz sand in potholes and pockets, on floors and on ceilings of passages. This indicated in the accessible caves a phase of former complete filling where the overlying landscape has been eroded. Later there was a phase with reactivation of the cave and transport of the sediments to a deeper level, which possibly has plugged its galleries. This is most likely the reason that it was not possible to get deeper into the cave systems.

7. Outlook

This very interesting region offers good possibilities for caving and research on cave development and the respective geologic and climatic influences during the past. Because the caves. It seems to be essential to investigate a wider area of the Arabian Penninsula for better comparison and to enhance dating of sediments and of speleothems.

Acknowledgments

The authors would like to express their gratitude to Prof. Dr. J. ZÖTL (Commission on Quaternary Research of the Austrian Academy of Sciences) for the invitation to undertake speleological work within the framework of the project. We are also indebted to the Arabian partners (Research Institute, King Fahd University of Petroleum and Minerals, Dhahran) for providing optimum working conditions and active interest in this aspect of earth sciences.

References

AL-SAYARI, S.S. & J. ZÖTL. 1978. Quaternary Period in Saudi Arabia, Springer, Vienna-NewYork, 335 p.

BRAMKAMP, R.A. & L.F. RAMIREZ. 1958. Geologic Map of the Northern Tuwayq Quadrangle, Kingdom of Saudi Arabia, U.S. Geol. Surv., Map I-207 A 1:500000, Washington.

BENISCHKE, R., FUCHS, G. & V. WEISSENSTEINER. 1987. Speläologische Untersuchungen in Saudi-Arabien (Eastern Province, As-Summan-Plateau, Region Ma'aqla). Die Höhle, 38 (3): 61-76.

BENISCHKE, R., FUCHS, G. & V. WEISSENSTEINER. 1993. Speläologische Untersuchungen. In: (H. Hötzl, S. Wohnlich, J.G. Zötl & R. Benischke): Verkarstung und Grundwasser im As Summan Plateau (Saudi Arabien). Steir. Beitr. z. Hydrogeologie, 44: 94-147.

COURBON, P. 1985. Puits sans Petrole au Pays de L'Or (Explorations en Arabie Saoudite). Grottes et Gouffres, 95: 19-21.

DAVIS, B.L. 1983. Voids between the Dunes. NSS News, Nov. 1983: 278-284.

HÖTZL, H., S. WOHNLICH, J.G. ZÖTL & R. BENISCHKE. 1993. Verkarstung und Grundwasser im As Summan Plateau (Saudi Arabien). Steir. Beitr. z. Hydrogeologie, 44, 5-158.

JADO, A.R. & J.G. ZÖTL. Eds. 1984. Quaternary Period in Saudi Arabia. Vol. 2: Sedimentological, Hydrogeological, Hydrochemical, Geomorphological, Geochrtonological and Climatological Investigations in Western Saudi Arabia. Springer, Vienna-New York, 361 p.

MIDDLETON, J.R. 1978. Some Notes on the World Caving Scene. Asia. Caves & Caving, No. 1(Aug. 1978): 2-11.

PETERS, D., J. PINT & N. KREMLA. 1990. Karst Landforms in the Kingdom of Saudi Arabia. NSS Bulletin, 52 (1): 21-32.

PHILBY, H.S. 1925. Das geheimnisvolle Arabien. 2 vol., Brockhaus, Leipzig, 365 p. + 320 p.

PINT, J. 1985. The Caves of Ma'aqla. NSS News, Sept. 1985: 277-282.

PINT, J. & D. PETERS. 1985. The Caves of Ma'aqla. Unpubl. Rep., 8 p.

Etude spéléo-karstologique du système Muruk-Bérénice (Monts Nakanaï ; Papouasie-Nouvelle Guinée) : résultats de l'expédition de 1995 et perspectives pour 1998

Fabien Hobléa et Philippe Audra,
CAGEP-URA 903 du CNRS, Institut de Géographie,
29 Avenue Robert Schuman, 13621, Aix-en-Provence Cédex, France.

Abstract

From january to march 1995, the french caving and diving expedition "Hémisphère Sud : 1er moins mille" took place in the Nakanaï mountains (East-New Britain, Papua-New Guinea). The main speleological aim was to continue the exploration of Muruk hole (alt. 1480 m) : after diving a sump at the depth of 637 meters, the exploration stopped at -1141 m. A water tracing showed that the underground river of Muruk is springing out from a big cave called Berenice (alt. 260 m, explored until +108-meter-spot height) in the canyon of the Galowe river. During this expedition were carried out a lot of observations about karst morphology and hydrology of this unknown equatorial area, which are summarised in this paper.

In january 1998, a new expedition will try to link up Muruk hole and Berenice Cave. The karst-research programme is ready and given to conclude.

Résumé

De janvier à mars 1995 s'est déroulée l'expédition française de spéléo-plongée "Hémisphère sud, 1er - 1000" dans le karst des Monts Nakanaï sur la côte sud-est de la Nouvelle-Bretagne (Papouasie-Nouvelle Guinée). Cette communication s'attache plus particulièrement à exposer les résultats des investigations scientifiques qui ont accompagné et parfois guidé les explorations spéléologiques, notamment dans le gouffre de Muruk, où un traçage à confirmé la liaison hydrogéologique rapide entre cette cavité et la résurgence de Bérénice, motivant la poursuite des explorations post-siphon en vue d'effectuer la traversée spéléologique intégrale du système.

Ce sera l'objectif principal d'une prochaine expédition prévue pour janvier 1998, et l'occasion de recueillir des données karstologiques complémentaires.

1. Introduction

Le gouffre de Muruk (5°28'15" S ; 151°21'48" E) s'ouvre à 1480 m d'altitude sur le plateau de la haute-Galowé dans les monts Nakanaï situés sur l'île de Nouvelle-Bretagne en Papouasie Nouvelle Guinée (figure 1). La cavité fut découverte par les membres d'une expédition française en 1985, qui s'étaient arrêtés sur un large siphon à la cote - 637 m. Le franchissement de cet obstacle et la poursuite des explorations post-siphon constituait le principal objectif de l'expédition française de spéléo-plongée "Hémisphère-sud : 1er - 1000" qui s'est rendue sur les lieux de janvier à mars 1995. Pendant que les plongeurs oeuvraient depuis le plateau, une partie de l'équipe s'est employée à atteindre et explorer une émergence repérée d'hélicoptère au fond du canyon de la Galowé entaillant le plateau sur sa bordure orientale. Cette magnifique source perchée 90 m au-dessus du talweg projette ses 2 m^3/s (à l'étiage) en une blanche cascade baptisée la Chevelure de Bérénice. Tandis que l'équipe de Muruk franchissait le siphon et poursuivait l'exploration dans de vastes galeries jusqu'à la cote - 1141 m, l'équipe de la résurgence parvenait à atteindre dans le canyon le porche pénétrable donnant accès à la rivière souterraine de Bérénice, qu'un traçage à démontré être l'aval des circulations rencontrées dans Muruk. Bérénice a été remontée sur 108 m de dénivellation. La corde et le temps ont malheureusement manqué pour effectuer jonction et traversée de ce système de 1220 m de dénivellation.

Dans ces contrées difficiles d'accès et peu connues, il est particulièrement important que les explorations, souterraines ou de surface, s'accompagnent d'observations et de mesures géographiques, (hydro)géologiques, géomorphologiques et biologiques.

Comme dans toutes les expéditions lointaines de ce type, la collecte des données s'effectue durant les temps d'explorations. Il s'agit d'avoir l'oeil ouvert à chaque instant, car il est difficile d'envisager des séances spécifiques aux recherches scientifiques, et bien entendu il n'est pas possible, lorsqu'on constate des lacunes après le retour de l'expédition, d'aller les combler au cours d'un week-end.

L'expédition de 1995 a permis de reconnaître le terrain sur le plan karstologique, de poser les problèmes morphogéniques en s'appuyant sur des relevés topographiques et spéléo-morphologiques concentrés sur le système Muruk-Bérénice, sans toutefois négliger le contexte des fonctions "entrées" et "sortie" du système, en étudiant aussi ce qu'il nous a été permis de parcourir du plateau et du canyon de la Galowé. Elle a en cela préparé le terrain à l'expédition prévue pour 1998, au programme scientifique balisé et étoffé.

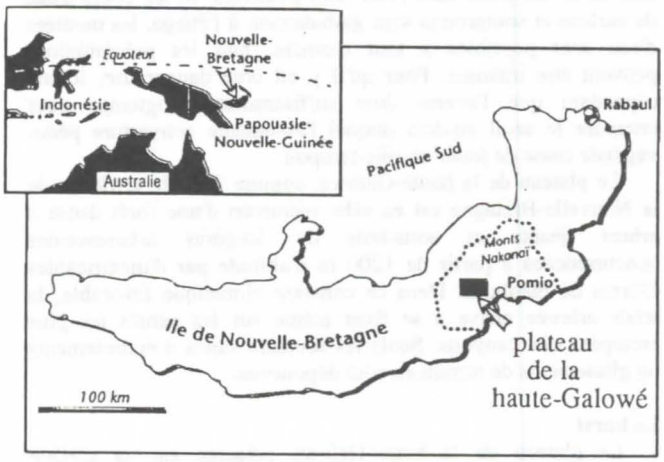

Figure 1 : Localisation de la zone explorée

2. Le karst de la haute-Galowé dans son cadre géologique et bioclimatique

Fort heureusement, les expéditions spéléologiques précédentes comprenaient également des karstologues qui purent déjà étudier des secteurs voisins aux caractères similaires (MAIRE, 1990). La Papouasie-Nouvelle-Guinée avait de plus fait l'objet de nombreuses recherches de la part de géoscientifiques issus des anciens pays colonisateurs de ce jeune Etat (LÖFFLER, 1977). Toutes ces données sont précieuses pour une approche à différentes échelles du pays en général ou du secteur en particulier.

Géologie

Au contact entre la plaque continentale australienne et plaque océanique du Pacifique, l'arc insulaire formé par la Nouvelle-Guinée, l'archipel Bismarck auquel appartient la Nouvelle-Bretagne, et les îles Salomon, est un maillon de la "ceinture de feu" du Pacifique. Il constitue une des zones les plus mobiles et instables de l'écorce terrestre, où se manifestent 5 à 10% de l'activité sismique mondiale ! Durant l'expédition, c'est en moyenne une secousse par semaine qui ébranlait sérieusement notre campement (magnitude supérieure à 4,5 Richter ?). Mais les équipiers évoluant alors sous terre n'ont jamais rien ressenti.

La tectonique du plateau de la haute-Galowé est assez mal connue à grande échelle. Cette partie de la plate-forme carbonatée des Monts-Nakanaï est constituée par les calcaires miocènes dits de Yalam (miocène inférieur et moyen), assez crayeux et épais de 1300 à 1500 mètres, reposant sur un socle volcano-sédimentaire dont la mise en place date de l'éogène. Le plateau de la haute-Galowé, dont le pendage est d'après nos observations de 5 à 10° vers l'Est/Sud-Est, serait sur le flanc Sud-Est d'un géanticlinal d'axe OSO-ENE (MAIRE, 1990), haché par des failles rectilignes Est-Ouest bien visibles sur photos aériennes.

Climat et végétation

Les données bioclimatiques sont caractéristiques des régions équatoriales, avec une moyenne annuelle de température supérieure à 25°C au niveau de la mer et des totaux annuels de précipitations parmi les plus importants de la planète (près de 6,5 m/an sur le littoral de la baie de Jaquinot au pied du plateau). Au camp de Muruk à 1500 m d'altitude,la température fraîchissait jusqu'à 17°C la nuit et dépassait difficilement les 25°C en journée. Du fait d'un régime pluviométrique de type mousson caractérisé par une bascule des vents dominants porteurs de pluie (N-O durant l'été austral de janvier à avril et S-E en hiver de mai à octobre), il est impératif que les expéditions sur la côte sud-est aient lieu durant l'été austral, période où cette façade est placée sous le vent, donc relativement plus sèche. Il n'empêche qu'il pleut quasiment tous les jours, mais seulement pendant quelques heures, et des jours sans pluie sont possibles. Si les cours d'eau de surface et souterrains sont globalement à l'étiage, les montées d'eau sont possibles à tout moment, tant les précipitations peuvent être intenses. Pour qu'il y ait crue dangereuse, il faut cependant que l'averse dure suffisamment longtemps pour atteindre le seuil au-delà duquel l'abondante couverture pédo-végétale cesse de jouer un rôle-tampon.

Le plateau de la haute-Galowé, comme 90% du territoire de la Nouvelle-Bretagne est en effet recouvert d'une forêt dense à arbres géants et sous-bois de fougères arborescentes concurrencées à partir de 1200 m d'altitude par d'inextricables fourrés de bambous. Dans ce contexte climatique favorable, la strate arborée arrive à se fixer même sur les pentes les plus escarpées des canyons. Seuls les secteurs sujets à écroulements ou glissements de terrain en sont dépourvus.

Le karst

Le plateau de la haute-Galowé présente sur sa surface sommitale entre 1000 et 1500 mètres d'altitude une morphologie typique des karsts intertropicaux humides. La partie amont de l'impluvium présente un modelé de type fluvio-karstique composé de nombreux talwegs guidés par la fracturation et partiellement imperméabilisés par une couverture argileuse enrichie d'apports volcaniques, à drainage temporaire absorbé par des pertes qui prennent parfois la forme d'un gouffre, comme celui de Muruk. A l'aval, ce modelé fait place à une bande de terrain où de vastes dolines jointives donnent un modelé polygonal (figure 2). Il faut se demander si la délimitation de ces modelés, bien visible sur photos aériennes, n'est pas en partie contrôlée par des paramètres lithologiques (contact entre récif et arrière-récif).

Indifférents à ces variations de modelés, des avens géants taillés à l'emporte-pièce dans le plateau nous rappellent que nous sommes dans la région des Kavakuna et autres Naré. Une énorme galerie-salle plongeante trépanée par l'érosion de surface à ainsi été survolée en hélicoptère au sud de la zone (photo 1). Baptisée provisoirement le "puits-haricot", elle constituera un des objectifs de la prochaine expédition, même si l'effondrement de la voûte à l'origine de cette dépression laisse peu d'espoir d'accès au karst profond...

Le canyon de la Galowé délimite le plateau au Nord et à l'Est. Il forme une entaille de plus de 1000 m de profondeur, extrêmement raide et étroite dans les 400 mètres inférieurs. Dans la partie amont du canyon, orientée Ouest-Est, le cours d'eau formant la haute-Galowé, alimenté par le ruissellement de surface, est des plus chétifs. La Galowé naît véritablement à l'exsurgence impénétrable de Mayang (20 m^3/s à l'étiage), située à l'entrée du coude infléchissant la direction du canyon vers le sud (figure 2). Entre Mayang et la mer, pas moins de 8 émergences ont été repérées en rive droite de la Galowé, dont la Chevelure de Bérénice, qu'il s'agissait d'atteindre et d'explorer, en s'assurant de sa relation avec les eaux de Muruk, hypothèse sur laquelle reposait tout l'intérêt de l'expédition.

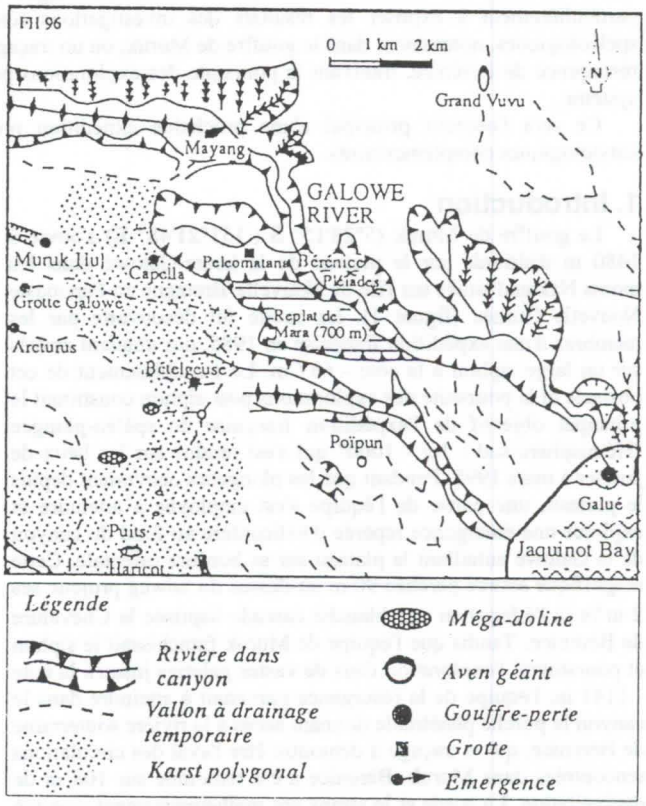

Figure 2 : Croquis morphologique du plateau de la Galowé (Mts Nakanaï, PNG)

3. Le système Muruk-Bérénice : grand gouffre équatorial... de type alpin !

Muruk et Bérénice ont fait l'objet d'une étude spéléo-morphologique combinant traçages, mesures des paramètres physico-chimiques des eaux, relevés spéléo-morphologiques, examen et échantillonnage des remplissages. L'ensemble des données recueillies peut être consulté dans deux publications facilement accessibles (HACHE et al., 1995 ; HOBLEA, 1995). Par souci de brièveté, nous nous contentons ici d'exposer les principaux résultats de nos recherches préliminaires, ainsi que les interrogations ayant servi de guide à l'établissement du programme d'étude de la prochaine expédition.

Hydrographie souterraine : l'apport des traçages

Deux traçages ont été effectués pour connaître la destination des rivières souterraines. La première coloration a permis de démontrer la liaison entre Muruk et Bérénice, motivant ainsi la poursuite des explorations post-siphon en quête du premier "moins mille" de l'hémisphère sud. La fluorescéine a été injectée post-siphon. La rapidité du transfert (300 m/h à plus d'1 km/h) laisse supposer qu'aucun autre siphon ne viendra entraver la traversée Muruk-Bérénice.Un second traçage a été réalisé pour lever un point d'interrogation sur l'organisation interne du drainage. La topographie et les observations directes in-situ ont permis de représenter l'organisation des circulations dans le système (figure 3). Au total, les parties connues du réseau montrent un système hydrographique fortement hiérarchisé autour d'un collecteur incliné et accidenté de nombreuses cascades, indépendant d'un quelconque écran étanche. Le volume des galeries est à la mesure des énormes débits de hautes eaux que l'on peut supposer s'écouler entre mai et octobre . Plusieurs affluents se greffent sur le collecteur après un parcours au profil plus raide, marqué par d'importantes verticales.

Vers - 1000 m se produit un phénomène remarquable : la galerie principale se ramifie en une dizaine de petits conduits tubulaires (le "Gruyère"), à l'image d'un barillet branché sur le canon d'un révolver. Dans la salle qui fait la jonction entre les deux morphologies, un actif arrive en cascade du plafond (la "cascade probabiliste") . Ses eaux se partagent en deux ruisseaux, de part et d'autre d'un cône d'éboulis : l'un dévale la pente caillouteuse pour rejoindre l'actif principal, l'autre continue sa route par une galerie différente, celle-là même suivie par les explorateurs pour atteindre la cote - 1141 m. On assiste ainsi à un spectaculaire (et rare) croisement de chemins de drainage karstique.

Débits et physico-chimie des eaux souterraines

Les débits d'étiage observés durant cette saison relativement sèche peuvent momentanément être gonflés par de violentes précipitations journalières, si l'intensité est suffisante pour qu'un écoulement apparaisse dans les talwegs de surface, conduisant les eaux de pluie vers une perte concentrée. Dans ces conditions, de brusques montées d'eau ont été observées dans Muruk comme Bérénice, sans cependant qu'ait été observé cette fois de véritable phénomène de vague de crue. Les actifs ont un débit d'étiage de quelques dizaines de l/s à l'amont du collecteur, quelques centaines de l/s dans la rivière à l'amont du siphon, 1,5 à 2 m^3/s à partir de la cascade rencontrée post-siphon à - 847 m, qui constitue le collecteur principal du système.

Des mesures plus précises ont pu être effectuées pour ce qui concerne les paramètres physico-chimiques des eaux. La température de la rivière souterraine variait entre 18°C dans la zone d'entrée de Muruk et 19,6°C dans Bérénice. le pH s'accroissait globalement d'amont en aval pour un même drain : entre 7,4 et 8, avec des pH toujours supérieurs à 8 pour les rivières de surface au fond des canyons (8,3 pour la Galowé).

De même, la conductivité comme la dureté et l'alcalinité allaient logiquement en s'accroissant d'amont en aval, mais se révélèrent caractéristiques d'eaux faiblement minéralisées, avec des valeurs de l'ordre de celles rencontrées dans la montagne calcaire tempérée (conductivités variant entre 185 et 270 µS/cm ; TH entre 9,25 et 13,5°F, TAC autour de 11°F). L'efficacité de l'érosion chimique dans les gros conduits s'explique ainsi plus par l'importance des débits écoulés que par la charge dissoute unitaire, peu élevée en raison de la grande vitesse de circulation dans les drains observés.

Morphologie des conduits et remplissages

Dans Muruk comme dans Bérénice, la forme de conduit dominante est de type canyon. Le surcreusement torrentiel semble cependant entailler sur toute sa largeur un (ancien ?) conduit de type phréatique. De rares tronçons de l'actif et de petits conduits secs adjacents ont conservé une morphologie tubulaire et s'ennoient très probablement en saison des pluies. Le profil en long est très tendu, avec une pente moyenne du collecteur, perché dans la masse calcaire, autour de 10°, supérieure au pendage. Le collecteur suit une trajectoire assez rectiligne dans le sens du pendage en direction du canyon, utilisant préférentiellement la fracturation Ouest-Est et ses dérivées comme fil directeur. La galerie prend à plusieurs reprises des allures de vaste salle (Puits du Visconte, Salle Elmira, Miroir de Galadriel). Ces gros volumes sont liés à des phénomènes de détente et d'écroulement des parois dans des zones faillées et broyées. Le siphon de - 637 m occupe un tronçon de galerie préservée entre deux grandes salles d'effondrement. Le plan d'eau siphonnant résulte du barrage de blocs et de cailloutis accumulés à l'entrée de la salle aval.

Formes de détail et micro-formes abondent dans tout le réseau : les parois sont très corrodées, tant par l'actif que par les ruissellements pariétaux (wandkarren). Le torrent souterrain a façonné un nombre incalculable de cascades et de marmites qui marquent et rythment la progression des spéléologues.

Les remplissages sont discrets. Les dépôts détritiques sont dominés par des formations à granulométrie grossière : épandages de galets dans les élargissements du lit torrentiel, couche à galets et graviers dans une matrice sombre sablo-limoneuse à éléments volcaniques abandonnée dans les rares parties fossiles ou semi-fossiles. La couverture meuble des talwegs du plateau est mobilisée dès la surface sous forme de galets d'argile qui s'engouffrent dans les pertes. Les concrétionnement peuvent abonder sur les parois hors d'atteinte de l'actif et soumises au ruissellement fissural, apparemment très encroûtant. La calcite est massive, à cristallisation en auréoles concentriques à gros cristaux. Les concrétions mises au jour par l'érosion de surface sont complètement altérées et se réduisent facilement en bouillie, quelle que soit leur taille...

Au total, l'ensemble donne un réseau d'allure "alpine" qui tranche avec les grottes-tunnels percées de méga-dolines habituellement rencontrées dans ce contexte.

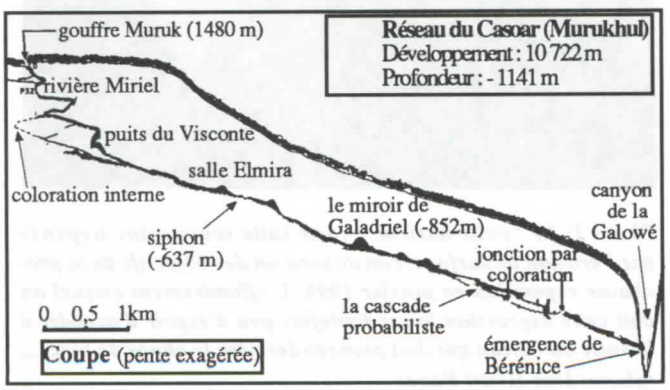

Figure 3 : coupe du système Muruk-Bérénice

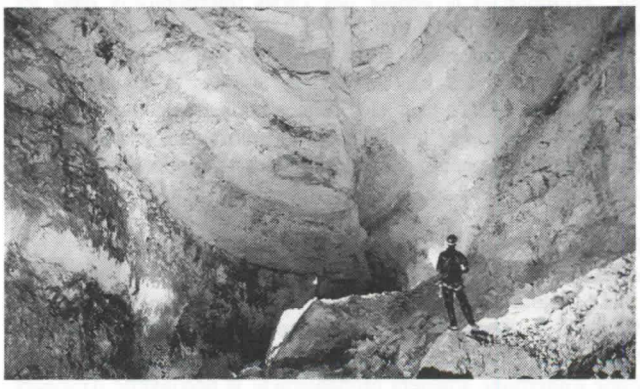

Photo 1 : La salle Elmira à - 630 m (cl. Sounier)

4 . Des problèmes karstogéniques à résoudre en 1998

Les relevés spéléo-morphologiques confrontés aux observations de surface permettent de soulever d'importantes questions spéléogénétiques et karstogéniques (reconnaissance et datation des phases de spéléogenèse, rapport entre le creusement de la cavité et l'incision du canyon où jaillissent en cascade les eaux du système etc...). Ce type de cavité apparaît d'ores et déjà comme fort intéressant pour rendre compte d'une possible spéléogenèse pré-quaternaire de nos grands réseaux des Alpes.

Une nouvelle expédition aura lieu en 1998, qui devrait permettre de recueillir des données complémentaires. Les thèmes d'étude envisagés se placent dans le prolongement des premiers résultats acquis, afin de préciser certaines données ou de vérifier des hypothèses.

Mieux connaître l'hydrogéologie du plateau

Le marquage des cheminements hydrogéologiques à l'aide de traceurs chimiques est l'un des principaux objectifs. Il s'agira par exemple de découvrir la destination des eaux de la rivière suivie jusqu'à la cote -1141m, qui semble s'écarter du drain principal (se dirige-t-elle vers les sources des Pléiades, reconnues quelques hectomètres à l'aval de Bérénice ?). Plus largement, la recherche de la limite entre les bassins-versants de Bérénice et de Mayang imposera certainement un multi-traçage entre les différentes cavités connues dans le secteur. Enfin, plusieurs liaisons hypothétiques avec le collecteur de Muruk restent à confirmer (Arcturus, Croix du Sud...). Compte-tenu des difficultés de parcours du terrain, la surveillance des différents points de sortie s'effectuera avec des fluocapteurs. Toujours dans le domaine des circulations souterraines, il reste à évaluer la part respective des apports provenant de l'infiltration directe des précipitations et de ceux provenant des talwegs fluvio-karstiques amenant de la montagne des torrents qui lors des crues atteignent les pertes.

Mieux connaître les modalités de l'érosion karstique

L'hydrochimie est un thème capital pour comprendre la répartition de la corrosion aux différents points du karst, que l'on soit en surface, en profondeur ou à proximité des émergences, voire même dans le canyon de la Galowe. La traversée du système offre une opportunité rare de pouvoir suivre tout au long du cheminement l'évolution des caractéristiques chimiques de l'eau, et donc les modalités de la corrosion. En revanche, la quantification de l'érosion mécanique, sans doute aussi efficace que la corrosion, semble beaucoup plus difficile à appréhender.

Mieux connaître la spéléogenèse en région intertropicale à forte surrection

La recherche sur les formes souterraines sera poursuivie en cartographiant la moitié aval du système. Nous chercherons en particulier des éléments de réponse pour interpréter la cause du profil en long tendu. De même, l'origine de la position perchée de l'émergence, vraisemblablement en relation avec l'évolution du canyon de la Galowe, pourrait apporter de précieuses indications sur l'évolution et la genèse des karsts intertropicaux dans les régions en forte surrection.

Cette approche morphologique s'appuiera sur une reconstitution chronologique, déduite de l'étude et de la datation des remplissages (U/Th sur les concrétions, paléomagnétisme). S'agissant d'un karst "jeune", sera-t-il pour autant possible de se caler temporellement dans les plages d'application de ces méthodes ?

Prendre en compte les autres composantes du milieu karstique

Le séjour dans cette région sauvage sera l'occasion de découvrir le fonctionnement de l'écosystème au travers de ses composantes les plus originales. La collecte d'échantillons de faune souterraine amènera probablement la découverte d'espèces nouvelles, adaptées aux conditions tout à fait particulières des karsts des forêts primaires équatoriales.

Malheureusement, l'avancée des compagnies forestières menace ces fragiles associations. Nous essayerons d'estimer la portée réelle de ces impacts, aussi bien sur la forêt elle-même, que sur les sols ou les écoulements. Sans compter les effets que peuvent avoir ces grandes entreprises sur la cohésion sociale des communautés villageoises locales.

Références

HACHE, Ph.; HOBLEA, F.; PHILIPS, M. ; SESSEGOLO, D. & SOUNIER, J. P. 1995. Muruk, hémisphère sud premier - 1000. *Spelunca* 60 : 35-54.

HOBLEA, F. 1995. Observations spéléo-morphologiques et hydrogéologiques dans le système karstique Muruk-Bérénice (île de Nouvelle-Bretagne, PNG). *Actes 5ème Rencontre d'Octobre*. Orgnac 1995. SCP, Paris : 50-69.

MAIRE, R. 1990. La haute-montagne calcaire. Thèse d'Etat. Karstologia Mémoires 3, 731 p.

LÖFFLER, E. 1977. Geomorphology of Papua New-Guinea. CSIRO, Camberra, 195 p.

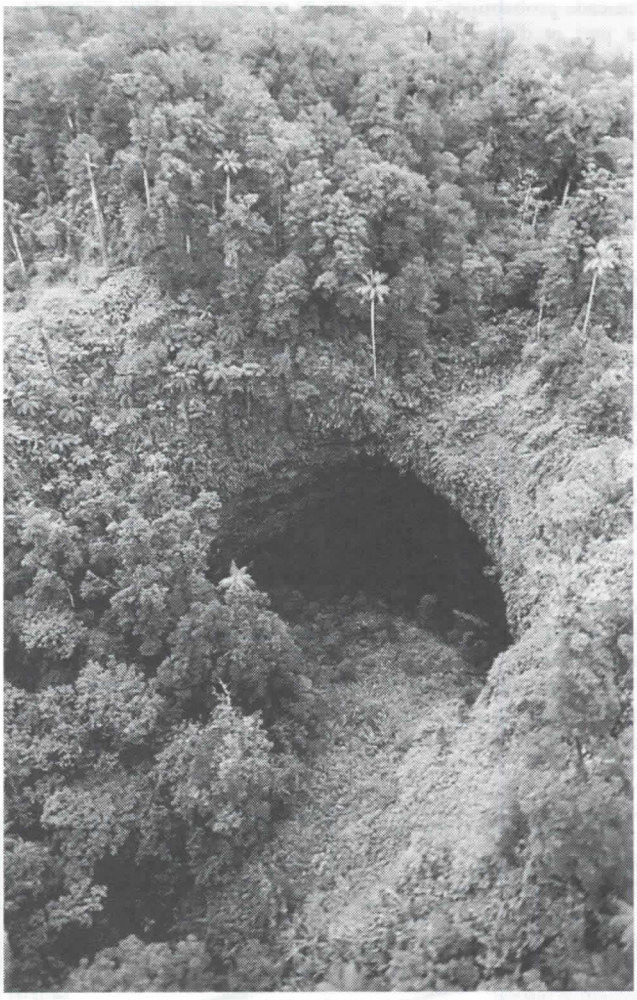

Photo 2: Le "puits-haricot", vaste salle souterraine trépanée par l'érosion de surface, constituera un des objectifs de la prochaine expédition en janvier 1998. L'effondrement auquel on doit cette dépression laisse toutefois peu d'espoir d'accéder à la suite du réseau qui doit plonger derrière le chaos de blocs... (photo: Luc-Henri Fage)

Lunan Shilin Landscape in China

SONG Linhua*, WANG Fuchang**
*Institute of Geography, Chinese Academy of Sciences, Beijing 100101, China
**Administration of Lunan Shilin National Park, Yunnan 652211, China

Abstract

The Lunan Shilin landscape mainly develop in the Lower Permian Qixia and Maokou limestone with a thickness of 480 m. The magic landforms made the geoscientists extensively study its origin and evolution. The Lunan shilin landscape has experienced 5 evolution stages. (1) Karst landform developed in the Lower Permian limestone. (2) In the late Permian, basalt and tuff covered the stone teeth and depressions. (3) Limestone and basalt-tuff ground surface experienced erosion and corrosion, the exposed or buried stone teeth and columns were developed from the late Permian to Mesozoic. (4) The Himalayan Tectonic Movement induced a strong uplift and created the fault basins in Yunnan Plateau. The Tertiary red deposits accumulated in Lunan Basin, covered the karst surface with its stone teeth and columns and filled the limestone fissures. The red deposits and weathering materials were eroded consequently. The subsoil erosion strongly separates the limestone block to form the subsurface stone teeth and forests. The upper part of columns are reformed by the rainwater to form the pinnacles.

The famous scenary of Lunan Shilin attracts more than 15 million visitors a year. The Lunan shilin was officially public in 1931, and the administration was set up in 1951. The main tourist areas are in good conditions for tourists, other subregions are reserved.

Physical Setting

The Lunan Shilin (Stone forest) landscape is 89 km far from Kunming, the capital of Yunnan Province, located in the central Yunnan Plateau (103°11' - 103°29' E, 24°40' - 24°56'). The altitude is about 1,500-1,900 m a.s.l.

From late Sinian to early Permian, carbonate rocks cover an area of 912 km^2, the shilin mainly developed in the lower Permian Qixia and Maokou limestone with a total thickness of 480 m. The limestone dips at 2 - 10°. The fractures with directions N40° W, N15° W and N50° E are well developed and their dipping angles drop in the range of 75-90°. Under the long term of warm and humid climatic condition, the karst strongly developed after the Maokou Limestone deposited. In the late Permian, the Emeishan basalt and tuff covered the karst surface and filled in the fissures of limestones. The fractured Emeishan basalt and tuff were benefit to the subjacent karst development. In the early Tertiary, the intensive uplift of the Himalayan Tectonic Movement caused faulted basins such as Lunan Basin, Luliang Basin and Kunming Basin. Red sediments with gypsum and marlite deposited in the Lunan Basin.

Karst is well developed in an area of 912 km^2, in which 350 km^2 of shilin landform have been defined as reserved areas including 17 subregions, such as the Major shilin, Minor Shilin, Outer Shilin, Naigu Shilin, Bucaowa Shilin, Weibuoye Shilin and Qingshuitan Shilin etc.

The shilin landscape may develop on the karst hills, slopes and in the depressions. The dimension of shilin in depressions is larger than that on the hills and slopes. The shilin landscape in Maokou limestone is more magnificent and beautiful than in other limestones.

Under the influence of deforestation, the intensive soil erosion has exposed the buried stone teeth and columns. The exposed shilin features are reformed by rainwater to create the pinnacles, solutional pots, gullies, fissures, through caves, wall troughs, holes and other features.

Evolution of Shilin Landscape

Based on the preliminary study, the shilin landscape has experienced long historical and complicated evolution stages (SONG, 1996):

The Maokou limestone was uplifted soon after deposition and formed the exposed karstic surface (Fig. 1-A); the stone teeth and forests developed at least 3-5 m high, the maximum pinnacle with depressions, sinkholes, pocket caves and other micro-features reaches a height of 10 m (Fig. 1-B).

The Emeishan basalts and tuffs covered the karst depressions, stone teeth, stone forests, sinkholes and shafts and filled in the limestone fissures. The fractures in basalts and tuff made rainwater percolate and dissolve the limestone to form the subjacent karst (Fig. 1-C). The fissures and cave passages in the Maokou limestone organized the maze structure within the epikarst.

In the Mesozoic, the Shilin area was in an environment of subaerial erosion, part of the basalt and tuffs were eroded away. A part of the limestone was re-exposed and eroded by rainwater to enlarge the fissures and form the

pinnacle features. In other places, the basalt and tuff still remained (Fig. 1-D). The new depressions developed well in the exposed limestone.

In the Eocene, the Himalayan orogeny caused the subsidence of the Lunan graben, and the red sediments deposited in the central basin up to 500 m. The limestone was deformed to develop two sets of vertical joints (N20-50°W and N40-60°E) controlling the gaps between the stone columns and pinnacles. The stone teeth and columns mainly developed near the lakes. At the end of Oligocene, the Lunan lake was dried out. In the Quaternary warm and humid climatic conditions, rainwater penetrated through the Eocene red beds to dissolve the limestone and intensify the subjacent karst to form larger stone teeth and columns (Fig. 1-E). Near the Shilin market, fissures filling with red sediments are about 10 m deep and 0.5-1.5 m wide.

In the Quaternary, a great amount of Eocene red beds were removed, but the weathered materials remained in the fissures and on limestone surface. Soil water rich in CO_2 strongly dissolved limestone to enlarge the karstic fissures in the exposed karst. The deepest fissure in the Heiqingdou Shilin reaches 30 m below surface. The most magnificent shilin and subsurface drainage systems were formed (Fig. 1-F). Sharp pinnacle crests, karren ridges, flutes and gullies are well developed. The features of Lunan shilin are very similar to the pinnacle karst in the Gunung Mulu National Park, Malaysia (SWEETING, 1979; WALTHAM, 1984, 1985).

Aesthetic values of Shilin Landscape and cultural heritage

In the main scenic spot of shilin park, the stone columns stand up to the blue sky. The rock lotus is blaming on the rock truck and out from the lake. After you snake in the gaps and climb to the top of the teeth, you may enjoy the stone elephant in the rock field and the beautiful phenics turning her neck to give you good wishes.

The Minor Shilin like the emperor garden, the small but beauty rock bamboo shoots grow up from the green land. The Sani girl Ashima with the flower and silver decorates and backing the flower basket is walking by the lake.

In the outer Shilin region, an old gentle man is walking around the shilin field and meets his daughter with her lovely son. The camel rides on the elephant, the rocket ranching, rocky towers and goat and sheep in the pasture, the mushroom grows in the dragon teeth field.

In Shilin area, the rocks dominate the Sani people life, animals like the elephant, camel, fish, cow, goal, horse, lion, tiger, birds, vegetation such as the mushroom, bamboo shoots, pine tree, weapons and house, what exists in the world you may see in the Shilin area.

As the excellent imagine of the rocks, the people copied the sceneries from Shilin to make the garden and the artists. The artists say that Shilin is their source to create the painting, novels, stories and dramas.

In Yunnan Province, there is a total population of 90,000 Sani people, a branch of Yi nationality. About 60,000 live in the Shilin area for a long time and created their own culture. Their pictographic characters remained on the rocky cliffs are very similar to the culture in Banpo Remains in Xian, that has 6000 year of history. The Sani people have their own dresses and hats decelerated with silver and cotton and silk embroider made by hand.

Management and protection of Shilin Landscape

The Lunan shilin landscape has been recognized since 300 B.C. many people visited and described it in poems and paints. In 1931, Mr. Long Yun, the chairman of Yunnan Province visited shilin and wrote the characters «Shi lin», late engraved on the stone column (WANG, 1994). The government then allocated the funds to build the trails through the gaps between stone columns and pavilion on the top of the highest columns.

During 1951-1960, the Shilin Administration Group was set up to manage and protect the landscape and environment. In 1962, the Administrative Office of the Shilin Scenic Area was established. In 1982, the first group of National Parks including Lunan Shilin was issued by the State Council of P.R. China. In 1987, the State Council approved the general plan of Lunan Shilin National Park, the park has been located and divided into 3 subregions based on the tourism development and scenery and environment protection. The Administration Bureau was officially set up. Now the environmental division of the Bureau is responsible for environment and landscape protection. The landscape and environment in the Lunan shilin Park will be protected following the Regulations of National Parks issued by the State Council and State Construction Ministry, Environmental Protection Law.

Many scientific research has been done. There are 50 papers and books which have been published.

Reference

CHEN ZHIPING, SONG LINHUA & M. M. SWEETING, 1985: The pinnacle karst of the stone forest, Lunan, Yunnan, China: an example of a subjacent karst. In: New Directions in Karst, Geobooks, Norwich. 597-607.

SONG LINHUA, 1986: Origination of Stone Forests in China. International Journal of Speleology. Vol. 15: 3-13.

SONG LINHUA, 1996. The Stone Forest landscape and its value as a tourist attraction. In FORNOS J. & GINES A., Karren Landforms. Universitat de les Illes Balears, 1996. 421-432

SWEETING M. M., 1979: Weathering and solution of the Melinan limestones in the Gunong Mulu National Park, Sarawak, Malaysia. Annales de la Societe Geologique de Belgique,T. 102.
WALTHAM A. C., 1984. Some features of karst geomorphology in South China. Transactions of British Cave Research Association, 11: 185-198.
WALTHAM A. C., 1995. The pinnacle karst of Gunung Api, Mulu, Sarawak. Transactions of British Cave Research Association, 22: 123-126.
WANG FUCHANG, LI ZHONGDE et al., 1994. Brief review of exploiting history of stone forest in LUNAN, YUNNAN. In: Song Linhua (Chief edi.); Study of Karst and Cave Scenicc Tourist Resources. Seismology Publishing House, 1994. Beijing. 219-222.
YE QINGTONG, 1982: Stone Forest and Karst (Unpublished).
YU JINBIAO, WANG XUEYU & WANG ZONGHAN, 1983: A preliminary study of age and palaogeographical environment of pinnacles in Lunan, Yunnan Province. Journal of Nanjing University. No.2 (1983): 362-374.
YUANG DAOXIAN, 1988: Glossary of Karstology. Geological Publishing house. Beijing.
ZHANG SHUYUE, 1984: The development and evolution of Lunan stone forest. Carsologica Sinica, Vol. 3, No. 3, 78-87.

This project is financed by the National Natural Science Fundation of China, No.49471008.

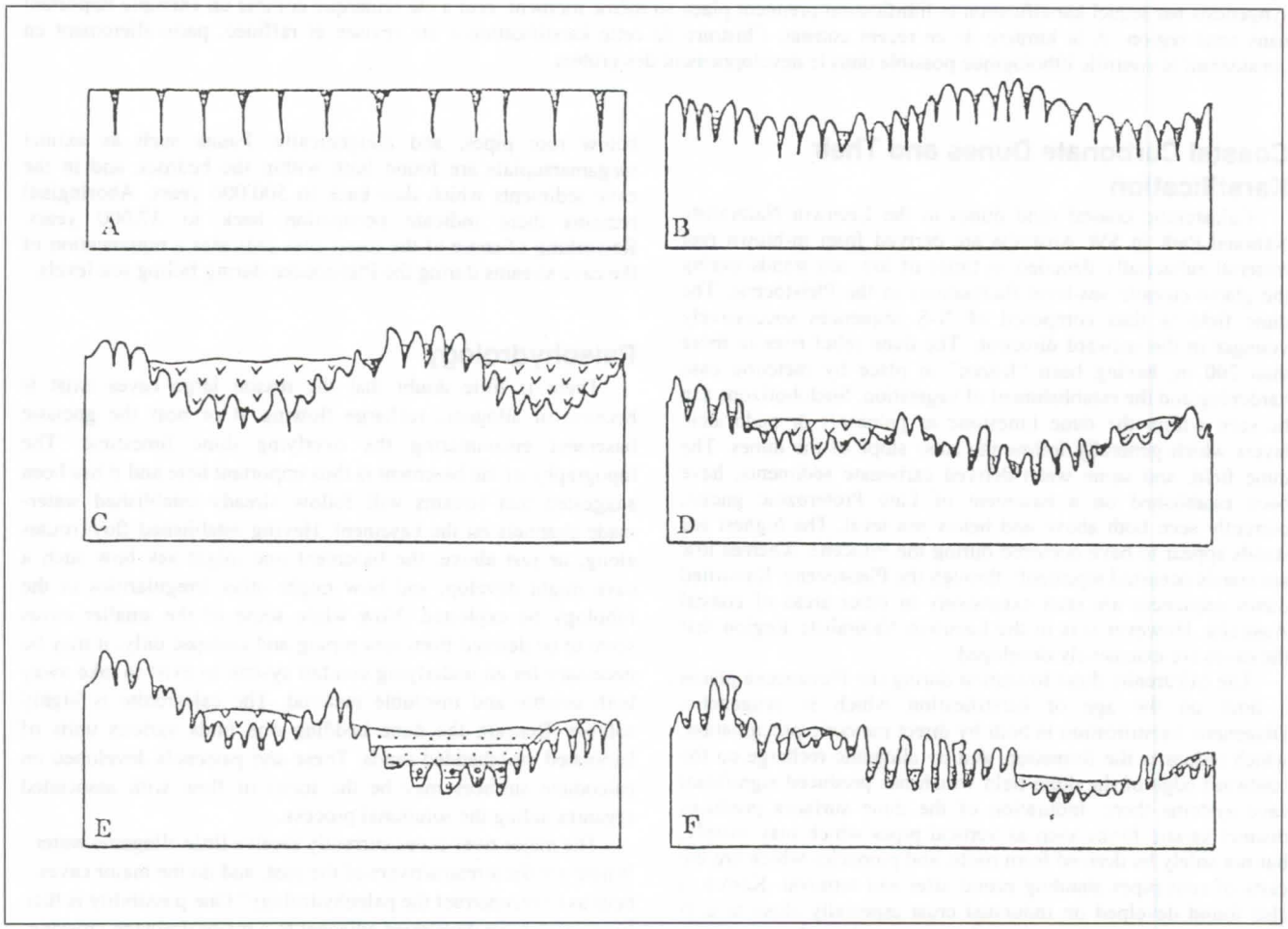

Fig. 1: A model of shilin landscape evolution in Lunan, Yunnan:

A. The original limestone surface after the Maokou limestone was deposited;
B. Karst surface features and epikarst developed in the late Permian;
C. The Emaishan basalts and tuffs covering the surface karst features in the expressions and basins during the upper Permian, with subjacent karst developed under the basalt
D. After erosion, part of the subjacent karst exposed to further development at the surface, with features including the stone teeth and stone forest;
E. Subsidence of the Lunan basin, and red sediments deposited in the lakes, covering the stone teeth and youthful stone forest; subjacent karst may be developed, and the exposed surface karst features were continuously modified;
F. With strong weathering and erosion, the subjacent karst under the red sediments has been exposed and the surface karst features have become well developed; the most spectacular stone forests develop in the valleys and depressions, and rainwater modifies the columns and stone teeth.

Speleogenesis of the Coastal Dune Karst of SW Australia

Charles J. Yonge[1], Jane Scott[2] and David J. Lowe[3]

[1] EIUDP, Universitas Sam Ratulangi, PO Box 1357, Manado 95013, Sulawesi Utara, Indonesia & Alberta KarstInstitute, PO Box 8213, Canmore, Alberta, Canada. E-mail: Yonge@manado.wasantara.net.id.

[2]Tourist Information Bureau, Margaret River, Western Australia. E-mail: mrshsst@griffin.bis.net.au.

[3]British Geological Survey, Keyworth, Notts, UK. E-mail: DJLO@WPO.NERC.AC.UK

Resume

Les dunes côtières de sable calcaire au Sud-Ouest l'Australie sont formées du matériel projeté du mur marin dénudé par le vent durant les marées basses de la période Pleistocène. La séquence des dunes est plus de 200 m d'épaisseur à certains endroits, ayant été consolidées sur place par un durcissement météorique, et s'étend dans le sous-sol gneissique Précambrien. La formation karstique contient d'énormes grottes, habituellement accessibles par de très grands effondrements ou des puits de grand diamètre. L'origine de ces grottes n'est pas entièrement comprise, même si des routes hydrologiques existent à partir de points recharge allogénique en direction des champs de dune et émergent en sources sur la rivage. La nature sableuse de cette pierre a comme résultat un bon nombre d'effondrement, avec de gros blocs ou des resserements de sable conduisant à de grandes cavernes, qui pourraient avoir leur origine comme les rivières de grottes. Comme résultat la karstification par l'action des racines du paléosol et l'imperméable sous-jacent jouent également un rôle important dans la spéléogenèse. Un des concepts l'évolution des karst, lequel a été grandement accepté, est celui de syngenesis par lequel karstification et lithification prennent place au même moment, ceci a été remarqué comme un exemple important dans cette région. A la lumière de ce récent constat, l'histoire de cette karstification a été revisée et raffinée, particulièrement en considérant le contrôle lithologique possible dans le développement des grottes.

Coastal Carbonate Dunes and Their Karstification

Calcarenitic coastal sand dunes in the Leeuwin Naturaliste National Park in SW Australia are derived from in-blown reef material subaerially denuded in times of low sea stands during the glacio-eustatic sea-level fluctuations in the Pleistocene. The dune field is thus composed of N-S sequences successively younger in the seaward direction. The dune relief rises to more than 200 m, having been "frozen" in place by meteoric case hardening and the establishment of vegetation. Such horizons can be seen within the dune limestone as paleosols or pedocalcic layers which generally follow the stoss slope of the dunes. The dune field, and some water-derived carbonate sediments, have been established on a basement of Late Proterozoic gneiss, currently seen both above and below sea level. The highest sea stands appear to have occurred during the Pliocene, whereas low sea stands occurred repeatedly through the Pleistocene. Karstified dunes sequences are seen extensively in other areas of coastal Australia. However it is in the Leeuwin Naturaliste Region that the caves are extensively developed.

The calcarenite dune formation during the Pleistocene places a limit on the age of karstification which is syngenetic. Diagenetic karstification is both by direct meteoric precipitation, which indurates the formation, and by allogenic recharge on the landward edge of the dune field which has produced significant cave systems there. Induration of the dune surfaces produces distinct karstic forms such as vertical pipes which may mainly, but not solely be derived from roots, and pinnacles which are the casts of root pipes standing proud after soil removal. Karren is also found develped on indurated crust especially close to cliff edges. Root pipes enlarge by subsequent vadose flow and may combine to create large shaft entrances. The significant speleogenic unit is the Tamala Limestone which comprises basal shallowing up sequences as well as overlying major dune units.

The Caves

More than 300 caves are reported between Cape Naturaliste to Cape Leeuwin, a N-S distance of some 90 km where the karstic dune field varies from 1-3 km wide. The Jewel-Easter Cave system is the longest with more than 8 km of passage reported. The southern caves are characterized by large, well-developed passsageways 10-20m wide, usually interrupted by collapse cones of boulders, sand and soil. The caves contain red-brown sediments that appear to be both derived from soil cones below root pipes, and allogenically. Fauna such as extinct megamarsupials are found both within the bedrock and in the cave sediments which date back to 500,000 years. Aboringinal remains there indicate occupation back to 37,000 years. Reworking of some of the fossil sites indicates a rejuvenation of the cave streams during the Pleistocene during falling sea-levels.

Paleohydrology

There is little doubt that the reason large caves exist is because of allogenic recharge flowing at or near the gneissic basement encountering the overlying dune limestone. The topography of the basement is thus important here and it has been suggested that streams will follow already established water-made channels on the basement. Having established flow routes along, or just above, the basement one might ask how such a cave might develop, and how might other irregularities in the lithology be exploited. Now while some of the smaller caves seem to be derived from root piping and collapse only, it may be necessary for an underlying conduit system to exist to take away both soluble and insoluble material. The calcarenite is highly soluble. Beneath the dune bedding one finds various units of laminated crossbedded sands. These and paleosols developed on paleodune surfaces may be the focus of flow with associated organics aiding the solutional process.

The major river caves currently receive little allogenic water. Where are the streams/rivers of the past, and do the major caves help us to reconstruct the paleohydrology? One possibility is that river caves have developed adjacent to a major drainage crossing the dune field that progressively stepped southwards due to tilting of the terrain against the Darling Fault. Three steps are suggested, the first two forming the Mammoth River Cave and then the Easter-Jewel Cave complex, with the final step steering drainage away from the dune field to the south giving the present-day Blackwood River. Rejuvenation, as evidenced by rapid flow scallops developed on large speleothems in Easter Cave, incision of the gneissic basement and re-excavation of sediments at other sites might be due to the -130m low sea stand at the Last Glacial Maximum (18,000 years BP).

Caves of the Republic of Mauritius, Indian Ocean

Gregory Middleton and William Halliday
Tasmanian Parks & Wildlife Service, G.P.O. Box 44a, Hobart, Tas. 7001 Australia and
IUS Commission on Volcanic Caves, 6530 Cornwall Court, Nashville, TN 37205, USA.

Abstract

In their *Underground Atlas,* MIDDLETON & WALTHAM (1986) dismissed Mauritius as: "very old volcanic islands with no speleological interest". Recent investigations indicate this judgement is inaccurate; there are over 50 significant caves, including lava tube caves up to 687 m long (one 665 m long was surveyed as early as 1769) and 35 m wide, and a karst cave over a kilometre in length (known since at least 1789). Plaine des Roches contains the most extensive system of lava tube caves with underground drainage rising at the seashore.

Notable fauna includes an insectivorous bat and a cave swiftlet *(Collocalia francica),* the nests of which are unfortunately prized for "soup". The caves are generally not valued by the people and are frequently used for rubbish disposal or filled in for agricultural development.

Résumé

Bien que les îles Maurice ne soient pas connues pour leur intéret spéléologique, de récentes recherches indiquent qu'il y a plus de cinquante cavernes importantes, comprenant des tunnels de lave allant jusqu'à de 687 m de long et 35 m de large, l'un d'entre eux, de 665 m de long a été découvert dès 1769, et un "karst" de plus d'un kilomètre de long, connu depuis au moins 1789.

La Plaine des Roches contient le système le plus étendu de tunnels de lave avec un écoulement souterrain qui s'élève au niveau du rivage. La faune importante de ces caves comprend de chauves-souris insectivores et de petites hirondelles (Collocalia francica), les nids desquelles sont malheureusement recherchés pour soupes de gourmets. Les caves ne sont généralement pas appréciées par les habitants qui trop fréquemment s'ent servent comme dépôts d'ordures ou d'entrepôts agricoles.

Location and geology

The Republic of Mauritius is comprised of two main islands in the southern Indian Ocean, the main one of 1,860 sq km, about 850 km east of Madagascar, and Rodrigues, 110 sq km, 560 km further east.

The main island is almost entirely volcanic, having originated about 13 million years ago in seabed eruptions which took until about 8 million years ago to reach the ocean's surface. The island's spectacular mountain chains and peaks are remnants of a large shield volcano, the centre of which subsided 5.5 million years ago to form the Mauritian caldera. The rest of the island was fashioned by suites of lavas (Hawaiian flows) emitted from 23 smaller, more recent volcanic structures. Lava flows have occurred as recently as 26,000 years ago in the Plaine des Roches area in the north-east (ANTOINE 1983). There are some limited exposures of calcareous aeolianite on the coasts of both islands and it comprises some small offshore islets.

The caves

Lava tube caves

Lava tube caves occur throughout the main island of Mauritius. Commonly they are the result of rapidly flowing basic (low silica) lavas cooling on the surface and forming a crust over the molten rock below. If the flow is cut off at its source and the lava continues to flow it can leave behind a void, the inner surfaces of which may contain a record of events during the cave's formation. Access to the tubes is generally only made possible by the eventual collapse of part of the roof.

These caves tended to form where conditions were optimal: small, non-explosive eruptions of basic lavas onto gently-sloping surfaces. By noting the orientation and extent of lava tubes it is possible to infer the sources of the relevant flows. Most lava tube caves are found in recent flows as these have had the least time to collapse and as later flows tend to obliterate features beneath them.

The principal localities in Mauritius where lava caves occur (see Fig. 1 and Table 1) are Plaine des Roches and

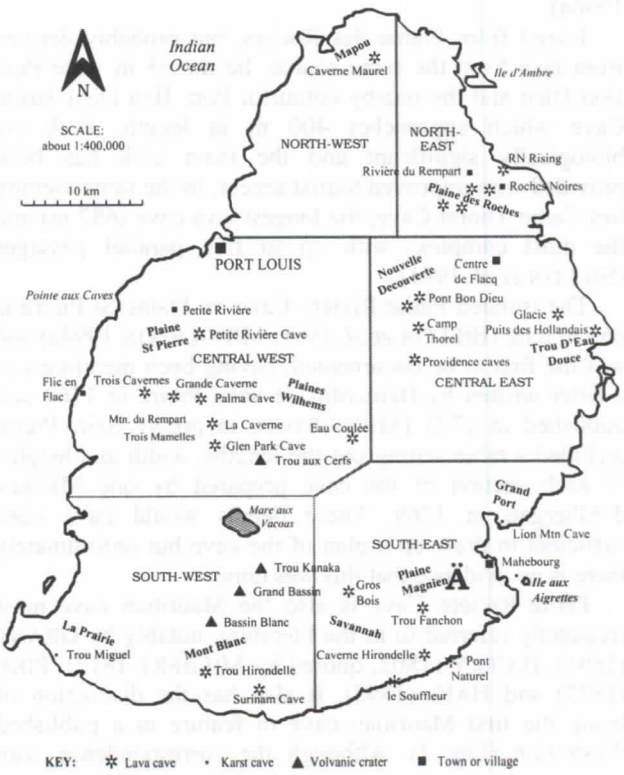

Fig. 1. Locations of the principle caves of the main island of Mauritius showing unofficial cave areas and regions.

Nouvelle Decouverte (originating from the Bar le Duc-l'Escalier volcanic system), Vacoas-Palma (Curepipe Point-Trou aux Cerfs-Verdun volcanic structures) and Mont Blanc-Surinam (Bassin Blanc volcanic system)(SADDUL 1995). In the south there is a scatter of small caves in the area extending from Savannah to Plaine Magnien and there is a single, isolated cave in the north at Réunion Maurel.

For convenience the main island has been divided into six regions and within these caves have been grouped into somewhat arbitrary 'cave areas', shown (in bold) on Fig. 1. The greatest concentration of caves occurs at Plaine des Roches. This is a flat to undulating area, comprised of probably the most recent lava flows on the island, derived from the Bar le Duc-L'Escalier volcanic system and partly from the Mont Pilon volcano (SADDUL 1995, p. 136). Middleton has documented some 29 cave entrances in this area and 16 discrete caves. The largest of these was surveyed by BILLON *et al.* (1991) at 520 m. It is a consistently large tube, 10 to 15 m wide and averaging about 10 m high. It contains one of the largest bat colonies in Mauritius, estimated at different times at from 10,000 individuals to 10 times that number. It also contains a small but important swiftlet colony of around 50 birds. Nine other lava tubes in the area exceed 100 m in length. A number of the Plaine des Roches caves contain water and, although no tracing has been done, it is believed that the water bodies are interconnected and that the whole system rises at an inlet on the coast. The rising was noted by CLARK (1859) and again by HAIG (1895) who suggested that the inlet was itself a collapsed cave.

Further south on the east coast, near Trou D'Eau Douce, lies the interesting Puits des Hollandais, a water filled circular hole over 10 m in diameter and around 28 m deep. The hole opens out with increasing depth attaining a diameter of over 40 m at the bottom (MIDDLETON, 1996a).

Inland from Plaine des Roches, but probably derived from lava from the same source, lie the 35 m wide Pont Bon Dieu and the nearby colourful Pont Bon Dieu Jardin Cave which approaches 400 m in length. Both are biologically significant and the main arch has been provided with improved tourist access. In the same vicinity lies Camp Thorel Cave, the longest lava cave (687 m) and the most complex, with up to five parallel passages (BILLON *et al.* 1991).

The isolated Petite Rivière Cave on Plaine St Pierre is 665 m long (BILLON *et al.* 1991; MIDDLETON 1994a) and was the first to be documented, having been mentioned in a letter written by Bernardin de Saint-Pierre in 1769 and published in 1773 (MIDDLETON, in press). Saint-Pierre included a table setting out the lengths, width and heights of each section of the cave prepared by one Marquis d'Albergati in 1769. These details would have been sufficient to draw up a plan of the cave but unfortunately there is no evidence that this was done.

Petite Rivière Cave is also the Mauritian cave most frequently referred to in the literature, notably by GRANT (1801), BAILLY (1802, quoted by MILBERT 1812), PIKE (1873) and HAIG (1895). It also has the distinction of being the first Mauritian cave to feature in a published illustration (Fig. 2). Although the correspondence with reality is slight, there can be little doubt that de Sainson's drawing of 1828, published in D'URVILLE (1830) is meant to be the Petite Rivière Cave.

South of Petite Rivière on Plaine St Pierre lie the Trois Cavernes, caves of considerable historical interest because FLINDERS (1814) recorded that the largest was used as a refuge by escaped slaves in the 1770s, over 50 having been caught there on one occasion by police. He recorded that "little oblong enclosures, formed with small stones by the sides of the cavern, once the sleeping places of the wretches, also [still] existed, nearly in the state they had been left" (FLINDERS 1814). MIDDLETON (in press) believes some of these stone arrangements persist to this day.

There are a few caves in the Plaines Wilhems area near the centre of the island, notably Glen Park Cave (440 m) and Palma Cave (210 m). The former frequently contains a significant stream while the latter is of considerable biological importance. A cave at La Caverne has clearly been known for a long time as it gave its name to the locality; it was modified with concrete in the past for the storing of cheese and butter.

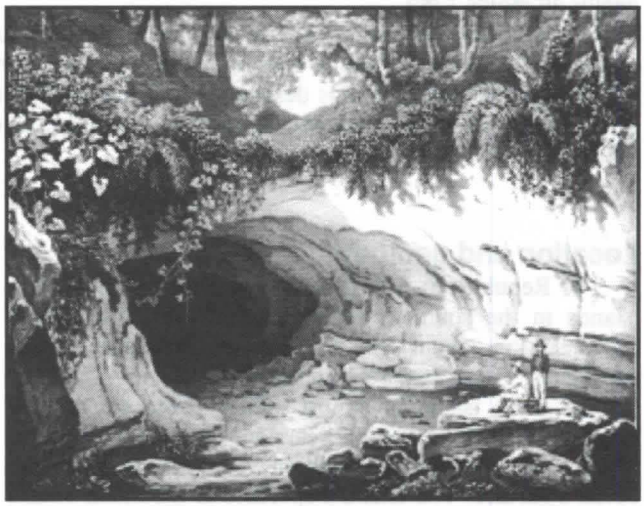

Fig. 2. "Une Grotte du quartier de la grande rivière (Ile Maurice)" by de Sainson - first published illustration of a Mauritian cave.

Of the caves in the south, probably associated with the Bassin Blanc volcano, Trou Hirondelle, 442 m long and containing a significant swiftlet colony, is worthy of mention (MIDDLETON 1994b), as is Surinam Cave which contains the largest known swiftlet colony (650 individuals in August 1996 - Hauchler, pers. comm.) and a unique sudden drop of about 12 m.

Karst caves

The country's second island, Rodrigues, has the most significant limestone caves (HALLIDAY & MIDDLETON 1996). Caverne Patate in Plaine Corail in the south-west, is the longest cave in Mauritius, totalling 1150 m (PC1-2-6), and the only show cave. Sadly, the use of flaming torches for lighting and speleothem collecting over many years have greatly detracted from the cave's aesthetic appeal (MIDDLETON 1996b). Other significant caves nearby are Caverne Safran and Caverne Tamarin. The Rodrigues caves achieved fame in scientific circles following the collection in them from 1786 of bones of the then recently-extinct flightless solitaire *(Pezophaps solitaria)*. Many

Table 1 - Documented caves by Region and Area

Region	Area	No. of caves	Total length (m)
North-West	Mapou	1	225
North-East	Plaine des Roches	16	2,500
Central West	Plaine St Pierre	6	900+
	Plaine Wilhems	9	930
Central East	Nouvelle Decouverte	11	1,535
	Trou D'Eau Douce	2	35
South-West	La Prairie*	2	70
	Mont Blanc	6	800+
South-East	Grand Port*	2	70
	Ile aux Aigrette*	1	7
	Plaine Magnien	1	20?
	Savannah	3	205
Rodrigues	Plaine Corail*	4	1,600
	TOTAL	64	8,900+

* Karst area, other areas are lava.

excavations for bones were conducted between 1831 and 1875 (NORTH-COMBES 1971).

Limestone, in the form of calcarenite/aeolianite, exists in fairly small deposits on the coast of the main island and comprises some offshore islets. Trou Miguel, on the south coast at La Prairie, is infamous as the site where two cave divers drowned in 1972 (LATTIMER 1977). There is a vertical drop 12 m to the normal water level and the water is reported to be at least a further 21 m deep. There are at least two further small but interesting limestone caves on the south east coast near Vieux Grand Port and at least one partly water-filled cave on Ile-aux-Aigrettes (MIDDLETON 1994c).

Since the areas of limestone on the main island are extremely small, only on Rodrigues is there any likelihood of further significant karst caves being found.

Cave fauna

The most obvious element of the cave fauna is the cave swiftlet, *Collocalia francica.* This bird, which navigates underground using audible echolocation 'clicks', nests in suitable caves all over the island and was once very numerous (CHEKE 1987). It is now threatened by sealing of caves and by thefts of its nests, apparently for making 'birds nest soup'. Populations in particular caves have dropped from 'thousands' to rarely more than a hundred. They also occur in Réunion, which is the western limit of the genus, but not on Rodrigues.

Another cave-dwelling vertebrate is the free-tailed bat, *Tadarida acetabulosus.* Very large colonies occur in two caves in the Plaine des Roches cave area but elsewhere colonies seldom number 2,000. A second species, the tomb bat, *Taphozous mauritianus,* is not known to inhabit Mauritian caves. Neither species occurs in Rodrigues but both are found in Madagascar and Africa.

Egg scars on the roofs of caves at Roches Noires and Plaine St Pierre indicate that these provided suitable sites for Gunthers gecko, *Phelsuma guentheri,* to attach its eggs. These are presumed to be very old as the species has been extinct on the mainland for about 200 years.

The shells of many species of land snails are regularly found at cave entrances and under daylight holes. Subfossil shells of *Tropidophora carinata* (extinct since the 1880s) are common in at least two caves at Plaine des Roches and Pont Bon Dieu. The fact that some still had their opercula in place indicates they died in situ and were not washed into the cave (O. Griffiths, pers. comm.).

Little has been published on the invertebrate fauna of Mauritian caves, but thanks to STRINATI (in press), Mauritius will soon be included in *Encyclopaedia Biospeologica II.* Strinati has collected at least one new species, an endemic thysanuran (MENDES 1996).

Threats to the caves

Most Mauritian caves have been damaged or are under some form of threat. An unknown number have had their entrances filled in the development of sugarcane plantations. This practice still continues, as does the widespread dumping of industrial and household waste into caves. At Palma a cave has been sealed by the construction of an underground temple.

Although water from caves is sometimes used for irrigation and domestic purposes, there are places where domestic waste, including sewage, discharges directly into the ground. There appears to be no realisation that the aquifer is at a shallow depth and that very limited purification takes place where there is conduit flow.

While the most unfortunate practice of using flaming torches for illumination has ceased in Caverne Patate, it is not unusual for local youths to burn tyres in the lava tube caves of Mauritius, with disastrous results. The worst case is at Caverne Maurel where most of the cave's surface is covered with a deposit of carbon. In at least one cave "black magic" is still being practiced; in the process material is burned on a stone "altar".

The numbers of cave swiftlets have declined steadily over the years and their nests are still taken indiscriminately despite the fact that this is illegal. Recent reports (Hauchler, pers. comm.) indicate this practice may be declining.

The only caves with any measure of protection are:

Caverne Patate where access is restricted to supervised parties of tourists (although a great deal of physical damage has already been done);

Pont Bon Dieu where the Ministry of Environment has built a fence to prevent rubbish dumping and local youth groups have tidied the access pit;

Palma Cave where the Ministry has, with the concurrence of the owner, built a fence around the entrance to try to prevent removal of swiftlet nests (unfortunately the fence has been cut and the padlock of the gate broken open); and

Petite Rivière Cave where the Medine Sugar estate has built a substantial grille across the entrance to try to protect the swiftlets (unfortunately the gate, which was regularly broken open, was demolished in August 1996 with explosive).

Attempts have been made to fence cattle out of *Caverne Tamarin* on Rodrigues, but so far without success.

Appreciation of the country's cave resources is coming only slowly and belatedly to Mauritius. It now seems likely that a concerted program to document, assess and conserve at least a representative sample of Mauritian caves will be undertaken.

Acknowledgments

Dr Trevor Shaw provided many of the historical references; Clement Moutou, Jörg Hauchler, Mario Allet and Paul Moolee made invaluable contributions to the field work; Owen Griffiths and Pierre Strinati contributed the de Sainson illustration and biological details; Carl Jones advised in relation to vertebrates; thanks to Prem Saddul for geological and geomorphological details and for constructive criticism; thanks to Jörg Hauchler for constructive criticism and updating; Yousoof Mungroo, Director of the National Parks & Conservation Service, made much of the work possible.

References

ANTOINE, R. 1983 La derniere coulée de laves à l'île Maurice. *Revue Agricole et Sucriere,* 62(2):91-92

BILLON, F., CHOJNACKI, P., BILLON, C., & ROUSSEAU, G. 1991 *Explorations souterraines à l'île Maurice* Spéléo-Club Nivernibou: Decize, France 46 pp.

CHEKE, A.S. 1987 The ecology of the smaller land-birds of Mauritius [IN] DIAMOND, A.W. (Ed.) *Studies of Mascarene island birds* Cambridge Univ. Press: UK pp. 151-207

CLARK, George 1859 A ramble round Mauritius with some excursions to the interior of that island … [in] Palmer & Bradshaw *The Mauritius register: historical, official and commercial* pp. i-cxxxii Port Louis: L. Channell. Reprinted in *La Revue Agricole,* 24(1):34-51; (2):96-114 (1945)

D'URVILLE, J.S.C. Dumont, le Comte 1830 *Voyage de la corvette l'Astrolabe. Exécuté par ordre du Roi, pendant les années 1826-29 sous le commandement de M. J. Dumont D'Urville.* J. Tastu: Paris. "Atlas", vol. 2, pl. 243.

FLINDERS, Matthew 1814 *A voyage to Terra Australis undertaken for the purpose of completing the discovery of that vast country* G. & A. Nicol: London 2 vols.

GRANT, Charles 1801 *The history of Mauritius or the Isle of France and the neighbouring islands ... composed principally from the papers and memoirs of Baron Grant, ... by his son* W. Bulmer & Co.: London

HAIG, H. de Haga 1895 Physical features and geology of Mauritius. *Quart. J. Geol. Soc. London,* 51(Aug. 1895):463-471.

HALLIDAY, W.R & MIDDLETON, G. 1996 A subdued karst on the island of Rodrigues, Mauritius pp. 345-354 [in] Fornós, J-J. & Ginés, A. (eds.) *Karren Landforms.* Universitat de les Illes Balears: Palma de Mallorca.

LATTIMER, R. 1977 *The Mauritius Underwater Group 1963-1977.* Michel Robert: Quatre Bornes, pp. 19-21.

MENDES, L.F. 1996 Further data on the Nicolettidae (Zygentoma), with a description of a new species from Mauritius. *Revue Suisse de Zoologie,* 103(3):749-756.

MIDDLETON, G. 1994a Rambles under Mauritius #1 — Petite Rivière. *J. Syd. Speleol. Soc.,* 38(8):131-133.

MIDDLETON, G. 1994b Rambles under Mauritius #2 — Chemin Grenier. *J. Syd. Speleol. Soc.,* 38(9):149-150.

MIDDLETON, G. 1994c Rambles under Mauritius #4 — Ile aux Aigrettes. *J. Syd. Speleol. Soc.,* 38(11):185-186.

MIDDLETON, G. 1996a Rambles under Mauritius #6 — Puits des Hollandais. *J. Syd. Speleol. Soc.,* 40(1):3-5.

MIDDLETON, G. 1996b Rambles under Mauritius #7 — Plaine Corail, Rodrigues. *J. Syd. Speleol. Soc.,* 40(6):83-94.

MIDDLETON, G. in press Early accounts of caves in Mauritius. Presented at Second Australian Seminar on Spelean History, Sydney, July 1994

MIDDLETON, J. & WALTHAM, T. 1986 *The Under–ground Atlas* Robert Hale: London. p. 134

MILBERT, J. 1812 *Voyage pittoresque à l'isle-de-France, au Cap de Bonne Espérance et à l'Isle de Ténériffe* Nepveu: Paris Vol. 1 pp. 358-360 and Vol. 2 pp. 102-104

NORTH-COMBES, A. 1971 *The island of Rodrigues.* The Author & Mauritius Advertising Bureau: Port Louis pp. 259-270 [Extracts reprinted in *J. Syd. Speleol. Soc.,* 35(9):171-175].

PIKE, Nicholas 1873 *Sub-tropical rambles in the land of Aphenapteryx: personal experiences, adventures & wanderings in and around the island of Mauritius* Sampson Low, Marston, Low & Searle: London

[SAINT-PIERRE, Bernardin de] 1773 *Voyage à l'Isle de France, à l'Isle de Bourbon, au Cap de Bonne Espérance par un officier du Roi* Amsterdam, Vol. 1, pp. 249-254

SADDUL, P. 1995 *Mauritius: A Geomorphological Analysis.* Mahatma Gandhi Institute: Moka 340 pp.

STRINATI, Pierre in press Ile Maurice [in] *Encyclopaedia Biospeologica II.*

Genèse de la dépression de Soulages (Causse de Sauveterre) : une explication nouvelle

par Bernard Loiseleur
Chemin de la Liasse 39, F-69570, Dardilly, France

Résumé

La région nord des grands causses (causse de Sauveterre et causse de Sévérac) présente un grand nombre de phénomènes volcaniques ayant affecté la série sédimentaire jurassique. Ceux-ci s'alignent d'ouest en est le long d'une série de failles dont la principale est la faille des Vignes. Ces manifestations sont au nombre d'une vingtaine et il s'agit le plus souvent de dicks ou de necks et de coulées basaltiques.

Mais il existe aussi au moins une dépression identifiée comme le vestige d'un cratère volcanique. Celle-ci, la doline des Croses, située sur le Causse de Sévérac, a été identifiée comme telle par des relevés d'anomalie magnétique. Par analogie, la doline de Soulages, située sur le Causse de Sauveterre et considérée comme l'archétype des mégadépressions endoréiques, paraît aussi devoir être identifiée avec un cratère de volcan aujourd'hui partiellement comblé par des remplissages.

Abstract

North part of the large Causses region (Causse de Sauveterre and Causse de Sévérac) presents some volcanic phenomenas which affect the jurassic sedimentary mantle. . They are lined up from west to east, along some faults, the main one is the Vignes fault .It is possible to count about twenty phenomenas, mostly dicks, necks and lava flows.

There is at least one explosion crater known, forming a very large dolina. This one, the Croses dolina (Causse de Sévérac), was such indicated by magnetic disturbances analysis. On the Causse de Sauveterre, the Soulages dolina, which is a typical exemple of large endoreic sink, seems to be also a volcano crater, today partly filled in by coarse wastes.

1. Introduction

Le phénomène karstique décrit ici est une très vaste doline située sur le causse de Sauveterre dans le département de la Lozère en France. Cette doline est considérée comme la plus vaste dépression endoréique des grands Causses. Jusqu'ici, sa genèse passait pour purement karstique. Cette explication traditionnelle ne rendait pas compte de l'ampleur de la dépression, disproportionnée avec son environnement.
Une comparaison avec la doline des Croses dont l'origine est maintenant considérée comme volcanique (Carte géologique de la France à 1/50 000 - notice) nous permet d'avancer une nouvelle explication quant à la formation de la doline de Soulages.

2. Le cadre régional : le volcanisme des grands causses

Le volcanisme qui a affecté l'Aubrac, les grands Causses et le Vivarais dans la partie méridionale du Massif central s'est étendu sur une période longue et assez tardive : du Miocène dans les Coirons (Ardèche) au Villafranchien pour les plateaux de l'Aubrac et les Grands Causses. Rappelons par ailleurs que des épisodes éruptifs beaucoup plus récents ont affecté le Vivarais et l'Auvergne (quelques milliers d'années seulement !). Ils résultent des contrecoups des mouvements affectant la chaîne alpine. Les dernières éruptions affectant la région de Clermont-Ferrand remontent même à la période historique.

Localement, la région allant du détroit de Rodez aux gorges du Tarn est parcourue d'une série d'accidents tectoniques importants dont l'importante faille des Vignes orientés grossièrement est-ouest. Le long de cette faille d'une part et à quelque distance au nord d'autre part, on trouve toute une série de phénomènes volcaniques qui ont affecté la série sédimentaire constituant les causses du Comtal, de Sévérac et du Sauveterre. Il s'agit soit de pointements basaltiques sous formes de dykes et necks amenés au jour par l'érosion comme à Buzeins, aux Croses, à Coussergues, et plus à l'est à Sauveterre, soit de coulées probablement aériennes comme à Montfalgous ou Aguès. La datation radiométrique de certains phénomènes (GILLOT P.Y., 1974) situe leur âge entre 4 millions d'années (Montfalgous) et 14 millions d'années (Coussergues). La coulée des Vignes recoupée par les Gorges du Tarn est d'origine différente et beaucoup plus ancienne (155 Ma).

3. La doline des Croses

La doline des Croses constitue notre site-type. Elle se situe sur le causse de Sévérac, environ 10 km au nord-ouest de Sévérac-le-Château, dans le département de l'Aveyron. Son diamètre au niveau du fond est de 500 mètres et elle offre une forme régulière en cuvette à bords peu redressés très remarquable. Son fond est très plat et présente vers le coin nord-ouest un entonnoir d'absorption.

Figure 1 : Neck basaltique de la dépression des Croses

Au printemps et lors de fortes pluies, le fond de la dépression est envahi par les eaux qui s'engouffrent alors dans cette perte. Le diamètre de la dépression au niveau de la couronne de sommets est de 1500 mètres.

Le fond de la dépression est bordé par de petites barres rocheuses établies dans les dolomies du bathonien. Son diamètre est disproportionné par rapport aux phénomènes karstiques environnants, nombreux mais, somme toute, de dimensions modestes . Sur les pentes menant aux sommets voisins, de nombreuses dolines aux bords rocheux de quelques dizaines de mètres de diamètre au plus parsèment la surface du causse. La doline est creusée de 130 mètres au plus par rapport aux sommets environnants : le fond en est situé à l'altitude de 750 mètres et le Puech de la Dreig au nord culmine à 879 mètres. Le point le plus bas de la couronne de crêtes qui l'entourent est à 800 mètres du coté est ou un col faiblement marqué assure la jonction avec la vallée sèche de Combelongue.

Sur le pourtour de la dépression, quatre avens d'une profondeur maximale de 30 mètres sont répertoriés. A 2 km au nord-nord-est, les importantes exsurgences de Lestang drainent un vaste secteur sur la bordure nord du causse de Sévérac limité au dessus de la vallée de la Serre par les escarpements dolomitiques du bajocien.

La carte géologique indique plusieurs affleurements basaltiques proches. Ils se présentent sous la forme de deux necks affleurants 200 mètres à l'ouest du fond de la dépression. Par ailleurs, de nombreux blocs de basalte isolés ou sous forme de coulées se trouvent épars sur son pourtour. Toutefois, malgré ces indices, jusque vers 1975, la doline des Croses était considérée comme d'origine purement karstique. A telle enseigne d'ailleurs qu'une désobstruction avait été entamée par l'auteur dans la perte qui draine la doline. Bien que la coloration n'ait pas été faite, les eaux qui y disparaissent resurgissent très probablement à Lestang. Aussi, la doline passait pour une forme endoréique particulièrement importante dont la genèse s'expliquait assez mal dans le contexte karstique local.

Des relevés magnétiques de surface, réalisés par G. Senaud et J. Roux, ont mis en évidence une structure très inattendue en cet endroit. Ils sont décrits dans la notice explicative de la carte géologique de la France (1/50 000) indiquée ci-après. En effet, ils révèlent une anomalie magnétique locale qui, pour les auteurs, s'explique par l'existence d'une masse basaltique assimilée à un lac de lave d'une épaisseur de 100 mètres au moins à 40 mètres sous la surface topographique actuelle. Ce lac occupe un cratère dont la genèse est rattachée à un épisode explosif antérieur.

De ce fait, il apparaît que l'on se trouve en face des vestiges d'un cratère de volcan aujourd'hui partiellement comblé par les matériaux détritiques provenant de l'altération des pentes environnantes. L'origine de la dépression est donc toute différente de ce que l'on imaginait avant la campagne de relevés magnétiques. L'épisode éruptif s'est déroulé en deux temps : tout d'abord une phase explosive amenant la création du cratère puis une phase effusive entraînant le remplissage du cratère par le lac de basalte aujourd'hui détecté en profondeur. Elle démontre l'existence de phénomènes originaux que l'on ne s'attend pas à trouver dans le contexte caussenard. Malheureusement aucune datation n'a été effectuée sur les laves basaltiques du site. Mais l'analogie avec les sites proches de Buzeins et de Montfalgous laisse supposer un âge compris entre 4 et 7 millions d'années, soit contemporain du début de l'enfoncement des cours d'eau actuels (Lot, Aveyron, Tarn) à partir de la surface d'aplanissement attribuée à la période ponto-pliocène.

4. La doline de Soulages

A 11 km à l'est de Sévérac-le-Château se trouve sur le causse de Sauveterre une dépression bien plus vaste et profonde que la précédente, connue sous le nom de doline de Soulages. Comme aux Croses, elle est drainée à proximité de son bord sud par un entonnoir d'absorption obstrué par des blocs, le puits de la Londe. Lors des fortes pluies, le fond de la doline est là aussi envahi par les eaux. Une zone marécageuse de plusieurs hectares alimente un ruisselet permanent qui se jette dans la perte. Un début de désobstruction de la perte a été entamé par un groupe spéléologique de la région. Cette désobstruction s'est opérée dans un remplissage de blocs à une trentaine de mètres du bord de la doline. L'épaisseur du remplissage à cet endroit est inconnue.

Figure 2 : Vue générale de la dépression de Soulages

Le fond de la dépression est elliptique et mesure 800 mètres sur 500. Le diamètre à la ligne de crêtes est de 2 km. La forme en est remarquablement régulière et ses dimensions sont tout à fait exceptionnelles pour le causse de Sauveterre où aucun autre phénomène karstique de même nature n'atteint une taille comparable. Il semble même s'agir de la plus vaste forme de doline en chaudron de l'ensemble des grands Causses. Le point bas de la dépression est à 774 mètres d'altitude, le point culminant de la couronne de sommets qui l'entourent est à 963 mètres au serre de la Garde. La profondeur maximale par rapport aux sommets environnants est de 190 mètres. Le point le plus bas est constitué, coté est, par un petit col à 838 mètres du côté du hameau de Soulages. Comme aux Croses, le bord de la doline est souvent formé par de petites barres rocheuses émergeant du remplissage.

Dans la littérature, cette dépression est considérée comme une forme endoréique très ancienne (ROUIRE J, 1973) qui aurait assuré le drainage de cette zone du causse du causse vers les exsurgences de Bouldoire et Fontmaure situées en rive droite du Tarn respectivement à 4700 et 5500 mètres en plan et 350 mètres plus bas. Une coloration, effectuée le 15 mai 1971 (POMIE J., 1974 et 1979), a mis en évidence cette liaison. L'auteur en a tiré des conclusions sur la genèse de la dépression. Il l'assimile à un poljé raccordé sur une vallée sèche aérienne dont les eaux auraient été évacuées par une grotte-tunnel aujourd'hui obstruées par les éboulis du fond de la dépression. Cette hypothèse est confortée par l'existence de plusieurs avens importants à proximité (aven de Cassan, -202 m).

Son creusement aurait dans ces conditions été nécessairement antérieur à celui du Tarn puisqu'il supposerait l'existence d'une nappe phréatique de haut niveau. Le niveau de

base aurait du alors être proche de l'altitude actuelle du fond de la dépression. Des dépression de ce type, aujourd'hui non fonctionnelles, existent par exemple sur le causse Méjean (plaine de Chanet, plaine de Carnac). Elles sont datées de la fin du tertiaire et présentent néanmoins une morphologie bien différente de celle de Soulages : typiquement celle de poljés, forme allongée et fond plat.

Figure 3 : Perte du puits de la Londe

Or la carte géologique mentionne sur la bordure sud de la dépression des affleurements de roches volcaniques. Par ailleurs, comme la dépression des Croses, la doline de Soulages est située 2 kilomètres au nord de la faille des Vignes. Précisément, l'observation des phénomènes volcaniques régionaux montre en fait deux alignements d'objets bien distincts L'un se situe exactement sur le trajet de la faille des Vignes (Coussergues, Buzeins, Lagarde, ...), l'autre est à peu près deux kilomètres au nord du trajet de la faille : Agués, Les Croses, Montsire. Celui d'Agués en particulier, absent de la carte géologique, est une coulée aérienne identique à celle de Montfalgous plus au nord-ouest. Pour expliquer cet alignement, il est possible de faire appel à l'existence d'un accident tectonique qui n'affecte pas la couverture sédimentaire du socle métamorphique, la carte géologique n'en faisant pas mention.

Il nous paraît alors possible de présenter une autre genèse pour la doline de Soulages. Il s'agirait des restes d'un cratère d'explosion semblable à celui des Croses rempli ensuite par un lac de laves basaltiques. Il est clair que par ailleurs, l'érosion a depuis profondément modifié le site, d'une part en entraînant un abaissement de la couronne sommitale du cratère, et d'autre part en comblant celui-ci par les débris ramenés des pentes sur plusieurs dizaines de mètres de hauteur. Par ailleurs, l'existence d'une telle dépression a entraîné lors des phases froides la mise en place d'un réseau aérien de drainage aujourd'hui fossilisé. Toutefois, l'allure générale de la dépression, par exemple lorsqu'on la voit depuis le petit col précédant le hameau de Soulages, ou depuis la route D32 au niveau de La Bastide, rappelle indiscutablement un cratère de volcan, aussi inattendu que celui-ci puisse être au centre du classique domaine karstique que constitue le Causse de Sauveterre.

Cette genèse n'est pas incompatible avec les résultats de la coloration montrant la relation entre le puits de la Londe et les exsurgences de la vallée du Tarn. En effet, les eaux infiltrées près du bord sud de la dépression peuvent parfaitement ruisseler sur la surface du dôme basaltique sous-jacent avant de rejoindre les roches karstifiables encaissantes. Par contre, elle rend improbable le succès d'une désobstruction de la perte.

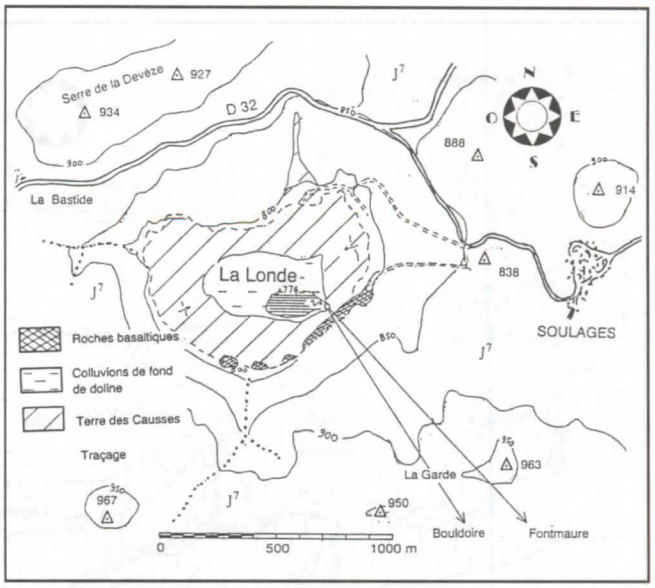

Figure 4 : Plan de la dépression de Soulages

Il nous semble donc nécessaire de reconsidérer la genèse de la dépression. Celle que nous avançons ne correspond pas à ce que l'on s'attend à trouver dans ce type de paysage. Elle a le mérite d'expliquer le gigantisme d'une forme jusqu'ici considérée comme purement karstique et de l'intégrer dans l'importante activité volcanique qui a caractérisé la région au villafranchien.

5. Conclusion

Il apparaît que certaines formes jusqu'ici considérées comme résultant d'une évolution karstique normale doivent être revues quant à leur genèse. L'existence de nombreux vestiges d'origine volcanique sur les causses de Sévérac et de Sauveterre permet d'avancer une nouvelle explication plausible quant à la formation de la méga-doline représentée par la dépression de Soulages. Une analyse d'anomalie magnétique permettrait de confirmer ou d'infirmer cette hypothèse.

Cartographie

DEFAUT B., BURG J.P., LEYRELOUP A.F., ROMNEY F., FUCHS Y., ALABOUVETTE B., LEFAVRAIS-RAYMOND A., 1990 - Notice explicative, carte géol. France (1/50 000), feuille Sévérac le-Château (885) - Orléans : BRGM, 58 p. Carte géologique par Alabouvette B. (coordinateur) et al. (1990).

Carte de France à 1/25000 - Sévérac-le-Château - feuille n° 7-8

Références

GILLOT P.Y., 1974 - Chronométrie par la méthode K/Ar des laves des Causses et du Bas-Languedoc. Thèse 3ème cycle Paris Sud.

POMIE J., 1974 - Le sotch de Soulages et la perte du puits de la Londe - Causse de Sauveterre (St Rome de Dolan - Lozère), Spelunca Mémoires n° 8, p. 131.

POMIE J., 1979 - Redécouvrons les possibilités géospéléologiques d'un grand causse oublié : le Cause de Sauveterre. Grands Causses, p. 26.

ROUIRE J., 1973 - Causses Cévennes Aubrac, Guides géologiques régionaux, p. 35.

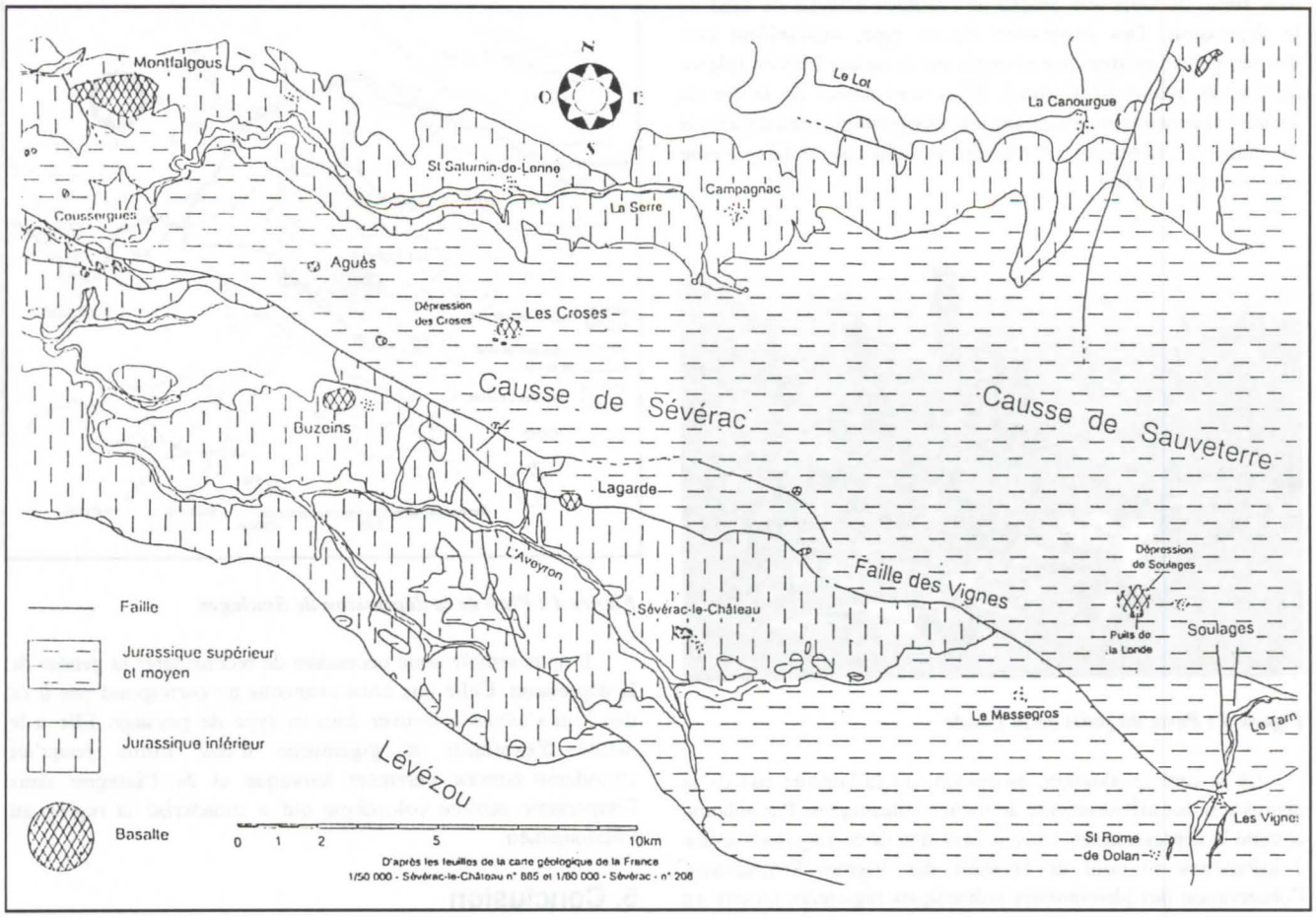

Figure 5 : Répartition générale du volcanisme des grands Causses

Lavafalls: a major factor for the enlargements of lava tubes on the Kilauea and Hualalai, Hawaii

by Stephan Kempe

Techn. Univer. Darmstadt, Geol.-Paleontol. Inst., Schnittspahnstr. 9, D - 64287 Darmstadt, Germany

Abstract

Extensive lava tube systems have recently been explored within the tholeiitic basalt flows of the Ai-la'au Shield Phase of the Kilauea Volcano (Keala Cave: 8.6 km total length, Keauhou Trail System: 3.0 km total length), and within the 1801 alkalic basalt flow of the Hualalai Volcano (Clague`s Cave: ca. 2 km total length). These caves in general have a much larger cross section (up to 15 x 10 m) than the lava river which formed them (often only 3 x 1 m). This can be explained by two processes secondarily widening the tube: downcutting and breakdown. The major agents responsible for downcutting are lavafalls and lava cataracts. They rapidly move upflow, becoming higher and higher and leave wide and winding canyons below. Several falls can join their erosive powers to form impressively tall canyons. At the foot of lavafalls large plunge pool rooms form which enlarge the tube by undercutting its sides. Blocks wedged loose from the walls and wedged from the floor float on the lava river because they are - due to their vesicularity - less dense than the molten lava. These blocks are coated with lava to form lavaballs and are transported downflow, sometimes wedgeing into ceiling spaces to form lava ball constrictions. The down- and undercutting can destabilize the primary roof, resulting in synflow collapse holes (hot pukas). Intrusion of cold air causes the lava surface to solidify forming secondary ceilings which divide the canyon passage. At places of lavafalls the secondary ceiling drops as well, often leaving spill holes through which lava is periodically splashed onto the secondary ceiling, thickening it. Erosion can continue below the secondary ceiling. In this way complex cave systems arise, composed of multiple levels, wide halls and narrow passages. Evidence of downcutting is visible in the caves at places where the ca. 10 cm thick glazing of the walls fell off. Older ash layers, which are not an integral part of a lava flow, or aa-lava from the surface of the underlying, older flows are often exposed.

Zusammenfassung

In den letzten Jahren wurden ausgedehnte Lavaröhrensysteme in den tholeiitischen Basalt-Flüssen der Ai-la'au Schildphase des Kilauea Vulkans (Keala Cave: 8.6 km Gesamtlänge; Keauhou Trail System: 3.0 km Gesamtlänge) und in den Alkalibasalten des Hualalai Ausbruches von 1801 (Clague's Cave: ca. 2 km Gesamtlänge) untersucht. Diese Höhlen haben in der Regel sehr viel größere Durchmesser (bis zu 15 x 10 m) als der Lavafluß, der sie durchfloß (oft nur 3 x 1 m groß). Diese sekundäre Erweiterung der Höhle kommt durch zwei Prozesse zustande: erosive Einschneidung und Versturz. Die Erosion nach unten wird hauptsächlich durch Lavafälle und -katarakte verursacht. Sie schneiden schnell rückwärts ein und werden höher und höher und schaffen weite und mäandrierende Canyons. Mehrere Lavafälle können ihre Erosionskraft vereinigen und beeindruckend hohe Canyons ausräumen. Am Fuß der Lavafälle entwickeln sich große Aufschlagbecken, die die Röhre durch Unterschneidung der Seitenwände ebenfalls erweitern. Blöcke, die von Wänden und Boden gelöst werden, schwimmen, da sie durch ihre vesikuläre Textur leichter als Lava sind, auf dem Lavafluß davon. Sie werden von der flüssigen Lava glasiert, zu Bällen gerundet und abtransportiert. Manchmal können sie sich über dem Lavafluß anstauen und zu Lavaball-Verstopfungen führen. Das Ein- und Unterschneiden kann das Primärdach destabilisieren, sodaß es noch während der aktiven Phase der Röhre einbricht. Durch solche „heißen Pukas" (hawaiianisch für Loch, Schacht, Eingang) kann kalte Luft eindringen, die die lokale Erstarrung der Oberfläche des Lavaflusses verursacht. Diese Sekundärdecken teilen denCanyon in obere und untere Passagen und fallen über Lavafällen steil ab. Häufig bilden sich dort Spritzlöcher, aus denen Lava auf die Sekundärdecke gelangt, die sich so von oben verdickt. Erosion und Rückverlagerung der Lavafälle kann unter der Sekundärdecke weitergehen. Auf diese Weise entstehen komplexe Lavahöhlensysteme mit multiplen Stockwerken, weiten Hallen und Engstellen. Beweise für die erosive Erweiterung der Höhlen finden sich dort, wo die ca. 10 cm dicke, glasige Wandkruste abgefallen ist. Dort kann man gelegentlich ältere Aschenlagen oder Aa-Blöcke finden, beide können nicht integraler Bestandteil eines Pahoehoe-Lavaflusses sein und zeigen, daß sich die Röhre in ältere Schichten eingetieft hat.

1. Importance and occurrence of lava tubes

Subaerial lava flows can propagate either as surface pahoehoe (rope lava), as tube-feed pahoehoe, or as aa (block lava). The same lava can occur either as pahoehoe or aa, depending on its viscosity. Viscosity is determined by temperature, chemical composition and gas content of the lava. Lava setting out as pahoehoe can change to aa while flowing but not vice versa. The longer lava can retain its heat content, the farther lava can flow. Tube-feed lava therefore has the best chance to form long lava flows. The longest reported lava flow on Earth is the basaltic 190 000 a old Undara flow, Australia, covering a distance of 160 km (ATKINSON, 1993). A total of 6 km of tube sections have been explored, showing that it was indeed a tube-feed flow.

Major lava tubes are known from Tenerife, Cheju Island (Korea), Kenya, the Western United States, Iceland, Japan and Hawaii. Most of these tubes have only been mapped for their total extent and have not been subject to extended geological analyses. Reports about them appear mostly in caving journals.

2. Lavatubes on Hawaii

On Hawaii lava tubes occur abundantly on the vol-canoes Kilauea, Mauna Loa and Hualalai. Only recently a cave in Mauna Kea lava has also been discovered. Kilauea and Mauna Loa produce tholeiitic basalt, the Hualalai erupts alkalic basalt.

Even though alkalic basalt is less viscous, the slope of the Hualalai (ca. 8°) is steeper than that of Mauna Loa (ca. 4°) and Kilauea (ca. 2°). This is due (LOCKWOOD pers. com.) to the fact that the Hualalai is coming to the end of its volcanic cycle and eruptions become less frequent and shorter, causing the flows to pile up steeper than on Mauna Loa and Kilauea (see also KEMPE & OBERWINDER this volume).

The largest single flow group containing the majority of the tubes so far explored are the flows belonging to the Ai-la'au shield phase of the Kilauea. These flows date to 500-350 aBP (HOLCOMB, 1987) and overlie older flows (Kalue Flows 500-750 aBP; Volcano Flows, 750-1000 aBP) which form so-called kipukas, vegetation islands. The flows covering the eastern flank of the Kilauea include the Kazumura and the older Keala tubes, plus the 6.25 km long John Martin/Pukalani System and the 15 km long Pahoa System plus a series of other tubes under investigation now. The southern branch of the Ai-la'au flows is steeper, because it crosses the South-Kilauea fault system. The Ainahou Ranch System and the Keauhou Trail System belong to this flow group (see KEMPE et al. this volume). On the Hualalai the tubes of the 1801-Huehue lava field (among them Clague's Cave) are the ones best know so far (see KEMPE & OBERWINDER this Volume)

Note that the term „cave" applies to one continuous cave while the term „system" applies to a series of caves, not directly connected but belonging to the same tube.

The Hawaii Speleological Survey, founded in 1989, is now taking a more systematic look at the lava tubes on Hawaii. K. ALLRED and his team have mapped Kazumura Cave totaling 59.33 km (e.g. KAMBESES, 1995). It is now not only the longest lava cave world-wide, but also the one with the largest difference in elevation, i.e. 1098 m.

I have looked at the internal structure of lava tubes while mapping Keala Cave (8.6 km), Keauhou Trail System (consisting of 5 individual caves, total length 3.0 km; plus Jens' Puka 0.42 km), Thurston Lava Tube (0.49 km) and Clague's Cave (2.0 km) in detail. These investigations plus the observations made in Charcoal Cave (1.5 km), Earthquake System (0.33 km) (KEMPE & KETZ-KEMPE, 1979, 1993) and in the Ainahou Ranch System (7.11 km) (mapped by WOOD, 1980) allow to uncover the rules by which lava tubes evolve on Hawaii and most probably elsewhere on Earth, on the Moon and on the terrestrial planets in general (FRANCIS, 1993).

3. Propagation of flows

The ability of pahoehoe lava to form tubes is responsible for the enormous length of Hawaiian lava flows. The flows associated with the Keala and Kazumura tubes are about 0.7-1.2 km wide (OBERWINDER, 1995), those of the Ainahou and Keauhou Trail tubes are < 0.5 km wide (HARTMANN, 1995; BUCHAS, 1996).

The internal structure of these flows is visible in collapse holes (pukas), which show that the tube roofs consist of up to ten laminae of lava, each several decimeters thick. They are separated by planes along which the laminae have slipped against each other. This structure is inconsistent with the frequently advanced idea that the tubes form from crusted-over channels. Crusting-over would involve relatively thin laminae which would have ropy surfaces and which should not extent across the tube without structural interruption. Crusting-over may occur near vents, but the tubes of the large flows certainly did not evolve from crusted-over channels.

Rather, the tubes seem to form inside of the massive flow, which as such is stationary and is extended at its flow front only. There lava, supplied by the forming tube, is injected, due to the weight of the melt, along the slip-planes inflating the tip from within its center. The injected melt takes the form of a new lamina, moving faster than the older laminae below and above it. In this way the flow propagates at a relatively constant width and velocity because the supply of new lava is limited by the capacity of the tube already established behind the propagating front. If the volcano supplies more lava than the tube can handle, then separate flows may begin to form near the vent. If the flow front reaches the ocean, lava is piped directly to the sea through an otherwise stationary flow. At obstacles, the flow may split. If the terrain is rather level, the flow may form more sheets and become thicker, before the tube can be prolonged, while on steeper slopes, fewer sheets are needed to advance the flow front. This model explains the observed structures of lava flows best. It is, however, difficult to verify in all its aspects and will need further investigation.

4. Evolution of tubes

In contrast, the further evolution of lava tubes can be inferred with more certainty because it leaves distinctive structures in the tubes which we can study directly.

4.1 Lavafalls

The most striking observation is that the tubes do not have cross-sections constant in size. Rather, the tube can be as wide as 15 m and as high as 10 m in places and then close down to the actual cross-section of the flow of perhaps 3 x 1 m. These variations form a repeating pattern: Going downslope, the tube begins to close down slowly until it suddenly opens up again. Where the cross-sections open up, lavafalls are encountered, i.e. the floor drops suddenly. In central Keala Cave (between the pukas Ladder and Flower), ca. 20 such segments occur (OBERWINDER, 1995). The highest lavafalls in the upper Kazumura system are over 10 m high, but they can also be as small as 10-20 cm. Below the lavafalls plunge pool rooms and large, mean-dering canyons are encountered. Going downslope, the canyons gradually become lower and narrower until the next segment begins.

Lavafalls occur both in caves with low and high gradients. In central Keala (3.69 km main tube length, 102 m vertical extension, 1.58° slope) at least 21.3 m or 20% of the altitude change is caused by lavafalls. In case of Clague's Cave (1.39 km main tube length, 157.1 m vertical extension, 6.49° slope) lavafalls contribute 40 m or 25.5% to elevation change. The occurrence of lavafalls seemingly does not depend on slope, it seems to be an intrinsic property of tube evolution itself.

The observed features are best explained by the assumption that the lavafalls are actively backcutting, i.e. eroding the underlying rock (Fig. 1). The analogy with waterfalls is obvious, both of them produce similar morphologies: plunge pool rooms, meanders, canyons and undercut walls.

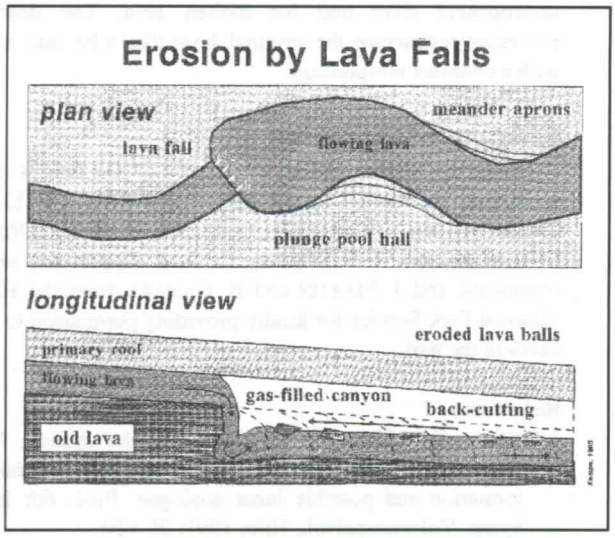

Fig. 1: Scheme of the erosion caused by lavafalls.

The higher the lavafalls become, the more effective-ly the falling lava hammers at the underlying strata. Rocks pounded loose will float up because solid and vesicular lava is less dense than molten lava. These blocks will be rolled over, coated with lava and form balls, often seen jammed into ceiling pockets (Fig. 2).

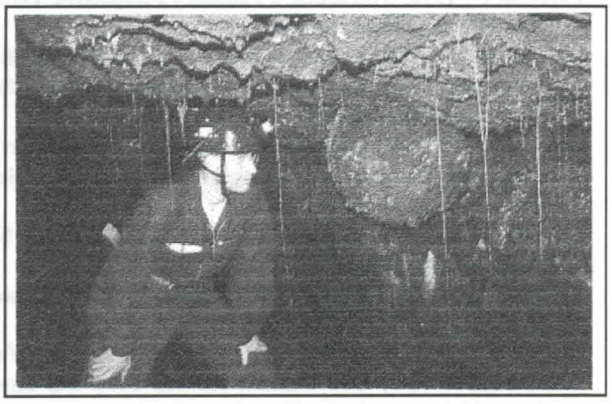

Fig. 2: Lava ball in the primary ceiling of Keala Cave.

Several lavafalls can follow each other and their backcutting can add up to carve impressively high canyon passages (Fig. 3). These canyons are gas-filled, only their lower section contains lava, flowing like a river in its bed with a free surface.

4.2 Direct evidence of lavafall erosion

In many tubes evidence of downcutting can be observed directly. This is possible because the flowing lava leaves only an about 10 cm thin glazing on the walls, which sometimes falls off. Behind, the country rock, through which the tube cut down, becomes visible. These rocks mostly are lava laminae, which are difficult to differentiate from the laminae of the tube-bearing flow. In some places, however, the tube has cut through older aa-flows and even through older ash layers. I observed aa outcrops in Ainahou Ranch Tube and in Clague's Cave. Ash deposits have been noticed in the Earthquake System and in Clague's Cave. Neither aa nor ash are integral parts of a pahoehoe flow and therefore offer firm proof of active tube downcutting.

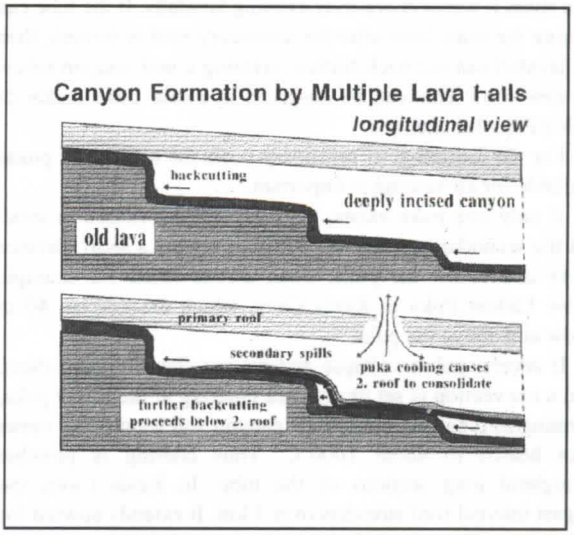

Fig. 3: Multiple lavafalls and the formation of a secondary ceiling.

4.3 Breakdown and puka collapse

The constant undercutting of the tube walls leads to instabilities and breakdown can enlarge the tube as well. Therefore, the walls may show alcoves and the ceiling may form irregular cupolas and domes exposing the internal structure of the primary roof. The breakdown blocks are carried away also, floating on the lava river. Collapse finally may puncture the primary roof causing a hot puka, i.e. a collapse hole, the breakdown of which has been carried away by the still active lava river. In Keala for example, all of the 8 pukas are hot pukas. In Clague's Cave at least 6 of the 8 pukas have formed hot while in the Keauhou Trail System most pukas (probably 7 out of 9) are cold pukas (i.e. collapsed after the activity terminated). Hot pukas occur very often above or makai of lavafalls. This is for example true for Josh's Puka in Keala, for Puka 2 in Keauhou Trail Cave, for Cannonball Puka in John Martin Cave and others.

4.4 Formation of secondary roofs

The collapse of pukas is the cause for another major alteration of the internal structure of lava tubes: The formation of secondary roofs inside the tube.

Frequently we observe in Hawaiian lava tubes double passages, one on top of each other, separated by a relatively thin roof. The lower passage is mostly more even in cross-section, while the upper passage is more irregular and usually contains more breakdown. Both passages unite at some point or may be connected through spillholes. Sometimes the separating floor collapsed, connecting both passages as well.

The observations and the analysis of the cave surveys show that these roofs are formed as a consequence of puka collapse: the puka introduces cold air into the gas space of the canyons, causing the lava river to solidify at its surface. This roof consists of one lava sheet to begin with. Later it may be reinforced by spills of lava which either inundate it from upslope or through spill holes. Spillholes often are found above lavafalls where the roof tends to be thin because of the rapid lava movement. Also gas, released by the stirring action of the fall, escaped through these holes. Sudden constrictions, caused for example by breakdown, can force thin and very hot spills of lava out of the holes, which then flows for some distance on top of the secondary roof strengthening it from above. Because the secondary roof follows the surface of the

lava river, it warps down over existing lavafalls. If the tube can operate for some time after the secondary roof is formed, then the lavafall can cut back further, creating a new canyon below the new roof. This can be observed in Keala Cave makai of Josh's Puka for example.

For the formation of secondary roofs the number of pukas available for air venting is important.

If only one puka exists, then the cooling caused is small and the secondary ceiling will extend only for a short distance above and below the puka. Such a roof exists for example below Ladder Puka in Keala Cave, which extends ca. 40 m below and above the puka.

If several pukas collapse and air can flow between them, then a convection is set up with air entering at the lower puka, warming as it passes through the canyon and leaving the upper puka heated to about 1000°C. Thus cooling is possible throughout long sections of the tube. In Keala Cave, the longest internal roof stretches over 1 km. It extends upward for 700 m from Grogan's Pukas 1 and 2 towards Josh's Puka, not quite reaching it because the air was already too hot to cause any significant cooling. The roof also extends for 300 m makai of Grogan's Puka, probably because cold air could flow down the - up to 6 m high - canyon for some distance as well.

Such secondary roofs caused by multiple pukas were also observed in Clague's Cave between Pukas 3 and 2 and between a now closed puka above „La Patisserie" and Puka 1. Significant secondary roofs are, however, missing in Keauhou Trail Cave, which is in accordance with the observation that most pukas collapsed only after the lava flow ended.

5. Mechanical versus thermal erosion

Observations show that lava tubes are enlarged by both back-cutting lavafalls and by breakdown. This erosion is mechanical in nature. It has often been claimed that lava tubes enlarge by „thermal erosion" (e.g. COOMBS & ROWLAND, 1994). Thermal erosion, i.e. melting of the tube downward, would cause enlargement throughout the tube, while lavafall erosion acts locally. Falling lava apparently acts as a kind of sledge hammer pounding at the underlying rocks.

This sort of erosion does not only cause downcutting, but undercutting of walls and collapse of the roof as well. Skylights open while the tube is still active (hot pukas). These pukas allow access of cold air which causes consolidation of secondary roofs. These internal roofs occur below pukas, therefore ensuring the continuity of the cave as an entity. This is the secret of the enormous length of Kazumura Cave in spite of its many collapse holes. Also the secondary roofs re-insulate the lava flow again and ensure its further function as an underground river bed for molten lava. The described processes restructure the original hose-like tube into a cave with a complex morphology.

6. Acknowledgments

Some of the observations were made during field work for a German Research Council project (DFG-Ke 287/13-1,2). Thanks are due to K. ALLRED, O. FULKS, W. R. HALLIDAY, J. LOCKWOOD and M. S. WERNER for field support and helpful comments, and J. MARTIN and B. CAMARA from the Hawaii National Park Service for kindly providing permission to enter caves in the park.

References

ATKINSON, A. 1993: The Undara lava tube system, North Queensland, Australia: Updated data and notes on mode of formation and possible lunar analogue. Proc. 6th Intern. Symp. Volcanospeleol., Hilo, 1991: 95-120.

BUCHAS, H., 1996: Differenzierung der Lavaflüsse der Ai-la'au Schildphase des Kilauea, Hawaii im Gebiet von Keauhou Trail anhand von Lavaröhren und Oberflächenmorphologie. Dipl. Kartierung, FB Geowiss., Techn. Univ. Darmstadt, 58 pp., unpubl.

COOMBS, C. & S.H. ROWLAND, 1994: Thermal erosion in a lava tube: Honoapo, Mauna Loa Volcano, Hawaii. Geol. Soc. Amer. Ann. Meeting Abstr. 26(7): A118-119.

FRANCIS, P., 1993: Volcanoes, a Planetary Perspective. Oxford Univ. Press, Oxford, 443 pp.

HARTMANN, J., 1995: Keauhou Cave System im Keauhouflow auf Hawaii. Dipl. Kartierung, F B Geowiss., Techn. Univ. Darmstadt, 74pp, unpubl.

HOLCOMB, R.T. 1987: Eruptive history and long-term behavior of Kilauea Volcano. In „Volcanism in Hawaii", US Geol. Surv. Prof. pa. 1350(1): 213-242.

KAMBESES, P. 1995: Kazumura Cave Project - 1995. Nat. Speleolo. Soc. 1995(11): 300-303.

KEMPE, S. & C. KETZ-KEMPE, 1979: Fire and ice atop Hawaii. Nat. Spel. Soc. News 37/8: 185-188.

KEMPE, S. & C. KETZ-KEMPE, 1993: Lava tube systems of the Hilina Pali area, Ka'u District, Hawaii. Proc. 6th Intern. Symp. Volcanospeleol., Hilo, 1991: 15-25.

OBERWINDER, M. 1995: Röhren und oberflächliche Verbreitung von Lavaflüssen der Ai-la'au Schildphase des Kilaueas/Hawaii. Dipl. Kartierung, FB Geowiss., Techn. Univ. Darmstadt, 65 pp, unpubl.

WOOD, C., 1980: Caves of the Hawaiian volcanoes. Caving Intern. Mag. 6&7: 4-11.

The upper Huehue flow (1801 eruption, Hualalai, Hawaii): An example of interacting lava flows yielding complex lava tube morphologies

by Stephan Kempe & Matthias Oberwinder
Techn. Univer. Darmstadt, Geol.-Paleontol. Inst., Schnittspahnstr. 9, D 64287 Darmstadt, Germany

Abstract

The Hualalai, Hawaii, erupted last 1800-1801. Alkalic basalt of the Kaupulehu and Huehue Flows formed extensive channel and tube systems. In March 1996, we investigated the 2 km long Clague's Cave in the upper Huehue flow (main passage length 1.4 km, vertical extent 157 m, average slope 6.56°, meander factor 1.18). Exploration ended at a breakdown choke. 1.1 km lower down, Medville et al. mapped 2.4 km (180.5 m vertical), probably of the same tube. The cave was enormously enlarged by lavafall erosion and breakdown (erosion factor 14). Collapse of pukas and air cooling have formed extensive secondary ceilings. Sides and roofs of some tube sections stand in aa, a contradiction in itself. This is explained by aa-lava derived from shield-forming rootless vents over a parallel tube (Mystery Tube) active at the same time, which transgressed Clague's Tube, causing collapse of its primary roof. Stooping upward of the cave roof caused the „aa-passages". Lava seeping through the aa formed unusually large stalactites and stalagmites. Comparison with Kilauea tholeiitic basalt tubes shows that slope and meander factor can be correlated but not slope and lava viscosity.

Zusammenfassung

Der Hualalai, Hawaii, brach zuletzt 1800-1801 aus. Die Alkalibasalte der Kaupulehu und Huehue Flows bil-deten lange Kanal- und Röhrensysteme. Im März 1996 erforschten wir die 2 km lange Clague's Cave im obe-ren Huehue Flow (Hauptgang 1.4 km lang, 157 m Höhenunterschied, Gefälle 6.56°, Mäanderfaktor 1.18). Die Höhle endet im Versturz, aber 1.1 km unterhalb vermaßen Medville et al., 2.4 km (180,5 m Höhenunterschied) vermutlich der selben Röhre. Die Höhle wurde stark durch Lavafall-Erosion und Versturz vergrößert (Erosions-faktor 14). Deckeneinsturz und Luftkühlung verursachten ausgedehnte Sekundärdecken. Wände und Dach eini-ger Gänge stehen in Aa, ein Widerspruch in sich. Diese Aa wurde von einer zeitgleich aktiven, parallelen Röh-re (Mystery Tube) über schildartige rootless vents gefördert, transgredierte Clague's Tube und löst den Einsturz ihrer Primärdecke aus. Weiteres Hochbrechen der Decke verursachte die „Aa-Gänge". Durch die Aa sickernde Lava bildete ungewöhnlich lange Stalaktiten und Stalagmiten. Der Vergleich mit den tholeiitischen Basalt-röhren des Kilaueas zeigt, daß Gefälle und Mäanderfaktor korrelieren, nicht aber Gefälle und Lavaviskosität.

1. Introduction

In March 1996, we investigated a lava tube in the upper part of the Huehue flow field north of Kona, Hawaii (for more details see OBERWINDER, 1996, unpublished). It was formed, together with the Kaupulehu flow, during the only historic eruption of the Hualalai in 1800-1801. These eruptions yielded alkalic basalts composed of phenocrists of olivine, plagioclase and pyroxene in a fine matrix of the same minerals.

The older part of the Huehue flow field was produ-ced by several spatter cones, called Puhia Pele, from which a large channel system extends seawards. The younger and smaller part of the flow field represents lava derived from inconspicuous vents south of the Puhia Pele cones. This flow contains the tube we have investi-gated (Fig. 1). Because no local name for the cave is known, we named it after the former director of the Hawaiian Volcanoes Observatory, Dr. DAVIDCLAGUE. He had brought the tube to our attention and also participated in the first reconnaissance trip in August 1994 together with Dr. W.R. HALLIDAY, DR. J. KAUAHIKAUA and S. KEMPE.

2. Survey Data

The grade 5 survey was conducted by M. OBERWINDER, S. KEMPE, H. BUCHAS and K. WOLNIEWICZ with a tripod-mounted digital compass, an electronic level (both readable to ± 0.1°) and a 50 m tape. Survey data were processed with the cave map program CAPS 7.3. Fig. 1 shows the plot of the survey line within the upper part of the Huehue flow. Maps, a longitudinal section (St. 0-78) (1:500), and cross-sections (1:200) were drawn to reveal the details of the internal tube structure and to contribute to the discussion about the tube's genesis.

In Table 1 main survey results are listed. The horizontal length of the main tube (without side passages) is 1367 m and the vertical distance amounts to 157 m; additionally ca. 625 m of side passages were explored, of which 355 m were mapped. The slope of the tube is 6.56°. However, if the direct distance (general strike WNW) between the upper and lower end of our survey is taken (1180 m), then the slope amounts to 7.6°.

The upper end of the tube is located shortly below the vent of the younger Huehue Flow at N 19° 45.571´/ W 155° 58.602´. Uphill the steep tube is blocked by welded lavaballs. The lower end was reached at N 19° 45.890´ / W 155° 59.183´. There the tube is blocked by breakdown, but air draft shows that the cave continues. In summer 1996 MEDVILLE & MEDVILLE (1997) mapped a 2413 m long (180.5 m vertical extent) section of a tube below (Goat Herd Cave), most probably the continuation of Clague's Cave (see Fig. 1). Their survey ended 1100 m below the breakdown plug. This section has yet to be explored.

3. Morphology of Clague's Cave

Clague's Cave is morphologically very complex. Up to 17 m wide halls are encountered and the main passage changes its slope, width and height constantly. Dividing the area of the cave (9000 m^2) (obtained by weighing the cut-out map of the cave) by the horizontal main passage length (1367 m) an average tube width of 6.6 m is ob-tained. Likewise the average hight was determined from the longitudinal section. It amounts

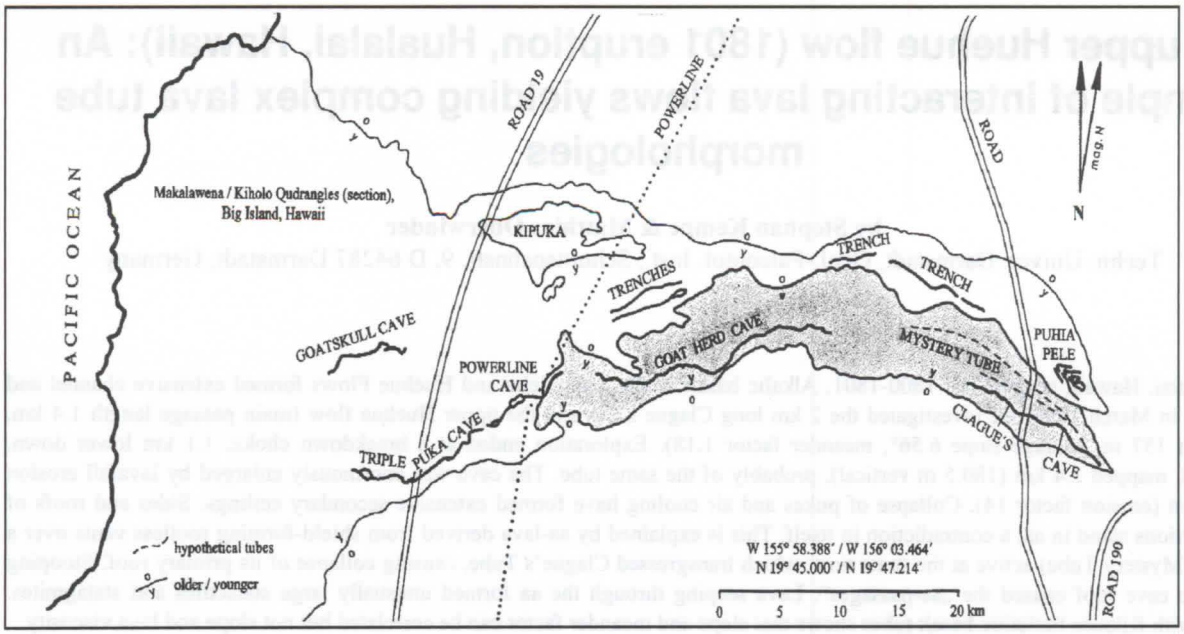

Figure 1: Geological map (after Moore & Clague, 1991) of the Huehue Flow field with survey lines of mapped caves (Goat Herd Cave and lower Huehue caves courtesy of D. & H. Medville).

Table 1: Clague's Cave, main survey results

main passage length	1389.86 m
main passage length, horizontal projection	1367 m
vertical extension	157.12 m
side passages, mapped	355.0 m
total length, mapped	1744.86 m
side passages, explored	ca. 270 m
total system length	ca. 2000 m
direct distance end to end	1180 m
meander factor	1.15
average slope	6.56°
slope of direct distance	7.58°
upper end of cave, altitude a.s.l.	512 m
lower end of cave, altitude a.s.l.	370 m
general direction of cave	290°
area of cave (horizontal projection) mapped passages only	9033 m^2
average width	6.61 m
widest passage	17.5 m
average height (above station 78)	5.47 m
highest passage	6.2 m
average cross-section $((6.61+5.47)/2/2)^2*p)$	28.7 m^2
number of pukas	7 (8)
cumulated height of lavafalls	ca. 40 m
percentage of lavafalls	ca. 25 %
number of survey stations	140
average station to station distance	13.08 m
total survey length	1831.0 m
surface slope over cave area	6.86°

to 5.5 m. On the assumption that the tube is oval in shape, a cross-section of ca. 29 m^2 can be calculated. This is much larger than the cross-section of the lava river which occupied the tube. At several places minimal passage cross-sections are encountered which show that the lava river probably was not wider than 2 m and not deeper than 1 m and that the large passages below these constrictions could never have been filled completely with lava at any time. The tube is, on average, 14 times (we call this ratio „erosion factor") wider than the lava river, i.e. the tube must have been enlarged substantially by secondary processes.

This enlargement was carried out by two processes: lavafall backcutting and breakdown. These processes are at work in all of the lava tubes we have investigated on Hawaii so far (KEMPE, 1996, 1997).

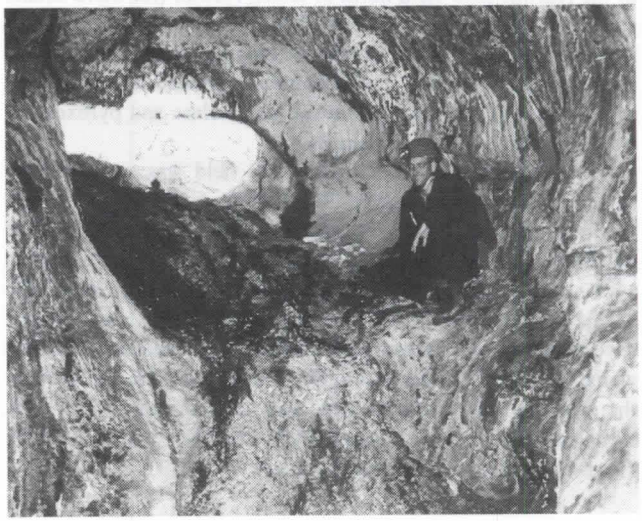

Figure 2: Lavafall (3 m high, St. 24) in Clague's Cave, note the minimal passage at its upper end.

The lavafalls (Fig. 2) in Clague's Cave can be up to 5 m high. They account for more than 40 m or 25 % of the elevation change in the mapped tube section. By backcutting, these falls increase in size and become evermore effective in hammering out tall canyons. Several of the falls can move upward through the same section of the tube deepening it more and more. The

loosened material is, because of the high vesicularity of the solid lava, less dense than the molten lava and will float on top of the lava river. There it is coated by lava and forms lava balls. Several places exist in Clague's Cave where the thin glazing of the tube has fallen away and where the rock, through which the downcutting occurred, is visible. One of them is found shortly above the breakdown plug, where aa-lava, covered by a red ash is exposed. Neither ash nor aa-lava are part of the tube forming pahoehoe flow. More aa is exposed at the wall of the „Plunging Passage" at the lower end of the „Wooden Vessel Hall" proving downcutting as well.

The second process to cause enlargement of the tube is breakdown. It can both increase the ceiling height irregularly and widen the tube when the side walls collapse and slump into the lava river. The loose material is also floated on top of the molten lava and carried downstream. Very often these lava balls are welded onto the ceiling or plug the entrances of once active sidepassages drained by the downcutting.

Downcutting and breakdown can cause the complete destruction of the primary tube roof and the opening of collapse holes (pu-kas). A total of eight pukas belong to the mapped section of the cave, most of them are hot pukas, i.e. they opened up while the tube was still actively transporting lava which removed the material of the collapsed roof. Only pukas 5 and 7 are clearly cold pukas, i.e. they formed after the tube flow subsided. Puka 1 also served as an overflow early in the tube history. It produced a thin flow of very hot surface pahoehoe almost devoid of rope structures.

As a consequence of the puka collapse, air was able to circulate through the tube. Because of the steep slope this current was directed upward between pairs of pukas with the cold air entering in the lower puka and the hot air exiting through the upper puka. The air cooled and consolidated the surface of the still flowing lava and caused the formation of a secondary roof, dividing the original canyon in an upper, gas-filled and a lower, lava-filled passage. Such a secondary roof starts for example a few meter below Puka 3 and extends upward until about 50 m below Puka 2. It contains a few spill holes, through which lava from the lower passage spilled on top of the secondary roof, thus thickening it from above. The longest secondary ceiling extends (with an interruption at around St. 129) from the end of the mapped section of the tube (where the collapse of the lower end of the secondary roof blocks the continuation of the cave) to about 100 m below Puka 5 (which is a cold puka, i.e. it did not serve as an air outlet) for over 350 m. It was most probably caused by air convection between Pukas 8 and 6. The secondary ceilings preserve the height of the lava level in the tube at the moment of their consolidation, i.e. they dip down steeply over active lavafalls. Since the lavafalls can continue their erosive activity below the secondary roof, the distance between the position of the bend in the secondary roof and the final position of the lavafall is a measure of the time be-tween the collapse of pukas and the end of the activity.

After the supply of lava subsided, the residual lava in the tube mostly was able to evacuate the passages below the secondary ceilings. In very steep sections of the tube („Wildwater Canyon") terminal lava flowed longer and was able to cool enough to turn into aa. It often formed steep rubble cones at the bottom of former lava cascades. Other terminal features include tube-in-tube structures and drained plunge pools.

All these morphological features are not unlike those seen in other Hawaiian caves. Clague's Cave however is unique because of its tube sections which have walls and ceilings entirely composed of aa. This is a contradiction in itself because aa is too viscous to form tubes.

Prominent aa sections include the large halls above Puka 2 and much of the upper passage between Puka 2 and Puka 3. This paradox can be solved by postulating the existence of an independent tube which runs parallel to Clague's Cave and was active at the same time (Fig. 3). This „Mystery Tube" must have run about 100 m north of Clague's Cave and is marked in the field by at least two rootless vents, which formed low shield-like rises (Fig. 1). These rootless vents most probably became active when sections of the Mystery Tube collapsed and forced the tube lava to rise to the surface. At the vent sites the lava formed small surface pahoehoe flows which quickly cooled and turned into aa flows. These covered also part of the roof of the adjacent Clague´s Cave to the south. In Puka 5, for example, at least three flow events can be seen, transgressing the original, thin primary pahoehoe roof of Clague's Cave. The load of the additional aa caused the collapse of the primary roof which was transported out of the tube by the still active flow. Further stooping upward into the fresh, welded aa layers and the formation of a secondary ceiling at a position not much below the original primary roof gives the impression of a lava tube composed entirely of aa (Fig. 3).

Credibility to this reconstruction of events is given by unusually large lava stalactites, stalagmites and columns. They represent portions of the melt from the transgressing Mystery Tube lava seeping through the hanging aa or through the remainders of the fractured primary roof. These stalactites also illustrate that both flows were active at the same time because the stalactites directly above the lava river of Clague's Cave do not have matching stalagmites. The material dripping to the floor must have fallen into the still hot lava river which was able to remove it. In addition, Pukas 2 and 3 received small aa-flows which drained into them.

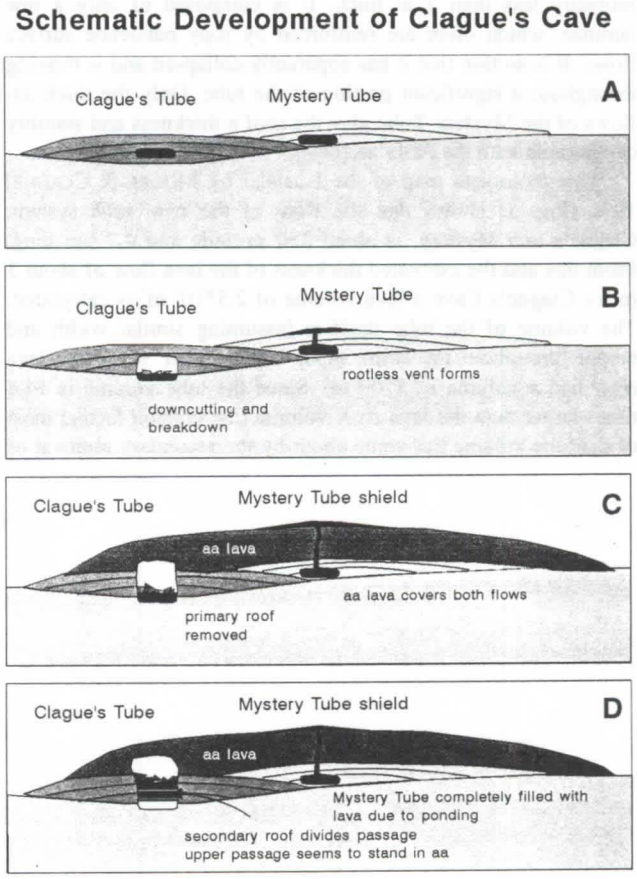

Figure 3: Scheme of the development of Clague's Cave. For explanation see text.

4. General Considerations

The slope of Clague's Cave (7.58°) (i.e. the slope calculated from the elevation difference and direct end-to-end distance of a tube) is much larger than for any of the Kilauea tubes known. The big Ai-la'au tubes Kazu-mura and Keala have a slope of 1.96° and 1.75°, respec-tively. Even the Keauhou Trail System, which extends a-cross one of the South-Kilauea faults, has a lower slope, i.e. 6.11°. These tubes developed in tholeiitic basalt, which is less fluid than alkalic basalt and should have a higher slope than the Hualalai tubes. This enigma is explained by the fact that the Hualalai is in a late state of its development and that its eruptions are shorter and less productive than those of the Kilauea and that therefore the slope of the volcano is steeper than that of the Kilauea. Slopes of tubes apparently are not directly linked to the fluidity of the lava. This is also shown by the fact that Goat Herd Cave, the presumed continuation of Clague's Cave, has a slope of 5.18°, because it occurs lower on the flank of the Hualalai, i.e., the tube slope decreases downhill even though the viscosity of the flowing lava increases due to ongoing cooling.

Dividing the horizontal passage length by the direct horizontal distance between the ends of a tube yields the meander factor. It amounts to 1.15 for Clague's and to 1.2 for Goat Herd Cave. This is smaller than the meander factors of Kazumura and Keala Caves (1.30 and 1.25, resp.) but similar to the Keauhou Trail System (1.13). Steeper slopes seem therefore to cause less meandering than more gentle slopes, on which the progressing lava can move around obstacles more freely.

There are other differences between Clague's Cave and the Kilauea caves. One of them is the thickness of the primary roof. Kazumura and Keala have 5 to 8 m thick roofs, composed of up to 10 lava sheets, while the primary roof of Clague's Cave is thin, probably less than 3 m thick. It is composed of only a few laminae, which often are reinforced by ropy pahoehoe surface flows. It is so thin that it has apparently collapsed and is missing throughout a significant portion of the tube. Only the thick aa-flows of the Mystery Tube give the roof a thickness and stability comparable with the Ai-la'au flows.

The geological map of the Hualalai by MOORE & CLAGUE, 1991 (Fig. 1) shows that the flow of the twin tube system, Clague's and Mystery, is about 350 m wide and 4.7 km long. From this and the estimated thickness of the lava flow of about 3 m for Clague's Cave a lava volume of $2.5*10^6$ m^3 is calculated. The volume of the tube itself is (assuming similar width and height throughout the entire tube) $1.4 * 10^5$ m^3 while the lava river had a volume of 9700 m^3. Since the tube volume is 14.4 times larger than the lava river volume (the erosion factor) most of the tube volume has come about by the secondary removal of rock, as already discussed. The ratio of total lava to tube volume is 18, i.e. the lava carried through the tube must have contained 1/18 of its volume in form of eroded material.

Furthermore, if one assumes that the lava flows with about a rate of 4 m^3sec^{-1} (as reported for the recent Pu'u O'o Flows, Kilauea) then the entire lava volume would have been deposited in only 7 days. In such a short time the observed erosion must also have occurred and all the internal features must have been formed. This is highly unlikely. We therefore suggest that the geological map needs correction and that Clague's Tube does not end after 4.7 km and 425 m vertical extent. It possibly extends well into the lower part of the Huehue flow field and may tie in with the tube called „Powerline Cave" (MEDVILLE & MEDVILLE, 1997) (Fig. 1). Then much more lava would have been carried through the tube, more time would have been available for erosion and the ratio of eroded material to lava would have been much less. This hypothesis will be tested during an expedition in March 1997.

Acknowledgments

This project was funded by the German Research Council (grant DFG-Ke 287/13-1,2), it is a contribution to the Hawaii Speleological Survey. We thank D. and H. MEDVILLE for kindly sharing their survey data with us, D. CLAGUE for showing us the entrance to „his" cave, J. KAUAHIKAUA for his field support, J. P. LOCKWOOD and W.R. HALLIDAY for helpful comments, and the manager Mr. A. NISHIYAMA and Mr. CLIFFORD of the Makalei golf course for their kind permission to enter the area.

References

KEMPE, S., 1996: Enlargement of lava tubes by downcutting and breakdown [Abstr.]. - Nat. Speleol. Conv., Salida Colorado, Aug. 5-9, 1996.

KEMPE, S., 1997: Lavafalls: a major factor for the enlargements of lava tubes of the Ai-la´au Shield Phase, Kilauea, Hawaii. - Intern. Congr. Speleol., La Chaux-de-Fonds, 1997, this volume.

MOORE, R.B. & CLAGUE, D.A., 1991: Geologic Map of Hualalai Volcano, Hawaii. - Mis. Invest. Ser., published by the U.S.G.S.

MEDVILLE, D. & H. MEDVILLE, 1997: Recent exploration of lava tube systems in Kona and on Mauna Loa, Hawaii. - Intern. Congr. Speleol., La Chaux-de-Fonds, 1997, this volume.

OBERWINDER, M., 1997: Genese und interne Struktur des oberen Teiles des Lavastromes von 1801 (Huehue Flow, Hualalai, Hawaii). - Dipl. Arbeit, FB. Geowiss., Techn. Univ. Darmstadt: 159 pp, unpubl..

Mapping lava flows by following their tubes: the Keauhou Trail/ Ainahou Ranch Flow Field, Kilauea, Hawaii

by Stephan Kempe, Holger Buchas, Jens Hartmann, Matthias Oberwinder, Jan Strassenburg & Klaus Wolniewicz

Techn. Univer. Darmstadt, Geol.-Paleontol. Inst., Schnittspahnstr. 9, D - 64287 Darmstadt, Germany

Abstract

During its last shield phase, 500-350 aBP, the Kilauea Volcano, Hawaii, issued large amounts of tube-fed pahoehoe lava eastwards and southwards. These Ai-la'au flows were deposited so rapidly that it was so far not possible to differentiate the individual flow events clearly. With the mapping of the tubes, this situation has changed. In the southern flow field we now mapped (in addition and in parallel to the already known, 7.11 km long Ainahou Ranch System) the Keauhou Trail System (KTS). The KTS is segmented by collapse holes into five individual caves totaling 2,999.5 m with a horizontal main tube length of 2,241.4 m, a vertical extent of 213.3 m and an average slope of 5.4°. The longest section is the Lower KT Cave with 1,217 m total length (974 m horizontal main passage length). Its vertical extent amounts to 132.2 m and its gradient to 7.73°. This high gradient is caused by one of the South-Hawaiian faults which the cave crosses. In its steepest section a slope of 25° is encountered. The cave ends at a second fault where recent movements caused the collapse of the tube roof and the downward displacement of the continuation. 50 m to the west of the KTS an earlier branch of the KTS was mapped, Jens' Puka, 427 m long in total. The upper end of the KTS is blocked by an intrusion of younger lava. Therefore we can now differentiate three individual flows: The Keauhou Trail Flow, the Ainahou Flow and a younger, intermediate flow. Age data and petrography leave, however, some doubts if these flows really belong to the Ai-la'au shield phase or to some independent eruption on the upper East Rift of the Kilauea.

Zusammenfassung

Während seiner letzten Schildphase, 500-350 aBP, produzierte der Kilauea Vulkan, Hawaii, riesige Mengen Lava, die durch Röhren nach Osten und Süden abflossen. Diese Ai-la'au Lavafelder wurden so schnell nacheinander abgelagert, daß es bisher nicht möglich war, die Sequenz der Ablagerung im einzelnen zu erfassen. Mit der Vermessung der Röhren hat sich diese Situation geändert. Im südlichen Lavafeld haben wir jetzt (zusätzlich zu der bereits bekannten und parallel laufenden, 7.11 km langen Ainahou Ranch Röhre) die Röhren des Keauhou Trail Systems (KTS) vermessen. Das KTS ist durch Deckeneinbrüche in fünf Höhlen segmentiert, sie sind insgesamt 2999.5 m lang, mit einer horizontalen Hauptröhrenlänge von 2241.4 m, einem Höhenunterschied von 213.3 m und einem Gefälle von 5.4°. Die längste Höhle ist die Lower Keauhou Trail Cave mit einer Gesamtlänge von 1217 m, einer horizontalen Hauptganglänge von 974 m, einer Höhendifferenz von 132.2 m und einem Gefälle von 7.73°. Dieser hohe Gradient entsteht, weil die Röhre über eine Verwerfungsfläche des Süd-Hawaii Abschiebungssystems verläuft und dort bis zu 25° Gefälle aufweist. Die Höhle endet an einer zweiten Verwerfung, an der rezente Bewegungen den Höhlengang nach unten setzten und das Höhlendach einbrechen ließen. 50 m westlich des KTS findet sich eine weitere Röhre, Jens' Puka, 427 m lang, die einen älteren Zweig des KTS darstellt. Das obere Ende des KTS ist durch eine Intrusion jüngerer Lava blockiert. Wir können daher jetzt drei Flüsse unterscheiden: Den Keauhou Trail Fluß, den Ainahou Ranch Fluß und einen dazwischen liegenden, jüngeren Fluß. Altersdatierungen und petrographische Daten lassen allerdings noch Raum für Zweifel, ob diese Flüsse wirklich zur Ai-la'au-Phase gehören oder zu einer unabhängigen Eruption des oberen East-Rifts des Kilaueas.

1. Introduction

The Kilauea Volcano, Hawaii, erupted mainly from its rift zones for the past 300 years. Prior to this phase, and before the collapse of the current caldera occurred, enormous amounts of tholeiitic basalt were produced from a vent forming a low shield at the top of the volcano, the Ai-la'au Shield. Flows extended to the east (towards Hilo) and to the south (Fig. 1). All of these flows formed tubes. Those flowing east have a gradient of less than 2°, those flowing south a gradient of ca. 5°. Among the eastern tubes are Kazumura Cave (the longest lava cave currently known world-wide, total length 59.33 km, vertical extent 1.099 km, mapped by K. ALLRED and his team; see KAMBESIS, 1995), the Pahoa System (15 km long, internal report by F. STONE), Keala Cave (8.6 km long, 180 m vertical extent, mapped by the authors) and the John Martin/Pukalani System, 6.26 km in length (FAVRE, 1993).

The southern tubes include the Ainahou Ranch System (7.11 km total length, 323 m vertical extent; WOODS, 1980) and the Keauhou Trail System (total length 2,999.5 m, vertical extent 213.3 m, mapped by the authors) (Fig. 2). Note that the term "system" indicates a tube segmented into several individual "caves".

2. The Keauhou Trail System

The Keauhou Trail System (KTS) system was mapped in April 1995, July 1995 and March 1996. (HARTMANN, 1995; BUCHAS, 1996). The survey data of the main tube of the KTS are given in Table 1.

Table 1 Main survey data of Keauhou Trail System

Main tube length	***2,272.8 m***
Horizontal main tube length	***2,241.4 m***
Total length (without Jens' Puka)	***2,999.5 m***
Distance end-to-end	***1992 m***
Meander factor	***1.13***
Vertical extent	***213.3 m***
Slope	***5.44°***
Number of stations along main tube	***133***
Average distances (horizontal)	***16.98 m***
Average distances (non-horizontal)	***17.22 m***

The main tube of KTS is interrupted by 9 pukas (roof collapses) numbered 7 from mauka (upslope) to -1 makai (downslope). This numbering system is identical to that of the Ainahou Ranch System, which has 22 entrances counted makai to mauka. KTS Pukas 0 and -1 were discovered only after the other numbers had already been established.

Some of the pukas segment the main KTS tube into five individual caves: Upper Keauhou Cave (upper end of tube to Puka 7), Keauhou Coconut Cave (Pukas 7 to 5), Keauhou Petroglyph Cave (Pukas 5 to 3), Keauhou Organ Cave (Pukas 3 to 1) and Lower Keauhou Cave (Pukas 1 to -1). Except for Pukas 7 and 2, all pukas are „cold" pukas, i.e. they collapsed after the flow subsided. To the west of the main tube a shallow tube is situated, which also belongs to the same flow. It forms two caves: Jens' Puka Mauka Cave and Jens' Puka. The survey data of these caves are listed in Table 2.

Table 2 Survey data of KT caves

Upper Keauhou Trail Cave	
Total length	*579.0 m*
Main passage length (non-horizontal)	*455.5 m*
Vertical extent	*28.0 m*
Keauhou Coconut Cave	
Ttotal length	*176.6 m*
Main passage length (non-horizontal)	*110.1 m*
Vertical extent	*5.4 m*
Keauhou Petroglyph Cave	
Total length	*164.9 m*
Main passage length (non-horizontal)	*61.4 m*
Vertical extent	*3.2 m*
Keauhou Organ Cave	
Total length	*862.0 m*
Main passage length (non-horizontal)	*590.0 m*
Vertical extent	*41.9 m*
Sum of above caves (upper KTS)	
Total length	*1782.5 m*
Main pas. length (horiz., incl. pukas)	*1235.4 m*
Vertical extent (incl. pukas)	*80.8 m*
Distance end-to-end	*1125 m*
Slope	*3.74°*
Meander factor	*1.10*
Lower Keauhou Trail Cave	
Total length	*1217.0 m*
Main passage length (non-horizontal)	*989.0 m*
Main passage length (horizontal)	*973.8 m*
Vertical extent	*132.2 m*
Distance end-to-end	*882 m*
Slope	*7.73°*
Meander factor	*1.10*
Jens´ Puka (total)	*401.5 m*
Jens´ Puka Mauka Cave (total)	*25.60 m*

2.1 Upper Keauhou Cave

This cave has only one entrance: Puka 7, also called Fern-Entrance because of the tree fern growing in it. The fern roots in a cone of ash from the 1969 Mauna Ulu eruption. This puka is classified as a hot puka (i.e., it opened up during the still active flow), because the breakdown from its collapse is missing and lava was spattered over its rim. A small lavafall has cut back below the puka (possibly causing its collapse) and is now found 25 m mauka of the entrance. It formed a small trench, accompanied by shelves and benches. Mauka of the fall, the tube widens and becomes lower. The floor is very uneven, covered with clinkery and rough lava formed in the terminal phase of the flow. Ca. 130 m in, we find the makai tip of black, ropy, intruded lava which covers the floor of the cave for the final 300 m to its mauka end. There the intruded lava broke through the ceiling of the tube and oozed through the breakdown. At this location the eastern side of a transgressing lava flow is encountered at the surface. The intrusion occurred at a section of the tube where a triple oxbow came to a close, most probably a place of roof weakness.

2.2 Keauhou Coconut Cave

This segment of the main tube is canyon-like (shaped by the backcutting lavafall already mentioned) and has two higher-level tubes branching off to the west (Coconut Passage and Matthias' Crawl). Coconut Passage probably was originally feeding the adjacent Jens' Puka tube before the downcutting of the main tube occurred. This tube was a distributary branches established during the early phase of the advancing lava flow.

2.3 Keauhou Petroglyph Cave

A 30 m long collapse trench (Puka 5) separates the Keauhou Coconut Cave from the Keauhou Petroglyph Cave. The main tube is buried by the breakdown of Puka 4, 15 m below Puka 5, but the higher-level Dwelling Passage branches off and, via an oxbow, reconnects with the main passage after Puka 4. The Dwelling Passage is another distributary branch of the tube ending in a lava seal after 60 m. At the surface it is marked by a failed branch in the lava flow.

2.4 Keauhou Organ Cave

Puka 3, which separates the Keauhou Petroglyph Cave from Keauhou Organ Cave occurred at a place where the main tube branched and where the roof was unstable. The branches reunite after 60 m. It is not the only oxbow occurring in this section of the tube, five more follow. Ca. 30 m makai of the first branch, the small Puka 2 is located, the second hot puka of the system. It formed due to a backcutting lavafall, which destabilized the roof at this location while the lava was still flowing. Air entering the tube through the puka cooled the surface of the still flowing lava and a short secondary ceiling formed, the only one to speak of in the entire system (see also KEMPE, this volume).

2.5 Lower Keauhou Cave

Puka 1, a 25 m long and 15 m wide collapse structure, separates Keauhou Organ Cave from Lower Keauhou Cave. Its collapse occurred at a place where two branches reunited and where the cave was very wide and the roof accordingly weak. Below Puka 1, the tube continues for almost 300 m as a rather uneventful tunnel, with an extremely rough floor. Then two oxbows follow and at 660 m makai of Puka 1 the tube becomes very steep (25°). At the discovery it was almost filled with terminal aa and we had to move some of it to proceed on through. Cracks cut across the tube, one of them showing downfaulting of the makai side by 25 cm. This is where the tube plunges over the first (ca. 30 m high) of the Poliokeawe fault faces. It is the steepest tube section yet recorded on Hawaii. Some 60 m beyond, a hole in the ceiling gives access to a small complex of low tubes (Stephan's System, some 80 m long) which must have formed in the cone of lava piling up below the fault during an early phase of the flow. These were later partly inundated by spills of lava rising up from the main passage. At 830 m makai Puka 1 the Red Channel Hall is reached, where terminal lava has formed two branches each with impressive levees. Their red color shows that they were able to cool slowly. 900 m below Puka 1 the main passage ends, because terminal lava fills it up to the ceiling. To the side very low tubes (Matthias' Maze and Klaus Connector) form a bypass to Puka 0 (collapsed over an older side-branch of the

flow) and eventually to Puka -1 where the main tube is reached again. The final section of the main tube (Stephan's Street) is about 60 m long and ends in a breakdown choke caused by the next lower fault, thus terminating the longest section of the Keauhou Trail caves just over 1 km below Puka 1.

2.6 Jens' Puka

Jens' Puka is situated ca. 50 m to the west of the Keauhou Trail Tube and runs in parallel to it. It consists of two caves (Jens Puka proper and the short Jens' Puka Mauka Cave) segmented by a cold puka. A second puka, a few meters makai of the first one, does not segment the cave. From here a crawl gives access to the lower part of the cave, probably the most sporting cave yet mapped in the National Park area because it is mostly only of crawling height. The few places, where duck-walking is permitted, are provided by breakout cupolas in the primary roof. All in all, the tube did not have much time to erode down (maximum height of some small lava cataracts is 50 cm) and must have been cut off its lava supply early in its history. In the middle part of the tube, up to five lava strands run in parallel, a good example of a distributary young lava tube. The cave ends at an impassable low tube section.

250 m makai of the end of Jens' Puka and in direct prolongation of it, a 480 m long and up to 60 m wide aa-tongue is noticed, overriding the surface pahoehoe of the Keauhou Trail Flow. This aa-tongue most probably represents the lava which drained out of the Jens' Puka tube after it had been cut off from its lava supply by the downcutting main Keauhou Trail Tube.

3. Ainahou Ranch System

The Ainahou Ranch Tube (data see Table 3) was mapped by a British expedition (WOODS, 1980). They reported a total length of 7.11 km. This length may not include some of the upper passages. It is also unclear, at how many of the 22 pukas the system is segmented. Reconnaissance trips in the upper, middle and lower sections of the cave show that it is deeply entrenched by lavafall erosion and that it has developed secondary roofs over long stretches of the tube. All in all, this tube has been active much longer than the Keauhou Trail System. Mauka the tube is choked by breakdown caused by the Kalanaokuaiki Fault, a recent uplift, which occurred after the tube formed. Makai the tube ends in a gaping opening at the same Poliokeawe fault face, on which the Keauhou Trail Tube ends in breakdown. From here the lava plunged down as surface pahoehoe. On the surface of the next fault block down (150 m deeper) apparently a new tube system formed. This however, has not been investigated as yet.

Table 3: Survey data of the Ainahou Ranch Tube (after WOOD, 1980)

Total length	**7.11 km**
Main passage length (horizontal)*	**4.82 km**
Distance end-to-end	**4.27 km**
Meander factor	**1.13**
Vertical extent	**323 m**
Slope	**4.26°**

*measured with distance wheel on map

4. The Keauhou/Ainahou lava flow field

In Fig. 2 the two tube systems discussed are plotted in relation to each other. They clearly define two separate flows (termed A and C) in this previously unstructured flow field (compare HOLCOMB, 1987). The intrusion at the upper end of Keauhou Trail System shows, that a younger flow (Flow B) transgressed in between the two tube-bearing flows. This flow can be identified on aerial photographs and in the field. Apparently it did not reach the Poliokeawe faults and was therefore more short-lived than the other two flows. We walked the entire length of the flow in an effort to find an entrance to its tube, without success. The flow is characterized by large tumuli, some of which had lava squeezed out of them like toothpaste. We also tried to follow the flow crest of Flow B north beyond the Chain of Craters road, but the thick ash of the 1969 Mauna Ulu eruption makes mapping impossible there. The old aerial pictures (taken in 1964) are of no help either, because the vegetation was very dense, also masking the topography. Therefore, the northern part of the route of Flow B is tentative.

At the rims, Flow B rests on both Flows A and C. It is possible that lava of Flow A reappears to the west of Flow B and is in contact with Flow C along the Chain of Craters Road (see „A?" on Fig. 2). If this is the case, then A (Keauhou) is the oldest of the flows, followed by C (Ainahou) and B (intermediate flow). This interpretation is substantiated by XRF (x-ray fluorescence) analyses of bulk rock samples taken from the individual lava flows. Cluster analysis of the 21 elements measured in each of the 6 samples shows that the two samples from Flow B and C cluster together closer than with the sample from A? and with the rest of the A-samples. It is therefore possible that B is a late flow of the same eruption which produced C. Both flows have higher Si- and Ca- and lower Mg-values than the samples from the A-Flow.

Along the Chain of Crater road pockets of ash from the 1790 Kilauea eruption are exposed. This finding shows that the flow field is older than 200 years. LOCKWOOD (pers. comm.) retrieved three charcoal samples from the area (see Fig. 2 for locations; L93-19, 400±55 aBP; L-78-35 620±70 aBP; L-82-07, 230±60 aBP). If the youngest sample represents the best „ante post quem" date (and if we assume that the older samples represent material from older trees burnt by the lava at the same time) then the entire flow field should be dated to ca.1720 AD This is too young to be included into the Ai-la'au shield phase. However, if L-93-19 is representative of the age of the flow-group, and sample L-82-07 is considered to derive from a younger forest fire, then the flows would have Ai-la'au age.

There is another difficulty with classifying these flows as Ai-la'au, and that is petrography. The Keauhou Trail Tube lava is very olivin-rich, almost picritic. This is uncommon for the Ai-la'au shield lavas. It is interesting to note, that north of the road the Kipuka Kahili'i forms a large shield-like hill. On it we were able to find three outcrops below the Mauna Ulu ash, all yielded picritic basalts. The KTS tube, however, does not point toward this hill.

Younger lavas have buried the Keauhou Flow field in the east. A very prominent aa- channel covers its northern part and Mauna Ulu 1969-74 lava has sent fingers even across the Lower Keauhou Trail Cave.

5. Acknowledgments

Field work was supported by a grant from the German Research Council (DFG-Ke 287/13-1,2). We thank J. LOCKWOOD, W. R. HALLIDAY, and M. S. WERNER for field support and helpful comments, and J. MARTIN and B. CAMARA from the Hawaii National Park Service for kindly providing permission to enter caves in the park and for much appreciated local support.

References

BUCHAS, H., 1996: Differenzierung der Lavaflüsse der Ai-la'au Schildphase des Kilauea, Hawaii im Gebiet von Keauhou Trail anhand von Lavaröhren und Oberflächenmorphologie. Dipl. Kartierung, FB Geowiss., Techn. Univ. Darmstadt, 58 pp., unpubl.

FAVRE, G., 1993: Some observations of Hawaiian pit craters and relations with lava tubes. Proc. 3. Intern. Symp. Volcanospeleol., Bend, Oregon, July 30-Aug. 1, 1982:37-41.

HARTMANN, J., 1995: Keauhou Cave System im Keauhouflow auf Hawaii. Dipl. Kartierung, FB Geowiss., Techn. Univ. Darmstadt, 74pp, unpubl.

HOLCOMB, R.T. 1987: Eruptive history and long-term behavior of Kilauea Volcano. U.S. Geol. Surv. Prof. Pap. 1350 (1): 213-242.

KAMBESIS, P. 1995: Kazumura Cave Project - 1995. Nat. Speleolo. Soc. 1995(11): 300-303.

WOOD, C., 1980: Caves of the Hawaiian volcanoes. Caving Intern. Mag. 6&7: 4-11.

Fig. 2: Geological map of lava flows of the Keauhou Trail area (St.Sys = Stephan's System, MS = Matthias' System)

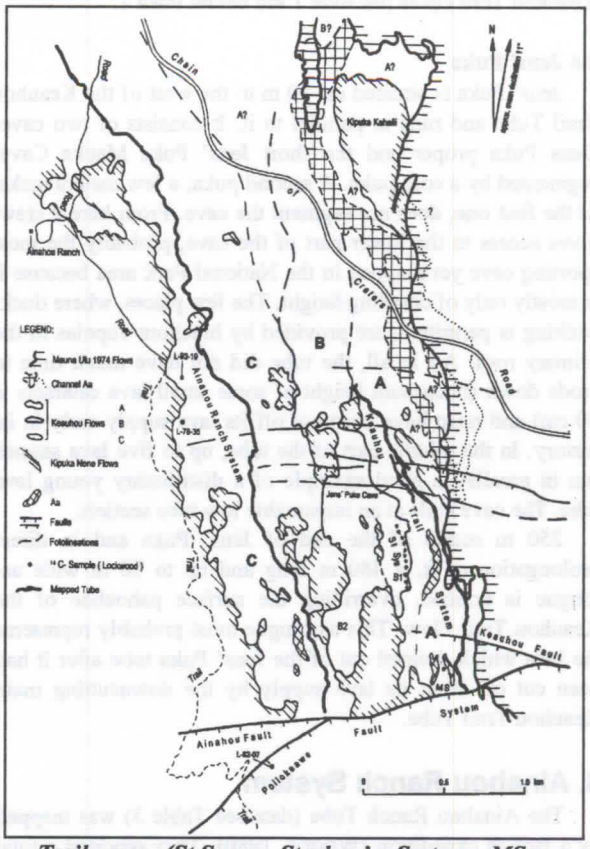

Trail area (St.Sys = Stephan's System, MS = Matthias' System.

Fig. 1: Extent of Kilauea Ai-la'au lava and major lava tubes

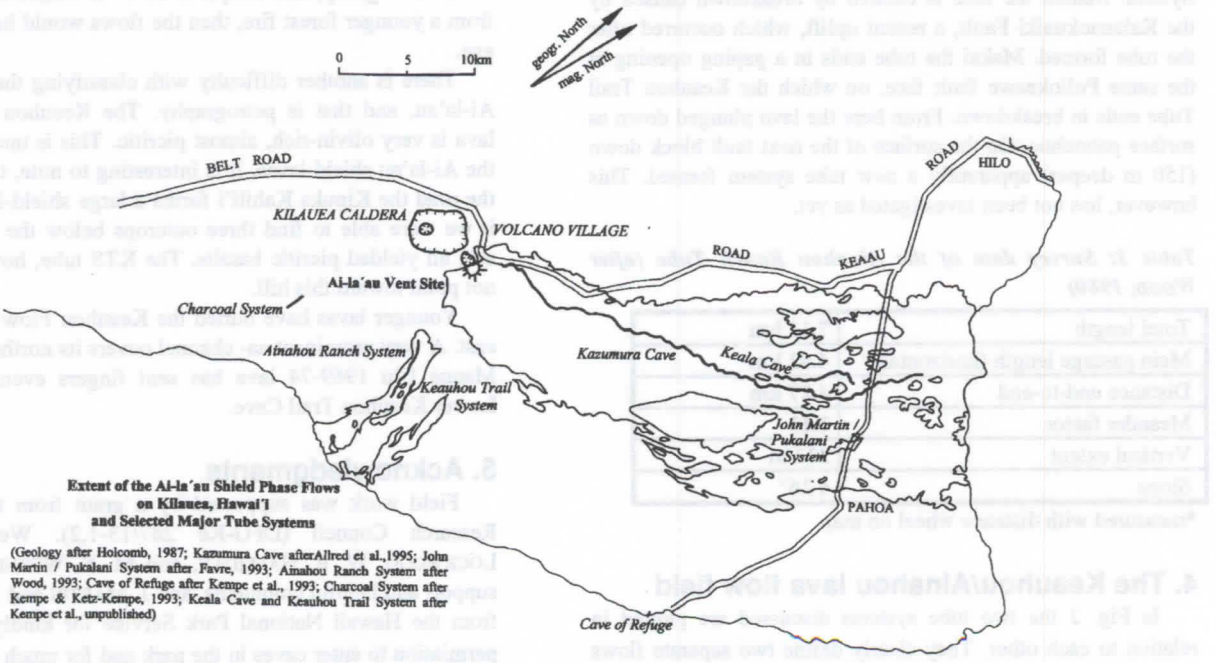

Recent Exploration of Lava Tube Systems in Kona and on Mauna Loa, Hawaîi

Douglas M. Medville and Hazel E. Medville
Hawaîi Speleological Survey
Reston, Virginia, USA

Abstract

The island of Hawaîi contains over 1,000 known lava tubes. Since the early 1990's, over 30 kilometers of lava tube has been found on the western slope of Hualalai, an older shield volcano on the island's west side, and on the north side of the largest volcano on Hawaîi; Mauna Loa. These tubes have linear extents of up to 6 km., diameters of up to 15 meters, and contain a variety of secondary mineralization, including sulfate crusts, crystals, and soda straws up to one meter in length. Some of the tube systems found in historic flows: e.g., the 1855 flow on Mauna Loa, consist of several sub-parallel but separate tubes. Also, several of the individual tubes are fairly complex, containing branching and braided passages resulting in a passage density comparable to that seen in limestone maze caves. The nature of the tubes in both areas will be described and contrasted: e.g., the tubes on Hualalai are near sea level and have a mean temperature of 26 degrees C while those on Mauna Loa are at elevations of up to 3400 meters and have mean temperatures as low as 4 degrees C.

Introduction

In the past several years, several substantial lava tubes have been found, explored, and surveyed in pahoehoe lava flows in several localities on the island of Hawaîi. In this paper, lava tubes in two of these localities will be described; these are found on the west side of Hawaîi north of the town of Kailua-Kona, and in the center of the island, to the north of the northeast rift zone on Mauna Loa.

Tubes North of Kona

The tubes to the north of Kailua-Kona are developed in historic and pre-historic flows from vents on the western flank of Hualalai, a volcano to the east of Kailua-Kona (summit elevation 2520 meters). Although the tubes here have been found in several flows, the greatest concentration of tubes have been found in three of these. In general, all of these tubes are at low elevations and thus, are hot: the mean temperature is 26 degrees C.

Tubes in the 1801 Flow

The longest and most voluminous tube complex is seen in the historic 1801 flow 14 km. north of Kona (Figure 1). This flow consists of at least two episodes (KAUAHIKAUA, 1995), the youngest of which contains a single large tube representing a unitary conduit having over 10 km. of surveyed passage and a vertical extent of495 meters. This tube, the Hue Hue Cave, is the second longest and deepest on the island of Hawaîi. In the upper (Clagues Cave) part of this system, 2.0 km of passage were surveyed in March 1996 (KEMPE, 1996) while just below another 2.7 km. were surveyed in Goat Herd Cave, also in 1996. These tubes were connected in March 1997 via another 1.7 km of survey. In the same flow episode but closer to the ocean and just down slope of the Clague's Cave/Goat Herd Cave complex, is another voluminous and extensive tube; the Power Line/Triple Puka complex with 3.1 km. of surveyed passage. In March 1997, these tubes were connected to each other and to the upper Clagues/Goat Herd complex, creating a single tube (the Hue Hue Cave) having a linear extent of 6.1 km. and, as noted above, a vertical extent of 495 meters, and a total surveyed length in excess of 10 km.

The tubes in the 1801 flow tend to be voluminous with widths of up to 10 meters and heights of 3 to 5 meters being fairly typical. The tubes are also unitary, with very little braiding observed and contain a variety of lava speleothems; primarily lava soda straws and ribbons up to a meter in length. In the higher gradient parts of the tubes, lava falls of up to 7 meters are also seen.

Tubes near the Kailua-Kona Airport

To the south of the 1801 flow and in the vicinity of the Kailua-Kona airport, several tubes are developed in prehistoric flows, dated by (CLAGUE, 1986a) at 2500 to 5000 years bp. The largest complex is found in a prehistoric flow and consists of about a dozen tubes having a combined length of 4 km. These tubes are aligned, are developed over a linear extent of 3 km., and several of them have been evaluated for their archeological significance. The tubes in this flow tend to have smaller volumes than those seen in the 1801 flow with widths of 3 to 5 meters and heights of up to 5 meters being common. Portions of the tubes are found at two levels about 3 meters apart. With an average depth beneath the surface of 3 to 4 meters, the tubes are also somewhat more shallow than the 7 to 10 meter deep tubes found in the 1801 flow. Consequently, individual tube segments tend to be shorter and are usually truncated by collapse.

The Tumuli Tubes

One of the most extensive and complex set of tubes is found 25 km. north of Kona, between State highway 19 and two circular collapsed tumuli, 2.75 km. to the southeast of the road and 180 meters higher. Here, in a prehistoric flow having an estimated age of 200-2500 years bp (CLAGUE, 1986b), 5.7 km. of tube has been surveyed. The three longest tubes in this flow have surveyed lengths of 1.4 to 1.8 km, are aligned, and are only separated by a few meters by rock fall that ends passages or by passage segments that become too low to traverse. Genetically, they are all part of the same tube. The tubes in this flow are quite complex. Braiding and branching is common with multiple (e.g., five) parallel but connected passage segments being observed in the same tube. These tubes are developed at several levels, increasing their complexity. The tubes are decorated and within them are found extensive areas containing white crusts; presumably of sulfate minerals.

In several places, intrusions of more recently emplaced lava terminate passages in these tubes or greatly reduce the passage size with tube heights of 0.3 meters frequently being encountered. The small passage size, combined with the maze-like nature of the tubes in this flow, has resulted in a substantial amount of effort being expended in their survey. This tube complex has been surveyed up to and around part of the perimeter of the lower tumulus and at this point, is 1 to 2 meters lower in elevation than the floor of the tumulus. The temporal and spatial relationship of the tubes to the tumuli is currently being studied.

North Mauna Loa

In contrast to the Kona-area tubes, the lava tubes found on the north side of the world's largest shield volcano, Mauna Loa, (summit elevation 4169 m) are at higher elevations: 2560-3400 meters and are colder with temperatures measured at 2 to 10 degrees C. Since 1992, 7.5 km. of tube has been surveyed in several historic and prehistoric flows originating on Mauna Loa's northeast rift zone.

Tubes in the 1855 Flow

The 1855 flow originates on Mauna Loa's NE rift zone at an elevation of 3170 meters and extends for 52 km. to the outskirts of the town of Hilo, almost at sea level. At elevations of 2500-2650 meters and 6 km. below (north of) the NE rift zone, over 6 km. of tubes have been surveyed since 1992 (Figure 2). These tubes extend over a linear distance of 1.8 km. The tubes in this flow are modestly complex, having braided passages usually about 4 to 6 meters below the local surface. Passages can be as much as 10 meters in width and 6 meters in height but are more typically 3-4 meters wide and 1-3 meters high.

The most notable aspect of tube development in this part of the flow is the parallel development of individual tubes as shown in Figure x. Here, three separate tubes, each having over a kilometer of surveyed passage, are found across a 530 meter lateral section of the flow. All of the tubes surveyed have been linked through surface surveys in order to determine the lateral separation between tubes. The tubes investigated in the 1855 flow to date represent a very small portion of the entrances seen in this flow and it is expected that many more kilometers of tube exist beneath this flow.

Other North Mauna Loa Tubes

In a prehistoric (750-1500 years bp) flow 3 km. west of the 1855 flow and at a elevation of 2800 meters, 700 meters of large passage have been surveyed in a cold, drafting tube complex (Wind Tunnel) that has developed on three levels over a vertical extent of 15 meters. At about the same elevation as wind Tunnel but another 3.6 km. to the west, about 700 meters of tube has been surveyed in a narrow prehistoric flow. To date, six short but highly decorated tubes have been surveyed and a mineralogical inventory has been conducted.

In addition to the above, several kilometers have been surveyed in many other lava tubes on the north side of Mauna Loa since 1992. The characteristics of these tubes depend on several factors; e.g., the age, thickness, and chemistry of the flows in which they are found. In addition, many large but inaccessible tube entrances have been seen from the air and it is expected that the lava tubes on the north side of Mauna Loa will be surveyed and studied for many years to come.

References

CLAGUE, D. A. and W. BOHRSON. 1985. Preliminary Geologic Map of Makalawena Quadrangle, Hawaii, U.S. Geological Survey Open File Report 85-595.

CLAGUE, D. A. and W. BOHRSON. 1986. Preliminary Geologic Map of Kiholo Quadrangle, Hawaii, U. S. Geological Survey Open File Report 86-336.

KAUAHIKAUA, J. 1995. U.S. Geological Survey, Hawaii Volcano Observatory, personal communication.

KEMPE, S. 1996. Technical University, Darmstadt, Germany, personal communication.

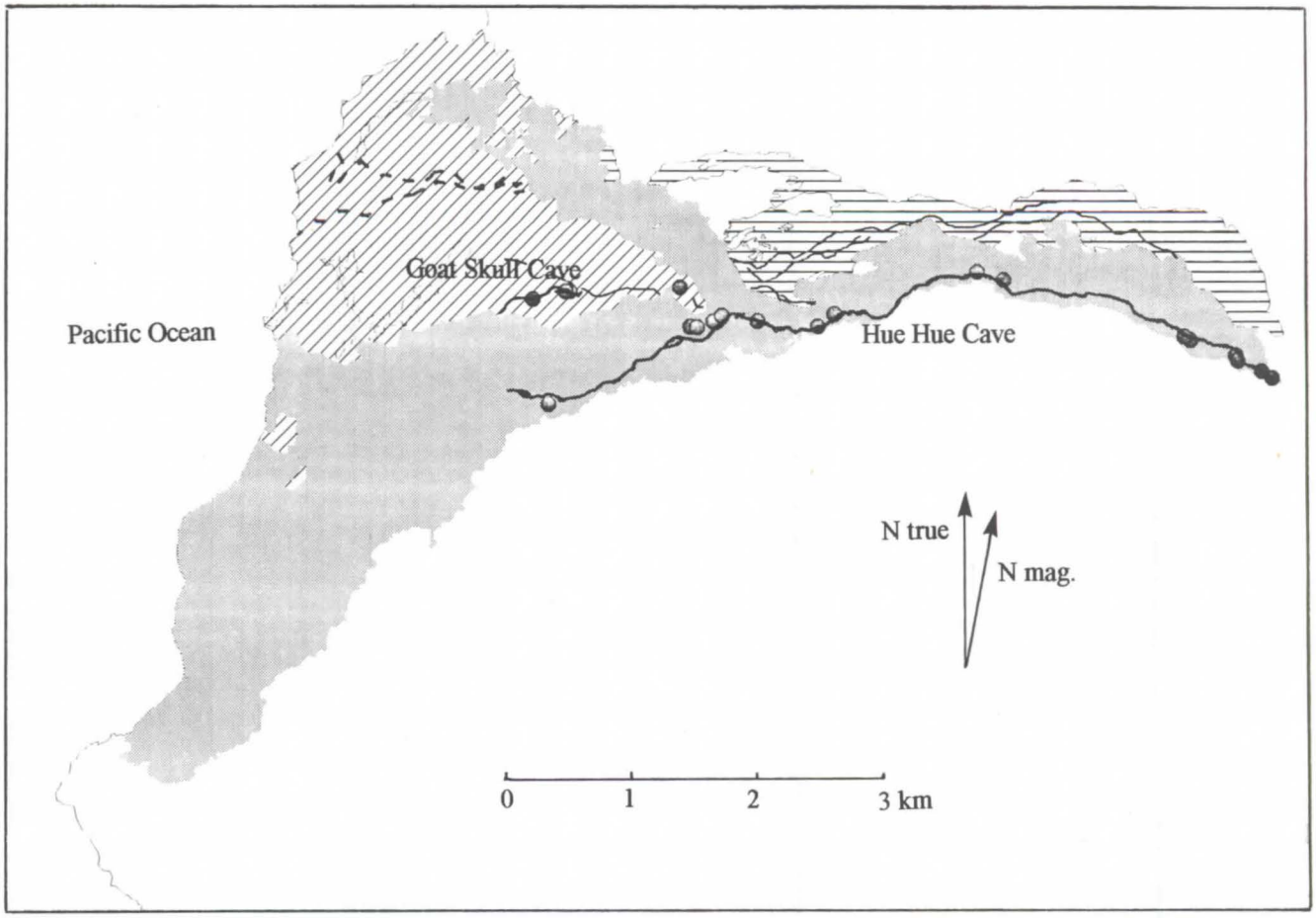

Figure 1: Map of the 1801 Hue Hue Flow and Caves

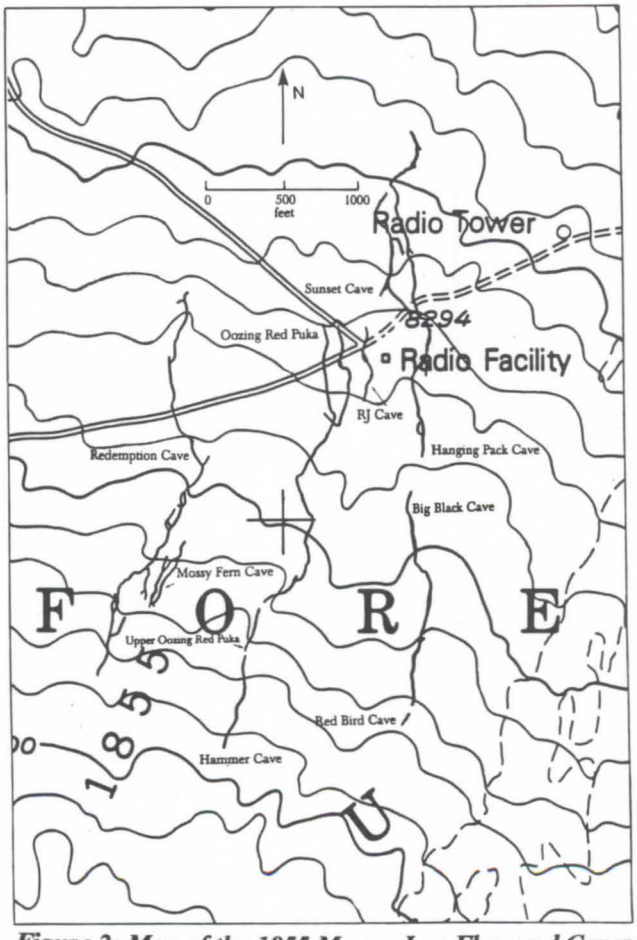

Figure 2: Map of the 1855 Mauna Loa Flow and Caves

Unusual Volcanic caves of Hawaii Island, Hawaii

by William R. Halliday
Hawaii Speleological Survey of the National Speleological Society
P.O. Box 1526, Hilo, Hawaii, U.S.A. 96721

Abstract

Numerous lava tube caves exist in Hawaii, including the world's longest cave of this type: Kazumura Cave on Kilauea volcano, Hawaii Island. Its mapped development is 59.33 km (slope length). Potentially of greater scientific interest, however, are some lesser known types of rheogenic caves and pit crater complexes, studied in this decade. On the floor of Kilauea crater are hollow tumuli (some of which are interconnected) and rheogenic caves within and adjacent to the boundary ridges of deflated lava tongues, lava rises, and related surface features. Some of these boundary ridge caves are complex horizontally and vertically. On Hualalai volcano, at the head of a very liquid 1800 basalt flow containing numerous ultramafic xenolith nodules are some small open vertical volcanic conduits (OVVCs) with short graded passages leading to open magma chambers 10 to 30 meters below the surface. These served as drainhack features and probably also as vents. A similar drainback cave was found beneath a deflated lava rise on the floor of Kilauea volcano. Also present on Hualalai volcano and elsewhere are notable sotano-like pit craters and complexes. Na One Pit is a complex of pit crater and OVVC 263 meters deep. Its OVVC opens on a ledge near the bottom of an otherwise typical pit crater of Hualalai volcano. Rift tube caves are present at the bottom of two pit craters of Kilauea volcano. Certain caves in the 1919 flow of Kilauea Crater are hyperthermic and their study requires special techniques discussed in a companion paper.

1. Introduction

Numerous lava tube caves exist in certain districts of Hawaii Island, including the world's longest: Kazumura Cave on Kilauea volcano. Its mapped development is 59.33 km (slope length). Other lava tube caves of this island also have slope lengths greater than 5 km (HALLIDAY, 1996). Also present on this island, however, are numerous caves of lesser known types, mostly studied only in this decade. These are much smaller than the dramatic lava tube caves, hut their scientific importance may be much greater. This paper classifies these lesser known types, and discusses some examples.

2. Hollow tumuli

In addition to lava tube caves with commonly noted features, sizable sub crustal spaces of several types exist on the floor of Kilauea Crater (and elsewhere). Most of these are due to deflation of partially stabilized volcanic structures enlarged or formed by injection of very fluid lava beneath a plastic crust. Most conspicuous are hollow tumuli, possibly first discus set by Walker who mapped and described the outer chamber of Tumulus E-l Cave (WALKER, 1991). It also has an inner room where the air temperature is at least as high as 51°C which apparently halted Walker's studies at a duck under connecting them. This room is beneath nearby Tumulus E-4, with a floor level about 2 meters lower than the start of the duckunder. On the surface there is no indication of the connection between the two tumuli. The outer room is 40 meters long, with a maximum width of 12 meters and ceiling height of 5 meters. The inner room is 20 meters long, up to 13 meters wide, and an estimated maximum ceiling height of 4 meters. (HALLIDAY, 1994; also in press). An example of a cave beneath a hollow "whaleback ridge" tumulus is Sleeping's Sister Cave, about 1/2 km east of Tumulus E-l Cave. It is 60 meters long, up to 12 meters wide and 2 meters high. When mapped, its maximum air temperature was 38°C but at times it filled by steam at much higher temperatures. Nearby, Almost Too Hot Cave is longer and hotter.

3. Boundary ridge and other caves of lava rises

Near Tumuli E-l and E-4 (and elsewhere in Kilauea Crater) are several low sunken areas with raised margins. WALKER (1991) termed these "lava rises". These are large crater-floor structures with centers deflated by withdrawal of very fluid lava after the margins had solidified. Small, irregularly rounded caves have been found beneath and adjoining the boundary ridges of at least two of these. The largest found to date has about 50 meters of passage. In the center of one lava rise, a vertical drainback OVVC can be entered beneath the partially collapsed floor of a small lava pond also. It has the form of an irregularly widened fissure about 10 meters long, 8 meters deep and up to about 3 meters wide.

4. Boundary ridge caves of deflated lava tongues

Similar but much more extensive boundary ridge caves exist along and adjacent to the margins of certain deflated lava tongues and flows in Kilauea Crater. To date, the largest and most complex example is Christmas Cave, a partially braided 2-level complex. It has a total of nearly 1/2 km of boundary ridge passages, rounded low chambers, and short lengths of rudimentary lava tube passages beneath a lava flat (possibly an atypical lava rise). The lower level is segmented and almost exactly beneath equivalent upper level passages. The overall pattern reveals complex subterranean piracy unsuspected from surface features, providing additional details of emplacement of flow fields of very fluid lava. This cave is normothermic to mildly warm, but others on the crater floor are as hot as 62°C. New techniques discussed in a companion paper have permitted studies up to 51°C.

5. Boundary ridge caves of related and/or complex features

The main entrance room of Sleeping Ohia Cave is within a hollow tumulus, much as in the case of the outer room of Tumulus E-l Cave. When steam conditions permit, however, it is possible to investigate a low tubular downflow extension 55 meters long which is not beneath this tumulus. Moreover, on the far side of the entrance breakdown are rounded extensions of the cave beneath low, inconspicuous ridges also unrelated to the central tumulus. Another example of a complex subcrustal cavern is Ring Cave. Its main section is beneath a low oval tumulus 20 by 30 meters in diameter, with a partially collapsed center (a common pattern). It also has a 12 meter downslope extension much like that of Sleeping Ohia Cave. In addition, however, a penetrable orifice about 1/2 meter above the floor connects it to a low boundary ridge cave about 25 meters long, at the head of a deflated tongue. Just beyond the latter is Ringleader Cave which has the appearance of a rudimentary, almost featureless lava tube cave 50 meters long, 6 to 7 meters wide, and 1 1/2 meters high, beneath a lava flat.

6. Open vertical volcanic conduit caves

In 1800, a short-lived eruption of very fluid basalt on Hualalai volcano deposited puzzling beds of ultramafic xenolith nodules. At and just below the head of these beds is a sequence of open vertical volcanic conduits (OVVCs) as defined by SKINNER (1992) and other cavernous volcanic features.

Unlike most OVVCs, small but significant caves can be entered at the bottom of some of these (HALLIDAY, 1992). The largest of these caves reaches a depth of 30 meters. It consists mostly of a large, steeply sloping chamber. Much of its ceiling is a "hanging wall" consisting of a single bed of very dense lava. In this matrix are ultramafic xenoliths of various types. Beds of xenolith nodules also are present in this cave. A small bed of the nodules also can be seen on the downslope lip of a cavernous-pahoehoe vent at the upper end of the nodule beds, but nowhere else in the OVVCs nor in the small chambers or passages at the bottom. These OVVCs clearly served as drainback routes forgery fluid lava; less clearly they also served as vents. This nodule-bearing flow is of special interest to planetary geologists (BALOGA et al, 1995). Unfortunately only one planetary geologist (with two of his graduate students) has been able to crawl into some of the most intriguing subsurface sites and the volcanology literature is almost wholly lacking in speleological observations of this fascinating site.

7. Sotano-like pit craters and complexes

Pit craters on Hualalai volcano are much more like Mexican sotanos than are their counterparts on Mauna Loa and Kilauea volcanoes. With a depth of 263 meters, the compound volcanic structure of Na One Pit shows especially clear similarities. Approximately half its depth consists of an OVVC shaped like an inverted, elongated funnel, much like Iceland's Prihnukargigur (STEFANSON, 1992). This vertical conduit opens upward on a ledge near the bottom of an otherwise typical pit crater about 150 meters in diameter and 135 meters deep. Most of the great pit craters of Hualalai volcano are on closely controlled private property where permission to enter is rarely granted. One of the deepest is estimated by the U.S. Geological Survey to be 200 meters deep (MOORE & CLAGUE, 1991). From the far side, the opening of a lava tube cave is visible perhaps 30 meters below the rim. Farther down the slope of Hualalai volcano a small, accessible vent complex has several interconnected OVVCs about 30 meters deep, a spatter pit with about the same depth plus three side chambers, and a largely unexplored deep cave passage leading downslope (HALLIDAY, 1995). Some recent proposals would transfer much of Hualalai volcano to public ownership. Much more should he heard of its caves and pits in the future.

8. Rift tube caves

Unless deeply buried by successive flows and later exposed by erosion or by the work of man, lava tube caves are rarely as much as 25 meters below the surface. Boundary ridge caves are even more superficial. On the other hand, during summit eruptions of Kilauea volcano open caves leading into the Southwest Rift Zone often have been recorded. In every

case, however, they soon have been closed by rockslides and rockfall. In two other locations, such caves have remained open long enough for at least limited studies: Mauna Ulu pit crater and the mis-named Wood Valley Pit Crater (FAVRE, 1993). Such caves are especially important for studies of cooling rates and processes, and of secondary volcanic minerals. Apparently neither has been reentered since Favre's 1981 expedition.

References

BALOGA, S., P. D. SPUDIS & J. E. GUEST 1995. The dynamics of rapidly emplaced terrestrial lava flows and implications for planetary volcanism. J. Geophys. Research 100: 24, 509.

FAVRE, G. 1993. Some observations on pit craters and relations with lava tubes. Proceedings of the 3rd International Symposium on Vulcanospeleology, Bend, Oregon, U.S.A., 1982. Vancouver, Washington,A.B.C. Publishing, p. 37-41.

HALLIDAY, W. R. 1992. Caves and associated features of open vertical volcanic conduits of the Kaupulehu Lava Flows xenolith nodule beds, Hualalai volcano, Hawaii: basic speleological considerations. Report #92-05, Hawaii Speleological Survey of the National Speleological Society, 12 p.

HALLIDAY, W. R. 1994. Caves of Kilauea Caldera: cave resource inventory and management recommendations. Report #94-05, Hawaii Speleological Survey of the National Speleological Society. 36 p. + maps.

HALLIDAY, W. R. 1995. Considerations of Puhia Pele for inclusion in the Hawaii Natural Area Reserve System. Report #95-02, Hawaii Speleological Survey of the National Speleological Society. 5 p.

HALLIDAY, W. R. 1996. Lava tube caves over 5 km currently in IUS files. IUS Commission on Volcanic Caves Newsletter #11, October 10, p.3.

MOORE, R. B, & D. A. CLAGUE. 1991. Geological map of Hualalai volcano. U.S. Geological Survey Misc. Invest. Series Map 1-2213, with text.

SKINNER, C. E. 1993. Open vertical volcanic conduits: a preliminary investigation of an unusual volcanic cave form with examples from Newberry volcano and the central High Cascades of Oregon. Proceedings of the 3rd International Symposium on Vulcanospeleology, Bend, Oregon, U.S.A. 1982. Vancouver, Washington, A.B.C. Publishing, p. 7-16.

STEFANSON, A. B. 1992. Prihnukargigur. Proceedings of the 6th International Symposium on Vulcanospeleology, Hilo, Hawaii, U.S.A. Huntsville, Alabama, National Speleological Society, p. 197.

WALKER, G. P. L. 1991. Structure, and origin by injection of lava under surface crust, of tumuli, "lava rises", "lava rise pits", and "lava inflation clefts" in Hawaii. Bull. Volcanol. 53: 546-558.

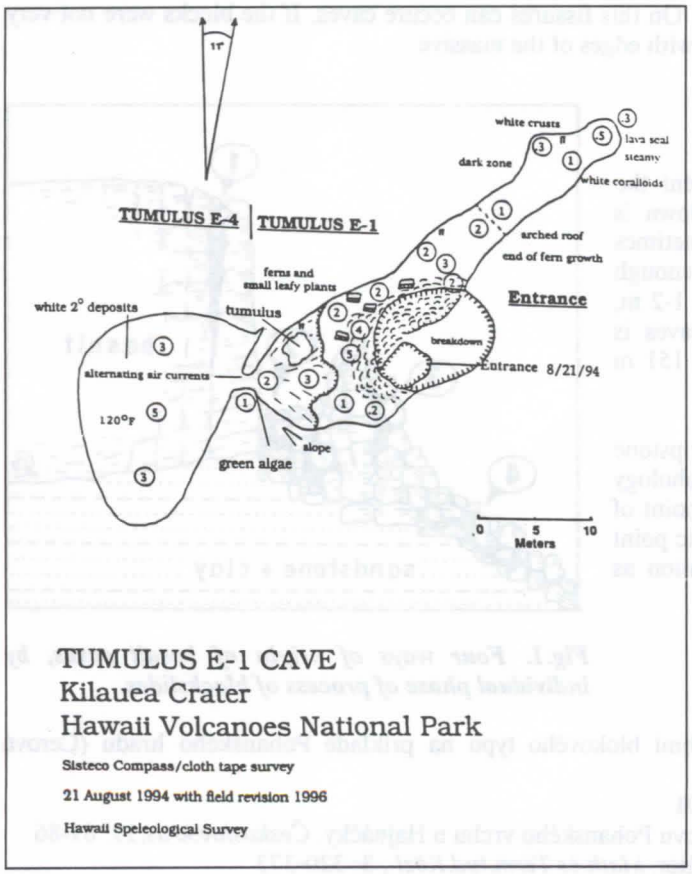

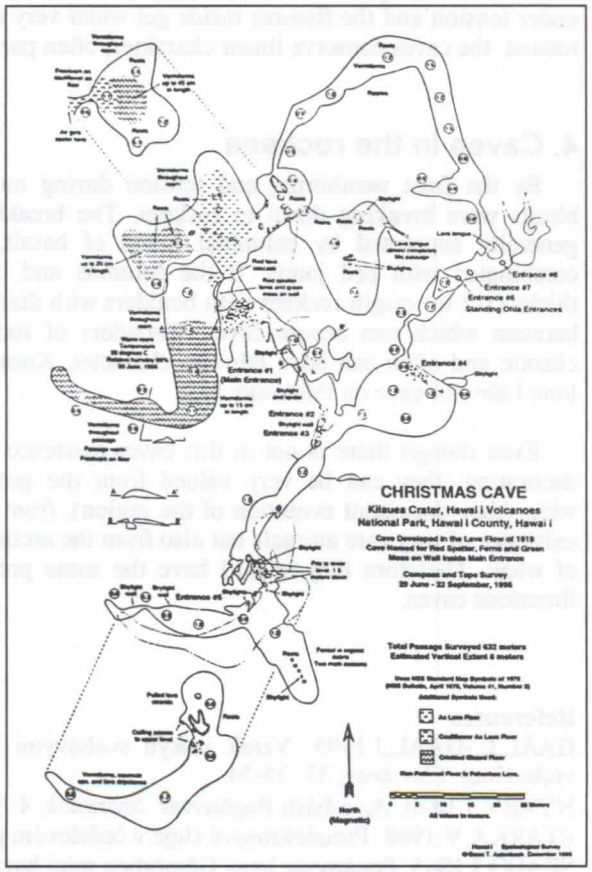

The model of development of basalt caves by slope movements

Ľudovít Gaál

Slovak Environmental Agency, Svätoplukova 40, 979 01 Rimavská Sobota, Slovakia

In the South of Slovakia, in the mountains Cerová vrchovina, is located a basalt cover named Pohanský hrad (V.STÁRKA 1967, Ľ.GAÁL-J.GAÁL 1995, or Pogányvár - J.SZABÓ 1865, J.NYÁRY 1869), where are created optimal conditions for development of caves by slope movements (plastic sandstone complex under rigide basalts, deep valleys around basalt plateau). At the present there are researched 31 caves in total area cca 1 km^2, with lenght from 3,2 m up to 182 m. According to the study of development of moving basalts blocks on the slope, the caves can be devided into following 4 categories:

1. Caves on the edges of the basalt plateau

Fissures on the edges of plateau represent initial stadium of the slope movements. Their are always parallel with the edge of the plateau. They where formed by growing of the pulling tension between margin blocks and massive, after erosion removal of stiff leaning from nearest basalt cover. If there is sufficient width of the fissure (generally up to 2 m) covered by the dropped boulders, the origin of caves begins. These caves are thin and always linear, ramificated only on diagonal lithoclases.

2. Caves in the fissures between the blockslide and massive

Between lower plastic (sandstone + clay) and higher rigide (basalt) complex were origined skid areas. By the gravitation the margin blocks slowly begin to separate from the massive and move down on the slope. Between slid blocks and massive origin fissures of different width (generally up to 5 m), which are covered by big boulders. Between boulders can occure caves, which have also linear character. Their width is limited by the width of fissure.

3. Caves inside the blockslides

By the measurement of leaking some of the blockslides brake down to a rocksea or they stay still sometimes even longer (there are knowen blocks, which are slide on slope 170 m). The movement of the blocks can have translated character on the plain or can come to the rotation with the backwords leaning. The blocks are during the movement under tension and the fissures inside get wider very often. On this fissures can occure caves. If the blocks were not very rotated, the caves conserve linear charakter, often parallel with edges of the massive.

4. Caves in the rocksea

By the frost weathering and tension during movement the blocks were breaking down to rocksea. The breaking down is generally supported by columnal joints of basalt, sometimes combinated with bed joints. If the columns and beds enough thicks (1-2 m) origin rocksea with boulders with diameter 1-2 m, between which can occure caves. Corridors of such caves is chaotic and often can have labyrint character. Known is 151 m long Labyrint cave on Pohanský hrad.

Even though there is not in this caves existence of dripstone decoration, they can be very valued from the geomorphology wiew (they document evolution of the region), from the point of existence of very rare animals but also from the archeologic point of wiew. Therefore they should have the same preservation as limestone caves.

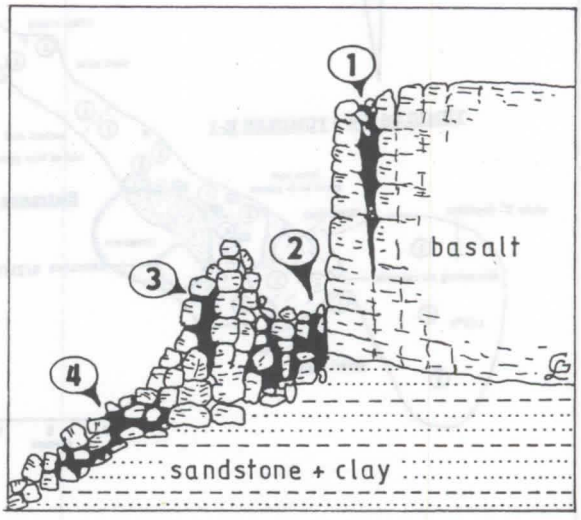

Fig.1. Four ways of origin of basalt caves, by individual phase of process of blockslides.

References

GAÁL,Ľ.-GAÁL,J.1995. Vznik jaskýň svahovými pohybmi blokového typu na príklade Pohanského hradu (Cerová vrchovina). *Slov.kras*, 33: 35-54

NYÁRY J.1870. Az ó-básti Pogányvár. *Századok*, 4: 97-101

STÁRKA,V.1968. Pseudokrasové sluje v čedičovém příkrovu Pohanského vrchu u Hajnáčky. *Československ.kras*,19: 81-86

SZABÓ,J.1865. Pogányvár hegy Gömörben mint bazaltkráter. *Math.és Term.tud.Közl.*, 3: 320-373

Gravity caves of the Siberian Platform

Andrey G. Filippov
East Siberian Research Institute of Geology, Geophysics and Mineral Resources,
Dekabrskih Sobitiy street 29, 664007 Irkutsk, Russia

Abstract

Gravity crevice caves include a special form, sometimes referred to as unloading caves or sherlopy. Such caves are frequently located on slopes and plateaus above river valleys of the Siberian Platform. Sherlopy are formed in vertical or steeply inclined cracks of unloading slopes, developing in basalts, tuffs, sandstones, dolomites and limestones. The cave's ceilings are formed from displaced rock blocks or wedged rock and earth obstructions. Sherlopy are known to reach depths of 144 m, and lengths of 820 m. The cave's microclimates may be either static, or dynamic, depending on whether the air is still or blowing. Microclimates are also described as warm or cold, depending on whether the temperatures in the caves are above or below 0°C during the winter. Lithogenesis is characterized by an intensive hypergene transformation of host rocks and debris, by the occurence of condensational formations in many caves, and by physical and chemical decomposition of minerals.

1. Introduction

The term "gravity caves" refers to caves formed as a result of displacement of rocks by gravity. There are several types of gravity caves. These are distinguished by the composition of their formation and include caves formed from breakdown or collapses, block landslides, and unloading. On the Siberian Platform, caves of the last type are widely distributed. Morphologically, they are represented by vertical or steeply inclined cracks, clefts, and horizontal fissure caves, distributed predominately along the edges of table plateaus in watersheds along deep river valleys. The caves are formed as a result of slope unloading, as described in 1932 by SOKOLOV (1933).

The essence of the phenomenon of unloading ist that one-sided removal of a lithostatic load occurs along the natural entrenchment created by a valley in a massif. This results in a slow displacement of rocks into the valley due to the influence of internal stresses and gravity. Deformation of the massif results in the formation of new joints or the opening of existing joints that are across or diagonal to the slope. Slope deposits and/or the debris crumbled from the walls of the joints crowds into these cracks, and acts as a wedge, opening the joint further (SOKOLOV, 1962a).

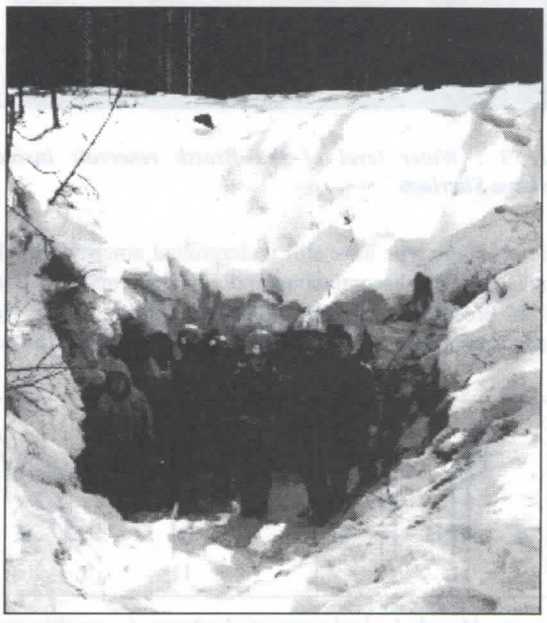

Figure 1 : Entrance sink of Volglaya Sherlopa on the Olkha River. Photo by S.I.Levashov

Caves of this type have been described by different authors as pseudokarstic caves (SOKOLOV, 1962; TURCHINOV, 1992), gravity caves (TURCHINOV, 1992), caves in unloading joints (SOKOLOV, 1962a; LUKIN, 1965), caves of dilatansion type (DUBLYANSKY & ANDREJCHOUK, 1989), corrosion gravitational caves (DUBLYANSKY, 1977), corrosion breaking caves (BERSENEV, 1989), thermokarstic caves in slope cracks (SPESIVTSEV & BELYAKOV, 1980), caves in slope cracks (TROFIMOVA, 1993), unloading caves (FILIPPOV, 1993, 1994), and sherlopy (FILIPPOV, 1994a).

The local Russian population along the Angara, Ilim, and Lena rivers call such caves "**øåðëîïû**" - "sherlopy" (singular "**øåðëîïà**" - "sherlopa"). I propose that this local name be accepted for wide use in the speleological literature for crevice caves large enough for human penetration consisting of hollow, gaping cracks formed by the unloading of slopes, and usually possessing roofs formed of displaced blocks of rock, wedged rock-earth chokes, and a soil layer (FILIPPOV, 1994a).

2. General characteristic

Sherlopy are usually accompanied by a number of surface features. These include linearly located sinks, blowing apertures and fissure wells, threaded along an unloading crack and by unloading ditches ranging from a few tens of centimeters up to several meters in depth (figure 1). During subfreezing winter weather, sherlopy are easily detected by columns of humid air which rise from the apertures to form plentiful hoarfrost on trees and bushes. Sherlopy are frequently located parallel to one another across the slope along linear segments of river valleys, and up to 1.5 km back from the river. Perpendicular sherlopa systems are sometimes formed on sites where two rivers valleys join.

The average length of the 51 surveyed sherlopy is 75 m and the mean depth is 28 m. Lengths range from 12 m up to 820 m. These lengths are characterized throughout by false passages and floors, formed by the debris of host rocks wedged into narrow parts of cracks. A more meaningful attribute is the length of the horizontal projection or plan view of a sherlopa. These range from 8 m to 125 m, with a mean of 34 m for the 51 surveyed

sherlopy. Sherlopy, irrespective of the composition and age of their host formations, have a similar structure and morphology. As a rule, sherlopy are steeply inclined or subvertical cracks with widths ranging from 30 cm (minimum size accessible to humans) up to 4 m in the largest cavities.The average width of passage ranges from 0.8 up to 1.2 m.

A characteristic feature of sherlopy is the progressive narrowing of the cross section of passages from the surface downwards. Many sherlopy have no floor, with the walls continuing to pinch below the survey. On vertical cross sections of such sherlopy these elements are shown conditionally by dotted lines, reflecting the narrowing of the crack beyond physically accessible limits (figure 2). The pinching cracks may continue downwards for many meters. Some sherlopy near the Bratsk, Ust-Ilim, Vilyuy and other reservoirs have been flooded by waters rising behind the dams. Examples are the sherlopa in

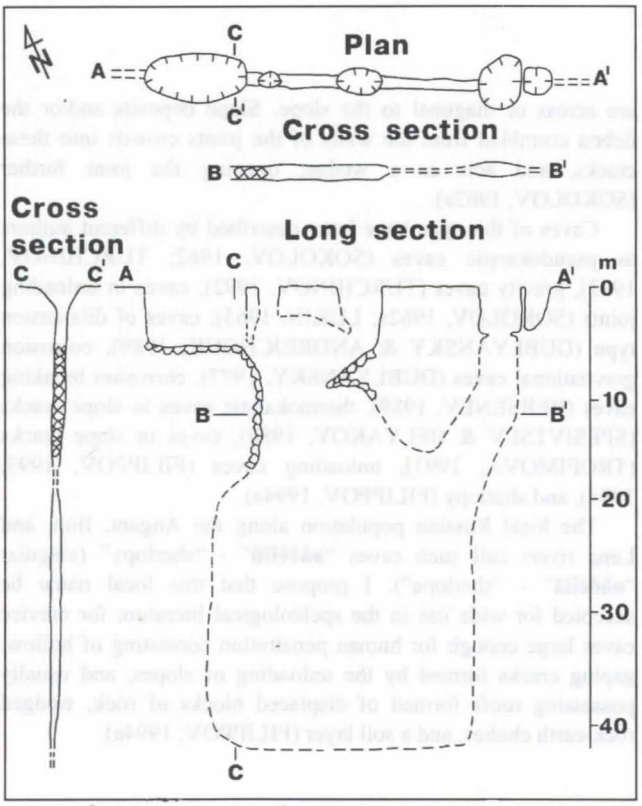

Figure 2 : Kunitsinskaya-10 Sherlopa. Dotted line shows the physically accessible limits to humans

basalts on the Vilyuy River, Yakutia (SPESIVTSEV & BELYAKOV, 1980), and the Spasskaya Sherlopa on the Angara River (personal observations, figure 3).

In other cases, false floors composed of wedged debris of different sizes are observed. Depending on local conditions these false floors may be composed of rock detritus, clay, or ice plugs. In zones of continuous permafrost, debris are, as a rule, cemented by ice. In "live" extended sherlopy, collapse apertures in false floors may be frequent, or the floors may be discontinuous. The false floors may also form at different levels, forming multiple false levels to the cave.

Sharlopy are rectilineal as a rule (figure 4A), but often they have insignificant knee-shaped bends in the plan and perpendicular cross section (figure 4B). Occasionally passages may join at acute (figure 4E, 5) or right (figure 4C,D), or obtuse angles (figure 4F). There is only one known example of a sherlopa with a horizontal labyrinthine structure on the Siberian Platform. It is situated an island in the Angara River. The crevice maze is formed by cave passages developed along crossed unloading cracks (SOKOLOV, 1962a: 75).

The sherlopy rather frequently are subvertical two-dimensional labirinths. They are guided between debris chokes, wedged blocks. The structure of some such sherlopy is not stable and are changed year after year due to breakdown of blocks. Such cavities are very dangerous.

The walls of sherlopy are formed by a rock plane of the mother massif and an unloading block, or by planes of two parallel unloading plates. As a rule, they are erratic and are complicated by rock ledges, shelves (figure 6), and overhanging cornices.

The sherlopy are divided into two microclimate types according to air regime: static and dynamic (blowing). The

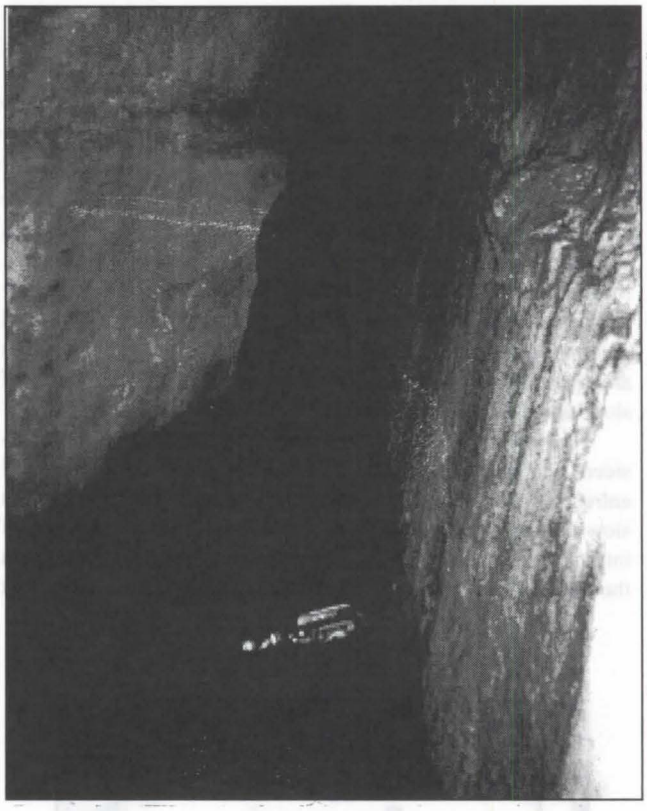

Figure 3 : Water level of the Bratsk reservoir inside of Spasskaya Sherlopa

cavities of static type have still underground atmospheres. They are rather rare in discontinuous and island permafrost, but are usual for areas of continuous permafrost. They contain frozen deposits, sometimes - frozen lakes or pools. Dynamic (blowing)

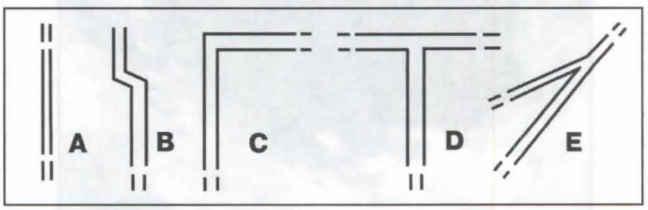

Figure 4 : Morphological types of sherlopy: A - rectilinear, B - rectilinear with knee-shaped bends, C - Γ-shaped, D - T-shaped, E - branching

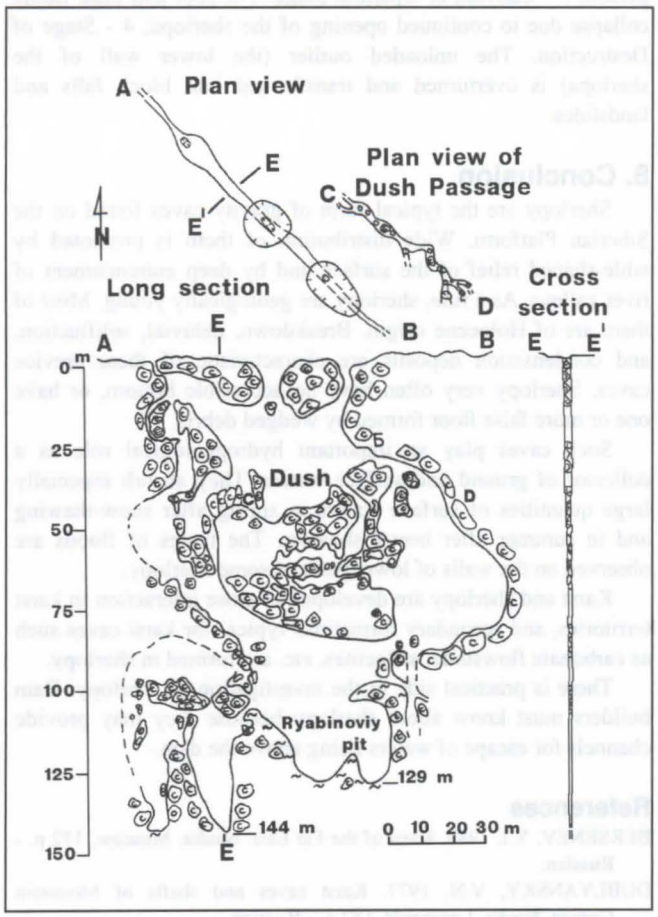

Figure 5 : Kurtujskaya Sherlopa, the Onot River

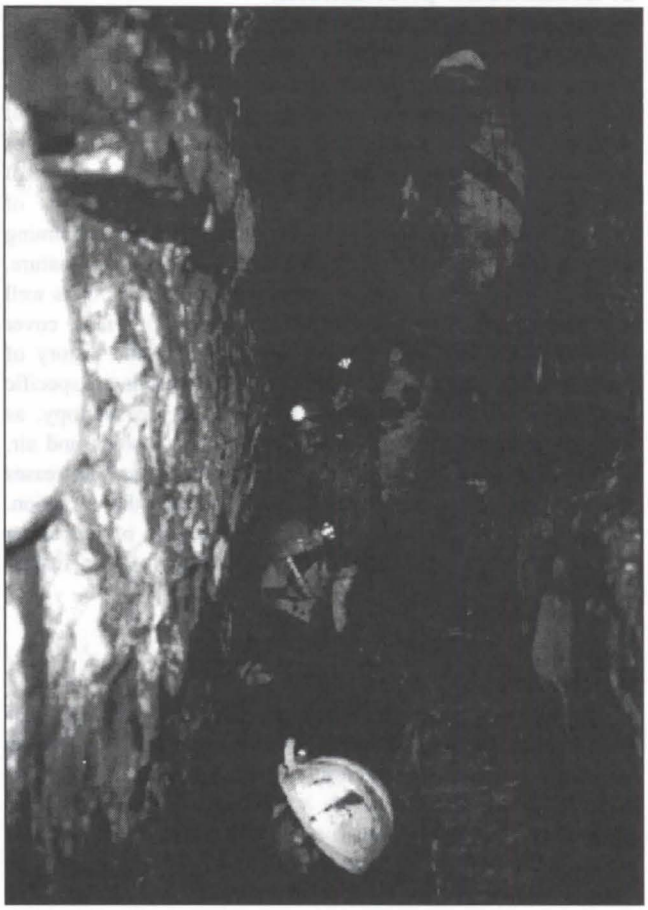

Figure 6 : Shelf on the wall of Volglaya Sherlopa

cherlopy are characterized by appreciable air movements. In a number cases, velocity of air flows taken by anemometers reaches 1-3 m/sec with calm weather on the surface. The rushes of wind are fixated in all large sherlopy characteried by the depth more than 30-50 m. In winter the air flows upwards forming the columns and wreaths of mist. The strong air movement plays a role for geochemical processes inside the sherlopy due to transportation and redistribution of moisture and aerosols, generation of condensational formations, and winter-proofing influence on subsurface parts of the cavities.

By thermic regime, sherlopy are divided into cold and warm types. The cold sherlopy have temperatures below 0°C in winter. Accordingly, the wintery temperature of warm caves is above zero. Winter air temperatures inside warm sherlopy usually are +0.4 - +4°C, with surface air temperatures of -10 - -45°C. The internal humidity of sharlopy is fixed at 95-98 %.

3. Geographical distribution

Presently, 51 sherlopy have been surveyed on the Siberian Platform. Among these, 26 sherlopy are situated on the Angaro-Lenskoe plateau in Middle - Upper Cambrian sandstones, Lower Ordovician sandstones and Lower Triassic basalts along the Lena, Angara, Ilim, Igirma, Yakurim rivers; Nineteen sherlopy are - in the Prisayan Foredeep in Vendian-Lower Cambrian carbonates, Lower Cambrian dolomites and Vendian sandstones along the Onot, Iret, Shamanka and Tojsuk rivers. Two are in the Pribaikal Foredeep in Lower Cambrian limestones and the Middle - Upper Cambrian sandstones along the Manzurka and the Lena rivers. Two are formed in Rephean shales along the Elovka River on the Primorsky Ridge; Three are in Western Yakutia in Upper Ordovician gypsum rocks and Lower Silurian limestones along the Vilyuy and the Alakit rivers. More of such crevice caves are known, but have not been surveyed.

4. An example of sherlopa

The largest known sherlopa is Kurtujskaya shaft (figure 5), located 260 m above the left bank of the Onot River in the Eastern Sayan foothills. It is developed in horizontally and thickly-bedded Lower Cambrian limestones. It has three entrances, two of which begin as pits at the bottom of deep conical sinks. The third entrance is a pit with a diameter of 0.5 m on a level surface. A circuit of suffosional sinks is located on the surface above the sherlopa. By descending into the entrance pits, one can confirm that the ceiling of the sherlopa is formed by angular blocks of shattered rock. This shattered ceiling has collapsed to form the entrance pits, leaving 1.5 to 4 m wide fissure shafts with vertical walls. The upper false level is located at a depth of 40 to 50 m. The floor is composed of a combination of scree and blocks of limestone. The fragments of an ancient karstic cavity, cleaved by the unloading crack, are observable at several sites. There are passages, leading to the bottom parts of Kurtujskaya Sherlopa in a number of places in the floor. As one descends, the walls gradually get narrower and the width of the gallery is only 30 to 50 cm at a depth of 120 to 144 m. The walls at these depths are covered by a 5-10 cm thick layer of sticky red-brown clay.

The air temperatures of Kurtujskaya Sherlopa are +2 - +4°C in winter, and +4 - +7°C in summer. The air humidity is about 100 %. During spring and summer, dense mist and underground rain are usually observed inside the cave.

5. Breakdown phenomena

Breakdowns are integral and regular events in the history of sherlopy. The wedged debris of the roof and false floors are always unstable. The reason for breakdowns and collapses include the suffosional removal of thin material from the roofs of sherlopy and false floors, seasonally wetting and drying of deposits, the progressive expansion of sherlopy as a result of unloading, freezing and melting of deposits in the tops of cavities, seismic pushes, and vibrating effects. The overwhelming majority of sherlopy have entrances of a collapsed nature. Entrances excavated by cavers in the bottoms of sinks in as well as lateral entrances on steep slopes nearly bare of friable cover are exceptions. Breakdown plays many roles in the history of sherlopy. The formation of debris deposits results in specific accumulational and destructional relief inside the sherlopy, as well as increasing the surface area of partition of rock and air. This results in a moisture increase in sherlopy and increases opportunities for condensation and freeze thaw action. Breakdown is also responsible for the wedging of unloading cracks at deeper and deeper levels, resulting in their further opening.

6. Deposits

Because of the morphologies and mechanisms of development, unusually dynamic microclimates, and intensive air and moisture exchange, sherlopy contain a characteristic set of deposits. Breakdown, deluvial, solifluction, and condensation formations are typomorphic (i.e. typical for caves of a given genesis). Breakdown deposits are the most typical, occuring as wedged debris and as block-debris chokes creating the false floors.

Lithogenesis inside sherlopy is characterized by intensive hypergene transformation of host rocks, debris, wide development of condensational formations, and physical and chemical decomposition of minerals. Condensational coralloids, buds, and crusts are incorporated in rocks, containing carbonates including limestones, dolomites, sandstones and marls. They are mostly found near the tops of sherlopy (0 to 20 m of depth), where the thermal regime allows plentiful condensation. The presence of other types of deposits is dependent on local natural conditions at individual sites. Such deposits are functions of the structure of the host rocks, the biological and other features of a site, and anthropogenic effects, and are not unique to the genesis of sherlopy (FILIPPOV, 1994).

7. Evolution

There are four major stages in the history of a sherlopa (figure 7): 1 - Initial Stage. An unloading crack with a gap up to 30 cm is formed; 2 - Slot-hole, or Pure-cave Stage. The unloading cracks open up to sizes necessary for passage by a person; 3 - Canyon, or Opening Stage. The roof and false floors collapse due to continued opening of the sherlopa; 4 - Stage of Destruction. The unloaded outlier (the lower wall of the sherlopa) is overturned and transformed into block falls and landslides.

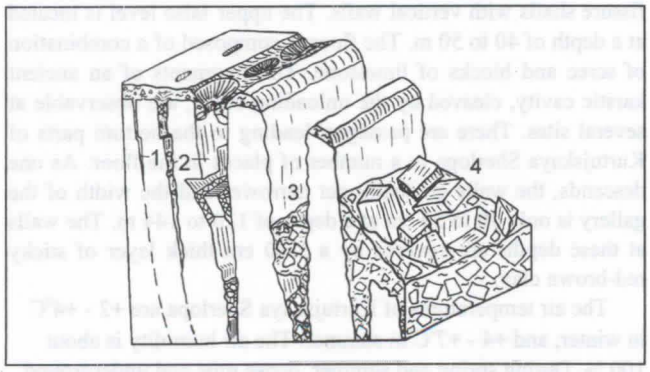

Figure 7 : Development stages (1 - 4) of a sherlopa

8. Conclusion

Sherlopy are the typical form of gravity caves found on the Siberian Platform. Wide distribution of them is promoted by table-shaped relief of the surface and by deep entrenchment of river valleys. As a rule, sherlopy are geologically young. Most of them are of Holocene origin. Breakdown, deluvial, solifluction, and condensation deposits are characteristic of these crevice caves. Sherlopy very often have no accessible bottom, or have one or more false floor formed by wedged debris.

Such caves play an important hydrogeological role as a collector of ground and surface waters. They absorb especially large quantities of surface waters in spring after snow-thawing and in summer after heavy showers. The traces of floods are observed on the walls of lower parts of some sherlopy.

Karst and sherlopy are developed in close interaction in karst territories, and secondary formations typical for karst caves such as carbonate flowstone, stalactites, etc. are formed in sherlopy.

There is practical side to the investigation of sherlopy. Dam builders must know about sherlopy because they may provide channels for escape of waters rising above the dam.

References

BERSENEV, Y.I. 1989. Karst of the Far East. Nauka, Moscow, 172 p. - Russian.

DUBLYANSKY, V.N. 1977. Karst caves and shafts of Mountain Crimea. Nauka, Leningrad, 182 p. - Russian.

DUBLYANSKY, V.N. & V.N. ANDREJCHOUK. 1989. Speleology. (Terminology, communication with other sciences, classification of cavities). Sverdlovsk, 33 p. - Russian.

FILIPPOV, A.G. 1993. Caves of Irkutsk Region. In: (K.A.Gorbunova, ed.): Caves. The results of investigations. Publishing House of Perm State University, Perm: 71-83. - Russian.

FILIPPOV, A.G. 1994. Genetic Classification of Unloading Caves Deposits. In: Scientific Readings. IV All-Urals meeting on underground waters of the Urals and of surrounding territories. Publishing House of Perm State University, Perm: 121-123. - Russian.

FILIPPOV, A.G. 1994a. Sherlopy. In: Karstic Collapses. Nauka, Ekaterinbourg: 22-25. - Russian.

KHOTINA, E.B. 1987. Deluvial Deposits. In: (G.S.Ganeshin, ed.): Manual on methods to be used in the studies and geological survey of the Quaternary deposits. Nedra, Leningrad: 51-52. - Russian.

LUKIN, V.S. 1965. Caves in unloading joints. In: (G.K.Mihailov, ed.): Caves. 5(6): 74-81. - Russian.

SOKOLOV, D.S. 1962. Main conditions of karst development. Moscow, 322 p. - Russian.

SOKOLOV, N.I. 1933. Geomorphology of Angara valley from a source up to the thresholds. In: Materials of First All-Union Geographical Congress, issue 2, Leningrad.

SOKOLOV, N.I. 1962a. About a parity relationship of karst and slope unloading phenomenon. In: (N.A.Gvozdetsky & N.I.Sokolov, eds.): General Questions of Karstology. Publishing House of Academy of Sciences of the USSR, Moscow: 70-77.

SPESIVTSEV, V.I. & L.P. BELYAKOV. 1980. The collapsed forms of relief in trapps on the slopes of the Vilyuy Reservoir. In: Labour of Gydroproekt Institute. 73: 69-81. - Russian.

TROFIMOVA, E.V. 1993. Chanchurskaya Cave in Irkutsk region. *Geography and natural resources.* 2: 182-184. - Russian.

TURCHINOV, I.I. 1992. Gravitational Caves of Kluch Ridge, the Ukrainian Carpathians. *The Light.* 4 (6): 15-17. - Russian.

Konsequenzhöhlen in vulkanischen Gesteinen

István Eszterhás
Isztimér, Köztársaság u. 157., H-8045, Ungarn

Abstract

The so called "consequence cave" as a genotype of caves was introduced only in 1991 and has therefore not become well-known yet. These caves were formed by further natural evolution - break-up and mass displacement - of man-made hollows like mines, cellars, casemates, etc. During men's hollow-making activity stress was arisen in rocks that then is dissolved on its natural way leaving behind caves in many cases, the mentioned "consequence" caves. Conditions of its forming are optimal where rigid rocks are situated over the former artificial hollows. This paper describes 13 consequence caves formed in volcanic rocks but it is plain that they can be found also in sedimentary and metamorphous rocks. Our aim is to make researchers pay more attention to learning these phenomena.

Begriff der Konsequenzhöhlen

Als Höhlen bezeichnen wir alle für Menschen begehbaren natürlichen Hohlräume. Von Menschen geschaffene Stollen, Keller, Kasematten usw. werden "künstliche Hohlräume" genannt.

Aber in welche Kategorie sind solche Hohlräume einzureihen, die auf eine natürliche Art, nämlich durch Einsturz von alten Stollen oder anderen künstlichen Hohlräumen entstanden sind?

Bei der Beurteilung dieses Problems gab es lange Zeit Unsicherheiten. Die meisten Behandlungen der Hohlräume lassen diese genetische Einstufung gegenwärtig beiseite. Das Vulkanspeläologische Kollektiv Ungarns hat fast eine halbe tausend Daten über Nicht-Karsthöhlen gesammelt. Diese hat der Verfasser aufgearbeitet und in der Behandlung des speläogenetischen Problems im Jahre 1991 zum ersten Male den Genotyp der Konsequenzhöhlen erläutert (ESZTERHAS, 1991). Seitdem habe ich den Begriff des neuen Höhlentyps öfters in Abhandlungen, in Publikationen und bei internationalen Tagungen (siehe Literaturliste) verwendet. In den letzten Jahren haben auch andere Forscher den Begriff übernommen (BELLA, 1995; HOLUBEK, 1995; PAS, 1996) und ihn bei der Beschreibungsanalyse der Höhlen benutzt. Seit der Einführung des Begriffes der Konsequenzhöhlen ist wenig Zeit vergangen, so dass der Gedanke nicht zu jeden Interessenten gelangen konnte. Deswegen möchte ich dieses Forum dazu nutzen, um das Thema weiter zu verbreiten.

Was bedeutet dieser Begriff? - Es handelt sich hierbei um wirkliche Höhlen, da sie auf eine natürliche Art, durch den Ausgleich der angewachsenen Spannung im Gestein entstanden sind. Solche Höhlen tragen überwiegend die Kennzeichen einer tektonischen Entstehung. Das Wort "Konsequenz-" weist darauf hin, daß die Höhlen dieses Genotyps durch den Einsturz eines früheren Hohlraumes entstanden sind und quasi dessen Erbe angetreten haben. Demzufolge liegen diese Höhlen in jedem Fall auf einem höheren Niveau als der ursprüngliche künstliche Raum.

Diese Erscheinung kommt auch durch den Einsturz wirklicher Höhlen vor. Solche Höhlen bezeichnen wir als "Versturzhöhlen" oder "jameo"-s. (Das Wort "jameo" wurde der guanchen Sprache der Kanarischen Inseln entliehen).

Solche Konsequenzhöhlen findet man hauptsächlich in den alten Bergwerksgegenden und in den alten Stadtteilen, die viele Kasematten beinhalten. Die Voraussetzungen zur Entstehung von Konsequenzhöhlen sind dann gut, wenn über den früheren Hohlräumen spröde Gesteine wie Basalt, Rhyolith, Kalkstein usw. vorhanden sind. Diese Gesteine sind fähig, die durch sekundäre Einstürze entstandenen Hohlräume, die Konsequenzhöhlen, zu bewahren.

Wegen des jungen Begriffes wissen wir nur wenig über solche Höhlen. Wir können sicher sein, daß solche Hohlräume in den verschiedensten Gesteinen auf vielen Gebieten der Erde vorhanden sind. Unseren Wissens wurden nur die Gebiete Ungarns (ESZTERHAS, 1995) und der Niederlande (PAS, 1996) in dieser Hinsicht stichprobenweise untersucht (im letzteren Falle sind die Konsequenzhöhlen im Kalkstein). Zudem wurden die Untersuchungen wurden auch in der Slowakei (HOLUBEK, 1995) begonnen. Nebst der Speläologie wäre die Ausweitung der Untersuchungen auf weitere Gebiete auch für die Statik, Mineralogie, Archäologie erfolgversprechend.

Im Folgenden möchte ich mich mit den Konsequenzhöhlen beschäftigen, die in den vulkanischen Gesteinen des Karpaten-Becken entstanden sind.

Die Höhlen des Szilvás-kös

Das Szilvás-kö (628 m) ist ein Basaltberg in Nordungarn bei der Stadt Salgótarján. Unter der fast 80 m dicken Basaltschicht aus dem Pleistozän finden sich miozäne Sedimentgesteine (Sandstein, Mergel, Kies usw.), in denen zwei Steinkohlenschichten von gesamthaft 3-3,5 m Mächtigkeit anzutreffen sind. Die obere, 2,2 m dicke Kohlenbank wurde bis 1910 gefördert. Nach der Beendigung der Bergwerksarbeiten ist der Stollenraum eingestürzt, und die bedeckende Basaltschicht ist abgesunken. Nach den Berechnungen gemäss "Menzel" und "Briggs" kann man eine Senkung von 0,55 m feststellen. Im Bereich des Zugangsschlotes erfolgte keine Unterförderung, so dass dort keine Senkung entstehen konnte. Infolgedessen "zerbrach" dort die Basaltschicht. In der Scheitelregion des Bergs ist ein 350 m langes, verzweigtes und tiefes Spaltsystem entstanden. An der Oberfläche vorhandene offene Spalten waren früher "mehr Etagen tief" (DORNYAI, 1929). Heutzutage sind sie schon stark aufgefüllt, der tiefste Teil reicht nur noch bis in 14 m Tiefe. Der obere Teil der Spalten ist an mehreren Stellen geschlossen, oder die Gesteinbrocken sind in den Spalten hängengeblieben und bilden damit Höhlen (ESZTERHAS, 1995). Auf dem verhältnismäßig kleinen Gebiet fand man bisher fünf Konsequenzhöhlen:

	Länge / Tiefe
Szilvás-kö-Höhle	68,0 / -13,5 m
Sárkánytorok-Höhle	28,4 / -14.0 m
Jansen-Höhle	20,2 / -5,8 m
Kis-Szilvás-kö-Spalthöhle	12,4 / -11,0 m
Vabot-Höhle	8,0 / - 4,7 m

Abb. 1: Speläogenetischer Plan des Szilvás-kös

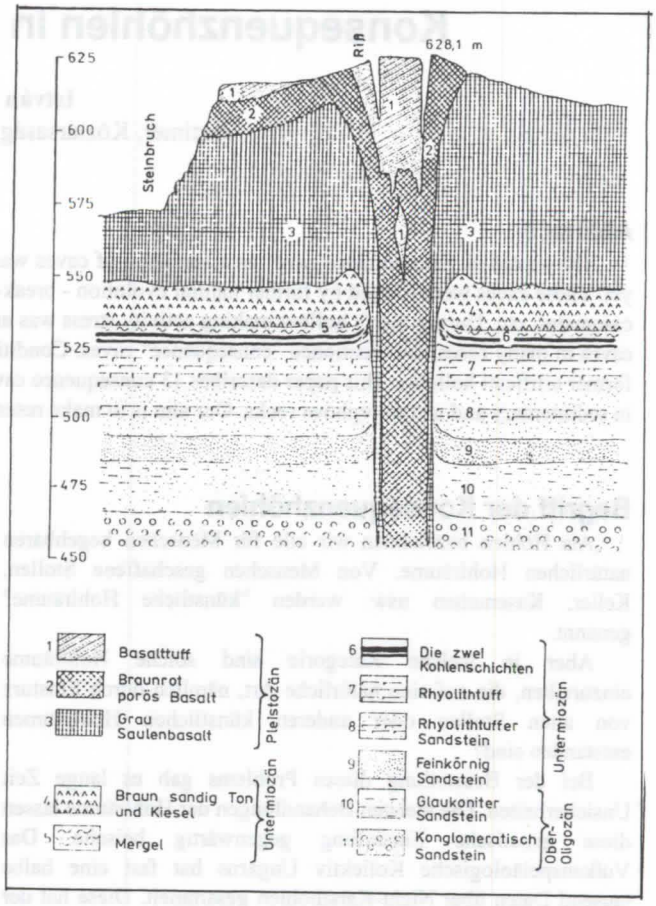

Abb. 2: Geologischer Schnitt des Szilvas-ko's

Das grösste Volumen enthält die Höhle Szilvás-kö mit einem Schuttlabyrinth in der Nähe des Eingangs und mit einem unteren geräumigen Saal (10 x 4 x 2 m). Die Gänge bestehen aus riesigen, verkippten Basaltblöcken. Die Sárkánytorok-Höhle ist durch die Kreuzung von zwei Spalten entstanden; sie zeigt einen X-förmigen Grundriss. Am Kreuzungspunkt ist sie als offene Schlucht ausgebildet. Ihre klimatologische Besonderheit ist, dass auf einem 628 m Höhe selbst im mitteleuropäischen Sommer noch Firnschnee zu finden ist. Die weiteren der Szilvás-kö Höhlen sind kleinere, weniger bedeutende Hohlräume.

Die Höhlen des Csák-kös

Das Csák-kö ist auf dem südlichen Teil des Matra-Gebirges, beim Dorf Gyöngyössólymos, ein sehenswürdiger Rhyolithfelsen aus dem Miozän. In den ersten Jahrhunderten der geschichtlichen Neuzeit wurde der harte, kleinblasige und körnige Rhyolith in situ für Mühlsteine gefördert. Vielenorts kann man die Bearbeitungsspuren auf der Oberfläche sehen. Dem qualitativ guten Stein folgend, hat man in den Felsen geräumige Hallen geschaffen. In den Wänden kann man halbfertig gemeisselte Mühlstein beobachtem. In einer Hälfte der grössten Grubenhalle ist die Decke heruntergebrochen und hat so praktisch zwei Konsequenzhöhlen hinterlassen:

	Länge / Tiefe
Grosshöhle des Csák-kös	133,0 /+14,5 m
Scheinhöhle des Csák-kös	5,1 / + 0,4 m

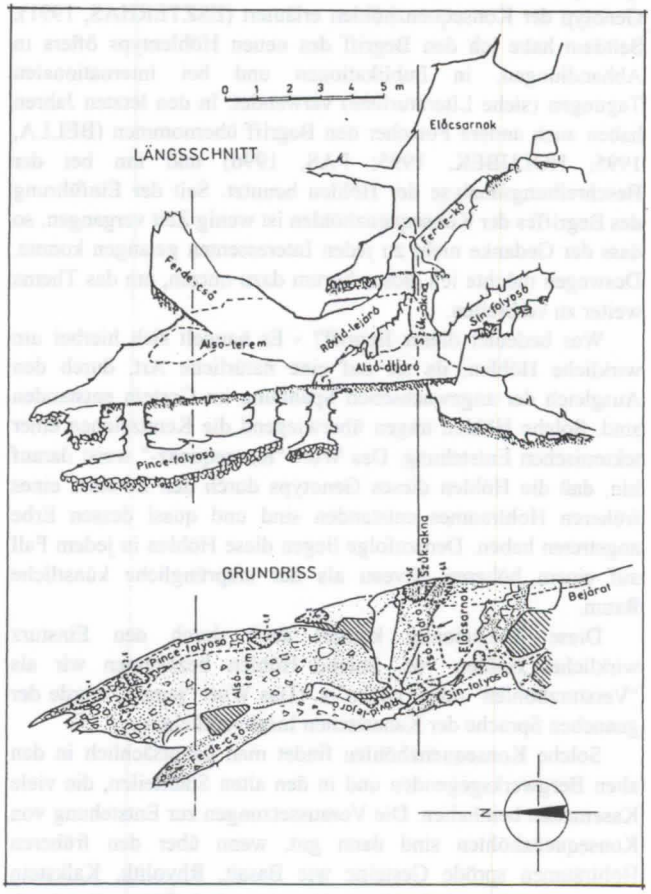

Abb. 3: Die Szilvás-kö-Höhle - eine Konsequenzhöhle (Längsschnitt und Grundriss)

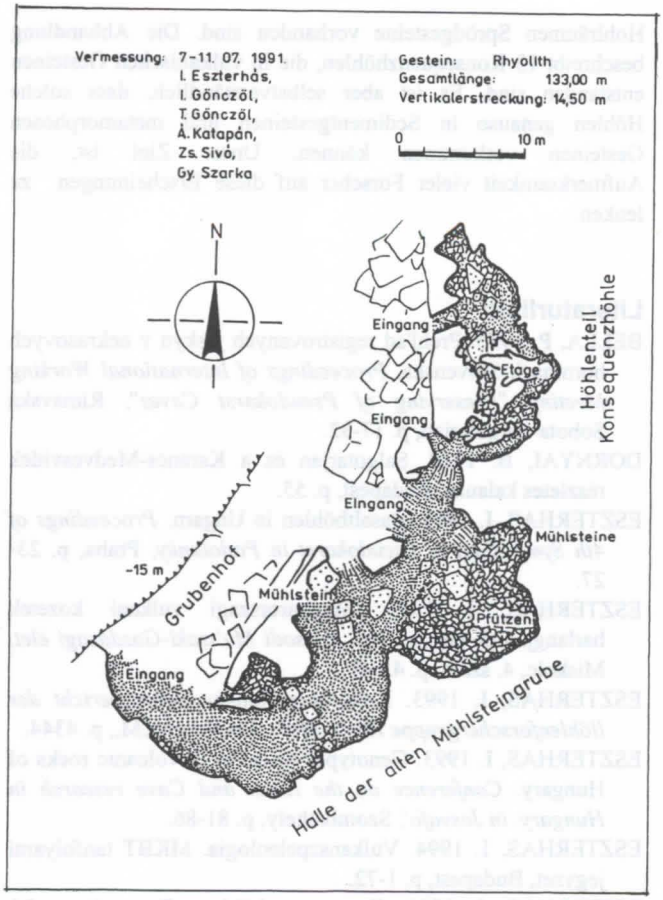

Abb. 4: In Csák-kö bildet sich die Grosshöhle durch Einsturz in einem alten Mühlsteinbruch

Ein Teil der Grosshöhle des Csák-kös bewahrt noch die ursprünglichen Formen der Grubenhalle. Die andere Hälfte hat sich bereits völlig umgebildet. Sie ist von der Urhöhle aus aufwärts gewachsen und wurde zum Schuttlabyrinth. Die Scheinhöhle des Csák-kös ist ein Hohlraum, der unter den heruntergefallenen größeren Rhyolithstücken entstanden ist (ESZTERHAS, 1995).

Die Höhle des Kečke (Ziegen)-Bergs

In der Slowakei, auf dem westlichen Teil des Schemnitz-Gebirges ([tiavnické vrchy), in der Nähe von Geletnek (Hliník) ist der Kečke-Berg, der aus einem miozänen Rhyolith besteht. Der Rhyolith wurde bereits vor hundert Jahren zur Herstellung von Mühlsteinen benutzt. Die Löcher, Hallen und Schächte des ehemaligen Stollens sind teilweise eingestürzt und aufgerissen. Deren Hohlräume gehen in die Konsequenzhöhlen über. Auf einem Gebiet von 40 x 60 m wurden vier Höhlen hinterlassen:

	Länge / Tiefe
Velká jaskyňa	58,0 /-12,0 m
Malá jaskyňa	44,0 / - 5,5 m
Tmavá jaskyňa	36,0 / - 9,0 m
Rozsadlina na Kečke	29,0 /-28.0 m

Die Velká jaskyňa hat die Umgestaltung zu einer Durchgangshöhle mit Schutt gemacht. Die schräge Decke. der Fussboden und die Wände bestehen aus grösseren Steinbrocken. Ähnlichen Charakter hat auch die Malá und Tmavá jaskyňa. Die Rozsadlina na Kečke ist ein aus den umgestalteten Schächten durch Aufriss entstandenes System. Über dem Scheidungspunkt des Stollens läuft der Aufriß bis zur Oberfläche und bildet eine

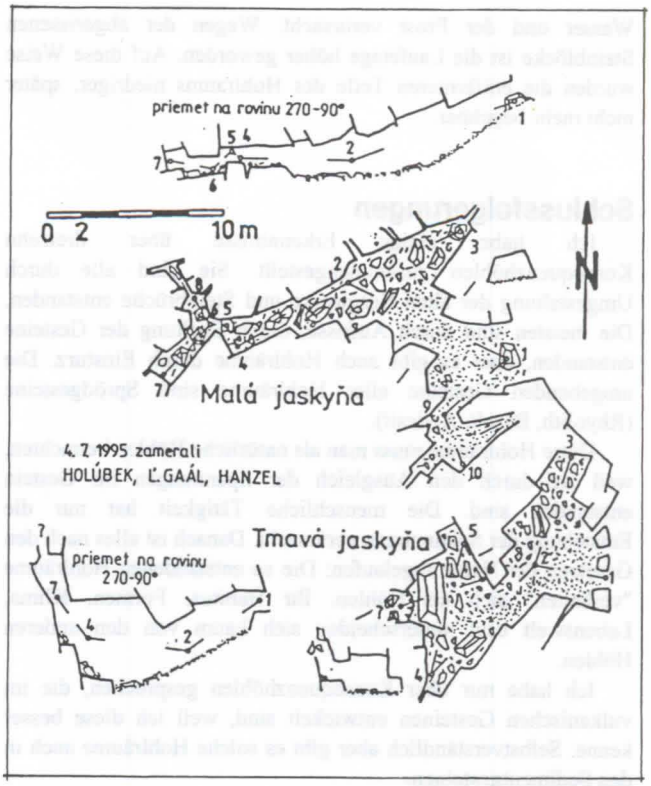

Abb. 5: Zwei Konsequenzhöhlen (Malá- und Tmavá-Höhle) beieinander am Kečke-Berg

28 m tiefe Konsequenzhöhle mit Schluchtähnlichkeit. Auf der Oberfläche zeichnen viele eingestürzte Löcher die Linie des Stollens nach (HOLUBEK. 1995).

Streuvorkommnisse von Konsequenzhöhlen

Auf dem südlichen Teil des Bakony-Gebirges, beim Dorf Badacsonytomaj, wurde bis in die 1950er Jahre ein grosser Basaltsteinbruch betrieben. Die Strebwand des früheren Steinbruchs bröckelt langsam herab, gestaltet sich um. Bei einem Abriß der Umgestaltung entstand in der früheren Steinbruchwand:

	Länge / Tiefe
Höhle des Basaltsteinbruchs von Badacsony	2,9 / + 1,4 m

Es handelt sich um eine kleine Nische. Ihre Decke und Steinwände werden von bisher nicht bewegten Basaltplatten umgrenzt, ihr Boden besteht aus lockeren Steinfelsen (ESZTERHAS, 1995).

Bei dem großen Bogen der Donau im Visegrader-Gebirge, an der Grenze zur Stadt Szentendre, ist der Andesitsteinbruch von Dömörkapu, wo seit 20-25 Jahren kein Stein mehr gefördert wird. Dies wurde auch durch Strebförderung am Übertagebau getrieben, aber auf der unteren Etage hat man eine Sprengstoffnische herausgebuddelt. Gegenwärtig zeigt dieser Stollen eine Umwandlung zur Konsequenzhöhle.

	Länge / Tiefe
Die Höhle von Dömörkapu	15,9 / +3,8 m

In der Eingangsnähe zeigt sich noch der charakteristische trapezförmige Schnitt der Schächte, aber der innere Teil des Firsts ist schon abgerissen. Den Abriss haben das durchsickernde

Wasser und der Frost verursacht. Wegen der abgerissenen Steinblöcke ist die Laufetage höher geworden. Auf diese Weise wurden die entfernteren Teile des Hohlraums niedriger, später nicht mehr begehbar.

Schlussfolgerungen

Ich habe einige Erkenntnisse über dreizehn Konsequenzhöhlen zusammengestellt. Sie sind alle durch Umgestaltung der alten Bergwerke und Steinbrüche entstanden. Die meisten sind durch Aufrisse, durch Spaltung der Gesteine entstanden, aber es gibt auch Hohlräume durch Einsturz. Die umgebenden Gesteine aller Hohlräume sind Sprödgesteine (Rhyolith, Basalt, Andesit).

Diese Hohlräume muss man als natürliche Höhlen betrachten, weil sie durch den Ausgleich der Spannungen im Gestein entstanden sind. Die menschliche Tätigkeit hat nur die Entstehung der Spannungen verursacht. Danach ist alles nach den Gesetzen der Natur abgelaufen: Die so entstandenen Hohlräume "verhalten" sich als Höhlen. Ihr Habitus, Formen, Klima, Lebenswelt usw. unterscheiden sich kaum von den anderen Höhlen.

Ich habe nur über Konsequenzhöhlen gesprochen, die im vulkanischen Gesteinen entwickelt sind, weil ich diese besser kenne. Selbstverständlich aber gibt es solche Hohlräume auch in den Sedimentgesteinen.

Der Natur- und Umweltschutz beschäftigt sich in den meisten Fällen nicht mit dem Schutz der Keller, Kasamatten und alten Stollen. So ist auch der Schutz der aus deren Weiterentwicklung entstehenden Konsequenzhöhlen nicht gegeben. Gegenüber den natürlichen Hohlräumen halten viele diesen Höhlentyp nicht für schutzwürdig. Es muss deshalb bewusst gemacht werden, daß die Weiterentwicklung der Hohlräume zu Konsequenzhöhlen auch unter Schutz stehen sollte. Wegen des häufigen Nachbruchs müsste zudem mehr Aufmerksamkeit auf die Sicherheit gelenkt werden.

Öfters ist der schädliche Einfluss auf die Höhlen durch Verfüllung, wie dies in Bergbaugebieten, aber auch in den Hohlräumen unter der Städten geschieht. In den Hohlräumen leben kurzzeitig oft Menschengruppen ohne Naturliebe und Kultur und verschmutzen bzw. verunstalten die Höhlen (z.B. Graffitti). In einigen Fällen sind diese Höhlen "Jagdgebiete" für Mineralsammler.

Zusammenfassung

Die Konsequenzhöhlen wurden erst im Jahre 1991 als ein Genotyp der Höhlen definiert und sind deswegen noch nicht so bekannt. Diese Höhlen sind von den Menschen geschaffene "künstliche Hohlräume" (Stollen, Keller, Kasamatten, usw.), welche sich auf natürliche Weise weiter entwickeln. Bei der Hohlraumschaffung des Menschen wurden Spannungen induziert. Diese Spannungen wurden nach den Gesetzen der Natur abgebaut und lassen in vielen Fällen Höhlen, sogenannte Konsequenzhöhlen, zurück. Die Voraussetzungen zu ihrer Entstehung sind dann gut, wenn über den ehemaligen Hohlräumen Sprödgesteine vorhandcn sind. Die Abhandlung beschreibt 13 Konsequenzhöhlen, die in vulkanischen Gesteinen entstanden sind. Es ist aber selbstverständlich, dass solche Höhlen genauso in Scdimentgesteinen und metamorphosen Gesteinen vorkommen können. Unser Ziel ist, die Aufmerksamkeit vieler Forscher auf diese Erscheinungen zu lenken.

Literaturliste

BELLA, P. 1995. Prehl'ad registrovanych jaskyn v nekrasovych horninach Slovenska. *Proceedings of International Working Meeting "Preserving of Pseudokarst Caves",* Rimavska Sobota-Salgotarjan, p. 17-32.

DORNYAI, B. 1929. Salgotarjan és a Karancs-Medvesvidék részletes kalauza, Budapest, p. 55.

ESZTERHAS, I. 1990. Basalthöhlen in Ungarn. *Proceedings of 4th Symposium of Pseudokarst in Podolanky,* Praha, p. 23-27.

ESZTERHAS, I. 1991. Magyarorszagi vulkani kozetek barlangjainak genotipusai. *Borsodi Mu'szaki-Gazdasagi élet,* Miskolc, 4. szam: p. 45-47.

ESZTERHAS, I. 1993. Konsequenzhöhlen. *Jahresbericht der llöhlenforschergruppe Rhein-Main,* Frankfurt a.M., p. 4344.

ESZTERHAS, I. 1993. Genotypes of caves in volcanic rocks of Hungary. *Conference on the Karst and Cave research in Hungary, in Josvafo',* Szombathely, p. 81-86.

ESZTERHAS, 1. 1994. Vulkanszpeleologia. MKBT tanfolyami jegyzet, Budapest, p. 1-72.

ESZTERHAS, I. 1994. Konsequenzhöhlen. *Proceedings 5th Pseudokarst Symposium in Szczyrk,* Bielsko-Biala, p. 25-28.

ESZTERHAS, I. 1995. Konzekvenciabarlangok genetikaja és védelme. *Proceedings of International Working Meeting "Preserving of Pseudokarst Caves",* Rimavska Sobota Salg6tarjan, p. 77-83.

ESZTERHAS, I. 1996. Natürliche und durch künstliche Hohlräume entstandene Risse in vulkanischen Gestein. *Proceedings of International Symposium on Volcanspeleology,* Santa Cruz de La Palma.

ESZTERHAS, I.; GAAL, L.; TULUCAN, T. 1996. Caves in the volcanic rocks of the Carpathian Ranges. Field Trip Guidc and Abstracts of 6th International Symposium on Pseudokarst, Galyateto p. 28; and (in press) *Proceedings of 6th Int. Symp. on Pseudokarst,* Galyateto.

HOLUBEK, P. 1995. Konzekvencné jaskyne v Stiavnickych vrchoch. *Proceedings of International Working Meeting of "Preserving Pseudokarst Caves",* Rimavska Sobota, Salgotarjan, p. 58-60.

OZORAY, Gy. 1960. The genesis of non-karstic natural cavities as elucidated by Hungarian examples. *Karszt- és Barlangkutato,* Budapest, II. évf.: p. 127-136.

VAN DER PAS, J. P. 1996. Consequence Caves in the Netherland. Field Trip Guide and Abstracts of 6th International Symposium on Pseudokarst, Galyateto, p. 26; and (in press) *Proceedings of 6th Int. Symp. on Pseudokarst,* Galyateto.

Karstification of sandstone in Central Europe: attempts to validate chemical solution by analyses of water and precipitates

by Thomas Striebel[1)2)] and Volker Schäferjohann[1)]
1) Department of Hydrology, University of Bayreuth, D-95440 Bayreuth
2) Höhlenforschungsgruppe (Cave Research Group) Blaustein,
T. Striebel, Am Sachsenberg 12, D-95448 Bayreuth

Abstract

Under temperate climatic conditions, non-carbonate sandstones are often regarded as non-karstificable. However, regarding solubility-conditions of quartzite and ferric oxide binders, the development of karstic forms seems to be possible. To validate or to exclude this assumption, chemical investigation of water and precipitates in a small, gorge-like, non-carbonate sandstone catchment was done.

The small stream flowing in the gorge carries silica concentrations around 8 mg/l (as SiO_2), pH is slightly alkaline and total iron contents are around 250 µg/l. Lateral tributaries show remarkably lower values of pH, silica concentrations between 9 and 16 mg/l and iron concentrations up to 900 µg/l. The water of stagnant pools has acid pH, often hydrogen sulphide is present, silica concentrations are in a moderate range, and iron concentrations may be high (up to 5.4 mg/l).

The concentrations of dissolved silica and total iron indicate that dissolution of both kinds of binders occurs. The development of solutional forms, at domains which are protected from physical weathering within the rock unit, would therefore seem to be possible.

Zusammenfassung

Nichtkarbonatische Sandsteine gelten unter gemäßigten Klimabedingungen oft als nicht verkarstungsfähig. Die Betrachtung der theoretischen Löslichkeit von quarzitischem oder ferritischem Bindemittel läßt jedoch vermuten, daß sich Karstformen entwickeln könnten. Chemische Untersuchungen von Wasser und Fällungsprodukten in einer kleinen Bachschlucht im Sandstein sollen Fakten zur Untermauerung oder Widerlegung dieser Vermutung liefern.

Der kleine Bach, der durch die Schlucht fließt, enthält Kieselsäurekonzentrationen um 8 mg/l (als SiO_2), der pH-Wert ist schwach alkalisch und die Konzentrationen des gesamten Eisens liegen bei 250 µg/l. Seitenzuflüsse zeigen deutlich niedrigere pH-Werte, Kieselsäurekonzentrationen zwischen 9 und 16 mg/l und Eisenkonzentrationen bis zu 900 µg/l. Das Wasser stehender Tümpel weist saure pH-Werte auf, oft ist Schwefelwasserstoff vorhanden, Kieselsäurekonzentrationen bewegen sich in einem mittleren Bereich und Eisenkonzentrationen können relativ hoch sein (bis zu 5,4 mg/l).

Die Konzentrationen von gelöster Kieselsäure und von Gesamteisen zeigen, daß beide Bindemittelarten gelöst werden. Deshalb erscheint die Entstehung von Lösungsformen zumindest innerhalb des Gesteinskörpers denkbar, weil dort das Gestein vor physikalischer Verwitterung geschützt ist.

1. Introduction

Under temperate or cool climatic conditions, the karstification of non-carbonate sandstone is normally regarded as unlikely or impossible (WILHELMY 1981). In opposition to this, karstic forms in sandstones may develop well under tropical or subtropical conditions (e. g., MARTINI 1990, SPONHOLZ 1989). With reference to the solubility conditions of quartzite (e. g., HURD ET AL. 1979, CASEY & NEAL 1986) and ferric oxide binding agents, the development of karstic forms should also be possible under temperate climatic conditions, so long as some chemical and microclimatic boundary conditions are present. Originating from studies done by RIMSTIDT & BARNES 1980, MARTINI 1984 developed a model to describe the solution of quartzite and the formation of caves. The assumption derived from these findings is that development of solutional caves may be possible at sandstone rock domains within the rock unit which are protected from physical weathering, but pervious to water due to the existence of joints and bedding planes.

Ferric binding agents may be attacked by acid and/or reduced water. There is a distinct increase of solubility of ferric oxides with increasing acid concentrations in the water. In addition, depletion of organic matter at boggy locations (due to the local occurence of claystone) causes a decrease of the redox potential with a subsequent reduction of ferric iron oxides to ferrous iron, which has a much better solubility than ferric iron.

To validate (or to exclude) the assumption that these processes are important enough to be relevant, different concepts of further research have been formulated and partly initiated already. One of them deals with the chemical investigation of surface water and precipitates in a small, gorge-like catchment in a sandstone area near Bayreuth, Germany (Teufelsloch bei Oberwaiz). Some preliminary results will be presented here.

2. Investigation site

The Rhätolias sandstone in which the gorge is embedded consists more or less of lithified sand- and claystone of Upper Triassic / Lower Jurassic age. The binding agents are mainly silica and ferric oxides (EMMERT 1977). Rock domains with low vulnerability to weathering commonly form rocks at valley slopes or small, deeply incised, water-carrying gorges. Resistant limonite crusts occur locally, forming knobby and wavy rock surfaces and supporting cellular weathering. Rocks at valley slopes often have been dislocated in Pleistocene times due to periglacial processes.

The genetic conditions of the caves or some special forms are already described (STRIEBEL 1994). Some of the forms mentioned there may have developed with the participation of solution processes, e. g., tube structures, cavettos, flat caves orientated along bedding planes and small dome-like chimneys.

Figure 1 illustrates the topography of the catchment and the locations of the sampling sites.

3. Some results of the chemical investigations

Sampling was carried out twice, once in December under average run-off conditions (T_{water} = 3.8 - 5.5°C) and at the end of summer under low run-off conditions (T_{water} = 8.6 - 9.7°C).

Measured values show only little variation in time, therefore no seasonal influences will be discussed here.

Sampling sites can be split up into three groups as follows:

a) principal stream (samples 2, 7, 12)
b) lateral tributaries (samples 3, 5, 6, 11)
c) stagnant surface water pools in contact with ground water (samples 8, 9, 10)

The chemical characteristics of each group are shown below.

Electrical conductivity, pH-values and dissolved oxygen concentrations were measured with electrodes (WTW pH91, WTW LF91, WTW Oxi323).

For the analyses of total iron (flameless atomic absorption spectroscopy) and calcium carbonate (flame emission) samples were taken in 100 ml polyethylene bottles and acidified with 14 M HNO_3 (0.2 Vol%).

Silica concentrations were determined in untreated samples by a photometric method according to DIN 38405.

In addition, total silicon (AAS), some macro ions (chloride, nitrate, sulphate, potassium, sodium, hydrogen carbonate as alkalinity) and heavy metals (zinc, cadmium, copper, lead) - dissolved and total contents - have been determined.

In the discussion we will focus on the more important variables for our topic. These are pH-values and oxygen saturation as indicators for the chemical boundary conditions, electrical conductivity as parameter for dissolved substances, and the concentrations of dissolved silica and ferric iron.

The principal stream flowing in the gorge contains calcium carbonate in concentration ranges similar to karstic waters (here 60 - 120 mg/l) due to its origin (some relict limestone can be found in surrounding soils plus a building waste disposal site is situated nearby). Typical values are around 800 µS/cm for the electrical conductivity, slightly alkaline pH-values, oxygen concentrations near 100% of the saturation value, silica concentrations around 8 mg/l (as SiO_2) and total iron concentrations around 250 µg/l.

Lateral tributaries show remarkably lower values of electrical conductivity (100 - 150 µS/cm), almost no calcium carbonate content, slightly or strongly acid pH-values between 6.8 and 3.8, oxygen concentrations near or distinctly below saturation (85% - 50%), silica concentrations between 9 and 16 mg/l and iron concentrations between 10 and 900 µg/l. The chemical conditions in these tributaries obviously vary across a wide range, and will have to be further investigated. At some boggy locations, oxygen-free reducing conditions with hydrogen sulphide production have been established.

In the stagnant surface water pools which are in contact with ground water, electrical conductivity is mostly below 100 µS/cm, the water is free of calcium carbonate, pH-values are acid (3.8 - 5.5), oxygen concentrations are far below saturation (< 30%), hydrogen sulphide is occasionally present, silica concentrations are within a moderate range (8 - 9 mg/l), and iron concentrations may be very extreme (up to 5.4 mg/l).

Some precipitates rich in iron have been observed. They develop at locations where acid and/or reduced water comes into contact with well-buffered and/or oxygen-rich environments. Such a typical location is the bed of the main stream where pore waters rich in iron penetrate the bed sediment and join the stream. There, red iron streaks and crusts are formed. At another location, some small, red and plastic stalactites have been discovered. Analyses have shown that the main cation is iron (231 mg/g).

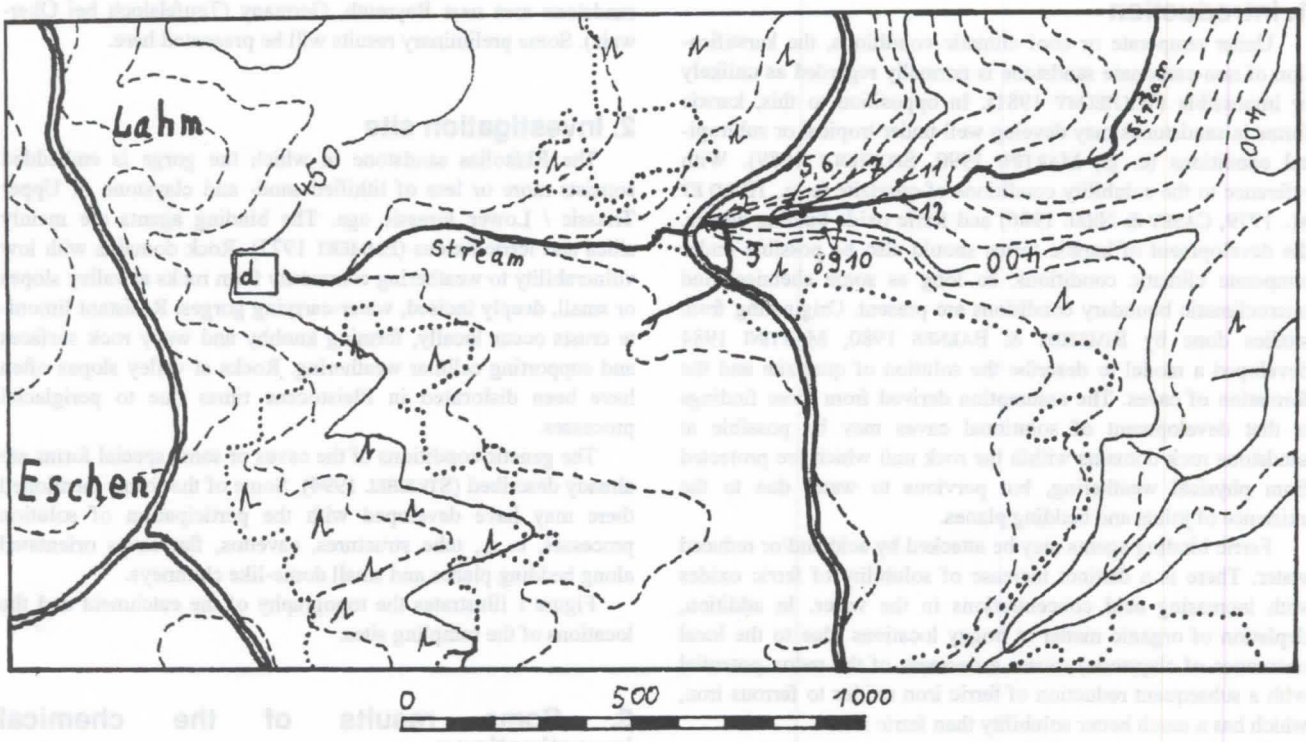

Figure 1: Sketchmap of the catchment. Altitudes and scale are given in meters. Eschen and Lahm are two small villages, 'd' is the building waste disposal site, and digits are sample numbers (cf. text and figure 2).

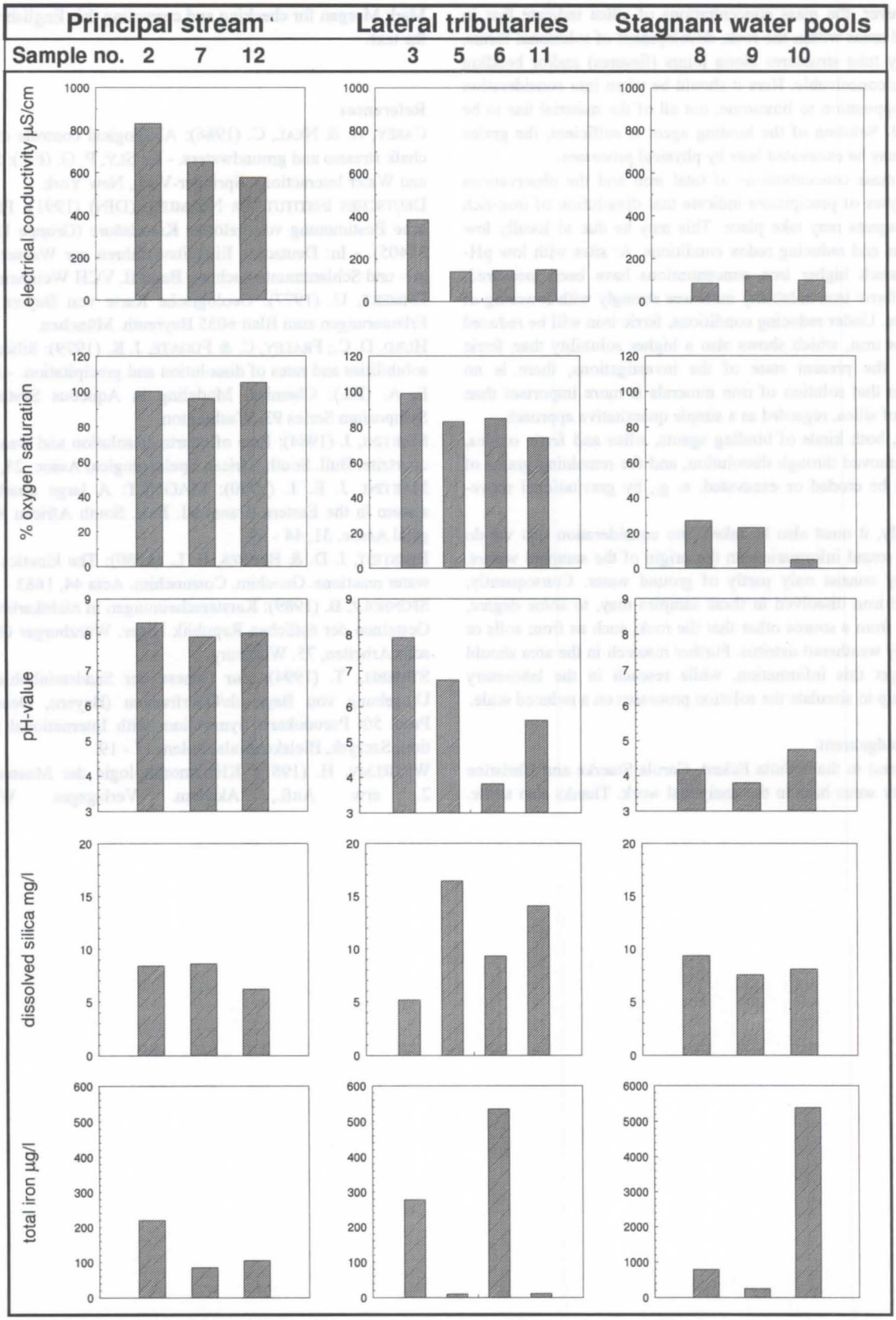

Figure 2: The most important results. Note: for each parameter the scale is the same, only for total iron the scale in the lower right bar graph was multiplicated with a factor of 10.

4. First conclusions

Due to the similar density of quartz and calcite, the volumes of dissolved silica and calcium carbonate show the same ratios as their mass concentrations. Thus, they may be compared directly. The concentrations of dissolved silica are one and a half orders of magnitude lower than typical mass concentrations of dissolved calcite in karstic waters of limestone areas. Therefore, at locations exposed to weathering, especially frost splitting, it is possible that no karst forms develop in sandstone. There, physical weathering is fast enough to destroy karst forms before they reach an observable state.

However, the mass concentrations of silica indicate that in protected areas within the rock, development of solutional forms, especially tube structures along joints (fissures) and/or bedding planes, is conceivable. Here it should be taken into consideration that, in opposition to limestone, not all of the material has to be dissolved. Solution of the binding agent is sufficient, the grains of sand may be excavated later by physical processes.

The mass concentrations of total iron and the observations and analyses of precipitates indicate that dissolution of iron-rich binding agents may take place. This may be due to locally low pH-values and reducing redox conditions. At sites with low pH-values, much higher iron concentrations have been measured, because ferric iron solubility increases strongly with lowering of pH-values. Under reducing conditions, ferric iron will be reduced to ferrous iron, which shows also a higher solubility than ferric iron. At the present state of the investigations, there is no indication that solution of iron minerals is more important than solution of silica, regarded as a simple quantitative approach.

Thus, both kinds of binding agents, silica and ferric oxides, can be removed through dissolution, and the remaining grains of sand can be eroded or excavated, e. g., by gravitational movement.

Finally, it must also be taken into consideration that we do not have sound information on the origin of the sampled waters. They may consist only partly of ground water. Consequently, silica and iron dissolved in these samples may, to some degree, originate from a source other that the rock, such as from soils or previously weathered detritus. Further research in the area should help to get this information, while reseach in the laboratory should help to simulate the solution processes on a reduced scale.

Acknowledgement

We want to thank Jutta Eckert, Carola Staerke and Christine Wörlen for some help in the analytical work. Thanks also to Dr. Mark Morgan for checking and correcting this English version of the text.

References

CASEY, H. & NEAL, C. (1986): Abiological controls on silica in chalk streams and groundwaters. - In: SLY, P. G. (Ed.): Sediments and Water Interactions. Springer-Verl., New York.

DEUTSCHES INSTITUT FÜR NORMUNG (DIN) (1991): Photometrische Bestimmung von gelöster Kieselsäure (Gruppe D21) (DIN 38405). - In: Deutsches Einheitsverfahren zur Wasser-, Abwasser- und Schlammuntersuchung Band II, VCH Weinheim.

EMMERT, U. (1977): Geologische Karte von Bayern 1:25000. Erläuterungen zum Blatt 6035 Bayreuth. München.

HURD, D. C.; FRALEY, C. & FUGATE, J. K. (1979): Silica apparent solubilities and rates of dissolution and precipitation. - In: JENNE, E. A. (Ed.): Chemical Modeling in Aqueous Systems. ACS Symposium Series 93. Washington.

MARTINI, J. (1984): Rate of quartz dissolution and weathering of quartzite. Bull. South African Spelaeological Assoc. 25, 7 - 10.

MARTINI, J. E. J. (1990): MAGNET: A large quartzite cave system in the Eastern Transvaal. Bull. South African Spelaeological Assoc. 31, 44 - 59.

RIMSTIDT, J. D. & BARNES, H. L. (1980): The kinetics of silica-water reactions. Geochim. Cosmochim. Acta 44, 1683 - 1699.

SPONHOLZ, B. (1989): Karsterscheinungen in nichtkarbonatischen Gesteinen der östlichen Republik Niger. Würzburger Geographische Arbeiten, 75. Würzburg.

STRIEBEL, T. (1994): Zur Genese der Sandsteinhöhlen in der Umgebung von Bayreuth/Oberfranken (Bayern, Deutschland). Proc. 5th Pseudokarst Symposium with International Participation, Szczyrk, Bielsko-Biala, Polen, 17 - 19.

WILHELMY, H. (1981): Klimamorphologie der Massengesteine. 2., erw. Aufl., Akadem. Verlagsges. Wiesbaden.

Karsts siliceux au Niger occidental

par Luc Willems
Université de Liège, Département de Géographie Physique
& Rue Tout Va Bien, 106, B-4420 Saint-Nicolas (Liège), Belgique

Abstract

Located in the Sahelian part, the area of Niamey presents a remarkable karstic network wich is developped in siliceous an non-carbonated rocks. The observation of several surface forms (collapse, closed depressions) and underground forms (caves) shows important hydric circulation networks in depth. We must consider the Sahel and its water resources like karstic aquifer.

Résumé

Située dans la bande sahélienne, la région de Niamey présente un réseau karstique remarquable par son développement dans un ensemble de roches principalement siliceuses et non carbonatées. L'observation d'un ensemble de phénomènes de surface (effondrements, dépressions fermées) et souterraines (grottes) montre des réseaux de circulations hydriques importants en profondeur. Les différentes observations nous font penser qu'il faut réenvisager le Sahel et ses ressources en eau en terme d'aquifères karsitifiés.

1. Introduction

Située dans la bande sahélienne, la région de Niamey présente un réseau karstique remarquable par son développement dans un ensemble de roches principalement siliceuses et non carbonatées. L'observation d'une grotte développée dans l'épaisseur des dépôts du Tertiaire, d'un effondrement et d'une cavité ouverte dans le socle précambrien permettent de dégager les grandes caractéristiques du relief karstique de cette région. D'autres formes tels que des dolines et des avens, des phénomènes de soutirrage, des cavités développées sous cuirasse latéritique indurée ont été également observés. A la fin de cet exposé un modèle d'évolution du relief dans cette région sera proposé.

2. Contextes géomorphologique et géologique

La zone d'étude présente, très schématiquement, un paysage constitué de plateaux disséqués par l'érosion. Entre ces reliefs se développent des oueds, "kori", et de grandes dépressions, "dallols".

La géologie de cette région est composée, outre des dépôts du Quaternaire, de deux ensembles principaux : un socle précambrien et une couverture sédimentaire du Tertiaire (Fig. 1). Le substrat précambrien est formé de massifs granitiques et de ceintures de roches volcano-sédimentaires, roches vertes à métavolcanites basiques et à métasédiments silico-alumineux.

Au Paléogène, il subit une profonde altération de type quartzo-kaolinique qui dépasse 100 mètres par endroits, formant une lithomarge (MACHENS, 1973; 1967). A l'Eocène, des formations détritiques fluvio-lacustres, sables, pélites, silts et argiles, se déposent en discordance majeure (GREIGERT 1966; Lang et al., 1990). Ces dépôts, appellés Continental terminal (Ct), sont interstratifiés de passées d'oolithes ferrugineuses qui, indurées à l'affleurement, jouent un rôle prédominant dans l'apparition de replats morphostructuraux.

Depuis la fin du Pliocène, une alternance de creusements et de comblements des vallées façonne un paysage de plateaux, entaille les dépôts cénozoïques et atteint par endroit le socle.

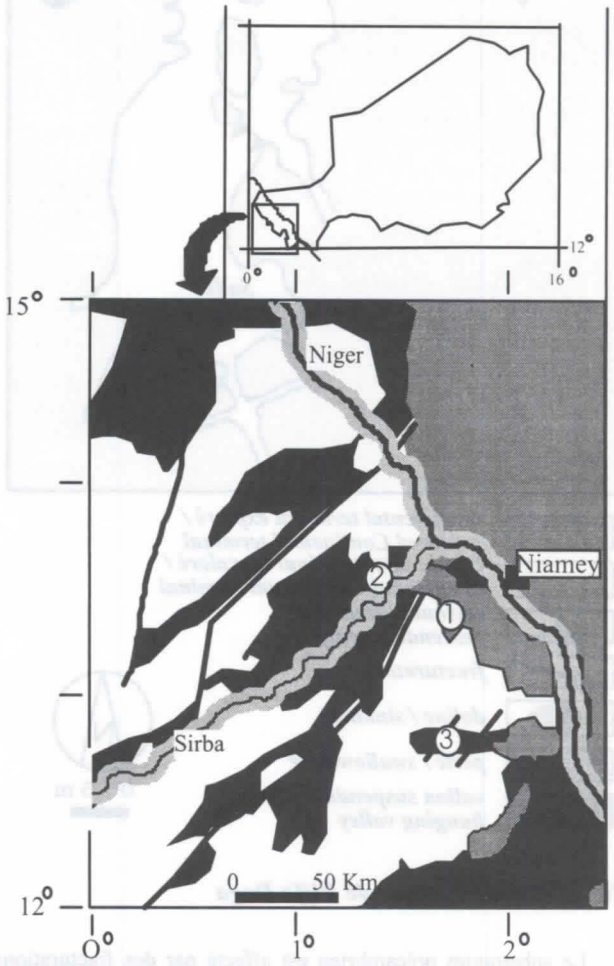

Fig. 1 Carte géologique de la région de Niamey

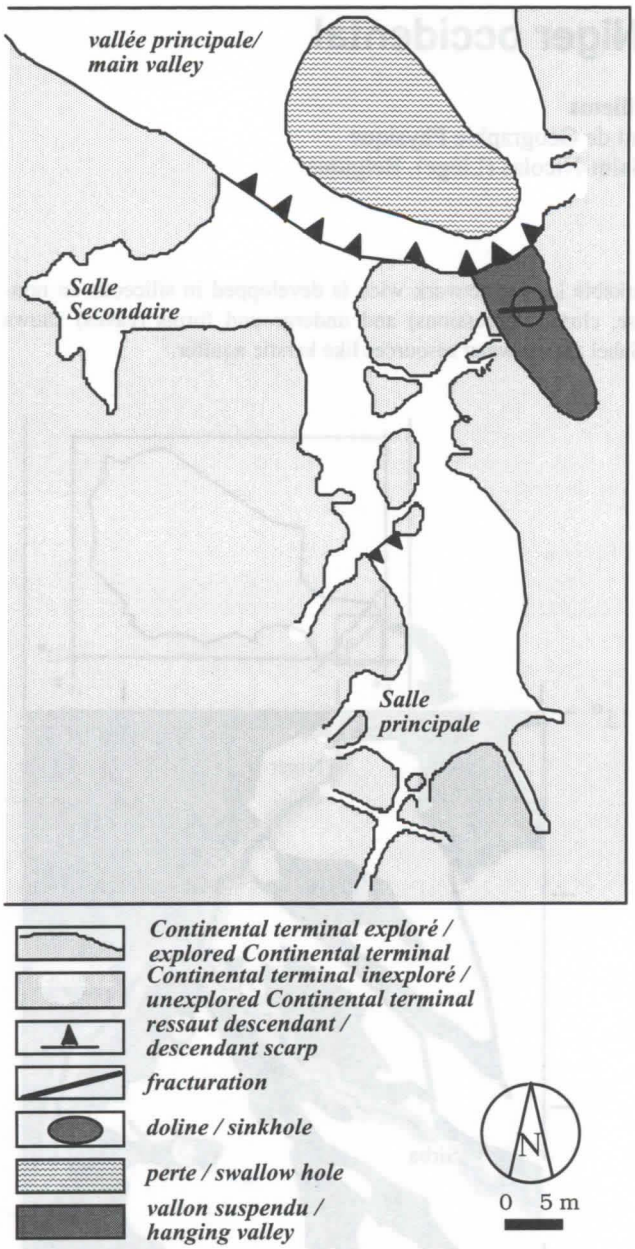

Fig. 2 Plan de la grotte de Diffa Doga

Le substratum précambrien est affecté par des fracturations très anciennes réactivées lors de l'orogenèse panafricaine (ABOUCHAMI et al, 1990); POUCLET et al.; 1990). Quant au Continental terminal, jusqu'il y a peu il était décrit comme non faillé.

Cependant une étude a mis en évidence un réseau de linéaments qui l'affecte et qui impose un système hydrographique régional (VICAT et al., 1993). Ce réseau traduirait le rejeu plio-quaternaire des accidents du socle, ou le prolongement, sous forme de plan de drainage, des fractures du socle dans les dépôts tertiaires comme nous le verrons par après.

3. Cavité dans l'épaisseur du Continental terminal-Diffa Doga

La grotte de Diffa Doga se développe dans l'épaisseur du Continental terminal, au pied d'une falaise d'une dizaine de mètres de haut (Fig. 2). En contre-bas de l'entrée s'ouvre une dépression elliptique encombrée de blocs écroulés. En saison des pluies, cette cuvette se remplit et s'assèche rapidement, se comportant come une perte. Sur le bord est de l'entrée et donnant sur cette dépression, un abrupt de quatre mètres de haut est occupé par une chute d'eau temporaire. Le Ct y présente la structure d'un ancien chenal d'écoulement. En amont, un petit vallon suspendu se perd rapidement sur la surface du plateau. Son fond est occupé par de petites "dolines" métriques dont certaines sont parcourues par une fracturation. Sur le versant abrupt de la vallée principale, à proximité de cette rupture de pente, s'ouvrent également quelques cavités de faible développement.

La grotte présente un important porche d'entrée d'une vingtaine de mètres de large et dépassant par endroit plus de quatre mètres de haut.

De celui-ci, deux couloirs donnant accès à deux salles principales sont accessibles. Ces couloirs sont encombrés par endroits de blocs métriques provenant du démantèlement de la voûte.

La plus grande salle fait une vingtaine de mètres de long, sur une dizaine de large, pour une hauteur avoisinant les 5 mètres. Son plancher est surbaissé d'environ 1,5 m par rapport à celui du couloir d'accès dont il est séparé par un seuil. Partant de cette salle et des couloirs principaux, un réseau de conduits de plus petites dimensions se développe dans des directions voisines de celles des fracturations du socle.

Certains de ces conduits se terminent brusquement en cul-de-sac, sous forme de demi-sphère incurvée. Cette morphologie est notamment observée pour le couloir secondaire qui s'arrête juste sous le vallon suspendu. Ces formes se retrouvent également sur certaines parois des salles. L'exploration plus poussée de cette grotte n'a pas été possible. L'abondance de chauves-souris limite la progression, de véritables bouchons vivants se formant dans les passages les plus étroits.

Retenons qu'aucune trace d'érosion mécanique sur les parois n'a été décelée, laissant supposer une action de dissolution chimique prédominante dans la genèse de la cavité, comme semble le montrer les formes semi-circulaires. Le développement principal des conduits s'est fait parallèlement aux fracturations parcourant le socle. Soulignons enfin la pérénité de l'axe d'écoulement occupé par la vallée et le vallon actuels qui est attesté par le chenal fossile du Ct au niveau de la chute (WILLEMS et al., 1995).

4. Effondrement de Guiddéré

Dans la vallée de la Sirba, à proximité du village de Guiddére, une dépression à parois subverticales faisant environ 3 m de profondeur, de 290 m de longueur et 17 m de largeur, s'est formée en quelques jours au cours de la saison des pluies de 1992 (Fig. 3) (WILLEMS et al.; 1993).

En coupe trois niveaux servent de repère : le sol actuel (70 cm) reposant sur un horizon bioturbé et induré (70 cm), lui-même recouvrant la lithomarge. De l'amont vers l'aval, peuvent être distinguées un tronçon amont, un tronçon aval et un seuil qui debouche sur un tributaire de la Sirba.

Le tronçon amont a sa tête évasée et occupée par une mare temporaire. De nombreux blocs effondrés, avec leur végétation en place occupent le fond.

Il n'y a pas de trace d'érosion par écoulement ni à l'extérieur ni à l'intérieur de ce secteur amont.

Le tronçon aval est tapisse de débris végétaux recouverts d'une pellicule argileuse. Des traces de rivage marquant les retraits successifs d'une flaque sont visibles sur les flancs de la dépression et signalent une vidange rapide.

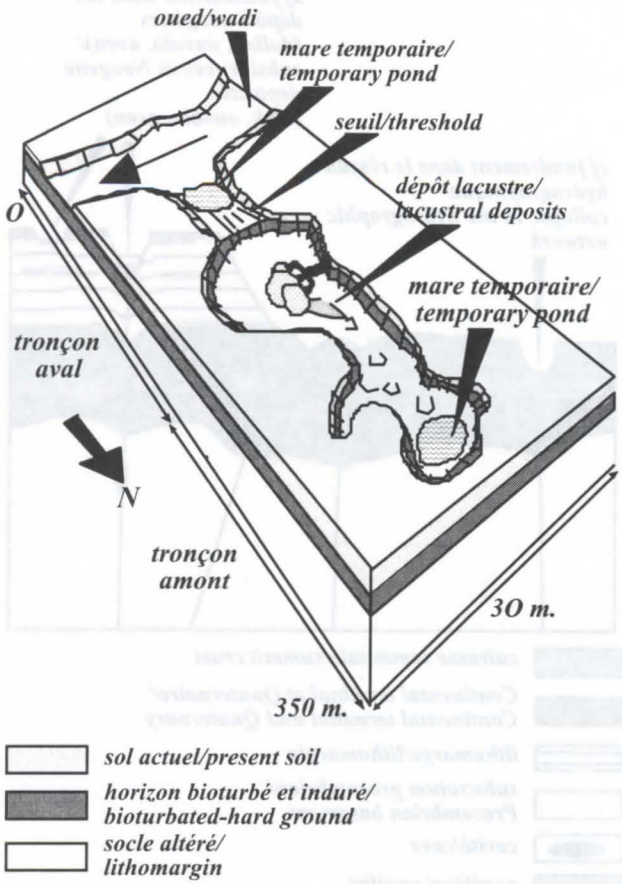

Fig. 3 Effondrement de Guiddéré

Le seuil correspond au toit de l'horizon bioturbé en place et ferme le tronçon aval à mi-pente des versants. Il sépare la dépression observée du lit de l'oued actuel, dont la tête de vallée est occupée par une mare temporaire. De petits chenaux et l'orientation des touffes herbacées indiquent le sens de l'écoulement qui a décape le sol actuel. Outre le témoignage des gens de l'endroit, les blocs éboulés, les racines sectionnées, l'observation de niveaux repères,

l'existence d'un seuil en place prouvent la rapidité de formation de cette dépression due à un effondrement.

L'allongement NS, conforme à l'orientation de failles du socle sous-jacent, témoigne des relations entre surface et profondeur.

5. Cavité développée dans le socle - Guéssédoundou

Développée dans le socle, la grotte de Guéssédoundou a été découverte au fond d'un effondrement, à une quinzaine de kilomètres au nord-est de Makalondi (Fig. 4).

Le site est constitué d'une colline surplombant d'une dizaine de mètres la plaine environnante. Au centre de ce relief, une dépression s'est ouverte, ovale et orientée NNE-SSW. Longue d'une vingtaine de mètres de long et profonde de trois à quatre mètres, son fond est occupé par des blocs anguleux mélangés à de la rocaille. Dans le flanc sud et dans l'axe de la dépression s'ouvre une grotte sur une longueur de deux à trois mètres. Son plafond, haut de 1,80 m à l'entrée, s'abaisse rapidement. Aucune trace d'exploitation humaine n'a été décelée dans ce site. La cavité s'ouvre dans des métagabbros à grains fins, fortement altérés et traversés par des filons quartzeux de largeur décimétrique. Une intense fracturation subverticale suivant le grand axe de la dépression est bien visible. Il s'agit d'un couloir de cisaillement le long duquel les roches ont subi une silicification et une ferruginisation importantes.

A l'entrée de la grotte et sur les parois subverticales de la dépression se développent des creux subcirculaires dont le diamètre varie de quelques centimètres à quelques décimètres, rappelant les formes observées sur les parois de la grotte de Diffa Doga. L'absence de traces d'écoulement et d'abrasion mécanique laisse supposer qu'il s'agit de phénomènes de dissolution. La position topographique en hauteur du site peut s'expliquer par une plus faible érosion du socle, rendu plus résistant à cet endroit par l'armature des filons de quartz et par la ferruginisation des roches le long du couloir de cisaillement. En contre-partie, les roches broyées, devenues poreuses, ont drainé les infiltrations des eaux météoriques, facilitant les processus de dissolution.

La grotte de Guéssédoundou s'est donc développée dans un ensemble de roches altérées et très fracturées, grâce à une circulation hydrique entraînant une forte mobilisation de la silice et du fer. La dépression résulterait de l'effondrement du toit d'une vaste cavité sous-jacente dont la grotte ne serait que le prolongement maintenant visible (WILLEMS et al., 1993).

6. Géomorphologie et karstologie au Niger occidental

L'ensemble des phénomènes décrits permet de proposer un schéma général de fracturation et de karstification ainsi qu'un modèle général d'évolution géomorphologique du paysage (Fig. 5).

Dans la couverture sédimentaire, la disposition des strates silico-pélitiques ou ferrugineuses et plus ou moins imperméables détermine une circulation des eaux phréatiques en nappes superposées. Ces dernières se raccordent par l'intermédiaire de drains subverticaux que sont les plans de fracture ou leur prolongement. Elles rejoignent la nappe de la lithomarge puis les réseaux aquifères discontinus du socle.

Des cavités subhorizontales s'étendent et sont compartimentées dans leur progression par les plans de drainage subverticaux. Des phénomènes karstiques se développent le long de ces plans. Peu à peu l'érosion creuse les vallées, elles-mêmes orientées par les directions de fracturation et de structure du socle. Des plateaux s'individualisent. Les nappes les plus hautes se fractionnent et trouvent des exutoires à l'air libre. Dès lors, elles s'assèchent progressivement, avec des remises en charge sporadiques lors des saisons des pluies. Les grottes ouvertes évoluent alors par dislocation des parois et transport mécanique des matériaux. L'écroulement des grottes entraîne la déformation des niveaux supérieurs et est responsable d'effondrements en surface.

L'évolution des réseaux hydrographiques, tant sur le socle que sur les dépôts du Continental terminal est donc largement conditionnée par la circulation des eaux souterraines au travers des altérites vers les fractures du socle. L'évolution des reliefs résulte donc, en grande partie, de la formation de karsts dans la lithomarge et dans les dépôts néogènes. L'observation de diaclases, de déformations affectant le Continental terminal ou les dépôts alluviaux quaternaires, d'effondrements et de nombreuses ruptures de pente non conformes à l'érosion régressive, attestent du fonctionnement actuel de ce système. Une étude récente menée portant sur le fonctionnement hydrologique d'une zone dont le bassin versant est de 6,1 km2 dans la région

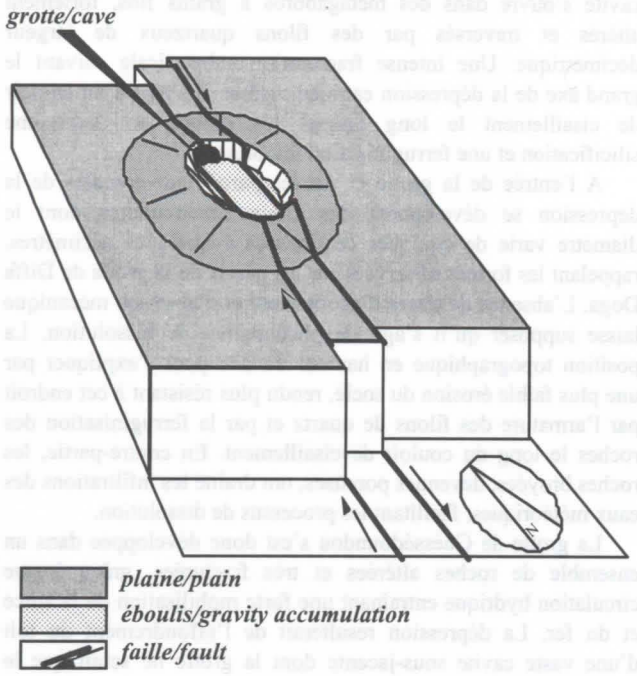

Fig.4 Site de Guessédoundou

de Niamey, menée par F. Lenoir et M. Esteves, montre qu'il faut moins de 3 heures pour que les eaux de surface traversent une épaisseur de 45 à 75 mètres de Continental terminal et atteignent la nappe phréatique. De plus, cette recherche estime qu'il faut de 2 à 3000 m^3 d'eau pour remplir le réseau qui aboutit à la nappe. L'existence de réseaux karstiques est ainsi confirmée par la rapidité de l'infiltration. et suppose des réseaux de circulation hydrique de grandes dimensions en profondeur. L'importance de réservoirs hydriques dans des roches réputées insolubles doit modifier complètement notre vision classique de l'hydrologie du socle à zones aquifères discontinues peu développées, et de sa couverture, à nappes temporaires en dehors des grandes vallées alluviales. Il nous faut donc repenser cette partie du Sahel et ses ressources en eau en terme d'aquifères karsitifiés.

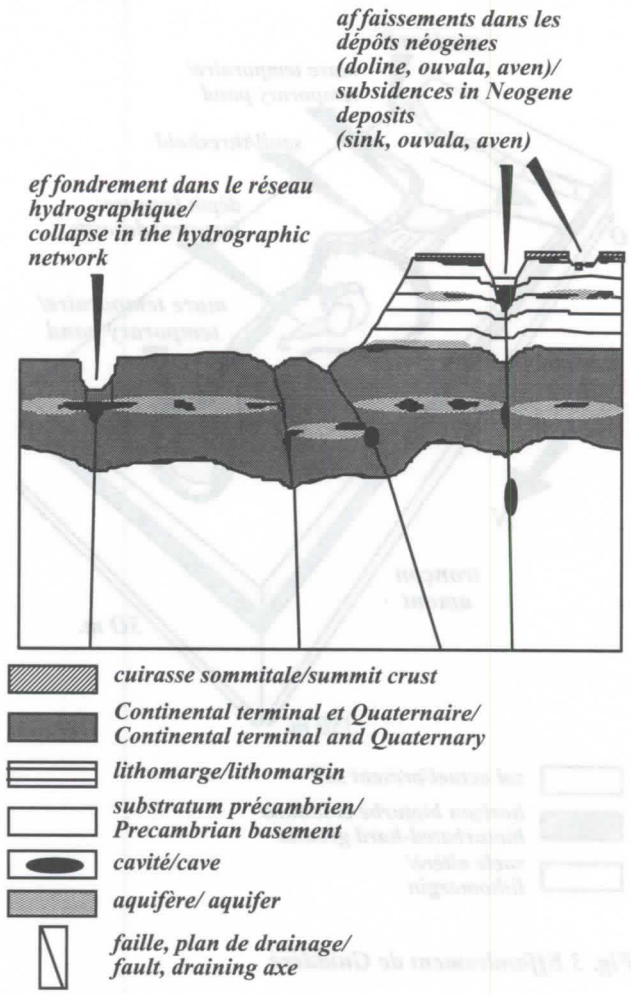

Fig. 5 Modèle général des réseaux karstiques au Niger occidental

Bibliographie

ABOUCHAMI, W., BONER, M., MICHARD, A., & F. ALBAREDE, 1990. A major 2.1 Ga event of mafic magmatism in West Africa: an early stage of crustal accretion. J. Geophys. Res., 95: 17,605-17,629.

ESTEVES, M. & F. LENOIR, 1994. Un exemple de fonctionnement hydrologique dans la région de Niamey : le bassin de Sama Dey. Journées Hydrologiques, ORSTOM, à paraître.

GREIGERT, J. 1966. Description des formations crétacées et tertiaires du bassin des Iullemmeden (Afrique occidentale). Pub. Dir. Mines et Géologie, Niger, 2, B.R.G.M. éd., 234 p.

LANG, J., C. KOGBE, S. ALIDOU, K.A. ALZOUMA, Y. BELLION, D. DUBOIS, A. DURAND, R. GUIRAUD, A. HOUESSOU, I. DE KLAZ, E. ROMANN, M. SALARDCHEBOLDAEFF & J. TRICKET, 1990. The Continental Terminal in West Africa. J. Af. Earth Sc., 10 : 79-99.

MACHENS, M. 1968, Notice explicative sur la carte géologique du Niger Occidental à l'échelle 1/200 000, Minis. TP, Transp. et Urb., Niamey, 35 p.

MACHENS, M. 1973. Contribution à l'étude des formations du socle cristallin et de la couverture sédimentaire de l'Ouest de la République du Niger, Mém. B.R.G.M., 82, 168 p.

POUCLET, A., A.E. PROST, I. AMA-SALAH & H. LAPIERRE, 1990. Les ceintures birimiennes du Niger occidental (Protorozoïque inférieur), nouvelles données pétrologiques et structurales des formations métavolcaniques. - C.R. Acad. Sci., Paris, 311, Sér. II : 333-340.

VICAT, J.P., J.M. LEGER, Y. AHMED & L. WILLEMS, 1994. Les indices de déformations plio-quaternaires de la bordure occidentale du bassin des Iullemmeden dans la région de Niamey. Au contact Sahara-Sahel, Milieux et sociétés du Niger , Rev. Géogr. Alp.Grenoble, Coll. Ascendances.Vol. 1, pp 15-24.

WILLEMS, L., F. LENOIR, J-M. LEVECQ & J-P. VICAT, 1993. Evolution du relief au Niger occidental : rôle de la fracturation du socle précambrien et de la formation de pseudo-karsts au sein de la lithomarge et de la couverture sédimentaire. C.R.Acad. Sci. Paris, Série II : 97-102.

WILLEMS, L., POUCLET , A., LENOIR, F. & JP. VICAT, 1996. Phénomènes karstiques en milieux non-carbonatés - Etudes de cavités et problématique de leur développement au Niger Occidental. Z. Geomorph. N.F., Suppl.-Bd 103 : 193-214.

Pseudokarst process and speleothems in Bohemia Cave

Havlicek D., Tasler R.

The Bohemia Cave is situated in alpine karst region Mt. Owen, Northwestern Nelson, South Island, New Zealand, and was discovered by the expedition of the Czech Speleological Society in the year 1990. Except of the first expedition in the year 1990, the cave was explorated by local cavers in the years 1991-1993 and by Czech expedition in the year 1994. This contribution does not embrance the results from the expedition 1997.

The entrance is at an altitude of 1250 m a.s.l. The system is about 8 km long, and denivelation is 663 m (-541, +122).

The area is built mainly of metamorphosed carbonates of Arthur Marble (Upper Ordovician) of Arthur Group (Upper Ordovician-Lower Silurian, WOPEREIS 1988). Carbonates are massive, occasionally bedded and contain silicified intercalations in places (TASLER 1991). Phyllites, probably belonging to the Pikikiruna Schist Formation, form the base of the marbles.

The cave has three different parts: 1) fossil phreatic passages and lateral labyrinth of phreatic channels with slight vadose premodeling, 2) classical fossil and active meanders and 3) giant rooms. We will deal only part 3 and the speleothems there.

The giant rooms form the main part of whole system (see fig. 1). They follow the contact between marbles and underlying phyllites. The active flow with several feeders and bifurcations follows the whole course of this gallery and is often covered by an accumulation of large blocks. Erosion has started along the contact, and the phyllites have been eroded to a considerable depth. The erosion reached a depth of 15 m and more in many places and the tectonically formed ceiling is affected very littly by karst processes in comparison with the volume of space created in the phyllites (see fig. 2). A more extensive karstification is not even present around ceiling tributaries. Near the exit of limestone tributaries, small domes are created in the phyllites beneath the contact. Some passages are developed only in phyllites, and the limestone ceiling is only tectonic.

The general dip angle/direction of the contact is 35-50° to the SSE. At some places, the contact is folded. The phyllites are black (graphite) and lower silver-green. The detailed petrology of the phyllites has not been studied so far.

Stalactites, stalagmites, stalagnates, straws and all excentric shapes are mainly aragonite. The excentrics may be divided into four basic groups, which are often combined and chaotically growing through each other: 1) anthoditic excrescences and fibres, 2) aragonite "iron blossoms" (giant-sized tufts up 1 m in diameter), 3) helictites, 4) straws growing out in every direction, from 1 mm to 10 mm in diameter and up to 50 cm long. X-ray diffraction analysis show a very pure aragonite, calcite is rare.

Hydromagnesite ($Mg(OH)(CO_3) \times 3H_2O$) soft balls occur on the ends of some shapes of aragonite.

References

WOPEREIS P., 1988: Geology of the Southern Part of Mt. Owen. N.Z. Speleological Society Bulletin 8/144/145: 134-140. Waitomo.

TASLER, R., 1991: Owen 90 - New Zealand. Czech Speleological Society - Alberice. Trutnov.

fig. 2

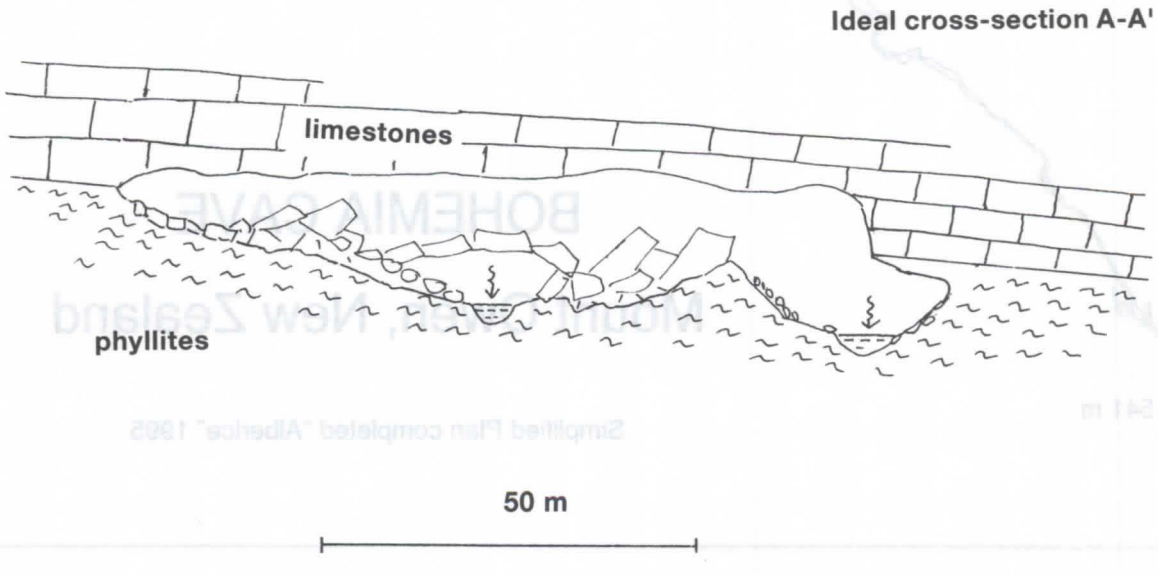

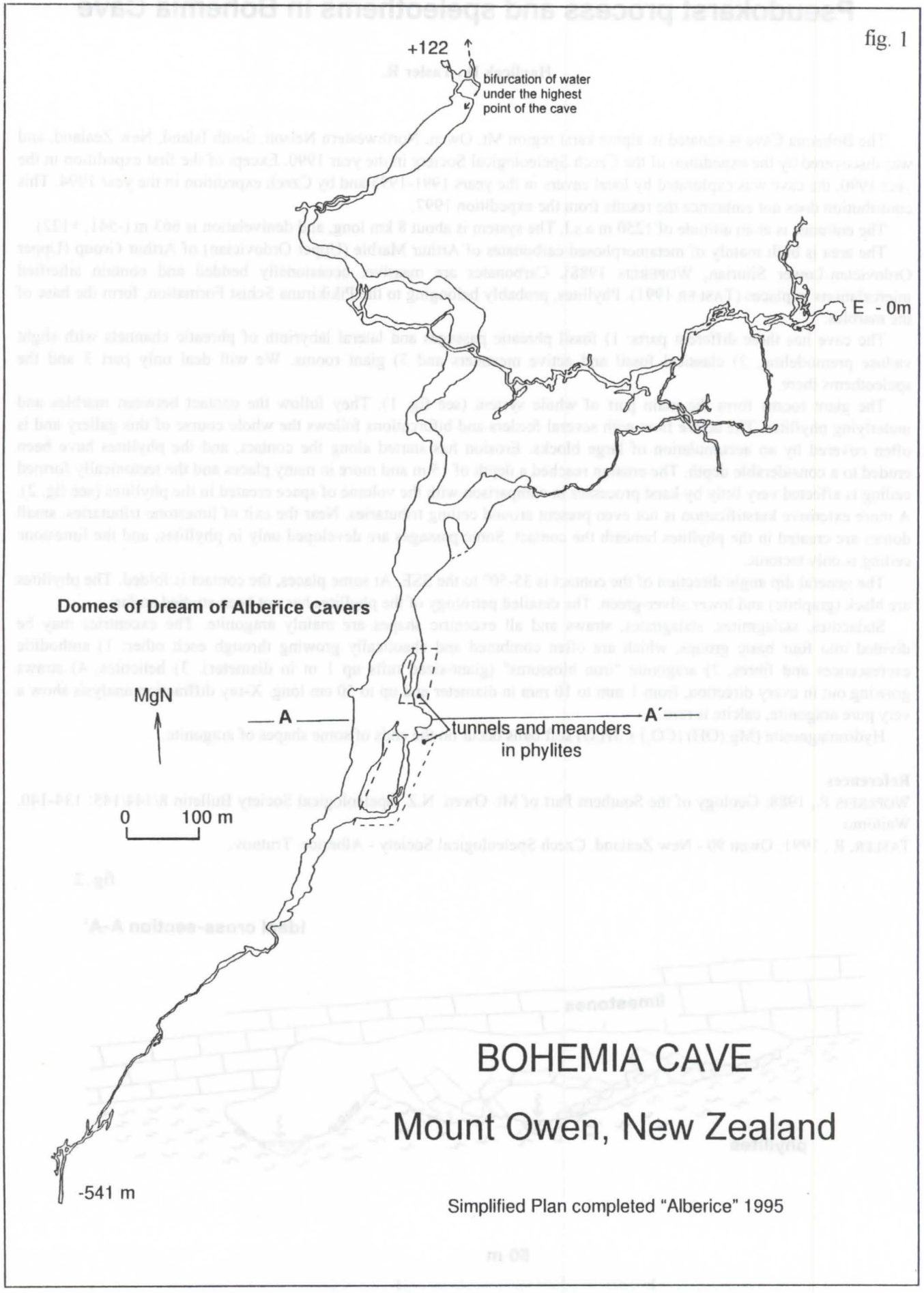
fig. 1
+122
bifurcation of water
under the highest
point of the cave
E - 0m
Domes of Dream of Albeřice Cavers
MgN
A
A´
tunnels and meanders
in phylites
0
100 m
BOHEMIA CAVE
Mount Owen, New Zealand
-541 m
Simplified Plan completed "Alberice" 1995

Present Status of Speleological Researches into the Patagonian Glaciers

Giovanni Badino (*), Adolfo Eraso Romcro (**), Marco Mecchia (+)
(*) Dip.to di Fisica Generale, Via Giuria 1, I-10125 Torino
(**) ETSIM, Rios Rosas, 21, 28003 Madrid
(+) Speleo Club Roma, Via Doria 79/f, I-00192 Roma

Abstract

The present status of deep water drainage researches on Patagonian glaciers is discussed. Their karstic phenomena appear to be the most interesting and perhaps the most penetrable encountered up to now. The reasons are probably the alimentation basin amplitude (the Hielo Patagonico Sur), the intense ablations due to singular climate conditions and the relative impermeability of glacier cores.

Introduzione

Il gruppo italiano che si occupa delle ricerche sul carsismo glaciale opera dall'84. Sono state condotte campagne prima sui ghiacciai alpini, il più interessante dei quali si è dimostrato il Gomergletscher, e poi all'estero: il Biafo in Karakorum (1987), l' Enilchek in Pamir (1992), il Batura in Karakorum (1993), il Moreno, il Viedma e il Marconi (1991, 1994, 1995) in Patagonia.

Come già delineato in precedenti lavori, il drenaggio delle acque di fusione avviene lungo reticoli di drenaggio semistazionan che si formano al di sotto della superficie.

Dalle osservazioni effettuate risulta che i mulinelli glaciali si trovano soprattutto su lingue glaciali estese, pianeggianti e poco erepacciate. Le morfologie osservate sono del tutto analoghe a quelle di inghiottitoi carsici e pertanto sono da considerarsi forme pseudocarsiche o, per usare un termine di nuova introduzione, "criocarsiche".

Al di sotto di 50-100 m di profondità i mulinelli assumono morfologie a forra con brevi salti occupati alla base da profonde vasche d'acqua. A profondità variabili da 70 a 150 m si raggiunge la superficie idrica di acquiferi che riempiono le cavità.

Esiste quindi una zona satura, o freatica, di struttura probabilmente complessa, sinora inesplorata.

I modelli numerici mostrano che le acque assorbite fluiscono attraverso una rete di condotte sommerse, all'interno della massa glaciale a profondità di 100-150 m, con struttura ad albero connettente i vari mulini. La rete di gallerie appare "schiacciata" sulla superficie delle falde acquifere del ghiacciaio.

In inverno, con il cessare della alimentazione, i reticoli di gallerie tendono a collassare a profondità superiori a 50-60 m, spingendo su l'acqua residente sino quasi prossimità della superficie.

"Ghiacciai carsici"

E' oramai evidente che i ghiacciai formati da ghiaccio a temperature prossime allo zero tendono a formare pozzi di drenaggio dei torrenti superficiali e a convogliare le acque in reticoli profondi.

Questi reticoli sono semi-stazionan, nel senso che migrano verso monte con la velocità con cui il ghiaccio migra a valle dato che sono legati alla forma del ghiacciaio, a sua volta legata alla struttua di contenimento. Di fatto le osservazioni indicano che quasi ovunque, eccetto che in Patagonia, la struttua a pozzi si riforma con periodicità annuale. I pozi fossili, annuali, vengono trascinati a valle, deformati dalla plasticità del ghiaccio.

Sinora non è stato possibile penetrare nei reticoli profondi ma i modelli a calcolatore stanno delincando abbastanza chiaramente le loro strutture. Che il ghiaccio sia "caldo" non basta però per formare reticoli profondi. Occorre anche che la morfologia estema permetta la formazione di grandi nussi d'acqua che possano applicare l'energia accumulata in pochi punti di entrata. Essi sono in genere quelli in cui lo stress da attrito fra gli scorrimenti differenziali delle lingue glaciali ha indotto depressione superficiale e un proto-reticolo di drenaggio interno. In altra comunicazione mostriamo che, come e più chiaramente che in altri materali anche la struttura complessiva del drenaggio è condizionata dallo stato di tensione della lingua glaciale.

Crediamo che sia molto naturale proporre per questo tipo di ghiacciai il termine "ghiacciai carsici".

La temperatura limite della massa del ghiaccio per la formazione di carsismo appare essere intonno a -3 o -5 °C. Questo esclude un cnocarsismo glaciale in zone polari. Il limite verso Nord appare essere alle Svalbard, dove infatti vi sono g~iacciai con fenomeni carsici (in genere abbastanza ridotti) accanto ad altn che ne sono privi.

Non abbiamo ancora determinato il limite Sud. Sulla base delle segnalazioni riteniamo che la penisola antartica sia ancora in situazione di carsismo mentre le coste del continente appaiono essere coperte da ghiacci non carsificati.

Nei ghiacciai della Patagonia

La peculiarità dei ghiacciai patagonici è il fatto che essi si spingono sino a quote molto basse. Questo è dovuto sia alla vastità del bacino di alimentazione sia alla loro velocità relativamente alta.

Questi fatti fanno si che enormi masse di ghiaccio arrivano ad essere sottoposte ad uno scioglimento estremamente rapido. L'ablazione osservata sul ghiacciao perito Moreno durante la spedizione del '95 è arrivata a superare 15 cm in un solo giorno. Questo causa una rapidissima evoluzione del reticolo superficiale e la riformazione di nuove entrate nello stesso punto, più volte all'anno. Quello che nei grandi ghiacciai carsici alpini e sub-tropicali awiene nel corso di un anno in Patagonia awiene nel corso di settimane: una sorta di "iper-carsismo" glaciale.

Altre particolarità del carsismo patagonico sono dovute al fatto che il rapido flusso del ghiaccio lo trasforma e ricristallizza. La luce impressionante che appare uscire da ogni fenditura ci sembra solo imputabile al fatto che il ghiaccio profondo è totalmente trasparente e fa da guida di luce per la radiazione che arriva sulle distese dello Hielo Continental. Il fatto che la luce sia azzurrina indica infatti che si tratta di luce "selezionata" da un filtro molto lungo e che trasmette solo le frequenze più alte della radiazione.

Questo ha importanti conseguenze sulla struttura del carsismo profondo: il nucleo dei ghiacciai appare essere praticamente impenetrabile ai flussi d'acqua se non nelle parti terminali delle lingue, dove la "guida d'onda" si spezza per fenomeni di distensione.

Il risultato è che le grotte nei ghiacciai pataonici sono estremamente superficiali e che viene fortemente soppressa la formazione di un reticolo freatico.

Le cavità sono dunque delle gallerie che corrono parallele alla superficie (in alcuni casi estremamente pericolose) coperte da spessori di ghiaccio che variano da poche decimetri sino ad una ventina di metri di spessore di ghiaccio.

Il drenaggio avviene dunque in ambienti vadosi e questo apre la prospettiva di esplorazioni che si potranno estendere per molti chilometri e per molte centinaia di metri di profondità.

Nel '94 e soprattutto nel '95 l'Associazione La Venta ha organizato campagne di ricerca sul Perito Moreno, realizando anche ricognizioni aeree sui ben più vasti ghiacciai Upsala e Viedma. Il primo, che pone problemi logistici molto ardui, non appare molto carsificato, anche se questo potrebbe essere in qualche modo collegato con un recente surge.

Il ghiacciaio Viedma appare invece straordinanamente carsificato, e risulta il principale obiettivo delle prossime ricerche per gli anni '97 e '98.

Bibliografia

BADINO 90, "Fisica dei buchi nell'acqua", Proc. of 1st Int. Symposium of Glacier Caves and Karst in Polar Regions, Madrid, 1990.

BADINO 92, "Ice Shaft Genesis: a Simple Numerical Approach", Proc. of 2nd Int. Symposium of Glacier Caves and Karst in Polar Regions, Miedzygorze, 1992.

BADINO 94, "In attesa del prossimo Jökulhlaup", Speleologia 30, 1994.

BADINO 94.1, "Phenomenology and First Numerical Simulations of the Freatic Drainage Network Inside Glaciers", Proc. of 3th Int. Symposium of Glacier Caves and Karst in Polar Regions, Chamonix, 1994.

BADINO 95, "L'estrema Thule: ultimo o penultimo limite dela speleologia?", Speleologia 32, 1995.

BADINO 96, G. BADINO, L. PICCINI, "Morfologie ed Evoluzione delle Cavità Endoglaciali di Origine Cnocarsica", Atti Convegno Naz. CGI, su Geogr. Fis. Din. Quat. 1996.

HOOKE 84. "On the role of mechanical energy in maintening subglacial water conduits at atmospheric pressure", Joumal of Glaciology, 30, 105, 1984.

MONTERIN 30, "Sulla costanza di posizione dei pozzi glaciali", Boll. Com. Glac. It., 10, 211, 1930, Nye 76, "Water Flow in Glaciers...", Journal of Glaciology, 17, 76, 181, 1976.

PATERSON 69, "The physics of glaciers", Pergamon Press, 1969.

ROTHLISBERGER 72, "Water Pressure in Intra and Subglacial Channels", Journal of Glaciology, 11, 62, 177, 1972.

SEABERG 88, "Character of the englacial e subglacial drainage system", Joumal of Glaciology, 34, 117, 1988.

SHREVE 72, "Movement of water in glacier", Joumal of Glaciology, 1l, 62, 1972.

WALDER 86, "Hydraulics of subglacial cavities", Joumal of Glaciology, 32, 112, 1986.

Investigations on the endorreic drainage of the south east part of Vatnajökull glacier

Adolfo Eraso[1], Sigurdur S. Jonnsson[2], Carmen Domínguez[3]
(1) Prof. Tit. de Hidrogeología, E.T.S.I.M.- Universidad Politécnica de Madrid.Spain
(2) HellarannsóknafélagIslands - Icelandic Speleological Society, Reykjavik. Iceland
(3) Prof. del Dpto. de Matemática Pura y Aplicada -Universidad de Salamanca.Spain

Abstract

During the "ISLANDIA 96" glaciological expedition, we explored two glacier tongues: Kviarjökull and (Virkis-Fall)jökull in the south part of Vatnajökull ice cap where we investigated a few moulins which generated endoglacier rivers.

We applied the Prediction Method of the main directions of subglacier drainage, quantifying the anisotropy of both glacier tongues, contrasting in each case the prediction obtained with the explored rivers.

The work we present here shows the results obtained by the application of the Prediction Method, its grade of accuracy and the discussion on its application.

Keywords: Iceland, Vatnajökull, Prediction Method, endoglacier drainage, tectoglyphs, eskers.

Résumé

Au cours de l'expédition glaciologique "ISLANDIA 96", nous avons exploré deux langues glaciaires: Kviarjökull et (Virkis-Fall)jökull emplacées au SE de la grande calotte glaciaire Vatnajökull où nous avons exploré quelques moulins qui génèrent des rivières endoglaciaires.

Nous avons appliqué la Méthode de Prédiction des principales directions du drainage sousglaciaire, quantifiant l'anisotropie des langues glaciaires, comparant dans chaque cas la prédiction faite avec les rivières explorées.

Le travail que nous présentons montre les résultats obtenus par l'application de la Méthode de Prédiction, son degré de justesse et la discussion sur son application.

Mots Clés: Islande, Vatnajökull, Méthode de Prédiction, drainage endoglaciaire, tectoglyphes, eskers.

1. Introduction

The investigations we present here were developped during the "ISLANDIA 96" Glaciological Expedition. During this expedition, we explored the Kviarjökull and Virkis-Falljökull ice tongues, both located in the southeastern (SE) part of the Vatnajökull ice cap which, with an extension of 8,300 km^2, is the larger one of Iceland and Europe.

One of the objectives of the Expedition was the localization of endo and subglacier rivers, apply on them the Prediction Method of the Main Directions of Drainage in Karst, and contrast the obtained results in the explorations with the prediction given by the referred Method.

The authors of the present work wish to express here their gratitude to the Icelandic Speleological Federation for their assistance as well as to the members of the Expedition: Donato Pérez, Ignacio Chavarría and Angel Sesma for their collaboration in the realized investigations.

2. Field works and methodology

The Kviarjökull and Virkis-Falljökull glacier tongues were selected because they present a karstical network of drainage in their ablation zone.

The exploration were made using speleological and climbing-in-ice techniques. The geodesic localizations were made through a TRIMBLE GPS, with the help of a BRUNTON compass. The magnetic declination in SE Iceland is 19ºW.

The applied Prediction Method (ERASO 1985/86) directionaly quantifies the anisotropy of a rocky massif (vgr. ice tongue) giving a percentage of probability associated with the obtained directional mode. It is essentially based on statistically quantify the extensional plans, or weakness plans which contain a $\sigma_1\sigma_2$ (major and intermediate components of the tensional elipsoid), with which the prediction is made.

We also used them to compare the visible eskers alignments in both ice tongues. These eskers represent paleo-drainages, dismantled by the glacier ablation.

3. Results and discussion

The investigations were made in the ablation zone of two different glacier tongues: Kviarjökull and Virkis-Falljökull (see figure 1), where we had observed, in previous explorations, the existence of several endoglacier rivers (ERASO, PULINA, 1994), some of which it was impossible to explore.

Kviarjökull

It is a 10 km long glacier tongue which goes downwards with an E slope and whose snout reaches a 2.5 km width.

The final part of the ablation zone, of 4 km long from the first barreer of seracs, has a lot of moulins (ponors) among which we choose the "Tatuk" Ponor where two supraglacier rivers disappear (see figure 1). After a wide 20 m deep well, the river flows through meanders we explored along 50 m (45.6 m of which we topographied) until it reached, at 32m deep, a "trop plein" which stopped our exploration.

The investigations made with the Prediction include 288 points of measurement of weakness plans which, distributed in 6 different stations, gather the information contained in the ablation zone.

Beside this, the alignments of eskers existing in the referred ablation zone and which show the evidence of former drainages, have been measured along 859.5 m.

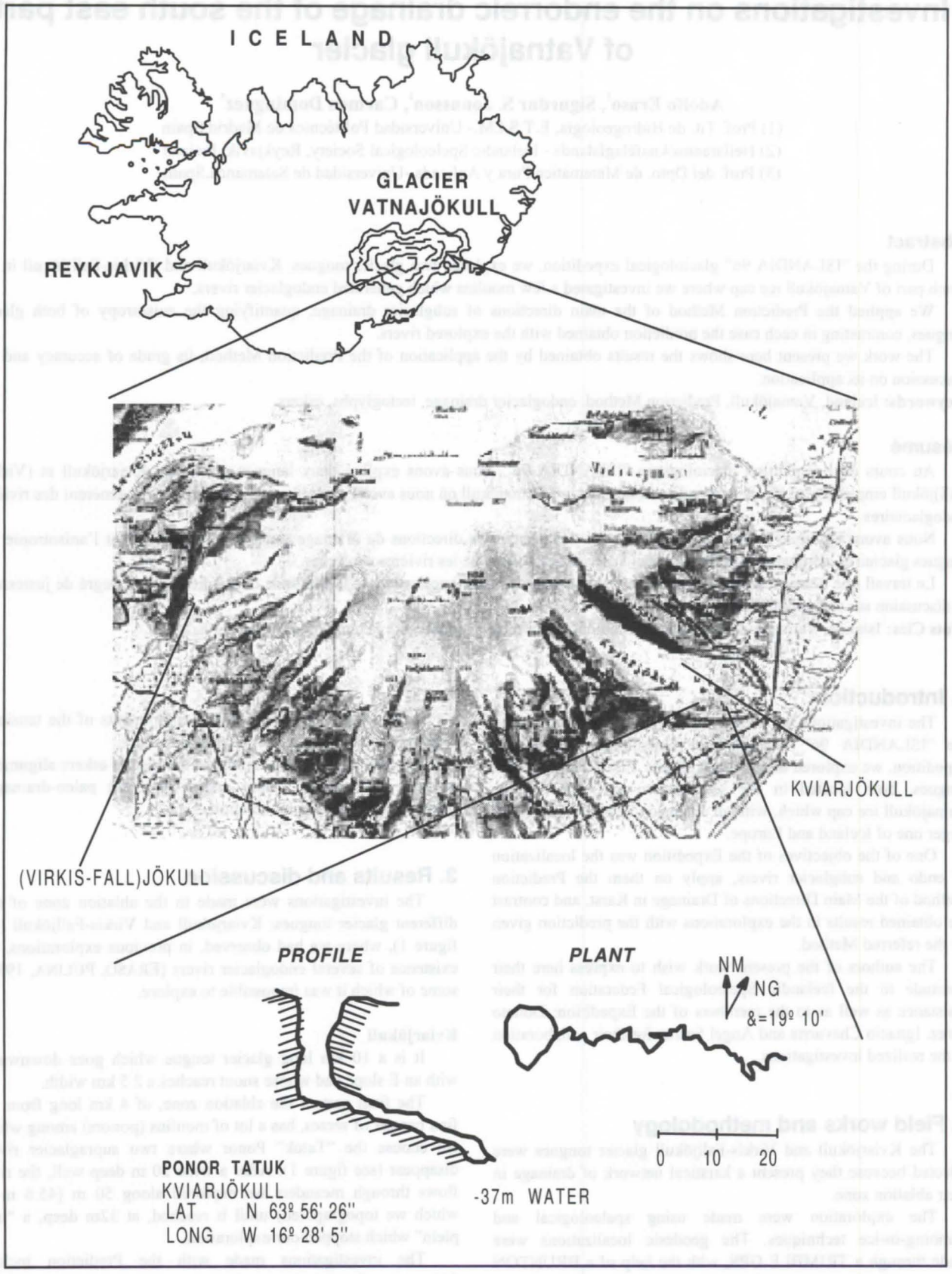

Figure 1: Location map.

The investigations made give us the following results:(see figure 2)

i)-. Tectoglyphs: The distribution law of the weakness plans given by the Prediction Method shows:

- A main mode according to N90º-105º (in class 7), with an associated probability of 27.4%.
- A secundary mode according to N120º-135º (in class 9), with an associated probability of 10.4%.

ii)-. Eskers: The measured alignments, indicating endoglacier paleodrainages show:

- A main mode according to N90º-105º (in class 7), with an associated probability of 38.8%.
- A secundary mode according to N60º-75º (in class 5), with an associated probability of 27.5%.

iii)-. Cave with endoglacier river: The prediction of the topographied streches develops according to:

- A main mode: N90º-105º (class 7), with a 35.7% probability.
- A secundary mode: N60º-75º (class 5),with a 17.5% probability.
- Two other accessory modes:
  N15º-30º (class 2), with a 9.4% probability.
  N120º-135º (class 9), with a 8.8% probability.

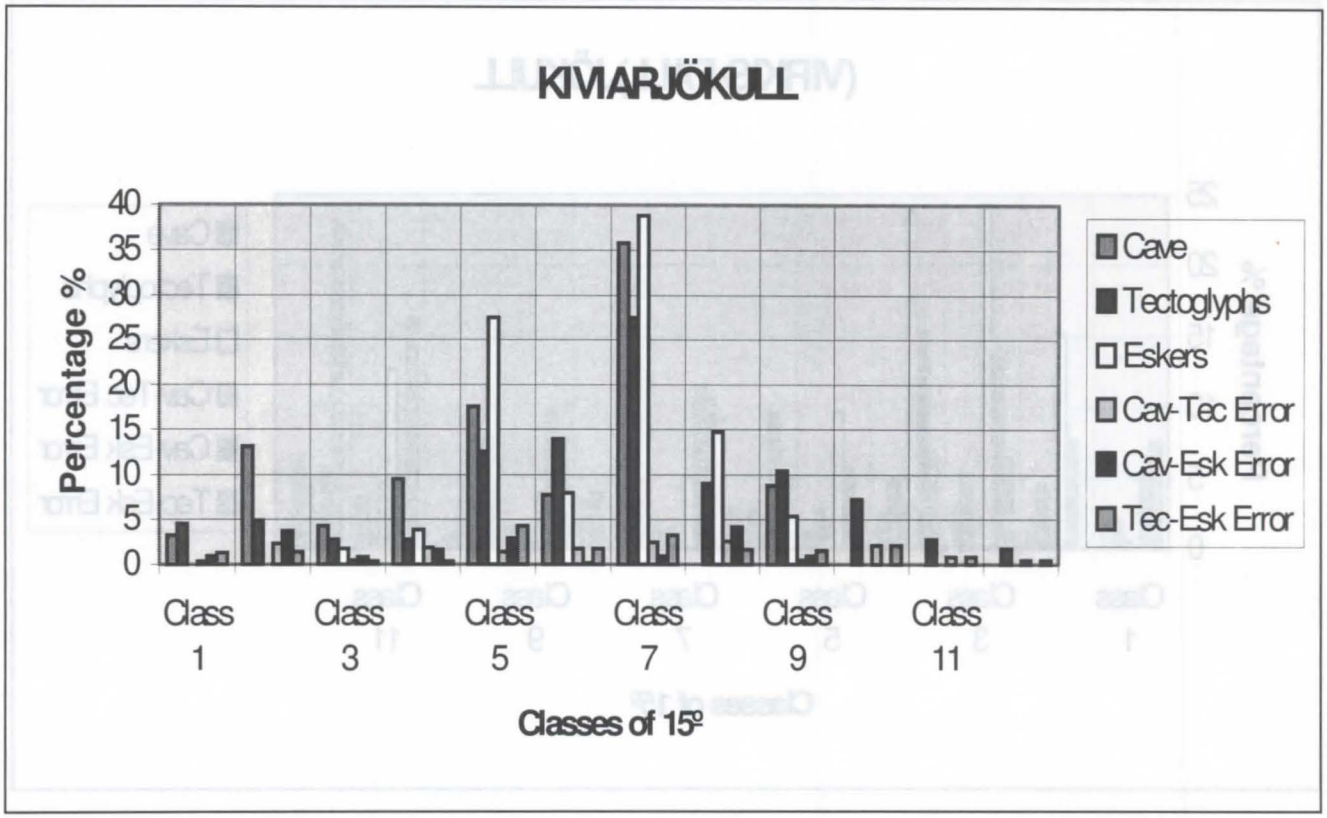

Figure 2: Histogram of tectoglyphs, eskers and cave of the Kviarjökull glacier tongue with the errors associated.

The grade of accuracy, comparing the prediction given by the Prediction Method (Tectoglyphs: **T**),the paleodrainages (alignments of eskers: **E**) and the directions of the underglacier river (glacier cave: **C**), will be given by the value of the maximum errors dragged along in the statistical classes where are the modes we got.

These errors are expressed in the table 1, according to the Kolmogorov-Smirnof test.

Class	T/C	T/E	C/E
7	2.4%	3.3%	0.9%
5	1.5%	4.3%	2.9%
9	0.5%	1.5%	1.0%
2	2.4%	1.4%	3.8%

Table 1: Errors of comparison of the Prediction Method (T), the paleodrainages (E) and the directions of the underglacier river (C) of the Kviarjökull glacier tongue, according to the Kolmogorov-Smirnof test.

And its small value shows the high grade of accuracy of the applied Prediction Method, where the main mode (class 7) is common for all the cases.

Virkis-Falljökull

The ablation zone of this glacier results in the comjunction of two different glacier tongues: Virkisjökull and Falljökull. Its slope is southwards. It has a maximum length of 6 km and its snout is 1.2 km wide.

The investigations made give us the following results: (see figure 3)

i)-. The Prediction Method has been applied here through the measurement of 52 tectoglyphs (**T**). The results indicate a distribution law of the weakness drainage plans with:

- A main mode according to N45º-60º (in class 4), with an associated probability of 15.4%.
- A wide mode according to N90º-120º (occupying classes 7 and 8), with an associated probability of 11.5% in each class.

ii)-. The alignments of eskers (**E**), with a total length of 197m, present the following directional modes:

• A main, wide mode, according to N30º-60º (classes 3 and 4), with an associated probability of 24% in each class.

•A secondary mode according to N150º-165º (class 11) with a 12.7% probability.

iii)-. The directions of the underglacier river, explored along 50m, has the following modes:

• A main mode: N165º-180º (class 12), with a 23% probability.

• Two other secundary ones:

N105º-120º (class 8) with a 13.6% probability.

N45º-60º (class 4) with a 6.8% probability.

In this example, the class 4 mode appears as the main one in the Prediction (**T**) and in the alignment of eskers (**E**) but it is secundary in the directions of the underglacier river (**C**).

The secundary mode of the Prediction (**T**), class 8, is also secundary in the underglacier river (**C**), but do not appear in the alignment of eskers (**E**).

The main mode of the underglacier river (**C**), class 12, do not appear in the Prediction (**T**), and in the alignment of eskers (**E**) appears displaced in class 11 as secundary character.

It is evident that here the Prediction is smaller than in the Kiviarjökull example, probably because the statistical weight of the measured populations is also very smaller.

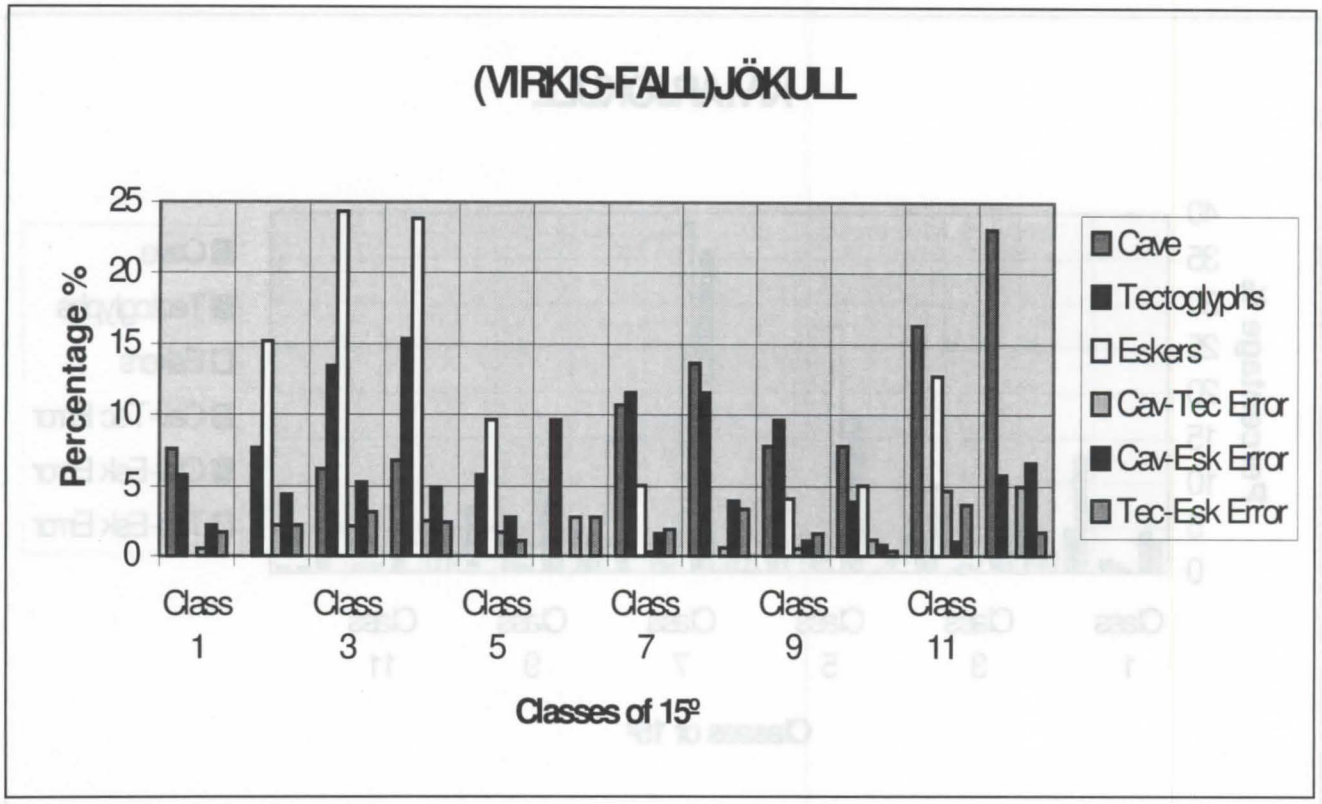

Figure 3: Histogram of tectoglyphs, eskers and cave of the Firkis-Falljökull glacier tongue with the errors associated.

Nevertheless, the maximum errors in the classes which present modes are expressed in the table 2, according to the Kolmogorov-Smirnof test.

So, major than in the former example, but still acceptable specially in reference to the applied Prediction Method.

CLASS	T/C	T/E	C/E
4	2.5%	2.4%	5.0%
3	2.1%	3.1%	5.3%
8	0.7%	3.3%	3.9%
7	0.3%	1.9%	1.6%
11	4.7%	3.7%	1.0%
12	5.0%	1.7%	6.7%

Table 2: Errors of comparison of the Prediction Method (T), the paleodrainages (E) and the directions of the underglacier river (C) of the Virkis-Falljökull glacier tongue, according to the Kolmogorov-Smirnof test.

4. Conclusions

- The Prediction Method applied in the investigation of the underground drainage of karsts developped in rocks such as gypsum, limstone, quartzite, etc... give also good results in karst in ice.
- The maximum errors in Kviarjökull between the Method and the endoglacier river **T/C** are 2.4%.
- In the case of the Virkis-Falljökull where the statistical population is much smaller, the maximum error is 5.0%.

Bibliography

ERASO, A. 1985/86. Método de predicción de las direcciones principales de drenaje en el karst. *Kobie (Serie Sc. Nat.) XV* pp. 15-165. Bilbao.

ERASO, A. & PULINA, M: 1994. Cuevas en hielo y ríos bajo los glaciares. *1 vol.* 242 pp. Ed. McGraw-Hill. Serie Div. Cient. Madrid.

Hydrologic systems in carbonate karst and in subpolar glaciers

Similarities and differences

by Jan Leszkiewicz & Marian Pulina
Department of Geomorphology, University of Silesia, ul. Bedzinska 60, 41-200 Sosnowiec, Poland

Abstract

Hydrological systems of chosen carbonate karst massifs and subpolar glaciers were compared. Beside obvious differences significant similarity in the course of hydrologic phenomena and in the relief was found. Glacier caves and forms similar to karst on the glacier surface are known. Water circulation inside glaciers is subject to similar rules as in karst hydrology. Caves are the most important elements of water discharge. Geometry and relief of caves in karst and in glaciers were compared, as well as water circulation in these caves. Beside the system of channel drainage in karst and glaciers other systems of drainage are active - fissured and porous. Terms used in karst were adopted to the similar to karst phenomena taking place in glaciers. Work is based mostly on own investigations of karst and Spitsbergen glaciers.

Résumé: Systèmes hydrologiques dans le karst carbonaté et dans les glaciers subpolaires. Analogies et différences

On a comparé les systèmes hydrologiques des massifs choisis du karst carbonaté et des glaciers subpolaires. A part les différences évidentes, on a constaté d'importantes analogies dans le déroulement des phénomenès hydrologiques et dans les formes du relief. On connaît des grottes glaciaires et des formes sur la surface des glaciers qui sont analogues aux formes karstiques. La circulation des eaux dans les glaciers est soumise à des lois analogues à l'hydrologie karstique.

Les grottes sont les éléments les plus importants du drainage. On a comparé la géométrie et le relief des grottes dans le karst et dans les glaciers, ainsi que la circulation des eaux dans ces grottes. A part du système de conduits, dans le karst et les glaciers fonctionnent d'autres systèmes de drainage - fissureux et poreux.

La terminologie appliquée au karst, a été adoptée pour des phénomènes analogues se produisant dans les glaciers. Le travail a été élaboré en grande partie à partir des propres recherches sur le karst et sur les glaciers du Spitsberg.

1. Introduction

Comparison of hydrological processes between karst regions (Caribbean - figures 1 and 2) and glaciers (figures 3 and 4) was made. Forms of surface and subterranean karst were chosen in relation to similar forms in the glaciers. Karst phenomena are very well known for participants of the Congress of Speleology so first of all analogous phenomena in glaciers were described, named cryokarst phenomena (PULINA, 1984, PULINA & REHAK, 1991).

2. Hydrological comparison

Hydrological systems of limestone karst and glaciers among obvious differences show considerable similarities. In both systems occurrence of four hydrogeological zones was found: vadose, transitional, phreatic shallow and phreatic deep. In karst massifs the zones mentioned above have been investigated for a long time which is documented in the rich bibliography of karst hydrology. In subpolar glaciers vadose and transitional zone were investigated in glacier tongues. Phreatic zone occurs in the bottoms of glacier cirques. In the case of glaciers ending in the sea (tide water glaciers) the lowest parts of the glacier are situated below the sea level, where a deep phreatic zone exists usually (e.g. the Hans Glacier in South Spitsbergen - JANIA, 1991). The main element of drainage in these zones are glacier channels being counterpart of karst channels. In the central part of glaciers horizontal caves exist ending by different outlets in the frontal zone: open glacier gates, glacier springs with siphon system. Complicated geometric networks of channels of the 'Swiss cheese' type were found in the outlet part of phreatic zones, where water is circulating under the pressure. Water flows into a glacial system by swallow holes (ponors), moulins and glacier blind valleys (closed glacier valleys fed by ablation water from glacier and water from unglaciated slopes). Percolation of water in the snow - firn layer in glaciers can be compared with filtration in pore systems, which in many cases are accompanying karst systems. In both cases the laws of seepage hydraulics can be used, but this broad problem will not be discussed here.

Below the glacier surface at the depth of few hundred meters in glacier cirques and on glacier plateaux the channels were found with diameter of few to a dozen millimetres in which water flows under pressure.

3. Comparison of caves

In comparison with limestone caves channels and caves in glaciers are characterised by considerably bigger dynamics of development. Their temporal development is restricted to tens or few years and sometime even to one year (season). Because of glacier movement and plasticity of ice, cave geometry is submitted to great changes. Cases of cutting off the channel fragments are met. Closed chambers with water or air are formed in the glacier this way.

Shifting of the glacier shafts (moulins) following the direction of the glacier movement is the characterictic phenomenon. Together with the increase of the distance from the place of their formation the shafts are gradually squeezed until they completly vanish. However in the region where earlier the old shaft emerged after some time the new shaft is formed. This process can be investigated on the example of Lipert Cave in the Werenskiold Glacier (figure 5). Apart from caves situated

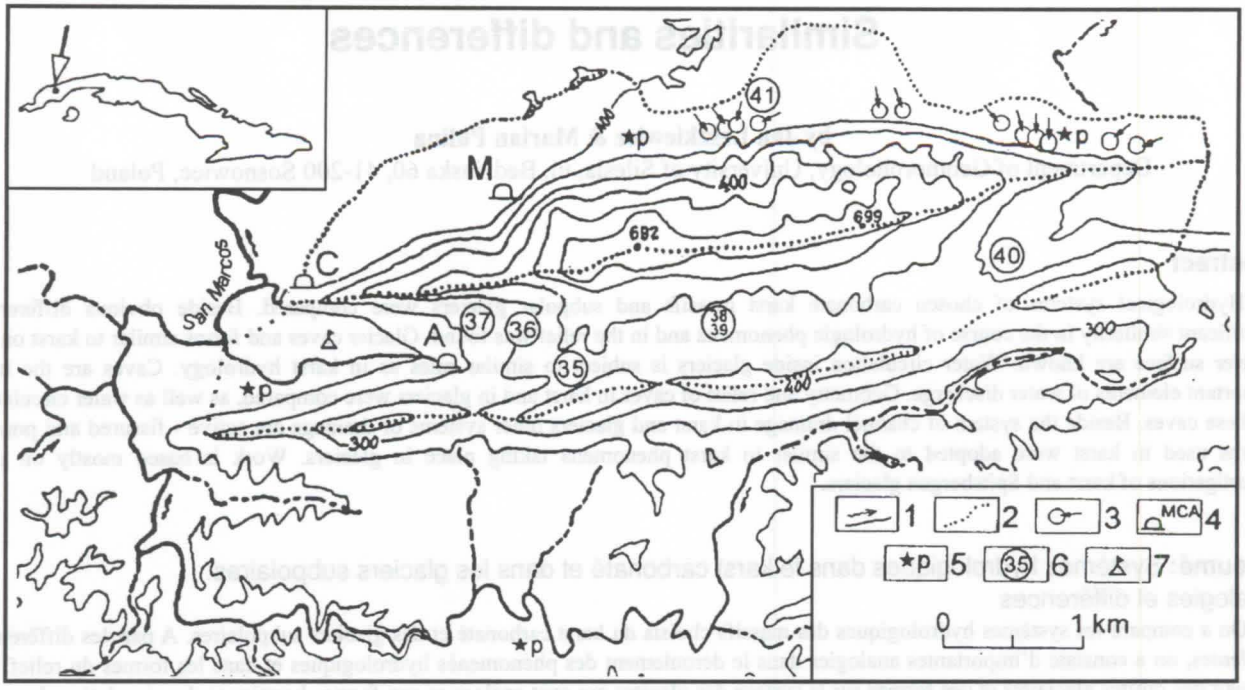

Figure1 : Pan de Guajaibon Massif (West Cuba): 1 - rivers, 2 - boundaries of the basins, 3 - swallow holes, 4 - caves (M - Mamey Cave, A - Ancon Cave, C - Canilla Cave), 5 - rain station, 6 - example of water from the surface of the massif, 7 - base of the expedition.

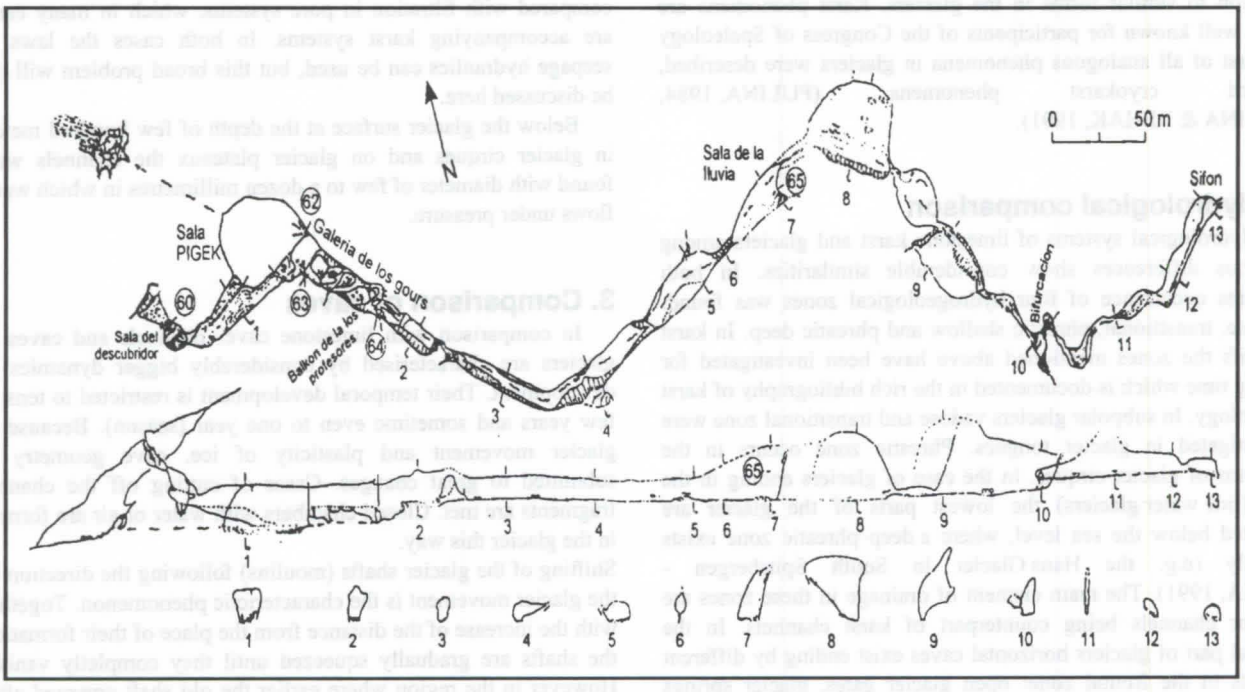

Figure 2: Ancon Cave in the Pan de Guajaibon Massif (West Cuba).

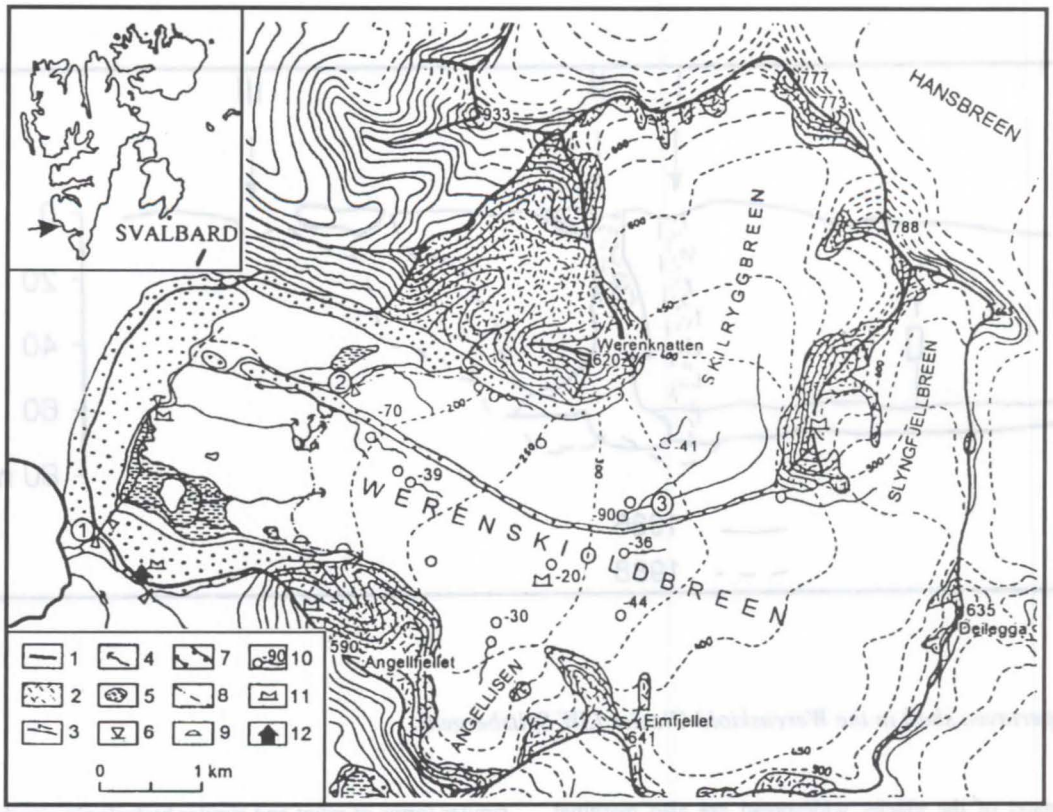

Figure 3: Basin of the Werenskiold Glacier (SW Spitsbergen):1 - boundaries of the basin, 2 - slopes of mountain massifs, 3 - supraglacial and proglacial rivers, 4 - springs, 5 - water reservoirs, 6 - hydrometric gauging stations, 7 - moraines, 8 - glacier front extent in 1983, 9 - horizontal caves, 10 - glacier shafts (numbers indicates depth), 11 - meteorological stations, 12 - Stanislaw Baranowski Glaciological Station of Wroclaw University.

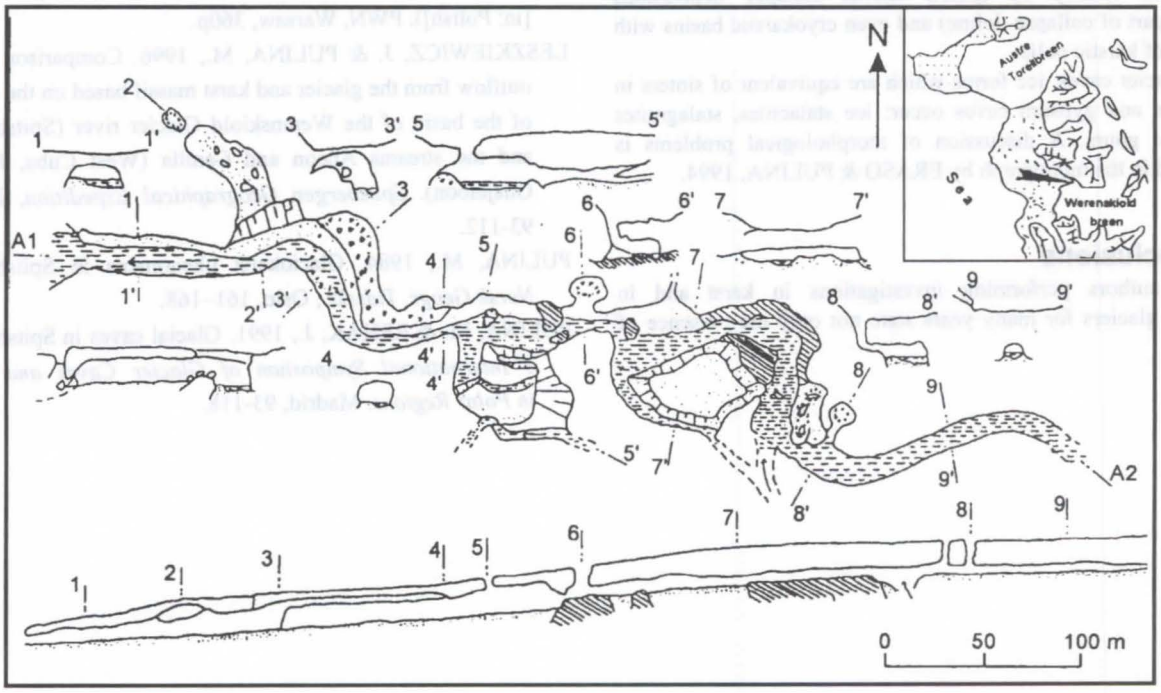

Figure 4: Kvisla Cave in the Werenskiold Glacier (SW Spitsbergen).

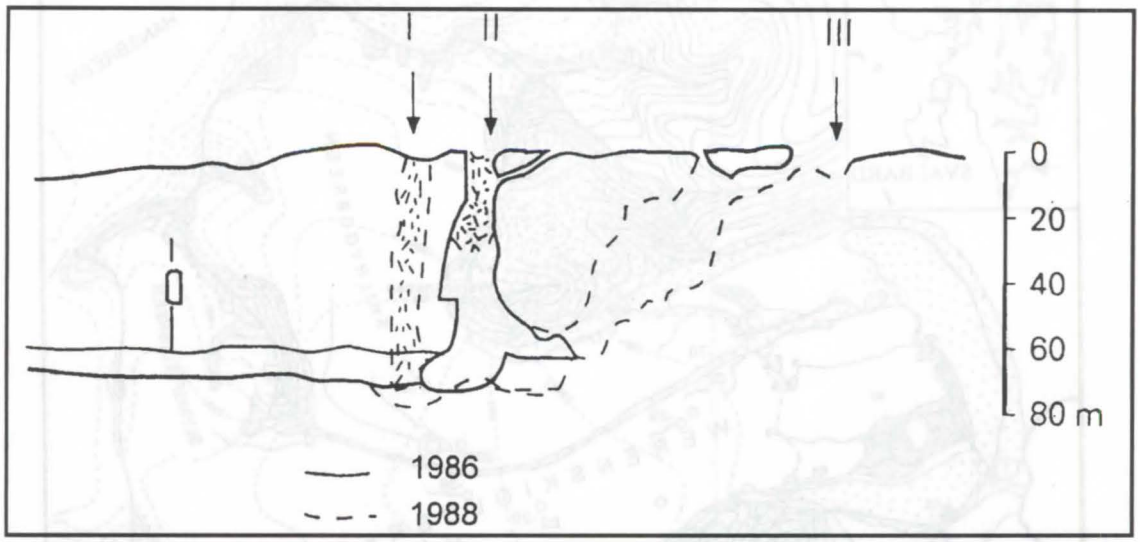

Figure 5: Lipertaven shaft in the Werenskiold Glacier (SW Spitsbergen).

in the main mass of the glacier widespread are also marginal caves fed from the outside of the glacier.

4. Morphological comparison

Water circulation in subpolar glaciers, similar like in karst, is closely related to the systems of channels and circulation - in this circulation on the surface and inside glaciers. Cryokarstic forms were distinguished, including typical cryokarstic depressions discharged usually by glacier shafts, collapse depressions (counterpart of collapse doline) and even cryokarstic basins with features of karstic polje.

In glacier caves, ice forms which are equivalent of sinters in limestone and gypsum caves occur: ice stalactites, stalagmites and even gours. A discussion of morphological problems is presented in the monograph by ERASO & PULINA, 1994.

5. Conclusions

The authors performing investigations in karst and in subpolar glaciers for many years state not only the presence of similar forms of relief and similar hydrologic circulation but also apply approximate geomorphological and hydrological models (LESZKIEWICZ & PULINA, 1996).

References

ERASO, A. & PULINA, M. 1994. Cuevas en hielo y ríos bajo los glaciares. McGraw-Hill, Madrid, 242p.

JANIA, J. 1991. Glacjologia. Nauka o lodowcach (Glaciology [in: Polish]). PWN, Warsaw, 360p.

LESZKIEWICZ, J. & PULINA, M., 1996. Comparison of the outflow from the glacier and karst massif based on the studies of the basin of the Werenskiold Glacier river (Spitsbergen) and the streams Ancon and Canilla (West Cuba, Pan de Guajaibon). *Spitsbergen Geographical Expedition,* Lublin, 93-112.

PULINA, M., 1984. Glaciokarst phenomena in Spitsbergen. *Norsk Geogr. Tidsskr.,* Oslo, 161–168.

PULINA, M. & REHAK, J., 1991. Glacial caves in Spitsbergen. *I[st] International Symposium of Glacier Caves and Karst in Polar Regions.* Madrid, 93-118.

Similarity between the hydrologic system of the Werenskiold Glacier (SW Spitsbergen) and a karst

by Wieslawa Ewa Krawczyk, Marian Pulina & Josef Rehák*
Department of Geomorphology, University of Silesia, ul. Bedzinska 60, 41-200 Sosnowiec, Poland
*Czech Speleological Society, Praha, Czech Republic

Abstract

An attempt was made to describe the development of the system of water circulation inside the subpolar glacier. It was done on the example of the Werenskiold Glacier, one of the best investigated glaciers in SW Spitsbergen. Based on detailed hydrochemical investigations of springs situated at the front of the glacier, performed in 1986, and conclusions drawn from it, the reconstruction of the temporal changes in glacier hydrologic system was made.

Two systems of water circulation in this type of glacier are known: summer and winter. During polar summer the system is filled up with ablation water and only when ablation is ceasing (and polar winter starts) it is possible, with simple chemical analysis based on macro-components, to distinguish water "reservoirs" inside the glacier.

Résumé: Les similarités du système hydrologique du glacier Werenskiold (en SW Spitsberg) et du karst

Le développement du système de circulation d'eau à l'intérieur d'un glacier sub-polair sur l'exemple de glacier Werenskiold est proposé. Le glacier choisi, c'est l'un parmi les mieux connus, au SW du Spitsberg. Après avoir effectué en 1986 les études hydrochimiques détaillées des sources situées sur le front du glacier, la reconstruction des changements temporaux du système hydrologique est obtenue.

A l' intérieur du glacier de ce type il existent deux systèmes de circulation d'eau: celui d'été et celui d'hiver. En été polaire le système est rempli avec de l'eau d'ablation. Lorsque l'ablation finit (et l'hiver polaire commence) il devient possible de distinguer les réservoirs de l'eau à intérieur par les analyses chimiques très simples des macro-composants.

1. Introduction

The Werenskiold Glacier is one of the best investigated glaciers in Spitsbergen. Scientific investigations have been performed in this region since late-fifties up to now (the last common expedition of Czech Speleological Society and University of Silesia, supervised by J.Rehák operated in the Werenskiold region in the summer of 1996). In the basin of the Werenskiold Glacier investigations were carried out during the whole polar hydrological year, also during polar winter (PULINA, PEREYMA, KIDA, KRAWCZYK, 1984).

The first caves in the Werenskiold Glacier were discovered in the late-fifties (BARANOWSKI, 1968). Speleological exploration of glacier shafts started in the end of the seventies (PULINA & REHÁK, 1991). One of the great achievements was reaching the depth of 130 metres in the Skilryggaven shaft. In 1986 and 1988 the Kvisla Cave and the system of Lipertaven shaft were investigated and mapped (REHÁK, OUHRABKA & BRAUN, 1990). A dozen or so caves are known in the Werenskiold Glacier at present (ERASO & PULINA, 1994). The system of englacial circulation is well recognised, by dye tracing (fluoresceine among others). Two caves, Kvisla and Angell are situated on the contact of the glacier with lateral moraines. Glacier shafts drain off supraglacial water which flows into the system of channels (reservoirs ?) in the glacier interior and emerges as springs in the snout. The location of caves, glacier shafts and springs in the Werenskiold Glacier is presented on figure 1. Exploration of caves and observations of phenomena and processes taking part in the glacier allow to conclude that this system is very similar to a karst system. Forms occurring in karst can be met also, different sinters and deposits on ice as well as tiny efflorescences.

Hydrochemical methods applied in karst can be used to study water circulation in the glaciers. Application of simple field methods of water analysis during investigations in 1986 enabled us to distinguish at least four water 'reservoirs' in the Werenskiold Glacier (KRAWCZYK, 1992). Observations and measurements performed suggested existence of two largely independent drainage systems in the glacier: summer and winter. The summer system is connected with an overflow of the englacial reservoirs. This is characterised by rapid water circulation, partly through the rock bed of the glacier, eroding it and transporting large amounts of crushed rock material. The most obvious results of this activity are springs emerging at the glacier front. The winter system is characterised by significantly smaller volumes of water, the lack of suspended material and a much higher total dissolved solids concentration. The loci of winter outflows are marked by fields of naled ice.

2. Caves in the Werenskiold Glacier

Two types of caves are known in the Werenskiold Glacier: horizontal and vertical.

Kvisla Cave System

Kvisla Cave is the system formed in the marginal part of the Skilrygg Glacier (in the northern part of the Werenskiold Glacier figure 1). This system discharges waters from non-glaciated slopes of the valley and from the surface and interior of the glacier. In the summer seasons of 1979, 1980 and 1983 the volume of water discharging from this part of the glacier was smaller than in the southern part. Kvisla river joined Glacial River near the frontal moraine. In 1985/86 some distinct changes in water circulation in this part of the glacier (probably in the upper part of the Skilrygg Glacier) took place. Kvisla river became the main river with the highest discharges in the basin (KRAWCZYK, 1994). These changes were rather short lived because in 1988 the Kvisla river discharged less water again (REHÁK, OUHRABKA & BRAUN, 1990). In 1986 the Kvisla Cave was enlarged - about 650 meters was mapped during the exploration in October 1986. But high amounts of outflowing water destroyed the cave quickly.

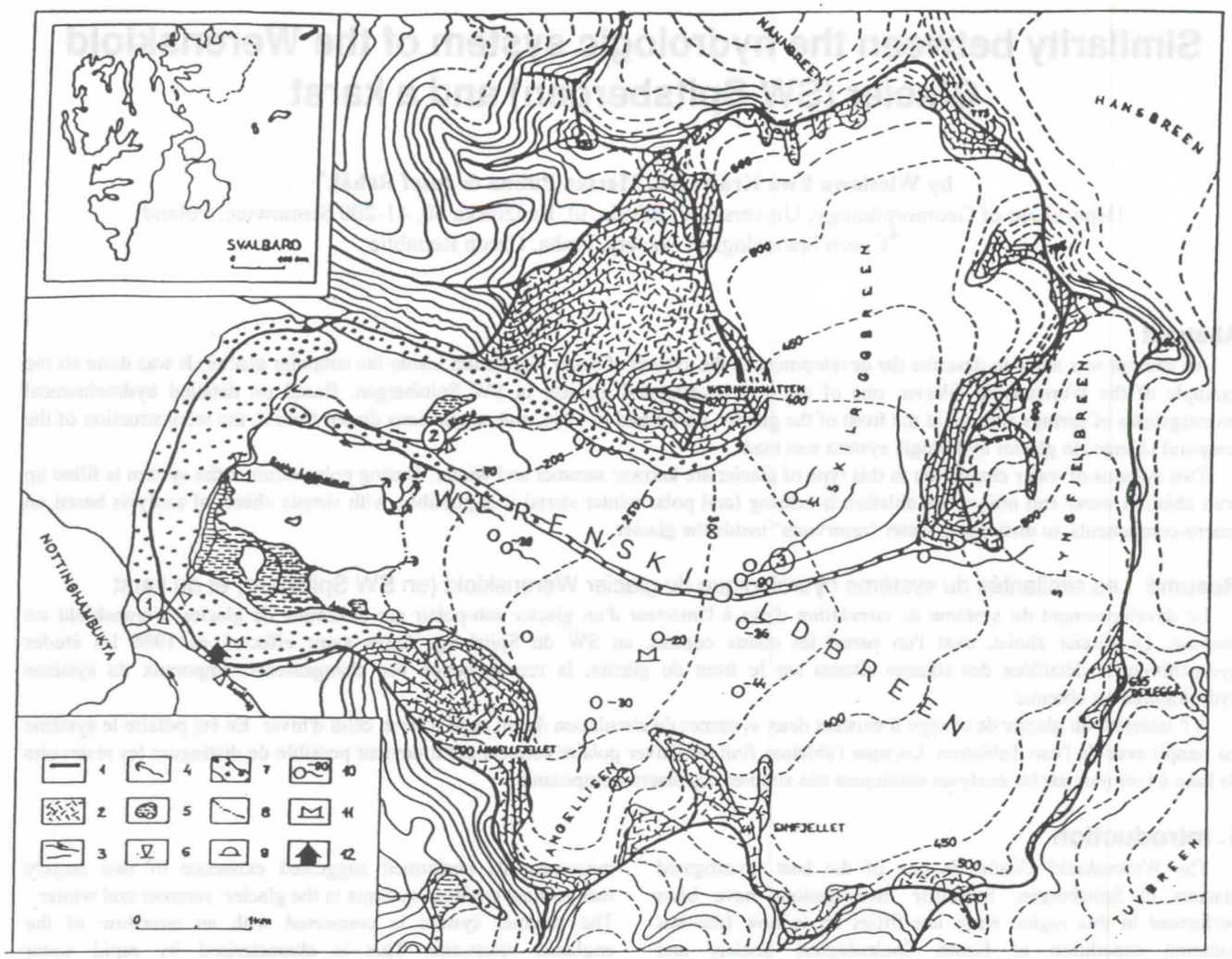

Figure 1: Basin of the Werenskiold Glacier: 1 - boundaries of the basin, 2 - slopes of mountain massifs, 3 - supraglacial and proglacial rivers, 4 - springs, 5 - water reservoirs, 6 - hydrometric profiles with limnigraph: ① Glacial River, ② Kvisla river, 7 - terminal and median moraines, 8 - range of glacier front in 1983, 9 - glacier caves, 10 - glacier shafts (number indicates depth), 11 - meteorological stations, 12 - S. Baranowski Glaciological Station of Wroclaw University

Difficulties in gaining access to the Kvisla Cave in summer caused that the chemical composition of waters issuing there was characterised by only few analyses (figure 2). During the polar summer, waters ouflowing from the Kvisla cave are so diluted by ablation waters that the ionic concentration sometimes dropped to less than 1 meq/l. After ceasing of ablation, in the second part of September, the prevailing ions were bicarbonate (HCO^{3-}) and calcium (Ca^{2+}), concentrations of agnesium (Mg^{2+}) and sulphates (SO_4^{2-}) also increased significantly. At the end of September, the sum of ions in the waters emerging from the cave exceeded 5 meq/l (figure 2). Specific electric conductivity (SpC) values of waters issuing from the Kvisla Cave in the first part of October (290 µS/cm on October 2, 1986, 380 µS/cm on October 8, 1983) increased significantly and during polar winter reached about 600 µS/cm (570 µS/cm on May 6, 1982, 620 µS/cm on May 10, 1980, 603 µS/cm on April 3, 1989).

It is interesting that samples taken from three channels inside the cave (a tributary from the Skilryggbreen side, the meander under the glacier and the Kvisla) were demonstrably of equal conductivity (290 µS/cm) during the exploration on October 2, 1986 which may indicate the existence of a common reservoir in this part of the glacier. Field observations show that during winter 1985/86 water discharged from the cave - in April 1986 near the cave outlet the vast naled ice field was formed. This field reached the height of 3 m and existed, partly melted, to the winter 1986/87. However during winter 1979/80 there was no outflow from the cave.

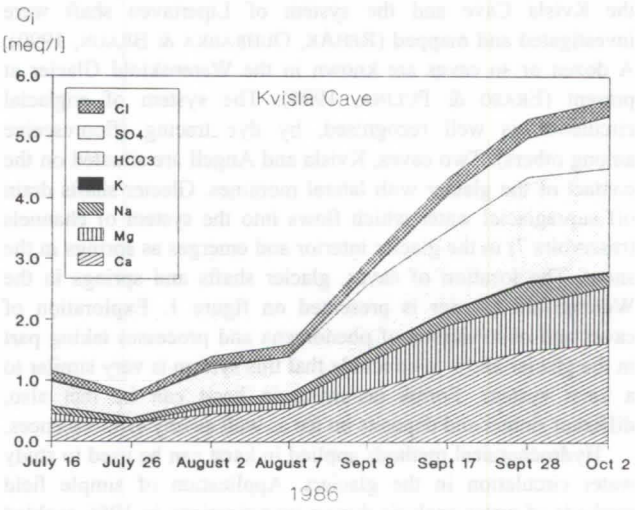

Figure 2: Changes of chemical composition (ion concentration in meq/l) of the waters outflowing from the Kvisla Cave

The system Lipertaven shaft - spring Kvisla II

At the end of glaciological expedition in 1986, in the last days of September, the outflow of water was observed in the place where during most of the summer the vast and thick naled ice fields existed. Measurements of conductivity showed that water discharging between naled ice was ablational in origin. Dye tracing carried out in the Lipertaven shaft situated on the opposite side of median moraine showed that the shaft is connected with this spring. On September 28, 1986 conductivity (SpC) of the waters of this spring was 410 µS/cm,which was higher than the outflow from the Kvisla Cave (270 µS/cm). The content of ionised silica was also relatively high, 2.5 mg/l SiO_2 compared to 1.7 mg/l SiO_2 in the Kvisla Cave (KRAWCZYK, 1992).

Important data were gathered during investigations carried out in the winter 1979/80. In the region of this spring (named Kvisla II) on April 3, 1980, three samples were taken with different values of SpC: 480, 930 and 1250 µS/cm. A nearly linear increase in concentration of calcium ions Ca^{2+}, sodium and potassium $Na^{+}+ K^{+}$, bicarbonates HCO_3^{-} and sulphates SO_4^{2-} can be noted (figure 3).

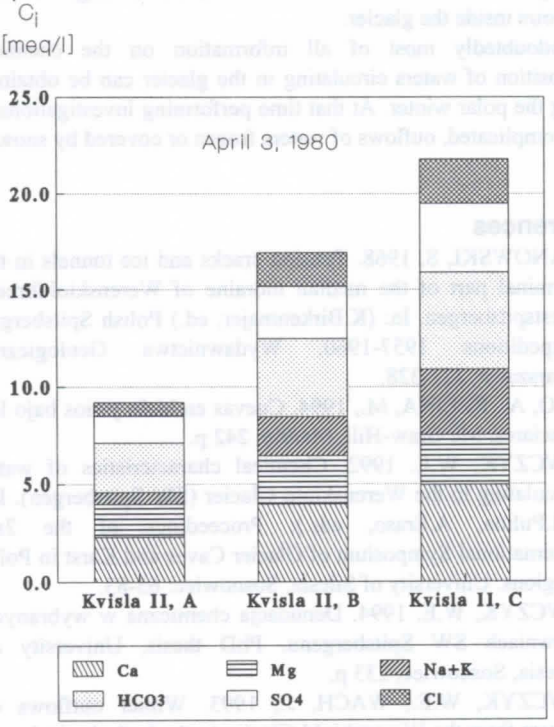

Figure 3: Chemical composition of the waters outflowing from the Kvisla II Spring on April 3, 1980.

Interpretation of this is complicated because low temperatures during sampling and transportation could cause freezing of samples. This may be the result of cryochemical processes (PULINA, 1990). Values of pH and ion concentrations in samples marked B and C (figure 3) show that sample B was in equilibrium according to calcite and in sample C carbonate precipitated from the sample as was seen on the walls of the sampling bottles.

Springs discharging the central system

Water in the central system is probably derived from the reservoir formed near to the bed of the glacier. Few outflows are connected with this system. In 1979 and 1980 the outflows in the esker zone were easy to distinguish and active both in summer and winter. They were marked as sources of the Glacial River.

The highest concentration of ions (40.9 meq/l) in the Glacial River Spring on April 9, 1980 (figure 4) is caused by cryochemical processes. The conductivity was 2100 µS/cm.

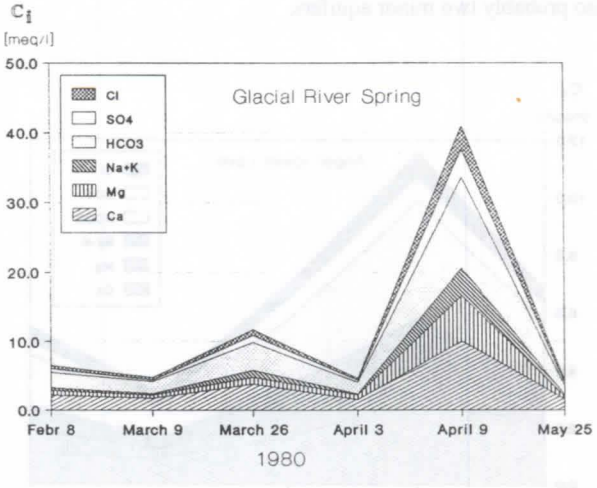

Figure 4: Changes of chemical composition (ion concentration in meq/l) of the waters outflowing from the Glacial River Spring during the polar winter in 1980.

During winter 1985/1986, vast naled ice covers were formed near the esker zone. However in the summer it was hard to distinguish any outflow because of large amounts of ablation water.

Two other springs were formed during summer 1986. Overflow of the intraglacial reservoirs resulted in an outflow of water under high pressure and creation of the 'Black' spring, so called because of the large amount of suspended material transported in its waters. The Second Black Spring became active one month later, after the highest precipitation of the summer season (28.6 mm). In summer of 1988 the Black Spring became even more spectacular - fountains of turbid water reached the height of 2 m and noisy rattle of gravel thrown up by this water was heard from long distance.

Angell Cave system

This system, situated like the Kvisla Cave on the contact of the glacier and slopes of Angellfjellet mountain was investigated in the winter 1980. Two caves were found in this region, one 100 m long. From the lower cave water issued with ion concentrations lower than in the Kvisla Cave (figure 5). The drop in ion concentration, from 11.4 meq/l to 3.20 meq/l on April 16, 1980 can be explained as the inflow of water from melting snow to the cave system. From meteorological data recorded in Polish Polar Station in Hornsund it is known that on April 16 and 17, 1980 air temperature was above 0°C and rain occurred.

In 1983 the upper cave did not exist, the lower one converted into a fissure. In winter 1985/1986 waters discharged from the small depression between the glacier and lateral moraine below Angellfjellet. These waters fed Angell stream which flowed into the Mewie (Sea gull) Lake. The field of naled ice started to form here in December 1985 and increased during next months. Values of electric specific conductivity were in the range 180 - 300 µS/cm (KRAWCZYK & WACH, 1993). This is the result of the geological foundation of this part of the Werenskiold valley (predominance of silicate rocks). The remnants of naled ice were observed in July 1986 but no spring was observed in this region.

Summer and winter systems of drainage

Detailed hydrochemical investigations performed in the summer of 1986 showed that at least two water reservoirs were active inside the Werenskiold Glacier in the summer. There were also probably two minor aquifers.

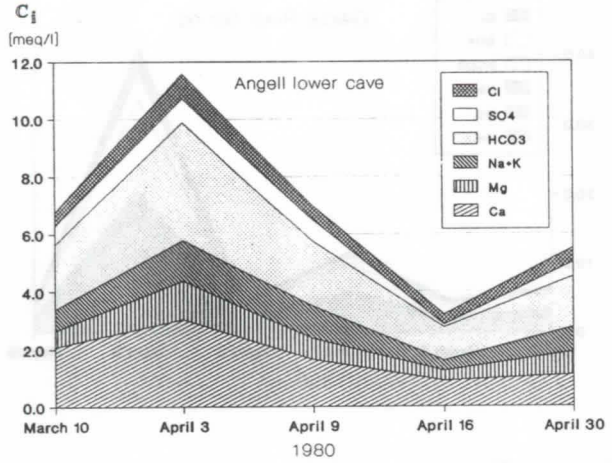

Figure 5: Changes of chemical composition of the waters outflowing from the Angell Cave during polar winter in 1980.

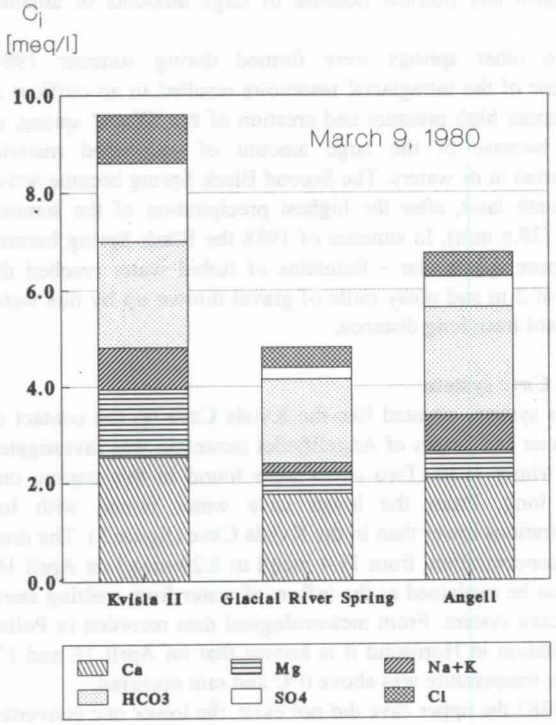

Figure 6: Chemical composition of different springs at the front of the Werenskiold Glacier on March 9, 1980.

Analysing data collected during polar winter seasons one may conclude that three or four water reservoirs exist in the glacier. They are similar to those in summer: central with outflow in Glacial River Spring, Angell connected with Angell Cave system and Kvisla II (figure 6). The system connected with the Kvisla Cave is probably not active every winter.

3. Conclusions

The cave system in the Werenskiold Glacier is well developed. It is formed by the central systems in which water circulation takes even few years and by marginal systems. The system is dynamic, changes occur even from year to year. Dynamics is enhanced by recession of the glacier.

Cave systems in glaciers are difficult to explore. Entrance to the cave is possible only after cessation of ablation, in the very short period from the second part of September to November. Low temperatures and short day make speleological activity complicated.

During polar summer the whole system of caves and fissures in the glacier is filled with ablation water and it is difficult to observe chemical differentiation in waters originating from the glacier. Not before cessation of ablation it is possible, with simple chemical methods similar to that used in karst investigations, to differentiate these waters and distinguish water reservoirs inside the glacier.

Undoubtedly most of all information on the chemical composition of waters circulating in the glacier can be obtained during the polar winter. At that time performing investigations is very complicated, ouflows of waters frozen or covered by snow.

References

BARANOWSKI, S. 1968. Tension cracks and ice tunnels in the terminal part of the median moraine of Werenskioldbreen, Vestspitsbergen. In: (K.Birkenmajer, ed.) Polish Spitsbergen Expeditions 1957-1960. Wydawnictwa Geologiczne, Warszawa: 321-328.

ERASO, A., PULINA, M., 1994. Cuevas en hielo y rios bajo los glaciares. Mc Graw-Hill, Madrid, 242 p.

KRAWCZYK, W.E. 1992. Chemical characteristics of water circulating in the Werenskiold Glacier (SW Spitsbergen). In: (M.Pulina, A.Eraso, eds.): Proceedings of the 2nd International Symposium of Glacier Caves and Karst in Polar Regions. University of Silesia, Sosnowiec: 65-83.

KRAWCZYK, W.E. 1994. Denudacja chemiczna w wybranych zlewniach SW Spitsbergenu. PhD thesis, University of Silesia, Sosnowiec, 233 p.

KRAWCZYK, W.E., WACH, J., 1993. Winter outflows of waters from the Werenskiold Glacier in the hydrological year 1985/1986. XX Polar Symposium, Lublin: 403-412.

PULINA, M., PEREYMA, J., KIDA, J., KRAWCZYK, W.E. 1984. Characteristics of the polar hydrological year 1979/1980 in the basin of the Werenskiold Glacier, SW Spitsbergen. *Polish Polar Research*, 5, 3-4: 165-182.

PULINA, M. 1990. Geomorphological effects of the cryochemical process. *Quaestiones Geographicae*, 13/14: 99-112.

PULINA, M., REHAK, J. 1991. Glacial caves in Spitsbergen. In: (A.Eraso, ed.): Proceedings of the 1st International Symposium of Glacier Caves and Karst in Polar Regions, Madrid: 93-117.

REHAK, J., OUHRABKA, V., BRAUN J., New information about the interior drainage of subpolar glaciers and the structure of medial moraines of the Southwest Spitsbergen. *Studia carsologica*, 1: 15-56.

Inlandsis 1994:
Glacial Speleology into the Greenland Icesheet

by Marc Tremblay and Diana Gietl
11700 Avenue Royale, Beaupré, Québec G0A 1E0, email: jean.gosselin@crchul.ulaval.ca

The Greenland ice-sheet (inlandsis) margins are subject to a meltwater process making subglacial drainage tunnels. The exploration of those ice-caves is generally hazardous at the resurgence level but possible at the inlets, usually vertical shafts that require combining singe rope techniques with ice-climbing skills. This enables modern scientists a new approach to peer directly ino the glacier instead of staring at ice-cores. During September 1994, a team of 13 spent 2 ½ weeks on the inlandsis exploring ice-caves at about 50 km east of Kangerlussuaq, 25 km into the ablation zone. The site is located just north of the arctic circle on the west coast. Initiated by Janot Lamberton of France in 1989, Lamberton organises logistics and searches for sponsors full-time for annual expeditions.

In a karst-like fashion, the surface meltwater enters fractures which enlarge into immense shafts. These shafts were called "moulins" or watermills because of the groaning noise of water cascading down. There is a critical time period for visiting the moulins, too early in the season, the volume of 0°C water prohibits entry or too late, snowfalls cover the entrances. Studies of the inlandsis attract scientists like glaciologists researching mechanics and hydrogeology of the immense glacier or biologists looking for the tiny organisms trapped in the ice. The expedition explored and mapped eight moulins which averaged between 20 and 20 meters deep with the exception of Paaqitsoq, which was bottomed to a deep lake at 80 meters of depth. The same moulin was explored down to 175 m the previous year, still the deepest explored in ice.

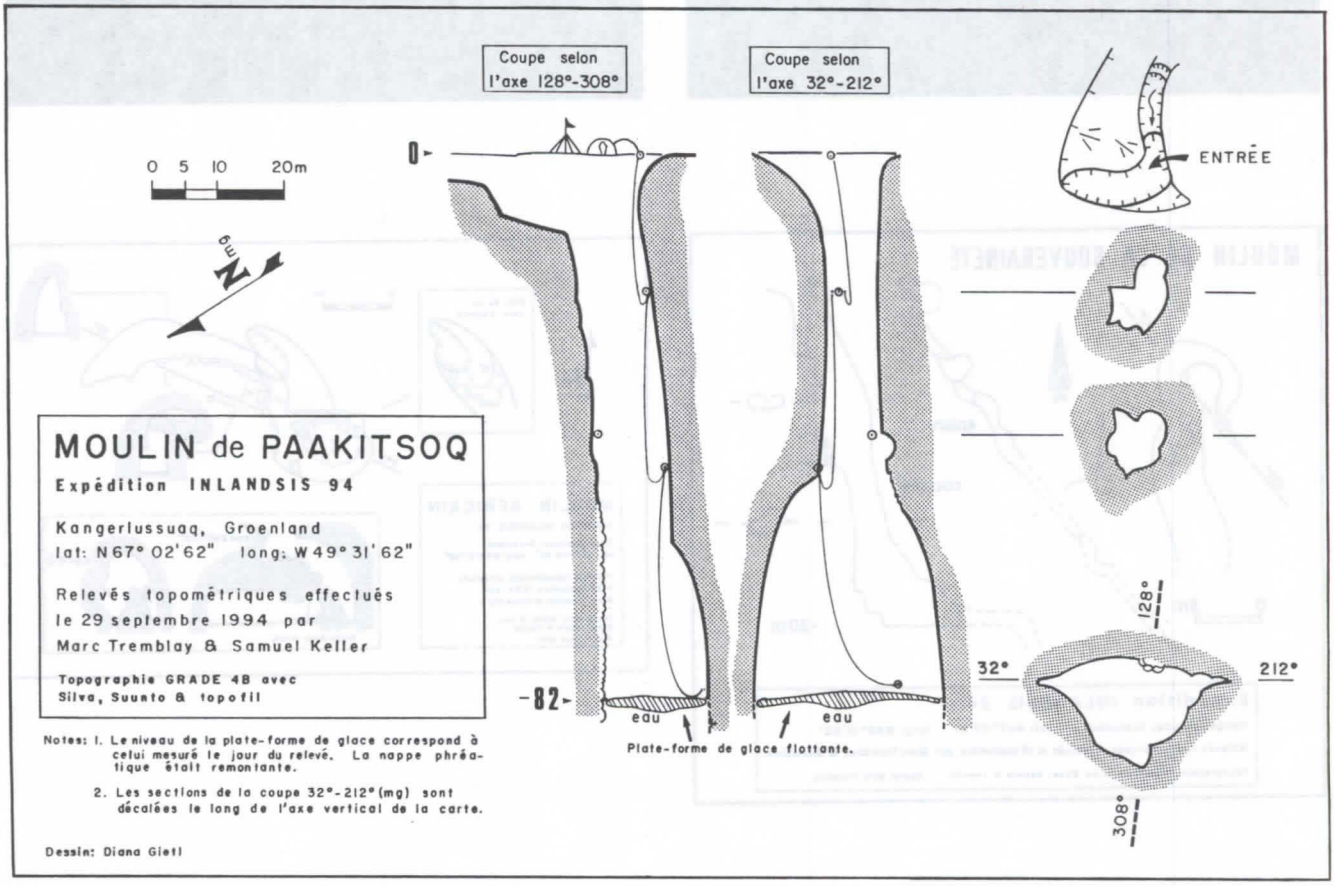

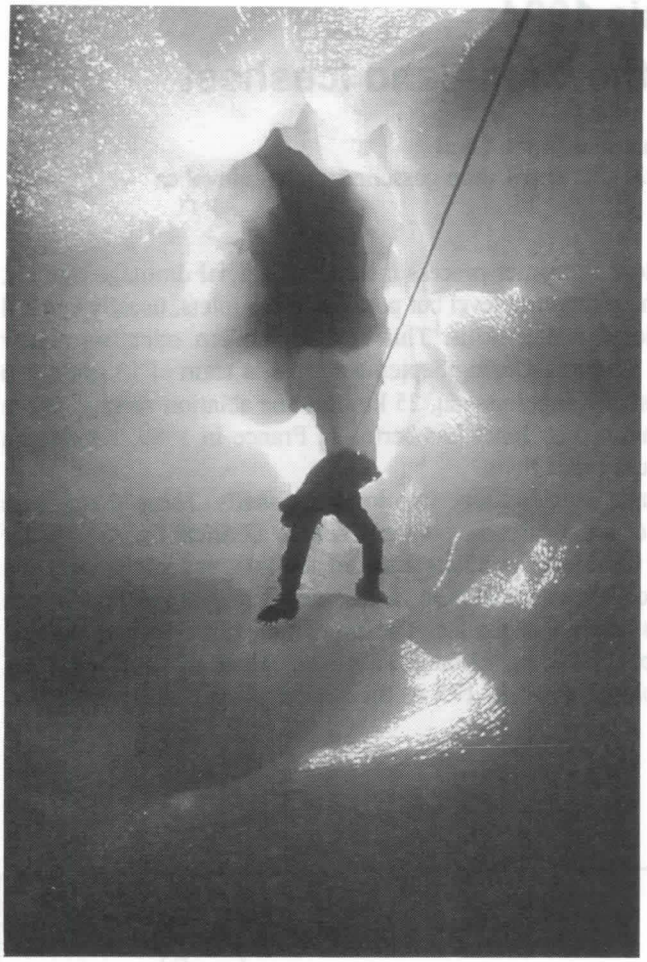

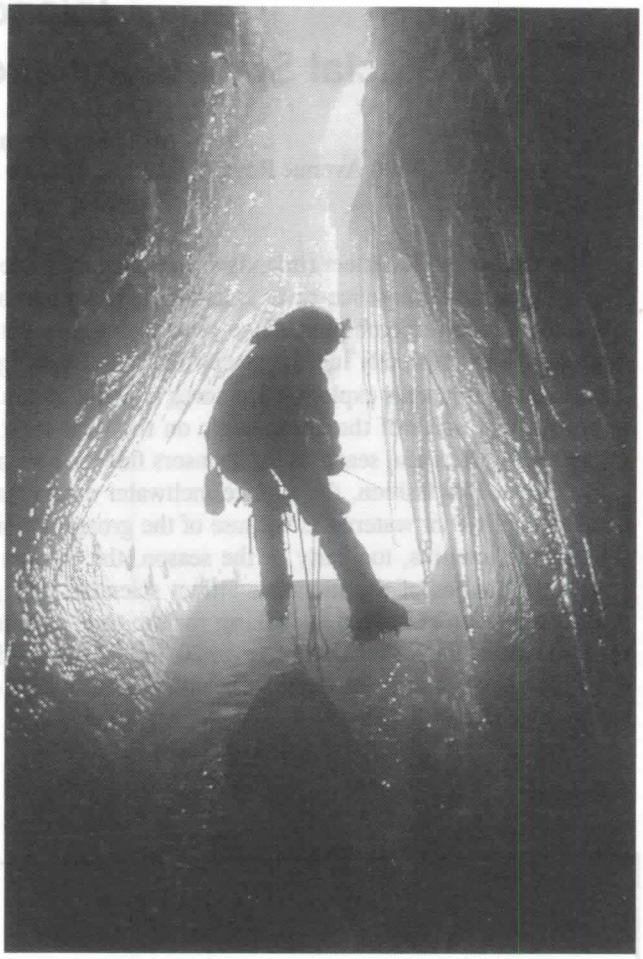

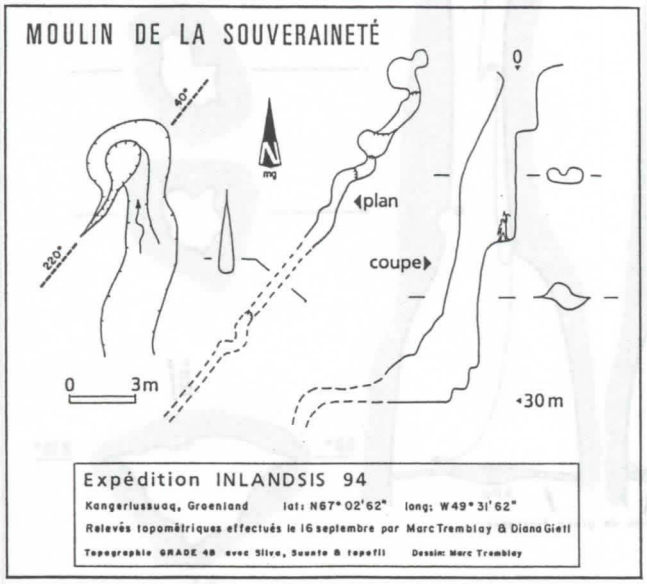
MOULIN DE LA SOUVERAINETÉ
0
40°
220°
mg
plan
coupe
0 3m
-30 m
Expédition INLANDSIS 94
Kangerlussuaq, Groenland lat: N67° 02'62" long: W49° 31'62"
Relevés topométriques effectués le 16 septembre par Marc Tremblay & Diana Gietl
Topographie GRADE 4B avec Silva, Suunto & topofil Dessin: Marc Tremblay

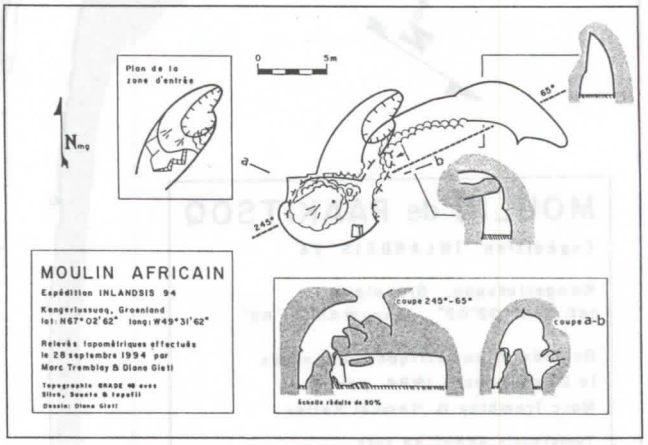
Plan de la zone d'entrée
0 5m
mg
a
b
65°
245°
MOULIN AFRICAIN
Expédition INLANDSIS 94
Kangerlussuaq, Groenland
lat: N67° 02' 62" long: W49° 31' 62"
Relevés topométriques effectués le 28 septembre 1994 par Marc Tremblay & Diana Gietl
Topographie GRADE 4B avec Silva, Suunto & topofil
Dessin: Diana Gietl
coupe 245°-65°
coupe a-b
Échelle réduite de 50%

Authors' Index

AAEMM III 191
Abbate R. II 205
Abdul-Nour Hani III 35
Abul-Hab Jalil III 369
Adank Markus IV 65
Adbesselam Malek II 247
Aigoun C. II 247
Aimé Gérard III 5
Allison Cara I 16
Ancel Bruno III 195
Ancel Bruno III 245
Ancel Bruno III 249
Andreev Sergiu P. III 321
Andreo B. II 251
Arcenegui Rocio I 183
Argant Alain III 105
Argant Alain III 160
Arlt Thilo III 203
Arlt Thilo III 253
Arlt Thilo III 257
Armand Dominique III 109
Arrigo Cyril IV 13
Astruc J.-G. I 424
Atteia Olivier II 125
Atteia Olivier II 141
Audra Philippe I 165
Audra Philippe I 337
Audra Philippe I 429
Auler A. II 271
Ayub Soraya IV 45
Ayub Soraya V 35
Badescu Adrian I 25
Badino Giovanni I 483
Bakalowicz Michel II 23
Bakalowicz Michel II 55
Balbi A. I 69
Balderer Werner II 275
Banton O. II 283
Barczewski M. II 55
Barredo Silvia P. I 69
Barsanti Cecilia M. III 217
Bartholeyns Jean-Pierre V 103
Bärtschi Hans-Peter III 233
Bayle Christian II 1
Becker José Henrique V 35
Bedos Anne IV 47
Bella P. I 85
Benderev Alexey II 255
Bengeanu Monica I 235
Benischke Ralf I 425
Bernasconi Reno III 333
Bernasconi Reno III 337
Berstad Ida Malene I 53
Bini Alfredo I 345
Bitinskaya L. N. V 31
Bitterli Thomas IV 5
Bitterli Thomas I 349
Bixio Roberto III 269
Bland J. I 111
Blinov S. M. II 319
Blondel C. I 424
Bock Matthias III 199
Bodin Jacques II 259
Boehm Peter III 203
Bohly Bernard III 221
Bolanz Jean-Jacques IV 75
Bolliger Thomas III 141
Bonacci Ognjen II 27
Borowsky Richard III 359
Borsato Andrea I 247
Borsato Andrea I 77
Borsato Andrea II 57
Boutin Claude III 350
Boyd Clifford C. III 37
Brandt Cyrille IV 71
Brouquisse François II 299
Brouquisse François II 61
Brouquisse François IV 47
Buchas Holger I 453
Bulichov Anatoly V 89
Bundschuh Jochen II 129
Burri Ezio II 201
Buzjak Nenad III 301
Calvet Jean-Paul III 261
Cañaveras J. C. II 103
Capellini Dante Terence III 145
Cappa Emanuele III 9
Cappa Emanuele IV 79
Cappa Giulio III 9
Cappa Giulio IV 79
Carlson Kent R. III 347
Carrasco F. II 251
Casati Luigi IV 67
Cassou Jean-Pierre V 53
Castellani Vittorio III 265
Castellani Vittorio III 269
Cech Brigitte III 209
Chabert Jacques IV 83
Chabert Jacques V 111
Changyun Zhang IV 55
Chauve Pierre II 247
Chazine Jean-Michel III 101
Choppy Jacques I 3
Choppy Jacques I 367
Choppy Jacques I 401
Choppy Jacques IV 83
Christe Romain II 221
Cigna Arrigo A. I 203
Cimino Antonio II 205
Cinq-Mars J. II 287
Clarck I. D. II 287
Clemens Torsten I 301
Clemens Torsten II 107
Clemens Torsten II 65
Clemens Torsten I 307
Closson Damien V 13
Closson Damien I 322
Clottes Jean III 103
Clottes Jean III 4
Coca Spencer IV 87
Codrea Vlad III 179
Coineau N. III 350
Collet Guy-Christian III 83
Collignon Bernard II 263
Collignon Bernard IV 57
Cordonnier M. II 69
Cortel Adriano I 183
Cortel Adriano I 179
Coste Thierry V 85
Cours Serge III 79
Cox Nicholas J. I 285
Craven Stephen Adrian V 15
Crochet Jean-Yves I 424
Cruz C. M. II 95
Cruz de la A. V. II 95
Dalmeri Gianpaolo I 77
Damyanov Y. I 111
Damyanov Y. I 105
Damyanov Y. I 107
Damyanov Y. I 110
Damyanova A. I 110
Damyanova A. I 111
Damyanova A. I 105
Damyanova A. I 107
Daoxian Yuan I 300
Daoxian Yuan II 123
Day Michael J. I 133
Day Michael J. I 215
de Bonis L. I 424
De Broyer C. V 103
De Paola Marco I 202
Décréau Frédéric III 91
Deflandre G. I 93
Deharveng Louis IV 47
Delaby Serge IV 111
Delaby Serge IV 115
Delannoy Jean-Jacques I 61
Delannoy Jean-Jacques II 69
Delannoy Jean-Jacques I 257
Dematteis Antonio II 291
Denneborg Michael I 341
Denys Christiane I 424
Denys Christiane III 165
Denys Christiane III 178
Destombes Jean-Luc I 257
Destombes Jean-Luc II 69
Destombes Jean-Luc I 61
Dimuccio Luca Antonio I 202

Dimuccio Luca Antonio I 400
Djurovic Predrag I 421
Dodelin Christian V 73
Doerfliger Nathalie II 133
Doerfliger Nathalie II 209
Doerfliger Nathalie II 47
Dogwiler Toby I 178
Dominguez Carmen I 485
Dragan-Bularda Mihail III 285
Dragoni Walter III 265
Draily Christelle III 61
Dreybrodt Wolfgang II 75
Dreybrodt Wolfgang II 81
Drouin Philippe IV 119
Drouin Philippe III 113
Drysdale R. N. I 73
Du Fayet de la Tour Alain III 79
Dublyansky Yuri V. II 267
Dublyansky Yuri V. I 271
Dubois Paul I 3
Ducimetière Pascal IV 13
Duday Henri III 79
Duffaud S. I 424
Dumont Laurent IV 13
Ehret Michel III 221
Einevoll Sølvi I 53
Eisenlohr Laurent II 81
Eiswirth Matthias II 213
Ek Camille I 297
Ek Camille I 322
Ek Camille V 13
Emblanch Christophe II 17
Emblanch Christophe II 5
Engel Scott I 21
Epis Lorenzo V 29
Eraso Adolfo Romero I 483
Eraso Adolfo Romero I 485
Espinasa Luis III 359
Eszterhás István I 469
Faeh A. II 9
Fage Luc-Henry III 101
Faillat Jean-Pierre II 111
Faillat Jean-Pierre II 85
Fairchild Ian J. I 247
Fang Jinfu I 395
Farina Daniele I 143
Favre Gérald IV 13
Felici Alberta IV 79
Felici Alberto III 9
Felisiak Ireneusz I 17
Ferguson Lynn M. III 315
Fernandez-Jalvo Yolanda III 165
Fiedler Suzana III 301
Filippov Andrey G. I 465
Fischer M. J. I 73
Fluck Pierre III 187
Foltete Jacques I 169
Font Estramar, Ass. Rech. IV 71
Ford Derek C. I 44
Ford Derek C. I 88
Ford Derek C. II 120
Ford Derek C. II 195
Ford Derek C. I 105
Ford Derek C. I 107
Ford Derek C. I 111
Ford Derek C. I 146
Ford Derek C. I 261
Ford Derek C. I 262
Forgeot Olivier I 9
Fornos Joan J. I 37
Forti Paolo I 187
Forti Paolo I 226
Fosse Philippe III 149
Fratila Gheorghe III 179
Fratila Gheorghe I 231
Frisia Silvia I 247
Frisia Silvia I 77
Frumkin Amos I 139
Fuchs Gerald I 425
Funcken Luc III 205
Funcken Luc IV 7
Funcken Luc IV 9
Furquim Scaleante Oscarlina A. I 363
Gaál Lúdovít I 464
Gabrovsek Franci IV 23
Gadat J.-Y. II 69
Gaiffe M. I 297
Galdenzi Sandro I 187
Gale S. J. I 73
Galik Alfred III 65
Gallerini Giuliano I 143
Garasic Mladen IV 123
Garasic Mladen IV 125
Garasic Mladen I 147
Garcia A. E. II 95
Garcia Michel III 79
Gaspar E. I 41
Gaspar Radu D. II 175
Gaspar Radu D. II 217
Genereux D. II 199
Genty Dominique I 61
Genty Dominique I 257
Georgiev L. N. I 105
Georgiev L. N. I 107
Ghergari Lucretia I 231
Ghergari Lucretia I 227
Giannandrea Paolo I 202
Gietl Diana I 497
Gillieson David I 327
Ginés Angel I 37
Ginés Joaquin I 37
Glazek Jerzy I 85
Glazek Jerzy I 405
Glazek Jerzy I 45
Glowacki Piotr I 366
Gobrunova K. A. II 319
Goggin Keith E. I 381
Gogniat Stéphane II 229
Goldie Helen S. I 285
Goodbar James V 3
Grady Frederick III 175
Gradzinski Michal I 275
Gradzinski Michal I 81
Gradzinski Michal I 85
Gradzinski Michal IV 91
Grandgirard Vincent I 331
Grasso Alessandro D. II 91
Guadelli Jean-Luc III 117
Guardiario J. D. A. II 199
Guglielmi Yves II 137
Guyot Jean Loup IV 51
Guyot Jean-Loup II 271
Guzvica Goran III 121
Habermann Dirk I 251
Halliday William R. I 437
Halliday William R. I 199
Halliday William R. I 461
Hanneberg Armin III 203
Hanneberg Armin III 253
Hanneberg Armin III 257
Hapka Roman III 3
Hapka Roman III 57
Harlacher Christof I 307
Hartenberger J.-L. I 424
Hartmann A. II 239
Hartmann Jens I 100
Hartmann Jens I 453
Hassan H. A. III 371
Hauns Michael II 141
Häuselmann Philipp II 31
Häuselmann Philipp IV 1
Havlicek David I 481
Heaton Tim I 77
Heijnis H. I 73
Heller Martin V 127
Hercman Helena I 45
Hercman Helena I 85
Hercman Helena I 87
Hermann Felix II 141
Herold Thilo II 275
Hill Carol A. I 226
Hill Carol A. I 390
Hobbs III H. H. III 345
Hobléa Fabien II 35
Hobléa Fabien I 429
Hof Alex I 137
Hofenpradli Angelica I 235
Hoffmann Guido V 65
Holland Ernst V 39
Holler Cato Jr. III 305
Holmgren K. I 55
Holsinger John R. III 347
Horat Peter II 9
Hoti Makir IV 129
Hötzl Heinz II 187
Hötzl Heinz II 213
Hötzl Heinz II 303
Hoyos M. II 103
Huang Yiming I 77
Hubbard David III 37

Hubbard David III 175
Hubbard David A. Jr. III 311
Hückinghaus Dirk II 107
Hückinghaus Dirk II 145
Hückinghaus Dirk II 65
Huff Warren I 25
Huggenberger Peter II 221
Huntoon Peter W. I 311
Imper David III 229
Isayevitch A. G. V 31
Jaillet Stéphane I 171
Jalov Alexey IV 25
Jambresic Gordana III 157
Jan Vit I 45
Jeanbourquin Pascal II 13
Jeannin Pierre-Yves I 195
Jeannin Pierre-Yves II 149
Jeannin Pierre-Yves II 91
Jeannin Pierre-Yves IV 1
Jeannin Pierre-Yves I 293
Jeannin Pierre-Yves I 349
Jifang Shen IV 55
Johnson Jerald III 41
Jonnsson Sigurdur S. I 485
Jordan P. II 275
Jordi Martin V 77
Jull Timothy A. J. I 65
Junwei Wan IV 55
Kadlec Jaroslav I 13
Kadlec Jaroslav I 387
Kalmbach Uwe IV 29
Karlén W. I 55
Kashima Naruhiko III 281
Käß Werner II 187
Käß Werner II 55
Kawashti I. S. III 371
Kejonen Aimo III 53
Kejonen Aimo IV 93
Kempe Stephan I 100
Kempe Stephan I 453
Kempe Stephan III 13
Kempe Stephan I 445
Kempe Stephan I 449
Keppens E. I 93
Ketz-Kempe Christhild III 13
Kicinska Ditta I 168
Kienle J. II 163
Kiss Stefan III 285
Klimchouk Alexander I 157
Klimchouk Alexander I 161
Klimchouk Alexander I 306
Knez Martin II 279
Knez Martin I 156
Korshunov Viktor A. I 29
Korzhyk Vitali V 7
Kósa Attila V 129
Kosel Vladimir III 310
Kostov Konstantin I 409
Kovacevic Tihomir IV 125
Krasnoshtein Arkady E. V 31
Krawczyk Wieslawa Ewa I 493
Krekeler Mark P. S. I 21
Krklec Nevenka III 157
Krouse Roy H. P. I 105
Krouse Roy H. P. I 107
Krouse Roy H. P. I 65
Krutaj Farudin IV 129
Kusch Heinrich III 17
Labau V. I 41
Laiconas Erikas III 169
Lami H. II 247
Larocque Marie II 283
Lascu Cristian I 25
Lastennet Roland II 17
Lastennet Roland II 5
Laudet Frédéric I 424
Laudet Frédéric III 165
Laudet Frédéric III 178
Laureti Lamberto III 236
Lauriol Bernard II 287
Lauritzen Stein-Erik I 178
Lauritzen Stein-Erik I 45
Lauritzen Stein-Erik I 55
Lauritzen Stein-Erik I 57
Lauritzen Stein-Erik I 85
Lauritzen Stein-Erik II 320
Lauritzen Stein-Erik I 49
Lauritzen Stein-Erik I 53
Le Bec G. II 111
Le Pennec Robert II 39
Lee-Thorp J. I 55
Leel-Ossy Szabolcs I 116
Legendre S. I 424
Lesinsky Gabriel III 325
Leszkiewicz Jan I 489
Lewandowski Klaus III 213
Lhenaff R. I 297
Li Juzhang I 395
Liedl Rudolf II 107
Liedl Rudolf II 145
Liedl Rudolf II 153
Liedl Rudolf II 65
Liedl Rudolf I 195
Liessmann Wilfried III 237
Lignereux Yves III 71
Lin Junshu I 395
Linge Henriette I 49
Lips Bernard IV 41
Liu Zaihua I 300
Liyanyun X. C. C. II 21
Ljubojevic Vladimir I 421
Lochner Bernd III 241
Loiseleur Bernard I 355
Loiseleur Bernard I 441
Longinelli Antonio I 247
Looser Michel II 291
López-Chicano M. II 43
Lowe David J. I 436
Lozan Mina N. III 321
Lundberg Joyce I 178
Lundberg Joyce I 101
Macaluso M. II 205
MacDonald William D. I 105
MacDonald William D. I 107
MacDonald William D. I 60
Madry B. II 81
Magniez Guy J. III 341
Maire Richard I 359
Maltsev Vladimir A. I 29
Maltsev Vladimir A. I 219
Maltsev Vladimir A. I 267
Mangan C. II 137
Mangin Alain II 283
Mania Jacky II 247
Manolache Elena III 285
Marandat B. I 424
Maréchal Jean-Christophe II 149
Maréchal Jean-Christophe II 291
Marinova E. I 107
Martin Philippe I 129
Martín Rosales W. II 43
Martinek Klaus-Peter III 253
Martinek Klaus-Peter III 257
Martini Jacques E.J. I 223
Martini Sergio III 217
Martini Sergio I 315
Masotti Daniel V 21
Masotti Daniel V 25
Masotti Daniel V 9
Massoli-Novelli R. II 201
Matthews Peter V 72
Matthews Peter V 72
Matthews Peter V 72
Maucha Laszlo II 157
Maucha Laszlo II 321
Mauduit Eric III 261
Mavlyudov Bulat R. I 191
Maximovich N. G. II 319
McDermott Frank I 77
Mecchia Marco I 483
Medville Douglas M. I 381
Medville Douglas M. I 457
Medville Hazel E. I 457
Meier Edi II 221
Melloul Abraham J. II 225
Melo Filho Leonildes IV 51
Melo-Filho Leonildes II 271
Menichetti Marco I 187
Menne Benjamin II 119
Menne Benjamin IV 33
Menne Benjamin III 289
Messouli M. III 350
Meus Philippe II 55
Michel G. V 103
Michel J. V 81
Michel Raymond V 13
Michie Neville V 43
Middleton Gregory I 437
Mihevc Andrej I 57
Mijatovic Borivoje F. II 295

Miserez Jean-Jacques II 229
Mixon David I 21
Mohrlok Ulf II 163
Mohrlok Ulf II 167
Moldovan Oana III 319
Montandon Paul-Etienne II 229
Montero Garcia Ismael Arturo III 20
Montero Garcia Ismael Arturo V 80
Morel Laurent V 99
Morel Philippe III 3
Morel Philippe III 137
Morin Denis III 225
Motyka Jacek II 171
Motyka Jacek II 235
Mouret Claude II 299
Mouret Claude IV 57
Mouret Claude III 363
Mousny Vincent V 13
Mudry Jacques II 137
Mudry Jacques II 17
Mudry Jacques II 247
Mudry Jacques II 251
Mudry Jacques II 5
Mueller Robert J. I 215
Muglova Penka III 95
Muglova Penka I 207
Mulaomerovic Jasminko III 87
Müller Claudia I 301
Müller Elisabeth II 239
Müller Imre II 221
Müller Imre II 243
Muñoz Alfonso I 179
Munson Cheryl Ann III 45
Munson Patrick J. III 45
Mylroie John E. I 178
Naef F. II 9
Niggemann Stefan I 251
Niggemann Stefan I 151
Nini Roberto III 273
Oberwinder Matthias I 453
Oberwinder Matthias I 449
Oelze Rainer I 251
Onac Bogdan Petroniu I 235
Onac Bogdan Petroniu I 227
Onac Bogdan Petroniu I 231
Orecchio S. II 205
Otonicar Bojan I 417
Otz Martin II 31
Paar Werner III 209
Pacher Martina III 65
Pajón Morejon Jesús M. I 97
Pajón-morejón Jesús M. II 95
Pandurska Rumiana III 367
Partridge T. C. I 55
Pascu Maria II 175
Pashenko Serguei E. I 271
Patrick Rosenthal III 225
Paunica I. II 217
Paunica T. I 41
Pavuza Rudolf I 7
Pechhold Eberhard I 211
Pedde Sara III 67
Perego Renata III 124
Perego Renata III 136
Perna Giuliano I 397
Perret Catherine IV 65
Perret Jean François IV 51
Perrette Yves I 257
Perrette Yves I 61
Perrin Jérôme II 99
Perrin Jérôme IV 19
Petitta Marco II 201
Petrochilou Anna III 64
Philippe Michel III 113
Philippe Michel III 125
Philippe Michel III 136
Philippe Michel III 161
Pinto Ana Cristina III 171
Plagnes Valérie II 179
Plesa Corneliu III 329
Porter Megan L. III 345
Postawa A. II 235
Preiswerk Christian IV 37
Prokhorenko Vitaliy V 93
Prokhorenko Vitaliy V 95
Proudlove Graham S. III 351
Proudlove Graham S. III 355
Puech Vincent I 293
Puig J. M. II 5
Pulido-Bosch Antonio II 43
Pulina Marian I 323
Pulina Marian I 366
Pulina Marian I 489
Pulina Marian I 493
Quinif Yves I 93
Quinif Yves I 257
Quinif Yves I 61
Radanovic-Guzvica Biserka III 121
Rage J.-C. I 424
Ragsdale Michael I 21
Rathgeber Thomas III 153
Ravazzi Cesare III 124
Razack M. II 259
Razack M. II 283
Ré G. I 69
Redonte Gabriel Jorge IV 99
Rehák Josef I 493
Reichert Barbara II 303
Reiner Gerhard III 181
Reisinger Christian III 129
Reisner Victor IV 103
Remy J.-A. I 424
Renner Sven II 153
Reynard Emmanuel V 17
Reynaud A. II 137
Richter Detlev K. I 251
Rigal Didier IV 47
Rogers Bruce W. III 45
Rognon P. II 229
Rosendahl Wilfried III 25
Rospondek Mariusz I 81
Rossi Carlos I 179
Rossi Carlos I 183
Rousset Claude II 307
Rouvinez Fabienne III 57
Rouzaud François III 261
Rouzaud François III 49
Rouzaud François III 71
Rouzaud François III 79
Rouzaud François III 97
Rouzaud François III 91
Rouzaud Jean-Noël III 91
Rowling Jill I 263
Rozkowski Jacek I 323
Rubbioli Ezio IV 51
Ruggieri Rosario IV 61
Ruggieri Rosario I 125
Saiers J. E. II 199
Salvatori Francesco V 107
Salvatori Francesco V 115
Salvatori Francesco V 117
Sanchez-Moral S. II 103
Sanz-Rubio E. II 103
Sarbu Serban I 25
Sasowsky Ira I 25
Sauter Martin II 107
Sauter Martin II 145
Sauter Martin II 153
Sauter Martin II 167
Sauter Martin II 65
Sauter Martin I 195
Sauter Martin I 301
Sauter Martin I 307
Sauter Martin I 318
Sbai Abdelkader I 297
Sbai Abdelkader II 311
Schäferjohann Volker I 473
Scherrer Nadim C. I 73
Scherrer S. II 9
Schifferdecker François III 137
Schmid G. II 55
Schnegg Pierre-André II 47
Schöne Tilo III 277
Schwarcz Henry P. I 88
Schwarcz Henry P. II 120
Schwarcz Henry P. I 262
Scott Jane I 436
Sebela Stanka I 113
Seiler Klaus-P. II 239
Semikolennykh Andrei A. I 29
Semikolennykh Andrey A. V 87
Semikolennykh Andrey A. III 293
Shanov Stefan II 255
Shanov Stefan III 367
Shaw D. Patrick III 347
Shaw P. A. I 55
Shelepin Aleksey IV 103
Shen Jifang II 21
Shopov Yavor Y. I 105
Shopov Yavor Y. I 107

Shopov Yavor Y. I 110
Shopov Yavor Y. I 111
Shopov Yavor Y. I 65
Shopov Yavor Y. I 103
Shrivastava V. K. III 31
Siebenlist-Kerner V. III 203
Siemens H. II 75
Sigé B. I 424
Simões Washington III 83
Simon-Coinçon R. I 424
Singh Ramesh B. I 369
Slabe Tadej I 377
Smart Chris C. II 183
Smart Chris C. II 315
Smart Chris C. II 51
Smart Peter L. I 16
Smyk Boleslaw I 275
Soler V. II 103
Somelette Luc II 111
Song Linhua I 279
Song Linhua I 319
Song Linhua I 433
Souillac, Spéléo-Club de III 161
Soulier Michel III 71
Spahlinger Wolf IV 29
Spicher Michel I 331
Spiro Baruch I 77
Stibrányi Gustáv V 119
Stichler W. II 303
Stiefelhagen Willy II 221
Stoev Alexey I 207
Stoev Alexey III 95
Stoev Dimitar I 207
Stoeva Mina III 95
Strassenburg Jan I 453
Striebel Thomas I 473
Stroutchkova Tatiana III 78
Stuart-Williams Hilary I 88
Sudre J. I 424
Summers Engel Annette I 21
Summers Engel Annette I 25
Sustersic France I 117
Swinburne Nicola I 88
Szulc Joachim I 275
Szulc Joachim I 81
Tacchini Pascal IV 19
Tamas Tudor I 413
Tankersley Kenneth B. III 75
Tankersley Kenneth B. III 45
Tarhule-Lips Rozemarijn F. A. I 146
Tarhule-Lips Rozemarijn F. A. I 261
Tasler R. I 481
Terlau Craig A. I 133
Teutsch Georg II 163
Teutsch Georg II 65
Thys G. V 103
Tognini Paola I 345
Tomova Bisera V 131
Toth V. A. II 120
Toussaint Michel III 21
Tremblay Marc I 497
Trimbom P. II 303
Trofimova Elena I 391
Tsankov Ludmil T. I 105
Tsankov Ludmil T. I 107
Tsankov Ludmil T. I 110
Tsankov Ludmil T. I 111
Tsankov Ludmil T. I 65
Tuccimei Paola I 37
Tulis Ján IV 107
Turberg Pascal II 243
Turchinov Igor I 121
Turchinov Igor I 239
Tyc Andrzej I 289
Tyc Andrzej I 323
Tyson P. D. I 55
Tysseland Magne I 235
Uhrin Marcel III 325
Urbani Franco I 243
Usuloglu Ender V 123
Vacquié Jean-François IV 57
Vadillo I. II 251
Valdés J. J. II 95
Vallejos A. II 43
van Beyden P. E. II 120
Van Beynen P. E. I 262
Vanara Nathalie II 115
Vanara Nathalie I 359
Vasileva Danica I 175
Vasiliev Andrey G. III 321
Vendramini Guilherme IV 51
Veni George I 373
Verheyden Sophie I 93
Verheyden Sophie IV 111
Verheyden Sophie IV 115
Versa Dorotea V 69
Vianey-Liaud M. I 424
Viehmann Iosif I 227
Viehmann Iosif III 133
Vremir Matei I 413
Wan Junwei Y. II 21
Wang Daqing III 311
Wang Fuchang I 433
Watson Patty Jo III 29
Weber Dieter III 307
Weidmann Yvo IV 37
Weidmann Yvo IV 65
Weisgerber Gerd III 216
Weissensteiner Volker I 425
Werner Andreas II 187
White Elisabeth L. II 191
White Elizabeth L. I 155
White Elizabeth L. I 305
White William B. II 191
White William B. I 155
White William B. I 305
White William B. I 89
Wilcock John D. V 61
Willems Luc I 477
Williams Paul W. I 92
Wollman S. II 225
Wolniewicz Klaus I 453
Wookey V 57
Worthington Stephen R. H. II 195
Wutzig B. III 277
Xiying Xiao IV 55
Xuewen Zhu II 121
Yaseen Ahmed E. III 371
Yonge Charles J. I 107
Yonge Charles J. I 111
Yonge Charles J. I 436
Yonge Charles J. I 65
Yonge Charles J. I 105
Yonge Charles J. I 60
Zabo L. II 51
Zaenker Stefan III 307
Zambo Laszlo I 44
Zechner Eric II 199
Zhao Jingbo I 300
Zhaohui Zhang III 297
Zhu Xuewen I 385
Zhu Yuanfeng V 47
Zuber A. II 171
Zuccoli Luisa I 345
Zupan Hajna Nadja I 33
Zurbrügg Ch. II 9
Zwahlen François II 209

Glattalp, Switzerland (Photo Pali Berg)

Faustloch, Promenadegang, BE, Switzerland (Photo Urs Widmer)

Faustloch, Promenadegang, BE, Switzerland (Photo Urs Widmer)

Hölloch, Tempelgang, SZ, Switzerland (Photo Pali Berg)

Lechuguilla, New Mexico, U.S.A. (Photo Urs Widmer/Sura Ballmann)